Indexes
ENGINEERING-TRANSPORTATION
LIBRARY
THE UNIVERSITY OF MICHIGAN
MAY 11 1966
ENGINEERING LIBRARY

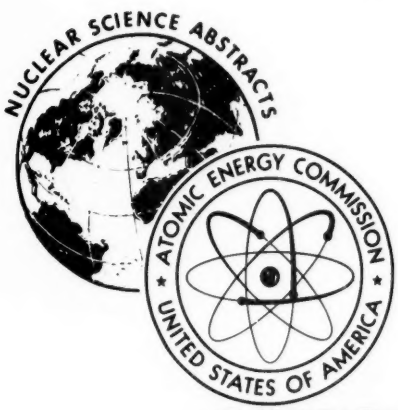

NUCLEAR SCIENCE ABSTRACTS

Volume 20 Number 7

Abstracts 10503–12562

April 15, 1966

UNITED STATES ATOMIC ENERGY COMMISSION
Division of Technical Information

DEPOSITED BY THE
UNITED STATES OF AMERICA

USAEC DEPOSITORY LIBRARIES

Collections of USAEC reports are maintained in the libraries of the organizations listed below for reference use by the general public. Facilities for making photocopies are available. The USAEC also makes available through these libraries atomic energy reports of countries other than the U. S. that are abstracted in *Nuclear Science Abstracts*.

ALABAMA
Auburn, Auburn University
ALASKA
College, University of Alaska
ARIZONA
Tucson, University of Arizona
ARKANSAS
Fayetteville, University of Arkansas
CALIFORNIA
Berkeley, University of California
Davis, University of California
Los Angeles, University of California
San Diego, Public Library
Stanford, Stanford University
COLORADO
Boulder, University of Colorado
Denver, Public Library
CONNECTICUT
New Haven, Yale University
DELAWARE
Newark, University of Delaware
DISTRICT OF COLUMBIA
Washington, Library of Congress
FLORIDA
Coral Gables, University of Miami
Gainesville, University of Florida
Tallahassee, The Florida State University
GEORGIA
Atlanta, Georgia Institute of Technology
HAWAII
Honolulu, University of Hawaii
ILLINOIS
Chicago, John Crerar Library
Chicago, University of Chicago
Evanston, Northwestern University
Urbana, University of Illinois
INDIANA
Bloomington, Indiana University
Lafayette, Purdue University
IOWA
Ames, Iowa State University
KANSAS
Manhattan, Kansas State University
KENTUCKY
Lexington, University of Kentucky
Louisville, University of Louisville
LOUISIANA
Baton Rouge, Louisiana State University
New Orleans, Tulane University
MARYLAND
Baltimore, Johns Hopkins University
College Park, University of Maryland
MASSACHUSETTS
Cambridge, Harvard University
Cambridge, Massachusetts Institute of Technology
MICHIGAN
Ann Arbor, University of Michigan
Detroit, Public Library
East Lansing, Michigan State University
MINNESOTA
Minneapolis, University of Minnesota
MISSISSIPPI
State College, Mississippi State University
MISSOURI
Kansas City, Linda Hall Library
Rolla, University of Missouri School of Mines and Metallurgy
St. Louis, Washington University
MONTANA
Bozeman, Montana State College
NEVADA
Las Vegas, Nevada Southern University
Reno, University of Nevada
NEW JERSEY
Princeton, Princeton University
Teaneck, Fairleigh Dickinson University
NEW MEXICO
Albuquerque, University of New Mexico
NEW YORK
Albany, The University of the State of New York
Buffalo, State University of New York at Buffalo
Ithaca, Cornell University
New York, Atomic Industrial Forum, Inc.
New York, Columbia University
New York, New York University
Rochester, University of Rochester
Schenectady, Union College
Syracuse, Syracuse University
Troy, Rensselaer Polytechnic Institute
NORTH CAROLINA
Charlotte, Public Library of Charlotte and Mecklenburg County
Durham, Duke University
Raleigh, North Carolina State College
NORTH DAKOTA
Grand Forks, University of North Dakota
OHIO
Cincinnati, University of Cincinnati
Cleveland, Public Library
OHIO (CONT.)
Columbus, Ohio State University
Toledo, University of Toledo
Youngstown, Youngstown University
OKLAHOMA
Norman, University of Oklahoma
Stillwater, Oklahoma State University
OREGON
Corvallis, Oregon State University
Portland, Reed College
PENNSYLVANIA
Philadelphia, University of Pennsylvania
Pittsburgh, Carnegie Library
University Park, Pennsylvania State University
PUERTO RICO
Rio Piedras, University of Puerto Rico
RHODE ISLAND
Providence, Brown University
SOUTH CAROLINA
Columbia, University of South Carolina
TENNESSEE
Knoxville, University of Tennessee
Memphis, Public Library
Nashville, Joint University Libraries
Oak Ridge, Oak Ridge Associated Universities
TEXAS
Austin, University of Texas
College Station, Texas A & M University
Dallas, Southern Methodist University
Houston, Rice University
Lubbock, Texas Technological College
San Antonio, Public Library
UTAH
Salt Lake City, University of Utah
VIRGINIA
Blacksburg, Virginia Polytechnic Institute
Charlottesville, University of Virginia
Norfolk, Old Dominion College
WASHINGTON
Pullman, Washington State University
Seattle, University of Washington
WEST VIRGINIA
Morgantown, West Virginia University
WISCONSIN
Madison, University of Wisconsin
Milwaukee, Public Library
WYOMING
Laramie, University of Wyoming

DEPOSITED BY THE
UNITED STATES OF AMERICA

Volume 20, Number 7, April 15, 1966

NUCLEAR SCIENCE ABSTRACTS

A semimonthly publication of the USAEC Division of Technical Information, Edward J. Brunenkant, Director.
Published by the USAEC Division of Technical Information Extension, Robert L. Shannon, Extension Manager.

Nuclear Science Abstracts covers the international literature on nuclear science and technology and provides the only comprehensive abstracting and indexing of this body of information. Published twice each month since 1947, *NSA* covers technical reports of the U. S. Atomic Energy Commission and its contractors, technical reports of U. S. Government agencies and other governments, universities, industrial and research organizations, as well as patents, books, and journal literature on a world-wide basis. Nearly 350,000 abstracts have appeared in *NSA* through Volume 19. The subject matter covered in *NSA* is described in issue Number 1 and in TID-4552, *Subject Scope of Nuclear Science Abstracts,* available free from the U. S. Atomic Energy Commission, Division of Technical Information Extension, P. O. Box 62, Oak Ridge, Tennessee 37830.

Abstracts are arranged according to a number of subject categories and subcategories. Definitions of categories appear in issues Number 1 and 13. If the language of the original item is not English, the language will be indicated. Translations are not abstracted where an abstract of the original item has appeared in *NSA*.

INDEXES TO NSA

Corporate author, personal author, subject, and report number indexes appear in each issue and are cumulated quarterly, semiannually, and annually. Multi-volume cumulations have been issued as indicated on the following page. Report number indexes for all volumes (1–18) were issued at the end of Vol. 18. At the end of Vol. 19, the indexes for Vols. 1–15 were reissued to include additional public availability information. This cumulation will be a permanent shelf item and will not be reissued. Report number indexes for Vol. 19 are included as a cumulation beginning with Vol. 16.

AVAILABILITY OF PUBLICATIONS ABSTRACTED

The public availability of all U. S. Atomic Energy Commission reports is indicated in the report number indexes. The availability of other reports, when known, is also indicated. The availability of some unnumbered reports is given in the abstract.

Dissertations abstracted in *Dissertation Abstracts* and included in *NSA* are available from University Microfilms, Inc., 315 N. First Street, Ann Arbor, Michigan 48103.

Most of the published literature abstracted in *NSA* is on deposit at the Library, Oak Ridge Associated Universities, Oak Ridge, Tennessee, (a USAEC depository library) and is available through interlibrary loan. When requesting papers from this source, it is important that *NSA* volume and abstract number be cited.

HOW TO OBTAIN NUCLEAR SCIENCE ABSTRACTS

NSA is available on an exchange basis to universities, research institutions, industrial firms, and publishers of scientific information. Inquiries should be directed to the U. S. Atomic Energy Commission, Division of Technical Information Extension, P. O. Box 62, Oak Ridge, Tennessee 37830.

Government agencies may obtain *NSA* free of charge.

NSA is available to the general public on a subscription basis from the Superintendent of Documents, U. S. Government Printing Office, Washington, D. C. 20402, as follows:

For the 24 regular issues, $30.00 domestic, $37.00 foreign. A single issue costs $1.75, plus 25 per cent for foreign mailing. Domestic rates apply to the United States, Canada, Mexico, and Central and South American countries except Argentina, Brazil, British and French Guiana, Surinam, and British Honduras. Foreign rates apply to the countries excepted above and to all other countries throughout the world.

For the quarterly, semiannual, and annual indexes, $22.00 domestic, $25.00 foreign.

Multivolume subject and author indexes are available as follows:

Vols. 1–4 (1948–1950) Johnson Reprint Corporation, 111 Fifth Avenue, New York, N. Y. 10003, $30.00.

Vols. 5–10 (1951–1956) Superintendent of Documents, U. S. Government Printing Office, Washington, D. C. 20402, $5.25.

Vols. 11–15, Subjects, Superintendent of Documents, U. S. Government Printing Office, Washington, D. C. 20402, $19.00.

Vols. 11–15, Personal Authors, Superintendent of Documents, U. S. Government Printing Office, Washington, D. C. 20402, $14.25.

Vols. 11–15, Corporate Authors, Superintendent of Documents, U. S. Government Printing Office, Washington, D. C. 20402, $2.50.

Cumulative Report Number Index, Vols. 1–15, Revised, is available from the Superintendent of Documents, U. S. Government Printing Office, Washington, D. C. 20402, $4.00.

Cumulative Report Number Index, Vols. 16–19, is available from the Superintendent of Documents, U. S. Government Printing Office, Washington, D. C. 20402, $2.50.

Annual Indexes are available separately from the U. S. Government Printing Office as follows:

Vol. 16, Subject and Authors, $9.75.
Vol. 17, Subject and Authors, $12.25.
Vol. 18, Subject and Authors, $12.50.
Vol. 19, Subject and Authors, $12.50.

ACKNOWLEDGMENTS

Agreements between the United States Atomic Energy Commission and the following organizations with regard to providing continuing services and specific literature coverage for *Nuclear Science Abstracts* are gratefully acknowledged:

American Institute of Physics; Atomic Energy of Canada Limited; Atomic Energy Research Establishment, United Kingdom; European Atomic Energy Community (EURATOM); Gmelin Institute; International Atomic Energy Agency; Japan Atomic Energy Bureau—Japan Atomic Energy Research Institute; Netherlands Patent Office; Reactor Centrum Nederland.

TABLE OF CONTENTS

Volume 20, Number 7, April 15, 1966

Category	Page
BIOLOGY AND MEDICINE	1297
General	1297
Ecology	1297
Metabolism, Tissue Distribution, and Toxicology	1298
Radiation Effects on Biochemicals	1304
Radiation Effects on Tissues	1306
Radiation Effects Therapy and Countermeasures	1321
Radiation Hazards and Protection	1323
Radiotherapy and Radiodiagnosis	1324
CHEMISTRY	1330
General	1330
Analytical Procedures	1330
Inorganic and Physical Chemistry	1335
Organic Chemistry	1342
Radiation Chemistry	1343
Radiochemistry	1351
Separation Processes and Procedures	1353
ENGINEERING	1357
General	1357
Applications of Nuclear Explosions	1357
Facilities and Equipment	1357
Heat Transfer and Fluid Flow	1359
Materials Testing	1361
Space Propulsion	1361
Vacuum Engineering	1361
GEOLOGY, METEOROLOGY, AND MINERALOGY	1362
General	1362
Meteorology	1362
Natural Radioactivity and Fallout	1362
Techniques and Equipment	1363
Thorium and Uranium Minerals	1364
HEALTH AND SAFETY	1365
INSTRUMENTATION	1369
General	1369
Radiation Detection	1371
Radiation Effects	1380
ISOTOPE TECHNOLOGY	1382
General	1382
Industrial Applications	1382
Power Application	1382
Separation and Production	1383
MATHEMATICS AND COMPUTERS	1384
METALS, CERAMICS, AND OTHER MATERIALS	1386
General	1386
Corrosion	1388
Fabrication	1389
Properties and Structure	1392
Radiation Effects	1401
PHYSICS	1404
General	1404
Accelerators	1405
Astrophysics and Cosmology	1410
Atomic Physics	1411
Cosmic Radiation	1421
Direct Energy Conversion	1424
Elementary Particles and Radiations	1425
Field Theory, Scattering Theory, and Symmetries	1438
Fluid Physics and Thermodynamics	1446
Geophysics	1450
Gravitation, Quantum Mechanics, and Relativity Theory	1457
Low Temperature Physics	1460
Neutron Physics	1464
Nuclear Properties and Reactions	1466
Plasma Physics and Thermonuclear Processes	1489
Shielding	1501
Solid State Physics	1502
REACTOR TECHNOLOGY	1510
General	1510
Auxiliaries and Components	1510
Criticality Studies	1512
Design and Feasibility	1515
Fuels	1515
Power and Power-Breeder Reactors	1516
Process Heat Reactors	1523
Production Reactors	1523
Propulsion and Space	1523
Research and Test Reactors	1526
WASTE DISPOSAL AND PROCESSING	1530
GENERAL AND MISCELLANEOUS	1532
CORPORATE AUTHOR INDEX	INDEX-1
PERSONAL AUTHOR INDEX	INDEX-10
SUBJECT INDEX	INDEX-54
REPORT NUMBER INDEX	INDEX-141

STAFF OF NUCLEAR SCIENCE ABSTRACTS

MANAGING EDITOR

John W. Norris

ASSISTANT MANAGING EDITOR

Donald D. Davis

ASSOCIATE EDITORS

Lawrence T. Whitehead
David E. Bost
Robert C. Kelly
Lee M. Thompson

SUBJECT INDEX EDITOR

Everett J. Hoffman

EVALUATORS

William D. Matheny
John H. Mitchell
Mary H. Newman

ABSTRACTORS

F. S. Armstrong (AECL)
Jane G. Buchanan
D. Lamar Cason
Helen G. Donald
James R. Dulaney
Wells L. Green
Mary Catherine Grissom
Fernando J. Hamilton
Phyllis C. Hansen
Thomas F. Heagerty
Carolyn D. Houston
Rose V. Jermain
Betty L. McDowell
Jean F. Peckham
Mona H. Raridon
Julia Redford
Lila B. Smith
Charles E. Stuber
Martha J. Thomas
Anne G. Ward
David C. West
Milton O. Whitson
Gabriel O. Ycaza

SUBJECT HEADING SPECIALIST

Robert E. Upchurch

CORPORATE AUTHOR SPECIALIST

Clara L. Fox

DESCRIPTIVE CATALOGING SPECIALIST

J. Paul Meredith

SCHEDULING AND PUBLISHING COORDINATOR

Brainard L. Patton

Communication concerning the editorial policy and content of *NSA* should be addressed to the Managing Editor, *Nuclear Science Abstracts*, AEC Division of Technical Information Extension, P. O. Box 62, Oak Ridge, Tennessee 37830.

Use of funds for printing this publication approved by the Director of the Bureau of the Budget, May 20, 1963

Volume 20, Number 7 April 15, 1966

NUCLEAR SCIENCE ABSTRACTS

BIOLOGY AND MEDICINE

General

10503 (BNWL–122) HANFORD BIOLOGY RESEARCH ANNUAL REPORT FOR 1964. Thompson, R. C.; Woods, S. W. (eds.). (Battelle-Northwest, Richland, Wash. Pacific Northwest Lab.). Jan. 1965. Contract AT(45-1)-1830. 229p. Dep. mn. CFSTI $6.00 cy, $1.25 mn.

Separate abstracts were prepared on forty-one sections of this report. Two sections were abstracted previously and appeared in NSA Vol. 19 as numbers 31856 and 40350. A list is included of 49 publications during the period covered by this report. (C.H.)

For abstracts of individual papers see: 10504, 10505, 10513–10538, 10596–10601, 10717, 10718, 11011, 11012, 11060, 11091, and 11184.

10504 (BNWL–122, pp 142) EFFECTS OF A SULFOXIDE COMPOUND ON FLOUR BEETLES EXPOSED TO X RAYS. Erdman, H. E. (Battelle-Northwest, Richland, Wash. Pacific Northwest Lab.).

The effects of various sulfoxide compounds on the sensitivity of flour beetles, Tribolium confusum and Tribolium castaneum to x radiation was investigated. Results are presented in tabular form. (C.H.)

10505 (BNWL–122, pp 146-9) LIVER INFILTRATES IN RADIATION CHIMERAS. Uyeki, E. M.; Palotay, J. L. (Battelle-Northwest, Richland, Wash. Pacific Northwest Lab.).

A numerical tally of microscopic foci of leukocytic infiltrates in the liver was shown to provide a sensitive means of detecting early graft-host interaction in radiation chimeras. The results suggest that the hepatomegaly of mouse-rat x radiation chimeras arises from an increase in all functional elements of the liver and that the infiltrates are a host response to graft versus host activity of donor cells. (auth)

10506 THE EFFECT OF 6-MERCAPTOPURINE AND OF X-RAYS ON SKIN HOMOGRAFTS. Bruzzese, E.; Patriarca, G.; Favuzzi, E.; Greco, G. (Sanita Militare, Rome). Giorn. Med. Mil., 114: 752-9(1964).

Survival of skin homografts in rats was doubled, compared to the controls, by the administration of 6-mercaptopurine during the 15 days after the graft. However, the same treatment was ineffective when begun with the appearance of the first necrotic area and when given conjunction with x-irradiation of the donor or recipient prior to grafting. (H.G.D.)

10507 THE STATUS OF REACTORS FOR BIOLOGICAL AND MEDICAL USE. Kitao, Kensuke (National Inst. of Radiological Sciences, Chiba, Japan). Nippon Genshiryoku Gakkaishi, 7: 694-702(Dec. 1965). (In Japanese).

The uses of nuclear reactors for biological and medical purposes, especially in therapeutic applications, health physics research, and radiobiological investigation, are summarized. The status of research work is reviewed. At present, the production of radioisotopes is the most important application of the reactor in biology and medicine. (auth)

10508 OBSERVATIONS ON THE SELECTIVE PERMEABILITY OF THE HUMAN PLACENTA TO PLASMA PROTEINS AND PROTEIN HORMONES. Gitlin, D. (Univ. of Pittsburgh Medical School. Heinz Memorial Labs. of the Children's Hospital, Pittsburgh). pp 197-204 of STI/DOC/10/45.

The selectivity of the human placenta in the transfer of plasma proteins and protein hormones between mother and fetus is considered briefly, and the significance of this selectivity on the survival of the newborn infant is discussed. (H.G.D.)

10509 ISOTOPES IN EXPERIMENTAL PHARMACOLOGY, CONFERENCE, CHICAGO, JUNE 7–9, 1964. Roth, Lloyd J. (ed.). Chicago, The University of Chicago Press, 1965. 502p. $12.50. (CONF-640628).

Thirty-six papers, authored by 40 authorities from the United States and 10 foreign countries, report the results of recent studies on the isotopic labeling of drugs, biological applications of activation analysis, autoradiographic studies of the distribution of drugs, the use of labeled pharmaceuticals in compartment analysis and dynamic measurements, drug biotransformation, biochemical pharmacology, and deuterium effects. This collection of papers illustrates the diversity and usefulness of isotopes in experimental pharmacology. (C.H.)

Ecology

10510 (BNL–9835) WEATHER MODIFICATION: THE EFFECT ON THE BIOLOGICAL EQUILIBRIUM IN THE PLANT COMMUNITY. Whittaker, R. H. (Brookhaven National Lab., Upton, N. Y.). [1966]. Contract AT-30-2-GEN-16. 24p. (CONF-651211–2). Dep. mn. CFSTI $1.00 cy, $0.50 mn.

From American Assn. for the Advancement of Science, Berkeley, Calif.

The effects of change in amount of mean annual precipitation, and increase in mean annual temperature on plant communities are discussed. Agricultural plant communities are excluded. Recommendations are given concerning further ecological studies along these lines. (P.C.H.)

10511 (BNL–9836) SPECIES-DIVERSITY PROBLEMS IN PLANT COMMUNITIES. Whittaker, R. H. (Brookhaven National Lab., Upton, N. Y.). Dec. 28, 1965. Contract AT-30-2-GEN-16. 13p. (CONF-651211–1). Dep. mn. CFSTI $1.00 cy, $0.50 mn.

From American Assn. for the Advancement of Science, Berkeley, Calif.

The forms of dominance-diversity curves, means of measuring diversity, and the perspective of interpretation as applied to plant communities are discussed. (P.C.H.)

10512 RADIOACTIVITY OF MINERAL WATERS RPR. XII. THE NATURAL RADIOACTIVITY OF THE WATER, DEPOSITIONS, AND CERTAIN SEA ORGANISMS OF THE BLACK SEA AND TECHIRGHIOL. Szabo, Arpad; Serbanescu, Octavian. An. Stiint. Univ. Al. I Cuza Iasi, Sect. II, 9: 157-62(1963). (In Rumanian).

The concentrations of some natural radioactive elements (U, Ra, and Rn) in the waters of the Black Sea and of Lake Techirghiol in relation to the concentration of some marine sediments, mud, and ashes of marine zooplankton were determined. The results are tabulated. A continuing study is being made on the selective accumulation capacity of various marine creatures and principally of marine phytoplankton for radioactive elements. (tr-auth)

Metabolism, Tissue Distribution, and Toxicology

Refer also to abstracts 11012 and 11054.

10513 (BNWL-122, pp 16-20) WHOLE-BODY RETENTION AND BIOLOGICAL EFFECTS OF INHALED ^{144}Ce-^{144}Pr AND ^{106}Ru-^{106}Rh OXIDES IN BEAGLES. Stuart, B. O. (Battelle-Northwest, Richland, Wash. Pacific Northwest Lab.).

In beagle dogs one-half to one-third of inhaled peroxide-prepared ^{144}Ce-$^{144}PrO_2$, calcined ^{144}Ce-$^{144}PrO_2$, or calcined ^{106}Ru-$^{106}RhO_2$ was rapidly cleared within 7 to 20 days. The remaining cerium and ruthenium were retained with biological half-lives of several years. Calcined ^{144}Ce-$^{144}PrO_2$ translocated to the liver and skeleton more slowly than ^{144}Ce-$^{144}PrO_2$ precipitated with peroxide; calcined ^{106}Ru-$^{106}RhO_2$ has remained in the region of the lungs for more than one year postexposure. One dog died eight months after depositing 2 mCi of peroxide-prepared ^{144}Ce-$^{144}PrO_2$; the remaining animals show varying degrees of lymphocyte depression. (auth)

10514 (BNWL-122, pp 21-4) SELECTIVE TISSUE ACCUMULATION OF URANIUM AND THORIUM IN RATS AFTER INHALATION OF URANIUM ORE DUST. Stuart, B. O.; Beasley, T. M. (Battelle-Northwest, Richland, Wash. Pacific Northwest Lab.).

Highly sensitive analytical techniques were developed to measure small amounts of U and Th present in tissues. Chemical separation and subsequent α counting were used. Groups of rats inhaled uranium ore aerosols semiweekly for two months. ^{230}Th activity levels in the lungs were twice those of ^{238}U by the end of exposures, increasing to nine times after four months due to selective removal of uranium. Levels of ^{230}Th in tracheo-bronchial lymph nodes were also higher than ^{238}U. Uranium levels in the kidneys and femurs were initially higher than thorium, but by two months post-exposure thorium activities were equal to or greater than those of uranium. This rapid in vivo separation of uranium and thorium is important for permissible limit considerations. These findings indicate that uranium and thorium become dissociated in the lung shortly after inhalation, each showing retentions similar to those of their pure oxides. (auth)

10515 (BNWL-122, pp 46-8) CYCLING OF ^{90}Sr IN MOLTING CRAYFISH. Dean, J. M. (Battelle-Northwest, Richland, Wash. Pacific Northwest Lab.).

Crayfish (Pacifastacus trowbridgi) injected with ^{90}Sr-^{90}Y while in the premolt stage concentrated the isotope in the gastrolith and fixed it in the exoskeleton. At molt the ^{90}Sr-^{90}Y in the gastrolith was mobilized and deposited in the postmolt exoskeleton. (auth)

10516 (BNWL-122, pp 49-51) BIOLOGICAL EFFECTS OF ^{131}I IN SHEEP AND CATTLE. Ragan, H. A.; McClanahan, B. J.; Horstman, V. G.; Shannon, R. O.; Bustad, L. K. (Battelle-Northwest, Richland, Wash. Pacific Northwest Lab.).

Peak thyroid uptake of ^{131}I in a group of ewes fed a single oral dose of 3 mCi ^{131}I seven years ago was not greatly different than results obtained two years ago (mean about 11%). Tissue ^{131}I concentrations in three cows are lower than those seen in sheep chronically fed ^{131}I. ^{131}I is present in detectable amounts in the distal colon of sheep within 20 min after receiving the isotope orally. Stable iodine administered to ewes several days prior to parturition reduced neonatal thyroid uptake of ^{131}I about 40% from that seen in control lambs. Continuing long term studies on the biological effects of ^{131}I in sheep are summarized. (auth)

10517 (BNWL-122, pp 52-4) SHEEP MILK PRODUCTION AND ITS ^{131}I CONTENT. Ragan, H. A.; Horstman, V. G.; McClanahan, B. J.; Bustad, L. K. (Battelle-Northwest, Richland, Wash. Pacific Northwest Lab.).

A study was undertaken in sheep to determine the secretion rate of milk as influenced by the time interval between milkings. Determined concurrently was the secretion of ^{131}I in milk following a single oral dose, the plasma levels of ^{131}I, and the influence of intravenously administered posterior pituitary extract on the protein-bound iodine (PBI) content of milk. Milk secretion in the groups of ewes studied appears to be linear over a 24 hr period with a daily secretion of about 1000 ml. Peak milk ^{131}I values occur near 5 hr postadministration and fall rapidly, whereas plasma ^{131}I levels have a diphasic pattern with a rapid peak, a decline, and then gradual rise again. Posterior pituitary extract apparently increases protein-bound iodine concentrations in milk when given intravenously shortly before sampling. (auth)

10518 (BNWL-122, pp 55-8) THYROID UPTAKE OF ^{131}I FROM SKIN EXPOSURE. Murray, J. L. (Battelle-Northwest, Richland, Wash. Pacific Northwest Lab.).

The maximum thyroid uptake in young swine following exposure of 150 cm area of swine skin to ^{131}I vapor was about 0.2 to 0.4% of the deposited dose and occurred on the fifth day. Following application of solution containing ^{131}I to a comparable area, allowing it to dry and then washing the area, peak thyroid concentrations of 0.1% of the total dose deposited occurred by the second day. Over 95% of the radioiodine was removed by washing. (auth)

10519 (BNWL-122, pp 59-63) ANALOG COMPUTER EVALUATION OF TELLURIUM-IODINE CONTAMINATION EVENTS. Watson, E. C.; Harvey, R. A.; Bustad, L. K. (Battelle-Northwest, Richland, Wash. Pacific Northwest Lab.).

Applications of analog computing for evaluating radionuclide kinetics especially following contamination events are discussed. A model was established limiting the compartments to total body, skin, lungs, gastrointestinal tract (stomach, small intestines, and large intestines), muscle, bone thyroid, liver, and kidneys. These compartments would satisfy the needs of all of the elements that result from the fission of ^{235}U. Transfer coefficients for ^{132}Te and ^{132}I used in the model are presented. Data are included on ^{132}Te-^{132}I burdens in several organs following the ingestion of 100 μC ^{132}Te. (auth)

10520 (BNWL-122, pp 64-6) RELATIONSHIP OF ^{137}Cs CONCENTRATION IN FEED AND RUMEN CONTENTS. Shannon, R. O.; Ragan, H. A.; Bustad, L. K. (Battelle-Northwest, Richland, Wash. Pacific Northwest Lab.).

A series of four studies were conducted with sheep to compare the ^{137}Cs concentration in the rumen contents with that in the feed ingested. The ^{137}Cs concentration in the rumen exceeded that in the feed in only those animals that received water on a regulated basis. (auth)

10521 (BNWL-122, pp 73-4) METABOLISM OF ^{137}Cs IN TROUT. Dean, J. M.; Eapen, J.; Nakatani, R. E. (Battelle-Northwest, Richland, Wash. Pacific Northwest Lab.).

Cesium-137 injected intravenously into yearling rainbow trout was distributed uniformly through the soft tissues with the exception of the white muscle. The effective half-life of ^{137}Cs in red muscle was 5½ days and in white muscle was 13 days. (auth)

10522 (BNWL-122, pp 79-80) EFFECT OF DIETARY AND HORMONAL MANIPULATIONS ON ^{237}Np-INDUCED

FATTY LIVERS. Mahlum, D. D. (Battelle-Northwest, Richland, Wash. Pacific Northwest Lab.).

Liver fat accumulation induced by injection of ^{237}Np into female rats can be reduced by prior hypophysectomy or adrenalectomy. Oral administration of glucose or butylated hydroxytoluene also resulted in a decreased fatty response to ^{237}Np. Thyroidectomy, ovariectomy, and testosterone treatment were without effect in female rats. Castration or injection of estradiol did not render the male more susceptible to ^{237}Np-induced fatty livers. (auth)

10523 (BNWL–122, pp 81-2) TRANSLOCATION OF SUBCUTANEOUSLY ADMINISTERED $^{239}PuO_2$. McClanahan, B. J.; Ragan, H. A. (Battelle-Northwest, Richland, Wash. Pacific Northwest Lab.).

The amount of plutonium deposited in soft tissues following subcutaneous injections of $^{239}PuO_2$ was about one-hundredth of that deposited when ^{239}Pu nitrate was injected in swine. The regional lymph nodes were an exception, accumulating up to one-half as much when $^{239}PuO_2$ was injected as when ^{239}Pu nitrate was injected. (auth)

10524 (BNWL–122, pp 83-4) EFFECT OF SPLENECTOMY ON ACUTE PLUTONIUM TOXICITY. Ballou, J. E. (Battelle-Northwest, Richland, Wash. Pacific Northwest Lab.).

The survival time of rats injected intravenously with either ^{238}Pu or ^{239}Pu was not altered by prior splenectomy. This would seem to eliminate spleen damage as a critical factor in explaining the greater acute toxicity of ^{239}Pu. (auth)

10525 (BNWL–122, pp 85-90) GASTROINTESTINAL ABSORPTION OF ^{144}Ce AND ^{147}Pm IN MINIATURE SWINE. McClellan, R. O.; Bustad, L. K.; Keough, R. F. (Battelle-Northwest, Richland, Wash. Pacific Northwest Lab.).

Miniature swine absorbed about 0.01% of an oral dose of ^{144}Ce chloride or oxide and about 0.001% of an oral dose of ^{147}Pm perchlorate. The majority of the absorbed material was found in liver and skeleton. (auth)

10526 (BNWL–122, pp 91-3) CHEMICAL CARCINOGENS AND RADIONUCLIDE METABOLISM. Mahlum, D. D. (Battelle-Northwest, Richland, Wash. Pacific Northwest Lab.).

The liver carcinogens, dimethylaminoazobenzene and diacetylaminofluorene, have been shown to increase the retention of $^{144}Ce-^{144}Pr$ and ^{238}Pu by the liver of rats. These carcinogens appear to act by decreasing biliary excretion of the radionuclides. (auth)

10527 (BNWL–122, pp 94-8) MILK SECRETION OF ^{65}Zn AND ^{115m}Cd IN SHEEP. McClanahan, B. J.; Ragan, H. A. (Battelle-Northwest, Richland, Wash. Pacific Northwest Lab.).

The concentration of intravenously administered ^{65}Zn in the milk of lactating ewes was approximately 8 times that in plasma, while the concentration of ^{115m}Cd in milk was 15 times its plasma concentration. Elevating the quantity of stable zinc simultaneously injected reduced the plasma clearance rate of ^{65}Zn and ^{115m}Cd, while their milk concentration was unchanged. Intramammary infusion of ^{65}Zn, ^{115m}Cd, and stable zinc via the teat canal demonstrated that both radionuclides were rapidly transferred from milk, but neither transfer rate was influenced by the presence of additional stable zinc in the milk. (auth)

10528 (BNWL–122, pp 101-6) EFFECT OF CHRONIC INGESTION OF ^{65}Zn IN TROUT. Nakatani, R. E.; Liu, D. H. W.; Clarke, W. J. (Battelle-Northwest, Richland, Wash. Pacific Northwest Lab.).

Three groups of rainbow trout fed ^{65}Zn at a daily rate of 0.01, 0.1, and 1.0 μCi/g fish for 17 weeks differed insignificantly from control fish in mortality, clinical hematology, and histology. However, damage was indicated when fish were fed at a rate of 10 μCi/g fish. The effective half-life for long term retention was 135 days. Trout with a body burden of 1600 μCi suffered no swimming performance decrement. Fish with more than 10,000 times the burden observed in river fish showed no effect. (auth)

10529 (BNWL–122, pp 110-12) ULTRAHIGH-SPEED GROSS ALPHA AUTORADIOGRAPHY. Hsieh, J. J. C.; Hungate, F. P.; Wilson, S. A. (Battelle-Northwest, Richland, Wash. Pacific Northwest Lab.).

High-speed gross alpha autoradiograms can be obtained using ZnS:Ag as an intensifier in conjunction with high-speed film. This technique requires approximately $^1/_{1000}$ of the exposure time needed by conventional methods using Kodak's NTB plates (nuclear track emulsion for beta particles). (auth)

10530 (BNWL–122, pp 113-17) EFFECT OF ^{127}I ON PASSAGE OF ^{131}I FROM COWS TO MAN VIA MILK. Watson, E. C.; Nelson, I. C.; Wood, D. H.; McClellan, R. O.; Bustad, L. K. (Battelle-Northwest, Richland, Wash. Pacific Northwest Lab.).

Milk from dairy cows fed ^{131}I and 0.002 to 2 g stable iodine was consumed by adult male volunteers. The resulting fractional thyroid uptake by eight men involved in both single and multiple intakes of ^{131}I was 0.1 to 0.3. Based on single intake data, the peak thyroid burden occurred at about 24 hr and decreased with an effective half-life of about 7 days. Increasing the iodine content of the cows' diet resulted in decreased amounts of ^{131}I appearing in both the cows' thyroids and milk and in the thyroids of volunteers consuming the milk daily from cows fed 2 g/day of stable iodine. (auth)

10531 (BNWL–122, pp 118-21) REMOVAL OF INTERNALLY DEPOSITED PLUTONIUM FROM RATS. Smith, V. H. (Battelle-Northwest, Richland, Wash. Pacific Northwest Lab.).

Deferoxamine (DFA) and diethylenetriaminepentaacetic acid (DTPA) when administered to the same rat showed a cooperative action wherein the plutonium deposition in bone reflected the DFA effect and the soft tissue response was that of DTPA. A similar response was not shown for the removal of well-fixed plutonium. (auth)

10532 (BNWL–122, pp 122-4) REMOVAL OF INTERNALLY DEPOSITED RUTHENIUM FROM RATS. Smith, V. H. (Battelle-Northwest, Richland, Wash. Pacific Northwest Lab.).

Several treatments were tested for the removal of ^{106}Ru from rats. None were successful on a practical basis. Results indicate that further study of reducing agents or sulfhydryl compounds in combination with chelons might lead to more effective treatments. (auth)

10533 (BNWL–122, pp 125-7) THE EFFECT OF DTPA ON TRANSLOCATION AND EXCRETION OF INHALED $^{144}Ce-^{144}Pr$ OXIDE IN DOGS. Tombropoulos, E. G.; Bair, W. J.; McDonald, K. E. (Battelle-Northwest, Richland, Wash. Pacific Northwest Lab.).

DTPA treatments increased the clearance of $^{144}Ce-^{144}Pr$ from all tissues after inhalation of $^{144}CeO_2$ which was prepared by precipitation with peroxide. However, after inhalation of calcined $^{144}CeO_2$, DTPA treatments caused the removal of only $^{144}Ce-^{144}Pr$ translocated to other tissues and did not appreciably reduce the lung burden. (auth)

10534 (BNWL–122, pp 168-9) INFLUENCE OF SOIL SODIUM ON PLANT UPTAKE OF ^{45}Ca, ^{85}Sr, AND ^{137}Cs. Cline, J. F.; Rickard, W. H. (Battelle-Northwest, Richland, Wash. Pacific Northwest Lab.).

The concentration of ^{85}Sr and ^{45}Ca in plants was reduced by 50% when grown in a high sodium soil. Cesium-137 concentration was reduced 25% by the same treatment. (auth)

10535 (BNWL–122, pp 176-80) RADIOACTIVITY IN ALASKAN ANIMALS AND FORAGE PLANTS. Watson, D. G.; Eberhardt, L. L.; Hanson, W. C. (Battelle-Northwest, Richland, Wash. Pacific Northwest Lab.).

Cesium-137 and ^{90}Sr were measured in large Alaskan herbivorous animals and their forage during 1963-64. In vegetation, lichens had highest concentrations of these radionuclides. The relatively high levels of ^{137}Cs and ^{90}Sr in reindeer and caribou were due to their consumption of lichens. Fallout concentrations in moose were about one-tenth that in caribou due to different food habits. Amounts of ^{137}Cs and ^{90}Sr have increased by a factor of four or more since 1960. (auth)

10536 (BNWL-122, pp 187-9) RADIONUCLIDE ACCUMULATION AND TRANSPORT BY PLANKTON IN THE COLUMBIA RIVER. Cushing, C. E. (Battelle-Northwest, Richland, Wash. Pacific Northwest Lab.).

A study was made of the accumulation and transport of ^{32}P and ^{65}Zn by net plankton in the Columbia River below the Hanford reactors. Net plankton, as used in this study, is defined as the free floating organic matter retained by a No. 20 mesh plankton net (68 meshes/cm) and includes both living and dead material. Cursory analysis of monthly averages of net plankton samples revealed that ^{32}P and ^{65}Zn concentration (nCi/g dry weight) was lowest during the summer months, probably related to dilution by runoff. Transport of these radionuclides by the plankton was highest in spring and late summer, coincident with seasonal increases of the plankton. The ability of the plankton to concentrate radioisotopes from the water varied seasonally with lowest values during the summer months. (auth)

10537 (BNWL-122, pp 190-3) RADIONUCLIDE ACCUMULATION AND PRODUCTIVITY OF PERIPHYTON IN THE COLUMBIA RIVER. Cushing, C. E. (Battelle-Northwest, Richland, Wash. Pacific Northwest Lab.).

The periphyton and the phytoplankton are important communities in the Columbia River in relation to radionuclide accumulation. Results are reported from a study of biological and environmental factors that are most influential in governing the amount of ^{32}P and ^{65}Zn accumulated from the river by the periphyton, and a comparison of the relationships among the commonly used production indices and certain environmental measurements. Data on the method of sorption of these nuclides were also evaluated. Best correlations among four biomass measurements of periphyton were between dry weight, ash weight, and chlorophyll a. Net production rate varied from 0.005 to 0.070 mg dry weight/cm^2/day and was closely related to chlorophyll a content and solar energy. The accumulation of ^{32}P and ^{65}Zn was best related to dry and ash weight, and chlorophyll a. Low correlations were found between radionuclide accumulation and the radionuclide content of the river. The data suggested that adsorption was the dominant mode of uptake. (auth)

10538 (BNWL-122, pp 198-201) REACTOR EFFLUENT MONITORING - 1964. Olson, P. A.; Nakatani, R. E. (Battelle-Northwest, Richland, Wash. Pacific Northwest Lab.).

Since monitoring of Hanford's reactor effluent started in 1945, the biological effects of the primary factors (heat, chemical toxicity, and radiation) have been defined in terms of growth and mortality for young chinook salmon. Comparisons between groups of chinook fingerlings reared in regular and cooled reactor effluent showed the importance of the accumulative effect of small temperature increments. Higher mortalities were observed in the present studies with local stock chinooks than in past studies with Puget Sound chinooks, due, perhaps, to physiological differences in racial stocks. Data are included on the content of ^{32}P and ^{65}Zn in fish reared in regular effluent for 10 weeks. (C.H.)

10539 (STI/DOC/10/45) RADIOISOTOPE TECHNIQUES IN THE STUDY OF PROTEIN METABOLISM, HELD IN VIENNA, JUNE 1–5, 1964. Technical Reports Series No. 45. (International Atomic Energy Agency, Vienna (Austria)). June 1965. 260p. (CONF-640629). IAEA: $4.50; S115,50; £1.13.0; F Fr 22,–; DM 19,25.

Twenty-four-papers were presented; separate abstracts were prepared for each. (H.G.D.)

For abstracts of individual papers see: 10508, 10558–10574, and 10941–10946.

10540 (HW-SA-3728) THE UTILIZATION OF TRYPTOPHAN BY NEUROSPORA. Matchett, William H. (General Electric Co., Richland, Wash. Hanford Atomic Products Operation). Dec. 18, 1964. Contract AT(45-1)-1350. 29p. Dep. mn. CFSTI $2.00 cy, $0.50 mn.

When Neurospora grows in media supplemented with tryptophan, 70–90% of the supplied tryptophan is converted in a series of reactions to anthranilic acid or derivatives of anthranilic acid. In certain strains (those blocked between shikimic acid and anthranilic acid) these reactions, coupled with the biosynthetic reactions, constitute a cycle involving the interconversion of anthranilic acid and tryptophan. Studies on the physiological control of these reactions revealed a marked effect of temperature upon the efficiency of utilization of tryptophan for the synthesis of protein. Subsequent investigation revealed that a small but significant quantity of indolepyruvic acid was accumulated in filtrates of cultures grown at the higher temperature and that this compound supported growth of strains requiring tryptophan. Studies with cell-free extracts of Neurospora indicate that the interconversion of tryptophan and indolepyruvic acid is mediated by a transaminase of nonspecific nature. (P.C.H.)

10541 STUDIES OF THE VENTROMEDIAL HYPOTHALAMUS WITH AUTORADIOGRAPHIC TECHNIQUES. Edelman, P. Michael; Schwartz, Irving L.; Cronkite, Eugene P.; Livingston, Linda (Brookhaven National Lab., Upton, N. Y. Univ. of Cincinnati). Ann. N. Y. Acad. Sci., 131: 485-501(Oct. 8, 1965). (BNL-8958).

Radioactivation techniques, radioautography, histological studies, and metabolic methods were employed to study the accumulation of gold in the hypothalamus and the development of hyperphagia and obesity in mice given intravenous goldthioglucose at various levels of blood glucose concentration. The findings indicate that the weight gain, the extent of the hypothalamic involvement, and the degree of hypothalamic gold accumulation generally reflect the blood goldthioglucose concentration in the first few minutes following the injection. The apparent selective permeability and/or transport of glucose into the ventromedial satiety area is considered to be a reflection of increased glucose metabolism in the glial cells of this area. A hypothesis is presented which correlates the blood glucose concentration with the degree of appetite inhibition. This hypothesis proposes that the degree of appetite inhibition of the ventromedial area is proportional to the number of nerve cells activated, that the generation of the action potential of the satiety neuron depends upon the metabolism of a specific quantity of glucose in the glial cell, and that there are different rates of glucose supply to, or different intrinsic rates of glucose metabolism in, the different neuron-glial complexes of the satiety area. (auth)

10542 UPTAKE OF ^{35}S-SODIUM SULFATE BY THE HEPATIC TISSUE OF NORMAL AND IRRADIATED RATS. Santagati, G.; Slaviero, G. E.; Cultrera, G.; Bosco, G. (Univ., Pavia, Italy). Arch. Sci. Med., 119: 48-56(1965).

The liver uptake of ^{35}S-labeled sodium sulfate was measured in normal rats and in rats irradiated with 500 and 1,000 R. The irradiated liver showed a reduced incorporation of the radioisotope. The reduced liver radioactivity was due mainly to a decreased incorporation of ^{35}S-labeled sodium sulfate in the residual organic fraction (mostly amino acids) in the liver and to a lesser extent in the proteins and polypeptides. (Exerpta Med.)

10543 QUANTITATIVE IN VIVO STUDIES ON THE COMPLETE INHIBITION OF THE WHOLE-BODY INCORPORATION AND RETENTION OF ^{131}I IN MAN. Heinrich, H. C. (Univ., Hamburg); Gabbe, E. E.; Meineke, B.; Whang, D. H.; Kuehnau, J. Jr. Atomkernenergie, 11: 83-8(Jan.-Feb. 1966). (In German).

The complete inhibition of the $^{131}I^-$-whole body incorporation and retention in man is required for the protection of the population against nuclear accidents and extended nuclear weapon test series as well as for studies on metabolism using labelled compounds. A 4π large volume radioactivity detector with a liquid organic scintillator and the ^{131}I-energy channel were used for ^{131}I-whole body retention measurements of the retained ^{131}I in man and its decorporation by oral iodide doses. The depression of the percentage of the oral $^{131}I^-$ test dose was used for the calculation of the ^{131}I decorporation effect. The ^{131}I-labelled portion of the organic iodine pool was reduced from 55–65% in control persons to about 0.1% by the oral administration three times of 200 mg KI at intervals of eight hours. The iodide

blockade has to be started as soon as possible after the oral $^{131}I^-$ uptake and has to be continued as long as free $^{131}I^-$ is introduced. The ^{131}I decorporated is excreted via urine with the biological half life of the inorganic iodine phase (~12 hours). Inhibitors of the iodide incorporation like ClO_4^- or SCN^- are not so efficient and harmless as iodide and their use is therefore inferior. (auth)

10544 STUDY ON THE HALF-LIVES AND EFFECTIVE EQUILIBRIUM OF RaD(^{210}Pb) AND RaF(^{210}Po) IN DOGS. Jaworowski, Z. (Inst. of Nuclear Research, Warsaw). Bull. Acad. Pol. Sci., Ser. Sci. Biol., 13: 439-45(1965).

The radiation dose absorbed in tissue from Ra decay products depends mainly on the high-energy α particles emitted by ^{210}Po. An attempt was made to determine the ^{210}Po/^{210}Pb ratios and the half life of ^{210}Po that originated from its parent ^{210}Pb after the intravenous injection of a mixture of ^{210}Pb, ^{210}Bi, and ^{210}Po in dogs. The dogs were sacrificed approximately 85 to 380 days after injection and the bones, liver, and muscles were analyzed for ^{210}Pb and ^{210}Po. Results indicate that the biological half lives of ^{210}Pb and ^{210}Po in mineral bone are 3300 days, and in liver are 3.8 and 719 days respectively. No information was obtained on the effective half life in muscles but the ^{210}Po/^{210}Pb ratio was found to be 0.14 in muscles, approximately 1.0 in bone, and 0.48 in liver. Factors affecting the ratio between ^{210}Po and ^{210}Pb in vivo are discussed. (C.H.)

10545 BALANCE OF NATURAL RADIOACTIVITY IN LEUKEMIA. Leonov, V. A.; Pavlova, M. P. (Minsk State Medical Inst.). Dokl. Akad. Nauk Belorussk. SSR, 9: 407-9(June 1965). (In Russian).

A study of the natural radioactivity balance in children with blood diseases and with massive leukemia was investigated. The results showed that there is a disturbance in the exchange of the natural radioisotopes in children with leukemia and this is probably based on a pathogenic change as a result of the leukemia. (J.S.R.)

10546 A STUDY OF THE RESPIRATORY INTAKE OF ^{45}Ca AND ^{204}Tl RADIONUCLIDES. Furnica, Gh., Racoveanu, N.; Toader, M.; Serban, D. (Inst. de Igiena si Protect. Muncii, Bucharest). Igiena (Bucharest), 13: 531-6(1964).

Respiratory uptake by man of an aerosol mixture consisting of ^{45}Ca and ^{204}Tl was studied. The total activity was 1,773 pC/l. After radiochemical separation the specific activity was 1,305 pC ^{204}Tl/l and 858 pC ^{45}Ca/l. Aerosols having a total activity of 8.06 μC ^{45}Ca and 12.26 μC ^{204}Tl were inhaled for five days. Immediate measurements revealed a radioactivity of 0.072 pC ^{204}Tl/ml and 1.70 pC ^{45}Ca/ml in the blood and 0.00124 pC ^{204}Tl/ml and 68.4 pC ^{45}Ca/ml in the urine. Determinations carried out 120 days after the contamination showed practically no ^{204}Tl activity ($1.49.10^{-5}$ pC ^{204}Tl/ml); the radioactivity of ^{45}Ca was 1.26 pC/ml. (Excerpta Med.)

10547 INTRAPULMONARY EXCHANGE OF THE STABLE ISOTOPE $^{18}O_2$ INJECTED INTRAVENOUSLY IN MAN. Lassen, N. A.; Fritts, H. W. Jr.; Caldwell, P. R. B.; Giuntini, C.; Dansgaard, W.; Cournand, A. (Columbia Univ., New York). J. Appl. Physiol., 20: 809-15(Sept. 1965).

After establishing the feasibility of injecting $^{18}O_2$ in solution, the authors compared the recovery of $^{18}O_2$ to that of the inert gas ^{85}Kr, tested the effect of changing the inspired oxygen concentration on the recovery of each of the two tracers, and contrasted the measured recoveries of $^{18}O_2$ with those which might be expected on theoretical grounds. Thus, $^{18}O_2$ was used to study the exchange of oxygen molecules between pulmonary capillary blood and alveolar gas in 16 patients with either normal lungs or limited lung disease. The technique entailed combining gaseous $^{18}O_2$ with blood, then mixing the blood anaerobically with saline containing T-1824 dye and ^{85}Kr in solution. After the combination of tracers had been injected into a vein, arterial blood was collected during the first passage of the indicators through the central circulation. Recoveries of the tracer gases were expressed as percentages of the amounts that would have been found had no loss from the blood stream occurred. The recoveries of $^{18}O_2$ were related to the oxygen concentration in the inspired gas, and averaged 55, 40, and 11% at inspired concentrations of 14, 21, and 65%, respectively. The recovery of ^{85}Kr was about 2%, and was independent of the inspired oxygen concentration. This study demonstrated that using $^{18}O_2$ as an intravenous tracer is a feasible procedure. It also indicated that the recoveries of $^{18}O_2$ and ^{85}Kr depend in part on different factors. For instance, at any particular blood oxygen tension the recovery of $^{18}O_2$ exceeded that of ^{85}Kr. Further, the recovery of ^{85}Kr was independent of the inspired oxygen concentration while that of $^{18}O_2$ was inversely related to it. This inverse relation could be predicted by considering a theoretical model in which the lung functions as a compartment wherein a gaseous tracer carried in the blood is allowed to equilibrate with the gas in the alveoli. (BBB)

10548 GLUTAMIC-OXALOACETIC (GOT) AND GLUTAMIC-PYRUVIC (GPT) TRANSAMINASE ACTIVITIES IN THE LIVER AND KIDNEY OF MICE DURING EXPERIMENTAL POISONING WITH URANYL NITRATE AND CARBON TETRACHLORIDE. Bastide, P.; Rigal, M. Th.; Bastide, J.; Turchini, J. P.; Dastugue, G. (Faculte Mixte de Medecine et de Pharmacie, Clermont-Ferrand, France). J. Physiol. (Paris), 57: 219-20(Jan.-Feb. 1965). (In French).

Mice were injected intraperitoneally with a 5% solution of CCl_4 in oil (0.2 ml/20 g body weight) or 400 mg/l uranyl nitrate solution (1ml/20 g body weight). Observations were made at 0, 24, 48, 72, and 96 hr after injection on histological changes and glutamic oxaloacetic (GOT) and glutamic pyruvic (GPT) transaminase activities in liver and kidneys. GOT and GPT activities decreased in mouse liver and kidney after intoxication with CCl_4 or uranyl nitrate. (BBB)

10549 EFFECTS OF DIETARY LEVELS OF PHOSPHORUS AND CALCIUM ON THE COMPARATIVE BEHAVIOR OF STRONTIUM AND CALCIUM. Kostial, K.; Vojvodic, S.; Comar, C. L. (Inst. for Medical Research, Zagreb. Cornell Univ., Ithaca, N. Y.). Nature, 208: 1110-11(Dec. 11, 1965).

The effects of dietary levels of Ca and P on the relative absorption and retention of Ca and Sr were studied in rats maintained on an experimental diet with tracer doses of ^{85}Sr or ^{45}Ca added to the drinking water for a 2-day period. The animals were maintained on the experimental diet for 2 days and then killed for analysis of the skeleton and soft tissues. The effects of Ca and P on the ratio of Sr/Ca of bone and diet were calculated. Results indicate that the minimum body burden of ^{85}Sr was attained when the Ca content of diet was increased to a maximum by the use of uncontaminated Ca and when, at the same time, the P content was increased was also increased to a maximum. (C.H.)

10550 HISTOLOGICAL INVESTIGATIONS OF THE MECHANISM OF STERILITY INDUCED BY DEUTERIUM OXIDE IN MICE. Hughes, Ann M. (Univ. of California, Berkeley); Glass, Laurel E. Nature, 208: 1119-20(Dec. 11, 1965).

Results of a histological investigation of the mechanism of sterility induced in male mice by deuterium oxide in the drinking water indicate that sterility was due to the failure of the sperm to fertilize the egg and not to a failure of the subsequent development of the fertilized egg. (C.H.)

10551 STUDIES ON THE NITROGEN METABOLISM IN FROG LIVER AFTER WHOLE-BODY IRRADIATION. I. NATURE OF THE NITROGEN COMPOUNDS EXCRETED FROM THE ISOLATED LIVER OF NON-IRRADIATED AND IRRADIATED FROGS. Furlan, M.; Antonijevic, M.; Lebez, D. (Nuclear Inst. Jozef Stefan, Ljublijana, Yugoslavia). Neoplasma, 12: 479-87(1965).

Perfused frog liver excretes increased amounts of protein and non-protein nitrogen after whole-body ^{60}Co γ irradiation of frogs. Paper chromatographic analysis show that amino acids excreted from the irradiated and non-irradiated frog livers are qualitatively similar though their amounts are increased with irradiation. The amino acid composition in the perfusate is very similar to the

composition of the hydrolysates of frog serum and liver tissue proteins. Frog serum proteins are not the main source of increased amino acid excretion in the liver after irradiation. Whole-body irradiation of frogs causes an enlargement of the livers with no significant differences in the liver composition. Mechanism of this change is discussed. (auth)

10552 COMBINED EFFECTS OF ^{90}Sr, ^{144}Ce, AND ^{239}Pu ON ORGANS OF RATS. Moskalev, Yu. I.; Budakov, L. A.; Koshurnikova, N. A.; Nifatov, A. P.; Reshetov, G. N. Radiobiologiya, 5: 836-41(1965). (In Russian).

The elimination of Sr, Ce, and Pu from critical organs at time intervals from 16 to 918 days followed an exponential dependence regardless of whether the isotopes were introduced separately or in combination. By joint introduction of isotope pairs with similar and different types of distribution the injuries were not only additive (Ce + Pu) but appeared sooner in some cases (Sr + Ce and Sr + Pu) than in separate use of the isotopes. The comparative biological effectiveness of Pu with respect to the β emitters has a variable significance for different criteria and also depends on the quantity of incorporated isotope. (tr-auth)

10553 ON THE RE-ABSORPTION OF BICARBONATES BY KIDNEYS INJURED BY URANIUM AND SECRETION OF URANIUM FROM AN ORGANISM. Ivannikov, A. T. Radiobiologiya, 5: 867-72(1965). (In Russian).

The destruction of uranyl bicarbonate complexes in the kidney leads to the reabsorption of the bicarbonate. The use of diacarb-sulfanilamide compound having an inhibitory effect on the carboanhydrase–causes a delay of the reabsorption of the bicarbonate which contributes to the elimination of uranium in urine and reduces the injury to the kidney. (tr-auth)

10554 ACCUMULATION OF RADIOIODINE IN THE OVARIES: EXPERIMENTAL DETERMINATIONS AND DOSIMETRIC CONSIDERATIONS. Martinenghi, C.; Castellano, E.; Riccardi, A.; Sanvito, R. (Univ., Milan). Radiol. Med., 51: 892-905(Aug. 1965). (In Italian).

The distribution of ^{131}I in the various tissues of rats and also its elimination, and the mean radioactivity concentration in the whole animal, thyroid, blood, ovaries, liver, and kidneys at different time intervals after intramuscular injection of ^{131}I were measured. The accumulation indices for the tissues considered were calculated supplementing the biological parameters with the physical properties of ^{131}I radioactivity. Extrapolating these data to women, even with all the reserves relative to the validity of such an extrapolation, guiding elements are obtained for calculating the order of magnitude of the doses absorbed in the ovary in relation to the quantity of ^{131}I administered. It is deduced from these evaluations that the doses to the ovary are very small when compared with those absorbed in the thyroid. During diagnostic tests with ^{131}I the doses to the ovary are equal to or slightly higher than those obtained on taking a radiogram of the chest. (tr-auth)

10555 STRONTIUM–CALCIUM DISCRIMINATION IN THE RAINBOW TROUT. Ichikawa, Ryushi (National Inst. of Radiological Sciences, Chiba, Japan). Rec. Oceanogr. Works Jap., 5: No. 2, 120-31(Mar. 1960).

The strontium-calcium discrimination observed between fish body and the water, the influence of the amount of calcium and strontium in the water to the rate of discrimination, the strontium-calcium discrimination observed between the fish body and the diet, and maximum probable concentration of strontium-90 in this fish derived from the contamination of the water and diet by the artificial radioactivity such as the radioactive fallout or the liquid waste effluence released from the nuclear energy plant were investigated in rainbow trout using ^{45}Ca and ^{90}Sr labeled water and diet. (auth)

10556 ELIMINATION OF RADIONUCLIDES (INVESTIGATION ON THE THERAPEUTIC INDEX OF TRIETHYLENETETRAAMINEHEXAACETIC ACID). von Wedelstaedt, Ekart; Catsch, Alexander (Kernforschungszentrum, Karlsruhe, Ger.). Strahlentherapie, 128: 385-95(Nov. 1965). (In German).

The lethal effect of the chronic parenteral administration of different TTHA chelates (triethylenetetraaminehexaacetic acid) was studied in mice. The toxicity increases in the following order: Zn_2-TTHA < CaZn-TTHA $\ll$ Ca-TTHA $\ll$ Zn-TTHA. The efficacy of the chelates in removing carrier-free ^{91}Y and ^{144}Ce from rats was studied and compared with that of diethylenetriaminepentaacetic acid. The relative potency of the chelates depends upon the radionuclide, organ, dosage, and time of administration. The practical implications of the experimental findings are discussed. (auth)

10557 DETERMINATION OF THE BODY WATER WITH ^{3}H. Buettner, K.; Langer, H. Z. Ges. Inn. Med. Ihre Grenz., 20: 176-80(1965).

From the methods for quantitative determination of body water available, the dilution method is commonly employed. Using tritium oxide, a simplified method of determination was developed. The results achievable by the method recommend it as a routine method for use in clinical practice and research. Average values obtained were for normal male persons: 55% total quantity of body water; for highly trained sportsmen: 68%. (TCO)

10558 THE MEASUREMENT OF THE SYNTHETIC RATE OF LIVER-SYNTHESIZED PROTEINS IN ANIMALS. Reeve, E. B. (Univ. of Colorado, Denver). pp 57-69 of STI/DOC/10/45.

A method for measuring the synthetic rate of proteins in animal liver is presented. Kinetic formulation of synthetic rate requires two assumptions: that essentially all urea is formed in the liver, and that the liver arginine forming urea is in very rapid equilibrium with that synthesized into proteins. However, the method holds only if the rates of formation of urea and liver-synthesized proteins are constant, or vary proportionately over the 2 to 3 hrs following injection of carbon-14-labeled arginine. Models and equations for protein synthesis in the liver are presented. (H.G.D.)

10559 COMMENTS ON THE MEASUREMENT OF PROTEIN SYNTHETIC RATE. McFarlane, A. S. (National Inst. for Medical Research, London). pp 71-2 of STI/DOC/10/45.

Advantages of using carbon-14-labeled carbonate in measuring rates of carbon-14-labeled urea synthesis are discussed. Results of experiments in which nitrogen-15-labeled urea was injected with carbon-14-labeled carbonate are reported. (H.G.D.)

10560 THE USE OF ^{15}N FOR THE STUDY OF PROTEIN METABOLISM, WITH PARTICULAR REFERENCE TO NUTRITIONAL PROBLEMS. Waterlow, J. C. (Univ. of the West Indies, Jamaica). pp 83-92 of STI/DOC/10/45.

Research on nutritional problems using ^{15}N is reviewed. Topics discussed include: utilization of non-specific nitrogen; measurement of cumulative excretion of ^{15}N; investigation of protein digestion and absorption; and measurement of total nitrogen turnover in the whole body. (H.G.D.)

10561 RADIOISOTOPE TECHNIQUES FOR THE STUDY OF PROTEIN TURNOVER. Jarnum, S. (Rigshospitalet, Copenhagen). pp 93-103 of STI/DOC/10/45.

Two methods for radioisotope-labeling of proteins are reviewed: biological labeling and in vitro labeling. Biological labeling involves the use of amino acids labeled with isotopes such as ^{35}S, ^{14}C, ^{3}H, or ^{15}N; whereas in vitro labeling normally involves radioiodinated proteins. Data on human plasma protein degradation obtained with radioiodinated plasma proteins are tabulated. (H.G.D.)

10562 THE USE OF COMPUTERS IN THE STUDY OF PROTEIN TURNOVER. Matthews, C. M. E. (Hammersmith Hospital, London). pp 105-18 of STI/DOC/10/45.

The use of analogue computers in the study of protein turnover is reviewed. Since computer methods all depend on compartment analysis, the mathematical methods that can be used are briefly discussed. The methods were used mainly for interpreting experiments in which ^{131}I-labeled plasma proteins are injected intravenously, but similar methods could be used for other proteins or labels. Com-

puter utilization to improve curve fitting and Berman and Schoenfeld analysis and to simulate the system either on a direct or a functional analogue are considered. An analogue computer analysis of plasmapheresis in rabbits is presented. It is concluded that the use of computers in studies of protein metabolism not only leads to increased accuracy and speed in analysis but also gives results that could not be obtained by more conventional methods. (H.G.D.)

10563 COMMENTS OF THE MINIMUM NUMBER OF OBSERVATIONS REQUIRED IN THE STUDY OF PROTEIN TURNOVER. Matthews, C. M. E. (Hammersmith Hospital, London). pp 119-23 of STI/DOC/10/45.

Recommendations are made for the minimum number of catabolic rate and extravascular pool and synthesis rate observations required in studies of protein turnover. Catabolic rate may be measured either by the clearance method or by using a whole-body counter. When using the clearance method, three urine collections and three blood samples should be taken, the blood samples being taken at times corresponding to the middle of the urinary collection period. Three blood samples taken simultaneously with three whole-body measurements are necessary for determining catabolic rates by the whole-body counter method. Extravascular pool and synthesis rate determinations use three measurements of intravascular and total activities. However if pool masses are not constant, daily measurement for 2 to 3 weeks are required. (H.G.D.)

10564 A SIMPLIFIED METHOD FOR THE CLINICAL STUDY OF PROTEIN TURNOVER. Koblet, H.; Diggelmann, H. (Univ., Bern). pp 125-8 of STI/DOC/10/45.

A simplified method for determining turnover rates of labeled proteins for clinical purposes is described. The following values must be known: the content of albumin in the serum; the distribution volume of albumin; and the slope of the line drawn on semilogarithmic paper, indicating the residual activity of ^{131}I in plasma at 3 to 5 points in time. Results show that the simplified method can be used for clinical purposes with certain limitations. (auth)

10565 THE INTERPRETATION OF RESULTS OF PROTEIN TURNOVER STUDIES. Diggelmann, H.; Koblet, H. (Univ., Bern). pp 129-31 of STI/DOC/10/45.

On the basis of modern knowledge of protein synthesis, a theory was developed that gives a simple interpretation of turnover data. As no disturbances leading to an endogenous hypercatabolism or hypocatabolism apparently exist, altered turnover results with labeled albumin can only be interpreted as follows: increased loss (renal, intestinal); decreased pool of building blocks (gastro-intestinal diseases, hunger); and disturbances of synthesis in the liver (acquired liver disease). (auth)

10566 RADIOISOTOPE TECHNIQUES FOR THE STUDY OF PROTEIN ABSORPTION. Jeejeebhoy, K. N. (Tata Memorial Hospital, Bombay). pp 141-8 of STI/DOC/10/45.

Properties of ^{131}I-labeled proteins and ^{3}H-labeled albumin are discussed, and methods for measuring intestinal absorption using ^{131}I-labeled calcium caseinate or albumin or tritiated albumin are reviewed. It is concluded that absorption studies with ^{3}H-labeled protein are more likely to be of value than those with ^{131}I-labeled protein in the study of the intestinal diseases found in tropical countries. However, it is suggested that the ^{131}I-labeled proteins may be of value in the demonstration of pancreatic disorders. (H.G.D.)

10567 THE MEASUREMENT OF GASTRO-INTESTINAL PROTEIN LOSS BY MEANS OF ^{131}I-LABELLED PROTEIN. Jarnum, S. (Rigshospitalet, Copenhagen). pp 149-63 of STI/DOC/10/45.

Measurement of gastrointestinal protein loss by labeled protein requires a test substance that: behaves like endogenous protein after intravenous injection; is non-toxic; is easy to detect and measure; and retains its label completely after passage into the gastrointestinal tract, so that it can be measured in stools. It is pointed out that none of the existing test substances fulfills all of these requirements. Physiological gastrointestinal protein loss is reviewed and it is concluded that nearly 50% of the normal degradation of albumin and γ-globulin may occur by a transfer of these proteins across the intestinal mucosa to the lumen of the gastrointestinal tract where they are rapidly broken down by enzymes. The use of ^{131}I-labeled albumin in detecting the source of protein loss in patients with idiopathic hypoproteinemia is discussed. Results suggest that ^{131}I-labeled albumin may be a useful test substance in the investigation of hypoprotein states, since it permits a diagnosis of abnormal gastrointestinal protein loss and at the same time gives information about the degradation and synthetic rates of serum albumin. Use of the combined ^{131}I-labeled albumin resin method was questioned as a reliable measurement of gastrointestinal protein loss. (H.G.D.)

10568 THE MEASUREMENT OF GASTRO-INTESTINAL PROTEIN LOSS BY MEANS OF ^{131}I-LABELLED POLYVINYLPYRROLIDONE. Barandun, S.; Aebersold, J.; Diggelmann, H.; Koblet, H. (Univ., Bern). pp 165-9 of STI/DOC/10/45.

The use of ^{131}I-labeled polyvinylpyrrolidone (PVP) for measuring gastrointestinal protein loss is evaluated. Other than simplicity and informational value, the method has the advantage that PVP is not digested in the gastrointestinal tract, an important attribute when evidence indicates that even under normal conditions, plasma proteins may be secreted into the gut. However, disadvantages of the method must also be considered such as: unpredictable behavior of PVP since it is not a physiological substance; unstable binding of ^{131}I to the PVP molecule; and variation from subject to subject of the rate of gastrointestinal transport. Diseases associated with protein-losing gastroenteropathy are tabulated. (H.G.D.)

10569 THE MEASUREMENT OF GASTRO-INTESTINAL PROTEIN LOSS BY MEANS OF ^{51}Cr-ALBUMIN AND ^{67}Cu-CAERULOPLASMIN. Waldmann, T. A.; Wochner, R. D. (National Cancer Inst., Bethesda, Md.). pp 171-81 of STI/DOC/10/45.

Advantages and limitations of ^{51}Cr-labeled albumin and ^{67}Cu-labeled ceruloplasmin for use in studies of gastrointestinal protein loss are discussed. In 60 studies on 40 patients with gastrointestinal protein loss, 1.2 to 3.2% of the intravenously administered ^{51}Cr-labeled albumin appeared in the subsequent four-day fecal collection. Because of the abnormally short survival of ^{51}Cr-labeled albumin following intravenous administration and in view of the inconsistency of the estimates of normal protein loss in studies with ^{51}Cr-labeled albumin and those with ^{131}I-labeled albumin and intubation, ^{67}Cu-labeled ceruloplasmin was evaluated as an agent for the study of the role of the gastrointestinal tract in the metabolism of serum proteins. Copper-67-labeled ceruloplasmin appeared to fulfill the major requirements of a technique for the quantitation of gastrointestinal protein loss. Data on metabolism were in accord with that obtained using ^{51}Cr-labeled albumin. However, the short physical half-life of ^{67}Cu and the difficulty of producing the labeled compound precludes its routine use in clinical studies. (H.G.D.)

10570 STUDIES OF PROTEIN METABOLISM IN DIGESTIVE DISEASES. Vesin, P. (Hopital d'Argenteuil, France). pp 185-96 of STI/DOC/10/45.

Data obtained by using labeled plasma proteins or protein-like substances in the study of protein metabolism in diseases affecting the stomach, small intestine, colon, and liver are presented. Major findings made in studies of protein metabolism in malignant disease are reviewed. (H.G.D.)

10571 THE DETERMINATION OF THE TOTAL CLEARANCE OF DIFFERENT PREPARATIONS OF GAMMA-GLOBULIN. Diggelmann, H.; Koblet, H.; Barandun, S.; Gerber, H. (Univ., Bern). pp 205-9 of STI/DOC/10/45.

The metabolic behavior of ^{131}I-labeled γ-globulin, pH 4-γ-globulin, and Gamma-Venin was studied in patients given intravenous injections of the test substances. Concentrations of total protein and γ-globulin in serum were

determined prior to and following the injections. Daily blood samples were taken and radioactivity followed for a period of 2 to 4 wks. Urine samples were collected at 24 hr intervals for one week. Distribution volumes and clearance constants were calculated. There was no significant difference between the mean values of the elimination constant for standard γ-globulin and pH 4-γ-globulin, and values for total clearance were of the same magnitude. In contrast, the slope of the elimination curve was much steeper in the case of Gamma-Venin. Total clearance values were also higher. (H.G.D.)

10572 METABOLISM OF GAMMA-GLOBULIN IN AGAMMAGLOBULINAEMIA AND HYPOGAMMAGLOBULINAEMIA. Koblet, H.; Diggelmann, H.; Barandun, S.; Kaeser, H. (Univ., Bern). pp 211-16 of STI/DOC/10/45.

Degradation capacity as a parameter of γ-globulin metabolism was studied in two agammaglobulinemic subjects in which normal γ-globulin pools were artificially created by infusing large quantities of standard γ-globulin. A classical turnover determination was done with ^{131}I-labeled γ-globulin in both patients. The distribution volume of γ-globulin remained normal in both cases, despite the sudden infusion. No answer was given as to the real degradation capacity, but it was clearly shown that the degradation capacity for γ-globulin of agammaglobulinemic subjects must be high. (H.G.D.)

10573 STUDIES OF PROTEIN METABOLISM WITH LABELLED PROTEINS AND PROTEIN-LIKE SUBSTANCES IN NUTRITIONAL DISORDERS. Hoffenberg, R. (Univ., Cape Town). pp 217-33 of STI/DOC/10/45.

Protein metabolism was studied in adult human volunteers using iodine-131-labeled albumin and iodine-131-labeled γ globulin. Subjects were given: a normal diet; an isocaloric low-protein diet for 3 to 6 wks; or a high-protein diet for a similar period of time. Results were analyzed by the equilibrium time method. Synthesis and transfer rates were derived. Evidence suggested that: the body reacts to protein deprivation by transferring albumin from the extravascular to the intravascular pool; the body adapts to protein depletion or deprivation by lowering the rate of albumin catabolism; and inadequacy of dietary protein is associated with a fall in albumin synthesis rate. (H.G.D.)

10574 OBSERVATIONS ON THE STUDY OF PROTEIN METABOLISM IN RELATION TO NUTRITION. Waterlow, J. C. (Univ., West Indies, Jamaica). pp 235-41 of STI/DOC/10/45.

The decrease in nitrogen excretion that occurs on a low protein diet must be regarded as a homeostatic response. It is suggested that a sensitive compensatory mechanism that causes a large change in the rate of excretion in response to a change in the total rate of entry which is proportionately much smaller. Therefore, a major factor in producing the economy is an increased re-utilization of amino acids, which is probably mediated largely by the liver. If this effect depends upon enzymic changes, it is not surprising that it takes several days to be established. Since the changes that occur in liver and muscle seem to be reciprocal, it might be expected that there would not be any great change in the over-all turnover rate of free amino acids in response to protein depletion. At present this question is being investigated by the method of constant intravenous infusion of labeled amino acid. Preliminary results in three children infused with ^{35}S-methionine showed no evidence of a decreased turnover in the malnourished state compared with the results after recovery. (TCO)

Radiation Effects on Biochemicals

See also CHEMISTRY — Radiation Chemistry

Refer also to abstract 10683.

10575 LATE CHANGES IN THE HUMAN BRAIN AFTER INTRAOPERATIVE IMPLANTATION OF ^{60}Co PELLETS. Afra, D.; Mueller, W.; Wilcke, O. (Univ., Cologne). Acta Neuropathol., 4: 299-311(1965).

Radiotherapy of brain tumors with ^{60}Co beads is evaluated in eight patients treated with surgery and irradiation. Results of autopsy are described for the three patients in which radiation effects were not obscured by surgical damage and infection. Cortical tissue in the autopsied cases was much less affected by radiation than was the white matter, damage in which was partly due to surgical trauma. Tumor tissue was found at death in 7 of the 8 cases. It was concluded that the treatment used was dangerous. (H.G.D.)

10576 THE HISTOCHEMICAL EFFECTS OF X-IRRADIATION UPON THE ADRENAL CORTEX. Chen, Chi-tang; Feng, Yue; Chien, Kuo-cheng. Chieh Pou Hsueh Pao, 8: 13-21(1965). (In Chinese).

Adult male rats weighing 140 to 200 grams were exposed to whole body x irradiation with a single dose of 1000 R and killed at intervals of 2, 5, 8, 12 hrs and 1, 2, 3 days after irradiation. The changes of RNA, glycogen, lipid and alkaline phosphatase in the adrenal cortex were studied by histochemical methods. The RNA content in the outer zona fasciculata began to increase as early as 5 hrs after irradiation. One day later the RNA of the whole zona fasciculata increased. At that time, the sizes of both the cells and nucleoli in the outer zona fasciculata became larger than the normal. On the 2nd day the granules of glycogen decreased or were depleted. The amount of lipid in the cortex decreased after 5 hrs. This change was first encountered in the zona reticularis and inner zona fasciculata, and then in the outer zona fasciculata. Three days later the lipid nearly disappeared in the zona fasciculata and reticularis, but in the zona glomerulosa no visible changes could be seen. There were no evident changes in alkaline phosphatase. The functional significance of the changes described above are discussed. (Excerpta Med.)

10577 FREE-RADICAL PROCESSES TAKING PLACE IN IRRADIATED HOMOGENATES OF ANIMAL TISSUES. Tarusov, B. N.; Kozlov, Yu. P.; Urtile, S.; Chou, Yung-tsen (Moscow State Univ.). Dokl. Akad. Nauk SSSR, 163: 752-3(July 21, 1965). (In Russian).

Gamma irradiation (^{60}Co) of brain, liver, and spleen tissue homogenates from white mice (male, 20 g) significantly disrupted the free-radical processes, apparently in connection with destruction of the lipoprotein complexes in the cell. The effect, as shown by graft-copolymerization with ^{14}C-labeled acrylamide, was greatest in brain tissue. The degree of copolymerization was determined by radiometric methods. Changes in the chemiluminescence of the tissues followed a similar pattern. Determinations, by modifications of standard methods, of free and bound lipids and proteins indicated considerable changes in the tissue lipoprotein. Gamma irradiation was also shown to affect linseed oil so that its components formed graft copolymers. The copolymerization effect was more sharply expressed here because of the higher proportion of unsaturated fatty acids. (TTT)

10578 ON THE NATURE OF SUPERWEAK LUMINESCENCE OF IRRADIATED SOLUTIONS OF DESOXYRIBONUCLEIC ACID. Zhizhina, G. P.; Kruglyakova, K. E.; Emanuel', N. M. (Inst. of Chemical Physics, Academy of Sciences, USSR). Dokl. Akad. Nauk SSSR, 163: 931-4 (Aug. 1965).

It was previously established that two compounds of differing stability are formed as the result of the decay of hydroperoxides obtained from irradiated DNA solutions. This study was extended by attempting to determine the character of the very weak luminescence noted in these irradiated solutions. Native 0.05 to 0.1% aqueous solutions prepared from calf thymus and dry, high-polymer DNA preparations were exposed to doses of 28 to 85 kr at 22°C. The luminescence was detected by means of a dry-ice cooled photomultiplier with a sensitivity in the 200 to 600 mμ range. The luminescence became stronger with increasing temperature and decreased exponentially within 150 to 300 sec. The decay rate constants of the luminescence of the various solutions lay within 0.8 to 2.0×10^{-2}

sec^{-1}. Further comparison of the intensity of the luminescence and the decay kinetics of the hydroperoxide compounds of DNA with the luminescence of DNA solutions exposed in an Ar atmosphere revealed that the luminescence is due to the presence of such hydroperoxides. The decay rate constants followed a 1/T relation with time in the 40 to 90°C range; the energy of activation of 13 ± 1 kcal/mole thus found agreed with chemically obtained data. It was assumed that the chemoluminescence arises from the recombination of radicals, probably peroxides. The presence of 4 to 10×10^{-4} wt % albumin and 1×10^{-4} M hydrogen peroxide in the irradiated solutions did not affect the luminescence. (TTT)

10579 THE EFFECT OF ^{32}P ON THE MULTIPLICATION OF GERMS: SALMONELLA TYPHIMURIUM AND AEROBACTER AEROGENES. THE POSITIVE POLYMETAPHOSPHATE. **Curatola, G.; Zaio, A. (Sanita Militare, Rome). Giorn. Med. Mil., 114: 661-73(1964).**

The action of ^{32}P on bacterial multiplication was studied in culture. A protective effect was seen, possibly due to the ^{31}P that was present at the same time in the culture medium. Intracellular reserves of polyphosphate (volutin) that were induced in A. aerogenes appeared to have a similar function. (Excerpta Med.)

10580 CERTAIN IMMUNE INDEXES IN NEWBORN MICE TREATED WITH ^{32}P. **Zaio, A.; Di Addario, A.; Stornelli, R. (Sanita Militare, Rome). Giorn. Med. Mil., 114: 674-82(1964).**

Bacterial and opsonic activity and serum properdin levels were studied in mice given ^{32}P intraperitoneally. There was a sharp decline in these defense properties, with a return to normal levels by the 20th day after injection. (Excerpta Med.)

10581 CHANGES OF THE ELECTROPHORETIC PATTERN OF THE SERUM PROTEINS OF THE MOUSE AFTER TREATMENT WITH ^{32}P. **Bruzzese, E.; Bonarelli Rulli, F.; Greco, G. (Sanita Militare, Rome). Giron. Med. Mil., 114: 695-705(1964).**

Modifications of serum protein electrophoretic pattern were investigated on mice given ^{32}P intraperitoneally at doses between 2 μc/g and 20 μc/g. Phosphorus-32 administration caused modifications noticeable with only 2 μc/g. With all of the doses a decrease of total serum proteins and the ratio of albumins and gamma-globulins and an increase of alpha-globulins was found. A good correlation was found between dose and observed effect. In mice given 2 μc/g, a return to normal was found by the 30th treatment day. (Excerpta Med.)

10582 THE EFFECTS OF ^{32}P ON THE URINARY EXCRETION OF AMINO-ACIDS IN THE MOUSE. METHODS OF DETERMINATION, AND DEFINITION OF A TECHNIQUE FOR QUALITATIVE AND QUANTITATIVE ANALYSIS. **Corbi, D.; Morselli, L. (Sanita Militare, Rome). Giorn. Med. Mil., 114: 706-15(1964).**

On the 10th day of treatment with progressively increasing doses of ^{32}P ranging between 2 and 20 μc/g. bodyweight, qualitative and quantitative changes of amino acid clearance in mouse urine were absent. Results are reported concerning the analysis of the different methods for determination of amino acids in mouse urine. (Excerpta Med.)

10583 THE VARIATIONS OF LACTIC ACID DEHYDROGENASE AND OF MALIC ACID DEHYDROGENASE IN THE LIVER AND IN THE SPLEEN OF RATS IRRADIATED WITH ROENTGEN RAYS. **Tocca, M.; Stornelli, R. (Sanita Militare, Rome). Giorn. Med. Mil., 114: 767-73(1964).**

Lactic dehydrogenase (LDH) and malic dehydrogenase (MDH) contents in extracts of liver and spleen of total body x-irradiated (900 R) rats were determined. It was found that a modification of MDH and LDH activities suggests an increased anaerobic glycolysis in irradiated tissues (liver and spleen). (Excerpta Med.)

10584 EFFECTS OF ULTRAVIOLET LIGHT ON THE TEMPLATE PROPERTIES OF POLYCYTIDYLIC ACID. **Ono, Joji; Wilson, Robert G.; Grossman, Lawrence (Brandeis Univ., Waltham, Mass.). J. Mol. Biol., 11: 600-12(Mar. 1965)**

Experiments are described involving uv-irradiation of polycytidylic acid and the subsequent effects of such irradiation on the template properties of this polymer in the RNA polymerase from Micrococcus lysodeikticus. When polycytidylate was irradiated, there was a loss of its characteristic uv absorbance, which could be restored by raising the temperature. The incorporation of guanosine-triphosphate (GTP) directed by polycytidylate, and catalyzed by the RNA polymerase, was sensitive to uv light, but could be restored under conditions of dehydration or on addition of unlabeled adenosinetriphosphate (ATP). Labeled ATP was incorporated in the presence of unlabeled GTP and irradiated polycytidylate. From nearest neighbor analysis, it was apparent that the ATP was directed into internucleotide linkage, and this incorporation could be reversed if the irradiated polycytidylate was heated to dehydration temperatures. It is suggested that each time a cytosine residue is converted to a water adduct by uv light, the sequential coding properties of the polymer stop at the point of the uv lesion. If such a lesion, in fact, codes for another and missing nucleoside triphosphate, then the coding or replicating process would continue when the missing nucleoside triphosphate is included in the reaction mixture. The homopolymer after the irradiation was converted to a copolymer, in which the uv-induced lesion coded in the replicating system as uracil and directed the incorporation of labeled ATP. (BBB)

10585 THE EFFECT OF LOCAL BETA-IRRADIATION ON THE CORNEAL METABOLISM OF RABBITS. **Korecz, K.; Szirmak, E. Klin. Monatsbl. Augenheilk., 146: 204-10(1965).**

By means of the direct Warburg method, O_2-consumption and glycolytic activity were measured in rabbit corneas that were irradiated with ^{90}Sr. The investigations were performed in 80 eyes of 40 rabbits. Six weeks after the administration of a local of 1000 to 1500 rep. dose, no differences could be established between the irradiated eyes and unirradiated control eyes. After 1500 to 3000 rep, there was a slight diminution, and after 5000 rep, a considerable decrease in O_2-consumption of the cornea and in anaerobic glycolysis. (Excerpta Med.)

10586 IN VITRO EFFECT OF GAMMA-RADIATION ON DIFFERENT CHOLINESTERASE PREPARATIONS. **Catalan, R. E.; Municio, A. M. (Inst. of Chemistry, Madrid). Nature, 208: 1227(Dec. 18, 1965).**

Experiments were designed to investigate the in vitro effect of γ rays on cholinesterase from various sources and of differing grades of purity. Irradiations were performed at 18°C in a thermostatically controlled cylindrical 2,000 c. ^{60}Co source. The dose-rate used was 2.5×10^5 r/h. Ten samples were simultaneously irradiated in sealed glass ampoules with a head space of 6 ml, containing air. Controls were handled in the same fashion, but they were not placed within the cobalt source. The preparations exposed to γ-radiation included bovine red blood cell cholinesterase preparations at different stages of purification. These stages were: whole heads; homogenate; and a purified fraction. The enzymatic activities of the samples were controlled within 1 h of irradiation. Cholinesterase activity was measured potentiometrically using as substrate a solution of 0.5 M sodium chloride – 0.04 M magnesium chloride-0.002 M acetylcholine bromide in 0.5 M phosphate buffer pH 7 and 38°C. The acetic acid liberated was automatically determined by titration with 0.005 N sodium hydroxide. Enzymatic activity was expressed as ml consumed alkali per min. The extent to which the pH of the samples was affected by the γ irradiation was also determined. Experimental results were evaluated by plotting the percentage of the remaining enzymatic activity as a function of irradiation dose. Results indicate that the more purified the samples were, the more was the inactivating effect of the irradiation. In the cholinesterase preparations from common fly, the order of inactivation was: purified sample > homogenate > whole heads. Assays carried out with red blood cells and cholinesterase from the electric eel showed a high grade of inactivation. (C.H.)

10587 GENERALIZED SKELETAL RESPONSE TO LOCAL RADIATION INJURY. Babicky, A.; Kolar, J. (Inst. for Biological Research, Prague. Charles Univ., Prague). Radiat. Res., 27: 108-18(Jan. 1966).

The results of some experiments with local x radiation damage to the soft tissues and bones of young white male Wistar rats are reported. After local irradiation, some whole-body skeletal reactions of the mineral metabolism were observed in areas not directly affected by irradiation. Some oscillating reactions exist in the uptake of radiocalcium. After local partial denervation of the irradiated extremity, the onset of such a general response was not observed, or it was retarded. A hypothesis is put forward as an explanation of this kind of reaction. This generalized response is considered as proof for regulatory mechanisms operating in the injured organism toward normalization of the state in the damaged area. (auth)

10588 EFFECTS OF α AND γ EMISSIONS ON THE SYNTHESIS OF DNA IN HeLa CELLS. Kuzin, A. M.; Vainson, A. A. (Inst. of Biological Physics, Moscow). Radiobiologiya, 5: 785-90(1965). (In Russian).

A quantitative investigation was made of the depression of the synthesis of DNA under the effects of α and γ radiation in HeLa cells in the S stage. It was found that the depressions of the DNA synthesis as a function of the dose is expressed by two-component curves both for γ and α radiation. The OBE of the α particles for the first and second components of the dose curve is less than unity (0.5) which does not permit the assumption of a causal bond between the disturbance of the DNA synthesis and the cell destruction (OBE greater than unity at 2.5 to 6). It was shown that the suppression of the DNA synthesis at a given radiation dose is equal in all synthesizing cells. The calculation of the sensitive volume for the first component of the dose curve was mol. volume $= 8 \times 10^8$ with a diameter of 24 Å and a length of 260 mk and for the second component 1.7×10^7, 28 Å, and 3 mk, respectively. (tr-auth)

10589 ON THE VARIABLE RADIOSENSITIVITY OF COMPONENTS OF ERYTHROCYTE MEMBRANE IN A NEW-BORN RAT. Trincher, K. S.; Orlova, L. V. (Inst. of Biological Physics, Moscow). Radiobiologiya, 5: 797-800(1965). (In Russian).

The kinetics of the radiation injuries in the erythrocytes of new-born rats was investigated by a photocolorimetric method. From the data it can be assumed that the α component consists of lipoid parts of the lipoprotide complex of the cellular membranes which are characterized by high radiosensitivity. The β components consist of albumin which has a significantly smaller radiosensitivity. (J.S.R.)

10590 EFFECTS OF WHOLE-BODY X RADIATION ON THE CONTENT OF IRIDINDIPHOSPHATE GLUCOSE IN THE LIVER OF RATS. Filippova, V. N.; Soldatenkova, L. I.; Seits, I. F. (Scientific Research Inst. of Blood Transfusion, Leningrad). Radiobiologiya, 5: 806-8(1965). (In Russian).

Every other day after whole-body x radiation at doses of 1000 r the quantity of iridindiphosphate glucose in the liver of rats was reduced by 40% on an average. The activity of the ferments of phosphoglucomutase, the pyrophosphorylase of iridindiphosphate glucose, and the percentage of glycogen in the irradiated animals is not affected. (tr-auth)

10591 RADIATION EFFECTS ON THE DESOXYRIBONUCLEASE ACTIVITY IN CELLULAR NUCLEI AND CYTOPLASM. Argutinskaya, S. V.; Salganik, R. I. (Inst. of Cytology and Genetics, Academy of Sciences, Novosibirsk, USSR). Radiobiologiya, 5: 815-21(1965). (In Russian).

In nuclei isolated from the thyroid from irradiated animals the hydrolysis is increased because of the effect of the desoxyribonuclease of type I and II. The desoxyribonuclease activity initially is detected in the cytoplasm of the cells and then in the nucleus, which leads to an hypothesis on the penetration of the ferments of the cytoplasm into the nucleus. In nuclei of thymus of irradiated animals the DNA is more sensitive to the effects of desoxyribonuclease in comparison with the DNA of the nuclei of unirradiated animals. This sensitivity is determined not only by the conditions of the nuclear membrane but also probably by the change of the conditions of the DNA in the cell nuclei of irradiated animals. During incubation of the recombining homogenates from cytoplasm and nuclei of irradiated and non-irradiated animals, the most intensive destruction of the DNA is found in the cases of the combination of nucleus and cytoplasm of irradiated animals which indicates the essential role of both the activation of the ferments and the condition of the nucleus structure in the increase of the post-irradiation hydrolysis of the DNA. (tr-auth)

10592 CHANGES IN THE BLOOD SERUM CHOLINESTERASE IN DOGS EXPOSED TO SINGLE AND FRACTIONATED DOSES OF IRRADIATION BY HIGH-ENERGY PROTONS. Uspenskaya, M. S. Radiobiologiya, 5: 822-6 (1965). (In Russian).

Single irradiation of dogs with high energy protons at 510 Mev at doses of 250, 400, and 500 rad produces a permanent reduction of the activity of cholinesterase in the blood serum in all degrees of radiation sickness independently of the dose effect. For fractionated irradiation of dogs with high energy protons at total doses of 690, 650, and 550 rad the changes of the cholinesterase in the blood serum has a wave-like character. The phase increase of the activity of the ferments and the subsequent decrease at the activity to levels close to the original values was noticed. For the effective dose of 650 rad in the terminal periods of life of the dog, an abrupt decrease in the activity of the cholinesterase in the serum was detected. (tr-auth)

10593 CHANGES IN ALANINE–2-OXOGLUTARATE AND ASPARTATE–2-OXOGLUTARATE-AMINOTRANSFERASE IN THE CENTRAL NERVOUS SYSTEM AND SKELETAL MUSCLES IN 6 WEEKS-OLD RATS EXPOSED TO X IRRADIATION. Pikulev, A. T.; Yakubovich, L. S. (Belorussian State Univ. Inst. of Physiology, Minsk). Radiobiologiya, 5: 910-12(1965). (In Russian).

Age changes in the activity of alanine–2-oxoglutarate and aspartate–2-oxoglutarate–aminotransferase in the different sections of the central nervous system and in the skeletal muscles were established. Whole-body x irradiation of six-week old rats at doses of 100 R produces in the large hemisphere of the brain, cerebellum, and spinal cord and in the skeletal muscles disturbances of the process of transamination of the catalyzing alanine and aspartate. In the central nervous system and the skeletal muscle the greatest displacements in the alanine and aspartateamino-transferase system at delayed time periods after ionizing irradiation. The catalyzing process of the aspartate seems to have the greatest sensitivity to the effects of x irradiation. (tr-auth)

10594 LEUKOCYTIC REACTIONS TO ADRENALINE IN DOGS EXPOSED AT EARLY AGE TO SMALL DOSES OF CHRONIC IONIZING RADIATION. Fokina, T. V. (Inst. of Pediatrics, Moscow). Radiobiologiya, 5: 914-16(1965). (In Russian).

Changes in the leukocytic reaction on adrenaline injection in dogs exposed at an early age to x-ray doses from 1 to 10 R were compared with that in healthy animals. The character of the changes of the leukocytic adrenal curve has a definite gradation and depends both on the total dose and on the individual resistance of the animals. The threshold of the total dose of X radiation at which changes in the leukocytic reactions to adrenaline occur is lower in dogs exposed at 5 days of age than in animals irradiated at six months of age. (tr-auth)

Radiation Effects on Tissues

Refer also to abstracts 10506, 10576, 10673, and 11185.

10595 (ABCC-60-61) ANNUAL REPORT [ON ACTIVITIES], 1 JULY 1960–30 JUNE 1961. (Atomic Bomb Casualty Commission, Hiroshima (Japan)). Contract AT(49-1)-Gen-72. 91p. Dep. mn. CFSTI $3.00 cy, $0.75 mn.

In Japanese and English.

Regular complete physical evaluations of about 20,000 persons exposed in 1945 to radiation from atomic bombs at Hiroshima and Nagasaki are conducted in such a way that each person is examined once every two years to detect any new disorders or increased incidence of disease that may be related to the radiation exposure. Control subjects are also examined making the total population sample approximately 100,000 persons. Data are presented from a preliminary analysis of mortality data, a study of the life span of children born to exposed parents, a mortality study of persons exposed in utero, pathological studies of tissues from exposed individuals, and a survey on the incidence of leukemia and other related disorders in residents of Hiroshima and Nagasaki. A list is included of 85 publications during the year covered by this report. (C.H.)

10596 (BNWL–122, pp 1-15) CHRONIC EFFECTS OF INHALED $^{239}PuO_2$ IN DOGS. Park, J. F.; Clarke, W. J.; Bair, W. J. (Battelle-Northwest, Richland, Wash. Pacific Northwest Lab.).

Inhalation of $^{239}PuO_2$ particles by 40 beagle dogs caused death in 10 animals 29 to 56 months postexposure. The body burdens at death ranged from 1 to 3 μCi with 40 to 75% of the body burden in the lungs, and 20 to 50% in the bronchial and mediastinal lymph nodes. The liver contained 2 to 15%, and the skeleton, 1 to 5%. Cardiopulmonary insufficiency and lymphopenia were the primary clinical signs. Pathologic effects in the lungs consisted primarily of severe fibrosis followed by alveolar cell hyperplasia, and bronchiolar and squamous types of metaplasia. Five of the animals showed bronchiolo-alveolar carcinomas, an incidence of 13% as compared to a primary lung tumor incidence of 0.2% in canine necropsy material. The bronchial lymph nodes were composed of dense sclerotic connective tissue devoid of any lymphoid element. Metastases of the pulmonary tumor to the bronchial lymph nodes were seen in one dog. (auth)

10597 (BNWL–122, pp 37-45) BIOLOGICAL EFFECTS OF ^{90}Sr IN MINIATURE SWINE. McClellan, R. O.; Clarke, W. J.; Palotay, J. L.; Ragan, H. A.; Vogt, Glenda S. (Battelle-Northwest, Richland, Wash. Pacific Northwest Lab.).

Biological effects of daily ingestion of ^{90}Sr are being studied in miniature swine fed from 1 to 3100 μCi ^{90}Sr/day. Approximately 300 animals are presently being maintained for lifetime observation. A total of five cases of neoplasia of the hematopoietic tissues have now been observed in 2.5 to 4.5-year-old miniature swine with chronic exposure to ^{90}Sr; four cases at the 125 μCi ^{90}Sr/day level and one case at the 25 μCi ^{90}Sr/day level. Three of these cases have been diagnosed as lymphosarcoma and two as myelogenous leukemia. Other animals at the 125 μCi ^{90}Sr/day level continue to have a moderate neutropenia, lymphopenia, and thrombocytopenia. Other animals at the 25 μCi ^{90}Sr/day have hematological values that are within the normal range. Effects related to ^{90}Sr ingestion have not yet been observed in animals fed 1 or 5 μCi ^{90}Sr/day. (auth)

10598 (BNWL–122, pp 107-9) TOXICITY OF COPPER AND X RAYS IN RATS. Hackett, P. L.; Clarke, W. J.; Palotay, J. L. (Battelle-Northwest, Richland, Wash. Pacific Northwest Lab.).

The administration of toxic levels of copper or x ray caused a depression of erythrocyte and lymphocyte values in rats. Copper administration produced a neutrophilic leukocytosis. Degenerative changes of the spleen, liver, and kidney were observed following treatment by either agent. High levels of copper increased ^{59}Fe levels in erythrocytes in contrast to the depression of these values following x irradiation. (auth)

10599 (BNWL–122, pp 128-30) BILE SALT ABSORPTION FROM THE IRRADIATED RAT INTESTINE. Sullivan, M. F. (Battelle-Northwest, Richland, Wash. Pacific Northwest Lab.).

Exposure of the abdomen of rats to 1500 R x radiation resulted in a 50% decrease in bile salt absorption at three days after exposure. This decreased function in the small intestine was shown to result in an increased excretion of bile salts. (auth)

10600 (BNWL–122, pp 131-4) THE EFFECT OF BILE ON ^{35}S INCORPORATION INTO INTESTINAL MUCOPOLYSACCHARIDES. Sullivan, M. F. (Battelle-Northwest, Richland, Wash. Pacific Northwest Lab.).

Sulphur-35 uptake was used as a measure of mucus synthesis in the intestine. Exposure of rats to 1000 R x radiation decreased ^{35}S uptake in the stomach, duodenum, ileum, cecum, and colon at three and four days after exposure. Draining the bile outside the lumen had the effect of preserving the mucus. This sparing effect was especially notable in the large intestine, where the quantity of mucus was greater than in the small bowel. (auth)

10601 (BNWL–122, pp 135-6) INFLUENCE OF FISSION NEUTRONS ON RAT REPRODUCTION. Sullivan, M. F. (Battelle-Northwest, Richland, Wash. Pacific Northwest Lab.).

Survivors of a neutron study were mated three successive times to determine the effect of fission neutrons on rat reproductivity. Males were temporarily sterile, but 2 of 11 recovered fertility. Doses of 145 to 265 rad did not render females infertile but litter size and the length of reproductive capacity were reduced. (auth)

10602 (CNAEM–32) THE EFFECT OF TRITIATED THYMIDINE AND GAMMA IRRADIATION ON THE MORTALITY OF ADULT DROSOPHILA MELANOGASTER LARVAE. [PART] II. Boeluekbasi, Esin Kent (Cekmece Nuclear Research Center, Atomic Energy Commission, Istanbul (Turkey)). Nov. 1965. 13p. Dep. mn.

The application of tritiated thymidine ($^{3}HTDR$) and ^{60}Co gamma irradiation at different times to the same adult Drosophila larvae caused a high but an additive mortality effect. The application of both irradiating agents to the larvae simultaneously caused a higher mortality rate which was even more than an additive one. Several factors that might affect the increase in mortality rate of Drosophila larvae when exposed to radiations were also studied. However it was found that irradiated tritiated thymidine was about the most influential factor for increased mortality in the larvae. (P.C.H.)

10603 (IAEA–2466-11) INVESTIGATIONS ON MUTABILITY OF POLYGENES AND ON UTILIZATION OF INDUCED GENETIC VARIABILITY. Progress Report. Scossiroli, R. E. (Pavia Univ. (Italy). Istituto di Genetica. Catania Univ. (Italy). Istituto di Genetica). Jan. 1, 1966. Contract 61/US. 33p. Dep. mn. CFSTI $2.00 cy, $0.50 mn.

Studies on radiation effects on genetics of maize and wheat are reported. Maize progenies selected from material grown the previous year were planted and fertilized using the intrafamily crossing method of pollination with the goal to maintain in the population the most of genetic variability present at the onset of selection and to allow a possible continuation of the response to selection in subsequent generations. Results on variability estimates suggest that a strong interaction effect takes place between genotypic and extranuclear factors. Using wheat, all treatments, with the exception of a 2000 R dose, showed significant differences between the means for the different groups for all characters considered. In other selection experiments, wheat was exposed to doses to 10,000 R and various characters, such as height of plant, number of stems, number of spikelets, and number of seeds in main spike, were studied in R_2 and R_3 generations. In spite of the fact that at early generations after selection the analysis of observation did not give estimates of genetic variation, the results of selections showed that phenotypic differences contain a genetic component. (P.C.H.)

10604 (NASA-TT-F–353) PROBLEMS OF RADIATION SAFETY IN SPACE FLIGHTS. PHYSICAL AND BIOLOGICAL STUDIES WITH HIGH-ENERGY PROTONS. Nefedov, Yu. G. Translation of Problemy Radiatsionnoi Bezopasnosti Kosmicheskikh Poletov; Fizicheskie i Biologicheskie Issledovaniya s Protonami Bol'shikh Energii, Atomizdat, Moscow, 1964. 244p. CFSTI $6.00.

Ten chapters on radiation effects under conditions of space flight and the development of permissible levels of radiation are included; separate abstracts were prepared for each chapter. (P.C.H.)

For abstracts of individual chapters see: 10605–10612, 10699, and 10719.

10605 (NASA-TT-F-353, pp 21-54) DOSIMETRIC INVESTIGATIONS AND SHIELDING STUDIES USING THE SYNCHROCYCLOTRON OF THE JOINT INSTITUTE FOR NUCLEAR RESEARCH. Afanas'ev, V. P.; Deev, Yu. S.; Keirim-Markus, I. B.; Kovalev, E. E.; Kuznetsova, S. S.; Litvinova, E. G.; Sakovich, V. A.; Smirennyi, L. N.; Sokolova, I. K.; Sychkov, M. A. Translated from Problemy Radiatsionnoi Bezopasnosti Kosmicheskikh Poletov; Fizicheskie i Biologicheskie Issledovaniya s Protonami Bol'shikh Energii, Atomizdat, Moscow, 1964.

Requirements of physical conditions for irradiation of animals by high-energy protons from a synchrocyclotron are given. In order to create a dose field meeting these requirements different methods for carrying out a number of dosimetric studies were used. Methods for measurement of an absorbed dose in a broad working range being the principal methods. It was concluded that dosimetry methods are suitable for measurements in fields of protons with energies of 100 to 600 Mev. Phantoms were used for study of the distribution of radiation in the bodies of animals. Radiation effects on shielding materials were also studied. The results showed that the radiation resistance of glass plastics is higher than for thermoplastics, whose properties must be modified by the introduction of matter protecting the polymer from the effects of penetrating radiations. Data are tabulated. (P.C.H.)

10606 (NASA-TT-F-353, pp 55-102) BIOLOGICAL EFFECT OF PROTONS WITH ENERGIES OF 510 Mev IN CASES OF MULTIPLE IRRADIATION. Bibikova, A. F.; Darenskaya, N. G.; Domshlak, M. P. (and others). Translated from Problemy Radiatsionnoi Bezopasnosti Kosmicheskikh Poletov; Fizicheskie i Biologicheskie Issledovaniya s Protonami Bol'shikh Energii, Atomizdat, Moscow, 1964.

The biological effects of high-energy protons on dogs and rats were studied. The dogs were subjected to fractional and single irradiation by protons with energies of 510 Mev in doses of 250 to 650 rad and rats in doses of 100 to 1200 rad. On the whole, the detected changes in dogs indicated that in addition to the other physiological systems the blood circulation apparatus is extremely sensitive to protons. At the same time, the cardiovascular system also possesses relative resistance to the effect of this factor. The fact that most of the observed changes were noted at the height of the illness, when the total dose reached about 550 to 600 rad, indicates the conservation of compensatory mechanisms which maintain the blood supply of the organism at the required rate over a long period of time. During morphological investigations of the internal organs of rats, there was development of changes characteristic of acute radiation sickness, and these were expressed most clearly in the first 2 or 3 weeks after termination of irradiations. (P.C.H.)

10607 (NASA-TT-F-353, pp 103-41) BIOLOGICAL EFFECT OF PROTONS WITH ENERGIES OF 510 Mev DURING SINGLE IRRADIATION. Bibikova, A. F.; Darenskaya, N. G.; Derbeneva, N. A. (and others). Translated from Problemy Radiatsionnoi Bezopasnosti Kosmicheskikh Poletov; Fizicheskie i Biologicheskie Issledovaniya s Protonami Bol'shikh Energii, Atomizdat, Moscow, 1964.

The biological effects of a single exposure of high-energy protons on dogs and rats were studied. Dogs were exposed to doses of 510, 550, 400, 250, and 330 to 690 rads and rats to 100 to 950 rads. Single irradiation of white rats with protons with doses of 330 to 620 rads, caused acute radiation sickness with uniform morphological changes of the internal organs. The height of the sickness in rats was observed approximately from the 3rd to the 10th day after irradiation. Acute radiation sickness also developed in all dogs after proton exposure. Radiation damages in the various organs and biological systems of the dogs and rats are described. (P.C.H.)

10608 (NASA-TT-F-353, pp 142-50) BIOLOGICAL EFFECT OF PROTONS WITH ENERGIES OF 126 Mev ON CORNEAL EPITHELIA OF MICE. Mastryukova, V. M.; Strzhizhovskii, A. D. Translated from Problemy Radiatsionnoi Bezopasnosti Kosmicheskikh Poletov; Fizicheskie i Biologicheskie Issledovaniya s Protonami Bol'shikh Energii, Atomizdat, Moscow, 1964.

Laboratory male mice were given total radiation with protons with an energy of 126 Mev in doses of 200 and 500 rad with a dose intensity of 0.3 rad/sec. The results showed a slowing of the mitotic activity of the corneal epithelium, a decrease of the number of cells in the field of view of the microscope and the development of pathological forms of mitosis. With an increase of the radiation dose the degree of suppression of mitotic activity increased and the intensity of restorative processes decreased. The appearance of pathological mitoses in irradiated tissue was taken as an indication of damage of the genetic structures of the cell. The mechanism of radiation effects is discussed. (P.C.H.)

10609 (NASA-TT-F-353, pp 151-6) DETERMINATION OF THE BIOLOGICAL EFFECT OF PROTONS WITH ENERGIES OF 510 Mev AND X-RAYS WITH ENERGIES OF 180 KV ON HEREDITARY STRUCTURES. Plotnikova, E. D.; Strashenko, S. I. Translated from Problemy Radiatsionnoi Bezopasnosti Kosmicheskikh Poletov; Fizicheskie i Biologicheskie Issledovaniya s Protonami Bol'shikh Energii, Atomizdat, Moscow, 1964.

The RBE of protons with energies of 500 Mev for hereditary structures in rats was studied. Dominant lethals were used as an index of hereditary changes caused by radiation. Nonlinear white rats were subjected to total irradiation by protons at doses of 55, 200, 360, 520, 780, and 1030 rad. The frequency of development of dominant lethals, established from the death of embryos of rats, increased with the irradiation dose. The mechanisms of the development of dominant lethals are discussed. The RBE of protons was determined to be 0.7. Results are compared with x-ray induced dominant lethals. (P.C.H.)

10610 (NASA-TT-F-353, pp 157-84) BIOLOGICAL EFFECT OF PROTONS WITH ENERGIES OF 130 Mev, X-RAYS WITH ENERGIES OF 180 KV AND ^{60}Co GAMMA RADIATION ON THE VESTIBULAR APPARATUS. Grigor'ev, Yu. G.; Sevan'kaev, A. V.; Sveshnikov, A. A. Translated from Problemy Radiatsionnoi Bezopasnosti Kosmicheskikh Poletov; Fizicheskie i Biologicheskie Issledovaniya s Protonami Bol'shikh Energii, Atomizdat, Moscow, 1964.

Studies were made of the effects of high-energy protons and gamma and x irradiation on the vestibular apparatus, the dose dependence of the studied effects, and functional impairments of the activity of the semicircular canals during different periods of radiation sickness in dogs and rabbits. Dogs were exposed to doses of 500 and 350 rad. Radiation illness transpired in a more acute form in the dogs receiving the higher dose. As the radiation sickness developed, the reaction of the vestibular apparatus decreased and it was possible to note phase states of retardation in the apparatus. A decrease of threshold sensitivity as a function of the lifetime of the irradiated animals and a decrease of the reaction of the vestibular apparatus was found. By experimentation on rabbits, a range of doses (500–5000 R) which leads to a considerable impairment of the functional state of the vestibular apparatus in most animals, which is expressed in a decrease of irritability and reaction of the vestibular apparatus was determined. Quantitative data characterizing the dependence between the dose of radiation and the effect are discussed. (P.C.H.)

10611 (NASA-TT-F-353, pp 185-93) BIOLOGICAL EFFECT OF MULTIPLE X-RAY IRRADIATION WITH ENERGIES OF 180 KV COMPARED WITH PROTON IRRADIATION (DOSES AND TEMPORAL DISTRIBUTION). Darenskaya, N. G.; Domshlak, M. P.; Grachev, V. I.; Ryzhov, N. I. Translated from Problemy Radiatsionnoi

Bezopasnosti Kosmicheskikh Poletov; Fizicheskie i Biologicheskie Issledovaniya s Protonami Bol'shikh Energii, Atomizdat, Moscow, 1964.

The relative biological effect of protons in fractional irradiation was determined by experiments with the corresponding irradiation of dogs and rats by x rays with a production energy of 180 kv. The condition of the animals and state of the peripheral blood and cardiovascular system were observed carefully and pathologic-morphological and histological investigations were made of the tissues and organs. In all dogs, acute radiation sickness with a sharply expressed hemorrhagic syndrome was found. However, multiple exposure to x rays in single doses of 15–110 R with intervals of 1–2 days and a total dose of about 750 R led to the development of a light form of radiation sickness in rats with the death of individual animals. In the case of a total dose of 1015 R there was a well-expressed picture of radiation damage with the death of 22% of the animals in 2 months and a loss of 60% when deaths at considerably later times were taken into account. (P.C.H.)

10612 (NASA-TT-F-353, pp 194-209) COMPARATIVE ANALYSIS OF BIOLOGICAL EFFECT OF PROTON RADIATION WITH ENERGY OF 510 Mev. Darenskaya, N. G.; Domshlak, M. P.; Grigor'ev, Yu. G.; Nefedov, Yu. G.; Razorenova, V. A.; Ryzhov, N. I. Translated from Problemy Radiatsionnoi Bezopasnosti Kosmicheskikh Poletov; Fizicheskie i Biologicheskie Issledovaniya s Protonami Bol'shikh Energii, Atomizdat, Moscow, 1964.

The RBE of proton radiation with an energy of 510 Mev was determined and compared with collected data on materials characterizing the effectiveness of x and γ radiation. Comparative characterization of the effectiveness was based on percentage survival and on the basis of a comparison of morphological changes in the organs and tissues and also from the depth and intensity of changes of individual physiological functions in dogs and white rats subjected under identical conditions to the effects of proton, x, and γ radiations. Special differences were observed in the coefficients of RBE of protons of small and large animals. The differences, which were rather large, can apparently be attributed to the fact that during the irradiation of small animals there apparently are no appreciable changes in the energy loss of particles. However, a considerable quantity of particles is absorbed completely in the body of the dogs (large animals). Data are tabulated. (P.C.H.)

10613 (NP-tr-1344) THE EFFECT OF IONIZING AND ULTRAVIOLET RADIATION ON CORN SEEDS. Sydorenko, I. D. Translated from Ukr. Bot. Zh., 19: No. 2, 3-12(1962). 11p. (TT-65-50025). CFSTI $1.00 cy, $0.50 mn.

The effects of presowing irradiated corn seeds on the growth and development of the plant were studied. The results showed that irradiation of corn seeds with low doses of all three types of radiation (x rays to a dose of 500 R, gamma rays to 1000 R, and uv radiation for as long as 120 min) had practically no effect on the germinating properties of the seeds. However, an entirely different situation was observed after irradiation of the seeds with doses of x rays from 500 to 1000 R, gamma rays from 1000 to 2000 R, and uv radiation from 120 to 240 min. Owing to the reduction in the germinating power of the seeds and the thinning of the shoots, growth inhibition of the plants as well as the considerable number of seedless ears, the inhibitory doses of ionizing radiation (22,000 R for x rays and 33,000 R for ^{60}Co gamma rays) caused a reduction in the yield of green mass and ears by an average of 50–70% as compared to controls. (P.C.H.)

10614 CHANGES IN THE OSMOTIC RESISTANCE OF WHITE BLOOD CELLS IN POSTRADIATION DISEASE IN RATS. Kocmierska-Grodzka, Danuta; Danysz, Andrzej; Kruszewska, Jadwiga. Acta Physiol. Pol., 16: 739-43 (Sept.-Oct. 1965). (In Polish).

The effect of irradiation on the osmotic resistance of white blood cells in adult rats of the Wistar strain was studied. In healthy rats, incubation of leukocytes in hypotonic sodium chloride solution for three hours caused changes in about 50% of the white blood cells. Irradiation of the animals with doses of 300 to 600 R x radiation lowered the osmotic resistance of white blood cells, the maximal effect occurring six hours after the irradiation. Compared with the initial values observed in the same animals before irradiation, the observed drop in osmotic resistance was not statistically significant. (auth)

10615 TREATMENT OF RADIATION DAMAGE OF THE SKIN. Ziegenbalg, H. (Medical Academy Carl Gustav Carus, Dresden). Aesthet. Med., 14: 74-84(1965).

Radiation induced changes in the femurs and soft tissues of the guinea pig were investigated histologically after ^{60}Co-irradiation with 5,000 R and 10,000 R. Bone tissue was found to be very resistant to the ultrahard ^{60}Co-gamma-rays. There was, however, considerable destruction of the irradiated soft tissue. From these results it can be concluded that human bone tissue will not be damaged with radiation doses used in the telecobalt treatment of deeper located tumors. The destruction of soft tissue by ^{60}Co-radiation must be investigated in more detail. (Excerpta Med.)

10616 EMBRYOTOXIC EFFECTS IN RATS. Lorke, Dietrich (Farbenfabriken Bayer AG, Wuppertal-Elberfeld, Ger.). Arch. Exp. Pathol. Pharmakol., 250: 360-82 (Mar. 4, 1965). (In German).

The authors report on the effects of embryotoxic doses of x irradiation in a strain of rats that is normally practically free of spontaneous malformations. X irradiation was administered to fetuses in a single dose of 150 R on the eleventh or thirteenth day of gestation. The single exposure resulted in fetal malformations that included lack of or excess of fingers, with and without fusion, bilateral aplasia of the tibiae and ulna, and micrognathy of the lower mandible. When fetuses were irradiated with 150 R of x ray on the fifth day of pregnancy, a large number developed ocular malformations. These consisted of macroscopically demonstrable microophthalmias and anophthalmias. The authors discuss the relative differences that define whether bone changes are the result of a distinct malformation, an indication of growth retardation, or a variation from normal development of the rat fetus. The bone changes observed after the single dose of x irradiation fall within the classification of an irradiation induced fetal malformation. (BBB)

10617 THE SYNTHESIS OF MACROGLOBULIN ANTIBODY TO A BACTERIAL ANTIGEN IN MICE AFTER TREATMENT WITH THOROTRAST. Jenkin, C. R.; Auzins, Ieva; Reade, P. C. (Univ. of Adelaide). Austral. J. Exp. Biol. Med. Sci., 43: 607-24(Oct. 1965).

In experiments designed to study the role of the macrophage in antibody formation, marked effects on the quantity and type of antibody formed were produced by treating mice with Thorotrast before or after the injection of antigen. The antigen used was a killed culture of Salmonella typhimurium which was injected either intravenously or intraperitoneally. The mice were injected intravenously with 25 mg of Thorotrast, and at various intervals (30 and 60 min, 2, 4, 7, 24, and 48 hr) following this teatment were challenged, again intravenously, with 1 μg of the bacteria. The antibody responses of these mice were examined up to 12 weeks later. In all the situations studied the macroglobulin antibody response was enhanced and maintained at a high level for the duration of the experiment. Mice that had been given a primary injection of antigen following Thorotrast responded with a secondary type macroglobulin antibody response, providing that Thorotrast was again given prior to the second antigen challenge. In this situation there was a very rapid, almost ten-fold, increase in the amount of macroglobulin antibody produced without much alteration in the level of presumably 7S antibody for a period of five days. In contrast, however, mice given a second challenge of antigen in the absence of any further Thorotrast injections gave a secondary response of 7S antibody. In these mice the titer of macroglobulin antibody rapidly declined. Histological examination of spleens from Thorotrast-treated mice indicated a degree of cellular damage followed by marked proliferation of lymphoid elements as evident by the number of mitotic figures. (BBB)

10618 RANDOMIZATION TESTS FOR COMPARING SURVIVAL CURVES. Cox, D. F.; Kempthorne, O. (Iowa State Univ., Ames). Biometrics, 19: 307-17(June 1963).

Randomization tests were used to study survival during the early postnatal life of pigs. Sexually mature males were treated with a single dose (300 R) of x rays. Comparisons were made between the mortality occurring in the first three weeks after birth among offspring from the untreated and treated males as a measure of the extent of the deleterious effects produced by paternal irradiation. The experiment consisted of 3552 animals born in 362 litters, 180 from irradiated males and 182 from control males. The results, assuming randomization had been carried out over all litters, support the hypothesis that paternal irradiation adversely affects the number of pigs born that survive to the end of each interval. (TCO)

10619 EXPERIMENTS ON THE INFLUENCE OF IONIZING RADIATIONS ON THE GROWTH OF BREWING BARLEY. Farkas, J.; Kiss, I.; Razga, Z., Vas, K. Brauwissenschaft, 16: 483-91(Dec. 1963). (In German).

The effects of 250-kv x rays in doses varying from 1.5 to 50 krad on the sprouting of barley to be used in brewing were investigated. The x rays were applied during steeping or at different points during germination to study the development of root growth in barley. It was found that radiation doses of over 12 krad exert an inhibitory action on the development of the roots but do not arrest the growth of tips and tendrils. The radiation could be used conveniently during storage of the barley since, in addition to its effect described above, it also has a lethal action on insect pests which normally contaminate the grain and thus prevents damage by them. On account of this, the action of radiation doses of 25–800 krad was investigated on air-dried barley (moisture content, 11.1%). On the basis of a 4-day growth test, it was established that steeped barley of moisture content of 35 to 45% is five times more sensitive to radiation than air-dried barley. Radiation sensitivity is increased both with increasing moisture content above 16.3% and when it is lowered from 13.7 to 9.5%. During storage of the irradiated air-dried barley for 7 months, no regeneration was observed. The retarding action of radiation on growth caused a decrease in malting loss. A close relation was found between the increase in malt yield and the reduction of the growth of roots obtained after irradiating the grain. After treating the air-dried barley with doses of 50 to 100 krad, the malting loss was reduced by 1 to 2%. All qualitative characteristics of the malts prepared from the irradiated barleys were satisfactory. The increase in malt yield obtained by irradiation occurred without disturbance of the enzymic processes which occur during germination. (BBB)

10620 THE RADIORESTORING ACTION OF A FRACTION EXTRACTED FROM TOBACCO LEAVES. Duarte, Maria Ivone; Kovoor, Aries (Univ., Paris). Compt. Rend., 261: 4202-5(Nov. 15, 1965). (In French).

A fraction extracted from tobacco leaves is capable of restoring the proliferating ability of x irradiated tobacco crown-gall in leaf tissues. (tr-auth)

10621 EFFECT OF X RAYS ON THE GROWTH OF TISSUE CELLS OF TOPINAMBOUR CULTIVATED IN VITRO. Spanjersberg, Genevieve (CPEM, Paris). Compt. Rend., 261: 4821-4(Nov. 29, 1965). (In French).

X rays inhibit the growth of Topinambour cells. This inhibiting effect is at a maximum at the time when cells are placed in the culture; it decreases when the cells begin to grow and becomes very weak when growth has begun. (tr-auth)

10622 THE ACID DESOXYRIBONUCLEASE OF THE SPLEEN AFTER IRRADIATION OF THE HEAD OR OF THE WHOLE BODY IN THE RAT. Goutier, R. (Centre d'Etude de l'Energie Nucleaire, Mol, Belg.). Compt. Rend. Soc. Biol., 159: 1001-5(1965). (In French).

The effects of whole-body or head irradiation on the acid desoxyribonuclease activity of the rat spleen was investigated. The rats were exposed to doses of 800 R x radiation. The results show that the total activity of the desoxyribonuclease decreased during the first 8 hrs following irradiation for both the partial and whole-body irradiation. Then the total activity continued to decrease in rats exposed to a whole-body irradiation but it was stabilized for rats exposed to head irradiation. (J.S.R.)

10623 INDUCTION OF LEUKEMIA IN THE C57 BL MOUSE BY MEANS OF TRITIATED THYMIDINE. Mewissen, D. J. (Univ., Brussels). Compt. Rend. Soc. Biol., 159: 1005-7(1965). (In French).

Two groups of C57 BL male and female mice were observed after the animals of the first group were injected at birth with tritiated thymidine at a dose of 0.3 μc per body weight. The animals of the control group received a physiological liquid. In the animals injected with tritiated thymidine, 5 deaths following the appearance of a lymphoid leukemia after a latency period from 315 to 524 days were observed. No leukemia or other malignant tumor was observed in the control group. (tr-auth)

10624 THE RADIOSENSITIZING EFFECTS OF N-ETHYLMALEMIDE ON VICIA FABA. Sharma, R. P. (Indian Agriculture Research Inst., New Delhi). Current Sci., 35: 21-2(Jan. 5, 1966).

Results are reported from a study designed to check the radiosensitizing ability of N-Ethylmalemide using the frequency of chromosome and chromatid aberrations in roots of Vicia faba as the radiation effect. The seeds were germinated in sand beds and the primary root-tips were cut off when they were 1 cm in length. The seedlings were then allowed to develop secondary roots, in glass vials containing tap-water at 25 ± 1°C. The secondary roots were treated for 24 hours with aqueous 10 μM solution of N-Ethylmalemide in phosphate buffer at pH 7. The concentration used is the maximum non-toxic dose and was selected after considerable trial. The chemically treated seedlings were divided into two sets. One set was kept in double distilled water for 24 hours and the second set was given 50 R of x rays at the dose rate of 25 R/minute. Another set of non-chemically treated seedlings was irradiated with 50 R of x rays, to serve as control for the chemical-radiation combination treatment. After 24 hours of recovery period the roots were pretreated with 0.05% colchicine, washed in water and fixed in acetic alcohol (1 : 3). Slides were prepared as feulgen squashes and scored for chromatid gaps (G′), chromosome gaps (G″), chromatid breaks (B′), chromosome breaks (B″) and also for both chromatid as well as chromosomal exchanges. Results show that N-Ethylmalemide is a poor chromosome-breaking agent, but when it is followed by radiation, there is a significant enhancement in the yield of chromosomal aberrations. The total number of chromosomal aberrations obtained in the combination treatment of chemical and radiation (27 · 24%) was more than additive of the aberrations produced separately by chemical (2 · 22%) and radiation (11 · 05%). (auth)

10625 FURTHER INVESTIGATION OF PARTICULAR MICROELEMENTS IN X-RAY DERMATITIS. Sosnovskii, A. T. (Minsk State Medical Inst. Belorussian Inst. of Dermatology and Venereal Diseases, USSR). Dokl. Akad. Nauk Belorussk. SSR, 9: 419-21(June 1965). (In Russian).

In rabbits with x-ray dermatitis with substantial accumulations of cobalt concentration in the blood, some reduction of its concentration in the liver was noted. In muscles and spleen there was no noticeable change in the quantity of cobalt. The increase of x-ray dermatitis in rabbits is not accompanied by a significant change of the concentration of nickel in the blood, liver, and muscle. In experimental animals there appeared some statistically unimportant increase of the copper in the liver, unessential decrease in the muscle, and significant decrease in the spleen. In the presence of some increase of zinc in the blood of experimental animals there was an increase in the liver and a statistically unimportant decrease in the muscle and spleen. (tr-auth)

10626 THE STIMULATING EFFECT OF CERTAIN DOSES OF IONIZING RADIATION ON THE OVOGENOUS FUNCTION OF BIRD OVARY. Karapetyan, S. K.; Vardan-

yan, V. A. (Inst. of Physiology, Academy of Sciences, USSR). Dokl. Akad. Nauk SSSR, 163: 745-6(July 21, 1965). (In Russian).

In chickens that were x irradiated, with doses of 4 to 500 R, at 112 days of age, sexual development was delayed 2 to 3 months. In a 12-month observation period, the 4-R-irradiated group laid 19 percent more eggs than the non-irradiated controls; the 12-R-irradiated group laid 26 percent more; and the 20-R-irradiated group laid 49 percent more. However, chickens irradiated to 100 or 500 R doses showed a sharply decreased overall egg production. At the tenth month of the experiments these last two groups showed some stimulation in egg production, but the effect was temporary. This alternation in stimulation and depression in egg laying is a characteristic response to the action of ionizing radiation. (TTT)

10627 ON THE PROBLEM OF ANTITUMORAL RESISTANCE IN ANIMALS SUBJECTED TO CHRONIC TREATMENT WITH SMALL DOSES OF ^{90}Sr. Lukash, N. I.; Gubareva, A. V.; Shimanovskaya, K. B. (Central Scientific-Research Inst. of Radiation Protection, USSR). Dokl. Akad. Nauk SSSR, 163: 747-9(July 21, 1965). (In Russian).

Histopathological observations and roentgenograms of 15 experimental animals and 15 controls indicated that ^{90}Sr administered in doses that are not carcinogenic when given alone induces sarcomas when a chemical carcinogen is also given. The experiments were carried out with adult white rats, which were given daily doses of ^{90}Sr so that in a 6-month period they received 0.68 to 3.4 rads irradiation. Systematic radiometric measurements were made to determine the ^{90}Sr in the skeleton. At the end of the ^{90}Sr administration period, 2.5 mg of 9,10-dimethyl-1,2-benzanthracene in 0.05 ml of sunflower seed oil was injected near the proximal metadiaphysis of the tibias; this is the main site of ^{90}Sr deposition and also of the origin of osteogenic sarcomas. Although the frequency of sarcoma occurrence is statistically significant, 71% in the experimental animals and only 7% in the controls, the work is considered preliminary. (TTT)

10628 THE EFFECT OF RADIATION ENERGY ON BONE TISSUE. Engstroem, Arne (Karolinska Institutet, Stockholm). Ergeb. Allgem. Pathol. Pathol. Anat., 45: 1-22(1964). (In German).

The effects of irradiation from ^{90}Sr and Ra on bone are reviewed and discussed. Induction of malignant tumors by irradiation of bone tissue have been obtained from studies made in experimental animals, using very high irradiation doses. Tumor formation took place after exposure to doses of several thousand rads. The irradiation dose from ^{90}Sr deposited in the skeleton is much less than the irradiation dose that was effective in the experimental studies. From the results of the experimental tumor studies which used such high irradiation doses it is difficult to draw conclusions as to the possibility of tumor induction from the present, rather very small concentrations of ^{90}Sr in bone because there are so many unknown factors which should be taken into account. As a result this problem still is unresolved. However, it can be said with some assurance that the risk of development of bone tumors as a result of the ^{90}Sr that has been incorporated into the skeleton from fallout is extremely small. In any case, though, it is impossible to differentiate between bone tumors that may arise spontaneously and any that are induced by deposited ^{90}Sr. Because statistics of spontaneously occurring bone tumors show wide variability normally, an increase in the additional number of tumors that might be induced by ^{90}Sr would be difficult to detect. (72 references cited.) (BBB)

10629 HOW RADIATION CAUSES CELL DEATH. Whitfield, James F. (EURATOM, Ispra, Italy). Euratom Bull., 4: 116-21(Dec. 1965).

Radiation effects on thymocytes from the thymus of 3-week-old Sprague-Dawley rats are discussed. The complete loss of nuclear structure was observed in irradiated thymocytes. Very shortly after the loss of nuclear structure large amounts of histone left the nucleus and accumulated in the cytoplasm. This histone had dissociated from DNA. This histone then depressed nuclear metabolism. It is suggested that the probability of a cell suffering interphase death may very well be a function of its histone content. The effect of changing the phosphate content of the cell culture medium was studied. The higher the phosphate concentration the more rapidly did the nuclei lose their structure after irradiation. It was concluded that the first change to occur after irradiation is the uncoupling of the formation of ATP from respiration, which, in turn, causes an accumulation of the free phosphate, which attacks and breaks the association between DNA and histone. DNP (2,4-dinitrophenol) stops phosphate uptake while increasing respiration. This inhibits the development of nuclear damage. A type of biological dosimeter was devised, which uses the proportion of lymphocytes from circulating blood that contain structureless nuclei as an indication of the amount of radiation received. (M.C.G.)

10630 THE EFFECT OF RADIATION ON LENTICULAR EPITHELIAL ENZYMES IN YOUNG RABBITS. Swanson, A. A. (Veterans Administration Hospital, McKinney, Tex.). Exp. Eye Res., 4: 231-6(Sept. 1965).

Biochemical comparisons were made between x irradiated and normal lenses of young animals which might reflect adverse changes in the enzymic equilibrium of the changing cell population. The mitochondrial fraction and the soluble fraction of the epithelial cells of the lens from 6-week-old New Zealand White male rabbits, exposed to 800 R of whole-head x irradiation, were evaluated for glucose-6-phosphate dehydrogenase, isocitrate dehydrogenase, malate dehydrogenase, glutathione reductase, glyceraldehydephosphate dehydrogenase, purine nucleoside phosphorylase, $NADPH_2$ diaphorase, and $NADH_2$ cytochrome c reductase activities. Increased enzyme activities were noted in the irradiated lenticular tissues for purine nucleoside phosphorylase, $NADPH_2$ diaphorase and $NADH_2$ cytochrome c reductase. Decreased activities for glucose-6-phosphate dehydrogenase, malate dehydrogenase, glutathione reductase, and glyceraldehydephosphate dehydrogenase were observed in the lenticular tissues of irradiated animals. The activity of isocitrate dehydrogenase was the same in the irradiated and control animals. The pronounced decrease in glutathione reductase in the combined lens capsule and epithelium was observed as early as 18 hr after exposure to x irradiation and long before any visible pathology was evident. The coenzyme for both glutathione reductase and malate dehydrogenase was NADP. However, the reduced state is required for glutathione reductase and the oxidized form for malate dehydrogenase. The irradiation response of the enzymes in the soluble fraction suggested that these enzymes are more sensitive to ionizing radiation than those of the mitochondrial fraction. This may be correlated with the rate of latent opacity formation in the lens and early damage to the rapidly dividing new epithelial cells in young rabbit tissues, which may give rise to abnormal metabolic fibers during the period of irradiation. (BBB)

10631 THE INFLUENCE OF CONTINUOUS IRRADIATION AND EXPERIMENTAL DIPHTHERIAL INTOXICATION UPON THE ORIGIN AND INCIDENCE OF NON-SPECIFIC NECROTIC CHANGES IN THE CARDIAC MUSCLE. Vasku, J.; Urbanek, E.; Dolezel, S.; Praslicka, M. (Univ. of Jan Ev. Purkinje, Brno. Safarik Univ., Kosice, Czechoslovakia). Experientia, 21: 651-3(1965).

Results are reported from studies on the interrelations between continuous γ irradiation and experimental diphtherial intoxication. Rats were divided into 4 groups. The first group received a relatively small dose of the diphtherial toxin, 250 MLD/150 g body weight. The second group was represented by the rats which were only continuously γ irradiated. In the third group the dose of the diphtherial toxin was the same as in the first group, but the animals were pretreated with continuous irradiation. The rats in the fourth group were treated with a massive dose of the diphtherial toxin: 1000 MLD/150 g body weight. The irradiation was continuous for 23 to 23½ hr a day. The daily dose was 90 R, total dose within 25 days 2250 R. The animals were kept in special cages in the γ field in a semicircular area around the ^{60}Co source. The characteristic

feature of the lesions in the cardiac muscle was the incidence of minute necroses in the myocardial fibers. Under the condition used it was concluded that the pathogenesis of infarctoid lesions in the myocardium is a non-specific stress process, which is initiated by the disturbance of the electrolyte metabolism in the isolated fibers of the cardiac muscle. (C.H.)

10632 ON THE POSSIBILITY THAT THYMUS-MEDIATED ALLOANTIGENIC STIMULATION RESULTS IN TOLERANCE RESPONSE. Vojtiskova, Marta; Lengerova, Alena (Inst. of Experimental Biology and Genetics, Prague). Experientia, 21: 661-3(1965).

The possible role of the thymus in the induction of transplantation tolerance was investigated in mice submitted to some or all of the following procedures: thymectomy, exposure to 400 R γ radiation, thymus grafting from a donor either irradiated or non-irradiated at the same time as the recipient, antigen (spleen cell) injection into the thymus graft, and skin grafting after 13 weeks. A long-lasting tolerance was induced in most of the irradiated animals when antigen was introduced into the preirradiated or non-irradiated thymus isograft and also when the antigen was given subcutaneously outside the irradiated thymic isograft. Results are discussed in relation to the hypothesis that an afferent blood-thymus bar prevents the entry of extrinsic antigens into the thymus. (C.H.)

10633 THE EFFECT OF RADIATION ON DEOXYRIBONUCLEOPROTEINS IN ANIMAL TISSUE. II. THE RELATIONSHIP BETWEEN THE RADIATION DOSE AND THE AMOUNT OF DEOXYRIBOPOLYNUCLEOTIDES IN RADIOSENSITIVE TISSUES AFTER A SINGLE AND REPEATED IRRADIATION. Skalka, M.; Matyasova, Jitka (Inst. of Biophysics, Brno). Folia Biol. (Prague), 11: 378-87(1965).

The increase in the amount of deoxyribopolynucleotides in mouse and rat spleen and thymus and in rat bone marrow four hours after whole-body irradiation shows a biphasic correlation to the radiation dose. In all the tissues examined, an almost linear increase in the concentration of these substances was found within exposure limits of 0 to 300 R x radiation, while after higher exposures the deoxyribopolynucleotide level remained unchanged. After the intraperitoneal administration of ^{32}P, an increase in the deoxyribopolynucleotide concentration was found in mouse spleen and thymus within the limits of the doses used (0 to 15 mC ^{32}P/kg body weight). In experiments on mice repeatedly irradiated after different intervals (2 hours to 11 days) with 600 R, it was found that the second irradiation exposure did not influence the deoxyribopolynucleotide level produced by the first exposure. Study of the relationship between the first radiation dose (exposure 0 to 1,200 R) and the deoxyribopolynucleotide level after the second irradiation (20 hours later, exposure 600 R) showed that the first irradiation with 0 to 300 R exposure caused a linear decrease in the response to the second irradiation; when irradiated the first time with exposures of over 300 R, the tissues no longer responded to the second irradiation. (auth)

10634 RELATIONSHIP OF RADIORESISTANCE AND IMMUNORESISTANCE IN AN EXPERIMENTAL TUMOR. Koldovsky, P.; Adamcova, Berta; Bubenik, J. (Inst. of Experimental Biology and Genetics, Prague). Folia Biol. (Prague), 11: 393-5(1965).

Radioresistant and immunoresistant forms of mouse sarcoma MC 1/C57BL were produced by exposure of a cell suspension to 500 R x radiation before each passage. The radioresistant form was found to be more sensitive to immunity than the initial tumor. The radiosensitivity of the immunoresistant form did not alter. A combination of radiotherapy and immunotherapy is therefore an advantage, particularly when immunotherapy is preceded by irradiation. (auth)

10635 EFFECT OF ULTRAVIOLET RAYS ON THE ERYTHROPOIETIC ACTIVITY OF THE KIDNEY. Wajdowicz, A. (Inst. of General and Experimental Pathology, Krakow). Folia Biol. (Warsaw), 13: 317-21(1965).

Irradiation with ultraviolet rays applied directly to the kidneys stimulated the production of the erythropoietic factor. The kidney is one of the principal organs producing this factor, which is evidenced by the result of control examinations, since irradiation of the liver and spleen has practically no effect on the activity of the hematopoietic system. The kidney of rats was directly exposed to ultraviolet rays, which brought about an increase in the number of reticulocytes from 29 to 106%. The renal venous blood of irradiated rat injected into a normal animal increased reticulocytosis from 24 to 67%. After unilateral nephrectomy the remaining kidney irradiated with ultraviolet rays showed a vicarious hormonal activity, the number of reticulocytes increasing from 28 to 143%. Renal venous blood of this kidney irradiated with ultraviolet rays and subsequently injected into a normal animal increased reticulocytosis from 27 to 83%. The results of all experiments were statistically significant. (auth)

10636 CHANGES IN THE CONTENT OF CEREBRAL LIPIDS DURING NORMAL DEVELOPMENT OF GUINEA PIGS AND AFTER PRENATAL X-IRRADIATION. Wender, M. (Dept. of Neurology, Medical Academy, Poznan, Poland). Folia Biol. (Warsaw), 13: 323-32(1965).

The content of various lipids in the guinea-pig brain was investigated at various stages of normal development and after prenatal x irradiation. Fetal guinea pigs were exposed to a single dose of 400 R x radiation in the 8th or 9th week of gestation. In the course of maturation of the brain, an increase in the contents of total phospholipids, cerebroside, sphingomyeline, and total and free cholesterol was observed. The developmental increase of cerebroside, sphingomyeline, and cholesterol content was more pronounced in the white than in the grey matter. The rapid rise of cerebroside, sphingomyeline, and, in a smaller degree, of cholesterol content, in the white matter occurs during the myelination of the nerve fibers. The ionizing radiation, acting during the final period of intrauterine life, caused only negligible alteration in the physiological changes of the lipid concentration in the developing nervous system. It is concluded that the ionizing irradiation acting in the final phase of gestation, i.e., just before or during the myelination, does not exert any remarkable effect on the laying down of lipids in the brain, including the process of myelination. (auth)

10637 OCCUPATIONALLY CAUSED BONE CHANGES BY EXTERNAL RADIATION BURDENS. Kolar, J.; Jirasek, L.; Vrabec, R. (Charles Univ., Prague). Fortschr. Geb. Roentgenstr. Nuklearmed., 103: 584-9(1965). (In German).

Investigations of bone changes in patients who were occupationally exposed to external chronic irradiation with small doses of ionizing radiation are discussed. In 76 patients it was possible to establish the following changes: osteoporosis, bone atrophy, osteosclerosis, dystrophy, osteomyelitis, arthritic changes of the joints, and radiation-induced primary and secondary bone tumors. The importance is stressed of these little known and insufficiently heeded symptoms for the assessment of somatic radiation injuries and of the most suitable therapeutic approach to the treatment of of skin damage. (tr-auth)

10638 HISTOCHEMICAL DETECTION OF GLYCOGEN AND MUCOPOLYSACCHARIDES IN THE BRAIN OF GUINEA PIGS AFTER X-RAY IRRADIATION. Lierse, W.; Gritz, K.; Franke, H. (Univ., Hamburg). Fortschr. Geb. Roentgenstr. Nuklearmed., 103: 612-18(1965). (In German).

The effect of x irradiation (200 kv) on the brain was studied in twenty male and female guinea pigs. They were given single treatments of 100, 500, 1,000, 1,500, 2,000, 2,500, 3,000, and 4,000 R, and killed twenty-four hours later. Following 500 R glycogen and mucopolysaccharides were visible in glial cells of the cerebral cortex. After 1,000 R these substances were found in the deeper layers of the cortex. After 2,000 and 3,000 R these substances were found in the entire cortex, in the cerebellar cortex, in the white substances of the cerebrum and cerebellum, not only in glial cells, but also in ganglion cells. Following

these doses microhemorrhages and karyolysis was observed in ganglion and glial cells. (tr-auth)

10639 THE MECHANISMS OF PROTECTION FROM AND REPAIR OF THE BIOLOGICAL LESIONS BROUGHT ABOUT BY IONIZING RADIATIONS. THE POSSIBILITIES AND LIMITS OF EXPERIMENTAL RESEARCH. **Bruzzese, E. (Sanita Militare, Rome). Giorn. Med. Mil., 114: 579-613(1965).**

A mechanism for the biological action of ionizing radiations was derived from a literature review. Possibilities and limitations of several experimental methods are discussed in view of the research program at the Army Medical Corp Research and Study Center. Radiation effects are considered as to: fundamental injuries caused by ionizing radiation and their possible reparation; the possibility of interfering with the action of radiations by outside agents; and experimental research in the fields of protection and radiation reparation. (H.G.D.)

10640 A QUANTITATIVE ANALYSIS OF THE BIOLOGIC EFFECT OF RADIOACTIVE PHOSPHORUS (^{32}P) IN THE MOUSE. **Bruzzese, E.; Buonerba, M.; Greco, G.; Mascioli, G. (Sanita Militare, Rome). Giorn. Med. Mil., 114: 614-44(1964).**

Possibilities of application of an experimental model utilizable for the quantitative definition of biologic effects caused by parenterally administered radioisotopes were studied. With such a model some quantitative aspects of the effects of ^{32}P given intraperitoneally in mice at progressively increasing doses were studied. Analysis of effects found at the tenth day from ^{32}P administration, demonstrated an effect proportional to the administered dose (from 2 to 20 μc/g of ^{32}P), causing modification of some more radiosensitive organs (thymus, spleen, testicle) and of radioactivity measurements in several organs and tissues. At successive times from the treatment, up to the 180th day, data relative to lethality, body-weight decrease, and successive weight increase correlated with dose. The experimental model employed appeared utilizable for a quantitative analysis of possible effectiveness of substances able to induce variation in the uptake of the isotope or to protect from radiation effects. (Excerpta Med.)

10641 AN ANALYSIS OF THE HEMATOLOGIC MODIFICATIONS PROVOKED IN THE MOUSE BY THE INTRAPERITONEAL ADMINISTRATION OF ^{32}P. **Maffei, G.; Mango, G. (Sanita Militare, Rome). Giorn. Med. Mil., 114: 645-9(1964).**

Modifications of blood and bone marrow patterns were induced in mice given ^{32}P intraperitoneally at doses ranging between 2 μc/g and 20 μc/g. A decrease of erythrocytes and leukocytes was observed at all dose levels; the leukocyte differential count did not show any appreciable modification. In bone marrow, hematopoietic cells were damaged in a dose-dependent manner. Within the limits of research duration, it was possible to obtain, with 2 μc/g dose, some information concerning reparative processes. (Excerpta Med.)

10642 THE EFFECT OF ^{32}P ON THE BACTERIAL FLORA OF THE INTESTINE OF THE NEWBORN MOUSE. **Curatola, G.; Zaio, A. (Sanita Militare, Rome). Giorn. Med. Mil., 114: 650-60(1964).**

In mice treated with ^{32}P intraperitoneally a modification of their intestinal microbial facies was noticed during the period of greatest damage: it consisted of a numerical reduction of viable bacteria, especially of gramnegative species, and change of the natural distribution in the intestinal segments. The degree of bacterial infection (10%) was less than that described for lethal and sublethal doses of x- and pan-irradiations. (Excerpta Med.)

10643 AN ANALYSIS OF THE ECG CHANGES OBSERVED IN THE MOUSE AFTER TREATMENT WITH ^{32}P. **Farina, A. (Sanita Militare, Rome). Giron. Med. Mil., 114: 683-94(1964).**

Literature on myocardial sensitivity to ionization is reviewed. Results of an electrocardiography in mice treated with a high dosage of ^{32}P are presented. Myocardial damage was expressed as alteration of repolarization in the electrocardiograph. (H.G.D.)

10644 SOME OBSERVATIONS ON THE MATING ACTIVITY AND FERTILITY OF DROSOPHILA MELANOGASTER MALES. **Kvelland, Ingerid (Univ. of Oslo). Hereditas, 53: 281-306(1965).**

Four groups of normal and x irradiated Drosophila melanogaster males: 022, 322 a, 322 b, and X 322, were mated to a surplus of virgin females both day and night for a variable number of days. During daytime all matings were observed, the inseminated females were isolated and the offspring counted. Likewise, the females inseminated during the nights were isolated every morning and their offspring counted. Individual males in all groups showed a great variation as to mating capacity, fertility, fecundity and productivity. The youngest males (group 022) showed an increase in mating frequency from the first day of mating up to a male age of seven days; thereafter a gradual decrease. The older males (group 322 a) showed a sharp drop in mating frequency from the first to the second day of mating, an increase to the seventh day, and thereafter a gradual decrease. The irradiated males (group X 322) showed a mating frequency on the first three days of mating similar to that found for the males in group 322 a; on the following seven days, however, the irradiated males showed a noticeably lower mating frequency than did the control males. (C.H.)

10645 MUTATIONS AND CROP IMPROVEMENT. VI. THE GENUS AVENA L. (GRAMINEAE). **Gustafsson, Ake; Gadd, Ivar (International Atomic Energy Agency, Vienna. Royal Coll. of Forestry, Stockholm). Hereditas, 53: 327-73(1965).**

Cultivated species of the genus Avena are either diploid, tetraploid, or hexaploid with their basic number x = 7. Hexaploid sativa oats rank fourth among cereals in world production. Tetraploid and hexaploid species have arisen through processes of amphi- and allopolyploidy. One genome A, occurring in the diploid Avena strigosa and brevis, is common to the polyploid species. Otherwise the genome formulas of the investigated tetraploid and hexaploid species seem to be different: AABB and AACCDD respectively. Results are reported from studies on the induction of mutations in several varieties and hybrids of oats by various treatments, including x radiation. Applications of induced mutations in crop improvement are discussed. (C.H.)

10646 THE INFLUENCE OF SMALL DOSES OF γ RAYS AT VARIOUS DOSE RATES ON THE SEED OF THREE SPECIES OF GRASS. **Starzycki, S.; Pala, J. (Inst. for Plant Breeding and Acclimatization, Radzikow, Poland). Hodowla Roslin, Aklim. Nasienn., 7: 593-604 (1963). (In Polish).**

The seeds of Festuca pratensis, Lolium perenne, and Poa pratensis were exposed to four different doses of ^{60}Co γ rays at two dose rates for each dose. Thus 500 R was given at 0.115 and 2.77 R/min, 1000 R at 0.231 and 5.55 R/min, 1500 R at 0.347 and 8.33 R/min, and 2500 R at 0.578 and 13.88 R/min. The exposures required up to three days to complete. For each of these rates and total doses he average values are tabulated for percentage germination, sprouting activity, length of roots, and length of the first leaf. The moisture content of the irradiated seeds varied from 10 to 12%. In some instances a stimulating effect of irradiation on sprouting was noted, usually only at 500-R doses, but in a few cases after 1000 R. Root length and first leaf length were also increased in some experiments at low doses, but there was considerable variation in response among the seed samples tested. In general, the more viable the seed the greater its growth stimulation by low doses of radiation. The low dose rates provided a greater degree of stimulation than higher dose rates, at comparable total doses. As expected, higher doses irrespective of dose rate impaired germination, sprouting, and root and leaf length. No correlation was noted between a stimulation in sprouting at low doses and length of roots or of first leaves. (BBB)

10647 CYTOGENETIC STUDIES IN CHRONIC MYELOID LEUKEMIA. **Padeh, B.; Bianu, G.; Akstein, E.; Schaki, R. (Government Hospital, Tel-Hashomer, Israel). Israel J. Med. Sci., 1: 791-3(July 1965).**

Several patients with chronic myeloid leukemia (CML) are described in which cytogenetic examinations revealed chromosome anomalies, which are discussed in terms of their possible relation to previous exposure to x rays and chemotherapeutic agents. (TCO)

10648 MODIFICATION OF RADIATION DAMAGE OF BACTERIA BY FOLIC ACID ANTAGONISTS. Pittillo, Robert F.; Lucas, Mary; Blackwell, Robert T.; Woolley, Carolyn (Southern Research Inst., Birmingham, Ala.). J. Bacteriol., 90: 1548-51(Dec. 1965).

The folic acid analogs, 2,4-diamino-6-methylpteridine, amethopterin, and aminopterin, have been found to sensitize certain bacteria, especially Escherichia coli, to the lethal action of ^{60}Co γ radiation. Data are presented which indicate that the compounds must be present during the irradiation period for maximal sensitization to be observed, the sensitizing effect can be nullified by cysteine or cysteamine, the sensitizing effect occurs in a number of diverse bacterial genera, and folic acid neither sensitizes bacteria to irradiation nor prevents the sensitization caused by these antifolic agents. (auth)

10649 THE EXPERIMENTAL DATA ON THE SURVIVAL OF CELLS UNDER SINGLE AND FRACTIONATED IRRADIATION AND THE SIGNIFICANCE OF THIS FOR THE RADIOTHERAPY OF TUMORS. Barendsen, G. W. (Toegepast Natuurwetenschappelijk Onderzoek, Delft, Netherlands). J. Belge Radiol., 48: 407-25(1965). (In Dutch).

Techniques of cell culture and tumor cell transplantation were developed, which yield quantitative data on the fraction of cells in a population retaining the capacity for unlimited proliferation after irradiation. From the shape of the experimental cell survival curves it can be deduced that the action of x rays and γ rays is partly cumulative. High doses are per unit dose more effective in producing damage than low doses. This cumulative effect is diminished with fractionated doses. On the basis of experiments this effect can be interpreted as a repair of sublethal damage at the cellular level that is completed within a few hours after irradiation at a given dose. On the basis of dose-effect curves obtained with cultured kidney cells of human origin, a curve can be derived that presents the relation between the number of fractions used and the total dose required to damage with a probability of 0.9 the reproductive capacity of all cells in a population containing 10^9 cells. The curve obtained shows a very good agreement with the Strandqvist curve obtained from clinical data which relates the number of fractions to the total tumor dose required to obtain a given degree of reaction. It is concluded that a clear relation exists between cellular phenomena that can be studied in detail in vitro and in vivo and fractionation effects in radiotherapy. (tr-auth)

10650 POSSIBILITIES FOR THE RECOVERY AFTER X IRRADIATION IN THE LIVING ORGANISM AND THE SIGNIFICANCE OF THESE RECOVERY PROCESSES IN THE IRRADIATION OF TUMORS. Vos, O. (Toegepast Natuurwetenschappelijk Onderzoek, Delft, Netherlands). J. Belge Radiol., 48: 426-41(1965). (In Dutch).

Different recovery processes can be detected in the living animal after x irradiation. Elkind described an intracellular repair that occurs a few hours after irradiation. In addition to this type of repair, a recovery by repopulation can take place. This repopulation involves the proliferation of cells that have survived earlier irradiations and the migration of cells from the unirradiated parts of the body. Elkind-type repair varies in magnitude in different cell types in the body. Epithelial cells of the intestine show a greater and faster recovery than bone marrow cells. Data reported in the literature, together with some new data on cell recovery, are presented. The importance of these recovery processes with respect to radiotherapy is discussed. It is concluded that there is, at the moment, an insufficent knowledge of recovery processes in vivo to predict the most effective radiation scheme. (tr-auth)

10651 THE INTERACTION BETWEEN TUMOR CELLS AND THEIR MEDIA UNDER THE EFFECT OF RADIATION. Reinhold, H. S. (Toegepast Natuurwetenschappelijk Onderzoek, Delft, Netherlands). J. Belge Radiol., 48: 442-52 (1965). (In Dutch).

The theory of cell survival has improved the understanding of the mechanisms that influence the effect of x rays on tumors. The lack of oxygen in numerous parts of a cell and the restoration of cells during the course of fractionated radiotherapy can explain to a large extent the resistance of tumors to x rays. The fact that many tumors can nevertheless be cured by irradiation is explained probably by additional mechanisms. The most important are the interactions between dead and living cells and the revascularization of the tumor tissue by which the oxygenization is improved. Thus the radiosensitivity of a tumor can be increased by fractionated irradiation. (tr-auth)

10652 THE ROENTGENOGRAPHIC DEVELOPMENT OF RADIOSTRONTIUM (^{90}Sr)-INDUCED OSTEOGENIC SARCOMA IN THE RAT. Poznanski, T. W.; Frankel, S. J. Bone Joint Surg., 47-A: 349-58(1965).

The development of the roentgenographic changes associated with radiostrontium (^{90}Sr)-induced osteogenic sarcomata in the young adult rat is described. Macroscopic and histological features of these neoplasms are also discussed. Intraperitoneal administration of 0.75 microcurie of ^{90}Sr per gram of body weight causes an incidence of osteogenic sarcoma of 65%. The greatest percentage of neoplasms (58.8%) occurred in the spine, followed by 28% in the long bones. The roentgenographic characteristics of ^{90}Sr-induced osteogenic sarcomata in the rat and mouse are compared. (Excerpta Med.)

10653 HISTOLOGICAL CHANGES IN PELVIC LYMPH NODES IN CANCER OF UTERINE CERVIX AFTER RADIOTHERAPY. AN ANALYSIS OF 596 LYMPH NODES. Chakravorty, A. P. (Univ. of Malaya, Kuala Lumpur). J. Obstet. Gynaecol. Brit. Commonwealth, 72: 182-4 (1965).

Pelvic lymph nodes removed from 50 cases of stage II cervical cancer that were previously irradiated were analyzed after histological study. Sinus cell hyperplasia in lymph nodes was noted in 277 nodes (46%). It may have followed a subcancericidal dosage of irradiation to the pelvic lymph draining area. (Excerpta Med.)

10654 RECTITIS AND ILEITIS AFTER TREATMENT OF CERVICAL CANCER WITH RADIUM AND X-RAYS. Bernard, A.; Gaudefroy, M. J. Sci. Med. Lille, 83: 11-18(1965).

Radiotherapeutic damage to the small intestine is rare. Factors favoring the complications are: fixation of the ileum by adhesions; particular individual radiosensitivity; and irradiation of the autonomic nervous ganglia, which is highly noxious. A rectitis patient is described in which two operations for subtotal occlusions had a good functional effect. After a 6 yr interval, the tumor recurred. (TCO)

10655 MODIFICATION OF DISTRIBUTION OF ^{35}S-LABELED MYCOBACTERIAL VACCINE IN MOUSE ORGANS BY X-RAY IRRADIATION. Tsukamura, Michio; Tsukamura, Sumio (Obuso National Sanatorium, Obu, Japan). Jap. J. Tuberc., 12: 41-5(Dec. 1964).

X-irradiation of the whole body of animals or cortisone administration depresses antibody production and the immunization process. To study the interaction between vaccine and host cells in the development of immunity, the influence of x irradiation and prednisolone administration on the distribution of ^{35}S-labeled vaccine in mouse organs was examined. Vaccination with heat-killed bacilli of Mycobacterium smegmatis (Jucho strain) was effective in preventing infection with Mycobacterium tuberculosis (H37Rv) in mice. The effect of vaccination was depressed significantly by x irradiation with a single dose of 4080 R given over the whole body. Distribution of the vaccine in mouse organs was followed using vaccine labeled with ^{35}S. In control animals most of the vaccine or its degradation products were found in the lungs, liver, and spleen as early as the first day after vaccination. The radioactivity derived from the labeled vaccine was maintained in these organs of controls even after seven days, but the specific activity in the organs decreased as swelling of the organs occurred

after seven days. On the other hand, the organs of x irradiated animals, especially the lungs and spleen, took up much less of the vaccine and released some of it after seven days. The organs of prednisolone-treated animals took up the vaccine to the same extent as those of control animals after one day, but released a considerable proportion of its radioactivity after seven days. It is suggested that x irradiation inhibits the incorporation of the vaccine in the cells of these organs and that organs of the irradiated animals can combine only loosely with vaccine degradation products. These results are discussed in terms of the two processes in the production of immune state; the first step is the fixation of vaccine by host cells and the second step is the production of antibody or the change of host cells to immune state. It is proposed that irradiation inhibits the first step. (BBB)

10656 INHIBITION OF PROTEIN SYNTHESIS IN ULTRAVIOLET-IRRADIATED MYCOBACTERIUM SMEGMATIS. **Tsukamura, Michio; Mizuno, Shoji (Obuso National Sanatorium, Obu, Japan). Jap. J. Tuberc., 12: 58-66(Dec. 1964).**

In the Mycobacterium, incorporation of ^{32}P into the DNA and RNA fractions is not inhibited in uv-irradiated cells, but incorporation of ^{35}S into the protein fraction is inhibited markedly. Further studies were conducted on the mode of protein synthesis inhibition in uv-irradiated cells. Thus, incorporation of acetate-1-^{14}C, leucine-1-^{14}C, and sulfate-^{35}S into cellular fractions were compared in uv-irradiated and nonirradiated cells of Mycobacterium smegmatis. Incorporation of acetate-1-^{14}C into glutamic acid was not inhibited in the irradiated cells, but its incorporation into the protein fraction was decreased markedly. Incorporation of acetate-1-^{14}C into lipid and nucleic acid fractions were decreased moderately. Incorporation of sulfate-^{35}S into sulfur-containing amino acids appeared to be maintained at normal levels in the irradiated cells. It is likely, however, that incorporation of the sulfur-containing amino acids into the protein was decreased in the irradiated cells. It is concluded that the uv-irradiated cells retain their ability to form amino acids, but incorporation of the acids into the protein is impaired in the irradiated cells. (BBB)

10657 MULTIVARIATE REGRESSION ANALYSIS OF THE SEX RATIO AMONG OFFSPRING FROM IRRADIATED WOMEN. **Watanabe, Mineo; Ito, Sadato; Horikawa, Masazumi; Hirata, Masashi; Sato, Hideo (Hiroshima Univ.). Med. J. Hiroshima Univ., 13: 79-85(Jan.-Feb. 1965). (In Japanese).**

Multivariate regression analysis was used to examine the relation of the sex ratio of offspring to parental exposure to radiation in infants delivered in the public hospitals of Fukuoka, Aiynan, Shimahane, and Hiroshima County, Japan, between Jan. 1953 and Aug. 1955. Irradiation dose from the atomic bombing irradiation exposure was calculated to the 1945 Hiroshima explosion in rads and the diagnostic x-ray abdominal exposure in mrad was estimated from medical records. Consideration of the radiation exposure period and pregnancy shows that sex ratio is lowest after exposure around the time of conception and increases with the period of irradiation before or after conception. When irradiation dose increases, sex ratio increased in groups parenteral exposed to atomic irradiation and irradiation before pregnancy. Sex ratio decreased after x irradiation before pregnancy, but slightly increases after exposure in the first 8 months of pregnancy. This analysis is based on the assumption that sex ratio changes according to the first order linear equation given, hence the results are limited in their interpretation. (BBB)

10658 POSSIBILITIES AND LIMITATIONS OF TREATMENT OF RADIATION INJURIES OF THE SKIN. **Micali, G. (Univ., Catania, Italy). Minerva Chir., 20: 167-74(1965).**

The macroscopic and microscopic changes that occur in the skin after exposure to radiotherapy are described and classified as reversible or irreversible. The incidence of cancers following these lesions is considered, and their peculiar chronic course is stressed. As regards their treatment, acute reversible forms can be treated by simple topical medications, avoiding the use of caustic or harmful substances. Irreversible forms should be treated surgically by excision of the affected area followed by adequate plastic surgery. (Excerpta Med.)

10659 GASCHROMATOGRAPHICAL ANALYSIS OF THE FATTY ACIDS OF THE LIVER IN NORMAL AND IRRADIATED RATS. **Notario, A.; Di Marco, N.; Doneda, G., Zanetti, A.; Slaviero, G. (Univ., Pavia, Italy). Minerva Nucl., 9: 237-47(July-Aug. 1965). (In Italian).**

Different groups of rats were treated with 500 and 1000 R and the content of the total lipids of the liver with respect to normal controls was studied. Gaschromatographical analysis was also made of methyl esters of the total lipids of the liver in the same normal and irradiated animals. In general it was observed that irradiation with 500 R caused an increase in total lipids. These, however, appeared to be practically unchanged in rats panirradiated with 1000 R. The most interesting alterations were seen in the fatty acids. As gaschromatographical analysis showed, irradiation caused in the liver, a drop in the content of palmitic acid and oleic acid. On the other hand the same treatment caused a slight increase in linoleic, linolenic, nonadecanoic, arachic, eicosanoic, arachidonic, trichosanoic, and saturated lignoceric acids. An attempt was made to interpret the recorded alterations and to judge their importance. (auth)

10660 HEMATOLOGIC CHANGES IN RADIATION DAMAGE. **Braunsteiner, H.; Huber, H. (Univ., Innsbruck). Mitt. Oesterr. Sanitaetsverwalt., 66: 99-103 (1965).**

After acute exposure to radiation the blood shows characteristic changes grossly related to the radiation dose absorbed. The earliest and most sensitive reaction concerns the lymphocytes; the leucocytes and thrombocytes show less distinct relationships to the dose, whereas the erythrocytes show a slight and delayed decrease only. Late damage after irradiation is seen in a small percentage of cases only. There is a relationship between increased incidence of leukemia and radiation dose. For supervision of chronic exposure to radiation, especially in occupational exposure, regular examination of the blood is necessary. As changes are late to occur and are mostly seen after the maximum permissible dose has been exceeded, physical methods (film strips, dosimeters) should also be used. (Excerpta Med.)

10661 STATISTICAL OBSERVATIONS OVER THE PAST FIVE YEARS ON THE HIROSHIMA ATOMIC BOMB IRRADIATED PATIENTS WHO ENTERED HIROSHIMA WITHIN THE THREE DAYS POSTATTACK PERIOD. (FIRST REPORT). **Shizumi, Kiyoshi; Watanaba, Mineo; Ito, Sadato; Yamamoto, Okimu (Hiroshima Univ.). Nagasaki Igakkai Zasshi, 38: Suppl., 36-45(Dec. 1963). (In Japanese).**

From 1957 to 1961 the number of atomic bomb irradiated patients in Hiroshima was 2246 (male 703, female 1543); 73.4% (138 persons) who entered Hiroshima within a 3-day-period (August 6 to 1945) after the attack. Among them were 60 men (78.1%) and 78 women (69.6%). The rate of persons entering the city was highest on August 7, 38.8% (73 persons), then August 6, 20.2% (38 persons), and the lowest on August 8, 14.4% (27 persons). The average age of persons entering Hiroshima was 35.4 years. The activities engaged in by persons entering the city was highest in terms wandering 71.0%, then in giving nursing care 13.8%, cadaver disposal 10.1%, and camping 5.1%. The average duration of the activity engaged in was highest in patient care, 13.4 days; then in body disposal, 7.5 days; lower in wandering around the city, 5.9 days. Except for the camping group, the incidence of liver disease was higher in these immigrants than in those directly exposed to the atomic bombing. Incidence of diseases in this immigrant population was as follows: anemia, 38.5%; liver disease, 29.7%; agranulocytosis, 7.9%; malignant tumors, 7.2%; anemia with hepatic disorders, 6.5%; hemorrhagic diathesis, 3.6%; agranulocytosis with hepatic disorder, 2.9%; and leukemia 2.2%. Malignancy was accounted for half as lung cancer (5 out of 10 cases), 3 cases of thyroid carcinoma, one of hepatoma, one of ovarian cancer. It is

noted that the occurrence of these diseases may be related to the absorption of the radiation by the body. (TCO)

10662 REPORT ON THE SURVEY OF THE HIROSHIMA COUNTY ATOMIC BOMBING SURVIVORS. Nakamura, Telhico (Hiroshima County Health Dept.). Nagasaki Igakkai Zasshi, 38: Suppl., 46-55(Dec. 1963). (In Japanese).

As of Oct. 1, 1961, a survey of the atomic bombing survivors was conducted by the questionnaire method. Hiroshima accounted for 163,624 survivors, among which 70,784 were living in Hiroshima County. There was a sex difference in survivors in Hiroshima County, with a male predominance, while a female predominance was noted in the city. About 29.8% of survivors was at a distance of 1501 to 2000 m from the hypocenter, and 9.3% at a distance of 1001 to 1500 m. The number of persons entering the city was high in the 3-day postattack period then lower in the next 7-day period. The total number of fetuses exposed in utero was 2310, among which the mother had been directly exposed in 1726 cases (74.7%). Among 161,314 survivors, 22,320 were in the age group of 30 to 34 yr (13.9%); in this age group the males slightly predominated over the female. In Hiroshima City there were more exposed persons under the age of 29 than in the county. Survivors were largely in low income groups. About 91.6% of the 30 to 34 yr age group was married; 91.4% of 15–19 age group was single. The widowed rate was higher among survivors than that of the general population in the above-70-yr age group (33.4%), and the divorce rate was higher in the 45–49 yr group. Among survivors there were 1438 in-patients (0.9%) while out-patients accounted for 13.3%. Administration of nutrients was required in 67.6% of the in-patients and 65.9% of the out-patients. (BBB)

10663 REPORT ON THE SURVEY OF NAGASAKI ATOMIC BOMBING CASUALTIES. Kurimoto, Sohei (Nagasaki County Health Dept.). Nagasaki Igakkai Zasshi, 38: Suppl., 56–60(Dec. 1963). (In Japanese).

Detailed statistical data on the citizenry of Nagasaki at the time of the atomic bomb attack are compiled. Of the total atomic bombing casualties of 101,601, 78% lived in Nagasaki City, comprising 230.5 exposed persons per 1000 population. The figure decreased as distance increased from the center of Nagasaki City. (TCO)

10664 A REDUCED OXYGEN ENHANCEMENT RATIO FOR X-RAY SURVIVAL OF HeLa CELLS IN VITRO, AFTER TREATMENT WITH "METHOTREXATE." Berry, Roger J. (Churchill Hospital, Oxford). Nature, 208: 1108-10(Dec. 11, 1965).

The reproductive survival of HeLa cells was determined by clonal growth after single and fractionated x radiation exposure under oxygenated or anoxic conditions. Methotrexate (4-amino-10-methylpteroylglutamic acid) added to the growth medium at the time of plating, removed 24-hr later by aspiration, and replaced with identical medium without the drug, sensitized the cells to x radiation even at concentrations of the drug that did not produce any cell killing. At a drug concentration of 0.3 μg/ml/24h, the x ray dose-response curve for methotrexate survivors showed a significantly reduced oxygen enhancement ratio. Possible applications of methotrexate in the radiotherapy of anoxic tumor cells are discussed. (C.H.)

10665 THE EFFECT OF X-IRRADIATION ON THE TAKE AND GROWTH OF THE GUERIN-TUMOR. II. HISTOLOGICAL EXPERIMENTS. Unger, E. (Frederic Joliot-Curie National Research Inst. for Radiobiology and Radiohygiene, Budapest). Neoplasma, 12: 509-16(1965).

The histological processes are described that were observed in connection with the take and growth of florid and necrotic parts from the Guerin-tumor in rats after transplantation of an x irradiated tumor, and after local x irradiation of the recipient of an unexposed tumor. The slackening in the growth of the tumor, experienced in many animals, is attributed to the change accomplished in the biological properties of the tumor-cells injured by irradiation. (auth)

10666 URINARY RADIOPHOSPHORUS ^{32}P LEVELS IN RATS AFTER A SINGLE 2,4-DINITROPHENOL ADMINISTRATION PRIOR TO X-IRRADIATION WITH THE DOSE OF 600 r. Kolousek, J.; Dienstbier, Z. (Charles Univ., Prague). Neoplasma, 12: 525-30(1965).

Urinary ^{32}P levels from injected $Na_2H^{32}PO_4$ were followed in rats after intraperitoneal 2,4-dinitrophenol administration (2.5 mg per 100 g of body weight) and after 2,4-dinitrophenol administration two hours before the rats were irradiated with a dose of 600 R/60 min of x rays. The values observed were compared with those found in animals that had received irradiation alone (600 R) and in control animals. Dinitrophenol administered 2 hours before irradiation caused a pronounced decrease in ^{32}P activity in the urine of rats. (auth)

10667 LATE EYE ALTERATIONS AFTER IRRADIATION. Nemeth, Gy. Orv. Hetilap, 106: 441-3(1965).

Ophthalmological alterations, which may develop after irradiation, are reported based on two cases with propagation of the tumor towards the bulbar cavity. Due to vital indication complete protection of the eye could not be achieved, and following irradiation therapy severe damage of the eye developed. (auth)

10668 FRACTURE OF PELVIS AFTER CURATIVE IRRADIATION. Landrgot, B.; Pribyl, T.; Sauer, J. (Karlova Univ., Plzen, Czechoslovakia). Plzensky Lekarsk Sb., 23: 125-8(1964).

A pelvic fracture is reported that occurred in a 76-year-old woman who was treated surgically and radiotherapeutically for a uterine adenocarcinoma. Complications first appeared one year postirradiation and were primarily attributed to osteoporosis. (H.G.D.)

10669 SUSCEPTIBILITY OF RADIATION CHIMERAS TO EXPERIMENTAL PSEUDOMONAS AERUGINOSA INFECTION. Watson, James R.; Hammond, Carolyn W. (Univ. of Illinois, Chicago). Proc. Soc. Exp. Biol. Med., 120: 585-7(Dec. 1965).

Lethally x-irradiated $B6D2F_1$ mice treated with syngeneic bone marrow cells were found to be no more susceptible to Pseudomonas aeruginosa challenge 43 days post-irradiation than unirradiated control animals. Allogeneic CF-1 chimeras proved to be substantially more susceptible to experimental Pseudomonas aeruginosa infection 43 to 46 days post-irradiation but at 175 to 177 days post-irradiation only a slight increase in susceptibility over control animals of the same age was observed. (auth)

10670 A STUDY OF THE INDIRECT EFFECTS OF X-RAY THERAPY. Cimellaro, M. (Univ., Rome). Quad. Clin. Obstet. Ginecol., 19: 571-80(1964).

On the basis of a study of the clinical course and of the variations of the leukocyte count in a group of patients subjected to supplementary x-ray therapy for cervical carcinoma the question of the indirect effects of x-ray therapy is reviewed. After a concise review of the extensive literature on the subject with special reference to the more recent findings, it is concluded that the indirect and systemic action of the x-rays, which manifests itself clearly only in a small number of cases, is in all probability to be attributed to deficiencies of protein synthesis, resulting from alterations of the pre-mitotic phase or of the processes of DNA synthesis. (Excerpta Med.)

10671 URETHAN-INDUCED LUNG TUMORS IN MICE: X-RADIATION DOSE-DEPENDENT INHIBITION. Foley, William A.; Cole, Leonard J. (Univ. of Minnesota, Minneapolis. Naval Radiological Defense Lab., San Francisco). Radiat. Res., 27: 87-91(Jan. 1966).

Adult male LAF_1 mice received single whole-body x-ray exposures of 100, 300, 500, or 700 rads, followed 1 day later by a single injection of urethan (1 mg/gm). The mice were sacrified 25 weeks later, and the lungs examined grossly and microscopically for tumors. All the mice in the group receiving 100 rads plus urethan exhibited lung tumors (alveolegenic carcinomas), with a mean of 3.1 tumors per mouse. This lung tumor incidence was identical with that occurring in the mice receiving urethan only. However, a definite reduction in lung tumor incidence and number of tumors per mouse was observed at the 500-rad dose (66% incidence and 1.8 tumors per mouse) and at 700 rads (59% incidence and 1.3 tumors per mouse). Thus,

the x-radiation suppression of urethan-induced lung tumors in mice is dose-dependent in the range of 500 to 900 rads. The data suggest that this tumor suppression is correlated with a direct radiation inhibition of alveolar cell proliferation. (auth)

10672 THE INFLUENCE OF PULSED MAGNETIC FIELDS ON THE CYTOGENETIC EFFECTS OF IRRADIATION. Pozolotin, A. A. (Inst. of Biology, Sverdlovsk, USSR). Radiobiologiya, 5: 809-11(1965). (In Russian).

The use of magnetic fields after irradiation increased the percent of anaphase chromosome aberrations. This increase is caused by the increase of the number of cells with fragments, and the mean number of chromosome aberrations in one cell does not vary under the effects of a magnetic field. The application of strong magnetic fields after irradiation delays the process of cellular reduction of primarily radiation damaged chromosomes. (J.S.R.)

10673 INHIBITING EFFECTS OF X RADIATION ON THE GROWTH OF NEW-BORN MICE. Nechaev, I. A. (Inst. of Genetics, Moscow). Radiobiologiya, 5: 833-5 (1965). (In Russian).

In newborn mice irradiation at doses of 300 R produced an inhibition of the growth. This effect was still greater after irradiation at doses of 400 R. The growth inhibition in mice in the radiosensitive line BALB/c was greater than in the radioresistant line $C_{57}Br$, which is connected not only with the greater damaging effects of the radiation on the radiosensitive animals but also with the difference in the tempo of restoration in the comparison line. (tr-auth)

10674 CERTAIN PECULIARITIES OF GASTRO-INTESTINAL DISTURBANCES BY CHRONIC RADIATION SICKNESS, INDUCED BY INJECTION OF VARIOUS RADIO-ISOTOPES. Lebedeva, G. A. Radiobiologiya, 5: 842-6 (1965). (In Russian).

The results of the investigation of the morphological changes of the gastrointestinal tract during chronic radiation sickness induced by the introduction of radioactive isotopes with different physical and chemical properties are reported. In the studies the isotopes investigated were ^{210}Po, an α emitter distributed evenly in the organism, ^{90}Sr a β emitter belonging to the group of oseotropic isotopes, and ^{144}Ce a β and γ emitter retained principally in the skeleton and liver. The results made apparent some peculiarities of the disturbance to the stomach and intestine under these irradiation conditions. It established their dependence on the degree of free sorption of the radioactivity, the character of its distribution, and the type of irradiation. (J.S.R.)

10675 A PARTICULAR FORM OF EYE DAMAGE IN DOGS EXPOSED TO IONIZING RADIATION IN ANTENATAL PERIOD OF DEVELOPMENT. Piontkovskii, I. A.; Airapetyants, M. G. (Inst. of Higher Nervous System and Neurophysiology, Moscow). Radiobiologiya, 5: 847-9 (1965). (In Russian).

Dog embryos aged 13, 20, 45, or 55 days were exposed to single x irradiations at a dose of 200 R. Of all the animals irradiated prenatally, eye damage was observed only in the animals irradiated on the 20th day. Cloudiness of the cornea was observed, sometimes in one eye and sometimes in both eyes. Differential diagnoses were made with respect to time to determine the form of the eye pathology. These results are discussed. (J.S.R.)

10676 REACTIONS OF TADPOLE TISSUES TO X RADIATION DURING STARVATION CONDITIONS. Gronskaya, N. F. (Central Scientific-Research Inst. of Roentgen-Radiological Inst., Leningrad). Radiobiologiya, 5: 850-4(1965). (In Russian).

Two- to three-week old tadpoles, kept in water at temperatures from 18 to 20°, were exposed to irradiation doses of 300 and 600 R. These doses did not cause the death of the animals within the 30 days of observation. The tadpoles were subjected to 6 days of starvation followed by resumption of nourishment. The epithelium of the cornea and the skin of the tail region were investigated histologically. The results are shown graphically. In both the control animals and the animals in starvation conditions the mitotic activity reached a minimum within 2 to 4 hrs after the radiation. Within 6 hrs a regeneration of the radiation damage had begun. In the animals irradiated on the sixth day of starvation a significant decrease of the mitotic activity caused by the starvation coincided with the moment of irradiation and with the beginning of the development of radiation injury. Starvation led to different reductions of the mitotic coefficients as a function of their regeneration activity. This reduction was greatest in the epithelium of the cornea. (J.S.R.)

10677 THE INFLUENCE OF RADIOINDUCED CHROMOSOME ABERRATIONS ON THE VITALITY OF TUMOR CELLS. Shapiro, I. M.; Faleeva, Z. N. (Severtsov Inst. of Morphology of Animals, Moscow). Radiobiologiya, 5: 873-7(1965). (In Russian).

According to the percentage of cells having chromosomal aberrations, single and fractionated irradiations of cells of Ehrlich ascites tumor in the stationary phase have the same effect. The absence of difference apparently is stipulated by the continued depression of mitosis produced by the first fraction of the dose and the preservation of damages in the non-dividing cells. The speed of development of the ascite tumor, judged from the number of tumor cells from the abdominal cavity of the mouse, after single and fractionated irradiation, agrees well in cases when a similar number of cells without chromosome aberrations is contained with the cells introduced. The test results confirmed the hypothesis of the lethal effects on tumor cells of a disturbance of the chromosome balance, caused from the division of cells with chromosome aberrations. (tr-auth)

10678 THE INFLUENCE OF IONIZING RADIATION ON THE CONTRACTIVE ABILITY OF MITOCHONDRIA. Rudakov, V. V.; Kukurudzyak, Yu. A.; Ivanov, I. I. (Kirov Military-Medical Academy, Leningrad). Radiobiologiya, 5: 878-81(1965). (In Russian).

The contractive ability of mitochondria, separated one hour after irradiation, is preserved from the effects of ionizing radiations even at very high doses. The mitochondria extract forms complexes with rabbit myosin capable of reacting with ATF and does not differ in this capacity from complexes formed with extracts of liver mitochondria with healthy animals which indicates the stability of the contraction of mitochondria albumin to the immediate effects of ionizing radiation at high doses. The contractive capacity of mitochondria isolated 48 hrs after x irradiation at doses of 2 and 6 kR has a tendency to depression, especially for mitochondria occurring in hypotonic medium. (tr-auth)

10679 EFFECTS OF THERAPEUTIC DOSES OF RADIO-IODINE ON THE COAGULATIVE PROCESSES. Marinosci, A.; Isidori, A.; Semprebene, L.; Cardone, U. (Univ., Rome). Rass. Fisiopatol. Clin. Terap, 36: 411-24(1964).

The effects of therapeutic doses of radioiodine on blood coagulation was investigated. Platelet count was not appreciably influenced although radioinduced hemorrahagic disorders are attributable mainly to injuries of platelet-producing tissue. Other than an effect on platelet adhesiveness, platelet functions essential in normal clotting process were not affected. Fibrinogen level was slightly increased, primarily because of the radioinduced stimulation of reticuloendothelial tissues. The increase, however, was not sufficient enough to have clinical importance. It was concluded that therapeutic doses of radioiodine affect the coagulative process very slightly and that hemorrhagic complications cannot be anticipated from its use. (H.G.D.)

10680 AN ANATOMOCLINICAL STUDY OF LATE LESIONS DUE TO THOROTRAST. Malaguti, R.; Cavagna, R. (Univ., Ferrara, Italy). Riv. Patol. Clin. Sperim., 5: 281-98(1964).

Thorotrast-induced injuries are reported in a 52-year-old man who was given a carotidograph with thorotrast for recurrent epilepsy a few months previously. Severe celiac attacks were ascribed to a lumboaortic adenopathy due to a large thorotrast deposit with connectival sclerosis and

fibrous periadenitis involving the celiac plexus. Large thorotrast deposits and non-cirrhogenous sclerosis were noted in the liver and spleen. Late effects of thorotrast are reviewed. (H.G.D.)

10681 THE MORPHOLOGIC ASPECTS OF INADEQUATE NEUTROPHILIC GRANULOPOIESIS IN BONE MARROW REGENERATION AFTER SUBLETHAL WHOLE-BODY IRRADIATION OF RATS. Stodtmeister, R. (Staedtisches Krankenhaus, Pforzheim, Ger.); Burrichter, M.; Fliedner, T. M. Schweiz. Med. Wochschr., 95: 1490-2 (Oct. 30, 1965). (In German).

Hematopoiesis was examined cytologically and histologically in rats after whole-body irradiation with a 600-R dose of 15-Mev electrons. Bone marrow and blood smears of rats were studied during the regenerative phase, 5 to 23 days after a single sublethal dose. Granulocytes and their precursors were found which were distinctly different in morphology from normal cells of comparable maturity, the major difference being in nuclear structure and form. In some of the atypical neutrophils the process of segmentation appeared to be disturbed. The nuclei and nuclear segments appeared swollen, and the formation of segments seemed to be inhibited in consequence. The chromatin of nuclei varied from a homogeneous to an irregular, coarse structure. Such anomalies were found not only in mature, segmented granulocytes, but could be traced through the immature precursors to cells thought to represent myelocytic stem cells. Cells were found showing all the signs of degeneration and degradation of the nucleus. In comparison with the frequency of these atypical cells in the marrow, only a few were found in blood smears. It is suggested that such atypical cells represent ineffective myelopoiesis in the recovery phase of the bone marrow. This may be caused by stem cells which have been injured by radiation in a manner whereby cell death occurs only after a number of divisions, thus suggesting a latent injury. (BBB)

10682 THE EFFECT OF STIMULATION OF THE VESTIBULAR ANALYZER ON BLOOD COAGULABILITY IN INTACT AND IRRADIATED DOGS. Abdurakhmanova, R. R. (Pavlov Medical Inst., Samarkand, USSR). Sezd Vsesoyuznog Fizioloyicheskogo Obshchestva Imeni I. P. Pavlova (Erevan), 11: No. 1, 4(1964). (In Russian).

In experiments on 12 dogs stimulation of the vestibular analyzer was shown to reduce the coagulation time in intact animals by 36.3%. Other tests, which included prothrombin time, recalcification time, and plasma tolerance to heparin, also indicated increased activity of the coagulation mechanism. General irradiation (300 R) extended the coagulation time which did not return to normal even after 90 days. Stimulation of the vestibular analyzer at any time after total body irradiation shortened the whole blood coagulation time and enhanced the activity of individual coagulation factors. (Excerpta Med.)

10683 THE EFFECT OF ^{90}Sr ON CERTAIN PHYSIOLOGIC INDICES IN ZEA MAYS L. Trifu, M.; Fabian, A.; Znamirovschi, V. Stud. Univ. Babes-Bolyai, Ser. Biol., 2: 59-63(1964).

Effects of ^{90}Sr β emission on radicle and coleoptile growth and on cellular and cytoplasmic pH in Zea mays seedlings are reported. Radiation exposures ranged from $2\frac{1}{2}$ to 96 hrs and source distances were from 1 to 3 cm. For 24 hr irradiation at a distance of 1.5 cm, stimulation of tissue growth was maximal, and shift of cytoplasmic pH toward the less acids zone was inhibited. Results suggest that nucleic acid synthesis is enhanced by this dose. (H.G.D.)

10684 REGULATION OF GROWTH AND ORIENTATION IN HAMSTER CELLS TRANSFORMED BY POLYOMA VIRUS. Stoker, Michael (Univ. of Glasgow). Virology, 24: 165-74(Oct. 1964).

A study was made of the effect of contact between polyoma-transformed hamster cells and various other cells. The polyoma-transformed cells (Py cells) were derived from clone 13 of the BHK21 line of hamster fibroblasts a after transformation by polyoma virus. For x irradiation, cells were exposed to 1700 R to give a survival of less than 10^{-5}. When the Py colony lies over an irradiated giant cell used in a feeder layer there may be a hole in the colony with Py cells reaching the edge of the giant cell but none lying on top. The same effect may be seen with irradiated giant cells from fresh hamster or mouse embryo cultures, untransformed BHK21 cells, or even Py cells. This suggested that Py cells were in some way sensitive to contact with nondividing cells and would not migrate over them. Irradiated Py cells, BHK21 cells, mouse embryo cells, and freshly cultured hamster embryo cells all inhibited Py colonies, and unirradiated mouse and hamster embryo cells were equally effective. X irradiation of the normal cells does not prevent this effect, and even transformed cells after irradiation will prevent the multiplication of unirradiated transformed cells. The orientation of transformed cells falling on a monolayer of normal cells could be due to the nonspecific phenomenon of contact guidance, but the distortion of a transformed colony meeting an advancing sheet of oriented cells, and the failure initially to overgrow these cells, suggests that some more active inhibition of movement, and avoidance of contact is taking place. These findings are explained by postulating that, in inhibiting each other, normal cells display two functions: an inhibition of other cells by contact, and response to these inhibiting factors, or signals, from other cells. Polyoma-transformed cells seem to be sensitive to normal contact signals, but they do not inhibit each other. It is therefore suggested that they have lost the ability to emit the contact signal without losing their ability to respond. (TCO)

10685 THE INFLUENCE OF IONIZING RADIATION ON THE CELLULAR RESPONSE IN THE LYMPH NODES OF RATS AFTER IMMUNIZATION. Yang, Kuei-chen; Chang, Shao-lun; Li, Hsing-chun; Wu, Keh-li, Peng, Ta-tsai; Wang, Chen-hai (Kirin Medical Inst., Changchun, China). Wei Sheng Wu Hsueh Pao, 11: 23-30(1965). (In Chinese).

Rats were immunized with two doses of diphtheria toxoid. One group of animals was exposed to irradiation of 400 R 24 hrs before the primary immunization. Another group received an additional 600 R 24 hrs before the secondary immunization. In both groups, the production of hemagglutinin suffered marked depression. In twice irradiated rats, the depression was complete, and the disturbance observed in the lymph node tissue was extensive. The weight of the lymph nodes and the number of cells in cell suspension decreased by roughly 10 and 100 times respectively. It was demonstrated in lymph node smears that the decrease in number was by far the most remarkable with the lymphocytes. Compared with rats immunized without irradiation, the irradiated animals showed a much greater diminution of the numbers of reticulocytes, transitional plasma cells, and plasma cells after immunization. In rats immunized after only a single dose of radiation, the hemagglutinin titre on the 7th day became 30 to 40 times as high as that on the 4th day. The weight of the popliteal lymph node was somewhat greater on the 7th day than on the 4th day, and such was also the case with cells of the plasmacyte series. On the other hand, in the group of animals irradiated two times, the majority died off on the 7th day; but, observation of the occasional survivors suggested that the lesion in the lymph nodes was still active. (Excerpta Med.)

10686 EFFECT OF CORTISONE AND X-RAY IRRADIATION ON MAST CELLS OF THE ADRENALECTOMIZED ALBINO RATS. Oh, Yung Keun; Pak, Soo Yun; Kwon Tai Su; Choi, Kum Duck (Yonsei Univ., Seoul, Korea). Yonsei Med. J., 5: 6-12(1964).

The effects of cortisone administration and whole-body x irradiation upon mesenteric mast cells of intact and adrenalectomized albino rats were studied. In intact rats, the administration of cortisone (50 mg/kg) and whole-body irradiation (800 R) caused severe degranulation and disruption of mesenteric mast cells within 24 hours. However their degranulation and disrupting effects upon mesenteric mast cells were markedly inhibited after the removal of the adrenal gland, although the adrenalectomy alone hardly caused these morphological changes of mesenteric mast

cells of the albino rats. According to this experiment it is fairly clear that the effects of cortisone and whole-body x irradiation inducing degranulation and disruption of mesenteric mast cells of the albino rats, were not direct phenomena but they indirectly affected the mesenteric mast cells through some special mechanism mediated by the adrenal gland. (auth)

10687 SEQUELAE OF RADIUM-IRRADIATED HEMANGIOMA. **Scheicher-Gottron, E. (Univ.-Hautklinik, Frankfurt am M.). Z. Haut-Geschlechtskrankh., 19: XLI-II(Oct. 1, 1965). (In German).**

Histologic studies were made of sections taken from the right ear of a 40-yr-old woman who in the first year of life had received radium treatments for a hemangioma. The histologic picture was one of long-standing radiodermatitis and developing basal cell carcinoma, both evidently resulting from Ra treatment of a hemangioma. (TCO)

10688 MAMMALIAN RADIATION GENETICS. **Grahn, Douglas (Argonne National Lab., Ill.). pp 127-55 of Methodology in Mammals. Burdett, W. J. (ed.). San Francisco, Holden-Day, 1963.**

Genetic effects of ionizing radiation are reviewed and radiation sources, temporal factors, and technics of exposure are discussed. Two principal methods of approaching radiation protection, preventive therapy and supportive therapy, are considered. The latter is typified by the successful use of postirradiation injections of bone marrow. Various chemicals, along with modifications of oxygen tension, have been tested for preventive therapy. No attempts have been made to study protection against specific mutational damage. The question of the genetic composition of animals chosen for experimentation is also considered. Whether inbred animals tend to express heterosis for induced mutation more readily than crossbred animals, or whether this expression will occur to any significant degree at all, is discussed. (BBB)

10689 IONIZING RADIATION: NEURAL FUNCTION AND BEHAVIOR. Kimeldorf, Donald J.; Hunt, Edward L. 343p. Academic Press, New York, 1965, $10.00.

Information is given on: ionizing radiations and radiobiological concepts; neural integration; ionizing radiation and neural development; neurophysiological effects of ionizing radiation; neuroregulatory effects of ionizing radiation; radiation effects on sensory capacities; radiation effects on performance capacity; radiation effects on psychological processes; and behavioral activation by exposure to radiation. (P.C.H.)

10690 METABOLISM OF BACTERIA SURVIVING LOW DOSE GAMMA IRRADIATION OF GULF OYSTERS [Thesis]. **Farag, Mohamed Kadri Ahmed. Baton Rouge, La., Louisiana State Univ., 1965. 138p.**

An attempt to isolate and identify bacteria from fresh Gulf oysters, which are resistant to radiation-pasteurization doses, and to ascertain if physiological changes are induced in the bacteria by the gamma radiation treatment is reported. Seventeen non-irradiated strains of bacteria (controls) were isolated. All of them were resistant to 0.1 Mrad irradiation but only four were resistant to 0.8 Mrad. These strains were identified and classed into genera and species. Irradiation of the cultures affected the optimum incubation temperature of three organisms, Pseudomonas erythra, Achromobacter butyri, and Bacillus laterospores. Other changes induced by radiation were culture chromogenesis in the agar stroke technique for Neisseria flavescene, Neisseria sicca, and Bacillus laterospores and indole production for Bacillus laterospores. Changes were also observed in the action of litmus milk by Bacillus laterospores. Irradiation did not alter the organisms' metabolism of nitrate, hydrolysis of gelatin, hydrolysis of urea, motility, production of hydrogen sulfide, reaction to MR-VP tests, and their growth characteristics in nutrient broth. All the organisms were tested for the utilization of eight different sugars. No variation was observed between non-irradiated and radiation-resistant organisms within each strain in utilizing these sugars, except in the genus Flavobacterium and Neisseria sicca. Low level gamma irradiation did not affect glycogen, sugar, total nitrogen, proteolytic activity, and trimethylamine nitrogen in oysters. The activity of two radiation-resistant and strongly proteolytic strains of Pseudomonas and Achromobacter were compared to the activity of other strains of resistant bacteria on fresh oysters during ice (32°F) and refrigerated storage (40°F) for 15 days. It was concluded that oyster tissue autolysis was not affected by gamma irradiation. Neither the nonirradiated nor the irradiated oysters displayed significant increases in proteolytic activity when they were ice stored for 15 days, but storage at 40°F for the same period resulted in significant increases in activity. Studies conducted on the level of gamma irradiation that reduces proteolytic activity of radiation-resistant bacteria showed that 0.2 Mrad was the level that could be used in this respect. It was concluded that the radiation-resistant bacteria are lower in their metabolic activity than their nonirradiated counterparts and that gamma irradiation is a useful tool for oyster pasteurization at levels of 0.2 Mrad. (Dissertation Abstr.)

10691 THE EFFECT OF X-IRRADIATION ON ENDOGENOUS RESPIRATION AND HISTONE SYNTHESIS IN EHRLICH ASCITES TUMOR CELLS [Thesis]. **Moorehead, Wells Rufus. Knoxville, Tenn., Univ. of Tennessee, 1965. 181p.**

Washed Ehrlich ascites tumor cells, harvested from Swiss mice 24 hr after 1250 R of whole-body irradiation, exhibited a significant increase in endogenous respiration as compared to an equal number of control cells when incubated in 0.5 molar phosphate buffer-saline. An electron-microscope study indicated that nuclei of irradiated cells exhibited a more heterogeneous electron density than nuclei of control cells. Histochemical studies indicated that 1250 R of x irradiation did not alter succinic dehydrogenase activity, lipid content, or the sulfhydryl content, although mitosis was completely suppressed for more than 24 hr. Mitochondria isolated from ascites cells 24 hr after irradiation exhibited normal oxidative phosphorylation. When cells were incubated in a series of 0.5 osmolar buffers of varying composition, it was found that high levels of phosphate greatly inhibited oxygen consumption by ascites cells when Mg^{2+} was absent. In hypertonic buffers containing high levels of phosphate and low levels of Mg^{2+}, it was noted that control cells underwent morphological change sooner than irradiated cells. Studies of histone synthesis in ascites tumor cells indicated that both irradiated and control cells incorporated labeled glycine into histone at a similar rate. (A.G.W.)

10692 LONG TERM EFFECTS OF ACUTE LOW-LEVEL X-RAYS ON THE POPULATION DYNAMICS OF THE YELLOW FEVER MOSQUITO, AEDES AEGYPTI [Thesis]. **Willard, William Kenneth. Knoxville, Tenn. Univ. of Tennessee, 1965. 50p.**

Four life history stages (eggs, larvae, pupae, and adults) of the yellow fever mosquito, Aëdes aegypti (Rockefeller strain), were subjected to acute low-level x rays. The stages were divided into seven groups; each group received a single dose of x rays, the dosage ranging from 0 to 3,200R. Radiation effects of acute low-level x rays on populations of Aëdes aegypti were most evident in the first generation and gradually disappeared in subsequent generations. The eggs were most radiosensitive, followed in rank by larvae, pupae, and adults. Egg viability was the characteristic most drastically affected, in that the viability of eggs produced by adults that arose from irradiated eggs, larvae, pupae, or young adults was reduced, in some cases, through three generations. A dose of 3,200R of x radiation delivered to Aëdes aegypti populations in each developmental stage resulted in the extinction of the populations in the first generation. Only a few eggs or larvae irradiated with an acute dose of 1,600R survived to the adult stage. Pupal populations irradiated with 1,600R of x rays had a lowered fecundity in the first generation followed by second generation recovery. The fecundity of adults irradiated with 1,600R was significantly lower than the controls in the first and second generations; however,

recovery occurred by the third generation. A dose of 800R to all stages resulted in a significantly reduced fecundity in the first generation; recovery occurred in all groups by the second generation. Doses of 50R to 400R resulted in variable effects (statistically significant only in isolated cases) such as increased or decreased fecundity, larval growth, and adult longevity. Recovery occurred in most cases by the second generation. (Dissertation Abstr.)

10693 REVERSION OF THE WHITE-IVORY MUTANT IN DROSOPHILA MELANOGASTER [Thesis]. Bowman, James Talton Jr., Davis, Calif., Univ. of California, 1965. 80p.

The sex-linked recessive mutant white-ivory (w^i) has been found to revert to an allele that is inseparable by several criteria from wild type. The frequency of spontaneous reversions is about 5×10^{-5} loci in homozygous females and about 0.2×10^{-5} loci in males and in females that are heteroxygous for deletions that include the white region. In females that are heterozygous for w^i and one of a variety of other white mutants, w^i reverts with a frequency comparable to that of homozygous females. Following treatment of females with 4,000R x rays, w^i reverts equally frequently in homozygotes and deletion heterozygotes although such treatment only rarely induces reversion in w^i in males. Induced reversion are commonly recovered as clusters, indicating that they are of gonial origin. The phenomenon is not correlated with recombination of outside markers, nor is its frequency increased by heterozygosity for autosomal inversion complexes. In an attempt to determine the mechanism of reversion, the mutants carried on the sister strands of four reversions of w^i were isolated and analyzed. One was found to revert at a frequency much lower than the other three, which reverted at the same frequency as the original w^i. These results are compatible with the hypothesis that w^i is associated with a tandem duplication of a portion of the white region and that reversion occurs by sister strand crossing over within a double loop formed by intrachromosomal pairing of the duplicated segments. The hypothesis leads to certain predictions concerning the behavior of small tandem duplications and to an explanation of the reversion of w^i with high frequency. (Dissertation Abstr.)

10694 THE EFFECT OF IONIZING RADIATION ON PASTEURELLA TULARENSIS [Thesis]. Tulis, Jerry John. Washington, D. C., Catholic Univ. of America, 1965. 90p.

Postirradiation survival and properties of the bacterial species Pasteurella tularensis were investigated as a function of various parameters. P. tularensis cells were suspended in a buffered gelatin-saline solution at pH 7.1 prior to ^{60}Co gamma irradiation. Inability of the bacterial cell to form macrocolonies was used as the criterion of radiation damage. Exponential survival data, characteristic of homogeneous radiosensitivity and the single-hit concept, were obtained. Cells surviving were normal morphologically and gave rise to typical colonies. Studies on the effect of cell concentration indicated that as cell population was increased radiation sensitivity was decreased. Cells that incorporated deuterium into their macromolecular structure and/or contained deuterated water of hydration were more radioresistant than cells where only free or readily exchangeable water was in the form of D_2O. Radioprotection of P. tularensis SCHU DT (deuterium-tolerant) cells was noted with cysteine, cysteamine, and glycerol. Radiobiological phonomena observed were indicative of the integrated effect of direct and indirect mechanisms of radiation damage. (A.G.W.)

10695 INDUCED MUTATION AND AMINO ACID PROTECTION AGAINST ULTRAVIOLET RADIATION IN HANSENULA WINGEI [Thesis]. Hunt, Dale E. Kingston, R. I., Univ. of Rhode Island, 1965. 70p.

In a study of induced antibiotic production in the yeast Hansenula wingei, suspensions of yeast cells were irradiated with ultraviolet light. The irradiated cells were transferred to agar plates to allow survivors to develop. The surviving yeast colonies were then covered with agar containing Staphylococcus aureus. If any of the mutant yeast colonies arising on the recovery plates produced antibacterial products, the bacteria seeded agar above such a yeast colony would reveal a zone of inhibition. In an effort to secure more survivors (and possibly more mutants) from irradiated cells, it appeared desirable to find some means of protecting the yeast cells against lethal uv damage. Yeast cells were grown in beef extract glucose broth enriched with certain amino acids. Suspensions prepared from these cultures, together with control cells grown in the basal broth, were irradiated and transferred to agar recovery plates. Protection afforded against uv inactivation was determined by the number of colonies on the recovery plates arising from the irradiated cells cultured in the amino acid enriched medium compared with the colonies arising from the irradiated control cells. An antibacterial mutant yeast was isolated, which produces a thermolabile or volatile inhibitory substance(s) that appears to be bacteriostatic for staphylococcus and pseudomonas, but bactericidal for Sal. typhosa. Preliminary cultivation of H. wingei in the presence of small concentrations of either tryptophan, cystine, tyrosine, phenylalanine, leucine, cysteine, threonine, isoleucine, ethionine, norvaline, or histidine protected against inactivating ultraviolet radiation. Methionine or proline conferred little protection, and valine or serine increased sensitivity to uv inactivation. The protection afforded by the amino acids tested is proportional to their concentration. (Dissertation Abstr.)

10696 MORPHOGENESIS IN EUPLOTES. [PARTS I AND II] [Thesis]. Wise, Benjamin Nathan. New Haven, Yale Univ., 1965. 147p.

The normal cycle of asexual reproduction in Euplotes eurystomus was subjected to a detailed morphological study. The cycle was divided into 7 stages characterized by cortical and nuclear events. Several features of the cycle were examined for their significance in relation to current hypotheses concerning the problem of ciliate morphogenesis. Developmental mechanisms in Euplotes plumipes were analyzed in terms of the response to damage produced by a uv microbeam. Individual animals, representing all stages of the morphogenetic cycle, were irradiated at a variety of cortical sites, including bases of mature cirri and membranelles, primordial structures, and non-ciliated regions; they were then fixed at intervals for silver-stain staining. No regenerative response ensues following such damage in these animals. Damage to cirri persists until these organelles are replaced during normal pre-division morphogenesis; damage to adoral membranelles, which are not normally replaced at division, persists indefinitely through succeeding generations of proters. It is concluded that destruction of infraciliary structures does not, in itself, provide a sufficient stimulus to regeneration in Euplotes. Irradiation of either mature or primordial cortical organelles can be effective, however, in causing the temporary arrest of normal predivision morphogenesis, including resorption of all primordial structures and the arrest or disappearance of macronuclear replication bands. The probability that resorption will occur depends, in part, on the development stage of the structures irradiated; irradiation of primordial structures during early stages induces this response more frequently than does irradiation of late stage primordia or mature organelles. These results are discussed in terms of the functional relationship between infraciliary structures and the mechanisms controlling development. (Dissertation Abstr.)

10697 PATHOLOGIC AND PATHOPHYSIOLOGIC MECHANISMS IN THE ACUTE INTESTINAL RADIATION SYNDROME AND THEIR MODIFICATION BY ADRENAL FACTORS [Thesis]. Eddy, Hubert A. Rochester, N. Y., Univ. of Rochester, 1964. 383p.

Comparative pathologic and pathophysiologic studies were made following single exposure to 1460 R of 250-kv x ray delivered to the whole body or the exteriorized intestine of saline-drinking rats that had been sham adre-

nalectomized or adrenalectomized and injected with placebo or adrenocortical extract. Whole-body irradiation of adrenal-containing, saline-drinking rats resulted in a diuresis similar to that in control animals, but polydipsia was inhibited. Both saline intake and urine output declined after the first day. Urine and plasma chloride concentrations indicated that the diuresis was a volume regulation rather than a regulation of salt concentration. Hemograms suggested a developing hemoconcentration. Histopathologic alterations showed progressive degeneration terminating in prominent mucosal atrophy and patchy terminal denudation that coincided with reduction of circulation occurring as a result of vascular occlusion. Irradiation of the exteriorized-intestine of adrenal-containing saline-drinking rats resulted in alterations qualitatively similar to those seen in adrenal-containing whole-body irradiated rats but both physiologic and pathologic changes developed somewhat slower and survival time was extended. With pre-irradiation adrenalectomy many of the differences between whole-body and exteriorized-intestine-irradiated rats were not seen and survival time was shortened. Diuresis was prominently reduced and hypodipsia occurred. Urine chloride concentrations were generally reduced and plasma chloride concentrations were similar to those seen in controls except for marked terminal changes. Injection of adrenocortical extract into adrenalectomized, irradiated saline-drinking rats restored the patterns and values of many of the parameters to those seen in adrenal-containing irradiated rats but was without influence on some. Survival time was extended only in exteriorized-intestine-irradiated rats. (A.G.W.)

10698 UNTERLAGEN ZUR NEUTRONENBIOLOGIE DES MENSCHLICHEN KOERPERS. (Basis of Neutron Biology of Human Bodies). Schreiber, Hans. Stuttgart, F. K. Schattauer-Verlag, 1965. 99p.

The literature on the biology of neutrons is relatively limited. Comprehensive reports on the properties of the biological objects with respect to the effects of neutrons are especially lacking. It is the purpose of the present volume to fill this gap. The properties and origins of neutrons are first discussed. The international standard man is described and the chemical composition of human organs and tissues are tabulated. The interrelations between neutrons and organic tissues in first collisions are considered. (J.S.R.)

Radiation Effects Therapy and Countermeasures

10699 (NASA-TT-F-353, pp 210-38) PROPHYLAXIS AND THERAPY OF RADIATION INJURIES CAUSED BY PROTONS. Balika, Yu. D.; Bibikova, A. F.; Lebedev, B. I.; Rogozkin, V. D.; Znamenskaya, K. M. Translated from Problemy Radiatsionnoi Bezopasnosti Kosmicheskikh Poletov; Fizicheskie i Biologicheskie Issledovaniya s Protonami Bol'shikh Energii, Atomizdat, Moscow, 1964.

Investigations on the therapeutic and prophylactic effectiveness of individual pharmacological materials and certain variants of protective-therapeutic complexes showed that the most clearly expressed protection was provided by 5-oxytryptamine and a combination of cystamine and amygdalin. A clearly expressed antihemorrhagic effect of 5-oxytryptamine during proton irradiation was established. An effective protective-therapeutic complex was developed, which consists of a minimum range of protective and therapeutic preparations used for the most part per os. Studies on dogs revealed that this complex is extremely effective in the case of absolutely fatal acute radiation injuries developing as a result of multiple irradiations of dogs by protons. However, this protective-therapeutic complex did not prevent the animals from developing aplastic anemia a considerable time after irradiation, and this resulted in their death. (P.C.H.)

10700 MODIFICATION OF RADIATION RESPONSE OF TUMORS BY ACTINOMYCIN D. CLINICAL EVALUATION. Ranniger, Klaus; Griem, Melvin L. (Univ. of Chicago). Amer. J. Roentgenol., Radium Therapy Nucl. Med., 96: 147-9(Jan. 1966).

Experiments on rats show that variation of the time interval between actinomycin D injection and administration of ionizing radiation modifies the radiation response of cells. Clinical studies suggest that certain radioresistant tumors, especially certain sarcomas, may exhibit enhanced radiosensitivity under similar conditions. (auth)

10701 THERMONUCLEAR INJURIES. Kellerbauer, A. (Univ., Munich). Arch. Klin. Chir., 308: 36-40 (Nov. 17, 1964). (In German).

Following a thermonuclear explosion about 15% of the total energy appears as radiation. About a third of this, consisting of very high energy γ radiation plus α, β, and neutron radiation, appears during the first minute after the explosion. The remaining two thirds consists of α, β, and γ radiation, but no neutrons. The primary cause of radiation sickness is the initial hard γ radiation which produces instantaneous, short term whole-body irradiation. This affects the blood-forming organs, the gastrointestinal system, and the central nervous system. The total dose received, organ radiosensitivity, the general body condition, wounds and other stresses, and the treatment facilities available all affect the course and severity of the irradiation injury. Irradiation injuries are usually accompanied by other types of trauma, except when the detonation amounts to less than 1 kt and irradiation injury from neutrons is most prominent. However, with increasing kt value, burn incidence increases proportionately more than injuries from irradiation. (BBB)

10702 STUDY OF THE VARIATIONS OF THE —SH GROUPS IN THE HUMAN SKIN AFTER IRRADIATION BY COBALT THERAPY. EFFECTS OF THE ADMINISTRATION OF GLUTATHION. Guerrier, Y.; Catayee, G.; De Varenne, D. (Faculte de Medecine, Montpellier, France). Compt. Rend. Soc. Biol., 159: 942-4(1965). (In French).

Experiments show that the –SH radicals are very sensitive to ^{60}Co γ radiation and with increase of the dose there is a decrease of the radicals. It is this decrease of the –SH radicals that is responsible for the epidermal disorders after ^{60}Co therapy. There is a ratio between the quantity of SH radicals present in the epidermis and scarring. The introduction of sulfur to the skin during the irradiation seems to facilitate the regeneration of different layers of the skin and the administration of glutathione during Co therapy treatment assures the sulfhydryl chains necessary for the normal evolution of the Malpighian layer. (tr-auth)

10703 PROTECTIVE ACTION OF WATER-SOLUBLE POLYSACCHARIDE FROM THE YEAST-LIKE MICROORGANISM OF PULLULARIA IN IRRADIATED MICE. Lobanok, A. G.; Bulanov, P. A. (Inst. of Experimental Botany and Microbiology, Academy of Sciences, Belorussian SSR). Dokl. Akad. Nauk Belorussk. SSR, 9: 477-9 (July 1965). (In Russian).

Nontoxic yeast polysaccharides were examined in order to determine the effect of biopolymers and microbic polysaccharides on the tissue and humoral factors involved in the nonspecific resistance to x radiation of mice. The water-soluble polysaccharide was prepared from 8-day old cultures of pullularia. Inbred, male mice were exposed to doses of 750 R x radiation, after the injection of the polysaccharide dissolved in sterile physiological solution. The results indicated that injection during the period from 3 to 24 hours prior to irradiation increased the survival rate and extended the life span of the animals; best results were obtained by injecting 25 mg/kg body weight 24 hours before exposure. A rate of 5 mg/kg was ineffective and 200 mg/kg actually reduced the survival rate. The injection also increased the resistance of the animals toward exogenous and endogenous infections and caused an earlier regeneration of hemopoiesis. It was not established whether the polysaccharide acts directly on the cell precursors or by another type of reaction on the organism. (TTT)

10704 THE PROTECTIVE ACTION OF A PHOSPHOLIPID EXTRACT OF SPLEEN ON MICE SUBJECTED TO A FATAL DOSE OF WHOLE-BODY IRRADIATION. Pasotti, C.; Del Favero, C.; Lami, L. (Univ., Pavia, Italy). Gazz. Intern. Med. Chir., 70: 123-32(1965).

The protective effect of a phospholipid extract of spleen was studied in mice after lethal whole-body irradiation. It was possible to observe positive effects on the mortality curve and the erythrocyte and leukocyte values. The spleen extract has a beneficial influence on liver lipids (diminution of the total lipids and the glycerides, increase of the phosphatides, unaltered steroid level) if the compound was given after irradiation. (Excerpta Med.)

10705 THE PROTECTIVE EFFECT OF A DUODENAL HEPARINOID ON THE MOUSE EXPOSED TO A LETHAL DOSE OF WHOLE-BODY IRRADIATION. Pasotti, C. Del Favero, C.; Lami, L. (Univ., Pavia, Italy). Gazz. Intern Med. Chir., 70: 241-49(1965).

The protective effect of a duodenal heparinoid was studied in the mouse after lethal whole-body irradiation. Positive effects on the mortality curve and on the level of the leukocytes were obtained, while the erythrocytes and the hemoglobin did not show any variation. The heparinoid had a positive influence on the liver lipids, since it corrected or limited the alterations of the lipid fraction caused by the radiation, with a diminution of the total lipids, normal phosphate levels, and a fall in the steroid levels. (Excerpta Med.)

10706 THE THERAPEUTIC EFFECT OF PRESERVED AUTOLOGOUS BONE MARROW ON THE HEMATOLOGICAL LESIONS PROVOKED BY RADIATION. Ferrara, A.; Maffei, G.; Mango, G. (Sanita Militare, Rome). Giorn. Med. Mil., 114: 745-51(1964).

Low temperature preservation of bone marrow with DMSO and its therapeutic effectiveness were studied on a group of 12 dogs made aplastic with radiation (900 R, telecesiumtherapy). (Excerpta Med.)

10707 LIFE-SHORTENING IN MICE EXPOSED TO RADIATION: EFFECTS OF AGE AND OF HYPOXIA. Lindop, Patricia J.; Rotblat, J. (St. Bartholomew's Hospital Medical Coll., London). Nature, 208: 1070-2 (Dec. 11, 1965).

Data are presented on the mean age at death of mice exposed to a single whole-body dose of 425 or 900 rads at age 1 day, 1 week, or 30 weeks while breathing air or N_2 atmosphere. In each age group the anoxia reduced the life-shortening effects of x radiation considerably, with a greater protective effects observed in the younger mice. (C.H.)

10708 THE RADIOPROTECTIVE EFFICIENCY OF CYSTAMINE AND ITS ACCUMULATION IN MOUSE THYMUS CELLS IN VIVO AND IN VITRO. Rass, I. T.; Tarasenko, A. G. Radiobiologiya, 5: 713-19(1965). (In Russian).

In contrast to cysteamine, cystamine was found ineffective by several authors as a radioprotective agent. The problem was further studied, examining the radioprotective ability of this agent and its accumulation in the thymus cells, using 14 to 16-g white mice for the experiments. For the in vivo tests the cystamine was injected subcutaneously 15 minutes after irradiation at a dose of 3 and 15 mg per animal. For the study of the in vitro protective efficiency, thymus cell suspensions were used with cystamine, irradiating the system after incubation. The radiation doses ranged from 100 and 200 R for in vivo to 4000 R in vitro. The results indicated that at a rate of 3 mg/mouse cystamine does not reduce the extent of radiation injury. Radiation damage after in vitro irradiation was reduced by using 0.1 to 0.5 mg/ml of cystamine. The accumulation of the compound was studied by using a labeled, 0.1-μC ^{35}C-cystamine; it was found to depend on the dose of the agent and the in vitro incubation temperature. By introducing 15 mg/mouse of cystamine, eight times more of the substance is accumulated than under in vitro conditions. The lack of in vivo radioprotective action and the high activity in vitro is not due to differential accumulation of the agent; it is assumed that there is a correlation between in vitro radioprotective action and the ability of cystamine to depress glycolytic processes in isolated issue. (TTT)

10709 ON THE EFFECTIVENESS OF HORMONE THERAPY IN RADIATION INJURIES. Akoev, I. G.; Lagun, M. A.; Klassovskii, Yu. A. Radiobiologiya, 5; 827-32 (1965). (In Russian).

In rats, 5 months after exposure to doses of 600 R, the following radiation effects were observed: decreased resistance to repeated radiation and to the effects of Bacterium perfringens toxin, intensity of erythropoiesis, and intensification of the thyroid function. These manifestations of irreversible irradiation injury have a determinative relation with the insufficiency of the endocrine apparatus. The introduction of thyroxine to the irradiated rats at intervals of 4 and 5 months after the irradiation liquidates the functional pressure of the thyroid gland and erythropoiesis and increases the resistance to repeated radiation at doses of $LD_{50/30}$ and less to the effects of the toxin at doses close to the minimum absolutely fatal dose. However the introduction of thyroxine reduces the resistance of the irradiated rats to repeated irradiation at doses of $LD_{95/30}$ and to the effects of the toxin at doses exceeding by 1.5 and 3 times the minimum absolutely fatal dose. The introduction of diethylstilbestrol to the irradiated female rats aged 1.5 years at intervals of 4 and 5 months after the irradiation produced a delayed increase of the functional pressure of the thyroid gland and erythropoiesis, reduced the resistance of the rats to repeated irradiations at doses of $LD_{50/30}$ and significantly impaired their resistance to the effects of the toxin at doses exceeding by 1.5 and 3 times the minimum absolutely fatal dose. (tr-auth)

10710 SOME PECULIARITIES OF OXYGEN EFFECTS IN THE CELLS OF THYROID GLAND IN MICE. Rass, I. T. (Severtsov Inst. of Morphology, Moscow). Radiobiologiya, 5: 855-9(1965). (In Russian).

Anoxia reduces the radiation damage to cells of the thyroid gland in mice during irradiation in situ at doses of 200 to 2000 R and in vitro at doses at 200 to 10,000 R. The number of cells with pycnotic nucleus at 6 hrs after irradiation was used as the criteria of radiation damage. The singularity of the anoxia defense during irradiation appearing in the absence of the usually observed reduction of the effective radiation dose was shown. The increase of the anoxia defense with respect to the increase of the dose and the presence of anoxia defense on the background of paradoxial resistance at 10,000 R was detected. (tr-auth)

10711 LABILE SAMPLES AS CRITERIA OF EFFECTIVENESS OF RADIOPROTECTION. Lavrenchik, E. I. (Inst. of Industrial Hygiene and Occupational Diseases, Moscow). Radiobiologiya, 5: 882-5(1965). (In Russian).

The use of AET and AETF before irradiation at an absolutely lethal dose increases the survival of 82 and 64% of the animals respectively and significantly decreases the gravity of the labile reaction to injections of distilled water. Preliminary injection for irradiation with lethal doses does not essentially affect the survival and the gravity of the labile reaction. Labile tests reflect the degree of gravity of the radiation sickness and correlates with the survival of the irradiated animals. (tr-auth)

10712 RADIOPROTECTIVE EFFECTS OF INERT GASES AND LOW-MOLECULAR NARCOTICS. 4. PROTECTIVE EFFECTS OF COMPRESSED NITROGEN AGAINST PHOTODYNAMIC DAMAGE OF PLANT CELLS. Paribok, V. P.; Krupnova, G. F.; Koroleva, Yu. I. (Inst. of Cytology, Leningrad). Radiobiologiya, 5: 886-9(1965). (In Russian).

Visible (white) light in the presence of oxygen causes chromosome damage in the meristem cells of bean roots, sensitized with acridine orange. Nitrogen under a pressure of 40 atm added to the oxygen during the light period reduces the photodynamic damage—the number of cells with chromosome breaks. The results make it possible to alter the hypothesis on the protective effect of gas layers as the cause of the protective effect of compressed gases. (tr-auth)

10713 THE INFLUENCE OF MARROW INJECTION INTO SPLEEN ON THE SURVIVAL AND WEIGHT OF MICE OF $C_{57}/_6B$ LINE. Pareishvili, E. A.; Organdzhanyan, E. E. (Division of Radiobiology, Erevan). Radiobiologiya, 5: 890-1(1965). (In Russian).

The intrasplenic injection of suspensions of bone marrow increases the survival of irradiated mice by 45 to 54%. The therapeutic effect was observed during introduction of bone marrow suspensions 24 hrs after the irradiation. The introduction of large quantities of bone marrow cells (from 2 donors) accelerates the restoration process in the organ. The restoration of the weight of the diseased animals is equal to and proceeds with greater speed than after the injection of the suspensions from only one donor. (tr-auth)

10714 ON THE RADIOPROTECTIVE AND PHARMACEUTICAL EFFECTS OF β-MERCAPTOPROPYLAMINE. Kozlov, V. A. Radiobiologiya, 5: 892-5(1965). (In Russian).

β-mercaptopropylamine appears to be an effective protective agent significantly alleviating the clinical pattern of acute radiation sickness and increasing the survival of the animals by 57 to 80% (mice) and 65 to 75% (rats). The protective effect is observed only with the parenteral method of injection and is maintained in the tract for 1.5 hrs after its introduction. The clearest prophylactic effect was noted with use of the drug in the maximum permissible dose. β-mercaptopropylamine reduces the level of exchange processes in the organism: reduces the consumption of oxygen by the organism; increases the resistance of the animal to oxygen starvation; in rats, rabbits, guinea pigs, and dogs reduces the temperature of the body by 1.5 to 5.5°; and possesses an antidiuretic effect. (tr-auth)

10715 METABOLISM OF ASCORBIC ACID IN ADRENAL GLAND IRRADIATED WITH OR WITHOUT MERCAMINE AND CYSTAMINE PROTECTION. Polikarpova, L. I. (Inst. of Experimental Medicine, Leningrad). Radiobiologiya, 5: 896-8(1965).

Acute radiation sickness produces disturbances in the metabolism of ascorbic acid in the adrenal gland of rats, shown by the decrease of reduced ascorbic acid and the appearance of its oxidation product, dehydroascorbic acid. Preliminary exposure of the rats to small doses (15 and 30 R) contributes to the reduction of the ascorbic acid in the adrenal gland of animals subjected to the repeated effects of ionization radiation in large doses (800 R). The injection of mercamine in healthy animals produces changes in the metabolism of ascorbic acid in the tissues of the adrenal gland, similar to the changes produced by ionizing radiation. The prophylactic injection of mercamine to the animals, irradiated with a lethal dose, causes oxidation of the ascorbic acid in the tissues of the adrenal gland. The injection of mercamine (before irradiation at a dose of 800 R) to animals irradiated at doses of 30 and 800 R, does not cause the oxidation of ascorbic acid in the adrenal glands. The injection of cystamine affects the metabolism of ascorbic acid in the tissue of the adrenal gland in healthy and irradiated animals. (tr-auth)

10716 STUDIES ON-EFFECTS OF ACRIFLAVINE ON UV-INDUCED LETHALITY AND PHOTOREACTIVATION IN NEUROSPORA CRASSA [Thesis]. Terry, Claude Emory Jr., Athens, Ga., Univ. of Georgia, 1965. 76p.

Studies were carried out on the ability of Neurospora crassa to repair lethal damage produced by ultraviolet irradiation. The mechanisms of repair considered possible were photoreactivation and dark repair. In addition, the effects of acriflavine on photoreactivation and on uv lethal effects were examined. Attempts to demonstrate dark repair by holding in liquid or water-agar, or by treating with cycloheximide or chloramphenicol were unsuccessful. Failure to obtain dark repair may be due to absence of the necessary enzymes in Neurospora. Photoreactivation of uv-induced lethal damage was found, amounting maximally to 12-fold and, on the average, to 10-fold. Acriflavine incorporation into plating media neither reduced survival of uv-treated cells nor prevented photoreactivation of uv damage. Pretreatment of conidial suspensions with acriflavine prior to photoreactivating illumination prevented photoreactivation. Pretreatment of conidial suspensions with acriflavine prior to uv-irradiation resulted in a 10-fold decrease in the lethal effects of uv. However, this protective effect did not extend to gamma radiation. (Dissertation Abstr.)

Radiation Hazards and Protection

See also HEALTH AND SAFETY

10717 (BNWL-122, pp 166-7) EFFECTS OF MOISTURE AND AIR TEMPERATURE ON DEPOSITION AND RETENTION OF $^{131}I_2$ ON PLANTS AND SOIL. Cline, J. F.; Hungate, F. P. (Battelle-Northwest, Richland, Wash. Pacific Northwest Lab.).

The effects of air temperature and moisture on the deposition and retention of I_2 on various surfaces were investigated. Increasing air temperature accelerated the loss of $^{131}I_2$ from leaf and other surfaces. Moist surfaces accumulated 1.2 to 2.3 times more I_2 than did corresponding dry surfaces. The amount of $^{131}I_2$ accumulated on a soil was dependent on the physical characteristics of the soil. (auth)

10718 (BNWL-122, pp 172-5) RADIOACTIVITY IN NORTHERN ALASKAN NATIVES AND THEIR FOODS DURING 1964. Hanson, W. C.; Palmer, H. E.; Braby, L. A.; Griffin, B. I. (Battelle-Northwest, Richland, Wash. Pacific Northwest Lab.).

A third survey of radionuclides in northern Alaskan natives and their foods was conducted during the summer of 1964. Cesium-137 body burdens were about double those found in 1963 in comparable ethnic groups of natives. The maximum value (3 μCi) found in whole-body counts of 380 residents occurred in a non-native male who consumed unusually large amounts of caribou. Seasonal variations were found in caribou flesh ^{137}Cs concentrations and in body burdens of natives that extensively utilized caribou as food. (auth)

10719 (NASA-TT-F-353, pp 3-20) CHARACTERISTICS OF THE RADIATION EFFECT UNDER SPACE FLIGHT CONDITIONS AND WAYS TO DETERMINE ADMISSIBLE RADIATION LEVELS. Dudkin, V. E.; Grigor'ev, Yu. G.; Kovalev, E. E.; Lebedinskii, A. V.; Levinskii, S. V.; Nefedor, Yu. G.; Ryzhov, N. I.; Smirennyi, L. N.; Sychkov, M. A. Translated from Problemy Radiatsionnoi Bezopasnosti Kosmicheskikh Poletov; Fizicheskie i Biologicheskie Issledovaniya s Protonami Bol'shikh Energii, Atomizdat, Moscow, 1964.

Radiation effects under space flight conditions and the means for determining admissible radiation levels are discussed. The intensity and composition of primary cosmic radiation were investigated in experiments on space rockets and artificial earth satellites and also in the launchings of geophysical rockets and pilot balloons. Primary cosmic radiation includes protons, α-particles, and heavy nuclei with energies of the order of 10^9 or more. In estimating the biological effect of radiation under space flight conditions, it is considered that the developed norms apply to a limited number of individuals, and genetic effects are not of decisive importance in this case. In addition, the great capacity of the human body for compensation and restoration of impaired functions is taken into account. (P.C.H.)

10720 HOW MUCH RADIATION DOES THE PATIENT RECEIVE PER SET OF DENTAL RADIOGRAPHS? Wainwright, W. W. J. Calif. Dent. Ass., 39: 493,536(Dec. 1963).

Criticisms are advanced against early estimates of radiation doses received in dental radiography, such as the estimates made by Nolan in 1953. He reports the radiation exposure to be a total of 315 R to the facial region during a full mouth exposure in one office using 25 films per set; in other offices it was 35 R. Nolan states further that to any 1 cm^2 of skin surface the dose will, in most instances, not exceed 100 R. The actual areas exposed on the face are illustrated. This shows the x rays are not centered on one

spot, but the erroneous figure of 300 R or more was obtained by assuming that the rays were centered on one spot and that older equipment is used with the slow films of the 1950's. Others who have repeated Nolan's work have shown that his figures are not representative of modern equipment. The beam collimators now required are smaller and films are more sensitive. With ultrafast film (Dupont LF and EK Ultraspeed) the skin exposure per 14 film set is 0.8 R. Dentists who use modern inspected equipment, full film development (based on 5 min at 68°) and ultrafast film, are giving only $^1/_{400}$th the amount of radiation dose that appears in the earlier report. (BBB)

10721 RISK OF INTERNAL CONTAMINATION IN INDUSTRIES EMPLOYING ^{137}Cs. Sbertoli, C.; Ghezzi, I. (Univ., Milan). Med. Lavoro, 55: 763-74(1964).

A case of accidental internal contamination with ^{137}Cs is reported. The accident was caused by an imperfection in the capsule containing the isotope, resulting in the escape of Cs salts. Radioactivity measurements were carried out on the body of the subject with a total body counter for 2 yrs after the accident, to determine the radioisotope incorporation (51.2 microcuries) and the dose of radiation absorbed by the worker in the first year after contamination (4.99 rem.). The latter dose was found to be markedly lower than the maximum allowable dose. The clinical findings excluded the presence of organic lesions attributable to the absorption of radioactive substances. The radiometric determination of ^{137}Cs in the urine showed that 3 yrs after the contamination there was still a persistent elimination of the radioisotope in a concentration about 10 times greater than that found in the general population (due to radioactive fallout). The case calls attention to the real danger of internal contamination from gamma radiations, when ^{137}Cs sources are employed. The danger is due to the fact that, on account of the chemico-physical characteristics of the Cs salts employed (alkalinity, powder form), the capsules containing them may easily break open, scattering their contents. Prophylactic and treatment measures for such accidents are discussed. (H.G.D.)

10722 FIELD SAMPLING OF ^{131}I IN MILK WITH ION EXCHANGE CARTRIDGES. Johnson, R. H.; Reavey, T. A. Public Health Rep. (U. S.), 80: 919-24(Oct. 1965).

The major advantages of the use of ion exchange cartridges for the field sampling of ^{131}I in milk are their simplicity, low cost, and the fact that all components are reusable. The iodine-131 can be stripped from the resin with 2M hydrochloric acid and the resin reconditioned with 2M sodium chloride. The resin can also be used 5 to 10 times without exceeding the exchange capacity after it is washed clean with water and the adsorbed iodine has decayed. The cartridges could be shipped in advance to a field location for use and then returned to a laboratory for counting. (C.H.)

10723 ^{137}Cs BODY BURDENS OF ALASKAN MEN, SPRING 1965. Bruce, Daniel W.; Remark, D. G.; Averett, W. J. Public Health Rep. (U. S.), 80: 949-53(Nov. 1965).

To assess the extent and the magnitude of the reportedly elevated cesium-137 body burdens in Alaska, 180 men in seven communities scattered throughout the State were counted in April and May 1965 to determine their cesium-137 body burdens. In addition, they were interviewed about their dietary consumption. The whole-body counting device consisted of a portable, unshielded, gamma scintillation detector coupled to appropriate instrumentation. The measurements indicated that body burdens higher than those recorded in the conterminous United States existed throughout Alaska. The data were divided according to whether or not the subject ate caribou (reindeer). The average body burdens for the caribou eaters were significantly high than for noncaribou eaters. However, the higher burdens did not exceed the radiation protection guidance recommended by the Federal Radiation Council. (auth)

Radiotherapy and Radiodiagnosis

10724 (ORINS-51) THE DESIGN OF A LOW-BACKGROUND WHOLE-BODY COUNTING FACILITY. Morris, A. C. Jr.; Ross, D. A. (Oak Ridge Inst. of Nuclear Studies, Inc., Tenn.). Jan. 1966. Contract AT-40-1-GEN-33. 51p. Dep. mn. CFSTI $3.00 cy, $0.50 mn.

The whole-body counter is described, and the selection of materials for use in the facility is discussed in detail. The construction of the facility is also outlined. (D.C.W.)

10725 COMBINED 5-FLUOROURACIL AND COBALT IRRADIATION EVALUATED BY DOUBLE BLIND TECHNIQUE. Howe, C. D.; Fletcher, G. H.; Samuels, M. L. Suit, H. D. (Anderson Hospital and Tumor Inst., Houston, Tex.). Acta Unio Int. Contra Cancr., 20: 400-3(1964).

A possible synergistic effect of 5-fluorouracil (5-FU) and ^{60}Co γ radiation was sought in 19 patients with locally advanced, previously untreated, squamous carcinoma of the posterior and lateral wall of the pharynx. The experiment was designed to answer two questions: (1) does a pharyngeal carcinoma treated with a dose of 1000 rad/week regress more rapidly if a near toxic dose of 5-FU is given at the start of the radiation therapy than if radiation at the same dose rate is given alone and (2) is the control of the primary lesion maintained longer if the treatment is 5-FU and 6000 rad in six weeks instead of 6500 to 7500 rad given over six to seven weeks. The 5-FU dose was 15 mg/kg for three days and 7.5 mg/kg for the next two days, and no daily dose exceeded 1 g. Cobalt-60 therapy was started on the last day of drug administration and given at the rate of 1000 rad per week for six weeks. The results indicated that a combination of 60 mg/kg of 5-FU and 1000-rad tumor dose per week for six weeks yielded a more rapid regression of pharyngeal wall carcinoma than a 1000-rad tumor dose given alone, but whether this was an additive synergistic or potentiating effect could not be determined. However, follow-up visits up to 23 months indicated no differences either in primary control or survival. It appeared that 6000 rad in six weeks plus 5-FU is equivalent to 6500 to 7500 rad in six and a half to seven weeks of radiation alone in producing control of locally advanced carcinoma of the pharyngeal wall. (BBB)

10726 TREATMENT OF CANCER OF THE CERVIX BY RADIATION AND ELECTIVE RADICAL HYSTERECTOMY. Greiss, Frank C.; Blake, Damon D.; Lock, Frank R. (Wake Forest Coll., Winston-Salem, N. C.). Amer. J. Obstet. Gynecol., 82: 1042-54(Nov. 1961).

Severe complications and survival data are reported for 149 patients undergoing standard or intensive radiotherapy and surgery for cervical carcinoma. There was no statistically significant difference in the survival of patients with Stage I cervical cancer treated with standard radiation therapy alone and those treated with supplemental elective radical operations. After operation, severe complications increased threefold and contraindicated postirradiation surgery. However, the survival rate of patients with Stage II or Stage III cervical cancer was improved after combined radiation and elective radical operation, the difference being highly significant. Increased therapy complications are compatible with the improved survival. Severe complications of therapy totaled 20%, 14% being considered as surgically induced and 6% as radioinduced. (TCO)

10727 FOLLOW-UP OF PATIENTS WITH ADENOCARCINOMA OF THE CERVIX AND CERVICAL STUMP. Peete, Charles H. Jr.; Carter, F. Bayard; Cherny, Walter B.; Parker, Roy T. (Duke Univ., Durham, N. C.). Amer. J. Obstet. Gynecol., 93: 343-56(Oct. 1, 1965).

Clinical results and complications of radiation and surgical treatment are discussed. In this series of 80 patients 51 were treated by irradiation alone, and 29 patients had operative therapy with or without irradiation therapy. Fourteen patients received adequate x ray alone and only one is known to survive. No patient was treated by radium alone. The total radiation dose varied from 7800 to 15,200 R. Complications of irradiation therapy are presented. No

deaths could be attributed directly to irradiation. Three patients developed vesicovaginal fistulas, but in two patients the fistula was attributed to persistent or recurrent tumor 3 and 6 months following therapy. One patient died with no attempted repair and the other died after unsuccessful ureterosigmoidostomy. The third fistula developed following vaginal hemorrhage 3 months after irradiation. No active tumor was identified and the fistula was closed successfully 8 years later. Other complications were as follows: 4 patients developed pyometra which responded to drainage; 3 patients had a rectovaginal fistula and one was successfully repaired; ureteral stricture was observed in one patient; proctitis was observed in 7 patients; one patient suffered a fracture of the right femur; symptomatic lymphedema was noted in 3 patients and thrombophlebitis in one patient. It is not possible to conclude from these results that there is a single best method of management of adenocarcinoma of the cervix; each patient's treatment must be individualized. The ultimate success of treatment depends upon many variables, including age, stage of disease, radiosensitivity of the tumor, general physical condition of the patient, presence of node or distant metastases, host resistance, and human error. The combination of full irradiation and radical Wertheim hysterectomy appears to offer the best hope for salvage in adenocarcinoma of the cervix. Even so, the over-all results can be expected to be discouraging. (BBB)

10728 NEUTRON CAPTURE THERAPY. **Knipping, H. W.; Pappas, A. (Univ., Cologne). Atomkernenergie, 11: 79-82(Jan.-Feb. 1966). (In German).**

The development of neutron capture therapy and especially the selective kinetics of Farr and Konikowski are discussed. The experiments with animals of the last years demonstrate that a high degree of selectivity of the therapy can be performed. In the future a vascular branch of the selective kinetic can be developed. (auth)

10729 TREATMENT OF CARCINOMA OF THE THYROID WITH RADIOIODINE. **Smithers, D. W.; Howard, Norman; Trott, N. G. (Royal Cancer Hospital, London). Brit. Med. J., 2: 969-74(Oct. 23, 1965).**

Problems associated with the use of radioiodine therapy in 59 patients with thyroid carcinoma are discussed. A description is given of the physical measurements carried out to determine the pattern of retention of the administered radioiodine, and hence the radiation dose to the whole body, to the blood, and to functioning thyroid tissue. Preparation for treatment and rationale of the treatment dosage and schedule are discussed. The amount of radioiodine given varied considerably, but 150 mC was found to be a satisfactory first treatment and was often given for subsequent ones as well; amounts ranging from 100 to 250 mC have been given at one time. The largest total amount of radioiodine administered to a patient in this series was 655 mC over a period of nine months. Higher total amounts have been given to later patients, however: over 1000 mC in two cases. A large amount of ^{131}I occasionally produced nausea. The white-cell count tended to fall temporarily, usually by about 2,000 cells/mm^3 in a patient with a normal count of between 5,000 and 10,000 cells/mm^3. Menstruation was sometimes affected temporarily. These 59 patients are discussed in two groups. The first comprises those in whom the disease was clinically confined to the neck, with persistent postoperative disease, with inoperable tumors, or with recurrent tumors. The second group comprises those with distant metastases, with no uptake, with limited uptake, or with good uptake of radioiodine in the tumor. Patients with anaplastic tumors, whether localized or generalized, all did badly. Good uptake of ^{131}I in a differentiated tumor may lead to regression and long survival, even in cases where wide dissemination has occurred. (BBB)

10730 THE QUANTITATIVE DETERMINATION OF CORONARY FLOW WITH A POSITRON EMITTER (^{84}Rb). **Cohen, Alberto; Gallagher, James P.; Luebs, Eide-Dittmar; Varga, Zoltan; Yamanaka, Jiro; Zaleski, Edward J.; Bluemchen, Gerhard; Bing, Richard J. (Wayne State Univ., Detroit). Circulation, 32: 636-49(Oct. 1965).**

A method employing ^{84}Rb in a coincidence counting system is described that was developed to measure coronary circulatory dynamics. The advantages of the coincidence method are enumerated. (TCO)

10731 POSSIBILITIES OF BONE MARROW TRANSFUSION IN THE TREATMENT OF BONE MARROW DISEASES. **Witte, S. (Medizinische Universitaetsklinik, Erlangen, Ger.). Deut. Med. Wochschr., 90: 1141-2 (June 18, 1965). (In German).**

The clinical possibilities of using bone marrow transfusions for treatment of bone marrow diseases fall into two different main groups. In primary bone marrow diseases homologous bone marrow can be given if a suitable donor is available. Nevertheless immunological complications may result. As long as only a transitory substitution of hematopoietic cells is necessary, transfer of homologous marrow cells is satisfactory. Homologous transfusions have been successful in idiopathic aplastic anemias, severe agranulocytosis, and in cytostatically induced marrow aplasia occurring during treatment for tumors or systemic diseases. If the bone marrow is involved in a systemic disease such as leukemia homologous transfusion can be considered only if the leukemia process has been essentially repressed. After exposure to a single whole-body irradiation, homologous transfusion is valuable only if the amount of irradiation has exceeded the capacity of the bone marrow to recover or symptomatic treatment is impossible. Autologous marrow transfusion requires a functioning bone marrow and availability of preservation equipment. There are no immunological dangers. Clinically, the most important possibility of use occurs when marrow removed before beginning of cytostatic therapy of a patient with an inoperable tumor can be administered for treatment of any impaired blood formation that may result. Because of the spontaneous ability for recovery of the bone marrow activity after short term treatment with cytostatics, usually only long term or combined cytostatic treatment justifies autologous transplantation of bone marrow. Although results are difficult to assess, autologous transplantation seems to permit higher dosages of cytostatic drugs to be administered, and induced pancytopenias may be corrected within 2 or 3 weeks. (BBB)

10732 LABELLING AND KINETICS OF BODY EXCRETION OF ^{131}I-IODOTHIAZIDE. **Bianchi, C.; Protto, C.; Sosi, S. (Univ., Pisa, Italy. Nuclear Research Center SORIN, Saluggia, Italy). Experientia, 21: 619-20(1965).**

Iodothiazide is a recently synthesized compound capable of producing a remarkable diuretic and natriuretic effect, similar to that of chlorothiazide. The method of labeling iodothiazide with ^{131}I-radioiodine and the patterns of distribution and excretion of this substance in man are described. ^{131}I-iodothiazide is excreted by the kidneys with a rather high excretion rate. This behavior lessens possible effects of accumulation when iodothiazide is given in therapeutical doses and may permit the use of ^{131}I-iodothiazide for renal function studies by external counting. (auth)

10733 THE SCINTIGRAPHIC DEMONSTRATION OF BRAIN TUMORS WITH ^{197}Hg-LABELED SUBSTANCES. **Haacke, Wolfram (Univ.-Klinik, Mainz). Fortschr. Geb. Roentgenstr. Nuklearmed., 102: 88-9(Jan. 1965). (In German).**

The authors report on the scintigraphic visualization of brain tumors with $^{197}HgCl_2$, administered at a dose level of 10 to 15 μC/kg body wt. The scanning study was started at 1 hr after the ^{197}Hg was administered. However, ^{197}Hg-labeled neohydrin has the advantage that it is more rapidly cleared from the blood so that the detectable background radiation is lower than with $^{197}HgCl_2$. The dose administered is the same for the two compounds. As compared to ^{203}Hg-labeled neohydrin, the ^{197}Hg-labeled compounds give scintigrams that are of equal quality. In contrast to ^{203}Hg, ^{197}Hg decays by K-capture so that there is almost no β irradiation. Since β radiation contributes the most to the irradiation burden received, and is practically without scintigraphic value, ^{197}Hg is preferable over ^{203}Hg for use in scanning. Because the irradiation dose delivered by the ^{197}Hg compound is much less than from the corresponding ^{203}Hg compound, larger doses of the ^{197}Hg can be adminis-

tered. This has the advantage that the pulse rate available can be increased. (BBB)

10734 RADIOISOTOPE NEPHROGRAPHY DURING CHILDHOOD. Hoer, G.; Heinze, H. G.; Frey, K. W. (Univ., Munich). Fortschr. Med., 82: 941-4(Dec. 17, 1964). (In German).

The use of isotope nephrography in children and adults is critically analyzed. (TCO)

10735 EFFECTIVENESS OF PREOPERATIVE IRRADIATION IN CONTROL OF MALIGNANT CELL CONTAMINATION DURING SURGERY. Mochizuki, Nobuyuki. Gan no Rinsho, 10: 532-42(July 1964). (In Japanese).

The containment of malignant cells is a major problem encountered during cancer operations. Patients were washed with physiological saline solution before and after operations, and the washings were found to show greater positive presence of cancerous cells after operations. Preoperation irradiation reduced the positive incidence significantly. Irradiation also reduced tumor progress by nearly a factor of three. Irradiated areas showed about half the number of cells with cancer symptoms compared to the areas outside the irradiation zone. It was found that preoperation irradiation was very effective in preventing the spread of cancerous cells particularly with stomach cancer cases of relatively limited size. The dissemination of cells into the abdominal cavity and the re-emergence of cancerous cells was controlled rather effectively by this technique. (TTT)

10736 RECENT PROGRESS IN RADIOLOGIC TREATMENT WITH FAST NEUTRONS AND MESONS. Fowler, J. F. (Hammersmith Hospital, London). Gazz. Sanit., 35: 501-5(1964).

Applications of fast neutrons, negative π mesons, protons, deuterons, and alpha particles in radiotherapy are reviewed. (H.G.D.)

10737 THE POSSIBILITIES OF THE THERAPEUTIC USE OF A SELECTIVE PERFUSION WITH RADIOISOTOPES WITH A SHORT HALF-LIFE. EXPERIMENTAL STUDIES WITH ^{165}Dy. Biagini, C.; Ficari, A.; Bruzzese, E.; Greco, G.; Buonerba, M.; Centi-Colella, A.; Daniele, G.; Bertolotti, A. (Univ., Rome). Giorn. Med. Mil., 114: 718-44 (1964).

The possible application of short-lived radioisotopes to regional selective perfusion techniques was studied. The following results were obtained by application of ^{165}Dy versenate: degree of chemical toxicity was shown to be low as regards the quantity of that compound, at the stable state, necessary to obtain a radiobiologically useful action on the interested field; the rate of ^{165}Dy versenate removal from the organism was favorable to its possible application with regional perfusion techniques; the method of distribution in different organs and tissues of normal and experimental tumor-bearing animals, did not suggest any elective uptake of the substance on tumor tissues; tissues and organs receiving highest doses during administration of the radioisotope, were bone, liver, and kidney; and necessity of employing high doses of radioisotope to obtain radiobiologic useful effect on the interested area required special provisions for radiation protection. (TCO)

10738 TREATMENT OF HYPERTHYROIDISM. Pittman, James A. Jr.; Pittman, Constance S. (Medical Coll. of Alabama, Birmingham). J. Amer. Acad. Gen. Pract., 31: 137-44(Apr. 1965).

The use of various drugs and radioiodine to treat hyperthyroidism is discussed. An objection to the use of radioiodine in children is the possibility that it may contribute to the subsequent development of thyroid cancer. Thyroid nodules have been reported in two adolescent patients who had been treated with radioiodine for hyperthyroidism. An additional case of this type is reported. A thyroid nodule containing papillary adenocarcinoma developed in a 12-year-old patient $2\frac{1}{4}$ years after the initial treatment with ^{131}I. Without adequate controls, however, these figures have little significance. More significant is the finding that 80% of a large series of patients with childhood thyroid cancer gave a history of prior exposure of the neck region to irradiation for such reasons as enlarged tonsils or an enlarged thymus. The use of radioiodine is avoided in children and not in older adults because the longer life expectancy of children offers more time for the development of late neoplasia and experiments in animals indicate that the rapidly growing tissues of children, including the thyroid, may be more susceptible to radiation damage than the tissues of adults. While these points do not prove conclusively that the radiation from radioiodine can cause thyroid cancer, the physician should consider them before using it in children. However, these arguments probably do not apply to the use of small diagnostic tracer doses since the radiation received is small compared with therapeutic dose. A second objection to the use of radioiodine is that it may induce leukemia. Many cases have been reported in which leukemia, usually acute, developed after use of radioiodine for hyperthyroidism. Two large studies, however, have failed to show that the incidence of leukemia among patients so treated is any higher than it is in other patients. A third objection to the use of radioiodine in children is the later development of hypothyroidism in a large proportion of cases. This point is discussed. (BBB)

10739 CAN RADIOSENSITIVITY AND HISTOPATHOLOGY OF CERVICAL CANCER BE CORRELATED? Glucksmann, Alfred (Strangeways Research Lab., Cambridge, Eng.). J. Amer. Med. Ass., 823-4(Sept. 6, 1965).

The histologic type of a carcinoma influences the local radiocurability, since the five-year symptom-free survival rates are significantly better with mature than anaplastic carcinomas. The initial response of an individual cancer to irradiation, as seen in serial biopsies, is closely correlated with the ultimate local radiocurability of the disease in the patient. Use of this method requires (1) the careful selection of biopsy samples taken prior to the insertion of radium, (2) the immediate fixation of the tissue in a suitable good fixative and (3) a good histologic technique. Radiation changes in serial biopsies can be interpreted in their prognostic significance only in relation to dose and time factors of the radiation treatment. In one series, 80% of the patients with a favorable histological prognosis survived symptom-free for five years, while only 30% of those with an unfavorable prognosis survived, the difference being highly significant. In another study a comparison of the prognosis given within 14 days of beginning treatment with the clinical results five years later for 1453 patients showed that the prognosis was accurate in 86% of the cases. The histological method can be made the basis of selection for additional surgical treatment. The histological assessment of radiosensitivity is practicable even in a routine manner. (BBB)

10740 IS CYTOLOGY A RELIABLE PROGNOSTICATOR OF RADIOSENSITIVITY? Graham, Ruth M. (Roswell Park Memorial Inst., Buffalo). J. Amer. Med. Ass., 193: 825(Sept. 6, 1965).

Attempts were made to determine whether vaginal exfoliative cytology can be used to detect radioresistant Stage II cervical cancers. Radioinduced changes in irradiated tumor cells and normal cells were examined. Vaginal smears were studied both before and during radiation treatment, with attention not on the malignant cells, but on the changes in the benign cells. Radiation changes in benign, squamous epithelial cells observed included vacuolization of the cytoplasm, enlargement of both cell and nucleus, changes in nuclear structure, and multiple nuclei. One hundred consecutive cells were counted to determine the percentage of response of the benign squamous epithelium to the radiation. The five-year results of this study show a marked difference in the survival rate of those who had a good cytological response to radiotherapy and those patients who had their radiotherapy stopped and radical surgery performed, the survival was 16% better than in the poor-response group. Thus radiation changes in the benign epithelial cells of the vaginal smear during radiation are reliable guides for prognosis. (BBB)

10741 CHOICE OF TREATMENT FOR CERVIX CANCER: RADIOSENSITIVITY TESTING. Gusberg, Saul B.

(Mount Sinai Hospital, New York). J. Amer. Med. Ass., 193: 826-7(Sept. 6, 1965).

Radiation-induced effects on cervical carcinomas were examined after a test dose of radiation, to ascertain whether cellular radiation response can be used to help decide whether further irradiation or surgery would be most effective. This test-dose technique with cytological and cytochemical appraisal of tumor response after one week was used for radiosensitivity testing of tumors of large stage I or stage II extent. A range of exposure between 1600 and 3000 R in two to five days was satisfactory to produce a spectrum of response great enough to indicate the sensitivity of the tumor to this type of treatment. Three types of tumor cell reaction indicating responsiveness to irradiation examined included death and dissolution of cells; increased differentiation of cells; and radiocytological reactions that suggest the probability of irreversible cell injury, including enlargement of cells and cell nuclei, disproportionate enlargement of nucleoli (RNA), and an early increase in chromatin material (DNA) followed by a relative decline. A good response was usually seen as a reaction in virtually all tumor cells, while a poor prognosis was indicated if unchanged tumor-cell nuclei predominate. The presence of more than 25% of tumor cells that are unchanged, frequently in the same high-powered field with reacting cells, indicates the so-called mixed response. These reactions are in accord with other experimental demonstrations that the reproductive apparatus of the cell (chromosomal DNA) is more sensitive to irradiation than the protein-forming apparatus (nucleolar RNA). About 70% of cervix cancers showed a good response and 30% a mixed or poor response. (BBB)

10742 CANCER OF THE CERVIX STAGE II: COMMENT. Rubin, Philip (Univ. of Rochester Medical Center, N. Y.). J. Amer. Med. Ass., 193: 827(Sept. 6, 1965).

The value of selecting patients for surgery or irradiation or both by means of a screening procedure such as the cytohistopathological techniques is briefly discussed. If it were possible to determine the biological aggressiveness of a neoplasm, host resistance of the patient, and radioresponsiveness of both tumor and normal tissue, a rational basis for therapeutic selection of patients could be made available. The main question yet to be answered is whether such selection can improve survival results by using various modalities of treatment. Or is the end result biologically determined and the ultimate outcome unaffected by the modality of treatment? Recent reports indicate that patients with poor radioresponsiveness can be salvaged by radical surgery. If this proves to be the case, application to other sites will follow and indeed is in progress to aid in case selection for specific treatment. (BBB)

10743 SOME ASPECTS OF FRACTIONATED IRRADIATION IN CLINICAL STUDIES. Kok, G. J. Belge Radiol., 48: 453-76(1965). (In Dutch).

Some fundamentals of radiobiology are discussed and the history of radiation fractionation is given. Observations previously made on the fractionated irradiation of the slightly radiosensitive skin carcinoma are cited and the tolerance of normal tissue is indicated. In recent years it has been shown that more tumor damage results if there is fractionated irradiation with an interval of 48 or 72 hrs and if there is an increase of the dose per fraction. Fractional irradiation given three times a week was introduced for patients to be exposed to megavoltage x rays. Provisional results showed that in carcinoma of the bladder the 20% correction factor given in the literature was too much and probably amounted to only 10%. This was later confirmed. There are indications, however, in the case of irradiation administered three times a week with a correction factor of 10% that the effect on tumors is as effective as with daily irradiations. For an evaluation of the results of irradiation between various radiotherapy departments, a better description of the dosage distribution used is required. The use of a computer for 2- and 3-dimensional dose distribution can be helpful for this purpose. It is currently under study and development. (tr-auth)

10744 THERAPEUTIC SCOPE OF RADIATION. den Hoed-Sijtsema, S.; Kaalen, J. (Rotterdam Radio-Therapeutisch Instituut). J. Belge Radiol., 48: 477-88 (1965). (In Dutch).

One-hundred and forty-two cases of carcinoma in the larynx were statistically analyzed with respect to local results of radiotherapy and various factors in the radiation techniques. In the case of good and fair mobility of the vocal cords there was a satisfactory cure rate, but it was poor in the case of complete or almost complete fixation. The therapeutic ratio was evaluated in the first group and the optimum radiation dose was calculated. A relation between the irradiation techniques and the time interval after which fibrinous mucositis appeared was established. Preliminary results obtained in a group of 34 patients treated with the optimum conditions derived from this analysis are encouraging. (tr-auth)

10745 THE RADIOLOGICAL REVIEW. Ruckensteiner, E. (Zentral Roentgen-Institut, Innsbruck). Klin. Med. (Vienna), 20: 240-5(May 1965). (In German).

Cavernous hemangiomas should be treated with small doses of irradiation repeated frequently rather than with large single doses. Overdosage can produce irreparable injuries, especially in children. Radiophosphorus is a pure β emitter, but it can only be used as an open source. For this reason enclosed sources consisting of $^{90}Sr-^{90}Y$ are preferred. This type of source has a tissue half-value layer of 1 mm, and at 2 mm depth 20% of the dose is still effective. The results achieved with $^{90}Sr-^{90}Y$ sources are reached more slowly than with other sources, but there is less danger of producing skin damage. Studies were made over 16 yr, including 322 cases of which 236 were children of 1 yr or less. Single doses administered were less than 150 R, given one/month, and the total dose administered was less than 2500 R. The treatments were successful, producing either complete removal of the hemangioma, and residual effects consisting of slight pigment changes, thinning of the cutis, loss of subcutaneous fat, or small teleangiectases. The cosmetic results were satisfactory. There was no evidence of functional injury, impairment of skeletal growth, or muscular injury. (BBB)

10746 BIOPTIC STUDIES ON THE PROBLEM OF THERAPY-INDUCED BONE MARROW FIBROSES IN CHRONIC MYELOID LEUKEMIA. Hunstein, W.; Harwerth, H. G.; Raju, S. (Medizinische Universitaetsklinik, Freiburg i. B.). Med. Klin. (Munich), 60: 991-5(June 18, 1965). (In German).

Results of studies in 20 cases of chronic myeloid leukemia indicate that marrow fibrosis can develop not only after use of myleran but also after x irradiation. The development of fibrosis appears to depend on the level of the dose and the length of time that treatment is administered. The anatomical picture was similar whether x irradiation or urethan was used. The fibrosis observed seemed to be a reparative process of the connective tissue subsequent to destruction of the leukemic cells. However, the sensitivity of connective tissue to myleran does not explain the bone marrow fibrosis observed after x irradiation. The process of fibrosis appears to involve a reactive increase in collagen fibers resulting from chronic marrow edema and proliferation. Thus, fibrosis may result from a reactive, reparative increase in connective tissue. Fibrosis is found in bone marrow more frequently and develops more rapidly after myleran use than after x irradiation. The question of whether marrow fibrosis is induced by either of these treatments for chronic myeloid leukemia can be resolved only by bioptic studies of its development made during the course of therapy itself. (BBB)

10747 THERAPY OF THYROTOXICOSIS. DeGroot, Leslie J. (Harvard Med. School, Boston). Mod. Treat., 1: 176-207(Jan. 1964).

The use of radioiodine, among other agents, to treat hyperthyroidism is reviewed, with attention to administered and absorbed doses, clinical results, and hazards. The simplicity of ^{131}I treatment is its chief recommendation. Radioiodine is especially useful when coincident organic disease, especially heart disease, increases the hazards of surgery, or if there has been prior thyroid surgery. The

total cost of ^{131}I therapy to the patient is less than for other forms of treatment. The main deterrent to the use of ^{131}I in hyperthyroidism has been the fear that radiation exposure (5,000 to 20,000 rad to the thyroid and 5 to 10 rad to the rest of the body) would eventually cause thyroid cancer or leukemia. Thyroid neoplasma, one possibly malignant, have developed in several children following ^{131}I therapy, but, to date, there has been no suggestion of an increased incidence of thyroid carcinoma following administration of ^{131}I to adults. There has been no increase in the reported incidence of leukemia among patients who have received ^{131}I treatment for thyrotoxicosis. It is also possible that irradiation of the gonads during ^{131}I therapy will induce genetic damage that will be transmitted from parent to child. However, the actual genetic hazard involved cannot be assessed with accuracy. The danger is probably slight, and the effects may even be imperceptible. (BBB)

10748 RADIOIODINE TREATMENT OF BENIGN STRUMAE IN THE ENDEMIC GOITER REGION OF SOUTHERN GERMANY. Frey, K. W.; Locher, D. W.; Heinze, H. G. (Univ., Munich). Muenchen. Med. Wochschr., 107: 1209-14(June 11, 1965). (In German).

The effect of radioiodine treatment of 60 euthyroid and 33 hyperthyroid benign goiters was studied over an average time of 18 months. The symptoms which indicated that radioiodine treatment would be beneficial were narrowing of the trachea, compression of the esophagus, obstruction in swallowing, and symptoms of hyperthyroidism. The strumas were classified as large (over 50 cm^2 in size, as measured by scintillation scanning) and small (25 – 50 cm^2). In general, the strumas markedly decreased in size after radioiodine treatment. On the average, the large goiters decreased by 4 cm and the small ones by 1.5 cm. The thyroid lobes decreased by about 20% (from 60 cm^2 to 48 cm^2). The estimated thyroid wt decreased in 80% of the patients by from 30 to 50%. The average increase in body wt amounted to 5.2 kg. The only important complications were thyroid hypofunction, which appeared in 4 cases, and myxedema that resulted in two cases. Thus frequency of appearance of posttreatment hypothyroidism was 9 times as great in small goiters as in large goiters. The ones most likely to become hypothyroid were the small goiters which recurred after earlier goitrectomy. A high blood cholesterol also seemed to be associated with increased frequency of posttreatment hypothyroidism, because 6 patients with euthyroid goiters and high cholesterol developed hypothyroidism following radioiodine treatment. References cited, 40. (BBB)

10749 THE PROBLEM OF CLINICAL INTERPRETATION OF HISTOLOGICAL FINDINGS IN Ca CORPORIS UTERI FOLLOWING THE RADIATION. Belohorsky, B.; Siracky, J. (Oncology Research Inst., Bratislava). Neoplasma, 12: 51-6(1965).

In 22 cases of Ca corporis uteri treated with a standard method of radium tamponade, the evaluation of radiocurability was made by control curettages carried out at 3 to 6 months' interval following the termination of the treatment. For the evaluation of radiocurability the interval of 3 months' duration was too short. Control curettage carried out after 6 months' interval was negative in a majority of cases. In cases in which the histologic finding demonstrated fragments of regressively changed carcinomatous tissue or isolated carcinomatous cells, histologic examinations were made at short time intervals. In each case, also with negative histologic findings, the passage of the cervical canal was maintained and cytologic examination was carried out at each clinical control examination in a course of 3 years. (Excerpta Med.)

10750 THE SYMMETRY OF ^{131}I 4-IODOANTIPYRINE UPTAKE BY BRAIN AFTER INTRAVENOUS INJECTION. Oldendorf, William H.; Kitano, Masami (Veterans Administration Center, Los Angeles). Neurology, 15: 994-9(Nov. 1965).

A technique for monitoring the distribution in the head of ^{131}I-labeled-4-iodoantipyrine following intravenous injection is described, and results from a large number of subjects (313) are given and compared with results obtained using ^{85}Kr and ^{133}Xe. The cranial counting system consisted of a large sodium-iodide scintillation unit on each side of the head. The two detectors were carefully equalized with a midline, mock-iodine source before each test. Every fourth pulse emerging from each photomultiplier unit having a pulse height greater than 0.2 Mev was recorded on 1 channel of a stereo tape recorder. The technique required abrupt intravenous injection of isotope; 8 μC of ^{131}I antipyrine in 1 ml of saline. The symmetry of the amount of intravenous tracer appearing in each hemicranium was used as an index of the symmetry of cerebral capillary blood flow. Results in 313 cases indicated that although uptake asymmetry approximated the changes anticipated, based upon clinical evaluation, this index of hemisphere blood flow symmetry correlated poorly with clinical data. (TCO)

10751 CARCINOMA OF THE CERVIX TREATED DURING PREGNANCY AND FOLLOWED BY SUCCESSFUL PREGNANCY: REPORT OF A CASE. Price, Joseph J.; Rominger, C. Jules (Misericordia Hospital, Philadelphia). Obstet. Gynecol., 26: 272-4(Aug. 1965).

This report considers a patient who had a successful pregnancy following a full course of radiation therapy including radium and x-ray therapy for carcinoma of the cervix. Pregnancy had progressed to the 20th week. X ray (220-kv) therapy was instituted prior to radium therapy because of a large tumor. Radiotherapy was administered through two anterior rectangular portals (10.5 × 14 cm) and two posterior portals (12 × 16 cm) delivering a total of 2100 R in air through each portal. Eighty mg of radium was left in place for 70 hr administering 3923 R to Point A, 2651 R to Point B, 19,668 R to the hot spot of the cervix (Point C), 4206 R to the rectum, and 2886 R to the bladder. A stillborn infant was delivered by classical cesearean section several weeks later. Less than a year later the patient became pregnant and the pregnancy progressed to normal. This is reputed to be the first case of a successful pregnancy following complete radiation therapy according to modern radiation technic. This patient has also survived 5 years with no evidence of recurrence of cancer. (BBB)

10752 PITUITARY DESTRUCTION BY IMPLANTATION OF ^{90}Y IN ADVANCED CASES OF BREAST CANCER. Jadresic, A.; Poblete, M.; Rahausen, A.; Pabst, Y. (Hopital San Juan de Dios, Santiago de Chile). Rev. Franc. Endocrinol. Clin., 5: 491-7(1965).

Sixteen cases of mammary carcinoma were treated by transfrontal stereotaxic implantation of ^{90}Y pellets in the turkish saddle. The implants administered varied between 7.1 and 13.4 M. In 6 out of the 13 cases studied an obvious hypothyreosis was obtained. In 7 cases gland destruction was estimated to be only partial. No operatory or post-operatory death was noticed. In 11 patients post-operatory diabetes insipidus developed. Post-pituitary therapy was necessary in six cases. Post-mortem examination in two cases revealed 60 and 80% pituitary destruction. The results obtained are compared with other intra-saddle implantation techniques of ^{90}Y. This method seems to offer some advantages in respect to the other methods, i.e., reduced morbidity and absence of mortality. It may be necessary to increase the dose of interstitial irradiation in order to obtain a greater percentage with complete hypophysectomy. (TCO)

10753 CRITICISM OF METHODS AND DIAGNOSTIC VALUE OF RADIOISOTOPE NEPHROGRAPHY AS COMPARED TO STANDARD FUNCTION TESTS. Hoer, G.; Pabst, H. W. (Univ., Munich). Schweiz. Med. Wochschr., 95: 445-53(Apr. 3, 1965). (In German).

The value of kidney function tests for detailed analysis of glomerular and tubular function, with particular reference to current concepts of mechanisms of tubular concentration is discussed and contrasted with conventional test methods. Radioisotope renography is described. The

parameters selected for quantitative evaluation of renal function, various technical procedures, and methods of interpretation are criticized. The value of radioisotopes renography for diagnosis of several types of renal lesions is discussed. The importance of such factors as the position of the patient, position of the detectors, and the state of hydration of the patient are considered. 118 references. (BBB)

CHEMISTRY

General

Refer also to abstract 11377.

10754 (IS-T-44) COMPARISON OF AXIAL DISPERSION AND RADIAL DIFFUSION MODELS FOR FIXED BED CATALYTIC REACTOR DESIGN [Thesis]. Shuck, David Leroy (Ames Lab., Iowa State Univ. of Science and Tech.). July 1965. Contract W-7405-eng-82. 70p. Dep. mn. CFSTI $3.00 cy, $0.75 mn.

An axial-dispersion model was compared with the radial-diffusion model as a basis for design of fixed-bed catalytic reactors. The catalytic oxidation of SO_2 to SO_3 was used since considerable data on the radial-diffusion model have been reported for this system. The axial-dispersion model predicted terminal conversions which ranged from 25 to 55% of the best estimated (0.27) available from experimental data. For the case of heat transfer only, good agreement was obtained between the computed temperature profiles for both models. In the corresponding reaction case, the terminal conversion predicted by the axial-dispersion model was less than 23% of that predicted by the radial diffusion model (0.22). The largest sources of error in the axial-dispersion model come from two sources. One is the assumption that the average rate of reaction evaluated at the average temperature and conversion. The other source of error occurs in the definition of a suitable heat transfer coefficient at the reactor wall. Since both of these sources of error are peculiar to a one-dimensional model, it is concluded that reactor design calculations should be based on a two-dimensional model, such as the radial diffusion model. (auth)

10755 (TID-4005(Pt.2a)(2nd ed.)) SUMMARIES OF THE USAEC BASIC RESEARCH PROGRAM IN CHEMISTRY (OFF-SITE). (Division of Research (AEC), Washington, D. C.). Jan. 1966. 158p. Dep. mn. CFSTI $1.75 cy, $1.00 mn.

Approximately 200 summaries are given of individual research projects supported by the Office of Chemistry Programs of the Division of Research under its offsite program. Attempts were made to include summaries for all contracts in effect on Dec. 1, 1965. The contract summaries are arranged in alphabetical order by contractor. Subject and author indexes are included. Each summary includes the name and address of the principal investigator, AEC contract number, and the date on which the summary was received. (P.C.H.)

10756 EFFECT OF STABLE COBALT ON ADSORPTION OF ^{60}Co BY PEAT. Berdnikov, A. I.; Oreshko, V. F. Radiokhimiya, 7: 494-6(1965). (In Russian).

The extent to which fission products penetrate plants and water depends to a large extent on their behavior in soil, slime, and various types of deposits. Experimental data were presented on the adsorption of ^{60}Co from solution by peat as a function of the concentration of stable Co. In order to evaluate the magnitude of the adsorption of ^{60}Co under these conditions the distribution coefficient was determined, the numerical value of which in the soil-solution system was calculated from the decrease of the activity of the starting solution. With increase of the concentration of stable Co at essentially constant pH the distribution coefficient was lowered to a minimum. When the concentration of stable Co exceeds 0.6 to 10^2 mg-equiv/g of peat the adsorption process practically ceased. (ATD)

Analytical Procedures

See also Separation Processes and Procedures

Refer also to abstracts 11365 and 11960.

10757 (BLG-353) PLUTONIUM URINANALYSIS. Valentin, N.; Weyers, C.; Boulenger, R. (Centre d'Etude de l'Energie Nucleaire, Brussels (Belgium)). July 1965. 23p. Dep. mn.

A simple method of urinanalysis, sensitive enough to detect 0.08 dpm of plutonium in 1500 ml of urine, is described. The method consists of a phosphate precipitation followed by the destruction of organic matters by ashing. Anion exchange is used to separate plutonium from other remaining inorganic ions and the final purified plutonium is deposited or electroplated on stainless steel discs and counted in a ZnS scintillator. Ten to twenty samples can be treated per day by two persons, the result being obtained three days after the beginning of the analysis. The recovery of about 3 dis./min of plutonium from a liter of urine is 78 ± 4% with 95% confidence. (auth)

10758 (EUR-2618.f) APPLICATION DE LA COULOMETRIE A POTENTIEL CONTROLE A DES DETERMINATIONS DANS DES SOLUTIONS RADIOACTIVES, CAS DES SOLUTIONS DE PRODUITS DE FISSION ET DES COMBUSTIBLES IRRADIES [Theses]. (Application of Controlled-Potential Coulometry to Determinations in Radioactive Solutions. Case of Fission-Product and Irradiated-Fuel Solutions [Thesis]). Denis, A. (Commissariat a l'Energie Atomique, Saclay (France). Centre d'Etudes Nucleaires). Nov. 1965. 33p. Dep. mn.

Submitted to Univ. Paris, France.

The technique of analysis by controlled-potential coulometry as applied to determinations in highly active solutions was studied. Coulometric determinations were carried out in connection with the analysis of four elements: uranium, molybdenum, chromium and iron. Determination of the H_2O_2 formed in the fission-product solutions was also undertaken, together with the application of this method as a means of checking the extraction yield as in the case of ^{129}I. (auth)

10759 (INP-427/C) BADANIA RADIOCHEMICZNE NAD EKSTRAKCJA I TRWALOSCIA CHELATOW ORAZ NAD ROZDZIELANIEM METALI METODA CHROMATOGRAFII EKSTRAKCYJNEJ. (Radiochemical Studies on the Extraction and Stability of Metal Chelates and on the Separation of Metal Salts by Extraction Chromatography). Stronski, Ignacy (Institute of Nuclear Physics, Krakow (Poland)). 1965. 119p. Dep.

The extraction of some metal ions by means of chloroform solutions of quadridentate, aromatic Schiff bases and 8-mercaptoquinoline (thiooxine) was investigated by the radioactive indicator method. The dissociation constants of some Schiff bases were determined spectrophotometrically, and the stability constants of nickel and uranium chelate complexes established by a graphical method. By means of thiooxine labeled with ^{35}S, the distribution coefficients of these compounds in the systems electrolyte–organic solvent were determined. Using radioactive isotopes, the optimum conditions for separation of various mixtures of transition and actinide metal salts by extraction chromatography in the system tri-n-butyl phosphate–hydrochloric acid, tri-n-octylphosphine oxide–mineral acid, and tri-n-octylamine–electrolyte, were determined. 135 references are cited. (auth)

10760 (IS-1305) THE SEPARATION OF HIGH PURITY LUTETIUM AND YTTERBIUM BY ION EXCHANGE AT 90 deg C. Powell, J. E.; Burkholder, H. (Ames Lab., Iowa State Univ. of Science and Tech.). Jan. 1966. Contract W-7405-eng-82. 15p. Dep. mn. CFSTI $1.00 cy, $0.50 mn.

An ion-exchange unit designed for continuous operation at 90°C and which includes a good method of preventing gas formation in heated columns, is described. The value of hot ion-exchange procedures for the production of lutetium and ytterbium oxides of very high purities is demonstrated. (auth)

10761 (IS-T-69) THE DESIGN AND PERFORMANCE OF A LONG-PATH OXY-ACETYLENE BURNER

FOR ATOMIC ABSORPTION SPECTROSCOPY [Thesis]. Fiorino, John Angelo (Ames Lab., Iowa State Univ. of Science and Tech.). Nov. 1965. Contract W-7405-eng-82. 63p. Dep. mn. CFSTI $3.00 cy, $0.75 mn.

The design and performance of a long-path premixed oxyacetylene slot burner for atomic absorption spectroscopy were studied. Design of the burner is described in detail. Many hours of successful burner operation provided ample proof that the burner is safe to use. The detection limits for a number of metallic elements were in most instances significantly reduced and equally important, and analytical sensitivities were greatly improved. The success of the burner was dramatically demonstrated by the observation of lanthanum and tungsten in absorption, neither of which could be observed at the 1% concentration level with the three-burner triple-pass system. The improvement of the detection limits and sensitivities combined with the low audible noise demonstrate the superior performance of the slot burner. The burner provides a good environment for the existence of free atoms and is thus a useful tool in atomic absorption spectroscopy. (auth)

10762 (IS-T-71) SEPARATION OF CADMIUM FROM THE LEAD-BISMUTH EUTECTIC BY HIGH VACUUM SINGLE STAGE DISTILLATION—CHAMBER DESIGN AND DISTILLATE PURITY [Thesis]. Murdoch, Lawrence Bryson (Ames Lab., Iowa State Univ. of Science and Tech.). Nov. 1965. Contract W-7405-eng-82. 59p. Dep. mn. CFSTI $3.00 cy, $0.75 mn.

A distillation chamber was evaluated to determine its effectiveness for separating liquid metals by a continuous high vacuum distillation process. This previously constructed chamber had an integral condenser which was cooled by a sodium–potassium eutectic. The metal to be separated flowed down an inclined distribution plate, opposite the condenser. The chamber was installed in a loop in which circulation of the liquid metal was effected by a remote diaphragm pump. Partial separation of cadmium from the lead–bismuth eutectic was achieved, verifying the method of operation. Distillate purity was found to be low, the cadmium concentration varying from 0.12 to 0.47 mass fraction. The cause of the low purity was investigated and determined to be the result of some design features of the distillation chamber. The distilland was short-circuiting from the distribution plate to the condensate receiver due to a combination of the steep slant of the distribution plate and the type of baffles on the plate. Contamination rates were determined to be related to the distilled flow rate through the chamber. Despite the effect of the contamination, distillation temperature and distilland concentration were found to have a strong effect upon the distillate purity. (P.C.H.)

10763 (KR-100) ON THE LIQUID SCINTILLATION DETERMINATION OF ^{239}Pu IN PURE AND CONTAMINATED SOLUTIONS. Joon, K.; Deurloo, P. A.; Hundere, I. A. (Institutt for Atomenergi, Kjeller (Norway)). Nov. 1965. 34p. Dep. mn.

The possibilities with respect to the application of liquid scintillation counting for routine determinations of Pu were investigated, using a scintillator solution composed of PPO, dimethyl-POPOP, and naphthalene in p-di-oxane. Regarding radiochemically pure Pu-solutions, it appeared that this technique is very well suited for the purpose, provided the Pu is prevented from adsorption on the wall of the counting vial. This can be obtained by addition of a suitable complexing agent to the scintillation liquid. The influence of quenching can be avoided by checking the place of the Pu-channel, by standardization of the composition of the scintillator-active sample mixture, or by integral counting. The counting efficiency is 100%. Radiochemical impurities may interfere to a greater or lesser extent, depending upon the nature of the activity (alpha or beta), the maximum energy of this radiation, the impurity to Pu ratio, and quenching conditions. For natural uranium and the fission products (Ce-Pr)-144, Cs-137, (Ru-Rh)-106, and (Zr-Nb)-95 this was investigated. Methods for correction are mentioned. (auth)

10764 (MITNE-64) NONDESTRUCTIVE ANALYSES OF IRRADIATED MITR FUEL BY GAMMA-RAY SPECTROSCOPY [Thesis]. Scientific Report No. 4. Sovka, Jerry A.; Rasmussen, Norman C. (Massachusetts Inst. of Tech., Cambridge). Oct. 1965. Contract AF19(604)-7492. 261p. (AFCRL-65-787). CFSTI $6.00 cy, $1.25 mn.

Submitted by Jerry A. Sovka.

Nondestructive analyses were made of irradiated MITR fuel elements with a lithium-ion drift germanium gamma spectrometer. Techniques for the preparation of Ge(Li) detectors were developed and are described in detail. Included are descriptions of the apparatus required for satisfactory performance of the spectrometers. Equipment used for scanning irradiated fuel elements in the MITR spent fuel storage tank is also described. Gamma spectra from fuel elements having different cooling periods show peaks attributed to the fission products Zr-95, Nb-95, Rh-106, Cs-134, Cs-137, Ba-140, La-140, Ce-144, and Pr-144. Fission product activities were determined from calculations of the intensities of the gamma rays in the spectra. Spatial variations of fission product content in the elements are shown. A method for interpreting the experimental results, requiring theoretical predictions of fission product activities in the fuel, is presented. The results of the application of this method include spatial distributions of absolute neutron flux, neutron exposure, and total U-235 burnup and irradiation time of the fuel. The operating pattern of each element and the time since its removal from the reactor could also be inferred. Some of the problems and limitations of the method are discussed and suggestions are made for improving the accuracy and precision of the results. (auth)

10765 (ORNL-3904) INDEXES TO THE ANALYTICAL CHEMISTRY DIVISION ANNUAL PROGRESS REPORTS, 1964–1965. Raaen, Helen P.; Haas, Ann K. (eds.) (Oak Ridge National Lab., Tenn.). Jan. 1966. Contract W-7405-eng-26. 72p. Dep. mn. CFSTI $3.00 cy, $0.75 mn.

Cumulative key word and author indexes to the annual progress reports from the Analytical Chemistry Division at ORNL are given for the periods following Nov. 15, 1963 including ORNL-3750 and -3889. The Key Word Index was prepared both from the numbered headings that appear within the reports and from the titles of the entries in the Presentation of Research Results and in the Translations. The form of the entries is that of a permuted title index. (P.C.H.)

10766 (TID-22511) IMPROVED ALUMINO SILICATE ION EXCHANGERS. Final Technical Report. Calmon, C.; Grundner, W. T. (Ionac Chemical Co., Birmingham, N. J.). Oct. 1962. Contract W-7405-eng-26, Subcontract No. 2133. 63p. (IONAC-5002). Dep. mn. CFSTI $3.00 cy, $0.75 mn.

For Oak Ridge National Lab., Tenn.

An investigation was conducted to determine the possibility of producing alumino-silicate ion exchangers with superior characteristics for the removal and/or recovery of cesium from radioactive wastes. The effect of changing certain variables in the preparation of these materials on the characteristics of the product, including such properties as the ion exchange capacity, selectivity for cesium, physical strength, stability to low and high pH, etc., was studied. Several materials were prepared which exhibit higher capacities than the standard commercially available materials. In addition to improved physical and chemical stability they also have improved (by factors as high as 7.5) selectivity for cesium present in very low concentrations in the presence of large amounts of sodium. (auth)

10767 (AD-620995) A METHOD OF DETECTING SUPERCONDUCTING INTERMETALLIC COMPOUNDS. Borovskii, I. B. Translated from Russian Patent No. 157, 557, Nov. 5, 1962. 4p. (FTD-TT-65-184). CFSTI $1.00 cy, $0.50 mn. JCL $1.10 fs, $0.80 mf.

A method of detecting intermetallic compounds in the diffusion layers formed at the interfaces of metals and alloys is proposed. (D.C.W.)

10768 (JPRS-33212) MESOTHORIUM-I CONCENTRATION IN THE BLACK SEA. Lazarev, K. F.; Grashchenko, S. M.; Nikolaev, D. S.; Drozhzhin, V. M. Trans-

lated from Dokl. Akad. Nauk SSSR, 164: 910-12(1965). 8p. (TT-65-33787). CFSTI $1.00 cy, $0.50 mn.

The results of determinations of the concentration of ^{228}Ra in the waters of different parts of the Black Sea and also the concentrations of ^{224}Ra in the coastal waters of the Black Sea are reported. The methods used are described. It was found that the ^{228}Ra concentration in the waters of the Black Sea is not a constant value and decreases somewhat with a transition from the northwestern shallow part of the sea, which receives the waters of the Danube, to the central parts of the sea. Reasons for this are given. Results for ^{224}Ra showed that its concentration virtually corresponds to an equilibrium value with the ^{228}Ra present in the water. (P.C.H.)

10769 RADIOCOULOMETRIC TITRATIONS. Braun, T.; Hradil, M.; Jesenak, V.; Toelgyessy, J. (Lorand Eoetvoes Univ., Budapest. Slovak Technical Univ., Bratislava). Acta Chim. Acad. Sci. Hung., 46: 35-44(1965).

An intermittent and a continous method are described that were developed for radiometric end-point determination of coulometric titrations based on precipitate formation and complexation. In the reactions involving precipitate formation, the titration is carried out with Ag^+ ions produced anodically. Cyanide ions are generated by electrolysis of the complex $[Ag(CN)_2^-]$ prepared previously. The applied instruments are described. As examples of application, radiocoulometric procedures for determining I^- and Ni^{2+} ions are presented. (auth)

10770 THE DETERMINATION OF URANIUM ISOTOPES BY ATOMIC ABSORPTION SPECTROPHOTOMETRY. Goleb, J. A. (Argonne National Lab., Ill.). Anal. Chim. Acta, 34: 135-45(Feb. 1966).

The uranium isotopes, ^{235}U and ^{238}U, can be determined easily by atomic absorption techniques. A water-cooled hollow-cathode discharge tube was used as an absorption tube. It was found that large amounts of uranium atoms in the ground state were produced by the discharge in the tube. Thus the inherently weak uranium resonance radiation coming from an emission source and passing through the absorption tube was absorbed. For the first time in an atomic absorption technique, samples and related standards were used in the emission source instead of an absorption source, and a high degree of accuracy and precision was obtained. Valid results were also obtained by conventional techniques; that is, the samples and related standards were employed in the absorption source. (auth)

10771 APPLICATION OF A FAST NEUTRON ACTIVATION METHOD TO THE DETERMINATION OF OXYGEN IN IRON AND STEEL. Fujii, I.; Miyoshi, K.; Muto, H.; Shimura, K. (Tokyo Shibaura Electric Co., Ltd.). Anal. Chim. Acta, 34: 146-53(Feb. 1966).

The determination of oxygen (0.001 to 0.2%) in iron and steel by fast neutron activation methods was investigated. The relative standard deviations of the method at oxygen levels of 0.1, 0.01, and 0.001%, were 3, 5, and 30%, respectively. The analytical results of the method were in good agreement with those of conventional methods in the range stated. (auth)

10772 LIQUID SCINTILLATION METHOD FOR DETERMINATION OF SOLVENT-EXTRACTED ^{32}P IN FOODS. Ellis, Mary K.; Wampler, Stanley N.; Yager, Robert H. (Walter Reed Army Medical Center, Washington, D. C.). Anal. Chim. Acta, 34: 169-74(Feb. 1966).

A method for solvent extraction of radioactive phosphorus, as phosphomolybdic acid from foods is described. The use of a carrier can be eliminated due to the quantity of the stable element present in foods. The use of a liquid scintillation technique for counting is discussed, showing the effective elimination of color and chemical quench. The efficiency resulting from the liquid scintillation method of counting makes possible the detection of 10^{-5} μC levels of activity in the original sample. (auth)

10773 SPECTROPHOTOMETRIC DETERMINATION OF YTTRIUM IN COPPER–YTTRIUM AND NICKEL–CHROMIUM ALLOYS WITH ARSENAZO-III. Hattori, Tadao; Tsukahara, Iwao; Yamamoto, Toshimi (Furukawa Electric Co. Ltd., Tokyo). Bunseki Kagaku, 14: 1044-8 (Nov. 1965). (In Japanese).

The sample is dissolved in nitric acid or perchloric acid, and an aliquot of the solution taken. When more than 40 mg of Cu or Ni and Cr are present, yttrium should be preliminarily isolated by TTA extraction. When the amount of Cu does not exceed 40 mg, it can be masked by thiourea. After the removal of the interference, Arsenazo-III is added and the 660 mμ absorbance measured at a pH of 2.5. Reference on the calibration line gives the amount of yttrium. The yttrium-Arsenazo-III complex obeys Beer's law over the range from 0 to 1 ppm Y, and the sensitivity of the determination is 0.1 ppm in the final solution. (auth)

10774 SPECTROGRAPHIC DETERMINATION OF STRONTIUM AND CALCIUM IN BONE ASH. Matsuda, Shunji (Gunma Univ., Kiriu, Japan); Kawamoto, Hiroshi; Yamagata, Noboru. Bunseki Kagaku, 14: 1061-5(Nov. 1965). (In Japanese).

A method is described for the spectrographic determination of strontium and calcium in bone ash. Two parts of carbon powder and 1 part each of potassium sulfate and bone ash were mixed, loaded into a graphite sample electrode, and burned in an interrupted a-c arc of 3 amp. The line pairs were: Sr 4077.7/Ca 3968.4 or 4226.7 and Ca 3644.4/Ti 3642.1 Å. The lower determinable limits by the method were 10^{-4} for Sr/Ca-ratio and 20% for calcium, and the coefficient of variation estimated statistically were below 5.3% for calcium and 12% for Sr/Ca-ratio. Mean values of calcium content and Sr/Ca-ratio in human bone ash, 34% and 0.36×10^{-3}, were obtained from results on 20 samples. (auth)

10775 SPECTROGRAPHIC DETERMINATION OF RARE-EARTH ELEMENTS OF THE YTTRIUM GROUP WITH A DFS-13 DIFFRACTION SPECTROGRAPH. Dopott, Z. M.; Sklyarova, Z. N. Byull. Nauch.-Tekh. Inform. Gos. Geol. Kom. SSSR, Otd. Nauch.-Tekh. Inform., 2: No. 52, 81-2(1964).

Rare earth elements were determined in fluorites in the spectral range from 3000 to 3500 Å (second order) by the three-standards method. Samples and standards were mixed (1 : 3) with buffer containing carbon powder (≈80%), $BaCO_3$ (≈20%), and Sc_2O_3 (internal standard) (0.01%), and the spectra excited in a vertical a-c arc. (Anal. Abstr., 12: (Dec. 1965))

10776 POTASSIUM ESTIMATIONS IN BIOLOGIC MATERIAL BY THE METHOD OF NEUTRON ACTIVATION ANALYSIS. Rakovic, M.; Talpova, H.; Langerova, I. (Karlova Univ., Prague). Cas. Lek. Ceskych, 104: 297-303(1965).

Non-destructive potassium detection by single or double filtration did not appear suitable for the detection of potassium in biological material when the method of neutron activation analysis was used. The method of assessing potassium in various types of animal tissues whereby the specimen is broken down in a fluid medium and potassium is separated as $KClO_4$ was suitable. The separated product is recrystallized after removal of sodium traces and the counting rate of recrystallized $KClO_4$ is assessed by a Geiger-Müller tube. (Excerpta Med.)

10777 DETERMINATION OF THE EQUIVALENCE POINT IN RADIOMETRIC PRECIPITATION TITRATION BY MEASUREMENT OF THE ACTIVITY OF THE PRECIPITATE. Klas, J. (Katedra Anorganickej Chemie Slovenskej Vysokej Skoly Technickej, Bratislava). Chem. Zvesti, 19: 689-94(1965). (In Czech).

A method of radiometric precipitation titrations ($A^+ + D^- = AD$) was studied in which the process of precipitation can be followed by means of the activity of the precipitates. The titration curve of activity of the precipitate as a function of the volume of the measuring solution was, in contrast to the titration curves of specific activity, independent of the radioisotope labeling. In the case of a weakly soluble precipitate the titration curve can be approximated by a straight line when the measuring solution consumption is under the equivalence point. After exceeding the equivalent point the activity remains constant. The equivalence

point can be determined graphically as the point of intersection of n and n_K or from the equation $v_E = v(n_K/n)$, where v_E = the equivalence consumption, v = the volume of the measuring solution, n_K the constant activity, and n = the activity of the precipitate. Construction of the titration curve from results is described. (tr-auth)

10778 THEORETICAL CONSIDERATIONS ON THE REFLECTION OF β RADIATION IN PRECIPITATION TITRATION. Klas, J. (Slovak Polytechnic Inst., Bratislava). Chem. Zvesti, 19: 783-91(1965). (In Czech).

Following the data reported by H. Müller (Anal. Chem. 29, 969(1957)), reflection of β radiation by the solution to be titrated was investigated, assuming that a precipitate AD with a solubility product K_s is formed during the titration, according to the reaction AC + BD = AD + BC. Equations were derived for determining the mean atomic number of the solution to be titrated from the ionic weights, densities, and volumes of the solution and the solvent. If the intensity of the reflected β radiation exhibited a linear dependence on the mean atomic number, the titration curve could be expressed by the equation $\bar{n} = k\bar{Z} + q$, where k and q designate constants dependent on the experimental system. If an insoluble precipitate was formed during the titration and the intensity of the reflected β radiation was not dependent on the density changes in the solution during the titration, the curve could be decomposed into two straight lines, which intersected at the equivalent point. The titration curve of the β radiation reflection method is similar to that obtained by conductometric titration. (TTT)

10779 COMPLEXOMETRIC DETERMINATION OF YTTRIUM(III) IN THE PRESENCE OF ALIZARIN RED S, THORON, AND MUREXIDE AS INDICATORS. Sangal, Satendra P. (Univ. Allahabad, India). Chim. Anal., 47: 596-8(Nov. 1965). (In French).

The complexometric determination of yttrium using alizarin red S, thorin, and murexide as indicators is described. The effect of pH on titration, the pH range, and the interferences due to foreign ions were studied. (tr-auth)

10780 STUDY OF THE SEPARATION OF ^{32}P FROM BIOLOGICAL RADIOACTIVE SOLUTIONS USING ION EXCHANGERS. Lambrino, V. (Inst of Medicine and Pharmacy, Bucharest). Compt. Rend. Acad. Bulg. Sci., 18: 751-4(1965). (In French).

The separation of ^{32}P from biological solutions using two bentonites as ion exchangers was investigated. The chemical composition of the bentonites, their ion exchange capacity, their pH, and their radiographic properties were determined. Decontamination of the solutions was determined as a function of the length of contact and the quantity of the bentonite used. The results showed that the degree of decontamination was a function of the nature of the bentonite. For the same bentonite the degree of contamination was directly proportional to the length of contact and to the quantity of bentonite used. The method seemed suitable for use in hospitals for routine determination of ^{32}P without necessitating special protection. (J.S.R.)

10781 THE USE OF A POLONIUM–BORON EMITTER OF NEUTRONS IN THE ANALYSIS OF ORES AND DRESSING PRODUCTS FOR ALUMINIUM. Plaksin, I. N.; Anchevskii, E. V.; Belyakov, M. A. Dokl. Akad. Nauk SSSR, 163: 1202-4(Aug. 11, 1965). (In Russian).

Neutron activation analysis results are difficult to interpret correctly if two different reactions yield the same radioactive isotope. Thus, ^{27}Al activated by thermal neutrons through an (n,γ) reaction yields ^{28}Al; at the same time, ^{28}Si which is usually present in Al ores also forms ^{28}Al by means of an (n,p) reaction with a 4.5-Mev threshold. The selective determination of Al and Si is based on the difference of the energy spectra of the neutrons involved in the above reactions. It was found that Al may be directly determined by a suitable discrimination of the high-energy neutrons. Po–B sources emit neutrons with a maximum energy of about 6 Mev with only a small percentage of 4.5-Mev neutrons, representing the threshold of the $^{28}Si(n,p)^{28}Al$ reaction; therefore the Si is only slightly activated. Tests were carried out with a 1.4×10^6 n/sec Po–B source. The results indicated that, while with the usual Po–Be source, a change of 1% of the SiO_2 content of the ore causes an error of 0.25% in the Al_2O_3 content, the error is reduced to 0.025% if a Po–B source is used. The method may be used to determine Al in ores and enriched products by a one-step activation with a sensitivity of about 0.5 to 1.0% Al_2O_3 within 15 to 20 min. (TTT)

10782 SEPARATION AND RECOVERY OF FALLOUT ^{137}Cs FROM Zr–^{95}Nb IN FORAGE SAMPLES. Johnson, James E.; Tengerdy, Catherine; Ward, Gerald M.; Wilson, Daniel W. (Colorado State Univ., Fort Collins). J. Agr. Food Chem., 13: 568-70(Nov.-Dec. 1965).

In forage samples contaminated with fallout, ^{137}Cs could not be calculated directly from a gamma spectrum of the sample because of Compton interference of other gamma-emitting radionuclides. The predominant interference was due to Zr–^{95}Nb, which was separated from the ^{137}Cs activity by digestion of ashed forage samples in concentrated NaOH. The recovery of ^{137}Cs by the method was 90% and the decontamination from Zr–^{95}Nb approximately 97%. (auth)

10783 ION EXCHANGE PAPER CHROMATOGRAPHY OF Tc(IV), Tc(V), AND Tc(VII) IN HYDROCHLORIC ACID. Shukla, S. K. (Istituto di Chimica Generale ed Inorganica, Rome). J. Chromatog., 21: 92-7(Jan. 1966).

The adsorption of Tc(IV), Tc(V), and Tc(VII) in 0.3 to 10N HCl on 3 cellulose paper, resin papers, and modified cellulose exchange papers was studied. The conditions under, which a separation of the three valency states can be obtained using HCl as the solvent were established. Only cellulose paper in the concentration range of 0.3 to 1.5N HCl was found to give complete separation. (auth)

10784 SEPARATION OF SOME FISSION PRODUCTS FROM URANIUM(VI) BY REVERSED-PHASE PARTITION CHROMATOGRAPHY. Tomazic, B.; Siekierski, S. (Inst. of Nuclear Research, Warsaw). J. Chromatog., 21: 98-104(Jan. 1966).

Reversed-phase partition chromatography with di-(2-ethylhexyl–ortho-phosphoric acid (HDEHP) retained on kieselguhr as the stationary phase was used for the separation of some fission products in trace amounts from macroamounts of U. The presence of U on the column caused incomplete elution of radiotracers under the usual experimental conditions. Increasing the temperature and decreasing the flow rate improve the separation. Group separation was performed on the synthetic mixture of Cs, Sr, Ba, La, Ce(III), Eu, Tb, Y, Zr, and U. The elutions were carried out with nitric acid of varying concentrations. Applying a flow rate of 0.2 ml · cm^{-2} · min^{-1} at 77°C, 95% recovery of the constituents of the mixture was achieved. (auth)

10785 STUDY OF THE ADSORPTION OF TRANSURANIC ELEMENTS BY ION-EXCHANGE PAPER CHROMATOGRAPHY. I. PLUTONIUM(IV) AND PLUTONIUM (VI) IN NITRIC MEDIA. Pages, Monique; Clanet, Frank (Institut du Radium, Paris). J. Chromatog., 21: 105-12 (Jan. 1966). (In French).

The adsorption of Pu(IV) and Pu(VI) on paper impregnated with ion-exchange resins was studied in nitric acid media in a concentration range of 0.5 to 15M. Evidence is presented for the existence of the species $Pu(NO_3)^{3+}$ and PuO_2^{2+} in 1 to 4M HNO_3. Some partition coefficients are given. (auth)

10786 AMPEROMETRIC STUDIES ON THE COMPOSITIONS OF THORIUM POLY-VANADATES. Saxena, R. S.; Sharma, O. P. (Malaviya Regional Engineering Coll., Jaipur India. Government Coll., Kota, India). J. Inorg. Nucl. Chem., 28: 195-8(Jan. 1966).

The stoichiometry of the compounds formed by the reaction of thorium salts and different alkali vanadates (ortho-, pyro-, meta-, and poly-) were investigated by means of amperometric titrations between the reactants at $E_{d.e.} = -1.5$ v (vs. S.C.E.). The end points obtained from the sharp breaks in titration curves provided definite evidence for the formation and precipitation of thorium ortho-$3ThO_2 \cdot 2V_2O_5$, pyro-$ThO_2 \cdot V_2O_5$, and meta-$ThO_2 \cdot 2V_2O_5$ vanadates at pH ranges from 7.50 to 6.00, 6.00 to 4.80, and 4.80 to

3.50, respectively. The precipitation of thorium orthovanadate was found to be quantitative and amperometric titrations offered a simple and rapid method for determination of Th^{4+} in solutions at suitable concentrations and pH ranges. The investigation was undertaken with a view to investigate compositions of thorium poly-vanadates more precisely by means of amperometric titrations. (auth)

10787 ELECTRON PROBE MICRO-ANALYSIS OF IRRADIATED UO_2. Bradbury, B. T.; Demant, J. T.; Martin, P. M.; Poole, D. M. (Atomic Energy Research Establishment, Harwell, Eng.). J. Nucl. Mater., 17: 227-36(Nov. 1965). (AERE-R-4845).

A white globular second phase was observed in UO_2 irradiated to 4.6% burnup at an estimated center temperature of 1500°C, and in the columnar grain growth region of UO_2 irradiated to 0.3% burnup at an estimated center temperature of 1970°C. An electron probe microanalyzer was used to identify the major constituents of these precipitates. The solid fission product elements molybdenum, ruthenium, cerium, and barium were detected in localized concentrations. (auth)

10788 THE DESAGA SCANNER: A NEW SCANNER FOR RADIOACTIVE SUBSTANCES ON THIN-LAYER CHROMATOGRAMS. Wilde, P. F. (Inst. of Animal Physiology, Cambridge, Eng.). Lab. Pract., 13: 741-5 (1964).

The instrument consists basically of three parts: a scanner that includes a gas-flow detector and preamplifier, a rate meter with power pack, and a pen recorder. It was tested for sensitivity, resolution, reproducibility, and rectilinearity of response. Universally labeled [^{14}C] linolenic acid and [9,10-^{3}H]-stearic acid, which were methylated with diazomethane, were used as test substances. The instrument, which can be used either for scanning or for recording radioactivity introduced into the gas stream through the detector, was found to be accurate and reliable; an attachment is available for simultaneous scanning of both sides of paper strips. (Anal. Abstr., 12: (Dec. 1965))

10789 THE ROLE OF THE RESONANCE ACTIVATION INTEGRAL IN THE ACTIVATION ANALYSIS DETERMINATION OF SILVER. Lux, F.; Koehler, W. (Technische Hochschule, Munich). Nukleonik, 7: 480-4(Oct. 1965). (In German).

In connection with the activation analysis of the silver content of cadmium, the determination of the resonance activation integral for the formation of ^{110m}Ag from ^{109}Ag is necessary. By simultaneous irradiation of gold and silver samples, the value $I(0)^{109}Ag \rightarrow {}^{110m}Ag = 47.5 \pm 6.6$ b was determined. The as yet unclear relations of the resonance absorption integral and the resonance activation integral of ^{109}Ag were discussed. (tr-auth)

10790 TIME-OF-FLIGHT MASS SPECTROMETRY AND ITS APPLICATIONS. PART I. Couchet, G.; Zvenigorosky, A. (Univ. de Toulouse). Rev. Quest. Sci., 136: 167-84(Apr. 1965). (In French).

The principle of the time-of-flight mass spectrometer is discussed. Its advantages are the rapidity with which a spectrum may be obtained, relative invariance between peak heights, and the simple dependence of the resolving power. Its main disadvantage is the low resolving power attainable. The history of the instrument is reviewed. The functioning of the ion source is described, and the method of calculating the time of flight of an ion of a specific given charge is outlined as well, with a numerical example given. The resolving power is discussed. A method for calculating the variation in time of flight of ions of mass M is given. Resolution masses of four types are described: energy-resolved mass, space-resolved mass, minimally resolved mass, and totally resolved mass; typical values for these are 210, 530, 150, and 150 to 210, respectively. The final value, total resolution, is the one that, in practice, characterizes the mass spectrometer. (BBB)

10791 TIME-OF-FLIGHT MASS SPECTROMETRY AND ITS APPLICATIONS. PART II. Couchet, G.; Zvenigorosky, A. (Univ. de Toulouse). Rev. Quest. Sci., 136: 334-50(July 1965). (In French).

The detection and amplification of ions is discussed. An electron multiplier in which there are parallel bands of semiconductor material separated by several mm is described. It has low response time, wide passing band, low noise level, and, under typical conditions, a gain of 10^7. Final detection systems described include: the oscilloscopic display method, digital detection, and analog detection. Detection by the analog method is discussed in connection with the semiconductor multiplier. Application of time-of-flight mass spectrometry to several areas of research, the detection of free radicals, utilization with a gas chromatograph, measurement of ionization potentials, study of ion-molecule reactions, and analysis of residual gas in high vacuums, is reviewed. (38 references). (BBB)

10792 THE USE OF EDTA FOR RADIOMETRIC DETERMINATION OF TRACES OF METALS BY MEANS OF ELECTROPHORESIS. Knobloch, V.; Stary, J. (Joint Inst. of Nuclear Research, Dubna, USSR). Zh. Anal. Khim., 20: 1160-3(1965). (In Russian).

The possibility of using EDTA for radiometric determination of traces of metals by means of electrophoresis is discussed. A method was developed for the determination of as little as 10^{-10} g of radioactive yttrium and europium. (auth)

10793 A METHOD OF TWO STANDARDS FOR ELIMINATING SYSTEMATIC ERRORS IN THE MEASUREMENT OF ISOTOPIC COMPOSITION ON A MASS-SPECTROMETER. Ustinov, V. I.; Galimov, E. M.; Grinenko, V. A. (Vernadskii Inst. of Geochemistry and Analytical Chemistry, Academy of Sciences, USSR. Inst. of Petroleum Chemistry and Gas Industry, Moscow). Zh. Anal. Khim., 20: 1180-4(1965). (In Russian).

By analysis of systematic errors occurring during the determination of isotopic ratios due to calibration of the value of the difference between the isotopic compositions of the sample and the standard at the last stage of recording (in the compensation scheme), it was concluded that it is necessary to calibrate at the inlet of the mass spectrometer using two standards. Calculation formulas and an experimental record chart of isotopic ratios obtained by the two standards method are given. (auth)

10794 A GRAVIMETRIC METHOD FOR THE DETERMINATION OF LARGE AMOUNTS OF NIOBIUM AND TUNGSTEN WHEN THEY ARE PRESENT TOGETHER. Sheskolskaya, A. Ya. (Baikov Inst. of Metallurgy, Moscow). Zh. Anal. Khim., 20: 1250-1(1965). (In Russian).

An accurate gravimetric method is suggested for determination of niobium and tungsten in binary Nb–W alloys. The method is based on the precipitation of niobium with ammonia at pH > 10 in the presence of complexone III. After the niobium is separated tungsten is precipitated with tannin and β-naphthoquinoline in a weakly acid medium. (auth)

10795 THE EVOLUTION OF THE ACCURACY OF ISOTOPIC ANALYSIS BY THERMAL IONIZATION FROM 2 PERCENT TO 0.02 PERCENT. Shields, W. R. (National Bureau of Standards, Washington, D. C.). Vienna, International Atomic Energy Agency, 1965, Preprint No. SM-67/41, 13p. (CONF-650803-44). ORINS.

From IAEA Symposium on Nuclear Materials Management, Vienna.

The parameters that affect the precision, both internal and external, of an isotopic analysis were studied. The magnitude of the effects of some of these parameters on the analysis of transuranic elements is shown. The effects of pH, concentration, and composition or purity on an analysis are discussed. By changes in the analytical method or by modification of the mass spectrometer, the magnitudes of the effects can be altered from a point at which the bias terms are generally additive to one at which they are compensating. Provable accuracy statements are contingent on identification and control of all bias factors, including those involved in sample preparation and analytical procedure as well as those involving the collector system and measuring circuit. A table of the best estimates of the isotopic compositions of 16 uranium isotope standards distributed by

the National Bureau of Standards is presented. The current level of analytical proof of these values is given along with a discussion of the work (in progress) that is necessary to change the analytical precision statements to accuracy statements. (auth)

10796 DETERMINATION OF ^{239}Pu CONTENT IN IRRADIATED NUCLEAR FUEL BY NEUTRON TRANSMISSION TECHNIQUE. Weinzierl, P.; Putz, F.; Al-Kafaji, T. (Oesterreichische Studiengesellschaft fuer Atomenergie GmbH, Vienna). Vienna, International Atomic Energy Agency, 1965, Preprint No. SM-67/6, 11p. (CONF-650803-50). ORINS.

From IAEA Symposium on Nuclear Materials Management, Vienna.

A procedure for determination of the ^{239}Pu content in nuclear fuel is discussed. The suggested method takes advantage of the fact that a neutron beam passing through a sample containing an appreciable amount of ^{239}Pu is highly attenuated in the energy region that is at the lowest resonance at 0.3 ev. In this energy region the total microscopic cross section of ^{239}Pu may be assumed to surpass the total microscopic cross sections of the other materials contained in the sample. Therefore, the sensitivity of the neutron transmission to changes of the ^{239}Pu concentration is increased in the energy range around 0.3 ev. To simplify calculation of the attenuation of the neutron beam, all the materials but ^{239}Pu can be replaced by a single fictitious absorber. For the total cross section of this absorber a reasonable energy dependence is assumed (the validity of this approximation must be examined by experiments). In this way the problem is reduced to the determination of two constants. This determination can be made by means of two transmission measurements; one of these is performed with well-thermalized neutrons, the other one with neutrons of energies covering a small range in the area of 0.3 ev. In both cases the neutron attenuation is calculated by numerical integration as a function of the two unknown constants. The latter ones can be determined by comparison with the results of the measurements. (auth)

10797 AN APPRAISAL OF METHODS FOR PLUTONIUM AND THEIR APPLICATIONS TO THE ANALYSIS OF NUCLEAR MATERIALS. Milner, G. W. C.; Phillips, G. (Atomic Energy Research Establishment, Harwell, Eng.). Vienna, International Atomic Energy Agency, 1965, Preprint No. SM-67/51, 16p. (CONF-650803-30). ORINS.

From IAEA Symposium on Nuclear Materials Management, Vienna.

Methods available for determination of the plutonium content of nuclear materials are reviewed. For milligram amounts of plutonium the available methods include differential spectrophotometry using the color of PuIII, gravimetry based on PuO_2, gamma counting, and redox methods including potentiometric and amperometric titrations and controlled-potential coulometry. Alpha counting, isotopic dilution, and polarographic methods are suitable for microgram amounts. The advantages and limitations of the above methods are described and accuracy, precision, sensitivity, and features of special interest are discussed. The use of anion exchange and reverse-phase chromatographic techniques for separation of plutonium from other sample constituents is discussed with emphasis on their suitability for radioactive samples. Consideration is given to the problems in successful application of these methods to the analysis of plutonium alloys, ceramics, and cermets in various systems containing uranium, thorium, iron, chromium, molybdenum, cerium, and cobalt. Difficulties occurring in the dissolution of samples and in the adjustment of the plutonium to the required valency state are described. The respective merits of dissolving in mixtures of common mineral acids and with the aid of fusion techniques are commented upon with examples. Outlines of procedures, together with analytical results for typical samples, are given for the analysis of Pu–U, Pu–Ce–Co, and Pu–U–Mo alloys, Pu–U oxides and carbides, and Pu–U carbide cermets with Fe, Mo, and Cr. (auth)

10798 PLASMA JET GENERATOR. Takei, Sachio; Yamamoto, Manabu (to Kabushiki Kaisha Hitachi Seisakusho). U. S. Patent 3,225,245. Dec. 21, 1965. Priority date Dec. 16, 1961, Japan.

A plasma jet generator is described for use as the light source and sample atomizer for spectroscopic analysis. The generator includes a hollow electrode having a nozzle portion and a rod-shaped electrode disposed around the central portion of the hollow electrode and pointed toward the nozzle portion. A first means is provided for creating an arc discharge between the tip of the rod-shaped electrode and the inner wall surface of the hollow electrode. A first inactive gas current introduced into the space between the two electrodes in the direction toward the nozzle portion, and pointed toward the tip of the rod-shaped electrode is provided for introducing a second gas current in the opposite direction to the first inactive gas current so as to cause suppression of the fluctuation of the path of the arc discharge and to effect mixture of the two gases current to the hottest point of the arc. (B.L.M.)

Inorganic and Physical Chemistry

Refer also to abstracts 10997, 11255, 11256, 11272, and 11938.

10799 (AD-625735) THE THERMODYNAMICS OF THE GRAPHITE–CARBON VAPOR SYSTEM. Krieger, F. J. (RAND Corp., Santa Monica, Calif.). Dec. 1965. Contract AF49(638)-1700. 32p. (RM-3326-1-PR). CFSTI $2.00 cy, $0.50 mn.

A thermodynamic investigation of graphite was made over a range of temperatures up to 6000°K and pressures up to 10^3 atmospheres. Two sets of equilibrium composition equations were used: one representing a pure gas phase, the other a heterogeneous system of gas and solid carbon. The heterogeneous chemical system was unique in that, although it involves two phases and a variety of chemical species, it comprises only one chemical element. The mathematical solution of the system of equations representing the heterogeneous chemical system was subject, therefore, to the physical constraint of one degree of freedom. The results of the computational program are presented in both tabular and graphic form. The latter is a conventional Mollier diagram in which specific enthalpy is plotted against specific entropy with cross plots of temperature, pressure, molecular weight, and moles of condensed carbon. (auth)

10800 (ANL-7113) A METHOD FOR AUTOMATIC ANALYSIS OF DATA ON THE KINETICS OF FAST CHEMICAL REACTIONS IN THE FORM OF PICTURES OF OSCILLOSCOPE TRACES. Sauer, Myran C. Jr. (Argonne National Lab., Ill.). Oct. 1965. Contract W-31-109-eng-38. 15p. Dep. mn. CFSTI $1.00 cy, $0.50 mn.

The CHLOE system for direct digitization of photographic data was used in conjunction with the Control Data Corporation 3600 Computer system to analyze data, in the form of pictures of oscilloscope traces, on the kinetics of fast chemical reactions. All measurements and analytical processes were done by machine in a completely automatic method. (auth)

10801 (CEA-R-2777) CONTRIBUTION A L'ETUDE DU SYSTEME URANIUM–HYDROGENE [Theses]. (Contribution to the Study of the Uranium–Hydrogen System [Thesis]). Chevallier, Jacques (Commissariat a l'Energie Atomique, Grenoble (France). Centre d'Etudes Nucleaires). 1965. 54p. Dep. mn.

Submitted to Grenoble Univ. (France).

The $U-H_2-UH_n$ equilibrium was investigated at pressures below one atmosphere and at temperatures lower than 430°C. The hydride obtained at equilibrium is deficient in hydrogen ($UH_{n<3}$), the hydrogen deficit increasing as the temperature rises. The thermodynamic increases relative to the formation and the saturation of the hydride and to the formation of a hydrogen vacancy were derived from the equilibrium pressures. A U–H phase diagram model was proposed. The hydrogenation of U–UC alloys was also examined at pressures below one atmosphere with regard

to the equilibrium: (free U + UC) – H_2–UH_n. The equilibrium conditions were found different from that observed for pure uranium. 86 references are cited. (auth)

10802 (COO–1020–9) CHELATION AND OLATION REACTIONS OF METAL IONS IN AQUEOUS SOLUTION. PART III. A POTENTIOMETRIC STUDY OF THE INTERACTION OF U(IV) WITH VARIOUS LIGANDS IN AQUEOUS SOLUTION. Progress Report. Carey, G. H.; Martell, A. E. (Illinois Inst. of Tech., Chicago). 1964. Contract AT(11-1)-1020. 19p. Dep. mn. CFSTI $1.00 cy, $0.50 mn.

Potentiometric data provide ample evidence that U(IV) reacts with multidentate ligands in aqueous solution to produce stable metal chelates when the number of donor groups provided by the ligand is sufficient to completely satisfy the coordination requirements of the metal ion (e.g., the 1:1 U(IV)-DTPA, 1:2 U(IV)-NTA systems). When the number of donor groups is less than eight, or are so arranged that less than eight groups can be completely effective, chelate formation at low pH is followed by successive hydrolysis steps, attendant with polymerization to polynuclear chelates with olate (hydroxo) bridges. The results were compared with thorium. (P.C.H.)

10803 (EUR–2466.e) STUDIES ON MOLTEN SALTS. Plenary Lectures of the Symposium Discussions on Molten Salts, September 16–17, 1964. (Liege Univ. (Belgium)). 1965. 80p. (CONF-640922). Dep. mn.

Five articles on molten salts are included; each was abstracted separately in NSA. (P.C.H.)

For abstracts of individual papers see: 10804–10808.

10804 (EUR–2466.e, pp 9-19) PROPERTIES OF IONIC LIQUIDS AND MIXTURES. Ketelaar, J. A. A.; Dammers-de Klerk, A. (Amsterdam Univ. (Netherlands)).

Differences and similarities of ionic and molecular liquids are discussed, and results obtained in a study of molten mixtures of silver and alkali nitrates are presented. By means of a stable and reversible nitrate electrode, emf data were obtained which, combined with thermochemical data, permitted a reliable estimation of the excess entropy for such mixtures. The excess entropy is by no means small, compared to the excess enthalpy. This conclusion holds true for fairly ideal systems and for pronouncedly non-ideal ones. (auth)

10805 (EUR–2466.e, pp 21-30) ION DIFFUSION AND MIGRATION IN MOLTEN SALTS. ATTEMPTS AT INTERPRETATION BY MEANS OF A MODEL. Perie, J.; Lantelme, F.; Chemla, M. (College de France, Paris).

The results of three types of experiment concerning ion transfer in molten salts are described; binary systems of alkaline salts with common anion, subjected to counterflow electromigration, show the existence of a critical composition at which the migration velocities of the two cations become equal. Measurements of transport numbers in the same systems show that the curves, representing cation mobility in function of the composition or of the temperature of the mixture, generally intersect. On the other hand, variations in the diffusion coefficients of these same cations are parallel. Depending on temperature or concentration, Einstein's formula appears sometimes to be exactly confirmed; in other cases, discrepancies between experimental and theoretical values are as much as 100%. These results as a whole are interpreted by a model of ionic liquid structure involving association equilibria and competition between cations for group formation with the anions. (auth)

10806 (EUR–2466.e, pp 31-8) ION MOBILITIES IN MOLTEN SALTS. Klemm, A. (Max-Planck-Institut fuer Chemie, Mainz (West Germany)).

Mass and electric transport properties in molten salts are discussed in the light of the most recent experimental acquisitions. The comparison between diffusion coefficient and electric conductivity by means of the Nernst-Einstein equation showed discrepancies from the value expected for non-associated liquids. A method is outlined for evaluation of the type and degree of association. (auth)

10807 (EUR–2466.e, pp 39-57) CHEMICAL EQUILIBRIA IN MOLTEN SALTS. Blander, M. (North American Aviation, Inc., Thousand Oaks, Calif. Research Center).

The use of molten salt thermodynamics for calculating chemical equilibria is discussed. The various theories on molten salt structures are analyzed and their previsions compared with experimental data. The discussion involves binary systems with common anion, reciprocal systems consisting of two anions and two cations, and ternary systems having one single anion. Few specific chemical reactions are finally discussed in detail. (auth)

10808 (EUR–2466.e, pp 59-80) CONTRIBUTION TO THE STUDY OF MOLTEN SALTS. Murgulescu, I. G.; Sternberg, S. (Academie R. P. R., Bucharest. Institutul de Cercetari Chemice).

A review is given of the research on molten salts carried on at the Institute of Physical Chemistry of Bucharest. Thermodynamic quantities were derived by means of emf measurements, melting diagrams, vapor pressure and calorimetric determinations. A discussion of the results follows. The viscosity of single salts and their mixtures was also investigated in order to study the mass transport in these systems and to obtain a better understanding of their constitution. 49 references are cited. (auth)

10809 (EUR–2531.f) PREPARATION ET PURIFICATION DU GERANYLLINALOL TRITIE. (Preparation and Purification of Tritiated Geranyllinalol). Verly, W. (Liege Univ. (Belgium)). Mar. 13, 1965. 8p. Dep. mn.

Purification of geranyllinalol on silica gel did not seem sufficient to give radiochemical purity when the substance was tritium labeled by exchange following Wilzbach's method. Other studies are also reported. Acetyl-L-phenylalanyl-L-glutamic acid and its D-L diastereoisomer have quite different partition coefficients between water and butanol–chloroform. Tritiated carnitine and crotonbetaine, with specific activities of 0.9 mC/m mole were kept without appreciable radiolysis at –20°C during 12 months. Chemically pure ethyl methanesulfonate was prepared with 100% yield from ethyl iodide and silver methanesulfonate. (auth)

10810 (JEN–153-DMa/I-19) ESTUDIO DE LIMPIEZA DE FILTROS POROSOS EN REACTORES DE LECHO FLUIDIZADO. (Cleaning of Porous Filters in Fluidized Bed Reactors). Rodrigo Otero, A.; Sancho Rod, J. (Junta de Energia Nuclear, Madrid (Spain). Division de Materiales). 1965. 33p. Dep. mn.

The optimum conditions for the cleaning of filters by the reverse flow of gas are established. The reasons for which it was previously impossible to control the pressure in a fluidized-bed calcination reactor are analyzed, and a criterion is established for calculating the optimum flow for the efficient cleaning of a porous filter by this technique. (D.C.W.)

10811 (LA-DC–6806) THE HEAT CONTENT OF MOLTEN TIN. Levinson, L. S. (Los Alamos Scientific Lab., Univ. of California, N. Mex.). [1963]. Contract W-7405-eng-36. 7p. Dep. mn. CFSTI $1.00 cy, $0.50 mn.

Using a drop calorimeter, the heat content of molten tin was measured between 1222 and 1745°K. Values for the heat content ranged from 7655 to 11,243 cal $mole^{-1}$. (J.G.B.)

10812 (NAA-SR-Memo–11569) INTERACTION OF MERCURY AND METAL HYDRIDES. Korst, W. L. (Atomics International, Canoga Park, Calif.). Aug. 31, 1965. Contract AT(11-1)-Gen-8. 6p. Dep. mn. CFSTI $1.00 cy, $0.50 mn.

A brief review of the literature concerning the interaction of mercury with metal hydrides is given. Particular emphasis is given to the rare earth hydrides, which possess many of the characteristics typical of transition metal hydrides. Mercury wets transition metal hydrides, apparently forming dispersions rather than true solutions. The rare earth hydride dispersions in mercury evolve hydrogen when heated, and react vigorously with air and

with water. Formation of ternary compounds (R–H–Hg) on the surface of rare earth hydride particles in mercury apparently occurs. (auth)

10813 (ORNL–3906) A METHOD FOR PURIFICATION AND GROWTH OF KCl SINGLE CRYSTALS. Butler, C. T.; Russell, J. R.; Quincy, R. B. Jr.; LaValle, D. E. (Oak Ridge National Lab., Tenn.). Feb. 1966. Contract W-7405-eng-48. 39p. Dep. mn. CFSTI $2.00 cy, $0.50 mn.

A method is described by which large, uniform KCl crystals of high purity can be obtained, starting with reagent grade material. Chemical means were employed to produce pure polycrystalline ingots which were then used to grow single crystals by pulling from the melt under semi-clean room conditions. The resulting crystals contain less than 1 μg/g of any foreign alkali or halide element, show OH^- concentrations of less than 10 ppB and conductivity knees which indicate typically less than 300 ppB total heterovalent cation content. Analytical methods are discussed and analyses of these as well as crystals from various commercial sources are given. (auth)

10814 (SCL-DC-65-96) QUALIFICATION TESTS OF SPRAY-DEPOSITED AND LIGHT-INITIATED SILVER ACETYLIDE–SILVER NITRATE EXPLOSIVE. Final Report. Langner, Carl G.; Hoese, Fred O. (Southwest Research Inst., San Antonio, Tex.). Jan. 1966. Contract AT(29-1)-789. 119p. Dep. mn. CFSTI $4.00 cy, $0.75 mn.

For Sandia Corp., Livermore, Calif.

Qualification tests on spray-deposited and light-initiated silver acetylide–silver nitrate explosive are described. The purpose of the tests was to demonstrate the merits of this explosive as a predictable energy source for flyer plate tests and as a direct means of impulsively loading structures. The test results provided values of impulse, pulse duration, and detonation simultaneity, as well as impact sensitivity and drying rate data, versus explosive coating thickness and density. (auth)

10815 (UCRL–16338) SPECTRA OF CaO [Thesis]. Hauge, Robert H. (Lawrence Radiation Lab., Univ. of California, Berkeley). Oct. 1965. Contract W-7405-eng-48. 49p. Dep. mn. CFSTI $2.00 cy, $0.50 mn.

Photographic extreme-infrared bands of CaO were characterized by a vibrational and rotational analysis as part of a known $A^1\Sigma - X^1\Sigma$ transition. Isotopic shifts with ^{18}O were measured for the infrared and green bands. Head measurements for the orange system are given. A discussion of low-lying levels of CaO and a way of determining the absolute v numbering in levels which perturb the $A^1\Sigma$ state are presented. (auth)

10816 (NASA-TT-F-285) CHEMICAL THERMODYNAMICS IN NONFERROUS METALLURGY. VOL. III. THERMODYNAMICS OF TUNGSTEN, MOLYBDENUM, TITANIUM, ZIRCONIUM, NIOBIUM, AND TANTALUM AND OF THEIR MORE IMPORTANT COMPOUNDS. Gerasimov, Ya. I.; Krestovnikov, A. N.; Shakhov, A. S. Translation of Khimicheskaya Termodinamika v Tsvetnoi Metallurgii. Spravochnoe Rukovodstvo. Tom 3. Termodinamika Vol'frama, Molibdena, Titana, Tsirkonoiya, Niobiya, Tantala i ikh Vozhneishikh Soedinenii, Metallurgizdat, Moscow, 1963. 245p. (TT–65–50111). CFSTI $6.00 cy, $1.25 mn.

Information is given on the thermodynamic properties of W, Mo, Ti, Zr, Nb, and Ta and their compounds, including oxides, halides, carbides, and in some cases nitrides, borides, sulfides, silicides, and hydrides. 796 references are cited. (P.C.H.)

10817 THE LATTICE CELL AND SPACE GROUPS OF EuOOH. Baernighausen, H. (Univ., Freiburg i. B.). Acta Crystallogr., 19: 1047(Dec. 10, 1965). (In German).

Crystallographic data are presented to show that the powder diagram of EuOOH can be interpreted on the basis of a small monoclinic cell. The following lattice constants were determined: a = 6.109 ± 0.005, b = 3.748 ± 0.003, and c = 4.347 ± 0.003 Å and β = 108.6 ± 0.2. EuOOH was assigned to the space group $P2_1/m$. (J.S.R.)

10818 PRODUCTION AND CRYSTAL DATA OF α-$LiEuO_2$. Baernighausen, H. (Univ., Freiburg i. B.). Acta Crystallogr., 19: 1048-9(Dec. 10, 1965). (In German).

α-$LiEuO_2$ can be prepared by heating equal molecular mixtures of Eu_2O_3 and Li_2O with LiCl in a high vacuum at 650°C or by heating Li_2O and Eu_2O_3 in the mole ratio of 2:1 for 8 hr at 600°C. The α-$LiEuO_2$ crystallizes in the monoclinic space grou $P2_1/c$ with the lattice constants a = 5.6815 ± 0.005, b = 5.9885 ± 0.0005, and c = 5.6221 ± 0.0005 Å and β = 103° 10′ ± 3′. (J.S.R.)

10819 COMPARISON OF THE HYDROGEN AND DEUTERIUM BONDS BY ULTRAVIOLET ABSORPTION SPECTROMETRY. Bellon, Louis; Luis-Abboud, Jose (Faculte des Sciences, Rabat, Morocco). Compt. Rend., 261: 3106-8(Oct. 18, 1965). (In French).

The association reactions (1) $Cl_3CD + A \rightleftharpoons Cl_3CD \ldots A$ and (2) $Cl_3CH + A \rightleftharpoons Cl_3CH \ldots A$ in which A designates a proton acceptor were compared by differential spectrometry in an inert solvent S. Whatever the nature of A (ether oxide, ketone, nitrile, or amide) and of S (n-heptane, cyclohexane, tetrachloromethane), the ratio K_D/K_H of the association constants of the reactions (1) and (2) was found very close to 1:1.01 ± 0.04 at 21°C. The difference of the absolute values of the association enthalpies is $|\Delta H_D| - |\Delta H_H| = 0.3 \pm 0.3$ kcal/mole. (tr-auth)

10820 KINETIC ISOTOPIC EFFECT IN THE REACTION OF CCl_3 RADICALS WITH MOLECULAR HYDROGEN. Hautecloque, Simone (Univ., Paris). Compt. Rend., 261: 3613-16(Nov. 3, 1965). (In French).

The reactions involving removal of an atom of hydrogen or deuterium from H_2 or D_2 molecules by $\dot{C}Cl_3$ radicals, produced by photolysis of bromotrichloromethane, were studied. From 500 to 573°K the ratio of the velocity constants observed k_{H_2}/k_{D_2}, varied from 3.6 to 3.1. The isotopic effect was calculated by the Bigeleisen method; the Johnston BEBO method made it possible to evaluate the properties of the activated complex and the activation energy of each of the two reactions studied. Good agreement was obtained between the theoretical and experimental values. (tr-auth)

10821 CONTRIBUTION TO THE STUDY OF THE IONIZATION OF CHROMIUM FLUORIDE AND CHROMIUM OXIDE IN SOME FUSED CHLORIDES AND FLUORIDES. Mergault, Pierre; Duffault-Devred, Marylis (Laboratoire de Physique-Enseignement, Paris). Compt. Rend., 261: 4392-5(Nov. 22, 1965). (In French).

Anhydride and hydrated La_2O_3 gives LaOF with fused NaF just as does hydrated La_2O_3 with fused LiF. The hydrated oxide reacts slightly with fused NaCl and more with fused KCl to give LaOCl. Anhydride or hydrated La_2O_3 added to a solution of CrF_3 in fused NaCl, KCl, NaF, or LiF gives either Cr_2O_3, if CrF_3 is in excess or $LaCrO_3$, or Cr_2O_3, if CrF_3 is deficient. (tr-auth)

10822 STRUCTURE AND PROPERTIES OF THE INTERMEDIARY PHASES OF SYSTEMS FORMED BY LIME WITH RARE EARTH OXIDES OF THE TYPE $C(Tl_2O_3)$. Queyroux, Francine (CNRS, Vitry-sur-Seine, France). Compt. Rend., 261: 4430-2(Nov. 22, 1965). (In French).

The systems formed by lime with the oxides of Dy, and Yb are described. The samples were prepared by solid-state reactions between anhydrous calcium carbonate and the M_2O_3 oxide. Equilibrium diagrams of M_2O_3–CaO system were obtained. There was a solid monoclinic solution whose range of homogeneity extended from 20 to 30 mole % CaO at 1800°C and ended at 1500°C with the eutectic point corresponding to the composition 72% Dy_2O_3–28% CaO. The dissolution of lime in the Yb_2O_3, also caused formation of a β monoclinic phase although this form did not exist for the pure oxide. The solid solution was stable at the fusion temperature at a region extending from 33 to 45 mole % CaO. The limit of existence and the structure of the compounds CaM_2O_4, $Ca_2M_2O_5$, and $Ca_3M_2O_6$, where M is the rare earth, were determined and reported. (J.S.R.)

10823 ABSORPTION SPECTRA OF WATER AND HEAVY WATER IN THE ULTRAVIOLET. Larzul, Helene;

Gelebart, Francois; Johannin-Gilles, Andree (Univ., Brest, France). Compt. Rend., 261: 4701-4(Nov. 29, 1965). (In French).

The extinction coefficient of water and heavy water were determined experimentally between 4000 and 2300 Å. The results are given in the form of curves. (tr-auth)

10824 CONSTITUTION IN SOLUTION OF COMPLEX CARBONATES OF THE RARE EARTHS. Fromage, Francine; Gobron, Roland (Faculte des Sciences, Reims, France). Compt. Rend., 261: 4764-6(Nov. 29, 1965). (In French).

It is shown using cryoscopic measurements that complex carbonates of the rare earth elements correspond in solution to the general formula $[M(CO_3)_4]^{5-}$. (tr-auth)

10825 COMPLEXES OF URANYL PERCHLORATE WITH NEUTRAL LIGANDS. Vdovenko, V. M.; Mashirov, L. G.; Suglobov, D. N. (Inst. of Chemical Studies, Academy of Sciences, USSR). Dokl. Akad. Nauk SSSR, 163: 100-2(July 1, 1965). (In Russian).

The large perchlorate anion is more easily and more completely substituted in the coordination sphere of the central ion by other ligands than most of the simpler ions; therefore, the uranyl ion may be expected to react strongly with electron-donor molecules. As a polyatomic anion, the perchlorate ion follows a mono- or bidentate coordination; determination of this factor from the infrared bands makes it possible to derive the coordination number of UO_2^{2+}. Strong organic bases, such as pyridine and antipyrine, weak donors, such as nitromethane, and intermediate bases, such as camphor, tributyl phosphate, dibutyl ether, methanol, and acetonitrile were used as ligands. It was found that in uranyl perchlorate complexes, the uranyl ion has a coordination number of 5. The distance of 2.41 Å between O atoms in the ClO_4^- molecule is probably close to the upper limit at which complexes with a coordination number of 6 are still stable. The degree of substitution of ClO_4^- depends on the basicity of the ligands and the polarity of the medium from which the compound is crystallized. When precipitating the complexes from pyridine, methanol, and water, the anions are completely replaced in the outer sphere. The alkalinity and polarity factors prevailing in the case of acetonitrile suffice only to cause a partial replacement of the ClO_4^-. (TTT)

10826 GROWING OF CERIUM ALUMINATE SINGLE CRYSTALS. Zonn, Z. N. (Inst. of Silicate Chemistry, Academy of Sciences, USSR). Izv. Akad. Nauk SSSR, Neorg. Mater., 1: 1128-9(July 1965). (In Russian).

To prepare cerium aluminate single crystals, three problems had to be solved: creation of a reducing atmosphere under conditions permitting crystallization in accordance with a predetermined heating schedule; selection of a solvent stable in this atmosphere; and selection of crucible material stable in this atmosphere and inert toward the solvent. The crucible (made of molybdenum, nickel, or fused graphite) was placed in a corundum capsule and covered with a mixture of activated carbon and Kryptol. Potassium fluoride was used as the solvent. The material to be crystallized was prepared in three ways: combined grinding of CeO_2 and Al_2O_3 in stoichiometric proportion; coprecipitation with ammonia from solutions of cerium nitrate and aluminate nitrate, and roasting to drive off the ammonium salts; and preliminary synthesis of $CeAlO_3$ at 1600°C in an ammonia atmosphere. A mixture 30% $CeAlO_3$ and 70% KF was used, and the crystallization was carried out by raising the temperature to 1300°C, then lowering it at 4 to 5 degrees per hour to 840°C. A radiogram of the $CeAlO_3$ single crystals obtained is given. (CFSTI)

10827 CONCERNING INTERPRETATION OF THE ABSORPTION SPECTRA OF SOME ORGANIC URANYL COMPLEXES. Shevchenko, A. N.; Umreiko, D. S. (Belorussian State Univ., USSR). Izv. Akad. Nauk SSSR, Ser. Fiz., 29: 1349-52(Aug. 1965). (In Russian).

The absorption and luminescence spectra of a number of uranyl complexes were investigated, and results obtained for dinitrouranyl and trinitrouranyl ions are reported. The complex trinitrouranyl compounds were prepared in anhydrous acetone or cyclohexanone solutions of uranyl nitrate hexahydrate, using tetraethylammonium nitrate or tetrabutylammonium nitrate as NO_3^- donors. The absorption spectra at room temperature of acetone solutions of uranyl tetraethylammonium nitrate and uranyl nitrate are compared. In the long wavelength region the absorption bands of the complex ion appeared in the same positions as those of the nitrate, but were much more prominent. The complex ion showed absorption bands in the ultraviolet, where the absorption spectrum of the nitrate is continuous. The frequency separations of the absorption bands are analyzed and it is concluded that three partly overlapping electron transitions are involved. The absorption and luminescence spectra of uranyl dinitrate and uranyl trinitrate were recorded at several temperatures between +20 and −183°C and are presented graphically. The trinitrate spectra are much more strongly temperature dependent than the dinitrate spectra. Two series of emission bands with different temperature behavior were observed in the trinitrate spectra, and it is concluded that two different complexes are present. This conclusion is supported by the different temperature dependences of the luminescence quantum efficiency and the fluorescence lifetime. (ATD)

10828 ON THE INFRARED SPECTRA OF LANTHANUM GERMANATES. Tenisheva, T. F.; Lazarev, A. N.; Pavlyukevich, T. M. (Inst. of Chemistry of Silicates, Academy of Sciences, USSR). Izv. Akad. Nauk SSSR, Ser. Khim., No. 9, 1553-6(1965). (In Russian).

The infrared spectra of compounds in the $La_2O_3-GeO_2$ system were investigated. Interpretation of the spectra confirmed the structural formulas of the compounds $La_2(GeO_4)O$ and $La_2(Ge_2O_7)$. The hypothesis on the coexistence of germanium tetrahedrans and octahedrans is suggested in the compound with the composition $La_2O_3 \cdot 3GeO_2$ with no analogy to the corresponding silicate system. (tr-auth)

10829 FORCE FIELDS IN KrF_2 AND XeF_2. Coulson, C. A. (Oxford Univ.). J. Chem. Phys., 44: 468-9 (Jan. 15, 1966).

A possible simple explanation is given of the different signs of the bond–bond interaction constants f_{rr} for the vibrations of KrF_2 and XeF_2. The magnitude and sign of f_{rr} are related to the ionization potential of the central rare-gas atom and the net charge distribution in the molecule. In KrF_2 the negative sign may be due to the greater weight of a no-bond structure in a resonance description. (auth)

10830 OPTICAL SPECTRA OF THALLIUM IN GLASSES AS RELATED TO CRYSTALS AND SOLUTIONS. Ghosh, Amal K. (Argonne National Lab., Ill.). J. Chem. Phys., 44: 535-40(Jan. 15, 1966).

The absorption and emission spectra of thallium in fused silica, aluminoborate, and phosphate glasses are similar to those of thallium-doped alkali halides and solutions. The absorption and emission bands in the different systems can be attributed to transitions within the central Tl^+ ions in a center with a $(TlX_n)^{(n-1)-}$ configuration, where X stands for the anions neighboring the Tl^+ ion. There is a shift in the absorption bands with the nature of the anions and cations neighboring the Tl^+ ion. This shift may be related to the chemical shift observed in NMR studies. The thallium centers in glass are possibly present in ordered regions in the glass structure. The minimum size of such an ordered region is estimated to be about 15 Å. There are indications of dimers being formed in thallium-doped fused silica. (auth)

10831 RELATIONS BETWEEN VIBRATIONAL SPECTROSCOPY AND THE ISOTOPE EFFECT ON VAPOR PRESSURES. Gordon, R. G. (Harvard Univ., Cambridge, Mass.). J. Chem. Phys., 44: 576-81(Jan. 15, 1966).

The vapor-pressure difference between isotopes of diatomic molecules is calculated for systems in which the rotational and translational molecular motion show small quantum deviations from classical behavior. Four

different terms contribute significantly to the isotope effect on vapor pressures. (1) The mean-squared force on a molecule in the condensed phase; (2) The mean-squared torque about the center of mass of a molecule; (3) The change in mean-squared torque when the position of the center of mass is changed by isotopic substitution; (4) The mean change in intermolecular potential due to isotopic substitution. The last three of these four terms are shown to be observable separately in the infrared or vibrational Raman spectrum of the system. Therefore by combining the thermodynamic and spectroscopic data, it is possible to derive experimental values of the mean-squared force on a molecule and the mean-squared torque as a function of the point on the molecular axis about which the torque is measured. Thus, the "center of force," the point about which the mean-squared torque is a minimum, may be experimentally determined. The analysis is applied to liquid and solid carbon monoxide. (auth)

10832 STUDIES OF LITHIUM HYDRIDE SYSTEMS. II. SOLID-LIQUID EQUILIBRIUM IN THE SODIUM CHLORIDE–LITHIUM HYDRIDE SYSTEM. Johnson, Carl E.; Wood, Scott E.; Crouthamel, Carl E. (Argonne National Lab., Ill.). J. Chem. Phys., 44: 880-3(Feb. 1, 1966).

Thermal analysis was used to determine the temperature-composition solid-liquid equilibrium diagram for the lithium hydride–sodium chloride reciprocal system. A eutectic composition of 55.2 mole % lithium hydride was observed, which melted at 565.7°C. No evidence for the formation of solid solutions was observed. The values of chemical potential of each component were calculated along the equilibrium curves where the solutions were saturated with respect to the pure solids. The limiting slopes of the saturation curves were consistent with the interpretation that sodium chloride exists primarily as an unionized monomer when dissolved in lithium hydride and that lithium hydride also exists primarily as an unionized monomer when dissolved in sodium chloride. (auth)

10833 STUDIES OF LITHIUM HYDRIDE SYSTEMS. III. SOLID-LIQUID EQUILIBRIUM IN THE LITHIUM BROMIDE–LITHIUM HYDRIDE AND LITHIUM IODIDE–LITHIUM HYDRIDE SYSTEMS. Johnson, Carl E.; Wood, Scott E.; Crouthamel, Carl E. (Argonne National Lab., Ill.). J. Chem. Phys., 44: 884-9(Feb. 1, 1966).

Thermal analysis was used to determine the temperature-composition solid-liquid equilibrium diagrams for the two binary systems, LiBr–LiH and LiI–LiH. Both are simple eutectic systems with no experimental evidence for the formation of solid solutions. Eutectic compositions of 29.7 mole % lithium hydride, mp 453.3°C, and 23.5 mole % lithium hydride, mp 390.8°C, were observed for the bromide and iodide systems, respectively. The values of the chemical potential of each component were calculated along the equilibrium curves where the solutions were saturated with respect to the pure solids. The limiting slopes of the saturation curves were consistent with the interpretation that lithium bromide and lithium iodide both exist primarily as unionized dimers when dissolved in lithium hydride and that lithium hydride exists primarily as an unionized monomer when dissolved in either lithium halide. (auth)

10834 ALKALI-ATOM–HALOGEN-MOLECULE REACTIONS IN MOLECULAR BEAMS; THE SPECTATOR STRIPPING MODEL. Minturn, Robert E.; Datz, Sheldon; Becker, Richard L. (Oak Ridge National Lab., Tenn.). J. Chem. Phys., 44: 1149-59(Feb. 1, 1966). (ORNL-P-1717).

Crossed-molecular-beam techniques was used to study reactive collisions in some alkali metal–halogen systems ($Cs + Br_2$, $K + I_2$, $K + Br_2$, and Rb + IBr). Both the absence of rainbow scattering in elastic-scattering distributions and the magnitude of the reactive collision yield suggested large reaction cross sections in the order of 100 $Å^2$ for all the systems studied. The position and width of the angular distributions of alkali halide product molecules indicated forward scattering in the center-of-mass system with recoil energies close to zero. These observations suggested a stripping mechanism for these reactions, and a model, based on the simplest possible stripping mechanism, was proposed to explain the observations. This model, called spectator stripping, predicted the gross features of the distributions and led to a prediction of the maximum intermolecular distance at which reaction can occur. This corresponded to a reaction cross section of approximately 100 $Å^2$. The effect of electron transfer from the alkali atom to the halogen molecule at large distances is shown to be almost equivalent to spectator stripping for these reactions if the vertical electron affinity of the halogen molecule is used. Even larger cross sections would be predicted if the adiabatic electron affinity were used; however, an evaluation of the probability of adiabatic adjustment of the halogen internuclear distances during the collision time appears to preclude this possibility. (auth)

10835 ^{17}O NMR IN POLYCRYSTALLINE H_2O AND D_2O ICE. Rabideau, Sherman W.; Waldstein, Peter (Los Alamos Scientific Lab., N. Mex.). J. Chem. Phys., 44: 1304-5(Feb. 1, 1966). (LA-DC-7241(Rev.)).

A search was made for the ^{17}O resonance in polycrystalline ice samples of oxygen-17-enriched H_2O and D_2O. The NMR derivative signal was observed in both samples in the absorption as well as in the dispersion mode. Measurements of $H_2{}^{17}O$ polycrystalline ice were made at frequencies of 4, 6, and 8 Mc/sec and the average shifts of the center of the oxygen resonance from Larmor frequency in kilocycles per second were 13.6, 7.6, and 4.4, respectively. The chemical shift was directly proportional to frequency. The peak-to-peak width was somewhat greater for the ^{17}O resonance in the D_2O ice. Therefore, the dipole-dipole contribution must be small. (F.J.H.)

10836 THE PREPARATION AND PROPERTIES OF SOME HYDROXY COMPOUNDS OF BERYLLIUM. Mercer, R. A.; Miller, R. P. (National Physical Lab., Teddington, Eng.). J. Inorg. Nucl. Chem., 28: 61-76(Jan. 1966).

The conditions governing precipitation of the polymorphic forms of beryllium hydroxide from sodium beryllate solutions were established, and the preparation of a series of hydroxy complexes of beryllium with calcium and strontium is described. The thermal decomposition reactions of these compounds were followed by thermogravimetric analysis (TGA), differential thermal analysis (DTA), and x-ray powder photography. (auth)

10837 PHOTOCHROMISM OF METAL OXIDES. I. THE LIGHT SENSITIVITY OF MoO_3 OR WO_3 COPRECIPITATED WITH TiO_2. Chopoorian, J. A.; Dorion, G. H.; Model, F. S. (American Cyanamid Co., Stamford, Conn.). J. Inorg. Nucl. Chem., 28: 83-8(Jan. 1966).

Photoreduction of sodium polymolybdates and tungstates was found to be sensitized by interfacial contact with a critical amount of anatase TiO_2. Reflexion changes at λ_{max} approached 60% and certain of these systems showed reversibility at room temperature. A coloration mechanism is proposed, which involves absorption of light by TiO_2 with subsequent electron transfer to the molybdate or tungstate phase. It was found that there is no new compound formation in the coprecipitated mixture, and that there is a dependence of coloration on the effective concentration of TiO_2. Activating wavelengths for the sensitizing process corresponded to a region of strong ultraviolet absorption for anatase. (auth)

10838 URANATES AS A FORM OF URANYL HYDROLYTIC COMPLEXES. Baran, V.; Tympl, M. (Nuclear Research Inst., Czechoslovak Academy of Sciences, Rez). J. Inorg. Nucl. Chem., 28: 89-98(Jan. 1966).

An attempt was made to relate the properties of uranyl hydrolytic complexes in solutions and hydrolytic precipitates. All data are expressed in terms of the independent parameter NaOH/U (degree of alkalization, i.e., molar ratio of hydroxide added to total uranium). All fundamental properties found may be explained by assuming that hydrolytic complexes in the liquid as well as in the solid phase are not higher than dinuclear, containing nonequivalent hydroxyl groups. (auth)

10839 A THERMOGRAVIMETRIC STUDY OF THE OXIDATION OF PARTICLES OF UO_2 PREPARED FROM U_3O_8 CALCINATED UNDER VARIOUS CONDITIONS. Imris, P. (Nuclear Research Inst., Czechoslovak Academy of Sciences, Rez). J. Inorg. Nucl. Chem., 28: 99-109(Jan. 1966).

The oxidation of UO_2 with a surface area from 1 to 6 m^2/g UO_2 and prepared from U_3O_8 calcinated at temperatures from 610 to 1000°C under various conditions, was studied. The distribution of particles in UO_2 samples was determined with the aid of sedimentation analysis. The activation energy was computed from experimental data obtained during the oxidation of UO_2 to $UO_{2.333\pm0.012}$. A study was also made of the oxidation of narrow fractions of UO_2 prepared from a single sample of UO_2, separated by sedimentation. Great differences were found to exist in the oxidation of such fractions. A study of the oxidation of UO_2 prepared by direct reduction of ADU in H_2 and of various fractions of such UO_2's was carried out for comparison. (auth)

10840 THE EVAPORATION BEHAVIOUR OF NEPTUNIUM DIOXIDE. Ackermann, R. J.; Faircloth, R. L.; Rauh, E. G.; Thorn, R. J. (Argonne National Lab., Ill.). J. Inorg. Nucl. Chem., 28: 111-18(Jan. 1966).

The evaporation behavior of neptunium dioxide in vacuo was studied over the temperature range from 1850 to 2475°K. The gaseous oxides NpO_2 and NpO were the only species observed and the temperature dependence of the major species NpO_2 was measured by mass spectrometry. The total mass effusion rates were determined by collecting known fractions of effusate, which were subsequently assayed by alpha counting of ^{237}Np. The effect on the partial pressures due to the variation of sample size and the fractional amount evaporated indicated that the solid dioxide becomes substoichiometric and produces a bivariant system. The extent of substoichiometry, although unknown, grossly affected the partial pressure of NpO(g) but had an insignificant influence on the partial pressure of NpO_2(g). The experimental results were combined with known and estimated thermodynamic data to yield the standard free energy of formation of NpO_2(g), $\Delta G_f^0(NpO_2,g) = -114{,}000 + 3.5T$, the dissociation energy of NpO_2(g), 14.3 ± 0.3 ev, and an estimated value for the dissociation energy of NpO(g), 7.4 ± 0.3 ev. (auth)

10841 HYDROLYSIS OF URANYL NITRATE SOLUTIONS AT ELEVATED TEMPERATURES. Robins, R. G. (Univ. of New South Wales, Kensington, Australia). J. Inorg. Nucl. Chem., 28: 119-23(Jan. 1966).

A phase diagram is predicted for the system UO_2^{2+}–UO_3–H_2O under hydrothermal conditions and variable pH, from low-temperature thermodynamic data. Experimental results substantiated the existence of the hydrates $UO_3 \cdot 0.5H_2O$, $UO_3 \cdot 0.8H_2O$, $UO_3 \cdot H_2O$, and $UO_3 \cdot 2H_2O$, each of which is shown to be precipitated from uranyl nitrate solutions at high temperature depending on the pH of the initial solution. (auth)

10842 2,2'-DIPYRIDYL COMPLEXES OF RARE EARTHS. III. CHANGE IN FLUORESCENCE INTENSITIES OF EUROPIUM AND TERBIUM CHELATES ON LIGAND SUBSTITUTION. Sinha, S. P. (Cyanamid European Research Inst., Cologny, Switzerland). J. Inorg. Nucl. Chem., 28: 189-93(Jan. 1966).

A semiquantitative comparison of the fluorescence intensities of unsubstituted and para dimethyl substituted dipyridyl chelates of trivalent europium and terbium is presented. The electron-donating methyl groups increased the overall intensity for both europium and terbium chelates. However, in the case of europium the intensity ratio $\eta_{Dimp/Dip}$, for the two transitions from $^5D_0$ to $^7F_1$ and $^7F_2$ levels were not of the same order of magnitude. The $\eta_{Dimp/Dip}$ values for all transitions of terbium were roughly the same. (auth)

10843 RESOLUTION IN CRYSTAL SPECTRA OF URANYL ACETYLACETONATE. Basu, G.; Belford, R. L. (Univ. of Illinois, Urbana). J. Inorg. Nucl. Chem., 28: 252-3(Jan. 1966).

Single crystals of uranyl acetylacetonate were prepared and the spectra examined. The spectrum was similar to that of solutions. Cooling was accompanied by the appearance of sharper absorption bands. Two distinct band maxima and a shoulder were observed beginning at 18.75 kK and spaced apart by approximately 0.750 kK, which corresponded to a typical OUO symmetric stretch frequency for the first excited state. (M.C.G.)

10844 SOLVENT AND TEMPERATURE EFFECTS ON FLUORESCENCE EMISSION OF EUROPIUM β-DIKETONATES. Filipescu, N. (George Washington Univ., Washington, D. C.); McAvoy, N. J. Inorg. Nucl. Chem., 28: 253-9(Jan. 1966).

The effects of temperature and solvent on the fluorescence intensity of several europium β-diketonates with different substituents attached to the chelate ring were studied. The following diketonates were used: dibenzoylmethide, benzoylacetonate, thenoyltrifluoroacetonate, p-methoxydibenzoylmethide, di-p-methoxydibenzoylmethide, m-methoxydibenzoylmethide, and di-m-methoxydibenzoylmethide. The relative intensity of the $^5D_0 \rightarrow {}^7F_2$ transition was determined over the freezing point-boiling point temperature range and the results are presented in diagrams. It was found that the radiationless conversion from the upper singlet to the triplet occurs with about the same efficiency in ordinary liquid solutions as in solids and rigid solutions. In general a higher fluorescence intensity was recorded at the same temperature for the same chelate in a solvent of higher dipole moment. There was a decrease in relative intensity with increasing temperature. (M.C.G.)

10845 RHENIUM NITROGEN FLUORIDE AND RHENIUM TETRAFLUORIDE. LaValle, D. E.; Steele, R. M.; Smith, Wm. T. Jr. (Oak Ridge National Lab., Tenn. Univ. of Tennessee, Knoxville). J. Inorg. Nucl. Chem., 28: 260-3(Jan. 1966).

Preparation of the lower rhenium fluorides by reduction of the hexafluoride or by decomposition of the ammonium salts of the hexafluoro complexes is described. ReNF was formed in the thermal decomposition of $(NH_4)_2ReF_6$. Large quantities of ReF_4 were prepared by reduction of ReF_6. ReF_4 is a medium to dark blue compound very sensitive to decomposition by traces of atmospheric gases. Its chemical properties were studied. (M.C.G.)

10846 REACTIONS OF SAMARIUM ISOPROPOXIDE WITH METHYLACETOACETATE. Sankhla, B. S.; Kapoor, R. N. (Univ. of Jodhpur, India). J. Less-Common Metals, 10: 116-20(Feb. 1966).

The reactions between samarium isopropoxide and methylacetoacetate led to the formation of mono-, di-, and tri-substituted derivatives of the type $(OPr^i)_2Sm(Meacac)$, $(OPr^i)Sm(Meacac)_2$, and $Sm(Meacac)_3$, but with excess of the ligand the addition of another mole of the ligand results in the formation of $Sm(Meacac)_3$ Meacac. The (OPr^i) groups in the first two derivatives are replaced by (OBu^t) on treatment with tert-butyl alcohol. The reactions of samarium isopropoxide with methylacetoacetate are all exothermic but the interchange reactions of the compounds $(OPr^i)_2Sm(Meacac)$ and $(OPr^i)Sm(Meacac)_2$ with tert-butyl alcohol are endothermic. (auth)

10847 HEATS OF DILUTION OF SOME ELECTROLYTE SOLUTIONS IN D_2O AND COMPARISON OF THERMODYNAMIC EXCESS FUNCTIONS IN D_2O AND H_2O. Wu, Yung-Chi; Friedman, Harold L. (IBM Watson Research Center, Yorktown Heights, N. Y.). J. Phys. Chem., 70: 166-72(Jan. 1966).

Heats of dilution of LiCl, NaCl, and NaI solutions in D_2O were measured in the range from 1 to 3M to supplement earlier results of Birnthaler and Lange. The solvent isotope effect on the excess enthalpies was much larger than that on the excess free energies found by Frank and Kerwin. The excess entropies in D_2O were calculated from these data and compared with those in water with the result that, within experimental error, S^{ex} (in H_2O) – S^{ex} (in D_2O) = $k_s m$, where m is the aquamolality (moles of salt per 55.51 moles of solvent). It was found that $Tk_s = 54$ for LiCl, 35

for NaCl, and 35 for NaI, all in units of cal mole^{-1} M^{-1}. These results, as well as the solvent-isotope effects on the entropies of solvation, seemed to be consistent with the model of aqueous solutions. (auth)

10848 A SPECTROPHOTOMETRIC STUDY OF THE Nd^{3+}-NO_3^- ASSOCIATION. Coward, Nathan A.; Kiser, Robert W. (Kansas State Univ., Manhattan). J. Phys. Chem., 70: 213-17(Jan. 1966).

A differential spectrophotometric method was used to study the association of Nd^{3+} and NO_3^- ions in aqueous solutions. The 579-mμ band was selected for quantitative determinations. Results indicated that $NdNO_3^{2+}$ is the only important absorbing species (at 579 mμ) other than Nd^{3+} in these solutions and that the $NdNO_3^{2+}$ is formed with an association constant of 0.77 at an ionic strength of 4.2. The differential technique was employed to produce the apparent visible spectrum of the pure $NdNO_3^{2+}$ complex. (auth)

10849 THERMODYNAMIC PROPERTIES OF LITHIUM HYDRIDE BY AN ELECTROMOTIVE FORCE METHOD. Johnson, Carl E.; Heinrich, Robert R.; Crouthamel, Carl E. (Argonne National Lab., Ill.). J. Phys. Chem., 70: 242-6(Jan. 1966).

The standard free energy of formation of solid lithium hydride was determined from emf measurements over the temperature range from 675 to 885°K. The cell utilizes an iron flag over which hydrogen is passed as the cathode and a molten lithium anode. The emf of the cell over this temperature range is expressed as $\epsilon^0 = 0.9081 - 7.699 \times 10^{-4}T$. Derived values of the standard free energy, enthalpy, and entropy at 800°K are $\Delta G_f^0 = -6740$ cal mole^{-1}, $\Delta H_f^0 = -20{,}940$ cal mole^{-1}, and $\Delta S_f^0 = -17.7$ cal deg^{-1} mole^{-1}. The values at 298°K calculated with the use of the best available heat capacity data are ΔG_f^0 (298) = −16,160 ± 50 cal mole^{-1}, ΔH_f^0 (298) = −21,790 ± 290 cal mole^{-1}, and ΔS_f^0 (298) = −18.9 ± 0.4 cal deg^{-1} mole^{-1}. (auth)

10850 PREPARATION OF DEUTERIUM ALCOHOLATES. Jakli, Gyoergy; Jancso, Gabor; Illy, Jozsef. Magyar Tud. Akad. Kozp. Fiz. Kut. Int. Kozlemen., 13: 235-9(1965). (In Hungarian).

The isotopic exchange reaction which leads to an equilibrium represents one of the most convenient methods for the substitution of D in the hydroxyl group of alcohols. In the presence of certain catalysts, the D is distributed between the alcohol and water: ROH + D_2O ⇌ ROD + HDO. Similar results are obtained by conducting gaseous D_2 over alcohols in the presence of catalysts: ROH + D_2 ⇌ ROD + HD. Nearly 100% deuterized ROD was prepared by the deuterolysis of Na, Al, and Mg alcoholates. Care was taken to remove all the moisture from the ambient air, eliminating also the traces of excess alcohol from the alcoholates and carrying out the operation in vacuum. The results indicated that D methylate and ethylate are best prepared by using Na alcoholate as the starting material because their volatility does not affect the removal of the traces of the alcohol. For the preparation of higher-C deuterated alcohols, it was found preferable to use the Mg or Al alcoholates. (TTT)

10851 INVESTIGATIONS ON SODIUM–AIR REACTIONS. Muenster, Horst (Interatom, Bensberg, Ger.). Nukleonik, 7: 477-80(Oct. 1965). (In German).

Reactor installations, that operate with liquid sodium as coolant, are protected against sodium fires by structural precautions. It is however of interest to know the consequences (pressure construction, temperature increase, release of radioactivity, etc.) of a sodium fire in a safety container. In order to prove how accurately the pattern of such a reaction can be predicted in a sealed space, a theoretical model was derived and compared with two experimental works. The results of the calculations agree well with the measuring results. (tr-auth)

10852 PREPARATION OF URANIUM HEXAFLUORIDE BY FLUORINATION OF UF_4. Deptula, Andrzej. Nukleonika, 10: 455-6(1965). (In Polish).

Fluorine gas was produced by electrolysis of anhydrous HF with KF, and was used for the fluorination. The fluorination was accomplished by means of the reaction, $2UF_4 + O_2 \rightarrow UF_6 + UO_2F_2$, which took place in a reactor chamber containing a nickel boat pretreated for 15 minutes at 500°C in uranium tetrafluoride. Gettering was accomplished in two stages with sodium fluoride. The procedures involved in the purification of the reagents, the preparation of the chamber, the fluorination process, and the subsequent treatment of the chamber for the recovery of pure uranium hexafluoride are described. The method, which was investigated on a laboratory scale, produced 50 g of sublimated uranium hexafluoride with a yield of 70 to 80% theoretical. (TTT)

10853 EFFECT OF DEUTERATION ON THE NEEL TEMPERATURE OF $CoCl_2.6H_2O$. Sahri, D. S. (Univ. of British Columbia, Vancouver). Phys. Lett., 19: 625-7 (Jan. 1, 1966).

When the protons in $CoCl_2 \cdot 6H_2O$ were replaced by deuterons, the Néel temperature T_N was found, using NMR techniques, to increase monotonically with the number of deuterons. T_N increased by 6% when the percentage of deuterons was changed from 0% to 92%. (auth)

10854 NAPHTHALENE EXCIMER EMISSION. Kazzaz, A. A.; Munro, I. H. (The Univ., Manchester, Eng.). Proc. Phys. Soc., 87: 329-30(Jan. 1966).

Concentrated solutions of naphthalene in toluene and in cyclohexane show a pronounced structureless excimer emission band, whose profile is unchanged in the presence of various quenching agents. (auth)

10855 ADSORPTION OF RUTHENIUM BY NATURAL ADSORBENTS. ADSORPTION OF NITROSONITRATO-, NITROSOCHLORO-, AND CHLORO-COMPLEXES OF ^{106}Ru. Sinitsyn, N. M.; Rovinski, F. Ya. Radiokhimiya, 7: 394-400(1965). (In Russian).

The purpose of this investigation was to determine the effect of the chemical state of ^{106}Ru in solutions on its adsorption by various natural adsorbents. The effect of the nature of the adsorbent on the adsorption of ruthenium was investigated. Adsorption of nitrosonitrate complexes of ruthenium increases in the following order: sand < clay < soil (chernozem) < peat < sludge. The effect of the chemical nature of radioactive ruthenium compounds is discussed. Regardless of the nature of the adsorbent, nitrosonitrate complexes are adsorbed better than nitrosochloro or chloro complexes. On the basis of adsorption curves it was established that in almost all cases radioactive ruthenium is adsorbed better from solutions containing it in the form of hydrolyzed complexes. It was found that the percent of adsorption is significantly related to the length of time of contact of adsorbent with radioactive ruthenium solution. The nature of the adsorbent and the chemical state of the radioactive ruthenium in solution markedly changes the time of maximum adsorption on the adsorption curves. Change of the pH of the solution from 2 to 11 leads to increase of the adsorption of radioactive ruthenium in the form of nitrosochloro- and chloro complexes. Nitrosonitrate complexes are adsorbed most intensely at about pH 9. (ATD)

10856 PREPARATION OF OXYNITRIDES FROM REFRACTORY OXIDES. STUDY OF THEIR STRUCTURES AND PROPERTIES. Gilles, Jean-Claude (Centre d'Etudes de Chimie Metallurgique, Vitry-sur-Seine, France). Rev. Hautes Temp. Refract., 2: 237-62(July-Sept. 1965). (In French).

Mixed phases of metal–oxygen–nitrogen can be obtained by solid-state reactions, under a neutral atmosphere, between the oxide and nitride of a same metal (Ti, V, Ge, or Al) or by reactions of ammonia gas with the oxide (Al_2O_3 or ZrO_2). These phases (oxynitrides) have structures that can be deducted either from the structure of the corresponding sub-oxide (type Ti_nO_{2n-1}) or from that of the oxide (Al_2O_3, GeO_2, or ZrO_2). The zirconium oxynitrides can be considered as intermediate phases between zirconia and the nitride Zr_3N_4. Their structures were deducted of that of cubic zirconia by partial substitution of nitrogen to oxygen, with creation of ordinated gaps in the anion network. The study of oxynitrides of aluminum, titanium, and zirconium was completed by infrared spectroscopy. (auth)

10857 SOLID SOLUTIONS FORMED BY THE ADDITION OF SELENIDES OF THE RARE EARTHS TO MSe SELENIDES OF THE FACE-CENTERED CUBIC NaCl TYPE. Golabi, Sayed Mehdi; Flahaut, Jean; Domange, Louis (Faculte de Pharmacie, Paris). Rev. Hautes Temp. Refract., 2: 263-73(July-Sept. 1965). (In French).

The systems formed at 1200 and 1300°C between rare earth selenides and CaSe were studied. Solid solutions of the type Th_3P_4 were observed on the L_2Se_3 side for the first rare-earth elements (La to Dy). Solid solutions of the NaCl type or derived structures, were observed on the CaSe side for the last elements (Gd to Lu). With elements Dy, Er, Yb, Lu, and Y, the solid solution, starting from the NaCl structure, had two superstructures, which appeared successively and without discontinuity when the content of rare-earth increased; one was cubic and the other was rhombohedral. The extent of the domains was considerable and in most cases covered ¾ of the diagrams. Anomalies were observed in the system formed with ytterbium as a result of the formation of Yb^{2+} ions under certain conditions. (auth)

10858 THE UNIT CELL AND SPACE GROUP OF GADOLINIUM MOLYBDATE AND OF SCANDIUM TUNGSTATE. Bernstein, J. L. (Bell Telephone Labs., Inc., Murray Hill, N. J.). Z. Kristallog., 122: 315-16(Nov. 1965).

Gadolinium molybdate, $Gd_2(MoO_4)_3$, belongs to the tetragonal system, with lattice constants a = 10.396 ± 0.006 and c = 10.697 ± 0.004 Å. The most probable space group is $P4/mbm-D^5_{4h}$, $P4bm-C^4_{4v}$, or $P4b2-D^7_{2d}$. Scandium tungstate is orthorhombic (pseudo tetragonal), with lattice constants a = 9.596 ± 0.004, b = 13.330 ± 0.003, and c = 9.512 ± 0.004 Å. The space group is $Pnca-D^{14}_{2h}$. (auth)

10859 A STUDY OF THE KINETICS OF THE OXIDATION OF GRAPHITE BY CARBON DIOXIDE [Thesis]. Biederman, David Leslie. University Park, Pa., Pennsylvania State Univ., 1965. 113p.

The chemical kinetics of the carbon-carbon dioxide reaction were investigated under very low pressure conditions in the temperature range 960 to 1120°C and with mixtures of carbon monoxide and carbon dioxide at a total pressure of one atmosphere in the temperature range of 1060 to 1200°C. The rate of reaction was first order with respect to the carbon dioxide concentration up to as much as 90 per cent carbon dioxide consumption for experiments performed at pressures ca 50 millitorrs. The experimental observations were found to be consistent with the following reaction mechanism: (1) $C_f + CO_{2g} \underset{j_1}{\overset{i_1}{\rightleftharpoons}} C(O) + CO_g$ and (2) $C(O) \rightarrow CO_g$. The specific rate constant for each step in this mechanism was evaluated along with its temperature dependence. The nature of the proposed carbon-oxygen surface intermediate was investigated and a heat of formation of 44 kcal/mole was calculated for this complex. The addition of small amounts of hydrogen to ca 50 millitorrs of carbon dioxide caused the rate of the carbon-carbon dioxide reaction to decrease ten fold. Hydrogen was found to adsorb on the graphite surface and a low pressure adsorption isotherm at 1100°C was measured. A stable one-to-one carbon-hydrogen surface complex was proposed. It was postulated that this complex chemi-sorbed on a substantial portion of the active surface and that the observed inhibition was due to a reduction of the unoccupied active area of the graphite. The addition of hydrocarbons such as methane and ethylene dichloride also caused the reaction rate to decrease sharply. It was thought that inhibition by these compounds was caused by a covering of the active surface also. (Dissertation Abstr.)

10860 THE CRYSTAL FIELD OF SOME MONOCLINIC RARE EARTH CHLORIDES [Thesis]. Harrop, Ian Hugh. Baltimore, Johns Hopkins Univ., 1965. 216p.

A fifteen-parameter crystal field was obtained, which accounts for the observed Stark and Zeeman splittings of Er^{3+} in the monoclinic crystal, $ErCl_3 \cdot 6H_2O$. It was shown that the same field is appropriate for the ions Yb^{3+}, Tm^{3+}, Ho^{3+}, and Dy^{3+} in the hydrated chloride lattice, and that altogether more than two hundred independent experimental data are adequately explained. The indentification of the M, N, and O absorption groups of Er^{3+} was confirmed, the upper Stark level of $^2F_{5/2}$ in $YbCl_3 \cdot 6H_2O$ was identified, and a large Zeeman splitting is predicted for the ground state of $TmCl_3 \cdot 6H_2O$. Although the parameters A^q_k are approximately the same for all ions in a given host lattice, the field for even electron ions appears to be significantly different from the field for odd electron ions. The Zeeman splittings of the A and B groups in $GdCl_3 \cdot 6H_2O$ were explained, and it was shown that the Gd^{3+} ion can be used as a probe to investigate the field of monoclinic and orthorhombic crystals. (Dissertation Abstr.)

Organic Chemistry

Refer also to abstract 10872.

10861 (CEA-R-2770) SYNTHESE ET PURIFICATION DE QUELQUES ALCOYLPHENANTHRENES ET PRESENTATION DE LEURS SPECTRES D'ABSORPTION INFRAROUGE, ULTRAVIOLETTE, DE RESONANCE MAGNETIQUE NUCLEAIRE ET DE MASSE [Theses]. (Synthesis and Purification of Some Alkylphenanthrenes and Presentation of Their Infrared, Ultraviolet, Nuclear Magnetic Resonance and Mass Spectra [Thesis]). Persaud, Kim (Commissariat a l'Energie Atomique, Grenoble (France). Centre d'Etudes Nucleaires). 1965. 205p. Dep. mn.

Submitted to Grenoble Univ. (France).

Phenanthrene, its five monomethyl derivatives, three dimethyl derivatives, and two trimethyl derivatives were prepared and purified. Low voltage mass spectrometry was used to establish purity at 99.5 per cent or better in most cases. The infrared, ultraviolet, nuclear magnetic resonance, and mass spectra of these products were recorded. (auth)

10862 (MLM-1252) PENTAERYTHRITOLTETRANITRATE: A BIBLIOGRAPHY. Kantz, Melvin R. (Mound Lab., Miamisburg, Ohio). Feb. 1, 1965. Contract AT-33-1-GEN-53. 20p. Dep. mn. CFSTI $1.00 cy, $0.50 mn.

References (176) on pentaerythritol tetranitrate and its homologs are given to journals and reports published from 1958 through 1964. A few pertinent references prior to 1958 are also included. Separate author and subject indexes are given. (P.C.H.)

10863 VALENCE, FUNDAMENTAL, AND HARMONIC VIBRATIONS OF PIPERIDINE $C_5H_{10}NH$ AND THE N-DEUTERATED PIPERIDINE $C_5H_{10}ND$. Levi, Georges (Univ., Paris). Compt. Rend., 261: 4007-9(Nov. 15, 1965). (In French).

The valence vibration spectra of piperidine and n-deuterated piperidine, which possess only a single vibrator NH or ND, have, both in the gaseous and the liquid phases, two components for the fundamental band ν(NH) or ν(ND) and for harmonic 2ν(NH) or 2ν(ND). Several interpretations are proposed. (tr-auth)

10864 INFRARED ABSORPTION SPECTRA OF DEUTERATED CYCLOHEXANE IN THE SOLID STATE. Roy, Alain Le (Univ., Paris). Compt. Rend., 261: 4022-4 (Nov. 15, 1965). (In French).

The infrared absorption spectra of deuterated cyclohexane, both pure and in solid solution in cyclohexane, were obtained at 77°K in the region from 1500 to 400 cm^{-1}. They have a multiplet structure. In pure molecular solids the components of the vibration spectrum are due to the static field and to the intermolecular coupling. (tr-auth)

10865 NEUTRON SCATTERING IN STRETCH-ORIENTED POLYETHYLENE. Myers, W.; Summerfield, G. C.; King, J. S. (Univ. of Michigan, Ann Arbor). J. Chem. Phys., 44: 184-7(Jan. 1, 1966).

Measurements on stretch-oriented polyethylene held at 100°K were undertaken in an attempt to clearly identify the frequency limit of the calculated stretch-bend acoustic mode. A simplified "constant-Q" scattering technique was used in order to isolate the longitudinal C-C-C motion. A frequency limit was observed at 525 ± 15 cm^{-1}. The per-

sistence of the torsional mode response in the longitudinal experiment is unexpectedly large. (auth)

10866 VAPOR PRESSURES OF THE DEUTERATED ETHANES. **Van Hook, W. Alexander (Univ. of Tennessee, Knoxville). J. Chem. Phys., 44: 234-51(Jan. 1, 1966).**

The vapor pressures of all 10 deutero–protio-ethane isomers $C_2H_iD_{6-i}$ ($0 \leq i \leq 6$) were measured over the temperature range 115° to 200°K [~1 mm C_2H_6 to 1600 mm C_2H_6] by direct manometry. The isotope effects are inverse and go through maxima between 125° and 140°K. At the maxima they are on the order of 1.2% per D atom. Deviations from the law of the mean are small, but for the three sets of equivalent isomers 1,1- and 1,2-$C_2H_4D_2$; 1,1,1- and 1,1,2-$C_2H_3D_3$; and 1,1,1,2- and 1,1,2,2-$C_2H_2D_4$ significant differences in vapor pressure are observed. The more unsymmetrically substituted compound has the higher vapor pressure in all cases. The data are interpreted in the light of the statistical theory of isotope effects in condensed systems. A model calculation is made within the framework of this theory in its harmonic-cell approximation using reasonable force fields. It is necessary to invoke temperature-dependent force constants for the low-energy ($u = h\nu/kT < 2\pi$) modes in order to rationalize the temperature dependency below 140°K. The agreement between the model calculation and experiment is excellent. The calculations reveal that the torsional motion, which must be blue shifted on condensation, is the single most important contributor to the isotope effects between equivalent isomers. The results constitute the second independent confirmation of the statistical theory of isotope effects in condensed systems as applied to molecules exhibiting higher-order quantum effects. (auth)

10867 EXPERIMENTAL AND THEORETICAL STUDIES OF PHOTOIONIZATION-EFFICIENCY CURVES FOR C_2H_2 AND C_2D_2. **Botter, R.; Dibeler, V. H.; Walker, J. A.; Rosenstock, H. M. (National Bureau of Standards, Washington, D. C. J. Chem. Phys., 44: 1271-8(Feb. 1, 1966).**

Photoionization-efficiency curves for C_2H_2 and C_2D_2 were remeasured in the wavelength region from onset of ionization to 600 Å, using a gold-coated grating and the Hopfield continuum as a photon source. The curve shapes of the molecular ions near threshold were compared with calculations of the Franck–Condon factors. Nearly exact agreement between experiment and calculation was obtained by taking into account hot bands. A general discussion is given for the shape of the molecule-ion curve and for that of the fragment ions, C_2H^+ and C_2D^+. The observed onsets of ionization for the latter ions are 17.2 and 17.3 ev, respectively. (auth)

10868 SYNTHESIS OF SALICYLIC ACID-(^{14}COOH). **Falecki, J.; Szuchnik, A. (Institut fuer Atomkernforschung, Warsaw). J. Prakt. Chem., 28: 119-22(1965). (In German).**

Freshly distilled o-bromophenol was methylated with dimethyl sulfate and potassium hydroxide in aqueous ethanol. The Grignard reagent was prepared from 1 g Mg turnings and 2.0 ml freshly distilled o-bromoanisole in ether with I_2 as catalyst; the reaction was complete in 2 hr. Carboxylation of the reagent proceeded in an apparatus described by Medenwald and Haberland (Ann. Chem., 306: 229(1957)). The reaction mixture was frozen in liquid N_2 and then shaken for 1.5 to 2 min. After repeated freezing the reaction mixture was hydrolyzed carefully with 10 ml 10% HCl and the ether layer removed. This was combined with two 5-ml washes of the water layer and extracted with 15, 10, and 5 ml $NaHCO_3$ solution. The aqueous solution was washed with 2 ml ether, and evaporated to 5 ml at 80°C. o-Methoxybenzoic acid was precipitated by 10% HCl and collected after 24 hr. From the combined ether layers bis(o-methoxyphenyl)ketone-^{14}Co was obtained and recrystallized from petroleum ether. The methoxybenzoic acid was demethylated either with freshly distilled HI at 125°C in the dark for 15 min or by treatment of Na o-methoxybenzoate with concentrated HCl in ether-methanol solution (2 : 1) at 0°C. After collecting the product, it was dissolved in 5% NaOH; the filtrate was washed with a small amount of 30% H_2O_2, reduced in volume, and the acid obtained by 10% HCl addition at 0°C. The product was collected after 24 hr and dried in vacuo. (BBB)

10869 CONCENTRATION OF 24 TRACE ELEMENTS IN HUMAN HEART TISSUE DETERMINED BY NEUTRON ACTIVATION ANALYSIS. **Wester, P. O. (Karolinska Institutet, Stockholm). Scand. J. Clin. Lab. Invest., 17: 357-70(1965).**

Human heart samples were irradiated in the reactor with a thermal neutron flux of 2.10^{12} n/cm^2 sec for 75 hr. Other heart samples were irradiated in the reactor with a thermal neutron flux of 2.10^{13} n/cm^2 sec for 24 to 65 hr. The irradiated heart samples were allowed to cool for 2 or 3 days before chemical separation, in order to reduce the very high ^{24}Na activity. In this way, neutron activation analysis was applied to heart tissue from autopsy of 20 victims of traumatic accidents to determine the concentration of 24 different trace elements. A recently developed ion-exchange technique combined with γ spectrometry was used which permitted simultaneous determination of a large number of trace elements. The following trace elements were determined quantitatively: Ag, As, Au, Ba, Br, Ca, Cd, Ce, Co, Cr, Cs, Cu, Fe, Hg, La, Mo, Pt, Rb, Sb, Sc, Se, Sm, W, and Zn. In some heart samples, Hf and Os were determined qualitatively. The mean and standard deviation are given for the elements Cu, Fe, Se, and Zn. Since none of the other quantitatively determined trace elements was normally distributed, the median is given as the central value. When possible, comparisons with values from other investigations were made. No marked differences in the trace-element concentrations with age or sex could be detected. Most of the concentrations of trace elements showed a skew distribution, with a large number of low values. Thus, the mean was higher than the median for all elements not normally distributed, except Co. (BBB)

Radiation Chemistry

See *also* BIOLOGY AND MEDICINE — Radiation Effects on Biochemicals
Radiation Effects on Tissues

Refer also to abstracts 10809, 11027, and 12429.

10870 (BMI–1753) RADIATION-INDUCED FORMATION OF ORGANOMETALLIC COMPOUNDS WITH PARTICULAR EMPHASIS ON ORGANOTINS. **Fentiman, Allison F. Jr.; Wyant, Robert E.; McFarling, James L.; Kahler, E. Jack; Kircher, John F. (Battelle Memorial Inst., Columbus, Ohio). Jan. 3, 1966. Contract W-7405-eng-92. 21p. Dep. mn. CFSTI $2.00 cy, $0.50 mn.**

Effects of variables on the yield of alkyltin halides and product distribution were studied. Yields corresponding to a G-value greater than 10^3 were obtained with tin and 1-bromobutane under the best conditions. An activation energy of 30.8 kcal/mole was found for the tin/1-bromobutane system and 20 kcal/mole for tin/1-bromopentane system. It was further observed, for the tin/bromobutane reaction, that the G-value is proportional to $I^{-\frac{1}{2}}$, where I is the intensity of the radiation. Thus, at low dose rates very high G-values were obtained. The product distribution appears to depend only on the degree of conversion. At a conversion of less than 10 wt % of 1-bromobutane, the product contained about 90 wt % dibutyltin dibromide, whereas at a conversion of 60 wt %, the dibutyltin dibromide content dropped to about 80 wt %. The crude product can be purified by thermal disproportionation, yielding dibutyltin dibromide with a purity greater than 95 percent. The radioinduced reaction of tin and the alkyl bromides appeared to be general, although the alkyl chlorides could not be made to react with tin under the radiation conditions examined. (auth)

10871 (EUR–2288.f) BOUCLES SOUS ELECTRONS SR_2–SR_3–SR_4. (SR_2–SR_3–SR_4 Electron Irradiation Loop). **Houiller, A.; Jayet, C.; Moneger, H. (Societa Progil, Lyon (France). Laboratoire Centrea de Recherches). Sept. 1965. 37p. Dep. mn.**

The SR_2, SR_3, and SR_4 loops which were developed for

use, in conjunction with accelerators, in studies of the radiolytic behavior of terphenyls, the fouling of heat-transfer surfaces under electron irradiation, and the radiolytic behavior of terphenyl substitutes, respectively, are described. (D.C.W.)

10872 (EUR-2517.f) ETUDE SUR LES SUBSTITUTS AUX TERPHENYLES ET SUR LE TERPHENYLE OM2. (Study of Terphenyl Substitutes and Terphenyl OM2). (Commissariat a l'Energie Atomique, Grenoble (France). Centre d'Etudes Nucleaires). 1965. 144p. Dep. mn.

The behavior of terphenyl OM2 in pyrolysis and radiolysis was studied. Pyrolysis tests showed that the pyrolysis speed of radiolyzed terphenyl is 4 to 6 times greater than that of pure terphenyl, and that this phenomenon might be related to the presence of paramagnetic active centers. In-pile radiolysis tests carried out between 200 and 450°C showed that there are two very distinct zones (separated by a transition zone between 350 and 390°C), in which the variation in the decomposition speed of terphenyl as a function of temperature differs considerably. In the lower temperature-zone, the activation energy was slight and corresponded to pure radiolysis. In the upper zone, the activation energy progressively climbed up to that of pure pyrolysis. The preparation and characteristics of alkyl-phenanthrene and the analytical investigation of these products are also discussed. The dosimetric methods used for the in-pile loop and the results obtained are described. (P.C.H.)

10873 RADIATION-INDUCED FORMATION OF FREE RADICALS IN STYRENE-GRAFTED CELLULOSE. Kroh, J.; Walicki, M. (Technical Univ., Lodz, Poland). Bull. Acad. Pol. Sci., Ser. Sci. Chim., 13: 635-7(1965).

Energy transfer phenomena were studied in irradiated cellulose grafted with styrene. The effects of radiation were evaluated by EPR measurements. ^{60}Co gamma rays were used to induce grafting and for irradiation after grafting. The presence of styrene grafted on the cellulose did not cause any marked change in the shape of the EPR spectrum. However, the number of unpaired spins strongly depended on the degree of grafting. It was concluded that small quantities of styrene introduced into the system facilitate stabilization of free radicals in the polymer. (M.C.G.)

10874 PHOTOLYSIS AND RADIOLYSIS OF SOME SIMPLE NITROALKANES. II. NITROETHANE. Paszyc, Stefan (Univ., Poznan, Poland). Bull. Soc. Amis Sci. Lett. Poznan, Ser. B, 18: 19-28(1965).

Photolysis of nitroethane in both the vapor and liquid states, as well as radiolysis in the liquid state, were carried out. Particular attention was devoted to investigation of the liquid systems. Photolysis of nitroethane vapor was carried out in specially assembled glass apparatus by introducing an immersion quartz lamp rich in radiation of wavelengths 366 and 313 mμ. The products of photolysis and radiolysis of the compound were analyzed by gas chromatography and infrared spectrophotometry. Photolysis was also carried out in the presence of cupric oxide. Radiolysis of liquid nitroethane yielded a number of products, both liquid and gaseous, among which simple saturated hydrocarbons prevail. The mechanism of formation of products by prolonged photolysis and radiolysis of nitroethane is discussed, as well as the role of oxygen evolving in the photolytic decomposition of NO_2. (auth)

10875 ROLE OF THE CHEMICAL SPECIES RELEASED BY THE RADIOLYSIS OF WATER IN THE SATURATION OF DOUBLE CARBON-CARBON BONDS. Nofre, Claude; Le Roux, Yvonne; Cier, Andre (Centre de Recherches du Service de Sante des Armees, Lyon). Compt. Rend., 261: 2887-90(Oct. 11, 1965). (In French).

The effect of pH or of oxygen on the formation of succinic, malic, and tartaric acids by the γ radiolysis of aqueous solutions of fumaric acid was studied; only the species H and OH permit the deocupling of the double carbon-carbon bonds into a carbonyl radical suited to react with e^-_{aq} or O_2. (tr-auth)

10876 A HYPERFREQUENCY SPECTROGRAPH FOR THE STUDY OF IRRADIATED SUBSTANCES FROM 20 TO 300 deg K. Petit, Pierre (Institut d'Electronique, Orsay, France). Compt. Rend., 261: 4717-20(Nov. 29, 1965). (In French).

A description is given of a hyperfrequency cavity in the 3-cm band, which permits the study by electron resonance from 20 to 300°K of monocrystals irradiated by electrons at 1.5 Mev. (tr-auth)

10877 THE HYDROGEN BONDS AND THE RADIO-RESISTANCE OF POLYNUCLEOTIDES IN THE SOLID PHASE. Rajalakshmi, K. V.; Venkateswarlu, K.; Van de Vorst, Albert (Kerala Univ., Alwaye, South India. Univ., Liege. Institut d'Astrophysique, Cointe-Sclessin, Belg.). Compt. Rend., 261: 4879-81(Nov. 29, 1965). (In French).

The radiolytic yield from the adenine uracil copolymer exposed in the solid phase to the effect of x and γ rays was compared to that of its components taken individually. The results obtained seemed to show that the hydrogen bonds characterizing the complex play practically no role in determining its radioresistance. A confirmation of the general validity of this conclusion was obtained by the demonstration that the denaturation of DNA does not alter the value of the yield in induced free radicals. (tr-auth)

10878 CAUSES RESPONSIBLE FOR THE INCREASED YIELD OF PHENOL IN THE RADIOLYSIS OF AQUEOUS SULFATE SOLUTIONS OF BENZENE CONTAINING DIVALENT IRON IONS AND OXYGEN. Kartasheva, L. I.; Pikaev, A. K. (Inst. of Physical Chemistry, Academy of Sciences, USSR). Dokl. Akad. Nauk SSSR, 163: 1155-8 (Aug. 11, 1965). (In Russian).

The increased yield of phenol in irradiated, aerated sulfate solutions of benzene containing Fe^{2+} ions was studied. A mechanism for this reaction was proposed which includes a chain reaction with water radicals (HO_2 and H_2O_2) leading to the formation of additional OH radicals which attach themselves to the benzene ring increasing the phenol yield. To clarify the role of the chain reactions in this process, the sulfate solutions were studied by radiolysis using a ^{60}Co source and 0.9-Mev electrons from a Cockcroft-Walton accelerator. The yields of phenol, Fe^{3+} ions, and carbonyl compounds were determined as a function of the Fe^{2+} and benzene concentrations. It was concluded that the very large yields of phenol and of Fe^{3+} ions must be due to a chain reaction which produced oxycyclohexadienyl radicals: $C_6H_6 + OH \rightarrow C_6H_6OH$; $C_6H_6OH + O_2 \rightarrow O_2C_6H_6OH$. The $O_2C_6H_6OH$ radicals may decompose to yield HO_2 and phenol, or may react with Fe^{2+} ions (which are also oxidized by HO_2 and H_2O_2 radicals). Other possible decomposition or recombination reactions of $HOOC_6H_6OH$ and $O_2C_6H_6OH$ radicals were also given. (G.O.Y.)

10879 THE MECHANISM OF THE NON-ADDITIVE FORMATION OF RADICALS IN THE RADIOLYSIS OF FROZEN $CCl_4 + CH_3OH$ SOLUTIONS. Roginskii, V. A.; Kotov, A. G.; Pshezhetskii, S. Ya. (Karpov Inst. of Physics and Chemistry, Academy of Sciences, USSR). Dokl. Akad. Nauk SSSR, 163: 1433-6(Aug. 21, 1965). (In Russian).

Following previous findings that radiolysis of frozen solutions of CCl_4 in methanol results in increased yields of stabilized radicals with respect to the additive value, an attempt was made to clarify the role of the reaction of hydrogen ions, electrons, and atoms with CCl_4 molecules in the formation of the stabilized radicals. Methanol containing 5% water was used in order to obtain amorphous specimens; the radiation dose amounted to 1 to 2 Mrad. The electron paramagnetic resonance spectrum of the system after irradiation was found to change on exposure to visible light: the lines belonging to formyl radicals and the singlet of the solvated electrons disappeared while the concentration of the triplet increased. The spectrum was improved and the original coloration of the sample disappeared but the total concentration of paramagnetic particles did not change. Addition of H_2SO_4 (H^+ ions) resulted in a decrease in the intensity of the singlet. Addition of CCl_4 to the CH_3OH suppressed the formation of solvated electrons

but resulted in a higher concentration of radicals. The following reactions were assumed to take place when amorphous CH_3OH is exposed to γ radiation at 77°K: $CH_3OH \rightsquigarrow CH_2OH^+ + H + e$, $CH_3OH \rightsquigarrow CH_2OH + H$, $H + H \rightarrow H_2$, $e \rightarrow (e)_{solv.}$. If CCl_4 was present, the following additional reactions were expected to occur: $e + CCl_4 \rightarrow CCl_3 + Cl^-$, $H + CCl_4 \rightarrow CCl_3 + HCl$. The latter reaction was responsible for the increased yield. (TTT)

10880 ACTIVATION ANALYSIS OF DRUGS. Schlesinger, H. L. (Internal Revenue Service, Washington, D. C.); Pro, M. J.; Hoffman, C. M.; Cohan, M. J. Ass. Offic. Agr. Chem., 48: 1139-47(Dec. 1965).

Activation analysis has been employed to compare and determine the source of manufacture of drugs. The irradiations were carried out with the DASA-TRIGA and Naval Research Laboratory nuclear reactors, and the induced radionuclides were identified by nondestructive gamma-ray spectrometry. The results show that the technique can be a useful tool for the identification of trace elements which serve to characterize drugs. (auth)

10881 VACUUM-ULTRAVIOLET PHOTOCHEMISTRY. IV. PRIMARY PROCESSES IN THE PHOTOLYSIS OF WATER AT 1470 A. Stief, L. J. (Melpar, Inc., Falls Church, Va.). J. Chem. Phys., 44: 277-9(Jan. 1, 1966).

Water was photolyzed at 1470 Å in the absence and presence of ethylene which acts as a scavenger for hydrogen atoms. Mixtures of D_2O and C_2H_4 were used to distinguish between hydrogen from the photolysis of water and from the photolysis of ethylene. In the presence of 5% and 20% C_2H_4, the rate of D_2 production from the photolysis of D_2O is 6% of that in the absence of C_2H_4. It is concluded that in the photolysis of D_2O at 1470 Å, there are two primary processes occurring: $D_2O + h\nu_{1470Å} \rightarrow D + OD$, $D_2O + h\nu_{1470Å} \rightarrow D_2 + O$. Direct production of molecular hydrogen and atomic oxygen accounts for 6% of the primary processes. (auth)

10882 ESR SPECTRUM OF FOO. Fessenden, Richard W.; Schuler, Robert H. (Mellon Inst., Pittsburgh). J. Chem. Phys., 44: 434-7(Jan. 15, 1966). (RRL-2310-161).

The ESR spectrum obtained during the electron irradiation of liquid CF_4 containing trace amounts of oxygen consists of a 12.83-G doublet at g = 2.0038. Under the conditions of the experiments the radical producing this spectrum has a mean lifetime of ~20 min. This observed spectrum is similar to the doublet which has been found in various oxides of fluorine. Addition of small amounts of oxygen enriched in ^{17}O shows that the radical contains two nonequivalent oxygen atoms which have appreciable hyperfine constants. The ^{17}O coupling constants, $a_0' = 22.17$ and $a_0'' = 14.50$ G, are similar to those found in RO_2. The simplest radical which can be proposed to explain these results is FO_2. Upon prolonged irradiation the CF_4 shows a second, transient spectrum which is tentatively assigned to $CF_3OCF_2\cdot$. (auth)

10883 H_2S AS A FREE-RADICAL INTERCEPTOR IN THE GAS-PHASE RADIOLYSIS AND PHOTOLYSIS OF PROPANE. Ausloos, P.; Lias, Sharon G. (National Bureau of Standards, Washington, D. C.). J. Chem. Phys., 44: 521-9(Jan. 15, 1966).

The gas-phase photolysis (1236 Å) and the γ-ray radiolysis of C_3D_8 were investigated in the presence of varying concentrations of H_2S. When 10% or more H_2S is added to C_3D_8, the majority of the D, CD_3, C_2D_3, and C_2D_5 radicals abstract an H atom from H_2S to form HD, CD_3H, C_2D_3H, and C_2D_5H, respectively. The fully deuterated molecules formed in these mixtures result from the unimolecular elimination of a stable molecule from C_3D_8 or $C_3D_8^+$ and from fast bimolecular processes such as ion–molecule reactions. The mechanisms of the radiolysis and the photolysis proposed in earlier studies were re-examined in the light of the information derived from the $C_3D_8-H_2S$ experiments and of some additional photolysis experiments on $CD_3CH_2CD_3-NO$ mixtures. The results indicate that the modes of decomposition of the neutral excited propane molecule are as follows: $C_3D_8^* \rightarrow C_2D_6 + CD_2$, $\rightarrow CD_4 + C_2D_4$, $\rightarrow D_2 + C_3D_6$, $\rightarrow CD_3 + C_2D_5$, $\rightarrow D + C_3D_7$. The internally excited C_2D_4, C_2D_5, C_3D_6, and C_3D_7 species formed in these primary processes decompose to form D, CD_3, C_2D_2, C_2D_3, and C_2D_4 unless they are collisionally stabilized. In the radiolysis of $C_3D_8-H_2S$ mixtures, yields of the free radicals can be adequately accounted for by taking into account the modes of fragmentation of the parent ion and of the excited propane. The $C_2D_5^+$ ions are shown to react with H_2S in part by the deuteron-transfer reaction $C_2D_5^+ + H_2S \rightarrow C_2D_4 + DH_2S^+$. The effect of pressure and the effectiveness of HI as a free-radical interceptor in the radiolysis were examined. (auth)

10884 ENERGY TRANSFER IN RADIOLYSIS OF RARE-GAS–C_2F_6 MIXTURES. Kevan, Larry (Univ. of Chicago). J. Chem. Phys., 44: 683-6(Jan. 15, 1966).

The gas-phase gamma radiolysis of C_2F_6 with He, Ne, Ar, Kr, and Xe was examined as a function of the fraction of energy deposition in the rare gas. For 90% energy deposition in the rare-gas energy-transfer efficiencies of 5%, 47%, 92%, 78%, and 36% in the respective mixtures of He to Xe were observed. The transfer efficiency is shown to depend on the difference between the recombination energies of C_2F_6 and the rare gas. This dependence indicates the existence of charge-transfer processes although some excitation transfer also takes place. In $Xe-C_2F_6$ mixtures charge transfer is endothermic and the change in product distribution supports the expectation that only excitation transfer occurs. (auth)

10885 CROSS SECTIONS FOR IONIZATION BY ELECTRONS. I. ABSOLUTE IONIZATION CROSS SECTIONS OF Zn, Cd, AND Te_2. II. COMPARISON OF THEORETICAL WITH EXPERIMENTAL VALUES FOR ATOMS AND MOLECULES. Pottie, R. F. (National Research Council, Ottawa, Can.). J. Chem. Phys., 44: 916-22(Feb. 1, 1966).

Ionization cross sections for Zn, Cd, and Te_2 vapors, were measured by collection of the total positive ion currents produced from electron impact by 50-ev electrons in the specially designed ion source of a mass spectrometer. The results are: $\sigma_i(Zn) = 5.03 \pm 0.45 \times 10^{-16}$ cm^2, $\sigma_i(Cd) = 8.54 \pm 0.33 \times 10^{-16}$ cm^2, and $\sigma_i(Te_2) = 17.46 \pm 0.48 \times 10^{-16}$ cm^2. These results were combined with available data to set up a compilation of absolute ionization cross sections for 27 atoms. Very limited agreement was found with theoretical ionization cross sections: It is shown that ionization cross sections of molecules cannot be calculated reliably by summation of the ionization cross sections of the constituent atoms. (auth)

10886 IONIC PROCESSES IN γ-IRRADIATED ORGANIC SOLIDS: ELECTRONS IN 3-METHYL PENTANE. Gallivan, James B.; Hamill, William H. (Univ. of Notre Dame,, Ind.). J. Chem. Phys., 44: 1279-87(Feb. 1, 1966).

Gamma-irradiated 3-methylpentane (3MP) and solutions of biphenyl (ϕ) were examined at –196°C at doses of 1 to 26×10^{18} ev ml^{-1}. The half life for decay of the trapped electron (e^-) in 3MP was independent of dose for t < 1 hr and the rate was approximately second order to t > 1 hr. This behavior, as well as very efficient formation of ϕ^- at small % ϕ, requires electron track lengths of $\sim 10^{-4}$ cm. The 100 ev yield of (e^-) shortly after γ irradiation was ~0.9, in terms of the measured extinction coefficient $\epsilon(e^-) \cong 3.0 \times 10^4$ liter mole^{-1} · cm^{-1} at 2.3×10^{18} ev ml^{-1}, but only 60% as great at 10-fold greater dose. At 0.04% ϕ, the rate of (e^-) decay was much faster and approximated first order. The ratio of reaction cross sections of (e^-) with positive holes and ϕ was ~120. Addition of 2% 2-methylpentene-1 as positive hole trap increased the yield of (e^-) and decreased the rate of decay, which became second order throughout. Recombination luminescence intensity from TMPD at t > hr decayed at the same rate following uv and γ excitation. The evidence for randomization of relatively large yields of ion pairs and very long track lengths, as well as trapping and escape, may require a new theoretical framework. (auth)

10887 ON THE THERMAL-SPIKE MODEL OF LOW LET RADIOLYSIS. Yang, John Y.; Burr, John G. (North American Aviation Science Center, Thousand Oaks, Calif.). J. Chem. Phys., 44: 1307-8(Feb. 1, 1966).

The thermal spike model proposed (Ingalls, Spiegler, and Norman, J. Chem. Phys., 41: 837 (1964)) to account for the low apparent activation energies observed in ^{60}Co gamma radiolysis of toluene is discussed. It is suggested that the reported low activation energies may be explained by reactions involving nonthermalized hydrogen atoms. Also, hydrogen formation by unimolecular detachment may account for that observed in the radiolysis of toluene. (M.C.G.)

10888 CHEMICAL CONSEQUENCES OF NUCLEAR RECOIL FOLLOWING THE RADIATIVE CAPTURE OF NEUTRONS BY COBALT IN METAL ACETYLACETONATES: RADIATION ANNEALING. Shankar, J.; Venkateswarlu, K. S.; Lal, M. (Atomic Energy Establishment, Trombay, India). J. Inorg. Nucl. Chem., 28: 11-16(Jan. 1966).

It was previously reported that γ and x radiation causes annealing in pure trisacetylacetone Co(III) following radiative neutron capture. These measurements were extended to the cobalt complex dispersed in a matrix of pure aluminum and rhodium acetylacetonates, which are isomorphous with the cobalt complex. The results with such diluted samples of cobaltic acetylacetonate showed a change both in the initial separable activity, as well as in the subsequent annealing compared to the results for the pure cobalt complex. The kinetics of thermal annealing in all these systems showed that the γ-rays prior to radiative neutron capture in the pure cobalt complex indicated that the inorganic yield increases with increasing gamma dose. For these samples also, thermal annealing rates were found to show a marked increase. A detailed study showed the close similarity of radiation and thermal annealing. Results of a study with ^{58m}Co dispersed in trisacetylacetone Co(III), both as an interstitial impurity and as in the form of the complex, are presented. (auth)

10889 ANNEALING EFFECTS IN NEUTRON IRRADIATED CRYSTALLINE COBALT COMPLEXES. I. HALOPENTAMMINE COBALT COMPLEXES. Yasukawa, T. (Tokyo Univ.). J. Inorg. Nucl. Chem., 28: 17-24(Jan. 1966).

The chemical behaviors of ^{60}Co and ^{82}Br produced by thermal neutron capture in the crystalline salts of the series, $[Co(NH_3)_5Y]X_2$, were investigated by solvent extraction and ion exchange procedures. Although the thermal recombination rate of ^{60}Co in $[Co(NH_3)_5Br]X_2$ increased in the order, nitrate, iodide, bromide, and chloride, the differences among them were less remarkable than in the series, $[Co(NH_3)_6]X_3$. In chlorides and bromides almost all the recombined ^{60}Co activity was found in the form, $[Co(NH_3)_5X]^{2+}$. In iodides and nitrates, however, about 30% of the recombined ^{60}Co activity assumed the chemical form, $[Co(NH_3)_6]^{3+}$, and this ratio increased when samples were annealed in a stream of ammonia. In all the complexes, $[Co(NH_3)_5Cl]Br_2$, $[Co(NH_3)_5Br]Cl_2$, and $[Co(NH_3)_5Br]Br_2$, the behavior of ^{82}Br was identical. This was interpreted as evidence for the existence of the disorder zone around recoil atoms. (auth)

10890 THE NATURE OF THE INORGANIC ^{82}Br IN NEUTRON-IRRADIATED BROMOBENZENE. Katsanos, N. A.; Varvoglis, A. G. (Nuclear Research Centre Democritus, Aghia Paraskevi Attikis, Greece). J. Inorg. Nucl. Chem., 28: 249-51(Jan. 1966).

The method of repeated extractions was used in an attempt to find the number and relative concentrations of extractable ^{82}Br-species in neutron-irradiated bromobenzene. After each extraction the ^{82}Br activity was counted with a well-type NaI(Tl) gamma scintillation spectrometer. The results were consistent with the presence of two extractable species in irradiated bromobenzene. Both species were more or less equally "reactive" with regard to their returning to organic combination. At least one of the species appeared to be acidic. (M.C.G.)

10891 RADIATION CHEMISTRY OF IONIC SOLIDS. IV. MODIFYING NITRATE RADIOLYSIS IN CRYSTALS BY COMPRESSION. Cunningham, Joseph (Illinois Inst. of Tech., Chicago. Argonne National Lab., Ill.). J. Phys. Chem., 70: 30-9(Jan. 1966).

Samples of crystalline alkali metal nitrates maintained under hydrostatic compression by several hundred atmospheres of rare gases were exposed to ^{60}Co γ radiation simultaneously with unpressurized samples. Growth of radiolytic product was followed by chemical solution analysis by two methods after irradiation. Compression-induced changes depended on whether the kinetics being observed correspond to: region 0, growth of primary product at low dose, which was increased by 15% in $NaNO_3$ irradiated at 77°K; region I, diffusion-controlled growth of secondary products at intermediate doses, which was decreased by 4, 9, 23, and 19% in KNO_3, $NaNO_3$, $RbNO_3$, and $CsNO_3$ irradiated at 300°K; or region II, growth of secondary product altered by crystal modifications at high dose, which was unaffected by compression. Product growth in region 0 at 77°K or region I at 400°K was sensitive to low partial pressures of oxygen. Detailed mechanisms of nitrate radiolysis are presented to account for the pressure and oxygen effects. (auth)

10892 THE EFFECT OF γ IRRADIATION ON A POLYAMIDE. Krasnansky, Victor J.; Parker, Midgett S.; Florin, Roland E. (National Bureau of Standards, Washington, D. C.). J. Phys. Chem., 70: 40-6(Jan. 1966).

Electron spin resonance and optical spectroscopy were used to study the kinetics of intermediates produced by the irradiation of a polyamide MXD-6. This polymer derived from m-xylylenediamine and adipic acid showed remarkable stability to radiation in previous studies. It was concluded that the colored intermediate is a radical species whose molar extinction coefficient is $\sim 10^5$ at 300 mμ. At temperatures above 85°C the decay of the active species measured by both methods tended to become second order after an initial rapid decay. This complex decay rate during the initial period was attributed to radicals having a very high decay rate or a diffusion-controlled bimolecular reaction of pairs. The derived activation energy for diffusion was 19 to 29 kcal/mole. (auth)

10893 THE MECHANISM OF DECAY OF VINYL UNSATURATION DURING THE RADIOLYSIS OF MARLEX-50 POLYETHYLENE. Dole, Malcolm; Fallgatter, M. B.; Katsuura, K. (Northwestern Univ., Evanston, Ill.). J. Phys. Chem., 70: 62-70(Jan. 1966).

Vinyl group decay during the γ irradiation of Marlex-50 polyethylene was reinvestigated by studying the distribution of vinyl unsaturation between sol and gel. Equations were derived for the theoretically expected distribution. It is shown that the initial number-average molecular weight of the molecules incorporated in the first bit of gel to be formed should be equal to the initial over-all weight-average molecular weight. The experimental results were in good agreement with theory provided that the vinyl groups in the gel decayed at the same rate as vinyl groups in the sol. This fact, as well as the results of Kitamaru, Mandelkern, and Fatou, ruled out the end-linking mechanism of vinyl decay. Calculations indicated that the disappearance of unsaturation is too rapid to be explained on the basis of scavenging by thermal hydrogen atoms, and it was concluded that vinyl decay is mainly the result of ion-molecule dimerization reactions. (auth)

10894 REACTION OF THE HYDRATED ELECTRON WITH WATER. Hart, Edwin J.; Gordon, Sheffield; Fielden, E. M. (Argonne National Lab., Ill.). J. Phys. Chem., 70: 150-6(Jan. 1966).

The reaction of a hydrated electron, e^-_{aq}, with water at 25°C, $e^-_{aq} + H_2O \underset{k_1'}{\overset{k_1}{\rightleftharpoons}} H + OH^-$, was investigated by pulse radiolysis techniques. Because the above reaction is about 10^{-3} times as fast as $e^-_{aq} + H_3O^+$, O_2, and H_2O_2, these and other adventitious e^-_{aq} scavengers were minimized by purification, preirradiation, and adjustment of pH. The rate constant was measured at impurity concentrations less than 5×10^{-9}M, in a hydrogen-saturated solution at pH 8.3 to 9.0 with a 1- and 2-rad x-ray analyzing pulse introducing $\sim 5 \times 10^{-9}$M e^-_{aq}. After computer analysis of the data, it was found that the value of $k_1 = 16 \pm 1 M^{-1}$ sec^{-1} encompasses all of the results. The possibility that this

value is an upper limit only was examined. Combined with a value for k_1' of $2.3 \times 10^7 M^{-1}$ sec^{-1}, the equilibrium constant for the reaction becomes 7.0×10^{-7}, and the pK becomes 9.6. Some applications of these results to radiation chemistry are discussed. (auth)

10895 GAS PHASE RADIOLYSIS AND VACUUM ULTRAVIOLET PHOTOLYSIS OF 2- AND 3-PENTANONE. Scala, A.; Ausloos, P. (National Bureau of Standards, Washington, D. C.). J. Phys. Chem., 70: 260-9(Jan. 1966).

In the photolysis of 3-pentanone and 2-pentanone at 1470 and 1236 Å, the major modes of fragmentation of the electronically excited ketones are $C_2H_5COC_2H_5^* \rightarrow C_2H_5 + CO + C_2H_4 + H$ or $\rightarrow CH_3 + CH_2COC_2H_5$ (or $CH_2CO + C_2H_5$) and $CH_3COCH_2CH_2CH_3^* \rightarrow CH_3CO$ (or $CH_3 + CO$) $+ C_2H_4 + CH_3$ or $\rightarrow CH_3CO$ (or $CH_3 + CO$) $+ C_3H_6 + H$. On the basis of experiments carried out with $C_2H_5COC_2H_5 - C_2D_5COC_2D_5$ mixtures, it was concluded that molecular elimination of methane does also occur to a minor extent. Isotopic analysis of the products formed in the photolysis of $CD_3COCD_2-CH_2CH_3$ further indicated that the elimination process $CD_3COCD_2CH_2CH_3^* \rightarrow CD_3COCD_2H + C_2H_4$ does take place, but to a lesser extent than at 2537 and 3130 Å. In radiolysis neutral excited molecules and ions were produced. When an electrical field was applied during radiolysis, increased excitation by electron impact occurred. At low field strengths molecules were mainly excited to the first upper singlet and/or triplet state and decomposed in much the same way as reported in the earlier near-ultraviolet photolysis studies. When the field strength was increased, the ketone was excited to a higher singlet state and decomposed according to the first and fourth processes. Products not affected by the application of an electrical field, such as C_3H_4 and $1\text{-}C_4H_8$, can be ascribed to ion–molecule reactions. It is proposed that, in the radiolysis, transfer of a proton from various fragment ions to the pentanone molecule does occur and that this is followed by neutralization of the protonated pentanone to yield hydrogen as a product. (auth)

10896 INVESTIGATIONS IN THE FIELD OF RADIATION-INDUCED SOLID STATE POLYMERIZATION. IX. THE GAMMA-RAY INITIATED POLYMERIZATION OF TRIALLYL CYANURATE IN THE LIQUID AND SOLID STATES. Hardy, Gyula; Nagy, Lajos. Magyar Kem. Foly., 71: 442-7(Oct. 1965). (In Hungarian).

The initial period of gamma-initiated polymerization of triallyl cyanurate in the liquid and solid states had linear character with respect to time. At temperatures near the melting point, an acceleration of the rate of polymerization was observed in the solid state. The activation energy for liquid-phase polymerization was 6.00 kcal/mole and in the solid state 2.42 kcal/mole. Under definite conditions, solid-state polymerization could be retarded by diphenylpicrylhydrazil and p-benzoquinone, which may be regarded as evidence for the radical mechanism of the process. Depending on the conditions of liquid and solid-state polymerization, after a definite conversion, insoluble polymers were formed with cross-linked structure. Swelling of these products in acetone was characteristically different depending on the conditions of their formation (liquid or solid state) and on the degree of conversion. (auth)

10897 INVESTIGATIONS IN THE FIELD OF RADIATION-INDUCED SOLID STATE POLYMERIZATION. X. THE COPOLYMERIZATION OF VINYL CHLOROACETATE WITH ACRYLIC ACID. Hardy, Gyula; Boros-Gyevi, Janosne; Koronczay, Laszlo. Magyar Kem. Foly., 71: 447-50(Oct. 1965). (In Hungarian).

The copolymerization of vinyl chloroacetate and acrylic acid is characterized in the liquid state by the copolymerization constants $r_1 = 0{,}1$ and $r_2 = 6$. The phase diagram of the solid system of this pair of monomers had an eutectic point at the composition containing 62 mole-% of vinyl chloroacetate. The rate of copolymerization in the solid state was maximum at the eutectic point, and the copolymer formed had a composition identical with this eutectic. In the supercooled liquid state the rules governing copolymerization were similar, but the rate of the processes was ten times as high as in the solid state. (auth)

10898 EFFECT OF PRESSURE ON THE RADIATION-INDUCED SOLID STATE POLYMERIZATION OF ACRYLAMIDE. Tabata, Y.; Suzuki, T. (Tokyo Univ.). Makromol. Chem., 81: 223-33(1965).

Effects of pressure on the ^{60}Co gamma-radioinduced solid-state polymerization of acrylamide were studied in a pressure range of 1 to 5000 atm and over a temperature region of 28 to 70°C. Rates of polymerization and molecular weights were measured. The rate of polymerization was suppressed by pressure at the lower temperatures; but, the rate was accelerated near the melting point. The rate of polymerization was decreased by pressure at an initial stage of polymerization, but accelerated at later stages of polymerization at the same temperature. The number of polymer chains obtained was not affected by pressure; it depended only on the radiation dose. These results indicated that pressure has very little effect on the rate of initiation but that the propagation rate constant is markedly affected by pressure. The effect of pressure on the solid-state polymerization of acrylamide was attributed to the pressure dependence of the activation enthalpy ($\Delta H^{\ddagger}$) and the activation entropy ($\Delta S^{\ddagger}$) of the propagation step. Thus, the effect due to an increase of $\Delta H^{\ddagger}$ by pressure exceeded that of $\Delta S^{\ddagger}$ in a rigid monomer crystal below about 60°C, while, the effect due to an increase of $\Delta S^{\ddagger}$ exceeded that of $\Delta H^{\ddagger}$ at temperatures above about 60°C. (BBB)

10899 SITE OF ATTACK IN THE RADIOLYSIS OF PYRIMIDINE COMPOUNDS. Myers, L. S. Jr; Ward, J. F.; Tsukamoto, W. T.; Holmes, D. E. (Univ. of California, Los Angeles). Nature, 208: 1086-7(Dec. 11, 1965). (UCLA-12-570).

The site of attack in radiolysis of pyrimidine compounds and their nucleosides and nucleotides in dilute aqueous solution by ^{60}Co γ radiation was investigated. Strongly acid, neutral, and strongly basic aqueous solutions of amino, methyl, ribose, deoxyribose, ribose phosphate, and deoxyribose phosphate substituent groups were exposed to γ radiation. Ultraviolet absorption spectra were measured and a loss of absorption in the region of 260 to 280 mμ was determined on a Cary recording spectrophotometer. Results indicated that in acid solutions the initial radiolytic attack occurs chiefly at the 5,6-double bond of the pyrimidine ring; amino and methyl groups do not appear to be attacked, and the presence of a pentose or pentose phosphate unit diverts no more than 20% of the attacking species from the double bond. In alkaline solutions, where the molecules are ionized, both methyl and ribose groups are more sensitive. Ribose appears to be somewhat more sensitive than desoxyribose when attached to cytosine. The phosphate group appears to play no important part in the initial radiolytic attack under any of the conditions studied. (C.H.)

10900 GAMMA-RAY-INDUCED CHLORINATION OF BENZENE. Faw, Richard E. (Kansas State Univ., Manhattan); McCabe, John M.; Isbin, Herbert S. Nucl. Appl., 1: 548-55(Dec. 1965).

The radiation-induced reaction between benzene and chlorine in the liquid phase was studied using a continuous stirred-tank reaction system. The reaction was studied at higher exposure dose rates [2.66×10^{17} ev/(ml min)] and lower chlorine concentrations [0.025 M] than heretofore reported. In agreement with previous studies of both the ultraviolet- and the gamma-ray-induced reactions, the reaction was found to be a chain reaction, first order with respect to chlorine concentration, resulting in the formation of a mixture of the stereoisomers of 1,2,3,4,5,6-hexachlorocyclohexane. No effects of temperature or reaction-vessel surface-to-volume ratio were observed. An observed decrease in reaction rate with increasing holdup time in the reaction vessel was attributed to buildup of an inhibitor during the course of the reaction. (auth)

10901 PRODUCTION OF CARRIER-FREE ^{132}Cs AND ^{129}Cs. Wilson, Virginia H.; Bishop, W. N.; Hillman, Manny (Brookhaven National Lab., Upton, N. Y.). Nucl. Appl., 1: 556-9(Dec. 1965). (BNL-9356).

Carrier-free ^{132}Cs and ^{129}Cs were produced by the $^{129}I(\alpha,n)^{132}Cs$, $^{129}I(\alpha,4n)^{129}Cs$, and $^{127}I(\alpha,2n)^{129}Cs$ reactions using thallous iodide as a recoverable target. Upper limits for the production yields of these isotopes are 25 $\mu C/(\mu A\ h)$ for ^{132}Cs and 2 $mC/(\mu A\ h)$ for ^{129}Cs, for 35-Mev alpha particles. (auth)

10902 ABSOLUTE LIQUID-SCINTILLATION RATE CONSTANTS AND FLUORESCENCE EFFICIENCIES. Lukens, H. R. Jr. Nucl. Appl., 1: 597-602(Dec. 1965).

A method of measuring absolute numbers of photons from beta-particle-induced fluorescence of liquids was used to obtain absolute rate-constant values for fluorescence and fluorescence quenching in toluene and toluene-base scintillator solutions. The average number of fluorescent-state toluene molecules produced by ^{14}C beta particles and fluorescence efficiencies based on that number were obtained. (auth)

10903 MOESSBAUER EFFECT IN SOME HAEMOGLOBIN COMPOUNDS. Lang, G.; Marshall, W. (Atomic Energy Research Establishment, Harwell, Eng.). Proc. Phys. Soc., 87: 3-34(Jan. 1966).

A number of ferrous and ferric compounds of ^{57}Fe-enriched rat hemoglobin were studied by observing nuclear resonant absorption by the iron of the hem group. The ferrous compounds, reduced hemoglobin and hemoglobin carbon monoxide, show only quadrupole splittings at all temperatures, with values characteristic of high and low spin materials respectively. The ferrous compound hemoglobin nitric oxide exhibits a broad spectrum with an effective field value of about 200 kilogauss at all temperatures. This phenomenon is interpreted in terms of a very strong covalent bond between the π orbitals of the NO molecule and the t_{2g} orbitals of the Fe ion; this bonding is so strong that the distinction between ferrous and ferric assignments is blurred. The observed quadrupole Mössbauer absorption spectra of oxygenated hemoglobin suggest a similar intermediate assignment. At 4°K the ferric compounds with CN^-, N_3^-, OH^-, H_2O, and F^- exhibit magnetic hyperfine interactions with characteristic effective magnetic fields of the order of 500 kilogauss. At 195°K all except the fluoride show simple quadruple spectra, with splittings which are unusually large for ferric compounds. The spectra are interpreted, with the help of g values where known, to deduce the electronic state of the ion. (auth)

10904 THE X-RAY-INDUCED DAMAGE TO THE p-AMINOBENZOIC ACID MOIETY OF FOLIC ACID AND SOME OTHER p-AMINOBENZOIC ACID CONJUGATES IRRADIATED IN SOLUTION. Nakken, Karl Ford; Pihl, Alexander (Norsk Hydro's Inst. for Cancer Research, Oslo). Radiat. Res., 27: 19-31(Jan. 1966).

The x-radioinduced degradation of folic acid and the p-aminobenzoic acid conjugates N-(p-aminobenzoyl)glutamic acid and N-(p-aminobenzoyl)glycine was studied in neutral solutions flushed with air or nitrogen. The radiation damage to N-(p-aminobenzoyl)glutamic acid and N-(p-aminobenzoyl)glycine was found to be preferentially localized to the p-aminobenzoic acid moiety that was degraded with a slightly higher yield (G = 1.08) that was free p-aminobenzoic acid (G = 0.99). The results indicate that the aliphatic residues of the conjugates studied are unable to compete effectively for the radicals degrading p-aminobenzoic acid. Folic acid was degraded with a total yield of G = 1.20. Results indicate that folic acid is degraded by OH radicals and reflect the high rate of interaction of OH radicals with benzene rings activated by amino groups. (H.G.D.)

10905 THE STUDY OF LIFETIMES OF POSITRONIUM IN TEFLON IRRADIATED BY GAMMA RAYS. Chandra, Girish; Kulkarni, V. G.; Lagu, R. G.; Patankar, A. V.; Thosar, B. V. (Tata Inst. of Fundamental Research, Bombay). pp 210-14 of Nuclear Physics and Solid State Physics Symposium, 1965. Solid State Physics. Bombay, Atomic Energy Establishment, 1965.

The effect of free radicals produced in the gamma irradiation of Teflon on the quenching of the triplet state of positronium in Teflon was investigated. The concentration of free radicals was measured as a function of dose by ESR techniques, and the lifetime of positronium was measured with a fast-slow coincidence system. (D.C.W.)

10906 PULSE RADIOLYSIS. Proceedings of the International Symposium held at Manchester, April 1965. Ebert, M.; Keene, J. P.; Swallow, A. J.; Baxendale, J. H. (eds.). London-New York, Academic Press, 1965. 347p. 70s. (CONF-650447).

Twenty-two papers are included; a separate abstract has been prepared for each. (B.L.M.)

For abstracts of individual papers see: 10907–10928.

10907 THE TECHNIQUE OF PULSE RADIOLYSIS BY OPTICAL ABSORPTION. Keene, J. P. (Christie Hospital and Holt Radium Inst., Manchester, Eng.). pp 1-14 of Pulse Radiolysis. Ebert, M. (ed.). London-New York, Academic Press, 1965.

The history, development, techniques, and equipment of pulse radiolysis are discussed briefly. Special attention is given to both flash spectroscopy and kinetic spectrophotometry as methods for detecting chemical changes resulting from pulse radiolysis. Some discussion of linear accelerators, which produce electron pulses of 2 μsec or less duration, and other suitable electron beam apparatus is presented. (B.L.M.)

10908 SOME CONTRIBUTIONS OF THE ELECTRON PULSE TECHNIQUE. Baxendale, J. H. (The Univ., Manchester, Eng.). pp 15-27 of Pulse Radiolysis. Ebert, M. (ed.). London-New York, Academic Press, 1965.

A survey of the major contributions of the electron pulse technique to basic chemistry is presented as well as its contributions of a confirmatory nature for information and data previously obtained by more conventional techniques. Examples of both types of information, such as rate constants for free radicals and hydrated electron and yields, relative reactivities, and reaction mechanisms for organic reactions, are presented. Absorption spectra obtained by pulse radiolysis techniques for many species are presented. (B.L.M.)

10909 POLAROGRAPHIC STUDY OF AQUEOUS OXYGENATED SOLUTIONS IRRADIATED WITH 10 Mev ELECTRON PULSES. Zagorski, Z. P. (Inst. of Nuclear Research, Warsaw); Sehested, K. pp 29-41 of Pulse Radiolysis. Ebert, M. (ed.). London-New York, Academic Press, 1965.

Polarographic methods were applied to the study of pulse radiolysis of solutions of perchloric and sulfuric acids to prove definitely that active intermediate compounds are polarographically more active than oxygen. The dropping mercury electrode was chosen, and only the zone around the DME was irradiated with as high dose as possible. In acidic aqueous solutions saturated with oxygen, the presence of an intermediate with a lifetime of several seconds (half life 1.4 sec) was determined, and the intermediate was found only at a pH lower than 4.8. The redox potential of the intermediate is higher than +0.5 v. (B.L.M.)

10910 PULSE RADIOLYSIS OF LIQUID AMMONIA. Compton, D. M. J.; Bryant, J. F.; Cesena, R. A.; Gehman, B. L. (General Atomic Div., General Dynamics Corp., San Diego, Calif.). pp 43-9 of Pulse Radiolysis. Ebert, M. (ed.). London-New York, Academic Press, 1965.

Samples of liquid ammonia distilled into irradiation cells after standing in contact with Na metal for 24 hr were subjected to pulses of 30 Mev electrons. The pulse widths could be varied from 10 nsec to 4.5 μsec, and a typical pulse delivered 1 to 5×10^4 rads. A strong transient absorption was observed which peaked in the infrared and is similar to the well-known absorption curve for alkali-metal solutions in liquid NH_3. The absorption was made up of two parts; the initial absorption showing a fast decay and a long-lived absorption having a lifetime of ~1 sec that is tentatively identified with the solvated electron. The G-value for formation of this species was determined to be 0.45 ± 0.05. (B.L.M.)

10911 RADICAL YIELDS AND KINETICS IN THE PULSE RADIOLYSIS OF POTASSIUM BROMIDE SOLU-

TIONS. Sutton, H. C. (Univ. of Edinburgh); Adams, G. E.; Boag, J. W.; Michael, B. D. pp 61-81 of Pulse Radiolysis. Ebert, M. (ed.). London-New York, Academic Press, 1965.

Oxygen-saturated neutral solutions of KBr were irradiated with 0.2 μsec pulses of electrons having an average energy of 1.8 Mev to doses of 260–1600 rads. The pulse radiolysis of these solutions was studied by kinetic spectroscopy of the Br_2^- ions and is found to proceed largely by the same mechanism as for γ-radiolysis at low dose rates. Rate constants were measured for most of the reactions involved, and these constants along with G-values for the intermediate species are reported. (B.L.M.)

10912 PULSE RADIOLYSIS OF AERATED AQUEOUS POTASSIUM BROMIDE SOLUTIONS. Cercek, B.; Ebert, M.; Gilbert, C. W.; Swallow, A. J. (Christie Hospital and Holt Radium Inst., Manchester, Eng.). pp 83-98 of Pulse Radiolysis. Ebert, M. (ed.). London-New York, Academic Press, 1965.

Studies of transient species, spectra, and yields in the pulse radiolysis of aqueous-aerated H_2SO_4 solutions of KBr are reported. The results indicate that in the reaction scheme for the radiolysis the Br_2^- ion should be included. The rate constants for the various reactions and the G-values for the various intermediates are reported. In some of the air-saturated solutions the G(OH) yields were found to be pH independent between pH 1 and 9.5. (B.L.M.)

10913 PULSE RADIOLYSIS STUDIES OF CARBOXYL AND RELATED RADICALS. Keene, J. P.; Raef, Y.; Swallow, A. J. (Christie Hospital and Holt Radium Inst., Manchester, Eng.). pp 99-106 of Pulse Radiolysis. Ebert, M. (ed.). London-New York, Academic Press, 1965.

Pulse radiolysis of deaerated solutions of CO, CO_2, sodium formate, formic acid, and sodium bicarbonate yielded a transient species absorbing at 250 ± 5 nm. Both the absorption spectra and the kinetic studies were carried out spectrophotometrically. The transient species is identified as CO_2^- or in its acid form COOH. In solutions of sodium formate saturated with CO_2, pH = 5, the transient species were shown to carry a negative charge. The molar extinction coefficient of the CO_2^- is 2400 $mole^{-1}$ cm^{-1} at 250 nm, and the second-order rate constant for the reaction $CO_2^- + CO_2^- \rightarrow O_2CCO_2^-$ is 1×10^9 $mole^{-1}$ sec^{-1}. In formic acid solutions saturated with CO_2, pH = 2.4, the molar extinction coefficient and its second order rate of decay are almost the same as at pH = 5. Neither H atoms nor OH radical react appreciably with CO_2, but OH reacts with HCO_3^- to produce the CO_3^- (HCO_3) radical ions that absorb at 600 nm; the rate constant for the reaction is 1×10^7 $mole^{-1}$ sec^{-1}; and the molar extinction coefficient is 2900 $mole^{-1}$ cm^{-1}. (B.L.M.)

10914 DETERMINATION OF SOME FAST REACTION RATES USING THE PULSED RADIOLYSIS OF PERMANGANATE SOLUTIONS. Baxendale, J. H.; Keene, J. P.; Stott, D. A. (The Univ. Manchester, Eng. Christie Hospital and Holt Radium Inst., Manchester, Eng.). pp 107-15 of Pulse Radiolysis. Ebert, M. (ed.). London-New York, Academic Press, 1965.

Pulse radiolysis techniques were used to investigate the reaction of Cr^{2+}, Ni^+, Co^+, Cd^+, Ag^0, and Cu^+ with MnO_4^-, and the bimolecular rate constants for the respective reactions in units of 10^9 $mole^{-1}$ sec^{-1} were found to be 3.7, 7.5, 10.6, 13.0, 12, 5, and 10. The reaction of H + O_2 was studied, and the rate constants for H and HO_2 were found to be 23.5 and 0.008, each in units of 10^9 $mole^{-1}$ sec^{-1}. (B.L.M.)

10915 THE PULSE RADIOLYSIS OF AQUEOUS SOLUTIONS OF THIOCYANATE ION. Adams, G. E.; Boag, J. W.; Currant, J.; Michael, B. D. (Mount Vernon Hospital, Middlesex, Eng.). pp 117-29 of Pulse Radiolysis. Ebert, M. (ed.). London-New York, Academic Press, 1965.

The kinetics of the formation and decay of the CNS radical and its primary yield were investigated as a function of CNS^- concentration, pH, and added O_2 and N_2O by pulse radiolysis techniques. The studies indicate the CNS radical disappears in solution by dimerization, but at low pH the reaction of HO_2 with CNS contributes to the decay. At high pH the yield of CNS depends upon the competition for OH and O^- by the CNS and for O^- by oxygen. The kinetic studies confirmed the pK(OH) = 11.9. G-values are given for the radical under various conditions of pH and with the addition of both O_2 and N_2O to the solution. (B.L.M.)

10916 ABSOLUTE RATE CONSTANTS FOR THE REACTION OF THE HYDROXYL RADICAL WITH ORGANIC COMPOUNDS. Adams, G. E.; Boag, J. W.; Currant, J.; Michael, B. D. (Mount Vernon Hospital, Middlesex, Eng.). pp 131-43 of Pulse Radiolysis. Ebert, M. (ed.). London-New York, Academic Press, 1965.

Since no definite absorption maximum for the hydroxyl radical has been found, a competition technique using solutions of CNS^-, which reacts with OH to yield the radical CNS with a maximum near 500 nm, was used to study the reaction of some organic compounds with the OH radical as a result of irradiation with a pulse of electrons. The electron pulse was 0.2 μsec with a mean electron energy of about 1.8 Mev, and the peak current in the pulse was generally set at about 0.2 amp. The absolute reactivities of the OH radical with 21 aliphatic alcohols, 27 organic acids, esters, and carbonyl compounds; and 12 aromatic compounds of various types are tabulated. The effect of pH on the reactivity, and the comparative reactivities of certain organic solutes for free radicals are discussed. (B.L.M.)

10917 PULSE RADIOLYSIS STUDIES OF AQUEOUS SOLUTIONS OF NUCLEIC ACID AND RELATED SUBSTANCES. Scholes, G.; Shaw, Patricia; Willson, R. L. (Univ. of Newcastle upon Tyne, Eng.); Ebert, M. pp 151-64 of Pulse Radiolysis. Ebert, M. (ed.). London-New York, Academic Press, 1965.

The electron-pulse technique was used to follow the rates of reaction of radiation-produced electrons and hydroxyl radicals with DNA, nucleotides, nucleosides, and with free purine and pyrimidine bases. Reactions with certain amino acids and with di- and tri-peptides were investigated also, and the rate constants obtained are compared with those obtained by competitive stationary methods. (B.L.M.)

10918 REACTIONS OF THE HYDRATED ELECTRON WITH GLYCINE AND OTHER AMINO ACIDS AND PEPTIDES. Davies, J. V.; Ebert, M.; Swallow, A. J. (Christie Hospital and Holt Radium Inst., Manchester, Eng.). pp 165-70 of Pulse Radiolysis. Ebert, M. (ed.). London-New York, Academic Press, 1965.

Irradiation of de-aerated solutions of glycine, some other common amino acids, and a few simple peptides with pulses of electrons of 100–200 rads were studied to determine the reactions of the hydrated electron with these substances. Reaction rate measurements were obtained at 510 and 650 nm for the hydrated electron, and an absorption in the ultraviolet region is probably attributable to the hydroxyl radical. Second-order rate constants were measured for the various reactions and do not demonstrate any considerable dependence on chemical structure. Estimates of both the influence of ionic form on the reaction rate and the activation energy for the reaction e_{aq}-glycine have been made. (B.L.M.)

10919 REACTIONS OF THE HYDRATED ELECTRON WITH AMINO ACIDS, PEPTIDES AND PROTEINS. Braams, Reinier (Argonne National Lab., Ill.). pp 171-80 of Pulse Radiolysis. Ebert, M. (ed.). London-New York, Academic Press, 1965.

The results of the measurements of reaction rates between the hydrated electron and all common amino acids, a number of peptides, and a few proteins are summarized; and an attempt is made to analyze the reactivity of ribonuclease in terms of the reactivities of its constituent amino acids. A large difference in reactivity was noted between different ionic forms of the amino acids, with the reactivity generally being greater at neutral pH than at alkaline pH. Two different explanations of these reactivity differences are offered. The overall findings of the work would indicate that an explanation of the radiation effects

in proteins in terms of reactivities of specific reaction sites is possible. (B.L.M.)

10920 PULSE RADIOLYSIS OF AQUEOUS CARBOHYDRATE SOLUTIONS. **Davies, J. V. (Christie Hospital and Holt Radium Inst., Manchester, Eng.); Griffiths, W.; Phillips, G. O. pp 181-91 of Pulse Radiolysis. Ebert, M. (ed.). London-New York, Academic Press, 1965.**

The pulse radiolysis technique was applied to aqueous carbohydrate systems in an attempt to elucidate the mechanism of destruction by ionizing radiation, and in particular to compare the dependence concentration with that previously observed in low dose rate experiments. With D-glucose solutions, a transient species with an absorption maximum at 260–270 nm on pulsing was observed, which decays by second order kinetics within a solute range of $5-500 \times 10^{-3}$ M in argon or N_2O. The concentration of the transient increases with D-glucose concentration up to 5×10^{-3} M and then remains constant. The second-order rate constant measured for the reaction e^-_{aq} + D-glucose (and similar monosaccharides) was $\leq 10^7$ mole^{-1} sec^{-1} at concentrations of 5×10^{-3} M or less. At higher concentrations, the half life of the electron decreases. Saturation of the carbohydrate-solution with N_2O produced a doubling of the yield of the 280 nm transient indicating that the OH radicals are the predominant species causing the decomposition below 5×10^{-3} M. Above this concentration, another process further increases the radiation decomposition, and possible mechanisms are discussed. (B.L.M.)

10921 PULSE RADIOLYSIS STUDIES OF AQUEOUS POLYMER–THIOUREA SYSTEMS. **Charlesby, A. (Royal Military Coll. of Science, Shrivenham, Eng.); Fydelor, P. J.; Kopp, P. M.; Keene, J. P.; Swallow, A. J. pp 193-201 of Pulse Radiolysis. Ebert, M. (ed.). London-New York, Academic Press, 1965.**

The pulse radiolysis technique was applied to the study of the polymer polyethyleneoxide (PEO) both with and without the thiourea as an additive. In the PEO solutions, a spectral peak was observed at 240 nm: and since the electron does not react with the polymer, the peak is ascribed to polymer radicals that decay slowly by a bimolecular reaction. Pulse radiolysis of the dilute solution of thiourea revealed two peaks, a major one at 400 nm and a lesser one at 290 nm, in addition to the usual electron peak. Neither of these two peaks is attributed to the reaction of the electron with thiourea. For a composite PEO–thiourea solution, the 400 nm peak found in the thiourea was absent. A more rapid decrease of the broad peak at 290 nm than in the PEO solutions is interpreted as evidence that PEO–radicals react with one of the thiourea radiolytic products. (B.L.M.)

10922 PULSE RADIOLYSIS OF Ag^+ SOLUTIONS. **Baxendale, J. H.; Fielden, E. M.; Keene, J. P. (The Univ. Manchester, Eng. Christie Hospitale, Manchester, Eng.). pp 207-16 of Pulse Radiolysis. Ebert, M. (ed.). London-New York, Academic Press, 1965.**

Pulse radiolysis of Ag^+ solutions was found to give rise to three transient species, silver atoms Ag^0, Ag^{2+}, and a third that is tenatively identified as an excited silver ion. The Ag^0 has an absorption maximum at 310 nm ($\epsilon = 2.3 \times 10^4$ mole^{-1} cm^{-1}) and is formed from Ag^+ by reaction with the hydrated electron and by reaction with hydrogen. The Ag^0 decays by a second-order process in de-aerated solutions and in aerated solutions reacts with oxygen. Ag^{2+} is formed more slowly, probably by reaction of Ag^+ with OH and has an absorption maximum at 270 nm. The third species (X) has an absorption maximum at 360 nm; is formed from Ag^+ in a bimolecular reaction with a precursor Y; and decays in a bimolecular reaction with Ag^+. The Y may be an excited water molecule, and X is probably an excited Ag^+, either of which may be quenched by O_2, N_2O, H_2O_2, and $Co(NH_3)_6^{3+}$, all of which are known to prevent the formation of this third transient species. Rate constants for all reactions are given. (B.L.M.)

10923 FORMATION OF Cu^{III} IN THE RADIOLYSIS OF Cu^{2+} SOLUTIONS. **Baxendale, J. H.; Fielden, E. M.; Keene, J. P. (The Univ., Manchester, Eng. Christie Hospital, Manchester, Eng.). pp 217-20 of Pulse Radiolysis. Ebert, M. (ed.). London-New York, Academic Press, 1965.**

Solutions of aqueous cupric ion exhibit a transient absorption maximum at 300 nm in neutral solution and at 265 nm in acid solution after pulse radiolysis. These maxima are shown to be due to Cu(III) in the form of $CuOH^{2+}$ and Cu^{3+}, respectively. The equilibrium constant for the hydrolysis $Cu^{3+} + H_2O \rightleftharpoons CuOH^{2+}$ is reported to be 0.9×10^{-3}, and the rate constant for the reaction OH + $Cu^{2+} \rightarrow CuOH^{2+}$ as 3.5×10^8 mole^{-1} sec^{-1}. (B.L.M.)

10924 TRANSIENT ABSORPTION FROM 260-320 nm IN CERTAIN PULSE IRRADIATED AQUEOUS SOLUTIONS. **Brown, D. M. (Leeds Univ., Eng.); Dainton, F. S.; Walker, D. C.; Keene, J. P. pp 221-6 of Pulse Radiolysis. Ebert, M. (ed.). London-New York, Academic Press, 1965.**

Using the pulse radiolysis technique, the absorption spectra of pure water saturated with N_2O and 6×10^{-4}M aqueous H_2O_2 at natural pH were investigated. A weak transient absorption maximum was measured in the region of 260–320 nm and is probably due to the hydroxyl radical. The absorption for which $G\epsilon_{275nm} = 1120 \pm 260$ is present at the end of a 2 μsec, 5000 rad electron pulse. Qualitative decay kinetics of the transient are described. Evidence obtained with various hydroxyl scavengers supports the assumption that the maximum in the region of 260 nm is indeed due to the hydroxyl radical. (B.L.M.)

10925 A PULSE RADIOLYSIS STUDY OF METHYLENE BLUE. **Keene, J. P.; Land, E. J.; Swallow, A. J. (Christie Hospital and Holt Radium Inst., Manchester, Eng.). pp 227-45 of Pulse Radiolysis. Ebert, M. (ed.). London-New York, Academic Press, 1965.**

A detailed pulse radiolysis study of methylene blue in the presence of excess formate at various acidities is reported. In neutral solution bleaching of the dye by solvated electrons and formate radicals results in the formation of a semiquinone radical having an absorption maximum at 420 nm and a molar extinction coefficient of 10400 mole^{-1} cm^{-1}. This radical disproportionates to leuco methylene blue and methylene blue. In progressively acidic solutions up to 22.9 N H_2SO_4, the semiquinone undergoes two changes in its state of protonation, and the two acidic semiquinones have wavelength maxima at ~380 and ~440 nm. Structures are suggested for the three forms of semiquinones, and approximate rates of formation and decay of the two protonated forms of semiquinone were obtained by studying selected acidities. The doubly protonated semiquinone was stable indefinitely in 22.9 N H_2SO_4. In the absence of formate, pulse radiolysis studies suggested the probable formation of semi-oxidized methylene blue having a maximum at 520 nm in addition to the semiquinone. Rate constants are given for all reactions. (B.L.M.)

10926 SOME ASPECTS OF THE QUENCHING OF EXCITED STATES FORMED IN PULSE RADIOLYSIS. **Kemp, T. J.; Salmon, G. A.; Wardman, P. (The Univ., Leeds, Eng.). pp 247-57 of Pulse Radiolysis. Ebert, M. (ed.). London-New York, Academic Press, 1965.**

A group of experiments are described that were designed to investigate and elucidate some of the quenching effects of substances, e.g., polar organic solvents, on the excited states arising from pulse radiolysis as evidenced by the quenching of absorption maxima measured for these excited states. The experiments were aimed at providing information concerning the three following problems: the spectroscopic identification and estimation of positive and negative ions and excited states derived from dilute liquid and glassy solutions of electron scavengers in solvents of widely differing polarity; elucidation of mechanism of transfer of charge and energy from the points of initial formation and deposition respectively in the solvent to the solute; and the role of aggregates in solutions comprising two solvents. (B.L.M.)

10927 EXCITATION TRANSFER AND DECAY PROCESSES IN MULTI-COMPONENT SYSTEMS: CYCLOHEXANE + BENZENE + p-TERPHENYL. **Dillon, Michael A.; Burton, Milton (Univ. of Notre Dame, Ind.). pp 259-**

77 of Pulse Radiolysis. Ebert, M. (ed.). London-New York, Academic Press, 1965.

The results of kinetic studies of the intermolecular and intramolecular energy transfer in excited benzene are reported in which the transfers have been examined in time-dependent experiments with ultrafast pulse times and delays i.e., in the nanosecond region. Most of the important conclusions are derived from luminescence decay curves of the de-aerated three-component system; cyclohexane-benzene–p-terphenyl (as a scintillator). The new values obtained for the characteristic luminescence parameters are in good agreement with those previously reported in steady-state studies with ^{60}Co gamma-radiation. Variations in the parameters are attributed to simultaneous variations in the specific rates of self-quenching and of excitation transfer and quenching. The diffusion of the excited state itself via the intermediary of intervening benzene molecules was found to be an important contributor to the two processes. (B.L.M.)

10928 PULSE RADIOLYSIS OF CARBON TETRACHLORIDE-BENZENE MIXTURES. Buehler, R. E. (Eidgenoessische Technische Hochschule, Zurich); Gaeumann, T.; Ebert, M. pp 279-84 of Pulse Radiolysis. Ebert, M. (ed.). London-New York, Academic Press, 1965.

After pulse radiolysis of a de-aerated solution of benzene-CCl_4 mixture, a transient absorption spectrum in the visible region with a lifetime of a few microseconds was observed. The absorption maximum is at 486 ± 4 nm and the half-width is about 150 mm. If the benzene in the mixture is replaced by cyclohexane, the absorption band disappears entirely. The half life of the transient remains for a few microseconds throughout the concentration range from 10^{-3} to about 1 M benzene in CCl_4, but the rate law changes. At low concentrations of the benzene a pseudo first-order disappearance was found for dose rates less than 1500 rads/2 μsec. It is highly improbable that the transient has chlorine as a direct precursor, and the transient is not a charge-transfer complex between the chlorine atom and benzene. (B.L.M.)

10929 METHOD FOR THE PRODUCTION OF CIS-1,4-POLYISOPRENE. Mitsutani, Akio (to Kurashiki Rayon Co., Ltd.). Japanese Patent 1964-24285. Oct. 29, 1964. Filed Jan. 16, 1962.

A method is proposed to obtain polyisoprene polymer with a high content of cis-1,4 structure with a very small ratio of trialkyl aluminum to $TiCl_4$, i.e., with an Al/Ti ratio of 0.8 to 0.2, and thus to reduce the amount of trialkyl aluminum necessary as the polymerization catalyst. The catalyst system consists of $TiCl_4$ irradiated with ionizing radiation in the presence of an inert hydrocarbon solvent as one component and trialkyl aluminum, as another component, mixed with the $TiCl_4$ in an inert hydrocarbon solvent in the Al/Ti molar ratio of 0.8 down to 0.2. Substantially all of the linkages of the polyisoprene obtained from isoprene monomer by the use of this catalyst system are of the cis-1,4 structure. (NSA of Japan)

10930 METHOD FOR PRODUCING BIPHENYL AND TRIPHENYL. Tsuda, Yutaka (to Chief of the Agency of Ind. Sci. and Tech.). Japanese Patent 1964-26197. Nov. 18, 1964. Filed Aug. 18, 1961.

A new radiation chemical method for the production of a biphenyl-terphenyl mixture consists of adding C_6H_6 to N_2O-saturated H_2O and irradiating the whole by high-energy radiation. The yield of the biphenyl-terphenyl mixture produced is proportional to the radiation dose and is over four times as large as that with no N_2O present. Upon standing, the biphenyl and terphenyl forms precipitate as white, crystalline flakes and can be filtered off to obtain the pure product. (TCO)

10931 METHOD FOR STABILIZING VITAMIN B_1-HYDROCHLORIDE. Takeda, Kenichi (to Shionogi and Co., Ltd.). Japanese Patent 1965-2154. Feb. 4, 1965. Filed Nov. 9, 1961.

Vitamin B_1-hydrochloride is stabilized by irradiation to produce a good crystalline product that is only slightly hydroscopic. The product is stable when combined with other ingredients, such as calcium carbonate and vitamin C. Irradiation conditions are described in detail. (TCO)

Radiochemistry

See also Separation Processes and Procedures

Refer also to abstracts 10901 and 11129.

10932 (ORNL-P-1928) LOW ENERGY GAMMA AND X-RAY FROM RADIOACTIVE SOURCES. Pressly, R. S. (Oak Ridge National Lab., Tenn.). [nd]. Contract W-7405-eng-26. 31p. (CONF-660207-2). Dep. mn. CFSTI $2.00 cy, $0.50 mn.

From Radioisotope Applications in Aerospace Symposium, Dayton, Ohio.

The methods used in the fabrication of low-energy gamma, bremsstrahlung, and x-ray sources are described. The spectra of the radiation from several sources are given with efficiency measurements. The newer radioisotopes which are being investigated and their availability are discussed. (auth)

10933 (TID-22532) RADIOCHEMISTRY RESEARCH. Final Report, June 1, 1956–May 31, 1965. (Kansas Univ., Lawrence). Contract AT(11-1)-407. 27p. Dep. mn. CFSTI $2.00 cy, $0.50 mn.

Developments are reported for studies on: reactions of recoil tritium atoms; radio gas chromatography; production and use of radioactive tracers; hot atom chemistry of ^{212}Pb, ^{131}I, and ^{38}Cl; and hot atom reactions in geochemical studies. (P.C.H.)

10934 (UCRL-11743) THE INSTABILITY OF PYRUVATE-^{14}C. Moses, V. (Lawrence Radiation Lab., Univ. of California, Berkeley). Oct. 1964. Contract W-7405-eng-48. 8p. Dep. mn. CFSTI $1.00 cy, $0.50 mn.

Pyruvate-^{14}C was analyzed for impurities and decomposition by one-dimensional chromatography. In both stored and newly prepared pyruvate-^{14}C decomposition products and/or impurities were found. Thus, further attempts to use this substance as a metabolic substrate were abandoned. (P.C.H.)

10935 (USNRDL-TR-948) AN IODINE SOURCE FOR BETA COUNTING. Delucchi, A. A.; Greendale, A. E. (Naval Radiological Defense Lab., San Francisco, Calif.). Nov. 15, 1965. Contract AT(49-2)-1167. 11p. Dep. mn. CFSTI $1.00 cy, $0.50 mn.

A method for preparing lightweight silver iodide sources is described. By reacting gaseous iodine with an electroplated silver surface, sources weighing a fraction of a milligram are obtained. (D.C.W.)

10936 (CEA-tr-A-1855) L'INFLUENCE D'ADDITIONS RADIOACTIVES D'ATOMES MARQUES SUR LES MECANISMES DES REACTIONS. (The Influence of Radioactive Additions of Labeled Atoms on Mechanisms of Reactions). Spitsyn, V. I. Translated into French from Abhandl. Deut. Akad. Wiss. Berlin, Kl. Chem., Geol. Biol., No. 2, 26-41(1960). 41p. Dep. mn; JCL $4.60 fs, $1.43 mf.

Studies were undertaken to determine the effects of radiation on the physicochemical properties of some solids. The exchange velocity of sulfur isotopes at high temperature in the system $K_2SO_4-SO_3$ and of oxygen in the system $Na_2SO_4-O_2$ depended considerably on the specific radioactivity (in ^{35}S) of the sulfate studied. It was found that the specific radioactivity of ^{35}S or of Ra in the barium sulfate affected the rate of adsorption of some aqueous solutions of organic dyes. The positive effect of the radioactivity of the catalyst on the kinetics of cyclohexanol hydrogenation is discussed. (tr-auth)

10937 (NP-tr-1323) SYNTHESES OF ^{32}S- OR ^{35}S-LABELLED MALEIMIDES. Merz, H.; Pfleiderer, G.; Wieland, T. Translated by E. F. Towndrow (U.K.A.E.A. Atomic Energy Research Establishment, Harwell, Eng.), from Biochem. Z., 342: 66-75(1965). 26p. Dep. mn. JCL $2.60 fs, $0.98 mf.

Methods are described for the preparation on a gram and milligram scale of N-ethylmercaptoethylmaleimide, N-(4-sulfophenyl)-maleimide, and N-(N-acetyl-4-sulfamoyl)-maleimide. The reaction between the latter compound, labeled with ^{35}S, and cysteine at pH 6 was studied by paper chromatography. In general, the syntheses followed the same pattern, which is cleavage of maleic anhydride with the appropriate amine and ring closure of the maleic monoamide by dehydration with acetic anhydride. (P.C.H.)

10938 REACTIONS OF BROMINE ACTIVATED BY ^{82m}Br ISOMERIC TRANSITION AND RADIATIVE NEUTRON CAPTURE IN LIQUID AND SOLID CARBON TETRACHLORIDE AND n-HEXANE. Merrigan, Joseph A.; Ellgren, William K. Jr.; Rack, Edward P. (Univ. of Nebraska, Lincoln). J. Chem. Phys., 44: 174-80(Jan. 1, 1966).

New methods were developed for obtaining ^{82}Br and ^{82m}Br organic retentions produced by ^{82m}Br isomeric-transition reactions and radiative neutron capture by ^{81}Br, respectively. No isotope effect was found for ^{80m}Br and ^{82m}Br reactions activated by the (n,γ) process. The ^{82m}Br (I.T.) ^{82}Br process was found to produce ^{82}Br organic retentions nearly twice as high as the ^{80m}Br and ^{82m}Br organic retentions produced by the (n,γ) process. Effects of solidifying samples indicate a clumping of bromine molecules upon freezing. Product analyses indicate similar reaction mechanisms for the (n,γ) and (I.T.) activated reactions. (auth)

10939 THEORY OF THE LOW-TEMPERATURE CHROMATOGRAPHIC SEPARATION OF THE HYDROGEN ISOTOPES. King, James Jr. (California Inst. of Tech., Pasadena); Benson, Sidney W. J. Chem. Phys., 44: 1007-14(Feb. 1, 1966).

An electrostatic theory is presented, which quantitatively explains the chromatographic separation of the hydrogen isotopes on an alumina column at low temperatures. The theory is based on the interaction of the surface electric fields of the alumina with the polarizable hydrogen isotopes. By calculating the electric fields over an adopted Al_2O_3 surface, it was found that there are two active adsorption sites at 77.4°K, one over a vacancy in the Al_2O_3 structure, and the other over an Al^{3+}. The total interaction potential over either side is a function of the polarizabilities of the adsorbed molecules and the distance the molecules are from the surface. A 5 to 9 potential over a vacancy site gives results that favorably agree with experimental values. The rotational barrier, necessary to explain the separation of the ortho and para species, is shown to arise from the difference in the parallel and perpendicular components of the molecular polarizability of the hydrogen molecule. (auth)

10940 ANALYTICAL RADIOCHEMISTRY OF TECHNETIUM [Thesis]. Goldstein, Gerald. Knoxville, Tenn., Univ. of Tennessee, 1965. 133p.

Analytical methods studied include two methods for beta counting of ^{99}Tc, activation analysis with 14-Mev neutrons, and separation of technetium by solvent extraction with cyclohexanone. Attempts were made to prepare improved sources for $4\pi\beta$ counting by electrodeposition of technetium on the standard $4\pi\beta$ mount, which consists of a VYNS plastic film with a thin gold layer vacuum-evaporated onto its surface. It was possible to prepare a thin, uniform, metallic source in this way provided that the mount had no conducting material other than the gold surface. It was not possible to quantitatively electrodeposit microgram quantities of technetium with the simple apparatus and technique employed. A detailed study was made of an extrapolation technique for liquid-scintillation counting in which the integral counting rate is determined as a function of pulse-height discriminator voltage and extrapolated to zero discriminator bias. Counting efficiency of 100 per cent was obtained for beta groups above 200 kev in energy, with a relative standard deviation of less than 1 per cent. This method was also applied with isotopes that decay by $\beta-\gamma$ emission or by emitting several beta groups with equally good results; it is relatively insensitive to quenching agents. The half life and specific activity of ^{99}Tc were determined by measuring the activity of a known weight by the liquid-scintillation method and found to be $2.14\ (\pm 0.05) \times 10^5$ years and $3.75\ (\pm 0.07) \times 10^4$ disintegrations per minute per μg, respectively. Cross sections for the reactions of 14-Mev neutrons with ^{99}Tc were determined. The cross sections for the (n,α) and (n,p) reactions are 8 and 5 millibarns respectively. While the cross section for the (n,n′) reaction is larger (70 millibarns), bremsstrahlung from the beta decay of ^{99}Tc interfere in the measurement of the ^{99m}Tc product. The product of the (n,2n) reaction, ^{98}Tc, has a half-life of 10^6 years and was not detected. Extraction of technetium with cyclohexanone from sulfuric acid solutions was a rapid, efficient, and selective method of separation. This procedure was used for the separation of technetium from fission products. (Dissertation Abstr.)

10941 THE PREPARATION OF ^{131}I- AND ^{125}I-LABELLED PLASMA PROTEINS. McFarlane, A. S. (National Inst. for Medical Research, London). pp 3-6 of STI/DOC/10/45.

Procedures for labeling plasma proteins with iodine radioisotopes are reviewed. Factors discussed include: protein denaturation; iodination; levels of substitution; carriers; removal of ^{131}I; self-radiation effects; and testing of labeled proteins. (H.G.D.)

10942 THE LABELLING OF PROTEINS WITH ^{131}I. Huegli, H. (Eidgenoessisches Institut fuer Reaktorforschung, Wuerenlingen, Switzerland). pp 7-8 of STI/DOC/10/45.

A method for preparing a product containing approximately 150 μc ^{131}I per 10 mg of human albumin per ml with an average of 0.7 atoms of iodine per protein molecule is described. Solutions of iodine monochloride and human serum albumin are prepared, and labeling is carried out by injecting the labeling solution into the albumin solution. The reaction is complete after 3 min. When stored in a refrigerator at 5°C, less than 1% unbound iodine separates out in the course of a month. The method was used successful to label other proteins such as γ-globulin, bovine albumin, and glucagon. (H.G.D.)

10943 CONSIDERATIONS IN THE PREPARATION OF ^{131}I-LABELLED HORMONES. Berson, S. A.; Yalow, R. S. (Veterinary Administration Hospital, New York). pp 29-33 of STI/DOC/10/45.

Procedures for preparing ^{131}I-labeled hormones are reviewed. Problems unique to ^{131}I-labeled hormones are determined by the special purposes to which the labeled compound is to be put and distinctive physical and chemical characteristics of protein and polypeptide hormones. Iodine-131-labeled hormones have been used in turnover studies, in immunological investigations, and in the immunologic assay of hormones. For the last of these purposes labeling at rather high specific activity is particularly necessary. Methods for iodination and purification are discussed. (H.G.D.)

10944 THE PREPARATION OF ^{51}Cr-ALBUMIN. Waldmann, T. A. (National Cancer Inst., Bethesda, Md.). pp 35-40 of STI/DOC/10/45.

Chromium-51-labeled albumin was prepared from carrier-free chromium-51-labeled chromic chloride of high specific activity. Labeled chromic chloride was incubated with human serum albumin. Free and weakly bound Cr was removed by passage through a column packed with Amberlite resin. Sterilization was achieved by filtration through a 0.22-μ membrane filter. Biological controls consisted of pyrogen testing in female virgin rabbits and a sterility test in fluid thioglycolate and fluid Sabarauds medium. From 23 to 50% of the ^{51}Cr initially incubated with the albumin was found bound to the final product, and from 90 to 96% of the radioactivity in the final product was precipitated by 10% phosphotungstic acid. The electrophoretic mobility of ^{51}Cr-albumin was studied with curtain electrophoresis. Chromium-51 radioactivity migrated with the unlabeled albumin. (H.G.D.)

10945 THE PREPARATION OF ^{3}H-LABELLED PROTEINS. Jeejeebhoy, K. N. (Tata Memorial Hospital, Bombay). pp 41-7 of STI/DOC/10/45.

Preparation of tritium-labeled proteins by biosynthesis or by exchange labeling is reviewed. Biosynthetic preparations of ^{3}H-labeled albumin and ^{3}H-labeled antibody are presented. Exchange labeling has the advantage of producing high specific-activity compounds. However, exchange labeling may be associated with denaturation of the parent compound and the introduction of the label may alter the biological reactivity of the compound. Purification is the most important procedure in the preparation of exchange-labeled proteins. A brief review is presented of the three main steps of the purification process: removal of labile ^{3}H and insoluble denatured protein; dialysis to remove non-protein fragments of low molecular weight; and preparative chromatography, electrophoresis or crystallization to separate chemically labeled protein. Effects of ^{3}H-labeling by the exchange process on chemical properties of enzymes, albumin, antibodies, and insulin and on biological properties of antibodies, albumin, and insulin are discussed. (H.G.D.)

10946 THE PREPARATION OF ^{131}I-POLYVINYLPYRROLIDONE. Huegli, H. (Eidgenoessisches Institut fuer Reaktorforschung, Wuerenlingen, Switzerland). pp 49-53 of STI/DOC/10/45.

A preparation of ^{131}I-polyvinylpyrrolidone (PVP) is described that results in a stable product with fractions having accurately determined molecular weights. Starting with 100 g of vinylpyrrolidone and 200 mg of α,α'-azodiisobutyronitrile, 30 to 40 g of PVP with an average molecular weight between 65000 and 85000 are produced in the form of a pure white powder that remains unaltered for several months. PVP fractionation is achieved by precipitation. Labeling is done by adding ^{131}I-labeling-NaI to the PVP and exposing the solution to uv radiation for 5 to 6 hrs. Chromatographic examination yielded an Rf value for PVP of 0 to 0.1 and for ^{131}I of 0.9 to 1.0. (H.G.D.)

Separation Processes and Procedures

See also Analytical Procedures
ISOTOPE TECHNOLOGY — Separation and Production

Refer also to abstract 11032.

10947 (AERE-R-4786) METHODS OF DECREASING THE EXTRACTION BY PROCESSING SOLVENTS OF NITROSYLRUTHENIUM NITRATO COMPLEXES FROM NITRIC ACID SOLUTIONS. PART 3. MINIATURE EXTRACTOR RUNS ON SYNTHETIC SOLUTIONS CONTAINING NITROSYLRUTHENIUM NITRATO AND NITRO COMPLEXES. Scargill, D.; Streeton, R. J. W.; Lyon, C. E. (Atomic Energy Research Establishment, Harwell (England)). Nov. 1965. 16p. Dep. BIS $0.60, HMSO 3s.

Miniature-extractor runs with tri-n-butyl phosphate (TBP) and Butex as extractants were carried out to measure the change in the decontamination factor for ruthenium (DF_{Ru}) obtained by converting nitrato complexes of nitrosylruthenium to nitro complexes. For a 90% conversion, a tenfold improvement in DF_{Ru} was obtained with 20 or 30% TBP as predicted. DF_{Ru} was decreased by operating at short residence times. With Butex, there was no improvement in DF_{Ru} for 30% conversion, because of the high extractability of the dinitro complex. (auth)

10948 (HW-76472) PROPOSED CHEMICAL FLOWSHEETS FOR THE DECLADDING AND DISSOLUTION OF PRTR PLUTONIUM ALUMINUM FUEL. Hanson, G. L. (General Electric Co., Richland, Wash. Hanford Atomic Products Operation). Feb. 5, 1963. Contract AT(45-1)-1350. 9p. ORAU.

Zircaloy-clad plutonium–aluminum fuel elements from the Plutonium Recycle Test Reactor will be dissolved and processed in the Redox plant. The proposed flowsheets together with existing process flowsheets and dissolver operating specifications will provide the basis for plant operating procedures required to process this fuel. The dissolution requires a three-step dissolution process, and is based on the current standard flowsheet for dejacketing aluminum-clad uranium fuels. The flowsheet for dissolving the Zircaloy cladding and end fittings was developed from laboratory and pilot plant data and was successfully demonstrated in the Redox plant. (P.C.H.)

10949 (K-1469) THERMAL DIFFUSION COLUMN SHAPE FACTORS. PART I. SHAPE FACTORS BASED ON AN INVERSE POWER REPULSION MODEL. Greene, E.; Hoglund, R. L.; Von Halle, E. (Oak Ridge Gaseous Diffusion Plant, Tenn.). Feb. 7, 1966. Contract W-7405-eng-26. 177p. Dep. mn. CFSTI $4.00 cy, $1.00 mn.

The separation of a binary gaseous mixture which can be obtained in thermal diffusion columns can be calculated from the transport equation $\tau = Hx(1-x) - (K_c + K_d)\, dx/dz$. Two tables of shape factors are presented from which the transport coefficients H, K_c, and K_d can be calculated. Both sets of shape factors are based on an inverse-power repulsion model for the intermolecular forces. (D.C.W.)

10950 EXTRACTION OF SUBMICROGRAM AMOUNTS OF MANGANESE USING ^{54}Mn FROM BONE, MILK AND TEETH SOLUTIONS. Healy, W. B. (Dept. of Scientific and Industrial Research, Lower Hutt, N. Z.). Anal. Chim. Acta, 34: 238-40(Feb. 1966).

The efficiency of sodium diethyldithiocarbamate in the presence of citrate on the extraction of manganese in amounts as low as 10^{-9} g is reported. The pH optimum in the system was considered. ^{54}Mn was used as tracer. The extraction at pH 5.3 appeared to be the most efficient. (M.C.G.)

10951 STUDIES OF THE LIQUID-LIQUID PARTITION SYSTEMS. IV. THE SOLVENT EXTRACTION STUDY OF EUROPIUM(III) ADDUCT CHELATE COMPLEXES WITH SIX ACETYLACETONE DERIVATIVES AND TRIBUTYLPHOSPHATE. Sekine, Tatsuya; Ono, Masaru (Tokyo Coll. of Science). Bull. Chem. Soc. Jap., 38: 2087-94 (Dec. 1965).

The extraction of europium(III) in 0.1M sodium perchlorate with acetylacetone, benzoylacetone, trifluoroacetylacetone, benzoyltrifluoroacetone, furoyltrifluoroacetone, and thenoyltrifluoroacetone in chloroform and the adduct formation of the metal chelates with tributyl phosphate were studied at 25°C. It was concluded that the β-diketones with one trifluoromethyl group extract europium(III) better than those that have no trifluoromethyl group. The difference in the metal extraction with acetylacetone or trifluoroacetylacetone and the metal extraction with homologs of these β-diketones seemed to be mainly due to the aqueous chelate complex formation. A metal chelate with a β-diketone that had a trifluoromethyl group was a much better acceptor of tributyl phosphate to form adduct complexes than a metal chelate with a β-diketone that had no trifluoromethyl group. The ability of the acetylacetone chelate or the trifluoroacetylacetone chelate to form an adduct was not changed very much by the replacement of the methyl group with a benzoyl, furoyl, or thenoyl group. (auth)

10952 THE INFLUENCE OF THE RADIUS AND CHARGE OF THE ION ON EXTRACTION (THE POSITION OF ELEMENTS IN THE SEPARATION SERIES). Nikolaev, A. V. (Inst. of Inorganic Chemistry, Academy of Sciences, USSR). Dokl. Akad. Nauk SSSR, 163: 897-9(Aug. 1, 1965).

In previous separation studies of the extraction of the nitrates of La + Y and $Th^{4+} + UO_2^{2+} + Ce^{4+}$ by tributyl phosphate, it was often noted that the position of the element in the extraction series is independent of the concentration. The series of trivalent rare earths agreed with the elements' position in the periodic system. This is due to the relative stability of complex compounds, which increases with decreases in the element's ionic radius. The ion with the most stable solvate is accumulated in the organic phase; that with the least stable solvate is enriched in the aqueous, raffinate phase. It was difficult to establish which of the two ions, Ce^{4+} and UO_2^{2+}, forms

more stable solvates; therefore, the $UO_2(NO_3)_2-Ce(NO_3)_4-H_2O-(C_4H_9O)_3PO$ system was studied. The partition coefficients and the phase diagram were determined. It was found that, regardless of the concentration, Ce is accumulated in the extract and the uranyl nitrate in the raffinate, although the partition coefficients differ only slightly. This indicated that there is only a slight difference in the stability of the solvates. On the other hand, the stability of La and Th solvates differed markedly, that of Th being more stable. The stability of the trivalent element complexes followed the series: La < Y < Sc < Al. Although the partition coefficients and the thermochemistry of extractive processes must be further studied, the following series may be accepted for indicating the separation of lanthanides and actinides: La ... HNO_3 ... Sm ... Gd ... Y ... Yb ... Lu ... Th(IV) ... UO_2(II) ... Ce(IV). (TTT)

10953 THE REGULARITIES IN STABILITY CONSTANTS OF SOME RARE EARTH COMPLEXES. Fidelis, I.; Siekierski, S. (Inst. of Nuclear Research, Warsaw). J. Inorg. Nucl. Chem., 28: 185-8(Jan. 1966).

It was found that the separation factor β of the rare earths in the 2-ethylhexyl phenylphosphonate–aqueous hydrochloric acid system shows some regularities depending on the atomic number of the lanthanon. The changes in β, from La to Gd and from Gd to Lu, were similar. It was assumed that entropy is the main factor that determines the strength of the metal–ligand bond and that the regularities observed are caused by the entropy changes. (auth)

10954 SEPARATION OF NEPTUNIUM FROM NEUTRON IRRADIATED URANIUM BY REVERSED-PHASE PARTITION CHROMATOGRAPHY IN THE TBP–HNO_3 SYSTEM. Lis, S.; Jozefowicz, E. T.; Siekierski, S. (Inst. of Nuclear Research, Warsaw). J. Inorg. Nucl. Chem., 28: 199-207 (Jan. 1966).

A method of quantitative separation of radiochemically pure ^{239}Np from neutron-irradiated uranium samples was developed using reversed-phase partition chromatography. TBP adsorbed on hydrophobic kieselguhr was used as stationary phase and HNO_3 of various concentrations as the mobile phase. Neptunium was selectively reduced in the column from the VI to V oxidation state. The behavior of some fission products creating special difficulties in the separation process was investigated along with the neptunium yield. (auth)

10955 ANION EXCHANGE OF METAL COMPLEXES. XV. ANION EXCHANGE AND AMINE EXTRACTION OF LANTHANIDES AND TRIVALENT ACTINIDES FROM CHLORIDE SOLUTIONS. Marcus, Y. (Soreq Nuclear Research Centre, Yavne, Israel). J. Inorg. Nucl. Chem., 28: 209-19(Jan. 1966). (IA–1020).

The lanthanide and trivalent actinide complex species existing in concentrated aqueous chloride solutions were ascertained from anion exchange and amine extraction data. The dependence of the anion exchange distribution coefficients on the crosslinking of the resin and on the acidity of the solutions led to the species MCl_4^- in the resin, and the chloride concentration dependence led to MCl_2^+ as the major species in solution. The dependence of the distribution coefficients with amines on amine concentration, acidity, and chloride concentration also led to MCl_2^+ in the aqueous phase, in accord with the anion exchange data. For Am(III), the species in the organic phase is probably LiA_2AmCl_6, where A^+ is the result of the dissociation of one chloride ion from an amine hydrochloride aggregate. (auth)

10956 ANION EXCHANGE SEPARATION BETWEEN AMERICIUM AND CURIUM AND BETWEEN SEVERAL LANTHANIDE ELEMENTS. Kraak, W.; Van Der Heijden, W. A. (Reactor Centrum Nederland, Petten, Netherlands). J. Inorg. Nucl. Chem., 28: 221-4(Jan. 1966).

A complete separation between americium and curium was obtained from an anion-exchange column in concentrated aluminum nitrate medium. Distribution coefficients for a number of lanthanide elements were determined in batch experiments. The results suggested good separation possibilities for several of the rare earth elements. (auth)

10957 INFLUENCE OF THERMAL TREATMENT ON THE RATE OF ION EXCHANGE OF ZIRCONIUM PHOSPHATE. Alberti, G.; Conte, A.; Torracca, E. (CNEN, Rome. Univ., Rome). J. Inorg. Nucl. Chem., 28: 225-31 (Jan. 1966).

For thermally treated samples of zirconium phosphate (ZP) the variations of K_d for Cs^+ and titration curves as function of time were determined. It was found that condensation of phosphate groups to pyrophosphate groups starts at ~180°C. From determinations of water lost and of pyrophosphate formed at 260°C it was possible to estimate the anhydrous ZP content in given ZP samples dried at room temperature. The interrelation between pyrophosphates formed, loss in total ion-exchange capacity, and variation in selective properties of thermally treated ZP samples are discussed. (auth)

10958 ION EXCHANGE IN FUSED SALTS. I. A COMPARISON OF THE ION-EXCHANGER CHARACTERISTICS OF FIVE MINERAL EXCHANGERS IN FUSED SODIUM NITRATE WITH SELECTED ALKALI-METAL AND ALKALINE-EARTH CATIONS. Callahan, C. M.; Kay, M. A. (Naval Radiological Defense Lab., San Francisco). J. Inorg. Nucl. Chem., 28: 233-44(Jan. 1966).

The ion-exchange characteristics of the zeolitic minerals chabazite, heulandite, analcite, natrolite, and of the felspathoid mineral sodalite, were investigated in fused $NaNO_3$, using ^{22}Na, ^{86}Rb, ^{137}Cs, and ^{133}Ba as tracers. The distribution coefficients of these elements were measured. The selectiviity of the zeolites for the alkali metal ions paralleled that found in aqueous solutions. Some possible explanations for these results are discussed. (auth)

10959 ANION EXCHANGE SEPARATION OF THORIUM FROM THE RARE EARTH ELEMENTS IN AN ACETONE-NITRIC ACID MEDIUM. Korkisch, J.; Ahluwalia, S. S. (Univ. Vienna). J. Inorg. Nucl. Chem., 28: 264-6(Jan. 1966).

Separation of thorium from rare earths using a strongly basic anion exchanger Dowex 1 × 8 was studied. The eluent solutions were contained 10% 6N HNO_3 and varying amounts of acetone and water. The best solution was found to contain 55% acetone and 35% water along with the 10% 6N HNO_3. Under these conditions the rare earth elements were eluted far ahead of the thorium. (M.C.G.)

10960 PARTITION CHROMATOGRAPHY OF RARE-EARTH METALS WITH BIS-(2-ETHYLHEXYL) HYDROGEN PHOSPHATE. I. INFLUENCE OF OPERATING CONDITIONS ON THE SEPARATING POWER OF THE COLUMN. Grosse-Ruyken, H.; Bosholm, J. (Technical Univ., Dresden). J. Prakt. Chem., 25: 79-87(1964).

The operating conditions were determined for maximum efficiency of a column of bis-(2-ethylhexyl) hydrogen phosphate(I) supported on silica gel, with dilute HCl as the mobile phase. Adsorbed Eu, with added ^{152}Eu and ^{154}Eu, was eluted, and the radioactivity was measured with a proportional counter and a rate meter and recorded. The number of theoretical plates was calculated from the peak width. Under optimum conditions [stationary phase], 0.6 ml of 0.81M I in toluene per g of gel; elution (at 0.3 ml per min per cm^2 of column area) with 2.5N HCl (10 ml) and then with 0.1 to 0.01N HCl at 40°C a separating power equivalent to 700 theoretical plates was attained with a 24-cm column. (Anal. Abstr. (Dec. 1965)).

10961 INVESTIGATIONS ON THE CHLORINATING PREPARATION OF FUEL ELEMENTS. Parthey, Harry (Kernforschungszentrum, Karlsruhe, Ger.). Nukleonik, 7: 473-7(Oct. 1965). (In German).

UO_2–Mo sinter tablets were transformed with a Cl_2-CCl_4 mixture to U or Mo chloride. The chlorides were separated by fractional sublimation, since they have different volatilities. A good separation and at the same time a good chemical yield of the reaction products require homogeneous chlorination products. The necessary reaction conditions were worked out using metallurgical phase diagrams that were derived from chemical thermodynamic calculations. The advantages and disadvantages of the chlorinating preparation of fuel elements were discussed with respect to the fluorinating procedure. The possible

significance of chlorination as a supplementary step for the Purex Process was indicated. (tr-auth)

10962 REACTOR FUEL PROCESSING. Volume 8, Number 3. Lawroski, Stephen (ed.). Contract W-31-109-eng-38. One of the five Quarterly Technical Progress Reviews published for the Division of Technical Information, USAEC. Argonne National Lab., Ill., Summer 1965. 53p. GPO $0.70 Domestic, $0.90 Foreign.

Developments in this area are reviewed in five sections. A separate abstract was prepared for each section. (J.R.D.)

For abstracts of individual sections see: 10963—10966, and 12524.

10963 COMMERCIAL ASPECTS OF FUEL PROCESSING. Reactor Fuel Process., 8: 141-5(Summer 1965).

Information is presented on fuel processing plans, economics of fuel cycles, shipping of spent nuclear fuel, and AEC-owned patents made available for licensing. (J.R.D.)

10964 RESEARCH AND DEVELOPMENT ON AQUEOUS PROCESSING. Reactor Fuel Process., 8: 146-51(Summer 1965).

Information is presented on fuel processing plant and equipment design and operation, preparation of fuel for recovery, and solvent extraction processes. (J.R.D.)

10965 RESEARCH AND DEVELOPMENT ON NON-AQUEOUS PROCESSING. Reactor Fuel Process., 8: 152-71(Summer 1965).

Volatility processes for high- and low-enrichment fuels are described. Information is included on properties of UF_6, corrosion in the ORNL molten-salt fluoride-volatility-process pilot plant, EBR-II fuel cycle facility design and operations, EBR-II skull-reclamation process, processes for advanced reactor fuels, other pyrochemical purification processes, oxide-fuel processing, and carbide-fuel processing. (J.R.D.)

10966 PRODUCTION OF URANIUM, THORIUM, AND PLUTONIUM AND THEIR COMPOUNDS. Reactor Fuel Process., 8: 183-92(Summer 1965).

Information is presented concerning production of UO_2, production and properties of PuO_2, preparation of Pu carbides, nitrides, and phosphides, and Pu metal. Descriptions of processes for recovery of Pu from waste materials are included. (J.R.D.)

10967 THE ECONOMIC BASIS FOR ESTABLISHING THE NUMBER OF MEASUREMENTS ACCORDING TO THE VALUE OF THE MATERIAL. Moeken, H. H. P.; Bokelund, H. (Eurochemic, Mol, Belg.). Vienna, International Atomic Energy Agency, 1965, Preprint No. SM-67/2, 19p. (CONF-650803-31). ORINS.

From IAEA Symposium on Nuclear Materials Management, Vienna.

The monetary value of a batch of material is determined by variables that are fixed on the basis of measurements such as weight, volume, concentration, and isotopic composition. It is is assumed that the measurements are subject only to random errors, these errors in the variables, and thus the uncertainty in the monetary value of the batch, can be reduced by repeating the measurements. The uncertainty decreases in this case, but the total costs incurred for measurements increase. Normally both the shipper and the receiver of a batch of valuable material establish the value independently. In the case of irradiated reactor fuel it is impossible for it to be sampled before shipment to a reprocessing plant. This led to an arrangement between both parties, which gives the reactor operator the right to be present during the sampling and the measurements and to have access to all data produced to establish the monetary value of the shipments. This practice requires an agreement about the number of measurements that is acceptable to both parties. A criterion for establishing the number of measurements is proposed. This criterion is applied to the cases of the determination of the value of irradiated reactor fuel (input to the reprocessing plant) and the shipments of purified plutonium oxide and uranium nitrate solution (output of the plant). (auth)

10968 GENERATION OF QUANTITATIVE DATA WHILE SAMPLING ORES AND CONCENTRATES. Shelley, W. J.; Ziegler, W. A. (Mallinckrodt Chemical Works, St. Charles, Mo.). Vienna, International Atomic Energy Agency, 1965, Preprint No. SM-67/39, 27p. (CONF-650803-43). ORINS.

From IAEA Symposium on Nuclear Materials Management, Vienna.

Analytical methods for materials containing known ranges of constituents important in uranium processing are considered. Difficulties that existed in the evolving practices, their methods of recognition, and work to further improve the sampling process and secure appropriate accuracy and precision are discussed. Data relative to the current work is presented in tables. During the evolution of the sampling, handling, and analytical procedure in the United States, continuous attention was fixed on the reliability of the process. Since a wide variety of materials require sampling, constant evaluation through development of reference sampling techniques, duplicate sampling, assay sample exchange, and statistical examination of accuracy and precision is maintained. (auth)

10969 APPLICATION OF REACTOR PHYSICS CALCULATION METHODS TO CRITICALITY CONTROL OF NON-INHERENTLY SAFE SYSTEMS IN FUEL PROCESSING PLANTS. Raber, M. (United Nuclear Corp., White Plains, N. Y.). Vienna, International Atomic Energy Agency, 1965, Preprint No. SM-67/43, 28p. (CONF-650803-39). ORINS.

From IAEA Symposium on Nuclear Materials Management, Vienna.

The economics of fuel processing operations involving the handling of large quantities of fissionable materials can be significantly improved by utilizing reactor physics calculation methods to establish criticality-safe process parameters. Some of the calculation techniques used for this purpose are described. Both hand calculation techniques and computerized techniques are discussed, and generally useful data obtained with those methods are presented. Comparison of these calculation methods against experimental data, and the assumptions made in applying these methods to criticality safety work, are also discussed. Simple, modified one-group hand calculation procedures for determining the reactivity and critical mass of highly enriched uranium alloy-water systems are described. These procedures enable self shielding in heterogeneous systems to be taken into account, in order to establish the safety of larger mass limits for such systems than could be justified on the basis of experimental data for homogeneous solutions. Computer codes were used to establish the safety of greater than 5-in. diameter pipes filled with solutions of highly enriched uranium when the pipe material is constructed of or wrapped with nuclear poison material. The safety of standard 6-in. borosilicate glass pipes and of 6-in. steel pipes wrapped with boron material or cadmium was established. The application of simple control rod worth calculation techniques to large vessels utilizing fixed heterogeneous poison sheets for criticality safety is discussed. The safety of large arrays of unmoderated, highly enriched uranium materials (e.g., UO_2, large U alloy pieces) under dry and flooded conditions is discussed. A method of treating partially moderated arrays, based partly on transport theory calculations, is presented. (auth)

10970 CONTROL POSSIBILITIES ON THE BASIS OF THE MATERIALS BALANCE. Gilles, A. (Centre d'Etudes Nucleaires, Fontenay-aux-Roses, France). Vienna, International Atomic Energy Agency, 1965, Preprint No. SM-67/11, 11p. (In French). (CONF-650803-22). ORINS.

From IAEA Symposium on Nuclear Materials Management, Vienna.

For handling a basic material a breakdown between the different types of expenditures and the losses and information on production yield are necessary. Using the materials

balance, a study of the "law of the conservation of matter" over a given accounting period, is considered. The material balance can be written as: $q_e + q_{vi} = q_s + q_{vf} + q_p$, where q_e denotes the quantity of incoming material, q_{vi} the reserves at the beginning of the period, q_s the quantity of outgoing material, q_{vf} the reserves at the end of the period, and q_p the losses. Analysis of the different factors showed that these are variates defined by a mean value and a variance. There is thus an area of uncertainty for closing the balance sheet and, conversely, if the size of this area is fixed the variance to be applied to each factor contained in the expression for the materials balance can be deduced from it. If the balance does not come within the area of uncertainty, this means that there is a systematic error in the determination of at least one of the factors. A formula is given by which it can be estimated whether total output is higher or lower than the minimum specified. Practical application of the method to a natural uranium refinery is described. (auth)

10971 METHOD FOR SEPARATION OF ALUMINUM CLADDING FROM SPENT FUEL ELEMENT. Yamamoto, Hiroshi (to Japan Atomic Energy Res. Inst.). Japanese Patent 1964-27173. Nov. 27, 1964. Filed Feb. 13, 1962.

A method for separation of the Al cladding from a spent fuel element consists of separation of the Al cladding by melting and recovery of the U or U alloy in its solid state. The Al clad U spent fuel is immersed in a molten halide salt or the salt added with either a carbonate or a caustic alkali or both at 660 to 1100°C. The density of the salt or the salt mixtures should be higher than that of aluminum in this temperature range. The molten salt bath dissolves the Al cladding without dissolving the U or U alloy and prevents evaporation of the Al and oxidation of the U or U alloy. (TCO)

ENGINEERING

General

Refer also to abstract 10814.

10972 (NYO–3237–4) EXPERIMENTAL TEST AND EVALUATION OF A GAS-BEARING BRAYTON CYCLE TURBOCOMPRESSOR. Quarterly Progress Report, September 1–November 30, 1965. Curwen, P. W. (Mechanical Technology Inc., Latham, N. Y.). Dec. 17, 1965. Contract AT(30-1)-3237. 105p. (MTI–65TR64). Dep. mn; CFSTI $4.00 cy, $0.75 mn.

A description of the aerodynamic performance of the turbocompressor as determined from closed-loop tests using nitrogen as the cycle gas is presented. The performance of the bearing system is discussed along with the loop facility. (M.O.W.)

10973 (TID–21992) TOPICAL REPORT ON TURBULENT LUBRICATION. Arwas, E. B. (Mechanical Technology Inc., Latham, N. Y.). Nov. 30, 1964. Contract AT(11-1)-Gen-8; Subcontract N2S9-1599. 120p. Dep. mn. CFSTI $4.00 cy, $0.75 mn.

For Atomics International, Canoga Park, Calif.

The bearings of compact, liquid metal, Rankine Cycle turbomachinery for dynamic power conversion, operate in turbulent regime. This is due to combined effect of high speed of rotation and, low kinematic viscosity of liquid metals. The differences in load capacity, friction, and in the dynamic characteristics between laminar and turbulent bearings are large, amounting in some cases to an order of magnitude. Thus, a theory and design procedure for turbulent bearings is needed to permit rational design of the bearings. A theory of turbulent lubrication for finite length bearings was derived starting from the eddy diffusivity concept in turbulent flow. This theory is consistent with the classical treatment of turbulent flow and it is completely free of empirical coefficients (other than the universal constants of turbulent flow), so that it should be applicable to the various bearing geometries and over broad ranges of eccentricity ratio and Reynolds Numbers. Design procedures for turbulent bearings were prepared and programmed for ready calculation on digital computers. These permit calculation for either laminar or turbulent bearings including the effects of misalignment. Extensive comparisons were made between the theory and experiments conducted with easy to use fluids in both laminar and turbulent regimes. These comparisons were made with two basic bearing geometries: the 360° plain circular and the partial arc bearings. The experiments covered a range of eccentricity ratios from about 0.3 to 0.95 and a range of Reynolds Numbers from laminar to 1300. The comparisons given are of: load, attitude angle, and pressure profiles as functions of geometry, eccentricity ratio, and Reynolds Number. The degree of correlation is judged to be good, generally agreement was well within 20%. The degree of agreement found between theory and test in turbulent regime was comparable to that found between theory and test in laminar regime. Based on this it is concluded that the theory can be used to perdict the hydrodynamic performance of turbulent bearings for design purposes. The theory was extended to permit calculation also of the temperature map in turbulent bearing fluid film. Sample calculations were made for two types of bearings, indicating that high temperature rises can be encountered at high values of the Reynolds Number and eccentricity ratio. This agrees generally with practical experience, however, there was no accurate experimental data for quantitative comparison. In addition to the turbulent lubrication work, a rotor-bearing dynamics analysis leading to a cumputer program for calculating the critical speeds and the response to unbalance loads of flexible shafts supported in bearings of finite stiffness was reviewed. This program, together with the bearing performance programs, is used to design and to predict the mechanical operation of high speed coupled rotor-bearing units. (W.L.G.)

10974 (AEC-tr–6665) AEROSTATIC [EXTERNALLY-PRESSURIZED GAS LUBRICATED] THRUST BEARINGS. Loch, Erwin. Translation of Thesis Submitted to the Technical University of Graz, Austria. Dec. 1965. 180p. (T-A2049-26). Dep. mn; JCL $12.50 fs, $5.60 mf.

The static and dynamic characteristics of single- and double-acting thrust bearings of many geometrical forms are dealt with in detail. The extensive theoretical analysis of these bearings is matched by abundant experimental data. (M.O.W.)

Applications of Nuclear Explosions

10975 (UCRL–14294) THE PARTICLE SIZE DISTRIBUTION AND BULK PERMEABILITY OF OIL SHALE RUBBLE. Lombard, D. B. (Lawrence Radiation Lab., Univ. of California, Livermore). Aug. 12, 1965. Contract W-7405-eng-48. 12p. Dep. mn. CFSTI $1.00 cy, $0.50 mn.

A tabulation of the size distribution of fragments of oil shale shattered in a roof fall at the U. S. B. M. mine at Rifle, Colorado was obtained by counting particles in photographs of the rubble. This distribution is approximately lognormal. The theory of particle statistics was then invoked in a calculation of the bulk permeability of the rubble. In an extrapolation to a hypothetical underground nuclear chimney in oil shale, it is estimated that the bulk permeability of the chimney rubble would be about 3×10^{-5} to 3×10^{-4} ft^2. (auth)

Facilities and Equipment

10976 (IS-T–46) A COMPARISON OF RARE-EARTH CATHODES IN A DIODE ION PUMP [Thesis]. Lorenz, Peter Klaus (Ames Lab., Iowa State Univ. of Science and Tech.). Nov. 1965. Contract W-7405-eng-82. 55p. Dep. mn. CFSTI $3.00 cy, $0.50 mn.

The performance of diode ion pumps with yttrium, neodymium, erbium, and ytterbium cathodes is compared with a pump in which titanium is the cathode material. All of the pumps used in the study used an egg-crate shaped anode constructed of titanium. Performance tests were made with nitrogen, oxygen, argon, carbon dioxide, air, hydrogen, and methane. In general, ytterbium, yttrium, and erbium are more effective in pumping air, nitrogen, methane, carbon dioxide and oxygen than is titanium. Yttrium is more effective than titanium for pumping hydrogen. All of the rare-earth metals are more effective than titanium for pumping argon at pressures above 5×10^{-6} torr. No periodic pumping instability for argon was observed with neodymium, erbium, or ytterbium cathodes. One serious drawback to the use of ytterbium cathodes is the high erosion rate of the cathode under ion bombardments. (auth)

10977 (KFK–370) LABORATORIEN FUER ARBEITEN MIT RADIOAKTIVEN STOFFEN. BIBLIOGRAPHIE UEBER PLANUNG, BAU, EINRICHTUNG U. AUSRUESTUNG. (Laboratories for Work With Radioactive Materials. Bibliographie on Planning, Building, Arrangement, and Equipment). Brossmann, G. (Kernforschungszentrum, Karlsruhe (West Germany)). Oct. 1965. 120p. Dep. mn.

References (425) are given to journals and reports published from 1955 through 1964. (P.C.H.)

10978 (RMO–3006) THE DESIGNS AND DESCRIPTIONS OF MECHANICAL SUBSAMPLE CUTTERS USED IN REDUCING URANIUM CONCENTRATE SAMPLE SIZES. Johnston, R. L. (Pitkin (Lucius) Inc., Grand Junction,

Colo. Western Uranium Project). Dec. 1, 1965. Contract AT(05-1)-912. 40p. Dep. mn. CFSTI $2.00 cy, $0.50 mn.

A portable, mechanical, straight-line secondary sampler and a smaller mechanical arc-path type tertiary sampler were designed and fabricated for use in reducing a uranium concentrate primary sample. The secondary sampler can be set with a timer device to cut representative subsamples of any desired weight within a range of 500 to 2000 grams. It can cut representative subsamples in this range from quantities of minus ¼ inch particle size concentrate varying in weight from 50 to 1200 pounds. The tertiary sampler is used to subsample an unblended, unpulverized secondary sample. It is capable of cutting representative tertiary samples as small as 14 grams or as large as 125 grams. Descriptions, detailed sketches, and photographs of these two mechanical subsamplers are given, along with results obtained in evaluating their capabilities. (auth)

10979 (TID-22528) EXPERIMENTS ON AN ULTRA-STABLE GAS JOURNAL BEARING. Malanoski, S. B. (Mechanical Technology Inc., Latham, N. Y.). Nov. 1965. Contract AT(30-1)-3363. 36p. (MIT-65TR37). Dep. mn. CFSTI $2.00 cy, $0.50 mn.

Shallow grooving in a herringbone pattern has been proposed to enhance the stability of both gas and liquid lubricated journal bearings. It has been shown theoretically that this possibility is particularly advantageous for unloaded journal bearings. Corroborating experiments are described. The experiments included the running of an unloaded bearing up to speeds of 60,000 rpm and the collection of steady state load-displacement attitude angle data at intermediate speeds up to an including 60,000 rpm. No sign of bearing whirl instability was detected. There was good correlation between theoretical and experimental data. Design data are included as a guide for future designs. (auth)

10980 (AEC-tr-6469) GAMMA IRRADIATION FACILITIES. Bibergal', A. V.; Sinitsyn, V. I.; Leshchinskii, N. I. Translation of Izotopnye Gamma-Ustanovki, a publication of Atomizdat, Moscow, 1960. 117p. (IPST-Cat.-1247). CFSTI $4.00 cy, $0.75 mn.

Information is given on: radiation sources in gamma-installations; gamma-installation types and their requirements; gamma-installation design; methods for calculating fields for sources of various configurations; and gamma-installation shielding design and calculations. (132 references). (P.C.H.)

10981 A NUCLEARLY SAFE TRIANGULAR-SLAB TANK FOR HANDLING ENRICHED URANIUM. Newlon, C. E.; Clouse, R. J.; Mallett, A. J. (Oak Ridge Gaseous Diffusion Plant, Tenn.). Nucl. Appl., 1: 546-7(Dec. 1965).

An improved abrasive slurry tank for use with conventional liquid-honing machines was built and tested. Its shape, a 1.7-in.-(4.3-cm)-thick triangular slab, promotes good mixing by improving recirculation and is nuclearly safe for uranium enriched to 93% ^{235}U. (auth)

10982 ENGINEERING DEVELOPMENT OF A 1200 deg F SODIUM VAPOR TRAP. Kimont, E.; Smith, F.; Featherstone, M.; Wagen, D. 20p. (CONF-650602-64). Gmelin, AED-CONF-65-125-36.

From American Nuclear Society, 11th Annual Meeting, Gatlinburg, Tenn.

Measurements were made to provide engineering data to give reasonable assurance that vapor traps provided for a 1200°F FARET engineering test loop would not plug with condensed solid sodium. This loop features a test vessel, expansion tank, a free surface pump, and the necessity of maintaining a common liquid sodium level in all three vessels. Operating data were obtained to establish design criteria for any sodium vapor trap for any system requiring an inert gas vent operating at temperatures up to 1200°F. (F.J.H.)

10983 DEVICE FOR LIFTING AND LOWERING A HEAVY BODY. Omori, Norihiko (to Mitsubishi Atomic Power Ind., Inc.). Japanese Patent 1964-12695. July 6, 1964. Filed Oct. 16, 1961.

A device for lifting and lowering a heavy body in a non-lubricating corrosive liquid consists of a vertically movable, load carrying bar held by a fixed bearing, and a drive mechanism installed separate from the bar for driving it in the axial direction. The drive mechanism includes a drive screw shaft, a hollow drive cylinder interlocked with the driving shaft movable in the axial direction and sealed at the bottom, and a support arm at the bottom to engage with the load carrying rod. With the proposed device a heavy body can be placed accurately in the predetermined location, and the lubricant in the drive mechanism can be maintained in good condition with the entrance into the liquid being prevented. (NSA of Japan)

10984 ELECTRON-BEAM IRRADIATION APPARATUS. Kawashima, Masao (to Sumitomo Electric Ind. Co., Ltd.). Japanese Patent 1964-15099. July 30, 1964. Filed Oct. 6, 1961.

An electron-beam irradiation apparatus is proposed in which the objects to be irradiated are attached to a member that rotates at a high speed. This repeated rather than prolonged irradiation prevents overheating. Since the surfaces of the objects rotate, the electron-beam apparatus can be made small. The apparatus is simple to operate, efficient, and suitable for irradiation of many objects. (TCO)

10985 NUCLEAR FUEL TRANSPORT CONTAINER. Murota, Kazuo (to Nippon Atomic Ind. Group Co., Ltd.). Japanese Patent 1964-23458. Oct. 21, 1964. Filed Dec. 26, 1961.

The fuel transport container proposed facilitates heat removal from the spent fuel contained and is easy to handle. The entire transport container consists of an outer massive wall, which forms a cylindrical body, and an inner space for the fuel rods. When contained, these fuel rods are grouped into bundles with spaces between the rods; in each bundle, the rods are supported at the top and bottom by plates. Neutron-absorbing rods are placed at regular intervals in the spaces between the fuel rods. Water is introduced for cooling the fuel rods; then the lid of the container is placed on. The heat convection, hence, heat removal in the transport container is greatly improved by the spaces produced in the structure. (NSA of Japan)

10986 CONVEYOR SYSTEMS. Bailey, Peter John; Baines, Bernard Deryck; Lindstaedt, Horst Karl (to Nuclear Chemical Plant Ltd.). U. S. Patent 3,224,562. Dec. 21, 1965. Priority date Nov. 10, 1961, Great Britain.

A conveyor system is provided for moving articles adjacent to treatment means from at least two opposite sides to expose the articles to emission from the treatment means. The system is particularly, but not exclusively, applicable to a conveyor system for moving articles to be sterilized adjacent to a radioactive source of sterilizing radiation. The system comprises an endless conveyor having two substantially parallel, upright portions passing adjacent to the source on each of two opposite sides and disposed one beyond the other relative to the source. Support means carry the articles so that each article has the same orientation with respect to the system on all of the upright conveyor portions. Means are provided for removing the article from the conveyor system after a single circuit or for passing the articles past the source a number of times in different positions with respect to the source. (B.L.M.)

10987 ATOMIC IRRADIATOR. Gombert, Dieter W. (to Cook Electric Co.). U. S. Patent 3,225,203. Dec. 21, 1965. Filed June 5, 1961.

A device for subjecting specimens to atomic radiation includes an irradiation chamber surrounded by a housing or shell for preventing the escape of radiation from the chamber and a device for introducing specimens into the chamber. The device for introducing specimens is in the form of a wheel that is rotatable in the housing and has a specimen holder movable between the outside of the housing and the irradiation chamber when the wheel is rotated. The source is contained in a pool of Hg or other liquid in a receptacle that is sealed by a flexible bellows connected to

the receptacle and the operating rod for the radioactive body. An adjusting screw is connected to the operating rod by a swivel coupling so that the position of the radioactive body in the attenuating liquid can be varied. (B.L.M.)

Heat Transfer and Fluid Flow

See also PHYSICS — Fluid Physics and Thermodynamics

Refer also to abstracts 10871, 11793, 12331, 12341, 12354, and 12480.

10988 (CONF-12-5) LOCAL FILM COEFFICIENTS ON THE ML-1 FUEL ELEMENTS DUE TO BOUNDARY LAYER TURBULENCE PROMOTERS. Kattchee, N.; Mackewicz, W. V. (Aerojet-General Nucleonics, San Ramon, Calif.). [1961]. Contract AT(04-3)-368. 25p. (AN-AGCR-223). Dep. mn. CFSTI $1.00 cy, $0.50 mn.

From American Nuclear Society 8th Annual Meeting, Boston, June 1962.

Local convective heat transfer coefficients for a surface with integral boundary layer turbulence promoters were determined by naphthalene mass transfer tests, using the heat transfer-mass transfer analogy. All determinations were relative to a smooth surface with parallel flow. Local coefficients up to six times the smooth surface value were encountered on the faces of the turbulence promoters. In general, the front and top faces developed high transfer coefficient distributions which increased as turbulence promoter spacing decreased, while coefficient values on the back faces were not dependent upon geometrical parameters. Corner areas showed transfer coefficients lower than those for a smooth surface with parallel flow. The data from the surface between two turbulence promoters were correlated in terms of the dimensionless distance parameter x/d. A broad peak of 2.4 times the smooth surface values was found at about x/d = 4. Each test showed a narrow peak at the point of boundary layer separation at x/d = (N − 0.5). The tests showed a unique generalized distribution of the transfer coefficient for surfaces with boundary layer turbulence promoters of rectangular cross section. The upstream and downstream boundary layer separation regions were independent of turbulence promoter dimensions. The estimated error for this series of tests was ±20% of the maximum relative transfer coefficient values. (auth)

10989 (IDO-28595(Rev.)) ARMY GAS-COOLED REACTOR SYSTEMS PROGRAM. HECTIC-II—AN IBM 7090 FORTRAN COMPUTER PROGRAM FOR HEAT TRANSFER ANALYSIS OF GAS OR LIQUID COOLED REACTOR PASSAGES. Kattchee, N.; Reynolds, W. C. (Aerojet-General Nucleonics, San Ramon, Calif.). Dec. 1962. Revised Dec. 1965. Contract AT(10-1)-880. 80p. Dep. mn. CFSTI $2.00 cy, $0.75 mn.

HECTIC-II, a FORTRAN program for the IBM 7090 computer, provides a means of calculating coolant and surface temperatures for heat exchangers such as nuclear reactor cores with single phase, low Mach number, axial coolant flow. The code considers a minimum geometrical symmetry flow-tube of a reactor fuel element in which several heated surfaces (such as rods and plates) are present. The heat transfer and friction surfaces are divided to correspond with the arbitrarily divided flow passage. For a prescribed axial power distribution in each surface, under steady-state conditions, HECTIC-II calculates fluid and surface temperatures as functions of distance downstream from the inlet. A typical run requires approximately 0.5 to 5 minutes of machine time, depending on the number of plates and passages and various options incorporated in the program. HECTIC-II includes turbulent heat and momentum exchange between all considered flow passages. (auth)

10990 (NAA-SR-11586) STEADY-STATE SODIUM BOILING AND HYDRODYNAMICS. Lurie, H. (Atomics International, Canoga Park, Calif.). Jan. 15, 1966. Contract AT(11-1)-Gen-8. 49p. Dep. mn. CFSTI $3.00 cy, $0.50 mn.

A study of boiling heat transfer characteristics and critical heat flux for sodium in forced convection was performed for inlet velocities between 1.1 and 6.7 ft/sec, pressures of 2 to 8 psia, and average subcoolings to 116°F or qualities up to 14%. A study of two-phase pressure drops and void fractions was also performed for vertical upflow of sodium in an unheated annulus with velocities from 0.5 to 4 ft/sec, pressures of 1.5 to 10 psia, and qualities up to 14%. The data obtained in forced convection boiling show that ordinary convective heat transfer seems to dominate practically up to the critical heat flux, with only a very small range of nucleate boiling heat transfer noticeable. Critical heat fluxes up to 1.6×10^6 Btu/hr-ft^2 were obtained. Under two-phase conditions, the critical heat flux for sodium was found to be a strong function of both pressure and quality; it increased with pressure, and first increased then decreased with increasing quality. The two-phase frictional pressure loss was correlated in terms of the Martinelli parameters. Over the range of variables covered no parametric dependence on flow rates and pressures could be discerned. The void fraction during the two-phase flow was also correlated using the Martinelli parameter and indicates slip ratios considerably higher than, and void fractions lower than, those reported for water at the same value of the Martinelli parameter. (auth)

10991 (NYO-3114-12) TWO-PHASE FLOW AND BOILING HEAT TRANSFER. BUBBLY FLOW IN STRAIGHT PIPES. Meyer, P. E.; Wallis, G. B. (Thayer School of Engineering, Dartmouth Coll., Hanover, N. H.). Nov. 1965. Contract AT(30-1)-3114. 48p. (EURAEC-1530). Dep. mn. CFSTI $2.00 cy, $0.50 mn.

Work Performed Under United States–Euratom Joint Research and Development Program.

An investigation was made on existing non-accelerated and accelerated bubbly flow data. Homogeneous flow theory was applied to all the data using an existing correlation for the frictional pressure drop. Total pressure drop data are correlated within an absolute error of 20 lb/ft^2, the total pressure drops ranging from −20 to 220 lb/ft^2. Effects not included by this simple correlation are discussed. Homogeneous theory was applied to the non-accelerating horizontal data in an attempt to correlate frictional pressure drop. The results point to non-Newtonian flow characteristics of bubbly mixtures as a possible consideration. Various rheological techniques and models are discussed in relation to possible correlations. (auth)

10992 (RISO-116) AN EXPERIMENTAL STUDY OF THE TANGENTIAL VELOCITY PROFILE IN THE RANQUE-HILSCH VORTEX TUBE. Linderstroem-Lang, C. U. (Atomenergikomissionen, Risoe (Denmark). Forsoegsinstitut). Sept. 1965. 17p. Dep. mn.

The tangential velocity profile in Ranque-Hilsch vortex tubes was calculated using the results of pressure determinations in such tubes. (D.C.W.)

10993 (TID-22513) ARMY GAS-COOLED REACTOR SYSTEMS PROGRAM. MASS TRANSFER ANALOGY STUDIES OF SHAPED TURBULENCE PROMOTER PERFORMANCE. Kattchee, N.; Mackewicz, W. V. (Aerojet-General Nucleonics, San Ramon, Calif.). July 1965. Contract AT(10-1)-880. 38p. (AN-AGCR-919). Dep. mn. CFSTI $2.00 cy, $0.50 mn.

Mass transfer tests were performed to evaluate the convective heat transfer characteristics of various configurations of boundary layer turbulence promoters (fins). A ten times actual size cylindrical surface was used to test fins with upstream and downstream ramps in axial flow. Various configurations of grooves normal to the flow were also tested. Performance was compared with performance of a smooth surface. Local and average heat transfer coefficients are presented as ratios of finned-to-smooth surface coefficients. Fins with downstream ramps about four fin heights long produced average heat transfer coefficients greater than those produced by rectangular fins without ramps. Upstream ramps improved the axial distribution of coefficients along the interval between promoters. Various combinations of upstream and downstream ramps re-

sulted in average coefficients 85 to 90% higher than those of a smooth surface and in a low ratio of maximum-to-minimum local coefficients. The optimum combinations of h_{av}/h_{sm} and h_{max}/h_{min} resulted from fins with long upstream ramps and downstream ramps approximately four fin heights long. Narrow and deep rectangular grooves resulted in only a small improvement in heat transfer over that of a smooth surface. Long shallow grooves provided the best average convective transfer coefficients in this series of tests. V-shaped grooves resulted in lowest maximum-to-minimum ratios. (auth)

10994 (TID–22539) THE EFFECT OF LENGTH AND PRESSURE ON THE CRITICAL HEAT FLUX FOR A CLOSELY SPACED 19-ROD BUNDLE IN FORCED CONVECTION BOILING. Tropical Report No. 7. Matzner, Bruce; Casterline, J. E. (Columbia Univ., New York. Engineering Research Labs.). Dec. 1965. Contract AT(30-3)-187. 34p. Dep. mn. CFSTI $2.00 cy, $0.50 mn.

Over 150 critical heat flux points were obtained for 5 different 19-rod bundles using 0.780-in. rods with 0.040-in. rod-to-rod and 0.060-in. rod-to-wall spacings. Heated lengths of 18 in. to 9 ft were investigated for the following ranges of system parameters: pressures from 500 to 1200 psia, mass velocities from 0.1 to 3.0×10^6 lb/hr-ft^2, and inlet subcoolings from 14 to 189°F. The effect of stripping rings on the flow tube wall of the 6 ft bundle was also studied. The data are compared with other multi-rod test section data. Single-phase and two-phase pressure drop measurements were made. (auth)

10995 (UCRL–10696(Rev.)(Pt.1)) SEGMENTED LAMINAR FLOW AND OTHER MODELS FOR PACKED-BED LONGITUDINAL DISPERSION. Hennico, Alphonse; Jacques, Gabriel; Vermeulen, Theodore (Lawrence Radiation Lab., Univ. of California, Livermore). Nov. 16, 1964. Contract W-7405-eng-48. 45p. Dep. mn. CFSTI $2.00 cy, $0.50 mn.

For comparison with the diffusion, random-walk, and mixing-cell models of axial dispersion, a segmented-laminar-flow model was developed for packed beds, by analogy with Taylor's derivation for concentration distribution in laminar pipe flow. Two different radial distributions of velocity were assumed, the quadratic profile having its average velocity at one-half the peak value, and a quartic profile with the average at one-third the maximum. The latter gave substantially better agreement with experiment, but was still imperfect. A numerical evaluation is described for the concentration distribution, and the results are presented in graphical form. The techniques developed, when used with an effective velocity distribution still to be determined, are expected to provide a dependable and versatile description of liquid-phase laminar-flow breakthrough behavior. (auth)

10996 (WANL-TNR–154) FORCED CONVECTION BOILING HEAT TRANSFER TO HYDROGEN. Chi, J. W. H. (Westinghouse Electric Corp., Pittsburgh, Pa. Astronuclear Lab.). Feb. 21, 1964. 74p.

Based on experimental data obtained from the chill-down of aluminum and copper test sections by liquid hydrogen and nitrogen, the mechanisms of boiling two-phase flow and heat transfer were elucidated. The apparent mechanisms provided models for the development of a forced convective boiling heat transfer correlation for hydrogen. It was postulated that forced convective boiling heat flux is made up of two components: a convective flux superimposed on a boiling flux: $[Q/A = (Q/A)_{Conv.} + (Q/A)_{Bo}$. The convective contribution can be calculated from conventional heat transfer coefficients given by Dittus-Boelter type equations. Based on forced convective hydrogen boiling heat transfer data available, a correlation for the boiling flux was obtained for a wide range of temperatures and pressures (up to the critical). It was found that the correlation can predict transient forced convective boiling heat flux well within experimental errors. Applications to the analysis of transient start-up are discussed. (auth)

10997 (AERE-Trans–1038) INTERPRETATION OF THE CONDUCTIVITY OF POROUS AND DISPERSED MEDIA WITH THE AID OF CUBIC CELLULAR GEOMETRIC MODELS. Le Goff, P.; Prost, C. Translated by J. M. Jacobs (U.K.A.E.A. Atomic Energy Research Establishment, Harwell, Eng.), from Symposium held by the Societe de Chimie Industrielle, Paris, 21–23 April 1965, on Porous Media in Chemical Engineering. 68p. Dep. BIS $2.00. HMSO 10s.

Mathematical representation for the operation of the four applications of porous media in chemical engineering in order to express the efficiency of each exchanger or reactor in relation to the various structural and operational parameters is discussed. A geometric model of the unit cubic cell is defined. This model is more complicated, the greater the number of experimental data available. A general model is described, which consists essentially of a bundle of parallel pores of diameter x connecting cubic cavities of diameter z. The pores and cavities are interconnected by slits of width y and height w. The general model is used to describe the texture of any porous medium by stating the fractions of the void volume which are in the form of cavities, pores, and slits, respectively. Both isotropic and fibrous textures are considered. (P.C.H.)

10998 FLOW OF SLURRY THROUGH A PIPE. II. FRICTION COEFFICIENT. Michiyoshi, Itaru (Kyoto Univ.); Matsumoto, Ryuichi; Mizuno, Kenichi; Nakai, Masaru, Nippon Genshiryoku Gakkaishi, 7: 627-33(Nov. 1965). (In Japanese).

The correlations of Bingham viscosity and yield stress of an alumina-water slurry with volume fraction of alumina and temperature of slurry, measured in a narrow channel with circular cross section, are presented. Data on the friction coefficient for slurry in laminar and turbulent flows through a circular pipe are also presented. Results for the laminar region coincided with Hedström's theory. In the turbulent region, the slurry friction coefficient deviated from the Newtonian fluid in the positive direction with increasing Hedström number, but for a given Hedström number the friction coefficient approached Newtonian fluid when the Reynolds number exceeded a certain critical value. The critical points of the Reynolds number were about 4×10^4, 6×10^4, and 1.5×10^5 for Hedström numbers of 5×10^4, 1×10^5, and 5×10^5, respectively. (auth)

10999 LIQUID-METAL BOILING HEAT TRANSFER. Tang, Y. S. (General Motors Corp., Indianapolis, Ind.). Nucl. Appl., 1: 521-37(Dec. 1965).

The increasing number of investigations of boiling heat transfer with liquid metals reflects the current interest in and importance of this process. Its application to nuclear power systems is important. The trend of the literature, for practical reasons, leans toward seeking answers to specific applications rather than understanding of the boiling mechanism. The major progress in experimental and analytical investigations, the evidence of agreements and disagreements between different investigators, and the difficulties in areas caused by lack of information are reviewed and recommendations for future work are presented. (auth)

11000 MEASUREMENTS OF BURNOUT CONDITIONS FOR FLOW OF BOILING WATER IN VERTICAL 3-ROD AND 7-ROD CLUSTERS. Becker, Kurt M.; Hernborg, Gunnar; Flinta, Jan E. Nukleonik, 7: 457-73(Oct. 1965).

Measurements of burnout conditions for flow of boiling water in vertical 3-rod and 7-rod clusters are considered. Data were obtained for heating the rods only, as well as for simultaneous uniform and non-uniform heating of the rods and the shroud. A total of 520 runs was performed. In the case of equal heat fluxes on all surfaces of the channels, burnout always occurred on the rods, and the data were low by a factor of about 1.3 compared with round duct data. When only the rods were heated, the data showed very low burnout values in comparison with results for total uniform heating and round ducts. This disagreement was explained by considering the climbing film flow model and the fact that only a fraction of the channel perimeter was heated. For simultaneous and nonuniform heating of the rods and the shroud it was found that the shroud could be overloaded up to 50% without reducing the margin of safety

in respect of burnout for the rod cluster. Finally, a correlation for predicting burnout conditions in round ducts, annuli and rod clusters is presented. This correlation predicts the burnout heat fluxes for the present measurements and previously obtained annuli measurements within ±5%. (auth)

Materials Testing

11001 (BNWL-SA-438) DETECTION OF METAL OVERSTRESS BY ACOUSTIC EMISSION. Hutton, P. H.; Spanner, J. C. (Battelle-Northwest, Richland, Wash. Pacific Northwest Lab.). Dec. 27, 1965. Contract AT (45-1)-1830. 8p. Dep. mn. CFSTI $1.00 cy, $0.50 mn.

Experimental work conducted indicates a tremendous potential for application of acoustic emission as a nondestructive surveillance tool to assess structural integrity of operating systems such as reactor pressure systems. Possible applications for the study of fracture mechanics, brittle fracture, ductility changes due to nuclear irradiation are also indicated. The method and its advantages are described. (P.C.H.)

11002 AUTORADIOGRAPHY. Colombo, R. (CCR-EURATOM, Ispra, Italy). Ing. Nucl., 6: 202-5(July-Aug. 1965). (In Italian).

The processes used for obtaining autoradiographic pictures using nuclear emulsions are described. The development processes used for thin, thick, and liquid emulsions are discussed. Some examples are given. (tr-auth)

11003 DETECTION OF URANIUM FUEL ELEMENT FAILURES DURING INACTIVE TESTS IN CO_2 STREAMS. Zajic, Vladimir (Inst. for Nuclear Research, Czechoslovak Academy of Sciences, Rez); Vlcek, Jiri; Hudecek, Milan. Jad. Energ., 12: 3-7(Jan. 1966). (In Czech).

A radiometric method of the detection of uranium released in an inactive test loop by rod-type fuel element is described. In comparison with some chemical methods of analysis, the radiometric method for detection of uranium aerosols in the test loop is simple and sensitive. (auth)

11004 NONDESTRUCTIVE METHODS FOR DETERMINING BURNUP IN NUCLEAR FUEL. McGonnagle, W. J. (Illinois Inst. of Tech., Chicago). Vienna, International Atomic Energy Agency, 1965, Preprint No. SM-67/46, 26p. (CONF-650803-35). ORINS.

From IAEA Symposium on Nuclear Materials Management, Vienna.

Nondestructive methods for quantitative measurement of burnup in nuclear reactor fuel elements are considered. Radioactive and stable isotopes resulting from the fission process are a record of burnup. In the nondestructive as well as the destructive fuel assay methods the neutron spectrum, irradiation history, and cooling period influence this record. Another difficulty in nondestructive assay is the presence of high radiation fields, which contribute to the "noise" background of the measurements. Several nondestructive methods for determining burnup are described, evaluated, or proposed. Various types of spectrometers including bent-crystal, magnetic Compton, Compton coincidence, and scintillation can be used to analyze the gamma radiation from the radioactive material formed during the fission process. Other nondestructive methods include foil activation, x-ray fluorescence, neutron transmission, activation analysis, measurement of capture gamma rays, and the measurement of prompt and delayed neutrons. The basic principles of each of these instruments and methods, their sensitivities, and their limitations are reviewed. Nondestructive methods using stable isotopes produced during the fission process are proposed. In the use of stable isotopes, detailed irradiation history is of secondary importance and the cooling time is unimportant. Also, there is more precise nuclear data for the stable fission products. Of the stable isotopes produced during the fission process, zirconium, molybdenum, ruthenium, and neodymium appear to be the most useful. (auth)

11005 NEUTRON-RADIOGRAPHY. Ogawa, Kazuyuki (to Tokyo Shibaura Electric Co., Ltd.). Japanese Patent 1964-14949. July 28, 1964. Filed Oct. 5, 1963.

A neutron radiography procedure is applied to the testing of an object for weld cracks or flaws. A good absorber for thermal neutrons, such as Cd, B, Li, In, Au, or Hg, or its compound, or a mixture of these compounds, is applied to the flaws by either impregnation or deposition. The object is irradiated with neutrons from a radiation source, and the amount of neutrons penetrating the object is detected. (NSA of Japan)

Space Propulsion

See also **ISOTOPE TECHNOLOGY — Power Application**
REACTOR TECHNOLOGY — Propulsion and Space

Refer also to abstracts 11175, 12476, and 12492.

11006 (NP-15824) ION ROCKET ENGINE DEVELOPMENT. Quarterly Report No. 3, April 1, 1965–June 30, 1965. Thompson, S. A.; Garvin, H. L.; McKee, W. E.; Zuccaro, D. E.; Couvillion, A. J. (Hughes Research Labs., Malibu, Calif.). Dec. 30, 1965. Contract NAS 3-6271. 113p.

A series of three four-strip integral-focus ion engines was evaluated. The third engine was tested for 954 hr until the cesium supply was expended. Ion optics studies were also performed, and an Ir-coated porous W ionizer and a Re-coated porous W ionizer were evaluated. An attempt was made to minimize the erosion of acceleration electrodes due to ions from the tips of solid W integral-focus electrodes by coating the W tips with alumina. (D.C.W.)

11007 (NP-15831) ADVANCED VALVE TECHNOLOGY FOR SPACECRAFT ENGINES. Final Report, July 1964–August 1965. Salvinski, R. J.; Fiet, O.; Merritt, F. (TRW Space Technology Labs., Thompson Ramo Wooldridge Inc., Redondo Beach, Calif.). Aug. 17, 1965. Contract NAS7-107. 372p.

Current problems and future requirements of valves operating in the space environment were determined, and a literature search was conducted to update previously reported work and to obtain required information on the current program. Feasibility testing was conducted on several new concepts which included a zero-g vent valve, a high-temperature lightweight actuator, a leak measurement device, and a wet seal. Studies which were undertaken include sterilization, radioisotope-heated valves, thin films, pyrotechnic dynamic testing, and small clearance clogging during N_2O_4 propellant flow. (auth)

Vacuum Engineering

11008 ULTRAHIGH VACUUM. Roberts, R. W. (General Electric Research and Development Center, Schenectady, N. Y.). Sci. J., 1: 32-9(Dec. 1965).

Advances in ultrahigh vacuum technology in the past ten years are reviewed. Applications of vacuum technology are pointed out. Materials used in vacuum systems, vacuum pumps, methods of measuring the degree of vacuum, and seals and valves for use in vacuum systems are considered. (A.G.W.)

GEOLOGY, METEOROLOGY, AND MINERALOGY

General

Refer also to abstract 12518.

11009 (BNWL-SA-406) A SEQUENCE FOR PREDICTING WASTE TRANSPORT BY GROUND WATER. Nelson, R. William (Battelle-Northwest, Richland, Wash. Pacific Northwest Lab.). Apr. 15, 1965. Contract AT (45-1)-1830. 17p. (CONF-651207-1). ORAU.

From American Water Resources Assn., 1st Annual Meeting, Chicago.

An analysis sequence is presented to enable rational predictions of containment concentrations entering streams, rivers, or other potable waters traversing the region of study by ground water transport. The purposes are to give an over-all description of the sequence, briefly describe the methods developed, and indicate the computer programs available to assist in accomplishing the analysis. Throughout the analysis, major emphasis was on realistically evaluating actual situations. The natural sediments are assumed heterogeneous with respect to the permeability, potential measurements can be irregularly located, and boundary conditions may be both mixed and nonuniform. (P.C.H.)

11010 (HNS-1229-61) TRANSPORT OF RADIONUCLIDES BY GROUND WATER—SOME THEORETICAL ASPECTS. Lynch, Edward J. (Hazleton-Nuclear Science Corp., Palo Alto, Calif. Bradberry (Carroll E.) and Associates, Los Altos, Calif.). Nov. 30, 1964. Contract AT (29-2)-1229. 56p. Dep. mn; CFSTI $3.00 cy, $0.75 mn.

Radionuclides may be transported by flowing ground water from the site of a nuclear detonation to points of potential water use. To aid in evaluating the hazard from this condition, an analysis of water transport and contaminant movement was made. Equations are presented for predicting transport time and dispersion in uniform systems. The equations indicate that dispersion should have a negligible effect on transport time, except for flow through a single set of parallel fractures. This is at variance with observed cases of dispersion in granular rocks, and suggests that geologic inhomogeneities may play an important role. (auth)

Meteorology

See Site Survey and Selection

Refer also to abstract 11808.

Natural Radioactivity and Fallout

See also HEALTH AND SAFETY

Refer also to abstracts 10512, 10535, 10718, and 10722.

11011 (BNWL-122, pp 181-3) STUDIES OF FALLOUT NUCLIDES IN PLANTS AND BROWSING ANIMALS OF WASHINGTON. Eberhardt, L. L.; Rickard, W. H. (Battelle-Northwest, Richland, Wash. Pacific Northwest Lab.).

An effort was made to appraise the effects of season, precipitation, and elevation on fallout levels in food chains at sites on the Hanford Reservation, in the Blue Mountains (near Dayton), in the Cascade Mountains (between Yakima and Packwood), and in the vicinity of Quinault, Washington state. A regular series of samples of plants and browsing animals was obtained during 1963 and 1964 over areas encompassing a wide range of precipitation and elevation. Levels of radionuclides in both plants and animals showed marked seasonal variations as well as precipitational effects. (auth)

11012 (BNWL-122, pp 184-6) RELATIONSHIP OF ANNUAL FORAGE YIELD AND FALLOUT DEPOSITION IN A CHEATGRASS COMMUNITY. Rickard, W. H. (Battelle-Northwest, Richland, Wash. Pacific Northwest Lab.).

Cheatgrass, a winter annual, was harvested from an abandoned field habitat on the Hanford Reservation, Benton County, Washington, during the years 1961 through 64. During the period of study the vegetation of the field consisted of a nearly pure sward of cheatgrass with only a sparse scattering of herbs, mostly Salsola kali L. with Sisymbrium altissimum L. The concentration of ^{137}Cs in cheatgrass was little changed in 1964 as compared to 1963. However, the yield of cheatgrass was much greater in 1963 because of a favorable precipitational regime. Increased harvest yield resulted in a 12-fold increase of ^{137}Cs in the vegetation of a herbaceous plant community in 1963 as compared to 1964. (auth)

11013 (USNRDL-TR-940) PULSED REACTOR SIMULATION OF UNDERWATER NUCLEAR DETONATIONS—THERMAL ANALYSIS. Schrock, V. E. (Naval Radiological Defense Lab., San Francisco, Calif.). Apr. 9, 1965. Contract AT(49-5)-2084. 29p. Dep. mn. CFSTI $2.00 cy, $0.50 mn.

Calculations were made, using reasonable approximations, to estimate the degree of vaporization, if any, which would result when a small ^{235}U sphere is irradiated in a pulsed reactor facility. Conditions considered were a 10-mg sphere immersed in water (and in vacuum) and irradiated with a reactor period of 2 ms, resulting in a total fission energy deposition of 16 calories (2×10^{12} fissions). Results of these calculations indicate complete vaporization of the ^{235}U bead in a vacuum environment, with a peak temperature of between 13,900 and 28,800°K. This temperature is limited by expansion, radiation heat loss, and condensation of ^{235}U on the walls of the vacuum vessel. In the water environment, the bead would be vaporized, with peak temperature above 7000°K, resulting in complete chemical reaction with water vapor and the release of an additional 5.1 calories of heat. Again, radiation, condensation, and expansion limit the temperature. The final state of fuel and fission products is expected to be finely divided oxides suspended in liquid water, if not free molecules. Hydrogen will be generated (1.9 ml at STP). (auth)

11014 A SIMPLIFIED METHOD FOR MEASURING THE HALF-LIFE OF RADIOACTIVE AEROSOLS IN THE STRATOSPHERE. Petrovic, Pavel. Meteorol. Zpravy, 18: 17-18(Feb. 1965). (In Czech).

By use of simplifying assumptions, the mean half life of radioactive aerosols in the stratosphere was established for the time interval from 1961 to 1964 as 2.7 years. An exponential fallout of radioactive aerosols was assumed. (tr-auth)

11015 TOTAL RADIATION IN MILESHOVKA. Picha, Jaroslav; Cenek, Josef. Meteorol. Zpravy, 18: 75-7(June 1965). (In Czech).

Data on total radiation were calculated for the interval 1951 to 1960 using the modified Angstrom equation and the results are reported. The results were compared with results obtained using the Berljand equation. (tr-auth)

11016 EVALUATION OF ATMOSPHERIC RADIATION DURING 1964. Petrovic, Pavel; Zavodsky, Dusan. Meteorol. Zpravy, 18: 82-8(June 1965). (In Czech).

Results of the measurement of radioactivity in the air and of monthly, weekly, and daily fallout measurements in 1964 are reported. The measurements are based on the meteorological analysis of the radioactivity extremes previously reported. (tr-auth)

11017 EXAMINATION OF RADIOACTIVITY OF FOOD IN BADEN-WUERTTEMBERG. Bergner, K. G.; Jaegerhuber, P. (Chem. Landesuntersuch.-Anst., Stuttgart). Mitt. Geb. Lebensmitteluntersuch. Hyg., 55: 490-501 (1964).

A brief review is given of some aspects of supervising

radioactive contamination of food and of determining sampling sites. An ample series of tests confirmed that the 16 sites chosen for sampling milk in the Baden-Würtemberg region were representative. The effects of the last atomic tests in the atmosphere prior to the test ban are illustrated by the following measurements. Changes in contamination of milk by ^{131}I, ^{89}Sr, ^{90}Sr and ^{137}Cs were measured from one sampling site each in a dry and wet region from September 1961 to July 1964. Since May 1964, the ^{90}Sr and ^{137}Cs decreased. The degree of contamination of wheat and rye of the 1962 and 1963 harvests with ^{89}Sr, ^{90}Sr and ^{137}Cs in the various sampling sites clearly followed the amount of precipitation. A comparison was made with the contamination of water from a cistern. Due to the biological differentiation of radioactive isotopes studies of fallout and precipitation cannot be a substitute to examination of the food when fallout is increased. (Excerpta Med.)

11018 FALLOUT IN LONDON RAINWATER DURING 1964. **Wood, R.; Kerr, J. R. W.; Richards, L. A. (Lab. of the Government Chemist, London). Nature, 208: 1083-4(Dec. 11, 1965).**

Monthly samples of rainwater were collected in London during 1964 and analyzed for the presence of various fission products. Data are presented on the content of ^{137}Cs, ^{144}Ce, ^{54}Mn, ^{147}Pm, ^{90}Sr, ^{91}Y, and ^{95}Zr. Strontium-89 due to the American and Russian tests of 1962 was last positively identified in April 1964 when the level was 0.8 pC/l. The levels of ^{91}Y and ^{95}Zr were approaching the limits of detection by the end of the year. The peak levels of radioactivity occurred in May when 33 pC/l and 59 pC/l of ^{90}Sr and ^{137}Cs respectively were recorded. Fallout debris from the low-yield Chinese nuclear test on Oct. 16 did not substantially affect the concentration of radioactivity in London rainwater during the last 3 months of the year. (C.H.)

11019 DETERMINATION OF THE GROSS GAMMA RADIOACTIVITY OF INDIANA SOILS BY LARGE VOLUME LIQUID SCINTILLATION COUNTING. **Ziemer, Paul L.; Christian, John E. (Purdue Univ., LaFayette, Ind.). Proc. Indiana Acad. Sci., 40: 339-42(1965).**

Samples of soil from 63 counties in Indiana were collected prior to resumption of weapons testing in 1961. Representative 1000-g portions were counted in the Purdue Small Animal Counter, a large-volume liquid scintillation counter. The average gross γ activity for all counties was 4.6 pC/g. The highest individual sample was 5.9 pC/g for Jay County and the lowest was 2.5 pC/g for Jasper and Pulaski Counties. Since the method used was rapid and sensitive and involved no chemical treatment or processing, it should be useful for large-scale environmental monitoring programs. (A.G.W.)

11020 GROSS GAMMA RADIOACTIVITY IN INDIANA PRECIPITATION. **Ziemer, P. L.; Schaal, L. A.; Newman, J. E.; Rhykerd, C. L.; Christian, J. E. (Purdue Univ., LaFayette, Ind.). Proc. Indiana Acad. Sci., 40: 343-7 (1965).**

Precipitation catches in excess of 1 in./24 hr were collected from 29 official U.S. Weather Bureau gages geographically distributed over Indiana for a year from April 1962 through March 1963. Sampling was continued for another year at 14 of the stations. Catches were transferred to 1-liter polyethylene bottles at the weather stations and mailed to Purdue for gross activity determination in the Purdue Small Animal Counter. The only processing prior to activity determination was measurement of the volume and adjustment to one liter. Results are tabulated. All values were well below maximum permissible concentration for fission products in drinking water established by the National Committee on Radiation Protection. (A.G.W.)

11021 THE RADIOACTIVITY OF WATER AND ITS CONTROL. **Kosmowski, A. Wasser, Luft Betrieb, 8: 719-21(1964).**

Industrial and medical use of radioactive substances necessitates measures for careful control of population exposure, particularly in the area of water contamination by artificial radioactivity. However, it is also essential that water be monitored for the presence of natural contaminants such as radium, uranium, radon, thoron and the fission products of these elements. A third source of water contamination is fallout. Because of the filtering property of soil, little radioactivity is found in surface waters. However, radionuclides in water become concentrated in plant and animal tissues. Measurement of activity and analysis of radionuclides are recommended procedures for control of water contamination. (H.G.D.)

Techniques and Equipment

Refer also to abstract 11087.

11022 (AERE-R-5080) AN INVESTIGATION USING RADIOACTIVE TRACERS INTO THE SILT MOVEMENT IN AN EBB CHANNEL, FIRTH OF FOURTH, 1965. **Smith, D. B.; Parsons, T. V.; Cloet, R. L. (Research Group, United Kingdom Atomic Energy Authority, Wantage (England)). Nov. 1965. 15p. Dep. BIS $0.80. HMSO 4s.**

An investigation of a spoil ground in an ebb channel near Oxcars was undertaken using ground glass tracer labeled with lanthanum-140. The results show that the spoil would be widely distributed downstream of the deposition area without approaching existing harbors on the estuary. Upstream movement of spoil was very limited during the three day period of the investigation. (P.C.H.)

11023 ^{90}Sr AND ^{137}Cs IN COLUMBIA RIVER PLUME, JULY 1964. **Park, Kilho (Oregon State Univ., Corvallis); George, Marilyn J.; Miyake, Yasuo; Saruhashi, Katsuko; Katsauragi, Yukio; Kanazawa, Teruko. Nature, 208: 1084-5(Dec. 11, 1965).**

The extension of Columbia River outflow into the Pacific Ocean, or plume, was analyzed for ^{137}Cs and ^{90}Sr content in a study of ocean mixing processes. Samples of water were collected from the surface of the river, the river plume, and its vicinity during July 1964. The river water contains radionuclides from world-wide fallout and from Hanford atomic reactor waste. Both ^{137}Cs and ^{90}Sr contents in the Columbia River plume waters were found to be proportional to the contribution of the river waters as determined from salinity measurements. (C.H.)

11024 OBSERVATION OF PARTIAL SHRINKAGE OF STRATA. **Sano, S. I.; Kanaya, H. (Geological Survey of Japan, Kawasaki). Vienna, International Atomic Energy Agency, 1965, Preprint No. SM-68/30, 18p. (CONF-651023-17). ORINS.**

From Symposium on Radioisotope Instruments in Industry and Geophysics, Warsaw.

In order to investigate land subsidence caused by shrinkage of strata, a method for measuring partial shrinkage in a borehole was developed. Radioactive sources containing ^{60}Co pellets are shot into strata around a borehole at various depths by a gun-perforator and used as marks indicating the vertical position of a stratum. By repeating measurement of the depth, vertical displacement of the sources is obtained, and thus partial shrinkage is derived. A well logging system was designed to reduce the error of displacement to less than several millimeters. The relative depth of the source held in the stratum is measured from a reference radioactive source fixed to the casing pipe and the vertical interval between neighboring reference sources, which are moved with deformation of the casing pipe, is checked by comparing with the spacing of two detectors connected vertically. The dual detector system travels but a few meters in scanning these measurements and elongation of the cable due to loading weight and self-weight is negligible. A horizontally directional scintillation detector was designed to locate precisely the position of the source, and the optimum time constant and logging speed were discussed for recording steep variation by a counting rate-meter. A winch was designed to avoid cable slip. The logging speed is kept constant regardless of loading weight; however, the speed is adjustable from 1 centimeter per

minute to 3 meters per minute. Two actual observation wells 650 and 950 meters deep were constructed through the quaternary sediments producing natural gas of dissolved-in-water type at Niigata City, and the sources were shot into strata mostly every 40 meters, while the spacing of the reference sources was 20 meters. Observations have been carried out since 1961 by measurement at intervals of about a year. (auth)

Thorium and Uranium Minerals

Refer also to abstract 10768.

11025 (RME-4552(Rev.)) RECONNAISSANCE FOR URANIUM IN THE LONQUIMAY AREA, PROVINCE OF MALLECO, CHILE. Knowles, Paul H.; Bowes, William A.; Serrano C., Mario; Moraga B., Aldo (Division of Raw Materials (AEC), Washington, D. C. Instituto de Investigaciones Geologicas, Santiago (Chile)). Oct. 1962. 13p. Dep. mn; CFSTI $1.00 cy, $0.50 mn.

In a two-week reconnaissance of the Lonquimay area, south-central Chile, anomalies were noted in marl and in a sulfide-mineralized shear zone in continental black shales. Slight anomalies also were indicated in water samples from streams draining the general area of the shear zone. (auth)

11026 DIFFERENT BEHAVIOR OF URANIUM AND THORIUM DURING LITHOGENESIS OF MANY-COLORED DEPOSITS. Kovalev, V. A. (Lab. of Geochemical Problems, Academy of Sciences, Belorussian SSR). Dokl. Akad. Nauk Belorussk. SSR, 9: 537-40(Aug. 1965). (In Russian).

The quantitative characteristics of uranium in complex igneous rocks are well known, but the geochemistry of thorium is not sufficiently well established. In order to obtain comparable data on the behavior of these elements, their geochemical properties were examined in Lower Triassic deposits from the Pripyat Basin. Multicolored sand, sandstone, siltstone, and clay specimens were studied by chemical and physical methods. The coloration of the rocks was found to be due to their Fe^{3+}/Fe^{2+} ratio; if this value was >1, the color was reddish and for <1, it was greenish. Sandstone specimens were usually more markedly green-colored than the clay specimens. The reddish, primarily clay specimens contained more Th than the corresponding greenish specimens; the reverse was true for the U content. The Th/U ratio was 2.5 in the green and 10.7 in the red rocks. In view of the oxidizing ability of U, its secondary compounds predominated in the sedimentary deposits; for Th, acceptor minerals predominated in such deposits. The Th/U ratio changed regularly, reaching a maximum near the periphery of the depression and a maximum near its center. This ratio may be used to indicate the distance of the formation of the deposit from the origianl shore line of the sedimentary basin. The coloration serves as an indicator of the presence of organic matter. (TTT)

HEALTH AND SAFETY

See also BIOLOGY AND MEDICINE — Radiation Hazards and Protection
GEOLOGY, METEOROLOGY, AND MINERALOGY — Natural Radioactivity and Fallout

Refer also to abstracts 10604, 10605, 10719, 10981, 11010, 11930, 12333, and 12359.

11027 (AED-C-21-03) PHOTOGRAPHIC, CHEMICAL AND SOLID STATE DOSIMETRY. Series C. Bibliographies. Becker, K. (comp.) (Kernforschungsanlage, Juelich (West Germany)). July 1965. 118p. Dep. mn.

References (381) are given to reports and journals published from 1953 through March 1965. Separate author, subject, and report number indexes are included. (P.C.H.)

11028 (AERE-M-1664) EXTENDED FIRE TESTS ON TINPLATE CANS. Dixon, F. E. (Atomic Energy Research Establishment, Harwell (England)). Nov. 1965. 13p. Dep. BIS $1.40. HMSO 7s.

Experiments were performed to show that tinplate containers would withstand extended fire tests. The tests used were a torch test, to simulate a jet of flame, on a container for 4 hr, and a 4 hr fire test in a completely oxidizing atmosphere in an electric furnace. The results showed that a torching flame of 800°C for 4 hr had no significant effect on the functional strength of the can or on its ability to contain isotopes. The can, although heavily oxidized, was still capable of retaining isotopes. (P.C.H.)

11029 (DP-1006) SAVANNAH RIVER PLANT CRITICALITY DOSIMETRY SYSTEM. Wright, Charles N.; Hoy, John E.; Splichal, William F. Jr. (Du Pont de Nemours (E. I.) and Co., Aiken, S. C. Savannah River Lab.). Nov. 1965. Contract AT(07-2)-1. 27p. Dep. mn. CFSTI $2.00 cy, $0.50 mn.

Methods that would be used to segregate exposed and nonexposed personnel and to determine neutron and gamma doses received by those who were exposed are described. Manual and computer methods used in processing the data obtained are appended. (P.C.H.)

11030 (NBS-MON-76) AN ENGINEERING METHOD FOR CALCULATING PROTECTION AFFORDED BY STRUCTURES AGAINST FALLOUT RADIATION. Eisenhauer, Charles (National Bureau of Standards, Washington, D. C.). July 2, 1964. 20p. GPO $0.20.

Technical assumptions underlying the methods currently recommended by the Office of Civil Defense (OCD) for calculating protection afforded by structures against fallout radiation are discussed. Included are methods for calculating the contributions from radioactive sources on the roof and on the ground surrounding a simple one-story building. It is shown in detail how each technical chart in the OCD Professional Manual is derived from basic data on radiation penetration. Charts are included in order to make the report self-contained. (auth)

11031 (NP-15708) SECONDARY IGNITIONS IN NUCLEAR ATTACK. Final Report. McAuliffe, John; Moll, Kendall (Stanford Research Inst., Menlo Park, Calif.). July 1965. Contract N228(62479)65701. 208p. CFSTI $6.00 cy, $1.25 mn.

Secondary fires (i.e., fires caused by blast and other nonthermal effects) and other fires caused by disruptions to normal activities because of attack were analyzed. Secondary ignition frequencies were estimated at 0.006 per 1,000 sq ft of total floor area damaged by at least 2 psi blast pressure. This estimate is consistent with available data from atomic and conventional bombings, explosive disasters, and earthquake and tornado experiences. The estimate implies that secondary ignitions can be the major cause of nuclear fires. Existing contradictory conclusions from Hiroshima and Nagasaki were resolved on the basis of known physical effects. It was found from statistical analyses that the most hazardous structures are wooden ones; the most hazardous fire sources are electrical and heating equipment; and the most hazardous occupancies are storage of high-energy materials such as oil and chemicals. It attributes secondary ignitions mainly to the rupture of fuel lines and containers by flying debris and collapsing structures. It was concluded that fires during warning and postattack recovery periods are not potentially critical civil defense problems. However, hazards from such fires, as well as from nuclear- and disaster-caused fires, can be greatly reduced by cutting off electricity and other energy supplies. (auth)

11032 (ORNL-3891) DECONTAMINATION OF THE ORNL MOLTEN-SALT FLUORIDE-VOLATILITY PILOT PLANT AFTER PROCESSING IRRADIATED ZIRCONIUM-URANIUM ALLOY FUEL. Mann, S.; Youngblood, E. L. (Oak Ridge National Lab., Tenn.). Feb. 1966. Contract W-7405-eng-26. 48p. Dep. mn. CFSTI $2.00 cy, $0.50 mn.

The molten-salt fluoride-volatility process for recovering uranium from irradiated zirconium- or Zircaloy-2-clad fuel elements was demonstrated successfully in the ORNL Molten-Salt Fluoride-Volatility Pilot Plant. Decontamination methods that were used twice, following two periods of hot operation, to reduce radiation levels in excess of 2000 R/hr to values sufficiently low to permit extensive direct maintenance and equipment modification are described. Radiation dosage to individuals who did the mechanical work in no case exceeded the quarterly 1.3-R allowance. Final backgrounds were less than 100 mR/hr in the majority of cell locations, with maximum readings of 500 mR/hr adjacent to some parts of the process equipment. The decontamination sequence was based on laboratory development work. It includes flushing with a molten salt, followed by treatment with three types of aqueous solutions for removing salt film, metal scale, and deposited radiation emitters. This procedure is suitable for radiation levels at least as high as those encountered in the two radioactive operating periods cited. (auth)

11033 (SC-TM-65-398) GROUND DEPOSITION OF MICROSPHERES RELEASED FROM 50 KILOMETERS. Warnke, D. F. (Sandia Corp., Albuquerque, N. Mex.). Jan. 1966. Contract AT(29-1)-789. 28p. Dep. mn. CFSTI $2.00 cy, $0.50 mn.

The surface deposit densities which result from a distribution of microspheres being released at an altitude of 50 kilometers and dispersed by gravitation, wind, and diffusion were calculated and are presented for eight wind conditions. The results proved to be useful as a rough guide to the sensitivity of deposit densities to particle size distribution parameters, source altitude, vertical wind shear, and lateral dispersion rates as well as an aid in investigating the merits of any refinements to the TRC model. (auth)

11034 (TID-5360(Suppl.5)) A SUMMARY OF INDUSTRIAL ACCIDENTS IN USAEC FACILITIES, 1963-1964. (Division of Operational Safety (AEC), Washington, D. C. Industrial Safety and Fire Protection Branch). Dec. 1965. 49p. Dep. mn. CFSTI $3.00 cy, $0.50 mn.

Information on accidents and incidents occurring during 1963-64 in plants owned and operated by the AEC is reported. Descriptions of accidents and incidents involving radioactive materials, together with a table of radiation exposures for AEC contractor personnel are also included, along with industrial fatal accidents. (P.C.H.)

11035 (TID-8541, pp 249-319) TRANSPORTATION OF RADIOACTIVE MATERIALS. Zahn, L. L. (General

Electric Co., Richland, Wash. Hanford Atomic Products Operation); Brown, C. L. (Battelle-Northwest, Richland, Wash. Pacific Northwest Lab.); Langhaar, J. W. (Du Pont de Nemours (E. I.) and Co., [Wilmington, Del.]).

A discussion of past experience in shipping of radioactive materials within the United States is presented. The overall considerations and relations that govern transport-system designs as a function of the material to be shipped, the mode of transport, and other factors, are summarized. The current status of standards and regulations, research and development programs, and current transport practice throught the United States, are summarized. (M.O.W.)

11036 (JPRS–33502) REGULATIONS ON RADIATION SAFETY DURING GAMMA RAY DEFECTOSCOPY. Translated from Durzhaven Vestn., No. 95, 1-7(1965). 24p. (TT–65-34076). CFSTI $1.00 cy, $0.50 mn.

Regulations obligatory in Bulgaria in the design, operation, and use of laboratories for gamma defectoscopy, regardless of their purpose, location, and type of gamma defectoscope are listed. (P.C.H.)

11037 DEPENDENCE OF ENERGY LOSSES AVERAGED OVER THE ELECTRON SPECTRUM ON β-SPECTRUM ENERGY MAXIMUM, ATOMIC NUMBER OF β EMITTER, AND TYPE OF TRANSITION. Baranov, V. F. At. Energ. (USSR), 19: 450-1(Nov. 1965). (In Russian).

The energy losses of beta particles in aluminum and tissue (water) were calculated, averaging over the electron spectrum for emitters having an allowed and a first-order absolutely forbidden transition. Beta emitters with Z of 10, 20, 40, 60, and 80 and maximum spectral energies from 0.1 to 3.0 were taken. Results are presented, and their accuracy is discussed. The obtained energy variation of the ionization energy loss in tissue is used to calculate the energy dependence of the maximum permissible electron flux, assuming a dose rate of 0.1 rads/week and an exposure time of 40 hours/week. (M.J.T.)

11038 BERYLLIUM DISEASE: REPORT OF THE SECTION ON NATURE AND PREVALENCE. COMMITTEE ON OCCUPATIONAL DISEASES OF THE CHEST. AMERICAN COLLEGE OF CHEST PHYSICIANS. Hannon, John W. G. Dis. Chest, 48: 550-8(Nov. 1965).

The physical and chemical properties of Be are reviewed in relation to acute and chronic forms of disease (berylliosis) caused by occupational exposure to the metal and its compounds. Acute respiratory tract responses to Be exposure range from transient rhinitis, pharyngitis, or tracheobronchitis to severe pulmonary involvement, depending on the degree, duration, and type of exposure to mists, fumes, or dust. All the soluble Be compounds utilized in industry are hazardous. Rhino-pharyngitis and tracheobronchitis usually resolve spontaneously and rapidly after cessation of exposure. A typical case of insidious pulmonary involvement is described. Dermal manifestations are presented as four distinctive lesions each with a special etiology. Contact dermatitis can be caused by or result from undue and/or prolonged contact with the soluble salts of Be. Allergic dermatosis usually occurs within 15 days after initial exposure to the fumes or mists or BeF_2 and can be expected to involve about 1% of the population at risk. Chemical ulcer may be the result of neglected superficial laceration of abrasions contaminated with the fluoric compounds of Be. The fourth dermal manifestation, ulcerating granuloma, is the result of subdermal implantation of Be salts, especially the sulfate. In chronic Be disease, respiratory tract manifestations include pulmonary berylliosis. This lesion is considered part of a systemic disease, induced by the Be ion, which affects the pulmonary parenchyma. Current epidemiologic evidence indicates that the principal etiologic factor in the proved cases had been inhalation exposure to aerosols of BeO with distinctive physical and chemical characteristics. The chronic pulmonary form occurs usually after a latent period following the last exposure to Be. In an attempt to explain the variable period of latency before manifestations of the chronic form appear, the concept of autosensitization has been proposed. In this sense, lesions may arise in the lung not as an expression of the direct or primary reaction of tissue to Be, but because of more subtle, indirect and delayed immunologic responses to tissues to secondary biologic materials (denatured proteins, endo-antibodies, and other intrinsic factors) created through the prior contact of Be with tissue. Industrial hygiene precepts for controlling the incidence of berylliosis are outlined. (BBB)

11039 RADIOECOLOGY AND RADIOLOGICAL PROTECTION. Michon, G. (CEA, Paris). Energie Nucl., 7: 333-9(Sept.-Oct. 1965). (In French).

The basic standards of radiological protection are shown to be not directly applicable to certain practical aspects of population protection; especially in that which concerns environment contamination. It is possible (by using the same reasoning used to define the maximum admissible concentrations of air and water consumed by man) to define the maximum quantities and concentrations in a nuclear environment. Instead of using biological constants inherent in man, it is necessary to define ecological constants, which are described in general for certain types of radioactive effluent disposals. (auth)

11040 THE TRANSPORTATION OF RADIOELEMENTS. Vinarnick, L. (CEN, Saclay, France). Ind. At., 9: 54-60(1965). (In French).

Following a discussion on the characteristics of the radioelements as products on the market, the philosophy and the chief provisions of the regulations covering the transport of these radioelements as developed from the recommendations of the A.I.E.A. are summarized. Two categories of radioelements based on their life time and on the type of packet they constitute are given; the practical requirements for transporting each of them are described with emphasis on the composition of the packaging which makes it possible for them to be handled by standard transport agencies. (auth)

11041 APPLICATION OF DOSIMETRY BY THERMOLUMINESCENCE TO RADIOPROTECTION. Cluchet, Jean; Joffre, Henri (Service de Protection Contre les Radiations, Saclay, France). Ind. At., 9: No. 9-10, 83-90 (1965). (In French).

Physical problems in the dosimetry of photons to obtain a precise estimate of the biological risks at energies between 10 kev and 10 Mev are discussed. When applied to dosimetry by thermoluminescence, these principles lead to compounds with a low atomic number (LiF, $Li_2B_4O_7$) as the detecting medium. It was also necessary to make a careful study of the thickness and the characteristics of the walls and materials composing the dosimeter. (auth)

11042 SAFETY AND DOSIMETRIC PROBLEMS IN EXPLORATION OF NUCLEAR POWER PLANTS. Kabat, Miloslav (Research Inst. of Power Engineering, Prague). Jad. Energ., 11: 346-9(Sept. 1965). (In Czech.).

Radiation measurements required in the operation of a nuclear electric power station are summarized under two topics: biological control and technological dosimetry. Some of the instruments for measurement of the activity of solid, liquid, and gaseous effluents are enumerated, and some of the problems involved in making meaningful measurements of activity are discussed. Problems of making significant activity measurements in circulating systems of the reactor are considered. The reliability of electronic measuring apparatus is considered a definite limitation on reliability of nuclear reactor power stations. (TTT)

11043 THE ANALYSIS OF INDUCED ATMOSPHERIC RADIOACTIVITY. Behounek, Frantisek; Matouskova, Jirina. Jad. Energ., 11: 441-7(Dec. 1965). (In Czech).

The radioactivity arising in the atmosphere after nuclear weapon tests is of complex nature and may be divided into a short-lived component containing nuclides with $T \leq 1$ year, and into a long-lived component formed essentially from two nuclides (^{90}Sr and ^{137}Cs) with the half lives of 28 and 30 years, respectively. The short-lived component forms the main part of total activity of atmospheric fallout for several years and is decisive in increased radiation background for populations. The long-lived component is important in the food chain and its quantitative evaluation is difficult. On the basis of long-term analyses criteria

for precise evaluation of atmospheric fallout activity are discussed. (auth)

11044 DETERMINATION OF THE TOTAL ALPHA ACTIVITY OF DRINKING WATER USING A NUCLEAR EMULSION. Tyrrell, M. W.; Demetsopoullos, I. C.; Collinson, A. J. L. (Borough Polytechnic, London). Nature, 208: 1074-6(Dec. 11, 1965).

A method is described for estimating the total α activity of solutions using 50 μ Ilford G5 nuclear emulsions. A tentative value of approximately 10^{-13} C/l, with a statistical accuracy of 15%, was obtained for the α activity of a sample of drinking water from the London area. It was assumed that the measured α activity of the water was due mainly to Ra and its decay products. (C.H.)

11045 NUCLEAR SAFETY. Volume 6, Number 4. Cottrell, Wm. B.; Jordan, W. H. (eds.). Contract W-7405-eng-26. One of the five Quarterly Technical Progress Reviews published for the Division of Technical Information, USAEC. Oak Ridge National Lab., Tenn., Summer 1965. 165p. GPO $0.70 Domestic, $0.90 Foreign.

Information on nuclear safety is presented in 20 sections. Separate abstracts were prepared for 19 of these. The section for which no abstract was prepared is concerned with a review of publications related to radiation-protection standards, a symposium on packaging and transportation of radioactive materials, and power reactor siting. (J.R.D.)

For abstracts of individual sections see: 11046–11052, 11222, 12334, 12335, 12433–12437, 12510, 12521, 12522, and 12559.

11046 THE ADMINISTRATION OF RADIATION SAFETY AT HANFORD. Keene, A. R. (General Electric Co., Richland, Wash.). Nucl. Safety, 6: 343-53 (Summer 1965).

Methods used in administering radiation safety at Hanford from 1943 to 1965 are described. (J.R.D.)

11047 RADIATION IN PERSPECTIVE. Eisenbud, Merril (New York Univ., New York). Nucl. Safety, 6: 380-5(Summer 1965).

Adages concerning nuclear energy that have come into being in the last few years causing public apprehension about hazards of nuclear power are discussed. (J.R.D.)

11048 SAFETY-SYSTEM RELIABILITY Vs. PERFORMANCE. Epler, E. P. Nucl. Safety, 6: 411-14; 420 (Summer 1965).

The applicability of probabilistic techniques to reactor control and safety systems is discussed. Reactor operating experience is analyzed, and is used as the basis for suggestion that most effort should be expended in improving the performance reactor safety systems. (J.R.D.)

11049 RADIATION-MONITORING AND -WARNING SYSTEM AT ORNL. Lieber, L. F. Nucl. Safety, 6: 414-21(Summer 1965).

Design and operation of a comprehensive radiation-monitoring and -warning systems at ORNL are described. Information is included on components such as the laboratory control center, monitoring systems, and radio-communications networks. (J.R.D.)

11050 DESIGN CONSIDERATIONS FOR OFF-GAS SYSTEM MAJOR COMPONENTS. Fuller, A. B. Nucl. Safety, 6: 422-5; 431(Summer 1965).

Designs of gaseous waste handling systems are discussed. Most of the design approaches discussed have evolved from repeated trials of these and less effective methods of obtaining the required reliability of operation. (J.R.D.)

11051 INCIDENTS RELATED TO NUCLEAR SAFETY IN AEC OPERATIONS. Nucl. Safety, 6: 451-4; 467(Summer 1965).

A summary is presented of nuclear incidents that occurred in Atomic Energy Commission operations during calendar year 1964. (J.R.D.)

11052 SAFEGUARDS REPORTS AND SELECTED READING. Nucl. Safety, 6: 466-7(Summer 1965).

A list of recently issued safeguards reports and selected literature pertaining to hazards of reactors is presented. (J.R.D.)

11053 MIGRATION OF RADIOACTIVE STRONTIUM IN SOIL UNDER THE INFLUENCE OF AN ELECTRIC FIELD. Prokhorov, V. M.; Krasnoshchekova, R. Ya. Radiokhimiya, 7: 465-72(1965). (In Russian).

Under the influence of an electric field, the transport of cations adsorbed on soil particles takes place due to electromigration and electroosmosis. An equation is derived which describes both of these processes. Experiments were conducted to determine the feasibility of purifying the soil from radioactive strontium by means of an electric field. In electromigration of ^{89}Sr in a soil filled cell the maximum activity peak moves toward the cathode with some decrease of the peak height due to quasidiffusion spreading of the zone. It was thus shown that soil may be decontaminated from Sr by this method, although the process is rather slow. With 100-v output the consumption of energy for moving the ^{89}Sr peak was 400 to 100 kw-hr/m^3. After 1080 hrs in a cell containing equally distributed ^{89}Sr the fraction of the original specific activity in 60% of the soil between the anode and the cathode did not exceed 1 to 2%. The activity between the anode and 90% of the distance toward the cathode was 14% of the original activity in the whole cell. (ATD)

11054 AN IDEA ON THE MAXIMUM PERMISSIBLE CONCENTRATION OF RADIOACTIVE MATERIALS IN SEA WATER. Hiyama, Yoshio (Tokyo Univ.). Rec. Oceanogr. Works Jap., 5: No. 2, 98-104(Mar. 1960).

The author tried to find a relationship between the level of seawater contamination by several radionuclides and the level of radiation dose-rate inside the human body caused by these radionuclides of marine origin, using the recommendation of the ICRP and data on the chemical analysis of sea water and of the human body. Radionuclides which are important in view of their presence in waste and their effect on public health are considered. The evaluation of the importance of these radionuclides cannot be made merely on the basis of the amount of discharge and the speed of decay. Additional consideration should be given to the fact that some elements are concentrated more than others from seawater by marine organisms and from marine products by the human body. Furthermore, in the estimation of physical decay from the time of discharge to the time of human intake, the period of preservation and storage of the marine products, which possibly differs according to national food habits, must be considered in addition to the period of time required for the physical and biological transmission of the materials from the place of discharge to the food-producing zone of the sea. The speed of uptake of radionuclides from the environmental seawater is higher in microorganisms, which also collect nuclides adhering to the body surface, than in macroorganisms. The latter, which generally have more value as human food than the former, are contaminated either by intake of macroorganisms or by direct material exchange through the gill membranes to and from the seawater. The time required to get equilibrium between the seawater and the body of a fish varies according to the nature of the element and the physiological activity of the fish. Numerous experiments have shown that this time is rarely on the order of several hours but commonly several days or weeks. Thus short-lived radionuclides, with half lives of less than a day, cannot enter into consideration for this problem. The radionuclides considered include ^{90}Sr, ^{137}Cs, ^{60}Co, ^{65}Zn, ^{144}Ce, ^{131}I, ^{103}Ru, ^{99}Mo, ^{140}Ba, and ^{140}La, and radioisotopes of Cd and Fe. (auth)

11055 INVESTIGATIONS ON THE DISTRIBUTION OF RADIOACTIVE RAINFALL AT A DAM WITH THE HELP OF GAMMA SPECTROMETRY. Haberer, Klaus; Bernhardt, Heinz (Technische Hochschule, Karlsruhe, Ger.). Vom Wasser, 31: 43-84(1965). (In German).

Investigations on the distribution of dissolved and suspended radioactive materials in water used for drinking are discussed. Measurements were made of beta and gamma activity to determine the dependence of vertical distribution of fallout nuclides in standing water on the

time of year and the plankton population. Gamma spectrometry was used to identify the individual nuclides. The measurements were carried out in 1963 and data are presented in tables and graphs. A transport mechanism for the radioactive materials in the water is proposed. (M.C.G.)

11056 AIR PURIFICATION TECHNIQUES CURRENTLY USED IN NUCLEAR PHYSICS. Schuetz, H. Wasser, Luft Betrieb, 8: 11-20(1964).

In the special field of air purification many problems remain to be solved, and concerted efforts are needed to keep abreast of the exceedingly rapid developments in nuclear technology. In nuclear or related plants, there are several possibilities of seeking adequate solutions to the difficult problems in this special field of filter techniques. Filter questions concerning the air supplied to, available in, and exhausted from nuclear plants are discussed in detail with reference to the latest technical acquisitions. A description is given of the purpose, design, and function of air filters used in this field of application. The effective incorporation of such air-conditioning plants is discussed with reference to examples. (TCO)

11057 LUNG X-RAY VARIATIONS BY RARE EARTHS. Hoschek, R. Zentralbl. Arbeitsmed. Arbeitsschutz, 14: 281-4(Dec. 1964). (In German).

In several retouchers from the off-set copying division of a printing plant, who had inhaled the smoke of arc lamps for 10 years, variations of the x ray pictures of the lungs were found that resembled those found in silicosis. The intensity corresponds to approximately the duration of the exposure. In this operation, 40 to 50 off-set copies were prepared daily, approximately 10 times as many as is usual in this type of operation. The shadowing arose from the deposition of rare earth dust which was added to the carbon to increase the light intensity. No perturbation of the lung function or toxic effects were observed. It appeared to be similiar to baritosis and siderosis in being a reactionless deposition of the dust which causes a contrast in the lungs without inducing any illness. Research of American workers indicated no fibrous or granulomatus reactions of the tissues in men. (tr-auth)

11058 APPLIED DOSIMETRY. Aglintsev, K. K.; Kodyukov, V. M.; Lyzkov, A. F.; Sivintsev, Yu. V. London, Iliffe Books, Ltd., 1965. 239p. 50s.

A Translation.

The main types of ionizing radiations and their interactions with matter are described. Units used and main methods of recording radiation—by ionization and gas-filled detectors and by scintillation, photographic, and chemical means—are considered. The classification, components, and calibration of dosimetric instruments, including dosimeters, radiometers, and radiation monitors, are discussed. Measurement techniques are described, with discussions of permissible exposure levels, personnel monitoring, surface contamination, radioactivity of gases and aerosols, contamination of water, dose and dose rate, and neutron fluxes. Principles of calculation of doses from gamma radiation, beta sources, neutrons, and internal irradiation are given. Methods and tables for calculating shielding from gamma rays, neutrons, and alpha and beta particles are presented. (M.J.T.)

INSTRUMENTATION

General

Refer also to abstracts 11276, 11367, 11817, 11844–11847, 11862, 12249, and 12499.

11059 (BLG–345) THERMAL FLOW-METERS FOR ClF_3. De Wet, R. (Centre d'Etude de l'Energie Nucleaire, Brussels (Belgium)). Dec. 1964. 40p. Dep. mn.

Various models of three flowmeter types were constructed, and tested for stability, predictability of calibration, and rate of response to change in gas flow rate. A commercial model of one of the types was also tested. The calibration of all except the calorimetric type was affected by change of temperature of the incoming gas. All meters used with ClF_3 showed a change of calibration attributed to corrosion by the gas. The calibration of the calorimetric type was predictable from first principles. The tests showed that prediction of the calibration of the other types could be made if model experiments were first performed. The calorimetric type gave the fastest response, about 25 seconds for return to steady state after a step change in flow. Recommendations are made for the future improvement of flowmeters for this type duty. (auth)

11060 (BNWL–122, pp 33-6) A VERSATILE IODINE VAPOR AND PARTICLE SAMPLER. Snyder, M. D.; Bair, W. J. (Battelle-Northwest, Richland, Wash. Pacific Northwest Lab.).

A compact, versatile air sampler pack for collection of ^{131}I vapor and particles is described. Particles are collected on membrane filters and vapors are collected on charcoal or copper turnings in one dram vials for direct radioiodine counting in well-type counters. Iodine collected on membrane filters and copper turnings can be also analyzed by chemical methods. (auth)

11061 (IDO–17112) INSTRUMENT DEVELOPMENT BRANCH ANNUAL REPORT, 1964. Wilde, N.; Boland, T. J.; Anderson, S. D. (Phillips Petroleum Co., Idaho Falls, Idaho. Atomic Energy Div.). Dec. 1965. Contract AT(10-1)-205. 101p. Dep. mn. CFSTI $4.00 cy, $1.00 mn.

Separate abstracts were prepared for the three sections of the report. (D.C.W.)

For abstracts of individual sections see: 11174, 12498, and 12499.

11062 (RFP–649) A STUDY OF THERMISTOR STABILITY. Pippin, C. A. (Rocky Flats Div., Dow Chemical Co., Golden, Colo.). Dec. 14, 1965. Contract AT(29-1)-1106. 9p. Dep. mn. CFSTI $1.00 cy, $0.50 mn.

The stability of two Fenwall GB31J1 thermistors was investigated, using two crystal ovens. It was determined that the thermistors are stable within the accuracy normally required for use with accurate readout equipment. (D.C.W.)

11063 (RFP–672) AN ADHESION TESTER FOR EVAPORATED METAL FILMS. Beno, R. L. (Rocky Flats Div., Dow Chemical Co., Golden, Colo.). Jan. 11, 1966. Contract AT(29-1)-1106. 4p. Dep. mn. CFSTI $1.00 cy, $0.50 mn.

A tensile tester for measuring the bond strengths of vapor-deposited metallic coatings is described. Film adherence values are read directly in pounds pull from a precision-force gage. Accuracy of the force gage is ±0.5 percent of the full scale reading over the entire range. (auth)

11064 (RISO–102) PULSE-HEIGHT DISCRIMINATOR. Diamond, J. M. (Atomenergikomissionen, Risoe (Denmark). Forsoegsinstitut). May 1965. 42p. Dep. mn.

A solid-state pulse-height discriminator with a voltage range of 0.4 to 10 v is described. A detailed analysis of the operation of the discriminator is included, together with the results of some stability tests. (D.C.W.)

11065 (SC-TM–323-62(72)) A FAST-PULSE RECORDING AND READOUT DEVICE USING TUNNEL DIODES. Kelly, C. N. (Sandia Corp., Albuquerque, N. Mex.). Jan. 1963. Contract AT(29-1)-789. 15p. Dep. mn. CFSTI $1.00 cy, $0.50 mn.

A recording and readout system was developed for measuring very fast pulses. Using the ultrafast switching speed of the tunnel diode, the system records (to an accuracy of about 5 percent) pulse amplitudes in eight steps over 30 increments of 0.1 microsecond each. Interrogation speed of the recording portion of the system is compatible with almost all large-scale recording devices. (auth)

11066 (SLAC-PUB–146) ITERATIVE CHEBYSHEV APPROXIMATION TECHNIQUE FOR EQUALIZER SYNTHESIS. Temes, G. C.; Bingham, J. A. C. (Stanford Linear Accelerator Center, Stanford Univ., Calif.). Oct. 1965. Contract AT(04-3)-400. 14p. (CONF-651058–1). Dep. mn. CFSTI $1.00 cy, $0.50 mn.

From Allerton Conference on Circuit and System Theory, Urbana, Ill.

The Remez-Werner algorithm is extended to the Chebyshev approximation of general loss and phase characteristics. The resulting technique is useful for the design of equalizers, pulse-shaping networks, impedances, and delay lines. The application of the process to the synthesis of a video cable system is described. (auth)

11067 (UCRL–12095-T) PARALLELING AVALANCHE TRANSISTORS. Prince, Paul (Lawrence Radiation Lab., Univ. of California, Livermore). [1964]. Contract W-7405-eng-48. 8p. Dep. mn. CFSTI $1.00 cy, $0.50 mn.

A method for producing very high current nanosecond pulses by paralleling avalanche transistors is presented. Flat top pulses of more than 60 volts amplitude into 10-ohm loads with rise and fall times of about one nanosecond were demonstrated. Circuit diagrams are given. (M.O.W.)

11068 (WAPD-T–1815) DEVELOPMENT OF PHOTOGRAMMETRIC TECHNIQUES FOR MEASURING SURFACE CONTOURS OF SMALL SAMPLES. Solomon, Y.; Bohn, S. W.; Dimond, W. J. (Bettis Atomic Power Lab., West Mifflin, Pa.). Mar. 1965. Contract AT-11-1-GEN-14. 11p. (CONF-661001–1). Dep. mn. CFSTI $1.00 cy, $0.50 mn.

For Presentation at 14th Conference on Remote Systems Technology, Pittsburgh.

A photogrammetric technique using a steromicroscope that can be used in measurements requiring precision of ±50 μ in., by magnification at the various stages of photographing, printing, and projection, is described. Correction for lens distortion can be determined and eliminated by adjustment of the plotter or elimination of the distorted portion of the negative by enlargement and projection of the center portion. The system can be calibrated directly without interjection of empirical formulas, and provides a permanent visual record of the measured component. (P.C.H.)

11069 ON THE MOST ACCURATE MEASUREMENTS OF THE WAVELENGTHS OF X-RAY SPECTRAL LINES. Backovsky, J. (Inst. of Solid State Physics, Prague). Czech. J. Phys., 15: 752-9(1965).

The influence of statistical errors in measuring the intensity of a spectral line on the exact determination of its wavelength is discussed. Using simplifying assumptions, it is shown that the relative error in measuring the wavelengths of spectral lines of the same type, caused by the statistical character of x-ray intensity measurements and by the influence of the true width of the spectral line, is practically constant under the same conditions, i.e., it is independent of the lattice parameters of the crystals used and of the wavelength of the spectral line. It seems that the latest exact measurements of Bearden confirm this result. The greatest care should therefore be devoted to the neighborhood of inflection points of the

curve representing the spectral line profile when making exact measurements of the spectral position of the lines. (auth)

11070 PROGRESS IN HIGH-TEMPERATURE AND RADIATION RESISTANT STRAIN-GAGE DEVELOPMENT. Wnuk, Stephen P. Jr. Exp. Mech., 5: No. 5, 27A-33A (May 1965).

Performance characteristics of bonded resistance strain gages in high-temperature and nuclear-radiation environments are described. Typical electrical properties of ceramic-bonded strain gages are given for various environmental conditions. The methods used to minimize errors induced by the extreme environments are fully discussed. (Rev. Metal Lit.)

11071 VARIATION OF TIME-OF-FLIGHT OF ELECTRONS THROUGH A PHOTOMULTIPLIER. Rees, James D. Jr.; Givens, M. Parker (Univ. of Rochester, N. Y.). J. Opt. Soc. Amer., 56: 93-5(Jan. 1966).

A new experimental method utilizing a property of the gas laser was developed that permits the measurement of the variation of the time of flight of electrons through a photomultiplier as a function of the position on the cathode from which they are emitted. The measurement of time variation is accomplished by comparing it with the distance traveled by a light beam during the same time and is capable of a time resolution of approximately 10^{-11} sec. (auth)

11072 A TIME-OF-FLIGHT MASS SPECTROMETER. Matus, Lajos. Magyar Tud. Akad. Kozp. Fiz. Kut. Int. Kozlemen., 13: 251-8(1965). (In Hungarian).

A linear ion-path, time-of-flight mass spectrometer was designed and constructed on the basis of the principles laid down by W. C. Wiley and I. H. McLaren (Rev. Sci. Instr., 26: 1150(1955)). The instrument possesses a 1-m long flight tube and operates at an accelerating voltage of 1000 v, and a repeat frequency of 8 kHz, achieving a resolution of 100. It includes an ion source with an incandescent W wire, the flight tube and an ion detecting system. An avalanche is initiated in the electron multiplier, yielding enough current to allow examination of the data on an oscilloscope after further amplification. The electron multiplier is provided with diodes made of an Ag–Mg alloy. Because of the relatively short flight path, the time interval between the arrival of the various ion species is quite short, requiring a high upper limiting frequency for amplifying and measuring the ion current. The instrument was calibrated with an artificial gas mixture of N_2, O_2, Ar, and CO_2. The sensitivity of the instrument, i.e., the smallest gas volume that can be detected in the presence of another gas in a mixture of inert gases was found to be about 0.1% of the volume. (TTT)

11073 A CONSTANT SPEED DRIVE FOR MOESSBAUER EXPERIMENTS. Hackett, Charles F.; Hughes, Harold K. (Indiana State Univ.). Proc. Indiana Acad. Sci., 74: 298-301(1965).

An apparatus for Mössbauer experiments consists basically of a stainless steel foil rotated at such an angle to the γ-ray path that there is a longitudinal component for Doppler shifting the resonance curve. Both the angle and the speed of rotation are adjustable. The foil is rotated by a motor to which is coupled directly a generator tachometer whose voltage is directly proportional to the motor speed. The motor is controlled by a feedback system that must be manually adjusted upon starting, but, once operating conditions are achieved, the motor will run at constant speed automatically compensating for circuit element heating or line voltage variations. (A.G.W.)

11074 HIGH VOLTAGE IMPULSE SYSTEM. Finkelstein, David; Goldberg, Philip; Shuchatowitz, Joshua (Yeshiva Univ., New York). Rev. Sci. Instrum., 37: 159-62 (Feb. 1966).

An alternative to the Marx circuit for the production of high voltage, high current pulses is developed. It employs a water-immersed spiral-wound stepup transformer to go from a capacitor bank charged to 100 kv to an output of 1 Mv. A method for using such a transformer to pulse charge a second capacitor bank efficiently without very tight coupling is derived. It is shown that for total transfer of energy (except for dissipation) the two resonant frequencies of the primary and secondary LC circuits (each measured with the other circuit open) should be equal, while the two normal mode frequencies of the coupled circuit should be in the ratio of 2 : 1, implying a coupling coefficient of $\frac{3}{5}$. The design and operation of such a system is described. (auth)

11075 MODIFIED DEBYE-SCHERRER X-RAY DIFFRACTION CAMERA FOR RADIOACTIVE COMPOUNDS. Sherman, R. L.; Keller, O. L. Jr. (Oak Ridge National Lab., Tenn.). Rev. Sci. Instrum., 37: 240(Feb. 1966). (ORNL-P-1755).

A solution is described for the problem of taking powder patterns of alpha active compounds. This solution allows the use of ordinary darkroom and x-ray equipment. A beryllium cup, which is attached to a brass ring with epoxy cement, fits over a backplate attached to the camera, as is shown. The brass ring prevents abrasion of the beryllium. In order to prevent the appearance of beryllium lines in the diffraction pattern, the entrance and exit collimators must pass through the beryllium cup. A beryllium cup was also designed for an XRD powder camera. (J.F.P.)

11076 THERMOCOUPLE FOR MEASURING TEMPERATURES UP TO 2500K. Zuykov, N. V.; Tsvetaev, A. A.; Bardyukov, M. E. (Moscow Power Engineering Inst.). Teplofiz. Vysok. Temp., 3: 815(Sept.-Oct. 1965). (In Russian).

A graphite-carbon thermocouple for measuring temperatures from 1200 to 2900°K in a carbonized media of inert gas was developed. In order to remove the air from the space between the external and internal electrodes during heating, several holes, 1.5 mm in diameter, were made in the graphite bushing. The thermocouple's emf vs temperature curve obtained during three consecutive heatings up to temperatures of 3000°K indicated noticeable variations in the emf at temperatures up to 2300 to 2500°K; further heating to 2900 to 3000°K produced no effects. The thermocouple can thus be used for prolonged measurements of temperature in an inert gas media in the range from 2300 to 2500°K. It is also capable of withstanding short periods up to 3000°K. (CFSTI)

11077 A PENNING ION SOURCE FOR MASS SPECTROMETERS. Boehm, H.; Guenther, K. G. (Siemens-Schuckertwerke AG, Nuernberg, Ger.). Vakuum-Tech., 14: 192-3(Oct. 1965). (In German).

The collector current of argon ions and the 0 current of the Penning ion source at optimum electrode geometry were determined as a function of the delayed grid potential. The results showed a dependence of both parameters on the delaying grid potential. Data are given for a mass filter with a Penning ion source developed with these parameter variations taken into consideration. (J.S.R.)

11078 MANIPULATOR BRAKE ASSEMBLY (Engineering Materials). (Lawrence Radiation Lab., Univ. of California, Livermore). (CAPE-1091).

23 drawings.

An air-brake assembly for a Model 8 master-slave manipulator is described. There are 3 locks, one for each x, y, and z motion. Two lights show the indexing motion selected and a third light is used to indicate when the brake may be used. The brake is either released by pushing an index trigger or by changing the selector to the "x" motion. To make the system fail safe, a "normally open" valve is used. (For details, see TID-4100). (M.C.G.)

11079 GAMMA CAMERA: OPTIMIZATION OF THE LIGHT PIPE THICKNESS. Mueller, William C.; Cameron, John R.; Wilson, Charles R. (Univ. of Wisconsin, Madison). 5p. (CONF-650647-3). ORINS. Gmelin, AED-CONF-5-197-2.

From Society of Nuclear Medicine, 12th Annual Meeting, Bal Harbour, Fla.

A gamma camera was constructed. The system includes an eleven-inch diameter by one half-inch thick NaI(Tl) scintillation crystal, a two-inch thick light pipe, and nineteen three-inch diameter photomultiplier tubes arranged in

a close-packed hexagonal array. An attempt was made to determine the light pipe thickness for best mapping of the source locations. To simulate the system the fraction of the total solid angle subtended to each tube in the array from an arbitrary scintillation site in the crystal is determined. Several assumptions were made to simplify the calculations, which are shown. (J.F.P.)

11080 FLOW METER USING NEUTRONS. Inoue, Minoru (to Hitachi, Ltd.). Japanese Patent 1964-14183. July 21, 1964. Filed Dec. 2, 1960.

A flowmeter based on the counting of neutrons moderated in the fluid is proposed. The neutron source emitting fast neutrons and the counter, e.g., a BF_3 counter, for the moderated neutrons are placed some distance apart in the fluid flow and are joined together through their supporting bar. When the fluid does not flow, the area of neutron moderation is not in reach of the BF_3 counter, but with increasing flow rate of the fluid this spherically shaped area moves deeper into the space where the counter is located. The moderated-neutron counter is placed in the direction of fluid flow with respect to the neutron source. The count rate of moderated neutrons becomes larger with increased flow rate, and by measuring the count rate it is possible to obtain an indication of the flow rate. (TCO)

11081 DEVICE FOR TRANSMISSION OF THE PULSES TO THE HIGH VOLTAGE CIRCUIT. Watanabe, Masanori (to Matsushita Electric Ind. Co., Ltd.). Japanese Patent 1964-18499. Aug. 31, 1964. Filed Sept. 5, 1962.

An improved pulse transmitter is proposed, which can send an electric pulse wave having a very short rise-time to a high voltage line with no distortion of the wave shape. The transmitter includes an evacuated hard-glass tube and an electric gun used in the construction of a conventional Brown tube. The gun consists of a filament, cathode, grid electrode, focusing electrode, anode, deflection coil, and electron collector. The negative bias potential applied to the grid electrode cuts off the operation of the transmitter, and the positive pulse wave from the pulse generator passes the accelerated and focused electron beam to the collector electrode according to the pulse shape. The transmitter can send the pulse wave having a rise-time as low as 0.01 μ sec. (NSA of Japan)

11082 NEGATIVE ION GENERATING DEVICE. Suematsu, Shigeru (to Hitachi, Ltd.). Japanese Patent 1964-21420. Sept. 30, 1964. Filed Apr. 5, 1963.

In the proposed device for generating negative ions a space charge is produced at the connection between the accelerating tube and the positive ion source; then a beam of atoms or ions collides with the space charge already produced. When a coil-type hot cathode and a coiled grid-type anode located coaxially inside the cathode are energized, the electrons emitted from the cathode are accumulated in the hollow space of the anode and form a space charge. Atoms or ions, e.g., of hydrogen, in a beam are introduced into the space charge. Collisions result in the generation of negative hydrogen ions. (NSA of Japan)

11083 ION BEAM GENERATOR. Okazaki, Ikio (to Japan Electron Optics Lab. Co., Ltd.). Japanese Patent 1964-25940. Nov. 16, 1964. Filed Aug. 13, 1963.

A structure is proposed for producing an extremely high-intensity, stable ion beam. A chamber having an exhaust pipe is installed between the ionization chamber and the electrode to draw out the ions by high potential. (TCO)

11084 RELAY CIRCUIT USING A RADIATION COUNTER. Kanzaki, Shizuo (to Kobe Kogyo Corp.). Japanese Patent 1964-26654. Nov. 21, 1964. Filed Feb. 24, 1961.

A new electric relay circuit is proposed that uses a radiation counter as the detector. The relay circuit consists of a radiation counter, such as a G-M counter; a wave shaper, such as a monostable multivibrator; a band-pass filter; an a-c amplifier; rectifier; and relay. The relay contact for an alarm is energized or de-energized by the level of signal intensity measured by the radiation detector. Since the relay contact for the alarm is energized also by a signal from the radiation detector, a failure in the relay circuit can be detected automatically. (TCO)

11085 DIGITAL MEASURING APPARATUS UTILIZING A RADIOACTIVE SOURCE AND DETECTOR. Hyde, James L. U. S. Patent 3,223,842. Dec. 14, 1965. Filed Mar. 15, 1962.

A digital measuring apparatus is described for measuring such physical variables as pressure, temperature, or acceleration that can be sensed through a mechanical displacement. The apparatus includes a radioactive source, a radiation shield, a radiation detector, and terminal utilizing means for giving a digital representation of the variable being measured. The radiation shield has an effective aperture area and a displaceable shutter in proximity to the aperture area and controlled in position by the variable to be measured for controlling the rate of radiation particles transmitted through the shield. The flux gradient of the particles emitted from the source is substantially zero through the aperture in the direction of motion of the shutter. The detector provides individual electric pulses representative of the individual radiation particles transmitted through the shield, and output signals comprising a digital representation of the rate of the individual radiation particles transmitted through the shield are developed in response to the individual electric pulses. (B.L.M.)

Radiation Detection

Refer also to abstracts 10724, 10902, 11049, 11058, 11201, 11496, 11527, 11853, and 11976.

11086 (AAEC/TM-299) A LARGE, COAXIAL, LITHIUM-DRIFT GERMANIUM DIODE FOR GAMMA-RAY SPECTROSCOPY. Tavendale, A. J. (Australian Atomic Energy Commission Research Establishment, Lucas Heights). Sept. 1965. 14p. (CONF-650839-1). Dep. mn.

From Conference on Nuclear Physics, Melbourne.

A "single-ended," coaxial, lithium-drift germanium diode with an active volume ~30 cm^3 (1.8 $in.^3$) was fabricated and tested as a high resolution γ-ray spectrometer. Leakage currents at liquid nitrogen temperatures (77°K) were $<1 \times 10^{-10}$ amp up to 1000 v reverse bias. Diode junction capacitance was 42 pF. Resolutions (FWHM) of 4.3, 5.5, and 8.7 kev were obtained on the full-energy peaks from γ-rays at 122-, 1333-, and 2614-kev energy respectively. Intrinsic full-energy peak efficiencies were 8.4, 3.1, and 2.3% at 511-, 1333-, and 1840-kev γ-ray energy respectively for a source-to-detector distance of 10 cm (axial irradiation). γ-ray pulse rise times (10–90% levels) were ~50–100 nsec and pulser rise time was 30 nsec at 1000 v bias. The performance of this large detector at high γ-ray energies was characterized by a high full-energy peak to Compton background ratio; a peak to Compton ratio of 5:1 was measured at 2614-kev γ-ray energy. (auth)

11087 (AE-203) A SCINTILLOMETER ASSEMBLY FOR GEOLOGICAL SURVEY. Dissing, E.; Landstroem, O. (Aktiebolaget Atomenergi, Stockholm (Sweden)). Dec. 1965. 16p. Dep. mn.

An instrument for gamma radiation measurements in connection with geological survey is described. It consists of a scintillation detector with a 5 in. dia × 6 in. sodium iodide crystal and a pulse height analyzer with four independent channels. In field survey work these channels are usually set in fixed positions to record different components of the gamma radiation simultaneously in order to facilitate an identification of the radioactive mineral from which the radiation originates. However, the instrument can also be used for more detailed study of gamma spectra either in the field or in the laboratory. The methods for interpretation of gamma spectra from radioactive ores are briefly reviewed, and a few typical results are given from carborne and air-borne survey. (auth)

11088 (AED-C-28-01) SLOW NEUTRON DETECTORS. Series C. Bibliographies. Jex, H.; Muellner, M. (comp.) (Institut fuer Kernphysik, Universitaet Frankfurt (West Germany)). Mar. 1965. 130p. Dep. mn.

References (332) are given to reports, journals, and patents published from 1955 through 1964. The compilation is divided into 11 subgroups according to types of detectors. NSA reference numbers and information keywords are given for each entry. Nuclear reactions used in slow neutron detection are appended, along with separate author, report number, and subject indexes. (P.C.H.)

11089 (AERE-M-1671) THE RESPONSE OF A MOVING GEIGER PROBE TO DISCRETE SOURCES OF BETA RADIATION. Cook, J. E. (Atomic Energy Research Establishment, Harwell (England)). Nov. 1965. 24p. Dep. BIS $0.80. HMSO 4s.

Recent experiments have shown that the efficiency with which the average person detects contamination on his clothing with a contamination monitor is considerably less than was hitherto supposed. As a further contribution to this problem an investigation is made of the response of a standard instrument when its geiger probe is moved over radioactive sources at different distances and velocities. The results are compared with a simple theory which is applicable if the time constant of the ratemeter is greater than the time during which the moving probe records counts from the source. The peak response is found to be inversely proportional to velocity and not strongly dependent on distance. Detection thresholds in terms of source strength are in the range 0.01 to 0.1 μC. The X1 range, 0–5 counts per second, of the BN110 ratemeter is found to have a dead time of about 25 milliseconds which much reduces response, so much so that with the probe close to the surface being monitored 100% detection of any source becomes impossible for velocities above about 20 centimeters per second. It is concluded that on the X1 range the instrument is unsuitable for contamination monitoring. (auth)

11090 (BNL–9749) THE TRACK-SEGMENT GENERATOR. Strand, R. C. (Brookhaven National Lab., Upton, N. Y.). [nd]. Contract AT-30-2-GEN-16. 27p. (CONF-651039–3). Dep. mn; CFSTI $2.00 cy, $0.50 mn.

From Conference on Programming for Flying Spot Devices, Columbia, N. Y.

The generation of track segments for flying-spot analyzers by means of a rotating-comb histogram technique is described. Operation, performance, strategy, and basic features of the track-segment generator are outlined. (T.F.H.)

11091 (BNWL–122, pp 67-72) RADIATION DOSIMETRY OF ^{137}Cs IN SHEEP EVALUATED WITH THERMOLUMINESCENT DOSIMETERS. McClellan, R. O.; Watson, C. R. (Battelle-Northwest, Richland, Wash. Pacific Northwest Lab.).

A thermoluminescent dosimetry system employing powdered lithium fluoride in Teflon capsules was evaluated and used to measure gamma radiation in vivo. Dose rates of less than 50 mR/day were successfully measured in sheep ingesting 25 μCi ^{137}Cs/day with body burdens around 400 μCi. (auth)

11092 (CLOR–39/D) ALPHA CONTAMINATION LOCATOR WITH JUNCTION RADIATION DETECTOR. Bukowiecki, B. (Centralne Laboratorium Ochrony Radiologicznej, Warsaw (Poland)). 1965. 5p. Dep. mn.

An alpha contamination locator with semiconductor radiation detector is developed. The alpha contamination locator is designed as a small, portable instrument that provides a precise location of alpha contamination. Electronic circuits provide an audible acoustic signal for every alpha particle that loses, within the detector sensitive volume, at least 600 kev of its energy. The instrument works with or without an extension of about 50 cm, according to the conditions of the measurements actually performed. (auth)

11093 (COO–614-34, Sect. IIA) AUTOMATIC RETRIEVAL SPARK CHAMBERS. Bounin, J.; Miller, R. H.; Neumann, M. J. (Chicago Univ., Ill. Inst. for Computer Research). 83p.

A comparison of conventional automatic retrieval chamber systems was made and the advantages of having a computer in the system were discussed. A special setup was used to measure the Michel parameter in μ-meson decay. The setup is described in terms of chamber fabrication techniques, chamber readout, transmission to computer, and computer handling of data. Discussions are also presented on general logical problems with wire chambers, and chamber hardware developments and speculations. (M.O.W.)

11094 (COO–1226-10) DEVELOPMENT OF A HIGH-SENSITIVITY FAST NEUTRON DOSIMETER. Tenth Quarterly Report, August 1, 1965–October 31, 1965. Chase, B. H.; Hickman, J. S.; Swartz, D. L.; Swartz, J. M.; Thurston, M. O. (Phylatron Corp., Columbus, Ohio). Contract AT(11-1)-1226. 10p. Dep. mn. CFSTI $1.00 cy, $0.50 mn.

The design of a silicon-diode dosimeter was completed, and a preliminary badge design was tested. A comparative test of dosimeters was conducted. (D.C.W.)

11095 (CRGP–1224) LARGE-VOLUME COAXIAL GERMANIUM GAMMA-RAY SPECTROMETERS. Malm, H. L.; Fowler, I. L. (Atomic Energy of Canada Ltd., Chalk River (Ontario)). Oct. 1965. 35p. (AECL–2504). AECL $1.00.

Germanium lithium-drift p-i-n diodes for high resolution γ-ray spectroscopy were made with sensitive volumes in the range 16 to 54 cm^3 (1 to 3.3 in.^{3}) using the coaxial method of drift. Details of the construction, mounting, and preparation as spectrometers are given. The shape of the undrifted p-type core was determined by scanning with a collimated γ-ray beam and by copper plating the surface of a sectioned diode. The characteristics as spectrometers, using γ rays of energies in the range 0.1 to 7.5 Mev, are shown. At 122 kev energy, resolutions of 3.0 and 4.4 kev (fwhm) were obtained with diodes of sensitive volumes 23 and 54 cm^3 respectively. A 16 cm^3 volume diode had a resolution of 4.8 kev at 1333 kev γ-ray energy, and a 45 cm^3 diode had resolutions of 6.5 and 19 kev at energies of 1.1 and 5.1 Mev respectively. The diodes were operated at bias voltages in the range 600 to 1500 v. Intrinsic full energy peak efficiencies are shown for different diode sizes over a range of γ-ray energies. For the 54 cm^3 volume diode, these efficiencies are 21 and 8% respectively for γ-ray energies of 0.5 and 1.0 Mev with a source to diode distance of 30 cm. The larger diodes show a greatly enhanced peak/total ratio, and the higher efficiencies make these spectrometers extremely useful in reaction γ ray, γ-γ coincidence, and n,γ studies. (auth)

11096 (EUR–2491.e) CONSTRUCTION AND CALIBRATION OF A PROTON RECOIL TYPE NEUTRON SPECTROMETER. Cappellani, F.; Cecchi, P. F.; Fubini, A. (European Atomic Energy Community, Ispra (Italy). Joint Nuclear Research Center). Nov. 1965. 14p. Dep. mn.

A proton-recoil spectrometer for fast neutrons is described in which methane-filled proportional counters are used. The response function and efficiency of the spectrometer for neutron energies of 0.2 to 2.0 Mev are included. (D.C.W.)

11097 (INR–621/XV/I) SILICONE LITHIUM DRIFTED DETECTORS. Kuchcinski, A. (Institute of Nuclear Research, Warsaw (Poland)). Apr. 1965. 28p.

An investigation of lithium-drifted silicon detectors is summarized. The preparation of the detectors is described, and the performance of the detectors in detection of alpha particles and beta particles is discussed. (D.C.W.)

11098 (IS–1312) INSTRUMENTATION FOR CONTINUOUS AVERAGING OF MAGNETIC SPIN RESONANCE SPECTRA. Torgeson, David R. (Ames Lab., Iowa State Univ. of Science and Tech.). Jan. 1966. Contract W-7405-eng-82. 18p. Dep. mn. CFSTI $1.00 cy, $0.50 mn.

Details are presented for the adaptation of a 400-channel analyzer to be used with a magnetic spin resonance spectrometer for the continuous averaging of wide line spectra. The description includes details of so-called interface circuits between the spectrometer and the analyzer and

between the analyzer and the electromagnet power supply control circuits. Two types of studies made with the spectrometer-analyzer system are also described. (auth)

11099 (JINR-P-2436) DETEKTIROVANIE γ-KVANTOV S POMOSHCH'YU ISROVOI KAMERY I CHERENKOVSKOGO SCHETCHIKA POLNOGO POLGOSHCHENIYA. (γ-Quanta Detecting by Using a Spark Chamber and Total Absorption Cherenkov Counter). Azimov, M. A.; Kolesnik, V. G.; Pantuev, V. S.; Sil'vestrov, L. V.; Khachaturyan, M. N. (Joint Inst. for Nuclear Research, Dubna (USSR). Lab. of High Energy). 1965. 8p. Dep. mn.

A system consisting of a thin spark chamber and a total absorption Cherenkov counter is used to detect γ quanta from the decay of 3- to 5-Bev π^0 mesons. The accuracy of determining the γ energy is ±5%, and the accuracy of determining the γ emission angle is ±0.4°. The spark chamber is triggered from the Cherenkov counter, permitting the efficiency of selecting γ events in the charged pion beam to be improved considerably. (auth)

11100 (JINR-P-2467) VOSPROIZVEDENIE KINEMATICHESKIKH PARAMETROV CHASTITS PO SNIMKAM SLEDOV V TREKOVYKH KAMERAKH S UCHETOM NEODNORODNOSTI MAGNITNOGO POLYA, POTER ENERGII I KULONOVSKOGO RASSEYANIYA. (Reproduction of Kinematical Particle Parameters by Chamber Pictures With Account of Inhomogeneity of Magnetic Field, Energy Losses, and Coulomb Scattering). Vishnevskii, V. F.; Ivanchenko, I. M. (Joint Inst. for Nuclear Research, Dubna (USSR)). 1965. 6p. Dep. mn.

A method is described for computer calculations of kinematical parameters of particles from track measurements on track chamber pictures taking into account the inhomogeneity of the magnetic field, energy losses, and Coulomb scattering. (auth)

11101 (JINR-P-2468) ISSLEDOVANIE VLIYANIYA KHARAKTERISTIK FOTOKAMER NA TOCHNOST VOSSTANOVLENIYA PROSTRANSTVENNOI KARTINY REGISTRIRUEMYKH IMI SOBYTII. (Investigation of Influence of Camera Properties on Accuracy of Spatial Reconstruction of Recorded Events). Ivanov, V. G. (Joint Inst. for Nuclear Research, Dubna (USSR). Lab. of Nuclear Problems). 1965. 8p. Dep. mn.

Methods for determining the properties of cameras and their influence on the accuracy of calculating the spatial coordinates are considered. It is shown that the application, for stereophotography, of cameras with identical properties and small inaccuracies essentially simplifies the geometric reconstruction of events recorded in bubble chambers. Selection criteria of cameras are given to carry out accurate photogrammetrical investigations. (auth)

11102 (JINR-P-2487) PRIMENENIE ELEKTROFOTOGRAFII DLYA IZMERENIYA CHUVSTVITEL'NOI OBLASTI GERMANIEVYKH p-i-n-DETEKTOROV. (Application of Electrophotography for Measurements of Sensitive Region of Germanium p-i-n Detectors). Antonov, A. S.; Yuskeselieva, L. G. (Joint Inst. for Nuclear Research, Dubna (USSR). Lab. of Nuclear Problems). 1965. 10p. Dep. mn.

The width of the sensitive region in germanium pin detectors is determined by developing the p–n-junction with dry and liquid electrophotographic developers. (auth)

11103 (JINR-P-2489) O VYYAVLENII DEFEKTOV V KREMNIEVYKH p-i-n-DETEKTORAKH YADERNYKH IZLUCHENII. (On Revealing of Defects in Silicon p-i-n Detectors). Yuskeselieva, L. G. (Joint Inst. for Nuclear Research, Dubna (USSR). Lab. of Nuclear Problems). 1965. 14p. Dep. mn.

Defects in p–n junction of silicon p–i–n detectors are investigated by means of electrophotography and electrochemical depositing of copper. The study of the defects is associated with electric characteristics of detectors. (auth)

11104 (LNF-65/33) RISOLUZIONI RAGGIUNGIBILI CON ALCUNI TRC A DEFLESSIONE ELETTROSTATICA E LORO UTILIZZAZIONE IN UN DISPOSITIVO DI LETTURA DI FOTOGRAMMI DI CAMERE A SCINTILLA MONOGAP. (Resolution Obtainable with some TRC'S with Electrostatic Deflection and their Utilization in a Device for Scanning Photograms of Monogap Scintillation Chambers. Note No. 290). Avaltroni, M.; Pandarese, F. (Laboratori Nazionali di Frascati, Comitato Nazionale per l'Energia Nucleare (Italy)). Sept. 25, 1965. 20p. Dep. mn.

The preliminary work on the design and construction of some parts of a device for the automatic analysis of spark chamber photographs is reported. The resolution obtainable with a given type of cathode-ray tube is investigated with a quantitative determination of the effect of some factors such as contrast of the photograph and granularity of the phosphor of the cathode-ray tube. A simple device for the analysis of monogap chamber photographs is also described. (J.S.R.)

11105 (NAA-SR-Memo-11132) DETERMINATION OF PAIRED-PULSE RESOLUTION OF RANDOM COUNTING SYSTEMS. Beller, L. S.; Farrar IV, H. (Atomics International, Canoga Park, Calif.). Mar. 8, 1965. Contract AT-11-1-GEN-8. 116p. Dep. mn. CFSTI $4.00 cy, $0.75 mn.

The precise measurement of the paired-pulse resolution of random counting systems is important if the uncertainty in measurement of this time is not to be the limiting factor in experimental precision. A discussion of the sources of finite resolution and four methods of measurement of paired-pulse resolution is included. Two computer codes written for data analysis are described. (auth)

11106 (NP-15786) ISSLEDOVANIE EFFEKTIVNOSTI REGISTRATSII NEITRONOV S IMPUL'SOM NESKOL'KO Bev/s STSINTILLYATSIONNYMI SCHETCHIKAMI. (Investigation of Scintillation Counter Effectiveness in Registering Neutrons With Several Bev Energy). Report No. 372. Galaktionov, Yu. V.; Landsberg, L. G.; Lyubimov, V. A. (Gosudarstvennyi Komitet po Ispol'zovaniyu Atomnoi Energii SSSR, Moscow. Institut Teoreticheskoi i Eksperimental'noi Fiziki). 1965. 8p. Dep. mn.

The efficiency of Bev-neutron registration by scintillation counters was investigated. The detectors with efficiency of 0.5 to 0.7 Bev-neutrons were described. (auth)

11107 (RFP-462) THE ROCKY FLATS BODY COUNTER. Johnson, V. P. (Rocky Flats Div., Dow Chemical Co., Golden, Colo.). Nov. 12, 1965. Contract AT(29-1)-1106. 11p. Dep. mn. CFSTI $1.00 cy, $0.50 mn.

A body counting facility was completed for the detection of plutonium and uranium in humans. The facility includes two showers, a steel shield 8 by 9 by 8 feet high inside, and a crystal spectrometer. (auth)

11108 (RFP-637) A LARGE AREA GAS PROPORTIONAL DETECTOR FOR LOW ENERGY PHOTONS. Tyree, W. H. (Rocky Flats Div., Dow Chemical Co., Golden, Colo.). Jan. 6, 1966. Contract AT(29-1)-1106. 16p. Dep. mn. CFSTI $1.00 cy, $0.50 mn.

A large-area gas proportional detector developed for use in a whole-body counter is described. The photons associated with the alpha decay of ^{239}Pu are detected. A comparison of the sensitivity of the gas proportional detector and of an NaI(Tl) thin-crystal detector is included. (D.C.W.)

11109 (SGAE-E-5/1965) UNIVIBRATOR AS A TIME ELEMENT IN A MEDIUM FAST COINCIDENCE CIRCUIT. Halling, H.; May, F. (Oesterreichische Studiengesellschaft fuer Atomenergie G.m.b.H., Siebersdorf. Elektronikinstitut). 1965. 17p. Dep. mn.

In a medium fast coincidence circuit (resolution time variable from 100 nsec–11 μsec) a univibrator is used as timing element (delay and determination of resolution time). The univibrator is designed to have a constant but adjustable output pulse width. (auth)

11110 (STI/DOC/10/46) IN-PILE DOSIMETRY. Report of a Panel Held in Vienna, 13–17 July 1964. Technical Reports Series No. 46. (International Atomic Energy Agency, Vienna (Austria)). June 1965. 112p. (CONF-621). IAEA: $2.50; S 52.50; 15/-stg; F Fr 10.-; DM 8,-.

Separate abstracts are prepared for 9 of the 11 papers presented. The remaining 2 papers were previously abstracted in NSA as 18: 33879 and 19: 14463. Thirteen papers were included in summary form and were not abstracted for NSA. (J.F.P.)

For abstracts of individual papers see: 11144–11152.

11111 (TID-22550) DESIGN OF A SCANNING TEMPLATE FOR ASSOCIATING Λ^0 DECAYS WITH Ξ^0 PRODUCTION VERTICES. Technical Report No. 522. Adelman, Saul Joseph; Kehoe, Brandt (Maryland Univ., College Park. Dept. of Physics and Astronomy); Nov. 1965. Contract AT(40-1)-2504. 7p. Dep. mn. CFSTI $1.00 cy, $0.50 mn.

In order to study the events $K^- + p \rightarrow \Xi^0 +$ others, $\Xi^0 \rightarrow \Lambda^0 + \pi^0$ and $\Lambda^0 \rightarrow p + \pi^-$, a scanning template was designed to aid the identification of these events on the scanning table. This would reduce the number of accidental associations between the beam interactions and Λ^0 decays in the chamber. The template design was based upon the results of a Monte Carlo computer program. (J.F.P.)

11112 (TID-22553) A BINARY-CODED DIGITIZED HODOSCOPE. Technical Report No. 514. Beall, E. F. (Maryland Univ., College Park. Dept. of Physics and Astronomy). Nov. 1965. Contract AT(40-1)-2504. 12p. Dep. mn. CFSTI $1.00 cy, $0.50 mn.

A binary hodoscope was constructed. The design of this hodoscope is described, and the results of tests show that of the light injected into one end of a strip, typically 35% reaches each PM photocathode to which the strip is optically coupled. The pulse height from a wrong tube, that is, one which is not optically coupled to the strip under test, is typically 5% of the pulse height from a right tube. Based on the data it is estimated that a minimum-ionizing particle which traverses a strip along the $\frac{3}{8}$-in. direction should cause on the order of 500 photons to impinge upon each photocathode to which the strip is optically connected. This would be more than adequate to make the device function. (J.F.P.)

11113 (UCRL-16471) ISO—A FORTRAN PROGRAM FOR UTILIZING THE STRONG-FOCUSING PRINCIPLE IN BETA-RAY SPECTROMETER DESIGN. Owens, Herman (Lawrence Radiation Lab., Univ. of California, Berkeley). Oct. 21, 1965. Contract W-7405-eng-48. 9p. Dep. mn. CFSTI $1.00 cy, $0.50 mn.

An IBM FORTRAN II code to calculate beta-ray spectrometer characteristics of aberration, dispersion, transmission, and resolution, using azimuthally varying magnetic fields, is described. (auth)

11114 (UR-875-66) SPARK CHAMBER TESTS OF MULTIPLE PARTICLE DETECTION EFFICIENCY. Ryan, James W. (Rochester Univ., N. Y. Dept. of Physics and Astronomy). Dec. 10, 1964. Contract AT(30-1)-875. 17p. Dep. mn. CFSTI $1.00 cy, $0.50 mn.

Measurements of efficiency for detecting multiple particles were made on two different types of spark chambers. Using a non-conventional chamber incorporating a 0.015-inch nylon sheet between conducting electrodes, the efficiency per gap for particle detection was found to be nearly 100% for up to at least 12 particles traversing the chamber within the sensitive time. Similar tests performed on a conventional chamber indicate that the efficiency for detecting a particle in the presence of several others is quite strongly dependent upon the relative number of residual electrons. (M.O.W.)

11115 USE OF SURFACE-BARRIER SILICON DETECTORS FOR MEASURING FAST PARTICLE SPECTRA. Bogdanov, G. F.; Maksimenko, B. P. At. Energ. (USSR), 19: 449(Nov. 1965). (In Russian).

Silicon surface-barrier detectors were used to measure the spectra of plasma ions and charge-exchange neutrals with energies of 10 to 200 kev. Calibration of the detectors using 28- to 70-kev protons indicated their response was linear. A sample spectrum of atoms and molecules from the Ogra device is presented and discussed. (M.J.T.)

11116 DETERMINATION OF SPECTRAL CHARACTERISTICS OF ISOTOPE NEUTRON SOURCES BY MEANS OF PAIRED SCINTILLATION CRYSTALS OF THE TYPE LiI(Eu). Gruzin, P. L.; Kichev, A. Z.; Minaev, V. M.; Samosadnyi, V. T.; Hsi, Chang-sung. At. Energ. (USSR), 19: 454-6(Nov. 1965). (In Russian).

A method is considered for subtracting the gamma background in measurements of spectra from neutron sources. Two paired LiI(Eu) crystals were used, one enriched 90% in ^{6}Li and the other 99.4% in ^{7}Li. The response of the two crystals to gamma radiation was assumed equal; the efficiency of the ^{6}Li-enriched crystal for fast neutrons was 150 times greater than that of the ^{7}Li-enriched crystal, so it could be assumed the latter was practically insensitive to fast neutrons. The neutron intensity at a given energy was thus the difference in the pulse heights from the two crystals. Differential neutron spectra measured for Po–Be, Pu–Be, and Po–B sources are presented and discussed. (M.J.T.)

11117 A PULSE TRANSFORMER WITH TWO SEPARATE CORES FOR TIME-TO-PULSE-HEIGHT CONVERSION. Ibel, K.; Stanek, F. W. (Technische Hochschule, Munich). Atomkernenergie, 11: 30-4(Jan.-Feb. 1966). (In German).

A very simple time-to-pulse height converter is described; it is a special pulse transformer consisting of two separate ferrox-cube-cores with three windings. The linear conversion-range is about 300 nsec, a resolution of 15 nsec can be obtained. Test measurements with generator pulses and with two scintillation detectors were performed. This TPC is used for time of flight measurements of recoil-atoms at alpha decay. The obtained resolution was sufficient for this purpose. (auth)

11118 ON THE INFLUENCE OF TEMPERATURE ON THE SCINTILLATIONS OF NaI(Tl). Brunner, G. (Institut fuer Angewandte Radioaktivitaet, Leipzig). Atomkernenergie, 11: 59-64(Jan.-Feb. 1966). (In German).

As a consequence of a corresponding temperature dependence of the scintillation decay τ_S the pulse height U_{max} at a clipping time of ≈ 0.8 μs and the light efficiency Q' of the examined NaI(Tl) scintillators show contradictory behavior: a positive temperature coefficient of +0.4%/°C was found for U_{max}, but a coefficient of about –0.6%/°C results for Q'. The temperature dependence of NaI(Tl) thoroughly agrees with a formula of Birks for the light efficiency. The formula was first set up from experimental results concerning the dependence on the activator concentration and the specific energy loss, but it is able to explain the temperature dependence in agreement with the assumption that only the fluorescence quantum efficiency essentially is dependent on the temperature. The experiments agree with the conception that the Tl^+ luminescence center consists of three excited levels i.e., the metastable level, the fluorescence level at an energy W_f above it, and a quenching level at an energy W_i above the fluorescence level, if the level spacings are $W_f = 0.15 \pm 0.05$ ev and $W_i = 0.10 \pm 0.02$ ev. In connection with this the fluorescence quantum efficiency is $q_{0y} = 0.5 \pm 0.1$. According to the experiments no reason was found for assuming a maximum in the light efficiency for normally activated NaI near room temperature and a connected temperature dependence of the exciton transfer from the lattice to the Tl^+ center. (auth)

11119 ON THE SUITABILITY OF NEUTRON SENSITIVE FOILS FOR THE DOSIMETRY OF THERMAL NEUTRONS BY MEANS OF POCKET ION CHAMBERS. Adler, P.; Matthe, P.; Bock, L. (Institut fuer Angewandte Radioaktivitaet, Leipzig). Atomkernenergie, 11: 65-70 (Jan.-Feb. 1966). (In German).

For the routine protection of the persons which are endangered by thermal-neutron radiation dosimeters were developed by assembly of neutron sensitive foils in commercial pocket ion chambers. Some investigations on metallic foils of cadmium, rhodium, and gold, methyl cellulose foils with amorphous boron, boron carbide of enriched ^{10}B, foils made of polytriethylene glycol boric acid ester and plast foils with lithium tetraborate are reported. The maximum neutron sensitivity was attained by use of lithium tetraborate foils in the pocket chambers.

Also it is possible to construct dosimeters that register integral dose of γ- and neutron radiation with identical sensitivity as well as double chambers. (auth)

11120 CORRUGATED-PLATE SPARK COUNTERS. Eichholz, G. G.; Templeton, W. M. (Georgia Inst. of Tech., Atlanta). Can. J. Phys., 44: 229-35(Jan. 1966).

Stacks of corrugated plates with symmetrical parallel ridges were employed as spark counters for the detection of alpha particles and neutrons. The counters were operated with various ridge pitches and plate spacings and with different counter gases. Such counters provide simple, rugged detectors with clearly localized corona discharges and are free from microphonics. When the grooves in the plates are filled with a hydrogenous or boron-containing material, such counters function as low-sensitivity neutron detectors with negligible sensitivity to gamma radiation. Such detectors are promising for measurements of reactor neutrons. (auth)

11121 CONTRIBUTION TO THE STUDY OF THE SENSITIVITY AND THE SENSITIZATION OF PHOTOGRAPHIC EMULSIONS. Rasigni, Georges (Faculte des Sciences, Marseille). Compt. Rend., 261: 2868-71 (Oct. 11, 1965). (In French).

It is shown that the study of the optical absorption of certain metals (Ag, Au, and Cu) in thin foils can yield new data for the interpretation of the fundamental phenomena of photography. (tr-auth)

11122 HIGHLY EFFECTIVE METHOD OF COUNTING ^{3}H. Pertsev, A. N.; Pisarevskii, A. N.; Soshin, L. D. (Belorussian State Univ., USSR). Dokl. Akad. Nauk Belorussk. SSR, 9: 509-10(Aug. 1965). (In Russian).

Tests were carried out to improve the efficiency of the scintillation method for counting the beta particles emitted by tritium. A 13-cascade photomultiplier with electrostatic screening was used. Background noise was 10 to 15 cpm under proper conditions. The apparatus permitted single electron pulses to be recorded. The recording efficiency was 85%, assuming that there is no deviation from the Fermi distribution in the low-energy range. (TCO)

11123 COMBINED PROTON SPECTROMETER FOR SPACE STUDIES. Savenko, I. A.; Savun, O. I.; Shavrin, P. I.; Yakovlev, B. M. (Moscow State Univ.). Geomagn. Aeronomy (USSR) (Engl. Transl.), 5: 420-2(1965).

Translated from Geomagn. Aeronomiya, 3: 546-9(1965).

A four-channel proton spectrometer, designed to measure the proton spectrum of the radiation belts of the earth in the energy range from 3 to 100 Mev in the presence of intense electron currents, is described. A silicon diffusion charged-particle detector is used as a dE/dx discriminator. The detector of E is a scintillation counter with a CsI crystal, surrounded by a plastic anticoincidence hood. (auth)

11124 INSTRUMENT FOR RECORDING PROTONS WITH E = 3 TO 14 Mev, α PARTICLES, AND NUCLEI OF Z > 2. Savenko, I. A.; Savun, O. I.; Yurovskii, A. V. (Moscow State Univ.). Geomagn. Aeronomy (USSR) (Engl. Transl.), 5: 423-5(1965).

Translated from Geomagn. Aeronomiya, 3: 550-3(1965).

An instrument is described in which surface-barrier type silicon detectors are used to record protons, α particles, and nuclei with Z > 2. Protons are recorded in three ranges: 0.3–8, 7–11, and 11–14 Mev. The advantages and possibilities of this method of recording particles without using amplitude analysis and pulse selecting logic circuits are described. (auth)

11125 METHOD OF DETERMINING THE DEAD TIME OF NUCLEAR RADIATION COUNTERS. Kapustin, I. N. (Polar Geophysical Inst., Academy of Sciences, USSR). Geomagn. Aeronomy (USSR) (Engl. Transl.), 5: 463-4 (1965).

Translated from Geomagn. Aeronomiya, 3: 594-5(1965).

A brief description is given of a highly accurate method of measuring the dead time of nuclear radiation counters while they are operating, which differs favorably from the two-source oscillographic methods. The circuit is illustrated. (L.B.S.)

11126 SEMI-CONDUCTOR DETECTORS OF NUCLEAR RADIATION. Coche, A. (Centre of Nuclear Research, Strasbourg). Ind. At., 9: 61-9(1965). (In French).

The principal characteristics of diodes with a n-p linkage and with surface barriers and their essential uses are examined. Next the principle of the method is given for compensating a material of the P type by the migration of lithium, and lastly the properties of n-i-p diodes of silicon and of germanium are studied, as well as their applications, with special attention to gamma spectrometry. (auth)

11127 CALCULATION OF THE GAMMA-RAY DETECTION EFFICIENCY OF ANNULAR AND WELL-TYPE SODIUM IODIDE CRYSTALS. Mishra, U. C.; Brar, S. S.; Gustafson, P. F. (Argonne National Lab., Ill.). Int. J. Appl. Radiat. Isotop., 16: 697-704(Dec. 1965).

Calculations of the detection efficiency of annular and well-type sodium iodide scintillation crystals were made for some of the commercially available sizes in the energy range from 0.1 to 6 Mev. The figures reported were obtained from geometrical considerations using values of mass absorption coefficients available in the literature. The values for 6 to 100 Mev can be estimated from the values reported by the method described. For annular crystals, calculations were made for different outer dimensions with a fixed diameter of the annulus. The results indicated the effects of outer diameter and length of the annular ring on the efficiency in various energy regions and thus are helpful in selecting a suitable annular crystal for use with a given central detector. For well-type crystals, the effects of well dimensions for a given outer geometry and source position inside the well are given. The effect of source position inside the well for a crystal of fixed dimensions is also discussed. All the calculations were made for a point source on the axis of the crystal using either 19-point of 25-point Weddle Rule for numerical integrations and an IBM-1620 computer for calculations. Where possible, results were compared with those obtained by other investigations. (auth)

11128 A LIQUID SCINTILLATION DETECTOR FOR EVALUATING PHOTOTUBES AND DETERMINING GAMMA-RAY ACTIVITIES. Meadows, H. L.; Ziemer, P. L.; Christian, J. E.; Kessler, W. V. (Purdue Univ., Lafayette, Ind.). Int. J. Appl. Radiat. Isotop., 16: 711-16(Dec. 1965).

The design and operating characteristics of a liquid scintillation test tank for evaluating large photomultiplier tubes are described. The detector tank was a 16-in.-dia by 6.5-in.-deep cylinder filled with PPO and POPOP in toluene and mounted with a 16-in. photomultiplier tube. The half resolution of the ^{137}Cs Compton "peak" for the system was 29.9%. Counting sensitivity for typical γ emitters were 62 pC/ml for ^{137}Cs, 27 pC/ml for ^{60}Co, and 11 pC/ml for ^{65}Zn based a 5-min count of 0.25 liter samples and a 1% counting error. Detector response to a collimated photon beam was found to be uniform over the surface of the detector tank, falling off only at the edges of the tank by 9.5%. Counting efficiencies up to 23.2% were obtained for a point source of ^{137}Cs. This type of detector is useful in testing individual 16-in. phototubes of the type used in whole-body counters. Such a "test tank" permits individual focusing of the tube, noise level determination, determination of resolution, and determination of uniformity of photocathode response prior to the installation of the tube in a whole-body counting facility. In addition, the test tank system itself may be used as a sensitive γ-detection system. (auth)

11129 SCINTILLATION PROPERTIES OF POLYPHENYLS. Matveeva, E. N., Medvedev, M. N.; Rubina, O. G.; Shafranov, M. D. (Joint Inst. for Nuclear Research, Dubna, USSR). Izv. Akad. Nauk SSSR, Ser. Fiz., 29: 1417-18(Aug. 1965). (In Russian).

The relative intensities of the scintillations initiated by ^{60}Co gamma rays in solutions of polyphenyls in polystyrene, toluene and phenylcyclohexane. The polyphenyls investigated were: diphenyl, n-terphenyl, n,n′-quaterphenyl, and pentaphenyl. The scintillation intensity increased with concentration at low concentrations, but this effect reached

a saturation; the maximum scintillation amplitude of diphenyl and terphenyl was reached at concentrations of 0.05 and 2%, respectively, and increasing the concentration even to 5% did not further increase the intensity. At concentrations up to 0.05% the scintillation intensity increased linearly with the number of phenyl rings in the molecule. The intensity of the scintillations was approximately the same in all three solvents. (ATD)

11130 SCINTILLATIONS AND ENERGY TRANSFER IN ARGON–NITROGEN MIXTURES. Schultz, Harvey A. (Argonne National Lab., Ill.). J. Chem. Phys., 44: 377-84 (Jan. 1, 1966).

Pulse-height measurements were made on scintillations produced by the complete stopping of alpha particles in gaseous argon, nitrogen, and argon–nitrogen mixtures. The results are correlated with the published results of spectrographic studies to derive information about energy transfer in collisions among Ar and N_2 molecules. The optical system responds to light within the spectral range 2200–6000 Å. Total pressures varied from 3.5 to 6 atm. It was observed that the pulse height is greatest for pure argon. As nitrogen is added, the pulse height decreases, then increases, and finally decreases again. From this behavior and the effect of total pressure, it is concluded that the detectable light consists of three components: (1) that emitted by argon excited directly; (2) that emitted by a nitrogen state, probably C $^3\Pi_u$, excited by energy transfer from an argon state that does not emit in the detection range, apparently the lower metastable state, (3) that emitted by nitrogen excited directly. The states that emit components (1) and (2) are quenched by nitrogen in the ground state. For three pairs of competing processes, one pair associated with (1) and two with (2), values of the product (lifetime) × (cross section) × (relative velocity) were obtained by fitting kinetic equations to the pulse-height data. The breakdown of the products into individual factors is discussed. (auth)

11131 EFFECTIVE CADMIUM CUT-OFF ENERGIES IN CYLINDRICAL GEOMETRY FOR FISSILE AND 1/V DETECTORS. Maunders, E. J. (Atomic Energy Establishment, Winfrith, Eng.). J. Nucl. Energy: Pt. A and B, 19: 959-69(Dec. 1965). (AEEW-R-403).

The importance of geometry in detector-filter arrangements used for integral neutron spectrum measurements is discussed, and cadmium transmission functions are presented for a number of detectors ranging from cylinders of 0.040 in. o.d. to slabs of finite thickness and infinite extent, with close-fitting filters of thickness 0.030, 0.040, and 0.050 in. The transmission function as defined is dependent on the physical size of the detector, and the importance of this consideration is demonstrated. In addition the transmission functions are used to determine the effective cadmium cut-off energies for ^{240}Pu, ^{235}U, ^{233}U, and 1/V detectors. (auth)

11132 COSMIC-RAY CONTRIBUTION TO THE BACKGROUND OF NaI SCINTILLATION SPECTROMETERS. Tanaka, Eiichi; Itoh, Susumu; Hiramoto, Toshiyuki; Iinuma, Takeshi A. (National Inst. of Radiological Sciences, Chiba, Japan). Jap. J. Appl. Phys., 4: 785-92(Oct. 1965).

The cosmic-ray contribution to the background of a 3-in. by 3-in. NaI detector in an iron room was studied by coincidence technique with a 4π plastic scintillator covering former detector. The NaI detector was surrounded by various materials inside the 4π guard detector in order to find the effect of the surrounding material. The observed counting rate due to the cosmic-ray component was about 19% of the total background in 0.1–0.4 Mev and 31% in 0.6–0.9 Mev when the NaI detector was surrounded by 5 cm lead. The cosmic-ray contribution did not critically depend upon the atomic number of the surroundings in the energy range of 0.6–0.9 Mev and in the annihilation peak but it decreased rapidly with increasing atomic number in 0.1–0.4 Mev. (auth)

11133 PERFORMANCE OF AN X-RAY SPECTRO-ANALYZER USING ^{147}Pm BETA-RAY SOURCE. Tanemura, Takashi (Rigaku Denki Co., Tokyo). Jap. J. Appl. Phys., 5: 51-8(Jan. 1966).

A high efficiency x-ray spectroanalyzer is described which is equipped with ^{147}Pm β-ray source and a Xe-CH_4 filled proportional counter. Unwanted scattered β-rays, were prevented from entering the counter by placing a 60 mg/cm^2 beryllium foil in front of the counter window. This allowed a geometry of much higher efficiency to be realized than that of an oridnary apparatus in which scattered β-rays are deflected away by a magnet. Thus K x rays above 10^4 counts/sec were able to be obtained by a 100 millicurie ^{147}Pm source for the elements from Cr to Zn. With this new apparatus, the intensity of K x rays and the intensity ratio background/K x rays were observed for Cr, Fe, Ni and Mo using a ^{147}Pm β-ray source on the one hand and using a ^{147}Pm β-excited x-ray source on the other. The comparison leads to the conclusion that the former is superior for the analyses of these elements except for low concentration Mo in a matrix of high atomic number. (auth)

11134 IMPROVEMENTS IN APPLIED GAMMA-RAY SPECTROMETRY BY GERMANIUM SEMI-CONDUCTOR DETECTOR. Brune, D.; Dubois, J.; Hellstroem, S. (Aktiebolaget Atomenergi Studsvik, Sweden). Nukleonik, 7: 484-8(Oct. 1965).

A germanium semiconductor detector was used in the investigation in four cases of applied gamma-ray spectrometry. In one case the weak activity contribution of ^{134}Cs to ^{137}Cs standard sources was determined. The second case concerns the determination of ^{42}K in samples of biological origin containing strong ^{24}Na activities. In the third case the ^{94}Nb and ^{95}Nb activities from neutron irradiated niobium foils used in the dosimetry of high neutron fluxes with long exposure times were completely resolved, and it was possible to determine the ratio of the two activities with a high degree of accuracy. Finally, a ^{95}Zr–^{95}Nb source was analyzed in a similar way with respect to its radiochemical composition. The resolution obtained also made possible a determination of the branching ratio of the two gamma-transitions in ^{95}Zr and the energies of the gamma-transitions of both nuclides. (auth)

11135 DEPOSITION OF ENERGY BY NEUTRONS IN SPHERICAL CAVITIES. Caswell, Randall S. (National Bureau of Standards, Washington, D. C.). Radiat. Res., 27: 92-107(Jan. 1966).

A theoretical description of the interaction of neutrons with a spherical cavity was developed in terms of four types of recoil particle interaction with the cavity. Energy loss distributions are calculated for polyethylene–ethylene and tissue cavities and are found to agree with experimental measurements within the probable uncertainty of these measurements. Conditions for optimum use of proportional counter cavity dosimeters and the interpretation of measurements made with these instruments are discussed. (auth)

11136 CERTAIN FACTORS THAT INFLUENCE THE RESPONSE OF PHOTOGRAPHIC DOSIMETERS FOR ROENTGEN AND GAMMA RAYS. Ladu, M.; Ramacciotti, D. (Univ., Camerino, Italy). Rendic. Ist. Sci. Univ. Camerino, 5: 226-32(1964).

The effects of fading, time and temperature of development, and the dose rate were studied in photographic dosimeters. It was found that the fading effect is negligible up to 5 R doses, even for 10 weeks of delay between the end of exposure and the development. The time and temperature of development affect the response of the dosimeter, which is correct only if these factors are unvaried. The dose rates between 500 mR/h and 10 R/h did not influence the response up to 10 R dose. (Excerpta Med.)

11137 GAMMA-RAY PULSE DOSIMETER. Furuta, Yutaka; Kinbara, Seturo (Japan Atomic Energy Research Inst., Tokyo). Rev. Sci. Instrum., 37: 176-80(Feb. 1966).

A gamma dosimeter, which has a response expressible in roentgens and high sensitivity with a small active volume, is described. The major parts of this dosimeter (gamma pulse dosimeter) are a scintillation counter using an organic scintillator and an electronic integrator, with special care to reduce the counting loss. This dosimeter is sensitive to x or gamma rays with energies above 50 kev, and has an air equivalent response for energies above

200 kev with maximum response at 80 kev (+14%). A linear temperature dependence (0.5%/°C) is obtained under 40°C. (auth)

11138 PULSE HEIGHT DEFECT AND ENERGY DISPERSION IN SEMICONDUCTOR DETECTORS. Haines, Eldon L.; Whitehead, A. Bruce (California Inst. of Tech., Pasadena). Rev. Sci. Instrum., 37: 190-4(Feb. 1966).

The contributions of the atomic (screened Coulombic) scattering process to the pulse height defect and energy dispersion observed when heavy ions expend their energies in semiconductor detectors were calculated. Atomic scattering appears to account qualitatively for the pulse height defect observed for most heavy ions in both silicon and germanium detectors. Atomic scattering also contributes substantially to the energy dispersion. (auth)

11139 HIGH EFFICIENCY SOLID STATE NEUTRON TELESCOPE FOR 15–35 Mev NEUTRONS. Flynn, E. R. (Los Alamos Scientific Lab., N. Mex.); Bryant, H. C. Rev. Sci. Instrum., 37: 215-23(Feb. 1966). (LA-DC-6929).

High detection efficiency for a neutron telescope spectrometer is achieved without the usual sacrifice in energy resolution by replacing the standard radiator by a series of radiators, each of which is backed by a silicon transmission detector. By adding the pulses from the transmission detectors, with appropriate gains, to the pulse from the final thick detector, in which the proton recoil stops, a signal is produced which is proportional to the energy of the proton recoil, with an energy uncertainty of one-half the energy lost by the proton in a single radiator. Thus the energy resolution is determined, for small recoil angles, by the thickness of a single radiator, whereas the detection efficiency is determined by the sum of the radiator thicknesses. Details of operation, efficiency calculation, data analysis, and several spectra demonstrating the performance are discussed. Possible extensions and improvements of the system are considered. (auth)

11140 RADIOPHOTO-LUMINESCENCE DOSIMETRY. Kiefer, H.; Maushart, R. (Kernforschszentrum, Karlsruhe, Ger.). Roentgen Bl., 18: 49-53(1965).

Photoluminescent dosimetry with the aid of silveractivated metaphosphate glasses is especially suitable for the control of personnel doses in nuclear technology. For control in x-ray installations, it can be used wherever the main share of the radiation energy is above 35 kev. In the case of low energies, it is necessary to calibrate each time otherwise only comparative measurements can be carried out with low energy radiations. Of special interest for radiologists is the glass dosimeter, because in vivo dosimetry is possible with rods of 6 mm length and 1 mm diameter. (Excerpta Med.)

11141 VACUUM AND CRYOGENIC ASSOCIATED TECHNIQUES. APPLICATION TO LARGE BUBBLE CHAMBERS. Florent, R. (CEN, Saclay, France). Vide, 20: 371-5(Sept.-Oct. 1965). (In French).

Vacuum and cryogenic techniques are fundamental in the engineering of hydrogen bubble chambers which are basic apparatus to visualize tracks of elementary particles. Volumes of several hundred liters of liquid hydrogen must be kept in equilibrium state with temperature gradients below 0.05°C and minimum losses. Refrigeration equipment supplies several kilowatts of cold. Multilayer insulation, new retrodirective material for optics, superconducting alloys open the way to giant bubble chambers containing 40 or 50 cubic meters of liquid hydrogen. Such instruments will play a leading part in nuclear physics. (auth)

11142 A NEW HIGH VOLTAGE POWER SUPPLY FOR STREAMER CHAMBERS. Rudenko, N. S. (Tomsk Polytechnic Inst., USSR). Zh. Eksp. Teor. Fiz., 49: 1394-8 (Nov. 1965). (In Russian).

Results of theoretical calculations and experiments are presented that were carried out with the aim of obtaining bright and narrow charged-particle tracks in a streamer chamber by applying a number of pulses of alternating polarity. Tracks are obtained which are almost of the same size and are identical with respect to the glowing centers (δ = 1 to 2 mm) along the field direction as well as perpendicular to it. The experimental results are in satisfactory agreement with the calculations. It is shown that the new high voltage power supply yields high quality tracks more consistently than when single high voltage pulses are imposed on the chamber plates. (auth)

11143 THE MICHIGAN STATE UNIVERSITY IRON-FREE DOUBLE FOCUSING BETA-RAY SPECTROMETER [Thesis]. Velinsky, Libor Jiri. East Lansing, Mich., Michigan State Univ., 1965. 258p.

A 30-centimeter-radius iron-free $\pi\sqrt{2}$ beta-ray spectrometer using the Moussa focusing coil configuration and some features of the Vanderbilt University instrument was designed and constructed. The design, construction, and testing of the machine are discussed in detail. With stable environment a $\pm 2 : 10^6$ short range and a $\pm 5 : 10^5$ long range stability was achieved. To test the performance of the instrument, the internal conversion spectrum of ^{137m}Ba was examined with 0.047% resolution. The relative line intensities obtained were: K : L(I) : L(II) : L(III) : M(I) : M(II,III) : M(IV,V) = (1 ± 0.04) : (0.140 ± 0.007) : (0.0207 ± 0.0046) : (0.0171 ± 0.0041) : (0.0233 ± 0.0030) : 0.0145 ± 0.0020) : (0.0047 ± 0.0016). The K and L shell results are in agreement with those of Geiger et al. The M shell results are new. The internal conversion spectrum of ^{210}Bi was obtained with 0.18% resolution. The relative line intensities are: L(I) : L(II) : L(III) : M(I) : M(II) : M(III) : N(I) : N(II) : N(III) : N(IV−VII) + O(I) + P(I) = (1 ± 0.034) : (0.111 ± 0.007) : (0.0094 ± 0.0028) : (0.229 ± 0.007) : (0.023 ± 0.003) : (0.0029 ± 0.0022) : (0.0597 ± 0.0038) : (0.0069 ± 0.0011) : (0.0012 ± 0.0005) : (0.015 ± 0.003). The intensity ratios in the L shell and the M(I)/M(II) ratio agree with theory for pure M-1 radiation. In both experiments the M shell line intensities fall considerably below Rose's calculated values. The discrepancies are consistent and agree with measurements of Bäckström et al., for ^{199}Hg. (Dissertation Abstr.).

11144 REPORT OF PANEL ON IN-PILE DOSIMETRY. pp 1-15 of STI/DOC/10/46.

The difficulties of measuring the dose in research reactor experiments are reviewed, and recommendations for specific methods are given. In-reactor fluence and dose measurements are discussed including reactor characteristics, fast, intermediate, and thermal neutron measurements; the determination of energy absorbed from reactor radiation including energy absorption processes, a definition of irradiation conditions, assessment of radiation heating, studies in radiation chemistry, biology, corrosion, etc., determination of absorbed dose or dose-rate, and standardization are considered. (J.F.P.)

11145 A STATUS REPORT ON IN-PILE DOSIMETRY IN CANADA. Boyd, A. W. (Atomic Energy of Canada Ltd., Chalk River, Ontario). pp 17-20 of STI/DOC/10/46.

The in-pile dosimetry work in Canada consists of thermal, intermediate, and fast-neutron flux measurements by activation methods, thermal-neutron flux monitoring by self-powered detectors, and calorimetric, ion chamber, and chemical measurements of absorbed due to neutrons and gamma rays. Work in each of these fields is summarized. (J.F.P.)

11146 STATUS OF DOSIMETRY IN FRANCE. Delattre, P.; Droulers, Y. (Commissariat a l'Energie Atomique, Paris). pp 20-35 of STI/DOC/10/46. (In French).

In order to present a comprehensive view of the actual state of in-pile dosimetry which is precise enough, the essence of these problems is given. What is considered acquired knowledge is distinguished from the problems which still present difficulties and are objects of study. Topics considered are thermal, intermediate, and fast neutrons, and gamma rays. Within each category the spectra, instantaneous flux, and the doses integrated with respect to time are examined. (J.F.P.)

11147 STATUS REPORT ON IN-PILE DOSIMETRY IN THE FEDERAL REPUBLIC OF GERMANY. Kapulla, H. (Gesellschaft fuer Kernforschung, Karlsruhe, Ger.). pp 35-9 of STI/DOC/10/46.

A brief review is given of the methods of in-pile dosimetry employed in the reactor stations of the Federal Republic of Germany. The topics covered include determination of thermal and intermediate neutron flux, in which activation detectors are used for flux measurements, activation detectors for spectrum measurements of intermediate neutrons, the beta current detector, and the thermopile. Determination of fast neutron flux, special detection methods for neutron flux and fluence, and the dosimetry of reactor irradiation with calorimeters are also discussed. (J.F.P.)

11148 A STATUS REPORT ON IN-PILE DOSIMETRY IN HUNGARY. Szabo, F. (Central Research Inst. for Physics, Budapest). pp 40-2 of STI/DOC/10/46.

In-pile dosimetry at the Central Research Institute of Physics is concerned with thermal, epithermal, and fast neutron flux measurements by the activation method, and calorimetric and chemical measurements of energy absorbed from reactor radiation. The flux measurement technique applied in the WWR-S research reactor is determined primarily by aspects of isotope production. Microflux distribution and neutron temperature measurements are carried on within the scope of the reactor physical experiments performed on the ZR-2 critical assembly. In-pile irradiation experiments on organic liquids required the development of methods for measuring the energy absorbed. Neutron flux, microflux, neutron temperature, and absorbed radiation energy measurements are discussed. (J.F.P.)

11149 STATUS REPORT ON IN-PILE RADIATION METROLOGY IN THE NETHERLANDS. Zijp, W. (Inst. for the Development of Peaceful Applications of Nuclear Sciences, Petten, Netherlands). pp 43-7 of STI/DOC/10/46.

The work on in-pile dosimetry in the Netherlands includes thermal, fast, and intermediate neutron measurements, and nuclear heat generation measurements. Also a list of the research reactors in operation in the Netherlands is given. (J.F.P.)

11150 CERTAIN PROBLEMS IN DOSIMETRY AROUND REACTORS. Kramer-Ageev, E. A. pp 48-51 of STI/DOC/10/46. (In Russian).

Problems encountered in measuring neutron doses and flux around reactors and in reactor channels are outlined, and methods for solving these problems are discussed. The types of dosimeters used are also briefly discussed. (C.E.S.)

11151 A STATUS REPORT ON IN-PILE DOSIMETRY IN THE UNITED KINGDOM. Loosemore, W. R. (Atomic Energy Research Establishment, Harwell, Eng.). pp 51-6 of STI/DOC/10/46.

Some problems of in-pile dosimetry currently being examined in the United Kingdom are reviewed. These are the measurement of reactor radiations, including fluence, fluence rates, and spectrum characteristics, and measurement of absorbed dose in materials by reactor radiations. In these discussions the basic difference between absorbed dose and exposure is pointed out. (J.F.P.)

11152 A STATUS REPORT ON IN-PILE DOSIMETRY TECHNIQUES IN YUGOSLAVIA. Raisic, N.; Draganic, I. G. (Boris Kidric Inst. of Nuclear Sciences, Vinca, Belgrade). pp 62-6 of STI/DOC/10/46.

Work in the field of reactor dosimetry is concentrated on determination of integral values of thermal, epithermal, and fast neutron fluxes, and measurements of absorbed doses of reactor radiation in various materials. A brief description is given of the most frequently used techniques for routine neutron flux measurement. The development of some new methods, such as semiconductor counters and specially constructed calorimeters and the aqueous oxalic acid dosimeter, are discussed. The measurements were performed in the core or reflector of the heavy water 2% enriched uranium 10-MW RA research reactor. (J.F.P.)

11153 POSTFOCUSING ACCELERATION FOR A $\pi\sqrt{2}$ SPECTROMETER. Krisciokaitis, R. J.; Haynes, S. K. (Michigan State Univ., East Lansing). 23p. (CONF-758-54). ORINS; Gmelin, AED-CONF-65-003-101.

From American Physical Society Meeting, New York, Jan. 1965.

Low-energy electrons (≤5 kev) were detected by using an electrostatic accelerating potential between the detector and the wall of a $\pi\sqrt{2}$ spectrometer. The accelerating voltage was kept below 10 kev and a negative retardation potential was incorporated into the accelerator. Tests indicated that the accelerator-introduced noise was about 1% of beam strength. Accelerator performance is demonstrated by studies of L and K Auger groups of ^{113}In. (A.G.W.)

11154 NEUTRON MEASUREMENTS IN HIGH GAMMA BACKGROUNDS. Bluestein, I. 21p. (CONF-650710-9). ORINS. Gmelin, AED-CONF-65-192-25.

From American Nuclear Society Meeting on Reactor Operating Experience, Jackson Lake Lodge, Wyo.

Experiments on neutron detection in high gamma backgrounds indicated that significant improvements could be attained by decreasing the diameter of the tube and reducing gas fill pressure in relation to conventional tubes. A cluster of 13 boron-lined tubes was manufactured, each of which was 9 in. long and ¼ in. in diameter and filled with argon-carbon dioxide to a pressure of 20 mm Hg. The tube cluster was installed against the beryllium reflector of a testing reactor facility and measurements were made for a six-day period after shutdown. The measured neutron flux decay closely approximated the calculated neutron flux decay. The equipment was then used to make transfer function measurements at different shutdown reactivities. (A.G.W.)

11155 A COMPARISON OF RADIOTHERMOLUMINESCENT AND RADIOPHOTOLUMINESCENT DOSIMETERS. Malsky, S. J.; Amato, C. G.; Roswit, B. (Manhattan Coll., Riverdale, N. Y.). 5p. (CONF-650616-10). ORINS. Gmelin, AED-CONF-65-153-5.

From Health Physics Society Annual Meeting, Los Angeles.

Miniature in vivo radiothermoluminescent (RTL) and radiophotoluminescent (RPL) dosimeters were developed and studied for possible application to dosimetric problems of therapeutic radiology, nuclear medicine, and environmental health. The characteristics established for these systems are summarized. Both systems seem suited to certain applications with RTL dosimeters having a wider range of sensitivity and therefore a wider range of possible applications. (A.G.W.)

11156 A MATRIX METHOD FOR RESOLUTION AND BACKSCATTERING CORRECTIONS IN SCINTILLATION BETA-SPECTROMETRY. Sen, P.; Patro, A. P. (Saha Inst. of Nuclear Physics, Calcutta). pp 305-8 of Nuclear Physics and Solid State Physics Symposium, 1965. Nuclear Physics. Bombay, Atomic Energy Establishment, 1965.

A matrix method for backscattering and resolution corrections in scintillation beta spectrometry is outlined, and the results obtained in applying the method to the ^{22}Na positron spectrum and to the spectrum of 620-kev conversion electrons from ^{137}Cs are summarized. (D.C.W.)

11157 A BETA-SPECTROMETER FOR MEASUREMENT OF LOW-ENERGY ELECTRONS ASSOCIATED WITH AURORAL PHENOMENA. Skovli, Gunnar (Univ. of Oslo). pp 147-51 of Proceedings of a Symposium on High Latitude Particles and the Ionosphere, Alpbach, 1964. Maehlum, B. (ed.). New York, Academic Press, 1965.

A miniaturized double-focusing beta spectrometer is described. This instrument may be used for measurements of primary electrons in the energy range from 3 to 40 kev. Some problems associated with this device are discussed. (auth)

11158 SOME COMMENTS ON ELECTROSTATIC ANALYSERS. Hultqvist, Bengt (Goddard Space Flight Center, Greenbelt, Md.). pp 153-57 of Proceedings of a Symposium on High Latitude Particles and the Ionosphere, Alpbach, 1964. Maehlum, B. (ed.). New York, Academic Press, 1965.

The electrostatic deflection type of particle spectrometer usually contains spherical or cylindrical surfaces with a practically homogeneous electrostatic field between them. The electrostatic deflection spectrometer used in a rocket or satellite instrument has some advantages over other types of particle spectrometers. For example, the geometric factor can be made bigger than for the magnetic spectrometers, but not bigger than the retarding potential type of devices. Such a design is shown. The deflection type of electrostatic spectrometer has the advantage over the retarding potential type in that it gives the differential energy spectrum instead of the integral one. An additional advantage over the magnetic analyzer is that it can be made small and of low weight. But the electrostatic analyzer has one important drawback on space vehicles in that it measures in only a narrow energy interval at one time. (J.F.P.)

11159 AUTOMATIC SCANNING INSTRUMENT FOR CHARGED-PARTICLE SPECTROMETER. (to Kabushiki Kaisha Hitachi Seisakusho). British Patent 1,012,912. Dec. 8, 1965. Priority date Dec. 27, 1961, Japan.

An automatic scanning instrument is provided in which scanning of any charged particle ray, particularly beta, within any desired energy range can be accomplished automatically, rapidly, and accurately. The instrument has means by which the current for creating the magnetic field of the spectrometer is caused by program signals to vary automatically and in a stepwise manner. Means are provided for automatically converting the current into a digital quantity and recording it. (B.L.M.)

11160 HOLDER OF A FLUOROGLASS ROD FOR USE IN RADIATION DOSIMETRY. (to Tokyo Shibaura Electric Co. Ltd.). British Patent 1,012,919. Dec. 8, 1965. Priority date Aug. 27, 1962, Japan.

A holder for a fluoroglass rod for use in radiation dosimetry comprises a pair of spaced outer frames each having a bore of a diameter smaller than that of the rod. A pair of supporting plates are mounted in the lower portions of recesses on the inner side of the outer frame, and each plate is provided with a notch to support the ends of the glass rod in axial alignment with the bore. An intermediate frame having a circular inner wall positioned between the supporting plates and a movable holding member adapted to hold the rod are provided. The inner surfaces of the supporting plates and outer frame, the surface of the holding member, and wide circular recesses on the outer frames around the bores are all painted black. The intermediate frame is plated to reflect fluorescent rays. A cover plate for excluding dust is provided on the holder. (B.L.M.)

11161 SCINTILLATION SCANNER. Ueyanagi, Hidero (to Shimazu Seisakusho Ltd.). Japanese Patent 1964-24780. Nov. 4, 1964. Filed Apr. 3, 1961.

In the two-dimensional movement mechanism of the proposed scintillation detector two devices are installed: one of which produces the electrical signals changing in proportion to the amount of movement of the respective dimensions, and another which records and indicates the relation between the signal and time, together with the detector output. The output circuit of the scintillation detector includes two circuits: one for making the output-pulse heights a given value, and the other for changing this pulse height according to the pulse count rate. The electrical signals along with the detector output are memorized in a magnetic tape, and these signals are reproduced on a Braun tube, when required, to obtain a scintigram. The scintillation detector is moved two-dimensionally, and the detector output at each position on the surface is memorized and reproduced individually on the scintigram. (TCO)

11162 RADIATION MONITOR USING A MAGNETIC AMPLIFIER. Kobayashi, Akira (to National Railway Div., Ministry of Transport). Japanese Patent 1964-26655. Nov. 21, 1964. Filed Aug. 18, 1961.

A radiation monitor includes a radiation counter, a pulse rate converter, a magnetic amplifier, a rectifier, and a relay. The circuit of the magnetic amplifier consists of an in-put coil for the pulse rate signal caused by the incident radiation, an in-put coil to energize the saturable magnetic core, an out-put coil to measure the radioactivity followed by the rectification of the pulse rate signal of the incident radiation, and an out-put coil to energize the relay contact of an alarm. The relay contact of the alarm is energized by a certain low level of pulse rate and by some failure occurring in the monitor; it is de-energized by a certain high level of pulse rate and no pulse rate signal. (NSA of Japan)

11163 RADIATION DETECTOR USING AN ELECTRIC DISCHARGE PHENOMENON. Morita, Tatsuo. Japanese Patent 1964-26932. Nov. 26, 1964. Filed Nov. 4, 1960.

A new radiation detector is proposed, which uses an unexpected interaction between the electric discharge and radiations, such as β rays. In the radiation detector, the anode and cathode are so arranged as to produce an extremely unsymmetrical and ununiform electric field in the vicinity of the anode. The electric discharge between the anode and cathode ceases when irradiated by radiation of a certain intensity under some conditions of the geometrical arrangement of the electrodes and the ambient gas. (NSA of Japan)

11164 ELECTRODE FOR A SMALL DOSIMETER. Kawahara, Masao (to Inst. Phys. and Chem. Res.) Japanese Patent 1964-26933. Nov. 26, 1964. Filed May 30, 1962.

The electrode for use in a small dosimeter is shaped in an inverted U and is supported in the dosimeter plug by its two legs. It is further supported at the top by another support protruding and penetrating through the insulator plug and connected electrically to the electrode. A quartz fiber is attached onto the electrode for dose-reading purposes. This structure of the electrode provides a structural stability against vibrations, shocks, etc. (TCO)

11165 PLASTIC SCINTILLATOR. Aoki, Ryozo (to Hitachi, Ltd.). Japanese Patent 1964-26934. Nov. 26, 1964. Filed Dec. 14, 1961.

A scintillator with high detection efficiency for gamma rays is made by imbedding a foil of a metal of sufficiently large atomic number and with high surface reflective power in the scintillating plastic body. (TCO)

11166 STABILIZED SCINTILLATION COUNTER USING PHOTOMULTIPLIER. Scherbatskoy, Serge A. U. S. Patent 3,218,460. Nov. 16, 1965. Filed Mar. 26, 1962.

In a scintillation counter employing a scintillation crystal optically coupled to a photomultiplier, a light source is arranged to illuminate the photocathode with a steady, unvarying, continuous, standard illumination during the measurement of nuclear radiation. This illumination produces a d-c photomultiplier anode current, and the scintillations produce photomultiplier anode pulses. A first electric signal channel selectively transmits variations in the d-c photomultiplier current, and a second electric signal channel selectively transmits pulses. Means controlled by the first signal channel automatically increases at least one of the potential differences when the d-c current decreases and decreases at least one of the potential differences when the d-c current increases so as to maintain the sensitivity of the counter substantially constant despite variations in the voltage of the source. (B.L.M.)

11167 STABILIZED SCINTILLATION TYPE RADIATION DETECTOR. Scherbatskoy, Serge A. U. S. Patent 3,225,195. Dec. 21, 1965. Filed Mar. 25, 1963.

A scintillation detector is described in which the sensitivity variations in the photomultiplier tube are compensated by continuously comparing the intensity of the light flashes generated in a scintillation phosphor to the intensity of a standard light pulses. The source of the standard light pulses is a small scintillating phosphor having dispersed in it, by inclusion in the melt, a radioactive material that emits monochromatic charged particles. These particles interact with the materials of the

phosphor and produce a succession of light pulses having uniform intensity, directly related to the energy of the charged particles emitted by the radioactive material. (B.L.M.)

11168 DEVICE FOR MEASURING DOSES OF THERMAL NEUTRONS. Gigon, Jean; Mayer, Guy (to Commissariat a l'Energie Atomique). U. S. Patent 3,225,196. Dec. 21, 1965. Priority date Nov. 8, 1957, France.

An analyzer for thermal neutrons consists of a glass body having a number of glass parts with different density response to neutrons and means to measure the dimensional response or deformation of the body to irradiation. After the glass has been deformed by density changes, it is restored to its original form by a heating process. (B.L.M.)

11169 FAST NEUTRON DETECTION AND FLUX DENSITY MEASUREMENT. Basso, Michael J. (to U. S. Army). U. S. Patent 3,225,197. Dec. 21, 1965. Filed May 10, 1963.

A method and apparatus embodying the phenomena of nuclear magnetic resonance are provided for detecting and measuring fast neutron flux as a function of time. A sample of a material having a high content of hydrogen nuclei is contained in a nonmagnetic receptacle and supported in a neutron free enviornment. A magnetic field is applied to the sample so that some of the gyromagnetic bodies in the material will be oriented in a common altitude. A radio frequency coil is disposed within the magnetic field with its turns arranged to produce a field having a longitudinal axis extending at 90° to the lines of the magnetic field and passing through the sample. The coil is energized, and the frequency of the input current is adjusted to that of the resonant frequency of the sample. The input current is measured, and then the sample is immersed in a high intensity fast neutron environment while the nuclei are in their resonant state so that the neutrons will collide with some of the nuclei to momentarily disrupt their resonance. The radio frequency input to the coil is again measured. The summation of the effects of the collisions indicates the changing neutron flux of the environment and corresponds to the change in absorption of the radio frequency input as a function of time. (B.L.M.)

11170 METHOD OF MEASURING NUCLEAR RADIATION UTILIZING A SEMICONDUCTOR CRYSTAL HAVING A LITHIUM COMPENSATED INTRINSIC REGION. Mayer, James, W. (to Hughes Aircraft Co.). U. S. Patent 3,225,198. Dec. 21, 1965. Filed May 16, 1961.

A device for measuring nuclear radiation consists of a silicon semiconductor crystal having a lithium compensated intrinsic region between the P and N type regions and means for measuring the electrical pulses generated between the P and N type regions. The crystal is maintained at a temperature below 100°C, and the bias voltage is maintained between 10 and 500 v. The bias and the width of the intrinsic region are sufficient to produce a depletion region in the crystal in excess of 1 mm thick. (B.L.M.)

11171 RADIOISOTOPE IDENTIFIER. Tolmie, Ronald W. (to Atomic Energy of Canada, Ltd.). U. S. Patent 3,225,199. Dec. 21, 1965. Priority date Jan. 8, 1962, Canada.

An apparatus for measuring the energy of local radiation includes a pair of radiation detectors of the counting pulse type, whose rate of counting depends upon the number of radiations quanta intercepted in a given time interval. A radiation absorbing shield is provided for absorbing a proportion of the radiation falling on one of the detectors, and this proportion is dependent upon the energy of the radiation. The shield is formed of two dissimilar materials having different absorption coefficients for a given energy of radiation to provide different attenuation for radiation encountering one of the detectors from separate chosen directions. The rate of counting of one detector is thus determined by that material which is interposed between the detector and the source of radiation. The number of counts from the shielded detector and the sum of the number of counts of both the detectors is derived as a potential difference. (B.L.M.)

Radiation Effects

Refer also to abstract 12276.

11172 (AD–623963) COMPARISON AND EVALUATION OF THREE AUTOMATED CIRCUIT ANALYSIS PROGRAMS: PREDICT, NET-1, AND CIRCUS. Dickhaut, R. H. (Boeing Co., Seattle, Wash. Aero-Space Div.). May 1965. 13p. CFSTI $1.00 cy, $0.50 mn.

The results of a comparison and evaluation of the existing circuit analysis programs as of early 1965 are presented. The radiation responses predicted by the three digital computer programs are essentially identical for each circuit. (D.C.W.)

11173 (D2-84071-1) THE RESPONSE OF P-I-N DETECTORS TO VARIOUS NUCLEAR RADIATION ENVIRONMENTS. Lowrey, A. R.; Friddell, K. D. (Boeing Co., Seattle, Wash.). [1964]. Contract AF29(601)-6425. 50p.

Si and Ge p-i-n detectors are exposed to various transient and steady-state radiation environments, and the theoretical and experimental variations in response are tabulated, compared, and analyzed. The radiations to which the detectors are exposed include gamma rays, x rays, and electrons. (T.F.H.)

11174 (IDO–17112, pp 81–91) INSTRUMENT DEVELOPMENT. (Phillips Petroleum Co., Idaho Falls, Idaho. Atomic Energy Div.).

The measurement of pressure in fuel capsules by the use of strain gages attached to the capsule walls was investigated, and transient radiation effects on electric cables and on a variety of transducers were studied. The strain in SPERT I fuel pin cladding was measured, and two devices were developed for measuring axial and radial deformations of PBF fuel elements. Instrumentation for testing PBF and SPERT III control-rod drives was evaluated. (D.C.W.)

11175 (NP–15823) DEVELOPMENT OF A MODEL EXPERIMENTAL DESIGN FOR NERVA INSTRUMENTATION RADIATION-EFFECTS TESTS. Drennan, James E.; Cote, Roger W.; Wyler, Eugene N. (Battelle Memorial Inst., Columbus, Ohio). July 19, 1965. 103p.

To demonstrate the application of experimental design principles to the radiation-effects program pertaining to the development of instrumentation for the NERVA environment, a model design based on the test for a LVDT linear displacement transducer described in Test Document 23/W205 was prepared. For this model experimental design, one experimental problem concerns determining whether the transducer internal temperature will remain within acceptable limits at the level of radiation flux expected for the NRX-A3 application; another pertains to establishing whether or not the transducer performance parameter values will meet the NERVA requirements at the level of integrated fast-neutron exposure expected for NRX-A3 use. A data reduction and analysis procedure based on regression techniques was developed and verified. The analysis procedure yields statements of the probability of successful transducer performance and the confidence appropriate to these statements. The precision and accuracy required for the experimental measurements and the experimental procedure were defined. The mechanics of the experimentation were summarized as a test specification. Although the model experimental design is directed toward specific problems and a specific instrument, its format and logic are applicable generally to radiation-effects testing of instrumentation. It is believed that the data reduction and analysis procedures documented may be applicable in detail to a wide variety of the radiation-effects experiments that will be planned during the NERVA development program. (auth)

11176 (NP–15835) INVESTIGATION OF TRANSIENT RADIATION DAMAGE IN SEMICONDUCTOR MATERIALS. Quarterly Progress Report No. 9, February 1–April 30, 1965. Lichtenstein, Roland M.; Willard, H. James Jr.; Corelli, John C.; Frederickson, A. Robb; West-

head, James W. (Rensselaer Polytechnic Inst., Troy, N. Y.). Contract DA-36-039-AMC-02165(E). 28p. CFSTI $2.00 cy, $0.50 mn.

Transient radiation effects induced by ≈48-Mev-electron beam pulses in 10 and 100 ohm-cm n-type silicon (phosphorus doped) and in ≈100 ohm-cm p-type silicon (boron doped) were studied using the transient resistivity voltage as the damage probe. The n-type silicon samples were irradiated at temperatures in the range 80°K up to ≈300°K, the p-type sample was irradiated at only one temperature namely, 288°K. In this first series of experiments the main results are briefly given as follows: The resistivity voltage for all samples appears to be saturated for a time which is in general much longer than the electron beam pulse width. Typical electron beam pulse widths used were from about 0.007 to 4.5 microseconds. The saturation time lasts ~70 microseconds for p-type silicon and is observed to markedly decrease when the total electron flux in the pulse is lowered. The saturation time becomes shorter as the irradiation temperature of the sample is lowered. In the n-type silicon a long-lived voltage decay which can persist up to several milliseconds following a burst of electrons is observed. This long-lived decay effect (or trapping) becomes more pronounced as the temperature at which the sample is irradiated is lowered below ≈300°K. (auth)

11177 (UJV-1388/65) PRESNA SYNCHRONIZACE, MERENI PROSTOROVEHO UHLU A KRUHOVY DIAGRAM REAKCNICH SYNCHRONNICH MOTORU. (The Precise Synchronization, the Measurement of the Spatial Angle, and the Circular Diagram of Reactionary Synchronous Motors). Plasil, V. (Ustav Jaderneho Vyzkumu, Ceskoslovenska Akademie Ved, Rez). 1965. 72p. Dep. mn.

An analysis is presented of the precise synchronization of two motors with the aid of a transmission. At the conditions considered, a mean deviation of the spatial angle of ±3.5 angular minutes was attained. An analysis of the measurement of the spatial (load) angle of a motor by means of current phase is also included. With suitable retarding compensation, the relative error is not greater than 5%. A derivation of a circular diagram of an actual motor is given with an examination of the losses in the copper, the iron, and dissipation. A method of directly deducing the performance and loss from a circular diagram is outlined. By means of collinearity, the construction of an angular scale for the spatial angle on a circular diagram is derived. (TTT)

11178 RADIATION DAMAGE AND ANNEALING OF GaAs LASER DIODE. Saji, Manabu; Inuishi, Yoshio (Osaka Univ.). Jap. J. Appl. Phys., 4: 830-1(Oct. 1965).

The effect of γ irradiation on GaAs laser diodes and annealing of this effect are discussed. Besides the decrease of quantum efficiency, it was found that the lasing peak wave length at 8414 Å before irradiation shifted slightly to shorter wave length with increasing gamma irradiation, as is shown. The output light intensity of each spectral peak versus forward injection current, annealing curves of threshold currents, wave length of emission peak, and reverse saturation currents are also shown. The change of reverse saturation current of laser junction due to irradiation and following annealing seems to be due to change in minority carrier density and life time. (J.F.P.)

11179 SUMMARY OF DESIGN CONSIDERATIONS ASSOCIATED WITH USE OF MICROELECTRONIC CIRCUITRY IN A SPACE RADIATION ENVIRONMENT. Sorkin, Rodney B. (Battelle Memorial Inst., Columbus, Ohio). 6p. (CONF-650707-12). ORINS. Gmelin, AED-CONF-65-152-12.

From IEEE Annual Conference on Nuclear and Space Radiation Effects, Ann Arbor, Mich.

The types and extent of microcircuit degradation caused by radiation and those parameters that are most critical in determining the radiation tolerance of microcircuits are briefly outlined. In general the transistor in the microcircuit structure is the single most sensitive component to radiation, and the most important microcircuit parameter for radiation resistance is speed. When commercially available microcircuit types were exposed to 3-Mev electrons, the failure mode for all circuits was an increase in the low-level output voltage above the specified maximum. The possibilities for minimizing deleterious effects are discussed from the points of view of both the manufacturer and the designer. (A.G.W.)

11180 SYSTEM QUALIFICATION PROCEDURES FOR A PULSED NUCLEAR ENVIRONMENT. Long, David M. (Martin Co., Baltimore). 3p. (CONF-650707-14). ORINS. Gmelin, AED-CONF-65-152-10.

From IEEE Annual Conference on Nuclear and Space Radiation Effects, Ann Arbor, Mich.

A procedure for rigorously qualifying an electronic system for a pulsed nuclear environment is outlined. The necessary inputs for the qualification analysis consist of environmental requirements, performance requirements, system characteristics, and radiation effects information. The analysis procedure consists of three principal steps for each item in the system: determination of radiation response, determination of failure criteria, and comparison of radiation response with failure criteria. The item is qualified only if the radiation response definitely satisfies the performance requirements. (A.G.W.)

11181 TESTING OF SPACE VEHICLE FLUID POWER CONTROLS IN NUCLEAR RADIATION. Billet, A. B. (Vickers Inc., Detroit). 23p. (CONF-650719-1). ORINS. Gmelin, AED-CONF-65-190-2.

From 4th Annual Reliability and Maintainability Conference, Los Angeles.

A complete aircraft-type hydraulic system was exposed to radiation from a pool-type reactor. During the first 52 hr of irradiation, the reactor was brought up to power in steps; this was followed by two irradiation periods of 250 hr each, one at 100 kw and the other at full power level of 500 kw. Throughout the entire test the hydraulic system operated satisfactorily. A postirradiation inspection showed that the metals in the system were not significantly affected but various elastomers, fluids, and plastics in the system were damaged. Other tests of hydraulic-system components and servo systems gave similar results. Environmental conditions in space, particularly sources and intensity of radiation expected, are summarized briefly. It is concluded that, with expected technological advances in materials, fluid power control systems can be made to operate satisfactorily under radiation conditions encountered in space. (A.G.W.)

11182 HIGH-ENERGY RADIATION DAMAGE IN SILICON TRANSISTORS. Brucker, G.; Dennehy, W.; Holmes-Siedle, A. G. (Radio Corp. of America, Princeton, N. J.). 10p. (CONF-650707-16). ORINS.

From IEEE Annual Conference on Nuclear and Space Radiation Effects, Ann Arbor, Mich.

Electron and gamma damage in silicon transistors was investigated. At low values of fluence ($\Phi_e < 10^{14}$ electrons/cm^2), loss in common-emitter d-c current gain of medium-frequency n-p-n planar transistors at collector currents of 1 to 10 ma was attributed to changes in the surface recombination velocity. Displacement-induced recombination centers in the base region caused a reduction in gain when Φ_e was greater than 10^{14} electrons/cm^2. A technique of saturating the surface damage with low energy electrons (E = 125 kev) so as to permit a separation of surface and bulk damage is demonstrated. The minority-carrier lifetime-damage constant, K_τ, was estimated from the separated bulk-damage curve. It agreed with the value determined from electron irradiation of a low-frequency ($f_{\alpha b}$ = 1.25 Mc/sec) mesa n-p-n transistor, which was found to suffer degradation in gain only from bulk recombination current losses within the base region. Surface damage from both electrons and gamma rays was annealed at 250°C or by injecting emitter currents of 200 ma, which generated a high internal temperature. In contrast to this behavior, electron irradiation of p-n-p transistors caused loss in gain, which was attributed to bulk damage. Damage constants, K_τ, determined from the data showed that p-n-p transistors suffered bulk radiation damage about five times greater than n-p-n transistors. (auth)

ISOTOPE TECHNOLOGY

General

11183 (ORNL-P-1900) PREPARATION OF ISOTOPE TARGETS BY ELECTRON-BOMBARDMENT TECHNIQUES. Kobisk, E. H. (Oak Ridge National Lab., Tenn.). Dec. 28, 1965. Contract W-7405-eng-26. 10p. (CONF-651055-2). Dep. mn. CFSTI $1.00 cy, $0.50 mn.

From Preparation and Standardization of Isotopic Targets and Foils Conference, Harwell, Eng.

In order to achieve maximum efficiency in the preparation of thin films of isotopically enriched normal elements using vacuum evaporation-condensation techniques, an electron-bombardment vaporization source using high electron currents and low acceleration voltages was developed. A minimum of about 20 and a maximum of 90% efficiency of vapor condensation were obtained with this system. The vaporization source uses special crucibles to attain mechanical collimation, permitting the use of milligram quantities of evaporant in cases where previously several hundred milligrams were required with other evaporation techniques. Materials having very high vaporization temperatures (about 3,000°C) were evaporated successfully by this method. Examples of these are oxides of neptunium, uranium, plutonium, and thorium. The electron-bombardment heat source can be installed in all standard vacuum chambers at low cost and is suitable for use at pressures of 10^{-10} torr. (J.F.P.)

Industrial Applications

Refer also to abstracts 11202–11204.

11184 (BNWL-122, pp 137-9) X-RAY AND FAST NEUTRON EFFECTS ON PRODUCTIVITY OF FLOUR BEETLES. Erdman, H. E. (Battelle-Northwest, Richland, Wash. Pacific Northwest Lab.).

Effects of temperature, x ray, and the sex irradiated were studied for the day-old flour beetle, Tribolium castaneum (Herbst). Onset of reproduction was earlier and productivity greater as temperature increased. A 4 kR exposure of females delayed reproductive onset by two to three days. Productivity was reduced by 2 and 4 kR. Radiation effect on productivity was additive when both sexes were x rayed. The ratio of doses required to produce 50% dominant lethals was 2.4:1 relative to 250 kV potential x rays and 4.6 Mev fast neutrons. (auth)

11185 VITAMIN B_{12} IN LYOPHILIZED MEAT AND IN MEAT IRRADIATED WITH THE γ-RAYS OF ^{60}Co. Curatola, G.; Stornelli, R.; Di Addario, A. (Sanita Militare, Rome). Giorn. Med. Mil., 114: 760-6(1964).

Cobalt-60 radiation given in sterilizing quantities caused about 60% destruction of vitamin B_{12} in natural meat, but only 20% in lyophilized meat. (Excerpta Med.)

11186 EFFECT OF GAMMA RADIATION UPON CHERRIES. Massey, L. M. Jr.; Robinson, W. B.; Spaid, J. F.; Splittstoesser, D. F.; Van Buren, J. P.; Kertesz, Z. I. (Cornell Univ., Geneva, N. Y.). J. Food Sci., 30: 759-65(Sept.-Oct. 1965).

The effect of ^{60}Co γ radiation upon the quality of stored sweet cherries was studied. Softening was detected which progressed rapidly above a threshold dose of about 50 krad and was related to the degradation of pectic constituents of the fruit. Although respiratory O_2 consumption and CO_2 evolution were stimulated during irradiation, the response subsided slowly after irradiation ceased. Color bleaching occurred only at the high doses. Despite a marked initial reduction in microbial contamination, extended storage periods showed increased microbial spoilage. A reduction in the development of brownrot during high-temperature short-time storage resulted from krad doses of radiation. There was a slightly increased rate of sulfur dioxide bleaching and increased yield of brined cherries, but this was accompanied by loss of texture of the finished product. In comparison with other plant tissues, cherries appear to have an intermediate susceptibility to softening. The calculated threshold dose (TD) of 50 krad was similar to the value of 35 krad found as the average softening TD value for apples. However, this value is lower than that found for the softening of carrots (166 krad), beets (316 krad), and lettuce (800 krad). Softening appears to be related directly to the degradation of pectic substances in the tissues in a manner similar to that known with several other tissues. The results show that cherries were relatively insensitive to radiation-induced respiratory activity stimulation. (TCO)

Power Application

See also ENGINEERING — Space Propulsion

Refer also to abstract 12394.

11187 (AGN-8138) MILITARY VEHICLES—MISSION ANALYSIS USING RADIOISOTOPE SUBMERSIBLE ENGINES. Finkle, Earl (Aerojet-General Nucleonics, San Ramon, Calif.). Mar. 1965. Contract AT(04-3)-368. 50p. Dep. mn. CFSTI $2.00 cy, $0.50 mn.

A mission analysis was undertaken for a variety of underwater platforms and vehicles in order to determine the most promising applications of radioisotope propulsion systems. (D.C.W.)

11188 (BLG-330) L'UTILISATION DES RADIOISOTOPES POUR LA PRODUCTION D'ENERGIE ELECTRIQUE A BORD DES ENGINS SPATIAUX. (Utilization of Radioisotopes for Production of Electric Energy Aboard Space Vehicles). Bemelmans, P.; Contzen, J.-P. (Centre d'Etude de l'Energie Nucleaire, Brussels (Belgium)). [1964]. 34p. Dep. mn.

Comparing the characteristics of the primary energy sources available on board space vehicles, it is shown that radioisotopes exhibit definite potentialities for missions of intermediate to long duration, involving but moderate power levels. A survey of the suitable conversion systems was given, and the different criteria a radioisotopic source must meet before it can be applied to the production of auxiliary electric energy on board space vehicles were discussed. On this basis, eleven isotopes were selected for their best fitted characteristics; the latter are summarized in tabular form and then separately discussed for each of the considered radioelements. (auth)

11189 (MND-3062-25) PARAMETRIC RE-ENTRY ABLATION STUDY OF HYPOTHETICAL ^{90}Sr FUEL FORMS. Final Report. Osmeyer, William E.; Carter, Edward L. (Martin Co., Baltimore, Md. Nuclear Div.). Jan. 1966. Contract AT(30-1)-3062. 182p. Dep. mn. CFSTI $5.00 cy, $1.00 mn.

Analytical computer programs were used to describe the re-entry trajectory, heat flux, ablation and molten droplet behavior of hypothetical strontium-90 fuel capsules exposed to a re-entry environment during the descent from orbit of a radioisotopic generator. A detailed parametric study was performed which covered a wide range of capsule designs and fuel form properties. Although gross capsule trajectory and ablation computer programs were available, new programs were generated to consider deceleration, breakup and ablation of micron size droplets. The capsule design and material property influence upon ablation was investigated for three major phases of the capsule re-entry ablation history: encapsulation material ablation; fuel form ablation; and molten droplet breakup and ablation. The most influential ablation parameters for each phase were determined. (auth)

Separation and Production

See also CHEMISTRY — Separation Processes and Procedures

Refer also to abstract 12394.

11190 (BLG–332) PRODUCTION DE SOURCES D'IRIDIUM-192 A HAUTE ACTIVITE SPECIFIQUE. (Production of ^{192}Ir Sources of High Specific Activity). Mekers, J.; Morel de Westgaver, A.; Constant, R.; Collignon, E. (Centre d'Etude de l'Energie Nucleaire, Brussels (Belgium)). July 1965. 10p. Dep. mn.

The production of high specific activity iridium-192 sources for industrial use is reported. The installations designed for the production are described. The method used for measuring the activity of ^{192}I with a precision of ±2% is also described. Since the total activities manipulated amount to ±2000 C per month, an easy and simple storage allowing operation under perfect conditions of security is necessary. (P.C.H.)

11191 (JEN–150-DQ/I-51) THE PRODUCTION OF STABLE ISOTOPES IN SPAIN. Urgel, M.; Uglesias, J.; Casas, J.; Saviron, J. M.; Quintanilla, M. (Junta de Energia Nuclear, Madrid (Spain). Division de Quimica). Dec. 1964. 15p. Dep. mn.

Developments in the production of stable isotopes by means of ion-exchange chromatography and thermal diffusion techniques are reported. The first method was used to study the separation of the nitrogen and boron isotopes, whereby the separation factor was determined by the breakthrough method. Values ranging from 1,028 to 1,022 were obtained for the separation factor of nitrogen by using ammonium hydroxide solutions while the corresponding values as obtained for boron amounted to 1,035-1,027 using boric acid solutions. Using ammonium chloride or acetate and sodium borate, respectively, resulted in the obtention of values for the separation factor approaching unity. Isotopic separation was carried out according to the method of development by displacement. Separation of the isotopes of the noble gases, oxygen, nitrogen, and carbon was accomplished by the method of thermal diffusion. (auth)

11192 (SGAE-PH–30/1965) ERGEBNISSE MIT EINEM MEHRZWECKISOTOPENTRENNER. (Yields with Multiphase Isotope Separator). Viehboeck, F. P. (Oesterreichische Studiengesellschaft fuer Atomenergie G.m.b.H., Seibersdorf). [1965]. 29p. Dep.

Experience gained in the use of the Seibersdorf Isotope Separator in its application to mass spectrometry, solid state physics, preparation of targets for nuclear spectroscopy, and separation of stable isotopes is reported. Improvements made to the instrument are also indicated. (J.S.R.)

11193 RECENT DEVELOPMENTS IN URANIUM ISOTOPE SEPARATION. Fiocchi, Roberto (Univ., Milan). Comit. Naz. Energia Nucl., Notiz., 11: No, 10, 38-49(Oct. 1965). (In Italian).

Methods developed since 1958 for the isotopic separation of uranium are reviewed. The theoretical bases for separation procedures and the elements indispensable for evaluation of the economic advantages of the methods are emphasized. (J.S.R.)

11194 PREPARATION OF HIGHLY ENRICHED ^{13}C BY THERMAL DIFFUSION OF METHANE. Rutherford, W. M.; Keller, J. M. (Mound Lab., Miamisburg, Ohio). J. Chem. Phys., 44: 723-9(Jan. 15, 1966). (MLM–1298J).

Methane, enriched to 93% in ^{13}C, was prepared by thermal diffusion in an 11-column, nine-stage isotope separation cascade. The experimental thermal-diffusion cascade was successfully operated at essentially steady-state conditions after a transient period of 292 days. Behavior of the cascade during steady operation was found to be in good agreement with the predictions of binary cascade theory. (auth)

MATHEMATICS AND COMPUTERS

Refer also to abstracts 10519, 11440, 11553, and 11609.

11195 (COO–614-34) ICR QUARTERLY REPORT, NUMBER 5, MAY 1, 1965. Miller, Richard H. (Chicago Univ., Ill. Inst. for Computer Research). Contract AT (11-1)-614. 203p. Dep. mn; CFSTI $6.00 cy, $1.25 mn.

Separate abstracts were prepared for the 7 included papers. (M.O.W.)

For abstracts of individual papers see: 11093, 11196–11199, 11440, and 11553.

11196 (COO–614-34, Sect. IIB) EXPERIMENTAL INVESTIGATION OF UNNORMALIZED ARITHMETIC. Ashenhurst, R. L. (Chicago Univ., Ill. Inst. for Computer Research). 51p.

Results of some numerical experiments carried out on the the Maniac III computer are presented. The experiments are based on two algorithms, one for matrix inversion and one for extracting and factoring zeros of polynomials. Experiments for inversion of Hilbert matrices are described. Also experiments performed on polynomial manipulation are described. These experiments seem to imply that careful use of unnormalized arithmetic can yield dividends in error monitoring, without undue sacrifice of accuracy over normalized calculation, for which a comprehensive error evaluation may be extremely difficult. (M.O.W.)

11197 (COO–614-34, Sect. IIIA) ON THE EXTENSION AND THE SOLUTION OF NONLINEAR OPERATOR EQUATIONS. Petryshyn, W. V. (Chicago Univ., Ill. Inst. for Computer Research). 38p.

A theory of nonlinear functions Pu = f was previously developed in Hilbert and reflexive Banach spaces involving monotone operators P satisfying certain very mild continuity conditions which guarantee the existence and the uniqueness of the solution for every f in a given space. The extension of certain densely defined nonlinear operators in Hilbert space is discussed in detail. (M.O.W.)

11198 (COO–614-34, Sect. IIIB) A DUALITY THEOREM IN COMBINATORIAL SWITCHING. Krishnamurthy, E. V.; Bodfish, E. (Chicago Univ., Ill. Inst. for Computer Research). 6p.

The duality theorem in combinatorial switching is stated and proven. The relation between AND-OR, majority and threshold logics and the property of self-duality in majority logic on this basis are indicated. (M.O.W.)

11199 (COO–614-34, Sect. IIIC) AN ALGEBRA FOR (m, p) SWITCHING NETS. Krishnamurthy, E. V. (Chicago Univ., Ill. Inst. for Computer Research). 6p.

The manner in which the (m,p) switching networks combine is described. It is shown that this logic (algebra) is isomorphic to the many-valued logic of Post. Application of this logic in designing error-free logic systems is indicated. (M.O.W.)

11200 (HMI-B-41) LOESUNG DER ERSTEN UND ZWEITEN RANDWERTAUFGABEN DES INNEN- UND AUSSENGEBIETES FUER DIE POTENTIALGLEICHUNG IN R_3 DURCH RANDBELEGUNGEN. (Solution of First and Second Boundary Value Problems of Inner and Outer Regions for the Potential Equations in R_3 Through Boundary Coverings). Wendland, W. (Hahn-Meitner-Institut fuer Kernforschung, Berlin (West Germany)). Sept. 1965. 104p. Dep. mn.

The inner and outer regions of the first and second boundary value problems for the potential equation R_3 were investigated. The boundary $\dot{G}$ is a simple closed surface consisting of many finite continuously curved parts. For the solution the potential of the simple and double coverings of the boundary were used. This method considers in its numerical solutions the geometric properties of the boundary. The problem for boundaries $\dot{G}$ with edges and angles was formulated. The original relations in $\dot{G}$ lead to the Fredholm integral equation of the second type for the coverings. The method used for the solution for continuously curved boundaries was represented. The Radon considerations were translated to the spatial case. The numerical methods described is independent of edges and angles in $\dot{G}$. Some examples of numerical calculations are given. (J.S.R.)

11201 (NYO–3136-2) STATISTICAL ANALYSIS OF ENVIRONMENTAL AND TOTAL BODY GAMMA-RAY SCINTILLATION SPECTRA. Annual Report, October 1964–September 1965. Pasternack, Bernard; Liuzzi, Anthony (New York Univ., N. Y. Inst. of Environmental Medicine). Sept. 30, 1965. Contract AT(30-1)-3136. 157p. Dep. mn; CFSTI $5.00 cy, $1.00 mn.

The statistical analysis of pulse-height distribution data from γ scintillation counting is discussed. Emphasis is placed on the concept of model adequacy, the development of procedures for detecting inappropriate or inadequate models, and the statistical properties of the estimates derived from the calculational procedures. The results of an empirical sampling study designed to investigate the use of overall model confirmed the validity of the method of analysis. A procedure is described that was developed for calculations of instrument gain and baseline discrepancy compensation. Appendixes I through IV contain an IBM 7094 Fortran program, PARANA, for the pulse-height analysis of radionuclide assay; a test for regression model adequacy in radionuclide assay; results of an empirical sampling study to evaluate the suitability of a statistical model used in analyzing the pulse-height distributions arising from the scintillation counting of radioactive materials; and a statistical study of probability of failure of an idealized light bulb while in use. (C.H.)

For abstracts of individual sections see: 11202–11205.

11202 (NYO–3136-2, App. 1) PARANA [PULSE-HEIGHT ANALYSIS FOR RADIONUCLIDE ASSAY]—A FORTRAN PROGRAM LISTING. (New York Univ., N. Y. Inst. of Environmental Medicine). 14p.

A computer code, PARANA, written in Fortran II for use with the IBM 7094 digital computer is presented. The program was written for the pulse height analysis of radionuclide assay data and was designed to handle up to 20 reference spectra and up to 300 channels of pulse-height data. The program will perform a test of model adequacy based on the ratio statistic (q^2) at a standard programmed significance level of 5% or at any integral level between 1% and 15%, if specified. The plotting routine was programmed to plot normalized residuals automatically if the value of q^2 falls below a given computed significance level. An option is provided for specifying the plot of residuals regardless of the value of q^2. (C.H.)

11203 (NYO–3136-2, App. 2) PATTERNS IN RESIDUALS: A TEST FOR REGRESSION MODEL ADEQUACY IN RADIONUCLIDE ASSAY. Pasternack, Bernard; Liuzzi, Anthony (New York Univ., N. Y. Inst. of Environmental Medicine). 38p.

Application of a modified form of weighted least squares estimation in radioactivity assay utilizing the entire pulse-height distribution (spectrum) obtained from the scintillation counting of radionuclide mixtures is discussed. It is assumed, in the model used in applying this procedure, that the pulse-height spectrum resulting from a mixture of radionuclides is a linear combination of the spectra associated with the constituent nuclides with superimposed statistical variations described as the error structure. Problems associated with incomplete and overspecified regression models, as applied to radionuclide assay, are discussed from the point of view of residual analysis. Use is made of a modified von Neumann ratio statistic as an overall index for judging model adequacy, and its approximate probability distribution is empirically evaluated by using radioactivity as a random distribution generator.

Examples are given of applications to ashed tissue samples. Illustrations of the manifestations of model inadequacies are also presented. (auth)

11204 (NYO–3136-2, App. 3) EMPIRICAL SAMPLING USING RADIOACTIVITY AS A GENERATOR OF RANDOMICITY. Pasternack, Bernard; Liuzzi, Anthony (New York Univ., N. Y. Inst. of Environmental Medicine). 24p. (CONF-650950–1).

From International Statistical Inst., 35th Session, Belgrade.

The results are presented of an empirical sampling study designed to evaluate the suitability of a statistical model used in analyzing the pulse-height distributions arising from the scintillation counting of radioactive materials. A random set of pulse-height distributions was accumulated by the repeated counting of a single prepared mixture of three radionuclides. The empirical results were obtained from the analyses of these distributions. A brief introduction and discussion of the radionuclide assay problem, the modified weighted least squares solution, and some actual applications of this method of analysis precede the presentation of the empirical sampling results. The results obtained confirm the applicability of this method of analysis. (auth)

11205 (NYO–3136-2, App. 4) LIGHT BULB STATISTICS. Mantel, Nathan; Pasternack, Bernard (New York Univ., N. Y. Inst. of Environmental Medicine). 14p.

Using the concept of an idealized light bulb, one subject to a constant probability of failure while in use, certain distribution problems are solved heuristically. These include: (1) The distribution of sums, or differences, of products of pairs of independent standard normal deviates; (2) The distribution of the difference of 2 chi squares, each with even degrees of freedom or, equivalently, the difference between 2 total waiting times; (3) the distribution of the ratio of 2 chi squares, each with even degrees of freedom or, equivalently, the ratio of 2 total waiting times; (4) Distributions arising in a simple exponential growth process. (auth)

11206 (TID–22529) CHEBYSHEV POLYNOMIAL APPROXIMATIONS FOR THE L-MEMBRANE EIGENVALUE PROBLEM. Mason, J. C. (Maryland Univ., College Park. Inst. for Fluid Dynamics and Applied Mathematics). Jan. 1966. Contract AT(40-1)-3443. 28p. (BN–428). Dep. mn. CFSTI $2.00 cy, $0.50 mn.

A method is proposed for the solution of partial differential equations in terms of two-dimensional Chebyshev series. The method is a generalization of the "selected points" method described by Lanczos for solving ordinary differential equations. Some indications are given of the possible applications of the method, and it is applied in detail to a particular example, the eigenvalue problem for a vibrating L-shaped membrane. (auth)

11207 (UCRL–7737) FORTRAN-FORTRAN. Mendicino, S.; Storch, D.; Sutherland, G. (Lawrence Radiation Lab., Univ. of California, Livermore). Nov. 11, 1964. Contract W-7405-eng-48. 15p. Dep. mn. CFSTI $1.00 cy, $0.50 mn.

The implementation of a machine-independent FORTRAN II compiler written in the FORTRAN II language is described. The hierarchy, path of flow, and assembly passes are discussed. (auth)

11208 (UCRL–12220) AUTO-DEBUG—A MACHINE-LEVEL DEBUGGING PROGRAM. Schoonover, Edward (Lawrence Radiation Lab., Univ. of California, Livermore). Dec. 3, 1964. Contract W-7405-eng-48. 34p. Dep. mn; CFSTI $2.00 cy, $0.50 mn.

An intensified effort is currently in progress to give the user of the various systems a cross compatibility in Fortran source language for computers. A working tool, Auto-Debug, whose purpose is to answer questions of why codes don't perform as planned, or why a code runs on one machine but not on another, and to rapidly seek out errors and give the status of operating efficiency is described. (auth)

11209 ON EXPANDING THE EXPONENTIAL. Kumar, Kailash (Australian National Univ., Canberra). J. Math. Phys. (N. Y.), 6: 1928-34(Dec. 1965).

Systematic methods for generating various expansions of the function $\exp(a + \lambda b)t$, of noncommuting operators a and b, are presented. The usual perturbation expansion in powers of λ, and several other formulas found in the earlier literature occur as special cases. Brief remarks about relative merits and physical applications are made. (auth)

11210 MEASURES ON INFINITE DIMENSIONAL VECTOR SPACES. Umemura, Yasuo (Kyoto Univ.). Pub. Res. Inst. Math. Sci., Ser. A, 1: 1-47(July 1965).

A proof is given of non-existence of translationally quasi-invariant measure on infinite dimensional vector spaces using a modification of Weil's theorem on invariant measures on groups, which was firstly proved by Sudakov. Minlos' theorem is proved for nuclear spaces. The original Minlos' theorem required more restrictions, but actually only the nuclearity condition is necessary. Infinite dimensional Gaussian measures are discussed, and it is proved that a rotationally invariant measure can be characterized as a superposition of Gaussian ones. For this fact, infinite dimensionality is essential. Some applications are noted. (auth)

11211 CARRIERS OF CONTINUOUS MEASURES IN A HILBERTIAN NORM. Umemura, Yasuo (Kyoto Univ.). Pub. Res. Inst. Math. Sci., Ser. A, 1: 49-54(July 1965).

From the standpoint of the theory of measures on the dual space of a nuclear space, the carrier of Wiener measure is discussed, regarding it as a measure on (D′) (= Schwartz's space of distributions). This may be contrasted with the usual treatment which regards it as a measure on the space of paths. It is shown that for $\alpha > 1/2$, integral operator I_α is nuclear on $L^2(0, 1)$ ($\equiv H_0$). Using this fact, we see that Wiener measure lies on the space $I_\beta(H_0)$ ($\beta < 1/2$) which consists of Hölder continuous functions of the β-th order in the sense of L^2. This result is true for any measure whose characteristic functional is continuous on $L^2(0, 1)$. (auth)

METALS, CERAMICS, AND OTHER MATERIALS

General

11212 (BMI-X-10143) FISSION-PRODUCT REACTIONS WITH AND RELEASE FROM FUEL-ELEMENT CLADDINGS. Quarterly Progress Report for July–September 1965. Sunderman, Duane N.; Morrison, David L.; Howes, James E. Jr.; Jablonowski, Edward J. (Battelle Memorial Inst., Columbus, Ohio). Oct. 1, 1965. Contract W-7405-eng-92. 8p. (EURAEC-1496). Dep. mn; CFSTI $1.00 cy, $0.50 mn.

Work Performed under United States–Euratom Joint Research and Development Program.

Experiments were undertaken to determine the effects of fission product concentration on diffusion in specimens of high-purity Fe–20 wt % Cr, on Fe–29 wt % Ni–13 wt % Cr specimens and on Fe–19 wt % Ni specimens. Experiments were also conducted to determine the fission-product diffusion rate in high-purity alloys during high-temperature irradiation. Data are included on irradiation conditions. Results of calculations of diffusion coefficients for Fe–Ni, Fe–Ni–Cr, and Fe–20 wt % are included. (J.R.D.)

11213 (BNWL-37) PLUTONIUM METALLURGY NOTEBOOK. Hasbrouck, M. E. (comp.); Burns, M. P. (ed.) (Battelle-Northwest, Richland, Wash. Pacific Northwest Lab.). Sept. 1965. Contract AT(45-1)-1830. 211p. Dep. mn. CFSTI $6.00 cy, $1.25 mn.

A compilation of data on the structure and properties of plutonium and its alloys is presented. Included are phase diagrams, crystal structure data, transformation kinetics, physical and mechanical properties, corrosion and corrosive properties, and radiation effects information. The information is current to September 1964. (W.L.G.)

11214 (NASA-CR-54717) SNAP-8 MATERIALS REPORT FOR JANUARY–JUNE 1964. VOLUME II. DEVELOPMENT OF COMPONENT MATERIALS. Report No. 2880. Derow, H.; Farwell, B. E. (Aerojet-General Corp., Azusa, Calif.). July 1964. Contract NAS-5-417. 68p.

Post-test analyses were performed on two experimental single-tube Hg boilers, each of which operated for approximately 250 hr. One boiler utilized type 316 stainless steel Hg-containment tubing, and the other utilized 9Cr–1Mo steel. The stainless steel boiler tube was attacked by the Hg, but no attack on the 9Cr–1Mo boiler tube was discernible. A typical leached corrosion layer was found on the stainless steel boiler tube. An evaluation of cold pressure welds between Ni and 6061-T6 Al alloy was completed. Specimens were evaluated by means of tension and torsion tests and metallographic study in the as-received condition and after thermal cycling between 70 and 500°F. The joint was found to be sound. Prototype refractory/316 stainless steel bimetal tubes were evaluated. Pure Nb and Nb–1Zr alloy were used as tube-liner materials. Only the pure Nb/316 stainless steel combination was found to be satisfactory. Thermal exposure of flat, multimetal-layered sheet specimens was started. These specimens contain various candidate interface systems that are being considered as means of preventing potentially detrimental diffusion effects and brittle-phase formation at the Nb/316 stainless steel interface. Work was started on the development of a rolled and welded tube-to-tube-sheet joint to replace a welded and back-brazed joint. The tube-to-tube-sheet weld parameters required modification because the rolling operation, which is performed prior to welding, produced a more intimate fit between the tube and the tube sheet. A slight increase in the weld current produced satisfactory weld penetration. More consistent weld contours and penetrations were produced in welding the rolled tube as compared with the non-rolled design. Eleven different turbine blade and nozzle materials were evaluated for resistance to erosion by elevated-temperature wet Hg. Twenty-one samples of these materials were exposed to 85%-quality vapor at 640°F flowing at 1000 ft/sec. Stellite 6B exhibited the greatest resistance to erosion and was recommended as the material to be used. Studies were conducted to facilitate the welding of various SNAP-8 system components. A procedure was devised for local stress relief of welds connecting Conoseal flanges to components fabricated from 9Cr–1Mo steel. These welds must be stress-relieved without heating the Conoseal above approximately 500°F to maintain critical flange dimensions for proper sealing. A procedure was devised whereby the weld is heated to the stress-relieving temperature, using an induction heater, and the Conoseal flange and component are protected by water-cooling coils wrapped around the pipe approximately ½ in. on both sides of the weld. Short-time elevated-temperature and room-temperature tensile tests were performed on welded and unwelded 9Cr–1Mo steel sheet. The unwelded specimens exhibited greater strength at all temperatures (1250 to 1325°F), although all the specimens had been heat-treated together. At 1300°F the ultimate tensile strength of the welded material was approximately 14% lower than that of the unwelded material, and the yield strength was approximately 20% lower. The reason for the difference is not apparent. Test capsules were completed that contained a 9Cr–1Mo/316 stainless steel transition joint that was fabricated using type 310 stainless steel weld-filler metal. The specimens were exposed to a nominal temperature of 1325°F and a nominal tube-wall stress of 1100 psi. Thirteen cycles of a scheduled 25-cycle test series were completed. (W.L.G.)

11215 (NASA-CR-54718) SNAP-8 MATERIALS REPORT FOR JULY–DECEMBER 1964. Report No. 2989. Derow, H.; Farwell, B. E. (Aerojet-General Corp., Azusa, Calif.). Jan. 1965. Contract NAS5-417. 90p.

Investigations of materials were initiated, or continued, in areas where the established state of the art was not well enough developed to permit a reliable material selection, and to assist in the design, development, fabrication, and testing of various SNAP-8 components. A Hg forced-convection corrosion-loop investigation was continued with the aim of evaluating the corrosion resistance of 9Cr–1Mo alloy steel for 10,000-hr service. Work was also initiated or continued, on evaluation of the resistance to Hg corrosion of candidate backup Hg-containment materials. Data were developed to substantiate the selection of 9Cr–1Mo steel as the Hg-containment material for the SNAP-8 system, and to evaluate potential problems related to its use. (auth)

11216 (PEL-79) AN ELECTROLYTIC JET MACHINING METHOD FOR CUTTING SINGLE CRYSTAL AND POLYCRYSTALLINE URANIUM CARBIDE. Louw, H. N. J.; Schmitt, R. J.; Sole, M. J. (Atomic Energy Board, Pelindaba (South Africa)). June 1965. 9p. Dep. mn.

A goniometer is used to position the specimen at the desired angle to the high-pressure knife-like jet of electrolyte. A large d-c voltage is applied between the specimen and the cathode, which is incorporated in the jet nozzle. The construction of the jet nozzle and the electrolyte pumping system is described and the composition of electrolyte used is given. (W.L.G.)

11217 (WANL-PR(Q)-007) DEVELOPMENT OF DISPERSION STRENGTHENED TANTALUM BASE ALLOY. Quarterly Progress Report No. 6, February 20–May 19, 1965. Buckman, R. W. Jr.; Goodspeed, R. C. (Westinghouse Electric Corp., Pittsburgh, Pa. Astronuclear Lab.). Contract NAS-3-2542. 64p. (NASA-CR-54658).

Development of dispersion strengthened Ta-base alloys for use in advanced space power systems continued with the melting of the first 4-in. dia ingot sheet and tubing alloy composition (Ta–8W–1Re–0.7Hf–0.025C). Three additional alloys were produced into 2-in. dia ingots as part of the composition optimization phase of the program. Six of

the planned seven ingots to be produced for this optimization study are in various stages of preparation and evaluation. Phase identification and morphology studies were initiated on a number of alloys using optical and electron microscopy, x-ray, and electron diffraction techniques, and electron beam microprobe analysis. Metallographic procedures for these alloys are detailed. (auth)

11218 ZONE REFINING OF MOLYBDENUM IN HIGH VACUUM. Ivanovskii, G. F.; Zagorskaya, T. N. Izv. Akad. Nauk SSSR, Metal., No. 3, 65-9(May-June 1965). (In Russian).

The effectiveness of high-vacuum zone refining in the absence of oil vapors and gases was investigated. Mo rods 5–7 mm in dia were zone refined in a vacuum of 10^{-7} torr with the oil vapor in the melting chamber removed by means of an ion-getter pump. Prior to zone refining the specimens were outgased at a temperature increasing gradually from 500 to 2500°C. Two passes at a speed of 0.8 mm/min yielded single crystals 3–4 mm in dia and 30–70 mm long with a hardness of 140–160 kg/mm^2, compared to the original 350 kg/mm^2. The crystals could be easily bent into rings. The ratio of room-temperature electrical conductivity to that at the liquid-He temperature varied from 1400 to 1600 compared with 900 in conventionally zone-refined single crystals. The main gas components evolving during outgasing and melting were H_2, CO, CO_2, CH_4, and H_2O. CO and CO_2 are formed from O_2 and H_2 dissolved in Mo; CH_4 is probably formed by dissolved H_2 and C. It is assumed that the quality of single crystals significantly depends on the ratio of C and O_2 in the original Mo, since the removal of these impurities proceeds mainly via CO and CO_2. H_2 is the most difficult to remove. (ATD)

11219 PRODUCTION OF COPPER, MOLYBDENUM, AND TUNGSTEN POWDERS BY ATOMIZATION WITH A PLASMA JET. Krasnov, A. N.; Samsonov, G. V.; Sleptsov, V. M. Izv. Akad. Nauk SSSR, Metal., No. 3, 70-2(May-June 1965). (In Russian).

The production of Cu, Mo, and W powders with spherical particles 100–400 μ in size by means of plasma-jet atomization was investigated. Metal wire 1 mm in dia was fed at a speed of 7.0 m/min and the plasma-forming gas (Ar) was fed under a pressure of 1.2 atm at a rate of 35 l/m. The arc gap was 7 mm. Atomized powders were cooled in water or engine oil. The distance between the torch nozzle and the cooling medium was varied from 120 to 1500 mm. Cu and Mo powders with spherical particles were produced with cooling in water or oil, regardless of the distance between the torch nozzle and the cooling medium. W powders with spherical particles were obtained when the torch nozzle was more than 1200 mm distant from the cooling medium, regardless of the nature of the cooling medium. At smaller distances the powder particles had irregular shapes. (ATD)

11220 ON THE TECHNIQUES FOR OBSERVING FISSION GAS BUBBLES IN URANIUM. Bainbridge, J. E.; Hudson, B. (Atomic Energy Research Establishment, Harwell, Eng.). J. Nucl. Mater., 17: 237-44(Nov. 1965). (AERE-R-4965).

Replicas taken from cathodically vacuum etched and fractured surfaces were compared with the results from thin-film electron microscopy to determine the limitation of each technique. Cathodic etching enlarged bubbles ~150 Å diameter by a factor of ~2; only cleavage surfaces from the fracture produced results comparable with the bubble size distributions obtained by using other techniques. With bubbles >500 Å the thin-film technique was no longer reliable. An experimental value for the surface energy of α-uranium of 1000 erg/cm^2 was obtained. (auth)

11221 HYDROGEN PICK-UP IN ZIRCONIUM ALLOYS. Nippon Genshiryoku Gakkaishi, 7: 703-12(Dec. 1965). (In Japanese).

The effect of hydrogen on Zr alloys used for fuel cladding is considered. Corrosion tests were performed to clarify the relation between coolant water conditions and hydrogen pickup. The factors considered were the composition of the alloys (Zircaloy-2 and -4), as well as the gas content (oxygen, hydrogen, and fluorine ion), pH, temperature, and pressure of the water. Among these, the amount of fluorine ion and temperature were found to be the only factors with appreciable effect on hydrogen absorption. The effects of alloying elements (Be, V, Y, and Nb) on hydrogen distribution in Zircaloy under a temperature gradient were examined. The shift of the hydrogen peak was observed to be influenced in different ways according to the alloying element added. The effects of hydrogen content on the mechanical properties of the alloys were studied. In the tensile test no appreciable effect of hydrogen content up to 300 ppM was observed. In the burst test little influence of absorbed hydrogen on the burst strength of Zircaloy-2 tubing was discerned, but severer cracking in the tubing as well as increasing tendency toward brittleness was apparent with increasing hydrogen content. (auth)

11222 INTEGRITY OF REACTOR FUELS. Peterson, Sigfred Nucl. Safety, 6: 398-403; 404-7(Summer 1965).

A review of information on reactor fuel integrity is presented. Discussions are included on U-base fuels, Al-base fuels, miscellaneous metallic fuels, stainless-steel-base dispersions of UO_2, UO_2 performance in water reactors and gas-cooled reactors, graphite-base fuels and other ceramic fuels. (J.R.D.)

11223 REACTOR MATERIALS. Volume 8, Number 4. Dayton, R. W.; Simons, E. M.; Endebrock, R. W. (eds.). Contract W-7405-eng-92. One of the five Quarterly Technical Progress Reviews published for the Division of Technical Information, USAEC. Battelle Memorial Inst., Columbus, Ohio, Winter 1965-1966. GPO $0.70 Domestic, $0.90 Foreign.

Separate abstracts were prepared for the 5 sections in the review. (W.L.G.)

For abstracts of individual sections see: 11224–11227, and 11260.

11224 FUEL AND FERTILE MATERIALS. Reactor Mater., 8: 175-95(Winter 1965-1966).

A review of recent research developments in fuel and fertile materials is presented. (86 references). (W.L.G.)

11225 MODERATOR MATERIALS. Reactor Mater., 8: 196-203(Winter 1965-1966).

A review of recent research developments in moderator materials is presented. (24 references). (W.L.G.)

11226 NUCLEAR POISONS. Reactor Mater., 8: 204-5 (Winter 1965-1966).

A review of recent research developments in nuclear poisons is presented. (6 references). (W.L.G.)

11227 CLADDING AND STRUCTURAL MATERIALS. Reactor Mater., 8: 206-24(Winter 1965-1966).

A summary of recent research developments in cladding and structural materials is presented. (93 references). (W.L.G.)

11228 INVESTIGATION OF THE CONDITIONS OF CARBON AND BORON SURFACE SATURATION IN REFRACTORY TRANSITION METALS. Samsonov, G. V.; Epik, A. P. pp 132-9 of Issled. Stalei i Splavov. Moscow, Nauka, 1964. (In Russian).

The processes of C and B diffusion saturation of Ti, Zr, Mo, and W, and those of B diffusion saturation of Nb and Ta, were investigated by x-ray, chemical and metallographic methods. Nb, Ta, Mo, and W were borated at 1100-1400°C, Ti and Zr at 1100-1500°C, Ti and Zr were carburized at 900-1300°C, Mo at 1400-1700°C, W at 1600-1900°C. The holding time at each temperature was 1, 2, 4, 6, and 8 hr. The phase composition of the layers was determined and dependence of their structure on the conditions of preparation investigated. It is shown that the layers grow as a result of the one-sided diffusion of C or B atoms in the metal through the phase which is formed on the surface. It was established that the technological properties of the diffusion layer become worse with the increase in its thickness: the cohesion with the base becomes weaker, the porosity, brittleness, the number and

dimensions of cracks in the layer increase. Layers less than 50–70 μ thick have satisfactory properties. The reaction diffusion constants and the temperature dependence of the coefficient of C and B in the investigated metals are determined. (Rev. Metal Lit.).

11229 RADIATION-SHIELDING CONCRETE INCORPORATING BORON CARBIDE. Ito, Norio (to Onoda Cement Co., Ltd.). Japanese Patent 1964-24897. Nov. 5, 1964. Filed June 8, 1962.

A radiation-shielding concrete is proposed in which boron carbide is used as an aggregate. It differs from shields in which boron carbide is mixed with aluminum and a plastic such as a synthetic resin. (NSA of Japan)

Corrosion

Refer also to abstracts 12330, 12380, and 12457.

11230 (BM-RI-6715) CORROSION PROPERTIES OF MOLYBDENUM, TUNGSTEN, VANADIUM, AND SOME VANADIUM ALLOYS. Acherman, W. L.; Carter, J. P.; Kenahan, C. B.; Schlain, David (Bureau of Mines, Washington, D. C.). Apr. 1965. 63p. Bureau of Mines Free.

Mo, W, and V were found to possess generally superior chemical and galvanic corrosion properties in many aqueous corrosive media at temperatures up to the boiling point. The corrosion resistance of V in certain solutions was further improved by alloying it with such metals as Nb, Ta, and Ti. W was susceptible to a type of crevice corrosion in mercuric chloride solutions, but no other instances of crevice corrosion were encountered. With few exceptions, Mo, W, and V were not adversely affected when coupled with dissimilar metals in galvanic corrosion experiments; in some cases one or both members of a couple were protected by contact. When exposed to aqueous ammonia spray at 60°C, all three metals were moderately attacked, but they were resistant in spray environments of substitute ocean water and ammonium dihydrogen phosphate. (auth)

11231 (CEA-R-2815) CONTRIBUTION A L'ETUDE DE LA CORROSION PAR PIQURES DU MAGNESIUM ET DE SES ALLIAGES [Theses]. (Contribution to the Study of Pitting Corrosion of Magnesium and its Alloys [Thesis]). Blanchet, Jean (Commissariat a l'Energie Atomique, Saclay (France). Centre d'Etudes Nucleaires). 1965. 51p. Dep. mn.

The pitting attack of magnesium and its alloys was studied by means of potentiokinetic polarization curves; the following parameters have been considered: structural state and composition of the metal; chloride concentration; and pH of the medium. The electrochemical data obtained demonstrate that at pH 12, a localized corrosion might appear as soon as a 10^{-3} M NaCl concentration is reached; on the other hand, at pH = 13, a much higher concentration (five times) has no effect. In the same conditions, the coupling of magnesium with various noble materials (graphite, platinum, 18/10 stainless steel) also severely increases its susceptibility to pitting, but only when chloride ions are present in the solution. Usual corrosion tests confirmed these electrochemical results. A micrographic study of the pits showed that their morphology is connected with the metallurgical state of the specimens. (auth)

11232 (INR-644/XIV/PS) INTERNAL OXIDATION OF Fe–Al ALLOYS. Matyja, Henryk; Bieszkiewcz, Jan (Institute of Nuclear Research, Warsaw (Poland)). July 1965. 27p.

The oxidation conditions that do not lead to formation of external zone of iron oxides were found. The kinetics of the internal oxidation process were studied, and from the parabolic growth rate law: $x^2 = kt$ for 800, 900, 1000, and 1050°C, the activation energies were calculated. It was proved that as the concentration of Al increases the depth of penetration decreases and on the samples with 5.18 wt % Al the internal oxidation process was not observed. (auth)

11233 (COO-1319-32) A STUDY OF THE MECHANISM OF STRESS CORROSION CRACKING IN THE IRON–NICKEL–CHROMIUM ALLOY SYSTEM. Quarterly Report, June 17, 1965–September 16, 1965. Staehle, R. W. (Ohio State Univ. Research Foundation, Columbus). Nov. 12, 1965. Contract AT(11-1)-1319. 54p. Dep. mn. CFSTI $3.00 cy, $0.50 mn.

Developments are reported for experiments on: time to cracking as affected by alloy, stress, dissolved oxygen, and sodium chloride; tensile properties as affected by temperature and alloy content; frequency of annealing twins as affected by alloy, cold work, and annealing temperature; electron metallography; and electrochemical studies. Work is under way to modify the circulating autoclave system in order to improve monitoring of data and to obtain better control of variables. (auth)

11234 (IS-1300) VAPORIZATION OF SOLID UO_2. Held, Peter Christian; Wilder, D. R. (Ames Lab., Iowa State Univ. of Science and Tech.). Nov. 1965. Contract W-7405-eng-82. 122p. Dep. mn. CFSTI $4.00 cy, $0.75 mn.

Uranium dioxide pellets were heated to 1890 to 2070°C in oxidizing, neutral and vacuum atmospheres. The condensed vapors were studied to determine the vaporization mechanism of uranium oxides. The condensates had nearly the same composition as the surface of the heated pellets at these temperatures, irrespective of the ambient atmosphere or pressure. This indicates that the percentage of oxide species, as opposed to oxygen vapor, over uranium oxides increases at high temperatures. Oxidation-reduction mechanisms for the vaporization of uranium oxides are thus ruled out since they would imply a memory for the parent material. An exception could occur in the vaporization of U_3O_8 as UO_3 gas, which would break down to U_3O_8 when condensed, due to the instability of UO_3 as a solid phase. A discussion of the vaporization behavior of uranium oxides from previous research efforts is included. (auth)

11235 (MSAR-65-194) EFFECT OF HIGH TEMPERATURE SODIUM ON AUSTENITIC AND FERRITIC STEELS. TOPICAL REPORT NO. 4. RESULTS OF MECHANICAL PROPERTIES TESTS OF 316 SS SPECIMENS IN 1200 F SODIUM CONTAMINATED WITH CARBON. Andrews, R. C.; Hiltz, R. H.; Kirschler, L. H.; Rodgers, S. J.; Tepper, F. (MSA Research Corp., Callery, Pa.). Dec. 1965. Contract AT(11-1)-765. 135p. Dep. mn. CFSTI $4.00 cy, $1.00 mn.

The mechanical properties of one heat of type 316 stainless steel were measured in a dynamic sodium system contaminated with carbon at 1200°F. The effects of carburization were evaluated by comparing these mechanical properties in the high-carbon sodium environment with the mechanical properties of the same heat in air, helium, and low-oxygen sodium. Both as received and 4000-hr exposed material were tested. Creep rupture and fatigue tests were conducted in the flowing sodium system, while tensile tests were conducted in air and helium at both room temperature and test temperature on exposed material. Impact tests were conducted in air at room temperature. In addition, monitoring tabs of type 316 and 304 stainless steels, 2¼ Cr–1 Mo steel, and Armco Iron were exposed to the high-carbon sodium environment for durations in excess of 5000 hrs. Metallurgical techniques used in post-test evaluation of the specimens and tabs included carbon analyses, microhardness measurements, microprobe analyses, metallographic analyses, standard x-ray diffraction, and chemical analyses of the extracted carbide phases. Carburization rates of the type 304 and 316 stainless steels are discussed and long-time predicted rates from short-time exposures were compared with actual measured long-time rates. Sodium chemistry, with emphasis on carbon analyses, is discussed as well as operation and post-test examinations. (auth)

11236 SILICONIZING TO PROTECT MOLYBDENUM. Colan, H.; Domsa, A.; Palfalva, A.; Nicholae, V.; Botha, I. Bul. Stiint. Inst. Politeh. Cluj, No. 7, 237-47(1964). (In Rumanian).

A method of applying protective silicide coatings to a Mo article from a Cu–Si system is described. Powder

metallurgical methods were used to make the Cu–Si alloy, of roughly eutectic composition, with 12–20% Si. The Mo article was immersed in the alloy, melted at 1200 to 1250°C in a protective atmosphere. At the point of contact of Mo and the Cu–Si alloy, a layer of $MoSi_4$ appears on the Mo surface. Residence of 50–75 min gives a layer 100 to 150 μ thick. As a result of diffusion, silicides Mo_3Si_2 and Mo_3Si form on the Mo–$MoSi_2$ boundary, but these layers are only a few parts of a μ thick. $MoSi_2$ affords reliable protection for Mo and the Mo article can be used in an oxidizing atmosphere at 1600°C. The SiO_2 film formed on the surface of the Mo article in such a case protects it from further oxidation. Siliconizing from a fused system gives dense coatings of sufficient thickness, firmly bonded to the Mo base. (Rev. Metal Lit.).

11237 DISINTEGRATION OF TUNGSTEN DISILICIDES DURING OXIDATION IN AIR. Nechiporenko, E. P.; Efimenko, L. N.; Matyushenko, N. N.; Verkhorobin, L. F. (Inst. of Physics and Tech., Academy of Sciences, Ukrainian SSR). Fiz. Metal. Metalloved., 20: 531-4(Oct. 1965). (In Russian).

Specimens of tungsten disilicide, prepared from 99.9%-pure W and Si powders either by hot compacting at 1700°C, by cold compacting and sintering in an Ar atmosphere at 1000°C for 1 hr, or by siliconizing of W in a vacuum of 10^{-5} mm Hg at 1250°C, had a porosity of 3, 40, or 0%, respectively. All specimens were tested for oxidation behavior in air at 600 to 1100°C. Hot compacted, and cold compacted and sintered specimens gradually disintegrated into yellow powder at 700 to 1000°C. On specimens obtained by vacuum-siliconizing, an oxide layer was formed which prevented disintegration. These results showed that the oxidation failure of homogeneous WSi_2 was not a specific property of the material but was caused by macrodefects (pores). In all cases, disintegration occurred in the temperature range where the oxidation products are not volatile. The oxidation behavior of poreless WSi_2 indicated that disintegration of porous WSi_2 specimens is associated with the accumulation of oxidation products and the accompanying increase in volume. (JPRS)

Fabrication

Refer also to abstracts 12377, 12396, 12397, and 12404.

11238 (CONF-650449-1) DEVELOPMENT AND EVALUATION OF A HOMOGENEOUS W–25Re ALLOY FOR 2600 deg C APPLICATIONS. Baxter, W. G.; Tarr, C. O.; McGurty, J. A. (General Electric Co., Cincinnati, Ohio. Nuclear Materials and Propulsion Operation). [1965]. Contract AT(40-1)-2847. 15p. (GE-TM-65-2-18). Dep. mn. CFSTI $1.00 cy, $0.50 mn.

From 6th Annual Structures and Metals Conference, Palm Springs, Calif.

Fabrication procedures were developed which result in an homogeneous W – 25Re alloy. Sheet, tubing, and rods were successfully fabricated with homogeneous structures. The properly processed alloy has low impurity content, is resistant to forming porous areas in welding, and has room-temperature bend ductility after heating at 2200 to 2600°C. Creep-rupture properties at 2600°C in H_2 are improved in laboratory-produced homogeneous W – 25Re sheet when compared to commercially produced sheet. Brazed commercial sheet and electron-beam welded homogeneous sheet creep-rupture specimens demonstrated acceptable strength at 1600°C in hydrogen. (auth)

11239 (EURAEC-1468) METHODS FOR THE FABRICATION OF PRESSURE VESSELS. Quarterly Report No. 13, April 1–June 30, 1965. (Neratoom, N. V., The Hague (Netherlands)). Contract 069-61-12RDN. 43p. (EUR-2391). Dep. mn. CFSTI $2.00 cy, $0.50 mn.

Work Performed under United States–Euratom Joint Research and Development Program.

The microstructures, mechanical properties, and chemical analyses of welds in 200 mm thick plates of 1.2 MD07 steel are given. The welds were produced by the boxed CO_2 method using three electrodes. (W.L.G.)

11240 (EURAEC-1520) STUDIES ON THE BRITTLE FRACTURE STRENGTH OF HEAVY-GAGE STEEL PLATE. Final Report No. 1. Constant; Prudhomme (Institut de Recherches de la Siderurgie, St. Germaine-en-Laye (France); Weisz; Le Bret; Obermosser (Commissariat a l'Energie Atomique, Saclay (France). Centre d'Etudes Nucleaires). [1965]. Contract 038-60-12-RDF. 29p. (EUR-2672). Dep. mn. CFSTI $2.00 cy, $0.50 mn.

Work Performed under United States–Euratom Joint Research and Development Program.

The development of a bend test to obtain detailed data on the brittle fracture phenomena encountered in welded and unwelded steel plates 200 mm thick is described. Preliminary results indicate that the transition temperature of specimens containing five scattered welds is higher than that of specimens containing one single central weld, regardless of whether this weld consists of one bead or five jointed beads. The brittle zone caused by several beads deposited alongside each other was not greater than that caused by one bead. (W.L.G.)

11241 (TID-8541, pp 71-148) THE REMOTE FABRICATION OF REACTOR FUELS. Shuck, A. B. (Argonne National Lab., Ill.); Lotts, A. L. (Oak Ridge National Lab., Tenn.); Drumheller, Kirk (Battelle-Northwest, Richland, Wash. Pacific Northwest Lab.).

Fabrication of fuels for the following three fuel cycles is reviewed; plutonium recycle in thermal-converter reactors, plutonium recycle in fast breeder reactors, and the Th–^{233}U cycle for thermal-converter and breeder reactors. The hazards associated with the fabrication process are discussed. (M.O.W.)

11242 (UCRL-12153) THE FUSION BONDING OF PLASMA-SPRAYED TUNGSTEN COATINGS TO STEEL. Landingham, Richard L.; Damon, Robert A.; Murphy, Daniel J. (Lawrence Radiation Lab., Univ. of California, Livermore). Nov. 2, 1964. Contract W-7405-eng-48. 22p. Dep. mn. CFSTI $1.00 cy, $0.50 mn.

Methods and conditions for obtaining strong fusion-bonding of plasma-jet-sprayed coatings were investigated using a basic system of tungsten sprayed on 1020 steel. Bonds were evaluated by various metallurgical, mechanical, and thermal-shock tests to determine the coating conditions and techniques which produced optimum bonding. (auth)

11243 (WANL-PR(EE)-001) EVALUATION OF REFRACTORY/AUSTENITIC BIMETAL COMBINATIONS. First Quarterly Progress Report, June 22, 1965–September 22, 1965. Godshall, J. L.; Buckman, R. W. Jr. (Westinghouse Electric Corp., Pittsburgh, Pa. Astronuclear Lab.). Contract NAS 3-7634. 32p.

Sixteen refractory/austenitic bimetal combinations produced by explosive bonding were evaluated for bond integrity by ultrasonic resonance and dye penetrant techniques, metallographic examination, and reverse bend and tensile tests. Nine combinations were selected for complete evaluation of thermal stability. (auth)

11244 (Y-MA-450) THE PREPARATION OF HIGHLY ENRICHED U_3O_8 FOR THE HIGH FLUX ISOTOPE REACTOR CORE. Barkman, J. R. (Union Carbide Corp., Oak Ridge, Tenn. Y-12 Plant). Feb. 1, 1966. Contract W-7405-eng-26. 11p. Dep. mn. CFSTI $1.00 cy, $0.50 mn.

Uranium fuel for the core of the High Flux Isotope Reactor (HFIR) was prepared in the form of a sintered U_3O_8 with a size range of 44 to 88 μ. The basic preparation method consisted of the precipitation of a solution of uranyl nitrate with H_2O_2, followed by calcining and sizing operations. The process was essentially a batch-type operation utilizing laboratory-type equipment because of the geometry restrictions imposed by nuclear safety and the availability of the equipment from other oxide production programs. Chemical and physical test data are appended. (P.C.H.)

11245 PREPARATION AND PROPERTIES OF URANIUM FUEL. Cordfunke, E. H. P. Atoomenergie Haar Toepass., 7: 171-81(Sept. 1965). (In Dutch).

After a brief description of the production of uranium

from ores, the preparation of the principal uranium compounds is described. The properties of uranium in connection with its utilization as a reactor fuel are discussed, with emphasis on uranium dioxide. (tr-auth)

11246 AUTOMATIC INERT GAS TUNGSTEN ARC WELDING APPLIED TO NUCLEAR ENGINEERING PROBLEMS. Gotch, R. W. Brit. Weld. J., 12: 276-80(June 1965).

A description of the pressurizer electric heater root welding torch (argon cooled) and of the water-cooled internal tube welding torch, which is based on the argon tungsten arc principles, is given. Details of the method devised for fusion welding of tubes to headers in nuclear steam generators are reported. The process is suitable for welding the following materials: 1% Cr–0.5% Mo steels, low (less than 0.17%) carbon mild steels and AISI type 321, 304 stainless steels. (Rev. Metal Lit.).

11247 C.N.E.N.'S FUEL ELEMENT FABRICATION AND CONTROL LABORATORIES AT SALUGGIA. Colombi, G.; Gabaglio, M.; Liscia, A. (CNEN, Saluggia, Italy). Comit. Naz. Energia Nucl., Notiz., 11: No. 10, 25-37(Oct. 1965). (In Italian).

The equipment at the fuel element fabrication and control laboratories is described and the work performed is discussed. The fabrication of the fuel elements for the Avogadro reactor is described. (J.S.R.)

11248 NON-STOICHIOMETRIC ZIRCONIA AND STABILIZATION OF TETRAGONAL ZIRCONIA. Livage, Jacques; Mazieres, Charles (ENSCP, Paris). Compt. Rend., 261: 4433-5(Nov. 22, 1965). (In French).

A radiocrystallographic study was made of the effect of heat treatments on black nonstoichiometric zirconia obtained by dehydration and heating under vacuum (or under argon) of hydrated zirconium oxide precipitates. The tetragonal form obtained during the crystallization had good stability contrary to what was observed when the procedure was carried out in air ("normal" white zirconia). This stabilization was attributed to oxygen holes. It made it possible to predict the preparation of a pure black zirconia refractory no longer having, at least in inert atmospere, the inconvenience of monoclinic transformation near 1000°C. (tr-auth)

11249 EFFECT OF THE CONDITIONS OF HOT PLASTIC DEFORMATION ON THE STRUCTURE AND PROPERTIES OF MOLYBDENUM, NIOBIUM, AND TITANIUM. Gurevich, Ya. B.; Orzhekhovskii, V. L. Izv. Akad. Nauk SSSR, Metal., No. 4, 137-43(July-Aug. 1965). (In Russian).

An investigation was made of the gas content, structure, and mechanical properties of vacuum-arc melted Mo, Nb, and Ti, hot rolled with a total reduction of 50% in air, Ar, or a vacuum of $5 \cdot 10^{-5}$ mm Hg at temperatures up to 800–1200°C. Hot rolling in air appreciably increased the gas content in Ti and Nb, especially at 800–1200°C. The greatest increase was in the O_2 content; the increases in N_2 and H_2 were somewhat smaller. No noticeable increase in the gas content was observed in Mo rolled at 1000–1200°C, although there was intense oxidation of the metal. No noticeable gas absorption occurred during heating and rolling in vacuum. Heating and rolling of Ti and Nb in an Ar atmosphere, as well as heating in vacuum with subsequent rolling in air, resulted in gas absorption to a degree intermediate between those produced with hot rolling in vacuum and in air. Nb and Ti hot rolled in vacuum were satisfactorily cold rolled at room temperature. However, in Nb and Ti hot rolled in air, a more or less satisfactory plasticity in cold rolling was achieved only after the removal of the surface gas-saturated layer, which was about 1 mm thick. An additional hot rolling in vacuum or in air at 1200°C (Nb and Mo) or at 1100°C (Ti) with a total reduction of 80% resulted in some fragmentation of the α'-phase of Ti. The recrystallized structure of Mo and Nb with almost equiaxial grains became fibrous, with the grains elongated in the direction of rolling. Nb and Ti hot rolled in vacuum had lower tensile and yield strengths and higher ductility than after rolling in air. The metals rolled in air failed in a brittle manner; those rolled in vacuum had a ductile fracture. Rolling in vacuum or in air produced no significant difference in the mechanical properties of Mo. (ATD)

11250 INVESTIGATION OF THE PROCESS OF ACTIVATED SINTERING OF TANTALUM AND HAFNIUM CARBIDES. Panasyuk, A. D. (Inst. of Power Metallurgy and Special Alloys, Academy of Sciences, USSR). Izv. Akad, Nauk SSSR, Neorg. Mater., 1: 1065-70(July 1965). (In Russian).

The process of activated sintering of tantalum or hafnium carbides was investigated. Carbide powders with the addition of 3% ammonium chloride or 2% cobalt chloride were cold compacted and sintered at 2200 to 2800°C for 20 to 100 min. The addition of ammonium chloride was found to reduce substantially the porosity of the carbides. Carbides sintered at 2600 to 2750°C had a porosity of 20 to 25% compared to 38 to 40% in carbides sintered at 2800°C without ammonium chloride. Still better results were obtained in sintering the carbides at 2600 to 2750°C with the addition of 2% cobalt chloride. In this case, the porosity of the sintered products obtained amounted to only 15 to 17%. (CFSTI)

11251 PREFERRED ORIENTATIONS IN ZIRCALOY-2 TUBING MANUFACTURED BY VARIOUS ROUTES. Hindle, E. D.; Slattery, G. F. (United Kingdom Atomic Energy Authority, Salwick, Eng.). J. Inst. Metals, 93: 565-70 (Dec. 1965).

The results are described of preferred-orientation measurements on Zircaloy-2 tubing produced by eleven fabrication routes. The basic orientation of the hot-extruded stock has the basal (0001) poles lying tangential to the circumference, while the poles of the prism planes $(10\bar{1}0)$ are in the axial direction. The effects of tube reduction, cold drawing, or planetary swaging are to spread the orientation of the basal poles and to shift their position of maximum intensity to either side of the tangential direction. A duplex texture (0001) $(11\bar{2}0)$ in the tangential direction was found with two tubes and is probably attributable to variations between end and center of the extruded stock. The highest bursting-stress criterion should be exhibited by tubing with the basal poles oriented radially and this single orientation can be achieved by incorporating a hammer-swaging process. (auth)

11252 THE REDUCTION AND SINTERING OF HYPERSTOICHIOMETRIC CARBIDES IN HYDROGEN. Harder, B. R.; Read, Julia; Sowden, R. G. (Atomic Energy Research Establishment, Harwell, Eng.). J. Nucl. Mater., 17: 203-14(Nov. 1965). (AERE-R-4877).

The reduction by hydrogen of hyperstoichiometric UC and (U,Pu)C to single phase material was studied. It affords a means of removing di- and sesqui-carbide phases and sintering to high density in a single operation. The technique can be used to obtain dense monocarbide pellets from mixtures of UC and Pu_2C_3. Use of undiluted hydrogen is essential to achieve a high rate of carbon removal. (auth)

11253 BEHAVIOR OF MOLYBDENUM POWDERS DURING PRESSING AND SINTERING. Domsa, A.; Palfalvi, A.; Filipescu, Miahela; Nicolae, V.; Botha, L. Metalurgia (Bucharest), 16: 156-8(1964). (In Rumanian).

Mo bars were pressed at 1–10 tons/cm^2 and sintered in H_2 at 1100°C for 90 min. Final sintering was carried out with direct heating of the bars by an electric current, or in a Tammann furnace at 1500 to 2100°C. Experience showed, however, that the best artefacts are obtained by pressing 3–5 tons/cm^2. Where higher pressures are employed, sintering results in cavities, cracks, and flaws on the surface. Sintered bars with 6–10% porosity can be forged, upset or rolled at 1400°C. The specific gravity of the bar can reach the theoretical value once the section of the part is reduced to 50–60% of its original size. (Rev. Metal Lit.).

11254 PYROLYTIC-CARBON COATINGS ON CERAMIC FUEL PARTICLES. Beatty, R. L.; Carlsen, F. A. Jr.; Cook, J. L. (Oak Ridge National Lab., Tenn.). Nucl. Appl., 1: 560-6(Dec. 1965). (ORNL-P-999).

The effects of varying deposition conditions on the properties, especially the structural features, of pyrolytic carbon deposited on ceramic fuel particles in a fluidized bed were systematically investigated. The carbon was formed by thermally decomposing methane on 200-μm-dia uranium carbide particles. Variables considered were deposition temperature, between 1300 and 2000°C, and methane flow rate, between 0.0167 and 2.53 $cm^3/(min\ cm^2)$. It was shown that these variables strongly influence microstructure, density, crystallite size, and preferred orientation of the pyrolytic-carbon coatings. The results are presented as contour maps for property dependence and as a montage of photomicrographs for microstructure dependence. The microhardness of coatings deposited at 1400°C increased with methane flow rate by a factor of 3 over the range of flow rates employed. (auth)

11255 FLUIDIZED-BED PROCESS FOR PRODUCTION OF TUNGSTEN. Oxley, J. H. (Battelle Memorial Inst., Columbus, Ohio); Beidler, E. A.; Blocher, J. M. Jr.; Lyons, C. J.; Park, R. S.; Pearson, J. Nucl. Appl., 1: 567-74(Dec. 1965).

A process was developed for the preparation of high-purity tungsten with unusual resistance to grain growth at elevated temperatures. The hydrogen reduction of tungsten hexafluoride in a fluidized bed of tungsten seed particles was used to prepare the granular product. These granules were then consolidated into various shapes by a gas-pressure-bonding technique. Consolidated bars were rolled to premium quality sheet and strip. (auth)

11256 VAPOR DEPOSITION AND CHARACTERIZATION OF TUNGSTEN–RHENIUM ALLOYS. Federer, J. I.; Leitten, C. F. Jr. (Oak Ridge National Lab., Tenn.). Nucl. Appl., 1: 575-80(Dec. 1965). (ORNL-P-1017).

Deposition of tungsten–rhenium alloys by the simultaneous hydrogen reduction of tungsten and rhenium hexafluorides was studied over the temperature range 450 to 700°C using a total system pressure of 10 torr and a $H_2/(WF_6 + ReF_6)$ ratio of about 20. Deposits formed on the inner wall of heated copper deposition tubes through which the reacting gases passed. Under these conditions the greater ease of reduction of ReF_6 compared to WF_6 resulted in nonuniform deposits having a higher rhenium content near the inlet to the reaction zone than farther downstream. Deposits containing up to 46 wt % Re were prepared. The use of argon with the reacting gases was found to improve homogeneity. The deposits were found to contain total interstitial impurities as low as 50 parts/10^6. The grain structure was typically columnar. X-ray diffraction revealed the presence of two phases that coexisted throughout part of the composition range: an alpha–tungsten (bcc) structure, which was the principal phase in low rhenium deposits, and a previously unreported beta–tungsten phase, which was favored by high rhenium contents. (auth)

11257 THERMOCHEMICAL REDUCTION OF URANIUM HEXAFLUORIDE FOR THE DIRECT FABRICATION OF URANIUM DIOXIDE CERAMIC FUELS. Heestand, R. L.; Leitten, C. F. Jr. (Oak Ridge National Lab., Tenn.). Nucl. Appl., 1: 584-8(Dec. 1965).

A one-step conversion of uranium hexafluoride to uranium dioxide was effected by combining the uranium hexafluoride with hydrogen and oxygen at elevated temperatures and reduced pressures. The product may be deposited as a submicron powder, dendritic crystallites, or a solid approaching theoretical density depending upon reaction pressure and gas-mixing techniques. The stoichiometry of the solid deposit may be controlled by adjusting the ratios of the gaseous reactants. It is anticipated that the process might be optimized for fuels having high enrichments or for reprocessing contaminated fuels, thus giving more-efficient controlled conversion to a desired form. The results also indicate that other refractory oxides may be produced as free-standing bodies through the use of similar techniques. (auth)

11258 FABRICATION OF 20 wt percent Ti–V ALLOY TUBING FOR NUCLEAR FUEL CLADDING. Burt, W. R. Jr.; Krammer, W. C.; Karasek, F. J.; Mayfield, R.M. (Argonne National Lab., Ill.). Nucl. Appl., 1: 589-96(Dec. 1965).

A recently developed technology for the consolidation and fabrication of high-quality small-diameter (<5 mm) thin-wall (<0.55 mm) tubing of 20 wt % Ti–V alloy is described. Compacted vanadium chip and titanium sponge feed rods are electron-beam melted, followed by arc melting of the electron-beam ingot. The arc-cast ingot breakdown is by extrusion. Tube blanks are produced by a secondary extrusion operation. The tube blanks are cold finished by swaging and drawing to the final tube size with intermediate vacuum anneals as required. Problems and solutions are discussed. (auth)

11259 SAFETY REQUIREMENTS FOR WELDING STAINLESS STEEL FOR NUCLEAR REACTOR PLANTS. La Velle, E. B. Oerlikon Schweissmitt, 23: No. 53, 17-25(1965). (In German).

Seam design and corrosion damage as caused by the use of incompatible filler material are described. (Rev. Metal Lit.).

11260 SPECIAL FABRICATION TECHNIQUES. Reactor Mater., 8: 225-33(Winter 1965-1966).

A review of recent developments in special fabrication techniques is presented. (39 references). (W.L.G.)

11261 NUCLEAR SUBMARINES—TECHNIQUES FOR WELDING HY-80. Alm, Robert D. Weld. Design. Fabr., 38: No. 4, 57-61(Apr. 1965).

Yield strength, tensile strength, elongation and Charpy V-notch strength of wrought plate, extrusions, forgings and castings of HY-80 steel are reported. Temperatures for welding, including preheat for welding and tacking, preheat for arc gouging and welding heat input are given. Typical joint design and operational data (welding position, electrode type, flux, preheat temperature and interpass temperature for HY-80 submerged arc welded, metallic inert gas welded and manual metal-arc (coated electrode) welded butt joints are described. Explosion bulge testing of welded HY-80 assemblies and use of radiography, magnetic-particle, liquid penetrant and ultrasonic sound waves in inspecting welds are described. Application of HY-80 steel to construction of nuclear submarine hulls is described. (Rev. Metal Lit.).

11262 ORGANIZATION OF BASIC MATERIALS AUDITING IN A FUEL ELEMENT FABRICATION PLANT. Pinochet, J.; Nadal, J. (Commissariat a l'Energie Atomique, Paris). Vienna, International Atomic Energy Agency, 1965, Preprint No. SM-67/9, 21p. (In French). (CONF-650803-38). ORINS.

From IAEA Symposium on Nuclear Materials Management, Vienna.

The plant chosen as an example is that of the Société Industrielle de Combustibles Nucléaires (SICN) at Annecy, which produces, principally from natural uranium provided by the CEA, fuel elements for reactors of the graphite-gas type. The auditing is carried out by following the movement of basic material from a single casting batch through the fabrication process. The auditing program at Annecy was based on a specific unit, the casting batch. The warehouse is divided into five sections: ingots, batch preparation, scrap, rough-cast rods, and slugs. Records kept include: stock slips and the melting control card, which is filled in at the warehouse when the batch to be sent to the melting shop is made up. At the melting shop, further entries are made in the melting control card and three additional forms are prepared: a card showing the results of melting; the machining and materials-balance card, on which are entered the number of the batch, the total weight and the number of rough-cast rods obtained; and individual rod cards bearing the batch number, which, like the machining cards, accompany the rods back to the warehouse. When rods leave the uranium warehouse a record of their removal is made on a rod stock card; they are delivered to the machine shop accompanied by the appropriate machining and materials-balance card as well as by the individual rod cards. After machining, the useful rods are sent on for degreasing and sandblasting, accompanied by the machining and materials-balance card,

while the recoverable waste is accompanied by the machining waste card. The turnings are sent to the turnings shop accompanied by a transfer slip. The scrap is degreased and returned to the warehouse along with the machining waste card. The useful rods are weighed, and the weight of each is entered in the form of a plus or minus variation from the theoretical weight on the machining card and the individual rod card. They are then sent on for cladding, accompanied by their individual rod cards. After cladding of the useful rods, a slug card is prepared and attached to the individual rod card. Thereafter the batch ceases to exist; each useful rod, and then each slug, is defined by its own number. The useful slugs are individually packed and returned to the warehouse for crating with a packing list. A provisional factory acceptance form is made out for each useful slug. (auth)

11263 WELDING METHOD FOR A CAPSULE. Komuro, Kojiro (to Hitachi, Ltd.). Japanese Patent 1964-18226. Aug. 28, 1964. Filed Sept. 10, 1962.

A welding method for scaling a capsule consists of placing the sample material in the cylindrical or other capsule, closing one or both ends of the capsule with plugs with a hole in the center for introducing a helium or other gas and welding the end plugs on with the holes left open. Then, a heat-conducting gas, such as He, is introduced into the capsule; and the holes are closed with tapered pins, which finally are welded onto the plugs. (TCO)

Properties and Structure

Refer also to abstracts 11063, 12377, 12378, and 12401.

11264 (ACF-14) CRYOGENIC AND ELEVATED TEMPERATURE PROPERTIES OF 7039 ALUMINUM PLATE AND WELDMENTS. Dillon, J. J.; Wallace, L. A. (ACF Industries, Inc., Albuquerque, N. Mex.). Oct. 8, 1965. Contract AT(29-1)-1352. 45p. (ACF-412-262). Dep. mn. CFSTI $2.00 cy, $0.50 mn.

Design-type data for 7039 aluminum base-metal and weldments are reported. Thermal conductivity of 7039-T61 was determined in the temperature range of +400°F to −320°F. The longitudinal and transverse, notched and unnotched, tensile properties of ½ and 1½ in. thick 7039-T61 base-metal were determined at −423, −320, −100, ambient, +200, +300, and +400°F. Similar mechanical properties were obtained for ½ and 1½ in. thick weldments (using X5039 filler wire). Additional mechanical properties were obtained for filler alloys D1495 and D1707 from 1½ in. thick 7039 weldments at temperatures of −423, −320, −100, ambient, and +200°F. All weldments were post-weld heat-treated to the T61 temper. (auth)

11265 (AD-626375) INVESTIGATION OF FRACTURE IN CONNECTION WITH HOT DEFORMATION PROCESSING OF METALS. Final Report. Grant, Nicholas J.; Bridenbaugh, Peter; Greene, Barry; Kane, Robert (Massachusetts Inst. of Tech., Cambridge. Dept. of Metallurgy). Sept. 1965. Contract NOw-65-0106-d. 38p. CFSTI $2.00 cy, $0.50 mn.

Results of stress-rupture measurements on Udimet 700, TZC molybdenum alloy, Ferrovac E, and Armco Iron at high temperatures and high strain rates are given. A tension-type machine capable of achieving strain rates up to 10,000%/sec was used for the measurements. (W.L.G.)

11266 (BNWL-167) HIGH TEMPERATURE CREEP-RUPTURE PROPERTIES OF HASTELLOY X IN VACUUM. Nyman, D. H. (Battelle-Northwest, Richland, Wash. Pacific Northwest Lab.). Nov. 1965. Contract AT(45-1)-1830. 17p. Dep. mn. CFSTI $1.00 cy, $0.50 mn.

The creep-rupture properties of Hastelloy X in vacuum were determined at 1950 and 2100°F. Grain growth occurred at 2100°F for times greater than 20 hrs and caused a marked reduction in both ductility and time to rupture from values extrapolated from lower temperature data. (W.L.G.)

11267 (BNWL-SA-488) PROMETHIUM COMPATIBILITY AND ENCAPSULATION STUDIES. Kirby, L. J.; Allemann, R. T.; Fullam, H. T. (Battelle-Northwest, Richland, Wash. Pacific Northwest Lab.). Dec. 27, 1965. Contract AT(45-1)-1830. 5p. (CONF-660305-2). Dep. mn. CFSTI $1.00 cy, $0.50 mn.

For Presentation at American Nuclear Society Topical Meeting, Augusta, Ga.

The compatibility of densified promethium oxide sources with potential cladding materials was determined for a large number of pure metals and alloys. Samarium oxide and neodymium oxide were used as stand-ins for promethium oxide. For Sm_2O_3 and Nd_2O_3 prepared exactly as originally planned for Pm_2O_3, the most encouraging results were obtained for rhenium, iridium, molybdenum−50% rhenium, molybdenum, Haynes-25, Hastelloy-C, Hastelloy-X, and stainless 304L in long term tests at 1100°C. By treating the final oxide powders to improve on their impurity levels and alter their defect structures, it may be possible to add to this list of potential cladding materials. Techniques of encapsulation which make maximum use of the encapsulation and shielding properties of the alloys and metals studied include fabrication of multilayered right cylindrical capsules and the use of powdered metal from which to form the shielding layer. Densification of the oxide sources was accomplished by step-pressing and high-energy-rate pneumatic impaction. (P.C.H.)

11268 (EIR-82) A CONTRIBUTION TO THE MECHANISM OF DISSOLUTION AND DIFFUSION OF OXYGEN IN ZIRCONIUM. Doerffler, W. W. (Eidgenoessisches Institut fuer Reaktorforschung, Wuerenlingen (Switzerland)). Sept. 1965. 34p. Dep. mn.

Values of the diffusion coefficient of oxygen in zirconium were determined from the dissolution rates of anodic oxide films in vacuum at elevated temperatures and from the penetration of oxygen in thermally oxidized specimens as a function of time of oxidation. Further information about the distribution of oxygen in the metal was obtained from studies of the proton radioactivation of oxygen-18. Diffusion coefficients at 550 and 600°C calculated from the depth of penetration of oxygen in the metal were found to be of the same order of magnitude as the values of diffusion coefficients calculated from the dissolution rates of anodic oxide films. Preferential line diffusion along grain boundaries, which was detected by using the nuclear reaction $^{18}O(p,n)^{18}F$, caused oxygen to diffuse into perfect lattice areas from more than one direction. These areas, therefore, fill up with oxygen relatively fast. The rate of oxide growth as a function of oxygen dissolved in the metal and of the diffusion coefficients of oxygen in the metal and in the oxide is discussed. (P.C.H.)

11269 (EUR-2483.f) PLASTICITE DES ALLIAGES A PHASE DISPERSEE TYPE Al/Al_2O_3. (Plasticity of Dispersed-Phase Type Al–Al_2O_3 Alloys). Guyot, P. (European Atomic Energy Community, Ispra (Italy). Joint Nuclear Research Center). Sept. 1965. 100p. Dep. mn.

The plastic deformation mechanisms of SAP, an alloy consisting of a dispersion of alumina particles in a polycrystalline aluminum matrix, were studied. The SAP structure was investigated in detail and a lack of coherence at the aluminum-alumina interface was found. The processes of plastic deformation were considered with regard to the deformation temperature. At low temperatures (from −196°C to room temperature), the deformation was controlled by the cutting through the forest, of which the density is high and rapidly increased with strain by the indirect presence of oxide particles. At high temperatures (from room temperature to 660°C) different processes successively occurred: cross-slip of screw dislocations and climb of edge dislocations by diffusion of jogs controlled the deformation of the aluminum matrix to about 350°C; above 350°C, the high values of activation energy and volume were partially explained by the thermal activation of the gliding of mobile dislocations pinned by the oxide particles, and by thermal activation of the by-passing of attractive trees. It is finally shown that the aluminum grain size has no influence. (auth)

11270 (LA-3424) A COMPARISON OF DIFFERENT METHODS OF PARTICLE SIZE ANALYSIS. Hipp, A. L.

(Los Alamos Scientific Lab., Univ. of California, N. Mex.). Sept, 1965. Contract W-7405-eng-36. 27p. Dep. mn. CFSTI $2.00 cy, $0.50 mn.

Particle size analyses were performed on several tungsten powders using four different methods for comparison. Two of the methods measured only specific surface and the other two measured particle size distributions. An application of log normal transformations was made to calculate specific surface from the size distributions and to compare the distributions obtained by different methods. (auth)

11271 (LFEN-24) ESTUDO DO SISTEMA TERNARIO U-V-Cr. (Study of the Ternary System U-V-Cr). Sampaio, Armando de Oliveira; Pinto, Maria de Lourdes (Laboratorio de Fisica e Engenharia Nucleares, Junta de Energia Nuclear, Sacavem (Portugal)). 1964. 30p. (CONF-640711-5). Dep. mn.

From 27th Portugo-Spanish Conference on Progress in Sciences, Bilbao, Spain.

The system U-V-Cr was studied using microscopic, thermal, dilatometric, chemical, and x-ray methods. Isothermal sections at 1000, 730, and 645°C and three temperature-concentration sections were investigated. No intermetallic compounds or four-phase equilibria were observed. The mechanism of retention of uranium β-phase in this ternary system seemed to be identical to those previously reported for the binary systems U-V and U-Cr. (auth)

11272 (NP-15661) CITRIFLEX—DECLADDING OF FUEL ELEMENTS CLAD WITH ZIRCONIUM OR ZIRCALLOY-2 BY AN AMMONIUM FLUORIDE-CITRIC ACID SOLUTION. Final Report of Laboratory Studies. Marchant, Y.; Van Caeneghem, J. (European Company for the Chemical Processing of Irradiated Fuels, Mol (Belgium)). Feb. 1965. 19p. (ETR-170). Dep. mn. CFSTI $1.00 cy, $0.50 mn.

Advantages of the Citriflex process compared to the Zirflex process for decladding fuel elements are discussed. These are listed as: absence of ammonia removal, therefore the elimination of its distillation into the vapor during the operation; attainment of a final stable solution with a zirconium concentration as high as 1 to 1.5 M; and distinctly lesser attack on the uranium oxide which makes up the interior of the clad fuel. The reagent is a mixed solution of ammonium fluoride and citric acid at concentrations of 3 and 2.5 M, respectively. (auth)

11273 (NRL-6364) METALLURGICAL CHARACTERISTICS OF HIGH STRENGTH STRUCTURAL MATERIALS. Eighth Quarterly Report. Puzak, P. P.; Lloyd, K. B.; Goode, R. J.; Huber, R. W.; Howe, D. G.; Judy, R. W. Jr.; Crooker, T. W.; Morey, R. E.; Lange, E. A.; Freed, C. N. (Naval Research Lab., Washington, D. C.). Oct. 12, 1965. 96p. CFSTI $3.00 cy, $0.75 mn.

Fracture toughness studies on the 12% Ni maraging and 9 Ni-4Co-0-XXC steels, a variety of Ti alloy gas metal-arc, electron-beam, and plasmarc weldments, and some Al alloys are presented. Current fracture toughness index diagrams are presented for steels, Ti alloys, and Al alloys. Results are presented of a study of the plane-strain fracture toughness of Ti-6Al-4V and Ti-6Al-6V-2.5Sn alloys over respective yield strength ranges of 130-140,000 and 147-186,000 psi; heat-treatment studies on several Ti alloys; and a low cycle fatigue crack propagation study of 5Ni-Cr-Mo-V steel in dry and wet environments in which considerable microcrack formation and growth were encountered. (auth)

11274 (NYO-3504-2) ON THE EFFICIENCY OF DISLOCATION CLIMB IN METALS. Balluffi, R. W.; Seidman, D. N. (Cornell Univ., Ithaca, N. Y.). Oct. 1965. Contract AT(30-1)-3504. 59p. Dep. mn. CFSTI $3.00 cy, $0.75 mn.

A wide variety of dislocation climb experiments was analyzed quantitatively with the object of determining in each case the magnitude of the maximum possible force driving climb and the ability of the dislocations to climb in response to this force. In general, the results indicate that the Frank three-dimensional dislocation network is very often capable of climbing with a high efficiency in pure metals. In the case of the high stacking fault energy metal, aluminum, climb appears to be highly efficient in the presence of large to moderate driving forces. Climb in the low stacking fault energy metal, gold, ranges from highly efficient to moderately efficient in the presence of large to moderate driving forces. No data are available for establishing lower limits of the climb efficiency under very small driving forces. The very limited climb data available for the Frank dislocation network in alloys over a wide range of driving forces indicate that climb efficiencies are generally lower in alloys than in pure metals. Climb during dislocation loop shrinkage appears to be highly efficient. Kinetic data are needed for loop growth. A number of aspects of dislocation climb were discussed and some assessment of the present status of the climb problem was attempted. (auth)

11275 (ORNL-TM-1338) MICROSTRUCTURAL EXAMINATION. Picklesimer, M. L. (Oak Ridge National Lab., Tenn.). Jan. 1966. Contract W-7405-eng-26. 24p. (CONF-412-2). Dep. mn. CFSTI $1.00 cy, $0.50 mn.

From Thermal Conductivity Conference, Gatlinburg, Tenn., Oct. 1963.

The ease of examination of the microstructures of specimens and its importance in the characterization of the specimens and in the interpretation of the data are discussed. Details of the methods of examination, equipment used, and techniques of quantitative microscopy are given. (P.C.H.)

11276 (PAEC(A)IN-657) SINGLE CRYSTALS. A Literature Search. (Philippine Atomic Energy Commission, Manila). June 1965. 23p. Dep. mn.

References (102) are given to journals and reports abstracted in NSA from Nov. 1951 through May 1964. The entries are included under the headings: chemistry, engineering, instrumentation, metals, ceramics and other materials, and physics. Separate corporate and personal author indexes are included. (P.C.H.)

11277 (RFP-659) EVALUATION OF BINDERS FOR MACHINABLE UNFIRED CERAMICS. Teter, A. R. (Rocky Flats Div., Dow Chemical Co., Golden, Colo.). Dec. 10, 1965. Contract AT(29-1)-1106. 8p. Dep. mn. CFSTI $1.00 cy, $0.50 mn.

Twenty-seven different combinations of binders were mixed with alumina powder to study tensile strength in unfired oxide parts and its relationship to machinability. Isostatically pressed oxides were impregnated with waxes to further increase their mechanical strengths for machining. Alumina, magnesia, zirconia, and zircon bars containing 4.0% polyvinyl alcohol were tested to compare the strength of equal amounts of binder in different oxides. In these bars the variation in tensile strengths was found to be due mainly to difference in particle size. Machinability was found to improve as the binder tensile strength increased. (auth)

11278 (RISO-48(Suppl.2)) BIBLIOGRAPHY ON DISPERSION-STRENGTHENED MATERIALS, 1964. Hansen, Niels; Lilholt, Hans; Jensen, Monika (Atomenergikomissionen, Risoe (Denmark). Forsoegsinstitut). Aug. 1965. 99p. Dep. mn.

References (502) are given to books, bibliographies, reports, and journals published during 1964. Report number and subject indexes are included. (P.C.H.)

11279 (SC-DC-64-1477X) DIELECTRIC STRENGTH AND FERROELECTRIC BEHAVIOR OF CERAMICS. Final Report, January 28, 1963-June 30, 1964. Lupfer, David A.; Nussbaum, Theodore; Onufer, Robert J.; Schroeder, Herbert S. (Rutgers-The State Univ. of New Jersey, New Brunswick, School of Ceramics). Contract AT(29-1)-789. 126p. Dep. mn. CFSTI $4.00 cy, $1.00 mn.

For Sandia Corp., Albuquerque, N. Mex.

Ceramics were prepared using high purity materials, preparation methods to give homogeneity, and techniques of firing for maximum density and uniformity. The samples were shaped and electroded with a contour on one

side such that there was a center area having a uniform field, and the edge had a reduced gradient. Ferroelectric and dielectric strength tests were performed using controllable d-c fields. The dielectric strength data were plotted using a number of statistical models, and it was found that a good fit was obtained with a skewed or extreme value distribution. This is related to a weak-link physical model of failure, and indicates that the breakdown is dependent on flaws in the ceramic. Dissection of the samples reveals gross flaws and imperfections. (auth)

11280 (UCRL–12001) THE PROPERTIES AND THE PREPARATION OF THIN BISMUTH FILMS. Condas, George A. (Lawrence Radiation Lab., Univ. of California, Livermore). Nov. 1, 1964. Contract W-7405-eng-48. 15p. Dep. mn. CFSTI $1.00 cy, $0.50 mn.

The optical transmission-surface density (thickness) relationship is given for thin, uniform, vacuum-deposited bismuth films for the thickness range 0–200 Å for white light. The transmission of these films in the wavelength range 2400–6800 Å is also given. The monochromatic transmissions of the thicker films (≈200 Å) were found to be remarkably equal over the range studied. The rapid deterioration with time (increase in transmission and resistance) in air of these films was also examined. The most significant mechanism was found to be due to the absorption of oxygen, although nitrogen and water vapor were also found to have some effect. Techniques and problems related to the production of thin films of bismuth are also discussed. (auth)

11281 (UCRL–12107) PROPOSED METHOD FOR MICROGRAM SURFACE DENSITY MEASUREMENTS BY OBSERVATION OF PROTON-PRODUCED X RAYS. Khan, J. M.; Worley, R. D.; Potter, D. L. (Lawrence Radiation Lab., Univ. of California, Livermore). Nov. 12, 1964. Contract W-7405-eng-48. 21p. Dep. mn. CFSTI $1.00 cy, $0.50 mn.

X-ray production by proton bombardment may be used to determine the surface density of thin films. Two conditions must be satisfied by the film: energy loss of the proton must be small (≤10%), and there must be negligible self-absorption of the produced x ray. The surface density must in general be less than 70 $\mu g/cm^2$, with a lower limit set by detector noise and beam current. To illustrate the method, aluminum is considered, indicating that for a 5-$\mu g/cm^2$ film on a substrate not contributing conflicting radiation, (e.g., carbon) a signal to noise ratio of at least 100 is obtainable: [conditions: 10 μA per cm^2 of protons at an energy of 100 kev; detector geometry ≈3,000]. The method was successfully applied to carbon films of $\mu g/cm^2$ surface density. Apparatus and method are described, and limitations are discussed. (auth)

11282 (UCRL–12119-T) $LiMg_2Tl$: PREPARATION AND STRUCTURE. Ramsey, William J. (Lawrence Radiation Lab., Univ. of California, Livermore). Oct. 1, 1964. Contract W-7405-eng-48. 4p. Dep. mn. CFSTI $1.00 cy, $0.50 mn.

The compound $LiMg_2Tl$ was prepared and its structure and properties were compared to those of Li_2MgPb. X-ray powder patterns showed preparations of the compound to be single phase and to have a face-centered cubic structure with a = 6.83 Å. On the basis of neutron diffraction data, the $L2_1$ structure type was ascribed to $LiMg_2Tl$. Data are tabulated. (P.C.H.)

11283 (UCRL–12142) RAPID PHASE TRANSFORMATIONS IN TITANIUM INDUCED BY PULSE HEATING. Parker, Robert (Lawrence Radiation Lab., Univ. of California, Livermore). Oct. 22, 1964. Contract W-7405-eng-48. 23p. Dep. mn. CFSTI $1.00 cy, $0.50 mn.

Measurements of the latent heat of transformation from alpha to beta Ti were made using a pulse heating technique. Rapid heating was accomplished electrically by discharging a low-inductance, 14-μF, 0–6-kv capacitor bank through thin strips of high-purity Ti and Ti containing 2700 ppm of O_2. An electrical resistivity technique and a plot of energy input versus temperature rise was used to monitor the phase change. It was concluded that: the latent heat of transformation is 800 cal/mole; phase change occurred in less than 200 μsec; the percentage phase change that occurs is linearly a function of the energy available for phase change. In addition, this experiment provides a unique, accurate, and inexpensive means of determining the specific heat of any metal through any desired temperature range. (auth)

11284 (UCRL–14599) THE EFFECT OF STRAIN RATE ON MECHANICAL PROPERTIES OF SOME WIDELY USED ENGINEERING METALS. Hoge, K. G. (Lawrence Radiation Lab., Univ. of California, Livermore). Dec. 14, 1965. Contract W-7405-eng-48. 36p. Dep. mn. CFSTI $2.00 cy, $0.50 mn.

A summary of the effects of strain rate on some of the mechanical properties of various types of structural materials is presented. Dynamic tensile data were obtained on a Dynapak machine at strain rates up to 200 in./in./sec and at temperatures from 75 to 900°F. Dynamic data from other sources are also presented. Some of this data are at strain rates as high as 9000 in./in./sec. Static data were obtained on a universal test machine at strain rates of 10^{-5} to 10^{-1} in./in./sec. Several theories on mathematical relationships between stress and strain rate were examined and evaluated in terms of experimental data. (auth)

11285 (UCRL–16434) HIGH-TEMPERATURE COMPRESSIVE DEFORMATION EQUIPMENT. Hulse, C. O.; Copley, S. M. (Lawrence Radiation Lab., Univ. of California, Berkeley). Oct. 27, 1965. Contract W-7405-eng-48. 18p. Dep. mn. CFSTI $1.00 cy, $0.50 mn.

Three apparatus for deforming ceramic materials in compression at elevated temperatures were developed. Methods used for loading, alignment, and measurement of stress and strain are described. (auth)

11286 (UJV–1405/65) SPECIFIKACE NEKTERYCH OCELI PRO TLAKOVE NADOBY JADERNYCH REAKTORU. (Specifications of Certain Steels for Nuclear Reactor Pressure Vessels). Cervasek, Jiri (Ustav Jaderneho Vyzkumu, Ceskoslovenska Akademie Ved, Rez). 1965. 27p. Dep. mn.

Steels used in the pressure vessels of various nuclear reactors are listed. The examples cited are all in the United States except for one application in Sweden. Complete specifications, chemical analysis, mechanical, and metallographic characteristics, are given for the steels. These are listed under different types as follows: ferritic-pearlitic carbon steels — ASTM A 212 grade B and steel No. 2103/R3; low-alloy Mn–Mo steels — ASTM A 302 grade B and steel No. 345; and high strength steels — Fortiweld Steel. The results of extensive laboratory tests on samples of the steels are presented. (TTT)

11287 (WAPD-T–1809) AN EXAMINATION OF THE EFFECTS OF THERMAL TREATMENT ON THE DISTRIBUTION OF ALLOYING ELEMENTS IN ZIRCALOY-2 [Thesis]. Gessner, R. F. (Bettis Atomic Power Lab., Pittsburgh, Pa.). Dec. 1965. Contract AT-11-1-GEN-14. 27p. Dep. mn. CFSTI $2.00 cy, $0.50 mn.

Submitted to Carnegie Inst. of Tech., Pittsburgh, Pa.

Electron microprobe analyses were performed on specimens of Zircaloy-2 which were slowly cooled from the $\alpha + \beta$ and β regions as well as on as-rolled specimens. Tin was found to concentrate in α grains formed during the cooling with concomitant tin depletion in the grain boundaries. Grain boundaries were enriched in iron, chromium, and nickel, but the grains themselves showed no evidence of depletion of these constituents. This anomaly was attributed to the analytical method utilized where a very fine electron beam was focused on the specimen. (auth)

11288 (AD–622477) EFFECT OF ALLOYING ON PHYSICO-MECHANICAL PROPERTIES OF NIOBIUM. Tarasov, N. D.; Ul'yanov, R. A.; Mikhailov, Ya. D. Translated from Fiz. Metal. Metalloved., 18: 740-5 (1964). 13p. (FTD-TT–65-915). CFSTI $1.00 cy, $0.50 mn.

Twelve different elements were alloyed with Nb and the

effects on the strength and plasticity to 1100°C and on the elastic modulus to 1300°C measured. Cr, Re, Zr, and Ir additions had the more pronounced effect on the strength of Nb. Increasing the concentration of Ta, W, Re, Mo, and Ir in the alloys produced an increase in the elastic modulus and strength and a decrease in the thermal expansion coefficient. Ti and Pd had little effect on the properties of Nb. Heterogeneous structures were obtained in alloys with B, La, and Si; maximum strengthening was obtained with B. (W.L.G.)

11289 (IS-Trans-26) ON THE MECHANISM OF ELECTROOSMOSIS IN LIQUID METALS. Belashchenko, D. K. Translated by E. E. Conrad (Ames Lab., Ames, Iowa), from Zh. Fiz. Khim., 39: 808-9(1965). 4p. Dep. mn. CFSTI $1.00 cy, $0.50 mn. JCL $1.10 fs, $0.80 mf.

Equations are given to show that the electroosmosis effect may be measured by the speed of transfer of a liquid from one communicating (connected) container into another with the same levels in them. The electroosmotic effect under consideration allows the speed of the charge carriers and their sign to be measured directly and may be applied for analysis of the state of the electrons in liquid solutions. Its distinguishing characteristic trait is the proportionality of the effect to the square of the current density. (P.C.H.)

11290 DIFFUSION OF URANIUM IN MOLYBDENUM, NIOBIUM, ZIRCONIUM, AND TITANIUM. Pavlinov, L. V.; Nakonechnikov, A. I.; Bykov, V. N. At. Energ. (USSR), 19: 521-3(Dec. 1965). (In Russian).

The diffusion of U in Mo, Ni, Zr, and Ti was studied. The coefficients of diffusion were determined by the method of measuring the integral activity of a sample using the alpha emission of U enriched to 90% in ^{235}U, at temperatures from 1500 to 2000°C for Mo and Ni and 915 to 1200°C for Zr and Ti. Expressions for the temperature dependence of the diffusion coefficients are given. The substantial differences in the diffusion mobility and the values of the activation energy of Mo and Ni, on one side, and Zr and Ti, on the other, are probably caused by the influence of defects of the crystal lattice, e.g., the excess vacancies arising in Zr and Ti during polymorphic transformation. (tr-auth)

11291 CHARACTERISTICS AND APPLICATIONS OF HIGH-DENSITY TUNGSTEN-BASED COMPOSITES. Larsen, E. I.; Murphy, P. C. Can. Mining Met. Bull., 58: 413-21(Apr. 1965).

Physical and mechanical property data are given for a series of W-base composites containing from 90 to 98.5% W, with the balance being either Ni–Cu or Ni–Fe. Such materials are fabricated by powder metallurgy techniques utilizing the principle of liquid phase sintering. Densities of 17 to 19 gm/cc and ultimate strengths of 80,000 to 150,000 psi with elongations of 2 to 15% can be obtained in as-sintered composites. The tensile properties of a W–Ni–Cu composite can be increased by about 50% by cold working. Tensile properties of various composites at elevated temperatures are given. Materials are easily machined on conventional equipment. Procedures are discussed for various means of protecting the composites from corrosion and oxidation at elevated temperatures. Various types of fabrication techniques are reviewed. Typical applications for high-density composites are included. (Rev. Metal Lit.).

11292 EFFECT OF CARBON ON THE FORMATION OF TEMPERING STRUCTURES IN URANIUM-MOLYBDENUM ALLOYS. Giraud-Heraud, Francois (Laboratoires de la Societe Industrielle de Combustible Nucleaire, Veurey, France). Compt. Rend., 261: 4407-10(Nov. 22, 1965). (In French).

Electron microscopy of U–2% Mo alloys welded by electron bombardment showed an inversion of the fast cooling structures between the fused zone and the zone where the metal passed into the γ phase. This inversion, as well as the preferential martensite reaction in the vicinity of precipitated carbides, can be explained by the displacement of the TTT curves with the carbon concentration of the matrix. (tr-auth)

11293 CRYOGENIC DESIGN PROPERTIES OF THE HARD CARBIDE ALLOYS. McCleary, Gail P. Cryog. Eng. News, 1: No. 2, 38-40(Oct.-Nov. 1965).

Low-temperature properties of the hard carbides of W and Ti were investigated. Tests concerning the crystalline structure of the carbides support the theory that at cryogenic temperatures the structure of the binder used is the predominant element and the carbides should retain their room-temperature properties. Coefficients of thermal expansion down to –320°F are shown for tungsten carbide with Co and Ni binders and titanium carbide with Ni binder. Applications of tungsten and titanium carbides in the cryogenic temperature range are suggested. (A.G.W.)

11294 BERYLLIUM—CANNING MATERIAL. Mallen, Jose-Maria; Weisz, Michel (CEN, Saclay, France). Ind. At., 9: No. 9-10, 78-82(1965). (In French).

Because of its neutron characteristics, beryllium is considered a good material for nuclear metallurgy, despite its brittleness at ambient temperature and around 600°C. A process was perfected for making beryllium tubes whose mechanical properties are adequate to allow their being used as a canning material. (auth)

11295 PHASE DIAGRAM OF THE IRON-NEODYMIUM SYSTEM. Terekhova, V. F.; Maslova, E. V.; Savitskii, E. M. Izv. Akad. Nauk SSSR, Metal., No. 3, 128-30(May-June 1965). (In Russian).

Fe–Nd alloys containing 0–100 wt % Nd were vacuum melted from 99.9%-pure Fe and 99.0%-pure Nd in a nonconsumable W electrode arc furnace in an atmosphere of He, under a pressure of 300–400 mm Hg. Depending on the composition, the alloys were vacuum annealed at temperatures ranging from 900 to 600°C for 130 hr and subjected to various methods of physicochemical analysis. On the basis of the results obtained, a phase diagram of the Fe–Nd system was plotted. The alloy containing 24 wt % Nd was found to be a single-phase chemical compound corresponding to the stoichiometric Nd_2Fe_{17} composition. A second chemical compound was found in alloys containing more than 50 wt % Nd. The largest amount of this compound was in alloys similar in composition to $NdFe_2$ compound. A fine-grain eutectic was observed in the system at 88.5% Nd. The Nd_2Fe_{17} and $NdFe_2$ compounds are formed with peritectic reactions at 1185 and 1130°C ± 10°C, respectively. Nd_2Fe_{17} has a Th_2Zn_{17}-type structure with the lattice parameters a = 8.59 Å, c = 12.47 Å, and c/a = 1.451. The structure of the second metallic compound was not identified, but preliminary data show it is not a Laves phase. Additions of Nd increase the hardness of α-iron solid solutions. With increasing content of the second phase, the hardness of the alloy increased. In the concentration range of 15–60 wt % Nd, the alloys became very brittle. The microhardness of Nd_2Fe_{17} was 730 kg/mm^2 and that of $NdFe_2$, 560 kg/mm^2. (ATD)

11296 THE HIGH-TUNGSTEN SECTION OF THE TUNGSTEN-SILICON PHASE DIAGRAM. Efimenko, L. N.; Verkhorobin, L. F.; Matyushenko, N. N. Izv. Akad. Nauk SSSR, Metal., No. 4, 163-7(July-Aug. 1965). (In Russian).

A brief survey of the literature shows contradictory information on the high-tungsten section of the W–Si phase diagram. Therefore a careful study of the tungsten-rich phases with particular regard to the products of diffusion between tungsten and its silicides was made. The tungsten specimens were annealed in WSi_2 powder at 1500°C. The metal was completely converted to a single-phase silicide by protracted silicidizing of sheet specimens 0.1 mm thick. Cylindrical tungsten samples 2 and 0.4 mm in dia were silicidized until a diffusion layer ~100 μ thick was formed. All experiments were carried out in a vacuum of $5 \cdot 10^{-5}$ mm Hg. X-ray analysis showed the presence of a W_5Si_3 phase. Analysis for the x-ray pattern of this phase is tabulated. It might be assumed that the necessary conditions for formation of the lower silicide would be created during silicidization of the metal in W_5Si_3 powder. However, x-ray diffraction revealed no silicide phase on the surface of tungsten specimens after annealing at 1500°C for 34 hrs. A comparison of x-ray patterns from the specimen and from the original metal shows a noticeable reduction in the lattice period of tungsten in the surface layer of the specimen, which is explained by diffusion of silicon in the tungsten. An oriented layer of W_5Si_3 phase is formed when tungsten

is silicidized in disilicide powder. The preferred orientation of the crystals in this layer is along the [001] axis. No silicide of composition W_3Si was observed at the W_5Si_3–W boundary, in contrast to the situation in the Mo–Si system, in spite of the similarity in phases. The intermediate silicide W_5Si_3 melts incongruently above 2300°C. (ATD)

11297 PHASE DIAGRAM AND THE PROPERTIES OF ALLOYS OF THE ALUMINUM–SCANDIUM SYSTEM. Naumkin, O. P.; Terekhova, V. T.; Savitskii, E. M. Izv. Akad. Nauk SSSR, Metal., No. 4, 176-82(July-Aug. 1965). (In Russian).

A large series of Al–Sc alloys melted from 98.16- or 99.5%-pure Sc and 99.99%-pure Al was studied. On the basis of the results obtained, a phase diagram of the Al–Sc system was plotted. The investigations showed that Al and Sc have unlimited solubility in the liquid state. The room-temperature solubility of Sc in Al is approximately 0.5 at.% and that of Al in Sc approximately 4 at.%. Four compounds: $ScAl_3$, $ScAl_2$, ScAl, and Sc_2Al were identified. All the compounds are brittle and crack during solidification. The microhardness is 255, 530, 370, and 460 kg/mm for $ScAl_3$, $ScAl_2$, ScAl, and Sc_2Al, respectively. Alloying with Sc increases the tensile strength at room and elevated temperatures without a noticeable decrease in ductility. The strengthening effect of Sc is much stronger than that of rare-earth metals. (ATD)

11298 METALLIC COMPOUNDS OF RHENIUM WITH RARE EARTH METALS. Savitskii, E. M.; Khamidov, O. Kh. (Inst. of Metallography, Academy of Sciences, Ukrainian SSR). Izv. Akad. Nauk SSSR, Neorg. Mater., 1: 1873-82(Nov. 1965). (In Russian).

From studies of rhenium–rare earth metal alloys it was experimentally established that metallic compounds of the Laves type–AB_2 are formed when rhenium is alloyed with praseodymium, gadolinium, terbium, erbium, holmium, and dysprosium. There was observed a polymorphic transformation of the compound $PrRe_2$, the high temperature modification which belongs to the $MgCu_2$-type cubic structure, and the low temperature modification which belongs to the $MgZn_2$ hexagonal structure. The formation of Laves phases with a different structure (cubic or hexagonal) is apparently due to a change of valence of the B-element in compounds of the AB_2-type or due to a valence change of the A-element. It is pointed out that the formation of Laves phases upon interaction of rhenium with transition metals are observed in the interval of atomic radii ratios (r_A/r_B) equal to 1.10 to 1.40. (JPRS)

11299 PRECIPITATION ON DISLOCATIONS IN A BERYLLIUM–3 percent IRON ALLOY. Koda, Shigeyasu; Morozumi, Shotaro; Tsuno, Nobuo (Tohoku Univ., Sendai). J. Inst. Metals, 93: 520(Oct. 1965).

Specimens were solution-treated at 1100°C for 30 min, oil-quenched, aged at appropriate temperatures for various periods, and the resulting structures studied by transmission electron microscopy. A precipitate formed on what appears to be helical or linear dislocations. On further aging, the precipitate assumed a hexagonal, platelike form of increased width and thickness. Fine dislocations, situated around or between the particles of the precipitate, are believed to result from the misfit caused by the form of the hexagonal lattice structure of the precipitate $Be_{11}Fe$, whose basal plane is parallel to that of the matrix. (W.L.G.)

11300 THE NOTCH-IMPACT BEHAVIOUR OF CHROMIUM AND A CHROMIUM–35 AT.-percent RHENIUM ALLOY. Gilbert, A.; Allen, B. C. (Battelle Memorial Inst., Columbus, Ohio). J. Inst. Metals, 93: 529-35 (Nov. 1965).

Studies were made of the notch-impact properties of Cr and a Cr–35 at. % Re alloy, and fractographic examinations performed on broken samples. The notch-impact transition temperature of iodide Cr is 240°C in the wrought condition and up to 380°C in the recrystallized condition. Optical and electron-replica fractography show that failure occurs by cleavage, and that the transition represents that for crack propagation. The transition temperature of the Cr–35% Re alloy is ~260°C, and fracture occurs by grain-boundary separation, ductile parting, cleavage, or failure at the twin/matrix interface. (auth)

11301 YIELDING EFFECTS IN A MAGNESIUM–0.5 percent THORIUM ALLOY. Kent, K. G.; Kelly, A. (Cambridge Univ., Eng.). J. Inst. Metals, 93: 536-42 (Nov. 1965).

Yield points and strain-ageing effects were studied in a Mg–0.5% Th alloy. In polycrystalline material yield points were recorded between ~100 and 300°C. The lowest temperature at which a yield point was observed depended inversely on grain size. The electron microscope showed precipitate particles preferentially nucleated at the dislocations, after very long ageing times. Yield points are thought to be due to a Cottrell interaction followed by the formation of small clusters of solute atoms along the dislocations. In lightly aged material the initiation and propagation of yielding involves unpinning of dislocations, but in recrystallized material fresh dislocations are nucleated. The absence of a yield point in polycrystals at room temperature is due to the fact that the stresses required for non-basal slip are high, so that the stress required to propagate yielding is greater than the stress required to initiate yielding. (auth)

11302 SUBSTITUTIONAL NIOBIUM ALLOYS OF HIGH CREEP STRENGTH. McAdam, G. D. (B.S.A. Group Research Centre, Birmingham, Eng.). J. Inst. Metals, 93: 559-64(Dec. 1965).

A study was made of the effects of various substitutional elements on some of the properties of niobium alloys. Analyses of room-temperature hardness data, and creep results at temperatures close to 0.5 T_m, provided some general rules for alloy development. The hardening of binary alloys at room temperature is a function of the differences between the rigidity moduli of niobium and the solute elements; this is also extremely important in high-temperature applications, but in this case there is a definite correlation with the melting point of the alloys. The strain caused by atomic size-mismatch is of secondary importance in both instances. The contributions of individual elements to the rupture strength have been estimated quantitatively at one stress and temperature. Comments are made on the changes that occur at other temperatures. (auth)

11303 DISLOCATION STRUCTURE IN CHROMIUM, CHROMIUM–RHENIUM, AND CHROMIUM–IRON ALLOYS. Reid, C. N.; Gilbert, A. (Univ. of Birmingham, Eng. Battelle Memorial Inst., Columbus, Ohio). J. Less-Common Metals, 10: 77-90(Feb. 1966).

Electron-transmission microscopy experiments were performed on chromium, chromium–rhenium, and chromium–iron alloys to investigate the effect of alloying on dislocation multiplication and configuration. It was found that the increase of dislocation density with strain was largely independent of composition, but that large alloying additions produced a uniform distribution of dislocations, rather than the cell-like structure observed in pure chromium. In unalloyed chromium, a cross-slip event was observed, which was consistent with a dislocation of ⟨100⟩ Burgers vector. (auth)

11304 HEATS OF SOLUTION OF SOME RARE-EARTH ELEMENTS IN LIQUID TIN. Pratt, J. N.; Morris, A. W. H. (Univ. of Birmingham, Eng.). J. Less-Common Metals, 10: 91-7(Feb. 1966).

Using a liquid-metal solution calorimeter, the heats of solution of some rare-earth metals in liquid tin were determined at temperatures conducive to optimum solution rates. The values obtained for lanthanum (632°K), cerium (631 to 634°K), praseodymium (724 to 768°K), and ytterbium (770°K) are, respectively, −66,240 ± 600, −68,408 ± 600, −61,341 ± 400, and −35,241 ± 330 cal/g-atom. Approximate values of −55 to −60 kcal/g-atom were also obtained for neodymium and samarium at 828°K. The data are discussed in terms of the characteristics of the rare-earth elements and liquid tin. (auth)

11305 THE STRUCTURES OF THE RARE-EARTH TRIALUMINIDES. Van Vucht, J. H. N.; Buschow, K. H. J.

(Philips' Gloeilampenfabrieken, Eindhoven, Netherlands). J. Less-Common Metals, 10: 98-107(Feb. 1966).

An extensive study was made of the trialuminides of the rare-earth metals. In addition to showing the existence of several Ni_3Sn-type trialuminides hitherto unknown (those of Ce, La, Pr, and Nd) the detailed structures are given of a number of rhombohedral trialuminides (those of Y and Tb, which are isotypic with $BaPb_3$, and those of Ho and Dy, which have the $HoAl_3$ type of structure). These structures, together with the Ni_3Ti type, encountered with the ternary trialuminides $(Gd_x, Er_{1-x})Al_3$ and $(Y_x, Er_{1-x})Al_3$, and the $PuAl_3$ type form a family of transition structures between the Ni_3Sn and Cu_3Au types. As the rare earth/Al radius ratio decreases the trialuminides adopt structures passing from predominantly hexagonal to predominantly cubic, subject to the two rules that the layer repeat period of the lattice tends to be a minimum and that the alternation of hexagonal and cubic stacking is a maximum. (auth)

11306 THE SOLUBILITY OF TANTALUM IN EIGHT LIQUID RARE-EARTH METALS. Dennison, D. H.; Tschetter, M. J.; Gschneidner, K. A. Jr. (Iowa State Univ., Ames, Iowa). J. Less-Common Metals, 10: 108-15(Feb. 1966). (IS-1231).

The solubilities of tantalum in liquid gadolinium, terbium, dysprosium, holmium, erbium, and thulium were determined from the melting point of the rare earth metal to ~1800°C, to ~1900°C for scandium, and to ~2000°C for lutetium. The change of the transition and melting points by tantalum was measured, and the partial molal heats of tantalum in the rare earth metals calculated from these data. The liquid solubility of tantalum was found to depend on the atomic size difference between the rare earth solvent and the tantalum solute, i.e., the smaller the size difference the greater the solubility at a given common temperature (e.g., 1700°C). (auth)

11307 THE SYSTEM ALUMINUM–HOLMIUM. Meyer, Andreas (Siemens and Halske AG, Munich). J. Less-Common Metals, 10: 121-9(Feb. 1966).

Differential thermal analysis, microscopic, and x-ray investigations enabled a phase diagram to be derived for the aluminum–holmium system. The melting points and peritectic temperatures of the compounds $HoAl_3$, $HoAl_2$, HoAl, Ho_3Al_2, and Ho_2Al are reported, as well as the eutectics occurring in the system, with the associated melting temperatures. Holmium is practically insoluble in aluminium. X-ray investigations confirmed results concerning the structures of $HoAl_3$, HoAl, and Ho_3Al_2. In addition, the lattice constants of the compound Ho_2Al were determined. The aluminum–holmium system is compared with the other known rare earth metal–aluminum systems. (auth)

11308 NOTE ON THE STRUCTURES OF $GdFe_3$, $GdNi_3$, $GdCo_3$ AND THE CORRESPONDING YTTRIUM COMPOUNDS. van Vucht, J. H. N. (Philips' Gloeilampenfabrieke, Eindhoven, Netherlands). J. Less-Common Metals, 10: 146-7 (Feb. 1966).

The intermetallic compounds $GdFe_3$, $GdCo_3$, $GdNi_3$, YFe_3, YCo_3, and YNi_3 were prepared and x-ray powder diagrams obtained. Unit cell dimensions indicated a close-packed structure. The measured densities, however, and the x-ray reflection intensities made it clear that the structure is not close-packed. The compounds were found to be isomorphous with $PuNi_3$. (M.C.G.)

11309 ORDERED AB AND AB_3 PHASES IN T_6–T_9 ALLOY SYSTEMS AND A MODIFIED Mo–Ir PHASE DIAGRAM. Giessen, B. C.; Jaehnigen, U.; Grant, N. J. (Massachusetts Inst. of Tech., Cambridge). J. Less-Common Metals, 10: 147-50(Feb. 1966).

The T_6–T_9 systems (Mo–Rh, Mo–Ir, W–Rh, and W–Ir) were examined to establish whether ordering of the ϵ phase exists in the concentration range from AB to AB_3. The occurrence of ordered structures was established for MoIr, $MoIr_3$, MoRh, WIr, and WRh_3 systems. The ordered AB phases, MoRh, MoIr, and WIr, have an orthorhombic structure of the B19-MgCd type, space group D^4_{2h}-Pmcm, 4 atoms per unit cell with A in 2(e): $\pm(0, y_e, 1/4)$; B in 2(f): $\pm(1/2, y_f, 1/4)$, with $y_e \sim 1/6$ and $y_f \sim 4/6$. The calculated and observed line positions and intensities were in good agreement. The ordered AB_3 phases $MoIr_3$ and WRh_3 are of the $D0_{19}$–$MgCd_3$ type, space group D^4_{6h}–$P6_3/mmc$, 8 atoms per unit cell, with A in 2(c): $\pm(1/3, 2/3, 1/4)$; and B in 6(h): $\pm(2\underline{X}, \underline{X}, 1/4; \underline{X}, \underline{X}, 1/4;$ and $\underline{X}, 2\underline{X}, 1/4)$, with $\underline{X} \sim -1/6$. The calculated line positions and intensities, assuming the ideal parameter $\underline{X} \sim -1/6$, agreed with those observed. The ordered phases at AB and AB_3 followed the principle of forming a maximum of unlike first nearest neighbors. (F.J.H.)

11310 THE METALLOGRAPHIC PREPARATION OF SOME RARE-EARTH METALS. Roman, W. A. (General Electric Co., Schenectady, N. Y.). J. Less-Common Metals, 10: 150-2(Feb. 1966).

The metallographic preparation of rare earths is begun by mounting the specimen in epoxy resin and grinding in turn on 180, 400, and 600 grit silicon carbide abrasive papers using kerosene as a lubricant. After cleaning with acetone, the specimen is coarse polished with 9μ diamond paste. This is repeated after acetone washing with 3μ diamond paste. It is chemically polished using a solution containing 20 ml lactic acid, 5 ml phosphoric acid, 10 ml acetic acid, 15 ml nitric acid, and 1 ml sulfuric acid. An etching solution of 10 ml phosphoric acid, 10 ml lactic acid, 30 ml nitric acid, and 20 ml acetic acid may be used. (M.C.G.)

11311 THE EFFECTS OF THERMAL HISTORY ON THE KINETICS OF THE $\beta \rightarrow \alpha$ PHASE CHANGE IN URANIUM AND URANIUM–CHROMIUM ALLOYS. Townsend, R. D.; Burke, J. (Univ. of Liverpool). J. Nucl. Mater., 17: 215-26(Nov. 1965).

The effects of various heat treatments on the kinetics of the $\beta \rightarrow \alpha$ phase change in pure uranium and two uranium–chromium alloys was examined using an electric resistivity technique. The heat treatments were arranged to enable the effects associated with β grain size to be separated from those due to submicroscopic effects determined by the quenching temperature. Transformation at temperatures near the equilibrium transition temperature was retarded by increasing the β quenching temperature. In the alloys this retardation is shown to be due to an increase in β grain size; in the pure metal the position is less clear but results suggested that while β grain size is the most important factor it is not the only one. Transformation at temperatures in the martensitic and bainitic ranges was accelerated by increasing the quenching temperature because of the removal of the β grain boundaries, which arrest growth of α crystals. (auth)

11312 DIFFUSION OF HEAVY ELEMENTS IN NUCLEAR FUELS: ACTINIDES IN UO_2. Schmitz, F. (Institut fuer Kern- und Radiochemie, Brunswich); Lindner, R. J. Nucl. Mater., 17: 259-69(Nov. 1965).

To measure the diffusion in solids of alpha-active elements, the surface-decrease method was supplemented by two others: a differential method based on measurement of the reduction in relative height of the alpha peaks and an absolute method based on the degradation of the alpha spectrum. These three methods give comparable results, as demonstrated by a study of the diffusion of plutonium in UO_2. The diffusion of the actinide elements 90 to 95 (Th to Am) in dense sintered compacts of UO_2 was measured in the range from 1250 to 1600°C. Taking as point of reference the experimentally determined activation energy of 98 kcal/mole for the transport of plutonium in UO_2, the following activation energies (in kcal/mole) were found by comparison: Th = 98, Pa = 108, U = 104, Np = 110, Am = 92. (auth)

11313 CREEP BEHAVIOR OF A MAGNESIUM–ALUMINUM–ZIRCONIUM ALLOY AT 450 deg C. Wells, T. C. (International Research and Development Co. Ltd., Newcastle upon Tyne, Eng.). J. Nucl. Mater., 17: 274-6 (Nov. 1965).

The behavior, at 450°C and a stress of 350 psi, of a magnesium alloy containing 0.84 wt % Al and 0.54 wt % Zr with smaller quantities of zinc (0.15 wt %) and calcium (0.1 wt %) was investigated. The creep rates for two specimens continually accelerated during the course of the tests from

minimum rates of 1.0×10^{-4} and 2.3×10^{-4}/hr. The specimens ultimately ruptured with elongations of 60 and 69% at 820 and 600 hr, respectively. (M.C.G.)

11314 TOTAL EMISSION CAPACITY OF NIOBIUM. Hoerz, G.; Duerrschnabel, W.; Gebhardt, E. (Max-Planck-Institut fuer Metallforschung, Stuttgart). J. Nucl. Mater., 17: 277-8(Nov. 1965). (In German).

A degassed niobium wire was stretched between two water-cooled copper electrodes in a high vacuum and heated to the desired temperature by direct current passage. The total emission capacity was determined as a function of temperature. (M.C.G.)

11315 THE M_s TEMPERATURE FOR PURE URANIUM. Townsend, R. D.; Burke, J. (Univ. of Liverpool). J. Nucl. Mater., 17: 279-81(Nov. 1965).

An attempt was made to determine the isothermal TTT diagram for pure uranium using a resistometric technique. A study was also made of the $\beta \rightarrow \alpha$ transformation temperature during continuous cooling. Data are presented in graphs. It was found that $M_s = 590 \pm 10°C$. (M.C.G.)

11316 THE INVESTIGATION OF URANIUM AND ZIRCONIUM COMPATIBILITY BY MEANS OF A MICRO-ANALYSER WITH ELECTRON PROBE. Karnikova, Eva; Vanicek, Oldrich (State Inst. on Conservation of Materials, Prague). Jad. Energ., 11: 411-14(Nov. 1965). (In Czech).

Quantitative investigations were made of uranium and zirconium diffusion. The principle of measurement and evaluation using Casting's microanalyzer is discussed. The diffusion coefficient, activation energy, and activation heat of the process in the temperature range from 500 to 900°C were calculated. (auth)

11317 SEVERAL ALLOY PHASES CONTAINING YTTRIUM AND DYSPROSIUM. Laube, E.; Kusma, J. B. Monatsh. Chem., 95: 1504-13(1964). (In German).

The ternary Y–Zn–Hg and Dy–Cd–Hg specimens were prepared by melting at 350 to 800°C in vacuo. The phases formed were studied by x-ray diffraction. The intermediate phases DyZn, $DyZn_2$, $DyZn_5$, YZn_2, YZn_5, and YHg_2 were identified. (Rev. Metal Lit.)

11318 OCTAHEDRAL PHASE STRUCTURES OF TRANSITION METALS. Rieger, W.; Nowotny, H.; Benesovsky, F. Monatsh. Chem., 96: 232-41(Feb. 1965).

Alloys within the ternary systems: (Zr, Hf, V, Nb, Ta)–(Ni, Cu, Ag, Au)–(Zn, Al, Ga, Sn, Pb) were prepared mainly in the domain of 50-60 at. % transition group, 10-30 at. % 8a- and one Ib group and 15-40 at. % 2b- and 4b group metals of the periodic chart. The phases Zr_3Cu_2Zn, Zr_3Ag_2Zn, Zr_3Au_2Al, Hf_5Cu_2Zn, Hf_3Au_2Al are found to be isostructural with the Ti_2Ni-type. Hf_5Sn_4 crystallizes with Ti_5Ga_4-type, while homogeneous samples having almost the same crystal structure such as Zr_5Pb_3Cu, Hf_5Sn_3Ni, Hf_5Sn_3Cu and Hf_5Pb_3Cu can also be considered as a filled Mn_5Si_3-structure. The small Ni- and Cu-atoms do play the same role as nonmetal atoms. $V_3(Au,Ga)_2N_x$, $Nb_3(Au,Ga)_2N_x$ and $Ta_3(Au,Ga)_2N_x$ possess a partially ordered parent lattice of the beta-Mn-type. It appears however that for stabilization of Nb_3Au_2 nonmetals, such as oxygen, nitrogen, or carbon have to be present. The phase of formula $Nb_{55}Au_{45}$ having beta-Mn-structure reported in the literature cannot be observed in purely binary Nb–Au-alloys. (auth)

11319 HEAT TREATMENT OF DILUTE U–Fe ALLOYS. Watanabe, Hitoshi (Japan Atomic Energy Research Inst., Tokyo). Nippon Genshiryoku Gakkaishi, 7: 686-93(Dec. 1965). (In Japanese).

Metallographic structure precipitation hardening, and distribution of precipitates were studied on γ-quenched U–Fe alloys containing from 400 to 900 ppm of Fe. Neither β nor γ phases were retained in the water-quenched specimens from 800 to 850°C, and only the α phase was observed. During subsequent annealing, hardening was found to occur in one or two steps, caused by the precipitation of U_6Fe. This hardening appeared to be similar in nature to that experienced with Al–Cu alloys. The size and number of precipitates in various heat-treated specimens were measured by electron micrography. The results obtained are discussed, with particular reference to the effect of precipitates on swelling, and compared with data on the bubble density in α-U irradiated to 0.5 at. % burnup. (auth)

11320 SUPPRESSION OF GRAIN GROWTH IN VAPOR-DEPOSITED TUNGSTEN UP TO 2500 deg C. Weinberg, A. F.; Lindgren, J. R.; Elsner, N. B.; Mills, R. G. (General Atomic Div., General Dynamics Corp., San Diego, Calif.). Nucl. Appl., 1: 581-3(Dec. 1965).

Electropolishing removal of the layer of small equiaxed randomly oriented grains of tungsten initially deposited during the hydrogen reduction of WF_6 eliminates variance in subsequent grain-growth behavior in the overlying columnar crystals. (auth)

11321 CRYSTALLITE SIZE, STRAIN AND SHAPE DETERMINATIONS ON THORIA FROM X-RAY LINE BROADENING STUDIES. Ferguson, I. F. (Atomic Energy Research Establishment, Harwell, Eng.). Phil. Mag. (8), 12: 1115-22(Dec. 1965).

The breadths of reflections on x-ray powder diffraction photographs of thoria specimens prepared at different temperatures are examined. It is shown how, by using appropriate values of the Scherrer constant and a statistical treatment of the data, a mean crystallite shape, size and strain may be inferred. The results are compared with those obtained by electron microscopy and B.E.T. surface area measurements. The strain measurements are discussed and it is shown that the strain energy represents only a small fraction (0.1%) of the surface energy of the crystallites. (auth)

11322 ELECTRON PROBE SURFACE MASS SPECTROMETRY STUDY OF OXYGEN ON MOLYBDENUM. Lichtman, D.; Kirst, T. R. (Honeywell Research Center, Hopkins, Minn.). Phys. Lett., 20: 7-9(Jan. 15, 1966).

The adsorption of oxygen on a polycrystalline molybdenum ribbon was studied using the electron-probe surface mass spectrometry technique. The existence of two adsorption states was confirmed. (D.C.W.)

11323 POSITRON ANNIHILATION AND THE ELECTRONIC STRUCTURE OF RARE-EARTH METALS. Williams, R. W.; Loucks, T. L.; Mackintosh, A. R. (Ames Lab., Ames, Iowa). Phys. Rev. Lett., 16: 168-70(Jan. 31, 1966).

The angular correlation of the photons from two-quantum positron annihilation in single-crystal discs of the rare-earth metals holmium and erbium and in yttrium, which has a similar electronic structure, were measured. A conventional parallel-slit geometry and a magnetically focused ^{58}Co positron source were used. The independent-particle model was used to calculate the angular distribution of photons in yttrium; qualitative agreement between the calculated values and the experimental results was obtained. (G.O.Y.)

11324 ULTRASONIC STUDY OF THE DISTRIBUTION OF CRACKS AND PORES IN SINTERED BERYLLIA. Levavasseur, G.; Frisby, H. (IRCHA, Paris. Centre d'Etudes Nucleaires, Saclay, France). Rev. Hautes Temp. Refract., 2: 275-82(July-Sept. 1965). (In French).

Preliminary studies made with a commercial device led to the development of an ultrasonic apparatus of high performance well-suited to the problems raised in the control of sintered beryllia. A study of pieces of this material by ultrasonics showed two distinct features: the location of large faults ($\phi > 0.01$ mm) by the echo method; and the statistical evaluation of the distribution of small faults ($\phi < 0.1$ mm) by analysis of acoustic absorption diagrams. The presence of these two types of faults revealed by ultrasonics in the sinters was confirmed by optical examination. (auth)

11325 AN X-RAY DIFFUSE-SCATTERING DETERMINATION OF SHORT RANGE ORDER IN Ni–Mo ALLOYS. Hsieh, Tai-ho; Kuo, Ke-hsin (Academia Sinica, Shenyang, China). Sci. Sinica (Peking), 14: 1704-6(Nov. 1965).

In order to clarify the relation between the short range order and the K state in Ni–Mo alloys, the short range

order parameters in alloys containing 10.7, 16.2, and 20.2 at. % Mo respectively (calculated from their lattice constants) were determined by the diffuse-scattering method. The diffuse scattering on an absolute intensity scale caused by the short range order and size effect from an alloy containing 16.2 at. % Mo is shown. The existence of a pronounced positive deviation from the Laue monotonic scattering in the region just prior to the (111) Bragg reflection is characteristic of the presence of short range order in this alloy. The alloys containing 10.7 and 20.2 at. % Mo show similar diffuse scattering curves. A summary of the short range order and size-effect parameters in Ni–Mo alloys is also shown. (J.F.P.)

11326 THE ACTIVATION ENTHALPY OF BERYLLIUM DIFFUSION IN Ni–Be ALLOYS. Baumgaertner, G.; Sizmann, R. (Technische Hochschule, Munich). Z. Angew. Phys., 20: 21-6(Nov. 1965).

The time-temperature dependence of the precipitation of beryllium from a quenched, supersaturated nickel–14% (per atom)–beryllium alloy was studied with a sensitive magnetic technique. The diffusion enthalpy of the beryllium atoms was found by two independent methods to be q = 2.36 ± 0.01 ev. (auth)

11327 THE CONSTITUTION OF THE SYSTEMS OF EUROPIUM WITH SILVER, CADMIUM AND INDIUM AND THE SYSTEM CADMIUM–STRONTIUM. Koester, Werner; Meixner, Johann (Max-Planck-Institut fuer Metallforschung, Stuttgart). Z. Metallk., 56: 695-703(Oct. 1965). (In German).

All phases show no measurable range of solubility. Ag_5Eu, Ag_5Sr, and Ag_5Ba are isotype with $CaZn_5$. $Cd_{11}Sr$ and $Cd_{11}Eu$ have a $BaCd_{11}$ structure. Cd_6Eu and Cd_6Sr have a large cubic elementary cell. Both phases are related to Cd_6Ce. Ag_5Eu_3, Cd_2Eu, Cd_2Sr, Ag_5Sr, and Ag_5Ba_3 belong to the orthorhombic $CeCu_2$-type. In_2Eu is hexagonal and isotype with In_2Ca. A CsCl-structure was confirmed for CdSr. Cd_5Eu_6 has the same x-ray-diffraction lines as CsCl and some additional lines. AgEu is not isotype with CsCl. Eu showed no solubility in Ag, Cd, and In. The susceptibility changes linearly from the values of Ag, Cd, and In to those of Eu. The behavior of Eu in its binary alloys with Ag, Cd, and In corresponds more to that of an alkaline earth than to that of a rare earth metal. (W.L.G.)

11328 ON SEVERAL T–Zn AND T–Cd ALLOY SYSTEMS. Rossteutscher, Werner; Schubert, Konrad (Max-Planck-Institut fuer Metallforschung, Stuttgart). Z. Metallk., 56: 730-4(Oct. 1965). (In German).

The crystal structures of intermetallic compounds in alloys of Zn with Ti, Zr, Hf, Nb, and Ta and Cd with Hf and Zr were determined. Ti_2Zn, Zr_2Zn, Hf_2Zn, Zr_2Cd, and Hf_2Cd had the Zr_2Cu-type structure; ZrCd and HfCd had the TiCu-type structure; $HfZn_2$ had the Ni_2Mg-type structure; and $HfZn_{22}$ had the $ZrZn_{22}$-type structure. There was evidence for the presence of other compounds in some of the systems. The bonding relation in these alloys was discussed. (W.L.G.)

11329 THERMAL CONDUCTIVITY OF Tm, Yb, AND Lu AT LOW TEMPERATURES. Aliev, N. G.; Volkenshtein, N. V. (Inst. of Physics of Metals, Academy of Sciences, USSR). Zh. Eksp. Teor. Fiz., 49: 1450-2(Nov. 1965). (In Russian).

The thermal conductivity of Tm, Yb and Lu was measured in the 2 to 100°K temperature range. An effect of the antiferromagnetism—paramagnetism transition on the thermal conductivity of Tm was observed at 53°K. The Lorentz numbers calculated for Yb and Lu at 4.2°K, which do not possess magnetic order, were found to exceed the theoretical values. It is anomalously large in Tm, which possesses a magnetically ordered state. It is suggested that in Yb and Lu samples at this temperature besides an electron thermal conductivity there exists an appreciable lattice conductivity and in the Tm samples also a magnon thermal conductivity. (auth)

11330 REFRACTORY CARBIDE ALLOYS FOR PARTS OF APPARATUS WORKING AT HIGH TEMPERATURES. Paderno, V. N. pp 117-24 of Novye Mater. v Mashinostr. Moscow-Leningrad, Mashinostroenie, 1964. (In Russian).

Methods of preparing carbide alloys in a homogeneous state, their physical properties and the possible use of a number of alloys for parts of apparatus working at elevated temperatures were studied. Alloys of type TiC–HfC, ZrC–HfC, HfC–NbC, HfC–TaC, NbC–TaC, ZrC–NbC were investigated. The melting points of the alloys were found to be higher than those of the initial components and the coefficient of thermal expansion was found to be somewhat lower than that of the individual carbides. The alloys NbC–ZrC can be used as materials for heaters in high-temperature furnaces. (Rev. Metal Lit.)

11331 THE STRAIN-AGING BEHAVIOR OF TANTALUM AND ASSOCIATED PROBLEMS IN THE THEORY OF PLASTIC DEFORMATION OF METALS [Thesis]. Hartley, Craig Sheridan. Columbus, Ohio, Ohio State Univ., 1965. 180p.

A theoretical and experimental investigation of the early stages of strain-aging in single-crystal and polycrystalline tantalum was conducted. For polycrystalline material, it was found that the time-temperature dependence of the strain-aging parameter, $P = 2(\sigma_a - \sigma_f)/(\sigma_a + \sigma_f)$, where σ_a is the lower yield stress or the intercept of the flow curve with the elastic portion of the stress-strain curve measured after aging for a time, t, at a temperature T_a, may be represented by an equation of the form $P = A + B(t/T_a)^{\frac{1}{3}}$. It is shown that this relationship may be derived theoretically by assuming that aging only reduces the total length of free dislocation line and that deformation after aging proceeds by the multiplication of long unpinned segments of dislocations existing as a result of the prestrain. The principal interstitial solute contributing to the strain-aging of polycrystalline tantalum, which was prestrained and retested in compression at room temperature with intermediate aging in the range 100–200°C, was found to be oxygen. Studies on high-purity single crystals indicate that strain-aging in this material may not be fully described by the same model that apparently holds for polycrystalline material. Two studies of the properties of dislocations in crystals indicate that (a) the products of reactions between $a/2\langle 111\rangle$ dislocations in body-centered cubic crystals may serve as important barriers to plastic flow and sources for the nucleation of twins and fracture and (b) mutual forces exerted on pairs of non-parallel, non-coplanar dislocations may account for the various types of debris, such as dipoles and tangles of dislocations, observed in deformed metals. Finally, an analysis of the resolutions of stresses in single crystal deformation resulted in the development of three master plots which, when used in conjunction with an appropriate stereographic projection, enable one to determine rapidly the ratio of the resolved shear stress on a particular slip system to the applied stress for various common states of stress. (Dissertation Abstr.)

11332 INVESTIGATION OF ALLOYS OF THE TERNARY Ti–Al–Zr SYSTEM. Pylaeva, E. N.; Volkova, M. A. pp 38-42 of Metalloved. Titana. Moscow, Nauka, 1964. (In Russian).

The alloys of the ternary Ti–Al–Zr system in the radial section at a ratio Al : Ti = 9 : 91 were studied by microstructural and thermal analyses and their electrical resistivity and hardness determined. The existence of a continuous series of solid solutions was detected, with the exception of those (of alpha + $alpha_2$ alloys) which, as regards their composition, adjoin the alloy with 9% Al and 91% Ti (for example, at 500°C the content of Zr in alpha + $alpha_2$ alloys is 0-10%). All alloys in the section investigated undergo a polymorphic transformation which is similar to the transformation in pure Ti and Zr and in the Ti–Zr system. Moreover, the temperature of the polymorphic transformation varies along curves with a minimum (660°C at 65% Zr). The electrical resistivity and the hardness of the alloys after quenching from 1100, 800, and 500°C vary along curves with humps. Moreover, the alloys quenched from the region of the beta-solid solution have the highest hardness numbers. (Rev. Metal Lit.)

11333 PHASE EQUILIBRIUM OF ALLOYS IN THE Ti_3Al–Zr SECTION OF THE TERNARY Ti–Al–Zr SYSTEM. Kornilov, I. I.; Nartova, T. T.; Savel'eva, M. M. pp 43-6 of Metalloved. Titana. Moscow, Nauka, 1964. (In Russian).

Specimens were prepared by induction levitation melting, homogenized in a vacuum at 1200°C for 6 hr and at 1100°C for 50 hr and water quenched from 1200, 1100, 1000, 950, 850, 750, 700, and 500°C after holding for 6 to 750 hr. At the same time specimens of the alloys were peened and subjected to prolonged annealing at 800°C for 2500 hr and at 500°C for 3000 hr. The investigation was carried out by thermal analysis, micrography, and x-ray micrography. The dependence of the density, hardness, microhardness, and electrical resistivity at room temperature on the composition of the alloys was studied by using standard methods for these investigations. It was established that the chemical interaction between the alloys of the Ti_3Al–Zr section is similar to the interaction between Ti and Zr in the binary Ti–Zr system and characterized by the presence of a continuous series of alpha- and beta-Ti(Zr)-base solid solutions. (Rev. Metal Lit.)

11334 INVESTIGATION OF THE PHASE STRUCTURE OF ALLOYS OF THE Ti–Al–Zr SYSTEM IN THE Ti_2Al–Zr SECTION. Kornilov, I. I.; Boriskina, N. G. pp 47-53 of Metalloved. Titana. Moscow, Nauka, 1964. (In Russian).

A tentative diagram of the polythermal section of the alloys Ti_2Al–Zr was plotted by microstructural, x-ray and thermal analyses and by measuring the electrical resistivity, the macro- and microhardness. A three-phase equilibrium region alpha + beta + Zr_2Al is formed in the alloys of this section. The existence of this region is confirmed by the results of thermal analysis of alloys containing 10-70% Zr. With the increase in the Zr content from 10 to 70%, the ternary eutectoid transformation temperature of the beta-phase drops from 975 to 780°C. (Rev. Metal Lit.)

11335 CREEP BEHAVIOR OF ALLOYS OF THE QUATERNARY Ti–Zr–Al–Sn SYSTEM AT 750 C. Kernilov, I. I.; Nartova, T. T.; Savel'eva, M. M. pp 218-21 of Metalloved Titana. Moscow, Nauka, 1964. (In Russian).

The creep behavior of alloys of the quaternary Ti–Zr–Al–Sn system in the section extending from pure Zr to the composition of alloys corresponding to the pseudoternary system Ti_3Al–Zr–Ti_3Sn was investigated. The alloys were prepared by arc melting in a furnace with a nonconsumable W electrode in an atmosphere of Ar. The alloys were annealed at 850°C for 30 min. To evaluate the dependence of the creep resistance of the alloys on their composition, phase structure and temperature, the tests were made by using the centrifugal bending method at 700-750°C, stress 15-25 kg/mm^2, for a total testing time 400-1000 hr. V, Nb, and Mo additions increase the heat resistance of the $TiAl_3$ compound-base quaternary solid solution. Additions of up to 0.5% V to the quaternary alloy increase the time required to reach the given bending deflection during the tests by centrifugal bending method more than by 2.5 times. An insignificant decrease in the heat resistance, owing to the formation of a two-phase alpha + beta structure, can be observed in alloys with 1 and 1.5% V. Nb within the limits of solubility in the compound Ti_3Al (up to 2%) increase its heat resistance. The alloy with 3% Nb and with a two-phase alpha + beta structure has the lowest heat resistance. A decrease in the heat resistance of the alloys with Mo can already be observed at a content of about 1% Mo. This is connected with the formation of a beta-phase in the structure. The investigation makes it possible to select the best compositions for heat resistant alloys working at temperatures from 700 to 750°C. (Rev. Metal Lit.)

11336 THE HEAT RESISTANCE OF ALLOYS OF THE QUATERNARY Ti–Al–Mo–V SYSTEM. Pylaeva, E. N.; Ge, Chzhi-min. pp 236-9 of Metalloved. Titana. Moscow, Nauka, 1964. (In Russian).

The dependence of the heat resistance of alloys of the Ti–Al–Mo and Ti–Al–(Mo:V = 1:1) systems on their composition and structure was investigated by means of stress-rupture, hot hardness, and centrifugal bending tests. The Ti alloys, whose compositions are near the boundary of transition from the alpha-solid solutions (ternary and quaternary) into the region of alpha + beta phases, are the most heat resistant. Of the alloys studied, those from the region of the quaternary gamma-solid solution on the base of the TiAl compound were found to be the most heat resistant. The high heat resistance of the compound TiAl is due to its strong chemical binding. Alloys of the given series are not deformable and can only be used as heat resistant casting alloys. (Rev. Metal Lit.)

11337 THE CRYSTAL STRUCTURE OF THE COMPOUND Zr_5Si_3. Karpinskii, O. G.; Evseev, B. A. pp 54-6 of Issled. Stalei i Splavov. Moscow, Nauka, 1964. (In Russian).

The unit cell constants of the compound Zr_5Si_3 were determined by subjecting the single crystals of this compound to x-ray analysis. The constants were found to be $a = 7.945 \pm 0.001$ Å, $c = 5.559 \pm 0.001$ Å, $c/a = 0.699_7$. The compound Zr_5Si_3 belongs to the Fedorov group of symmetry D^3_{6h} and in the lattice of the compound Zr_5Si_3 occupies two structurally nonequivalent positions: 4 (d) and 6 (g). The results obtained agree with the data on the structural type Zr_5Si_3 determined by the powder method but their coordinates and unit cell dimensions differ somewhat. (Rev. Metal Lit.)

11338 INVESTIGATION OF ALLOYS OF THE Cb–$CbCr_2$–$CbAl_3$ SYSTEM. Svechnikov, V. N.; Shurin, A. K.; Dimitrieva, G. P. pp 104-7 of Issled. Stalei i Splavov. Moscow, Nauka, 1964. (In Russian).

The solubility of Al in Nb in the Nb–Al system was determined and was found to be 2.8 and 1.7% at 1500 and 1200°C respectively. The isothermal sections of the phase diagram of the Nb–$NbCr_2$–$NbAl_3$ system at 1500 and 1200°C were plotted. These sections are characterized by the regions of the phases gamma (Nb_3Al), sigma (Nb_2Al), delta ($NbAl_3$), beta (low-temperature modification of $NbCr_2$), epsilon (high-temperature modification of $NbCr_2$), the extent of which hardly changes with temperature. The oxidation resistance of the alloys Nb–Al, Nb–Cr, and Nb–$NbCr_2$–$NbAl_3$ was studied. The alloys Nb–$NbCr_2$–$NbAl_3$ containing 5-6% Al and 4-7% Cr have the lowest oxidation rate at 1100°C. (Rev. Metal Lit.)

11339 PLASTICITY AND STRENGTH OF TUNGSTEN DURING SHORT-TIME TESTS. Severdenko, V. P.; Kal'nitskii, R. M. pp 114-17 of Issled. Stalei. i Splavov. Moscow, Nauka, 1964. (In Russian).

An investigation was made of powdered-metal W (99.95%) at 20–1000°C and tension rates 2.36×10^{-2}–5.55×10^{-1} sec^{-1}. The brittle-elastic transition point shifts toward higher temperatures with the increase in the strain rate and radial tensile stress. In the zone of brittleness at strain rate less than 10^{-1}sec^{-1}, the strength does not change, at higher strain rates it decreases with the drop in temperature. Moreover, the rate of change decreases with the increase in the strain rate radial tensile stress. A slight increase in strength and a decrease in plasticity is noticeable when the strain rate is increased. (Rev. Metal Lit.)

11340 FERROMAGNETISM AND ANTIFERROMAGNETISM OF RARE EARTH METALS AND ALLOYS. Belov, K. P.; Levitin, R. Z. pp 42-54 of Vopr. Teor. i Prim. Redkozem. Met. Moscow, Nauka, 1964. (In Russian).

A review of results of investigation on the magnetic properties of metals of the groups Y and Ce and also of rare-earth metals. (50 references). (Rev. Metal Lit.)

11341 MAGNETIC PROPERTIES OF GADOLINIUM ALLOYS WITH IRON, CERIUM AND YTTRIUM. Chechernikov, V. I.; Pop, I.; Burov, I. V. pp 55-9 of Vop. Teor. i Prim. Redkozem. Met. Moscow, Nauka, 1964. (In Russian).

The magnetic properties of Gd alloys with Fe, Ce and Y in the whole range of concentrations and temperatures from liquid N_2 to the melting point were studied. Gd–Fe alloys were studied both in the ferromagnetic and paramagnetic regions. The temperature dependence of the

intensity of magnetization for a series of alloys in this system is complex. The alloys containing up to 35% Gd satisfy the Curie-Weiss law. The paramagnetic Curie point and the effective atomic moment were determined. Curie point and atomic moment decrease with the increase in the Gd content in the alloy (up to 60% Gd); on approaching the compound of the Fe_2Gd type, minima could be observed on the curves for the concentration dependence of Curie point and atomic moment. The paramagnetic susceptibility of Gd–Y alloys with 25, 50, 65, 75, and 95 at. % Gd obeys the Curie-Weiss law. Curie point and atomic moment of these alloys decrease with the increase in the Y content. Curie point is less than zero for alloys containing up to 20% Gd. The dependence of the inverse of the susceptibility on temperature is nonlinear for Gd–Ce alloys containing up to 30% Gd. Susceptibility of alloys containing 40% Gd is constant at low temperatures. At higher temperatures the temperature dependence susceptibility is nonlinear and gradually changes into a linear dependence. (Rev. Metal Lit.)

Radiation Effects

See also CHEMISTRY — Radiation Chemistry

Refer also to abstracts 10605, 12442, and 12457.

11342 (EURAEC–1502) REACTOR TANKS STEELS. IRRADIATION OF TENSILE-TEST PIECES IN EL.3 AT DIFFERENT TEMPERATURES AND POST-IRRADIATION TESTS. Final Report. Cibois, [E.]; Lemaire, J.; Weisz, M. (Commissariat a l'Energie Atomique, Paris (France)). [1964]. Contract 039-61-12RDF. 64p. (EUR–2660). Dep. mn. CFSTI $3.00 cy, $0.75 mn.

Work Performed under United States–Euratom Joint Research and Development Program.

Fast neutron irradiation hardening in steels was studied as a function of irradiation temperature and steel type. Carbon steels with C contents from 0.03 to 0.05%, ASTM A302B steel, and low-alloy Ni–Cr–Mo steels, commonly used for reactor pressure vessels, were irradiated to 3×10^{19} n/cm^2 at 100 to 400°C. Maximum hardening occurred between 100 and 200°C regardless of steel type, but the hardening obtained decreased with increasing C content in the carbon steels. At 300°C, irradiation hardening was negligible, but recovery studies revealed a secondary hardening occurring in the ASTM A302B steel. The Ni–Cr–Mo steels showed recovery at lower irradiation temperatures than the carbon steels, however, they possessed a residual hardening at irradiation temperatures of 400°C. (W.L.G.)

11343 (LA–3367) THE BEHAVIOR OF COATED PARTICLES IN A LARGE NUCLEAR TRANSIENT (KIWI TNT). Geer, W. U.; Hoffman, C. G.; Kerrisk, J. F. (Los Alamos Scientific Lab., Univ. of California, N. Mex.). Sept. 1, 1965. Contract W-7405-eng-36. 78p. Dep. mn. CFSTI $3.00 cy, $0.75 mn.

Capsules containing extruded graphite fuel samples, loaded with 19 different types of coated particles, were exposed to the neutron pulse generated by the Kiwi Transient Nuclear Test (Kiwi TNT). The effects of flux, particle core material (UC_2 and UO_2), core diameter, coating thickness, and sample temperature on the graphite matrix damage and the coated particle damage were investigated. Visual, metallographic, and radiographic examination of the recovered samples produced the following conclusions: the total energy deposition was by far the most significant variable giving complete destruction of the samples at the highest energy depositions and little or no change at the lowest; particles with large core sizes showed more damage than those with small cores; neither coating thickness nor sample temperature significantly affected damage; and particles with UO_2 cores were more easily damaged than those with UC_2 cores. (auth)

11344 (N65–35361) POLYMERIC MATERIALS IRRADIATION DATA SUBMITTAL. (Lockheed-Georgia Co., Marietta). May 1965. 55p. (NASA-CR–67342; ER–7887).

A compilation of physical and electrical measurements performed on polymeric materials after exposure to 5.0×10^5 R and 7.7×10^{11} n/cm^2 (E ~ 0.5 Mev) or to 1.4×10^6 R and 1.2×10^{14} n/cm^2 is reported. The specimens were located in a vacuum chamber during irradiation. The tests included: dielectric constant, dissipation factor, volume resistivity, dielectric strength, compression strength, tensile strength, and hardness. (P.C.H.)

11345 (NASA-CR–54787) EFFECT OF NUCLEAR RADIATION ON MATERIALS AT CRYOGENIC TEMPERATURES. Quarterly Report No. 1, July 21, 1965–October 21, 1965. (Lockheed Nuclear Products, Marietta, Ga.). Nov. 1965. Contract NAS3-7985. 93p. (LAC-ER–8231).

The preparation and modification of existing test loops and equipment for tensile testing and low-cycle fatigue testing of irradiated materials are reported. Titanium and several Ti alloys and alloy conditions were selected for engineering studies and aluminum 1099 was selected for fundamental as well as engineering studies. Test specimens for the tensile testing phase of the test program were fabricated. (P.C.H.)

11346 (NP–15611) RADIATION DAMAGE TO SEMICONDUCTORS BY HIGH-ENERGY ELECTRON AND PROTON RADIATION. Progress Report, March 15, 1965–September 15, 1965. Corelli, John C. (Rensselaer Polytechnic Inst., Troy, N. Y.). 93p.

Separate abstracts were prepared for the five included sections. Diagrams of results for all five sections are presented on pages 50–89. (M.O.W.)

For abstracts of individual sections see: 11347–11351.

11347 (NP–15611, pp 5-18) A STUDY ON INFRARED ABSORPTION BANDS IN SILICON INDUCED BY 45-Mev ELECTRONS. PART I. THE 1.8 MICRON BAND. Cheng, L. J.; Gaerttner, M. (Rensselaer Polytechnic Inst., Troy, N. Y.).

Infrared spectroscopy, using polarized light and stress alignment experiments on defects induced in Si by approximately 45-Mev electrons, was used to show that the 1.8 μ absorption band is due to a divacancy. Detailed results are presented. (M.O.W.)

11348 (NP–15611, pp 19-27) INFRARED STUDIES OF 48 Mev ELECTRON-IRRADIATED (AT 125 deg K) OXYGEN-DOPED GERMANIUM. Gaerttner, M. (Rensselaer Polytechnic Inst., Troy, N. Y.).

The study of radioinduced oxygen-defect complexes in oxygen-doped germanium was extended by performing cold temperature irradiation (≈ 125°K) with approximately 48-Mev electrons and examining the defects using infrared spectroscopy. In addition to yielding a simpler defect absorption band pattern, sufficient evidence is given that leads to the conclusion that a defect band at 618 cm^{-1} may be the germanium A-center, i.e., a simple complex consisting of a substitutional oxygen coupled to a single vacancy similar to the analogous radioinduced defect found in Si (Si–A center). Results of the annealing experiments run on this sample from 125 to 370°K are presented. (M.O.W.)

11349 (NP–15611, pp 28-38) LIFETIME AND TRAPPING IN 6- TO 50-Mev ELECTRON-IRRADIATED GERMANIUM. Fischer, John E. (Rensselaer Polytechnic Inst., Troy, N. Y.).

The study of lifetime and trapping in 6- to 50-Mev electron-irradiated germanium was extended to include measurements of carrier concentration and conductivity on bridge-type samples cut from the same ingot as the parallelopiped lifetime samples. The irradiations were made at 85°K (49-Mev electrons) and detailed annealing experiments were run on the electrical property sample and the lifetime sample from 90°K to 600°K. (M.O.W.)

11350 (NP–15611, pp 39-46) ELECTRICAL PROPERTIES OF 50-Mev ELECTRON-IRRADIATED GERMANIUM. Kalma, Arne H. (Rensselaer Polytechnic Inst., Troy, N. Y.).

Electric properties (temperature dependence of carrier

concentration and conductivity) of 50-Mev electron-irradiated germanium were studied on samples irradiated at 325°K and at 82°K. In the 82°K irradiation 1Ω-cm n-type germanium samples doped with oxygen (1.2×10^{17} cm^{-3}) and antimony were compared and marked differences were observed in the defect energy levels produced and in the annealing behaviors of the two samples. In the 325°K irradiations the n-type germanium samples were exposed to high fluxes in order to study the ultimate position of the Fermi level. (M.O.W.)

11351 (NP–15611, pp 48-9) PHOTOCONDUCTIVITY STUDIES IN 10- TO 50-Mev ELECTRON-IRRADIATED SILICON. Cheng, L. J.; Kalma, A. H. (Rensselaer Polytechnic Inst., Troy, N. Y.).

A brief summary of work on photoconductivity studies in electron-irradiated Si is presented. In studies on the uniaxial stress effects on the radiation induced 1.8 μ infrared absorption band, it is concluded that the band is due to the electronic excitation of the silicon divacancy in one of its charged states. (M.O.W.)

11352 (NP–15707) FERROELECTRICS—THEIR ELECTRICAL BEHAVIOR DURING, AND SUBSEQUENT TO, IONIZING RADIATIONS. Lefkowitz, I.; Kramer, K.; Kroeger, P. (Frankford Arsenal, Philadelphia, Pa.). Nov. 1965. 142p. (R–1779). CFSTI $4.00 cy, $1.00 mn.

A study was made on certain ferroelectric materials which are among those used extensively in military applications, both in a polarized condition in such items as impact fuzes and in an unpolarized condition as capacitors. The transient voltages across a load produced by charge generated on the surface of various types of ferroelectric specimens during irradiation were measured. These outputs were found to vary widely in amplitude and polarity even from specimens ostensibly alike (i.e., from the same lot of a given manufacturer), and even from a single specimen pulsed repeatedly with gamma and neutron radiation. Pulses were found to vary from background levels to a high of 300 volts on a large specimen with a load of 10^7 ohms and radiation of 5.4×10^{14} fast (Pu) neutrons and associated gammas. The maximum voltage possible is unknown, as are the factors causing the variation. Both polarized and unpolarized specimens showed outputs well above background transients. Some specimens were identical to those used in impact fuze applications and were in simulated housings which reproduce the mechanical environment of the device. Some fuze circuits in present use are discussed with reference to their use of ferroelectric materials and a calculation of the energy transferred by a voltage pulse to a load is presented. (P.C.H.)

11353 (ANL-Trans–259) INTERPRETATION OF ELECTRON-MICROSCOPIC CONTRAST PHENOMENA IN VACANCY AGGLOMERATES OF NEUTRON-IRRADIATED COPPER. Ruehle, M.; Wilkens, M.; Essmann, U. Translated by Elmar K. Wilip (Argonne National Lab., Ill.), from Phys. Status Solidi, 11: 819-29(1965). 15p. Dep. mn. JCL $1.60 fs, $0.80 mf.

Contrast experiments of Essmann and Wilkens (Phys. Stat. Sol. 4, K53(1964)) on neutron irradiated copper indicated that the black-white contrasts (SW-contrasts) observed were due to small Frank dislocation loops. To explain this the electron microscope contrast of this kind of defects was calculated as a function of loop depth within the foil, of dimensions of loops, and of the electron microscope focusing conditions. Comparison of theory with experiment showed that other defects apart from those induced by radiation damage are present. To demonstrate this, non-irradiated, well annealed monocrystalline copper foils were investigated. Depending on the polishing conditions, different numbers of SW-contrasts having the same properties as Frank loops were observed in these samples. However, they lay only near the sample surface turned to the electron gun. Under well defined polishing conditions disturbing SW-contrasts were eliminated. The properties of remaining SW-contrasts in neutron irradiated copper agreed with the calculations. (auth)

11354 INVESTIGATION OF THE EFFECT OF NEUTRON IRRADIATION ON PROPERTIES OF THE ALLOY Zr–3Nb–1Sn. Jung-Koenig, W. (Metallgesellschaft A. G., Frankfurt am Main); Richter, H.; Spalthoff, W.; Starke, E. Atomkernenergie, 11: 47-58(Jan.-Feb. 1966). (In German).

The effect of neutron irradiations on mechanical and corrosion properties of the alloys Zr–3Nb–1Sn and Zircaloy-2 was tested at the swimmingpool reactor FRG-1. Tensile and impact specimens received an integrated fast flux (E > 1 Mev) of up to 4.5×10^{19} n/cm^2 at 45°C in contact with the pool water. Corrosion specimens were irradiated up to 820 hours in autoclaves in steam of 400°C and 100 at; in this case the maximum integrated fast flux (E > 1 Mev) was 1.5×10^{19} n/cm^2. For both alloys the irradiation yields an increase of the 0.2% offset yield strength and the ultimate tensile strength and a decrease of the elongation. The impact strength of Zr–3Nb–1Sn was increased, but that of Zircaloy-2 was not altered essentially by the irradiation. The mechanical properties of both alloys attain saturation values at an integrated fast flux of about 3×10^{19} n/cm^2. Zr–3Nb–1Sn has a higher strength than Zircaloy-2. With respect to the corrosion behavior in steam both alloys are nearly equivalent. The hydrogen pick up and the growth of mass are increased by the factor 2 to 3 under irradiation. (auth)

11355 THE SCIENTIFIC WORK OF THE RCN IN NATIONAL AND INTERNATIONAL CONTEXTS. Goedkoop, J. A. Atoomenergie Haar Toepass., 7: 204-11 (Oct. 1965). (In Dutch).

Several examples were given of the scientific investigations performed by the RCN to determine the shrinking of graphite under irradiation, the magnetic structure of cobalt oxide, and the irradiation of cobalt oxide with fast neutrons. A large number of the investigations of the RCN were concerned with the development of reactors, especially in the area of marine reactor development. (tr-auth)

11356 CALCULATION OF THE DENSITY OF ELASTIC ATOMIC DISPLACEMENTS PRODUCED IN SILICON AND GERMANIUM BY PROTONS AT 30 Mev TO 1 Bev. de Lafond, Yann Gervais; Cambou, Francis; Daspet, Danielle (Faculte des Sciences, Toulouse). Compt. Rend., 261: 4709-12(Nov. 29, 1965). (In French).

Equations were derived for calculation of the density of elastic atomic displacements taking into consideration the Coulomb contribution and the nuclear contribution. The numerical results obtained are presented graphically. The importance of the nuclear contribution is shown. (J.S.R.)

11357 THE METALLOGRAPHIC EXAMINATION OF URANIUM–METAL FUEL ELEMENTS IRRADIATED IN CALDER HALL REACTORS TO 4660 MWD/te OR LESS. Jepson, M. D.; Hindmarch, P. (United Kingdom Atomic Energy Authority, Sellafield, Eng.). J. Inst. Metals, 93: 495-504(Oct. 1965).

The microstructure and density are reported of samples of Springfields uranium bars irradiated in the Calder Hall reactors to 4660 Mwd/te element average irradiation or less. There is a progressive increase in the structural distortion as the irradiation level increases, but above 450°C, even at high irradiation levels, the original structure appears to be retained apart from slightly enhanced twinning. Intergranular cracks and voids were observed in material irradiated to >4000 Mwd/te at >450°C. A change in the mechanism of irradiation damage at 450°C seems probable. The volume changes estimated to have occurred during irradiation confirm the suggested linear relation of 1.0% swelling per 1000 Mwd/te. Recrystallization is noted and a possible explanation for its spasmodic occurrence is discussed. The anticipated channel average irradiation of 3000 Mwd/te was achieved in Calder reactors with no indication of impending failure. (auth)

11358 EFFECTS OF NEUTRON IRRADIATION ON THE STRESS-RUPTURE PROPERTIES OF HIGH-TEMPERATURE PRECIPITATION HARDENING ALLOYS. Moteff, J.; Robertshaw, F. C.; Kingsbury, F. D. (General Electric Co., Cincinnati). J. Nucl. Mater., 17: 245-58 (Nov. 1965).

Studies to determine the threshold neutron dosage in which observable changes in the stress-rupture proper-

ties of an iron base (A-286) and a nickel base (René 41) precipitation-hardened alloy may be detected are described. Specimens were irradiated at a temperature of approximately 650°C to fast ($E_n \geq 1$ Mev) and thermal neutron dosages as low as 8.3×10^{14} and 4.4×10^{15} nvt, respectively. Post irradiation stress-rupture tests were conducted at 650°C. The results indicated that there are observable changes in the stress-rupture properties of these alloys even at relatively low neutron exposure. The rupture ductilities, especially, were significantly reduced as a result of the irradiations. A preliminary model explaining the observed effects of neutron irradiation on elevated temperature embrittlement is presented. This model is based on the concentration of boron in the grain boundaries and the changes in the substructure of the grain boundary region as a result of the $^{10}B(n,\alpha)^7Li$ thermal neutron reactions. (auth)

11359 A COMPARISON OF NEUTRON DAMAGE IN ZINC OXIDE AND BERYLLIUM OXIDE. **Hickman, B. S. (Australian Atomic Energy Commission Research Establishment, Lucas Heights, Sydney). J. Nucl. Mater., 17: 270-3(Nov. 1965).**

Single crystals of zinc oxide were irradiated and the effects compared with those on beryllium oxide. The samples were irradiated at 75 to 100°C in HIFAR to doses of 5×10^{19} to 4×10^{20} nvt > 1 Mev. Lattice parameter changes were determined as a function of dose. The expansion was highly anisotropic with the a parameter change apparently saturating at a value of 0.03 to 0.04% and the c parameter change increasing steadily with dose up to 0.4% at the highest dose investigated. Little recovery occurred up to 600°C but one hour at 800°C resulted in complete annealing of the lattice growth. (M.C.G.)

11360 HALL EFFECT MEASUREMENT OF RADIATION EFFECT ON P-TYPE SILICON. **Tanaka, Toshikatsu; Inuishi, Yoshio (Osaka Univ.). Jap. J. Appl. Phys., 4: 725-30(Oct. 1965).**

The Ev + 0.27 ev center was produced by γ irradiation at room temperature in p-type silicon single crystals. The introduction rate was found to be proportional to the density of the acceptor as dopant. It suggests that this center might be dopant vacancy complex as in the case of E center in n-type materials. It was revealed that this radiation-induced level is closely related to the dislocation density in both formation and annealing behaviors. At the same time, oxygen concentration reduces the indroduction rate of the Ev + 0.27 ev center and influences its annealing behaviors, which is similar to the case of E center. (auth)

11361 MEASUREMENT OF THE HOMOGENITY OF A SEMICONDUCTOR WITH AN ELECTRON BEAM. **Munakata, Chusuke (Hitachi Ltd., Tokyo). Jap. J. Appl. Phys., 4: 815(Oct. 1965).**

A p-type Ge bar was irradiated by a pulsed electron beam. The energy of the electrons was 20 kev, and the beam current was 50m μA. Using the scanning technique the beam spot was moved along the surface of the sample. The distribution of the specific resistance and the voltage due to electron bombardment are shown. The output of the integrator is also shown. It is noted that the results for the specific resistance and those from the integrator output coincide qualitatively well. (J.F.P.)

11362 ON THE RECOVERY OF ALUMINIUM AFTER NEUTRON IRRADIATION AT 78 deg K. **Federighi, T.; (I.S.M.L., Novara, Italy); Ceresara, S.; Pieragostini, F. Phil. Mag. (8), 12: 1093-1103(Dec. 1965).**

The recovery after neutron irradiation at 78°K of annealed and vacancy doped Al 99.995% purity, was compared with the recovery observed after quenching from 600°C; from the analysis of the results it appears that stage III (160 to 280°K) can be fairly well interpreted as due to the migration of single vacancies to interstitial clusters formed at the irradiation temperature. Since this interpretation is in contrast with the point of view advanced by others, who assume that interstitial defects move in stage III, a new analysis of the low temperature recovery stages is advanced. From a comparison of the results of several investigators it appears that all experimental results can be fairly interpreted by the assumption that crowdions move at about 34°K and that normal interstitials move at about 80°K. Both the interstitials interact selectively with impurities and have a large tendency to form stable clusters, which can be eliminated only at higher temperatures (during stage III) by the migration of single vacancies. (auth)

11363 CONVERSION OF CRYSTALLINE GERMANIUM TO AMORPHOUS GERMANIUM BY ION BOMBARDMENT. **Parsons, J. R. (Atomic Energy of Canada Ltd., Chalk River). Phil. Mag. (8), 12: 1159-78(Dec. 1965).**

Of particular interest in the theory of radiation damage are the size and structure of the damaged regions produced in crystalline solids by fast particle irradiation. Crystalline germanium at room temperature or at 30°K was bombarded in a Siemens electron microscope with 100 kev oxygen ions emanating from oxide-coated emission filaments. The size and structure of the damaged regions generated by the incident ions were examined at both temperatures using transmission electron microscopy. Detailed evidence is presented which shows that the damaged regions had a size which was dependent on the temperature of the specimen during bombardment and a structure which was amorphous and less dense than the crystalline matrix in which they were located. Further, as the ion dose was increased to 2×10^{15} ions cm^{-2} the entire surface region to a depth of ~600 Å was observed to undergo a gradual transition from a crystalline to an amorphous state. In terms of radiation damage models these results are shown to be consistent with the concept of a temperature spike superimposed on a depleted zone. (auth)

11364 ENERGY AND ORIENTATION EFFECTS OF ELECTRON IRRADIATION IN SILICON. **Haddad, I. N.; Banbury, P. C.; Grimshaw, J. A. (Univ. of Reading, Eng.). Phil. Mag. (8), 12: 1203-7(Dec. 1965).**

Measurements are reported of Hall effect and conductivity on thin oriented specimens of n-type Si subject to room temperature electron bombardment at energies from 0.3 to 2.0 Mev. The carrier removal rate was found to be greater for irradiation in the ⟨100⟩ direction than in the ⟨111⟩ direction throughout the energy range. (auth)

11365 ELECTRON PROBE MICRO ANALYSIS OF IRRADIATED UO_2. **Waldron, M. B. (United Kingdom Atomic Energy Authority, Harwell, Eng.). pp 31-6 of ANS-100(Suppl.).**

Electron microprobe analysis of irradiated (to about 4.6% burnup) UO_2 pellets is reported. White inclusions are detected, and the concentrations of solid fission products, Cs, and Xe are measured inside and outside these inclusions. (T.F.H.)

11366 POSSIBILITIES AND PROSPECTS OF STRENGTHENING METALS AND ALLOYS BY IRRADIATION. **Konobeevskii, S. T.; Levitskii, B. M.; Sokurskii, Yu. N.; Andreev, G. A. pp 104-8 of Protsessy Uprochneniya Detalei Mashin. Moscow, Nauka, 1964. (In Russian).**

A brief survey on the mechanism of radiation damage and data on the nature of change in the properties of metals subjected to irradiation are given. The possibilities of using irradiation to improve the properties of materials or to prepare materials with unusual properties (for instance, alloys with elements which cannot be smelted in usual conditions, but which are formed during the nuclear reactions under neutron irradiation) are examined. It is emphasized that, in a number of cases, a favorable effect can be obtained by combining irradiation (neutron or gamma-quantum irradiation) with subsequent heat treatment. The surface hardening of metals and alloys by electron and heavy ion irradiation is very promising. (Rev. Metal Lit.)

PHYSICS

General

Refer also to abstracts 11130 and 11183.

11367 (D1-82-0448) THE PRODUCTION OF LARGE-DIAMETER LOW-VOLTAGE ELECTRON BEAMS IN THE ABSENCE OF A MAGNETIC FIELD. Kofoid, M. J.; Zieske, P. (Boeing Scientific Research Labs., Seattle, Wash. Plasma Physics Lab.). June 1965. 45p.

The production of long 10 mm-diameter electron beams in the absence of a magnetic field was studied experimentally. The gun design is described at length. Pencil beams of several hundred ev energy were obtained in noble gases in the 1–20 microns pressure range. However, measurements disclosed that in these space-charge focused beams there may be a severe diminution of beam electron current with axial distance from the gun. Analyses showed that a large low-energy electron population exists in the beam volume, forming with the neutralizing positive ions a plasma in which two-stream instabilities can develop and produce the spread found in the energy of the primary beam electrons. Space potential measurements showed that a positive potential well existed in the beam volume, resulting in the trapping of the low-energy electrons. The unavoidable presence of this relatively large population of low-energy electrons in the beam volume prevented precise measurements of the high-energy beam electron current; reasonable measurements were obtained through special experimental precautions. The beams were studied over a range of the parameters of pressure and beam current, energy, and length. (auth)

11368 BEAM DECOMPOSITION IN THE LINEAR OR ELLIPTICAL REFLECTION OF POLARIZED PLANE WAVES ON THE SEPARATION PLANE BETWEEN ABSORBING MEDIA. Schilling, Heinz (Technische Hochschule Otto von Guericke, Magdeburg, Ger.). Ann. Phys. (7), 16: 122-34(1965). (In German).

The behavior of an astigmatic bundle of given polarization on the separation plane between two absorbing media was investigated with respect to its wave optics, and the beam decomposition in the linear or elliptical reflection of polarized plane waves was determined. The calculations show that the decomposition of the reflected beam from one component is generally parallel to the incident plane and orthogonal from the other component. (tr-auth)

11369 STATISTICAL-MECHANICAL DERIVATION OF THE GENERALIZED DIFFUSION EQUATION. Ebeling, W. (Univ. Rostock, Ger.). Ann. Phys. (7), 16: 147-59(1965). (In German).

For solid, liquid, or gaseous solutions of N interacting particles closed equations for the purely place-dependent distribution functions were derived using the resolvent formalism and the Zwanzig method. The starting points are the stochastic Bergmann-Lebowitz equation for N dissolved particles or the Liouville equation for the total system. Equations of the diffusion type were obtained in which tensors occur in place of the diffusion constants. For liquid solutions an estimation of these magnitudes was given on the basis of hydrodynamic methods. (tr-auth)

11370 TRAJECTORIES OF ELECTROMAGNETIC WAVES IN AN IONIZED TOROID AND ITS EFFECTIVE REFLECTING SURFACE. Mar'in, N. P. Geomagn. Aeronomy (USSR) (Engl. Transl.), 5: 437-41(1965).

Translated from Geomagn. Aeronomiya, 3: 568-73(1965).

The ray trajectories of electromagnetic waves in toroids and the magnitude of the effective reflecting surface of a ring are determined using the method of geometric optics. (L.B.S.)

11371 MATERIALY XIII SOVESHCHANIYA PO LYUMINESTSENTSII (ORGANICHESKIE LYUMINOFORY I MOLEKULYARNAYA LYUMINESTSENTSIYA, KHARKOV, 25 IYUNYA–1 IYULYA, 1964). (Proceedings of the 13th Conference on Luminescence, Kharkov, USSR, June 25–July 1, 1964). Izv. Akad. Nauk SSSR, Ser. Fiz., 29: 1258-1438(Aug. 1965). (In Russian). (CONF-640627).

Forty-one papers are included; separate abstracts were prepared for two. (L.B.S.)

For abstracts of individual papers see: 10827 and 11129.

11372 PROTON TUNNELING IN THE HYDROGEN-EVOLUTION REACTION. Bockris, J. O'M.; Matthews, Dennis B. (Univ. of Pennsylvania, Philadelphia). J. Chem. Phys., 44: 298-309(Jan. 1, 1966).

The quantum-mechanical theory of tunneling was applied to the proton-discharge step of the hydrogen-evolution reaction. An unsymmetric Eckart barrier with allowance for zero-point energies was employed. The quantum-mechanical rate i_q was calculated by integration with a digital computer for a large number of combinations of barrier width, barrier heights, heats of reaction, and temperatures over a large potential range for protium, deuterium, and tritium. From these results the quantum-mechanical transmission coefficient τ and the quantum-mechanical correction Γ to the separation factor, Tafel slopes, and activation energies were calculated. By comparison to observed values of $S_{H,T}$, and $S_{H,T}$ as a function of temperature and potential the most probable barrier parameters were obtained. These values were tested by comparison of calculated and observed activation energy, Tafel slopes, $S_{H,D}$ as a function of potential, and the rate of protium evolution at high cathodic overpotentials as a function of temperature. The degree of proton tunneling was found to be significant being 69% at a cathodic overpotential of 1 v for Hg in acid solution. (auth)

11373 COMPLEX SPACE-TIME AND CLASSICAL FIELD THEORY. I. Das, A. (Carnegie Inst. of Tech., Pittsburgh). J. Math. Phys., 7: 45-51(Jan. 1966).

This is the first of the series of three papers which introduces complex space–time to describe physical phenomena. The objective of this generalization is twofold: firstly, to geometrize gauge transformations and electromagnetic fields, and secondly, to quantize space–time in order to remove serious divergences from the field theory. Classical fields are discussed in complex space–time with a view of subsequent generalization to quantum field theory in quantized space–time. (auth)

11374 PRODUCTION OF IONS OF ALKALI METALS, OTHER METALS, AND HALOGEN IN AN rf SOURCE. Lockwood, Grant J. (Sandia Lab., Albuquerque, N. Mex.). Rev. Sci. Instrum., 37: 226-7(Feb. 1966).

A method is reported by which a commercially available r-f source can be used to produce ions of alkali metals, other metals, and halogens as well as the usual gases. The method consists simply of placing a small quantity of appropriate material in the ion source bottle and maintaining a stable r-f discharge in the bottle by admitting a gas. Thus far the method has been used to produce ion beams of cesium and iodine from CsI crystals, lithium and chlorine from LiCl, sodium and fluorine from NaF, lithium and fluorine from LiF, and aluminum and mercury from the pure metals. Beam intensities produced by this method are not as high as those from sources designed specifically for their production, but they are sufficient for many laboratory experiments. Beam intensities are shown at 50 kev for the various ions obtained by this method. (J.F.P.)

11375 QUANTUM FIELD THEORETICAL METHODS IN STATISTICAL PHYSICS. Second Edition. Abrikosov, A. A.; Gor'kov, L. P.; Dzyaloshinskii, I. E. International Series of Monographs in Natural Philosophy. Volume 4. New York, Pergamon Press, 1965. 377p. $12.00.

Translated from the Russian by D. E. Brown.

Topics considered are properties of many-particle systems at low temperatures, quantum field theoretical methods at T = 0, the diagram technique at finite temperatures, Fermi liquid theory, system of interacting bosons, electromagnetic radiation in an absorbing medium, the theory of superconductivity, and the transport equation for excitations in a Fermi liquid. Only one possible variant of the statement of quantum statistics in the language of field theory is used—the Green function method. (M.J.T.)

11376 A COLLECTION OF PROBLEMS IN ATOMIC AND NUCLEAR PHYSICS. Irodov, I. E. New York, Pergamon Press, 1966. 249p. $9.50.

Translated from the Russian by Stevan Dedijer.

A collection of some 850 problems in atomic and nuclear physics is presented. Topics include thermal radiation, corpuscular properties of light, the Rutherford-Bohr atom, wave properties of particles, the Schrödinger equation, alkali-metal spectra and fine structure, the atom in a magnetic field, diamagnetism and paramagnetism, x rays, many-electron atoms and the periodic system, molecules, nuclear reactions and decay, nuclear properties, elementary particles, and experimental methods in atomic physics. A set of comprehensive answers to the problems and derivations of the important theoretical facts and formulas are given. (M.J.T.)

11377 YADERNAYA KHIMIYA. (Nuclear Chemistry). Goldanskii, V. I.; Lavrukhina, A. K. Moscow, Izdatel'stvo Nauka, 1965. 330p.

Seventeen articles are included on fast-proton reactions in meteorites, composition and origin of galactic cosmic rays, fragmentation by high-energy particles, production of tritium and more complex particles in high-energy proton reactions, secondary reactions of formation of At in high-energy bombardment of Bi and Pb, direct nuclear reactions at high energies, mechanism of heavy-ion induced nuclear reactions, origin of rare-earth isotopes in the solar system, chemistry of hot atoms in condensed organic systems, momentum distribution of annihilating electron-positron pairs from photon angular correlations, Hartree-Fock method in positron annihilation in condensed ionic media, Mössbauer effect in analytic chemistry and geochemistry, annihilation of positrons from polarized states in alkali-halide crystals, positron capture by defects in alkali-halide crystals, molecular neutron spectroscopy, physics and chemistry of muonium, and study of chemical reactions by depolarization of muons. (M.J.T.)

Accelerators

11378 (AD-626633) ON A PROCEDURE FOR EVALUATING SPACE-CHARGE EFFECTS IN A BEAM BENDING MAGNET SYSTEM. Preliminary Report, May–June 1964. Yadavalli, S. V. (Stanford Research Inst., Menlo Park, Calif.). Contract Nonr-2728(00). 17p. CFSTI $1.00 cy, $0.50 mn.

A procedure for evaluating the effect of space charge on the electron trajectories in the presence of a beam bending magnet system is outlined. The above procedure employs a particle trajectory equation derived from the principle of least action. A simplified trajectory equation applicable for a beam whose cross section is not far from circular is given. Also, it is mentioned that a beam whose cross section is elliptical can be treated in a similar manner employing results reproduced in an Appendix. An analogous procedure can be employed in the case of ion beams. (auth)

11379 (ANL-7118) SURVEY OF POLARIZED ION SOURCES IN EUROPE. Hess, D. C.; von Ehrenstein, D. (Argonne National Lab., Ill.). Nov. 1965. Contract W-31-109-eng-38. 103p. Dep. mn. CFSTI $4.00 cy, $0.75 mn.

A survey of polarized ion sources in Europe was made. The various ion sources discussed are located in England, France, Germany, Italy, Netherlands, and Switzerland. (M.O.W.)

11380 (BNL-9772) PULSED PHASE MEASURING AND CONTROL SYSTEM FOR THE RF SEPARATOR. Cassel, R. L.; Halama, H. J. (Brookhaven National Lab., Upton, N. Y.). Nov. 9, 1965. Contract AT-30-2-GEN-16. 9p. Dep. mn; CFSTI $1.00 cy, $0.50 mn.

Proper operation of the r-f separated beam in the Brookhaven AGS requires that the phase difference between the two deflectors remain constant within a few degrees. A long (200 ft) cable is used to transmit the microwave power from a central control station to the two deflectors. Circuits are described that measure the phase difference between the end of the cable and the input to the deflector. The error signal produced by these circuits can be used to drive a pulsed servo loop and provide a continuous phase correction. (T.F.H.)

11381 (BNL-9833) NORMAL MODE ANALYSIS OF STANDING WAVE LINACS—FIELD EXCITATION AND BEAM LOADING IN LINAC CAVITIES. Nishikawa, T. (Brookhaven National Lab., Upton, N. Y.). Nov. 15, 1965. Contract AT(30-2)-Gen-16. 52p. Dep. mn. CFSTI $3.00 cy, $0.50 mn.

Previous studies of the normal modes of standing-wave linacs were extended to include the time dependent properties of both the dominant and associated higher modes when the cavity is excited by a well-padded oscillator and a bunched beam passing along the axis. The transient phenomena of cavity excitation and beam loading were studied. The cases of drift-tube and multiple-cell cavities were studied. The results agree with those obtained by equivalent circuit analysis. (M.O.W.)

11382 (CEAL-TM-151) SYNCHROTRON COLLIDING BEAM FACILITY AT THE CEA. Livingston, M. S. (Cambridge Electron Accelerator, Mass.). Dec. 7, 1965. Contract AT(30-1)-2076. 31p. Dep. mn. CFSTI $2.00 cy, $0.50 mn.

A qualitative description of the proposed colliding beam facility is presented. The following successive steps in the development are described; electron linac injector, positron source and accelerating linac, multi-cycle injection and storage, storage with d-c magnetic fields, bypass sector and straight sector, separation of beams, vacuum system, and luminosity and duty factor. A cost estimate for the facility is also presented. (M.O.W.)

11383 (CEAL-TM-152) A 9-MAGNET BYPASS IN THE TARGET AREA. Mieras, Harry (Cambridge Electron Accelerator, Mass.). Dec. 9, 1965. Contract AT(30-1)-2076. 8p. Dep. mn. CFSTI $1.00 cy, $0.50 mn.

Following the proposals for a colliding beam facility for the CEA, calculations were made on a transport system for a bypass in the target area. Linear effects were only considered. Included is a list of associated magnetic and electrostatic components. (M.O.W.)

11384 (CEAL-TM-156) CALCULATION OF RADIATION EFFECTS FOR BYPASS. Robinson, K. W. (Cambridge Electron Accelerator, Mass.). Dec. 10, 1965. Contract AT(30-1)-2076. 8p. Dep. mn. CFSTI $1.00 cy, $0.50 mn.

Synchroton radiation effects which are of interest for the bypass storage ring of the Cambridge Electron Accelerator CEA were investigated. For purposes of scaling to other energies and conditions, the equilibrium density was calculated in synchrotron oscillation phase space due to quantum emission and radiation damping in the CEA at 3 Bev. (M.O.W.)

11385 (CEAL-TM-157) VACUUM REQUIREMENTS FOR THE BYPASS. Winick, H. (Cambridge Electron Accelerator, Mass.). Dec. 20, 1965. Contract AT(30-1)-2076. 29p. Dep. mn. CFSTI $2.00 cy, $0.50 mn.

The modifications required to the CEA vacuum system in order to meet the pressure requirements for storage are described. Quantitative estimates were made of the amount of gas expected due to synchrotron radiation. Average pressures and resulting lifetimes were com-

puted. The vacuum system of the bypass section itself is briefly described. (M.O.W.)

11386 (CERN-65-35) CONTRIBUTION A L'ETUDE DE L'ORBITE FERMEE. (Contribution to the Study of the Closed Orbit). Baconnier, Y. (European Organization for Nuclear Research, Geneva (Switzerland)). Nov. 1965. 58p. Dep. mn.

An optimization principle is defined that makes it possible to work on measurable parameters while one is selective on the harmonics of these parameters. It is based on a method of least squares and it limits to the maximum the effect of errors. Some preliminary results obtained are given. (tr-auth)

11387 (CONF-650922-28) INSULATION STRUCTURE AND COIL RELIABILITY. Brechna, H.; Oster, E. (Stanford Linear Accelerator Center, Stanford Univ., Calif.). [1965]. Contract AT(04-3)-400. 45p. Dep. mn. CFSTI $2.00 cy, $0.50 mn.

From 1st International Symposium on Magnet Technology, Stanford, Calif.

Insulation voids due to impregnation and potting failure, and delamination of insulation due to magnetomechanical and thermomechanical forces lead frequently to coil deficiencies such as corona, accelerated aging, electrical breakdown between conductors and adjacent pancakes, or flashover from coil to magnet core or structural parts. The prevention and evaluation of cavities and the determination of their size and distribution over the coil is a formidable task. However, an approach to determine the stresses on the insulation and corona, ionization effects on the thermoset, and reduction of the corona threshold due to environmental influences is discussed. Methods of prevention, detection, and evaluation of cavities are given. A nondestructive coil test program to evaluate the soundness of insulation is proposed. (auth)

11388 (CONF-650922-29) AN ADJUSTABLE CURRENT SHUNT FOR TRIMMING THE AMPERE TURNS IN A MAGNET OPERATING FROM A CONSTANT DC SOURCE. Hicks, John W. (Midwestern Universities Research Assn., Stoughton, Wis.). [1963]. Contract AT(11-1)-384. 22p. Dep. mn. CFSTI $1.00 cy, $0.50 mn.

From 1st International Symposium on Magnet Technology, Stanford, Calif.

A simple practical method for maintaining the current division between a coil and a shunt in the kilowatt power range was developed. The design equations are presented with their sample calculations. Factors considered for obtaining ±5% adjustability, while maintaining ±0.01% stability of field coil ampere turns, are field coils turns and resistance, temperature and pressure of the cooling supply, and effects of the thermocouple junctions. Experimental and calculated performances are compared for various operating conditions. (auth)

11389 (DESY-65/12) EICHMESSUNGEN MIT FARADAYKAEFIG, KALORIMETER, QUANTAMETER UND SEKUNDAEREMISSIONSQUANTAMETER AM EXTERNEN ELEKTRONENSTRAHL 1 Gev BIS 5 Gev. (Calibration Measurements with Faraday Cup, Calorimeter, Quantometer on the External Electron Beam 1 to 5 Gev). Ladage, A.; Pingel, H. (Deutsches Elektronen-Synchrotron, Hamburg (West Germany)). Aug. 1965. 76p. Dep. mn.

Calibration measurements were made on the external electron beam at DESY in the energy region 1.5 to 5 Bev with a Faraday cup, a calorimeter, several gas-filled quantometers, and a secondary emission quantometer, using a thin secondary emission monitor of 2.10^{-2} radiation length as an intermediate standard. The response of the monitors was investigated over a wide range of intensities, energies and for various beam positions across the aperture. Plateaus were measured and short and long term stability was checked. Comparisons of the response of these monitors are presented. (M.O.W.)

11390 (JINR-P-2446) EKSPERIMENTAL'NOE OPREDELENIE FUNKTSII PROSTRANSTVENNOGO RASPREDELENIYA NEITRONOV VOKRUG SINKHROFAZOTRONA NA 10 Gev. (An Experimental Determination of a Function of the Spatial Neutron Distribution Around the 10 Gev Synchrophasotron). Lebedev, V. N. (Joint Inst. for Nuclear Research, Dubna (USSR). Lab. of High Energy). 1965. 19p. Dep. mn.

Results are presented of investigating the distribution of the flux density and the dose equivalent of neutrons with energies less than 20 Mev around the 10-Bev synchrophasotron. The quality factor of the effective energy of the fast neutrons is given as a function of distance. The value of the effective energy of the equilibrium spectrum is close to 3 Mev. The measurement results are compared with data obtained on other high-energy accelerators. Empirical formulas are given for calculating the flux density and dose equivalent of neutrons at large distances from the accelerator. (auth)

11391 (NP-15274) ENTWICKLUNG EINES 100 Mev FFAG-ELEKTRONENSYNCHROTRONS: MAGNETOFELDMESSUNGEN AN ZWEI MODELLSEKTOREN. (Development of a 100-Mev FFAG Electron Synchrotron: Magnetic Field Measurements on Two Model Sectors). Report No. 20. Arendt, F. (Freie Universitaet, Berlin (West Germany). I. Physikalisches Institut). Feb. 20, 1965. 8p. Dep. mn.

Magnetic field measurements in the radial and the azimuthal direction were reported. Representative measurement results were given with examples. (tr-auth)

11392 (NP-15275) ENTWICKLUNG EINES 100 Mev FFAG-ELEKTRONENSYNCHROTRONS: ZUR STRAHLSTROMMESSUNG UND STRAHLFUEHRUNG. (Development of a 100-Mev FFAG Electron Synchrotron: On Beam Current Measurements and Beam Guides). Report No. 19. Hoffmann, G. (Freie Universitaet, Berlin (West Germany). I. Physikalisches Institut). Feb. 20, 1965. 6p. Dep. mn.

An induction current monitor selected for the beam current measurement was developed. It has the advantage of not disturbing the beam and having an energy-independent reading. It is simple in construction, operation, and calibration. The basic principle of the induction current monitor is briefly outlined. The results obtained are given. With this instrument the current and voltage can be measured with an error ±3%. (J.S.R.)

11393 (NP-15715) ETUDE D'UN SYSTEME DE GROUPEMENT DES ELECTRONS A L'ENTREE D'UN ACCELERATEUR LINEAIRE ET ETUDE DES COEFFICIENTS D'HARMONIQUES D'ESPACE DE LA STRUCTURE ACCELERATRICE [THESES]. (Study of a System of Electron Grouping at the Input of a Linear Accelerator and Study of the Coefficients of Space Harmonics of the Accelerating Structure [Thesis]). Hirel, Renee (Paris Univ. (France). Faculte des Sciences). 1965. 20p. Dep. mn.

Electron grouping at the input of an accelerator and a deflector system that makes it possible to eliminate the electrons that cannot be grouped in such a way that operation of the machine is not disturbed were studied theoretically. The method of measurement of the coefficients of space harmonics of the iris structures used for the accelerator guide was studied experimentally. The values of these coefficients were compared for different disc thicknesses. (J.S.R.)

11394 (NP-15788) IMPUL'SNYI IONNYI ISTOCHNIK S KATODNOI IGLOI. (Pulsed Ion Source With Point Cathode (Needle)). Report No. 380. Lapitskii, Yu. Ya.; Khoroshkov, V. S. (Gosudarstvennyi Komitet po Ispol'zovaniyu Atomnoi Energii SSSR, Moscow. Institut Teoreticheskoi i Eksperimental'noi Fiziki). 1965. 10p. Dep. mn.

The pulsed cold cathode ion source with fixed discharge region is described. The ion emission current is 0.3. The working resource of the source is several thousand hours. Gas consumption is 25 cm^3/hour. Power dissipated in the source is 35 watts. (auth)

11395 (ORNL-TM-1172(Rev.)) MAGNETIC FIELD STORAGE CODES AND ORBIT CALCULATIONS. Rankin,

Mozelle (Oak Ridge National Lab., Tenn.). June 18, 1965. Contract W-7405-eng-26. 21p. Dep. mn. CFSTI $1.00 cy, $0.50 mn.

Two useful codes for studying single particle orbits are described. After calculating the magnetic field quantities and their derivatives for an axisymmetric coil system, the first code stores them on magnetic tape. The second code then integrates the equations of motion using the magnetic quantities previously stored on tape. Since the values are only stored for a finite grid, a Taylor series expansion is used to obtain the field at the point called for in the integration procedure. Plots are produced to facilitate analysis of these orbits. (auth)

11396 (ORNL-TM-1382) BEAM ENERGY MEASUREMENTS AT THE OAK RIDGE ISOCHRONOUS CYCLOTRON. Santoro, R. T.; Bertrand, F. E.; Love, T. A.; Peelle, R. W. (Oak Ridge National Lab., Tenn.). Jan. 13, 1966. Contract W-7405-eng-26. 17p. Dep. mn. CFSTI $1.00 cy, $0.50 mn.

Measurements have been made of the beam energy of the Oak Ridge Isochronous Cyclotron for protons at acceleration frequencies of 17.04 and 21.22 Mc, H_2^+ ions at 11.32, 11.91, and 12.61 Mc, and alpha particles at 11.32 Mc. The energy was determined from measurements of the particle path length in Al using a remotely controlled range wheel to vary the absorber thickness. The experimental results are given in tabular form. A curve of measured proton energy as a function of the r-f acceleration frequency is included. (auth)

11397 (SC-RR-65-111) A SMALL ORBIT BETATRON. Mogford, J. A.; Law, W. B. (Sandia Corp., Albuquerque, N. Mex.). Sept. 1965. Contract AT(29-1)-789. 54p. Dep. mn. CFSTI $3.00 cy, $0.50 mn.

A small orbit betatron (equilibrium orbit radius ~3.3 cm) was designed, built, and studied to determine its operational characteristics. Two modifications of the basic design were made operational and a comparison between them is discussed. The design was facilitated by a computer program which calculates the magnetic field and vector potential as a function of the coordinate for cylindrical current sheets. The investigation concentrated on three areas: injection, ejection, and output pulse. The dependence of the output characteristics on such parameters as time, radius, energy, and angle of injection, and time of ejection is reported. Maximum energy of operation is about 0.60 Mev, but a more typical energy is ~0.2 Mev. It is estimated that a maximum of $\sim 10^8$ particles are accelerated onto the target to produce an output pulse with a duration which can be controlled by variation of the time of orbit expansion. (auth)

11398 (UCID-10028) A "MONOCHROMATIC" NEUTRINO BEAM FROM A HIGH INTENSITY 200 Gev PROTON SYNCHROTRON. Peterson, Vincent Z. (Lawrence Radiation Lab., Univ. of California, Berkeley). Nov. 30, 1964. Contract W-7405-eng-48. 42p. Dep. mn. CFSTI $2.00 cy, $0.50 mn.

A preliminary study is made of whether or not a monochromatic beam of neutrinos of adjustible energy and reasonable intensity appears to be possible using conventional bending magnets and focusing lenses to define a pencil beam of mesons (π) and mesons (K) decaying into neutrinos which are detected in a liquid hydrogen/deuterium bubble chamber. It is shown that a high intensity proton synchrotron operating at 200 Bev is well suited to provide facilities for experiments. Together with an appropriate detector for such high energies the higher energy and intensity make neutrino experiments of 10% resolution in neutrino energy practicable. A specific beam design is sketched which uses conventional magnets and does not require special focusing devices. (J.F.P.)

11399 (UCRL-7566(Rev.1)) POSITRON FOCUSING IN AN ACCELERATING FIELD. Hong, Gay (Lawrence Radiation Lab., Univ. of California, Livermore). Jan. 1, 1965. Contract W-7405-eng-48. 13p. Dep. mn. CFSTI $1.00 cy, $0.50 mn.

The equation of motion of positrons (or electrons) in an accelerating field and a focusing magnetic field is analyzed with relativistic effects included. An iterative procedure is used to solve the resulting nonlinear differential equation. An example is included to illustrate this technique; it is found that the assumptions involved are consistent with the numerical calculations. The feasibility of the proposed focusing scheme can be determined from the results obtained by this method of analysis. (auth)

11400 (UCRL-16323) SOME EXPERIMENTAL SHIELDING STUDIES AT THE 6.2-Bev BERKELEY BEVATRON. Smith, Alan R. (Lawrence Radiation Lab., Univ. of California, Berkeley). Nov. 10, 1965. Contract W-7405-eng-48. 61p. (CONF-651109-20). Dep. mn. CFSTI $3.00 cy, $0.75 mn.

From 1st Symposium on Accelerator Radiation Dosimetry and Experience, Upton, N. Y.

Three kinds of shielding measurements performed at the Berkeley Bevatron are described. In each case quantities related to the fast-neutron component of the radiation field were measured. The improvement in shield effectiveness brought about by installation of a complete shield enclosure around the accelerator is described. Two sets of measurements were made while identical beam-target conditions prevailed. Detectors were located at 24 equally spaced stations along the crane walkway, which overlooks the entire circumference of the accelerator. The initial measurements were taken when the shield was essentially a ring without a roof. A second set was taken after this ring was thickened and a roof shield was added, to handle the greatly increased proton-beam intensity. Goldfoils in moderators and aluminum-disk threshold detectors were used for this evaluation; the importance of aluminum disk data is clearly demonstrated here. The second experiment describes some measurements of the radiation field inside a thick concrete shield when this shield is bombarded by a well-focused beam of 6.2-Bev protons extracted from the Bevatron. The shield array permitted insertion of detectors at regularly spaced intervals along the beam axis to a depth of 24 feet and laterally to 11 feet off the beam axis. Activation threshold elements were used as detectors. The third experiment relates to the energy spectrum of neutrons emerging from the accelerator shield in the vicinity of a thick target. A mixed system of threshold detectors was used. (M.O.W.)

11401 (UCRL-16502) ON THE APPLICATION OF DIRECT DIGITAL CONTROL TO HIGH ENERGY PARTICLE ACCELERATORS. Machen, Donald R. (Lawrence Radiation Lab., Univ. of California, Berkeley). Nov. 8, 1965. Contract W-7405-eng-48. 12p. (CONF-651130-1). Dep. mn. CFSTI $1.00 cy, $0.50 mn.

From DECUS Symposium, Stanford, Calif.

The performance of a PDP-5 computer for the control of the 200 Bev synchrotron is described. The topics covered include developmental research at the bevatron, details of the bevatron computer control system, and interface details. (J.F.P.)

11402 OBSERVATIONS OF MAGNETICALLY SELF-FOCUSING ELECTRON STREAMS. Graybill, S. E.; Nablo, S. V. (Ion Physics Corp., Burlington, Mass.). Appl. Phys. Lett., 8: 18-20(Jan. 1, 1966).

Experiments for evaluation of self-focusing periodic phenomena in fully and partially neutralized beams were carried out using the Ion Physics Corporation prototype 3.6-Mv pulsed power supply. A pulsed electron beam was transmitted by a window into a 10-cm-dia drift tube several meters long. The pressure dependence of the beam energy flux monitored by calorimetric probes 20 cm from the window is shown. Maximum compression of the beam was realized at a pressure of 0.2 torr. An isometric profile of the beam current density at a beam energy of 2.5 Mev and pressure of 0.2 torr is presented. The expected periodic motion of the drifting stream was observed over 3 nodes with a gradual degradation in definition of the sinusoidal shape of the envelope into cylindrical geometry. (A.G.W.)

11403 CHARACTERISTICS OF SYNCHROTRON RADIATION AT 1000 Mev. Missoni, Guido; Ruggiero, Alessandro (Istituto Superiore di Sanita, Rome). Atti Accad. Naz. Lincei, Rend., Cl. Sci. Fis., Mat. Nat., 38: 677-85 (May 1965). (In Italian).

Characteristics of synchrotron radiation at 1000 Mev are discussed. Measured angular distributions of synchrotron radiation, radiated by electrons accelerated up to 1000 Mev, are reported. Measurements refer to total distribution as well as to components polarized with electric vector parallel and perpendicular to the orbital plane. Data were obtained scanning the beam by means of a photomultiplier. Spectral distribution of radiation emitted, during the accelerating cycle, in the range 50–120 Å, is also given; finally a measurement of the distribution of power irradiated at 3800 Å, as a function of electrons energy is reported. (auth)

11404 RECENT DEVELOPMENTS AT THE PS (THE PS SHUT-DOWN, AND AFTERWARDS). CERN Cour., 5: 170-3(Nov. 1965).

Activity around the proton synchrotron tends to be at a peak during a shut-down period, because it is then that major changes are made to the installations and essential maintenance is carried out on those parts of the machine that are normally operating more or less continually. However, much development, testing, and other preparatory work is required on the major installations before the shutdown, and many additions and changes are also made to the accelerator during the shorter shut-downs every fortnight. The emphasis is more on the continuous development of the PS facilities than on the shut-down itself. (auth)

11405 IMPROVEMENT OF THE FOCUSING POWER OF AN ELECTROSTATIC ACCELERATOR TUBE WITH VERY HIGH OUTPUT. Burnot, Guy (Institut de Physique Nucleaire, Lyon). Compt. Rend., 261: 2876-9(Oct. 11, 1965). (In French).

An accelerator tube that would permit improved focusing of high intensity ion beams is proposed. The apparatus was determined by a method of rapid study which is described and by the numerical integration of very general equations. (tr-auth)

11406 MEASUREMENT OF THE SYNCHRONOUS PHASE IN AN ION ACCELERATOR. Boussard, Daniel (Univ. Paris, Orsay, France). Compt. Rend., 261: 4665-8 (Nov. 29, 1965). (In French).

A device for the measurement of the synchronous phase in an ion accelerator is described. Its originality is based on the use of a sampling technique not of a signal from the Faraday cage but directly on the secondary electron beam emitted by a target bombarded with fast ions. The schematics of the device are given, and its characteristics are discussed. Measurements show that the method permits a precise determination of the synchronous phase. (J.S.R.)

11407 BEAM PROFILE MEASUREMENT FOR ELECTRON ACCELERATORS. Okabe, Shigeru; Tabata, Tatsuo; Tsumori, Kunihiko (Radiation Center of Osaka Prefecture). Jap. J. Appl. Phys., 5: 68-73(Jan. 1966).

New methods were developed for monitoring the beam profile of electron accelerators. For electron energies above and below 3 Mev, the monitor utilizes the secondary emission from the probe and the partial absorption of the primary beam in it, respectively, and the probe consists of copper wire or thin aluminum plate. The performance of the monitor was investigated with electron beams of a 15 Mev linear accelerator and a 2 Mev resonance transformer. The advantages of these methods are simpleness and utility for high power accelerators. (auth)

11408 DEVELOPMENT OF THE PARTICLE DISTRIBUTION DENSITY DURING ACCELERATION TOWARD A STATISTICAL DISTRIBUTION LIMIT. Andrade e Silva, J.; Lochak, G. (Laboratoire Joliot-Curie de Physique Nucleaire, Orsay, France. Institut Henri Poincare, Paris). Port. Phys., 4: 7-16(1965). (In Portuguese).

It is shown that the evolution of the particles distribution density in a beam of accelerated particles inside a circular accelerator is due to convection currents. This evolution, which may be considered an example of a famous problem already studied by Maxwell, tends to approach the beam composition into a given limiting statistical distribution. (auth)

11409 THIN LIQUID SHEETS AT REDUCED PRESSURE AND APPLICATIONS IN NUCLEAR PHYSICS. Griffith, J. A. R.; Burge, E. J. (King's College, London). Rev. Sci. Instrum., 37: 147-54(Feb. 1966).

Thin sheets of flowing water, up to 10 cm^2 and 0.01–0.05 cm thick, were produced and investigated under reduced ambient pressures down to the natural vapor pressure. Their behavior was well represented by Taylor's theory. Measurements were made of the sheet thickness, and a schlieren system was used to estimate thickness variations, which could be limited to about 1% over areas of a few cm^2. Preliminary studies were also made with jets and sheets of liquid oxygen under reduced pressures. A practical water target is described for time of flight measurements on the reaction $^{16}O(p,n)^{16}F$ with 30 and 50 Mev protons. It is pointed out that such targets sometimes have advantages over gaseous, solid, and conventional liquid targets, particularly with regard to defined geometry, low background, single nuclear species, and ability to be used with high beam intensities. (auth)

11410 SPECIMEN HOLDER FOR DEUTERON IRRADIATION EXPERIMENTS IN METALS BETWEEN 4 deg K AND ROOM TEMPERATURE. Herschbach, K. (Douglas Aircraft Co., Inc., Santa Monica, Calif.). Rev. Sci. Instrum., 37: 171-2(Feb. 1966).

A specimen holder which permits annealing experiments to be carried out after deuteron bombardment at liquid He temperature is described. Utilizing the heat capacity of He gas results in lower He consumption and improved temperature regulation. For any temperature between 15 and 300°K, the temperature regulation is ±0.01°K or better. Details of the mounting of specimens are included. (auth)

11411 SYMMETRY PROPERTIES OF BEAM HANDLING MAGNET SYSTEMS. Herrera, J. C.; Bliamptis, E. E. (High Voltage Engineering Corp., Burlington, Mass.). Rev. Sci. Instrum., 37: 183-8(Feb. 1966).

Matrix methods are used to analyze particle-beam-handling magnet systems composed of a primary system followed by a symmetrical replica of itself. There are three such combinations, i.e., the primary system followed by its reflection, the system followed by its antireflection, and the system followed by the flipped over replica of itself. Explicit conditions are imposed on the primary system which due to the over-all symmetry result in desirable beam transport properties for the complete system. (auth)

11412 POSSIBILITIES OF APPLICATION OF SUPERCONDUCTORS TO PARTICLE ACCELERATORS. Septier, A. (Univ. Paris, Orsay, France). Vide, 20: 328-42 (Sept.-Oct. 1965). (In French).

The research work undertaken in recent years in order to compare the h-f surface resistance of common superconductors to that of copper, measured at room temperature, makes it possible to expect a gain of 5,000 over the h-f power dissipated in the walls of guides or cavities. It appears from the energy balance in h-f power and from the efficiency of refrigerators that, in the near future, linear accelerators or superconducting particle deflectors might be designed which would work continuously, or at least with a duty cycle approaching one. (auth)

11413 ELECTROSTATIC STEERING (Engineering Materials). (Lawrence Radiation Lab., Univ. of California, Livermore). (CAPE–1216).

9 drawings.

The electrostatic steering (bias) described is used in a system that applies 1500 v of d-c bias to a pair of deflection plates. One plate has +1500 v and the other has 0 v.

This results in beam-bending, which prevents the beam of particles from reaching a target. When a −1500 v pulse is applied to the deflection plate that initially was positive, the voltage plates are at 0 and the particles hit the target. (For Details, See TID-4100.) (M.C.G.)

11414 PULSE AMPLIFIER (Engineering Materials). (Lawrence Radiation Lab., Univ. of California, Livermore). (CAPE–1217).

13 drawings.

The pulse amplifier described is used in a system that controls deflecting plates, which control a beam of accelerated particles at the target. The amplifier consists of two stages. In the first stage, which is normally conducting, control and screen grids are driven to their full power rating 85 to 100% of the time. This stage suppresses any ringing introduced by the transmission cable. The second stage is driven directly from the first stage, thus providing the necessary bias. Grid and plate circuits are series peaked. During the leading edge switching transient, the screen operates at 400 v. To protect the tube, the voltage drops to about 250 v during the rest of the pulse. (For Details, See TID-4100) (M.C.G.)

11415 METHOD AND ARRANGEMENT FOR THE MEASUREMENT OF THE OUT-OF-PHASE CONDITION OF THE IONS IN A CYCLE TRACK IN AN ISOCHRONOUS CYCLOTRON IN RELATION TO THE ACCELERATING H-F VOLTAGE BY PASSAGE THROUGH A MEASURING PLANE. Feldmann, Hans-Helmut (to Licentia Patent-Verwaltungs-GmbH). German Patent 1,202,914. Oct. 14, 1965. Filed July 19, 1962.

The arrangement consists of an electrode in which a signal voltage is induced by the passing ion bunches, transposition means below or above the ion path and in the vicinity of the electrode (which transpose the signal voltage by means of a modulator voltage derived from the accelerating voltage and a low-frequency voltage into low-frequency signals), and a phase discriminator, which compares the low-frequency signals with the high-frequency accelerating voltage and delivers a signal proportional to the out-of-phase condition. (Gmelin Inst.)

11416 ELECTRON IRRADIATION METHOD. Ota, Susumu (to Nissin Electric Co., Ltd.). Japanese Patent 1964-12700. July 6, 1964. Filed Sept. 30, 1961.

An electron accelerator includes a device for changing freely the crest factor of the scanning magnetic field, and collectors, one at the center and the other at the edge of the beam, below the irradiation window for detecting beam current. The difference between the two detected values actuates the automatic control system connected to the collectors, which adjusts the shape of the scanning wave so as to level off the current difference. With this accelerator wide and uniform irradiation of the material is obtained. (TCO)

11417 PARTICLE ACCELERATOR. Suematsu, Shigeru (to Hitachi, Ltd.). Japanese Patent 1964-18500. Aug. 31, 1964. Filed Aug. 1, 1963.

In a linear accelerator using an insulated transformer an improved supply system is proposed for the focusing or anode electrodes. The system consists of the insulated transformer, the electric sources for the ion source, and the focusing electrodes, and is constructed so that the grounds of these sources are connected to the cabinet containing the high voltage electrodes. The voltage supply for the collector electrodes is independently accomplished by the high-voltage direct current supplier and by means of the divided resistor system. The optimum electric condition of the collector electrodes for the collection of electron beam is kept constant under the various electric conditions of the ion source and the focusing electrodes. (NSA of Japan)

11418 ELECTRON BEAM APPARATUS. Akabori, Hiroshi (to Hitachi, Ltd.). Japanese Patent 1964-24985. Nov. 6, 1964. Filed Sept. 6, 1962.

In the electron beam apparatus proposed, the structural wall with an electron absorbing lining is placed parallel to the beam direction and in the way of electrons scattered from the sample surface. The lining is made of a light metal such as aluminum or magnesium that absorbs the electrons while the primary and secondary x-rays are absorbed in the wall material behind the lining. (TCO)

11419 TRAVELLING-WAVE TYPE ELECTRON ACCELERATOR. Komai, Kenichiro (to Hitachi Co., Ltd.). Japanese Patent 1964-30370. Dec. 26, 1964. Filed Mar. 18, 1963.

A travelling wave type electron accelerator is proposed in which both electron acceleration and focusing are done simultaneously at the maximum phase of accelerating electric field in the accelerating tube. Consequently, the focusing coils can be reduced in size or can completely be eliminated to reduce the weight and cost of the accelerator. A simply constructed support for the accelerator also is applicable. The accelerator consists of a charged-particle source, a high-frequency electric wave source for the particle acceleration, and a number of accelerating electrodes arranged in the path of charged particles. Both an axial accelerating electric field and a radial focusing electric field are produced simultaneously in the vicinity of the maximum phase of accelerating electric field. To achieve the simultaneous accelerating and focusing the effective hole of one, at least, of the adjoining two accelerating electrodes in the forward direction is made smaller than that of the other electrode. (TCO)

11420 DEVICE FOR COOLING AN ACCELERATING TUBE. Iwashiia, Fumio (to Tokyo Shibaura Electric Co., Ltd.). Japanese Patent 1964-30372. Dec. 26, 1964. Filed Aug. 27, 1963.

A method is proposed for minimizing the differences in temperature in the wall of an accelerating tube. The accelerating-tube wall is cooled, as usual, by flowing the coolant along the tube wall and the heat is applied either by directly heating the tube wall or by heating the coolant itself. The heating methods may be used individually or in combination. (TCO)

11421 CHARGED-PARTICLE ACCELERATOR. Komai, Kenichiro (to Hitachi, Ltd.). Japanese Patent 1964-30373. Dec. 26, 1964. Filed Oct. 25, 1963.

A charged-particle accelerator is proposed, in which the deceleration effect produced near the end of an accelerating tube is reduced when the charged particle current is increased. Thus, the accelerating power of the charged particle accelerator can be maintained high. The accelerator consists of a charged-particle source and first and second accelerating tubes, which are connected together in one whole body. In the second accelerating tube, phase adjusting devices are provided for breaking the coincidence between the electric wave and the accelerated charged particles. This second accelerating tube is made of a high resistance material. If the devices for breaking the coincidence are installed in the first accelerating tube, the accelerating power is lowered; but the output energy of accelerated charged particles can be changed as required. (NSA of Japan)

11422 CHARGED-PARTICLE ACCELERATOR. Komai, Kenichiro (to Hitachi, Ltd.). Japanese Patent 1964-30374. Dec. 26, 1964. Filed Oct. 25, 1963.

A charged-particle accelerator is proposed in which the coupler of electric-wave exit and the electric-wave absorbing part usually installed at the end of an accelerating part are eliminated, and provision is made for the simultaneous acceleration and electric-wave absorption near the end of an accelerating tube. The accelerator consists of a charged-particle source; a high-frequency electric wave source; a wave-delaying structure, composed of discs with a hole in the center for the passage of charged particles; and first and second accelerating tubes, connected together in a series in the path of charged particles. The attenuation constant in the second accelerating tube fabricated of a high-resistance material is made much larger than in the

first accelerating tube. The diameter of the holes of the discs in the second accelerating tube is made much smaller than in the first accelerating tube. (NSA of Japan)

11423 POLE SHOE ASSEMBLY FOR A CYCLOTRON ELECTROMAGNET. Verster, Nico Frederick; Hagedoorn, Hendrik Lourens (to North American Phillips Co. Inc.). U. S. Patent 3,225,270. Dec. 21, 1965. Priority date Apr. 16, 1962, Netherlands.

An electromagnet is patented for use in a cyclotron in which in the central part at least an axial stability of the particles is improved by azimuthal dependence of the magnetic flux. The magnet has two pole shoes each having an equal number of segments of alternately large and small height. The shoes are arranged so that the segments of large height as well as those of small height are opposite one another. The difference between a segment of large height and a segment of small height is substantially zero in the vicinity of the center of each shoe, and the difference between the largest height and the height at the center of each pole-shoe is smaller than the difference between the height at the center and the smallest height. The variation between the level of the largest height and that of the height at the center being less steep (an angle between 20 and 90° to the axis) than the variation between the level of the height at the center and the smallest height (an angle between 10 and 90° to the axis). (B.L.M.)

Astrophysics and Cosmology

Refer also to abstracts 11830, 11852, and 12228.

11424 (NP–15629) SPALLATION, FISSION AND NEUTRON CAPTURE ANOMALIES IN METEORITIC KRYPTON AND XENON. Marti, K.; Eberhardt, P.; Geiss, J. (Berne Univ. (Switzerland). Physikalisches Institut). Nov. 1965. 51p. Dep. mn.

Measurements of the Kr and Xe concentrations and isotopic compositions in five meteorites are reported. Experimental techniques and reproducibility are discussed in detail. In the Stannern achondrite 75% of the total Kr and 30% of the total Xe are due to cosmic ray induced spallation reactions. Also Bruderheim and H-Ausson show distinct spallation components. The isotopic composition of pure spallation Kr is derived as $^{78}Kr : {}^{80}Kr : {}^{82}Kr : {}^{83}Kr : {}^{84}Kr = 0.179 : 0.495 : 0.765 : 1.00 : 0.63$ and of spallation Xe as $^{124}Xe : {}^{126}Xe : {}^{128}Xe : {}^{130}Xe : {}^{131}Xe : {}^{132}Xe = 0.590 : 1.00 : 1.45 : 0.97 : 3.9 : 0.9$. It is shown that the spallation components found were produced by the cosmic radiation late in the history of the meteorite during a period given by the radiation age. The observed $^{126}Xe/^{124}Xe$ spallation ratio rules out a substantial contribution of spallation products in the xenon of carbonaceous chondrites. The Xe fission spectrum derived by Rowe and Kuroda from Pasamonte is corrected for spallation and the following composition is obtained for fission Xe: $^{131}Xe : {}^{132}Xe : {}^{134}Xe : {}^{136}Xe = 0.22 : 1.00 : 1.02 : 1.00$. In Mezö-Madaras and Abee a ^{80}Kr, ^{82}Kr and ^{128}Xe excess is found, due to (n,γ) reactions on Br and I. It is shown that neutrons produced by the cosmic radiation during the radiation age can account for the observed effect in Abee and the evidence so far suggests that this is also true for Mezö-Madaras. (auth)

11425 (UCRL–7777) THE HYDRODYNAMIC BEHAVIOR OF SUPERNOVAE EXPLOSIONS. Colgate, Stirling A.; White, Richard H. (Lawrence Radiation Lab., Univ. of California, Livermore). July 1964. Contract W-7405-eng-48. 107p. Dep. mn. CFSTI $4.00 cy, $0.75 mn.

Detailed calculations of the stellar hydrodynamics were performed using a finite difference approximation to the differential equations. Spherical symmetry was assumed on the basis that magnetic fields and angular momentum are small and that the symmetrizing effect of the gravitational field ensures a high degree of azimuthal symmetry during the quasistatic phase of the star's evolution. Detailed results are presented. (M.O.W.)

11426 (UCRL–12267) THE EFFECT OF THE PLANETARY SYSTEM ON THE NEARLY-PARABOLIC COMETS. Brady, Joseph L. (Lawrence Radiation Lab., Univ. of California, Livermore). Jan. 6, 1965. Contract W-7405-eng-48. 12p. Dep. mn. CFSTI $1.00 cy, $0.50 mn.

The total effect of the planetary perturbations on the eccentricity of 30 nearly-parabolic comets is obtained by integrating from oscillation backward to the year 1800 and forward to the year 2000. Twenty-three of these 30 comets, over 75% of them, pick up energy and show an increased eccentricity after passing through the planetary system. After enough passes through the planetary system apparently all these comets will attain hyperbolic velocity and be ejected. (auth)

11427 INFLUENCE OF THE DISTRIBUTION FUNCTION OF ELECTRONS ON THE SPECTRUM OF NON-THERMAL RADIO SOURCES. Souffrin, Suzanne; Chesnay, Nicole (Institut d'Astrophysique, Paris). Compt. Rend., 261: 3541-4(Nov. 3, 1965). (In French).

In the case of a continuous injection of ultrarelativistic electrons it was found that the electron distribution function has an increasing part capable of provoking instabilities. Moreover, the collisions due to high energy electrons do not appear capable of explaining the ionization. (tr-auth)

11428 SOLAR COSMIC-RAY BURST OF SEPTEMBER 28, 1961. Dorman, L. I.; Miroshnichenko, L. I. (Inst. of Terrestrial Magnetism, Ionosphere and Radio Wave Propagation, Academy of Sciences, USSR). Geomagn. Aeronomy (USSR) (Engl. Transl.), 5: 293-7(1965).

Translated from Geomagn. Aeronomiya, 3: 377-83(1965).

A simple diffusion model is used to investigate the propagation of solar cosmic rays for the flare of September 28, 1961. The dependence of the diffusion coefficient and of the transport mean free path for scattering of nonrelativistic solar particles on their kinetic energy is estimated. It is shown that the scattering mean free path is practically independent of energy and is equal to $(6-8) \cdot 10^{11}$ cm in the energy range 10–500 Mev. The spectrum of solar cosmic-ray generation in the nonrelativistic energy range is obtained. The dependence of the scattering mean free path on the distance from the sun r is also found. It can be represented as $\Lambda \sim r^{\beta}$, where β varies from 0 for an energy of 30 Mev to 1 for an energy of 600 Mev. (auth)

11429 SOLAR COSMIC RAYS RECORDED IN THE STRATOSPHERE IN SEPTEMBER 1963. Lazutin, L. L. (Polar Geophysical Inst., Academy of Sciences, USSR). Geomagn. Aeronomy (USSR) (Engl. Transl.), 5: 432-5 (1965).

Translated from Geomagn. Aeronomiya, 3: 563-6(1965).

The results of radiosonde measurements of solar cosmic radiation associated with solar flares during September 1963 are reported and discussed. Data showing the relation between solar and geophysical phenomena from Sept. 13 to 24 are presented. (L.B.S.)

11430 XENON AND KRYPTON IN THE BRUDERHEIM METEORITE. Merrihue, Craig (Univ. of California, Berkeley. Smithsonian Astrophysical Observatory, Cambridge, Mass.). J. Geophys. Res., 71: 263-313(Jan. 1, 1966).

In a series of heating experiments, xenon, radiogenic ^{129R}Xe, and krypton contents and the xenon and krypton isotopic composition of the Bruderheim meteorite were studied for the separated minerals feldspar, pyroxene, olivine, and troilite and for numerous chondrule fractions. Important differences among the individual minerals and between minerals and chondrules were observed. (auth)

11431 ANALOGY FOR THE LABORATORY SIMULATION OF HYDROMAGNETIC PHENOMENA IN ASTROPHYSICS. Pneuman, G. W. (General Motors Defense Research Labs., Santa Barbara, Calif.). Phys. Fluids, 9: 218-20(Jan. 1966).

An analogy involving convective diffusion of a dye in a moving fluid is described which permits the laboratory simulation of many hydromagnetic phenomena believed to occur on a cosmic scale. (auth)

11432 ANALYSIS OF THE PROPOSED PLANETARY RADAR REFLECTION EXPERIMENT. Ross, D. K.; Schiff, L. I. (Stanford Univ., Calif.). Phys. Rev., 141: 1215-18(Jan. 1966).

An analysis is made of an experiment recently proposed by Shapiro as a new test of general relativity theory. This consists in measuring the transit times of radar signals reflected from one of the inner planets. It is found that if the observations are expressed in terms of measurable orbital parameters, as they must be eventually, this experiment has the unexpected property of being sensitive to a nonlinear term in Einstein's theory. Great care must be taken in deciding what is actually measurable, and it is shown that the process of reconciling the results of calculations performed with mathematically different but physically equivalent forms of the metric is of considerable help in making this decision. (auth)

11433 TESTING GENERAL RELATIVITY WITH RADAR. Shapiro, Irwin I. (Massachusetts Inst. of Tech., Lexington). Phys. Rev., 141: 1219-22(Jan. 1966).

A test of the influence of solar gravity on the echo times of radar waves reflected from planets is described. By deriving a theoretical expression solely in terms of measurable quantities, it is demonstrated for a simple model of planetary motion that radar determinations of interplanetary echo times will allow the predictions of general relativity to be distinguished from those of Newtonian theory. The basic idea involves estimating the unknown parameters of the planetary orbits from time-delay measurements made when the target planet is near the earth and using the measurements made when the path of the radar wave passes near the sun to distinguish the effect of solar gravity on delay. (auth)

11434 HYDRODYNAMIC CALCULATIONS OF GENERAL-RELATIVISTIC COLLAPSE. May, Michael M.; White, Richard H. (Univ. of California, Livermore). Phys. Rev., 141: 1232-41(Jan. 1966).

The general-relativistic equations governing the motion of a large mass under the influence of its own gravitational field and its own pressure were approximated by finite-difference equations. A spherically symmetric, co-moving frame of reference was used. The pressure was assumed to be zero at the outer boundary. Rest mass was assumed to be conserved and heat transfer by neutrinos, radiation, etc., was not taken into account. Numerical solutions were obtained on a computer for several simplified equations of state, chosen to bracket the behavior of stellar material in late stages of collapse, and several masses. The maximum stable masses obtained were of the same order of magnitude, but somewhat larger than the maximum stable masses calculated statically. The behavior of light signals, of the metric coefficients, and of the hydrodynamic quantities as functions of time is described for collapse past the Schwarzchild radius. Such collapse leads to regions where the surface area of concentric spheres decreases as the rest mass contained by the spheres increases. (auth)

11435 COMPLETE ANALYTIC EXTENSION OF THE SYMMETRY AXIS OF KERR'S SOLUTION OF EINSTEIN'S EQUATIONS. Carter, Brandon (Cambridge Univ., Eng.). Phys. Rev., 141: 1242-7(Jan. 1966).

The 2-dimensional metric on the symmetry axis of the Kerr solution is examined and it is shown that in the form usually given it is incomplete when $a^2 \leq m^2$. The method developed by Kruskal for completing the Schwarzschild solution is adapted to the distinct cases $a^2 < m^2$ and $a^2 = m^2$. In each case a singularity-free metric is obtained which is periodic with respect to a timelike coordinate, and which is shown to be a complete analytic extension. The generalization to the full 4-dimensional Kerr solution is discussed, and finally the question of uniqueness and causality are considered. (auth)

11436 NEUTRINO ASTROPHYSICS. Chiu, Hong-yee. Documents on Modern Physics. New York, Gordon and Breach, 1965. 113p. $5.00 Cloth; $2.50 Paper.

General properties of a star are reviewed, including gravitational binding and equilibrium, limits on stellar size, and lifetime and luminosity. Equations of stellar structure are presented. The theory of nuclear reactions and the specific reactions occurring in stars are described. The Hertzsprung-Russell diagram is explained. Neutrino processes, including the URCA process, neutrino bremsstrahlung, the photoneutrino process, pair annihilation, and the plasma process, are discussed, and stellar collapse is considered. An introduction to general relativity is given. The Schwarzschild solutions, equations of state, and observations of neutron stars are discussed. A brief note on cosmology is included. (M.J.T.)

11437 TWO TOPICS IN THE PHYSICS OF THE SOLAR WIND: 1. A MODEL OF FERMI ACCELERATION AT SHOCK FRONTS. 2. EFFECTS OF DIFFUSION ON THE COMPOSITION OF THE SOLAR CORONA AND SOLAR WIND [Thesis]. Jokipii, Jack Randolph. Pasadena, Calif., California Inst. of Tech., 1965. 84p.

A model of first order Fermi acceleration at shock fronts is developed. A "fast" hydromagnetic shock is assumed to be propagating toward an isolated magnetic mirror in an otherwise uniform magnetic field not parallel to the shock front. The behavior of an ensemble of particles trapped between the mirror and the shock is studied and a differential equation describing the balance of particle injection into the trapping region, loss through the shock of mirror, and energy gain is obtained. The general theory is then applied to the acceleration of electrons at the earth's bow shock. This leads to an attractive model for the energetic electron pulses observed beyond the magnetopause. The observations and their interpretation are discussed. A simple model is developed with which it is possible to estimate quantitatively the effects of radial diffusion on the composition of the solar corona and solar wind. The relative diffusion velocities of ions and protons are a substantial fraction of the local solar wind velocity. This diffusion is found to be mostly due to the coronal pressure gradient, with the effect of the temperature gradient relatively unimportant. Effects of magnetic fields and turbulent mixing are briefly considered. It is concluded that, in conjunction with the diffusion, they may lead to appreciable fluctuations of the composition as a function of time and heliocentric radius. The conclusions are in agreement with the observed behavior of the He/H ratio observed on Mariner-2. (A.G.W.)

11438 OBSERVATIONS OF SOLAR PARTICLES IN INTERPLANETARY SPACE. de Jager, C. (Sterrewacht Sonnenborgh, Utrecht). pp 299-311 of Proceedings of a Symposium on High Latitude Particles and the Ionosphere, Alpbach, 1964. Maehlum, B. (ed.). New York, Academic Press, 1965.

The various kinds of particles emitted by the outer solar layers and moving into interplanetary space originate from two different kinds of regions and are emitted by different mechanisms. The solar corona is the source of solar wind, and the transition between the photosphere and corona produces solar flares, which are related to the acceleration of particles by various and unknown mechanisms. Topics discussed are the solar wind, particle emission from activity regions, solar flares, flare associated particles, relativistic and subrelativistic particle emission, and nuclear reactions in flare regions. (J.F.P.)

Atomic Physics

Refer also to abstracts 11133, 11281, 11493, and 11681.

11439 (BNL-8800) VIRTUAL-STATE EIGENVALUE PROBLEMS. I. PHYSICAL AND MATHEMATICAL DESCRIPTIONS. Chen, Joseph C. Y. (Brookhaven National Lab., Upton, N. Y.). [1964]. Contract AT-30-2-GEN-16. 12p. Dep. mn. CFSTI $1.00 cy, $0.50 mn.

From symmetry consideration of time reversal, a projected Schrödinger equation is obtained for virtual states

having reasonably long lifetimes. Eigenvalue problems for such virtual states are discussed in terms of this equation. The phenomena of decay of virtual states are interpreted as transitions from the projected subspace to its complementary orthogonal subspace. Methods for the calculation of energy levels and level widths are presented. (auth)

11440 (COO–614-34, Sect. IID) MU-MESIC X-RAY EXPERIMENT. McKee, R. (Chicago Univ., Ill. Inst. for Computer Research). 5p.

The Maniac III computer was used on-line in a μ-mesic x-ray experiment. The computer was used to collect the data as they were produced and to store the accumulation on magnetic disks for later analysis, and to provide fast feedback to the experimenters for better control of the experiment. Various aspects of the computer operation are briefly discussed. (M.O.W.)

11441 (IC/65/94) GREEN FUNCTIONS FROM LIE ALGEBRAS. Budini, P. (International Centre for Theoretical Physics, Trieste (Italy)). Dec. 23, 1965. 6p. Dep. mn.

It is shown that the theory of a noncompact extension of the symmetry algebra of a system which contains the mass operator as a noncommuting operator and generates the spectrum of the physical system can solve completely the dynamical problem of the system without any explicit reference being made to the interaction or potential. The example of the hydrogen atom problem is considered. (J.F.P.)

11442 (MATT–280) THEORETICAL FINE STRUCTURE OF He II 4686 A IN MAGNETIC FIELDS TO 40 KILOGAUSS. Norem, P. C. (Princeton Univ., N. J. Plasma Physics Lab.). June 1964. Contract AT(30-1)-1238. 43p. Dep. mn. CFSTI $2.00 cy, $0.50 mn.

The wavelengths and intensities of the 146 fine structure components of the 3686 Å line of ionized helium were determined in vacuum for magnetic fields up to 40 kG. Following the work of C. G. Darwin and K. Darwin the line is treated as a group of doublet transitions with observed positions and separations. The wavelengths of these components are determined by more or less conventional methods and the intensities by solving general equations from the two papers listed for the specific component and magnetic field of interest. The lengthy computational work was carried out on an IBM 1410 computer. The F and D components, which give the dominant contribution to the total intensity, exhibit an almost complete Pashen-Back effect above 20 kG. A statistical population of the n = 4 level is assumed. (auth)

11443 (NASA-CR–54790) INVESTIGATION OF COLLISION PROBABILITY OF ELECTRONS AND IONS WITH ALKALI METAL ATOMS. Semiannual Report, April 22, 1965–October 21, 1965. Bullis, R. H.; Nighan, W. L. (United Aircraft Corp., East Hartford, Conn. Research Lab.). Nov. 1965. Contract NAS3-4171. 50p. (UACRL-D–920243-18).

Design and construction was initiated on a low energy electron beam experimental apparatus similar in concept to the modified Ramsauer system employed in the cesium ion-cesium atom cross-section measurements. This system will be used to measure the total collision cross section of electrons interacting with cesium atoms over an energy range from 0.5 to 2.5 ev. The most critical portion of this experiment, the design of which was completed, is the development of a region free of stray magnetic fields and the generation of uniform magnetic fields with intensities of 0.1 gauss for energy analysis of the electron beam. Measurements of the time required for the neutral cesium density in a scattering chamber to reach equilibrium after a temperature change occurs in the cesium reservoir were made with a surface ionization gauge detector. An analysis was conducted to determine the effect of using a 4-6-12 type interaction potential rather than only an inverse fourth power potential to determine the magnitude of the contribution of elastic scattering events to the measured total cesium ion-cesium atom collision cross section. The available experimental electron-atom and electron-molecule differential scattering cross sections reported in the literature were analyzed in an effort to determine the magnitude of the difference that can exist between the total and momentum transfer cross sections due to anisotropic scattering effects. (M.O.W.)

11444 (NASA-CR–54790(App. 1)) LOW-ENERGY ELECTRON-CESIUM ATOM COLLISION PROBABILITY INVESTIGATIONS. Nighan, William L. (United Aircraft Corp., East Hartford, Conn. Research Lab.). 17p.

The elastic electron-cesium atom momentum transfer collision probability was determined in the electron velocity range corresponding to 0.45 to 0.80 $\sqrt{ev}$. The collision probability was determined from an analysis of an effective electron-heavy particle collision frequency obtained from measurements of the plasma properties in a cesium arc discharge. The effective collision frequency was found to be strongly dependent on electron temperature in the 2000 to 5000°K range and significantly dependent on plasma degree of ionization for values of this parameter greater than 10^{-4}. The collision probability determined from an analysis of the integral equation describing the effective collision frequency was found to be a strong function of electron velocity having a pronounced minimum of approximately 100 to 300 collisions per cm mm Hg in the 0.45 to 0.65 $\sqrt{ev}$ range of electron velocities, rising to a value about an order of magnitude larger in the velocity range corresponding to 0.75 to 1.0 $\sqrt{ev}$. (auth)

11445 (NP–15793) O SKRYTOI SIMMETRII ATOMA VODORODA. (Latent Symmetry of Hydrogen Atom). Report No. 378. Perelomov, A. M.; Polov, V. S. (Gosudarstvennyi Komitet po Ispol'zovaniyu Atomnoi Energii SSSR, Moscow. Institut Teoreticheskoi i Eksperimental'noi Fikizi). 1965. 22p. Dep. mn.

Dynamical symmetry of the hydrogen atom is considered from the group-theoretical point of view. Transition from the compact group 0(4) to its noncompact analog (the Lorentz group) makes it possible to describe discrete and continuous spectra of the hydrogen atom. It is shown that wave functions of the continuous spectrum form the infinite-dimensional irreducible representation $D(0,\rho)$ of the Lorentz group ($\rho = \sqrt{2/E}$) belonging to the so-called "main series" of unitary representations. Wave functions of the discrete spectrum with given principal quantum number η form the finite-dimensional representation $D[(n-1/2), (n-1/2)]$ of the Lorentz group. A peculiar symmetry of the wave functions of the continuous spectrum in the case of Coulomb potential is found. The special case of the states with E = 0 (in attractive Coulomb potential) when the Lorentz group contracted into nonrelativistic Galilei group is also considered. (auth)

11446 (NP–15794) O FUNKTSII GRINA DLYA KULONOVSKOGO POTENTSIALA. (Green's Function for Coulomb Potentiai). Report No. 379. Perelomov, A. M.; Popov, V. S. (Gosudarstvennyi Komitet po Ispol'zovaniyu Atomnoi Energii SSSR, Moscow. Institut Teoreticheskoi i Eksperimental'noi Fiziki). 1965. 22p. Dep. mn.

An expansion of the Coulomb Green function (for E > 0) over irreducible infinite-dimensional representations of the Lorentz group is obtained. The special case when the dynamical symmetry group of the hydrogen atom contracts to nonrelativistic Galilei group is also considered. An explicit expression for the Green function of the Kepler problem in the n-dimensional space is obtained. (auth)

11447 (TID–22476) IONIZATION AND CHARGE TRANSFER CROSS SECTIONS. Technical Status Report No. 18. Progress Report, December 1, 1964–November 30, 1965. Martin, D. W.; Puckett, L. J.; Taylor, G. O. (Georgia Inst. of Tech., Atlanta. Engineering Experiment Station). Dec. 1, 1965. Contract AT(40-1)-2591. 35p. Dep. mn; CFSTI $2.00 cy, $0.50 mn.

Cross sections for positive-ion and electron production in He^{++}, He^{+}, and He^{0} beam reactions with He, Ar, H_2, and N_2 targets are measured, at beam energies of 0.15 to 1 Mev. Sources of error are discussed. (T.F.H.)

11448 (TID–22480) EMISSION AND EXCITATION CROSS SECTIONS. Technical Status Report No. 1. Progress Report, March 1–November 30, 1965. Thomas, E. W.; Bent, G. D. (Georgia Inst. of Tech., Atlanta. Engineering Experiment Station). Dec. 1, 1965. Contract AT(40-1)-2591. 37p. Dep. mn; CFSTI $2.00 cy, $0.50 mn.

Excitation and emission cross sections for atomic reactions of 0.15- to 1-Mev protons on helium are measured. The design of the instrumentation, beam transport systems, and target assembly required for these measurements is outlined. (T.F.H.)

11449 (TID–22530) APPROXIMATE FORMULAE FOR A VARIETY OF SOLUTIONS OF THE THOMAS-FERMI EQUATION. Mason, J. C. (Maryland Univ., College Park. Inst. for Fluid Dynamics and Applied Mathematics). Jan. 1966. Contract AT(40-1)-3443. 19p. (BN–430). Dep. mn. CFSTI $1.00 cy, $0.50 mn.

In the Thomas-Fermi method of determining the potential produced by an atom at zero temperature, electrons are considered as a spherically symmetric cloud charge, with positive charges of nuclei smoothed out over the surface of a sphere of given radius. Two rational approximations are produced which, together with an approximation given previously, will generate accurate solutions of the dimensionless Thomas-Fermi equation both inside and outside the sphere for any radius in a certain range. A new method is used for obtaining rational approximations directly from an ordinary differential equation. (auth)

11450 (UCRL–7842-T) HELIUM ISOELECTRONIC SEQUENCE WAVE FUNCTIONS AND ENERGIES FOR THE SECOND AND THIRD ROWS OF THE PERIODIC TABLE. Swain, J. E. (Lawrence Radiation Lab., Univ. of California, Livermore). Sept. 17, 1964. Contract W-7405-eng-48. 33p. Dep. mn. CFSTI $2.00 cy, $0.50 mn.

A Green's function technique allows Schrödinger's equation to be written as an integral with a Green's function kernel. For the electrostatic atomic problem the Green's function is represented as a bilinear expansion of products of hydrogen-like wave functions. For the helium atom and for members of the helium isoelectronic sequence the integral equation is solved by expanding the wave function into a series of products of hydrogen-like wave functions. The helium isoelectric sequence wave function expansion in hydrogen-like wave functions is shown to converge uniformly to the exact solution of the electrostatic Schrödinger's equation. The equations are simplified by truncation of sum-integrals that appear and the remaining implicit algebraic equations are solved by the use of a digital computer. The resulting wave functions and energies are presented for the first 18 members of the helium isoelectronic sequence, including the hydrogen negative ion. The calculated energies are accurate to within a few percent of the experimental values for helium and improve through the helium isoelectronic sequence ions to a few tenths of a percent for argon. Several bound states of the hydrogen negative ion are predicted. The calculated energies are closer to the experimental values than could be expected from the accuracy trend for the remainder of the helium isoelectronic sequence ions. In addition to the ground state wave functions and energies the wave functions and energies are presented for several excited states and states of multiple excitation. Results are compared with experimental values and the calculations of others. (auth)

11451 (UCRL–7941(Rev.1)) SOLUTION OF THE SECULAR EQUATION FOR THE ELECTROSTATIC HELIUM ATOM. Curnutte, B. Jr. (Kansas State Univ., Manhattan); Swain, J. E. (Lawrence Radiation Lab., Univ. of California, Livermore). Oct. 23, 1964. Contract W-7405-eng-48. 18p. Dep. mn. CFSTI $1.00 cy, $0.50 mn.

As a further study of wave functions obtained by solving the secular equation, two systems of equations, one 25 × 25 and the other 196 × 196, representing successive approximations to the problem of the electrostatic helium atom, are solved. Energies and wave functions are obtained for the 1^1S, 2^1S, 2^3S, 2^1P, and 2^3P states from the 25 × 25 approximation, and the 1^1S, 2^1S, 2^3S, 2^1P, 2^3P, 3^1S, 3^3S, 3^1P, 3^3P, 3^1D and 3^3D states from the 196 × 196 approximation. In addition, for both approximations, energies and wave functions for states of multiple excitation were obtained. The ground state energy was found to be −77.15282 ev from the 25 × 25 approximation and −77.41092 ev from the 196 × 196 approximation, as compared to the experimental value of −78.983 ev and a value within experimental error for the most recent variational calculation. The energies of the 2^1S, 2^3S, 2^1P, and 2^3P states, as obtained from the 196 × 196 secular equation, are within a few tenths or hundredths of an electron volt of the experimental values. The value of the wave function at various positions is found to vary markedly from the Hylleraas wave function. (auth)

11452 (UCRL–12042-T) QUANTUM CORRECTIONS IN THE THOMAS-FERMI MODEL. Schey, Harry M.; Schwartz, Judah L. (Lawrence Radiation Lab., Univ. of California, Livermore). Aug. 25, 1964. Contract W-7405-eng-48. 37p. Dep. mn. CFSTI $2.00 cy, $0.50 mn.

Quantum corrections to the Thomas-Fermi model of the atom derived by expansion procedures are examined numerically. Corrected potentials, one-electron eigenvalues and eigenfunctions, dipole oscillator strengths, diamagnetic susceptibilities and electron binding as a function of atomic number are considered. In all cases the corrected quantities either agree less well with experiment than the results of the simple zeroth order theory or show improvement which is inconsistent, unimpressive and unreliable, lending strong support to conjectures made by others that the expansion methods leading to the quantum corrections give rise to series which are asymptotic and which fail to include important oscillatory terms. (auth)

11453 (UCRL–12230) THE HYDROGEN NEGATIVE ION. Curnutte, B. Jr. (Kansas State Univ., Manhattan); Swain, J. E. (Lawrence Radiation Lab., Univ. of California, Livermore). Nov. 1964. Contract W-7405-eng-48. 17p. Dep. mn. CFSTI $1.00 cy, $0.50 mn.

The secular equation form of Schrödinger's equation was used to predict bound states of the hydrogen negative ion and to calculate the energies and wave functions of these states. The infinite degree secular equation was truncated at two points, producing two truncated secular equations one of degree 25 × 25 and the other of degree 196 × 196. Of the 25 states involved in the 25 × 25 case, all 25 are bound, but only the 1^1S state is more tightly bound than is the ground state of the neutral hydrogen atom. Of the 196 states involved in the 196 × 196 case, 186 are bound states; the 10 states that are not bound states are all states of multiple excitation. The only state of the 186 that is bound more tightly than is the ground state of the neutral hydrogen atom is, again, the 1^1S state. The energies calculated for these two cases are −14.01659 ev and −14.04182 ev, respectively, as compared to the experimental value of −14.344 ev. (auth)

11454 (UCRL–12233) THE ELECTROMAGNETIC MASS OF THE CLASSICAL ELECTRON. Zink, J. W. (Lawrence Radiation Lab., Univ. of California, Livermore). Jan. 7, 1965. Contract W-7405-eng-48. 21p. Dep. mn. CFSTI $1.00 cy, $0.50 mn.

The difference between the electrostatic mass of the classical electron, m_0, and the electrodynamic mass, $(4/3)m_0$, has caused a considerable amount of confusion because the theory of relativity seems to predict that, in the limit of small velocities, the two masses should be the same. It is shown that within the structure of relativity the two masses should not necessarily be the same. The nature of each of the two masses is brought out. (auth)

11455 (UCRL–14450) PRODUCTION OF METASTABLE ATOMS BY ELECTRON IMPACT [Thesis]. Dowell, Jerry T. (Lawrence Radiation Lab., Univ. of California, Livermore). Dec. 9, 1965. Contract W-7405-eng-48. 52p. Dep. mn. CFSTI $2.00 cy, $0.50 mn.

The excitation of metastable states in He, Ne, Ar, Kr, and Xe by electron impact is studied near threshold as a

function of electron energy. The RPD method is used for energy selection of the electron beam, yielding a resolution of 0.1 ev. Results in He, Ne, Ar, and Kr are consistent with those of other investigators. Metastable production in each of the gases studied exhibits two major peaks in addition to other structure. These peaks are associated in energy with groups of excited states and may be interpreted as resonances with compound states of the electron-atom collision complex having short lifetimes for decay by autoionization. In krypton, the lowest energy peak is due to excitation of the lowest metastable state alone. Both peaks in the xenon data are due to the lowest metastable state. The energy region close to threshold is studied in detail for each gas, and it is found that a peak or steplike rise occurs within 0.1 ev of threshold in Ar, Kr, and Xe. No such behavior is found in He or Ne. (auth)

11456 (AERE-Trans-1041) ON THE THEORY OF THE ZEEMAN EFFECT IN THE SALTS OF THE RARE EARTHS. Bethe, H. Translated by H. B. Andrews (U.K.A.E.A. Atomic Energy Research Establishment, Harwell, Eng.), from Z. Phys., 60: 218-33(1930). 16p. Dep. BIS $0.60. HMSO 3s.

The Zeeman effect in the spectra of the salts of the rare earths is discussed with the help of the quantum mechanics of atoms in crystals developed by Bethe. In complete qualitative agreement with the experimental results of Becquerel, there is found a splitting of each spectral line into a magnetic doublet with very wide spacing and frequently anomalous polarization, without special assumptions having to be made regarding the splitting factors g. (auth)

11457 (LA-tr-65-29) CAPTURE OF ELECTRONS BY α-PARTICLES. Brinkman, H. C.; Kramers, H. A. Translated for Los Alamos Scientific Lab., Univ. of California, N. Mex., from Koninkl. Ned. Akad. Wetensch., Proc., 33: 972-84(1930). 14p. Dep. mn. JCL $1.60 fs, $0.80 mf.

The capture of electrons by alpha particles in collisions with atoms was treated in the first Born approximation. It was found that the integral expressions which occur in the calculation of the capture of an electron bound in a Coulomb field can be evaluated exactly. (D.C.W.)

11458 RADIATIVE LEVEL SHIFTS. I. FORMULATION AND LOWEST ORDER LAMB SHIFT. Erickson, Glen W. (New York Univ., N. Y.); Yennie, Donald R. Ann. Phys., 35: 271-313(Nov. 1965). (COO-1371-4).

An attempt is made to develop and apply formal operator techniques for radiative level shift calculations. The general formulation of the method and its application to the evaluation of the lowest order Lamb shift is considered. An effort is made to keep it pedagogically coherent, and a detailed review of the various theoretical contributions and comparison with experiment is included. (auth)

11459 ASYMPTOTIC SOLUTION OF THE SCHROEDINGER EQUATION FOR THE THREE BODY PROBLEM. Vezzetti, David J. (New York Univ., N. Y.); Rubinow, S. I. Ann. Phys., 35: 373-95(Dec. 1965).

The WKB method is applied to determine the asymptotic expansion of the Schrödinger wave function for a system of three spinless particles which interact through central forces. An assumption is made concerning the form of the asymptotic wave function which is designed to take advantage of the fact that the total angular momentum of the system is constant. As a result, equations for the phase and amplitude of the wave function, different from those which follow from ordinary WKB theory, are obtained. In particular, the phase function satisfies a Hamilton-Jacobi-like equation of degree 2(2L + 1). The method is applied to the helium atom for S- and P-states. The wave functions and energy eigenvalues are determined by means of perturbation theory. A classical description of the various electronic motions in the helium atom is presented. Previous attempts to describe the helium atom in terms of the old Bohr theory are clarified. (auth)

11460 SPOT PATTERNS AND SILSBEE CHAINS ON A Cu SINGLE CRYSTAL. Harrison, D. E. Jr.; Johnson III, J. P.; Levy, N. S. (Naval Postgraduate School, Monterey, Calif.). Appl. Phys. Lett., 8: 33-6(Jan. 15, 1966).

The spot patterns in the sputtering of a single crystal of Cu by Ar^+ ions were studied using a computer simulation of the sputtering process. It was concluded that the Silsbee energy chain mechanism is not significant for sputtering at normal incidence with energies in the low kev region. (D.C.W.)

11461 VISCOSITY COEFFICIENTS OF ISOTOPES OF HYDROGEN (H_2,D_2), NEON (^{20}Ne,^{22}Ne), AND HELIUM (^{3}He) IN TEMPERATURE RANGE FROM −195 TO +25 deg C. Menabde, N. E. At. Energ. (USSR), 19: 453-4(Nov. 1965). (In Russian).

Results of measurements of the coefficients of viscosity of ^{3}He, ^{20}Ne, ^{22}Ne, H_2, and D_2 are given for temperatures from −195.8 to +26.5°C. The ratios of the viscosity coefficients of D_2 and H_2, ^{22}Ne and ^{20}Ne, and ^{4}He and ^{3}He are given for various temperatures, and their variation with the square root of the ratio of the molecular weights of the isotopes is discussed. The force parameters of the Lennard-Jones potential function for intermolecular interactions—the depth of the potential well and the diameter of molecular interaction—were calculated for the six isotopes from the temperature dependence of the coefficients of viscosity. (M.J.T.)

11462 SECONDARY ELECTRON EMMISSION OF IRON UNDER BOMBARDMENT OF Ar^+ IONS OF MEDIUM ENERGY. Fagot, Bernard; Colombie, Nicole; Fert, Charles (Laboratoire de Physique du Solide, Toulouse). Compt. Rend., 261: 2855-8(Oct. 11, 1965). (In French).

Measurements made from the free faces (100), (110), and (111) of iron for different directions of the ion beam make it possible to obtain values of the emission coefficient γ_0 under normal incidence for the principal directions. In the energy range investigated (10 to 100 kev), this study confirms for a body-centered structure the results obtained for copper (face-centered cubic lattices) on the importance of the role played by the opacity of the crystalline lattice for the beam of incident ions: γ_0 increases with opacity of the lattice, but there is no simple proportionality relation. (tr-auth)

11463 STUDY OF THE ENERGY OF IONS EMITTED BY A METALLIC TARGET BOMBARDED BY A LASER BEAM. Ducauze, Alain; Tonon, Gianfranco; Veyrie, Pierre (CEA, Villeneuve-Saint-Georges, France). Compt. Rend., 261: 4039-41(Nov. 15, 1965). (In French).

The energy and the intensity of ions emitted by a metallic target were studied experimentally as a function of the characteristics of the laser and of the nature of the metal. The phenomena observed are compatible with a thermal model. (tr-auth)

11464 NEW DETERMINATION OF THE IONIZATION POTENTIAL FROM THE ARC SPECTRUM OF THULIUM. Camus, Pierre; Blaise, Jean (CNRS, Bellevue, France). Compt. Rend., 261: 4359-61(Nov. 22, 1965). (In French).

A study of the Zeeman effect made it possible to identify the 3 deep levels of $4f^{13}6s8s$. It was deduced that the ionization potential of Tm I is 6.22 ± 0.02 v. A certain number of levels were added to the lists previously published. (tr-auth)

11465 RESONANCES IN ELECTRON SCATTERING FROM H_2, HD, AND D_2. Kuyatt, C. E.; Simpson, J. Arol; Mielczarek, S. R. (National Bureau of Standards, Washington, D. C.). J. Chem. Phys., 44: 437-9(Jan. 15, 1966).

Resonances in the transmission of electrons through H_2, HD, and D_2 were studied for electrons of energy 11 to 13 ev. In H_2 and HD pairs of resonances were observed, indicating that there exist two electronic states of H_2^- and HD^-, each with well-developed vibrational structure. In D_2 only one series of resonances is observed. The single series is attributed to the overlap of two states of D_2^- because of a smaller vibrational separation. The absolute energy scale for the resonances has been recalibrated to an estimated accuracy of 0.1 ev. (auth)

11466 INELASTIC ELECTRON SCATTERING FROM H_2. Heideman, H. G. M.; Kuyatt, C. E.; Chamberlain, G. E. (National Bureau of Standards, Washington, D. C.). J. Chem. Phys., 44: 440-1(Jan. 15, 1966).

Energy-loss spectra were measured for 13.7- to 50.7-ev electrons in H_2. For incident energies below about 16 ev, energy-loss peaks are observed due to either or both of the a $^3\Sigma_g^+$ and c $^3\Pi_u$ states of H_2. The excitation cross section of the v = 0 and v = 1 vibrational levels of the B $^1\Sigma_u^+$ state show sharp and large resonances, corresponding in energy with resonances in the total scattering. The absolute electron energy scale in H_2 was recalibrated to an estimated accuracy of 0.1 ev. (auth)

11467 INELASTIC COLLISIONS OF H_2^+ AND N_2^+ IONS WITH HYDROGEN MOLECULES. Vance, Dennis W.; Bailey, T. L. (Univ. of Florida, Gainesville). J. Chem. Phys., 44: 486-93(Jan. 15, 1966).

Absolute total cross sections were measured for some inelastic processes occurring in collisions of N_2^+ and H_2^+ ions with H_2 molecules. The reactions which were studied are: $H_2^+ + H_2 \rightarrow H_2 + H_2^+$, $H_2^+ + H_2 \rightarrow H_2 + H + H^+$, $N_2^+ + H_2 \rightarrow N_2 + H_2^+$, $H_2^+ + H_2 \rightarrow H_3^+ + H$, $N_2^+ + H_2 \rightarrow N_2 + H + H^+$. The cross sections were determined over the range of kinetic energy of the incident ions, 3 to 100 ev. The experimental method consists of energy and mass analyzing the products of collisions occurring when a beam of ions of known kinetic energy passes through a scattering chamber containing target gas at low pressure. The energy analysis provides considerable new information regarding the mechanisms of the reactions. The results are in reasonable agreement with previous measurements. Comparisons of the experimental results with existing theories are made. In the case of charge transfer, the symmetric atomic-resonance theory of Rapp and Francis is found to be a good qualitative description of the $H_2^+ - H_2$ charge-transfer process. (auth)

11468 ESR SPECTRA OF GASEOUS ^{129}I AND ^{127}I. Aditya, Sukumar; Willard, John E. (Univ. of Wisconsin, Madison). J. Chem. Phys., 44: 833-4(Jan. 15, 1966). (COO-32-112).

The conditions under which the I-atom spectra may be observed were investigated, using both ^{127}I and ^{129}I. The results of gas-phase experiments are reported, and a comparison is made of ESR spectral widths with nuclear magnetic moments for some halogen isotopes. (L.B.S.)

11469 HYPERSENSITIVE TRANSITIONS IN RARE-EARTH IONS. Judd, B. R. (Univ. of California, Berkeley). J. Chem. Phys., 44: 839-40(Jan. 15, 1966). (UCRL-16380).

It is argued that the dynamic mechanism depending on quadrupolar enhancement by dielectric inhomogeneity, which was previously proposed for the hypersensitivity of some absorption line intensities in the solution spectra of rare-earth ions to the solvent, contribute to some extent; but the hypersensitivity should be principally assigned to a simple change of point symmetry. (L.B.S.)

11470 A MODEL OF INTERACTING RADIATION AND MATTER. II. Willis, Charles R. (Boston Univ.). J. Math. Phys. (N. Y.), 6: 1984-94(Dec. 1965).

The investigation of the long time behavior of a model consisting of N two-level atoms interacting with radiation is extended to include dissipation, pumping, and center-of-mass motion. It is shown that when the effective expansion parameter $\tilde{\gamma}N\tilde{\gamma}$ is small, the self-consistent field approximation remains the solution to lowest order in $\tilde{\gamma}N\tilde{\gamma}$. The inclusion of the center-of-mass motion introduces another dimensionless parameter β into the theory. It is shown that when this parameter is small, the electromagnetic field amplitude varies slowly on the time scale of the center-of-mass motion. The equations of motion in this slowly varying limit are solved by an extension of the Bogoliuboff-Kryloff theory of quasilinearity to the problem of time-dependent integral kernals. The unique stable stationary state is found and it is shown that in the slowly varying limit the stationary state is approached independent of initial conditions. The frequency shift is calculated to second order in β. The first-order frequency shift is the same as that calculated by Lamb. The steady-state solution is compared with recent experiments with lasers. The effect of collisons in the steady state is included. (auth)

11471 CHARGE EXCHANGE OF PROTONS IN ALKALINE METAL VAPOR WITH FORMATION OF HIGHLY EXCITED HYDROGEN ATOMS. Il'in, R. N.; Oparin, V. A.; Solov'ev, E. S.; Fedorenko, N. V. (Ioffe Inst. of Physics and Tech., Leningrad). JETP Lett. (USSR)(Engl. Transl.), 2: 197-9(Oct, 1, 1965).

The charge exchange of 10- to 180-kev protons in vapors of Li, Cs, Mg, K, and Na was investigated. The atomic beam obtained by charge exchange of the protons in the metal vapors was purified to eliminate the charged particles and was fed into a region with a strong electric field of intensity $E \leq 160$ kv/cm. The ratio of the current of the secondary protons, produced upon ionization of the highly excited atoms in the field E, to the total current of atoms I(E) was measured and was used to characterize the relative charge-exchange yield of the highly excited atoms. It was concluded that vapors of alkaline and alkali-earth metals are more suitable targets for the production of highly excited atoms of hydrogen at energies below 50 kev and that molecular hydrogen and inert gases are preferable at higher energies. (G.O.Y.)

11472 ACCURATE ANALYTICAL HARTREE-FOCK POTENTIALS FOR NEUTRAL ATOMS AS A SUM OF YUKAWA TERMS. Strand, T. G.; Tietz, T. (Indiana Univ., Bloomington). Nuovo Cimento (10), 41B: 89-91 (1966).

Parameters are given for the screening factor as a sum of Yukawa terms, which reproduce to a high degree of accuracy the Hartree-Fock screening function, and which allow easy and accurate numerical evaluation of analytic expressions for the Born phase shift formula, the Mott polarization effect, and the formation of negative ions. (L.B.S.)

11473 FICTITIOUS NATURE OF "CORE TERM" IN EXCHANGE AMPLITUDE FOR ELECTRON-ATOM SCATTERING. Kang, Ik-Ju (Univ. of Massachusetts, Amherst); Sucher, J. Phys. Lett., 20: 22-4(Jan. 15, 1966).

The so-called "core-term" in the exchange amplitude for electron-atom scattering is shown to be fictitious. The theoretical foundations of some successful approximate calculations of such scattering are thereby clarified. (auth)

11474 MEAN LIVES OF SOME STATES IN ATOMIC HYDROGEN. Goodman, A. S.; Donahue, D. J. (Univ. of Arizona, Tucson). Phys. Rev., 141: 1-3(Jan. 1966).

Hydrogen atoms in excited states were produced by passing a beam of fast-moving hydrogen molecules through a thin carbon foil. Radiation from these atoms was studied as a function of time using filtered photomultiplier tubes. Measured values of the mean lives of the 3s, 3d, 4s, 4p, and 4d states in hydrogen are presented and compared with theory. Results of measurements of relative initial intensities of radiation from fine-structure states of the n = 3 and n = 4 levels in hydrogen are also presented. (auth)

11475 THREE-PARTICLE OPERATORS FOR EQUIVALENT ELECTRONS. Judd, B. R. (Univ. of California, Berkeley). Phys. Rev., 141: 4-14(Jan. 1966). (UCRL-16321).

Interaction between the electronic configurations $(nl)^N$ and $(nl)^{N\pm1}(n'l')^{\mp1}$ can be represented for $(nl)^N$ by the addition of effective three-particle operators to the hamiltonian, the effective two-particle parts being absorbed by operators already present in the elementary linear theory of configuration interaction. For *f* electrons, the three-particle operators are decomposed into nine operators t_i that are labeled by irreducible representations of R_7 and G_2. The effects of three of them can be reproduced by two-particle operators; hence, only six additional parameters are required to describe the interaction. Tables of matrix elements are given, and the properties of the operators

t_i with respect to symplectic symmetry and quasispin are examined. (auth)

11476 HYPERFINE STRUCTURE OF ^{73}Ge IN THE $^3P_1$ AND $^3P_2$ ATOMIC STATES AND THE NUCLEAR MAGNETIC DIPOLE MOMENT OF ^{71}Ge. Childs, W. J.; Goodman, L. S. (Argonne National Lab., Ill.). Phys. Rev., 141: 15-21(Jan. 1966).

The hyperfine-structure constants of ^{73}Ge in the $^3P_1$ and $^3P_2$ atomic states of the $3p^2$ electronic configuration were measured with the atomic-beam magnetic-resonance method. The values of the magnetic dipole hyperfine-interaction constant a are 15.5480(18) Mc/sec and –64.4270 (7) Mc/sec, respectively, for the $^3P_1$ and $^3P_2$ states. The nuclear electric quadrupole interaction constants b are –54.566(9) Mc/sec and +111.825(13) Mc/sec, respectively, for these two states. On the basis of these measurements of a, the known spin and nuclear magnetic dipole moment of ^{73}Ge and the measured spin and a factors of ^{71}Ge, the nuclear magnetic dipole moment of ^{71}Ge can be calculated. It is $\mu = 0.546(5)$ nm. (auth)

11477 LOW-ENERGY IONIZATION OF ARGON ATOMS BY ARGON ATOMS. Hayden, Howard C.; Amme, Robert C. (Univ. of Denver, Colo.). Phys. Rev., 141: 30-1(Jan. 1966).

A neutral atomic beam was used to measure the total ionization cross section for argon atoms incident on low-density argon gas. The beam was produced by symmetric charge transfer of argon ions produced in an electron-impact ion source with 20-ev electrons. Beam energies varied from 30 ev (just below threshold for electron production in ground-state atom collisions) to 2900 ev laboratory energy. As in earlier work, the neutral beam intensity was determined by measurements of slow and scattered ion currents in the charge-transfer process. The intensities were checked by measurements of secondary electron emission from a gold target. Comparison of these measurements with those made at higher energies by other investigators suggests additional broad structure, with possibly a minimum near 8 kev. (auth)

11478 RADIATIVE ABSORPTION CROSS SECTION OF AN ELECTRON IN THE FIELD OF AN ARGON ATOM. Ashkin, M. (Westinghouse Electric Corp., Pittsburgh). Phys. Rev., 141: 41-4(Jan. 1966).

The results of a numerical calculation of the radiative absorption cross section for an electron in the field of a neutral argon atom are reported. The atomic potential used is the same as used by Holtsmark in his treatment of the Ramsauer effect. The light frequency is 4.318×10^{14} cps. This exact cross section is compared with three approximations which contain the phase shifts for elastic scattering. One of these approximations, the one due to Holstein, is found to differ very little from the exact cross section over a large range of initial electron energies. (auth)

11479 ELECTRONIC g FACTORS OF THE LOW LEVELS OF Ni I. Childs, W. J.; Fred, M. S.; Goodman, L. S. (Argonne National Lab., Ill.). Phys. Rev., 141: 44-7(Jan. 1966).

Electronic g factors were obtained for the seven lowest levels in Ni I by means of the atomic-beam magnetic-resonance technique. The results, in order of increasing excitation energy, are $^3F_4$, 1.24968(3); $^3F_3$, 1.08285(3); $^3F_2$, 0.66954(3); $^3D_3$, 1.33358(3); $^3D_2$, 1.15106(3); $^3D_1$, 0.49804(2); and $^1D_2$, 1.01297(7). A re-analysis of the atomic spectrum involving configuration interaction with intermediate coupling has resulted in an improved set of parameters. The g values so computed are compared with the experimental results. (auth)

11480 ISOTOPE SHIFT IN THE MUONIC K X RAYS OF ^{16}O–^{18}O, ^{40}Ca–^{44}Ca, ^{116}Sn–^{124}Sn, AND ^{155}Gd–^{160}Gd. Cohen, R. C.; Devons, S.; Kanaris, A. D.; Nissim-Sabat, C. (Columbia Univ., New York). Phys. Rev., 141: 48-55(Jan. 1966).

Measurements were made of the isotope shift in the muonic K x rays for the pairs of isotopes ^{16}O–^{18}O, ^{40}Ca–^{44}Ca, ^{116}Sn–^{124}Sn, and ^{155}Gd–^{160}Gd. The measurements were limited in resolution by the conventional NaI detectors used: no fine or hyperfine structure was resolved. The results confirm the indications from optical isotope-shift measurements that the expansion in charge distribution of a nucleus on addition of neutrons is less than the expansion in the density distribution, and indicate that this trend is even more marked in the light nuclei examined. (auth)

11481 HYPERFINE SEPARATION OF DEUTERIUM. Crampton, S. B.; Robinson, H. G.; Kleppner, D.; Ramsey, N. F. (Harvard Univ., Cambridge, Mass.). Phys. Rev., 141: 55-66(Jan. 1966).

The hyperfine separation of deuterium was measured by a spin-exchange technique in which deuterium interacts with radiating hydrogen in a hydrogen maser. Resonance of the deuterium is detected by its effect on the hydrogen oscillation power level. The result is $\Delta\nu(D) = 327,384,352.3 \pm 0.25$ cps in the A1 time scale [$\Delta\nu(Cs) = 9,192,631,770$ cps]. A theoretical analysis of the technique and experimental details are presented. (auth)

11482 EXCITATION-TRANSFER COLLISIONS BETWEEN RUBIDIUM AND HELIUM ATOMS. Beahn, T. J.; Condell, W. J.; Mandelberg, H. I. (Lab. for Physical Sciences, College Park, Md.). Phys. Rev., 141: 83-7(Jan. 1966).

An experiment is described which measures the collision cross section for transfer of excitation in rubidium by helium. Rubidium atoms are pumped to either the $^2P_{\frac{3}{2}}$ or $^2P_{\frac{1}{2}}$ state by irradiation with one of the resonance lines. Some excited rubidium atoms are transferred to the other P state by collisions with helium atoms. The rubidium atoms then radiate both resonance lines. Measurements of the intensities of both resonance lines as a function of helium pressure are used to calculate the collision cross section. The cross section for $^2P_{\frac{1}{2}}$ to $^2P_{\frac{3}{2}}$ is 1.0×10^{-17} cm^2 ± 10% and for $^2P_{\frac{3}{2}}$ to $^2P_{\frac{1}{2}}$ is 1.2×10^{-17} cm^2 ± 10%. (auth)

11483 BINARY-ENCOUNTER ELECTRON-ATOM COLLISION THEORY. Vriens, L. (Univ., Utrecht). Phys. Rev., 141: 88-92(Jan. 1966).

Recently, various papers have appeared on binary-encounter collision theories of electron-atom collisions. In nearly all of these papers use is made of Gryzinski's collision model. A theoretically somewhat better justified and more useful model has been given by Burgess. In an introduction, both collision models are described. In the first section a set of (classical) differential-cross-section formulas is given for Grysinski's model as well as for Burgess's model. In the second section total (quantum) cross-section formulas are derived by means of Burgess's model for electron-atom collisions. These formulas are simpler than those previously given by Burgess. In the third section a comparison is made between differential cross sections for large electron energies predicted by the binary-encounter theory and by the Born approximation, respectively. In the fourth section a combined binary-encounter-quantum method, which is alternative to Burgess's exchange classical impact-parameter method, is suggested for calculating cross sections. (auth)

11484 ROTATIONAL MAGNETIC MOMENTS OF ALKALI-HALIDE MOLECULES. Mehran, F.; Brooks, R. A.; Ramsey, N. F. (Harvard Univ., Cambridge, Mass.). Phys. Rev., 141: 93-104(Jan. 1966).

The rotational magnetic moments of a number of alkali-halide molecules were measured by the molecular-beam magnetic-resonance technique. The gyromagnetic ratios in units of nuclear magnetons are: ^{7}Li^{19}F, (+)0.07367 ± 0.00050; ^{7}Li^{35}Cl, (+)0.0848 ± 0.0032; ^{6}Li^{35}Cl, (+)0.1042 ± 0.0033; ^{7}LiBr, (+)0.0911 ± 0.0089; ^{23}Na^{127}I, (+)0.0268 ± 0.0047; ^{39}K^{19}F, (–)0.0364 ± 0.0012; ^{85}Rb^{19}F, (–)0.0441 ± 0.0028; ^{85}Rb^{35}Cl, (–)0.0183 ± 0.0018; ^{133}Cs^{19}F, (–)0.0621 ± 0.0055; ^{133}Cs^{35}Cl, (–)0.0212 ± 0.0011. Only the absolute values were determined experimentally. However, the absolute values are reasonably consistent with the theoretical ones, so signs from the theory are listed above in

parentheses. It is shown that for weak fields the molecular rotational magnetic moments do not correspond directly to the peaks of the resonance curves. A statistical analysis was carried out to determine the rotational g values from the peaks of the observed resonances. Since the correction is large (up to 50%), the above results would be wrong by an amount beyond the indicated experimental error if the interpretation of the correction is not valid. No such uncertainty arises in the LiF measurements or in other rotational-moment measurements where the correction does not need to be made. The measured values determined in accordance with the above analysis are found to be in good agreement with the predictions from a theory of Foley. The spin-rotational interaction constant of ^{19}F in $^{133}Cs^{19}F$ was measured by a new method to be 13.5 ± 2.5 kc/sec. (auth)

11485 ASYMPTOTIC LARGE-Z ATOMIC WAVE FUNCTIONS. **Mendelsohn, Lawrence B. (New York Univ., New York). Phys. Rev., 141: 113-29(Jan. 1966).**

A new technique for calculating wave functions for atoms and ions is developed. Formal asymptotic expansions with largeness parameter Z (nuclear charge) of the form $\Psi = e^{-Zh}\Sigma a_n Z^{-n}$, where h and the set of a_n's are functions of the electron coordinates, are determined through first order in 1/Z. In so doing, the Schrödinger equation for a general atomic system with N electrons is reduced to a set of first-order partial differential equations for successive a_n. These equations are then solved recursively. Screening and correlation are exhibited explicitly in the resulting asymptotic atomic wave functions. Applications made to the ground state of 2-electron systems show that the asymptotic wave function obeys the virial theorem through first order. Magnetic susceptibilities within 5% of the accepted values are obtained for helium and singly ionized lithium. Other expectation values, $\frac{1}{2}(s_1 + s_2)$, s_{12}^2, and s_{12}, are found to be in excellent agreement with Pekeris's variational calculations utilizing many parameters. In the neighborhood of certain singular points the large-Z asymptotic solutions obtained by a "matching technique" are shown to satisfy the correct cusp conditions. In certain of these regions, (lnZ)/Z terms enter. The omission of such terms in ordinary variational-perturbation wave functions may result in a loss of accuracy when computing expectation values other than the energy. (auth)

11486 OPTICAL-PUMPING TRANSIENTS IN ^{87}Rb AND APPLICATION TO EXCITED-STATE DISORIENTATION CROSS SECTIONS. **Marrus, Richard; Yellin, Joseph (Univ. of California, Berkeley). Phys. Rev., 141: 130-6 (Jan. 1966). (UCRL-16065).**

Detailed studies were made of the light transmitted through rubidium-87 vapor during the optical-pumping process, both with and without buffer gas present. The observed transients are single exponentials with no buffer gas present, and double exponentials with buffer gas present, over a wide range of pumping intensities and relaxation times. These results are in excellent agreement with the predictions based on phenomenological equations in which nuclear spin is included and a single relaxation time is assumed. From a study of the amplitudes of the two exponential components of the optical-pumping transient, an effective cross section σ_{eff} is deduced for the disorientation of rubidium-87 within the $5^2P_{\frac{1}{2}}$ state as a result of its collision with a buffer-gas atom. It is shown that $\sigma_{eff} = \sigma_{\frac{1}{2}} + \sigma_{\frac{1}{2}}$, where $\sigma_{\frac{1}{2}}$ is the cross section for disorientation within the $5^2P_{\frac{1}{2}}$ level, and $\sigma_{\frac{1}{2}}$ is the cross section for transfer from the $5^2P_{\frac{1}{2}}$ level to the $5^2P_{\frac{3}{2}}$ level by means of collisions with the buffer gas. On the basis of recently measured values for $\sigma_{\frac{1}{2}}$, values are deduced for $\sigma_{\frac{1}{2}}$. The cross sections are: $\sigma_{\frac{1}{2}}$(Rb–He) = 1.5(0.8) × 10^{-17} cm², $\sigma_{\frac{1}{2}}$(Rb–Ne) = 4.4(2.2) × 10^{-17} cm², and $\sigma_{\frac{1}{2}}$(Rb–Ar) = 3.5(1.8) × 10^{-16} cm². These cross sections are deduced from a model in which the probabilities for ^{87}Rb to relax from any hyperfine level to any other are all equal. This model gives a better fit with the observed transients than the assumption that the electron spin only is randomized in the $P_{\frac{1}{2}}$ state with the nuclear spin unaffected. It is shown that accurate relaxation-time measurements can be made by measuring the time constants associated with the double exponentials as a function of light intensity, and extrapolating them to zero light intensity. Moreover, since no shutter is required, relaxation times <10^{-3} sec can be easily observed. (auth)

11487 POLARIZATION POTENTIALS FOR LOW-ENERGY SCATTERING: e^+-H AND e^--Li. **Stone, Philip M. (Sperry Rand Corp., Sudbury, Mass.). Phys. Rev., 141: 137-45(Jan. 1966).**

Polarization-potential calculations are given for positron scattering by hydrogen and for electron scattering by lithium. The potentials are obtained in the adiabatic approximation by a simple variational calculation of the energy of the disturbed atom. This approach is more general than perturbation theory and is valid even for the large interactions typical of the alkali elements. The l = 0 phase shifts are calculated for positron-hydrogen scattering with differing numbers of excited states included in the coupling. First, only the 2p state is considered, next, all p states, and finally all p states plus the 2s state. Phase shifts and cross sections of five partial waves (l = 0 to l = 4) are calculated for the lithium problem when the interaction of the first excited state (2p) is considered. This accounts for all of the experimentally observed polarizability. Comparison with close-coupling results in both cases shows the present method to be of similar accuracy when coupling with the same excited states is included. The adiabatic approximation, inherent in the polarization potential, is therefore not a serious limitation and the method can be used with confidence for more complex atoms. (auth)

11488 ION BEAM MEASUREMENTS OF CESIUM RECOMBINATION CROSS SECTIONS. **Hammer, J. M.; Aubrey, B. B. (RCA Labs., Princeton, N. J.). Phys. Rev., 141: 146-51(Jan. 1966).**

The recombination cross sections of both atomic and molecular cesium ions were measured using an ion-beam technique. An ion beam is passed through a modulated space-charge-neutralized electron cloud, and the emergent atoms and molecules are detected. This technique allows the molecular and atomic recombinations to be found independently. The atomic cross section at an effective electron temperature of 1540°K is found to be (1.7 ± 1.2) × 10^{-19} cm², corresponding to a recombination coefficient of (3.1 ± 2.3) × 10^{12} cm³/sec. The molecular recombination cross section at an effective electron temperature of 1380°K is (1.2 ± 1.0) × 10^{-15} cm², corresponding to a recombination coefficient of (2.5 ± 1.8) × 10^{-6} cm³/sec. (auth)

11489 ABSOLUTE CROSS SECTIONS FOR SINGLE IONIZATION OF ALKALI IONS BY ELECTRON IMPACT. I. DESCRIPTION OF APPARATUS AND Li^+ RESULTS. **Lineberger, W. C.; Hooper, J. W.; McDaniel, E. W. (Georgia Inst. of Tech., Atlanta). Phys. Rev., 141: 151-64(Jan. 1966). (TID-22341).**

The absolute cross sections for the single ionization of Li^+ ions by electron impact were measured over the electron-energy range from below threshold (75.6 ev) to 800 ev. The measurements were performed with an ultrahigh-vacuum crossed-beam facility operating under continuous, rather than the usual time modulated, beam conditions. A detailed description of the apparatus and experimental method is presented. Numerous checks were performed to justify the use of the continuous-beam measurement technique developed for this experiment, particular attention being paid to beam intensities, beam profiles, space charge, signal-to-noise ratio, and ion-beam composition. The error in the measured cross sections is believed not to exceed ±12% above 150 ev electron energy; it may be as large as ±21% at 90 ev. Of this possible error, an amount ±6% is considered systematic. (auth)

11490 ABSOLUTE CROSS SECTIONS FOR SINGLE IONIZATION OF ALKALI IONS BY ELECTRON IMPACT. II. Na^+ AND K^+ RESULTS AND COMPARISONS WITH THEORY. **Hooper, J. W.; Lineberger, W. C.; Bacon,**

F. M. (Georgia Inst. of Tech., Atlanta). Phys. Rev., 141: 165-73(Jan. 1966). (TID-22340).

The absolute cross sections for single ionization of Na^+ and K^+ ions by electron impact were measured over the electron-energy range from below threshold to 1000 ev. The measurements were performed in a crossed-beam facility operating under continuous-beam conditions. Numerous checks were performed to establish the validity of the data. For both Na^+ and K^+, the measured cross sections were zero below threshold, and thus no "correction" was required to obtain the actual cross section. The present Na^+ and K^+ data and the Li^+ data presented in a previous paper are discussed and compared with relevant theory and experiment. (auth)

11491 HYPERFINE STRUCTURE OF THE 9161-cm^{-1} $^2D_{3/2}$ STATE OF ^{197}Au AND THE NUCLEAR ELECTRIC-QUADRUPOLE MOMENT. Childs, W. J.; Goodman, L. S. (Argonne National Lab., Ill.). Phys. Rev., 141: 176-80 (Jan. 1966).

The hfs of the $5d^96s^2\ ^2D_{3/2}$ metastable atomic state at 9161 cm^{-1} in ^{197}Au was studied by the atomic-beam magnetic-resonance technique. The results, in conventional notation, are $g_J = 1.20000(2)$, $A = +80.236(3)$ Mc/sec, $B = -1049.781(11)$ Mc/sec, and $C = +0.0004(4)$ Mc/sec. A detailed comparison of these results with those of Blachman and Lurio on the $^2D_{3/2}$ member of the same term indicates that configuration interaction is very small in the ^2D term. The nuclear electric-quadrupole moment is calculated to be $Q(^{197}Au) = +0.59 \pm 0.12$ b. (auth)

11492 METHOD OF CORRELATED BASIS FUNCTIONS. Clark, John W.; Westhaus, Paul (Washington Univ., St. Louis). Phys. Rev., 141: 833-57(Jan. 1966).

The method of correlated basis functions provides a means of systematic investigation of real physical systems. An attempt is made especially to develop a formalism for describing systems of strongly interacting fermions, for example, nuclei and liquid He^3, using a complete set of correlated functions $\Psi_m = F\Phi_m/(\Phi_m, F^2\Phi_m)^{1/2}$. F is taken as a product of two-body factors, $\Pi_{i<j} f(r_{ij})$, the $f(r_{ij})$ embodying at least the correlations arising from strong short-range repulsions; and $\{\Phi_m\}$, a set of independent-particle-model functions which might serve as a basis in the absence of highly singular interactions. The matrix elements $\mathcal{H}_{mn}$, $\mathcal{N}_{mn}$ of the hamiltonian and identity operators with respect to the correlated basis $\{\Psi_m\}$ are evaluated by generalization of cluster-expansion techniques. A detailed technical discussion of the cluster expansions is given, with special emphasis on their symmetry properties upon truncation. An attempt is made to construct explicitly a second-quantized effective hamiltonian which generates the same matrix elements, to prescribed order in $\rho\omega$, when operating between independent-particle kets of the model occupation-number representation, as does the given hamiltonian in the configuration-space representation, between the corresponding correlated functions of the Löwdin basis. The quasiparticles described by this effective hamiltonian interact via well-behaved two-body, three-body, ... , Q-body, ... potentials, in contrast to the highly singular two-body interactions of the real particles. For small $|\rho\omega|$, the effective two-body forces predominate. An avenue to deeper understanding of the applicability of the nuclear-shell model and the dressed-quasiparticle theory of liquid ^3He has been opened. Only the formalism for a uniform extended medium is treated. (L.B.S.)

11493 MUONIC MOLECULES AND NUCLEON-DEUTERON CAPTURE. Carter, B. P. (Stanford Univ., Calif.). Phys. Rev., 141: 863-72(Jan. 1966).

Variational wave functions were computed for all S states of muonic molecules involving hydrogen isotopes. Results for the $p\mu d$ ground state were used to compare nucleon-deuteron capture cross sections with $p\mu d$ fusion rates. Using our molecular wave functions and the results of muonic-molecule experiments, the low-energy S-wave cross section for the reaction $D(p,\gamma)^3He$ is estimated. The result is in disagreement with measurements in the tens-of-kilovolts region, but is consistent with thermal neutron-deuteron capture data when Coulomb effects are taken into account by means of the usual penetration factor. Finally, the usual assumption that proton-dueteron capture occurs only from the doublet state is re-examined and it is shown how the doublet and quartet matrix elements could both be determined from a new measurement of the total yield of gamma rays from $p\mu d$ fusion in liquid hydrogen. (auth)

11494 ISOTOPIC MASSES OF HYDROGEN, CHLORINE, BARIUM, CERIUM, AND NEODYMIUM. Benson, Jay L.; Johnson, Walter H. Jr. (Univ. of Minnesota, Minneapolis). Phys. Rev., 141: 1112-22(Jan. 1966).

A 16-in. double-focusing mass spectrometer was employed to measure the atomic mass of ^1H and the atomic masses and isotopic mass differences of chlorine, barium, cerium, and neodymium. Recent improvements in instrumentation have increased the precision of both narrow and wide doublet measurements. The doublet $C_{11}H_{22}-C_{12}H_{10}$ was used to relate the H mass directly to the ^{12}C mass standard with a precision of ±30 ev. The chlorine masses obtained in this investigation have a precision greater than previous measurements and provide further information about disagreements which were present in previous work. Additional atomic masses are calculated from the stable-mass data of barium, cerium, and neodymium, together with alpha-decay, beta-decay, and nuclear-reaction energies. The resultant table of masses is used to calculate nuclear systematic energies in the region near N = 82. The systematics of the separation energies display very smooth characteristics except at the shell closure of N = 82 and are so regular as to be a powerful aid in the evaluation of some possible errors in reaction and decay data used in the calculation of these nuclear systematics. (auth)

11495 LOW-ENERGY ELECTRON SCATTERING FROM ATOMS AND MOLECULES: A MODEL. Lenander, Carl J. (Aerospace Corp., El Segundo, Calif.). Phys. Rev., 142: 1-7(Feb. 1966).

A simple model is proposed for the calculation of free-electron wave functions for low-energy electrons incident upon neutral atoms. The region of interaction of the electron with the atom may be separated into three important regions of potential: Coulomb plus exchange, Coulomb, and far-field induced polarization. The division of regions is based on mathematical and physical reasons for the characteristic behavior of wave functions in the scattering problem. Examples are given for the elastic scattering of electrons from nitrogen, oxygen, and argon. The agreement with experiment and effective-range theory is good. The application of the method to the prediction of low-energy electron scattering from homonuclear diatomic molecules is discussed. (auth)

11496 ABSOLUTE PHOTOELECTRIC CROSS SECTIONS OF 320-kev GAMMA RAYS IN Pb, Sn, AND Ag. Parthasaradhi, K.; Lakshminarayana, V.; Jnanananda, Swami (Andhra Univ., Waltair, India). Phys. Rev., 142: 9-11 (Feb. 1966).

A well-type plastic-scintillation spectrometer was assembled and used for the measurement of absolute photoelectric cross sections of 320-kev gamma rays in Pb, Sn, and Ag. The results are 76.5 ± 4.6, 10.2 ± 0.6, and 7.65 ± 0.46 barns per atom for Pb, Sn, and Ag, respectively. These values are found to be in agreement with the standard interpolated values from the NBS Circular 583 within the range of experimental errors. (auth)

11497 HYPERFINE STRUCTURE OF THE STABLE LITHIUM ISOTOPES. I. Schlecht, Richard G.; McColm, Douglas W. (Univ. of California, Berkeley). Phys. Rev., 142: 11-13(Feb. 1966). (UCRL-11773).

The atomic-beam magnetic-resonance technique was used to determine the hyperfine-structure separations and the hyperfine-structure anomaly between the isotopes ^6Li and ^7Li the $^2S_{1/2}$ ground state. The separated-oscillatory-field method of Ramsey was used to determine the hyperfine-structure separations. The hfs of ^6Li is $\Delta\nu_6 = 228.20528(8)$ Mc, and of ^7Li is $\Delta\nu_7 = 803.50404(48)$ Mc. By means of these values and the value for the ratio of

the g_I's obtained by Klein, the hyperfine-structure anomaly was determined to be $\Delta_{87} = +1.065(6) \times 10^{-4}$. The errors quoted are four times the statistical errors. (auth)

11498 HYPERFINE STRUCTURE OF THE STABLE LITHIUM ISOTOPES. II. McColm, Douglas (Univ. of California, Berkeley). Phys. Rev., 142: 14-19(Feb. 1966). (UCRL-16125).

A theoretical treatment of the hfs anomaly between ^{6}Li and ^{7}Li is given, and the result compared with experiment. The distribution of nuclear charge and magnetism, the polarization of the electron wave function by the nuclear electric-quadrupole moment, and the specific mass correction are treated. Agreement with experiment is obtained with a value for the p-nucleon radial parameter not inconsistent with that obtained from electron-scattering experiments. (auth)

11499 COLLISION-INDUCED MIXING IN THE FIRST EXCITED STATES OF SODIUM AND POTASSIUM. Jordan, J. A. Jr.; Franken, P. A. (Univ. of Michigan, Ann Arbor). Phys. Rev., 142: 20-5(Feb. 1966).

The cross sections for the collision-induced transfer of excitation from the $^2P_{\frac{3}{2}}$ level to the $^2P_{\frac{1}{2}}$ level of the first excited states of the alkali atoms were measured for several alkali-noble gas systems. The cross sections were determined with a conventional resonance fluorescence technique in which the radiation from a spectral source was absorbed and re-emitted by an alkali vapor at low pressure ($\sim 10^{-6}$ torr), and the scattered light analyzed with a scanning spectrometer. Provision was made for the introduction of various noble gases at controlled pressures into the alkali vapor. The determined cross sections are (in units of 10^{-16} cm^2): Na-He, 41.1 ± 2.9; Na-Ne, 36.1 ± 2.5; Na-Ar, 64.6 ± 5.2; Na-Kr, 68.2 ± 5.5; Na-Xe, 61.8 ± 4.9; K-He, 52.8 ± 5.8; K-Ne, 14.0 ± 1.2; K-Ar, 34.0 ± 3.1. The quoted errors are estimated 70% confidence intervals. The measurements are compared with other experimental results and with various estimated cross sections. (auth)

11500 THEORY OF LOW-ENERGY SCATTERING OF ELECTRONS BY HYDROGEN ATOMS. Levin, F. S. (Brookhaven National Lab., Upton, N. Y.). Phys. Rev., 142: 33-45(Feb. 1966). (BNL-9430).

The theory of low-energy electron-hydrogen atom scattering is reformulated to include, in any truncated coupled-channel calculation, the contribution from continuum states due to exchange effects. The existence of such a contribution was explicitly demonstrated by Castillejo, Percival, and Seaton, although the standard treatment does not include it. The formulation of the problem employs the expansion of the exact wave function $\Psi^{\pm}$ in terms of the complete set of hydrogenic states $\{\varphi_\alpha\}$ in the form $\Psi^{\pm} = \Sigma_\alpha \varphi_\alpha(1)\psi_\alpha^{\pm}(2)$. Although this expansion is not termwise symmetric or antisymmetric, the entire sum is made so by use of the integral equation for $\Psi^{\pm}$. The boundary conditions satisfied by the scattering coefficients $\psi_\alpha^{\pm}$ are automatically specified in this approach. Furthermore, it is now clear that the entire, exact elastic or inelastic amplitude is contained in the scattering wave function $\psi_0^{\pm}$. The elastic wave function $\psi_0^{\pm}$ (and also the set of open-channel wave functions) is shown to obey both homogeneous (optical potential) and inhomogeneous equations. The equivalence of these equations with each other and with the equation found using Feshbach's projection-operator method is demonstrated. A set of homogeneous equations are found for the case where only certain chosen channels are kept and the rest are truncated. This latter set of equations is identical to those obtained by Hahn, O'Malley, and Spruch as an adjunct to calculations establishing bounds on scattering parameters. Both the exact and the approximate sets of equations for the $\psi_\alpha^{\pm}$ differ from the corresponding equations used in all previous coupled-channel calculations. Using the results, the relation between the Born-Oppenheimer amplitude and first-order exchange amplitude of Bell and Moiseiwitsch is discussed. Each is shown to be a different first-order approximation to the exact amplitude, although the Born-Oppenheimer amplitude is seen to be an approximation to the amplitude derived from the inhomogeneous equation. Some simple single-channel calculations of phase shifts and scattering lengths were carried out. The triplet phase shifts and scattering length derived from the approximate homogeneous equation are identical to those of the standard static exchange approximation, a result expected on the basis of the antisymmetry of the Ψ^-. However, the singlet phase shifts and scattering length differ from those of the standard static exchange approximation. It is found that for $k^2 \leq 0.09$, the singlet phase shifts are larger than those calculated in the 1s-2s strong-coupling approximation, and that the singlet scattering length is 7.85, where quantities are given in atomic units. For $k^2 > 0.09$, the singlet phase shifts are less than those of the 1s-2s case and approach those of the static exchange calculation. Reasons for this behavior are discussed. (auth)

11501 ELECTRON BREMSSTRAHLUNG FROM PROTON-EXCITED TARGETS. Ogier, W. T.; Carlson, R. D.; Knoche, Jayne (Pomona Coll., Claremont, Calif.). Phys. Rev., 142: 50-2(Feb. 1966).

Formulas are derived for continuous x-ray quantum yields from proton-bombarded targets due to electron acceleration during collision and due to subsequent bremsstrahlung as the electrons stop. Measurements with a proportional counter of yields from a beryllium target bombarded with 1.6-Mev protons are in agreement within a factor of two with calculated bremsstrahlung yields, and they are in qualitative agreement with calculated acceleration yields, which fall in a band at roughly one-quarter of the bremsstrahlung quantum energies. (auth)

11502 HYPERFINE STRUCTURE AND OCTOPOLE INTERACTION IN STABLE BROMINE ISOTOPES. Brown, Howard Howland; King, John G. (Massachusetts Inst. of Tech., Cambridge). Phys. Rev., 142: 53-9(Feb. 1966).

The atomic-beam magnetic-resonance method was used to measure the hyperfine structure of the $^2P_{\frac{3}{2}}$ ground state of ^{79}Br and ^{81}Br. The values obtained for the nuclear dipole, quadrupole, and octopole constants, uncorrected for second-order perturbations, are in cps: ^{79}Br 884,811,540 ± 62 − 384,880,292 ± 200 and 163 ± 8 and for ^{81}Br 953,770,006 ± 62 − 321,520,344 ± 200 and 235 ± 8. The positive value of the nuclear dipole moment was confirmed. (auth)

11503 REORIENTATION OF H ATOMS BY PROTON IMPACT. Soltysik, Edward A. (Univ. of Massachusetts, Amherst). Phys. Rev., 142: 72-3(Feb. 1966).

The scattering amplitude in Born approximation is presented for the reorientation of H atoms by proton impact. A hydrogen atom originally in the state designated by the quantum numbers (n_0,l_0,m_0) may have its m quantum number altered through an impact with a proton. The results presented show that the scattering amplitude for this reorientation depends not only upon the magnitude of the momentum-transfer vector q ($|q| = 2k_0 \sin\frac{1}{2}\theta_s$), but also upon its direction with respect to the axis of quantization. It is suggested that this effect may be observable by measuring the change in the polarization of the emitted radiation as a function of the momentum of the proton. (auth)

11504 VARIATIONAL CALCULATIONS OF LONG-RANGE FORCES. Davison, W. D. (Queen's Univ., Belfast). Proc. Phys. Soc., 87: 133-43(Jan. 1966).

The coefficients of the R^{-4}, R^{-6}, and R^{-8} terms in the series representation of the long-range interaction between two atomic systems at separation R are evaluated by a two-center variational procedure, using highly refined ground-state wave functions. Calculations are carried out for all atom-atom and atom-ion pairs drawn from the one- and two-electron systems H, He^+, He, Li^+, and H^-. The values for the R^{-6} coefficient are in excellent agreement with the values previously derived from oscillator strength data. (auth)

11505 APPROXIMATIONS FOR EXCHANGE SCATTERING. I. ELASTIC COLLISIONS. Abiodun, R. A.; Seaton, M. J. (Univ. Coll., London). Proc. Phys. Soc., 87: 145-51(Jan. 1966).

The problem of elastic scattering of electrons by the hydrogen ground state is formulated using a variational principle. With trial functions $\Psi = (1/\sqrt{2})\{\Psi(r_1)\phi(r_2) \pm \phi(r_1)\psi(r_2)\}$ where ψ is the ground state functions, the exchange integro-differential equations for the functions ϕ are obtained. Results from exact solutions of these equations are compared with results obtained using (a) modified Born-Oppenheimer approximations, with trial functions $\phi(r) = [1/r(4\pi)^{\frac{1}{2}}] \sin(kr) + \alpha\psi(r)$ and various choices for the parameter α, (b) the approximation of Ochkur, in which only the leading term in the (1/k) expansion of the Oppenheimer exchange amplitudes is retained, and (c) the distorted wave approximation, in which the direct potential is allowed for exactly. (auth)

11506 ISOTOPE SHIFT IN Li AND B^{2+}. Prasad, S. S. Stewart, A. L. (Queen's Univ., Belfast). Proc. Phys. Soc., 87: 159-61(Jan. 1966).

The mass polarization or specific isotope shift of the $1s^22s\ ^2S$ and $1s^22p\ ^2P$ levels of Li and B^{2+} is calculated using the 45-parameter wave functions of Weiss. The specific shifts of the resonance lines of ^7Li relative to ^6Li and of $^{11}B^{2+}$ relative to $^{10}B^{2+}$ are calculated to be 0.186 and 0.843 cm^{-1} respectively, compared with the observed values 0.157 cm^{-1}, 0.930 cm^{-1} ($\Delta J = 0$), and 0.970 cm^{-1} ($\Delta J = 1$) of Burke and of Hughes. (auth)

11507 ATOMIC STRUCTURES AND ELECTRON SCATTERING IN THE RELATIVISTIC HARTREE APPROXIMATION. Schonfelder, J. L. (Univ. of Melbourne). Proc. Phys. Soc., 87: 163-9(Jan. 1966).

The problems of atomic structure and electron scattering from heavy atoms are investigated using the relativistic Hartree approximation. The results obtained from the self-consistent field calculation of structure indicate the necessity for including relativistic effects for heavy atoms. Previously reported scattering calculations, also made using the Hartree approximation, are extended, and it is shown that the approximation ceases to be valid for an incident energy below a few hundred ev. (auth)

11508 A NEW RESONANCE SCATTERING FORMALISM AND ITS APPLICATION TO ELECTRON–HYDROGEN SCATTERING. Phythian, R. (The Univ., Manchester, Eng.). Proc. Phys. Soc., 87: 171-92(Jan. 1966).

It is shown that the scattering of a particle by a potential can be described by a Fredholm equation with hermitian kernel. From this follows an expansion for the reaction matrix, the individual terms of this series having a resonance-type structure. A simple example is given which suggests that a few terms of the series are sufficient to yield a good approximation to the scattering cross section over a wide energy range. A similar expansion is then given for the reaction matrix in the case of electron–hydrogen scattering (or similar three-body scattering problems), the expansion being exact when the total energy of the system is negative and a close approximation for positive energies. Variational methods which may be useful in calculating terms of the expansion are derived, and methods of calculating cross sections are briefly discussed. (auth)

11509 ELECTRON LOSS AND FORMATION OF SLOW NEGATIVE IONS IN COLLISIONS BETWEEN HYDROGEN ATOMS AND NEGATIVE IONS WITH GAS MOLECULES. Pilipenko, D. V.; Gusev, V. A.; Fogel', Ya. M. (Inst. of Physics and Tech., Academy of Sciences, Ukrainian SSR). Zh. Eksp. Teor. Fiz., 49: 1402-7(Nov. 1965). (In Russian).

Results of measurement of the effective cross section for electron loss by negative hydrogen ions with energies between 3 to 30 kev in collisions with O_2, NO and CO gas molecules are presented. The cross sections for formation of slow negative ions in collisions between hydrogen atoms or negative ions and the same molecular gases are measured in the same energy range. The curve describing the dependence of the effective cross section σ_{-10} (ϵ) on fast particle energy for the H–CO pair possesses a structure which can be explained by invoking the adiabatic Massey criterion. The magnitude of the cross section σ^- and the shape of the curve σ^- (ϵ) depend on the nature of the target gas and on the binding energy of the electron in the fast particle. The position of the peaks of the plot of σ^- (ϵ) as a function of the primary beam energy corresponds to the adiabatic Massey criterion. (auth)

11510 ON EVALUATION OF THE POLARIZATION OF AN ATOM IN A STRONG ELECTROMAGNETIC FIELD. Kuznetsova, T. I.; Rautian, S. G. (Lebedev Inst. of Physics, Moscow). Zh. Eksp. Teor. Fiz., 49: 1605-10(Nov. 1965). (In Russian).

The interaction of a two-level quantum system with the sum of a weak and monochromatic strong radiation field is calculated. The conditions are obtained, at which combination frequencies components in the polarization are of the same order of magnitude as the weak field frequencies components. (auth)

11511 THE THEORY OF ATOMIC COLLISIONS. Third Edition. Mott, N. F.; Massey, H. S. W. The International Series of Monographs on Physics. Oxford, Claredon Press, 1965. 880p. £6.

The application of classical and quantum mechanics to collisions between atoms, electrons, ions, and nuclei is discussed. Aspects of the theory of the one-body collision problem are treated, including the use of the wave equation and Green's function; scattering of a beam of particles by a center of force and by a Coulomb field; central-force scattering using Born and semiclassical approximations and variational methods; the scattering matrix and dispersion relations; scattering by nonlocal, absorptive, and multicentral interactions; the electron spin; and polarization and scattering by spin-dependent interactions. Aspects of the many-body problem are considered, with discussions of non-relativistic two-particle collisions and of atomic-collision theory involving the Born and impulse approximations, the two-state approximation, the many-state problem and the generalized S matrix, and rearrangement collisions. Application of the theory to electron and positron collisions with H and complex atoms, collisions between atomic systems, nuclear collisions, transition probabilities, and radiation in relativistic two-body problems is discussed. (M.J.T.)

11512 THE STRUCTURE OF ATOMS AND MOLECULES. Kondratev, V. Dover Books on Physics and Mathematical Physics. New York, Dover Publications, Inc., 1965. 540p. $2.50.

Translated from the Russian by G. Yankovsky.

A study of quantum mechanics is presented, offering a descriptive survey of current knowledge of electronic, atomic, and molecular structure, including detailed work on the nuclei of atoms. Topics considered are electrons and quanta, the nucleus, electronic structure of atoms, atomic and molecular spectroscopy, the nature of chemical forces, and electric and magnetic properties of atoms and molecules. The book is useful as a senior undergraduate or first-year graduate text in atomic physics or as a high-level survey of atomic and molecular structure for researchers not primarily in this field. (M.J.T.)

11513 ELASTIC AND REACTIVE SCATTERING IN THE (H,H_2) SYSTEM [Thesis]. Tang, Kwong-tin. New York, Columbia Univ., 1965. 179p.

A quantum mechanical study is made of elastic and reactive scattering in the (H, H_2) system and its isotopic analogs. The scattering problem is formulated in terms of the appropriate differential-integral equations. From the three-body potential energy surface for the (H, H_2) system, approximate two-body potentials are constructed by introducing assumptions corresponding to limiting cases of physical interest. The elastic scattering for the different two-body potentials is evaluated in terms of a partial wave analysis, and the calculated differential and total cross sections are compared with the available data. The reactive scattering is first examined by a form of the distorted-wave Born approximation (DWBA) suitable for collisions in which all particles have finite mass. For

certain incident energies, differential and total cross sections, as well as other attributes of the reactive collision (e.g., reaction configuration), are determined. Since the DWBA method is too complicated for a general study of the (H, H_2) reaction, a much simpler approximation method, the "linear model," is developed. It is found that the linear model, when appropriately normalized, gives results in good agreement with the DWBA method. By application of the linear model to (H, H_2), (H, D_2) and (D, H_2), the energy dependence, rotational state dependence, and other properties of the total and differential reaction cross sections are determined. The conclusions obtained from the quantum mechanical treatment are compared with the classical trajectory calculations and with the experimental measurements. Finally, the reaction mechanism is discussed in the light of the new information obtained. (Dissertation Abstr.)

11514 INCOHERENT SCATTERING OF GAMMA RAYS BY K-SHELL ELECTRONS. Reddi, A. Ramalinga; Lakshminarayana, V.; Jnanananda, Swami (Andhra Univ., Waltair, India). pp 227-32 of Nuclear Physics and Solid State Physics Symposium, 1965. Nuclear Physics. Bombay, Atomic Energy Establishment, 1965.

The effects of K-shell electron binding on the incoherent scattering of 320-kev gamma rays were investigated. The incoherent scattering function was obtained for Pb, Sm, and Ta as a function of the scattering angle. The experimental results were compared with calculations by Koppe's interpolation method. The Z-dependence of the differential scattering cross section was analyzed using a formula of the type $d\sigma_k/d\Omega = kZ^n$. (D.C.W.)

11515 COMPTON SCATTERING OF LOW ENERGY GAMMA RAYS. Rao, P. V. Ramana; Rao, J. Rama; Lakshminarayana, V. (Andhra Univ., Waltair, India). pp 233-7 of Nuclear Physics and Solid State Physics Symposium, 1965. Nuclear Physics. Bombay, Atomic Energy Establishment, 1965.

The cross sections for the incoherent scattering of gamma rays by bound electrons in Al, Cd, C, and Cu at 100, 129, 145, and 280 Mev were determined. The results were compared with the predictions of the Klein-Nishina formula for incoherent scattering by free electrons. (D.C.W.)

11516 PHOTOELECTRIC CROSS SECTION OF GAMMA RAYS FOR HEAVY ATOMS. Ghose, A. M. (Bose Inst., Calcutta). pp 316-19 of Nuclear Physics and Solid State Physics Symposium, 1965. Nuclear Physics. Bombay, Atomic Energy Establishment, 1965.

A method developed for the measurement of the photoelectric cross sections of heavy atoms is described, and the results obtained for Pb and Hg using this method with a ^{60}Co source are presented. A comparison of experimental and theoretical cross sections as a function of atomic number is included. (D.C.W.)

11517 LOSS OF THE FAST NEGATIVE IONS IN ATOMIC COLLISIONS. Karmohapatro, S. B. (Saha Inst. of Nuclear Physics, Calcutta). pp 358-62 of Nuclear Physics and Solid State Physics Symposium, 1965. Nuclear Physics. Bombay, Atomic Energy Establishment, 1965.

The cross section for the reaction $Cl^- + Cl \rightarrow Cl + Cl^-$ in the energy range from 25 to 90 kev was calculated using the impact parameter method. (D.C.W.)

Cosmic Radiation

See *also* Elementary Particles and Radiations
Nuclear Properties and Reactions

11518 DYNAMIC FREQUENCY SPECTRA OF SHORT-PERIOD COSMIC-RAY INTENSITY FLUCTUATIONS. Kuklin, G. V.; Luzov, A. A. (Inst. of Terrestrial Magnetism, Ionosphere and Radio Wave Propagation, Academy of Sciences, USSR). Geomagn. Aeronomy (USSR) (Engl. Transl.), 5: 298-303(1965).

Translated from Geomagn. Aeronomiya, 3: 384-91(1965).

The spectral concepts of the theory of random processes are used to compute the spectra of short-period cosmic-ray intensity fluctuations. Use of the method of successive additions in spectral computations produces a representation of the dynamics of the change of the frequency components in time. A method is shown for allowing for the modifying properties of recording equipment and mathematical operators used in the processing of experimental data. (auth)

11519 STUDY OF PERIODIC VARIATIONS OF COSMIC-RAY INTENSITY BY MEANS OF SELECTIVE FREQUENCY FILTERS. Luzov, A. A.; Kuklin, G. V.; Pezhemski, A. I. (Inst. of Terrestrial Magnetism, Ionosphere and Radio Wave Propagation, Academy of Sciences, USSR). Geomagn. Aeronomy (USSR) (Engl. Transl.), 5: 304-10(1965).

Translated from Geomagn. Aeronomiya, 3: 392-400 (1965).

The characteristics and shortcomings of methods of determining the diurnal variations of cosmic-ray intensity are examined and reasons are given for the use of selective filters. Selective filters for determining diurnal variations are computed. The characteristics of diurnal and semi-diurnal variations are found from data on the neutron component at several stations. Note is made of the global character of cyclic diurnal variations and of the significant modulation of semidiurnal variations by meteorological factors. (auth)

11520 EQUIPMENT AND TECHNIQUES FOR RADIATION DAMAGE STUDIES. Lee, William (Hazleton-Nuclear Science Corp., Stanford, Calif.). J. Environ. Sci., 7: 28-34(Apr. 1964).

Various aspects of testing materials to be used in space exploration are reviewed. Some properties of various sources of radiation which may be encountered in space are considered as well as certain radiation effects of interest to space scientists. (TCO)

11521 SURVEY OF COSMIC-RAY INTENSITY IN THE LOWER ATMOSPHERE. Coxell, H.; Pomerantz, M. A.; Agarwal, S. P. (Franklin Inst., Swathmore, Pa.). J. Geophys. Res., 71: 143-54(Jan. 1, 1966).

Observations of the intensity of the nucleonic component were obtained with a neutron monitor on an aircraft in a worldwide survey extending from the equator to the north and south geomagnetic poles. The data were reduced to a standard pressure altitude (500 mm of Hg), and the effects of temporal variations were removed by a normalization procedure involving four ground-based neutron monitor stations distributed over a wide range of latitude. Representation of the results in the form of an isocosm map revealed general agreement with the Quenby and Wenk calculations of threshold rigidities. Discrepancies are attributable to the inexactness of the approximation adopted for taking into account the effects of the penumbra. The location of the cosmic-ray equator, determined at seven points, was in accordance with calculations using the sixth-order expansion of the geomagnetic potential. The variation in intensity along the equator was in agreement with earlier results obtained during a different phase of the solar cycle. Measurements in the arctic and antarctic regions reveal that, during a period of extreme solar cycle modulation, the intensities in the northern and southern polar caps were equal within less than 0.5%. The latitude dependence of the atmospheric attenuation length of the nucleonic component, L, was determined from observations of the dependence of intensity upon altitude. In the plateau region, the mean value of L was 136.1 ± 0.3 g/cm^2. L increased by about 11% over the range of threshold rigidity from 2.5 to 16 Gv. The absorption mean free path, λ_a, deduced from L, was 160 g/cm^2 in the plateau region. Calculations based on currently accepted models of nuclear collision and of the process of nucleon propagation through the atmosphere yielded a value for the interaction length, λ_i, of about 80 g/cm^2. This increased to 85 g/cm^2 when the effects of charge exchange were considered. (auth)

11522 FERMI ACCELERATION OF CHARGED PARTICLES IN TRANSITION REGION BEYOND MAGNETOSPHERE. Shen, C. S. (Purdue Univ., Lafayette, Ind. Catholic Univ. of America, Washington, D. C.); Chang, C. C. J. Geophys. Res., 71: 241-51(Jan. 1, 1966).

Recent experiments of the Imp 1 satellite show the existence of high-energy electrons with $E \geq 30$ kev in the transition region between the shock and the magnetosphere. It is suggested that electrons are locally accelerated by means of a Parker-Wentzel version of the Fermi mechanism. The trapping and acceleration dynamics of a typical electron along the distorted background magnetic field line is studied. It is found that the magnetic bottleneck just outside the shoulders of the magnetopause can reflect the gyrating electron toward upstream of the solar wind, whereas a large-amplitude magnetohydrodynamic wave that originated near the shock front can push the electron downstream. The electrons thus trapped increase in energy about 3 to 4 times before they can penetrate the advancing wave. Because of the scattering of small-scale magnetic irregularities, some of the electrons that have penetrated redistribute their pitch angle and can be trapped again by another advancing wave train. The high-energy electrons found in the Imp experiment can be built up by this process in a time on the order of a few minutes. (auth)

11523 POSITION OF THE SOUTH LATITUDE COSMIC-RAY PLATEAU. Gauger, J. (Boeing Scientific Research Labs., Seattle, Wash.). J. Geophys. Res., 71: 335-6(Jan. 1, 1966).

Measurements of the charged-particle and neutron fluxes produced within the atmosphere by the primary cosmic radiation were made on two aircraft flights in January 1964. Data on the count rates of a G-M tube array and a moderated BF_3 counter as functions of the aircraft position in terms of the L parameter at 10-km altitude are presented, for L from 1 to 3.5. Clear evidence for a flat south-latitude polar plateau is not found. (M.J.T.)

11524 SIDEREAL COMPONENT OF THE DIURNAL VARIATION OF COSMIC-RAY INTENSITY. Kane, R. P. (Physical Research Lab., Ahmedabad, India). Nuovo Cimento (10), 41A: 90-114(1966).

Sidereal variation is studied for cosmic-ray intensity recorded during the last decade. The neutron monitors show a 6 to 12 hr sidereal component (roughly towards the Milky Way direction of 07 hr) in 1954 and throughout 1952-55 with a monthly average amplitude of about 0.05% in contrast to about 0.10% in 1954. A spectrum with negative exponent is indicated. In the peak solar activity period 1956-59, this direction was considerably disturbed, and most of the sidereal vectors lay in the other three quadrants. Whereas no discernible latitude or altitude effect was observed, a striking longitude effect was noticed for European longitudes between 12 to 18 hr and far eastern longitudes between 18 to 24 hr. In 1960-64, most of the sidereal vectors lay in the 0 to 6 hr and 6 to 12 hr quadrants, indicating partial revival of the 1954 conditions. The 1964 minimum did not seem to be as deep as the 1954 minimum. The solar diurnal vector almost disappeared in 1954 but not in 1964. Hence, the problem raised by Dorman about the 22 year cycle in the phase of diurnal variation remains unresolved. A disconcerting feature about neutron monitor data was the inconsistency between the results of some nearby stations. A similar study of the temperature-corrected meson intensities revealed oppositely oriented sidereal vectors from the northern and southern hemispheres. It seems, therefore, that there are multiple sources of sidereal variation, some oriented towards the center of the galaxy, some along the spiral arms, and perhaps some others in other directions. (auth)

11525 MODULATIONS OF GENERICALLY RELATED GALACTIC COSMIC RAYS. Hildebrand, B.; Silberberg, R. (Naval Research Lab., Washington, D. C.). Phys. Rev., 141: 1248-60(Jan. 1966).

A method of analysis of the spectra of generically related cosmic-ray species is formulated. The effects of various spatial modulations between the cosmic-ray sources and the earth are separated from the effect of fragmentation in interstellar space. Predictions are made on how the ratios of the intensities of related cosmic-ray species, for both rigidity and energy/nucleon intervals, would be expected to vary with geomagnetic latitude, solar activity, and energy. These predictions are compared with the experimental results. Variations in the reported abundance ratios of helium isotopes and the light ($3 \leq Z \leq 5$) to medium ($6 \leq Z \leq 9$) elements can be explained in terms of solar and geomagnetic modulation, rather than by invoking the hypothesis of longer interstellar path lengths for low-energy cosmic rays. At a geomagnetic latitude of 55°, on 21 April 1961, the relative transmission of ^3He to ^4He through interplanetary and geomagnetic fields in the energy/nucleon interval 250–350 Mev/nucleon is found to be 0.38 ± 0.2. Statistically limited data favor a rigidity-dependent rather than velocity-dependent solar modulation above a rigidity of 1.2 BV. The local interstellar intensity of cosmic-ray helium (i.e., before solar modulation) at 1.7 BV is 0.6 ± 0.4 of that at 1.3 BV. Assuming the differential rigidity (R) spectrum of local interstellar helium to vary as $1/R^q$, the exponent q is found to be 1.8 ± 2 in the rigidity interval 1.2–1.7 BV. The result suggests that considerable solar modulation of the intensity of low-energy cosmic rays may occur even at solar minimum. Based upon the limited available data, the mean interstellar path length for cosmic rays in the region 200–400 Mev/nucleon is found to be 5 ± 2 g/cm^2. The values of the mean path length of cosmic rays and the exponent of the local interstellar helium spectrum are consistent with the values obtained for higher energy cosmic rays. The effects of modulations occurring in the cosmic-ray source regions are also explored. (auth)

11526 THE MOMENTUM SPECTRUM OF COSMIC-RAY MUONS AT LARGE ZENITH ANGLES. Ashton, F.; Kamiya, Y.; MacKeown, P. K.; Osborne, J. L.; Pattison, J. B. M.; Ramana Murthy, P. V.; Wolfendale, A. W. (Univ. of Durham, Eng.). Proc. Phys. Soc., 87: 79-88(Jan. 1966).

The momentum spectrum of cosmic-ray muons was measured as a function of zenith angle in the range 77.5 to 90° and covering the momentum band 3 to 500 Bev/c. Based on knowledge of the experimentally determined muon energy spectrum in the vertical direction, an accurate analysis is made of the inclined muon spectra expected as a function of the ratio of kaons to pions produced in high energy interactions. Inclusion of the various kaon decay modes reduces the sensitivity of the inclined intensities to the K/π ratio, and despite the good statistical accuracy of the measurements only an upper limit can be set to the ratio, the conclusion being that $K/\pi \lesssim 0.4$ at production in the nuclear collisions of high energy nucleons in the energy range 6×10^2 to 4×10^4 Bev. It is pointed out that an accurate estimate of the ratio will be possible when improved measurements of both the vertical and near-horizontal muon intensities are available in the region of 1000 Bev/c. (auth)

11527 AN INVESTIGATION OF COSMIC RAYS UNDERGROUND USING A SCINTILLATOR STACK. I. THE APPARATUS. Barton, J. C. (Northern Polytechnic, London). Proc. Phys. Soc., 87: 89-100(Jan. 1966).

A description is given of the construction, testing, and performance of an apparatus which consists of six liquid scintillation counters, each of area 1×1 m^2, interleaved with sheets of lead of thickness 2.5 radiation lengths. The pulse height from each of the counters is converted into digital form and recorded, together with hodoscope information from index counters above and below the stack, on standard five-hole tape. At a depth of 60 mwe below sea level the total event rate is about 2 sec^{-1}. The classification system used for distinguishing the various types of events is also described. (auth)

11528 AN INVESTIGATION OF COSMIC RAYS UNDERGROUND USING A SCINTILLATOR STACK. II. THE ELECTROMAGNETIC INTERACTIONS OF HIGH-ENERGY MUONS. Barton, J. C. (Northern Polytechnic, London);

Rogers, I. W.; Thompson, M. G. Proc. Phys. Soc., 87: 101-7(Jan. 1966).

The probability of a high-energy cosmic-ray muon undergoing an electromagnetic interaction in lead with energy transfer in the range 0.1 to 20 Bev was determined, using a scintillation apparatus described previously. The energy transfer in the process is determined by a comparison of the ensuing shower produced in the stack with theoretical shower curves due to Buja. The results indicate that up to energy transfers of 20 Bev there is no significant discrepancy between the theoretical and experimental values for the sum of the electromagnetic cross sections. (auth)

11529 THEORETICAL APPROACH TO VERY HIGH ENERGY PHENOMENA. Kobayashi, Tetsuro (Waseda Univ., Tokyo); Namiki, Mikio. Progr. Theoret. Phys. (Kyoto), Suppl., No. 33, 1-34(1965).

Reviews of the theory on very high energy phenomena are presented. After an introductory sketch on historical development, models of multiple particle production are discussed first from the point of view of structure of the nucleon, and it is shown that a model based on the inner cloud excitation is fairly well supported by recent experiments of cosmic ray jets. Secondly, the interrelation of high energy elastic scattering and multiple particle production are examined in connection with the model and the field aspect of boson. (auth)

11530 FOUR MOMENTUM TRANSFER IN JET SHOWERS AND MULTI-FIREBALL MODELS. Kobayakawa, Keizo (Univ. of North Carolina, Chapel Hill). Progr. Theoret. Phys. (Kyoto), Suppl., No. 33, 35-54(1965).

Two methods of evaluating the four momentum transfers in high energy jet showers are compared with each other. Some physical considerations are carried out based on the experimental information analyzed by the two methods. It is confirmed that multi-fireballs are produced and the number of them increases with the incident energy rather than with the multiplicity of secondary particles. Some theoretical models are examined concerning the four momentum transfers. It is shown that the mass of the linked boson is larger than the pion mass and the mass of a fireball is larger than twice the nucleon mass in the multilinked model which generalizes the multi-peripheral model. Some difficulties appear in the model in which the virtual particles are regarded as Pomeranchuk particles. The 2πNS model in which the four momentum transfer is proportional to the incident energy is also tested and found not to be inconsistent with the experiment. (auth)

11531 TWO-CENTER MODEL AND FOUR MOMENTUM TRANSFER IN JETS. Kobayakawa, Keizo (Univ. of North Carolina, Chapel Hill); Nishikawa, Kiyoshi. Progr. Theoret. Phys. (Kyoto), Suppl., No. 33, 55-75(1965).

A method of evaluating the four-momentum transfer in high-energy jet showers is proposed. This method is based on the two-center model. The values of the Lorentz invariant square of the four momentum transfer are obtained from eighty-one jets with $N_h \leqq 3$ which contain nearly equal numbers of primary and secondary jets. Their distribution and their relations with the incident energy, multiplicity etc. are studied. Also the energy transfer for each jet is obtained. Attention is paid to some differences between primary and secondary jets. Several theoretical models are examined concerning the four momentum transfer. It is shown that the models where a pion is exchanged between colliding particles can not explain the general features of high energy jets. One needs to take a heavy boson into account instead of a pion. Difficulties appear in the model where the virtual particle is regarded as a Pomeranchuk particle. The 2πNS model in which the four momentum transfer is proportional to the incident energy is also tested. (auth)

11532 ANALYSIS OF THE HIGH ENERGY JET SHOWERS. I. A PROPOSAL OF NEW KINEMATICS. Yajima, Nobuo (Nagoya Univ., Japan); Hasegawa, Shun-ichi. Progr. Theoret. Phys. (Kyoto), Suppl, No. 33, 76-91(1965).

A method is introduced for the kinematic analysis of data obtained from the study of multi-pion production at very high energy, without making use of a symmetry assumption for the angular distribution of pions in the center of mass system. Expressions are derived which, for constant and known transverse momentum of the emitted pions, give the inelasticity in the mirror system, the four-momentum transfer and the tranverse momentum of the target particles. Introducing the asymmetry factor, which is obtainable appropriately in the practical case, it is shown to be possible to derive formulas which, also for constant and known pion transerse momentum, yield, in good approximation, the total energy and the angular momentum of the pions in the center of mass system, and the Lorentz factor of the center of mass. The new formula for the Lorentz factor is compared with Castognoli's formula, for the case in which a true asymmetry exists. (auth)

11533 ANALYSIS OF THE HIGH ENERGY JET SHOWERS. II. MONTE CARLO TEST OF THE NEW FORMULAE. Hasegawa, Shun-ichi (Univ. of Tokyo); Outi, Akizi; Yajima, Nobuo. Progr. Theoret. Phys. (Kyoto), Suppl, No. 33, 92-108(1965).

The method, introduced for the kinematic analysis of high energy nuclear jet showers, is examined by using the Monte Carlo method. The angular distribution and the distribution of the transverse momentum of emitted pions are assumed to be of the type of $\cos^m\theta$ and $P_T \exp[-P_T^2/P_0^2]$, respectively. Furthermore, the number of emitted charged pions is assumed to be two thirds of the total number of emitted pions. For each artificial jet thus obtained, the reliability of the formulas previously proposed is examined. These numerical experiments show that the formulas are in good approximation for the practical use. (auth)

11534 ANALYSIS OF THE HIGH ENERGY JET SHOWERS. III. ANALYSIS OF EXPERIMENTAL DATA. Borello, T. (Sao Paulo Univ., Brazil); Cattani, M.; Cruz, M. T.; Hasegawa, Shun-ichi; Lattes, C. M. G.; Okuno, E.; Orsini, C. M.; Pacca, I. G.; Sequeiros, H.; Yajima, Nobuo. Progr. Theoret. Phys. (Kyoto), Suppl., No. 33, 109-33(1965).

A systematic method that was previously introduced for the kinematic analysis of cosmic ray jet phenomena is applied to experimental data. The results of the analysis are presented for a selection of about one-hundred jet showers of the type $N_n = 0$ and 1. The special relations obtained among the physical quantities are discussed on the bases of three phenomenological models of multiple-meson production. In particular, the H-quantum hypothesis is studied in a quantitative manner. It is concluded that the H-quantum hypothesis seems to be most satisfactory to explain cosmic ray jet phenomena. (L.B.S.)

11535 ANALYSIS OF THE HIGH ENERGY JET SHOWERS. IV. FOUR MOMENTUM TRANSFER AND TRANSVERSE MOMENTUM OF RECOIL NUCLEON. Yajima, Nobuo (Nagoya Univ., Japan); Hasegawa, Shun-ichi; Kobayashi, Tsunehiro; Ohsawa, Akinori; Shibata, Toru. Progr. Theoret. Phys. (Kyoto), Suppl., No. 33, 134-42(1965).

Formulas are introduced for obtaining the four-momentum transfer Δ^2 and transverse momentum P_T of the recoil proton in high-energy jet showers. A method is presented for discriminating recoil proton among secondary thin tracks, taking into account the experimental knowledge of the behavior of secondary pions. A practical analysis of the experimental data is made and the results are discussed. P_T distribution is presented for nineteen jets of $K_M \leq 0.2$, which are identified with good reliability as the recoil proton. (L.B.S.)

11536 STUDIES ON X-AGENT. XLV. FLUCTUATION OF THE EFFECT OF LIGHT ON THE PATTERNS OF X-AGENT AROUND A WATER BOTTLE. Moriyama, Hideo (Shonan Hygiene Inst., Kamakura, Japan). Yokohoma Med. Bull., 16: 155-64(Aug. 1965).

The variability of X-agent, a hypothetical cosmic radi-

ation, was alleged to have been demonstrated in the effect of an artificial light (100-w incandescent lamp) on the pattern of secondary X-agent produced around a water bottle. In some cases, the light proved to be effective in altering the pattern, whereas in other cases it was found to have little or no effect. In general, the effect of the light varied with its intensity, and its effect tended to be reversed depending on its intensity. The intensity of the secondary X-agent, which originated from the light, was not influenced by the intensity of the light. In general, the effect of the light varied gradually over the course of a day, indicating that X-agent was undergoing a gradual change during the day. However, on some days the agent rapidly altered during the course of the day. The difference in the intensity of the light resulted, in most cases, in the difference in the intensity of secondary radiation. Such a difference in intensity is considered to be due to the production of a new X-agent from the light by the interaction between the light and the X-agent. Evidence is presented which suggests that X-agent produced from strong light by this interaction acts antagonistically to an agent produced by weak light. Atmospheric pressure and X-agent show related fluctuations. (BBB)

11537 DETECTION OF SOLAR NEUTRINOS BY MEANS OF THE $^{71}Ga(\nu,e^-)^{71}Ge$ REACTION. Kuzmin, V. A. (Lebedev Inst. of Physics, Moscow). Zh. Eksp. Teor. Fiz., 49: 1532-4(Nov. 1965). (In Russian).

The possibilities of detecting solar neutrinos by means of the low threshold reaction $^{71}Ga(\nu,e^-)^{71}Ge$, which can be efficiently employed for recording neutrinos from the $^{1}H(p,e^+\nu)^{2}H$ and $^{7}Be(e^-,\nu)^{7}Li$ reactions, are examined. The merits of the radiochemical method based on this reaction are compared with those of other reactions. The cross section for absorption of solar neutrinos by the ^{71}Ga nucleus and the magnitude of the effects on the earth due to neutrinos from various reactions occurring in the depths of the sun are presented. It is pointed out that transitions to the excited states of the ^{71}Ge nucleus may be important for neutrino absorption. (auth)

Direct Energy Conversion

Refer also to abstract 12421.

11538 (65RL-3814E(Rev.)) GRAVITATIONAL INSTABILITY IN A VERTICAL MAGNETIC FIELD. BenDaniel, D. J.; Hurwitz, H. Jr. (Research Lab., General Electric Co., Schenectady, N. Y.). Aug. 1965. 12p.

Liquid phase magnetohydrodynamic generators require the efficient transfer of energy from an expanding vapor to a liquid metal. A longitudinal magnetic field may influence the efficiency of this process by reducing the growth rate of the gravitational instability that is encountered. The reduction in growth rate of this instability is calculated for arbitrary electric conductivity of the liquid. (auth)

11539 (65RL-3888E) CALCULATION OF CURRENT AND POTENTIALS FOR A SEGMENTED ELECTRODE MHD GENERATOR. Kilb, R. W. (Research Lab., General Electric Co., Schenectady, N. Y.). Feb. 1965. 10p.

The work of Hurwitz, Kilb, and Sutton was extended to derive complex plane mapping functions which allow one to analyze currents and potentials in an idealized segmented MHD duct when the insulator and electrode segments are unequal in length. This mapping function is used to obtain suitable expansions of parameters required in relating electrode current and voltage across and along the duct. These expansions apply particularly to the case of very thin electrodes. (auth)

11540 (AD-626444) THE DEVELOPMENT OF A LOW-WORK-FUNCTION COLLECTOR FOR THERMIONIC ENERGY CONVERTERS. Annual Technical Summary Report No. 3, November 1, 1964-October 30, 1965. Shefsiek, P. K.; Buzzard, R. J. (Radio Corp. of America, Lancaster, Pa. Direct Energy Conversion Dept.). Contract NONR-4012(00)-FBM. 121p. CFSTI $4.00 cy, $0.75 mn.

An equation was developed which describes the performance of a thermionic converter in terms of the output potential, current density, emitter temperature, collector temperature, cesium reservoir temperature, and electrode spacing. The correlation between values predicted by the equation and a variety of experimental data was checked. In addition, a number of materials were evaluated for use in collectors. A current-voltage curve was obtained at four different collector temperatures for the following collector materials: Tr matrix, arc-cast Mo, Mo matrix, Ni matrix, Ta matrix, and W matrix. The results were plotted as maximum output power and output voltage vs collector temperature. (D.C.W.)

11541 (AERE-R-5107) STUDY OF GAS DISCHARGES THAT ARE EXPECTED IN A CLOSED CYCLE MAGNETOHYDRODYNAMIC GENERATOR. Sakuntala, M. (Atomic Energy Research Establishment, Harwell (England)). Dec. 1965. 68p. Dep. BIS $2.00. HMSO 10s.

An investigation of plasmas of interest for closed-cycle MHD generators, reveals the dominant mechanisms determined by the space charge distribution, the production of positive ions by thermal ionization and electron collisions, and thermionic emission and backscattering. Depending on the magnitude of the applied voltage between the electrodes, three regions were distinguished in which the current is either independent, uniformly or rapidly rising until a transition to the low voltage arc occurs when the current suddenly changes by a factor 10^{13} or more. The variation of current with voltage and the transition point were analyzed and the results agree satisfactorily with experiments. (M.O.W.)

11542 (EUR-2534.e) OPTIMIZATION OF HEAT PIPE THERMIONIC CONVERTERS FOR SPACE POWER SUPPLIES. Busse, C. A. (European Atomic Energy Community, Ispra (Italy). Joint Nuclear Research Center). Dec. 1965. 16p. Dep. mn.

A relation for the electric power output of a cylindrical heat pipe thermionic converter is derived, taking into account ohmic losses in the emitter, the collector, and the lead wire. The maximum power output is determined for a given specific mass of the converter, emitter radius, and lead-wire length by optimizing the load voltage, the length of the emitter, and the cross sections of the emitter, the collector, and the lead wire. (auth)

11543 (GIC-2605-3) LOW POWER THERMOELECTRIC COMPONENT DEVELOPMENT PROGRAM. Final Report. Lemanski, E. J. (General Instrument Corp., Newark, N. J. Thermoelectric Div.). Mar. 1, 1965. Contract AT(30-1)-2605. 132p. Dep. mn. CFSTI $4.00 cy, $1.00 mn.

Several types of bonds for bismuth telluride power producing material were evaluated for stability and physical strength in a 1000 hour test at hot junction temperatures ranging up to 530°F under conditions of moderate vacuum (50 microns mercury). A bond consisting of a layer of plasma sprayed molybdenum, to serve as a diffusion barrier, followed by a layer of plasma sprayed nickel, to facilitate attachment to shoe materials was found to meet all the requirements of a good bond. Based on test results, in which no degradation was noted over an extended 1700 hour period at 530°F hot junction temperature, years of operation can be extrapolated. A thermal syphon loop operating as a heat dump device, between the temperature of the heat source (~500°F) and a water cooled heat sink, carried a heat load up to 3630 Btu/hr. The heat source was maintained at a constant temperature over a range of power inputs by manually regulating the flow rate with a throttling valve. In its present form the heat dump can regulate the temperature of a decaying heat source of a 12.5 watt (electrical) generator for 2.3 half lives. The reduced pressure insulation characteristics of powdered opacified insulation mixtures were measured. Powdered aluminum and ferrosilicon were used as the opacifiers with silica aerogel

powdered insulation. A Santocel C-aluminum mixture was the best combination, giving an apparent K of 0.002 Btu/hr ft°F at 100 microns mercury absolute pressure. The qualities of the insulation mixtures were found to be dependent upon particle size—a close match in particle size between silica aerogel and opacifier gave the best insulation characteristics. A Santocel A-ferrosilicon insulation mixture was successfully degassed, as evidenced by operation in a stable, static vacuum over a period of almost one year at 500°C. As of this date, the system is still in operation with no indication of outgassing. The insulation was altered as a result of the degassing process, but the thermal conductivity (0.0025 Btu/hr ft°F at 100 microns mercury, absolute) was close to the best combination tested. Although special handling is required after processing, the Santocel A-ferrosilicon mixture meets the requirements of an efficient, vacuum-stable insulation at moderate-to-high temperatures (up to ~800°C). (auth)

11544 (LA-DC-7390) SPACING AND CESIUM PRESSURE DEPENDENCE OF ELECTRON TEMPERATURES AND ION DENSITIES IN A THERMIONIC CONVERTER. Reichelt, Walter H.; Kruer, William L. (Los Alamos Scientific Lab., Univ. of California, N. Mex.). [1965]. Contract W-7405-eng-36. 9p. (CONF-651049-2). Dep. mn. CFSTI $1.00 cy, $0.50 mn.

From IEEE Thermionic Conversion Specialist Conference, San Diego, Calif.

Electron temperature and ion density profiles in the interelectrode gap were determined spectrographically for a thermionic diode operating in the ignited mode for spacings of 1.0, 1.5, and 2.0 mm. At an emitter temperature of 1730°K, the cesium reservoir temperatures between 550 and 598°K, the maximum electron temperature and density were of the order of 2800°K and 5×10^{14} ions/cm^3, respectively. Electron temperature and density profiles near the emitter display a flattening or "turning down" which commences about 0.2 mm from the emitter. Departures from local thermodynamic equilibrium are not resolvable in the region of operation. (auth)

11545 (LA-DC-7555) SURVEY OF LOS ALAMOS AND EURATOM HEAT PIPE INVESTIGATIONS. Ranken, W. A.; Kemme, J. E. (Los Alamos Scientific Lab., Univ. of California, N. Mex.). [1965]. Contract W-7405-eng-36. 12p. (CONF-651049-3). Dep. mn. CFSTI $1.00 cy, $0.50 mn.

From IEEE Thermionic Conversion Specialist Conference, San Diego, Calif.

A review is presented of investigations of heat pipes for thermionic diode uses. The theory of heat pipes is presented. Experimentally obtained properties of heat pipes and several possible pipe designs are discussed. (M.O.W.)

11546 (SC-RR-65-671) ^{147}Pm-SILICON BETAVOLTAIC BATTERY FEASIBILITY. Windle, W. F. (Sandia Corp., Albuquerque, N. Mex.). Jan. 1966. Contract AT(29-1)-789. 25p. Dep. mn. CFSTI $1.00 cy, $0.50 mn.

Betavoltaic battery work is summarized and expected characteristics of optimized ^{147}Pm-Si betavoltaic batteries are discussed. ^{147}Pm source output calculations and data on experimental batteries are presented. (auth)

11547 EXPERIMENTAL INVESTIGATIONS ON CYLINDRICAL NOBLE GAS-FILLED THERMIONIC CONVERTERS FOR A THERMIONIC-REACTOR. Mayer, R.; Pruschek, R. (Technische Hochschule, Stuttgart). Atomkernenergie, 10: 346-52(Sept.-Oct. 1965). (In German).

The results of two experiments on the influence of position and distribution of auxiliary emitters in a cylindrical noble gas-filled thermionic converter are dealt with. The spatial arrangement of the auxiliary emitters influences the current-voltage characteristic current and power gain as well as a and c generation. Uniform current density distribution across the emitter surface will be obtained if several auxiliary emitters are arranged within the electrode space. The performance of a converter constructed on these lines is discussed. (auth)

11548 MAGNETIC SYSTEMS OF MAGNETOGASDYNAMIC GENERATORS. Bertinov, A. I.; But, D. A.; Kalugin, V. N. Magnit. Gidrodin., No. 3, 145-54(1965). (In Russian).

Two design variants of the magnetic systems of MGD generators are examined: with an inner magnetizing coil and with an outer magnetizing coil. The advantages and shortcomings of both systems are discussed. General formulas are presented for calculating the scattering factor and determining the weight of the systems for any value of the inlet and outlet channel radii, height of channel, and induction in the channel. (ATD)

11549 PHOTOIONIZATION OF CESIUM ATOMS BY SOLAR RADIATION. APPLICATION TO A LOW-TEMPERATURE CESIUM THERMIONIC DIODE. Luke, Keung P. (Unified Science Associates, Inc., Pasadena, Calif.). Solar Energy, 9: 110-12(July-Sept. 1965).

The photoionization of cesium atoms by solar radiation is studied as means for producing sufficient ionization in cesium diodes at low emitter temperatures. (D.C.W.)

11550 MINIATURE MAGNETOHYDRODYNAMIC GENERATOR. Biehl, Arthur T. (to MB Associates). U. S. Patent 3,225,227. Dec. 21, 1965. Filed July 2, 1962.

A miniature MHD generator is patented, which is capable of delivering an average power of about 50 megawatts for a duration of 5 μsec providing a short high energy power pulse suitable for many applications. The generator includes a first inner electrically conductive material and a second outer electrically conductive material coaxially aligned with the first material and defining an annular space between them. A source of electrical energy is connected to the first and second materials for generating a magnetic field in the annular space. Conductive means interconnect the materials at one of their ends; and an explosive charge surrounds the second material, while detonating means are provided adjacent to the other ends for initiating an axially progressing wave in the charge to progressively collapse the second material toward the conductive means. Means are provided for extracting the generated electrical energy from the compression of the magnetic field. (B.L.M.)

Elementary Particles and Radiations

See also Field Theory, Scattering Theory, and Symmetries

Refer also to abstracts 11111, 11503, 11528, 11912, 11965, 11975, and 12084.

11551 (CONF-650837-3) K^-p INTERACTIONS FROM 900 TO 1100 Mev/c AND THEIR BEARING ON $Y^*(1765)$ AND $Y_1^*(1815)$. Technical Report No. 513. Yodh, G. B. (Maryland Univ., College Park. Dept. of Physics and Astronomy). Oct. 1965. Contract AT(40-1)-2504. 36p. Dep. mn. CFSTI $2.00 cy, $0.50 mn.

From Boulder Conference on Particle Physics, Boulder, Colo.

A summary is presented of experimental data on K^--p interactions from 900 to 1100 Mev/c K^- momentum (total cms energy of the K^-p system from 1740 to 1840 Mev). The bearing of these results on the K^-p resonances Y_1^* (1765) and Y_0^* (1815) is discussed. Previous data are reviewed. Results of the neutral V channels and the Σ channels from bubble chamber experiments are discussed. Results on the energy, width, decay channels, spin-parity, and isospin of the resonances are summarized. (M.J.T.)

11552 (CONF-651015-3) BOSON RESONANCES PRODUCED IN K^-p INTERACTIONS. Leitner, Jack ([Syracuse Univ., N. Y.]). [nd]. 16p. Dep. mn. CFSTI $1.00 cy, $0.50 mn.

From American Physical Society, Chicago.

Four mesons from K^-p interactions are discussed. The ϕ (1020) and the η^* (960) or the χ^0, are reviewed and new knowledge regarding them is discussed. The f* (1500) and the K** (1410) are treated in some detail. Their possible SU(3) classification is considered. It is emphasized that the remarks on classification are speculative on many counts, but the nonet and mixing scheme appear to be attractive enough to warrant further investigation especially with regard to SU(6) which in principle should account for the degree of mixing in the various multiplets. (J.F.P.)

11553 (COO-614-34, Sect. IIC) EXPERIENCE WITH ON-LINE EXPERIMENTATION. Ehrlich, R. D.; Fryberger, D.; Powers, R. J.; Sherwood, B. A.; Telegdi, V. L.; Bounin, J. (Chicago Univ., Ill. Inst. for Computer Research). 5p.

On-line computation was used to measure the electron momentum spectrum in muon decay. A brief description of on-line modifications for the experiment is presented. A comparison of ALGOL and FORTRAN for the above purposes was made. (M.O.W.)

11554 (COO-1195-27) $K_2^0 \rightarrow \pi^- + \pi^+$, EEN VREEMD VERVAL VAN EEN VREEMD DEELTJE. ($K_2^0 \rightarrow \pi^- + \pi^+$—A Strange Decay from a Strange Particle). Nefkens, B. M. K. (Illinois Univ., Urbana). [1964]. Contract AT(11-1)-1195. 19p. Dep. mn; CFSTI $1.00 cy, $0.50 mn.

Two experiments in which the decay $K_2^0 \rightarrow \pi^- + \pi^+$ was observed are summarized, and the various theories of this decay mode are discussed. (D.C.W.)

11555 (DESY-65/13) DETERMINATION OF THE $\pi\pi$ SCATTERING PHASE SHIFTS UP TO 1.3 Gev CMS ENERGY. Wolf, Guenter (Deutsches Elektronen-Synchrotron, Hamburg (West Germany)). Oct. 1965. 18p. Dep. mn.

The experimental data on elastic $\pi\pi$ scattering were combined and analyzed in terms of the $\pi\pi$ scattering phase shifts up to cms energies of the $\pi\pi$ system of 1.3 Bev. Most of these data come from the application of the one-pion exchange model to reactions of the type $\pi N \rightarrow \pi\pi N$. The analysis resulted in a set of phase shifts which give a good fit to the existing data. For the width of the meson (ρ) a value of 170 Mev was obtained. The behavior of the asymmetry parameter $R = (F - B)/(F + B)$ in $\pi^+\pi^-$-scattering implies the existence of a $T = 0$, $J = 0$ $\pi\pi$ resonance. A mass of 0.74 Bev and a width of 90 Mev were found for this resonance. (auth)

11556 (DESY-65/14) STRAHLUNGSKORREKTUREN ZUR e-p-STREUUNG FUER WINKEL- UND ENERGIEKOINZIDENZ-EXPERIMENTE. (Radiative Corrections for e-p Scattering for Angular and Energy Coincidence Experiments). Kohaupt, R. D. (Deutsche Elektronen-Synchrotron, Hamburg (West Germany)). Oct. 1965. 44p. Dep. mn.

Calculations of radiative corrections to e-p-scattering are performed for experiments in which the final particles are detected in coincidence and both the angles and energies of the outgoing particles are measured. The dependence of radiative corrections on angle and energy resolution parameters is discussed in detail. (auth)

11557 (JINR-E-2457) A POSSIBLE TEST OF CPT INVARIANCE IN $\bar{p}$-p SCATTERING. Bilenky, S. M. (Joint Inst. for Nuclear Research, Dubna (USSR). Lab. of Theoretical Physics). 1965. 5p. Dep. mn.

A method is suggested to test the CPT-invariance in $\bar{p}$-p scattering. The method is essentially as follows: the antiproton (proton) polarization in scattering of unpolarized antiprotons by unpolarized protons is compared with the asymmetry in scattering of unpolarized antiproton beam by a polarized proton target (a polarized beam by an unpolarized target). (auth)

11558 (JINR-E-2496) ON A POSSIBILITY OF SPECIFIC INTERACTIONS OF MUONS AND ν_μ-NEUTRINOS AT SUPERHIGH ENERGIES. Markov, M. A. (Joint Inst. for Nuclear Research, Dubna (USSR). Lab. of Theoretical Physics). 1965. 4p. Dep. mn.

In the light of cosmic ray particle data and neutrino experiments a possibility is considered of specific interactions for muons and ν_μ essential only at $E \geq 10^{12}$ ev. (auth)

11559 (JINR-P-2445) LEPTONNYE RASPADY Ω^--GIPERONA V MODELI KVARKOV. (Leptonic Decay of the Ω^--Hyperon in the Quark Model). Tikhonin, F. F. (Joint Inst. for Nuclear Research, Dubna (USSR). Lab. of Theoretical Physics). 1965. 6p. Dep. mn.

The leptonic decay of a Ω^- hyperon is considered on the basis of the quark model. An expression for the decay width $\Omega^- \rightarrow \Xi^0 + e^- + \tilde{\nu}$ is obtained. (auth)

11560 (JINR-P-2449) OPREDELENIE OTNOSITEL'NOI VEROYATNOSTI RASPADA $K_2^0 \rightarrow \pi^\mp + e^\pm + \nu(\tilde{\nu})$. (A Determination of Relative Probability of $K_2^0 \rightarrow \pi^\mp + e^\pm + \nu(\tilde{\nu})$ Decay). Mestvirishvili, A. N.; Nyagu, D.; Petrov, N. I.; Rusakov, V. A.; Wu, Tsung-fan (Joint Inst. for Nuclear Research, Dubna (USSR). Lab. of Nuclear Problems. Joint Inst. for Nuclear Research, Dubna (USSR). Lab. of High Energy). 1965. 4p. Dep. mn.

The relative probability of the $K_2^0 \rightarrow \pi^\mp + e^\pm + \nu(\tilde{\nu})$ decay was determined by means of a cloud chamber in the magnetic field. Use was made of the identification of the decay electrons by the momentum loss which they suffer in passing through a lead plate 5.8 g/cm^2 thick which is placed in the middle of the fiducial volume of the chamber. (auth)

11561 (JINR-P-2450) EKSPERIMENTAL'NOE OPREDELENIE OTNOSITEL'NOI VEROYATNOSTI RASPADA $K_2^0 \rightarrow 3\ \pi^0$. (An Experimental Determination of Relative Probabilities of $K_2^0 \rightarrow 3\ \pi^0$ Decays). Mestvirishvili, A. N.; Nyagu, D.; Petrov, N; Rusakov, V.; Wu, Tsung-fan (Joint Inst. for Nuclear Research, Dubna (USSR). Lab. of High Energy. Joint Inst. for Nuclear Research, Dubna (USSR). Lab. of Nuclear Problems). 1965. 11p. Dep. mn.

On the basis of the identification of 29 Dalitz pairs among 7520 V^0 events from the decay of long-lived neutral K mesons recorded in the magnetic cloud chamber, the relative probability of $K^0 \rightarrow 3\pi^0$ decay was determined. It was found to be $W(K_2^0 \rightarrow 3\pi^0)/(K_2^0 \rightarrow \text{charged products}) = (31^{+7}_{-6})\%$. (auth)

11562 (JINR-P-2454) ANALIZ REAKTSII π N $\rightarrow$ $\pi_1\ \pi_2$ N' V OBLASTI ENERGII DO 1 Gev. (Analysis of Reactions π N $\rightarrow$ $\pi_1\ \pi_2$ N'). Zhukov, V. A.; Nemenov, L. L.; Yuang Rung-fang (Joint Inst. for Nuclear Research, Dubna (USSR). Lab. of Nuclear Problems). 1965. 14p. Dep. mn.

The cross sections for the $\pi N \rightarrow \pi + N^*_{\frac{3}{2}}$ processes are determined in the energy range 290-905 Mev. (auth)

11563 (JINR-P-2456) OB OPREDELENII SPINA I CHETNOSTI Ω^--GIPERONA. (On Determination of the Spin and Parity of the Ω^--Hyperon). Bilen'kii, S. M.; Ryndin, R. M. (Joint Inst. for Nuclear Research, Dubna (USSR). Lab. of Theoretical Physics). 1965. 10p. Dep. mn.

It is shown that the spin and parity of the Ω^--hyperon can be uniquely determined by studying the nonleptonic decays of Ω^--hyperons produced in the reaction $K + p \rightarrow \Omega^- + M_1$ (M_1 is a newly discovered boson with strangeness $s = 2$) on a polarized target. The consideration is based on invariance principles only. No assumptions are made on the dynamics. (auth)

11564 (JINR-P-2462) OBRAZOVANIE π-MEZONOV V (n-p)-STOLKNOVENIYAKH PRI ENERGII 600 Mev. (Pion Production in (n-p) Collisions at 600 Mev). Kazarinov, Yu. M.; Simonov, Yu, N. (Joint Inst. for Nuclear Research, Dubna (USSR). Lab. of Nuclear Problems). 1965. 18p. Dep. mn.

Angular distributions of charged pions and total production cross sections of neutral pions generated in n-p collisions at 600 ± 10 Mev were measured. It was found that $\sigma_{\pi^\pm}(\theta) = [(0.115 \pm 0.005) \mp (0.004 \pm 0.013)\cos\theta + (0.04 \pm 0.02)\cos^2\theta] \times (1.073 \pm 0.104) \times 10^{-27}$ cm^2/sterad, in the cms of the colliding nucleons. The total cross sections of the reactions are $\sigma(np \rightarrow \pi^0) = (4.6 \pm 0.6) \times 10^{-27}$ cm^2 and

$\sigma(np \rightarrow \pi^+) = \sigma(np \rightarrow \pi^-) = (1.68 \pm 0.17) \times 10^{-27}$ cm^2. The obtained data do not contradict the hypothesis of charge independence of nuclear forces. The cross sections for pion production in collisions of two nucleons in states with total isotopic spin T = 0 and T = 1 are equal to $(4.4 \pm 0.6) \times 10^{-27}$ and $(10.85 \pm 0.42) \times 10^{-27}$ cm^2, respectively. (auth)

11565 (JINR-P-2469) PROTON-ANTIPROTONNOE RASSEYANIE V SU(6)$_w$ SIMMETRII. (Proton-Antiproton Scattering in SU(6)$_w$ Symmetry). Dao Wong Duc (Joint Inst. for Nuclear Research, Dubna (USSR). Lab. of Theoretical Physics). 1965. 5p. Dep. mn.

The proton-antiproton scattering process in SU(6)$_w$ symmetry is considered. Simple relations for the differential cross sections (forward, backward) are found. They can be verified with experiment. (auth)

11566 (JINR-P-2472) VNUTRIYADERNYE KASKADY PRI SVERKHVYSOKIKH ENERGIYAKH. (Internuclear Cascades at Superhigh Energies). Artykov, I. Z.; Barachenkov, V. S.; Eliseev, S. M. (Joint Inst. for Nuclear Research, Dubna (USSR). Lab. of Theoretical Physics). 1965. 6p. Dep. mn.

It is shown that the generally accepted model of internuclear cascades considered as series of independent two-particle interactions for T $\gg$ 10 Bev is in a strong disagreement with experiment. The difference is mainly due to the contribution of a leading core particle. (auth)

11567 (LAL-1144) PROTON FORM FACTORS FROM PROTON OBSERVATION. Frerejacque, D.; Benaksas, D.; Drickey, D. (Laboratoire de l'Accelerateur Lineaire, Univ. de Paris, Orsay (France)). 1965. 25p. Dep. mn.

A determination of the electric and magnetic form factors of the proton was made by studying the elastic scattering of electrons from a polyethylene target by observation of the recoiling proton at 0 and 30° for values of q^2 between 1 and 1.8 fermi^{-2}. From these measurements, the charge radius and the magnetic radius of the proton were determined; the two radii are equal within the experimental errors. (D.C.W.)

11568 (UCRL-11749) CALCULATION OF THE CHARACTERISTICS OF THE ω^0 BY THE FADDEEV EQUATIONS. Ahmadzadeh, Akbar (Lawrence Radiation Lab., Univ. of California, Berkeley). Oct. 13, 1964. Contract W-7405-eng-48. 22p. Dep. mn. CFSTI $1.00 cy, $0.50 mn.

The Faddeev equations are applied to the calculation of resonances in a state of three mesons (π) with the quantum numbers of the ω^0 particle. Only the kinematics is made relativistic and the meson (π)-meson (π) scattering amplitude which appears in the kernel of the equations is approximated by the ρ contribution alone. Two resonances are found, one of which has a mass and a width reasonably close to those of the ω^0. The second resonance has an approximate mass of 1600 Mev. (auth)

11569 (UR-875-118) ALGEBRA OF CURRENTS AND THE MAGNETIC MOMENTS OF HYPERONS. Mathur, V. S.; Pandit, L. K. (Rochester Univ., N. Y. Dept. of Physics and Astronomy). Jan. 7, 1966. Contract AT(30-1)-875. 11p. Dep. mn. CFSTI $1.00 cy, $0.50 mn.

Using equal time commutations relations of the strangeness-changing axial-vector "charges" with the isoscalar and isovector electromagnetic current densities, the magnetic moments of Σ^+ and Λ and the Σ^0-Λ transition magnetic moment were calculated in terms of strange particle photoproduction amplitudes, which are evaluated using low lying baryon resonant states. The results agree very well with the experimental values available for Σ^+ and Λ magnetic moments. (auth)

11570 (ANL-Trans-258) USE OF BEAMS OF POLARIZED DEUTERONS AND DETERMINATION OF THE PARAMETERS OF AN OPTICAL MODEL. Raynal, Jacques (Commissariat a l'Energie Atomique, Saclay (France). Centre d'Etudes Nucleaires). Translated for Argonne National Lab., Ill., from report CEA-R-2511. 1965. 115p. Dep. mn; JCL $9.60 fs, $3.65 mf.

A descriptive formalism of a generalized polarized beam is presented. Any reaction whatsoever is described in terms of a collision matrix written in helical formalism. The optical model is discussed for particles of spin 1. The discussion includes possible potential forms, separation into partial waves, resolution of partial wave equations, diffusion amplitudes, and approximate calculations. A Watanabe calculation of the effective potential for deuterons is presented. Also generalization of the calculation of form factors are discussed. Optical model calculations were made with simple form factors, central potentials and free $\overline{LS}$ coupling, and a nucleon-nucleus potential. (M.O.W.)

11571 STUDIES OF THE BACKGROUND OF PROTONS IN EXPERIMENTS WITH NEUTRINOS. Aguilar, J.; Aguilar, R. (Facultad de Ciencias, Madrid). An. Real Soc. Espan. Fis. Quim. (Madrid), Ser. A, 61: 135-9(May-June 1965). (In Spanish).

The background of protons produced by leakage neutrons was studied by means of the bubble chamber technique applied to the neutrino interactions. 141 small low-energy stars involving only one or more protons were found, all of which have visible energy smaller than 250 Mev. The energy distribution was very different from that of the presumed neutrino events. (auth)

11572 ONE-PARTICLE EXCHANGE THEORY OF PION PHOTOPRODUCTION. I. GENERAL CALCULATION. Harun-ar-Rashid, A. M. (Technische Hochschule, Karlsruhe, Ger.); Moravcsik, Michael J. Ann. Phys., 35: 331-50(Dec. 1965). (UCRL-12110-T).

A calculation of single pion photoproduction from single nucleons was made using one-particle exchange model involving the exchange of one pion, one ρ, one ω, one ϕ, one nucleon, one N*, and one N**. Cross diagrams were also included in the calculation. An imaginary part of the amplitudes was included using a Breit-Wigner-type formula and experimentally observed widths. (auth)

11573 ABSORPTIVE CORRECTIONS TO THE NUCLEON EXCHANGE TERM IN ELASTIC πN SCATTERING. Smrz, Pavel; von Baeyer, Hans C. (McGill Univ., Montreal). Can. J. Phys., 44: 105-8(Jan. 1966).

The absorption model of Gottfried and Jackson is justified in the case of backward elastic scattering. The model is then applied to the nucleon exchange term in π^+p scattering at 4 and 8 Bev. It is found that the data can be fitted only if a phenomenological form factor is introduced. (auth)

11574 A SCALAR PION-NUCLEON INTERACTION. Coombes, Charles A. (Univ. of Alberta, Calgary, Can.). Can. J. Phys., 44: 285-6(Jan. 1966).

It is suggested that the pion-nucleon cross section for scattering at low energy and the branching ratio of the processes $\pi^- + p \rightarrow n + \pi^0$ and $\pi^- + p \rightarrow n + \gamma$ might be explained if pions behave both as scalars and as pseudoscalars with respect to nucleons. It is also shown qualitatively that this possibility is not prohibited by some other observations. (AECL)

11575 PRINCIPAL RESULTS FURNISHED BY ANTIPROTON-PROTON ANNIHILATIONS AT REST OR AT LOW ENERGY. Leprince-Ringuet, Louis (College de France, Paris. Univ. of Liverpool. CERN, Geneva). Compt. Rend., 261: 3509-11(Nov. 3 1965). (In French).

The principal results relative to resonances observed in antiproton-proton annihilations either at rest or at low energy when these annihilations take place with the emission of two heavy mesons, K and $\overline{K}$, and a variable number of π mesons are summarized. The annihilations were observed with a liquid hydrogen bubble chamber placed in almost pure beams of antiprotons having a maximum momentum of the order of 1 Bev/c. The experiments showed the existence of three new resonances. (J.S.R.)

11576 THE SELF-CONSISTENCY CONDITION AND THE πNN-VERTEX FUNCTION. Petras, M.; Noga, M. (Komensky Univ., Bratislava). Czech. J. Phys., 16: 54-6 (1966).

It is shown that the πNN-vertex function, which is calculated within the framework of the self-consistency theory,

has the usual analytic properties prescribed by unitarity. (L.B.S.)

11577 DISCRIMINATION OF THE NONPOLARIZED STATE IN LEPTON RADIATION PRODUCED BY NEUTRINO INTERACTIONS WITH MATTER. Shishkin, G. V. (Inst. of Heat and Mass Transfer, Academy of Sciences, Belorussian SSR). Dokl. Akad. Nauk Belorussk. SSR, 9: 443-5(July 1965). (In Russian).

Previous studies on the effects of neutrino interactions are extended to the problem of isolating out the nonpolarized state arising from neutrino processes of the $\nu + N \rightarrow B + L$ type, where ν designates a neutrino or antineutrino, N the target nucleon, B the product baryon, and L a lepton. By using the method based on the Dirac-particle theory, an expression is obtained for determining the degree of polarization of the leptons in the above process for the (V,A) variant of the weak four-fermion interaction, deriving also an equation for the transverse polarization of the leptons in the neutrino + lepton momentum plane. Equations are also obtained for the case of a nonpolarized state in the lepton beam. It is concluded that the leptons are completely polarized only when the spins of the target nucleons and of the neutrinos in the lepton beam are completely polarized; in other cases, a nonpolarized state also exists. (TTT)

11578 ANGULAR ASYMMETRY OF μ DECAY AND NEUTRAL WEAK CURRENT ($\nu_e \nu_\mu$). Shishkin, G. V. (Inst. of Heat and Mass Transfer, Academy of Sciences, Belorussian SSR). Dokl. Akad. Nauk Belorussk. SSR, 9: 514-15(Aug. 1965). (In Russian).

The possibility that a weak neutral current may exist as a result of the angular asymmetry of electrons and positrons emitted during muon decay is considered. The decay $\mu^\mp \rightarrow e^\mp + \nu + \nu$ may be described by deriving the hamiltonian of the interaction either on the basis of lepton currents ($e\mu$) and ($\nu\nu$) or of charged particle currents (νe) and ($\nu\mu$), as was done by Lee and Yang and by Feynmann and Gell-Mann, respectively. The calculations carried out indicate that, by making certain assumptions, Lee and Yang's hamiltonian allows asymmetry coefficients identical with the experimentally derived value to be obtained. Thus, the experimental μ-decay data may be considered as an argument in favor of Lee and Yang's hamiltonian and of the existence of a weak neutral current ($\nu_e \nu_\mu$). (TTT)

11579 STRUCTURE OF THE NUCLEONS. Latal, H.; Urban, P.; Zingl, H. (Univ., Graz). Fortschr. Phys., 13: 481-98(1965).

Some of the recent developments in the theory of the structure of nucleons are surveyed including discussions on experimental verifications of theoretical treatments. (auth)

11580 EXPERIMENTS WITH HIGH ENERGY NEUTRINOS. Plass, G. (Univ. of Berlin. CERN, Geneva). Ind. At., 9: 39-53(1965). (In French).

Observing the interaction of high energy neutrinos is considered among the most important of the experiments which have been conducted with large proton accelerators. After an introduction to the problem, the techniques employed for the formation of a beam of neutrinos are described, as well as the detectors used in the experiments, and the principal results obtained. In conclusion, a few projects now being planned are indicated. (auth)

11581 PHOTOPRODUCTION OF MESONS ON NUCLEONS AND SU(6) SYMMETRY. Rekalo, M. P. JETP Lett. (USSR)(Engl. Transl.), 2: 203-5(Oct. 1, 1965).

The consequences of SU(6) symmetry for the processes of meson photo-production on nucleons were studied under the assumption that the use of SU(6) symmetry is justified in the case of meson production in the s-state. (D.C.W.)

11582 POSSIBLE VERIFICATION OF NONCONSERVATION OF TIME PARITY IN COLLIDING BEAM EXPERIMENTS. Baier, V. N. (Novosibirsk State Univ., USSR). JETP Lett. (USSR)(Engl. Transl.), 2: 209-11(Oct, 1, 1965).

Some colliding-beam experiments are discussed by which the nonconservation of time-parity could possibly be verified. The most realistic experiment would be an investigation of the asymmetries of the products of interactions of the type $e^+ + e^- \rightarrow \pi^+ + \pi^- + \gamma$ and $e^+ + e^- \rightarrow K^+ + K^- + \gamma$. (D.C.W.)

11583 CONTRIBUTION TO THE THEORY OF WEAK INTERACTION. Vanyashin, V. S. (Dnepropetrovsk State Univ., USSR). JETP Lett. (USSR)(Engl. Transl.), 2: 211-13(Oct. 1, 1965).

The baryon-lepton weak interaction is analyzed on the basis of the hypothesis that there exists an intermediate boson possessing baryon and lepton charges. (D.C.W.)

11584 CHARGE ASYMMETRY IN RADIATIVE DECAYS OF K AND ρ MESONS UPON VIOLATION OF CP INVARIANCE. Solov'ev, V. V.; Terent'ev, M. V. JETP Lett. (USSR) (Engl. Transl.), 2: 213-16(Oct. 1, 1965).

It is shown that no large charge asymmetry will arise under any violation of CP invariance in decays of the type meson $\rightarrow \pi^+ + \pi^- + \gamma$ if a decay to $\pi^+\pi^-$ without emission of a photon is allowed. (D.C.W.)

11585 ON THE MASSES OF PARTICLES (RESONANCES) WITH STRANGENESS S = −4 AND S = +1. Zel'dovich, Ya. B. JETP Lett. (USSR) (Engl. Transl.), 2: 216-18(Oct. 1, 1965).

A supermultiplet containing states with strangeness from S = −4(Y = −3) up to S = +1(Y = +2) was studied in the context of the quark model. The variation of the particle mass with strangeness or hypercharge was considered, with particular emphasis on the masses of the S = +1 and S = −4 members. (D.C.W.)

11586 EFFECT OF MASS SPLITTING WITHIN THE BARYON OCTET ON BB SCATTERING. Zakharov, V. I.; Tyutin, I. V. JETP Lett. (USSR) (Engl. Transl.), 2: 240-2(Oct. 15, 1965).

It was previously noted that the differences in the masses of the pseudoscalar mesons can strongly violate the unitary-symmetry character of the baryon-baryon interaction. It is shown that even if such symmetry breaking is foregone, an account of the baryon mass difference can qualitatively change the scattering picture. The two-channel Λp scattering process with zero spin is treated as an example. (G.O.Y.)

11587 SEARCH FOR $\pi^0 \rightarrow 3\gamma$ DECAY. Kut'in, V. M.; Petrukhin, V. I.; Prokoshkin, Yu. D. (Joint Inst. for Nuclear Research, Dubna, USSR). JETP Lett. (USSR) (Engl. Transl.), 2: 243-5(Oct. 15, 1965).

The photons from the decay of the meson (π^0) in the interaction $\pi^- + p \rightarrow \pi^0 + \eta$ were detected using three Cherenkov spectrometers arranged in a plane perpendicular to the meson (π^-) beam. The upper limit of the branching ratio ($\pi^0 \rightarrow 3\gamma/\pi^0 \rightarrow 2\gamma$) was found to be $<5 \times 10^{-6}$ at the 90% confidence level. (D.C.W.)

11588 THE LEPTON DECAY OF THE Λ^0 HYPERON BY A MODIFIED VECTOR BOSON PROPAGATOR. Huszar, Miklos. Magyar Tud. Akad. Kozp. Fiz. Kut. Int. Kozlemen., 13: 213-20(1965). (In Hungarian).

In recent studies of weak interactions it has been pointed out that $[1/(2\pi)^4i][9mn - (k_m k_n/m_w^2)](1/m_w^{-2} - k^2)$ vector boson propagator, where m_w designates the mass of the boson, may be used to renormalize the theory of weak interactions. By means of this propagator, the energy spectrum and the average lifetime of electrons in the $\Lambda^0 \rightarrow p + e^- + \gamma^-$ decay was calculated. The results indicated a good agreement with Fermi's theory. Quantitative determinations were carried out for cases in which the spectrum derived from this propagator could deviate from the predictions of Fermi's theory. The cases examined included the Λ decay, the μ-meson decay and the neutron decay. For μ mesons, the spectrum reflects closely the Fermi theory; however, in the case of neutron decay marked deviations from that theory may be expected at the lower portion of the electron spectrum and in the energy dependence of the longitudinal polarization of electrons. (TTT)

11589 LOW ENERGY ASSOCIATED PRODUCTION: $\pi^- + p \rightarrow K^0 + \Lambda$. Hoffman, Herbert S.; Schnitzer, How-

ard J. (Brandeis Univ., Waltham, Mass.). Nucl. Phys., 76: 481-90(1966).

The process $\pi^- + p \rightarrow K^0 + \Lambda$ is studied near threshold by means of a resonance model based on the Cini-Fubini approximation using only known resonances. Thus the only term contributing an imaginary part to the amplitude is the $N^*(1688)T = \frac{1}{2}$, F^+ resonance. Reasonable agreement with the total cross section and angular distribution data is obtained, but the predictions for the polarization are not satisfactory. It is concluded that either several small, complex amplitudes make important contributions to the polarization, or that there are other large partial waves in addition to the $F_{\frac{5}{2}}$ resonance. It may be difficult to distinguish between these two possibilities within the framework of this or other conventional resonance models. (auth)

11590 THE PROCESS $\pi^- + p \rightarrow \tilde{p} + d$ AND REGGE POLES. Hsien, T. C.; Mihul, El. C. (Joint Inst. for Nuclear Research, Dubna, USSR). Nucl. Phys., 76: 491-504(1966).

The process $\pi^- + p \rightarrow \tilde{p} + d$ is considered for which the possible intermediate states are fermionic. Using partial helicity amplitudes the analytical continuation of the partial wave amplitudes into the complex plane of the orbital angular momentum J is studied. Regge-poles are defined and expressions for the helicity amplitudes in the crossing-channel are given. The behavior of the differential cross section was obtained as a function of the two kinematical invariants s and t that define the process. (auth)

11591 POLARIZATION IN ELASTIC p-p SCATTERING AT HIGH ENERGIES. Kanavets, V. P.; Levintov, I. I.; Morosov, B. V. (Inst. for Theoretical and Experimental Physics, Moscow). Nucl. Phys., 76: 505-12(1966).

Measurements on polarization of protons with energies of 4.9 Bev and 8.5 Bev and $|t| \approx 0.3$ Bev^2 showed that the value of polarization considerably decreases with the increase of proton energy. The analysis of experimental data shows that of the two possible reasons for this effect, (1) decrease of the absolute value of spin flip amplitude and (2) decrease of the difference between the phase shifts of the amplitudes with and without spin flip, the second reason is more probable. Using the general internucleon potential an approximate formula for p-p scattering polarization at high energies is obtained. (auth)

11592 A POSSIBLE NEW OCTET. Clegg, A. B. (Nuclear Physics Lab., Oxford). Nucl. Phys., 76: 545-50 (1966).

Attention is drawn to evidence for strong interactions in elementary particle states with $J^\pi = \frac{1}{2}^+$, Y = 0 and respectively I = 0 and I = 1. These strong interactions are similar to that in the $J^\pi = \frac{1}{2}^+$, Y = 1, I = $\frac{1}{2}$ state, which is seen in the $\pi^- p \rightarrow n\pi^+\pi^-$ reaction, and are seen in the $K^- p \rightarrow \Lambda^0\pi^+\pi^-$ and $K^- p \rightarrow \Sigma^0\pi^+\pi^-$ reactions, respectively. These strong interactions are possibly members of a new octet of which the Y = −1, I = $\frac{1}{2}$ member would then remain to be found. A possible candidate for the missing Y = 0, I = 1 member of a $J^\pi = \frac{3}{2}^-$ octet is also noted. (auth)

11593 A GENERALIZATION OF QUANTUM ELECTRODYNAMICS WITH AN APPLICATION TO THE ELECTRON-PROTON SCATTERING. Hellman, O. (Univ. of Turku, Finland). Nucl. Phys., 76: 556-76(1966).

An attempt to extend the validity of quantum electrodynamics to small distances is continued. The generalized equations of quantum electrodynamics previously suggested appear here in a modified form. The theory now satisfies also the following requirements: (a) the S-matrix expansion must have all the gauge transformation properties of quantum electrodynamics, (b) the free field equations, must define the future history of the free field, (c) the masses of the theory must be real, (d) since the theory will have a fermion mass spectrum and a boson mass spectrum, it must be impossible that a fermion would decay into lower fermions and vector particles and (e) the self-energy of the photon must be zero. The generalized Dirac equation which satisfies the above conditions is expressed in terms of a spectral function whose explicit form remains to be determined. It is shown, however, that this function could be chosen so as to reproduce any given fermion mass spectrum. As an illustration a spectral function is given such that the stable fermions of the theory would be the neutrino, the electron and the proton. The differential cross section for the scattering of electrons from protons is derived from the theory. The Dirac and Pauli form factors obtained, when the elementary length of the theory is given the value $l_0 = 0.38$ fm, show the same trend as experimental form factors. An exact agreement could not be expected, however, since the theory does not contain the zero-spin particles. The Fourier transform of the Dirac form factor is of exponential nature as was concluded from experiments by Chambers and Hofstadter. The theory embodies the electron and the proton with both positive and negative masses and two different neutrinos. This is, partly, a consequence from the Lagrangian principle, and leads to the vanishing of the self-energy of the photon. The theory allows, however, no particles with negative masses as products in processes involving particles with positive masses. The generalized Maxwell equation is obtained with a modification due to the requirement (b) above. There are indications that a generalization of the kind discussed in this paper would imply a quantization of time. (auth)

11594 ANALYSIS OF LIGHT Λ HYPERFRAGMENTS ON THE SEPARABLE POTENTIAL MODEL. II. Bhamathi, G.; Seshadri, Indumathi (Univ. of Colorado, Boulder). Nucl. Phys., 76: 625-37(1966).

The hyperfragments ${}_\Lambda H^3$ and ${}_\Lambda H^4$ are analyzed on the separable potential model. The interaction strength parameters in the singlet and triplet states of Λ-N interaction ($\lambda^s_{\Lambda N}$ and $\lambda^t_{\Lambda N}$) are obtained from the binding energy data of ${}_\Lambda H^3$ and ${}_\Lambda H^4$, respectively. It is found that $\lambda^t_{\Lambda N}$ is less than $\lambda^{max}_{\Lambda N}$ only on the assumption of a Λ + d + N structure for the ${}_\Lambda H^4$ system. The total cross sections for Λ-N scattering calculated from these parameters $\lambda^s_{\Lambda N}$ and $\lambda^t_{\Lambda N}$ are in reasonable agreement with the available experimental data. (auth)

11595 PHOTOPRODUCTION OF VECTOR MESONS. Achuthan, P.; Srinivasan, S. K. (Indian Inst. of Tech., Madras). Nucl. Phys., 76: 638-56(1966).

The amplitude for photoproduction of vector mesons is studied using the approach of dispersion theory. The contribution to the amplitude from the nearest singularities is estimated and numerical results for total and angular distributions of the ω meson are discussed. (auth)

11596 ANALYTIC PROPERTIES OF TRIANGLE GRAPHS WITH DECAY MASSES AND THREE-PARTICLE PRODUCTION. Anisovich, V. V.; Dakhno, L. G. (Ioffe Physical Technical Inst., Leningrad). Nucl. Phys., 76: 657-64(1966).

The analytical properties of triangle graphs are considered and the amplitude of the $\pi + N \rightarrow N + \pi + \pi$ process is given for the case when the logarithmic singularity originating from such graphs comes close to the physical region of this reaction. (auth)

11597 HEAVY MESONS AND NUCLEON-NUCLEON POTENTIALS. Babikov, V. V. (Joint Inst. for Nuclear Research, Dubna, USSR). Nucl. Phys., 76: 665-71(1966).

Local, velocity-dependent nucleon-nucleon potentials are obtained for the exchange of pseudovector ($J^\pi = 1^+$), tensor ($J^\pi = 2^+$) and pseudotensor ($J^\pi = 2^-$) heavy mesons. The recoil effects are taken into account exactly. The relativistic corrections leading to the velocity dependence of the potentials are calculated in the p^2/m^2 approximation, used by Wong for the exchange of scalar, pseudoscalar and vector mesons. (auth)

11598 THE φ MESON AND LOW-ENERGY INTERACTIONS OF ELEMENTARY PARTICLES. Soloviev, L. D.; Shchelkachev, A. V. (Joint Inst. for Nuclear Research, Dubna, USSR). Nucl. Phys., 76: 684-90(1966).

The simple resonance model for nucleon form factors is considered. The ρ, ω, and φ mesons with experimental

masses are taken into account and all other contributions are approximated by constants. For the isovector form factors this model is applicable for $|q^2|$ not far from m_ρ^2, i.e. for $|q^2| \leq 20$ fm^{-2}. It is shown that the model agrees quite well with experiment in this region. The kaon form factors are also considered and the φ-meson-nucleon coupling constant is estimated. (auth)

11599 THE ABSORPTION OF K^- MESONS IN DEUTERIUM. Fowler, G. N.; Poulopoulos, P. N. (Univ. of Newcastle upon Tyne, Eng.). Nucl. Phys., 77: 689-95 (1966).

The two-nucleon capture rate of K^- mesons in deuterium is evaluated using the impulse approximation and taking account of Y* production. The results are compared in detail with previous calculations which neglect the Y* processes considered here. (auth)

11600 CONTRIBUTIONS OF PION PAIRS AND UNSTABLE INTERMEDIATE STATES TO γ-γ SCATTERING. De Tollis, B. (Univ., Rome); Violini, G. Nuovo Cimento (10), 41A: 12-21(1966).

The contribution to photon-photon scattering, graphically represented by lowest-order perturbation diagrams containing charged pions in the closed loops, is evaluated. This contribution is found to be not important compared with the one of diagrams with internal electron lines. Moreover the possible effects arising from the presence in the intermediate states of an unstable system (such as π^0, η, positronium) are briefly discussed. (auth)

11601 S-WAVE KAON-PION SCATTERING. Huq, M. (Univ. of Durham, Eng.). Nuovo Cimento (10), 41A: 48-66(1966).

The inverse amplitude method is used to find iterative self-consistent solutions for S-wave kaon-pion scattering. The experimental values for the K* resonance and the ρ-meson are used in addition to the one-pole approximation for the I = 0, T = 0 pion-pion amplitude, given by Hamilton, representing the ABC anomaly. Crossing symmetry for the real part of the scattering amplitude and a sum rule for $A^{(-)}(s,u,t)$ enable the results to be expressed in terms of only one parameter, $a_0^{(+)}$. Numerical results are given for negative values of this parameter. (auth)

11602 THE INTERACTION OF 16.3 Gev π^--MESONS WITH COMPLEX NUCLEI. Finney, P. J.; Major, J. V. (Univ. of Durham, Eng.) Nuovo Cimento (10), 41A: 77-89(1966).

The interactions of 16.3-Bev negative pions with emulsion nuclei were examined to test the Castagnoli and Duller-Walker formulas for the determination of the energy of a primary particle from the angular distribution of the secondary particles. It is found that these formulas may be applied with confidence to collisions in which the produced mesons do not interact within the nucleus. (auth)

11603 DECAYS $\pi^0 \rightarrow 2\gamma$ AND $\eta \rightarrow 2\gamma$. Faier, H. (Northwestern Univ., Evanston, Ill.). Nuovo Cimento (10), 41A: 127-31(1966).

The rates for $\pi^0 \rightarrow 2\gamma$ and $\eta \rightarrow 2\gamma$ are calculated using the vector-meson dominant model and the ω-φ mixing hypothesis. It is shown that these rates have no dependence on the mixing ratio and are functions of one fundamental constant which also determines the rate of $\eta \rightarrow \pi^+\pi^-\gamma$. For $\Gamma_{\pi^0} = 6.3$ ev the η rates are $\Gamma_\eta(2\gamma) = 38$ ev and $\Gamma_\eta(\pi\pi\gamma) = 9$ ev. (auth)

11604 A STUDY OF THE J = I = 0 $\pi\pi \rightarrow N\bar{N}$ AMPLITUDE AND ITS EFFECT ON πN SCATTERING. Der-Sarkissian, M. (Univ. of Alberta, Can.). Nuovo Cimento (10), 41A: 132-41(1966). (UCRL-14256-T).

It is assumed the main contribution from the J = I = 0 $\pi\pi \rightarrow N\bar{N}$ amplitude to πN scattering comes from the Abashian-Boothe-Crowe (ABC) anomaly. The ABC anomaly is treated as a just barely bound s-wave combination of 2 pions and the coupling of this particle to the $N\bar{N}$ system is studied in the following way: let γ_π denote the coupling ABC $\rightarrow \pi\pi$ and γ_A the coupling ABC $\rightarrow N\bar{N}$. The quantity $\gamma_\pi\gamma_A$ is expressed in terms of the J = I = 0 $\pi\pi \rightarrow \pi\pi$ amplitude and a potential which is calculated in terms of the analytic structure of the πN amplitudes. The result of this analysis suggests that ABC exchange produces an attractive force of about the same strength for all p-states of the πN system. (auth)

11605 EXCHANGE MECHANISM FOR $\pi^+p \rightarrow N^{*++}\rho^0$ REACTION AT 2.75 Gev/c. Armenise, N. (Univ., Bari, Italy); Ghidini, B.; Picciarelli, V.; Romano, A.; Kayas, G.; Laberrigue-Frolow, J.; Tridon, J.; Vigneron, L.; Yiou, T. P. Nuovo Cimento (10), 41A: 159-66(1966).

The reaction $\pi^+p \rightarrow p\pi^+\pi^+\pi^-$ is studied, particularly the channel $\pi^+p \rightarrow N^{*++} + \rho^0$. Experimental decay angular distributions of N^{*++} and ρ^0 resonances indicate that the production is dominated by the OPE model. Nevertheless the experimental cross section is not in agreement with the theoretical predictions, even if absorption effects are taken into account. (auth)

11606 ELASTIC n-p CHARGE-EXCHANGE SCATTERING AT 8 Gev/c. Manning, G. (Atomic Energy Research Establishment, Harwell, Eng.); Parham, A. G.; Jafar, J. D.; van der Raay, H. B.; Reading, D. H.; Ryan, D. G.; Jones, B. D.; Malos, J.; Lipman, N. H. Nuovo Cimento (10), 41A: 167-88(1966).

The differential cross section for elastic charge-exchange scattering of neutrons on protons was measured at 8 Bev/c over forward laboratory scattering angles 0 to 90 mrad [square of four-momentum transfer $0 < -t < 0.05$ (Bev/c)^2]. The method utilized acoustic spark chambers, and about 1900 elastic-scattering events were analyzed. A value of $(d\sigma/d\Omega)_{lab} = (20 \pm 6)$ mb/sr [$d\sigma/dt = (0.93 \pm 0.28)$ mb/(Bev/c)^2] was obtained for the forward differential cross section, and an estimated (0.06 ± 0.03) mb for the elastic charge exchange cross section. Both cross sections show the decreased values expected from Pomeranchuk's second theorem when compared with results at lower energies. Further comparison shows that the narrow forward peak in the distribution of $d\sigma/dt$ previously observed for $-t < 0.05$ is still present at 8 Bev/c, varying in shape only slowly, if at all, with energy. For $-t > 0.1$ however, energy dependence is apparent. The results also suggest that the interaction is spin-dependent and/or that the real parts of the scattering amplitudes in the isospin states 0 and 1 are different. Comparisons with the theoretical predictions show good agreement with the value of forward cross section given by the Regge pole approach of Ahmadzadeh. The model of Ringland and Phillips for single-pion exchange with absorption agrees with the results for $-t < 0.01$, but a predicted secondary peak at $-t \sim 0.08$ is not observed. (auth)

11607 AN EXACT CALCULATION OF THE BREAK-UP OF DEUTERONS BY NEUTRONS. Phillips, A. C. (Univ. of Sussex, Eng.). Phys. Lett., 20: 50-2(Jan. 15, 1966).

The breakup of deuterons is considered using the Faddeev equations and an approximation scheme which involves the use of nonlocal separable potentials. The theoretical results for the energy spectra of the final particles are in reasonable agreement with the experimental data. (auth)

11608 DIRECT TESTS OF CP INVARIANCE. Roos, M. (CERN, Geneva). Phys. Lett., 20: 59-62(Jan. 15, 1966).

The $\pi^+\pi^-$ decay mode of the meson (K^0) is considered. Four predictions are made on the basis of which a distinction can be made between CP-invariant theories and CP-violating linear theories. (D.C.W.)

11609 ON THE NUMBER OF CASIMIR OPERATORS ASSOCIATED WITH ANY LIE GROUP. Beltrametti, E. G.; Blasi, A. (Univ., Genoa). Phys. Lett., 20: 62-4 (Jan. 15, 1966).

A formula which gives the number of Casimir operators associated with any Lie algebra is proved. For simple groups it is explicitly shown how the formula gives back the known result (the rank of the group). The connection with semi-simple groups is also discussed. (G.O.Y.)

11610 ALGEBRA OF CURRENTS AND A GENERALIZED ADEMOLLO-GATTO THEOREM. Guralnik, G. S.;

Mathur, V. S.; Pandit, L. K. (Univ. of Rochester, N. Y.). Phys. Lett., 20: 64-7(Jan. 15, 1966). (UR-875-114).

Within the framework of the $\overline{W}_3$ symmetry, it is shown that the conservation of axial-vector current implies no renormalization, and that if the symmetry is broken in any arbitrary manner, the renormalization effects on both vector and axial-vector currents are of second order in the symmetry-breaking parameter. The results are generalized to any symmetry group for which the generators are conserved (vector or axial-vector) "charges." (auth)

11611 NON-DYNAMICAL SPIN AND PARITY DETERMINATIONS. Csonka, P. L.; Moravcsik, M. J.; Scadron, M. D. (Univ. of California, Livermore). Phys. Lett., 20: 67-70(Jan. 15, 1966).

A general prescription, supplemented by a table of examples, is given of nondynamical methods for determining the spin and/or parity of a particle participating in an interaction. (G.O.Y.)

11612 SUM RULES FOR THE WEAK AXIAL-VECTOR COUPLING CONSTANTS. Chan, C. H. (Univ. of California, San Diego, La Jolla). Phys. Lett., 20: 70-2(Jan. 15, 1966).

Sum rules for the weak axial-vector coupling constants are obtained on the basis of the assumption of the axial-vector current algebra suggested by Gell-Mann and the hypothesis of a partially conserved $\Delta Y = 0$ axial-vector current. (auth)

11613 NOTE ON MASS SHELL CORRECTIONS IN CURRENT ALGEBRA CALCULATIONS. Renner, B. (Cambridge Univ., Eng.). Phys. Lett., 20: 72-4(Jan. 15, 1966).

The Adler-Weisberger relation for the ratio of the axial-vector and the vector coupling constant is rederived. Information from the K-π system about the Cabibbo angle is also discussed, together with extensions of the SU(3) algebra. The value of the pole approximation in avoiding off-the-mass-shell amplitudes is stressed. (D.C.W.)

11614 A SECONDARY PEAK AT $t = -1$ (GEV/c)^2 IN HIGH ENERGY π^-p CHARGE EXCHANGE SCATTERING. Sonderegger, P.; Kirz, J.; Guisan, O.; (and others) (CEN, Saclay, France). Phys. Lett., 20: 75-8(Jan. 15, 1966).

The second peak in the interaction $\pi^- + p \rightarrow \pi^0 + n$ was investigated at six momenta between 3 and 18 Bev/c. The differential cross section was obtained at each momentum, together with the total cross sections over the forward peak and the second peak as functions of pion momentum in the laboratory system. (D.C.W.)

11615 ANALYSIS OF πN CHARGE EXCHANGE SCATTERING FROM 4 TO 18 Gev/c. Hoehler, G. (Technische Hochschule, Karlsruhe, Ger.); Baacke, J.; Schlaile, H.; Sonderegger, P. Phys. Lett., 20: 79-82(Jan. 15, 1966).

It is shown that the π^-p charge exchange data above 4 Bev/c and for momentum transfers up to $t = 2$ (Bev/c)^2 are in good agreement with the Regge pole model, assuming that the interaction is dominated by the ρ-exchange in the t-channel. (G.O.Y.)

11616 RARE DECAY MODES OF ρ, A_1 AND A_2 MESONS. Deutschmann, M. (Technische Hochschule, Aachen); Steinberg, R.; Weber, H.; (and others). Phys. Lett., 20: 82-5(Jan. 15, 1966).

The possible decay modes of the meson (ρ) into 4π and $\pi\eta$ and of the mesons (A_1) and (A_2) into 3π, $\pi\eta$, πX^0 and $K\overline{K}$ were investigated in a study of the interactions produced by 8-Bev/c mesons (π^-) in a hydrogen bubble chamber. The c-violating $\pi\eta$ decay mode of the meson (ρ) was not observed. For the mesons (A_1) and (A_2), it was found that the $\pi\rho$ decay mode is clearly the dominant mode. The modes $\pi\eta$ of A_1 and A_2 and $K\overline{K}$ of A_2 occur in a few percent of the cases at most; there is no serious violation of the conservation of the Bronzan-Low quantum number. (D.C.W.)

11617 RE-NORMALIZATION OF POLARIZATION IN n-p SCATTERING AT MEDIUM ENERGIES. Rose, B. (Atomic Energy Research Establishment, Harwell, Eng.). Phys. Lett., 20: 86-8(Jan. 15, 1966).

Published data on polarization in n-p scattering at medium energies are reconsidered, and certain renormalizing factors and normalization errors are proposed. (D.C.W.)

11618 AN UPPER LIMIT FOR THE PARTIAL WIDTH $\Gamma(\rho \rightarrow \pi\gamma)$. Huson, F. R.; Allard, J. F.; Drijard, D.; Hennessy, J.; Lloret, A.; Six, J.; Veillet, J. J. (Faculte des Sciences, Orsay, France. Ecole Polytechnique, Paris). Phys. Lett., 20: 91-3(Jan. 15, 1966).

The electromagnetic production of the meson (ρ) was studied using the reaction $\pi^- + Pb \rightarrow \pi^- + \pi^0 + Pb$ at 15 Bev/c. An upper limit for the partial width $\Gamma(\rho \rightarrow \pi\gamma)$ was obtained on the basis of the results. (D.C.W.)

11619 EXPERIMENTAL BRANCHING RATIOS FOR φ DECAY. Lindsey, J. S.; Smith, G. A. (Univ. of California, Berkeley). Phys. Lett., 20: 93-6(Jan. 15, 1966). (UCRL-16527).

Analysis of 100,000 K^-p interactions in a 72-in. bubble chamber yielded branching ratios for φ decay, particularly for the rarer modes ($\rho\pi, \eta\gamma$) for which little data are available. Partial decay rates were compared with predictions of the Sakurai-Glashow "$\varphi\omega$" mixing theory and were used to determine the φ spin. (auth)

11620 THREE-QUANTUM ANNIHILATION OF POSITRONS IN IONIC CRYSTALS. Bisi, A.; Bussolati, C.; Cova, S.; Zappa, L. (CNR, Milan). Phys. Rev., 141: 348-51(Jan. 1966).

The three-quantum decay of positrons annihilating in lithium hydride, alkali halides, and alkaline-earth oxides was investigated using a triple-coincidence method. Relative measurements were made by comparing the three-quantum yield in each substance with that in aluminum, taken as a standard. In some cases the three-quantum yield was measured as a function of temperature and employing multicrystalline specimens or single crystals with and without color centers. The results suggest that the essential features of positron decay in alkali halides are connected with the properties of ideal crystals, while this is not true in alkaline earth oxides. (auth)

11621 POSITRON DECAY IN HALOGEN COMPOUNDS. Germagnoli, E.; Poletti, G.; Randone, G. (Laboratori Centro Informazioni Studi Esperienze, Milan). Phys. Rev., 141: 419-22(Jan. 1966).

The decay of positrons was investigated in the halogen derivatives of benzene, both at room temperature and at −100°C, and in a number of halogen compounds. A lifetime of the order of 4×10^{-10} sec is found in all the investigated compounds but fluorobenzene, and suggests the presence of a positron-halogen bound state; a search for the excited levels of such a bound state, whose decay features were predicted by Goldansky and co-workers, was inconclusive. (auth)

11622 DETERMINATION OF THE NUCLEON-NUCLEON ELASTIC-SCATTERING MATRIX. IV. COMPARISON OF ENERGY-DEPENDENT AND ENERGY-INDEPENDENT PHASE-SHIFT ANALYSES. Arndt, Richard A.; MacGregor, Malcolm H. (Univ. of California, Livermore). Phys. Rev., 141: 873-88(Jan. 1966). (UCRL-14252-T).

(p,p) and (n,p) scattering data in six energy bands centered at 25, 50, 95, 142, 210, and 330 Mev, were analyzed. First an energy-dependent analysis was carried out. Then phase-shift energy derivatives were extracted from this analysis and used in carrying out accurate energy-independent analyses. The energy-dependent phase-shift forms were chosen to have a singularity structure consistent with the requirements of partial-wave dispersion equations. A very rapid search procedure was utilized. The isotopic spin-1 scattering matrix was accurately determined over the energy range under consideration. The isotopic spin-0 scattering matrix was also determined, but not to the same accuracy, because of the incompleteness of the (n,p) data selection. The phase-shift analyses were carried out, and the pion-nucleon coupling constant g^2 was determined, using first (p,p) and then (p,p) plus (n,p) data selections. The results were a further substantiation of the charge independence hypothesis. Matrix methods used for the search pro-

cedures are discussed, and it is shown how the data normalization constants can be eliminated from the search. A discussion is also included of the use of the inverse error matrix in obtaining quantitative fits with theoretical models. (auth)

11623 THEORY OF THE TRITON WAVE FUNCTION. Amado, R. D. (Univ. of Pennsylvania, Philadelphia. Univ. of California, Los Angeles). Phys. Rev., 141: 902-13(Jan. 1966).

The exact bound state of the three-nucleon system with separable interactions between pairs is studied. The method for extracting the bound-state wave function from the equations for the scattering amplitude is outlined. The wave function is used to study the proton- and neutron-body form factors of the triton. S-wave spin-dependent forces between nucleon pairs are used and a parameter represents the effects of tensor forces. Although this theory gives good answers for the binding energy of the triton and for low-energy neutron-deuteron scattering, rms triton radii are slightly small and the form factors too large at large momentum transfers. This difficulty is due to the neglect of a short-range repulsion. The experimental splitting of the proton and neutron form factors due to spin dependence of the forces is present. The percent of mixed-symmetry S state is calculated. (auth)

11624 MEASUREMENT OF THE N^{*-}-N^{*++} MASS DIFFERENCE. Gidal, George; Kernan, Anne; Kim, Sedong (Univ. of California, Berkeley). Phys. Rev., 141: 1261-7 (Jan. 1966). (UCRL-16096; UCRL-16096(Rev.)).

A measurement of the N^{*-}-N^{*++} mass and width differences is described, where N* is the nucleon resonance with $I(J^P) = {}^3/_2({}^3/_2{}^+)$ and mass approximately 1240 Mev. The resonances were produced in the inelastic reactions $n\,n \rightarrow p\,n\,\pi^-$ and $p\,p \rightarrow n\,p\,\pi^+$, which are known to proceed almost entirely via N^{*-} and N^{*++} production, respectively, in the observed energy region. A comparison of the $(n\pi^-)$ and $(p\pi^+)$ effective-mass distributions gives a mass difference of 7.9 ± 6.8 Mev and a width difference of 25 ± 23 Mev for N^*-N^{*++}. This result agrees with predictions based on the SU(3) and SU(6) symmetry schemes. (auth)

11625 MEASUREMENT OF PROTON ELECTROMAGNETIC FORM FACTORS AT HIGH MOMENTUM TRANSFERS. Chen, K. W.; Dunning, J. R. Jr.; Cone, A. A.; Ramsey, N. F.; Walker, J. K.; Wilson, Richard (Harvard Univ., Cambridge, Mass.). Phys. Rev., 141: 1267-85(Jan. 1966).

Elastic electron-proton scattering cross sections were measured using the internal beam of the 6-Bev Cambridge Electron Accelerator at laboratory scattering angles between 31 and 90° for values of the four-momentum transfer squared ranging from $q^2 = 0.389$ to 6.81 $(Bev/c)^2$ ($q^2 = 10$ to $175 F^{-2}$). Incident electron energies ranged from 1.0 to 6.0 Bev. Scattered electrons from an internal liquid-hydrogen target were momentum-analyzed using a single quadrupole spectrometer capable of momentum analysis up to 3.0 Bev/c. Čerenkov and shower counters were used to help reject pion and low-energy background. The cross sections presented are absolute cross sections with experimental errors ranging from 6.8 to 20%. Separation of proton electromagnetic form factors were made for all but the two highest momentum transfer points, using the Rosenbluth formula. Both form factors, G_{Ep} and G_{Mp}, were observed to continue to decrease as the momentum transfer increases. An upper limit to the possible asymptotic values of the proton electromagnetic form factors was established. (auth)

11626 QUASI-ELASTIC ELECTRON-DEUTERON SCATTERING AND NEUTRON FORM FACTORS. Dunning, J. R. Jr.; Chen, K. W.; Cone, A. A.; Hartwig, G.; Ramsey, N. F.; Walker, J. K.; Wilson, Richard (Harvard Univ., Cambridge, Mass.). Phys. Rev., 141: 1286-97(Jan. 1966).

The cross section for inelastic electron-deuteron scattering was measured in the four-momentum transfer region corresponding to $q^2 = 0.389$ to 6.81 $(Bev/c)^2$ ($q^2 = 10$ to 175 F^2). The impulse approximation was used in the form given by Durand to interpret the deuteron cross sections as the sum of free-proton and free-neutron scattering cross sections. Using elastic electron-proton scattering cross sections obtained with a hydrogen target and using the Rosenbluth equation, neutron form factors were obtained at $q^2 = 0.389$, 0.623, 0.857, 1.17, and 1.75 $(Bev/c)^2$. Upper limits on the form factors were extracted from the $q^2 = 2.92$, 3.89, and 6.81 $(Bev/c)^2$ data. No evidence for possible core terms was found in either form factor. (auth)

11627 NUCLEON FORM FACTORS AND THEIR INTERPRETATION. Chan, L. H.; Chen, K. W.; Dunning, J. R. Jr.; Ramsey, N. F.; Walker, J. K.; Wilson, Richard (Harvard Univ., Cambridge, Mass.). Phys. Rev., 141: 1298-1308 (Jan. 1966).

All available elastic electron-proton and quasielastic electron-neutron cross sections are analyzed assuming one-photon exchange. The model in which the form factors are caused entirely by vector mesons is discussed. A good fit cannot be obtained assuming ρ, ω, and ϕ alone. An acceptable fit with an additional meson (ρ') is discussed. Possible connections with elastic pp scattering are also discussed. (auth)

11628 PROTON FORM FACTORS FROM OBSERVATION OF RECOIL PROTONS. Frerejacque, D.; Benaksas, D.; Drickey, D. (Ecole Normale Superieure, Orsay, France). Phys. Rev., 141: 1308-12(Jan. 1966).

A determination of the electric and magnetic form factors of the proton was made by studying the elastic scattering of electrons from a polyethylene target by observation of the recoiling proton at 0 and 30° for values of q^2 between 1 and 1.8 F^{-2}. From these measurements the charge radius R_c and the magnetic radius R_m of the proton were deduced and equality within the experimental errors ($R_c = 0.800 \pm 0.025$ F; $R_m = 0.810 \pm 0.029$F) was found. (auth)

11629 UNSUCCESSFUL SEARCH FOR AN EXCITED ELECTRON. Budnitz, R.; Dunning, J. R. Jr.; Goitein, M.; Ramsey, N. F.; Walker, J. K.; Wilson, Richard (Harvard Univ., Cambridge, Mass.). Phys. Rev., 141: 1313(Jan. 1966).

F. Low has recently conjectured on the existence of heavy electrons. A search for a heavy electron in the mass range of 300 to 700 Mev is described. No evidence for the existence of such an object was observed within this mass range. (auth)

11630 LOW ENERGY K^--d ELASTIC SCATTERING: EFFECT OF THE $\bar{K}^0$-K^- AND n-p MASS DIFFERENCES. Hetherington, J. H.; Schick, L. H. (Univ. of Minnesota, Minneapolis). Phys. Rev., 141: 1314-20(Jan. 1966). (COO-1371-17).

A Faddeev type of multiple-scattering formalism with nonlocal separable S-wave potentials for the two-particle interactions is applied to K^--d scattering for incident meson(K) momentum up to 300 Mev/c. Coulomb scattering is neglected but calculations are performed both neglecting and including the $\bar{K}^0$-K^- and n-p mass differences. K^--d elastic angular distributions, elastic cross sections, and total cross sections are calculated using the Kim $\bar{K}$-N scattering lengths and values of the K^--N range parameters from 0.05 to 0.20 F. The corrections due to the mass differences run about 3–9%, being larger at the smaller values of the incident meson(K) momentum. (auth)

11631 PHOTODISINTEGRATION OF THE DEUTERON FROM 500 TO 1000 Mev. Ching, R.; Schaerf, C. (Stanford Univ., Calif.). Phys. Rev., 141: 1320-1(Jan. 1966).

The photodisintegration of the deuteron was studied at energies comparable with the second and third meson(π) nucleon isobars using linear electron accelerator. No evidence was found for any resonant behavior in the energy region of interest. (auth)

11632 DYNAMICS OF THE Y_{05}^* (1815-Mev) $\bar{K}N$ RESONANCE. Agarwal, S. C. (National Physical Lab., New Delhi, India). Phys. Rev., 141: 1325-7(Jan. 1966).

An exact N/D calculation is done in $\bar{K}N$ scattering by taking ρ and ω exchanges in the t channel. The calculation

shows a resonance (Y_{05}^*) at ≃13 m_π with a width of $\Gamma \simeq 100$ Mev in the I = 0, $f_{5/2}$ state. No resonance occurs in the I = 0, $d_{3/2}$ partial wave, suggesting the spin-parity assignment $5/2^+$. (auth)

11633 RADIATIVE HYPERON DECAYS, $\Sigma^\pm \to n + \pi^\pm + \gamma$. Li, Ming Chiang (Univ. of Maryland, College Park). Phys. Rev., 141: 1328-42(Jan. 1966).

The observation of the $\Sigma^\pm \to n + \pi^\pm + \gamma$ radiative-decay spectra was proposed as a method of determining the s- or p-wave nature of the Σ meson(π) decay. The previous theoretical treatment is based on a phenomenological interaction that neglects all form-factor effects. Calculations were made to investigate the sensitivity of the theoretical predictions to structure effects by using two models: a self-consistent pole model that includes the $\Sigma^+ \to p + \gamma$ vertex in a natural way; a loop model that serves as a demonstration of the radiative influence of a virtual light particle. The results show that the simple phenomenological calculation is not changed significantly. Hence, the reliability of the radiative-decay method to determine the s- or p-wave nature of Σ meson(π) decay is improved. (auth)

11634 CONSEQUENCES OF C-VIOLATING INTERACTIONS IN η^0 AND X^0 DECAYS. Barrett, Barbara (Columbia Univ., New York); Jacob, Maurice; Nauenberg, Michael; Truong, Tran N. Phys. Rev., 141: 1342-9(Jan. 1966). (NYO–2262-101).

Several decay modes of the meson(η) and the (heavy η) meson(X^0) are discussed under the assumption that there exist C-violating interactions which conserve parity and strangeness. Various speculations about the strength, symmetry, and electromagnetic properties of this interaction are considered to find out how these properties might be determined experimentally from these decays. From available experimental data, several limits for the strength of C-violating interactions are obtained. (auth)

11635 PHOTOPRODUCTION PROCESSES AND SU(6) SYMMETRY. Tripathy, K. C. (Univ. of Delhi). Phys. Rev., 141: 1350-1(Jan. 1966).

The consequences of SU(6) symmetry for photoproduction processes are investigated with restriction to $S_{1/2}$ channel only. In addition to the well-known SU(3) sum rules, some new sum rules are derived and discussed. (auth)

11636 ELECTRON-NUCLEON SCATTERING CROSS SECTION INCLUDING ALL POLARIZATION CORRELATIONS. Scofield, James. Phys. Rev., 141: 1352-3 (Jan. 1966). (UCRL–14348).

The first-order Born-approximation cross section for the electromagnetic scattering of two nonidentical spin one-half particles is given, including the dependence on arbitrary initial and final spin states of both particles. Both particles are treated relativistically with charge and magnetic-moment interactions. (auth)

11637 AN ANALYSIS OF SOME PION-PION SCATTERING MODELS. Kreps, R. E. (Univ. of California, Berkeley). Phys. Rev., 141: 1380-4(Jan. 1966).

A numerical investigation is made on some model calculations based on a suggestion of Blankenbecler. The models satisfy threshold conditions, elastic unitarity, and nearest crossed-channel singularities exactly. The internal parameters are chosen so as to minimize crossing dissatisfaction. No physically sensible result emerges. (auth)

11638 DECAYS OF THE Y_0^* AND CP-NONINVARIANT ELECTROMAGNETIC INTERACTIONS. Barshay, S. (Rutgers Univ., New Brunswick, N. J.). Phys. Rev., 141: 1385-6(Jan. 1966).

Although the study of this reaction may not be experimentally feasible at present, it is worth noting that the decay Y_0^* (1405) $\to \Lambda + e^+ + e^-$ allows a test for time-reversal noninvariance in a transition between different spin-$1/2$ baryons involving a virtual photon. Assuming the Y_0^* to have $J^P = (1/2)^-$, we give the expression for the polarization of the Λ in a direction normal to the decay plane. Unlike the the corresponding Λ polarization in the decay $\Sigma^0 \to \Lambda + e^+ + e^-$, the T-violating observable will not vanish in the limit of unbroken SU(3) symmetry. The same expression is applicable to the idea of Schwartz to measure the T-violating normal component of the neutron polarization in the much more accessible reaction $\pi^- + p \to n + e^+ + e^-$ induced by stopped π^- in hydrogen, if it is assumed that the initial state corresponds to a $J^P = (1/2)^-$ "particle." It is noted that a study of the branching ratios for the decays $Y_0^* \to \Lambda + \gamma$, $\Sigma^0 + \gamma$ allows for a test of the SU(3) transformation properties of a possible T-violating electromagnetic interaction, and also bears on the question of the existence of nonminimal electromagnetic interactions. (auth)

11639 RELATIVISTIC THREE-PION CALCULATION. [PART] I. Basdevant, Jean-Louis; Kreps, Rodney E. (Univ. of California, Berkeley). Phys. Rev., 141: 1398-1403(Jan. 1966). (UCRL–16233).

In order to do a reasonably simple relativistic three-meson calculation, a relativistic analog to the Faddeev equations proposed by Alessandrini and Omnes is examined. An explicit angular-momentum decomposition, following the method of Omnes, is given. Some remarks are made about suitable approximations for the relativistic off-shell two-body amplitude, and a separable form of this is used to reduce the equations to their final form. As an example, the explicit equations are written in the three-pion I = 0, $J^P = 1^-$ case. (auth)

11640 RELATIVISTIC THREE-PION CALCULATION. [PART] II. Basdevant, Jean-Louis; Kreps, Rodney E. (Univ. of California, Berkeley). Phys. Rev., 141: 1404-9 (Jan. 1966). (UCRL–16255).

The calculation of the I = 0, $J^P = 1^-$ three-pion state is done on the basis of previously derived equations. The two-body amplitude is assumed to be well represented by the pole of the ρ. Particular choices for the resonance form factors appearing in the equations are discussed. The behavior of the eigenvalues of the Faddeev kernel is exhibited, and it is explained why the ω meson does not appear in such a model. A resonance is found at relatively high energy which does not depend on the choice of the form factors. This resonance seems to correspond to the experimental E meson. (auth)

11641 RELATIVISTIC THREE-PION CALCULATION. [PART] III. Basdevant, Jean-Louis; Kreps, Rodney E. (Univ. of California, Berkeley). Phys. Rev., 141: 1409-12 (Jan. 1966). (UCRL–16331).

A model for three-spinless-meson relativistic resonances, based on the Alessandrini-Omnes generalization of the Faddeev equations, which was explained previously, is studied in all three-pion states with angular momentum J < 3. The only part of the two-body amplitude which is taken into account is the ρ resonance. The separation of isospin is shown explicitly, and it is explained how the momentum-space equations reduce to only one when Bose statistics is taken into account. The results do not suggest the dynamical origin of the A_2, and many isoscalar resonances are found in a small energy region. (auth)

11642 PRODUCTION AND ABSORPTION OF S-WAVE PIONS AT LOW ENERGY BY TWO NUCLEONS. Koltun, D. S.; Reitan, A. (Univ. of Rochester, N. Y.). Phys. Rev., 141: 1413-18(Jan. 1966). (UR–875-88).

The cross sections for the reactions $p + p \to d + \pi^+$ and $p + p \to p + p + \pi^0$ are calculated for s-wave pions at threshold. The meson (π) is produced by either nucleon and emitted directly or rescattered in an s wave by the second nucleon, through a modified static interaction. The two nucleons interact through a phenomenological potential. For the Hamada-Johnston potential both calculated cross sections agree with experimental results. Application of the method of calculation to the nuclear absorption of s-wave pions is discussed. (auth)

11643 N/D CALCULATION WITH INELASTIC UNITARITY OF πN SCATTERING. Coulter, Philip W.; Shaw, Gordon L. (Stanford Univ., Calif.). Phys. Rev., 141: 1419-24(Jan. 1966).

The real part δ of the πN phase shifts for partial waves

$J \leq 3/2$ was calculated using the N/D equations with inelastic unitarity. The generalized potential is determined by considering single-exchange diagrams for the nucleon, the N* (1238 Mev) and the ρ (760 Mev). The inelastic factor η is taken from the recent, extensive complex phase-shift analyses. A straight cutoff W_c on the dispersion integrals in the energy plane W is used to eliminate the high-energy divergences associated with the exchange of particles with spin ≥ 1. Full numerical solutions of the integral equation for the N function are obtained by the matrix-inversion technique. The single cutoff W_c is separately adjusted for each J to give the best fit to the two coupled waves $l = J - 1/2$ and $J + 1/2$. For comparison, the δ's are also calculated using elastic unitarity, i.e., $\eta(W) \equiv 1$. By including inelastic effects, better agreement with the phase-shift analyses is obtained, except for the S_{31} and P_{13} partial waves. In particular, the calculation of the D_{13} phase shift agrees with the phase-shift analyses for $\delta_{D_{13}}$ up to $E_L \approx 450$ Mev (whereas the solution for $\eta \equiv 1$ gives a δ which is much too small). The P_{11} partial wave is of special importance since (in addition to the nucleon pole) it contains a possible resonance at $E_L \sim 570$ Mev which is very inelastic. Two different calculations of the $I = 1/2$, $J = 1/2$ partial wave were performed: W_c was adjusted to yield the nucleon pole as a bound state. The residue (related to $g_{\bar{N}N\pi}$) is approximately twice what it should be. Both the S_{11} and P_{11} phase shifts are in violent disagreement with the phase-shift analyses. (The calculations with inelastic effects gave only a slight improvement over the $\eta \equiv 1$ calculations.) The nucleon pole was included in the direct channel at the correct position with the correct residue and W_c was adjusted so that no zero appeared in the D function. Quantitative fits to the low-energy S_{11} and P_{11} phase shifts were then obtained. (auth)

11644 ELASTIC ELECTRON-DEUTERON SCATTERING. Grossetete, B.; Drickey, D.; Lehmann, P. (Ecole Normale Superieure, Orsay, France). Phys. Rev., 141: 1425-34(Jan. 1966).

Results on elastic electron-deuteron experiments performed at Orsay are presented. The range of momentum transfers is 0.6 to 2 F^{-2}. Two kinds of measurements were taken detecting the scattered electron: one with a solid CD_2 target, the other with a liquid target. The data are analyzed with the nonrelativistic theory, which gives slightly positive neutron form factors and a magnetic neutron form factor nearly equal to the magnetic proton form factor. (auth)

11645 ELECTRODISINTEGRATION OF THE DEUTERON AROUND $q^2 = 3.5$ F^{-2}. Grossetete, B.; Jullian, S.; Lehmann, P. (Ecole Normale Superieure, Orsay, France). Phys. Rev., 141: 1435-40(Jan. 1966).

The absolute cross sections of the electron-deuteron scattering at $q^2 = 3.5$ F^{-2} were measured and the complete inelastic spectrum was obtained. Three points for each spectrum are given with a 4% accuracy. The scattering angles, 60 and 130°, were chosen to allow the separation between electric and magnetic scattering. Calculations of radiative corrections were made in order to permit the comparison of the spectra with the inelastic-scattering theories. (auth)

11646 INELASTIC ELECTRON-DEUTERON SCATTERING AND THE RESCATTERING CORRECTIONS. Bosco, B.; Grossetete, B.; Quarati, P. (Ecole Normale Superieure, Orsay, France. Univ. Cagliari, Turin). Phys. Rev., 141: 1441-53(Jan. 1966).

The inelastic electron-deuteron scattering is completely re-examined on the basis of the recent Orsay experiments. The expression for the differential cross section is derived on a more general basis, the rescattering corrections predicted by different methods are compared extensively, and their effects on the nucleon form factors are discussed. (auth)

11647 REGGE POLES IN πN SCATTERING. Joshi, G. C. (Univ. of Delhi). Phys. Rev., 141: 1471-8(Jan. 1966).

Exploiting the unitarity and analyticity properties of relativistic partial-wave amplitudes for pion-nucleon scattering, the partial-wave amplitude was analytically continued in the complex J plane. The Froissart-Gribov (F-G) representation in π-N scattering is holomorphic in the domain $\mathrm{Re}J > \alpha + 1/2$ provided the invariant amplitudes and their absorptive parts in the t and u channels are bounded by t^α, u^α for fixed s and large t,u. Using the N/D method of analytic continuation it was shown that it is possible to continue the F-G representation in the interesting region $\mathrm{Re}J \leq \alpha + 1/2$ and it is meromorphic there. This was done under some reasonable assumptions on the asymptotic growth of the spectral function. It is further shown that the N/D method of analytic continuation does not work beyond the line $J = -1/2$ and at $J = 0$ there is an accumulation of an infinite number of poles at threshold. (auth)

11648 $T = 1/2, 3/2$ P- AND S-WAVE Kπ PHASE SHIFTS. Gupta, K. C.; Saxena, R. P.; Mathur, V. S. (Univ. of Delhi). Phys. Rev., 141: 1479-83(Jan. 1966).

Using the N/D technique, $T = 1/2, 3/2$ P- and S-wave phase shifts are calculated. The $T = 1/2$ P- and S-wave phase shifts are also calculated in the Khuri-Regge representation. For the purpose of comparison with experiments, the phase shifts are used to calculate the angular distributions in the reaction $K^-p \rightarrow \bar{K}^0p\pi^-$. (auth)

11649 n-n AND n-p SCATTERING LENGTHS AND CHARGE INDEPENDENCE. Henley, E. M.; Morrison, L. K. (Univ. of Washington, Seattle). Phys. Rev., 141: 1489-93(Jan. 1966). (TID-22233).

The degree of charge-independence violation for the low-energy nucleon-nucleon system is studied on the basis of a semiphenomenological meson theory. The difference between the singlet n-p and n-n scattering lengths induced by the $\pi^\pm$-π^0 and $\rho^\pm$-ρ^0 (Δm) electromagnetic mass splittings is investigated for the one-meson(π)-, two-meson (π)-, and meson(ρ)-exchange potentials. A charge-independent boundary condition is used to replace the short-range behavior. It is found that approximately 60% of the measured difference between the scattering lengths can be accounted for by the one- and two-meson (π) potentials with charge-independent pseudoscalar coupling. The calculated results are sensitive to parameters of the ρ-exchange potential, such as Δm and coupling constants, which are not well known. The dependence of the scattering lengths on these parameters is found. Finally, it is noted that a negative Δm, or a change of the order of 2% in the boundary condition or in the ratio of charged to neutral coupling constants, can account for the discrepancy that remains after meson(π) electromagnetic mass splittings are included. (auth)

11650 THREE-NUCLEON INTERACTION. Harrington, David R. (Rutgers Univ., New Brunswick, N. J. Oak Ridge National Lab., Tenn.). Phys. Rev., 141: 1494-6 (Jan. 1966). (ORNL-P-1617).

A contribution to the long-range part of the three-nucleon potential arising from the interaction of virtual mesons (π) with the cloud of s-wave, two-meson(π) resonances around a nucleon is investigated. Crude estimates are made for the effect of this potential in nuclear matter and in triton. In nuclear matter the corresponding effective two-nucleon interaction at small distances is repulsive and strong enough to dominate the one-meson (π)-exchange potential. The contribution to the triton binding energy is about 1.1 Mev. (auth)

11651 MESON EXCHANGE EFFECTS ON THE ELECTROMAGNETIC STRUCTURE OF THE DEUTERON. Adler, R. J. (Univ. of Washington, Seattle). Phys. Rev., 141: 1499-1508(Jan. 1966).

Adler and Drell recently reported on a calculated effect of the $\rho\pi$ mesonic exchange current on the electromagnetic interactions of the deuteron. The method of calculation used is described more fully and the confrontation of the results with more recent large-angle elastic electron-deuteron scattering experiments is discussed. The most

striking aspect is that at q^2 values of 6, 7, and 8 (fermi)$^{-2}$ the recent data are in excellent agreement with the present theory, but the magnetic scattering does not agree with the predictions of the older and well-studied impulse approximation. (auth)

11652 DYNAMICAL INELASTICITY AND HIGH-ENERGY p-p SCATTERING. Islam, M. M. (Brown Univ., Providence). Phys. Rev., 141: 1524-8(Jan. 1966).

A recently proposed method for calculating partial-wave inelasticity dynamically is applied to the high-energy p-p scattering. The two nucleons are considered spinless. Their left-hand-cut contribution is calculated by making a δ-function approximation of the absorptive part in the crossed channel. Partial waves with $l \leq l_a$ are taken to be completely imaginary and those with $l > l_a$ are considered to be given by the Born term. Certain interesting features of the present model are discussed. (auth)

11653 EFFECTIVE NONLOCAL ENERGY-INDEPENDENT POTENTIAL AND THE POSSIBILITY OF A REPULSIVE CORE AT SMALL DISTANCES. Balazs, Louis A. P. (Tata Inst. of Fundamental Research, Bombay). Phys. Rev., 141: 1532-41(Jan. 1966).

An effective nonlocal potential is constructed by requiring that its Born expansion give the same amplitude as the peripheral-interaction expansion of Cutkosky. The latter is a modified perturbation expansion based on dispersion theory in which each line of a Feynman graph represents not only discrete states, but also all states lying in the continuum which have a limited angular momentum; in higher order diagrams one also has to subtract out certain contributions which are already included in lower order diagrams, so as to avoid double counting. It can then be argued that, at least if we go up to fourth order, there should be a repulsive core in the potential. The Schrödinger equation is thus solvable without cutoff in configuration space. Because of the difficulties of such a program, only a rough momentum-space calculation was carried out for $\pi\pi$ scattering with ρ exchange. (auth)

11654 K_{e4} DECAY AND s-WAVE π-K SCATTERING. Martin, B. R. (Univ. of Copenhagen). Phys. Rev., 141: 1571-80(Jan. 1966).

A study of K_{e4} was made in an attempt to deduce information about the low-energy s-wave π-K interaction. Using a method due to Van Hieu, the decay amplitude is written in terms of the s- and p-wave amplitudes for $\pi\pi \rightarrow K\bar{K}$ and the known $K_{\mu 2}$ decay rate. The latter amplitudes are calculated from physical π-K scattering and s- and p-wave π-π phase shifts, via the Omnès method. Two simple nonresonant parameterizations are used for the s-wave π-π phases. For physical π-K scattering the existence of K* (891) is assumed and the s waves are parameterized. A sum rule is used to reduce the number of parameters to one, which is adjusted to give the observed decay rate. Two solutions are found, and comparison with the two-meson(π) decay spectrum are made in order to choose between them. The best solution is a nonresonant $T = \frac{1}{2}$ s-wave π-K interaction, with s-wave scattering lengths $a_{10} = 0.06 \pm 0.03$, $a_{30} = -0.06 \pm 0.03$. A second solution, with a resonant $T = \frac{1}{2}$ interaction and scattering lengths $a_{10} = 0.11 \pm 0.03$, $a_{30} = -0.01 \pm 0.03$ is also possible, although less likely than the former solution. (auth)

11655 POSITRON ANNIHILATION IN DIATOMIC CRYSTALS. Brandt, Werner (New York Univ., N. Y.); Eder, Leslie; Lundqvist, Stig. Phys. Rev., 142: 165-73 (Feb. 1966).

The angular correlation between the two photons created by annihilating positron–electron pairs in lattices with a basis is derived in various approximations. The effects of temperature as introduced through the momentum distribution of the positrons and through lattice vibrations are examined. Self-consistent electron wave functions with exchange are calculated for the LiH crystal in the cell approximation. The resulting x-ray structure factors are in close agreement with the recent extensive experimental data of Calder et al. The positron wave function is obtained in the same approximation and the momentum distribution of annihilating positron-electron pairs is calculated. The apparent discrepancy noted by Stewart and March between their angular-correlation data and the electron density distribution in the LiH crystal consistent with the x-ray structure factors can be traced to the phase relations between the wave functions within the unit cell of a lattice with a basis. (auth)

11656 SPIN-PARITY DETERMINATION OF THE $Y_1^*(1765)$. Bell, Robert B.; Birge, Robert W.; Pan, Yu-Li; Pu, Robert T. (Univ. of California, Berkeley). Phys. Rev. Lett., 16: 203-7(Jan. 31, 1966). (UCRL-16451).

The interaction $K^- + n \rightarrow \Sigma^- + \pi^+ + \pi^-$ at 828, 930, 1025, and 1112 Mev/c was investigated. The results confirm the existence of the $Y_1^*(1765)$ resonance with a mass of 1760 ± 10 Mev, a width of 60 Mev, and a spin-parity assignment of $5/2^-$. (D.C.W.)

11657 QUANTUM NUMBERS AND MASSES OF MESONS AS QUARK-ANTIQUARK SYSTEMS. Sinanoglu, Oktay (Univ. of Miami, Coral Gables, Fla). Phys. Rev. Lett., 16: 207-10(Jan. 31, 1966).

The mesons are studied in terms of quark-antiquark systems with particular consideration of the implications of SU(6) (or U(6) ⊗ U(6)) symmetry. (D.C.W.)

11658 BRANCHING RATIOS INTO $K_{\mu 2}$, AND K_{e3}, AND K_{e4} IN THE PARTIALLY CONSERVED AXIAL-VECTOR CURRENT. Suzuki, Mahiko (California Inst. of Tech., Pasadena). Phys. Rev. Lett., 16: 212-15(Jan. 31, 1966).

The branching ratios of the K_{12}, K_{13}, and K_{14} decays were calculated in the framework of the partially conserved axial-vector current hypothesis. (D.C.W.)

11659 CURRENT ALGEBRAS AND THE SUPPRESSION OF LEPTONIC MESON DECAYS WITH $\Delta S = 1$. Oehme, Reinhard (Univ. of Chicago). Phys. Rev. Lett., 16: 215-17(Jan. 31, 1966).

A set of relations between the semileptonic amplitudes, which indicated that the suppression of $\Delta S = 1$ transitions relative to $\Delta S = 0$ decays can not be due to strong-interaction effects, was previously derived on the basis of the chiral U(3) ⊗ U(3) algebra of hadron currents, partially conserved axial-vector currents, and the assumption that the divergence of the axial-vector current acts approximately like a creation or destruction operator for the corresponding pseudoscalar mesons. It is shown that the same relations can be derived without the latter assumption, if one of the meson mass variables is allowed to be zero. It is concluded that the current algebra strongly indicates that the suppression of $\Delta S = 1$ decays must be due to effects which are related to the structure of the weak interactions. (D.C.W.)

11660 MOTION OF POSITRONS. Stewart, A. T.; Shand, J. B. (Univ. of North Carolina, Chapel Hill). Phys. Rev. Lett., 16: 261-2(Feb. 14, 1966).

The angular correlation of photons from positrons annihilating in sodium metal at four different temperatures was measured. The "effective temperature" of the positrons was obtained as a function of specimen temperature. On the basis of the results, it was concluded that the positron is thermalized but has an effective mass in sodium metal of approximately twice the rest mass. (D.C.W.)

11661 MAGNITUDE OF THE K_1^0-K_2^0 MASS DIFFERENCE USING STRONG INTERACTIONS. Meisner, Gerald W.; Crawford, Bevalyn B.; Crawford, Frank S. Jr. (Univ. of California, Berkeley). Phys. Rev. Lett., 16: 278-82(Feb. 14, 1966).

The magnitude of the mass difference $(K_1^0 - K_2^0)$ was measured using the strong-interaction method. The result was compared with other determinations. It was concluded that the strong-interaction and coherent-regeneration methods give compatible results. (D.C.W.)

11662 EXPERIMENTAL TEST OF TIME-REVERSAL INVARIANCE IN THE DECAY $K_L^0 \rightarrow \pi^- + \mu^+ + \nu$. Bartlett, D.; Friedberg, C. E.; Goulianos, K.; Hutchinson, D.

(Princeton Univ., N. J.). Phys. Rev. Lett., 16: 282-5 (Feb. 14, 1966).

The muon polarization transverse to the π-μ plane in the decay $K_L^0 \rightarrow \pi^- + \mu^+ + \nu$ was investigated. The result is clearly consistent with time-reversal invariance. (D.C.W.)

11663 POLARIZATION AS A TEST FOR REGGE BEHAVIOR IN BACKWARD π^+-p SCATTERING. Stack, John D. (Univ. of California, Berkeley). Phys. Rev. Lett., 16: 286-8(Feb. 14, 1966).

It is shown that the exchange of the crossed-channel baryon trajectories, since they are associated with fermions, gives rise to amplitudes which are highly spin-dependent. In particular, the measurement of the polarization of the recoil proton can provide an important test for Regge behavior in these trajectories. (D.C.W.)

11664 π-p CHARGE-EXCHANGE PROCESSES IN THE REGION OF 2 Gev/c. Carroll, A. S. (Rutherford High Energy Lab., Chilton, Eng.). Phys. Rev. Lett., 16: 288-91 (Feb. 14, 1966).

The interactions $\pi^- + p \rightarrow n + \pi^0$ and $\pi^- + p \rightarrow (N^{*0}(1238) \rightarrow n + \pi^0) + \pi^0$ were studied at incident pion momenta of 1.715, 1.889, 2.071, 2.265, and 2.460 Bev/c. The results for the first interaction were fitted with a model in which the amplitude for exchange of a Reggeized meson(ρ) is dominant, interfering with weaker amplitudes due to π-N resonances. This analysis indicates that the 2190-Mev resonance has $J = 1 - 1/2$. It was also shown that the second interaction can be described by the same Regge-pole model. (D.C.W.)

11665 UNIVERSALITY: A DYNAMICAL PRINCIPLE FOR THE THEORY OF HADRONS. Freund, Peter G. O. (Univ. of Chicago). Phys. Rev. Lett., 16: 291-5(Feb. 14, 1966). (COO-264-294; EFINS-65-112).

It is shown that the central masses and the Gell-Mann-Okubo splittings of hadrons, as well as their electromagnetic and weak-interaction properties, can be accounted for under the assumption of the universality and M(12) symmetry of strong interactions. (D.C.W.)

11666 INELASTIC ELECTRON-DEUTERON SCATTERING WITH FINAL-STATE INTERACTIONS. Braess, D.; Kramer, G. (II. Institut fuer Experimentalphysik, Hamburg). Z. Phys., 189: 242-68(1966).

Measurements of the cross section $d^2\sigma/d\Omega\, dE'$ for the inelastic electron-deuteron scattering process $e + d \rightarrow e + n + p$ were used to determine the electromagnetic structure of the neutron. The effects on the theoretical cross section of the structure of the deuteron and of interactions between the outgoing nucleons are examined in detail. The relativistic invariant expressions of the one-nucleon exchange diagram including deuteron structure are used to obtain the interaction hamiltonian. For the disintegration near the quasi-elastic peak the d-n-p vertex function can be represented by nonrelativistic deuteron wave functions. The final state interaction is calculated from phenomenological nucleon-nucleon potentials. The rescattering corrections are found to lead to a decrease in the peak value of the cross section between -2 and -6% depending on the electron momentum transfer q^2 which has been varied between $2.5f^{-2}$ and $40f^{-2}$. These corrections are largest for small $q^2 < 5f^{-2}$. Furthermore the results show that the influence of our insufficient knowledge of the deuteron structure on the cross section is small. (auth)

11667 SCATTERING OF LASER PHOTONS ON FAST ELECTRONS. Krueger, H. (Univ., Freiburg i. B.). Z. Phys., 189: 302-11(1966). (In German).

The high laser intensity allows colliding-beam Compton scattering experiments of high-energy electrons with the photons of the red ruby laser light by which the latter are transformed into γ-radiation photons. Detailed calculations are given for the "average" polarization over the scattered beam and for the energy spectrum of the γ rays. (auth)

11668 VECTOR MESON IN A COULOMB FIELD. Karpenko, D. Ya.; Yaroshenko, A. P. (Dnepropetrovsk State Univ., USSR). Zh. Eksp. Teor. Fiz., 49: 1463-9 (Nov. 1965). (In Russian).

The motion of spin 0 and 1 bosons in a Coulomb field is considered on basis of the 16-row Kemmer representations. The integrals of motion which completely classify the states are determined. The radial and angular parts in the initial equation can be separated by employing the integrals of motion and set of projection operators. (auth)

11669 A SELF-CONSISTENT CALCULATION OF K* RESONANCE PARAMETERS. Isaev, P. S.; Radutskii, G. M. (Joint Inst. for Nuclear Research, Dubna, USSR). Zh. Eksp. Teor. Fiz., 49: 1475-82(Nov. 1965). (In Russian).

The position and width of the K*-meson are computed by the Balazs method. The solution depends on the following parameters: on ϵ, the slope of the K*-meson Regge trajectory; s_0—the reference point; function R(s), which describes the contribution of inelastic processes; and point t_d, which divides the physical energy region into two parts, in one of which the contribution of inelastic processes is small ($R(s) \approx 1$) and in the other it is appreciable ($R(s) \gg 1$). The value of the ρ-meson mass t_r and of its width Γ_1^t are taken from experiment. The following solutions were obtained for various values of the parameters ϵ, s_0, t_d and R(s): (1) $M_{K^*} = 832$ Mev and $\Gamma_{K^*} = 82.5$ Mev (the experimental values are 888 and 50 Mev respectively); (2) $M_{K^*} = 815$ Mev and $\Gamma_{K^*} = 51.4$ Mev. (auth)

11670 BREMSSTRAHLUNG ON MEDIUM ELECTRONS AND HARD VAVILOV-CHERENKOV RADIATION. Batygin, V. V. (Leningrad Polytechnic Inst.). Zh. Eksp. Teor. Fiz., 49: 1637-49(Nov. 1965). (In Russian).

The additional effect on bremsstrahlung of charged particles due to interaction between the particles and the long wave electromagnetic field in matter and electron ensemble of the outer shells is considered. The latter effect is taken into account via the transverse and longitudinal permeabilities of the matter. General expressions are derived for the probabilities of emission of a hard photon accompanied by a soft photon or by absorption of a soft photon. Two-quantum Vavilov-Cherenkov radiation is considered for the case when one of the emitted photons is hard and the other soft. This radiation is a new type of mechanism of hard photon production. It is much weaker than bremsstrahlung but nevertheless should be observable. The correction to bremsstrahlung of electrons on electrons obtained by taking into account electron coupling in matter is calculated for a certain model of the electron plasma. The correction may be as large as 50%. (auth)

11671 DOUBLE NN SCATTERING WITH A POLARIZED BEAM AND A POLARIZED TARGET. Bilenskii, S. M.; Lapidus, L. I.; Ryndin, R. M. (Joint Inst. for Nuclear Research, Dubna, USSR). Zh. Eksp. Teor. Fiz., 49: 1653-63 (Nov. 1965). (In Russian).

Possible experiments for measuring the polarization of nucleons produced as a result of scattering of a polarized beam by a polarized proton target are discussed. In such experiments it should be possible for the first time to determine the components of the third rank polarization tensor M_{ikq}. Polarization correlation is also considered in the case when one of the initial particles is polarized. Relativistic formulas for measurable quantities are derived. The problem of reconstructing the scattering matrix is discussed. (auth)

11672 INTERACTIONS OF POSITIVE PI MESONS WITH PROTONS AT 2 Bev [Thesis]. James, Frederick Edward. New Haven, Yale Univ., 1965. 138p.

Interactions of positive π mesons of momentum 2.08 Bev/c incident on protons were studied using the 20-in. hydrogen bubble chamber at Brookhaven National Laboratory's Alternating Gradient Synchrotron. A total of 12,000 events, was used to measure both the elastic differential cross section and the partial cross sections for all available inelastic reactions involving non-strange particles. The ρ^+, ρ^0, ω^0, and η^0 resonances are all produced strongly and emerge predominantly in the forward direction in the

center-of-mass system, suggesting a peripheral mechanism for their production. The possibility of explaining these reactions on the basis of certain specific particle exchange models is investigated. The neutral resonant states are usually accompanied by the ($\frac{3}{2}$, $\frac{3}{2}$) nucleon isobar at 1238 Mev. Also observed was a nucleon isobar of mass 1670 Mev, which decays into π^+n. (Dissertation Abstr.)

11673 THE EXPERIMENTAL DETERMINATION OF THE BRANCHING RATIOS FOR THE DECAY OF THE ρ^0, ω, AND ϕ MESONS INTO LEPTON PAIRS [Thesis]. Hertzbach, Stanley Shipley. Baltimore, Johns Hopkins Univ., 1965. 135p.

An experiment was performed at the Brookhaven AGS to study the decays of the neutral vector mesons ρ^0, ϕ, and ω into lepton pairs, a decay mode expected to occur with a frequency about 10^{-3} to 10^{-4} times that of the dominant mode. The data discussed were obtained with a total of 1.3×10^9 negative pions of momentum 3.0 Bev/c incident upon a 1.5-foot liquid hydrogen target. The pair, produced via the reactions $\pi^- + p \rightarrow n + V^0$ and $V^0 \rightarrow l + \bar{l}$, was identified by a system of scintillation counters and spark chambers. Electrons were electronically identified by their shower characteristics in a shower chamber that accepted less than one out of 10^4 pion pairs. Muons were identified by their ability to traverse many pion mean free paths of material. A Monte Carlo technique was employed to calculate the expected spectrum of pair opening angles and the detection efficiencies. A good fit to the data was obtained only when direct lepton pair decays of the ρ^0, ω, and ϕ mesons were included in the expected spectrum. The branching ratios for the electron pair decays of the ρ^0 and ω mesons were found to be on the order of 10^{-4}. The results for the decay of the ϕ are inconclusive because of the lack of knowledge concerning its production. For the muon branching ratios, only an upper limit, equivalent to that quoted for previous experiments, was obtained. In the case of electron pairs, the branching ratios obtained are an order of magnitude smaller than previously quoted upper limits. (Dissertation Abstr.)

11674 POSITRON LIFETIME IN LITHIUM AMMONIA SOLUTIONS [Thesis]. Deiterman, Louis Henry Jr. Austin, Tex., Univ. of Texas, 1965. 193p.

The lifetimes of positrons in lithium ammonia solutions and in pure ammonia were measured with an instrumental time resolution of 0.5 nsec. The temperature of the solutions was held constant at −65°C during the experiments. The range of concentrations studied was from .013 to 3.30 moles lithium per liter of ammonia. The short component half life was resolved and varied from 0.3 to 0.25 nsec as the lithium concentration increased. The half life of the long component decreased from 28% in the case of pure ammonia to a value of 12.5% in the concentrated range. Also, an additional third component in the half life was evident in the range between 0.1 and 1.2 moles lithium per liter NH_3. The intensity of this third component was about 1% over the range studied and vanished when the solution was warmed to −45°C at a concentration of .1 moles lithium per liter NH_3. The data can be interpreted by the mathematical method of Dixon and Trainor and results in conversion rates of $\gamma = (.52 + 12.5C) \times 10^9$ sec^{-1} at $0 < C < .04$, $\gamma = (1.11 + 5.2C) \times 10^9$ sec^{-1} at $.04 < C < .12$, and $\gamma = 2.28 \times 10^9$ sec^{-1} at $.12 < C < 3.3$. The transition regions of .04 and .12 moles lithium per liter NH_3 suggest phase changes in the ordering of the liquid. (Dissertation Abstr.)

11675 A SEARCH FOR THE PROCESS $K^+ \rightarrow \pi^+ + \pi^0 + \gamma$ [Thesis]. Macek, Robert James. Pasadena, Calif., California Inst. of Tech., 1965. 226p.

A search for the process $K^+ \rightarrow \pi^+ + \pi^0 + \gamma$ was made using counter and spark chamber techniques. The experiment was designed to detect all of the products of the process and measure sufficient quantities to overdetermine the kinematical parameters. Positive pions from K^+ decays at rest were detected in a scintillation counter hodoscope sensitive to pions with energies between 55 and 105 Mev. Positive identification of the π^+ was achieved by observing the $\pi - \mu$ decay on photographs of the hodoscope counter pulses displayed on a fast oscilloscope. The primary photon and the two π^0 decay photons were observed by the showers produced in spark chambers constructed of several radiation lengths of steel plate. Additional spark chambers determined the π and K trajectories, which, combined with a measurement of photon angles, overdetermine the $K_{\pi_2\gamma}$ kinematics by two parameters. A total of 4.3×10^6 stopping K's were counted by the apparatus whose overall efficiency for detecting $K_{\pi_2\gamma}$ events is 2.5×10^{-3}. One or possibly two events survived all the $K_{\pi_2\gamma}$ selection criteria. Because approximately one or two background events would be expected to survive the same selection criteria; the results must be presented as an upper limit of about 2×10^{-4} on the $K_{\pi_2\gamma}$ branching ratio for the portion of the π^+ spectrum from 55 to 85 Mev. This upper limit is in agreement with the prediction based on the internal bremsstrahlung mechanism and with other experiments that obtain the branching ratio by another approach. (Dissertation Abstr.)

11676 Λ POLARIZATION AT 90° IN K^+ Λ PHOTOPRODUCTION [Thesis]. Groom, Donald Eugene. Pasadena, Calif., California Inst. of Tech., 1965. 155p.

The polarization of Λ hyperons in the reaction $\gamma + p \rightarrow K^+ + \Lambda$ was measured, using the Caltech synchrotron. The measurements were made at 90° in the cms system, at laboratory photon energies of 1100, 1200, and 1300 Mev. Protons from the asymmetric decay of the Λ were detected by counters placed symmetrically above and below the plane defined by the photon beam and the mean kaon momentum. Kaons were detected in a 16 to 18 counter range telescope. If preliminary logic was satisfied, all pulse heights from counters in the telescope were digitized and recorded on paper tape, along with relevant coincidence information. A detailed fit to the Bragg curve was made in a digital computer to establish the kaon identification. The results were $P_\Lambda = +0.34 \pm 0.09$ at 1100 Mev, $+0.30 \pm 0.07$ at 1200 Mev, and $+0.08 \pm 0.07$ at 1300 Mev, where P_Λ is measured in the $\hat{k}_\gamma \times \hat{p}_\Lambda$ direction. These data, together with those of other groups, add support to the suggestion that the effects of the third πN resonance are evident in K_Λ photoproduction. (Dissertation Abstr.)

11677 ASSOCIATED PARTICLE METHOD FOR THE D(d,n)^{3}He REACTION. Divatia, A. S. (Atomic Energy Establishment, Trombay, Bombay); Bernard, D. L.; Bonner, B. E.; Philips, G. C.; Poppelbaum, C. pp 297-302 of Nuclear Physics and Solid State Physics Symposium, 1965. Nuclear Physics. Bombay, Atomic Energy Establishment, 1965. (TID-21420).

The possibility of using the D(d,n)^{3}He for the investigation of neutron-deuteron interactions was studied. The detection of the ^{3}He particles at various angles and energies was considered in some detail. Neutron energies, ^{3}He energies, and the energies of elastically scattered deuterons with an incident deuteron energy of 5.0 Mev were measured, as well as the charged-particle spectrum. The absolute efficiency of a neutron counter was measured by counting the associated ^{3}He particles. (D.C.W.)

11678 POSITRON ANNIHILATION IN MAGNESIUM–INDIUM AND INDIUM–LEAD ALLOYS. McKee, B. T. A.; Langstroth, G. F. O.; MacKenzie, I. K. (Dalhousie Univ., Halifax, Nova Scotia). 12p. (CONF-650721-2). ORINS. Gmelin, AED-CONF-65-211-9.

From Positron Annihilation Conference, Detroit.

Measurements were made of the temperature dependence of the angular correlation of two-quantum annihilation radiation in In-Pb and In-Mg alloys. Results were compared with anomalous temperature effects previously observed in In. Temperature effects corresponding to those of pure In were found in the In−Pb system with the size of the effect almost proportional to the amount of In present. No such effects were found in the In−Mg system even though the alloy proportions were selected to produce anisotropic variation of lattice parameters resembling those due to thermal expansion in In. It is concluded that the temperature dependence of positron annihilation in In is not due to

thermal expansion of the lattice and is not a characteristic of the lattice phase. (A.G.W.)

Field Theory, Scattering Theory, and Symmetries

See also Elementary Particles and Radiations

Refer also to abstract 12016.

11679 (CONF-650927-21) HIDDEN SYMMETRIES AND THE QUESTION OF MASSLESS PARTICLES. Bludman, S. A. (Pennsylvania Univ., Philadelphia. Dept. of Physics. California Univ., La Jolla, San Diego). Aug. 1965. Contract AT(30-1)-3489. 26p. Dep. mn. CFSTI $2.00 cy, $0.50 mn.

From American Physical Society, Honolulu, Hawaii.

The dynamical breakdown of symmetry is considered. In this the Goldstone theorem, which states that if a continuous symmetry is broken by the vacuum, then there must exist massless excitations of a definite symmetry character determined by the broken symmetry, is treated. The merits of the hidden symmetry approach are that states which do not transform covariantly under the group are admitted while maintaining the symmetry of the lagrangian, and the existence of massless particles is apparently associated with an invariance principle. It is shown that while the theorem is formally true, under conditions which themselves assume something about the dynamics, nevertheless no physical conclusion can be drawn directly from the broken symmetry alone. This is not to deny that massless particles may very well appear in broken symmetry theories as a consequence of a dynamical calculation or approximation. (J.F.P.)

11680 (IC/65/84) THE SL(6,c) SYMMETRY. (Lecture Notes). White, R. (International Centre for Theoretical Physics, Trieste (Italy)). Dec. 1965. 24p. Dep. mn.

The method of creation and destruction of operators as proposed by Feynman and Gell-Mann is used to construct the ladder representation of SL(6,c), a group proposed as being the most economical noncompact extension of SU(6), and most extensively developed. The representations are constructed with simple decompositions according to the maximal compact subgroup, SU(6). These representations correspond to highly degenerate representations of the discrete series. (J.F.P.)

11681 (IC/65/85) NON-COMPACT EXTENSIONS OF SYMMETRY GROUPS. Budini, P. (International Centre for Theoretical Physics, Trieste (Italy)). Dec. 3, 1965. 14p. Dep. mn.

An attempt is made to give a general method for obtaining the mass formula once the symmetry algebra of the system is known, and this is applied to simple systems. The harmonic oscillator and the hydrogen atom are considered. It is shown that the noncompact extension of symmetry algebras can not only generate the eigenstates spectrum of the physical system, but it can also furnish a method for obtaining mass formulas exact in the frame of the symmetry, the degeneracy of the invariants being connected to the degeneracy of the multiplets. One general condition is that the mass operator does not commute with some of the operators of the noncompact algebra or, exceptionally, be contained in the compact one. (J.F.P.)

11682 (IC/65/89) THE MOST DEGENERATE REPRESENTATIONS FOR THE COMPACT AND NON-COMPACT ROTATION GROUPS. Niederle, J.; Raczka, R. (International Centre for Theoretical Physics, Trieste (Italy)). Nov. 1965. 16p. Dep. mn.

The most degenerate representations of any compact as well as non-compact rotation groups are considered and their properties are discussed in detail. The explicit construction of the corresponding harmonic functions is given. The coordinate systems are chosen in such a way that Cartan subalgebra of considered groups is diagonal and the harmonic functions are denoted only by discrete numbers except one. (auth)

11683 (JINR-E-2475) ELECTROMAGNETIC CURRENT AND FORM FACTORS FOR THE MESON 35-PLET IN THE SL(6,C) SYMMETRY. Winternitz, P.; Zubarev, A. L.; Makarov, A. A. (Joint Inst. for Nuclear Research, Dubna (USSR). Lab. of Theoretical Physics). 1965. 7p. Dep. mn.

The structure of the electromagnetic meson current is investigated in the framework of the SL(6,c) symmetry and it is shown that the current depends on three form factors. The results are compared with the U(6,6) theory. (auth)

11684 (JINR-P-2442) RELYATIVISTSKAYA SOSTAVNAYA MODEL VYSSHIKH MEZONNYKH I BARIONNYKH REZONANSOV. (A Relativistic Composite Model of Meson and Baryon Resonances). Bogolyubov, P. N.; Matveev, V. A.; Struminskii, B. V. (Joint Inst. for Nuclear Research, Dubna (USSR). Lab. of Theoretical Physics). 1965. 21p. Dep. mn.

A relativistic composite model of mesons and baryons is developed. Highest meson resonances are considered as bound states in the p-wave of the quark-antiquark system, and baryon resonances as bound states in the p-wave of the three-quark system. Some mass relations are obtained, on the basis of which new particles are predicted. The electromagnetic interactions of new resonances are studied under the assumption of a minimal electromagnetic interaction of quarks. (auth)

11685 (JINR-P-2444) OKTET BARIONNYKH REZONANSOV V SKHEME UNITARNOI SIMMETRII. (An Octet of Baryon Resonances in Unitary Symmetry Scheme). Bokov, O. G. (Joint Inst. for Nuclear Research, Dubna (USSR). Lab. of Theoretical Physics). 1965. 7p. Dep. mn.

Decays of an octet of resonances $J^P = 3/2^-$ into octets of baryons and pseudoscalar mesons are treated under the SU(3) symmetry. Relations are obtained between the coupling constants of the fields and the decay widths. A comparison of the obtained results with the available experimental data favors an assignment to an octet of the resonance Λ (1668) not yet found experimentally by comparison with the well-known isotopic singlet Λ (1520). (auth)

11686 (JINR-P-2447) ZAPRESHCHENNYE KONFIGURATSII V SISTEME TREKH FOTONOV. (Forbidden Configurations in a Three-Photon System). Kopylov, G. I. (Joint Inst. for Nuclear Research, Dubna (USSR). Lab. of High Energy). 1965. 13p. Dep. mn.

The effective matrix elements of decay of particles with spin 0 and 1 into three photons are listed. It is proved in a general form that the spin 0 unlike the spin 1 and 2, forbids the collinear configurations and the configurations with monoenergetic photons. Characteristic distributions over the photon energies are given. (auth)

11687 (JINR-P-2485) ANALITICHESKIE SVOISTVA EVKLIDOVYKH AMPLITUD. (Analytical Properties of Euclidean Amplitudes). Efimov, G. V. (Joint Inst. for Nuclear Research, Dubna (USSR). Lab. of Theoretical Physics). 1965. 19p. Dep. mn.

The Cutkosky rule is proved for normal thresholds in the case of arbitrary Feynman graphs in the Euclidean formulation of quantum field theory. (auth)

11688 (JPL-TR-32-797) PARTICLE SYMMETRIES. Zmuidzinas, Jonas Stasys (Jet Propulsion Lab., Calif. Inst. of Tech., Pasadena). Dec. 15, 1965. Contract NAS7-100. 50p.

A theory of particle symmetries is proposed based on general principles of quantum mechanics and special relativity. Starting with a modest generalization of the Poincaré group and using techniques of group theory and operator algebras, the construction of composite-particle state vectors labeled by external (i.e., pertaining to space-time properties) and internal quantum numbers of physical significance is demonstrated. Macroscopic space-time be-

haves in exactly the same manner under both the Poincaré group and its generalization, the augmented Poincaré group. It is found that there exists a hierarchy of groups, Sp (1) ⊂ SP (2) ⊂ Sp (3) ⊂ ···, which characterizes internal symmetries of the composite particles. These groups are all noncompact. However, it is argued that physical particle states are characterized by the compact subhierarchy of unitary groups U (1) ⊂ U (2) ⊂ U (3) ⊂ ···. Thus, it is shown that the essential features of fundamental-particle symmetries can be derived in a general way from basic properties of space-time. These results are believed to form a theoretical framework for attacking dynamical problems such as the correlation of masses and spins with internal quantum numbers furnished by the hierarchy of unitary groups. (auth)

11689 (LA-DC-6912) ASYMPTOTIC PHASE AND AMPLITUDE FOR A MODIFIED COULOMB POTENTIAL IN SCATTERING THEORY. Beyer, W. A. (Los Alamos Scientific Lab., Univ. of California, N. Mex.). [1964]. Contract W-7405-eng-36. 18p. Dep. mn. CFSTI $1.00 cy, $0.50 mn.

A new representation is derived for the asymptotic phase and amplitude of the solution of the partial-wave Schroedinger equation in the case where a Coulomb potential is present. The derivation of this representation is an application of invariant imbedding. (J.F.P.)

11690 (NP-15764) OPERATORY KAZIMIRA DLYA GRUPP U(n) i SU(n). (Casimir Operators for U(n) and SU(n) Groups). Report No. 338. Perelomov, A. M.; Popov, V. S. (Gosudarstvennyi Komitet po Ispol'zovaniyu Atomnoi Energii SSSR, Moscow. Institut Teoreticheskoi i Eksperimental'noi Fiziki). 1965. 32p. Dep. mn.

A simple method of finding the eigenvalues of the invariant operators (Casimir operators) C_p of arbitrary order p for the U(n) and SU(n) groups is developed. The relations between Casmir operators for the U(n) and SU(n) groups is established. Explicit formulas for the operators C_p with $p \leq 6$ are given. (auth)

11691 (ORNL-3914) R-MATRIX APPROACH TO COMPLEX ANGULAR MOMENTUM AND TO THREE-PARTICLE INTERACTION [Thesis]. Roskies, Ralph (Oak Ridge National Lab., Tenn.). Jan. 1966. Contract W-7405-eng-26. 91p. Dep. mn. CFSTI $3.00 cy, $0.75 mn.

Submitted to Princeton Univ., N. J.

A brief review of the R-matrix formalism for two-particle elastic scattering via a spherically symmetric potential is presented. Properties of the R matrix are developed as a function of complex energy, or of complex angular momentum. Regge poles in potential scattering are discussed from an R-matrix point of view. The analytic properties of the S matrix as a function of complex energy for arbitrary (i.e., nonintegral) real angular momentum, concentrating especially on the multivalued nature of S as a function of energy, and on the behavior of S near threshold are discussed. The analytic properties of S for real energy and complex angular momentum are discussed, studying the location of the poles of S, and their trajectories as functions of the energy. A brief analysis of some limitations of R-matrix theory is presented. R-matrix theory is generalized to discuss a restricted three-body problem, one in which there are no two-particle interactions. The analytic structure of the S matrix is then studied as a function of complex total energy, emphasizing the multivaluedness of S, its threshold behavior, and the location of its poles. Finally, the connection between the asymptotic form of the wave function for an incident plane wave, and our S matrix was investigated. Some general features of three-body elastic scattering are described. The three different types of collisions (two-body, sequential, and real three-body collisions) are distinguished. The diagrams in perturbation theory are identified that are associated with each collision and it is found that the different types of collisions give rise to T-matrix elements of different dimensions. A time-dependent account of three-body elastic scattering is discussed, and the analogs of cross section for each type of collision are defined. (M.O.W.)

11692 (UCRL-11768) A VARIATIONAL PRINCIPLE FOR THE FADDEEV EQUATIONS. Wright, Jon; Omnes, Roland (Lawrence Radiation Lab., Univ. of California, Berkeley). Nov. 9, 1964. Contract W-7405-eng-48. 7p. Dep. mn. CFSTI $1.00 cy, $0.50 mn.

The Faddeev integral formulation of the nonrelativistic scattering of three particles is briefly discussed. The off-the-energy-shell scattering amplitude was written by Faddeev as a sum $T(z) = T_1(z) + T_2(z) + T_3(z)$ where z is the total energy. A variational principle is proposed for finding bound states and resonances. (M.O.W.)

11693 (UCRL-12016-T) ANALYTIC CONTINUATION OF $a(\ell,s)$ FOR $\mathrm{Re}\,\ell < N$. Zimmerman, Robert L. (Washington Univ., Seattle. Lawrence Radiation Lab., Univ. of California, Livermore). [1963]. Contract W-7405-eng-48. 42p. Dep. mn. CFSTI $2.00 cy, $0.50 mn.

The positions of the singularities of the partial wave amplitude in the complex ℓ plane are investigated for that case of a relativistic, two-particle elastic scattering amplitude satisfying the Mandelstam representation. For a finite number of intermediate states it is shown that the convex hull of singularities in the ℓ plane is related to a growth indicator function. For an infinite number of intermediate states it is demonstrated that the imaginary parts of the singularities in the ℓ plane are unbounded from either above or below. (auth)

11694 BOOTSTRAP METHOD AND REGGE POLES. Kwiecinski, J. (Joint Inst. for Nuclear Research, Dubna, USSR). Acta Phys. Pol., 28: 749-62(Dec. 1965).

A bootstrap method is proposed where the resonances are treated as Regge poles. The Khuri representation is used to describe the contribution from Regge poles. This enables the threshold behavior of the partial wave amplitude to be factored in such a way that its asymptotic behavior is not spoiled. The unphysical singularities of the so obtained reduced partial wave amplitude are determined by the contributions from the crossed-channel Regge poles. An approximate method is described to calculate these contributions. The possibility of application of this method in a scheme of new form of the strip approximation is discussed. (auth)

11695 ON FUNCTIONAL FORMULATION OF THE S-MATRIX THEORY. PART II. GENERALIZATION TO SPIN 1/2 PARTICLES. Rzewuski, J. (Univ., Wroclaw, Poland. Inst of Phys., Polish Academy of Sciences, Wroclaw). Acta Phys. Pol., 28: 789-807(Dec. 1965).

The functional formulation of the S-matrix theory developed previously for the case of scalar functions is extended to the case of spinor functions. (auth)

11696 ON THE VALIDITY OF MARTIN'S PHYSICAL SUM RULE FOR THE FORWARD SCATTERING AMPLITUDE. Wit, Romuald (Jagellonian Univ., Krakow). Acta Phys. Pol., 28: 861-4(Dec. 1965).

The necessary condition for Martin's physical sum rule to be true is given. (auth)

11697 NEW RESTRICTION ON THE FORWARD SCATTERING AMPLITUDE IN LOCAL FIELD THEORY. Wit, Romuald (Jagellonian Univ., Krakow). Acta Phys. Pol., 28: 865-8(Dec. 1965).

From the general properties of the forward (symmetrized) scattering amplitude in local field theory an integral equality is derived that must be fulfilled by the scattering amplitude. Some applications for the case of $\pi^{\pm}$-p scattering are given. (auth)

11698 ANGULAR MOMENTUM CONSERVATION IN THE STATISTICAL MODEL OF THE MULTIPLE PRODUCTION OF PARTICLES. Zalewski, Kacper (Inst. of Physical Chemistry, Krakow). Acta Phys. Pol., 28: 933-40(Dec. 1965).

The high energy behavior of the statistical model with angular momentum conservation is examined. It is concluded that angular momentum conservation is insufficient to produce the observed anisotropy of the final state amplitude. (auth)

11699 CRITERIA FOR THE SOLUBILITY OF PARTIAL-WAVE DISPERSION RELATIONS. Balachandran, A. P. (Syracuse Univ., N. Y.). Ann. Phys., 35: 209-39 (Nov. 1965). (NYO-3399-12).

The properties of the function associated with the unphysical cut and the transmission factor (the "interaction terms") are derived, which would ensure that the partial-wave dispersion relations possess solutions. An important role in this investigation is played by the N/D decomposition introduced by Frye and Warnock and by Warnock where D is a so-called Herglotz function. General considerations show that if the dispersion relation is to be consistent, N in the physical region and D at threshold must be nonpositive, D must be Herglotz, and N and D must satisfy some asymptotic constraints. Certain inequalities are proved for the solutions of linear integral equations of a certain class and used to derive sufficient conditions on the interaction terms which would lead to these properties of N and D. These are also sufficient conditions for the solubility of dispersion relations. It is shown that if the phase shift is restricted to be less than a fixed multiple of π at infinity and the angular momentum is sufficiently large, the CDD ambiguities tend to disappear and the solution is likely to be unique. The restrictions on the CDD parameters of the present N/D decomposition are exhibited explicitly. These results are closely related to a theorem due to Frye and Warnock and to Warnock. It is also shown that if the transmission factor $\eta(s)$ decreases rapidly at high energies (that is, if absorption becomes complete rapidly at high energies), the solution is again likely to be unique if the phase shift at infinity is not too large. A proof is constructed to demonstrate that if $\eta(s)$ decreases so rapidly as $\exp[-\alpha s^{\frac{1}{2}}]$, $\alpha > 0$ or faster as $s \to \infty$, the solution is, in fact, unique independent of any consideration based on the N/D method or on the asymptotic behavior of the phase shift. An algorithm is outlined for calculating this unique solution. It is argued on physical grounds that such a rapid decrease of $\eta(s)$ is not unlikely. Some results are also found regarding the behavior of the phase shift for large angular momenta. For example, the sufficiency criteria developed earlier imply that when $l \geq 2$, there is at least one energy where the phase shift increases through an integral multiple of π. (auth)

11700 MODIFIED DETERMINANTAL METHOD. Roy, S. M.; Blankenbecler, R. (Princeton Univ., N. J.). Ann. Phys., 35: 314-27(Nov. 1965).

An improved version of the determinantal method for solving N/D equations is developed. Unlike the determinantal approximation, the accuracy of this method is not limited to small coupling constants. Further, this method guarantees a real residue at the position of a pole in the partial-wave amplitude whereas the determinantal approximation yields a complex residue when the pole lies on the left-hand cut in the s-plane. Both nonrelativistic and relativistic cases are considered. Numerical accuracy of the new method is examined in some typical applications. (auth)

11701 THREE PARTICLE SINGULARITIES IN SCATTERING AMPLITUDES. Branson, David (Cambridge Univ., Eng.). Ann. Phys., 35: 351-72(Dec. 1965).

A discussion is given, within the framework of the s-matrix postulates of analyticity and unitarity, of methods of defining reduced two-particle scattering amplitudes that lack the two-particle singularity; the extension to the multichannel case is briefly described. The same methods are used to remove one-, two-, and three-particle physical threshold singularities from a three-particle scattering amplitude. (auth)

11702 INFINITESIMAL GENERATORS OF THE POINCARE GROUP IN AN ANGULAR MOMENTUM BASE. Bertrand, Jacqueline. Compt. Rend., 261: 3053-5 (Oct. 18, 1965). (In French).

The zero mass representations with multiple helicity of the Poincaré group are studied using the Mackey induction-reduction theorem. Thus the expression of the infinitesimal generators for a base where the energy, the helicity, and the third component and square of the angular momentum are diagonal can be obtained directly. (tr-auth)

11703 RELATIVISTIC GENERALIZATION OF DYNAMIC EQUATION FOR JOST FUNCTION. Petras, M. (Komensky Univ., Bratislava). Czech. J. Phys., 15: 627-36(1965).

A system of dynamic equations for the simultaneous determination of the scattering amplitude and the relativistic Jost function is derived from the Mandelstam representation and the unitarity condition. The relativistic generalization of the de Alfaro, Regge and Rossetti dynamic equation for the Jost function is given. (auth)

11704 ON A LIE GROUP OF INFINITE ORDER AS A NON-TRIVIAL COUPLING OF INTRINSIC AND SPACE-TIME SYMMETRIES. Formanek, J. (Czech Technical Univ., Prague). Czech. J. Phys., 16: 1-7(1966).

A real Lie algebra of denumerable infinite order is derived. The algebra contains the Poincaré algebra P and the algebra SU(2) as sub-algebras. The algebra reduces to the direct sum $P \oplus SU(2)$ in the limit $M_n/M_p \to 1$. (auth)

11705 THE BOOTSTRAP APPROACH TO STRONG INTERACTION SYMMETRIES. Tarjanne, Pekka (Univ. of Oulu, Finland). Fortschr. Phys., 13: 533-56(1965).

A review is given of the development and achievements of the bootstrap approach to elementary particle theory with special emphasis on its relation to the exact as well as broken internal symmetries and on the weaknesses of the presently used calculational techniques. The conjecture that the origin of unitary symmetry is completely dynamical leads to the discussion of several proposed mechanisms for spontaneous breakdown of this symmetry. The phenomenological octet enhancement found to exist in strong, electromagnetic as well as weak processes is studied in connection with the dynamical content of solutions with different symmetry character. It is also shown that in the superconductor model of elementary particle symmetries the octet enhancement can be the consequence of simple stability criteria. (auth)

11706 SCATTERING BY THE SINGULAR POTENTIAL r^{-4}. Aly, H. H. (Max-Planck-Institut fuer Physik und Astrophysik, Munich); Mueller, H. J. W. J. Math. Phys., 7: 1-9(Jan. 1966).

The potential $1/r^4$ is the only known potential more singular than the centrifugal term, for which the Schrödinger equation can be solved exactly. The potential is considered in more detail. In particular the physical S-matrix is obtained, shown to be unitary, and compared with expressions of other derivations given in the literature. The eigenvalues of the Mathieu equation are finally discussed, and the behavior of the Regge trajectories is indicated. (auth)

11707 LOCAL APPROXIMATION IN RENORMALIZABLE AND NONRENORMALIZABLE THEORIES. I. Bardakci, K.; Schroer, B. (Inst. for Advanced Study, Princeton, N. J.). J. Math. Phys., 7: 10-15(Jan. 1966).

A framework of quantum field theory is presented which is wide enough to incorporate renormalizable, as well as nonrenormalizable theories. A universal high-energy bound for matrix element of fields is derived. The "string" approximation of the two-point function for various couplings is studied. (auth)

11708 LOCAL APPROXIMATIONS IN RENORMALIZABLE AND NONRENORMALIZABLE THEORIES. II. Bardakci, K. (Inst. for Advanced Study, Princeton, N. J.); Schroer, B. J. Math. Phys., 7: 16-26(Jan. 1966).

Previous investigations are generalized to two-point matrix elements. A principle is formulated, which yields unique finite Feynman rules in the renormalizable case, i.e., permits a unique separation of counterterms. For nonrenormalizable theories this principle yields uniqueness up to a "scaling" parameter. The results are generalized to a large class of Feynman graphs. For this subset of

graphs, field-theoretical principles do not determine this scaling parameter. (auth)

11709 THE QUANTIZED COMPLEX SPACE-TIME AND QUANTUM THEORY OF FREE FIELDS. II. Das, A. (Carnegie Inst. of Tech., Pittsburgh). J. Math. Phys., 7: 52-60(Jan. 1966).

A covariant quantization of complex space–time is proposed. As a consequence of this quantization each of the four real coordinates can take discrete values $n^{1/2}l$, and furthermore, measurements of these coordinates are noninterfering with each other. Next the general theory of quantized free fields is developed in the background of quantized space–time. As an example the case of complex scalar field was dealt with and it is found that the resulting Green's functions are nonsingular. (auth)

11710 ASYMPTOTIC BEHAVIOR OF THE SCATTERING AMPLITUDE IN THE LEFT HALF-PLANE OF COMPLEX ANGULAR MOMENTUM. Dilley, J. (Ohio Univ., Athens); Barut, A. O. J. Math. Phys., 7: 64-5(Jan. 1966).

It is shown, for a certain class of analytic potentials, that the previously reported result $A(\lambda,k) \xrightarrow[|\lambda|\to\infty]{} 1/k^2V(\pm\lambda/k)$, Re $\lambda \geq 0$, where the sign ± is chosen such that $-\pi/2 \leq \arg \pm (\lambda/k) \leq \pi/2$, is valid also for Re $\lambda < 0$ except for a discrete set of points on the negative real axis. The result holds for arbitrary complex $k \neq 0$, finite or infinite. (auth)

11711 PHYSICAL REGION DECOUPLING PROCEDURE FOR COUPLED CHANNEL SCATTERING AMPLITUDES. Fleming, Gordon N. (Univ. of Washington, Seattle). J. Math. Phys., 7: 76-80(Jan. 1966).

A method for expressing unitary, coupled channel, scattering amplitudes in terms of amplitudes satisfying "uncoupled" or "elastic" unitarity equations is presented. The method is given a physical interpretation by relating the equations to equations of the Heitler type. It is shown how continuous channels may be incorporated into the formalism, in some circumstances, without requiring the solution of integral equations. The influence of inelastic channels on pure elastic scattering is mentioned briefly and a pseudoelastic form of the exact unitarity equation is discussed. No applications of the method are undertaken. (auth)

11712 ASYMPTOTIC BEHAVIOR OF PHASE SHIFT IN λ FOR STRONGLY SINGULAR POTENTIALS. Jaksic, B.; Limic, N. (International Center for Theoretical Physics, Trieste, Italy). J. Math. Phys., 7: 88-97(Jan. 1966).

The asymptotic form of the phase shift is derived for strongly singular potentials for large complex λ, $|\arg \lambda| < \frac{1}{2}\pi$, and real k. This result is valid also for usual (regular) potentials. It is shown also that the S-matrix for strongly singular potentials must have an infinite number of poles in λ-plane accumulating asymptotically in a narrow region along the imaginary axis in the first and third quadrants. (auth)

11713 REPRESENTATION OF DISCRETE SYMMETRY OPERATORS. Mariwalla, K. H. (Univ. of South Carolina, Columbia. Univ. of Georgia, Athens). J. Math. Phys., 7: 114-22(Jan. 1966).

Representations of discrete symmetry operators (DSO's) connected with space (P), time (T), and generalized charge (C) are considered. It is shown that if a DSO is written as $\exp(i\pi\Omega) \times$ a phase transformation, then (under certain conditions on Ωs) to each DSO there corresponds a set of Ωs which is closed with respect a Lie algebra, which is isomorphic to the Lie algebra of generators of rotation in an n-dimensional Euclidean space; where n is the number of commuting observables that changes sign under this DSO in a given representation (e.g. linear momentum representation). In the particular case of the (TCP) operation, there are six Ωs, of which two are diagonal, viz. the generalized charge Q, and spin projection along the z axis Sz; corresponding Euclidean group is four-dimensional. For the sake of completeness, the representations are also given for the following cases: (i) nonrelativistic quantum mechanics, (ii) quantum theory of free fields, in terms of field operators. (auth)

11714 INTERACTING FERMIONS IN ONE DIMENSION. II. ATTRACTIVE POTENTIAL. McGuire, J. B. (Florida Atlantic Univ., Boca Raton). J. Math. Phys., 7: 123-32(Jan. 1966). (BNL-9132).

The exact energies and wavefunctions for a system of (N−1) one-dimensional fermions all of the same spin and one fermion of the opposite spin are calculated in the large volume, finite density limit, when the particles interact via an attractive delta function potential. It is found that the attractive potential gives rise to a bound state, but, in spite of the presence of this bound state, all of the physical properties which are calculated (ground-state energy, effective mass of a certain class of excitations, etc.) are analytic continuations in the coupling constant of the corresponding results in the repulsive case. In addition, it is possible to have eigenstates which do not have the bound state present. These excited states are also discussed and are found to exhibit a negative effective mass and to modify the particle density at very large distances from the different particle. (auth)

11715 ON A QUANTUM FIELD THEORY WITH DEGENERATE VACUUM AND A SPECIAL TYPE OF SYMMETRY. Lopuszanski, Jan; Reeh, Helmut (Inst. for Advanced Study, Princeton, N. J.). J. Math. Phys., 7: 148-54(Jan. 1966).

A frame of a model of quantum field theory with a degenerate vacuum is investigated. At least one vacuum is cyclic. The field is covariant under a gauge transformation. The existence of non-gauge-invariant vacuum states is shown. Observables are defined as gauge-invariant operators; the algebra of these does not coincide with the algebra of the field operator; the reduction of the former algebra reflects a superselection rule. (auth)

11716 LEHMANN–SYMANZIK–ZIMMERMANN FORMALISM IN A MODEL FIELD THEORY. Scarfone, Leonard M. (Univ. of Vermont, Burlington). J. Math. Phys., 7: 159-62(Jan. 1966).

The Lehmann-Symanzik-Zimmermann (LSZ) formalism is used as a calculational method to obtain an equation for the determination of the V + N potential energy in a slightly modified Lee model. This approach to the problem is compared with the standard eigenvalue technique and the dispersion theory treatment. It is found that an exact solution to the VN − 2Nθ sector can be obtained with one algebraic equation and this evidence gives additional support to the desirability of the LSZ method as a calculational tool for the model. (auth)

11717 TRANSLATIONS OF THE DISCRETE BOSE–EINSTEIN OPERATORS. Shelupsky, David (City Univ. of New York). J. Math. Phys., 7: 163-6(Jan. 1966).

The effects on a certain family of representations of the commutation relations of the operator-translations $a_k \to a_k + c_k$, $a_k^\dagger \to a_k^\dagger + c_k^*$, are investigated. Here a_k and $a_k^\dagger$ are the annihilation and creation operators of the representations, the c_k are complex numbers (scalar operators), and the representations considered are the discrete representations described by Gårding and Wightman, and Schweber and Wightman, generalizations of the usual Fock representation. Necessary and sufficient conditions on the translations are obtained for the resultant representations to remain in the family of discrete representations, and the resultant translation groups are investigated for their relevant structure. (auth)

11718 SPACE-TIME THEORY OF ELEMENTARY PARTICLES. I. BORN RECIPROCITY PRINCIPLE. Shin, Ernest E. H. (Massachusetts Inst. of Tech., Cambridge). J. Math. Phys., 7: 167-73(Jan. 1966).

The use of the Born reciprocity principle as a postulate applied to "internal" Minkowski space leads to a theory of elementary particles based on a purely "space–time"

point of view. The reciprocity transformations of Born $(x_\mu, p_\mu) \rightarrow (\pm p_\mu, \mp x_\mu)$, form a discrete subgroup of the x-p rotation group SU(2), which is associated with isotopic spin symmetry. The full dynamic symmetry of the eight-dimensional phase space with Minkowski metric is a 36-parameter group which contains the x-p rotation group SU(2) and the homogeneous Lorentz group $\mathcal{P}$ as disjoint subgroups. This gives the symmetry of "subquantic" matter which has oscillator-rotator properties. Some physical aspects of the generators and possible forms of mass formulas for both integer and odd-half integer spins are discussed. Finally, it is suggested that the nonrelativistic counterpart of the present formalism may explain the symmetry of atomic nuclei. (auth)

11719 SPACE-TIME THEORY OF ELEMENTARY PARTICLES. II. COMPLEX MINKOWSKI SPACE FORMALISM. **Shin, Ernest E. H. (Massachusetts Inst. of Tech., Cambridge). J. Math. Phys., 7: 174-80(Jan. 1966).**

The space–time formalism of elementary particles presented previously is generalized to a complex "internal" Minkowski space described by (z_μ, ω_μ) and $(z_\mu^\dagger, \omega_\mu^\dagger)$. In this way, the dual signatures of the "superselection" operator and the odd-half spins are considered in a natural manner. The full dynamic symmetry group of the 16-dimensional phase space is a 136-parameter group $\mathcal{G}$ of which the reciprocity-invariant content is a 64-parameter group isomorphic with the 64-parameter Lie group. The complete $\mathcal{P}$-invariant subgroup of $\mathcal{G}$ is a 10-parameter group, which is identified as the five-dimensional real "Lorentz" group and which is the "unitary spin" subgroup of $\mathcal{G}$. Discussions on the various reduced or subgroup structures of $\mathcal{G}$ are given. In particular, the physical nature of the $\mathcal{P}$-invariant generators and possible forms of mass formula are discussed. (auth)

11720 SPIN AND ISOSPIN IN S-MATRIX THEORY. **Taylor, John R. (Palmer Physical Lab., Princeton, N. J.). J. Math. Phys., 7: 181(Jan. 1966).**

The Gunson–Olive technique for exploiting physical region poles and the unitarity equations to derive the analytic properties of S-matrix elements is applied to particles which belong to isospin multiplets and to particles with spin. In the former case it is shown that, in the framework of S-matrix theory, crossing symmetry leads to the requirement that particles and antiparticles transform according to complex conjugate representations; and it is possible to clarify the origin of the familiar isospin crossing matrices. In the case of particles with spin the construction of appropriate "spinor" basic states is discussed and the analytic properties of the corresponding spinor S-matrix elements or "M-functions" are derived. (auth)

11721 ON THE REPRESENTATIONS OF THE SEMI-SIMPLE LIE GROUPS. V. SOME EXPLICIT WIGNER OPERATORS FOR SU_3. **Baird, G. E. (Northrop Space Labs., Huntsville, Ala.); Biedenharn, L. C. J. Math. Phys. (N. Y.), 6: 1847-54(Dec. 1965).**

A general method for the calculation of the [21 . . . 10] Wigner operators is presented and used to obtain specific results for the SU_3 group. General expressions for the SU_3 reduced Wigner operators are given for tensor operators transforming like the representations [100], [110], and [210]. (auth)

11722 GENERALIZED SOLUTIONS FOR MASSLESS FREE FIELDS AND CONSEQUENT GENERALIZED CONSERVATION LAWS. **O'Connell, R. F.; Tompkins, D. R. (Louisiana State Univ., Baton Rouge). J. Math. Phys. (N. Y.), 6: 1952-4(Dec. 1965).**

Generalized solutions to the equations for a massless free field with arbitrary spin are given. It is shown that they lead immediately to generalizations of all the usual conservation laws. (auth)

11723 REDUCTION OF A ONE-LOOP FEYNMAN DIAGRAM WITH n VERTICES IN m-DIMENSIONAL LORENTZ SPACE. **Petersson, Bengt (Univ. of Lund, Sweden). J. Math. Phys. (N. Y.), 6: 1955-9(Dec. 1965).**

An explicit formula is given for the evaluation of a diagram with one loop and n vertices in m-dimensional Lorentz space (n > m). The result is given as a sum of terms each corresponding to a one-loop diagram with m vertices and with a coefficient which can be obtained from rules analogous to the rules of residue calculus. (auth)

11724 THE FROISSART-GRIBOV CONTINUATION AND REGGEON UNITARITY CONDITIONS. I. **Polkinghorne, J. C. (International Centre for Theoretical Physics, Trieste). J. Math. Phys. (N. Y.), 6: 1960-6(Dec. 1965).**

An identity is derived which is useful in the discussion of unitary integrals. It is used to discuss single Regge pole insertions in the Froissart–Gribov continuation and with the help of perturbation theory models a derivation is given of reggeon unitarity conditions. The general form suggested by Gribov, Pomeranchuk, and Ter-Martirosyan is confirmed. Finally cancellation mechanisms are discussed and their relation to the mechanism generating Regge poles is emphasized. (auth)

11725 ISOTOPIC SPACE, COMPLEX CONJUGATION, AND U_3 SYMMETRY FOR PARTICLES. **Teitler, S. (Naval Research Lab., Washington, D. C.). J. Math. Phys. (N. Y.), 6: 1976-9(Dec. 1965).**

The inherent U_4 symmetry over spinor spaces of the regular decomposition indicated previously is discussed from the viewpoint of a single spinor space. It is noted that this symmetry does not yet include isotopic spin. Isotopic space is introduced by considering that the space-time vectors and its vector Clifford algebra are imbedded in the algebra of a six-dimensional Euclidean space. Three of the latter's dimensions are identified with ordinary space, and three are identified with isotopic space. The time vector corresponds to the pseudoscalar element in isospace, and the imaginary unit is expressed as a linear combination of the bivectors in isospace. The relation among complex conjugation, time inversion, and space inversion is thereby clarified. Some comments on the application of these ideas to particle symmetry discussions are made. In particular one obtains as the first extension of the SU_2 symmetry of isotopic spin, a U_3 symmetry for particles. (auth)

11726 MOMENTUM-SPACE ANALYTICITY PROPERTIES OF THE BERGMAN-WEIL INTEGRAL FOR THE THREE POINT FUNCTION. **Kaellen, G. (Univ. of Lund); Toll, J. S. J. Math. Phys. (N. Y.), 6: 1885-1901(Dec. 1965).**

The momentum-space analyticity domain of the Bergman–Weil integral representation of the vertex function or three-point function is investigated using the assumption that thresholds can be introduced simply as lower limits of integration for the mass variables in the representation. It is shown that this assumption leads to a regularity domain which is larger than the domain following from general physical assumptions of Lorentz invariance, local commutativity and reasonable mass spectrum. To simplify the discussion it is also assumed that the vertex function is regular when all three complex variables lie in the same half-plane. Standard techniques for the evaluation of Feynman diagrams have proved to be inconvenient for this investigation and new methods were developed taking explicit advantage of the fact that only two external vectors exist and, hence, a two-dimensional Lorentz space is used. Further, the vanishing of the masses for certain internal lines was also exploited. The techniques might be of interest also in other connections. (auth)

11727 ELECTROMAGNETIC PROPERTIES OF MESONS IN BROKEN SU(6) SYMMETRY. **Babaev, Z. R.; Samiralov, V. S.; Solov'ev, L. D. (Joint Inst. of Nuclear Research, Dubna, USSR). JETP Lett. (USSR) (Engl. Transl.), 2: 199-201(Oct. 1, 1965).**

The electromagnetic properties of mesons were studied within the framework of SU(6) symmetry. The effect of taking into account the medium-strong interaction that leads to mass splitting within unitary multiplets was investigated. It was found that the broken SU(3) and SU(6)

symmetries lead, in the general case, to the same relations. However, if the current is assumed to be an octet, both schemes give different results. (D.C.W.)

11728 INITIAL VALUE PROBLEM FOR ELEMENTARY AND COMPOSITE PARTICLES. Sekine, Katsuhiko (Institut Henri Poincare, Paris). Nucl. Phys., 76: 513-38(1966).

Equivalence between bound states (composite particles) and elementary particles with vanishing wave function renormalization constant Z is re-examined by solving explicitly the initial value problem for a simple model. The highly singular character of the limit Z = 0 is revealed and is investigated in detail. A singular perturbation scheme is developed in the context of quantum field theory. (auth)

11729 ASYMPTOTIC RELATIONS BETWEEN CROSS SECTIONS FOR THE BARYON RESONANCE PRODUCTION. Nguyen Van Hieu; Rerikh, K. V.; Khelashvili, A. A. (Joint Inst. for Nuclear Research, Dubna, USSR). Nucl. Phys., 76: 551-5(1966).

The asymptotic equality of the cross sections of crossed inelastic processes with baryon resonance production is proved. (auth)

11730 THE SELF-CONSISTENT DETERMINATION OF THE πNN AND πNN* VERTEX FUNCTIONS. Noga, M.; Dubec, M. (Univ. Komenskeho, Bratislava). Nucl. Phys., 76: 577-87(1966).

The self-consistent method of Zachariasen and Zemach is used to calculate the πNN and πNN* vertex functions. The calculated thresholds of the special representation of these vertex functions agree with those found by Karplus, Sommerfield and Wichmann. (auth)

11731 APPLICATION OF FUNCTIONAL METHODS IN QUANTUM FIELD THEORY AND QUANTUM STATISTICS. II. Fradkin, E. S. (Lebedev Physical Inst., Moscow). Nucl. Phys., 76: 588-624(1966).

It is shown that when the interaction involves Fermi particles the divergences of the theory can only be eliminated by a suitable non-linearity of the intermediate boson field. An operator solution for the Green function in an external field is obtained. A closed expression is found for the generating functional; with its aid it is possible to develop a modified perturbation theory convenient for finding different asymptotic behaviors for the Green function. (auth)

11732 DISPERSION RELATIONS IN THE COMPLEX ANGULAR MOMENTUM PLANE AND THE SOMMERFELD-WATSON TRANSFORMATION. Lopez, C. A. (Univ., Chile, Santiago). Nucl. Phys., 76: 672-6(1966).

Dispersion relations for the S-matrix in the complex plane $\lambda = l + \frac{1}{2}$ for the class of potentials considered by Regge are written down. From them, the values of $S_l(k)$ for integral l are obtained, which, after been introduced into the partial wave expansion for the scattering amplitude, turn into the Sommerfeld-Watson transformation. This transformation is therefore shown to be an immediate consequence of the dispersion relations. Finally, potentials which only differ from the previous ones by the addition of an attractive term of the form $1/r^2$ are considered, in order to get the modifications introduced by the presence of a cut along the real axis. (auth)

11733 THEORIES OF INTERACTING FIELDS WITH SPIN 1. Ogiyevetsky, V. I.; Polubarinov, I. V. (Joint Inst. for Nuclear Research, Dubna, USSR). Nucl. Phys., 76: 677-83(1966).

A new derivation is given of the symmetries characteristic for the theories of interacting vector fields with spin 1. A direct connection between the requirement that virtual vector quanta transfer spin 1 and the gauge invariance of such theories in the zero mass limit of vector fields is discussed. (auth)

11734 THE MASS RENORMALIZATION IN THE BROKEN SL(6) SYMMETRY. Nguyen Van Hieu (Joint Inst. for Nuclear Research, Dubna, USSR). Nucl. Phys., 77: 680-8(1966).

The renormalization of the masses and the coupling constants in the broken SL(6) symmetry is considered by means of the Lagrange formalism of quantum field theory. Some mass relations are obtained on the basis of the assumption that the part of the interaction Lagrangian which breaks the unitary symmetry is a component of some 35-plet. The existence of the meson multiplets containing spin-2 particles is also discussed. (auth)

11735 MESON-BARYON SCATTERING IN THE SPURION SCHEME OF BROKEN $U_{\mathcal{F}12}$-SYMMETRY. Lai, C. S. (Univ. of Chicago). Nuovo Cimento (10), 41A: 1-11(1966). (COO-264-260)

Meson-baryon scattering is discussed in the spurion scheme of broken $U_{\mathcal{F}12}$-symmetry. With the insertion of a momentum-dependent spurion S, there are now twelve amplitudes, instead of four in the strict $U_{\mathcal{F}12}$-scheme. The scattering amplitude T(s,t) for many meson-baryon reactions is calculated explicitly in terms of these twelve amplitudes. The validity of sum rules is discussed in some detail. (auth)

11736 AN INTEGRAL REPRESENTATION FOR HIGH-ENERGY SCATTERING AMPLITUDES. Luming, M.; Predazzi, E. (Univ. of Chicago). Nuovo Cimento (10), 41A: 22-34(1966).

The approximation of converting the partial-wave expansion into an integral over the impact parameter, at high energies, is reviewed in some detail. This approximation is independent of any dynamical assumptions and is not confined to small scattering angles, provided the momentum is sufficiently large so that the error, which is of order 1/p, can be kept small. The integral representation thus obtained for asymptotic scattering amplitudes has a spectral function that satisfies a simple unitary relation. An alternate form of the representation is also derived which turns out to be a natural extension of the usual eikonal approximation to large scattering angles. An example is presented to illustrate the application of the integral representation. (auth)

11737 UNITARY REPRESENTATIONS AND RELATIVISTIC COUPLING COEFFICIENTS FOR $SL_{2,C}$. Bisiacchi, G.; Fronsdal, C. (International Center for Theoretical Physics, Trieste). Nuovo Cimento (10), 41A: 35-47(1966).

$SL_{2,C}$ coupling coefficients are calculated for some unitary representations of physical interest. The connection between the unitary irreducible representations of $SL_{2,C}$ and the ordinary spin is shown and the expression of the invariant vertex function is given in terms of physical states. As an example a vertex that includes the decay of a spin-1 particle into two spin-0 particles is calculated. (auth)

11738 ON A PROBLEM OF MAXIMUM IN DISPERSION THEORY. Lukaszuk, L. (CERN, Geneva). Nuovo Cimento (10), 41A: 67-76(1966).

A technique is presented for finding maximal bounds on strengths of interaction when the general inequality of the type arising from dispersion relations is given. It is shown that for quite a large class of functionals involved in such inequalities the solution exists and is unique. (auth)

11739 SUM RULES IN POTENTIAL SCATTERING. II. Chadan, K. (Laboratoire de Physique Theorique et Hautes Energies, Orsay, France). Nuovo Cimento (10), 41A: 116-21(1966).

Sum rules obtained previously for potentials of finite radius are generalized to the case of potentials extending to infinity. (auth)

11740 SOME SU_n CROSSING MATRICES. Cook, C. L.; Murtaza, G.; Rashid, M. A. (Imperial Coll. of Science and Tech., London). Nuovo Cimento (10), 41A: 122-6(1966).

Generalized crossing matrices for arbitrary SU_n, covering many cases of physical interest, are given. They include those involving the regular representation and an arbitrary completely symmetric irreducible representation, and also

the one associated with the system [3] + [3] → [3] + [3]. (auth)

11741 ON SU_3 VECTOR COUPLING COEFFICIENTS. Ponzano, G. (Univ., Turin). Nuovo Cimento (10), 41A: 142-58(1966).

Algebraic techniques are used to calculate several particular SU_3 coupling coefficients. Two equivalent expressions for the general nonorthonormalized isoscalar factor are discussed. (auth)

11742 SINGLE-COLLISION APPROXIMATION. Trammell, G. T.; Chalk, J. D. (Rice Univ., Houston, Tex.). Phys. Rev., 141: 815-24(Jan. 1966). (TID-22113).

The scattering of a projectile by a target which is bound in a potential is considered. The collision matrix is represented as a power series in the free-projectile–target t matrix; the retention of only the first term of the series constitutes the single-collision approximation (sca). The impulse approximation follows from the sca upon neglecting the effect of the acceleration of the projectile-target center of mass during the collision; it may be called the short-time approximation (sta). An approximation to the sca is considered which takes into account the effect of the potential on the motion of the c.m. during the collision, but neglects the effect of the potential on the relative projectile-target motion during this time. Its validity depends upon the negligibility of the variation of the target potential over the range of the projectile-target interaction, and it is called the short-range approximation (sra). The sta and sra are supplementary and partially overlapping. Expressions are derived for the reaction amplitudes in the sra in terms of the free-particle scattering amplitudes (analytically continued to negative energies). In the sra the criteria for the validity of the sca are examined. A class of multicollision graphs are summed in order to include the effect of bound projectile-target intermediate states on the reaction amplitudes. These states then appear as resonances with finite widths if the energy is below pickup threshold. The results are generalized to allow for a third potential acting on the projectile, and to allow for a finite mass of the third (potential-producing) particle. (auth)

11743 BARYON MAGNETIC-MOMENT SUM RULES IN BROKEN SU_3 AND SU_6 SYMMETRIES. Kawarabayashi, K. (International Center for Theoretical Physics, Trieste); Wada, W. W. Phys. Rev., 141: 1322-4(Jan. 1966). (COO-1261-7).

The φ-ω mixing model for the breaking of SU_3 symmetry was used to obtain sum rules for the magnetic moments of the octet baryons in broken SU_3 and SU_6. The contributions of the vector couplings are assumed to be dominant over those of the tensor couplings in the self-energy effects of the model. It is found that the sum rules obtained are consistent with the magnetic moments of SU_6 symmetry (Coleman-Glashow relations plus $\mu_p = -\frac{3}{2}\mu_n$) modified by appropriate mass ratios only under very restrictive choice of values for the parameters that occur in the model. (auth)

11744 LINEAR AND NONLINEAR MASS-DIFFERENCE EFFECTS IN A MODEL OF THE BARYON MULTIPLETS. Ernst, Frederick J. (Illinois Inst. of Tech., Chicago); Warnock, Robert L.; Wali, Kameshwar C. Phys. Rev., 141: 1354-72(Jan. 1966).

The breaking of SU(3) symmetry is studied in two models: (a) the $J^P = \frac{3}{2}^+$ decuplet states formed as composites of baryons and mesons through baryon exchange, and (b) the $J^P = \frac{1}{2}^+$ octet states formed also as composites of baryons and mesons through decuplet exchange. In both models symmetry-breaking effects are introduced as mass splittings within the component baryon and meson octets. Expansion of dispersion integrals in powers of mass differences is employed to discuss sum rules for masses and coupling constants. In first order the expected results are obtained when the Gell-Mann–Okubo mass rule holds for the component particle masses; i.e., the GMO rule also holds for the composite particle masses, and the coupling constants of composite to component particles obey the known sum rules. However, a comparison of exact and first-order dispersion integrals in model (a) shows that the first-order approximation is quite poor. Therefore, the approximate propagation of the GMO rule from component to composite masses that was found in earlier work cannot be explained as merely a reflection of the first-order result. Significant higher order effects conspire to preserve nearly equal spacing of the decuplet masses. A mass-difference perturbation theory of eigenvalues and eigenvectors of the scattering matrix is presented, together with a review of the decomposition of perturbations by irreducible tensor operators. In the case of model (b), "octet enhancement" is verified (i.e., the intrinsic preference of the bootstrap equations for octet-type perturbations). This discussion of octet enhancement, and a similar one of Dashen and Frautschi, is criticized on two grounds: linearization in mass differences is not justified, and the neglect of decuplet states in external lines might be a serious error. Inclusion of the external decuplet states is necessary for vertex symmetry. It is found that vertex symmetry is difficult to reconcile with other general requirements in approximations based on the ND^{-1} method. (auth)

11745 LEE MODEL WITH AN UNSTABLE V-TYPE PARTICLE. Luke, T. M. (Univ. of Western Ontario, London). Phys. Rev., 141: 1373-80(Jan. 1966).

The solution is given to a modified Lee model in which there is a resonance having the quantum numbers of the usual V particle. It is demonstrated that all channels having the same quantum numbers are coupled by the integral equations; in particular, "unphysical" amplitudes involving unstable external particles are coupled to the physical amplitudes through solutions to homogeneous integral equations of the Omnes-Muskhelishvili type. (auth)

11746 THEORY AND CALCULATION OF SCATTERING WITH THE BETHE-SALPETER EQUATION. Schwartz, Charles; Zemach, Charles (Univ. of California, Berkeley). Phys. Rev., 141: 1454-67(Jan. 1966).

The Bethe-Salpeter equation studied describes the interaction of two scalar particles via the exchange of a third scalar particle in the ladder approximation. The properties of the Green's function and the potential in coordinate space are shown to permit a Wick rotation to an imaginary time variable, without appeal to information not contained in the original equation. The resulting four-dimensional (Euclidean) wave equation has a solution which grows exponentially for large time-like distances but behaves as an ordinary Schrödinger scattering wave for large space-like distances. A modification of the Schwinger variational principle is used to obtain, with a modest use of computing machinery, scattering phase shifts for various angular momenta and for energies below the inelastic threshold. The success of these calculations indicates that the Bethe-Salpeter equation can be accepted as a powerful and practical tool for the study of strong-interaction dynamics. (auth)

11747 APPLICATION OF THE SCHWINGER VARIATIONAL PRINCIPLE FOR SCATTERING. Schwartz, Charles (Univ. of California, Berkeley). Phys. Rev., 141: 1468-70(Jan. 1966).

The usual difficulty of having to evaluate double integrals with $G(x,x')$ is avoided by considering as the trial function $U(x) = V(x)\psi(x)$ and its Fourier transform. Numerical calculations of s-wave scattering by a Yukawa potential were carried out both by means of this form of Schwinger's method and also by using Kohn's variational principle. For comparable trial functions, the latter method appears to converge faster. (auth)

11748 CURRENT ALGEBRAS AND MESON SYSTEMS. Schnitzer, Howard J. (Brandeis Univ., Waltham, Mass.). Phys. Rev., 141: 1484-8(Jan. 1966).

The algebra of compact $U(6) \times U(6)$, obtained from integrated current components, is applied to meson systems. If the sums over intermediate states are limited to the lowest lying 36 SU(3)-invariant pseudoscalar and vector meson physical states at rest, then several of the predictions of SU(6) models are obtained. On considering the

commutation rules of magnetic-moment operators additional relations are also obtained. Among these are $\langle r_\pi^2 \rangle = \langle r_\rho^2 \rangle$ and $\mu_\rho^2 = 1/6 \langle r_\rho^2 \rangle$ relating the electric charge radii to the meson(ρ) magnetic moment, with a pole model giving 2 magnetons for the meson(ρ) total magnetic moment. Also $\langle r_\pi^2 \rangle/6 \simeq 1.6/M_{V\rho}^2$ is found using an additional consistency relation, in rough agreement with the vector-meson pole model. However, the radius of electric charge form factors is predicted to be the same as that of the divergence of the axial-vector current form factors, which disagrees with present ideas about these form factors. (auth)

11749 SELF-ENERGY LOOP OF THE CHARGED VECTOR MESON. Wellner, Marcel (Syracuse Univ., N. Y.). Phys. Rev., 141: 1497-8(Jan. 1966).

The vector-meson self-energy loop is examined to second order in the electric charge. The renormalizability of this diagram implies a simple relation between the electric and magnetic dipole moments of the meson. If parity is conserved, then two discrete values of the gyromagnetic ratio are allowed. For all other possible values of this ratio one must introduce an electric dipole (i.e., give up parity conservation and time-reversal invariance) to make the diagram renormalizable. (auth)

11750 VECTOR-MESON DECAYS IN U(6) CURRENT ALGEBRA. Fayyazuddin (Univ. of Wisconsin, Madison); Riazuddin; Razmi, M. S. K. Phys. Rev., 141: 1509-13 (Jan. 1966).

Decay constants for various decays of vector mesons and their magnetic and quadrupole moments are calculated by using equal-time commutation relations for weak hadron currents, which generate the algebra of U(6). (auth)

11751 THEORY OF REGGEIZED BOOTSTRAPS. Abbe, W. J.; Kaus, P.; Nath, P.; Srivastava, Y. N. (Univ. of California, Riverside). Phys. Rev., 141: 1513-23(Jan. 1966).

Using a representation for the partial-wave S matrix developed recently, a representation for the total scattering amplitude is constructed with Regge trajectories as the sole input. The resulting representation has the following properties regardless of the number of trajectories included: It has the correct analytic structure; namely, the double spectral function is nonvanishing in a region bounded by the curved boundaries implied by the Mandelstam representation. It is unitary. It gives the correct threshold behavior for both the real and imaginary parts of the total amplitude. It converges rapidly. A potential theory example is worked out explicitly and with one trajectory input, numerically an excellent agreement with the exact result for the total amplitude is obtained. The representation is then generalized to the relativistic case. Invoking crossing, a set of relatively simple bootstrap equations is obtained for a self-consistent determination of the Regge trajectories. Also, an alternative procedure is proposed which imposes approximate crossing symmetry in the unphysical region to determine the Regge parameters. The latter method is operationally more attractive since it obviates solving any dispersion integrals, and also has the added advantage of avoiding inelasticity. Finally, in this method, no statements (or approximations) regarding the I = 2 channel need be made, since the latter can be eliminated from the appropriate crossing relation. (auth)

11752 VECTOR-VECTOR-PSEUDOSCALAR INTERACTIONS. Kundu, S. K. (Australian National Univ., Canberra). Phys. Rev., 141: 1529-32(Jan. 1966).

Vector-vector-pseudoscalar (V-V-PS) interactions are interpreted exclusively in terms of baryon loops, and application is made to radiative decay of bosons. The model appears to give a highly satisfactory account of A-forbiddenness; it also agrees with at least one decay that is A-allowed, suggesting that intrinsic V-V-PS couplings are of secondary importance. (auth)

11753 SU_4 MASS FORMULA AND PARTICLE CLASSIFICATION SCHEMES. Antoine, J.-P. (Univ. Louvain, Heverle, Belg.); Speiser, D.; Oakes, R. J. Phys. Rev., 141: 1542-53(Jan. 1966).

The mathematical derivation of the general mass formula of SU_4 is given. The derivation is preceded by a survey of the mathematical aspects of the group SU_4 and its representations. The possible elementary-particle symmetry schemes based on the Lie algebra of SU_4, most of which have already been proposed, are classified and systematically discussed. The extension of SU_4 to SU_8 by inclusion of ordinary spin is discussed and shown to rule out two of the three classes of models. Finally, a simple SU_8 model is sketched. (auth)

11754 EQUIVALENT FIELD THEORIES AND ELEMENTARY-PARTICLE DEMOCRACY. Zimmerman, Robert L. (Univ. of California, Livermore). Phys. Rev., 141: 1554-9(Jan. 1966). (UCRL-14384-T).

It is shown how one can eliminate various fields from a lagrangian to obtain a new lagrangian, wherein the theories obtained from the two lagrangians are equivalent. In general the lagrangian obtained by eliminating various fields is nonlocal. In some cases under certain requirements it can be made local. These requirements are equivalent to having the wave-function renormalization constants of the eliminated fields vanish. The results are fully illustrated by various examples. In particular, for the case of the Yukawa coupling, it is shown that if we require the lagrangian obtained by eliminating the boson field to be local then this is equivalent to the vanishing of the wave-function renormalization constant of the boson field. From the examples it is surmised that the creation of elementary-particle democracy is achieved by eliminating various fields from the lagrangian and requiring all the final self-interacting lagrangians to be local. (auth)

11755 RELATIVISTIC COMBINATION OF INTERNAL AND SPIN SYMMETRIES IN S-MATRIX FORMULATION. Ekstein, H. (Argonne National Lab., Ill.). Phys. Rev., 141: 1560-71(Jan. 1966).

The relativistic combination of internal and spin symmetries is considered as a restriction on the scattering operator. A physical principle for the statement of symmetries other than space-time is formulated. In the simplest case, the intuitive idea that interactions do not depend on some observables is expressed by the statement that the S operator belongs to a subring of the ring of observables. This principle leads to the usual results for purely internal symmetries, for spin independence of forces, and also for their combinations as in Wigner's supermultiplet theory. The combination of Poincaré group, spin independence, and internal symmetry leads to a group which is not a (finite-dimensional) Lie group and not locally compact. Nevertheless, simple homomorphic representations of the little group exist and suffice for physical applications. The nonrelativistic SU(6) multiplet structure and the selection rules are unchanged in the relativistic case. In addition to the deficiencies of the nonrelativistic model, the relativistic S operator has highly unrealistic properties, although it is not trivial ($S \neq 1$). A scheme for symmetry breaking is described which may be expected to remedy these deficiencies. (auth)

11756 THREE-BARYON STATES IN SU(6) THEORY. Ram, Budh (Univ. of North Carolina, Chapel Hill). Phys. Rev., 141: 1581-2(Jan. 1966).

Three-baryon states with hypercharge Y = 3 and Y = 2 are classified in SU(6) theory of strong interactions. Some examples of the reactions in which these states might be observed are given. (auth)

11757 FREDHOLM METHOD FOR BETHE-SALPETER EQUATION. Graves-Morris, P. R. (Cambridge Univ., Eng.). Phys. Rev. Lett., 16: 201-3(Jan. 31, 1966).

A method for making the Bethe-Salpeter equation Fredholm is outlined. The method is essentially one for systematic removal of poles or logarithms in kernels of linear integral equations, when both the inhomogeneous term and kernel have the same functional dependence on the parameter variables as distinct from integration variables. (G.O.Y.)

11758 COMPLEX INHOMOGENEOUS LORENTZ GROUP AND COMPLEX ANGULAR MOMENTUM. Roffman, Eric H. (Brandeis Univ., Waltham, Mass. New York Univ., New York). Phys. Rev. Lett., 16: 210-11(Jan. 31, 1966).

It is shown that the property of generalizing integral or half-integral angular momentum and the property of characterizing the asymptotic behavior of the S matrix in the crossed channel can both be derived from group-theoretical arguments. (G.O.Y.)

11759 PARTICLES OF ARBITRARY SPIN IN CURVED SPACES. Dowker, J. S.; Dowker, Y. P. (The Univ., Manchester, Eng.). Proc. Phys. Soc., 87: 65-78(Jan. 1966).

A generalization of two-spinor calculus, useful in the discussion of particles with arbitrary spin, is extended to generally covariant form. The spinor connection and curvature are derived in general form, and the analogy between spin and charge is made explicit by consideration of commutators of covariant derivatives. The generation of the gravitational field by the Yang-Mills trick is briefly discussed. (auth)

11760 THE BINARY COLLISION EXPANSION OF DOUBLE-TIME-TEMPERATURE-DEPENDENT GREEN'S FUNCTIONS. Tsai, C. H.; Hsu, H. H. (Nanking Univ., China). Wu Li Hsueh Pao, 21: 1785-97(Oct. 1965). (In Chinese).

The method of binary collision expansion was employed to obtain series developments in powers of the scattering length between two particles for double-time-temperature-dependent Green's functions of statistical mechanics. The cases of Bose and Fermi statistics were studied as well as the case of a Bose system in the presence of a condensed phase, and rules were established for computation of the successive terms of expansion with the aid of diagrams. The present method is applicable to many particle systems with strong and short-ranged mainly repulsive two-body interactions. (auth)

11761 SCATTERING MATRIX FOR FINITE TIMES IN INTERACTING PARTICLE WAVE FUNCTION SPACE. Alekseev, V. V. (Moscow State Univ.). Zh. Eksp. Teor. Fiz., 49: 1470-4(Nov. 1965). (In Russian).

For a nonrelativistic system with a given number of particles it is shown how an operator $S(t,t_0)$ which transforms the exact solution in the interaction representation $\Psi_{B3}(t_0)$ at a time t_0 to an exact solution $\Psi_{B3}(t)$ at time t can be found by a method which somewhat differs from the usual one. In the space of these states the S-matrix is unitary and the coefficient functions $S(t,t_0)$ can be expressed in terms of the wave functions of the problem, including the bound states. (auth)

11762 AXIOMATIC CONSTRUCTION OF THE SCATTERING MATRIX. 4. LAGRANGIAN FORM OF THE THEORY. Medvedev, B. V. (Steklov Inst. of Mathematics, Academy of Sciences, USSR). Zh. Eksp. Teor. Fiz., 49: 1518-25(Nov. 1965). (In Russian).

It is shown that the axiomatic theory can, at least formally, be presented in a lagrangian form. Conditions that should be imposed on the lagrangian in order to ensure that the scattering matrix be causal and unitary are considered. (auth)

11763 ON NONUNIQUE SOLUTIONS FOR THE PROBLEM ON SCATTERING. Kirzhnits, D. A. (Lebedev Inst. of Physics, Moscow). Zh. Eksp. Teor. Fiz., 49: 1544-55 (Nov. 1965). (In Russian).

The dynamic, axiomatic and dispersion methods as applied to the scattering model of nonrelativistic particles with point interaction are compared. The number of solutions of the corresponding equations, the analytic properties of the scattering amplitude and the origin of superfluous solutions are determined. A short summary of the results is presented. (auth)

11764 RESTRICTIONS ON THE ELASTIC SCATTERING CROSS SECTIONS IN THE DIFFRACTION PEAK REGION. Malkov, E. I. (Ioffe Inst. of Physics and Tech., Leningrad). Zh. Eksp. Teor. Fiz., 49: 1558-61(Nov. 1965). (In Russian).

It is shown that if the real part of the elastic scattering amplitude is smaller than the imaginary part in the diffraction peak region, then the unitarity condition imposes an upper limit on the elastic scattering cross section. (auth)

11765 QUANTUM FIELD THEORY EQUATIONS IN THE AXIOMATIC APPROACH. Kallosh, R. E.; Fainberg, V. Ya. (Lebedev Inst. of Physics, Moscow). Zh. Eksp. Teor. Fiz., 49: 1611-23(Nov. 1965). (In Russian).

It is shown that within the framework of the axiomatic formulation of quantum field theory the indefinite quasilocal terms can be expressed through the R-functions for fixed values of some invariants. The invariant properties of the retarded matrix elements or ν-function are effectively used in this case. It is shown that on the mass shell the ν-functions in the physical region of variation of 4-momenta depend only on the invariant scalar products of the 4-vectors. The procedure for excluding the quasilocal terms yields explicit equations for an arbitrary matrix element (n-tail graph) in an integro-differential and difference form. The equations contain a finite number of arbitrary parameters, boundary values or charges, which are equal to the number of amplitudes which do not vanish at infinity. (auth)

Fluid Physics and Thermodynamics

See also Plasma Physics and Thermonuclear Processes

Refer also to abstract 11431.

11766 (AWRE-O-82/65) THE FUNDAMENTAL EQUATIONS OF RADIATION HYDRODYNAMICS. Fraser, A. R. (Atomic Weapons Research Establishment, Aldermaston (England)). Jan. 1966. 24p. Dep. BIS $0.80. HMSO 4s.

The radiative transfer equation is derived for an absorbing and scattering fluid in motion. The equations of hydrodynamics are extended to include terms due to the radiation field. (auth)

11767 (HMI-B-42) STATIONAERE UEBERSCHALLSTROEMUNGEN UM ALLGEMEINE KEGEL UND DIE GRUNDLAGEN IHRER NUMERISCHEN BERECHNUNG. (Stationary Supersonic Flow in a Common Cone and the Basis of its Numerical Calculation). Bruhn, G. (Hahn-Meitner-Institut fuer Kernforschung, Berlin (West Germany)). Sept. 1965. 59p. Dep. mn.

The problem of stationary supersonic flow in a common cone was formulated considering the special flow symmetry through the use of two independent variables. The basic assumptions are given and are represented in an integral form. The general non-isotropic case is considered. The case of constant entropy was studied as an approximation. Numerical calculations based on the equations derived are given. (J.S.R.)

11768 (JUL-327-PP) IONIZATION OF HYDROGEN AND NITROGEN IN AN UNIFORM MAGNETIC FIELD INCREASING WITH TIME. Beerwald, Hans (Kernforschungsanlage, Juelich (West Germany). Institut fuer Plasmaphysik). Nov. 1965. 9p. (CONF-650836-2). Dep. mn.

From 7th International Conference on Phenomena in Ionized Gases, Beograd, Yugoslavia.

The temporal growth of electron density during the formation of ring discharges in damped oscillating strong magnetic fields was studied. Discharges of this type can be produced in magnetic fields, generated by the discharge of a capacitor bank. The electron density shows characteristic jumps each time when the magnetic field passes through zero. Near zero the magnetic field depends linearly on time. The study of ionization can be limited to these time intervals, since for the rest of the time ioniza-

tion seems to be negligible. The multiplication of the electron density was measured in hydrogen and nitrogen by means of microwaves. A simplified interpretation of the results is given. (auth)

11769 (LGI-65/30) THE EXPERIMENT ON THE ELECTRICAL BREAKDOWN IN VACUUM AT LABORATORIO GAS IONIZZATI. Gourlan, C.; Maisonnier, Ch.; Samuelli, M. (Laboratorio Gas Ionizzati, Comitato Nazionale per l'Energia Nucleare, Frascati (Italy)). Nov. 1965. 23p. Dep. mn.

A review is made of the theories of breakdown in vacuum, and an experiment is described in which electron prebreakdown currents are prevented to reach the anode by means of a transverse magnetic field. (auth)

11770 (ORNL-P-1005) ON THE POSSIBILITY OF EXCITATION-HEATING OF IONS TO HIGH TEMPERATURE. McNally, J. Rand Jr. (Oak Ridge National Lab., Tenn.). [1964]. Contract W-7405-eng-26. 3p. Dep. mn. CFSTI $1.00 cy, $0.50 mn.

The observation of carbon ions up to 100 times hotter than the electrons in very long, steady state, high current, magnetically-confined, carbon and gas-fed carbon arcs suggest the presence of a new type of energy pumping mechanism, which is referred to as excitation-heating. The particular pumping cycle under consideration is discussed. (M.O.W.)

11771 (NP-tr-1346) MAGNETOHYDRODYNAMICS OF LIQUID METALS. Kirko, Igor' Mikhailovich. Translation of Zhidkii Metall v Elektromagnitom Pole, Publishing House Energiya, Moscow, 1964. 85p. Consultants Bureau. $17.50.

The physics of MHD phenomena is discussed. Solutions to MHD problems involving plane-parallel flow with transverse magnetic field and traveling magnetic fields are obtained. Technical applications of the magnetohydrodynamics of liquid metals are discussed. Specific applications toward electromagnetic conduction and induction pumps are discussed. (M.O.W.)

11772 BASIC CONCEPT OF THE GENERAL RELATIVISTIC MAGNETOHYDRODYNAMICS FOR IDEAL CONDUCTORS. Schoepf, Hans-Georg (Univ. Greifswald, Ger.). Ann. Phys. (7), 16: 114-21(1965). (In German).

As the basis of the derivation of general relativistic magnetohydrodynamics for ideal conductors it is assumed that the method developed earlier for relativistic continuum mechanics can be treated in a very transparent manner to lead to some new significant results. It is shown first that in the reference system which moves relative to the matter purely magnetostatic behavior occurs. This fact leads to a quasimechanical determination of the electromagnetic energy-pulse-voltage complex. The possibility of treating weak collision waves is obtained from this. Some non-relativistic relations given by Carstoiu were generalized for the case of rigid motion of material. (tr-auth)

11773 THE OPTICAL EXCITATION IN NEGATIVE GLOW DISCHARGE LIGHT OF A HOLLOW CATHODE DISCHARGE. Falk, Heinz (Institut fuer Optik und Spektroskopie der DAW, Berlin). Ann. Phys. (7), 16: 160-73(1965). (In German).

The excitation of impure gases in the hollow cathode was investigated using the example of chlorine with helium as a carrier gas. It can be shown that the electron velocity in the glow discharge light was limited by the carrier gas. The limiting energy for the excitation of the impure gases in the hollow cathode were found to be in agreement with experiment. Metastable atoms of the carrier gases could play a role only for the excitation of low levels of the impure gas or its ionization. The hollow cathode can be explained only from the increase of the photoeffect through the cathode geometry. The current dependence of the intensity of the chlorine spectrum was discussed and the increase of the ionization degree of the chlorine with increasing current was determined. (tr-auth)

11774 MIXING PHENOMENA IN NON-STATIONARY GLOW DISCHARGES. Deutsch, H. (E.-M.-Ardnt-Univ., Greifswald, Ger.). Ann. Phys. (7), 16: 174-83(1965). (In German).

Systematic investigations were carried out on the frequency dependence of the alternating current mixing phenomena. It was shown that the mixing phenomena is limited to low-frequency alternating-current discharges. In the studies it was proven advantageous to produce the mixing phenomena with pulse discharges. The supposed origin of the mixing phenomena in non-stationary discharges was indicated. (tr-auth)

11775 MEASUREMENTS OF THE DISTRIBUTION OF PRESSURE BEHIND STRONG SHOCK WAVES. Fedulov, V. I.; Borman, V. D. At. Energ. (USSR), 19: 446-8(Nov. 1965). (In Russian).

The pressure distribution on the front of a shock wave produced in an electric-discharge shock tube was studied. The energy of the electric discharge is used to increase the temperature of the propelling gas in the tube. The circumstances that the time of the electric discharge is comparable to that of the opening of the diaphragm and that the discharge power is not constant in time contribute to the excitation of inhomogeneities in the shock-wave front. Results of the dependence of the pressure at the shock-wave front on the velocity of the wave are shown. (M.J.T.)

11776 SLOW STEADY MAGNETODYNAMIC MOVEMENT OF AN ELECTRICALLY CONDUCTING VISCOUS FLUID IN A SPHERICAL ENVELOPE. [PART] I. Agostinelli, Cataldo. Atti Accad. Naz. Lincei, Rend., Cl. Sci. Fis., Mat. Nat., 38: 296-303(Mar. 1965). (In Italian).

The questions which relate to a slow steady motion of a viscid and electrical conducting fluid, in a moving spherical rigid envelope, which is plunged in a uniform magnetic field, has particular interest for the study of the inner magnetism of the earth. The stationary magnetohydrodynamic equations in the case of small velocity and weak induced magnetic field are considered, and meanwhile it is shown that the vortex vector and the conductive current verify a differential equation of the fourth order. After the vortex vector and the conductive current are determined in a point within the sphere when their values are assigned on the surface. (auth)

11777 SLOW STEADY MAGNETODYNAMIC MOVEMENT OF AN ELECTRICALLY CONDUCTING VISCOUS FLUID IN A SPHERICAL ENVELOPE. [PART] II. Agostinelli, Cataldo. Atti Accad. Naz. Lincei, Rend., Cl. Sci. Fis., Mat. Nat., 38: 448-53(Apr. 1965). (In Italian).

The slow steady motion of a viscid and electrical conducting fluid, in a moving spherical rigid envelope, plunged in a uniform magnetic field is considered. First it is shown that the velocity of the fluid particles verifies the same differential equation of the fourth order which is satisfied by the vortex vector and the conductive current. After this the velocity of the fluid particles and the inducted magnetic field at a point within the sphere are determined when their values are assigned on the surface. (auth)

11778 HYDROMAGNETIC FLOW AGAINST A ROTATING DISC. Jagadeesan, K. (Indian Inst. of Tech., Kharagpur). Bul. Inst. Politeh. Iasi, 10: 81-6(1964).

Hydromagnetic flow against a rotating disk is investigated theoretically. Equations for the flow are developed, and Karman's integral method is used to study the boundary value problem. Tables and figures show the effects of magnetic field strength on velocity profiles and boundary layer thickness. It is observed that torque increases with increasing magnetic field. (A.G.W.)

11779 STUDY OF THE STRUCTURE OF A SHOCK WAVE FOR A GAS WITH DISCRETE DISTRIBUTIONS OF VELOCITIES. Gatignol, Renee (Institut Henri Poincare, Paris). Compt. Rend., 261: 2841-4(Oct. 11, 1965). (In French).

The structure of a shock wave is discussed in the cases of compression and reflection on a plane wall, for a gas consisting of identical particles of which the number of possible velocities is reduced to 6; these particles, opposed

two by two, have the same modulus and have for support the edges of a trirectangular trihedron. (tr-auth)

11780 THE INITIATION OF HIGH-FREQUENCY ELECTRIC DISCHARGE IN RARE GASES IN THE PRESENCE OF A LONGITUDINAL MAGNETIC INDUCTION. Bacri, Jean; Benoit-Cattin, Pierre; Blanc, Daniel; Dagnac, Rene; Ferre, Jean (Faculte des Sciences, Toulouse). Compt. Rend., 261: 2859-61(Oct. 11, 1965). (In French).

With a capacitive coupling, the role that a uniform magnetic induction, parallel to the high frequency electric field (80 MHz), plays is established as a function of the pressure (from 10^{-4} to 1 torr). A theoretical calculation shows the importance of the geometric dimensions of the discharge tube. (tr-auth)

11781 INDUCTIVE CHARGED FLUIDS OF FINITE CONDUCTIVITY. Bruhat, Yvonne. Compt. Rend., 261: 3545-8(Nov. 3, 1965). (In French).

It is shown that the equations of relativistic inductive charged fluids of finite conductivity, such as were obtained by Pichon from the non-symmetrized momentum-energy tensor, form a non-strict hyperbolic system in the sense of Leray and Ohya. (tr-auth)

11782 THERMODYNAMICS OF CHARGED FLUIDS. Bruhat, Yvonne; Pham-Mau-Quan (Institut Henri-Poincare, Paris. Institut de Mathematiques, Lille, France). Compt. Rend., 261: 3987-90(Nov. 15, 1965). (In French).

A relativistic model of charged fluids in the presence of electromagnetic inductions and thermal exchanges was studied. The equation of heat and the equations of motion are derived. The Cauchy problem and characteristic varieties are considered and discussed. (tr-auth)

11783 CONSTRUCTION OF A MAGNETOHYDRODYNAMIC MODEL OF A CYCLONE. [PART] II. Khantadze, A. G. (Inst. of Geophysics, Academy of Sciences, Georgian SSR). Geomagn. Aeronomy (USSR) (Engl. Transl.), 5: 320-2(1965).

Translated from Geomagn. Aeronomiya, 3: 413-16(1965).

The motion of a rotating ideal compressible, conducting fluid is analyzed. (auth)

11784 KINETIC THEORY OF NUCLEAR SPIN RELAXATION IN GASES. Gordon, R. G. (Harvard Univ., Cambridge, Mass.). J. Chem. Phys., 44: 228-34(Jan. 1, 1966).

A theory of nuclear spin relaxation in linear molecules is developed for dilute gases and mixtures. The main assumptions used are those often employed in the kinetic theory of dilute gases: binary collisions, no correlation between the effects of successive binary collisions, and classical mechanics for the molecular translational and rotational motion. The calculations result in expressions relating the spin relaxation times to the rotational angular momentum transferred by collisions. Using the results, it is possible to calculate the spin relaxation times for any given intermolecular potential which includes angle-dependent terms. (auth)

11785 VIBRATIONAL RELAXATION OF DEUTERIUM BY A QUANTITATIVE SCHLIEREN METHOD. Kiefer, John H.; Lutz, Robert W. (Los Alamos Scientific Lab., N. Mex.). J. Chem. Phys., 44: 658-67(Jan. 15, 1966). (LA-DC-7384).

A quantitative schlieren method is described which uses photomultiplier detection of the deflection of a narrow gas-laser beam to obtain a close approximation to a point measure of density gradient. This method is very sensitive to rapid density changes (a gradient of 5×10^{-5} g/liter·mm can be detected in argon) and laboratory relaxation times as short as 0.2 μsec can be measured in the shock tube. The application of this technique to studies of vibrational relaxation is discussed in detail, and the method is compared with the integrated schlieren of Resler and Scheibe for this application. This technique was applied to a shock-tube study of the vibrational relaxation of mixtures of D_2 in Ar with the results, in atmosphere·seconds, $P\tau = (2.7 \pm 0.3) \times 10^{-10} \exp[(110.5 \pm 1.5)/T^{1/3}]$, (1100°–3000°K) for pure D_2, and $P\tau = (1.0 \pm 0.7) \times 10^{-9} \exp[(118 \pm 10)/T^{1/3}]$, (1600°–3000°K) for D_2 dilute in Ar. The experimental results are in serious disagreement with both the correlation scheme of Millikan and White and the SSH theory. (auth)

11786 VIBRATIONAL RELAXATION OF HYDROGEN. Kiefer, John H.; Lutz, Robert W. (Los Alamos Scientific Lab., N. Mex.). J. Chem. Phys., 44: 668-72(Jan. 15, 1966). (LA-DC-7480).

The laser schlieren technique was applied to a shock-tube study of hydrogen vibrational relaxation. Mixtures of 30%, 50%, and 70% normal hydrogen in argon were investigated in the range 1100°–2700°K. The results yield an expression for relaxation in pure hydrogen, $P\tau_{H_2-H_2} = (3.9 \pm 0.8) \times 10^{-10} \exp[(100.0 \pm 2.6)/T^{1/3}]$ atm·sec (1100°–2700°K), and allow an approximate determination of the relaxation time for hydrogen dilute in argon, $P\tau_{H_2-Ar} = 4.1\ P\tau_{H_2-H_2}$ (1500°–2700°K). These results are in adequate agreement with previous data and the theoretical calculations of Salkoff and Bauer. However, they are in serious disagreement with both the correlation of Millikan and White and the SSH theory. (auth)

11787 ON THE SURFACE TENSION OF ISOTOPIC MIXTURES. Bellemans, A.; Fuks, S. (Univ. Libre, Brussels). J. Chem. Phys., 44: 834-5(Jan. 15, 1966).

Recent data on the surface tension of H_2-D_2, H_2-HD, and HD-D_2 mixture are compared to Englert-Chwoles and Prigogine's theory, which expresses the excess surface tension of an isotopic mixture as the sum of a dynamic term and an adsorption term. (L.B.S.)

11788 DISTRIBUTION OF ZEROS OF THE GRAND PARTITION FUNCTION. Hemmer, P. C.; Hauge, E. Hiis; Aasen, J. O. (Norges Tekniske Hoegskole, Trondheim, Norway). J. Math. Phys., 7: 35-9(Jan. 1966).

The distribution of zeros of the grand partition function is calculated in the thermodynamic limit for a class of one-dimensional gas models in two ways: from the equation of state and directly from the partition function. In this way (for these cases) a verification of the assumptions that were made in order to associate a unique distribution of zeros with a given equation of state is obtained. In the Appendix some numerical evidence for the validity of these assumptions is presented also in the case of the van der Waals gas. (auth)

11789 THERMODYNAMIC EVOLUTION EQUATION FOR A QUANTUM STATISTICAL GAS. Fujita, S. (Pennsylvania State Univ., University Park). J. Math. Phys. (N. Y.), 6: 1877-85(Dec. 1965).

It is shown by a perturbation diagram method that partial Green's functions satisfy closed evolution equations exact in the thermodynamic limit except for the neglect of the contribution of initial particle correlations. This contribution is negligible for a system at a time $t \gg r_c$ (average collision duration) when the main interaction processes are localized in space and time. In particular this makes unnecessary the often imposed assumption of the absence of initial particle correlations for the derivation of the usual Boltzmann equation or its generalizations. (auth)

11790 MAGNETOHYDRODYNAMIC BOUNDARY LAYER. Lyubimov, G. A. Magnit. Gidrodin., No. 3, 3-20(1965). (In Russian).

A survey is presented of studies of the theory of a laminar magnetohydrodynamic boundary layer for magnetic Reynolds number $Re_m \leq 1$ and $Re \gg 1$, with the principal attention being paid to the physical and mathematical formulations of the problem. The applications of the one-dimensional theory to the calculation of flow core are considered. Magnetohydrodynamic interaction is examined with respect to flow in channels. It is shown that for the case of the magnetohydrodynamic boundary layer Maxwell's equations of the electric field must be added to the boundary layer equations. A system of equations for a viscous magnetohydrodynamic boundary layer, with $Re_m \leq 1$, is derived for the elementary case of an isotropically con-

ducting, weakly ionized medium. The characteristic features of this system are analyzed. It is shown that friction and heat transfer decrease with increase in the magnetic field applied. The problem of the flow of an incompressible fluid around a dielectric plate in a uniform field normal to the plate in the presence of fixed and variable conductivity is discussed. (ATD)

11791 PLANE MAGNETOHYDRODYNAMIC FLOW. Tsinober, A. B.; Shcherbinin, E. V. Magnit. Gidrodin., No. 3, 21-9(1965). (In Russian).

General solutions for two-dimensional jets of conductive fluid in the presence of a random transverse magnetic field were obtained. Induced magnetic field is neglected, i.e., $Re_m \ll 1$. (auth)

11792 INTEGRAL METHODS IN ELECTROCONDUCTING FLUID JET THEORY. Shcherbinin, E. V. Magnit. Gidrodin., No. 3, 30-6(1965). (In Russian).

An example of the integral relation method for solving laminar electroconducting jets in the uniform transverse magnetic field is presented. (auth)

11793 EFFECTS OF TRANSVERSE MAGNETIC FIELD ON CONVECTIVE HEAT TRANSFER IN CONDUCTING FLUID FLOW IN A CHANNEL. Krasilnikov, E. Yu. Magnit. Gidrodin., No. 3, 37-40(1965). (In Russian).

The effect of a transverse magnetic field on the convective heat transfer is considered in the case of conducting fluid flow in a channel formed by two parallel plates. For turbulent flow the solution is obtained by a numerical method. The results of calculations give a simple approximate relation for conductive heat transfer computation. (auth)

11794 ON DISSIPATIVE INSTABILITY IN MAGNETOHYDRODYNAMICS. Sanochkin, Yu. V. Magnit. Gidrodin., No. 3, 61-6(1965). (In Russian).

The effect of energy dissipation and temperature dependence of transfer coefficients on the development of short-wave disturbances in magnetohydrodynamics is considered. Criteria for stability and disturbance growth rate near the stable region boundary for different cases are obtained. (auth)

11795 FLOW NEAR THE STAGNATION POINT IN THE PRESENCE OF MAGNETIC FIELDS PARALLEL AND NORMAL TO THE BODY SURFACE. Denisov, Yu. N.; Zalogin, G. N.; Kalashnikov, V. K. Magnit. Gidrodin., No. 3, 81-6(1965). (In Russian).

Two-dimensional inviscid flow of an incompressible fluid with finite electric conductivity is investigated near the stagnation point before a cylindrical magnet. The shock-wave near the stagnation point is considered to be coaxial with the cylinder. Equations of motion in cylindrical co-ordinates with boundary conditions given by the Hugeniot relations were obtained. Numerical calculations of the equations are performed by Runge-Kutte's method provided constant density in the shock layer. In case of a parallel magnetic field, contrary to the normal one, there are no substantial changes in radial and tangent velocity components near the stagnation point with varying MHD parameter S. (auth)

11796 REFLECTION OF A HYDROMAGNETIC SHOCK ON A RIGID WALL. Verma, B. G. (Univ. of Gorakhpur, India). Nuovo Cimento (10), 41B: 9-14(1966).

Conditions were obtained for regular stationary reflection of a hydromagnetic shock on a rigid wall. Certain other theorems in the same connection were derived. (auth)

11797 RELATIVISTIC TRANSFORMATION LAWS FOR THERMODYNAMIC VARIABLES. Kibble, T. W. B. (Imperial Coll. of Science and Tech., London). Nuovo Cimento (10), 41B: 72-8(1966).

General remarks are given on the relativistic transformation laws of thermodynamic variables. The specific case of the total energy is discussed, and is illustrated with the example of cavity radiation. The work done in changing the volume or pressure of the system is then considered. A demonstration is given of the necessity for, and physical reality of, the kind of energy flux that plays an important role in the conventional treatment of the stressed lever. The conclusions are briefly summarized. (L.B.S.)

11798 SCALAR FORMULATION OF IDEAL CHARGED GAS FLOW. Schmid, Lawrence A. (Goddard Space Flight Center, Greenbelt, Md.). Phys. Fluids, 9: 102-10(Jan. 1966).

In the case of adiabatic flow of an ideal electron or ion gas in the presence of gravitational and electromagnetic fields, it is possible to derive a system of scalar equations of motion for the gas that provides an alternative to the Euler formulation. The new dynamical variables that replace the velocity are three scalars, one of which is a generalization of the flow potential and satisfies a generalized Hamilton–Jacobi equation. The other two are constants of motion that specify the intrinsic vorticity, which is that part of the total vorticity that is not produced by the external fields, but rather is simply a residue of the initial conditions of the gas. It is this intrinsic vorticity that satisfies the generalization of the simple vorticity conservation theorem. The same formalism can be adapted to the case of constant-temperature flow and to the flow of an arbitrary barotropic fluid. (auth)

11799 EXISTENCE OF TWO PHASES IN ONE-DIMENSIONAL CLASSICAL FLUIDS. Andrews, F. C.; Benson, J. M. (Univ. of Wisconsin, Madison). Phys. Lett., 20: 16-17(Jan. 15, 1966).

The equilibrium position of 1000 classical, one-dimensional particles interacting through a square-well potential of finite energy range were studied using Monte Carlo techniques. At a low temperature, the particles form condensed droplets separated by essentially empty space. (auth)

11800 ON THE THEORY OF DROPLET FORMATION IN ONE-DIMENSIONAL FLUIDS. Andrews, F. C. (Univ. of Wisconsin, Madison). Phys. Lett., 20: 17-19(Jan. 15, 1966).

A heuristic argument is given to show why droplets form in one-dimensional classical fluids at sufficiently low temperatures. The average droplet size was then calculated exactly for nearest-neighbor square-well interaction in the limit of a large system. (auth)

11801 ANALYSIS OF A BOSON MODEL DISPLAYING A PHASE TRANSITION. Bassichis, W. H. (Centre d'Etudes Nucleaires de Saclay, Gif-sur-Yvette, France. Weizmann Inst. of Science, Rehovoth, Israel); Disantnik, Y. Phys. Rev., 141: 217-21(Jan. 1966).

The simple boson model proposed by Foldy, which displayed a discontinuity in its energy as a function of interaction strength, is studied using symmetry arguments, the method of linearized equations of motion, and perturbation theory. The particular symmetry responsible for the discontinuity, or phase transition, is pointed out. The method of linearized equations is shown to predict the transition value of the interaction strength and, like the Bogoliubov approximation, to accurately describe the energy of the first excited state. It is further shown that simple perturbation theory is quite accurate except in the transition region. The validity of that feature of the Bogoliubov method in which excited states are described by independent quasiparticles is examined. This description is found to be excellent in the normal region. All comparisons are made with a numerical solution which provided the complete energy spectrum and the associated eigenvectors. It is hoped that these arguments can be applied in considerations of the validity of the various approximations for realistic systems. (auth)

11802 BROWNIAN MOTION OF CHARGED PARTICLES IN CROSSED ELECTRIC AND MAGNETIC FIELDS. Liboff, Richard L. (Cornell Univ., Ithaca, N. Y.). Phys. Rev., 141: 222-7(Jan. 1966).

A new method for evaluating the Brownian motion of

charged particles in crossed electric and magnetic fields is presented. In the problems considered, a steady B_z field and radial electric field are embedded in a viscous medium. Calculations are made for the three-dimensional mean-square displacement of particles migrating away from the cylindrical axis. The results are applied to the theory of sheaths to uncover the manner in which the wall charge affects the familiar Debye displacement. The resulting formula is independent of the presence of a magnetic field parallel to the wall. Relaxing the electric conditions yields the Brownian motion of a neutral particle in a neutral viscous fluid. (auth)

11803 ELECTRIC FIELD IN A MAGNETOHYDRODYNAMIC CHANNEL IN THE PRESENCE OF A MOVING MEDIUM WITH AN ALTERNATING ELECTRIC CONDUCTANCE. Regirer, S. A.; Rutkevich, I. M. Prikl. Mat. Mekh., 29: 870-8(Sept.-Oct. 1965). (In Russian).

The motion of an isotropic conducting medium in a rectangular channel in a magnetic field is studied, assuming that the velocity of the longitudinal flow is everywhere constant, that the magnetic field, having longitudinal and transverse components, is independent of time, and that the conductivity of the medium is a periodic function of time and the longitudinal coordinate. Equations for the flow are obtained, and solutions for the electric-field distribution in the fluid are considered for specific functions describing the conductivity, magnetic field, and velocity. (M.J.T.)

11804 ON THE DAMPING OF HOMOGENEOUS TURBULENCE IN A MAGNETIC FIELD. Eliseev, B. V. Prikl. Mat. Mekh., 29: 961-5(Sept.-Oct. 1965). (In Russian).

The linearized MHD equations for the motion of a conducting incompressible fluid in a magnetic field are written and solved, using a Fourier transformation, for arbitrary initial values of the kinetic and magnetic energies. The solution is studied for $R = 1$ and $R \to \infty$, where $R = 4\pi\sigma\nu/c^2$, σ being the conductivity and ν the kinematic viscosity of the fluid. For $R = 1$, when the magnetic and kinematic viscosities are equal, correlations between the velocity and the magnetic field fall faster than other correlations; the magnetic and kinematic energies decrease asymptotically as $t^{-3/2}$. Fulfillment of the condition $R \gg \tau \gg 1$, where τ is the dimensionless time, is studied for $R \to \infty$; here, the magnetic energy and the correlations between velocity and magnetic field decrease asymptotically as $t^{-3/2}$. It is shown that taking the electric-field fluctuations into account would not change the results obtained. (M.J.T.)

11805 NOTE ON THE MOTION OF LOW-ENERGY HYDROGEN IONS IN HYDROGEN. Dutton, J.; Williams, E. M. (Univ. Coll. of Swansea, Eng.). Proc. Phys. Soc., 87: 339-41(Jan. 1966).

Values of the mobility and collision cross section obtained for ions of measured mean energy in hydrogen are discussed in relation to other, recently published, values of mobility. The discussion shows that further measurements of mobility are required for ions of experimentally established identity and measured mean energy. (auth)

11806 ELECTRICAL CORONAS, THEIR BASIC PHYSICAL MECHANISMS. Loeb, Leonard B. Berkeley, Calif.; Los Angeles; University of California Press, 1965. 713p. $14.00.

Phenomena involving corona discharges are analyzed in terms of basic mechanisms. Various gap forms in use are presented, and fundamental relations pertinent to electrical breakdown are summarized. Discussions are given of true coronas produced by highly stressed positive electrode with negligible cathode influence; true coronas produced by highly stressed cathode with the anode playing a minor role; asymmetrical gaps with both electrodes participating, producing pseudo coronas in coaxial cylindrical geometry, for highly stressed anode and cathode; and symmetrical gaps with nonuniform fields at both electrodes. Gases are treated in which the electrons exist as free electrons and in which the electrons attach to make negative ions. (M.J.T.)

Geophysics

Refer also to abstracts 11783, 12194, and 12228.

11807 (UCRL-7495(Rev. 1)) CHERENKOV ELECTROMAGNETIC RADIATION FROM A NUCLEAR DETONATION IN SPACE. Colgate, S. A.; Yee, K. S. (Lawrence Radiation Lab., Univ. of California, Livermore). Dec. 12, 1964. Contract W-7405-eng-48. 43p. Dep. mn. CFSTI $2.00 cy, $0.50 mn.

It is predicted that a nuclear detonation above the earth's atmosphere will give rise to an electromagnetic pulse that is in phase with the emitted gamma ray pulse. The maximum electric field at the earth's surface several hundred kilometers from a detonation may reach a limiting breakdown value of 300 v/cm with the electric vector directed opposite to the direction of gamma ray propagation. The origin of the pulse depends upon the Cherenkov-like radiation from the gamma ray produced Compton electron current distribution moving across the top of the earth's atmosphere at a phase velocity greater than that of light. The time behavior of the pulse in first order is independent of the thickness of the earth's atmosphere in which the gamma rays are absorbed. (auth)

11808 TWO-DIMENSIONAL FLOW OF AN ELECTRICALLY CONDUCTING MEDIUM IN THE PRESENCE OF MASS FORCES AND A FLAT MAGNETIC FIELD. Khantadze, A. G. (Inst. of Geophysics, Academy of Sciences, Georgian SSR). Geomagn. Aeronomy (USSR) (Engl. Transl.), 5: 323-6(1965).

Translated from Geomagn. Aeronomiya, 3: 417-22(1965).

Some particular solutions of equations of magnetohydrodynamics are obtained that are of interest in the study of gradient winds and cyclonic motion in a conducting atmosphere. (auth)

11809 RELATIONSHIP BETWEEN E_s AT MIDDLE AND LOW LATITUDES AND ELECTRODYNAMIC CONDITIONS IN THE IONOSPHERE. Fatkullin, M. N. (Inst. of Terrestrial Magnetism, Ionosphere and Radio Wave Propagations, Academy of Sciences, USSR). Geomagn. Aeronomy (USSR) (Engl. Transl.), 5: 335-9(1965).

Translated from Geomagn. Aeronomiya, 3: 435-41 (1965).

An attempt is made to relate the origin of the most characteristic types of E_s in the ionosphere at middle and low latitudes with S_q currents in the E region. The E_s-layer effect in S_q variations is discussed briefly. (auth)

11810 IONOSPHERIC-MAGNETIC DISTURBANCES IN YEARS OF MAXIMUM SOLAR ACTIVITY. Dolgova, E. I. (Inst. of Terrestrial Magnetism, Ionosphere and Radio Wave Propagation, Leningrad). Geomagn. Aeronomy (USSR) (Engl. Transl.), 5: 340-5(1965).

Translated from Geomagn. Aeronomiya, 3: 442-9(1965).

Charts of the distribution of L disturbances are constructed, and the presence of a maximum in intensity and in the latitude of propagation of L disturbances at definite hours of universal time is established. $D_{st}(\Delta f_0F_2)$ are determined for several high-latitude stations. Differences are found in the diurnal variation of $(\Delta \int_0 F2)$ and absorption for types SC and G storms. (auth)

11811 INTERPRETATION OF OBSERVATIONS OF SUDDEN COMMENCEMENTS OF MAGNETIC STORMS IN SPACE. Ivanov, K. G. (Inst. of Terrestrial Magnetism, Ionosphere and Radio Wave Propagation, Academy of Sciences, USSR). Geomagn. Aeronomy (USSR) (Engl. Transl.), 5: 362-6(1965).

Translated from Geomagn. Aeronomiya, 3: 471-6(1965).

It is shown that simultaneous observations of the magnetic field and plasma in space during the SC of March 27, 1961, satisfy the conditions at the front of an oblique magnetohydrodynamic shock wave and serve as an argument for the fact that this sudden commencement was caused by a shock wave. It is assumed that the sudden decrease of the magnetic field in space during the SC of December 2, 1963, was caused by the passage of a tangential disconti-

nuity, formed during the supersonic motion of a corpuscular stream with a force-free magnetic field in interplanetary space. (auth)

11812 DISTURBED SOLAR-DIURNAL VARIATIONS AT HIGH LATITUDES DURING THE IGY. Fel'dshein, Ya. I.; Zaitsev, A. N. (Inst. of Terrestrial Magnetism, Ionosphere and Radio Wave Propagation, Academy of Sciences, USSR). Geomagn. Aeronomy (USSR) (Engl. Transl.), 5: 367-74 (1965).

Translated from Geomagn. Aeronomiya, 3: 477-86(1965).

The space-time distribution of the disturbance vector at high latitudes during the IGY is examined. It is shown that the maximum values of the horizontal projection of the disturbance vector in local winter corresponds to the location of the auroral zone. A westerly current flows along the oval zone. (auth)

11813 PROPERTIES AND NATURE OF GEOMAGNETIC MICROPULSATIONS WITH PERIODS FROM 10 SEC TO SEVERAL MINUTES. Zybin, K. Yu. (Inst. of Terrestrial Physics, Academy of Sciences, USSR). Geomagn. Aeronomy (USSR) (Engl. Transl.), 5: 380-3(1965).

Translated from Geomagn. Aeronomiya, 3: 494-8(1965).

The main patterns of behavior of geomagnetic pulsations with periods from 10 sec to several minutes are described. The two types of pulsations found in the above range of periods, regular (Pc) and irregular (Pi), possess significantly different properties. Possible mechanisms of the formation of these types of micropulsations are discussed. (auth)

11814 STATISTICAL ANALYSIS OF THE MAIN PART OF THE GEOMAGNETIC FIELD. I. GENERAL THEORY. Kautzleben, H. (Geomagnetic Inst., Academy of Sciences, German Democratic Republic). Geomagn. Aeronomy (USSR) (Engl. Transl.), 5: 387-93(1965).

Translated from Geomagn. Aeronomiya, 3: 502-10(1965).

The spherical analysis of the main part of the geomagnetic field is supplemented by a study of statistical parameters. A method is proposed for taking several exactly comparable samples from world magnetic charts. A method of analyzing the samples from the viewpoint of probability theory is described. (auth)

11815 STATISTICAL ANALYSIS OF THE MAIN PART OF THE GEOMAGNETIC FIELD. II. ANALYSIS OF WORLD MAGNETIC CHARTS OF THE 1955.0 EPOCH. Kautzleben, H. (Geomagnetic Inst., Academy of Sciences, German Democratic Republic). Geomagn. Aeronomy (USSR) (Engl. Transl.), 5: 394-401(1965).

Translated from Geomagn. Aeronomiya, 3: 511-21(1965).

The world magnetic charts of the U. S. Navy Hydrographic Office for the 1955.0 epoch are subjected to statistical analysis. Three samples of 306 points each are examined individually and jointly. A mathematical model of the main part of the field is obtained in the form of a series of the magnetic potential with coefficients for the internal part of order up to n = 6 and for the external part of order up to n = 2 inclusive. The scatter of observations with reference to this model is ~250 γ. Some conclusions are made concerning the properties of the interior of the earth. (auth)

11816 COMPUTATION OF THE GEOMAGNETIC FIELD AT GREAT HEIGHTS. Adam, N. V.; Ben'kova, N. P.; Tyurmina, L. O. (Inst. of Terrestrial Magnetism, Ionosphere and Radio Wave Propagation, Academy of Sciences, USSR). Geomagn. Aeronomy (USSR) (Engl. Transl.), 5: 402-7(1965).

Translated from Geomagn. Aeronomiya, 3: 522-8(1965).

The distributions of the Z component of the magnetic field at heights of 1000, 5,000, and 10,000 km, for the 1955 epoch, computed by the integral method and by spherical analysis, are compared. It is found that the differences between the computed Δ do not exceed 400 γ at the 100-km level, 100 γ at the 5000-km level, and 50 γ at the 10,000-km level. The planetary distribution of Δ is similar to the distribution of the external part of the constant field, obtained from spherical analysis. Recommendations are made for computing the magnetic field at great heights from surface data. (auth)

11817 OPTIMUM METHOD OF RECORDING THE FREQUENCY OF FREE NUCLEAR PRECESSION IN THE PRESENCE OF NOISE. Blagoveshchenskaya, E. E.; Gol'tsman, F. M.; Rotshtein, A. Ya. (Leningrad State Univ. Inst. of Terrestrial Magnetism, Ionosphere and Radio Wave Propagation, Academy of Sciences, USSR). Geomagn. Aeronomy (USSR) (Engl. Transl.), 5: 426-31 (1965).

Translated from Geomagn. Aeronomiya, 3: 554-62(1965).

The statistical theory of reception is used to obtain mathematical algorithms of optimum signal analysis when measuring the frequency of free nuclear precession. The maximum measurement accuracy is estimated and the dependence of accuracy on various signal analysis parameters is investigated. Some possibilities of using electronic digital computers and similar devices for practical optimum analysis are discussed. The data obtained can be used in the design of nuclear geomagnetometers. (auth)

11818 TWENTY-SEVEN-DAY VARIATIONS OF GEOMAGNETIC FIELD DISTURBANCE ON ZERO-DAYS OF COSMIC-RAY INTENSITY. Dorman, L. A.; Koiava, V. K.; Koridge, V. G.; Shatashvili, L. Kh. (Inst. of Geophysics, Academy of Sciences, Georgian SSR). Geomagn. Aeronomy (USSR) (Engl. Transl.), 5: 435-7(1965).

Translated from Geomagn. Aeronomiya, 3: 566-8(1965).

A study was made of the relation of 27-day cosmic-ray variations with the geomagnetic field variations. The principal method of analysis consisted of comparing Chree diagrams for K indices, averaged over eight latitudinal zones, as well as the characteristics of geomagnetic disturbance, Kp. It is concluded that the most sensitive solar wind indicator is the characteristic disturbance of geomagnetic field in the auroral zone. (L.B.S.)

11819 SOME CHARACTERISTICS OF THE RELATIONSHIP BETWEEN AURORAS AND MAGNETIC DISTURBANCES. Zaitseva, S. A. (Polar Geophysical Inst., Academy of Sciences, USSR). Geomagn. Aeronomy (USSR) (Engl. Transl.), 5: 454-7(1965).

Translated from Geomagn. Aeronomiya, 3: 585-8(1965).

The results of observations with an S-180 camera are compared with the records of the magnetic variation station at Murmansk (ϕ = 64°N) to ascertain how the sign of a bay is determined by the structure and movement of auroras (i.e., how auroras are associated with emf), what forms are associated with ionospheric currents, and how the relative orientation of arcs and currents varies throughout the day. An attempt is also made to establish the character of relation between the δH component of the magnetic disturbance vector and auroral intensity from observations at Laparskaya (ϕ = 64°N) in the winter of 1963–1964. (L.B.S.)

11820 LIMIT ON STABLY TRAPPED PARTICLE FLUXES. Kennel, C. F.; Petschek, H. E. (Avco-Everett Researh Lab., Everett, Mass.). J. Geophys. Res., 71: 1-28 (Jan. 1, 1966).

Whistler-mode noise leads to electron pitch angle diffusion. Similarly, ion cyclotron noise couples to ions. This diffusion results in particle precipitation into the ionosphere and creates a pitch angle distribution of trapped particles that is unstable to further wave growth. Since excessive wave growth leads to rapid diffusion and particle loss, the requirement that the growth rate be limited to the rate at which wave energy is depleted by wave propagation permits an estimate of an upper limit to the trapped equatorial particle flux. Electron fluxes >40 kev and proton fluxes >120 kev observed on Explorers 14 and 12, respectively, obey this limit with occasional exceptions. Beyond L = 4, the fluxes are just below their limit, indicating that an unspecified acceleration source, sufficient to keep the trapped particles near their precipitation limit, exists. Limiting proton and electron fluxes are roughly equal, suggesting a partial explanation for the existence of larger

densities of high-energy protons than of electrons. Observed electron pitch angle profiles correspond to a diffusion coefficient in agreement with observed lifetimes. The required equatorial whistler mode wide band noise intensity, 10^{-2}_{γ}, is not obviously inconsistent with observations and is consistent with the lifetime and with limiting trapped particle intensity. (auth)

11821 EXPERIMENTAL OBSERVATIONS OF PROTON WHISTLERS FROM INJUN 3 VLF DATA. Shawhan, Stanley D. (Univ. of Iowa, Iowa City). J. Geophys. Res., 71: 29-45 (Jan. 1, 1966).

A new vlf phenomenon named a proton whistler was identified in the vlf data from Alouette 1 and Injun 3 satellites. Two independent analyses on 12% of the proton-whistler Injun 3 data were conducted: a semimonthly sample of data for Injun 3's 10-month lifetime to determine the gross features of proton whistlers; and a local nighttime and local daytime study of proton whistlers. Six assertions are made from these experimental observations: (1) Proton whistlers are observed only after the reception of an upward-propagating electron whistler. (2) At a frequency termed the crossover frequency (ω_{12}), the initial electron whistler frequency-time trace and the proton whistler trace are coincident in time. (3) Proton whistler traces show initially a rapid rise in frequency which starts at ω_{12} and which asymptotically approaches the proton gyrofrequency Ω_1 (200–650 cps for altitudes of 2700 to 400 km). (4) Proton whistlers occur more frequently during local nighttime than during local daytime, and they have not been observed to occur below 442 km during local nighttime or below 640 km during local daytime. (5) The ratio of the crossover frequency to the proton gyrofrequency increases with decreasing altitude and approaches unity at an altitude of approximately 440 km around local midnight and approximately 640 km around local noon. (6) There is an apparent northern hemisphere–southern hemisphere asymmetry in the occurrence of proton whistlers; they occur 3 times more frequently in the northern than in the southern hemisphere. Also, there is a high-latitude boundary in the occurrence of proton whistlers that seems to correspond with the auroral zone. The theory describing proton whistlers due to Gurnett is summarized. (auth)

11822 FRACTIONAL CONCENTRATION OF HYDROGEN IONS IN THE IONOSPHERE FROM VLF PROTON WHISTLER MEASUREMENT. Shawhan, Stanley D.; Gurnett, Donald A. (Univ. of Iowa, Iowa City). J. Geophys. Res., 71: 47-59 (Jan. 1, 1966).

The derivation and the accuracy of an expression relating the fractional concentration of H^+, $\alpha_1 = n(H^+)/n_e$, to the crossover frequency ω_{12} for a vlf proton whistler are discussed. To an accuracy of $\pm 3\frac{1}{2}\%$ it is found that $\alpha_1 = (264/255)(1 - \Lambda_{12}^2)$, where $\Lambda_{12} = \omega_{12}/\Omega_1$ and Ω_1 is the proton gyrofrequency. Values of α_1 are deduced from measurement of proton whistler spectrograms for some of the satellite Injun 3 vlf data and plotted against altitude (400–2600 km) and against invariant latitude (20–63°) for summer daytime and winter nighttime of 1963. The fractional concentration of H^+ is found to be higher for winter nighttime than for summer daytime at all altitudes and latitudes; the ratio is approximately 3:1 at 1000 km. At 1000 km the value of α_1 drops from 0.43 in the 20–30° invariant latitude range to 0.27 in the 40–45° range for summer daytime. For winter nighttime α_1 is nearly constant at 0.82 for 1000 km from 30 to 50° latitude, but drops to 0.75 in the 50–63° latitude range. Near 2400 km for summer daytime, α_1 drops from 0.65 at 46° latitude to 0.20 at 56° latitude. This same tendency is observed for winter nighttime, apparently being due to auroral-zone heating. These observations are consistent with the assumption that the heavier ions tend to predominate with increasing latitude for a given altitude. Comparison of these vlf proton whistler results for α_1 is made with reasonably good agreement to rocket ion mass spectrometer results of NASA 8.23 and to Alouette 1 vlf results deduced from lower hybrid resonance frequency. This general agreement establishes the vlf radio technique as an independent method for determining ion concentrations in the ionosphere. The general equations for uniquely determining the concentration of O^+, He^+, and H^+ from observation of the critical frequencies (crossovers, hybrid resonances, and cutoffs) due to the presence of ions are presented, and their usage is discussed. (auth)

11823 LOW-ENERGY ELECTRONS IN THE DARK MAGNETOSPHERE. Serlemitsos, P. (Univ. of Maryland, College Park). J. Geophys. Res., 71: 61-77 (Jan. 1, 1966).

A number of observations on satellite data are presented which pertain to low-energy (~100 kev) electrons in the dark magnetosphere and which were obtained with a scintillation counter aboard Explorer 14. It is shown that the trapping region near the magnetic midnight meridian and at low magnetic latitudes extends on quiet days to distances in excess of 12 R_e. The extent of this region and the morphology of electrons near its outer boundary are shown to have a pronounced dependence on geomagnetic activity. Electrons trapped in the distant geomagnetic field are shown to have a pitch-angle distribution whose maximum is along the field lines and which undergoes a 90° change through a region of near isotropic electron fluxes, generally located at about 7 to 8 R_e, near the equatorial plane. Evidence is presented to the effect that the distant field as deduced from the anisotropic features of trapped electrons is highly distorted, having an almost radial appearance and showing a tendency to align itself along the earth-sun direction. A case was found in which trapped electrons in this region displayed a net flow away from the earth over a 3-minute interval. Finally, it is shown that electron fluxes outside the trapping region and specifically in the tail of the magnetosphere are essentially isotropic, that they appear in pulse-like events clustered around the geomagnetic equatorial plane (at least up to 16 R_e), and that the frequency of their occurrence decreases with geocentric distance. (auth)

11824 MIDLATITUDE TRANSITION BAYS AND THEIR RELATION TO THE SPATIAL MOVEMENT OF OVERHEAD CURRENT SYSTEMS. Rostoker, Gordon (Univ. of British Columbia, Vancouver). J. Geophys. Res., 71: 79-95 (Jan. 1, 1966).

An analysis of the occurrence frequency of midlatitude geomagnetic bays gives strong support to the polar electrojet configuration of Akasofu, Chapman, and Meng. Modifications of that current system, combined with an emphasis on the importance of differential movement of the overhead current system with respect to an observer, result in consistent explanations of the form of most geomagnetic bay phenomena. A study is made of phenomena termed transition bays, and the dependence of the form of geomagnetic bays on latitude is investigated. It is shown that D bays show a drop in occurrence frequency around local midnight relative to the number of events before and after. This dip is shown to identify the demarcation line for the average current system for the bay. Subauroral and polar-cap stations may lie in a cancellation zone so that the H component of the disturbance has its contribution from the electrojet almost canceled by the contribution from the overhead return current. It is shown that there are two separate causes of geomagnetic bays, and their manifestations are discussed in detail. (auth)

11825 TRAPPED PROTONS OF THE INNER RADIATION BELT. Fillius, R. Walker (State Univ. of Iowa, Iowa City). J. Geophys. Res., 71: 97-123 (Jan. 1, 1966).

Satellite Relay 1 performed a thorough mapping of the energy spectrum and spatial distribution of protons in the inner zone. New intensity maps are presented for six energy ranges between 1.1 and 63 Mev as of January 1, 1963. With these six distributions and previously published intensities accurate energy spectra can be constructed at arbitrarily selected locations throughout most of the inner zone. The Relay 1 data compare favorably with those of other experiments and unify the knowledge of the proton distributions. In any energy range the maximum intensity is found at the equator, and varies along a line of force near the equator as the third or fourth power of 1/B. There

are fewer high-energy than low-energy protons, and they are found closer to the earth. Neutron albedo sources, both cosmic ray and solar proton sources, are weaker than required by as much as four orders of magnitude at 1 Mev. Adiabatic breakdown theories are in disagreement with the spatial dependence of the energy spectrum and can not be controlling factors. Injection and diffusion of solar wind particles is a possible source, but more theoretical work is needed to clarify the expected results. (auth)

11826 SPATIAL AND TEMPORAL CHARACTER OF FAST VARIATIONS IN AURORAL-ZONE X RAYS. **Barcus, J. R.; Brown, R. R.; Rosenberg, T. J. (Univ. of California, Berkeley). J. Geophys. Res., 71: 125-41(Jan. 1, 1966).**

Fast pulsations, characterized by half-widths of 2 to 10 seconds and temporal spacings of 4 to 30 seconds, in the intensity of auroral-zone x rays were investigated using simultaneous pairs of balloon-borne detectors with spatial separations of approximately 100 to 200 km. Such events, usually of an hour's duration, occur almost exclusively in the midnight to dawn sector (0200 to 0800 local hours) and appear preferentially on the equatorward side of the auroral zone. Spectral analysis shows the phenomena to be nonstationary but suggests that quasi-periods of 5 to 10 seconds ought to be considered a significant feature of the process responsible for such variations. Cross-correlation studies confirm the limited spatial extent of individual pulsations, on the average, and further indicate the possibility of longitudinal motions. Microburst events, characterized by scores of transient bursts of about 200-msec half-width, occur most frequently around local noon, favoring the late morning and early afternoon. There appears to be little average latitude dependence across the auroral zone. Individual events, however, may be quite restricted in latitude. On one occasion, microbursts were observed for the better part of 3 hours at L = 5.5 in the absence of similar activity at L = 6.5, suggesting a rather localized magnetospheric origin. (auth)

11827 TRANSITION REGION MAGNETIC FIELD AND POLAR MAGNETIC DISTURBANCES. **Fairfield, D. H. (Pennsylvania State Univ., University Park); Cahill, L. J. Jr. J. Geophys. Res., 71: 155-69(Jan. 1, 1966).**

The Explorer-12 measurements of the magnetic field outside the magnetosphere are compared with ground magnetograms from arctic observatories. Results indicate that an exterior field with a southerly component tends to be associated with ground disturbance whereas a northward field is associated with quiet conditions. Examples are presented showing how a north-to-south field-direction change accompanies an increase in ground activity, and also how south-to-north changes may produce quiet intervals between substorms. Results are discussed in terms of breaking and reconnection of the interplanetary field to the dipole field as the solar wind carries the variously directed interplanetary fields past the earth. (auth)

11828 IONOSPHERIC HEATING BY MAGNETIC CONJUGATE-POINT PHOTOELECTRONS. **Carlson, H. C. Jr. (Cornell Univ., Ithaca, N. Y.). J. Geophys. Res., 71: 195-9(Jan. 1, 1966).**

Regular observations of incoherent backscatter spectra of the ionosphere at the Arecibo Ionospheric Observatory in Puerto Rico since June 1964 establish presunrise and postsunset ionospheric heating above the F_{max} to be present during the winter, though less evident toward either equinox, and absent during the summer. The observed heating is interpreted in terms of a streaming of photoelectrons from the sunlit magnetic conjugate ionosphere. The detailed timing of the onset of the heating supports this hypothesis, and a semiquantitative model for the heating mechanism explains further details of the observations. (auth)

11829 GROWTH AND DECAY OF THE RING CURRENT AND THE POLAR ELECTROJETS. **Akasofu, S.-I.; Yoshida, S. (Univ. of Alaska, College). J. Geophys. Res., 71: 231-40(Jan. 1, 1966).**

It is shown that, although intense polar magnetic substorms tend to occur frequently when the ring current is rapidly growing, there is a tendency for the ring current to grow prior to the growth of well-defined polar magnetic substorms. It is shown also that earlier estimates of the rate of energy injection to produce the ring current are too low, because the simultaneous dissipation was not considered. It is shown that, when this is taken into consideration, an unreasonably high energy conversion would be necessary to produce the ring current if the energy were carried by protons in the solar plasma. (auth)

11830 GEOMAGNETIC AND SOLAR DATA. **Lincoln, J. Virginia (Inst. for Telecommunication Sciences and Aeronomy, Boulder, Colo.). J. Geophys. Res., 71: 316 (Jan. 1, 1966).**

Selected geomagnetic and solar data for August 1965 are presented, giving K_B, C_i, C_p, A_p, K_{Fr}, R_z, and selections of quiet and disturbed days. (M.J.T.)

11831 CORRELATED MAGNETIC TAIL AND RADIATION BELT OBSERVATIONS. **Ness, Norman F. (Goddard Space Flight Center Greenbelt, Md.); Williams, Donald J. J. Geophys. Res., 71: 322-5(Jan. 1, 1966).**

Simultaneous observations from two satellites during a sudden commencement magnetic storm on April 1, 1964, are reported, showing the correlation between changes in the earth's magnetic tail and the radiation belts within the magnetosphere. It is indicated that during a magnetic storm the midnight latitude profile of trapped electrons at 1100 km changes in a manner consistent with the behavior of the magnetic tail field at $\approx 30\ R_E$. (M.J.T.)

11832 STARFISH DEBRIS MEASUREMENTS FROM COSMOS 5. **Manley, Oscar P.; Carpenter, Jack W. (American Science and Engineering, Inc., Cambridge, Mass.). J. Geophys. Res., 71: 333-4(Jan. 1, 1966).**

An analysis of published data from Cosmos-5 observations after the Starfish high-altitude detonation on July 9, 1962, is presented. A limit on the amount of fission debris over Johnston Island for $L \geq 1.25$ at H + 1 sec is computed from the reported initial G-M count rates in the satellite. It is contended that the increasing electron flux at H + 8 min may be due to high-energy electrons injected at L = 1.4 which drifted around the earth and caught up with the satellite. The G-M count rate reported at H + 20 min at the geomagnetic equator is used to estimate the debris in the view of Cosmos 5 as no more than 0.3 Mt. (M.J.T.)

11833 SPATIAL PROPERTIES OF RAPID GEOMAGNETIC FLUCTUATIONS. **Lawrie, J. A. (Univ. of Sussex, Eng.). J. Geophys. Res., 71: 337-9(Jan. 1, 1966).**

Rapid geomagnetic fluctuations at Apia, Amberley, Christchurch, and Scott Base are analyzed, examining correlations between distant stations, epoch differences between distant stations, distributions of azimuths, and Parkinson's plane effects. Possible causes of the fluctuations are considered, including rotational and compressional hydromagnetic disturbances, ionospheric currents, and cosmic particles. (M.J.T.)

11834 MAGNETIC FIELD DATA FOR TRAPPED-PARTICLE EVALUATIONS. **Hendricks, S. J.; Cain, J. C. (Goddard Space Flight Center, Greenbelt, Md.). J. Geophys. Res., 71: 346-7(Jan. 1, 1966).**

An analysis for the geomagnetic field epoch 1960.0, using only internal coefficients, was made, fitting a selection of 197,000 survey observations from 1945 to 1964 with a series of 99 spherical harmonics and 48 first derivatives. Results are tabulated. Availability of a digital magnetic tape of hourly values of the ring current magnetic index Dst is explained. (M.J.T.)

11835 CORRECTIONS AND ADDITIONS TO THE PAPER ENTITLED "ON THE INTERCHANGE STABILITY OF THE VAN ALLEN BELT." **Chang, D. B.; Pearlstein, L. D.; Rosenbluth, M. N. (General Atomic Div., General Dynamics Corp., San Diego, Calif.). J. Geophys. Res., 71: 351-5(Jan. 1, 1966).**

Inadequacies in an approximate expression for $\partial F(\mu,J,\alpha)/\partial\alpha$ in the previous paper are pointed out, and the complete expression is derived; the effects of the error amounted to ignoring the large stabilizing effect associated with the fact that the volume of a flux tube in a dipole field increases rapidly with increasing radial distance. The energy change from interchanging the plasma in two unit flux tubes separated by a given angle is constructed. The distribution used previously for energetic protons is considered, and a conservative sufficient condition for stability is derived, taking into account the effects of a resistive ionosphere. (M.J.T.)

11836 CRITICAL STOERMER CONDITIONS IN QUADRUPOLE AND DOUBLE RING-CURRENT FIELDS. Urban, Eugene W. (George C. Marshall Space Flight Center, Huntsville, Ala.). J. Math. Phys. (N. Y.), 6: 1966-75 (Dec. 1965).

A theoretical study was made of the behavior of the critical Störmer pass points for general axially symmetric magnetic configurations. A topological method was derived to predict the occurrence of the critical Störmer conditions for charged-particle exclusion. This analytic technique, when applied to geomagnetically interesting fields, should be a useful aid to the understanding of experimental data. The method is applied here to three magnetic geometries: double ring currents with parallel dipole moments and with antiparallel dipole moments, and the axial magnetic quadrupole. The topology of the regions representing allowed motion is treated systematically and the behavior of the critical pass points is illustrated in typical Störmer plots. For the quadrupole and the antiparallel ring system critical pass points are found to occur only out of the equatorial plane. For the parallel ring system, critical points can occur in or out of the equatorial plane. For certain special conditions as many as three simultaneous critical pars points are found, and two simultaneous points occur for a wide range of parameters. (auth)

11837 STOCHASTIC ACCELERATION. Sturrock, P. A. (Stanford Univ., Calif.). Phys. Rev., 141: 186-91 (Jan. 1966).

Charged particles moving under the influence of randomly time-varying electromagnetic fields may be expected to experience a net acceleration. This process is analyzed for the special case of nonrelativistic motion in a static uniform magnetic field and time-varying electric field. Acceleration parallel and transverse to the magnetic field are considered separately. In the weak-field approximation, the motion may be described by a Fokker-Planck equation. The coefficients of this equation are expressible in terms of the correlation functions for the electric fields. In certain cases, the coefficients may be expressed in terms of the energy spectrum of the field. The Fokker-Planck equation derived for motion along the magnetic field is closely related to an equation of the quasilinear theory of plasma instability. One may also show that the equation is closely related to the phenomenon of Landau damping. Longitudinal acceleration is effected by waves with phase velocities slightly greater than the particle velocity. A similar statement is true for transverse acceleration, except that the "resonant" waves are in addition shifted by the particle gyrofrequency. In the absence of any other effects (such as "loading" of the accelerating field by the accelerated particles), the transverse energy distribution tends to a Maxwellian form with a temperature which increases linearly with time. The same is true for longitudinal acceleration if the spectrum of the electric field is flat over the range of phase velocities of interest. The equations related to transverse acceleration show that the high-energy electrons observed in the transition region outside the earth's magnetosphere may have been accelerated by quite weak random or quasirandom electric fields. (auth)

11838 SOME THEORETICAL INVESTIGATIONS AND MODEL EXPERIMENTS ON THE STRUCTURE OF RADIATION BELTS AND ITS VARIATION DURING A MAGNETIC STORM. Sci. Sinica (Peking), 14: 1645-62 (Nov. 1965).

The important results of some theoretical investigations and model experiments concerning the variation of the structure of the radiation belts during a geomagnetic storm are summarized. The configuration of the forbidden region in connection with the magnetic field, the variation of the micro-structure of the radiation belts during a magnetic storm, the asymmetrical character of the magnetospheric boundary under the action of solar wind, and a possible way of penetration of solar plasma into the magnetosphere through the neutral point are presented. The outcome of these investigations is compared with the findings of the space exploration as well as the morphology of geomagnetic field with satisfactory results. (auth)

11839 CORRELATIONS BETWEEN AURORAL AND GEOMAGNETIC MICROPULSATIONS [Thesis]. Victor, Laurence Joseph. New Haven, Yale Univ., 1965. 344p.

A comprehensive analysis of both the experimental characteristics of and proposed mechanisms for geomagnetic micropulsations is presented. The relation between micropulsations and related magnetospheric phenomena is discussed in detail. Part A is a brief presentation of the relevant characteristics of and models for the related magnetospheric phenomena. Part B is a detailed presentation and critical analysis of the nature of micropulsations as reported in the literature. Part C presents an analysis of research on micropulsations and pulsating aurora during the Antarctic winter of 1961. Examples of excellent correlation between long-period auroral pulsations, giant pulsations (Pc 5), pearls of Pc 1 in the Antarctic, and long-period pulsations of radio noise absorption in the conjugate area are reported. Details of this correlation lead to a model for Pc 5 where resonant hydromagnetic waves generate electrojets and associated auroral arcs, which drift rapidly over a station producing the observed polarization of Pc 5 and its correlation with the aurora. The extraordinary and ordinary hydromagnetic waves produce oppositely directed electrojets, each having different correlation characteristics. The close correlation between Pc 5 and Pc 1 pearls suggests a model whereby the Pc 5 hydromagnetic waves excite lower exospheric resonance. The periodic drift of the center of the Pc 5 disturbance produces the rising-tone fine structure of Pc 1, and the nature of the coupling in the exosphere produces the observed 180° phase shift between hemispheres. Excellent correlation is also reported between Pc 2 and Pc 3 and pulsating aurora. A model is proposed whereby oscillating bunches of very low energy electrons can produce these correlated pulsations. The importance of very low energy electrons ($E < 1$ kev) in the production of auroral zone phenomena is discussed in detail. (Dissertation Abstr.)

11840 DEFINITION OF SPACE RADIATION ENVIRONMENT. Gordon, Frederick Jr. (Goddard Space Flight Center, Greenbelt, Md.). 18p. (CONF-650707-13). ORINS. Gmelin, AED-CONF-65-152-7.

From IEEE Annual Conference on Nuclear and Space Radiation Effects, Ann Arbor, Mich.

The general radiation environment that may be encountered by earth satellites is outlined. Figures show general radiation fluxes encountered in an equatorial circular orbit, intensity patterns and energies of protons and electrons in the Van Allen belt, energy and intensity distributions at various times from 1962 to 1965 of electrons from the nuclear explosion Starfish, and radiation doses received by satellites in various orbits. (A.G.W.)

11841 PROCEEDINGS OF A SYMPOSIUM ON HIGH LATITUDE PARTICLES AND THE IONOSPHERE, ALPBACH, 1964. Maehlum, B. New York, Academic Press, 1965. 325p. $16.00. (CONF-640307).

The conference included 27 papers. Separate abstracts were prepared for each paper. (J.F.P.)

For abstracts of individual papers see: 11157, 11158, 11438, and 11842–11865.

11842 SPACE RESEARCH IN POLAR REGIONS. Boyd, R. L. F. (London Univ.). pp 1-13 of Proceedings of a Symposium on High Latitude Particles and the Ionosphere, Alpbach, 1964. Maehlum, B. (ed.). New York, Academic Press, 1965.

Attention is drawn to the revolution in polar physics that is coming about because of the availability of spacecraft. The changes in the basic approach that are demanded by the new techniques are examined, and some of the available facilities are reviewed. Topics considered are the scope of polar space research, co-ordination of ground-based studies, quantities to be observed, available techniques, and crucial problems of instrumentation. (J.F.P.)

11843 THE IMPORTANT ATMOSPHERIC PROCESSES IN THE D REGION. Reid, George C. (National Bureau of Standards, Boulder, Colo.). pp 15-19 of Proceedings of a Symposium on High Latitude Particles and the Ionosphere, Alpbach, 1964. Maehlum, B. (ed.). New York, Academic Press, 1965.

The salient features of the important processes in the D region of the ionosphere are summarized. Since all the important reaction rates are rapid compared with drift and diffusion processes, it is possible to express the time derivative of the electron density, N, in the simple form, $dN/dt = q - A + P + D - R$, where q is the rate of production of electrons by the ionizing source, A is the rate of attachment to form negative ions, P is the rate of photodetachment of negative ions in sunlight, D is the rate of other detachment reactions, and R is the rate of recombination of electrons and positive ions. A similar equation can be written for the time derivative of the negative ion density. Each of these processes is considered and also that of the mutual neutralization. (J.F.P.)

11844 PROBE TECHNIQUES. Willmore, A. P. (London, Univ.). pp 21-32 of Proceedings of a Symposium on High Latitude Particles and the Ionosphere, Alpbach, 1964. Maehlum, B. (ed.). New York, Academic Press, 1965.

A critical assessment of the measurements which can reliably be made by probe techniques in the polar atmosphere at the present time is made. The experimental problems implicit in probe measurements are briefly surveyed, and the different probe techniques are discussed. The experimental problems in probe measurements include the passage of the spacecraft through the ionosphere, photoemission, and variations in spacecraft potential. The types of measuring probes considered are Langmuir probes, r-f probes, Gerdien condensers, and the resonance probe. A critical evaluation of the merits and demerits of the various probes is given. (J.F.P.)

11845 DIRECT SATELLITE PROBE MEASUREMENTS OF IONOSPHERIC IRREGULARITIES IN THE POLAR CAP. Pfister, W.; Ulwick, J. C.; McInerney, R. E. (L. G. Hanscom Field, Bedford, Mass.). pp 33-41 of Proceedings of a Symposium on High Latitude Particles and the Ionosphere, Alpbach, 1964. Maehlum, B. (ed.). New York, Academic Press, 1965.

A standing wave impedance probe was flown on polar orbiting satellites through the F2 layer. Continuous measurements for entire orbits were recorded and stored on magnetic tape. The data were processed and plotted completely automatically from the telemetry magnetic tapes. Of special interest are irregular structures observed in the south polar region above the peak of the F layer. The satellite passes through the region at the same local time but covers the whole region geographically in the course of a day. One system of irregularities appears to be aligned with the magnetic latitude, while another structure appears consistently at a geographic latitude near 70°. (auth)

11846 LOW FREQUENCY PROPAGATION AND PROBE EXPERIMENTS. Kaiser, T. R. (Univ. of Sheffield, Eng.). pp 43-52 of Proceedings of a Symposium on High Latitude Particles and the Ionosphere, Alpbach, 1964. Maehlum, B. (ed.). New York, Academic Press, 1965.

The attraction in using low radio frequencies for rocket investigations of the ionosphere rests in the relatively large effects that may be expected with low ambient electron densities, as, for example, in the D region. There is, however, considerable difficulty in interpreting the results. A low frequency propagation experiment is described, which has successfully yielded a D region ionospheric profile. The theory of radio-frequency impedance probes is considered, and formulas are given which may be useful in deriving ionospheric profiles, especially in the D region. (auth)

11847 SIMULTANEOUS MEASUREMENTS OF IONOSPHERIC PLASMA DENSITY BY THREE DIFFERENT METHODS. Buechau, J.; Jacobs, K. G.; Kaiser, P.; Rawer, K.; Reinisch, B. (Ionosphere Inst., Breisach, Ger.). pp 55-62 of Proceedings of a Symposium on High Latitude Particles and the Ionosphere, Alpbach, 1964. Maehlum, B. (ed.). New York, Academic Press, 1965.

During a Veronique firing on 1 May, 1963, at Hamaguir, in the Sahara, the following three measurements were made simultaneously: impedance probe with variable frequency, dispersive Doppler measurements on 5 and 20 Mc, and field strength records of several r-f transmissions by an r-f spectrometer. The fundamental theory, the experimental arrangement, and some preliminary results are presented. (J.F.P.)

11848 ELECTRON DENSITY AND COLLISION FREQUENCY OBSERVATION FROM A ROCKET EXPERIMENT DURING AN AURORAL ABSORPTION EVENT. Jespersen, M. (Technical Univ. of Denmark, Copenhagen); Olesen, J. K.; Landmark, B. pp 63-67 of Proceedings of a Symposium on High Latitude Particles and the Ionosphere, Alpbach, 1964. Maehlum, B. (ed.). New York, Academic Press, 1965.

Results from observations of electron density and collision frequency obtained during a rocket firing from Andøya in northern Norway are described. The rocket was fired on 12 September, 1963, into an auroral absorption event, and the riometer absorption at 27.6 Mc was 3.5 db. The results are compared with those obtained from previous flights. (auth)

11849 SOME ASPECTS OF PARTICLES AND FIELDS IN THE MAGNETOSPHERE. Faelthammar, C-G. (Royal Inst. of Tech., Stockholm). pp 71-102 of Proceedings of a Symposium on High Latitude Particles and the Ionosphere, Alpbach, 1964. Maehlum, B. (ed.). New York, Academic Press, 1965.

The interaction of charged particles with the fields of the magnetosphere is discussed, and the particles are classified into categories according to the character of the interaction. It is shown that the long mean free paths of plasma particles in certain regions may have important consequences for the properties of the magnetosphere — in particular its response to electric fields. A brief survey is given of existing theoretical magnetosphere models. Scale model experiments are described that were designed to cast light on the applicability of the various theoretical models. (auth)

11850 METHODS AND RESULTS OF PARTICLE OBSERVATIONS. Maehlum, Bernt (Norwegian Defence Research Establishment, Kjeller). pp 103-12 of Proceedings of a Symposium on High Latitude Particles and the Ionosphere, Alpbach, 1964. Maehlum, B. (ed.). New York, Academic Press, 1965.

Some particle observations which may be of importance for ionospheric phenomena are discussed. Most of the observations refer to published results from the satellites Injun I and III. (auth)

11851 COMMENTS ON MEASUREMENTS OF PARTICLE PRECIPITATION WITH THE INJUN SATELLITES. O'Brien, B. J. (Rice Univ., Houston, Tex.). pp 113-18 of Proceedings of a Symposium on High Latitude Particles and the Ionosphere, Alpbach, 1964. Maehlum, B. (ed.). New York, Academic Press, 1965.

Several of the more significant measurements made by

the satellites Injun I and Injun III are briefly summarized. The flux of electrons precipitated at L = 6.0, and 6.5 during January 1963, is given and it is shown that precipitation is generally more intense during magnetic storms. Samples of precipitated fluxes over North America in January 1963, aurora and precipitated particle simultaneous measurements, and samples of the intensity of auroral light measured by a photometer over North America are given. (J.F.P.)

11852 SOLAR FLARE PARTICLES IN SEPTEMBER 1963. **Burrows, J. R.; McDiarmid, I. B.; Wilson, Margaret D. (National Research Council, Ottawa). pp 119-36 of Proceedings of a Symposium on High Latitude Particles and the Ionosphere, Alpbach, 1964. Maehlum, B. (ed). New York, Academic Press, 1965.**

Solar protons from flares in September 1963 were observed at an altitude of 1000 km by satellite instrumentation. A possible impact zone effect was measured 1 h after the 21 September flare. A differential spectrum $dN/dE \alpha E^{-3.2}$ is calculated. Latitude distribution and cutoff latitudes for selected proton energies from 1 to 165 Mev are determined. Time variations and decays of proton fluxes from the 21 and 26 September flares are studied and relations between the proton flux and cosmic noise absorption measurements, planetary magnetic index, and possible interplanetary field configurations are discussed. (auth)

11853 AN ELECTRON-PROTON SPECTROMETER FOR ROCKETS USING SOLID STATE DETECTORS. **Riedler, W. (Kiruna Geophysical Observatory, Sweden). pp 137-45 of Proceedings of a Symposium on High Latitude Particles and the Ionosphere, Alpbach, 1964. Maehlum, B. (ed.). New York, Academic Press, 1965.**

An instrument is described which was designed to measure integral energy spectra of auroral electrons and protons in the range from 40 to 104 kev. Silicon junction particle detectors were used for this purpose. Preliminary results from a successful launch on 12 March 1964 from Andøya, Norway, are given. (auth)

11854 MEASUREMENT OF CHARGED PARTICLES IN THE AURORAL ZONE, ANDOEYA, NORWAY. **Soeraas, F.; Trumpy, B. (Univ. of Bergen, Norway). pp 159-63 of Proceedings of a Symposium on High Latitude Particles and the Ionosphere, Alpbach, 1964. Maehlum, B. (ed,). New York, Academic Press, 1965.**

Solid state detectors were used on rockets fired from Andeoya in order to measure the energy and pitch-angle distribution of electrons and protons. The integral proton energy spectra measured on 11 December, 1962, the counting rate of particles with energy greater than 0.125, 0.600, and 1.15 Mev, and the modulation of the proton counting rate as a function of spin angle are shown. (J.F.P.)

11855 BALLOON MEASUREMENTS OF SOLAR PROTONS AND AURORAL X-RAYS. **Pfotzer, G. (Max Planck-Institut fuer Aeronomie, Lindau/Harz, Ger.). pp 167-204 of Proceedings of a Symposium on High Latitude Particles and the Ionosphere, Alpbach, 1964. Maehlum, B. (ed.). New York, Academic Press, 1965.**

Balloon measurements are complementary not only to ground based records but also to rocket and satellite work. Also small groups are able to perform balloon flights at relatively low expense and thus contribute valuable results to the exploration of various auroral and polar cap phenomena. In contrast to satellites, balloons can be kept for periods of many hours at about the same geographic location allowing continuous records of variations of various phenomena with local time to be made. Flight techniques, instrumentation, and interpretation of the measurements are discussed. Results of some balloon flights are also considered. Typical features of polar cap or auroral phenomena are illustrated by selected measurements related to solar flare nucleonic radiation and to auroral x rays. (J.F.P.)

11856 A NETWORK TO TEST THE RELIABILITY OF VLF PHASE RECORDINGS ON TRANSPOLAR PROPAGATION PATHS TO BE USED AS A METHOD TO INDICATE THE PRECIPITATION OF SOLAR COSMIC RAY PARTICLES IN POLAR CAP REGIONS. **Lange-Hesse, G. (Max-Planck Inst. for Ionospheric Physics, Lindau, Ger.). pp 205-10 of Proceedings of a Symposium on High Latitude Particles and the Ionosphere, Alpbach, 1964. Maehlum, B. (ed.). New York, Academic Press, 1965.**

Suitable vlf equipment was developed for the purpose of obtaining additional confirmation from a polar observatory operating riometers to check whether the cosmic-noise absorption has increased in the polar cap, when a sudden vlf phase shift occurs at a station in middle latitudes. If this is the case then the prepared launching of the sounding balloon can begin. At the final stage two vlf sets will operate at Lindau and two at Sodankyla. A wireless circuit exists between these two points to exchange first results of the phase recordings. It is intended to operate the complete vlf network for several years mainly with the air of testing the reliability of such vlf phase and amplitude recordings, in order to observe the precipitation of solar cosmic ray particles in the polar cap region. (J.F.P.)

11857 OPTICAL EFFECTS OF PARTICLES. **Omholt, A. (Univ. of Oslo, Blindern). pp 213-20 of Proceedings of a Symposium on High Latitude Particles and the Ionosphere, Alpbach, 1964. Maehlum, B. (ed). New York, Academic Press, 1965.**

The current theories for excitation of aurora, of the general excitation and ionization by fast particles in air, and the relation between luminosity and ionization in aurora are reviewed. The angular distribution and the energy spectrum of the primary electrons and protons are discussed in view of the observed height distribution of the auroral luminosity and Doppler broadening of the hydrogen lines. (auth)

11858 IONOSPHERIC EFFECTS OF PARTICLES. **Reid, George C. (National Bureau of Standards, Boulder, Colo.). pp 221-31 of Proceedings of a Symposium on High Latitude Particles and the Ionosphere, Alpbach, 1964. Maehlum, B. (ed.). New York, Academic Press, 1965.**

A review is given of the influence of energetic particles on the ionosphere. Restriction is made to the direct ionization effects since these are on firmer observational and theoretical grounds. The auroral sporadic-E layer, radio-aurora, electron density irregularities, high-frequency radio absorption, both polar cap and auroral, and the flux and energy spectrum of protons during a polar cap absorption event are considered. (J.F.P.)

11859 THE DEVELOPMENT OF THE RADIO-AURORA. **Brooks, D.; Kaiser, T. R. (Univ. of Sheffield, Eng.). pp 233-7 of Proceedings of a Symposium on High Latitude Particles and the Ionosphere, Alpbach, 1964. Maehlum, B. (ed.). New York, Academic Press, 1965.**

From observations of 17 Mc radio-auroras following stormy sudden commencements it is found that the delay in onset of the aurora depends on the local time of occurrence of the s.s.c. If this is close to 1500 or 2300 local time, then an aurora is observed virtually immediately, otherwise the onset of the aurora tends to be delayed until the next evening auroral sequence is due. (auth)

11860 ENHANCED ELECTROMAGNETIC RADIATION BETWEEN 500 AND 1000 C/S IN THE AURORAL ZONE. **Egeland, Alv (Kiruna Geophysical Observatory, Sweden); Aarons, Jules; Barron, Williams. pp 239-46 of Proceedings of a Symposium on High Latitude Particles and the Ionosphere, Alpbach, 1964. Maehlum, B. (ed,). New York, Academic Press, 1965.**

Electromagnetic radiation in the audio frequency range was studied at Kiruna Geophysical Observatory (geomagnetic latitude 65.3°N) since 1958. Several hundred emission bands between 500 and 1000 c were recorded by a swept frequency battery-operated analyzer. The most important characteristics of this enhanced radiation are the

following: the maximum signal strength is observed at a fixed frequency (700 ± 100 c). The bandwidth of the emission is less than 500 c. The shape of the emission band is asymmetrical. The diurnal variation of the 700 c emissions shows a pronounced maximum between 06 and 11 local time. The hypothesis that these emission bands are due to radiation at the gyro-frequency of protons is discussed. (auth)

11861 ON THE LONGITUDINAL EXTENT OF AURORAL IONIZATION. **Ortner, J.; Riedler, W. (Kiruna Geophysical Observatory, Sweden). pp 247-55 of Proceedings of a Symposium on High Latitude Particles and the Ionosphere, Alpbach, 1964. Maehlum, B. (ed.). New York, Academic Press, 1965.**

Auroral type of riometer absorption and magnetic disturbances are studied for stations situated at different longitudes in the auroral zone. A smooth type of riometer absorption occurring during the local morning hours is especially investigated. It is concluded that this special type of absorption is also produced by precipitation of electrons and that auroral ionization occurs at the same time on a large scale around the auroral zone. (auth)

11862 THE USE OF MULTIPLE ANTENNAS IN STUDIES OF ABSORPTION AT CONJUGATE POINTS. **Chivers, H. J. A.; Hargreaves, J. K. (National Bureau of Standards, Boulder, Colo.). pp 257-64 of Proceedings of a Symposium on High Latitude Particles and the Ionosphere, Alpbach, 1964. Maehlum, B. (ed.). New York, Academic Press, 1965.**

As part of a program of absorption measurements in magnetically conjugate regions, a multiple antenna based on the corner reflector was constructed. The use of this antenna is described and some preliminary results are mentioned. (auth)

11863 RECENT SOLAR COSMIC RAY EVENTS. **Masley, A. J.; Goedeke, A. D.; Adams, G. W. (Douglas Missile and Space Systems Div., Santa Monica, Calif.). pp 265-74 of Proceedings of a Symposium on High Latitude Particles and the Ionosphere, Alpbach, 1964. Maehlum, B. (ed.). New York, Academic Press, 1965.**

A discussion is given of recent solar cosmic ray events observed at stations located within the polar cap regions, removed toward the magnetic poles from the auroral zones so that relatively clean solar cosmic ray data are collected with minimum auroral interference. The lack of auroral contamination of data is encouraging for solar cosmic ray studies, as is evidenced by the agreement obtained with satellite measurements. The differences in the measurements at the conjugate points imply a rather complex interaction between the geomagnetic field and the solar particles. (J.F.P.)

11864 THE HEIGHT OF AURORAL ABSORPTION OBTAINED FROM SATELLITE OBSERVATIONS. **Hultqvist, Bengt (Goddard Space Flight Center, Greenbelt, Md.). pp 275-83 of Proceedings of a Symposium on High Latitude Particles and the Ionosphere, Alpbach, 1964. Maehlum, B. (ed.). New York, Academic Press, 1965.**

Statistical data from Alouette and Injun III on the average precipitation rate of electrons in the auroral zone as a function of energy, are discussed with regard to the average absorption produced by the energy ranges 1–40 and 40–250 kev. From the satellite data, it is found that the higher energy range for the primary electrons is the dominating one in producing absorption at riometer frequencies. From this it follows that the majority of auroral absorption takes place below 90 km altitude in the auroral zone. (auth)

11865 SOME PARTICULAR PROBLEMS IN THE POLAR IONOSPHERE AND THEIR POSSIBLE RESOLUTION BY ROCKET AND SATELLITE EXPERIMENTS. **Dalziel, R. (Radio Research Station, Slough, Eng.). pp 285-96 of Proceedings of a Symposium on High Latitude Particles and the Ionosphere, Alpbach, 1964. Maehlum, B. (ed.). New York, Academie Press, 1965.**

During the IGY a large quantity of data was collected. Statistical analysis of these data has shown that polar ionospheric phenomena exhibit certain patterns of behavior in space and time. Not only must this behavior be explained by any theory of particle precipitation mechanisms, but direct measurements on events selected according to the pattern should throw some light on the mechanisms. A few suggestions are made for rocket and satellite experiments based on problems associated with the diurnal variation of polar cap absorption, the differences in vertical extension of visual aurorae and sporadic-E, the geographic and local time distributions of auroral blackout and sporadic-E, the excitation of auroras by protons and the universal time effect in the F region. (auth)

Gravitation, Quantum Mechanics, and Relativity Theory

Refer also to abstracts 11432–11435, 11441, 11459, and 11759.

11866 (JINR-E-2478) TIME AND ENERGY IN QUANTUM MECHANICS. Shirokov, M. I. (Joint Inst. for Nuclear Research, Dubna (USSR). Lab. of Theoretical Physics). 1965. 12p. Dep. mn.

Time and energy are conjugate operators (like coordinate and momentum) in a theory based upon all the usual quantal postulates preceding the Schroedinger equation. In treating a physical system obeying this equation, time may be considered as a parameter. The relation $\Delta E \Delta t \approx h$ and the problem whether the energy of an isolated system is conserved in time are discussed. (auth)

11867 (NP-15762) GRAVITATSIYA I KONECHNYE PERENORMIROVKI V KVANTOVOI ELEKTRODINAMIKE. (Gravitation and Finite Renormalization in Quantum Electrodynamics). Khriplovich, I. B. (Akademiya Nauk SSSR, Novosibirsk. Institut Yadernoi Fiziki). 1965. 19p. Dep. mn.

Electromagnetic self-energy and wave function renormalization constant of the electron become finite when taking into consideration some model of its gravitational interaction. In the first order in e^2 the self-energy totals 20% of the physical mass. The semiclassical calculation of the electrostatic energy of the Dirac electron when taking into account the space curvature leads to nearly the same result. (auth)

11868 (UCRL-14546) A NOTE ON PARALLELISM. Neuman, M. (Lawrence Radiation Lab., Univ. of California, Livermore). Nov. 22, 1965. Contract W-7405-eng-48. 22p. Dep. mn. CFSTI $1.00 cy, $0.50 mn.

The concept of parallelism is presented in a manner which is believed to be in better agreement with the global viewpoint. (D.C.W.)

11869 NON-STATIC SPHERICALLY SYMMETRIC CLUSTERS OF PARTICLES IN GENERAL RELATIVITY. [PART] II. Datta, Bidyut Kumar (Surendra Nath Coll., Calcutta). Acta Phys. Pol., 28: 883-9(Dec. 1965).

The case of a non-stationary cluster of particles moving freely under the influence of the gravitational field produced by all of them together is discussed on the basis of the equations of general relativity. The gravitating mass of the cluster is shown to be equal to the sum of the particle masses in the limiting case. (auth)

11870 ON A GENERALIZED LORENTZ TRANSFORMATION. Strauss, M. Ann. Phys. (7), 16: 105-13 (1965).

The generalized Lorentz group of Romain is reconstructed and analyzed as to both its mathematical structure and its possible physical interpretations. Apart from the "formal" interpretation intended the generalized group is shown to possess a "realistic" interpretation referring to a hypothetical situation and also a nontrivial interpretation

in terms of general relativity referring to the presence of a scalar gravitational potential. (auth)

11871 INTERACTING FIELD OF SPIN 2 AND THE EINSTEIN EQUATIONS. Ogievetsky, V. I.; Polubarinov, I. V. (Joint Inst. for Nuclear Research, Dubna, USSR). Ann. Phys., 35: 167-208(Nov. 1965).

The possible local theories of an interacting symmetric tensor field $h_{\mu\nu}$ are considered, in which the equations of motion are compatible with a general Hilbert-Lorentz type condition to exclude spin 1. It is shown that in the case of massless tensor field there exists only one such a theory under the assumption of minimal interactions, and the equations of motion coincide exactly with the Einstein equations including all nonlinearities of the latter. That is, the field theoretical derivation of the Einstein equations is given. In this approach space-time remains flat and the nonlinearities peculiar to the Einstein theory are generated by the requirement for interacting gravitons to have spin 2 but not spin 1. As to the massless field this requirement is guaranteed by an invariance under gauge transformations, which on the one hand are analogous to the gauge transformations in electrodynamics and on the other hand are formally equivalent to the general covariant transformations. The generalization of the Einstein equations to the case of a massive tensor field is obtained. Mass terms violate the general covariance and the equivalence principle but the equality of inertial and "gravitational" masses remains valid. (auth)

11872 SEMIGENERALLY COVARIANT EQUATIONS OF MOTION—II. THE SIGNIFICANCE OF THE "TAIL" AND THE RELATION TO OTHER EQUATIONS OF MOTION. Carmeli, Moshe (Temple Univ., Philadelphia). Ann. Phys., 35: 250-70(Nov. 1965).

The semigenerally covariant equation of motion of a particle of finite mass moving in an external gravitational field, obtained previously, is further discussed. At first it is decomposed into four scalar equations along four orthonormal vectors moving with the particle. It is shown that if the particle moves along a geodesic line in the external field, then the "tail" vanishes. The vanishing of the "tail," on the other hand, implies a motion that tends to be geodetic, without the appearance of any runaway solution. The "tail" term is then determined for the case of slow motion (to an accuracy up to the seventh order in c^{-1}) of two finite mass particles. It is shown that its structure is very similar to that obtained for the (test) charged particle moving in a static gravitational field, i.e., it depends on the velocity of the particle and the Riemann tensor of the external field. It is then shown that both the Einstein-Infeld-Hoffmann and the Havas-Goldberg equations of motion can be obtained as limiting cases of the semigenerally covariant equation when the latter is expanded in c^{-1} and G, respectively. (auth)

11873 MACH'S PRINCIPLE AND MASS IN AN EXPANDING UNIVERSE. Rosen, Nathan (Israel Inst. of Tech., Haifa). Ann. Phys., 35: 426-36(Dec. 1965).

The extent to which Mach's principle is realized in the homogeneous isotropic closed model of the universe is studied. The variation of the mass of a given particle with time is investigated. (D.C.W.)

11874 COSMOLOGY WITHOUT GENERAL RELATIVITY. Harrison, E. R. (Goddard Space Flight Center, Greenbelt, Md.). Ann. Phys., 35: 437-46(Dec. 1965).

It is assumed that the universe contains a perfect fluid and is homogeneous and isotropic at every point in space. The concept of a partitioned universe then leads to the boundary conditions necessary for isolating a small region or cell of space. A microcosmic model of the universe, which is based upon an infinitesimally small isolated cell embedded in flat space, is studied. When the fluid is pressure-free, the model obeys the Newtonian equations accurately. By working within the framework of special relativity, the cosmological equations are obtained for the more general case of a non-zero pressure. (D.C.W.)

11875 COMPLEX SPACE-TIME AND GEOMETRIZATION OF ELECTROMAGNETISM. III. Das, A. (Carnegie Inst. of Tech., Pittsburgh). J. Math. Phys., 7: 61-3(Jan. 1966).

It is shown here that if the covariance under general circular transformations (rotations in complex planes) is demanded, the electromagnetic potentials can be geometrized as the affine connections necessary for such covariance. The geodesic hypothesis yields the Lorentz equation of motion with an interesting correction term. (auth)

11876 MATHEMATICAL ASPECTS OF THE WEYL CORRESPONDENCE. Pool, James C. T. (Ford Motor Co., Dearborn, Mich. Brandeis Univ., Waltham, Mass.). J. Math. Phys., 7: 66-76(Jan. 1966).

The Weyl correspondence between classical and quantum observables in rigorously formulated for a linear mechanical system with a finite number of degrees of freedom. A multiplication of functions and a *-operation are introduced to make the Hilbert space of Lebesgue square-integrable complex-valued functions on phase space into a H*-algebra. The Weyl correspondence is realized as a *-isomorphism $f \to W(f)$ of this H*-algebra onto the H*-algebra of Hilbert-Schmidt operators on the Hilbert space of Lebesgue square-integrable complex-valued functions on configuration space. Moreover, the kernel of $W(f)$ is exhibited in terms of a Fourier-Plancherel transform of f. Elementary properties of the Wigner quasiprobability density function and its characteristic function are deduced and used to obtain these results. (auth)

11877 SOME EXACT SOLUTIONS OF THE FIELD EQUATIONS OF GENERAL RELATIVITY. Misra, M. (Temple Univ., Philadelphia). J. Math. Phys., 7: 155-8 (Jan. 1966).

A method for generating nonstatic solutions of the Einstein–Maxwell field equations in vacuo from nonstatic solutions of the empty space–time field equations is given. It is shown that under certain conditions one of the metrics under investigation admits algebraically degenerate vacuum solutions. The necessary and sufficient condition in order that the vacuum solutions for this metric be of type null is obtained. Some exact solutions are listed. (auth)

11878 QUANTUM ELECTRODYNAMICS OF THE STIMULATED EMISSION OF RADIATION. II. Bevensee, R. M. (Univ. of California, Berkeley). J. Math. Phys. (N. Y.), 6: 1857-70(Dec. 1965).

The equations of motion for the resonant modes in a lossy cavity, which couples them through the nonresonant thermal loss mechanism described by Senitzky, are examined. The second-order perturbation treatment of dissipation is justified for long time intervals by reference to an intermittent similarity transformation. Self-consistent expressions for commutators such as $\langle [P_n(t_1), P_m(t_2)] \rangle_d$, P_n being the operator-amplitude of the electric field in the nth mode, as averaged over the loss mechanism d with respect to its diagonal density matrix, are obtained from Laplace transform expressions for these operators. These averaged commutators describe correlations of fluctuations in different modes, in a way compatible with the ordinary commutation relations for lossless modes. The selfconsistent anticommutator expressions, averaged over the loss mechanism, imply the Bose–Einstein formula for thermal energy in each mode at time $t_2 = t_1$. This is shown from direct examination of anticommutators and also from an integration of the correlation function. Commutators for the total electric and magnetic fields at two space-time points in the cavity have the proper causal properties. The dissipation terms in the field equations of motion cannot be derived from an equivalent Hamiltonian unless a modified analysis such as that of Kemeny is undertaken. Finally, the approximate equations of motion for the mode operator-amplitudes of a parametric amplifier are derived in the creation-annihilation operator framework and the spectral density of noise obtained at the signal frequency. The

equilibrium noise present due to coupling with the idle modes is proportional to the number of photons in the idle frequency mode instead of that number plus one, in contrast to the conclusion of Wagner and Hellwarth. In this system the loss-averaged operators evolve from initial thermal equilibrium values to parametric equilibrium values according to nonlinear equations of motion containing time dependent commutators. (auth)

11879 CARTESIAN TENSORS IN SPACES WITH AN INDEFINITE METRIC WITH APPLICATIONS TO RELATIVITY. **Foldy, Leslie L. (Case Inst. of Tech., Cleveland). J. Math. Phys. (N. Y.), 6: 1871-6(Dec. 1965).**

A new formalism for dealing with Cartesian tensor analysis in flat spaces with an indefinite metric with the same ease as in Euclidean spaces is introduced. It avoids the necessity of distinguishing covariant and contravariant indices and the consequent use of the metric tensor in raising and lowering indices; neither does it require the introduction of imaginary coordinates and components of tensors. It is based on the use of a modified Einstein summation convention combined with a modified differentiation with respect to tensor components in such a way that all formal manipulations are essentially identical with those employed in Cartesian tensor analysis in Euclidean spaces. The further introduction of a modified matrix multiplication and a modified definition of a determinant serves to round out the formal analogy with the Euclidean space. The convenience, simplicity, and typographical economy of the new formalism is illustrated by examples drawn from special relativity. The formalism can be trivially generalized to complex linear vector spaces with an indefinite metric. (auth)

11880 A NEW PHASE-SPACE DISTRIBUTION FUNCTION IN THE STATISTICAL THEORY OF THE ELECTROMAGNETIC FIELD. **Kano, Yutaka (Univ. of Rochester, N. Y.). J. Math. Phys. (N. Y.), 6: 1913-15(Dec. 1965).**

A new probability distribution function q(z) relating to blackbody radiation was previously introduced. The properties of this function for a general radiation field are studied. Unlike the phase-space distribution function of Sudarshan (1963), this function is nonnegative and is an ordinary function. A series expansion for q(z) is given, and it is shown that the series is absolutely convergent for all eigenvalues z of the destruction operator. It is also shown that the density matrix in the Fock representation can be uniquely determined from this probability distribution function, and vice versa. The relation between q(z) and the Sudarshan's phase-space distribution function is discussed. (auth)

11881 NULL FIELDS IN EINSTEIN-MAXWELL FIELD THEORY. **Wyman, M.; Trollope, R. (Univ. of Alberta, Can.). J. Math. Phys. (N. Y.), 6: 1995-2007(Dec. 1965).**

The role of the electromagnetic null field, within the framework of classical relativistic electrodynamics, was never fully established. A large class of exact solutions to the Einstein–Maxwell null field equations is presented with the hope that the physical implications of these solutions may lead to a more thorough understanding of these fields. In the analysis, it appears that the nature of the solutions depends on the form of the propagation vector. In the cases for which the divergence of this vector vanishes, an extensive class of solutions is obtained and particular examples are considered. The analysis of the case when the divergence is nonzero is far from complete and only a particular solution is given. (auth)

11882 PROPER TIME FORMULATION OF THE DIRAC ELECTRON THEORY. **Saavedra, I. (International Center for Theoretical Physics, Trieste, Italy). Nucl. Phys., 77: 673-9(1966).**

In terms of the proper time of the particle, a covariant hamiltonian formulation of Dirac's electron theory is given, and the formalism is applied first to discuss the motion of the particle and second, to construct a new conserved spin angular momentum operator. (auth)

11883 PRECESSION OF SATELLITE ORBITS AND GENERAL RELATIVITY. **Goldberg, I.; Madey, R. (Clarkson Coll. of Tech., Potsdam, N. Y.). Nuovo Cimento (10), 41B: 1-8(1966).**

The orbits of artificial satellites about celestial bodies can be chosen to optimize the precision of a measurement of the precession of satellite perihelia. Experiments with satellites in optimized orbits appear capable of testing the precessional formula of general relativity with greater precision than heretofore. Maximizing a precessional figure of merit based upon the observational techniques of planetary astronomy leads to the optimal orbital condition that the ratio of the semi-major axis to the semi-minor axis of the elliptical orbit is equal to $\sqrt{3}$. In MKS units, the magnitude of the angular advance of satellite perihelia is ψ_0(seconds of arc/century) = $5.0 \cdot 10^{-19}(M^{3/2}/r^{5/2})$, where M is the mass of the celestial body, and r is the perihelion distance. For a given ratio of perihelion distance to the radius of the celestial body, the Sun causes a satellite to precess from about two to three orders of magnitude more than the jovian planets and from about three to four orders of magnitude more than the terrestrial planets. Although the precession of the perihelion of a satellite in an optimized orbit about the Earth is comparable with that from the planet Mercury about the Sun, the observational figure of merit for an optimized Earth satellite is several times that of Mercury. The observational figure of merit for an optimized Moon satellite is comparable with that for the planet Mercury. (auth)

11884 CONSISTENCY OF SUBTRACTION METHOD FOR GRAVITATIONAL MASS. **Tangherlini, F. R. (George Washington Univ., Washington, D. C.). Nuovo Cimento (10), 41B: 62-5(1966).**

The consistency of the subtraction technique developed previously is further verified for calculating gravitational mass in nonquasi-rectangular coordinates directly from the surface integrals provided by von Freud superpotentials. A point mass and a bar in Weyl's cylindrical coordinates are considered. The Einstein and de Sitter universes are also briefly studied as a preliminary to investigating cosmologies by these techniques. Some results for the stationary metric of Kerr are presented. (L.B.S.)

11885 POSSIBLE CAUSAL VIOLATIONS AT RADII GREATER THAN THE SCHWARZSCHILD RADIUS. **Anderson, J. L.; Gautreau, R. (Stevens Inst. of Tech., Hoboken, N. J.). Phys. Lett., 20: 24-5(Jan. 15, 1966).**

The reflection of light signals from a Schwarzschild source is studied. If such reflections are possible, apparent violations of causality occur. (D.C.W.)

11886 KRUSKAL SPACE WITHOUT WORMHOLES. **Belinfante, F. J. (Purdue Univ., Lafayette, Ind.). Phys. Lett., 20: 25-7(Jan. 15, 1966).**

It is proposed that the points (u, v, θ, φ) and (–u, –v, θ, φ), usually interpreted as different points on two sides of a wormhole, are two different representations of one single point event. (D.C.W.)

11887 QUANTIZED ENERGY DISTRIBUTIONS FOR THE HARMONIC OSCILLATOR. **Rankin, Bayard (Case Inst. of Tech., Cleveland). Phys. Rev., 141: 1223-30(Jan. 1966).**

An earlier study of quantum-mechanical time has suggested that, from the quantum-theoretic point of view, time is a random variable. An investigation is made of how such a description of time can be used to bring greater detail into the analysis of the one-dimensional harmonic oscillator. Specifically, the classical equations for harmonic motion are used as a point transformation between phase space and time-energy space, permitting probability distributions in the two spaces to be different representations of the same thing. The familiar energy-quantization hypothesis is supplemented with the hypothesis that quantized energy values are means (averages) of energy distributions characteristic of each energy state. With the probability distribution of time determined from the previously cited study, the desired quantized energy distributions

follow from the requirements: (1) that they should be normalized, non-negative, and with means equal to the quantized energy values; (2) that the equivalent representation of distribution in position-momentum space should have marginal densities that are proportional (except near the origin) to the densities in position and momentum, $|\varphi(q)|^2$ and $|\psi(p)|^2$, which are postulated in quantum theory. Requirement (2) is a weakening of the Born postulate. In the time-energy space, the probability distributions exclude energies smaller than the mode (energy value with maximum probability). In position-momentum space this exclusion requirement becomes the dynamical restriction: $q^2m\omega^2/2 + p^2/2m \geq \Lambda_n\hbar\omega/2$, where, for the first three energy states, $\Lambda_0 = 0$, $\Lambda_1 = 3/2$, $\Lambda_2 = 2 + \sqrt{3}/2$. In general terms it is thus shown that the quantized harmonic oscillator can be described as a statistical ensemble of classical oscillators. Some comparisons with work on phase-space formulations of quantum mechanics (especially with the work of Wigner) are made and some aspects of the theory that should submit to experimental verification are pointed out. (auth)

11888 GRAVITATIONAL WARD IDENTITY AND THE PRINCIPLE OF EQUIVALENCE. Brout, R.; Englert, F. (Univ. Libre, Brussels). Phys. Rev., 141: 1231-2(Jan. 1966).

The Ward identity for a gravitational field interacting with a scalar field is given. It is shown that in the limit in which the scalar field is taken on the mass shell, this identity becomes the principle of equivalence. (auth)

11889 STABILITY AND DYNAMICS OF SPHERICALLY SYMMETRIC MASSES IN GENERAL RELATIVITY [Thesis]. Bardeen, James Maxwell. Pasadena, Calif., California Inst. of Tech., 1965. 134p.

The Einstein equations for a spherically symmetric distribution of matter are recast in comoving (Lagrangian) coordinates in a form similar to that of the classical hydrodynamic equations. The jump conditions for a shock wave in an ideal fluid are found in these coordinates. The equation of radiative transfer in general relativity is derived, and analyzed with respect to the non-gravitational interaction of the radiation and the matter as reflected in the equations arising from the zero covariant divergence of the energy-momentum tensor. The radiative transfer equation is solved assuming the radiation is in local thermodynamic equilibrium with the matter. Some examples are presented of numerical calculations of the equilibrium, stability, and dynamics near equilibrium of spherically symmetric masses for a simple, although physically reasonable, type of equation of state, in which the thermal energy density is given solely in terms of the pressure and an adiabatic index Γ_1 independent of density and pressure. One numerical method follows the growth of instabilities to all orders in the fractional change in radius away from equilibrium. This formulation of the Einstein equations is applied to the analytical study of the stability, and it is proved that, regardless of the equation of state, a maximum or minimum of the binding energy as a function of central density along a sequence of masses in hydrostatic and convective equilibrium with constant number of baryons and constant rest mass per baryon implies some mode of radial oscillation has zero frequency there. As a result of this theorem, the stability properties of models in convective equilibrium can be read off a plot of fractional binding energy against the ratio of gravitational radius to radius. One example is presented of a numerical difference equation calculation of the collapse of a large mass inside the gravitational radius. (Dissertation Abstr.)

11890 INTRODUCTION TO SPECIAL RELATIVITY. Smith, James H. New York, W. A. Benjamin, Inc., 1965. 230p. $2.95 domestic; $3.25 foreign.

Discussions are given of classical relativity, the relativity postulates, light waves, time dilation, length contraction, velocity and acceleration, and the twin paradox, using the gedanken-experiment approach. The Lorentz transformation is explained, and an introduction is presented to proper velocity, momentum and energy conservation, zero-mass particles, center-of-mass and particle systems, four-vectors, and the relativistic treatment of electric and magnetic fields and forces. (M.J.T.)

Low Temperature Physics

Refer also to abstracts 10767, 10996, and 11410.

11891 (COO-264-224) ON SURFACE SUPERCONDUCTIVITY IN THE SUBCRITICAL REGION. Maki, Kazumi (Enrico Fermi Inst. for Nuclear Studies, Univ. of Chicago, Ill.). Nov. 1964. Contract AT(11-1)-264. 13p. (EFINS-64-59). Dep. mn. CFSTI $1.00 cy, $0.50 mn.

As a simple application of the general Ginzburg-Landau equation previously deduced, surface superconductivity in a strong magnetic field is considered. The expression of local density of state and surface impedance is obtained. Also the critical current in superconducting sheath is calculated by using Abrikosov's procedure. (auth)

11892 (LA-DC-6824) A HYDRODYNAMIC MODEL OF He(II) NEAR T_λ. Bendt, Philip J. (Los Alamos Scientific Lab., Univ. of California, N. Mex.). [1964]. Contract W-7405-eng-36. 9p. Dep. mn. CFSTI $1.00 cy, $0.50 mn.

The temperature dependence of the torque on a Rayleigh disk in rotating helium II is investigated. A model of He II is described. In the model, He II consists of two interpenetrating components, both of which rotate with the vessel. (M.O.W.)

11893 PHONON-ROTON MODEL FOR COMPRESSED He II. Mills, R. L. (Los Alamos Scientific Lab., N. Mex.). Ann. Phys., 35: 410-25(Dec. 1965). (LA-DC-7269).

Some data on the isobaric thermal expansion coefficient of He II in the temperature range from 0.5 to 1.5°K and at pressures between the vapor curve and the melting curve were analyzed in terms of the Landau model of phonon-roton excitations. (D.C.W.)

11894 MAGNETIC PINNING IN A TYPE-II SUPERCONDUCTOR. Alden, T. H.; Livingston, J. D. (General Electric Research and Development Center, Schenectady, N. Y.). Appl. Phys. Lett., 8: 6-7(Jan. 1, 1966).

Dispersions of spherical Fe particles in Hg-13 at. % In were prepared and cooled to 4.2°K. A state of remanent magnetization was induced in the Fe by applying and removing a field of 6000 Oe; the sample was then cooled to the superconducting state in zero field. Magnetization curves to 400 Oe and back to zero were then taken either parallel or antiparallel to the remanent particle magnetization. The hysteresis observed is markedly different in these two directions. The interaction between flux threads and ferromagnetic particles is considered. The results demonstrate the effectiveness of magnetic particles in increasing critical currents, the superiority of attractive centers over repulsive ones, and the possibility of directional superconductors whose properties depend on the sense of the applied magnetic field. (A.G.W.)

11895 FLUX JUMPS AND TRAINING EFFECT IN MULTILAYER Nb-Zr SUPERCONDUCTING COIL. Iwamoto, M.; Kaneseki, N.; Kawai, T. (Mitsubishi Electric Corp., Amagasaki, Japan). Appl. Phys. Lett., 8: 38-40 (Jan. 15, 1966).

The flux jumps which seem to be responsible for the training of superconducting coils were observed using a coil wound with two pieces of Nb-Zr wire in parallel. (D.C.W.)

11896 SUPERCONDUCTIVITY OF OSMIUM AND RUTHENIUM UNDER PRESSURE. Bucher, E. (Univ. of Geneva); Mueller, J.; Olsen, J. L.; Palmy, C. Cryogenics, 5: 283-4(Oct. 1965).

Measurements of superconducting transition temperature as a function of pressure were made on electron-beam-melted samples of Os and Ru up to 30,000 atm. The results were compared with available data on the isotope effect, and the correlation was found to be less simple than previously suggested. (A.G.W.)

11897 ON THE QUANTUM-MECHANICAL PAIR-CORRELATION FUNCTION OF ^{4}He GAS AT LOW TEMPERATURES. **Larsen, Sigurd Yves** (National Bureau of Standards, Washington, D. C.); Witte, Kathleen; Kilpatrick, John E. J. Chem. Phys., 44: 213-20(Jan. 1, 1966). (LA-DC-7459).

The density-independent part of the direct- and exchange-correlation functions for ^{4}He, using the de Boer and Michels Lennard-Jones potential, were calculated at 2, 1, 0.5, and 0.1°K. The necessary wave-functions were obtained by numerical integration of the Schrödinger equation. The peak of the direct-correlation function is much less than its classical value and occurs at a slightly larger radius. The tail (large r) agrees very well with the form given by the Wigner-Kirkwood expansion. The exchange-correlation function which represents the entire effect of the spin and statistics of the system vanishes very rapidly with increasing temperatures. (auth)

11898 GREEN'S FUNCTIONS AND SUPERFLUID HYDRODYNAMICS. **Kane, Joseph W.**; Kadanoff, Leo P. (Univ. of Illinois, Urbana). J. Math. Phys. (N. Y.), 6: 1902-12(Dec. 1965).

The two-fluid hydrodynamics of Landau and Tisza is related to the thermodynamic Green's function formulation of the many-body problem. A specific approximation for the self energies yields directly the superfluid hydrodynamics in the limit of slow space and time variation. The approximation chosen is the simplest possible form for the self energies which includes the effects of collisions and which also satisfies the differential conservation laws for the mass, momentum, and energy. Of course these self energies are not adequate for a realistic description of ^{4}He. Nonetheless the structure of this model may provide some insight into the exact theory. For example, in the model employed here the self-energies and Green's functions obey several integral identities which are utilized in the derivation of the two-fluid hydrodynamics, and which yield useful expressions for some thermodynamic quantities. It is speculated that the identities and the consequent expressions for the various thermodynamic quantities may have a wider range of validity than their derivation. (auth)

11899 THE OCCURRENCE OF SUPERCONDUCTIVITY IN SULFIDES, SELENIDES, TELLURIDES OF PT-GROUP METALS. **Raub, Ch. J.**; Compton, V. B.; Geballe, T. H.; Matthias, B. T.; Maita, J. P.; Hull, G. W. Jr. (Bell Telephone Labs., Inc., Murray Hill, N. J.). J. Phys. Chem. Solids, 26: 2051-7(Dec. 1965).

Superconductivity was discovered in Pd compounds with Se and Te, in $IrTe_3$ and in PtTe. The superconducting transition temperature of a Pd–Se alloy containing 85 to 87 at. % Pd is 0.66°K which is unusually high for its valence-electron concentration. A homogeneity range exists for the hexagonal $B8_1$-type compound PdTe and for the trigonal C6-type compound $PdTe_2$. The results of the low temperature heat capacity measurements of PdTe and $PdTe_{1.04}$ show that the large change in the transition temperature with composition is accompanied by a large change in the linear heat capacity coefficient, γ. (auth)

11900 CONCERNING THE ROTATION OF HELIUM II NEAR THE λ POINT. **Tsakadze, D. S.**; Shanshiashvili, L. G. (Tbilisi State Univ., USSR). JETP Lett. (USSR) (Engl. Transl.), 2: 194-5(Oct. 1, 1965).

The deflection of a Rayleigh disc in rotating liquid He was measured by observing the reflection of light from the disc and from a mirror located outside the liquid. The results verified that near the lambda point, liquid He II rotates, on the average, as a unit. (D.C.W.)

11901 TRANSITION OF SEMICONDUCTORS TO A SUPERCONDUCTING STATE UNDER THE INFLUENCE OF THE FIELD EFFECT. **Sandomirskii, V. B.** (Inst. of Radio Engineering and Electronics, Academy of Sciences, USSR). JETP Lett. (USSR) (Engl. Transl.), 2: 248-9 (Oct. 15, 1965).

On the basis of estimates for a semiconductor with the parameters of $SrTiO_3$, it is shown that, with the aid of the field effect, it is apparently possible to transform into the superconducting state a surface layer of a sample which would be in the normal state at the given temperature in the absence of charging. (D.C.W.)

11902 CURRENT MOTION IN SUPERCONDUCTORS CARRYING ALTERNATING CURRENTS IN A TRANSVERSE MAGNETIC FIELD. **Martinoli, P.**; Olsen, J. L.; Zoller, P. (Swiss Federal Inst. of Tech., Zurich). Phys. Lett., 20: 12-13(Jan. 15, 1966).

Flux variations close to current-carrying type I and type II superconductors in a transverse field were used to observe asymmetries in the distribution of current and magnetic moment. The sideways motion of the current in the mixed state agrees with a simple calculation. (auth)

11903 CAPTURE WIDTH OF VORTEX LINES FOR NEGATIVE IONS IN HELIUM II. **Douglass, R. L.** (Univ. of Beirut, Lebanon). Phys. Rev., 141: 192-7(Jan. 1966).

Negative-ion trapping was investigated in rotating liquid helium at temperatures above 1.2°K. Measurements are reported of the ion-capture width versus temperature and electric field (from 5 to 100 V/cm). The theory of the effect is reviewed and discussed and is shown to be in excellent agreement with experiment. Owing mainly to the insensitivity, at low ratios of electric field to temperature, of the capture width to the properties of the ion-vortex potential well, it is deduced only that the well must be larger than the ionic mean free path. (auth)

11904 RECOMBINATION LUMINESCENCE IN THE SCINTILLATION OF NORMAL AND SUPERFLUID LIQUID HELIUM. **Hereford, Frank L.**; Moss, Frank E. (Univ. of Virginia, Charlottesville). Phys. Rev., 141: 204-8(Jan. 1966).

The alpha-particle-induced scintillation of liquid helium was studied experimentally in the temperature range 1.23 to 4.2°K with an electric field (9 to 43 kv/cm) applied in the region of the alpha tracks. Simultaneously with observation of the scintillation intensity, the ion current extracted from the alpha tracks by the field was measured. The results indicate that recombination luminescence accounts for approximately 60% of the total scintillation intensity (with zero electric field) and that this component of the intensity is temperature-independent. However, the ion current extracted by the field and the corresponding reduction in scintillation intensity both have temperature dependences which exhibit anomalous behavior in the He II region. (auth)

11905 GROWTH OF PINNED QUANTIZED VORTEX LINES IN HELIUM II. **Glaberson, W. I.**; Donnelly, R. J. (Univ. of Chicago). Phys. Rev., 141: 208-10(Jan. 1966).

A model is proposed for the onset of instability of superflow in a narrow tube assuming growth of a primordial vortex pinned to irregularities on the wall. A description of subcritical and supercritical flow is obtained closely paralleling that proposed by Donnelly on a phase-slip argument. The critical velocity corresponds to the minimum radius of curvature of the pinned vortex line. The operation of a quantized-vortex-ring mill is described. (auth)

11906 THEORY OF SUPERCONDUCTORS CONTAINING MAGNETIC IMPURITIES. **Fulde, Peter**; Maki, Kazumi (Univ. of California, Berkeley). Phys. Rev., 141: 275-80 (Jan. 1966).

The recent theory of Gor'kov and Rusinov was studied in detail and extended, which describes superconductors with ferromagnetically aligned impurities, under the assumption that the electron mean free path due to spin-orbit interaction is small as compared with the coherence distance. It is shown that all usually considered physical quantities of such a system are identical to those of a superconductor containing magnetic impurities with randomly oriented spins, and those vertices for which differences should arise are pointed out. In addition, the magnetic properties of such systems were investigated. The upper critical field is calculated as a function of impurity concentration and temperature and it is shown

that the specific heat at the transition point in the presence of a field is a function of temperature only and does not depend on the magnetic-impurity concentration. The last results can explain the recent experimental findings by Finnemore et al. (auth)

11907 ELECTRODYNAMICS OF SUPERCONDUCTING ALLOYS IN HIGH MAGNETIC FIELDS. **Maki, Kazumi (Univ. of Chicago). Phys. Rev., 141: 331-5(Jan. 1966). (COO-264-263).**

The surface impedance of the superconducting alloys in high magnetic fields is explicitly calculated by restricting consideration to the critical region where the order parameter is small. It is shown that an expression can be obtained for the complex conductivity equivalent to that for superconductors containing paramagnetic impurity, as long as a gapless region is considered. A brief discussion is given on the complex conductivity in the weak-field region where the low-lying excitations associated with each flux line play a dominant role. (auth)

11908 THEORY OF NONHOMOGENEOUS SUPERCONDUCTORS. **Silvert, William; Cooper, Leon N. (Brown Univ., Providence). Phys. Rev., 141: 336-45(Jan. 1966).**

A variational principle is developed for calculating the properties of nonhomogeneous superconducting systems at finite temperatures. The quantity varied is the energy-gap function as it occurs in the Gor'kov equations, and the correct Green's function is obtained by minimization of the thermodynamic potential. The calculation may be simplified by expanding the potential in powers of the energy-gap function or by a technique of analytic continuation. The former is easier but can be used only near the transition temperature, while the latter is valid at all temperatures. The variational procedure is used to calculate the transition temperatures of superposed-film systems, using a one-parameter model to describe the intermetallic potential barrier. The results agree well with the experimental data and indicate that barrier effects are important. The theory is valid for all mean free paths and is in accord with the phenomenological analysis of Hilsch and Hilsch. (auth)

11909 SUPERCONDUCTING TRANSITION TEMPERATURE OF La_9S_4. **Guthrie, G. L.; Palmer, R. L. (General Atomic Div., General Dynamics Corp., San Diego, Calif.). Phys. Rev., 141: 346-7(Jan. 1966).**

The superconducting transition temperature of stoichiometric La_9S_4 was measured by two different methods and was found to be (8.25 ± 0.2)°K. A range of superconducting compositions exists in the metal-rich end of the γ phase of lanthanum sulfide. Part of the sulfur-rich end of the γ phase is nonsuperconducting. The superconducting transition temperature of γ-phase lanthanum sulfide appears to increase with increasing lanthanum content. (auth)

11910 ELECTRODYNAMIC STUDY OF JOSEPHSON TUNNELING IN SUPERCONDUCTING JUNCTIONS. **Silver, A. H.; Jaklevic, R. C.; Lambe, J. (Ford Motor Co., Dearborn, Mich.). Phys. Rev., 141: 362-6(Jan. 1966).**

A quantitative electrodynamic experiment on a Josephson oxide tunneling junction was performed. Using a current source at 30 Mc/sec, the time dependence of the Josephson equation, $j = j_0 \sin [\gamma_1 - \gamma_r - (2e/\hbar)\int A \cdot dl]$ was verified, where $(\partial/\partial t)[\gamma_1 - \gamma_r - (2e/\hbar)\int_1^r A \cdot dl] = -(2eV/\hbar)$. Thus the limiting voltage is shown to obey the quantum relationship, $2eV = \hbar\omega$. Measurements were made completely in the coherent state showing the diffraction nature of the junction as a function of applied magnetic field. The Josephson (parametric) inductance of the junction was directly observed and is in good agreement with the theory. (auth)

11911 MACROSCOPIC QUANTUM INTERFERENCE EFFECTS THROUGH SUPERCONDUCTING POINT CONTACTS. **Zimmerman, J. E.; Silver, A. H. (Ford Motor Co., Dearborn, Mich.). Phys. Rev., 141: 367-75(Jan. 1966).**

A small-area contact between two pieces of superconducting metal or alloy is a remarkably sensitive and convenient device for demonstrating long-range quantum interference effects. It has been shown in many experiments that the critical supercurrent through a pair of such contacts in a parallel superconducting circuit has a component periodic in the flux enclosed by the topological ring formed by the parallel circuit, the periodicity being h/2e, showing that the wave function is coherent around the ring. With this configuration coherence lengths of the order of millimeters or centimeters were demonstrated in Nb, V, Ta, Sn, Pb, and $Nb_{0.85}Zr_{0.15}$, in rings where the enclosed area was as large as 1 cm^2, so that the periodicity in applied field was of the order of 10^{-7} G. Both bulk and thin-film materials were used. These experiments provide general proof of London's concept of long-range phase coherence in both type-I and type-II superconductors, and in addition lead to useful laboratory instruments. Such devices were used to show quantized flux pinning in bulk type-II superconductors and to measure the magnetic field of a rotating superconductor. (auth)

11912 POSITRON ANNIHILATION IN SUPERCONDUCTING LEAD. **Briscoe, C. V.; Beardsley, G. M.; Stewart, A. T. (Univ. of North Carolina, Chapel Hill). Phys. Rev., 141: 379-80(Jan. 1966).**

The angular correlation of photons was measured for positrons annihilating in normal and superconducting lead. Any effect on the Fermi surface due to superconductivity was, as expected, too small to be observed. (auth)

11913 CRITICAL MAGNETIC FIELDS OF SUPERCONDUCTING RUTHENIUM ISOTOPES AND SEARCH FOR AN ISOTOPE EFFECT. **Gibson, J. W.; Hein, R. A. (Naval Research Lab., Washington, D. C.). Phys. Rev., 141: 407-11(Jan. 1966).**

In order to investigate the isotope effect, i.e., the dependence of the superconducting transition temperature on the isotopic mass, the critical-magnetic-field curves of three samples of ruthenium were measured to temperatures below 0.1°K. The samples had mean isotopic masses of 99.2, 101.1 (natural), and 103.9. Detailed critical-magnetic-field curves were obtained, but no systematic dependence of the transition temperature on the mean isotopic mass was found. The transition temperature in zero external magnetic field characteristic of all three samples is $T_0 = 0.509 \pm 0.002$°K and the critical magnetic field at absolute zero in $H_0 = 70.0 \pm 0.5$ G. Plots of the critical-field curves are given, as well as plots of H_c versus T^2, which show deviations from parabolicity consistent with the weak-coupling limit of the BCS theory. Values for the electronic specific-heat coefficient γ were determined from the critical-field curves, and these give $\gamma \simeq 2.80$ mJ/mole deg^2. All three samples exhibited "ideal" or "Meissner" properties, that is, the transitions were reversible in a magnetic field. (auth)

11914 SUPERCONDUCTIVITY IN THE ALLOY SYSTEM CADMIUM–MERCURY AND THE EFFECT OF ORDERING UPON SUPERCONDUCTIVITY. **Claeson, T.; Luo, H. L.; Merriam, M. F. (Univ. of California, San Diego, La Jolla). Phys. Rev., 141: 412-18(Jan. 1966).**

The superconducting transition temperatures of Cd–Hg alloys covering the complete composition range were determined. The solubility of Cd in Hg was accurately determined; it is 1.5 ± 0.25 at.% at 193°K. The terminal solid solubility of Hg in Cd is found to be 26 ± 2 at.% at 418°K. Boundaries of the ω phase occur at 88 ± 1 at.% Hg at 193°K and at 35 ± 2 at.% Hg at 383°K. Ordering occurs in the intermediate ω phase at compositions based on Cd_2Hg and $CdHg_2$. The effect of ordering upon the superconducting transition temperature is observed for the first time. The transition temperature for the ordered phase is lower than the one for the disordered. This is presumably caused either by a reduced electron-phonon interaction, which is reflected also in a lower measured normal-state resistivity of the ordered phase, or by changes in the electronic density of states at the Fermi surface, which would be expected as a consequence of the subdivision of the Brillouin zones by the superlattice formation. (auth)

11915 ULTRASONIC STUDIES IN NORMAL AND SUPERCONDUCTING THALLIUM. **Weil, Raoul; Lawson, A. W. (Univ. of California, Riverside). Phys. Rev., 141: 452-60(Jan. 1966).**

The velocity and attenuation of ultrasonic waves were determined in thallium for the case $ql < 1$. The data are used to verify Pippard's semiclassical theory of the attenuation of sound by normal electrons. The elastic constants are given at 4.2 and 297°K. The value of the superconducting energy gap is determined for several directions of propagation and polarization of shear waves and found to be slightly anisotropic. A strain-amplitude dependence of the attenuation is found, which occurs after a minimum threshold is attained. (auth)

11916 THERMAL CONDUCTIVITY IN SOLID ^{3}He AND ^{4}He. **Bertman, B.; Fairbank, Henry A.; White, Clark W. (Duke Univ., Durham, N. C.). Phys. Rev., 142: 74-9 (Feb. 1966).**

The thermal conductivity of solid ^{4}He and ^{3}He was measured over the temperature range 0.5 to 2.0°K at a number of molar volumes. In the hcp phase the thermal conductivities of both isotopes show the usual low-temperature maximum. Below the maximum the conductivity is characteristic of boundary scattering with a T^3 dependence and a phonon mean free path comparable to the sample diameter. The conductivity above the maximum varies exponentially with $1/T$ over about three orders of magnitude. This is characteristic of umklapp scattering. In the bcc phase of ^{3}He the anomalous behavior found by Walker and Fairbank is confirmed and the extension of the measurements to lower temperature permits observation of more of the anomalous region. The thermal conductivity in the bcc phase of ^{4}He was also measured. (auth)

11917 THERMAL CONDUCTIVITY IN ISOTOPIC MIXTURES OF SOLID HELIUM. **Bertman, B.; Fairbank, H. A.; Guyer, R. A.; White, C. W. (Duke Univ., Durham, N. C.). Phys. Rev., 142: 79-85(Feb. 1966).**

Thermal-conductivity measurements in isotopic mixtures of solid helium at concentrations of 1%, 4%, 10%, and 50% of ^{3}He in ^{4}He and vice versa are reported. The data were taken at $V = 19.5$ and 20.2 cm^3/mole; the data at 19.5 cm^3/mole are analyzed using the phenomenological equation of Callaway. Resistance to heat flow is assumed to be due to boundary, normal-process, umklapp-process, and a Rayleigh-like scattering mechanism which may be a combination of mass-fluctuation and lattice-distortion scattering. The strength of these scattering mechanisms is determined by the analysis. The major contribution to the thermal resistance at low temperature is found to be the lattice distortion around the site of an isotopic impurity. The intrinsic strength of lattice-distortion scattering is evaluated and found to depend on concentration more strongly than the $x(1-x)$ expected by analogy to mass-fluctuation scattering. Two arguments are given in explanation of this increased concentration dependence. (auth)

11918 PROXIMITY EFFECTS BETWEEN SUPERCONDUCTING AND MAGNETIC FILMS. **Hauser, J. J.; Theuerer, H. C.; Werthamer, N. R. (Bell Telephone Labs., Murray Hill, N. J.). Phys. Rev., 142: 118-26(Feb. 1966).**

Superimposed normal-superconducting films can be used in conjunction with theory to investigate the nature and magnitude of the electron-electron interaction taking place in the normal metal. Studies are reported in which the normal metals were various types of magnetic materials: the ferromagnets Fe, Ni, and Gd; antiferromagnetic Cr; and the dilute magnetic alloys 1% Fe in Mo and 2.9% Gd in Pb (the last actually being a low-transition-temperature superconductor). The superconducting metal in all cases was pure Pb. Measurements of the transition temperature of the sandwich as a function of Pb film thickness were compared with a combined theory incorporating the de Gennes-Werthamer calculation of the proximity effect in nonmagnetic materials together with the Abrikosov-Gor'kov model of superconductivity in dilute magnetic alloys. Agreement for the alloy systems was satisfactory with no adjustable parameters, while extension of the theory to the concentrated, ordered systems with one parameter adjusted was qualitatively reasonable. Certain aspects of superimposed films in general were also studied: Diffusion of one metal into the other during and after deposition; dependence of the sandwich transition temperature on the order of deposition of the component films; recrystallization at room temperature; and interfacial cell reactions, selectively oxidizing one of the components at room temperature in ambient atmosphere. (auth)

11919 ACCELERATED CURRENTS IN SUPERCONDUCTORS. **Ambegaokar, Vinay (Univ. of Helsinki); Rickayzen, Gerald. Phys. Rev., 142: 146-51(Feb. 1966).**

It is shown that the ratio of the accelerated currents of energy and matter induced in a superconductor by a long-wavelength electric field is equal to the chemical potential of the system. (auth)

11920 HEAT CAPACITY OF DILUTE SOLUTIONS OF LIQUID ^{3}He IN ^{4}He AT LOW TEMPERATURES. **Anderson, A. C.; Roach, W. R.; Sarwinski, R. E.; Wheatley, J. C. (Univ. of Illinois, Urbana). Phys. Rev. Lett., 16: 263-4 (Feb. 14, 1966). (COO-1198-326).**

The heat capacity of dilute solutions of liquid ^{3}He in ^{4}He were measured for nominal ^{3}He concentrations of 1.3% and 5.0% down to about 10 millidegrees Kelvin. The results showed that in these concentrations the ^{3}He is soluble in ^{4}He to at least 10 millidegrees Kelvin and that the ratio of heat capacity to temperature is constant within an experimental error of 2% from the lowest temperature of 8 millidegrees Kelvin up to about 35 millidegrees Kelvin for the 5% mixture. (G.O.Y.)

11921 SHAPE OF THE COEXISTENCE CURVE IN THE CRITICAL REGION. **Mistura, L.; Sette, D. (Univ., Rome). Phys. Rev. Lett., 16: 268-70(Feb. 14, 1966).**

The shape of the coexistence curve in the critical region is studied on the basis of data on the orthobaric densities of ^{4}He. A previous analysis of the data in which the Landau expansion was carried out in terms of the density $\rho = N/V$ with V fixed instead of the specific volume $u = V/N$ with N fixed is extended to include second-order terms. (D.C.W.)

11922 THERMAL EQUILIBRIUM BETWEEN LIQUID ^{3}He AND POWDERED CERIUM MAGNESIUM NITRATE AT VERY LOW TEMPERATURES. **Abel, W. R.; Anderson, A. C.; Black, W. C.; Wheatley, J. C. (Univ. of Illinois, Urbana). Phys. Rev. Lett., 16: 273-5(Feb. 14, 1966).**

On the basis of an analysis of the temperature-time curves from measurements of the heat capacity, it was found that the thermal relaxation time of a mixture of powdered magnesium cesium nitrate and liquid ^{3}He is anomalously small at very low temperatures. (D.C.W.)

11923 NORMAL PROCESSES WHICH INHIBIT SUPERCONDUCTIVITY. **Ferrell, Richard A. (Univ. of Maryland, College Park). Z. Phys., 189: 335-8(1966).**

The effective interaction strength for the establishment of Cooper pairs in a degenerate fermion gas is shown to be reduced by a second-order exchange process. In physical terms, the reduction is a consequence of the normal polarization clouds surrounding the individual fermions. Because of the Pauli exclusion principle, these polarization clouds block the approach of further quasi-particles and thereby tend to prevent Cooper pairing. The effect is related to but simpler than that studied by Henley and Wilets in connection with the energy gap of nuclear matter. The second-order suppressive effect is considerable for strong interaction and large state density, and may even prevent the superconducting transition from occurring at all. (auth)

11924 MULTIPLE-TRANSITION EFFECTS IN SUPERCONDUCTING FILAMENTARY CRYSTALS OF TIN [Thesis]. **Webb, Donald Harris. Pasadena, Calif., California Inst. of Tech., 1965. 94p.**

Some effects involving stepped transitions from the superconducting to the normal state, and vice versa, in filamentary crystals (whiskers) are reported. The crystals

were produced by extrusion under high pressure from plates of tin and mounted on glass; the transitions were observed by measuring voltage across the samples as they passed through the transitions induced by varying the temperature in a constant external magnetic field. The resistance was observed to change from zero to normal, and vice versa, in discrete steps. In each particular stage of the transition, the resistance was apparently constant, even though the temperature was continuously changing. The effect was most prominently evinced when the sample axis was inclined slightly to the field. The effect was found only in the first-order transition region. The conjectured interpretation proceeded along lines of work reported by Little and Parks, who first found evidence of quantized Abrikosov vortex lines in the intermediate state of filamentary samples. The dependence of the new effect on the angular orientation was investigated. The data regarding the upper limit of transition regions are consistent with Tinkham's predictions, based on a vortex-line model. The lower limit of the transition regions was found to be irregular and not very sensitive to field orientation. If the proposed interpretation is correct, then quantized vorticity is verified because the observed jumps are sharp and because they are observed (generally) throughout the intermediate state not merely in the limit where R/R_N is small. (Dissertation Abstr.)

11925 HEAT TRANSFER BY THE CIRCULATION OF SUPER-CRITICAL HELIUM. Kolm, H. H.; Leupold, M. J.; Hay, R. D. (Massachusetts Inst. of Tech., Cambridge). 17p. (CONF-650802-8). ORINS. Gmelin, AED-CONF-65-193-6.

From Cryogenic Engineering Conference, Houston, Tex.

Two prototype systems for maintaining cryogenic environments by forced circulation of supercritical He were designed and built. The first system consisted of a compact circulating pump and heat exchanger immersed in a He storage dewar and connected by two lines of small-diameter tubing to the apparatus to be cooled. The transfer line and experimental apparatus were contained in communicating vacuum jackets that could be cryo-pumped upon immersion into the storage dewar. The system was able to cool down a 20-g Cu block from room temperature in 30 sec and to sustain a limiting temperature of 16°K. In the second system the pump was located in the He line above the storage dewar, and the cryostat vacuum was isolated from the rest of the system so that the cryostat could be opened for sample changes and adjustments without losing the insulating vacuum in the immersed parts of the apparatus. (A.G.W.)

11926 FLUX-TRAPPING OF RF FIELDS IN SUPERCONDUCTORS. Haden, C. R.; Hartwig, W. H. (Univ. of Texas, Austin). 10p. (CONF-758-55). ORINS. Gmelin, AED-CONF-65-003-99.

From American Physical Society Meeting, New York, Jan. 1965.

A non-zero asymptotic loss at 0°K observed in previous studies of the microwave surface impedance of superconductors was investigated. Experimental results for Sn with Cu impurities, pure Ta, and 3 at. % In in Sn were compared with a simple model for flux trapping of the r-f magnetic field, which is valid in a local sense for a single typical trapping center. Good agreement between the model and experiment indicates that the loss is due to flux-trapping and that the essential features of the model are correct. (A.G.W.)

Neutron Physics

See also REACTOR TECHNOLOGY — Criticality Studies

Refer also to abstracts 12309 and 12364.

11927 (AE-208) MEASUREMENT OF THE NEUTRON SLOWING-DOWN TIME DISTRIBUTION AT 1.46 eV AND ITS SPACE DEPENDENCE IN WATER. Moeller, E. (Aktiebolaget Atomenergi, Stockholm (Sweden)). Dec. 1965. 30p. Dep. mn.

The use of the time dependent reaction rate method for the measurement of neutron slowing-down time distributions in hydrogen was analyzed and applied to the case of slowing down in water. Neutrons with energies of about 1 Mev were slowed down, and the time-dependent neutron density at 1.46 ev and its space dependence was measured with a time resolution of 0.042 μs. The results confirm the well known theory for time-dependent slowing down in hydrogen. The space dependence of the distributions is well described by the P_1-calculations by Claesson. (auth)

11928 (BNL-9790) INTERMEDIATE RESONANCE ABSORPTION. Goldstein, Rubin (Brookhaven National Lab., Upton, N. Y.). Dec. 1965. Contract AT(30-2)-Gen-16. 14p. (CONF-660203-3). Dep. mn. CFSTI $1.00 cy, $0.50 mn.

From National Topical Meeting on Reactor Physics in the Resonance and Thermal Regions, San Diego, Calif.

The difficulty of obtaining an exact analytical solution to the equations for the slowing down of neutrons has led to a number of approximate solutions to the problem. The intermediate resonance IR approximation is discussed. The extension of the IR formulation to nonhomogeneous systems is described. (M.O.W.)

11929 (CEA-R-2849) ASPECTS THEORIQUES ET EXPERIMENTAUX DE L'INTERACTION NEUTRONIQUE ENTRE MILIEUX MULTIPLICATEURS DE NEUTRONS. (Theoretical and Experimental Aspects of the Neutronic Interaction Between Multiplying Media). Mougniot, Jean-Claude (Commissariat a l'Energie Atomique, Saclay (France). Centre d'Etudes Nucleaires). Oct. 1965. 92p. Dep. mn.

A theoretical study of neutronic interaction of multiplying media is presented. The use of the surface multiplication constant and of the effective multiplication constant is considered. Three classical methods of interaction calculations are studied in parallel and the application of the K_{eff} method to problems of nuclear safety is discussed. (auth)

11930 (CEX-65.03) OPERATIONS PLAN—OPERATION HENRE. Haywood, F. F.; Provenzano, T. G.; Auxier, J. A. (eds.) (Oak Ridge National Lab., Tenn.). June 1965. Contract W-7405-eng-26. 48p. Dep. mn; CFSTI $1.00 cy, $0.50 mn.

A series of experiments, designated Operation HENRE (High Energy Neutron Reactions Experiment), to be held at the Nevada Test Site in the summer of 1965 is described. The objectives and methods of measurement of the 9 planned experimental programs are discussed in detail, along with the organization and responsibilities of Operation HENRE, the neutron source and support facilities, safety, and operating schedule. The studies are aimed at neutron and gamma distribution calculations to be used in characterizing radiation fields from nuclear weapons. (P.C.H.)

11931 (CONF-651101-53) THERMAL NEUTRON DIFFUSION IN HEAVY WATER. Parks, P. B.; Baumann, N. P. (Du Pont de Nemours (E. I.) and Co., Aiken, S. C. Savannah River Lab.). Nov. 1965. Contract AT(07-2)-1. 29p. Dep. mn. CFSTI $2.00 cy, $0.50 mn.

From 13th Conference on Remote Systems Technology, Washington, D. C.

A series of pulsed measurements were made to accurately determine the diffusion coefficient for thermal neutrons in pure D_2O. All known sources of error, both experimental and analytical, were closely examined. The calculated value of the D_2O absorption cross section (18 sec^{-1}) was used. The other coefficients were determined from the measured decay constants. A wide range of bucklings was used to maximize sensitivity. Detailed information on the experimental and theoretical techniques used is presented. (M.O.W.)

11932 (GA-6637) GAROL—A COMPUTER PROGRAM FOR EVALUATING RESONANCE ABSORPTION INCLUDING

RESONANCE OVERLAP. Stevens, C. A.; Smith, C. V. (General Atomic, San Diego, Calif. John Jay Hopkins Lab. for Pure and Applied Science). Aug. 24, 1965. Contract AT(04-3)-167. 131p. Dep. mn. CFSTI $4.00 cy, $1.00 mn.

A computer program, GAROL, was written to study resonance absorption. The program is an improvement over other programs, presently in use, by virtue of its ability to handle overlap effects between resonances of a resonance absorber and of mixtures of resonance absorbers. In addition, a wide choice of geometry, energy mesh spacings, and cross section representation is available to the user. (auth)

11933 (INR-630/IX-A/PR(Pt.2)) TABLES OF THE FUNCTIONS $x(c,-\nu)$ AND $x\pm(c_1,c_2)$ FOR THE NUMERICAL SOLUTION OF SLAB GEOMETRY NEUTRON TRANSPORT PROBLEMS. Kowalska, K. (Institute of Nuclear Research, Warsaw (Poland)). May 1965. 201p. Dep.

Numerical tables are presented for $1.00 \leq c_1 \leq 2.00$ in increments of 0.01 where at each value of c_1, c_2 takes on all values between 0.01 and 0.99 in increments of 0.01. (M.O.W.)

11934 (ORNL-TM-1325) REACT AND CONVRG FORTRAN SUBROUTINES FOR DETERMINING SOURCE CONVERGENCE FOR THE 05R MONTE CARLO NEUTRON TRANSPORT CODE. Morrison, G. W.; Mihalczo, J. T.; Irving, D. C. (Oak Ridge National Lab., Tenn.). Jan. 10, 1966. Contract W-7405-eng-26. 22p. Dep. mn. CFSTI $1.00 cy, $0.50 mn.

REACT is a FORTRAN subroutine for analyzing the neutron history tapes from the 05R Monte Carlo neutron transport code and for calculating the probability that a neutron born in one region will produce a neutron in another region. CONVRG is a FORTRAN subroutine for forming a matrix of the probabilities calculated by REACT and then iterating on the initial source distribution with this matrix until convergence is obtained. The number of iterations required for convergence is the average number of batches (generations) required for spatial convergence. The largest eigenvalue of this matrix, the neutron multiplication factor, is also calculated by CONVRG. (auth)

11935 (RFR-154) MONTE CARLO BERAEKNINGAR AV NEUTRON TERMALISERING I ETT HETEROGENT SYSTEM. II. NUMERISKA RESULTAT. (Monte Carlo Calculations in Neutron Thermalization in a Heterogeneous System. II. Numerical Results). Hoegberg, T.; Ljunggren, S.; Persson, P. E. (Aktiebolaget Atomenergi, Stockholm (Sweden)). Sept. 26, 1961. 18p. Dep. mn.

Numerical results on the calculation on the thermalization in plane geometry using the Monte Carlo method are reported. The results are analyzed by the method of Tretiakoff. (tr-auth)

11936 THE SPECTRUM OF THE MONOENERGETIC BOLTZMANN EQUATION IN PLANE GEOMETRY WITH LINEAR-ANISOTROPIC SCATTERING FUNCTION. Haungs, G. (Technische Hochschule, Karlsruhe, Ger.). Atomkernenergie, 11: 19-24(Jan.-Feb. 1966). (In German).

The multiplication factor c and anisotropy parameter γ_t dependence of the linear anisotropic scattering function is considered ($\gamma_t = \Sigma_t/\Sigma$, Σ_t = macroscopic transport cross section). It is shown that the positiveness of the scattering function limits the range of the physically possible γ_t values. Using an approximation the eigenvalues of the Boltzmann equation were found and their distribution in a γ_t-c-plane is represented graphically. It turns out that only two discrete eigenvalues belong to the physically allowed γ_t-region. These eigenvalues are tabulated for different γ_t- and c-values. (auth)

11937 AN EXACT DETERMINATION OF NEUTRON TEMPERATURE IN A NEUTRON FIELD VARIABLE IN TIME. Fleck, C. M.; Steuer, M. (Oesterreichische Hochschule, Vienna). Atomkernenergie, 11: 25-29(Jan.-Feb. 1966). (In German).

A method permitting the measurement of the neutron temperature, even if there are epithermal and fast neutrons, in a nonstationary, collimated neutron beam with the transmission method is described. The use of Dy, which combines a 1/v-activation cross section with a high Cd ratio, permits the determination of the Cd-difference of the foil arrangement in a single exposure to the neutron beam. Due to the rotational symmetry of the detector foils one needs not to worry about field gradients perpendicular to the field axis. Assuming a Maxwellian distribution the error of the temperature determination is 1.6% and therefore compatible with differential methods. (auth)

11938 USE OF TOTALLY REFLECTED COLD NEUTRONS FOR MEASUREMENT OF THE TEMPERATURE DEPENDENCE OF THE (n,p) CROSS SECTION FOR CHEMICALLY BOUND PROTONS. Schmidt, U. (Univ., Kiel). Atomkernenergie, 11: 39-46(Jan.-Feb. 1966). (In German).

A beam of cold neutrons was produced by total reflection from iron plates of a special constructed collimator. The reflected beam contains all energies up to a limiting energy, which is determined by the angular position of the collimator. This method was used to determine the cross section of the (n,p) scattering in C_6H_{12} in the temperature range between −25 and 30°C for a neutron beam with a limiting energy of 0.0018 ev. The cross section increases slightly with temperature and shows a step of 5 barns at the melting point. (auth)

11939 HALF-SPACE NEUTRON TRANSPORT WITH LINEARLY ANISOTROPIC SCATTERING. McCormick, N. J.; Kuscer, I. (Univ. of Michigan, Ann Arbor). J. Math. Phys. (N. Y.), 6: 1939-45(Dec. 1965).

The method developed by Case is used to solve four time-independent, one-speed problems for neutron transport in a homogeneous medium where the scattering function is linear in the cosine of the scattering angle. The solutions to the albedo, Milne, Green's function, and constant isotropic source problems for a half-space are facilitated by the use of half-range bi-orthogonality relations between the eigenfunctions of the homogeneous transport equation. Expressions are also derived for the emerging angular densities and the densities and net currents on the surface of the half-space. (auth)

11940 TIME-DEPENDENT NEUTRON SPECTRA IN GRAPHITE. Nicholson, K. P.; Poole, M. J. (Atomic Energy Research Establishment, Harwell, Eng.). J. Nucl. Energy: Pt. A and B, 19: 949-57(Dec. 1965). (AERE-R-4842).

The experiments of Barnard, Khan, McLatchie, Poole, and Tait were repeated using improved equipment to give neutron spectra in a graphite cube (of ~120 cm side) at 80 μsec intervals after the injection of a fast neutron pulse, over the interval 50 to 5010 μsec. Spectra calculated from a semiempirical energy transfer kernel agree well with the experiment provided leakage effects are properly treated. In particular the calculation is very sensitive to the form chosen for the transport cross section and to the treatment of the spatial distribution of flux in the block. (auth)

11941 RESONANCE ABSORPTION FOR HEAVY MODERATORS IN HOMOGENEOUS MEDIA. Sehgal, B. R. (Brookhaven National Lab., Upton, N. Y.). J. Nucl. Energy: Pt. A and B, 19: 921-34(Dec. 1965). (BNL-9136).

Resonance absorption is investigated in homogeneous media with heavy moderators. An intermediate resonance approximation is developed in which intermediate parameters are introduced for both the absorber and the moderator scattering, and a method for calculating these intermediate parameters is developed. Monte Carlo calculations of resonance capture are done for some ^{238}U resonances and for a set of moderator masses. The second-order methods of Chernick and Vernon and of Spinney, the intermediate resonance method of Forti, and the intermediate resonance approximation developed in this paper are compared against Monte Carlo calculations.

It is found that the intermediate resonance method developed in this paper compares best with the Monte Carlo results. Doppler coefficients calculated by this intermediate resonance approximation method are generally in agreement with the Monte Carlo calculations. An equivalence among homogeneous systems is established which states that homogeneous media with moderators of different mass but having the same effective moderator scattering cross section per absorber atom have the same resonance absorption for an individual resonance. (auth)

11942 RECONSTRUCTION OF THE NG 200/1 NEUTRON GENERATOR. Pasztor, Endre; Veress, Imre. Magyar Tud. Akad. Kozp. Fiz. Kut. Int. Kozlemen., 13: 273-80(1965). (In Hungarian).

The neutron generator, designated as NG 200/1, built in 1957 in the Central Research Institute of Physics, was moved to another building and was completely rebuilt during 1962-4. The improved design was aimed at a better protection against radiation, creation of neutron fluxes that can be varied within the limits of 10^5 to 10^{10} n/sec, operation of the machine under steady-state and nanosecond pulsed modes, and creation of a reliable control system. Steps were taken to allow extended operation up to periods of 100 hours and to improve the location of the target area. The original 1-stage cascade was used as the voltage source, operating it at 200 kv nominal tension with Se rectifiers. Separate ion paths were built for operation under steady state and pulsed conditions. The accelerator tube contained a single accelerating lense provided with cylindrical electrodes. The system was operated at a vacuum of 1 to 2×10^{-5} mm of Hg. The distance from the ion source to the final target was about 10 m. The neutron yield of the machine was checked by counting the α particles emitted during the nuclear reactions. A 16-kva triphase generator supplied the power to the machine that was remotely controlled and partially automatized. (TTT)

11943 EXPERIMENTAL DETERMINATION OF THE NEUTRON SPECTRA AND THE DECAY TIME CONSTANTS IN ZIRCONIUM HYDRIDE AS A FUNCTION OF THE TEMPERATURE. Einfeld, Klaus; Ruppert, Edmund (Interatom, Bensberg, Ger.). Nukleonik, 7: 452-7(Oct. 1965). (In German).

On a sample of zirconium hydride ZrH_x with a hydrogen concentration of x = 1.65, the decay time constants of a pulsed neutron field were measured as a function of temperature in the range from 20 to 450°C. The thermal neutron spectrum was also determined by use of the neutron time-of-flight method at temperatures of 20, 340, and 555°C. (tr-auth)

11944 EXPERIMENTAL INVESTIGATION OF THE NEUTRON SPECTRA EMERGING FROM POSSIBLE COLD NEUTRON MODERATORS AT 80 deg K AND 20 deg K [Thesis]. Altschuler, Sidney Joseph. New York, Columbia Univ., 1964. 164p.

Neutron spectra emerging from various thicknesses of paraffin, n-hexane, ammonia, ammonium chromate, ammonium fluosulfonate, ammonium persulfate, ammonium hexafluophosphate, water, Lucite, and heavy water at 77° and 300°K and 2 inches of water, paraffin, and Lucite at 20°K were obtained by using a slow chopper and time-of-flight measurements. For moderators at 77°K, the space transient of the neutron temperature varied exponentially as predicted by the rethermalization theory of Kottwitz and rethermalization lengths were measured. Values of "effective masses" were obtained by several methods. The behavior of a substance as a low temperature moderator was found to depend upon its rethermalization length, equilibrium neutron temperature, and the presence of certain energy levels. These factors appeared to be totally independent of each other. Lucite appeared to be the best such moderator yielding a neutron spectrum with an effective neutron temperature of 68°K. Although not superior to liquid hydrogen, it was comparable to methane and far better than water. A method of estimating the net gain of cold neutrons was developed. (Dissertation Abstr.)

11945 A METHODOLOGY FOR NEUTRON RESONANCE CALCULATIONS [Thesis]. Yost, Kenneth John. Lafayette, Ind., Purdue Univ., 1964. 173p.

A mathematical model for neutron resonance calculations was developed. The nature of the model is such that it can be used in conjunction with any computer code that develops group average fluxes. Special emphasis is given to the problem of interference between resonances of different isotopes. A wide variety of approximations to the statistical variation of resonance parameters is possible within the framework of the method. A selected few are expanded. Others are either specifically mentioned or implied. A Doppler coefficient calculation was made for a pure uranium critical assembly at temperatures of 400, 600, and 800 degrees Kelvin. The temperature dependence of the Doppler coefficient based upon these three points was found to lie "between" those of T^{-1} and $T^{-\frac{1}{2}}$. (Dissertation Abstr.)

11946 PINETO—A FORTRAN CODE DESIGNED FOR THE SOLUTION OF NON-LINEAR DIFFERENTIAL EQUATIONS IN NEUTRONS DYNAMICS. Mongini Tamagnini, C. (EURATOM, Ispra, Italy); Bona, C.; Mathis, A.; Modonesi, O. 22p. (CONF-650501-20). ORINS. Gmelin, AED-CONF-65-115-13.

From the Application of Computing Methods to Reactor Problems, Argonne, Ill.

PINETO, written in Fortran for IBM 7090, solves a system made up of the following equations: (a) the one-group one-region kinetic equation; (b) up to 11 delayed neutron equations; and (c) up to 98 equations of the type $dV_i(t)/dt = r_i(t)V_i(t) + N_i(t)$, where $r_i(t)$ and $N_i(t)$ are completely arbitrary functions depending on time directly or through any combination of the system variables t, $V_i(t)$. If desired, equations of type (a) and (b) can be dumped, and the problem can be described entirely by equations of type (c). A method is provided for automatically handling problems in which some of the system equations change their form during transient. The user of standard PINETO needs no knowledge of programming. Three examples of use of PINETO in its standard form are given: the determination in three-group theory of the behavior of a fast pulsed reactor during one pulse of reactivity; the study of a startup accident in a fast reactor; the solution of differential equations of the Bessel type. (A.G.W.)

11947 DETERMINATION OF THE NUMBER OF NEUTRONS EMITTED SIMULTANEOUSLY BY A SOURCE. Gey, Albert; Jacquesson, Jacques (to Commissariat a l'Energie Atomique). U. S. Patent 3,225,200. Dec. 21, 1965. Priority date Aug. 11, 1961, France.

An apparatus for determining among the neutrons emitted by a source the proportion of the neutrons emitted simultaneously includes a detector means adapted to deliver a signal upon detection of a neutron with the time interval between the appearance of the neutron and the emission of the signal being less than a predetermined time delay. The indications of two counters receiving the signal issued from the detecting device are compared, one through a first line having a dead time that is negligible with respect to the predetermined time delay and the other by means of a second line having a dead time substantially equal to the time delay. (B.L.M.)

Nuclear Properties and Reactions

Refer also to abstracts 10901, 10935, 11134, 11143, 11409, 11476, 11491, 11498, 11511, 11566, 11677, 12303, and 12374.

11948 (AD-624318) QUASI-FREE PROTON-PROTON SCATTERING IN LIGHT NUCLEI AT 460 Mev. Tyren, H.; Kullander, S.; Sundberg, O.; Ramachandran, R.; Isacsson, P. (Enrico Fermi Inst. for Nuclear Studies, Univ. of Chicago,

Ill.); Berggren, T. (Nordisk Institut for Teoretisk Atomfysik, Copenhagen (Denmark)). [1964]. 150p.

Quasi-free proton-proton scattering was studied in a number of light nuclei at 460 Mev using two large identical magnetic spectrometers with two-directional focusing and a multichannel detector system. The experiments were performed in a symmetric geometry. Summed energy spectra and angular correlation distributions of separated components of the spectra are presented. The experimental results for the lighter nuclei are analyzed by comparing them with theoretical results obtained on the basis of the distorted-wave impulse approximation. Information on the radii and occupation numbers of the 1s and 1p orbitals in the nuclei considered is obtained. (auth)

11949 (AD–625747) TOTAL NEUTRON CROSS SECTIONS OF COPPER, IRON, AND ALUMINUM NEAR 14 Mev. Albergotti, Jesse C.; Ferguson, James M. (Naval Radiological Defense Lab., San Francisco, Calif.). Nov. 8, 1965. 11p. (USNRDL-TR–929). CFSTI $1.00 cy, $0.50 mn.

Total neutron cross sections of Mg, Al, Fe, and Cu were measured using T(d,n) neutrons in the energy range 12 to 14 Mev. The accuracy (counting statistics) is better than 1%. The energy resolution (two standard deviations of the energy resolution function) varies from 35 to 150 kev. Fluctuations of amplitude 2 to 3% and width of the order of 100 kev are found in the cross sections of Mg and Al. No such variations are found in the cross sections of Fe and Cu; a χ^2 test agrees with a straight line fit to the Fe and Cu data. (auth)

11950 (AE-202) A STUDY OF THE "384" Kev COMPLEX GAMMA EMISSION FROM ^{239}Pu. Forsyth, R. S.; Ronqvist, N. (Aktiebolaget Atomenergi, Stockholm (Sweden)). Nov. 1965. 15p. Dep. mn.

Gamma spectrometric studies of plutonium samples of several isotopic compositions were described using a sodium iodide detector and a lithium-drifted germanium detector. The 384-kev peak was shown to be a complex peak containing 12 gamma components due to plutonium-239 between 300 and 450 kev, and their relative intensities were estimated. Anion exchange and solvent extraction experiments also demonstrated that two further contributions due to uranium-237 are present in plutonium containing significant amounts of plutonium-241. (auth)

11951 (AE–205) SYSTEMATICS OF ABSOLUTE GAMMA RAY TRANSITION PROBABILITIES IN DEFORMED ODD-A NUCLEI. Loebner, K. E. G.; Malmskog, S. G. (Aktiebolaget Atomenergi, Stockholm (Sweden)). Nov. 1965. 60p. Dep. mn.

All known experimentally determined absolute gamma ray transition probabilities between different intrinsic states of deformed odd-A nuclei in the rare earth region ($153 \leq A \leq 181$) and in the actinide region ($A \geq 227$) are compared with theoretical transition probabilities (Weisskopf and Nilsson estimate). Systematic deviations from the theoretical values are found. Possible explanations for these deviations are given. This discussion includes Coriolis coupling, $\Delta K = \pm 2$ band-mixing effects and pairing interaction. (auth)

11952 (COO–238-46) THE GALILEAN TRANSFORMATION OF CONTINUOUS ENERGY PARTICLE DISTRIBUTIONS. Allison, Samuel K. (Enrico Fermi Inst. for Nuclear Studies, Univ. of Chicago, Ill. Chicago Univ., Ill. Dept. of Physics). Jan. 1965. Contract AT(11-1)-238. 55p. (EFINS–65-3). Dep. mn. CFSTI $3.00 cy, $0.50 mn.

Continuous-energy particle distributions are characteristically produced in collision processes from which more than two bodies result. The first step in interpretation of a continuum observed in the laboratory system is usually to consider it in the barycentric system of the collision. Such a transformation of a continuum will in general change both its shape and total intensity as observed per unit solid angle. The non-relativistic transformation equations in terms of velocity are given, and the Jacobian determinant is evaluated. A method of normalizing an observed continuum is suggested, and the transformation equations are given. The application of the transformation is demonstrated by transforming a simple numerical barycentric distribution to the laboratory system, thus obtaining velocity spectra at various angles and angular distributions of particles of the same laboratory velocity. (auth)

11953 (COO–347-17) MASS AND CHARGE DISTRIBUTION STUDIES IN THE FISSION OF ^{197}Au BY INTERMEDIATE ENERGY HELIUM IONS [Thesis]. Lisman, Frederick L. (Purdue Univ., Lafayette, Ind. Dept. of Chemistry). June 1965. Contract AT(11-1)-347. 277p. Dep. mn. CFSTI $6.00 cy, $1.50 mn.

The fission of ^{197}Au was studied radiochemically by bombarding thin targets of high-purity gold with 33.5-, 37.0-, and 40.0-Mev helium ions. The fission products were chemically separated and purified, and their activities were counted in low-level beta counters. The absolute fission cross sections, mass distributions, and charge distribution were determined. (auth)

11954 (COO–347-18) CHARGE AND MASS DISTRIBUTION STUDIES IN THE FISSION OF ^{237}Np AND ^{239}Pu BY INTERMEDIATE ENERGY HELIUM IONS [Thesis]. Wogman, Ned Allen (Purdue Univ., Lafayette, Ind. Dept. of Chemistry). Jan. 1966. Contract AT(11-1)-347. 292p. Dep. mn. CFSTI $6.00 cy, $1.50 mn.

The fission of ^{237}Np and ^{239}Pu induced by helium ions in the energy range from 20.0 to 40.5 Mev was studied radiochemically. The charge distribution, mass distribution, and absolute fission cross sections were determined. (D.C.W.)

11955 (COO–347-19) FISSION OF RHENIUM AT INTERMEDIATE EXCITATION ENERGY [Thesis]. Menninga, Clarence (Purdue Univ., Lafayette, Ind. Dept. of Chemistry). Jan. 1966. Contract AT(11-1)-347. 155p. Dep. mn. CFSTI $5.00 cy, $1.00 mn.

The fission resulting from bombardment of naturally occurring ^{185}Re and ^{187}Re with 40.9-Mev ^{4}He ions was studied radiochemically. The target materials were extensively purified before irradiation. Thin targets were prepared by electroplating rhenium metal onto silver foil, and absolute cross sections were determined for the production of six selected nuclides. Relative cross sections were determined for six additional nuclides in bombardments of thick rhenium targets. The fission products were purified, and the activities were measured using low-background beta counters. Decay curves were resolved by a least square fit using an IBM 7094 computer. Determinations were made of several impurities remaining in the target material, and appropriate corrections were applied to the data. The mass distribution was observed to be symmetric. The full width at half maximum of the mass yield curve was 23 ± 2 mass units. The average number of neutrons emitted per fission event was 1 ± 1 neutrons. The total fission cross section was found to be 2.4 ± 0.6 microbarns. (auth)

11956 (EUR–2632.d) ZUM ZERFALL DES ^{241}Am—DIE INTENSITAET DER KONVERSIONSELEKTRONEN DES 26.4 kev- UND DES 33.2 kev-UEBERGANGS IM ^{237}Np. (On the Decay of ^{241}Am—Intensity of Conversion Electrons in 26.4 kev and 33.2 kev Passages in ^{237}Np). Bambynek, W. (European Atomic Energy Community, Geel (Belgium). Central Nuclear Measurements Bureau). Nov. 16, 1965. 36p. Dep. mn.

Data on the decay of ^{241}Am published in literature are reviewed. It is shown that the absolute intensities of the conversion electrons of the 26.4 and the 33.2 kev transitions, which were calculated from measured β-spectrometer data, are too small by nearly a factor of 2. On the other hand the intensities $e(26) = (23.9 \pm 6.7)$ and $e(33) = (26.4 \pm 6.6)\%$, which were calculated essentially from α- and γ-intensities, could be confirmed by the measurements. The conversion coefficient $\alpha(26) = 9.5 \pm 3.4$ deduced from these figures is about 3 times larger than that calculated by Sliv and Band or Rose. (auth)

11957 (GA-6832) THE ENERGY DEPENDENCE OF THE NEUTRON CAPTURE CROSS SECTION OF THE TUNGSTEN ISOTOPES FROM .01 TO 10 EV. Friesenhahn, S. J.; Haddad, E.; Froehner, F. H.; Lopez, W. M. (General Atomic, San Diego, Calif. John Jay Hopkins Lab. for Pure and Applied Science). [1965]. Contract SNPC-27. 47p.

Capture cross section measurements from 0.01 to 10. ev on ^{182}W, ^{183}W, ^{184}W, and ^{186}W employing a totally absorbing gamma ray detector are described. The 2200 m/sec value of the capture cross section is compared with previously reported measurements, and the shape and magnitude of the cross section curve is compared to calculations using reported resonance parameters. Parameters of negative energy levels required to account for the discrepancy between measured and calculated cross sections for ^{182}W and ^{184}W are given. A measurement of the gold capture cross section is used as a check on the techniques employed. (auth)

11958 (GAMD-6562) FASDOP—A FORTRAN IV COMPUTER PROGRAM FOR COMPUTING CROSS SECTIONS FROM RESONANCE PARAMETERS. Stevens, C. A. (General Atomic, San Diego, Calif. John Jay Hopkins Lab. for Pure and Applied Science). Aug. 9, 1965. Contract AT(04-3)-167. 13p. Dep. mn. CFSTI $1.00 cy, $0.50 mn.

The FASDOP computer program evaluates pointwise cross sections from single level Breit-Wigner resonance parameters. For any single problem it can handle up to 500 resonances and compute cross sections for a maximum of 2500 energies. (auth)

11959 (HW-77389) WESTCOTT PARAMETERS DERIVED FROM THE RBU BASIC LIBRARY FOR A Δ-4 CUTOFF. Liikala, R. C. (General Electric Co., Richland, Wash. Hanford Atomic Products Operation). Apr. 25, 1963. Contract AT(45-1)-1350. 17p. Dep. mn. CFSTI $1.00 cy, $0.50 mn.

Westcott parameters were derived for the following isotopes; ^{235}U, ^{236}U, ^{238}U, ^{239}Pu, ^{240}Pu, ^{241}Pu, ^{242}Pu, ^{241}Am, ^{242}Am, ^{243}Am, ^{242}Cm, ^{243}Cm, and ^{244}Cm. Results are presented in tabular form. (M.O.W.)

11960 (IDO-14667) BURNUP DETERMINATION OF NUCLEAR FUELS. Project Report for the Quarter, July 1–September 30, 1965. Maeck, William J.; Rein, James E. (eds.) (Phillips Petroleum Co., Idaho Falls, Idaho. Atomic Energy Div.). Dec. 1965. Contract AT(10-1)-205. 48p. Dep. mn. CFSTI $2.00 cy, $0.50 mn.

Measurements were made of ^{235}U and ^{233}U thermal fission yields from the second irradiated capsules of ^{235}U and ^{233}U. Two capsules, one containing a weighed quantity of highly enriched ^{235}U, both irradiated to ~12 atom percent fission, were dissolved and analyzed for the number of atoms of each uranium isotope and for the number of atoms of the various stable and long-lived fission product nuclides. The absolute fission yield values determined on the second ^{233}U capsule are given. Also reported is the weighted average of the absolute ^{235}U fission yields determined on the first and second ^{235}U capsules. In addition the values for the thermal capture-to-fission ratio (α) of ^{233}U and ^{235}U were determined. (auth)

11961 (INR-602/VII/PH) NUMERICAL SOLUTIONS OF THE SUPERCONDUCTIVITY EQUATIONS FOR ODD-A NUCLEI IN THE RARE-EARTH REGION. Hassan, M. Y. M.; Skladanowski, Z.; Szymanski, Z. (Institute of Nuclear Research, Warsaw (Poland)). Feb. 1965. 37p. Dep.

Numerical solutions of the equations of superconductivity are tabulated for even-odd nuclei in the rare-earth region. Some values of parameters for odd-A nuclei in this region are also given. (auth)

11962 (INR-655/I/PL) ENERGY LEVELS OF ^{8}Be PRODUCED IN THE $^{11}B(n,\alpha)^{8}Li \rightarrow {}^{8}Be$. Jaskola, M.; Natanson, L.; Osakiewicz, W.; Turkiewicz, J. (Institute of Nuclear Research, Warsaw (Poland)). Sept. 1965. 7p.

The energy spectrum of alpha particles from ^{8}Be which was produced by beta emission from ^{8}Li formed in the reaction $^{11}B(n,\alpha)^{8}Li$ was measured. Only one peak, at 2.9 Mev, was observed. (D.C.W.)

11963 (INSJ-91) SHELL EFFECTS IN THE COULOMB DISPLACEMENT ENERGIES OF THE EXCITED STATES. Ejiri, Hiroyasu (Institute for Nuclear Study, Tokyo Univ. (Japan)). Nov. 29, 1965. 18p. Dep. mn.

The Coulomb displacement energies of the ground states and the excited states in light nuclei are obtained from the energy differences between the corresponding isobaric levels. The equivalent uniform radii of $T = \frac{1}{2}$ and $T = 1$ levels are extracted from the Coulomb displacement energy. The shell effects are indicated in the equivalent uniform radii of the excited states and the ground states. Each state is found to have the equivalent uniform radius which is characteristic of the shell orbit. The levels in the same shell orbit have nearly the same equivalent radii, while the excitations to another shell orbit give rise to a discrete change of the equivalent uniform radii. The rotational states have the equivalent uniform radii close to that of the intrinsic state. These features are consistent with the simple shell model picture. (auth)

11964 (JINR-E-2464) PROTON EMITTERS AMONG Te ISOTOPES. Ter-Akopyan, G. M.; Petrov, L. A.; Vertogradov, L. S.; Karnaukhov, V. A. (Joint Inst. for Nuclear Research, Dubna (USSR). Lab. of Nuclear Reactions). 1965. 7p. Dep. mn.

The delayed proton emitters produced by the bombardment of ^{92}Mo and ^{94}Mo with ^{20}Ne ions were investigated. Proton activities with (4.2 ± 0.2) sec; (19 ± 0.7) sec; (13 ± 2) sec, and (60 to 80) sec. halflives were found. It is most probable that the first two emitters are Te isotopes with mass numbers of 109 and 111, respectively. (auth)

11965 (JINR-P-2426) PRIMENENIE POLYARIZOVANNOI POLYARIZOVANNOI PROTONNOI MISHENI DLYA ISSLEDOVANIYA NUKLON-NUKLONNOGO VZAIMODEISTVIYA PRI NIZKIKH ENERGIYAKH. (Use of Polarized Proton Target in the Investigation of Low-Energy Nucleon-Nucleon Interactions). Winternitz, P.; Legar, F. (Joint Inst. for Nuclear Research, Dubna (USSR). Lab. of Theoretical Physics. Joint Inst. for Nuclear Research, Dubna (USSR). Lab. of Nuclear Problems). 1965. 168p. Dep. mn.

The possible use of a polarized proton target in the investigation of low-energy nucleon-nucleon interactions is reviewed. The reconstruction of the scattering matrix and verification of P-, T-, and isotopic invariance are briefly discussed. Possible sources and detectors of polarized particles are discussed. Detailed tables of experimental values are listed for the polarization of nucleons scattered on nucleons and complex nuclei and in nuclear reactions for energies from 0.1 to 25 Mev. All possible experimental quantities determined from the phase shift analysis are given in graphs, for the energy 23.1 Mev. 175 references. (auth)

11966 (JINR-P-2432) KOLLEKTIVNYE SOSTOYANIYA YADER V METODE TAMMA-DANKOVA. (Collective States of Nuclei in Tamm-Dancoff Method). Fogel, P. (Joint Inst. for Nuclear Research, Dubna (USSR). Lab. of Theoretical Physics). 1965. 11p. Dep. mn.

Equations for the energies of collective states are obtained for the weak multipole interaction on a quasiparticle basis. Conditions are found under which simple equations of the Tamm-Dancoff method are derived. It is shown that these conditions are very well fulfilled for vibrations of even-even deformed nuclei. (auth)

11967 (JINR-P-2455) RASCHET MNOGOKRATNYKH VZAIMODEISTVII DLYA EKSPERIMENTOV PO RADIATSIONNOMU ZAKHATU NEITRONOV. (A Computation of Multiple Interactions for Experiments on Radiation Capture of Neutrons). Mikhailus, F. F.; Pikel'ner, L. B.; Sharapov, E. I. (Joint Inst. for Nuclear Research, Dubna (USSR). Lab. of Neutron Physics). 1965. 18p. Dep. mn.

Methods and results of calculating multiple interactions

of neutrons in flat samples are considered. A comparison is made of calculations carried out by the Monte-Carlo method and experimental data obtained in measurements of radiative neutron capture. (auth)

11968 (JINR-P-2470) O SVOISTVAKH IZOTOPA ^{254}102. (On Properties of Isotope ^{254}102). Zager, B. A.; Miller, M. B.; Mikheev, V. L.; Polikanov, S. M.; Sukhov, A. M.; Flerov, G. N.; Chelnokov, L. P. (Joint Inst. for Nuclear Research, Dubna (USSR). Lab. of Nuclear Reactions). 1965. 8p. Dep. mn.

The isotope ^{254}No was synthesized on an external beam of the JINR 150-cm cyclotron in the reaction ^{243}Am(N-15,4n) ^{254}No. By recording the α decay of the parent and daughter nuclei it was established that the half life of this isotope lies between 20 and 50 sec and the energy of emitted α particles is 8.10 ± 0.05 Mev. The results obtained are in contradiction with available data. (auth)

11969 (JINR-P-2471) K VOPROSU O SVOISTVAKH IZOTOPA ^{254}No. (On Properties of a ^{254}No Isotope). Donets, E. D.; Shchegolev, V. A.; Ermakov, V. A. (Joint Inst. for Nuclear Research, Dubna (USSR). Lab. of Nuclear Reactions). 1965. 17p. Dep. mn.

The isotope ^{254}No was synthesized in the nuclear reactions ^{243}Am(N-15, 4n)^{254}No and ^{238}U(Ne-22, 6n)^{254}No. The ^{254}No was identified by its daughter product ^{250}Fm. The dependence of the cross sections of these reactions on the energies of the bombarding ions from 75 to 90 and 112 to 135 Mev, respectively, was investigated. It was shown that ^{254}No undergoes α decay with a lifetime of about 50 sec. (auth)

11970 (JINR-P-2473) O RAVNOVESNOI DEFORMATSII TYAZHELYKH YADER. (On the Equilibrium Deformation of Heavy Nuclei). Bal'butsev, E. B.; Mizhailov, I. N. (Joint Inst. for Nuclear Research, Dubna (USSR). Lab. of Theoretical Physics). 1965. 13p. Dep. mn.

Effects are discussed which are due to taking account of the space symmetry of wave functions approximating the heavy nuclear states. It is shown that projecting the wave functions on the states with fixed rotational quantum numbers is important especially when pairing correlations are present and can lead to a change in the magnitude of the equilibrium deformation parameters as well as to the appearance of a small deformation in many nuclei which are usually treated as spherical. (auth)

11971 (MLM-1251J) WEAK ALPHA AND ELECTRON-CAPTURE DECAY IN ^{208}Po AND ^{209}Po. Hagee, G. R. (Mound Lab., Miamisburg, Ohio. Cincinnati Univ., Ohio); Lange, R. C. (Mound Lab., Miamisburg, Ohio); McCarthy, J. T. (Cincinnati Univ., Ohio). Jan. 1966. Contract AT(33-1)-Gen-53. 48p. Dep. mn. CFSTI $2.00 cy, $0.50 mn.

The weak alpha and electron-capture decay modes of ^{208}Po and ^{209}Po were investigated. Previously unobserved alpha groups were found at 4.22 Mev with 2.44×10^{-4}% abundance in ^{208}Po decay and at 4.11 and 4.31 Mev with 5.66×10^{-4}% and 1.46×10^{-4}% abundances, respectively, in ^{209}Po decay. The 4.617 Mev alpha group in ^{209}Po was measured explicitly and found to have 0.48% branching. Electron-capture branchings in ^{208}Po and ^{209}Po were measured as 1.81×10^{-3}% and 0.263%, respectively. Predominant electron-capture feeding in ^{208}Po populates a 921 kev level in ^{208}Bi. The log ft. value of this transition was determined to be 13.7 in agreement with its assignment as a second forbidden transition ($\Delta I = 2$, $\Delta\pi$ = NO). Gamma-rays following electron-capture decay in ^{208}Po were found at energies of 65, 291, 534, 565, 599 and 865 kev. Measurements of internal conversion coefficients or K to L + M shell conversion electron ratios on the 291, 534, 565 and 599 kev transition in ^{208}Po or 263 and 900 kev transitions in ^{209}Po show them to be pure MI or mixed MI + E2 transitions. (auth)

11972 (NP-15716) CONTRIBUTION A L'ETUDE THEORIQUE DES REACTIONS A(t,p)B [These]. (Contribution to the Theoretical Study of A(t,p)B Reactions [Thesis]). Maguin, Claude (Lyon Univ. (France). Institut de Physique Nucleaire). [1964]. 82p. Dep. mn.

The processes of double stripping are calculated. The wave functions characterizing each method (triton plus target nucleus and proton plus residual nucleus) are given. The transition amplitude was calculated, and this leads to the differential cross section, simplified by a particular potential. Numerical applications are given for the reactions ^{28}Si(t,p)^{30}Si and ^{16}O(t,p)^{18}O. The results are discussed and compared with those obtained previously. (tr-auth)

11973 (NP-15791) O KOGERENTNOI VOZVUKHDENII YADER, PROLETAYUSHCHIKH CHEREZ KRISTALL. (On the Coherent Coulombic Excitation of Nuclei Passing Through Crystals). Report No. 357. Okorokov, V. V. (Gosudarstvennyi Komitet po Ispol'zovaniyu Atomnoi Energii SSSR, Moscow. Institut Teoreticheskoi i Eksperimental'noi Fiziki). 1965. 12p. Dep. mn.

The qualitative considerations are presented discussing the existence of the effect of the coherent Coulombic excitation of nuclei passing through a crystal. (auth)

11974 (ORNL-P-960) OPTICAL POTENTIALS AND HIGH-ENERGY INELASTIC PROTON SCATTERING. Haybron, R. M. (Oak Ridge National Lab., Tenn. Michigan State Univ., East Lansing). [1964]. Contract W-7405-eng-26. 10p. Dep. mn. CFSTI $1.00 cy, $0.50 mn.

Distorted-wave calculations of inelastic proton scattering on ^{12}C at 156 Mev were compared with experimental results to determine the sensitivity of the inelastic cross section to the choice of optical parameter. Excitation of the 2^+, 4.43-Mev and 3^-, 9.6-Mev levels of ^{12}C was considered. The cross section and polarization results are presented. (M.O.W.)

11975 (PAM-6502) MISE AU POINT SUR LE PROBLEME DES INTERACTIONS NUCLEAIRES DES MUONS ULTRA-ENERGETIQUES DU RAYONNEMENT COSMIQUE. (Comments on the Problem of Nuclear Interactions of Ultra-Energetic Muons of Cosmic Radiation). Kessler, Paul (College de France, Paris. Laboratoire de Physique Atomique et Moleculaire). Jan. 1965. 29p. Dep. mn.

The Kessler-Kessler formula for the equivalent photon spectrum of the muon is derived using more rigorous techniques than were originally used. The predictions of the K-K method and of the Williams-Weizsacker method are compared with some experimental observations on reactions of cosmic neutrons. The results indicate that the true representation probably lies somewhere between these two methods, but is more closely related to the K-K method. (D.C.W.)

11976 (TID-22504) I. INTERNAL CONVERSION COEFFICIENTS IN THE DECAY OF ^{57}Co. II. STUDY OF THE "FOCUSING EFFECT" OF THE VANDERBILT BETA-RAY SPECTROMETER POST ACCELERATION SYSTEM [Thesis]. Hall, Duane Charles (Vanderbilt Univ., Nashville, Tenn.). Aug. 1965. Contract AT(40-1)-2401. 60p. Dep. mn. CFSTI $3.00 cy, $0.75 mn.

The conversion coefficients for 14.4-kev transition in the decay of ^{57}Co were determined. Branching ratios for the 122- and 136-kev transitions were determined. The experimental techniques used are discussed. An investigation of the "focusing effect" of the Vanderbilt beta spectrometer post acceleration system was made. Results of this investigation are discussed. (M.O.W.)

11977 (TID-22536) A STUDY OF NON-MESIC DECAY OF HELIUM HYPERNUCLEI. Technical Report No. 519. Huang, Rosalind (Maryland Univ., College Park. Dept. of Physics and Astronomy). Sept. 1965. Contract AT(40-1)-2304. 61p. Dep. mn. CFSTI $3.00 cy, $0.75 mn.

The branching ratio for two-prong nonmesic to π^- mesic decays for helium hypernuclei is obtained. It is found to be: Q (two-prong) = 1.75 ± 0.55. Combining this with other similar experimental results, the ratio becomes: Q (two-prong) = 1.67 ± 0.22 from which Q($_\Lambda$He^5) is obtained and

compared with a theoretical prediction. One-prong helium hypernuclei were also investigated. An attempt was made to separate them from background events. The number of one-prong helium hypernuclei found in this experiment is estimated to be zero. Also presented is the ratio of proton stimulation to neutron stimulation in helium nonmesic decay. However the stimulation ratio for $_{\Lambda}He^{5}$ estimated from this experiment is inconsistent with the theoretical prediction. (auth)

11978 (UCRL-7961-T) AN ANALYSIS OF THE N + ^{4}He REACTION AND THE EFFECTS OF SPIN COUPLING n + ^{4}He TO d + T. DeFacio, W. Brian (Lawrence Radiation Lab., Univ. of California, Livermore). July 13, 1964. Contract W-7405-eng-48. 61p. Dep. mn. CFSTI $3.00 cy, $0.75 mn.

The total hamiltonian for a five-body system is solved in the lump-lump approximation with the quartet S state of (d + T) spin coupled to the doublet D($^{3}/_{2}$) state of (n + ^{4}He) via a square well phenomenological potential. The range and depth of the square well are adjusted to provide the proper (n + ^{4}He) channel elastic cross section and also the proper (d + T) channel total cross section. Angular distributions peak at backward angles quite naturally in this model (usually strong exchange processes are concluded for back angle peaking of differential cross sections, but in the lump-lump approximation there are no identical particles so this is desirable). Excellent agreement was obtained with the data of Shamu and Jenkins with a square well of range a_0 = 3.35f and depth 20 Mev. The dependence on observables upon both the depth and the range of the coupling potential is discussed. (auth)

11979 (UCRL-12152) ELASTIC AND INELASTIC SCATTERING OF PROTONS BY ^{18}O. Stevens, J.; Lutz, H. F.; Eccles, S. F. (Lawrence Radiation Lab., Univ. of California, Livermore). Dec. 7, 1964. Contract W-7405-eng-48. 36p. Dep. mn. CFSTI $2.00 cy, $0.50 mn.

Differential cross sections for elastic and inelastic scattering of protons by ^{18}O were obtained. Excitation curves from 7.89 to 16.28 Mev exhibit a large resonance at 10.5 Mev. Angular distributions were obtained at 11 values of the incident energy. The elastic angular distributions were fitted with the optical model and the inelastic scattering angular distributions were analyzed with both the distorted-waves Born-approximation and the generalized optical model. The DWBA analysis yield a $\beta \simeq 0.4$, while the generalized optical model allows the data to be fit with β = 0.28. (auth)

11980 (USNRDL-TR-935) NUCLEAR-CHARGE DISTRIBUTIONS OF SEVERAL FISSION PRODUCT MASS CHAINS. Strom, P. O.; Love, D. L.; Greendale, A. E.; Delucchi, A. A.; Sam, D.; Ballou, N. E. (Naval Radiological Defense Lab., San Francisco, Calif.). Nov. 5, 1965. Contract AT(49-2)-1167. 27p. Dep. mn. CFSTI $2.00 cy, $0.50 mn.

Information on the nature of nuclear charge distribution in thermal-neutron fission of ^{235}U was obtained from measurements of fission yields of the major constituents in each of three adjacent mass chains. A regular variation in the width of the charge distribution curves with mass number was observed, and values of the most probable nuclear charge were determined. No effects attributable to the 50-proton or 82-neutron closed shells were observed in the charge distribution curves examined. (auth)

11981 (USNRDL-TR-943) ^{115}Pd YIELD IN THERMAL NEUTRON FISSION OF ^{235}U. Weiss, H. V.; Reichert, W. L. (Naval Radiological Defense Lab., San Francisco, Calif.). Nov. 12, 1965. Contract AT(49-2)-1167. 8p. Dep. mn. CFSTI $1.00 cy, $0.50 mn.

The formation of ^{115}Pd in thermal neutron fission of ^{235}U was studied quantitatively. A procedure was developed which rapidly separated palladium from daughter elements silver and cadmium. Separations were made from 2.8–120 seconds after fission. The growth of ^{115}Cd from palladium separated at various times constituted a decay curve for ^{115}Pd. The half life thus determined was $40.5^{+4.0}_{-3.0}$ seconds, a value which agrees with that previously reported. The cumulative fractional yield of ^{115}Pd compared to the total ^{115}Cd yield was 90.5 ± 7.2%. (auth)

11982 (LA-tr-65-34) LEVELS OF THE NUCLEUS ^{166}Ho FROM THE REACTION (n,γ). Groshev, L. V.; Shadiev, N. (Gosudarstvennyi Komitet po Ispol'zovaniyu Atomnoi Energii USSR). Translated by Helen Chick (Los Alamos Scientific Lab., N. Mex.). 18p. Dep. mn. CFSTI $1.00 cy, $0.50 mn. JCL $1.60 fs, $0.80 mf.

The spectrum of γ-rays emitted in the capture of thermal neutrons by ^{165}Ho, in the energy range 4.5 to 6.35 Mev was measured by a magnetic Compton spectrometer. Thirty-eight lines were found in the γ-ray spectrum. On the basis of these data, the energies of excitation of the levels of ^{166}Ho were found. They are in good agreement with the energies of the levels of ^{166}Ho appearing in the (d,p) reaction. (auth)

11983 Q-VALUES AND CROSS-SECTIONS MEASUREMENTS OF THE (n,α) REACTION ON SOME NUCLEI. Benisz, J.; Jasielska, A.; Panek, T. (Inst. of Nuclear Physics, Krakow. Higher Pedagogical Coll. Katowice, Poland). Acta Phys. Pol., 28: 763-75(Dec. 1965).

The Q-values of the (n,α) reaction were measured for ^{17}O, ^{32}S, ^{33}S, ^{39}K, ^{40}Ca and ^{43}Ca, using the emulsion technique. The Q-values were found as follows ^{17}O, 2.76 ± 0.12 Mev; ^{32}S, 1.80 ± 0.11 Mev; ^{33}S, 3.62 ± 0.22 Mev; ^{33}S, < 1.04 Mev; (for the (n,α) reaction producing the first excited level of ^{30}Si); ^{39}K, 1.26 ± 0.16 Mev; ^{40}Ca, 1.76 Mev; ^{43}Ca, 3.63 Mev. The (n,α) cross sections were measured for ^{32}S, ^{33}S, ^{39}K. The plates were irradiated by thermal neutrons from a Po-Be source (0.025 ev) and from a nuclear reactor (0.035 ev). The values of cross sections were obtained for two neutron bombarding energies: E_n = 0.025 ev, ^{32}S: 3.9 ± 0.5 mb; ^{33}S: 151 ± 22 mb; ^{33}S: < 79 mb (the first excited level); ^{39}K: 4.3 ± 0.5 mb; E_n = 0.035 ev, ^{32}S: 3.2 ± 0.7 mb; ^{33}S: 148 ± 39 mb. The experimental cross sections were compared with cross sections predicted by theory based on the statistical nucleus model. (auth)

11984 THE CAPTURE RATIO P_L/P_K FOR THE ELECTRON CAPTURE DECAY OF ^{57}Ni. Winter, G.; Hohmuth, K.; Ross, R.; Kaestner, H.; Schintlmeister, J. (Zentralinstitut fuer Kernforschung, Rossendorf, Ger.). Ann. Phys., (7), 16: 207-8(1965). (In German).

The capture ratio P_L/P_K for ^{57}Ni was determined with a multiwire proportional counter. The Ni, produced by β irradiation of Fe, was separated with ion exchange and introduced into the compound nickelcyclopentadiene. Low masses of this substance were used together with argon and methane to fill a multiwire counter. The intensity of the K and L radiation was determined. The intensity ratio was evaluated as N_L/N_K = 0.108 ± 0.003. The evaluation of the capture ratio gave the value P_L/P_K = 0.102 ± 0.006, in good agreement with theoretical calculations. (J.S.R.)

11985 CROSS SECTIONS FOR NEUTRON INELASTIC INTERACTIONS WITH ^{7}Li, ^{12}C, ^{14}N, ^{27}Al, ^{56}Fe, Cu, Pb, ^{235}U, ^{238}U, AND ^{239}Pu. Degtyarev, Yu. G. At. Energ. (USSR), 19: 456-7(Nov. 1965). (In Russian).

Coefficients of transmission of neutrons of energies 8.1 and about 13 to 21 Mev through spherical samples were measured and used to derive the cross sections for nonelastic interactions. The results are presented, giving the percentage of multiple scattering in each case. (M.J.T.)

11986 CROSS SECTIONS FOR FAST NEUTRON RADIATIVE CAPTURE IN RHENIUM AND TANTALUM. Kononov, V. N.; Stavisskii, Yu. Ya. At. Energ. (USSR), 19: 457-8(Nov. 1965). (In Russian).

Radiative-capture cross sections of neutrons in Re and Ta were measured for energies from 30 to 170 kev, using a time-of-flight method. Results are presented and compared with those from previous experiments, and their accuracy is discussed. (M.J.T.)

11987 MEASUREMENT OF THE ABSORPTION CROSS SECTION OF ^{156}Gd. Grishanin, E. I.; Kukavadze, G. M.; Lependin, V. I.; Mamelova, L. Ya.; Morozov, I. G.; Orlov,

V. V.; Pilipets, D. T. At. Energ. (USSR), 19: 459-60(Nov. 1965). (In Russian).

Samples of gadolinium oxide were irradiated in a reactor with thermal neutrons to various integral fluxes. The thermal-neutron absorption cross section of ^{156}Gd was determined from the values of the ^{156}Gd and ^{157}Gd concentrations in the irradiated samples, measured on a mass spectrometer, and the value of the ^{157}Gd absorption cross section, obtained by averaging the cross section from resonance parameters over the neutron spectrum of the reactor. The cross section for 0.025-ev neutrons was found to be 13 ± 3 barns. (M.J.T.)

11988 THE (e,e'p) REACTION IN THE ^{9}Be NUCLEUS. Amaldi, Ugo, Jr.; Venuti, Gloria Campos; Cortellessa, Giorgio; Fronterotta, Gabriele; Reale, Armando; Salvadori, Paolo (Istituto Nazionale di Fisica Nucleare, Rome). Atti Accad. Naz. Lincei, Rend., Cl. Sci. Fis., Mat. Nat., 38: 499-504(Apr. 1965).

Some results on beryllium-9 are given. It is shown that the (e,e'p) reaction gives the same results as the (p,2p) reaction on some nuclei. The counting rate versus the binding energy is shown. It is concluded that there is further evidence of the existence of a proton group in the vicinity of 32 Mev binding energy, and that the $1s_{1/2}1p_{3/2}$ structure is confirmed, although lack of resolution does not add new knowledge about these binding energies. (J.F.P.)

11989 THERMONUCLEAR REACTIONS IN MEDIUM AND HEAVY NUCLEI. Truran, J. W. (Yale Univ., New Haven); Hansen, C. J.; Cameron, A. G. W.; Gilbert, A. Can. J. Phys., 44: 151-74(Jan. 1966).

A method is outlined by which thermonuclear reaction rates can be determined from the statistical properties of nuclei. Under the assumption that the contribution to the cross section of a given resonance is given by the Breit-Wigner single-level formula, the total rate is determined by integrating the product of the cross section, weighted by the nuclear level density, and the velocity over energy. The nuclear radiation widths are calculated on the assumption that electric-dipole transitions are dominant. The particle widths are determined by approximating the nuclear strength function by that value calculated for a black nucleus. Nuclear cross sections calculated in this manner are compared with experiment both for charged-particle reactions on lighter nuclei and for neutron-capture reactions proceeding on nuclei in the mass range A > 60. Good agreement is obtained in both cases. (auth)

11990 THE RATIO OF THE DIRECT TO THE CUMULATIVE YIELD OF ^{135}Xe IN THE THERMAL NEUTRON FISSION OF ^{233}U, ^{235}U, ^{239}Pu, AND ^{241}Pu. Okazaki, A.; Walker, W. H.; Bigham, C. B. (Atomic Energy of Canada Ltd., Chalk River, Ont.). Can. J. Phys., 44: 237-46(Jan. 1966). (AECL-2374).

The ratio of the direct to cumulative yields of ^{135}Xe produced in thermal neutron fission was determined by measuring the growth and decay of this nuclide in irradiated ^{233}U, ^{235}U, ^{239}Pu, and ^{241}Pu. After a short irradiation in a low neutron flux, the amount of ^{135}Xe increases and reaches a maximum at about 11 hours after the end of the irradiation. The direct yield of ^{135}Xe modifies the time this maximum is reached. The ratio of the direct to calculative yields was determined by measuring the time shift of the growth and decay curve. The amount of ^{135}Xe was measured as a function of time after the end of irradiation by counting the 249-kev γ ray accompanying the β decay of ^{135}Xe with a lithium-drifted germanium-diode spectrometer. The ratio of the direct to the cumulative yield was found to be 0.195 ± 0.016, 0.044 ± 0.017, 0.162 ± 0.025, and 0.070 ± 0.040 for ^{233}U, ^{235}U, ^{239}Pu, and ^{241}Pu fission respectively. (auth)

11991 THE STUDY OF K^- MESON INTERACTION WITH NUCLEI USING NUCLEAR EMULSION TECHNIQUE. Burhop, E. H. S. (Univ. of London). Cesk. Cas. Fys., 15: 484-98(1965). (In Czech.).

A review is presented of recent works in high energy physics and physics of nuclei (hyperfragments). Results have been obtained by means of nuclear emulsion technique, which during the past 20 years has made possible many outstanding discoveries in elementary particle physics. Nuclear emulsion technique has inevitably become a supplementary method of study of high energy processes because the other techniques, such as the bubble-chamber and spark-chamber, have shown indisputable advantage in the homogeneity of interaction volume and also in that they are readily adaptable to powerful and direct automatic methods of analysis and data handling. It is shown that a good many problems still exist in which emulsion technique is the only favored one for its very high spatial resolution power of tenths of microns. For comparison, the resolution power of other techniques is characterized by several tenths of millimeters. This high spatial resolution power has made possible the measurement of the lifetime of the neutral meson π^0 (which is of the order of 10^{-16} sec) and is the basis of physicists' confidence that there are no other commonly occurring unstable particles with lifetimes in the range 10^{-11} to 10^{-16} sec. All in all, it is shown that the already classical nuclear emulsion technique will continue to be well applicable in the future, provided that a careful selection of experiments is made. (auth)

11992 STUDY OF THE γ RADIATIONS EMITTED DURING THE TRANSMUTATIONS OF ^{227}Th (RdAc) TOWARD ^{223}Ra (AcX). Treherne, Jacqueline; Vieu, Charles (CNRS, Orsay, France). Compt. Rend., 261: 3100-2 (Oct. 18, 1965). (In French).

The γ-ray spectrum emitted during the transmutation of ^{227}Th to ^{223}Ra was studied using a germanium junction. This type of detector made it possible to observe new γ radiations. These results are reported and compared with previous studies. (J.S.R.)

11993 ENERGY SPECTRA AND ANGULAR DISTRIBUTION OF THE (n,α) REACTION PRODUCED ON ^{32}S BY NEUTRONS AT 3.2 Mev. Chambon, Bernard; Billerey, Roland; Salin, Raymond; Depraz, Jean (Univ. Lyon, Villeurbanne, France). Compt. Rend., 261: 3582-5 (Nov. 3, 1965). (In French).

The reaction $^{32}S(n,\alpha_0)^{29}Si$ was studied by means of junction detectors. The energy spectra and the angular distribution of the α_0's are obtained for a neutron energy of 3.2 Mev. (tr-auth)

11994 NUCLEAR LEVELS OF SULFUR FORMED BY THE (α,γ) REACTION ON SILICON. Langevin, Michel; Laurent, Henri; Vernotte, Jean (Univ., Paris). Compt. Rend., 261: 4055-8(Nov. 15, 1965). (In French).

The radiative capture reaction $^{28}Si(\alpha,\gamma)^{32}S$ was studied to E_α = 4.3 Mev. The majority of the resonances observed were attributed to the formation of excited levels of ^{32}S or to the formation of excited levels of ^{34}S by the reaction $^{30}Si(\alpha,\gamma)^{34}S$. (tr-auth)

11995 SCATTERING OF PROTONS BY NEON. Dumazet, Gerard; Gaillard, Michel,; Lambert, Michel; Meynadier, Christian (Institut d'Etudes Nucleaires, Alger, Algiers). Compt. Rend., 261: 4381-4(Nov. 22, 1965). (In French).

The elastic and inelastic angular distributions and the excitation curves for the scattering of protons by ^{20}Ne were determined in the vicinity of the resonance at 2.725 Mev in order to determine the characteristics of this resonance and the spin and parity of the corresponding levels at 5.05 Mev of ^{21}Na. The excitation and angular-distribution curves obtained are given. The angular distributions of the inelastic scattering are not isotropic or symmetric with respect to 90°, indicating the presence of at least two interferring levels of ^{21}Na. (J.S.R.)

11996 Lg ft-VALUES OF FORBIDDEN BETA-TRANSITIONS. Vinduska, M. (Inst. of Nuclear Research, Czechoslovak Academy of Sciences, Rez). Czech. J. Phys., 15: 637-43(1965).

The influence of the interference and nuclear charge on log ft-values is investigated. It is shown that interference by most of 1st and 2nd forbidden transitions is weak and,

further, that the nuclear charge influence, compared theoretically, is in good agreement with experimental results. (auth)

11997 SOLUTION OF THE BETHE-GOLDSTONE EQUATION FOR THE REACTION MATRIX IN FINITE NUCLEI. Blank, J.; Ulehla, I. (Czech Technical Univ., Prague). Czech. J. Phys., 15: 797-823(1965).

A method for solving the BG equation for the reaction matrix t in finite nuclei is presented. The application is demonstrated for a one-dimensional case, which is similar to the problem where the internucleon potential acts only in the relative s-state. The single particle potential has a harmonic oscillator form and the phenomenological internucleon potential v(r) contains a hard core and an attractive part of the Yukawa type. By taking the exclusion principle into account exactly an infinite system of integral equations is obtained. It is proved that the solution of the corresponding finite system converges to the exact solution. An iteration method for solving such a finite system with an arbitrary number of equations is developed. Its main feature consists in the exclusion of the dependence on the hard core part of v(r) (which is treated as the limit case of a rectangular repulsive potential with a variable height v_0). This exclusion transforms the original system to a system of integral equations depending only on the attractive part of v(r) and to a linear algebraic system. Both these systems can be solved by iteration for all values of v_0 as well as for $v_0 = +\infty$. The numerical results confirm the rapid convergence of the proposed iteration method and demonstrate that the solution of the finite system with a sufficiently large number of equations approximates the exact solution very precisely. (auth)

11998 RADIOACTIVE DECAY OF ^{188}Re. Maly, L.; Plajner, Z.; Dragoun, O.; Kuklik, A.; Bocev, B. (Inst. of Nuclear Research, Czechoslovak Academy of Sciences, Rez). Czech. J. Phys., 15: 824-31(1965).

The spectra of negatons, conversion electrons, and photoelectrons were measured with the iron-yoke double-focusing spectrometer. Two β-groups with end-point energies 2128 and 1973 kev and log ft values 8.04 and 8.41 respectively were observed. The K and L conversion coefficients of 155.0 kev transition were found to be in agreement with theoretical prediction within a few per cent. Three new γ transitions, 635, 1175 and 1461 kev, were observed and some corrections of the decay scheme were made. The possible interpretations of the excited states are discussed. (auth)

11999 SHELL-MODEL CALCULATION OF THE BRANCHING RATIO OF HYPERNUCLEAR BETA-DECAY. Chen-Tsai, C. T.; Lee, T. Y. (National Tsing Hua Univ., Hsinchu, Taiwan). Ho Tsu K'o Hsueh, 4: No. 3-4, 1-16 (Aug. 1965).

The branching ratio of the beta decay with respect to the π^--decay for several light p-shell hypernuclei is calculated on the assumption of the j-j coupling shell-model structure of hypernucleus. (auth)

12000 LIFE-TIME OF THE 619 Kev STATE OF ^{181}Hf. Shen, Pu; Lee, Yu Hao (National Tsing Hua Univ., Hsinchu, Taiwan). Ho Tsu K'o Hsueh, 4: No. 3-4, 17-23(Aug. 1965).

By the delayed-coincidence method, the lifetime of the 619-kev state of ^{181}Hf was determined as $(8.7 \pm 0.2) \times 10^{-10}$sec. (auth)

12001 TEMPERATURE DEPENDENCE OF THE ^{240}Pu RESONANCE ABSORPTION AT 1.05 ev IN HOMOGENEOUS SYSTEMS. Beonio-Brocchieri, F.; Diana, E. (CCR EURATOM, Ispra, Italy). J. Nucl. Energy: Pt. A and B, 19: 971-2(Dec. 1965).

The errors in the calculation of the ^{240}Pu resonance integral at 1.05 ev due to neglecting the thermal motion of the moderating atoms which produces a significant distortion of the neutron spectrum from 1/E behavior are evaluated in ideal homogeneous systems containing different quantities of ^{240}Pu at moderator and absorber temperatures from 300 to 1200°K. Formulas for the resonance escape probability and the temperature dependence of the resonance integral are obtained. (M.J.T.)

12002 APPLICATION OF SIMPLE MODELS OF DIRECT INTERACTION TO STUDY OF THE REACTION ^{28}Si(n,α)^{25}Mg AT 14.8 Mev. Massot, J. N.; El-Baz, E.; Lafoucriere, J. (Univ., Lyon). J. Phys. (Paris), 26: 527-8(Aug.–Sept. 1965). (In French).

The reaction ^{28}Si(n,α)^{25}Mg at 14.8 Mev was studied from the point of view of direct interaction with delta and gaussian interaction potentials. A system of $\sigma(\theta)$ curves shows the influence of parameters used. (auth)

12003 SMALL-ANGLE SCATTERING OF PROTONS BY ^{24}Mg. Hulubei, H.; Scintei, M.; Berinde, A.; Martalogu, N.; Neamu, I. (Inst. of Atomic Physics, Bucharest). JETP Lett. (USSR)(Engl. Transl.), 2: 207-9(Oct. 1, 1965).

The mechanism of small-angle scattering was investigated. The inelastic scattering of protons by ^{24}Mg at small angles was studied using semiconductor detectors. The angular variation of the ratio of the proton elastic scattering cross section to the Rutherford scattering cross section was also considered. (D.C.W.)

12004 TOTAL NUCLEAR DECAY REACTIONS. Shumilov, S. N.; Klyucharev, A. P.; Rutkevich, N. Ya. JETP Lett. (USSR)(Engl. Transl.), 2: 220-2(Oct, 1, 1965).

The reaction $^{14}N + {}^{10}B \rightarrow 6\alpha$ was investigated by bombarding type NIKFI-D nuclear emulsions with 100-Mev ^{10}B ions. The excitation function of the reaction was obtained, together with the energy and angular distributions of the alpha particles. (D.C.W.)

12005 EXCITATION FUNCTION OF THE REACTION ^{36}S(pγ)^{37}Cl IN THE INTERVAL $E_p = 1.4 - 2.1$ Mev. Koval', A. A.; Kopanets, E. G.; Korda, Yu. S.; Sukhotin, L. N.; Tsytko, S. P. JETP Lett. (USSR) (Engl. Transl.), 2: 252-4 (Oct. 15, 1965).

The excitation function of the reaction ^{36}S(p,γ)^{37}Cl was measured over the energy range of 1.4 to 2.1 Mev. Resonances corresponding to ^{37}Cl resonance levels were observed. The positions of the resonances and the corresponding excitation energies of the ^{37}Cl nucleus were determined. (D.C.W.)

12006 THE TWO-STEP (p, 2p) REACTION. Detenbeck, Robert W. (Univ. of Maryland, College Park). Nucl. Phys., 74: 199-218(1965).

A formal theory of two-step (p,2p) reactions was developed, based on a combination of the dispersion theory of compound-nucleus states and the formal reaction theory appropriate to a direct (p,p') reaction with final-state distortion. The formal theory yields an expression for the angular correlation between the two protons emerging from a two-step process involving an isolated intermediate state. This expression is obtained explicitly for the simplest plane wave Born approximation description of the (p,p') process. The effects of antisymmetric wave functions neglected in the early part of the paper, are discussed at the end in terms of the formal theory. (auth)

12007 CALCULATION OF PARITY IMPURITIES IN ^{203}Tl. Szymanski, Z. (California Inst. of Tech., Pasadena). Nucl. Phys., 76: 539-44(1966).

Parity admixtures in the wave functions of the ^{203}Tl nucleus are calculated with use of the shell model. The irregular electromagnetic transition E1 combined with the regular M1 give rise to the circular polarization P of outgoing gamma rays. The resulting calculated estimate is $P \approx -(0.6-1.2) \cdot 10^{-4}$. (auth)

12008 INELASTIC SCATTERING AND THE NUCLEAR SHELL MODEL. Satchler, G. R. (Oak Ridge National Lab., Tenn.). Nucl. Phys., 77: 481-512(1966). (ORNL-P-1695).

The application of a previously derived formalism to a microscopic description of the inelastic and charge exchange scattering of various projectiles by nuclei is discussed. The problem is reduced to the evaluation of certain nuclear form factors. The model appropriate for low ener-

gies assumes a central but spin- and isospin-dependent two-body force between the projectile and each target nucleon. The high-energy impulse approximation is also discussed. The nuclear wave functions are treated in an independent-particle (shell model) representation. Particular attention is paid to selection rules which may be imposed by assumptions about the nuclear structure. (auth)

12009 THE DECAY OF ^{191}Pt(3.0 d) TO ^{191}Ir. **Blichert-Toft, P. H.; Funk, E. G.; Mihelich, J. W. (Univ. of Notre Dame, Ind.). Nucl. Phys., 77: 513-26(1966). (COO-498-44).**

The electron capture decay of ^{191}Pt(3.0d) to excited states in ^{191}Ir was studied with a lithium-drifted germanium detector and a scintillation spectrometer. Singles and coincidence spectra were obtained. Previously reported transitions were verified. Hitherto unreported weak transitions of energy 659 ± 2 kev and 762 kev were observed. Evidence was found for a level at 588.3 kev recently postulated on the basis of an interpretation of resonance fluorescence measurements in ^{191}Ir. The present data are consistent with a level scheme with states at 82.45 kev ($1/2^+$), 129.45 kev ($5/2^+$), 171.25 kev ($1/2^-$), 179.0 kev ($3/2^+$), 351.4 kev ($5/2^+$), 539.3 kev ($3/2^+$), 569.1 kev ($7/2^+$), 588.3 kev ($5/2^+$), 624.5 kev ($5/2^+$), 762.2 kev and 838 kev. Ratios of experimental gamma-ray transition probabilities from the 539.3 kev, 351.4 kev and 179.0 kev states are presented. Absolute experimental M1 transition probabilities in the de-excitation of the 624.5 kev, 588.3 kev, 539.3 kev, 129.45 kev and 82.45 kev levels are compared with the Weisskopf and Nilsson estimates. (auth)

12010 FINAL STATE INTERACTION IN THE DECAY ^{8}Li → $e^- + \nu + 2\alpha$. **Lipperheide, R. (Univ., Heidelberg). Nucl. Phys., 77: 527-40(1966).**

The energy distribution of the α-particles in the β-decay of ^{8}Li is calculated by dispersion methods. The experimental α spectrum is explained in terms of the α-α scattering phase shifts and the structure of the ^{8}Li wave function. (auth)

12011 NOTE ON THE LABORATORY TO CENTER-OF-MASS TRANSFORMATION OF PARTICLE DISTRIBUTIONS CONTINUOUS IN ENERGY. **Allison, Samuel K. (Univ. of Chicago). Nucl. Phys., 77: 541-4(1966).**

It is noted that the Jacobian determinant for the transformation of $d^2\sigma/d\Omega dE$ from the laboratory to the center-of-mass coordinate systems is simply (v_{mC}/v_{mL}), the ratio of the center-of-mass velocity observed in the laboratory. It is shown that the numerical factors needed for such a transformation can be read from tables of the function $F(x,y) = (1 + x^2 - 2x \cos y)^{-1/2}$ and its square. (auth)

12012 THE ANGULAR MOMENTUM-DEPENDENCE OF THE NUCLEAR LEVEL DENSITY. **Lang, Donald W. (Argonne National Lab., Ill.). Nucl. Phys., 77: 545-58 (1966).**

It is shown that the separation of rotational and thermal excitation of nuclei, which has previously been presented as an approximation, is actually more accurate than several of the forms used to derive the "approximation". A set of functions to describe the independent-particle model of the nucleus under extreme conditions is derived, and experiments to test the predictions at high angular momentum are suggested. All derivations are based on an independent-particle model of the nucleus. Questions concerning the approximations used are considered. (auth)

12013 FOUR-PARTICLE CORRELATIONS IN LIGHT NUCLEI. **Bremond, B. (Laboratoire de Physique Theorique et Hautes Energies, Orsay, France). Nucl. Phys., 77: 559-64(1966).**

It is proposed to use, for light nuclei, trial wave functions describing dynamically independent groups of four particles formed of two protons and two neutrons, each group being of the most general form. The usual methods of the pairing problem cannot be generalized to this case. A variational method adapted to this wave function is developed. (auth)

12014 EXCITATION FUNCTIONS FOR ALPHA-PARTICLE INDUCED REACTIONS ON ^{139}La. **Furukawa, Michiaki (Tokyo Univ.). Nucl. Phys., 77: 565-76(1966).**

Excitation functions for the (α,n), (α,pn), (α,3n) and (α,4n) reactions of ^{139}La were measured with alpha particles up to 40 Mev by means of radiochemical techniques. The experimental results were compared with the predictions from the statistical theory using a level density expression of the form $W(E) = C \exp[4a(E-\delta)]^{1/2}$. The experimental results agree fairly well with the theoretical values for a = 4 Mev^{-1}, except for the high-energy "tail" of the (α,n) reaction. The cross sections for the (α,n) reaction are also compared with those for the ^{142}Ce(p,n) reaction. They do not agree with each other and this discrepancy may be a consequence of a shortcoming in the present theoretical treatment. The sum of the measured cross sections is compared with the optical model calculation of the total reaction cross section. At 38 Mev the agreement is within 15%. (auth)

12015 THE POSSIBILITY OF STUDYING THE DIPOLE-GIANT RESONANCES IN HEAVY DEFORMED NUCLEI BY MEANS OF HIGH-ENERGY ELECTRONS. **Scheck, Florian (Univ., Freiburg i. B.). Nucl. Phys., 77: 577-608(1966).**

The study of the dipole-giant resonances in heavy deformed even nuclei by means of inelastic scattering is suggested. The nuclear states are described by the hydrodynamical model of Jensen and Steinwedel, which has been extended by Danos and Greiner by including the well-known Bohr-Mottelson vibrations and rotations of the nuclear surface and their strong coupling to the dipole modes. This dynamic treatment is further examined and, in particular, the equation for the a_2 surface vibrations is solved by a variational calculation. The cross sections for the electro-excitation of the dipole resonances are then calculated using a complete partial-wave analysis for the electron wave functions and are discussed in detail. (auth)

12016 SOLUTIONS OF THE AITCHISON EQUATION FOR FINAL STATE INTERACTION. **Duck, Ian; Khanna, F. C. (Rice Univ., Houston, Tex.). Nucl. Phys., 77: 609-18(1966). (TID-21913).**

Numerical solutions to the Aitchison equation are presented for final state interactions in the process A → 3a for the special cases that the two particle interaction in the final state is given by a scattering length, effective range or resonance approximation. Non-relativistic kinematics are used throughout. The integral equations were solved by numerical iteration. In addition, the Aitchison equation was generalized to include a two particle bound state, but no solutions were found for this case. (auth)

12017 LIFETIMES OF E3 TRANSITIONS IN THE ODD-MASS Ho ISOTOPES. **Borggreen, J.; Frahm, H. J.; Hansen, N. J. Sigurd; Bjoernholm, S. (Univ. of Copenhagen). Nucl. Phys., 77: 619-24(1966).**

The halflives of the 206 kev E3 transition in ^{159}Ho and the 211 kev E3 transition in ^{161}Ho were measured to be 6.9 ± 0.3 s and 6.1 ± 0.3 s, respectively, and the existence of a 305 kev E3 transition in ^{163}Ho with a halflife of 1.1 ± 0.1 s was confirmed. (auth)

12018 DIRECT EFFECT AND EVAPORATION MECHANISM IN ^{27}Al(d,p)^{28}Al AND ^{27}Al(d,α)^{25}Mg REACTIONS. **Corti, M.; Marcazzan, G. M.; Colli, L. Milazzo; Milazzo, M. (CISE, Milan. Univ., Milan). Nucl. Phys., 77: 625-40(1966).**

The Al(d,α) and (d,p) reactions are studied from the point of view of the reaction mechanism in the energy interval of ≈1.5–3 Mev. Strong intensity fluctuations are found in the excitation functions of both reactions. They can be explained and analyzed on the basis of the Ericson theory for compound nucleus formation. In the (d,p) reaction the stripping mechanism is also present, giving rise to interference phenomena with the compound nucleus mechanism. From these measurements, the value of the average compound nucleus level width Γ' can be deduced. For the (d,p) reaction it is also possible to estimate the magnitude of the direct effect. (auth)

12019 A NEW DETERMINATION OF THE ^{16}N HALF-LIFE. Scott, S. A. (Israel Inst. of Tech., Haifa); Notea, A. Nucl. Phys., 77: 641-9(1966).

The irradiated primary circuit cooling water of the IRR-1 reactor was used as an intense source of ^{16}N. After scramming the reactor and bringing the cooling water to a standstill, the time decay of the gamma-ray activity was followed over more than four decades. The ^{16}N halflife was determined as 7.10 ± 0.03 sec. The possible influence of competing activities was considered, and their effect reduced to a minimum. (auth)

12020 LIFETIME MEASUREMENTS OF SOME ROTATIONAL LEVELS BY A NEW RECOIL METHOD. Ashery, D.; Assaf, N.; Goldring, G.; Sprinzak, A.; Wolfson, Y. (Weizmann Inst. of Science, Rehovoth, Israel). Nucl. Phys., 77: 650-6(1966).

Lifetime measurements of some rotational levels were carried out by observing the decay of the excited nuclei along the recoil path, following Coulomb excitation with backscattered oxygen ions. Mean lives were determined for levels in ^{153}Eu and ^{163}Dy and also, as a check, for the 2^+ levels is ^{152}Sm and ^{188}Os. As a consequence of these measurements the ratio of the M1 strengths of the transitions $9/2^+ \rightarrow 7/2^+$ and $7/2^+ \rightarrow 5/2^+$ in ^{153}Eu was found to agree with the rotational value. The E2 strength of the $9/2^+ \rightarrow 7/2^+$ transition was on the other hand found to be reduced by a factor of two relative to the pure rotational value. (auth)

12021 EXACT DESCRIPTION OF ELASTIC SCATTERING PROCESSES AND DEDUCTION OF OPTICAL NUCLEAR MODELS. Elk, K.; Macke, W. (Technische Univ., Dresden). Nucl. Phys., 77: 657-64(1966). (In German).

The elastic scattering of a single particle by a bound system of particles is considered. The matrix element $S_{1'1}$ characteristic for this process is formulated in a compact form, computable in principle by means of the time-dependent perturbation theory. By application of the linked cluster theorem of the S-matrix it is possible to separate and sum up all the terms contributing to $S_{1'1}$. Thereby, it can be demonstrated that the elastic scattering is described completely by an effective potential. However, inelastic scattering here appears only as an average "absorption". The formalism supports the phenomenological optical nuclear model but it is not identical with it. A rule is formulated for calculating the effective potential U from the exact two-particle interaction V. Thus U is equal to the sum over all irreducible one-particle clusters which can be calculated in principle from V and the unperturbed state Φ^0. Finally an approximate evaluation, consisting mainly in performing a partial summation, is briefly discussed. (auth)

12022 GAMMA RAYS FROM THE DECAY OF ^{75}Se. Naqvi, S. I. H.; Dilay, A. J. (Univ. of Manitoba, Winnipeg, Can.). Nucl. Phys., 77: 665-72(1966).

A γ-γ coincidence and angular correlation spectrometer capable of automatic operation is described. Gamma spectra in coincidence with the weak 199 and 121 kev γ-rays were investigated by a fast-slow coincidence method ($2\tau \approx 50$ ns) using NaI(Tl) scintillation detectors. No evidence is found for 81, 188 and 203 kev γ-rays. The 66-199 kev γ-γ angular correlation is found consistent with the spin $\frac{1}{2}$ for the 199 kev level in ^{75}As. The only high energy (>401 kev) γ-ray discovered is the one at 577 kev. The changes in the decay scheme are indicated. (auth)

12023 ENERGY LEVELS OF LIGHT NUCLEI. VII. A = 5–10. Lauritsen, T. (California Inst. of Tech., Pasadena); Ajzenberg-Selove, F. Nucl Phys., 78: 1-175 (1966).

A summary is presented of existing experimental information on the structure and properties of the nuclei with mass numbers five through ten. (auth)

12024 E2-SURFACE RESONANCE IN SPHERICAL NUCLEI. Faessler, Amand (Univ., Freiburg i. B.). Nucl. Phys., 78: 176-92(1966). (In German).

Quadrupole surface vibrations are considered for the proton and the neutrons separately in medium and heavy even mass spherical nuclei. The two kinds of oscillations are strongly coupled by the symmetry term in the mass formula. The coupling constant between the proton and the neutron oscillations is calculated with the help of the symmetry energy. With the strong coupling, vibrations of the protons and the neutrons in phase and in anti-phase are obtained. The former are the well-known low-energy quadrupole vibrations. The vibrations in anti-phase lie between 5 and 50 Mev in the case where there is no interaction between the oscillations in phase and in anti-phase. If they do not lie immediately near closed shells, the anti-phase resonances (E2 surface resonances) lie between 15 and 20 Mev. The γ-absorption cross section and the inelastic electron scattering cross section are considered for the detection of the E2 surface resonances. It is shown that the γ-absorption cross section is negligible compared to the cross section of the E1 giant resonance. The inelastic electron scattering cross section is of the same order as for the giant resonance. Thus it is proposed to search for the E2 surface resonance by comparing the shape of the γ-absorption and the electron scattering cross section in the excitation region between 10 and 25 Mev. (auth)

12025 SPINS OF EXCITED LEVELS OF ^{18}F. Chagnon, P. R. (Univ. of Notre Dame, Ind.). Nucl. Phys., 78: 193-206(1966).

Proton-gamma directional correlations through several excited levels of ^{18}F in the reaction ^{16}O(^{3}He,pγ)^{18}F were studied at ^{3}He energies of 3.6 to 4.0 Mev. Spin assignments of 3, (2), 1, 2, (2) and 1 were deduced for the 0.94, 1.082, 1.70, 2.53, 3.06 and 3.13 Mev levels, respectively. Limits were placed on the spins of the 2.10 and 3.35 Mev levels. Quadrupole-dipole mixing ratios for several γ-ray transitions were deduced. (auth)

12026 THE DECAY OF ^{132}Te AND LEVELS IN ODD ^{132}I. Fransson, K.; Bemis, C. E. Jr. (Research Inst. for Physics, Stockholm). Nucl. Phys., 78: 207-24(1966).

The properties of excited states in odd ^{132}I were investigated by a detailed study of the gamma-ray and conversion-electron spectra from the decay of ^{132}Te. Transitions of 49.72, 111.76, 116.30 and 228.16 kev were observed and their multipolarities determined from measurements of conversion electron intensity ratios K/L and $L_I/L_{II}/L_{III}$ and from the measured K-shell conversion coefficients. The mixing ratio, δ^2(E2/M1), was determined for those predominantly M1 transitions from measurements of the L-subshell conversion ratios. Reduced transition probabilities, B(M1) and B(E2), were deduced from existing lifetime data and compared with theoretical predictions for transitions in odd nuclei. Definite spin-parity assignments of 4^+, 3^+, 2^+ and 1^+ were made for the ground state, 49.72, 161.48 and 277.88 kev levels, respectively, in ^{132}I. (auth)

12027 ^{9}Be(^{3}He,α) REACTIONS TO THE 16.63 AND 16.92 Mev STATES OF ^{8}Be. Sullivan, D. J.; Treacy, P. B. (Australian National Univ., Canberra). Nucl. Phys., 78: 225-332(1966).

Coincidences were observed between successively emitted α-particles from the ^{9}Be(^{3}He,α)^{8}Be(α) reaction at a laboratory bombarding energy of 3 Mev. The reaction was shown to proceed predominantly by sucessive transitions via states in ^{8}Be. The observed angular correlations have been interpreted to show that the spins and parities of the 16.63 and 16.92 Mev states of ^{8}Be are both 2^+. (auth)

12028 TWO-PROTON RADIOACTIVITY OF HEAVIER-THAN-TIN NUCLEI. Goldansky, V. I. (Inst. of Chemical Physics, Moscow). Nucl. Phys., 78: 233-7(1966).

It is shown that two-proton radioactivity may be observed not only for light nuclei as has been assumed so far but also for elements heavier than tin. About half of all two-proton radioactive nuclei lie in the region Z > 50. A distinctive

characteristic of the two-proton radioactivity of heavy nuclei are unstable energetically to one-proton decay as well; however, two-proton decay proves to predominate definitely in many cases. Two proton radioactive decay differs from a chain of two successive proton decays by the spectrum of emitted protons, and their energy and angular correlation. (auth)

12029 THE GIANT RESONANCE IN INELASTIC ELECTRON SCATTERING. Ueberall, H. (Catholic Univ. of America, Washington, D. C.). Nuovo Cimento (10), 41B: 25-36(1966).

It is shown that Walecka's version of the Goldhaber-Teller model of the giant dipole nuclear collective oscillations, which is generalized to spin-isopin vibrational modes, may be used to describe the gross features of the inelastic electron scattering results in a semi-quantitative manner. Simple expressions are obtained for the longitudinal and transverse matrix elements leading to electric dipole (1^-) and magnetic quadrupole (2^-) collective states in ^{12}C and ^{16}O. The decay widths of these states are also calculated using Wigner's R-matrix theory, and are generally in good agreement with the observed widths. (auth)

12030 THE ANGULAR DISTRIBUTIONS OF THE α-PARTICLES LEADING TO THE FIRST EXCITED STATES OF ^{25}Mg IN THE REACTION $^{28}Si(n,\alpha)^{25}Mg$, AT A NEUTRON ENERGY OF 14.8 Mev. Forti, P. (CAMEN, Pisa, Italy); Gadioli, E.; Marini, A. Nuovo Cimento (10), 41B: 52-9 (1966).

The angular distributions of the α-particles leading to the first five levels of ^{25}Mg, in the reaction $^{28}Si(n,\alpha)^{25}Mg$, are analyzed. They were obtained by means of a telescope device consisting of two silicon semiconductor detectors. If it is assumed that the angular distributions are due partially to a statistical effect, partially to a heavy stripping process, both their shape and their absolute value can be correctly explained. (auth)

12031 EXCITATION OF A 4.5 Mev STATE IN ^{27}Al BY INELASTIC SCATTERING OF 14 Mev NEUTRONS. Bonazzola, G. C. (Univ., Turin); Chiavassa, E.; Bressani, T. Nuovo Cimento (10), 41B: 60-1(1966).

Differential cross sections for inelastic scattering of 14.2 Mev neutrons on ^{27}Al were measured to demonstrate the applicability of the excited-core model hypothesis to the first five levels. It is concluded that the neutron group near 4.5 Mev cannot be described as due to the excitation of an octupole state. (L.B.S.)

12032 INTERPRETATION OF THE (p,2p) REACTION IN ^{10}B AND ^{11}B. Jackson, D. F. (Battersea Coll. of Tech., London). Nuovo Cimento (10), 41B: 86-8(1966).

It was previously reported that three peaks corresponding to angular momentum transfer $l \neq 0$ were observed in the reactions $^{10}B(p,2p)^{9}Be$ and $^{11}B(p,2p)^{10}Be$. The difficulties of interpreting the peaks in terms of direct knock-out from single-particle states are pointed out, and a simple explanation of the reactions is offered in terms of excited states of the residual nucleus. (L.B.S.)

12033 ELASTIC ELECTRON SCATTERING FROM TITANIUM AT 53 Mev. Engfer, R. (Technische Hochschule, Darmstadt, Ger.). Phys. Lett., 19: 131-3(Oct. 1, 1965).

In order to provide accurate low-energy elastic electron scattering data, the elastic electron scattering from titanium (natural isotopic abundance) was measured at 53 Mev relative to carbon and beryllium. The elastic cross sections calculated for titanium at 53.01 Mev and various charge distributions with the same rms radius are shown. Ratios of the elastic cross sections for Ti and C and for Ti and Be are also shown. A phase-shift analysis of the cross sections was also carried out, and gave an rms radius for the titanium nucleus (averaged over natural isotopic abundance) of 3.61 ± 0.05 fm. (J.F.P.)

12034 STUDY OF THE PRODUCTION OF ^{32}P AND ^{33}P BY HIGH ENERGY PROTONS. Simonoff, G. N.; Vidal, C. (Faculte des Sciences, Bordeaux). Phys. Lett., 20: 30-1 (Jan. 15, 1966). (In French).

The production of ^{32}P and ^{33}P in proton reactions with targets with $59 \leq A \leq 238$ at 0.60 to 2.75 Bev was investigated. (D.C.W.)

12035 L SUBSHELL RATIOS OF PURE E2 TRANSITIONS. Hamilton, J. H. (Vanderbilt Univ., Nashville). Phys. Lett., 20: 32-4(Jan. 15, 1966).

A survey of some recent experimental data on the L subshell ratios of pure E2 transitions in even-even nuclei is presented. The experimental values are compared with theoretical predictions. (D.C.W.)

12036 THE MASS 13, T = 3/2 QUARTET. Cerny, J.; Pehl, R. H.; Butler, G.; Fleming, D.; Maples, C.; Detraz, C. (Univ. of California, Berkeley). Phys. Lett., 20: 35-7 (Jan. 15, 1966).

The isobaric multiplet mass equation was tested by predicting the mass of ^{13}O from the excitations of the lowest $T = 3/2$ states in ^{13}C and ^{14}N as determined by the reactions $^{15}N(p,t)^{13}N$ and $^{15}N(p,He\text{-}3)^{13}C$ and from the ground-state mass excess of ^{13}B. The ground-state mass of ^{13}O was measured using the $^{16}O(He\text{-}3,He\text{-}6)^{13}O$ reaction. (D.C.W.)

12037 THE Q VALUES OF THE REACTION $^{9}Be(p,d)$ ^{8}Be AND $^{8}Be \rightarrow 2\ ^{4}He$. Reichart, W.; Staub, H. H.; Stuessi, H.; Zamboni, F. (Univ., Zurich). Phys. Lett., 20: 40-2 (Jan. 15, 1966).

The Q-values of the reactions $^{9}Be(p,d)^{8}Be$ and $^{8}Be \rightarrow 2\ ^{4}He$ were measured. The results agreed with previous determinations within the limits of accuracy. (D.C.W.)

12038 DETERMINATION OF LIFETIME AND GROUND-STATE ENERGY OF ^{8}Be BY α-α ELASTIC SCATTERING AT 184 Kev. Benn, J.; Dally, E. B.; Muller, H. H.; Pixley, R. E.; Staub, H. H.; Winkler, H. (Univ., Zurich). Phys. Lett., 20: 43-5 (Jan. 15, 1966).

The binding energy and lifetime of ground-state ^{8}Be were measured by the elastic scattering of $^{4}He^{+}$ ions on He at 184 kev. (D.C.W.)

12039 MAGNITUDES OF SOME REDUCED TRANSITION PROBABILITIES IN ^{6}Li. Hansteen, J. M.; Kanestroem, I. (Univ. of Oslo, Blindern). Phys. Lett., 20: 48-50(Jan. 15, 1966).

The evidence for the alpha-deuteron cluster representation of the ^{6}Li nucleus was reviewed. The alpha-deuteron cluster prediction for the reduced transition probability $B(E2; 1 \rightarrow 3)$ was found to be within error limits for a value derived from a Coulomb breakup experiment. It was concluded that under the influence of the long-range Coulomb force, the alpha-deuteron cluster character of the ^{6}Li nucleus seems to be rather strikingly demonstrated. (G.O.Y.)

12040 DEPENDENCE OF (n,2n) CROSS SECTIONS ON THE SYMMETRY PARAMETER N-Z. Csikai, J.; Petoe, G. (Hungarian Academy of Sciences, Debrecen). Phys. Lett., 20: 52-3(Jan. 15, 1966).

The total (n,2n) reaction cross sections were measured using the activation method and a constant excess energy of 3 Mev above the threshold for $30 \leq N \leq 120$. It was found that the (n,2n) cross sections can be calculated from a simple formula relating the cross section to the symmetry parameter N-Z. (G.O.Y.)

12041 FISSION BY A RADIATIONLESS TRANSITION IN THE μ MESONIC ATOM ^{239}Pu. Cojocaru, V. (Inst. of Atomic Physics, Bucharest); Marinescu, L.; Petrascu, M.; Voiculescu, G.; Ignatenko, A.; Omelianenko, M. Phys. Lett., 20: 53-5(Jan. 15, 1966).

The time distribution of fission in the μ-mesonic atom ^{239}Pu was measured. It was found that the ratio prompt fissions/fissions by μ-capture is equal to 0.43 ± 0.09. This value indicates a radiationless transition contribution by an order of magnitude greater than in uranium and thorium. (auth)

12042 AN ISOMER OF SPIN $25/2^{+}$ IN ^{183}Re. Emmott, M. J. (Univ. of Manchester, Eng.); Leigh, J. R.; Ward, D.; Newton, J. O. Phys. Lett., 20: 56-8(Jan. 15, 1966).

A 1.0 msec isomeric state of ^{183}Re at 1907 kev was produced. The state decays to the $2\frac{1}{2}^+$ member of the ground-state rotational band and is assigned to be $2\frac{5}{2}^+$ and a three-quasi-particle state. Evidence was given for an alternating energy term in the rotational band. (auth)

12043 PRODUCTION AND DECAY OF A ^{13}B HYPERNUCLEUS. Mora, S. (Univ., Parma, Italy). Phys. Lett., 20: 89-91(Jan. 15, 1966).

The production of a hyperfragment by the capture of a hyperon (Σ^-) produced by a meson (K^-) interaction in a stack of K-5 emulsions was observed. It was concluded that the hyperfragment can be considered as probably an example of $_{\Lambda}B^{13}$; the binding energy of the hyperon (Λ^0) was calculated (from the decay) to be 12.5 ± 0.7 Mev. (D.C.W.)

12044 CROSS-SECTION AND POLARIZATION DETERMINATIONS FOR THE ^{12}C(d,n)^{13}N REACTION FROM 2.8 TO 4.2 Mev. Sawers, J. R. Jr.; Purser, F. O. Jr.; Walter, R. L. (Duke Univ., Durham, N. C.). Phys. Rev., 141: 825-32(Jan. 1966).

Using time-of-flight techniques, a 5° yield curve of the neutrons from the ^{12}C(d,n)^{13}N(g.s.) reaction was obtained from 2.8 to 4.2 Mev. Three peaks, each greater than 100 kev wide, at energies of 3.00, 3.35, and 3.96 Mev were observed. Seventeen differential cross sections were measured in this energy region for reaction angles from 5° to 145° in the center-of-mass system. All exhibited prominent l = 1 stripping distributions. A 5° yield curve of neutrons leaving ^{13}N in the first excited state was determined for bombarding energies greater than 3.5 Mev. Three angular distributions of these neutrons, obtained at 3.810, 3.895, and 4.150 Mev, exhibited the expected shape for l = 0 angular momentum transfer. In a second experiment eleven angular distributions of the ground-state neutron polarization were determined for the 2.8- to 4.0-Mev region over the same angular range. Scattering from helium served as the polarization analyzer. In the region of the forward maximum, the polarization is negative at all energies and ranged from about –0.08 to –0.44. From 3.1 to 3.4 Mev the polarization is noticeably dependent on energy at back angles. Above 3.5 Mev the angular dependence of the polarization does not change appreciably even though the values range from about –0.60 to +0.50. A comparison of these data above 3.5 Mev with the 11.8-Mev ^{12}C + d neutron polarization data and with the 6- to 15-Mev ^{12}C + d proton data shows similar angular dependence for all polarizations. (auth)

12045 COUPLED EQUATIONS FOR REARRANGEMENT COLLISIONS. Levin, F. S. (Brookhaven National Lab., Upton, N. Y.). Phys. Rev., 141: 858-62(Jan. 1966). (BNL-9462).

An exact set of coupled inhomogeneous equations for rearrangement collisions, analogous to the coupled equations used in ordinary scattering, is derived. The boundary conditions are obtained from the integral equation for scattering. The solutions describing rearrangement are the particular integrals and contain none of the complementary function. Both truncation procedures and distorted-wave approximations are discussed. (auth)

12046 EXPERIMENTAL STUDY OF THE REACTION ^{3}He(γ,π^+)^{3}H UP TO 260 Mev. O'Fallon, J. R.; Koester, L. J. Jr.; Smith, J. H.; Yavin, A. I. (Univ. of Illinois, Urbana). Phys. Rev., 141: 889-901(Jan. 1966).

The differential cross section for the reaction ^{3}He(γ,π^+)^{3}H was measured for photon energies of 180 to 260 Mev. A target of gaseous ^{3}He at 20.4°K and approximately one atmosphere pressure was irradiated by a 270-Mev bremsstrahlung x-ray beam. The reaction was observed by detecting π^+–^{3}H coincidences. Tritons with energies between 9.7 and 24.5 Mev (momentum transfer 1.2 F^{-1} to 1.9 F^{-1}) were observed at laboratory angles of 26°, 30°, 35°, and 40°. At 26° the cross sections in the center-of-mass system ranged from 2.55 ± 0.34 μb/sr to 0.78 ± 0.16 μb/sr, decreasing with increasing photon energy. Impulse-approximation calculations relate the cross section to the matter form factor of the 3-nucleon system under the assumption of identical wave functions for ^{3}He and ^{3}H. Cross sections found in this experiment lie from 25% to 50% below the values predicted by this theory with form factors form factors from electron-scattering data inserted. (auth)

12047 MICROSCOPIC THEORY OF THE OPTICAL-MODEL POTENTIAL AND THE HOLE-PARTICLE MODEL IN NUCLEAR SPECTROSCOPY. Van-Giai, Nguyen (Univ., Paris, Orsay, France); Sawicki, J.; Vinh Mau, N. Phys. Rev., 141: 913-26(Jan. 1966).

Approximate expressions for the optical-model potential v_{opt} in terms of the nucleon-nucleon interaction are discussed. The identity of all the A + 1 nucleons of the scattering problem is approximately taken into account in our final formulas. The imaginary part of v_{opt} is calculated for for the case of ^{12}C and the incident-nucleon energy of 20 Mev. The spherical-model random-phase-approximation (RPA) eigenvalues and eigenvectors are assumed for the complete set of intermediate nuclear states involved. The results are rather insensitive to the exchange-force mixture assumed for our zero-range nucleon-nucleon potential. The antisymmetrization of our V-matrix elements is extremely important as it reduces the Imv_{opt} by a factor of 2–3. For a reasonable set of RPA intermediate eigenvalues and eigenvectors a semiquantitative agreement is obtained with the best phenomenological Imv_{opt} available. The most important contribution to Imv_{opt} corresponds to the first excited T = 0, 2^+ state in ^{12}C. (auth)

12048 COMPETITION BETWEEN NEUTRON AND GAMMA EMISSION FROM NUCLEAR STATES WITH HIGH SPIN. Sperber, Daniel (Illinois Inst. of Tech., Chicago). Phys. Rev., 141: 927-32(Jan. 1966). (TID–22076).

The effect of the high spin of the compound nuclei on the ratio of the gamma width to the neutron width is studied. It is shown that this ratio increases with the increase of the spin of the compound nucleus. This is attributed to both model-independent and model-dependent factors. (auth)

12049 NUCLEAR PAIRING ENERGIES WITH SIMPLE INTERACTIONS. Jakeman, E.; Moszkowski, S. A. (Univ. of California, Los Angeles). Phys. Rev., 141: 933-40 (Jan. 1966).

A brief review is given of the estimation of nuclear pairing energies using interactions with constant matrix elements, in analogy with the theory of superconductivity. More realistic potentials are discussed in the solution of the nuclear-matter problem, and an analytic expression for the pairing parameter Δ is obtained using a simple separable S-state interaction which approximately fits the two-nucleon scattering data up to the point where the phase shift turns negative. The pairing energies obtained are of the same order as those obtained by other authors, and smaller than those found experimentally for finite nuclei. It is argued that since the interaction is a decreasing function of the kinetic energy, the average coupling will be increased by the low-density surface region, and the effect of the latter is then taken into account by assuming the validity of the Thomas-Fermi approximation. An average coupling constant is calculated using the same separable interaction as was used in the nuclear-matter case, and an expression for Δ in the case of uniformly spaced single-particle levels is obtained by making a simple approximation for the off-diagonal matrix elements. It is found that for a trapezoidal one-body potential $\Delta \approx 4.0A^{-\frac{1}{3}}$ in agreement with the empirical values, and this result is discussed in relation to the approximations made during its derivation, and to the various parameters entering into the theory. (auth)

12050 COMPARISONS OF BCS NUCLEAR WAVE FUNCTIONS WITH EXACT SOLUTIONS. II. PARTICLE-NUMBER-CONSERVING METHOD. Mang, Hans J. (Technische Hochschule, Munich); Rasmussen, John O.; Rho, Mannque. Phys. Rev., 141: 941-8(Jan. 1966).

It is investigated whether, in the nuclear pairing theory of the BCS type, a sudden transition from configuration

mixing to nonconfiguration mixing state at a critical force strength G_c is a physical phenomenon. The variational method taking the components of the BCS wave function with correct particle number shows that such a transition is an artificial feature of the theory arising mainly from the number fluctuation in the wave function. The effect of a 4-quasiparticle component in the number-conserving method is to improve higher order amplitudes of the wave function, to necessitate a reduction of Δ, and to modify the roles of the u and v parameters. The absence of a sudden transition is expected to have some bearing on the question of whether a discontinuous "Mottelson-Valatin effect" in the nuclear rotational spectra does exist in nature. (auth)

12051 NUMERICAL STUDY OF THE 8-32-PARTICLE EIGENSTATES OF THE PAIRING HAMILTONIAN. Richardson, R. W. (New York Univ., New York). Phys. Rev., 141: 949-56(Jan. 1966).

Exact eigenstates of the pairing-force hamiltonian were calculated for 2N particles in 2N equispaced, doubly degenerate single-particle levels for N = 4, 8, 12, and 16. The states calculated are the ground state and the first two excited seniority-zero and seniority-two states. These states were calculated for values of the interaction strength that give pairing energies that are typical of nuclear systems. Numerical results are given for the energies and occupation probabilities of these states and are compared with the corresponding results of the Bardeen-Cooper-Schrieffer (BCS) theory. It is shown that the BCS theory is a worse approximation for the larger values of N than it is for the smaller values, with errors as high as 140% (20%) for the excitation energies of the seniority-zero (-two) states. The methods used in the calculation of these states are outlined. (auth)

12052 ^{27}Al AND THE EXCITED-CORE MODEL. Thankappan, V. K. (Indiana Univ., Bloomington). Phys. Rev., 141: 957-61(Jan. 1966).

The nuclear properties of the low-lying levels in ^{27}Al are discussed in terms of a model in which a proton hole is coupled to the observed levels of ^{28}Si. The calculated electric E2 transition probabilities are found to be in good agreement with the experimental values, but the agreement between theory and experiment for M1 transition probabilities does not appear to be so good. It is found that the core-particle interaction required to fit the observed levels of ^{27}Al contains multipoles of order up to four. A possible explicit form for this interaction is suggested. (auth)

12053 LITHIUM–LITHIUM SCATTERING. Pinsonneault, L. L.; Blair, J. M. (Univ. of Minnesota, Minneapolis). Phys. Rev., 141: 961-5(Jan. 1966).

Elastic-scattering experiments were performed with ^{6}Li on ^{6}Li from 3.2 to 7.0 Mev and with ^{7}Li on ^{7}Li from 4.0 to 6.5 Mev. In the lower portion of this energy range the observations follow Mott's scattering formula but at higher energies fall below these predictions. An analysis of the data in terms of the rounded-cutoff Blair model resulted in a set of parameters which was not sharply defined and probably not unique but which gave curves which reproduced satisfactorily the fluctuations of cross section with angle. An analysis in terms of one parameter, the interaction distance, gave values of $r_0 = (1.38 \pm 0.03) \times 10^{-3}$ cm for ^{6}Li and $r_0 = (1.52 \pm 0.03) \times 10^{-13}$ cm for ^{7}Li. (auth)

12054 BETA DECAY OF ^{19}O: STATES OF ^{19}F. Olness, J. W. (Brookhaven National Lab., Upton, N. Y.); Wilkinson, D. H. Phys. Rev., 141: 966-74(Jan. 1966). (BNL-9465).

The beta decay of ^{19}O was re-examined in order to search for transitions to highly excited states of ^{19}F which are predicted by the independent-particle model (IPM) to have large matrix elements. Such a transition is found in the 0.16% beta branch to the 4.39-Mev state of ^{19}F: log ft = 3.54 ± 0.06. This state deexcites through gamma branches of (18 ± 7%) to the 2.79-Mev state of ^{19}F and (82 ± 7)% to the 0.197-Mev state; branches to other states below that at 2.79 Mev are less than 5%. These data make it certain that the 4.39-Mev state is of $J^\pi = 3/2, 5/2, 7/2^+$ (assuming that the ground state of ^{19}O is of $J^\pi = 5/2^+$). If, as is most likely, the 2.79-Mev state of ^{19}F is of $J^\pi = 5/2^+$, then $J^\pi = 7/2^+$ is strongly favored for the 4.39-Mev level. An IPM state of $J^\pi = 7/2^+$ enjoying a strong beta decay from ^{19}O is predicted at just this energy. Beta decay to the 2.79-Mev state of ^{19}F has log ft > 7.4. The decay of the 1.56-Mev state of ^{19}F is also examined and a ground-state branch of (2.4 ± 0.5)% is determined. This transition is expected to be weak by both the IPM and the collective models. The ^{19}O used in this experiment was made by the reaction ^{18}O(d,p)^{19}O, and the experimental techniques were exclusively those of NaI spectroscopy, including two-dimensional analysis. (auth)

12055 ^{17}O(d,p)^{18}O REACTION AND NUCLEAR STRUCTURE OF ^{18}O. Wiza, Joseph L.; Middleton, Roy; Hewka, Peter V. (Univ. of Pennsylvania, Philadelphia). Phys. Rev., 141: 975-9(Jan. 1966).

A target enriched to 40% in ^{17}O was bombarded with 10-Mev deuterons, and the emitted protons were analyzed with a broad-range magnetic spectrograph. Angular distributions of the groups corresponding to the ground and 12 excited states of ^{18}O were measured and analyzed using plane-wave theory. The predicted 3^+ state arising from the $(d_{5/2}s_{1/2})$ configuration was found to be at 5.37-Mev excitation. Relative reduced widths and spectroscopic factors were determined from the stripping analysis, and were found to be in good agreement with recent theoretically predicted wave-function amplitudes. This implies that several states of ^{18}O have an appreciable collective component. (auth)

12056 MEASUREMENT OF Fe(α,α')Fe* REACTIONS PRODUCED BY 21-, 27.5-, AND 47.9-Mev ALPHA-PARTICLE BOMBARDMENT: STATISTICAL-THEORY ANALYSIS. Benveniste, J. (Aerospace Corp., San Bernardino, Calif.); Merkel, G.; Mitchell, A. Phys. Rev., 141: 980-95 (Jan. 1966).

The energy and angular distributions of inelastically scattered α particles from Fe were measured at bombarding energies of 21, 27.5, and 47.9 Mev. The energy and angular distributions were analyzed with the semiclassical compound-nucleus theory of Ericson and Strutinski. In the analysis of the 21-Mev data, all of the inelastically scattered α particles are assumed to be emitted from the original compound nucleus. The angular distributions produced by the 27.5- and 47.9-Mev α-particle bombardment are found to be consistent with the nuclear moment of inertia determined from the 21-Mev data when multiple-particle-emission reactions such as Fe($\alpha,n\alpha$)Fe or Fe($\alpha,p\alpha$)Mn are included in the analysis. The inclusion of multiple-particle emissions in the statistical-theory analysis of the 27.5- and 47.9-Mev-induced reactions also significantly improves the agreement between experimental and theoretical energy distributions. In the statistical-theory analysis essentially two assumptions were made about the dependence of nuclear level density on nuclear spin and nuclear excitation energy. (L.B.S.)

12057 NEW TOTAL-CROSS-SECTION MEASUREMENTS FOR THE REACTIONS ^{14}N(^{14}N,^{13}N)^{15}N AND ^{10}B(^{14}N,^{13}N)^{11}B. Gaedke, R. M.; Toth, K. S.; Williams, I. R. (Oak Ridge National Lab., Tenn.). Phys. Rev., 141: 996-1002(Jan. 1966). (ORNL-P-1615).

Thick targets of AgCN and ^{10}B were bombarded with ^{14}N ions accelerated in the Oak Ridge Tandem Van de Graaff. The amount of ^{13}N present in each irradiated sample was determined by the detection of the 10-min positron activity characteristic of the isotope. In this manner cross sections were measured for the neutron-transfer reactions ^{14}N(^{14}N,^{13}N)^{15}N and ^{10}B(^{14}N,^{13}N)^{11}B. The (assumed equal) neutron reduced widths in ^{14}N and ^{15}N were determined by applying the tunneling theory to the ^{14}N-on-^{14}N measurements. The reduced width in ^{11}B was then calculated from the cross-section data for the reaction of ^{14}N on ^{10}B by the use of the now measured reduced width in ^{14}N. The ^{14}N and ^{11}B reduced widths were found to agree with the same values as determined from the bound-state, single-particle,

radial wave functions that have been calculated by using a Woods-Saxon potential. In resolving the experimental decay curves, 2- and 20-min components were found for the ^{14}N and ^{10}B targets, respectively. These activities were ascribed to the ^{15}O and ^{11}C which result from the proton-transfer reactions $^{14}N(^{14}N,^{15}O)^{13}C$ and $^{10}B(^{14}N,^{13}C)^{11}C$; cross sections for these reactions were also measured. (auth)

12058 $^{12}C(\gamma,n)^{11}C$ GIANT RESONANCE WITH GAMMA RAYS. Lochstet, William A.; Stephens, William E. (Univ. of Pennsylvania, Philadelphia). Phys. Rev., 141: 1002-6 (Jan. 1966).

The photonuclear reaction $^{12}C(\gamma,n)^{11}C$ was produced in natural carbon by means of the monochromatic gamma rays from $T(p,\gamma)He$ in the range of $21 < E_\gamma < 26.7$ Mev. The reaction was detected by means of the positron radioactivity of ^{11}C using coincidences of the annihilation gamma radiation from the positrons. The cross section was determined absolutely to an accuracy of 10%. The gamma-ray energy width or resolution varied from about 0.1 Mev at $E_\gamma = 22$ Mev to 0.2 Mev at $E_\gamma = 26$ Mev. The peak cross section is 7.8 mb at both 22.15 and 23.0 Mev, and additional structure is observed at 25.6 Mev. The integrated cross section from 20 to 27 Mev is 36 Mev mb. Comparison is made with other reported measurements and with theoretical calculations. Some agreement is found with the deformed-nucleus calculation of Nilsson, Sawicki, and Glendenning. Also, some indication is observed of transition to excited states of ^{11}C suggesting two-hole–two-particle excitation in ^{12}C. (auth)

12059 TOTAL CROSS SECTIONS AND ANGULAR DISTRIBUTIONS OF THE $^{12}C(^6Li,p)^{17}O$, $^{12}C(^6Li,d)^{16}O$, AND $^{12}C(^6Li,\alpha)^{14}N$ REACTIONS FROM 4.5 TO 5.5 Mev. Heikkinen, D. W. (Univ. of Iowa, Iowa City). Phys. Rev., 141: 1007-17(Jan. 1966).

The $^6Li + ^{12}C$ reaction was studied for bombarding energies in the range 4.5 to 5.5 Mev. Angular distributions and total cross sections were obtained at 100-kev intervals using a dE/dx-E system coupled to a computer. The reaction products which were studied are proton groups from the ground and first four excited states of ^{17}O, deuterons from the ground and first four excited states of ^{16}O (the 6.05–6.13-Mev doublet unresolved), and alpha particles from the ground and second excited states of ^{14}N. The angular distributions of certain of the particle groups show a rather strong energy dependence. The total cross sections, however, are smoothly increasing functions of energy. There is no strong (2J + 1) dependency in total cross sections that would imply a statistical compound-nucleus decay. The relatively smooth variation of the angular distributions of deuterons from the excited states of ^{16}O and alpha particles from the second excited state of ^{14}N suggests that these proceed predominantly via a direct reaction. The ground-state groups would appear to have significant compound-nucleus contributions. (auth)

12060 LIFETIME OF THE 1.02-Mev STATE IN ^{23}Ne. Fossan, D. B.; McDonald, R. E.; Chase, L. F. Jr. (Lockheed Palo Alto Research Labs., Palo Alto, Calif.). Phys. Rev., 141: 1018-20(Jan. 1966).

The lifetime of the $\frac{1}{2}^+$ 1.02-Mev state in the ^{23}Ne was measured with a fast time-to-height converter. A half-life of (178 ± 10) psec was obtained from the logarithmic slope of the distribution of time delays between protons from the $^{22}Ne(d,p)^{23}Ne$ reaction detected in a solid-state counter and gamma rays detected with a plastic scintillator. This lifetime measurement implies a $\frac{5}{2}^+$ assignment for the ground state in ^{23}Ne; the deduced B(E2) transition probability is consistent with the Nilsson model. (auth)

12061 INVESTIGATION OF HIGH SPIN LEVELS PREFERENTIALLY POPULATED BY THE (α,d) REACTION. Rivet, Ernest; Pehl, Richard H.; Cerny, Joseph; Harvey, Bernard G. (Univ. of California, Berkeley). Phys. Rev., 141: 1021-32(Jan. 1966). (UCRL-16200).

The energy spectra of deuterons from the (α,d) reaction on ^{12}C, ^{14}N, ^{15}N, ^{16}O, ^{20}Ne, ^{24}Mg, ^{26}Mg, ^{28}Si, ^{32}S, ^{40}Ar, and ^{40}Ca were observed. These reactions were induced by alpha particles ranging in energy from 42 to 53 Mev. All the energy spectra were dominated by one or more preferentially populated levels. Evidence that these levels have a common configuration is obtained from (a) the relation between their Q values of formation and the mass number of the recoil nuclei, and (b) the similarity of their angular distributions. It is proposed that the levels preferentially populated are of a $[J_T + (j_pj_n)_{I'}]_J$ configuration, with the proton-neutron pair captured in the $d_{\frac{5}{2}}$ or $f_{\frac{7}{2}}$ shell, and that the maximum final spin (5, 6, or 7) is favored. A self-consistent energy-level scheme for the low-lying levels of ^{42}Sc is also proposed. (auth)

12062 PROTON EMISSION IN 42-Mev ALPHA-PARTICLE BOMBARDMENTS OF SEVERAL ELEMENTS. West, R. W. (Univ. of Washington, Seattle). Phys. Rev., 141: 1033-52(Jan. 1966).

Measurements were made of the energy spectra, angular distributions, and absolute cross sections of protons emitted from bombardments of ^{59}Co, ^{58}Ni, ^{60}Ni, ^{62}Ni, ^{63}Cu, ^{65}Cu, Nb, Rh, Pd, and Pt targets by 42-Mev alpha particles. A dE/dX-E scintillation telescope was used in conjunction with an x, y oscilloscope to detect and identify protons in the energy range from 2 to 40 Mev. The data were compared with predictions of the statistical model of nuclear reactions. A calculation was made of the expected proton energy spectra based on this model. The cascade was restricted to neutron and proton emission only, and a level density of the form $\{\exp 2[a(U-\delta)]\}/(U-\delta)^2$ was used. Except for Pt, the calculated and experimental energy spectra matched in slope over a relatively wide intermediate-energy region with the observed spectrum, exceeding the calculated spectrum in both the lowest and highest energy regions. The lowest energy protons were assumed to be caused by compound-nuclear events and the data were separated into compound-nuclear and non-compound-nuclear portions. It was found that the compound-nuclear portions agree well with expectations of the statistical model for yields, spectra, and angular distributions, and they account for 90% of the proton yield for targets in the Ni region, 65% of the proton yield for targets in the Rh region, and probably less than 6% of the proton yield for Pt. The non-compound-nuclear component exhibits a relatively constant yield of ≈85 mb for all the targets studied. (auth)

12063 NUCLEAR ENERGY LEVELS OF ^{56}Fe AND ^{59}Co. Katsanos, A. A. (Argonne National Lab., Ill. Univ. of Chicago); Huizenga, J. R.; Vonach, H. K. Phys. Rev., 141: 1053-61(Jan. 1966).

Nuclear energy levels of ^{56}Fe and ^{59}Co were determined by analyses of particles from the $^{59}Co(p,\alpha)$, $^{56}Fe(p,p')$, and $^{59}Co(p,p')$ reactions with a broad-range single-gap magnetic spectrograph. In the first 6.7 Mev of excitation energy, 100 levels of ^{56}Fe, and in the first 4.0 Mev, 62 levels of ^{59}Co were resolved and investigated. In the excitation-energy region of ^{56}Fe examined previously, new levels was found at 3.748 and 4.802 Mev and the previously reported level at 4.676 Mev was resolved into a doublet with energies of 4.675 and 4.688 Mev. Information on the spins of a few levels of ^{56}Fe is obtained from their cross sections in the aforementioned reactions. The energy dependence of the level density is found to agree qualitatively with theoretical expectations for a finite superconducting nucleus. (auth)

12064 PULSED-BEAM MEASUREMENT OF THE GYROMAGNETIC RATIO OF THE FIRST EXCITED ROTATIONAL STATES IN ^{172}Yb, ^{174}Yb, AND ^{176}Yb. Tippie, J. W.; Scharenberg, R. P. (Case Inst. of Tech., Cleveland). Phys. Rev., 141: 1062-7(Jan. 1966).

The gyromagnetic ratio g of the first excited rotational states in ytterbium 172, 174, and 176 was measured using the pulsed-beam technique. The precession of the Coulomb-excited nuclei in an external magnetic field was detected by observing the angular distribution to the de-excitation gamma radiation as a function of time. The measured g factors and mean lives (τ) are: $g = 0.279 \pm 0.014$, $\tau = 2.46 \pm$

0.07 nsec for ^{172}Yb; g = 0.247 ± 0.013, τ = 2.59 ± 0.07 nsec for ^{174}Yb; g = 0.299 ± 0.015, τ = 2.54 ± 0.07 nsec for ^{176}Yb. The timing techniques which make possible an evaluation of the effect of target perturbations on the measurement are discussed. These measurements were made in ytterbium-metal targets where the magnetic field at the nucleus is essentially the applied external magnetic field. (auth)

12065 STUDY OF THE STRONGLY EXCITED 2^+ AND 3^- STATES IN THE ^{54,56}Fe AND ^{58,60,62}Ni ISOTOPES BY PROTON SCATTERING AT 18.6 AND 19.1 Mev. Eccles, S. F.; Lutz, H. F.; Madsen, V. A. (Univ. of California, Livermore). Phys. Rev., 141: 1067-77(Jan. 1966). (UCRL-14305).

Elastic and inelastic proton-scattering angular distributions were obtained at incident proton energies of about 19 Mev from ^{54}Fe, ^{56}Fe, ^{58}Ni, ^{60}Ni, and ^{62}Ni. The elastic angular distributions were fitted with the nuclear optical model and the parameters so determined were compared to ascertain systematic variations. Generally the fits are good. The parameters were also used as input for distorted-wave Born-approximation (DWBA) calculations of the inelastic scattering. Of special interest was the excitation of the collective 2^+ and 3^- states in these nuclei. The inelastic cross sections were assumed to be a result of a direct reaction exciting collective states, and in addition for the iron isotopes, calculations were made assuming single-configuration shell-model wave functions for the first 2^+ excited states. Although the calculated cross section is greater in ^{56}Fe than in ^{54}Fe, it is still far too small to explain the large difference seen experimentally. Cross sections for collective excitations were calculated assuming the DWBA, and also using the coupled-equation method. Comparison between the two methods are made in terms of the shapes of the angular distributions as well as the magnitude of the cross sections. The forward peak is reasonably fitted in all the isotopes by both the DWBA and coupled-equations calculations, but the remainder of the angular distribution is not as well reproduced. The cross section for excitation of the first 2^+ state in ^{54}Fe is not explained adequately by either the collective or particle model calculations. The identification of the collective 3^- excited state in ^{54}Fe could not be made unambiguously. (auth)

12066 NUCLEAR MATRIX ELEMENTS IN THE FIRST-FORBIDDEN 2.2-Mev β TRANSITION OF ^{140}La. Singru, R. M.; Simms, P. C.; Steffen, R. M. (Purdue Univ., Lafayette, Ind.). Phys. Rev., 141: 1078-81(Jan. 1966). (COO-1420-114).

The angular dependence of the circular polarization of the 1.6-Mev γ radiation following the 2.2-Mev β transition of ^{140}La was measured. The analysis of these data, together with β-γ directional-correlation and spectrum-shape data, was made using exact electron wave functions and taking into consideration finite-nuclear-size effects. The nuclear beta matrix elements determined in this manner show that the deviations of the 2.2-Mev β transition from the Coulomb approximation is caused by a cancellation effect of the vector-type matrix elements and not by a selection-rule effect. The experimentally determined ratio of the $\int i\alpha$ and the $\int r$ matrix elements does not agree well with the value predicted by Fujita on the basis of the conserved-vector-current theory. The discrepancy may be due to the presence of higher order effects in the 2.2-Mev β transition of ^{140}La. (auth)

12067 ENERGY SPECTRA AND RELATIVE YIELDS OF ^{24}Na FRAGMENTS EVAPORATED IN HIGH-ENERGY REACTIONS. Porile, Norbert T. (Purdue Univ., Lafayette, Ind. Brookhaven National Lab., Upton, N. Y.). Phys. Rev., 141: 1082-8(Jan. 1966). (BNL-9470).

The energy spectra and relative yields of ^{24}Na fragments emitted in the interaction of 1.84-Bev protons with copper, silver, and bismuth were calculated. It is assumed that the fragments are evaporated from the residual nuclei resulting from the knock-on cascade in competition with the emission of lighter particles. Account is taken of the motion of the emitting nuclides and of the emission of excited progenitors of ^{24}Na. The calculation is in approximate agreement with results of differential-range studies provided that the emitting nuclides are assumed to be sufficiently distorted at the scission point to reduce the Coulomb barrier against fragment emission to approximately half its classical value. The combined results of calculations for evaporation and spallation processes suggest that at 3 Bev the production of ^{24}Na from copper can be completely accounted for by the latter mechanism. On the other hand, both processes may contribute to the formation of ^{24}Na from silver at this energy. (auth)

12068 LOW LEVELS OF ^{128}Ba FROM ^{128}La DECAY. Li, A. C.; Preiss, I. L.; Strudler, P. M.; Bromley, D. A. (Yale Univ., New Haven). Phys. Rev., 141: 1089-96 (Jan. 1966).

The decay of ^{128}La produced in the ^{115}In(^{16}O, 3n)^{128}La reaction was re-examined with lithium-drifted germanium detectors and standard scintillation spectrometers. The level structure of ^{128}Ba was found to be much more complex than previously reported. The ^{128}La positron decay proceeds mainly to a group of close-lying states at an excitation of approximately 1.35 Mev; no direct branch to the ground state of ^{128}Ba has been observed. While the new level spectrum may include the previously suggested levels, the evidence for rotational spectrum characteristics is no longer compelling. Discussion of the experimental difficulties inherent in studies in this mass region is included. (auth)

12069 ISOMERISM IN ^{129}Ba. Li, A. C.; Preiss, I. L.; Strudler, P. M.; Bromley, D. A. (Yale Univ., New Haven). Phys. Rev., 141: 1097-1105(Jan. 1966).

Isomers of half-lives 2.13 ± 0.06 and 2.20 ± 0.15 hr were identified in ^{129}Ba. The relative ordering of the isomeric states, which most probably have assignments $^9/_2-$ and $^1/_2+$, was not established. Their energy separation is less than 700 kev. No evidence was found for an isomeric transition. These data are in qualitative accord with the Kumar-Baranger prediction of oblate-equilibrium nuclear shapes for odd-neutron nuclei in this mass region. However, the weight of evidence strongly suggests that the nuclides thus far studied lie in a collective transitional region of predominantly vibrational rather than rotational character. (auth)

12070 NUCLEAR MOMENTS OF ^{43}Sc AND ^{47}Sc. Cornwell, R. G.; Happer, William Jr.; McCullen, J. D. (Princeton Univ., N. J.). Phys. Rev., 141: 1106-11 (Jan. 1966).

The magnetic and quadrupole moments of the radioactive isotopes ^{43}Sc and ^{47}Sc were measured by atomic-beam magnetic resonance. Measurements were made of the hyperfine structure of these isotopes in the $^2D_{3/2}$ state of the scandium atom. The results (without diamagnetic or Sternheimer corrections) are ^{43}Sc: A = +105.7 ± 0.9 Mc/sec, B = −44 ± 10 Mc/sec, μ = +4.61 ± 0.04 nm, Q = −0.26 ± 0.06 b. ^{47}Sc: A = 122.2 ± 0.5 Mc/sec, B = −38 ± 6 Mc/sec, μ = +5.33 ± 0.02 nm, Q = −0.22 ± 0.03 b. The electronic g value in both cases was close to the LS-coupling value, and consistent with previous measurements on ^{44}Sc. The mean value of g_J was determined from ^{43}Sc, ^{44}Sc, and ^{47}Sc to be g_J = −1.20061 ± 0.00013. Using this, the ^{44}Sc moments were recalculated. A discussion of the interpretation of the moments of the scandium isotopes is included. (auth)

12071 NUCLEAR MOMENTS OF ^{147}Pm. Reader, Joseph (National Bureau of Standards, Washington, D. C.). Phys. Rev., 141: 1123-28(Jan. 1966).

The nuclear magnetic dipole and electric quadrupole moments of ^{147}Pm were derived from an analysis of the optical hyperfine structure of singly ionized ^{147}Pm. The hyperfine constants for the $[4f^5\ {}^6H_{5/2},6s]_2$ ground state are A = −10.24 ± 0.20 mK; B = −10.6 ± 2.6 mK. By using the known atomic-beam data for the $[4f^56s^2\ {}^6H_{5/2}]$ state of neutral Pm to determine the contribution of the $[4f^5\ {}^6H_{5/2}]$ core to the observed magnetic-splitting factor, the splitting factor of the 6s electron was found to be a_{6s} = +214.2 ± 4.9 mK. The nuclear moments deduced from the hyperfine

constants are $\mu_I(^{147}Pm) = +2.58 \pm 0.07$ nm and $Q(^{147}Pm) = +0.74 \pm 0.20$ b. (auth)

12072 NEUTRON RESONANCE PARAMETERS OF ^{109}Ag. Chrien, R. E. (Brookhaven National Lab., Upton, N. Y.). Phys. Rev., 141: 1129-32(Jan. 1966). (BNL-9412).

The transmission of a thick sample of 99.2% ^{109}Ag was measured for incident neutron energies from 20 kev to 30 ev. The total cross section from 320 to 30 ev was fitted in detail with the Breit-Wigner single-level parameters for 15 resonances in this energy region. An acceptable fit was obtained for a common radiation width of 120 ± 10 Mev and a radius parameter R′ of $(0.63 \pm 0.01) \times 10^{-12}$ cm. From the average cross section in the kev region a neutron strength function of $(0.54 \pm 0.10) \times 10^{-4}$ was obtained. (auth)

12073 NUCLEAR SPIN AND MOMENT OF ^{110m}Ag BY PARAMAGNETIC RESONANCE. Easley, Warren; Edelstein, Norman; Klein, Melvin P.; Shirley, D. A.; Wickman, H. Hollis (Univ. of California, Berkeley). Phys. Rev., 141: 1132-5(Jan. 1966). (UCRL-16002).

Paramagnetic resonance was observed in 253-day ^{110m}Ag, present as Ag^{2+} in the $[(iso\text{-}C_3H_7)_2NCS_2]_2Ag$ complex. Eleven hfs lines were observed, the positions of the other two lines being obscured by other absorptions present in the sample, and the nuclear spin of 6 was confirmed. A hfs constant $a_{110m} = (7.108 \pm 0.02) \times 10^{-3}$ cm^{-1} was determined. A hyperfine anomaly of $\Delta_{107,109} = -0.40\% \pm 0.1\%$ was observed for stable Ag^{2+} in this complex, indicating that the hfs arises from contact interaction. A nuclear moment of $\mu_{110m} = +3.55 \pm 0.04$ nm was derived after a 3.7% hyperfine-anomaly correction. It is pointed out that hyperfine anomalies can be infinitely large for very small moments, and that the anomaly may cause a finite moment to exhibit vanishing hyperfine structure or conversely. The nuclear moment does not agree with shell-model predictions using empirical g factors, being low by 1 nm. It is suggested that the $(g_{9/2})^7$ proton configuration might be coupled to spin $^7/_2$. This yields a moment of +3.54 nm. The hyperfine fields for Ag in Fe and Ni are corrected to -282 ± 20 kG and -87 ± 8 kG, respectively. (auth)

12074 ALPHA CLUSTERS IN A SPHERICAL NUCLEUS. Chang, F. C. (St. John's Univ., Jamaica, N. Y.). Phys. Rev., 141: 1136-7(Jan. 1966).

The probability of occurrence of an alpha cluster in a ^{212}Po nucleus is calculated on the basis of the assumption that the alpha cluster is always formed of a pair of equivalent neutrons, each pair coupling to zero angular momentum. It is shown that the calculated probability can be incorporated with Winslow's surface-well model to explain the decay rate of ^{212}Po. (auth)

12075 COLLECTIVE EXCITATIONS IN ^{207}Pb, ^{208}Pb, AND ^{209}Bi. Alster, J. (Univ. of Washington, Seattle). Phys. Rev., 141: 1138-45(Jan. 1966).

The nuclei ^{207}Pb, ^{208}Pb, and ^{209}Bi are investigated by inelastic scattering of 42-Mev α particles. The previously noted similarity in the excitation of these three nuclei is studied in detail. The excitation of collective levels is strongly favored in this experiment. The measured angular distributions show equally strong octupole levels in the three nuclei, at 2.6-Mev excitation. Levels in ^{207}Pb and ^{208}Pb around 3.2 Mev are found with the same strength as the known 5^- level at 3.198 Mev in ^{208}Pb. The previously reported level at 4.3 Mev in ^{208}Pb is shown to consist of two levels at 4.12 and 4.40 Mev and their angular distributions favor a 2^+ assignment. These levels are also found in ^{207}Pb with the same intensity as in ^{208}Pb. The conclusion is drawn that the excitations in these three nuclei are due to the collective excitations of the ^{208}Pb core and that the coupling to the ^{208}Pb core of a single proton or a single neutron hole is very weak. Collective parameters are extracted using the Austern-Blair model which is shown to give good agreement with the measured angular distributions. The Coulomb-excitation contribution to the inelastic scattering is demonstrated by extending the angular-distribution measurements to small angles. (auth)

12076 FRAGMENT ENERGY CORRELATION MEASUREMENTS FOR ^{252}Cf SPONTANEOUS FISSION AND ^{235}U THERMAL-NEUTRON FISSION. Schmitt, H. W.; Neiler, J. H.; Walter, F. J. (Oak Ridge National Lab., Tenn.). Phys. Rev., 141: 1146-60(Jan. 1966). (ORNL-P-1536).

Fission-fragment mass and energy distributions and mass-versus-energy correlations were obtained for ^{252}Cf spontaneous fission and ^{235}U thermal-neutron-induced fission. Silicon surface-barrier detectors were used in energy correlation measurements; absolute fragment energies were obtained by means of the mass-dependent energy calibration developed recently. Average total fragment kinetic energies before neutron emission are found to be 186.5 ± 1.2 Mev for ^{252}Cf and 171.9 ± 1.4 Mev for ^{235}U. Detailed experimental results are given and compared with those of other experiments. Observed fine structure in the fragment mass distribution and in the average total fragment kinetic energy as a function of mass is correlated with the energetically preferred even-even nucleon configurations in the fragments. New determinations of the root-mean-square width of the total-kinetic-energy distribution as a function of mass show structure which is also correlated with the energetically preferred even-even fragment configurations. Fission-neutron and gamma-ray data of other experiments are used with the new fragment kinetic energies presented to examine the total energy balance for fission for the two cases studied. (auth)

12077 DEFORMATION OF THE TRANSITION-STATE NUCLEUS IN ENERGETIC FISSION. Reising, R. F.; Bate, G. L.; Huizenga, J. R. (Argonne National Lab., Ill.). Phys. Rev., 141: 1161-6(Jan. 1966).

Fission-fragment anisotropy ratios, W(170°)/W(90°), from fission induced by 42.8-Mev helium ions, were measured for the targets ^{230}Th, ^{232}Th, ^{231}Pa, ^{233}U, ^{234}U, ^{235}U, ^{236}U, ^{238}U, ^{237}Np, ^{239}Pu, ^{240}Pu, ^{242}Pu, ^{241}Am, ^{243}Am, ^{244}Cm, and ^{249}Cf. By modifying values of the fission-to-neutron level-width ratio Γ_f/Γ_n from the literature, first-chance anisotropies were calculated to permit comparison of the targets at nearly uniform and rather high excitation energies. The resulting values of K_0^2 (the projection K of the total angular momentum I on the nuclear symmetry axis is assumed to have a Gaussian distribution, and K_0^2 is the squared standard deviation of the Gaussian) associated with first-chance fission in conjunction with the assumptions of rigid moments of inertia permitted evaluation of saddle deformations. The saddle deformations were found to be fairly insensitive to programmed variations in Γ_f/Γ_n values based on a semiempirical relation deduced for the (Z,A) dependence of the compound nucleus. The unrelieved disparity for the heaviest elements between the experimentally derived saddle deformations and those theoretically deduced from the conventional liquid-drop model has been interpreted to suggest a re-evaluation of the fissionability parameter, $(Z^2/A)_{crit}$. Qualitative extrapolation of the new data (assuming a nuclear level-density parameter a = A/8) yields $(Z^2/A)_{crit} \approx 44-45$ for saddle deformations based on first-chance anisotropies computed from experimental data (deleting higher chance fission contributions). This value compares favorably with results of a modification of the conventional liquid drop model, which allows the surface tension to vary with the curvature of the nuclear surface. (auth)

12078 ISOBARIC ANALOGUE STATES IN HEAVY NUCLEI. I. MOLYBDENUM ISOTOPES. Moore, C. F.; Richard, P.; Watson, C. E.; Robson, D.; Fox, J. D. (Florida State Univ., Tallahassee). Phys. Rev., 141: 1166-79 (Jan. 1966).

Isobaric analog states observed as compound-nucleus resonances in proton elastic scattering and (p,n) reactions were studied using the target isotopes ^{92}Mo, ^{94}Mo, ^{95}Mo, ^{96}Mo, ^{97}Mo, ^{98}Mo, and ^{100}Mo. The observed resonances which occur at high excitations in the target-plus-proton system were analyzed using a Coulomb-plus-single-level formula. The spectroscopic information for these resonances is compared with the analog states in the target-

plus-neutron system as observed in (d,p) reactions on the same targets. Level separations, l-value determinations and corresponding spectroscopic factors show remarkable agreement with the (d,p) data. A survey of the experimentally determined Coulomb displacement energies (ΔE_c) was performed via the relation $\Delta E_c = C Z/A^{1/3}$. It is found that C is fairly constant for all the molybdenum isotopes. (auth)

12079 ISOBARIC ANALOGUE STATES IN HEAVY NUCLEI. II. RESONANCES IN ^{69}Ga. Vourvopoulos, G.; Fox, J. D. (Florida State Univ., Tallahassee). Phys. Rev., 141: 1180-4(Jan. 1966).

Resonances in proton elastic scattering and (p,n) reactions on targets of ^{68}Zn are interpreted as isobaric analogs of the excited states of ^{69}Ga. Twelve resonances are identified and classified with respect to l_p. The resolution of a previously unresolved energy-level doublet is demonstrated. The Coulomb displacement energy for the isobaric-analogue system ^{69}Zn–^{69}Ga is found to be 9.60 Mev, in agreement with other work. (auth)

12080 GAMMA-GAMMA DIRECTIONAL CORRELATIONS IN ^{149}Pm. Gopinathan, K. P. (Tata Inst. of Fundamental Research, Bombay). Phys. Rev., 141: 1185-93 (Jan. 1966).

The directional correlations of six γ-γ cascades in ^{149}Pm from the decay of ^{149}Nd were studied. The results are given. From the measured spin of the ground state of ^{149}Pm as $\frac{7}{2}$ the excited states of ^{149}Pm are assigned spins as follows: 114 kev, $\frac{5}{2}$; 210 kev, $\frac{5}{2}$ ($\frac{7}{2}$); 272 kev, $\frac{7}{2}$ or $\frac{5}{2}$; 538 kev, $\frac{5}{2}$; and 650 kev, $\frac{3}{2}$ ($\frac{7}{2}$). The half lives of the 114- and 272-kev levels are found to be 2.4 ± 0.2 and 2.6 ± 0.2 nsec, respectively. The M1 retardation and E2 enhancement of the 114-kev transition in ^{149}Pm are estimated to be 608 and 15, respectively, and these values are compared with those for similar transitions in the neighboring nuclei. The 272- and 158-kev E1 transitions from the 272-kev level are retarded by factors of 3.0×10^5 and 1.7×10^5, respectively. (auth)

12081 REINVESTIGATION OF THE DECAYS OF ^{146}Eu AND ^{146}Pm AND THE EXISTENCE OF TWO CLOSE-LYING STATES AT 1381 kev IN ^{146}Sm. Buss, D. J.; Funk, E. G.; Mihelich, J. W. (Univ. of Notre Dame, Ind.). Phys. Rev., 141: 1193-9(Jan. 1966). (COO-498-45).

The decays of ^{146}Pm and ^{146}Eu were reinvestigated with the primary purpose of establishing the character of the second excited state previously reported at 1384 kev in ^{146}Sm. Gamma-gamma directional correlation data obtained from studies of both the beta decay of ^{146}Pm and the electron capture and positron decay of ^{146}Eu, along with the K-shell internal-conversion-coefficient data, establish the existence of two close-lying states in ^{146}Sm at 1380.7 and 1382.0 kev with spins and parities 3– and 4+, respectively. the gamma-ray spectra were studied with a lithium-drifted germanium detector. In the beta decay of ^{146}Pm the feeding to the 3– state is at least 9.7 times that to the 4+ state, while in the decay of ^{146}Eu the total feeding to the 3– state is ≈1.2 times that to the 4+ state. In addition, gamma-ray energies and intensities are presented for the transitions observed in the decay of ^{144}Pm to ^{144}Nd and ^{146}Pm to ^{146}Nd and ^{146}Sm, and for some of the more intense transitions observed in the decay of ^{146}Eu. Energy systematics of 3– and 4+ states for even-even nuclei in the transition region A = 142 to 152 are presented. (auth)

12082 HALF-LIVES OF THE 2+ ROTATIONAL STATES IN ^{158}Dy AND ^{158}Gd AND SEVERAL OTHER HALF-LIFE MEASUREMENTS FOR DEFORMED NUCLEI. Funk, E. G.; Prask, H. J.; Mihelich, J. W. (Univ. of Notre Dame, Ind.). Phys. Rev., 141: 1200-5(Jan. 1966). (COO-498-46).

The half lives of the 99.1-kev level in ^{158}Dy and the 79.6-kev level in ^{158}Gd were measured to be 1.64 ± 0.08 nsec and 2.47 ± 0.10 nsec, respectively, using a source of ^{158}Tb (150 yr) and a time-to-amplitude converter circuit. In addition, the following half lives were measured: 86.8-kev state in ^{160}Dy, 2.02 ± 0.09 nsec; 84.2-kev state in ^{170}Yb, 1.56 ± 0.08 nsec; 76.5-kev state in ^{174}Yb, 1.74 ± 0.09 nsec; 100.1-kev state in ^{182}W, 1.35 ± 0.7 nsec; 1289-kev state in ^{182}W, 1.06 ± 0.05 nsec. A compilation of the more recent data on first excited state half lives, B(E2) values, and deformation parameters is presented for the even-even rotational nuclei in the region Z = 60–68. A comparison is made between values determined from half life and Coulomb-excitation measurements. (auth)

12083 LIFETIMES OF FIRST 2+ AND 4+ STATES OF ^{192}Pt AND SOME SYSTEMATICS OF E2 TRANSITIONS IN EVEN-EVEN NUCLEI. Schwarzschild, Arthur (Brookhaven National Lab., Upton, N. Y.). Phys. Rev., 141: 1206-14(Jan. 1966). (BNL-9429).

The mean lifetimes of the first 2+ (316-kev) and 4+ (785-kev) states of ^{192}Pt were measured using the delayed-coincidence method. The results are $\tau_m(2+) = (5.1 \pm 0.4) \times 10^{-11}$ sec and $\tau_m(4+) = (1.7 \pm 0.3) \times 10^{-11}$ sec. The $2 \rightarrow 0$ transition is enhanced by a factor 69 and the $4 \rightarrow 2$ by a factor 31 relative to the single-particle estimate. Thus $B(E2; 4 \rightarrow 2)/B(E2; 2 \rightarrow 0) = 0.45 \pm 0.10$. The systematics of the 2+ states and B(E2) values for nuclei with $170 \leq A \leq 210$ are presented. In addition, a compilation of measured ratios $B(E2; 4 \rightarrow 2)/B(E2; 2 \rightarrow 0)$ for all nuclei is given. Comparison with these systematics indicate that in ^{192}Pt the $2 \rightarrow 0$ transition is unusually fast and $B(E2; 4 \rightarrow 2)/B(E2; 2 \rightarrow 0)$ is small. Studies of the conversion electron spectrum of ^{192}Pt show that the previous assignment of a $4 \rightarrow 2'$ transition is incorrect. (auth)

12084 HYPERTRITON WITH S' STATE AND THE Λ-N INTERACTION. Bodmer, A. R. (Argonne National Lab., Ill.). Phys. Rev., 141: 1387-97(Jan. 1966).

The hypertriton $_\Lambda H^3$ is considered with the inclusion of an S' state $\Psi_{S'}$ in the total wave function. For $\Psi_{S'}$ the nucleons are in a singlet spin state and the space part is correspondingly antisymmetric with respect to exchange of the nucleons. Only a spin dependence of the Λ-N interaction can give a nonzero admixture of $\Psi_{S'}$ to the dominant component Ψ_S, which is space-symmetric under exchange of the nucleons and which is the only component that was considered in previous investigations. Central, spin-dependent Yukawa potentials were used. The most flexible trial function used was one with 16 parameters for which Ψ_S has the same 6-parameter form as used by Downs and Dalitz and $\Psi_{S'}$ has a corresponding flexibility. In particular, for an intrinsic range b = 1.5 F (corresponding to a Yukawa interaction appropriate to two-pion exchange), the effect of $\Psi_{S'}$ is quite appreciable; the singlet strength is reduced, the triplet strength slightly increased, and the spin dependence reduced by about a third. For a range corresponding to meson (K) exchange (b = 0.84 F), the effect of $\Psi_{S'}$ is considerably less. With inclusion of $\Psi_{S'}$ (for a given b), the singlet strength is found to be quite insensitive to the value of the triplet strength and is therefore almost entirely determined by $B_\Lambda(_\Lambda H^3)$. The resulting total Λ-N cross sections at low energies (≲20 Mev) are compared with the experimental values σ_{exp}. If it is assumed that the singlet scattering length a_s and effective range r_s are most reliably determined from hypernuclei, then for b = 1.5 F (for which the estimated values with a hard core of radius 0.42 F are $a_s \approx -2.3$ F, $r_s \approx 3.6$ F), acceptable agreement with σ_{exp} can be obtained with only a modest increase of $|a_t|$ ($a_t \approx -1.3$ F, $r_t \approx 2.9$ F) above the value obtained from hypernuclei. (The maximum value consistent with the hypernuclear results is $a_t \approx -0.9$ F together with $r_t \approx 3.3$ F.) It is shown that an increase of this order of magnitude could be obtained through suppression of the coupling with the ΣN channel in $_\Lambda He^5$. Results are also given for a Yukawa potential with b = 2.07 F, which is the intrinsic range for an interaction with a hard core of radius 0.42 F and an attractive Yukawa tail appropriate to an exchanged boson with mass $3m_\pi$. Finally, it is argued that there is a tentative indication for the existence of a repulsive core in the Λ-N interaction. (auth)

12085 STOPPING OF ENERGETIC COPPER IONS IN ALUMINUM. Subrahmanyam, V.; Kaplan, Morton (Yale Univ., New Haven). Phys. Rev., 142: 174-8(Feb. 1966).

By means of differential-range experiments, the average

ranges and range straggling of 24-min ^{60}Cu and 3.3-h ^{61}Cu in Al were measured. These species were produced with initial recoil energies from 3 to 18 Mev by bombardment of thin targets of ^{59}Co and ^{55}Mn with ^{6}Li, ^{10}B, and ^{11}B heavy-ion beams. The average ranges increase smoothly with recoil energy and the distributions in range about the average values follow a Gaussian relationship. The experimental range-energy data are in good agreement with theoretical expectations, assuming total momentum transfer over the full energy region investigated. It is concluded that the nuclear processes which produced the recoiling ions are pure compound-nucleus reactions. Although theory and experiment yield consistent average-range values, the stopping-theory predictions for range straggling are much smaller than experimental estimates of the straggling inherent in the stopping process. The source of the discrepancy is discussed in terms of the relative contributions of electronic and nuclear stopping. (auth)

12086 FINITE-WELL, SINGLE-PARTICLE WAVE FUNCTIONS IN TWO-NUCLEON STRIPPING. Drisko, R. M.; Rybicki, F. (Univ. of Pittsburgh). Phys. Rev. Lett., 16: 275-8(Feb. 14, 1966).

The angular distributions for the reactions ^{40}Ca(He-3,p)^{42}Sc and ^{54}Fe(t,p)^{56}Fe were calculated using the distorted-wave Born approximation with oscillator and finite-well single-particle wave functions. The results show that finite-well single-particle functions, or some equivalent, should be used in DWBA calculations for two-nucleon transfers. (D.C.W.)

12087 FINE STRUCTURE IN NUCLEAR RESONANCES. Ferrell, Richard A.; MacDonald, William M. (Univ. of Maryland, College Park). Phys. Rev. Lett., 16: 187-90 (Jan. 31, 1966).

It is shown that a seemingly complicated behavior, such as that displayed by the fine-structure fluctuations in the nuclear cross section, may actually be only a superficial complication. Underlying the fluctuations, there may be a single doorway state which retains its simple nature and corresponds to some energy-independent angular distribution. In some cases, the fluctuations may be the result of other doorway states falling in the same energy range; the hallway-state theory of fine structure does not apply to these cases. (D.C.W.)

12088 $I^2(I+1)^2$ CORRECTION TO NUCLEAR ROTATIONAL SPECTRA. Marshalek, Eugene R. (Brookhaven National Lab., Upton, N. Y. Univ. of Notre Dame, Ind.). Phys. Rev. Lett., 16: 190-4(Jan. 31, 1966).

The β coefficients in the expression $E_I = \frac{1}{2}(\hbar^2/\mathcal{I})I(I+1) + \beta I^2(I+1)^2 + \ldots$ for the energies of members of the ground-state rotational band of even-even deformed nuclei were calculated, together with the corresponding moments of inertia (I). The results were compared with experimental values. (D.C.W.)

12089 TOTAL CROSS SECTION FOR 14-Mev NEUTRONS USING ALIGNED ^{165}Ho NUCLEI. Marshak, H. (National Bureau of Standards, Washington, D. C.); Richardson, A. C. B.; Tamura, T. Phys. Rev. Lett., 16: 194-7(Jan. 31, 1966). (ORNL-P-1878).

The effect of nuclear deformation on the total cross section of ^{165}Ho was measured using 14-Mev neutrons and an aligned target. The data were explained quite well in terms of the nonadiabatic coupled-channel calculation. (D.C.W.)

12090 NEW NUCLIDIC MASS RELATIONSHIP. Garvey, Gerald T.; Kelson, Itzhak (Yale Univ., New Haven). Phys. Rev. Lett., 16: 197-200(Jan. 31, 1966).

A simple relation between nuclidic masses, which is based on an independent-particle model of the nucleus and which is valid independently of the actual variation of mass with atomic number and charge, is proposed. (D.C.W.)

12091 FINITE-RANGE COULOMB STRIPPING AND HEAVY ION TRANSFER REACTIONS. El-Nadi, M.; Rihan, T. H. (Atomic Energy Establishment, Cairo). Proc. Phys. Soc., 87: 119-32(Jan. 1966).

An analytical method, based on some approximations, is given for the calculation of finite-range Coulomb stripping reactions. The case when the captured and emitted particles are initially in arbitrary radial states is considered. Comparison is made with previously derived formulas. By adopting the Morinigo wave function for the final bound state, it is shown that the finite-range interaction leads to an additional angular-dependent factor when the angular momentum of the captured particle is not equal to zero. This correction factor decreases at large angles, an effect which is also observed in the finite-range effects on the non-Coulomb stripping process. (auth)

12092 ENERGY SPECTRUM OF CHARGED PIONS FROM K^--CAPTURES IN CF_3Br. Abraham, F. (Univ. of Chicago); Beniston, M.; Levi-Setti, R.; (and others). Univ. Brux., Inst. Phys., Bull. No. 22, 1-17(Aug. 1965).

From about 30,000 stopped mesons (K^-) in the Ecole Polytechnique bubble chamber filled with CF_3Br a search was made for long range mesons (π^-) due to the reaction $K^- + Br \rightarrow {}_{\Lambda}Br + \pi^-$, in an attempt to determine a lower limit of the Λ-binding energy in ${}_{\Lambda}Br$. No event compatible with this reaction was found. Results from measurements of the total π^-- and π^+-energy spectra were used to investigate the production and trapping of hyperons (Λ) in K^--captures on complex nuclei. From the frequency of Λ production associated with the emission of mesons (π^-) with kinetic energy > 110 Mev, the fraction of directly produced hyperons (Λ) being trapped in the production nuclei was estimated as $0.29^{+0.5}_{-0.6}$. For Λ hyperons due to Σ-conversion a lower limit for the same quantity is 0.28 ± 0.05. (auth)

12093 THE EFFECT OF PAIR CORRELATION ON α DECAY IN THE NEIGHBORHOOD OF ^{208}Pb — AN ABSOLUTE CALCULATION OF REDUCED WIDTH. Kao, Mei-juan; Chen, Jin-quan; Sze, Shih-yuan (Nanking Univ., China). Wu Li Hsueh Pao, 21: 1725-43(Oct. 1965). (In Chinese).

By means of the BCS wave functions and projected wave functions the absolute values of α reduced width of even-even isotopes of Po and odd-even isotopes of At are calculated. The change of absolute values and the behavior of the relative values due to the change of the parameters b, R_0, and G were investigated, where b is the parameter of harmonic oscillator well, R_0 the channel radius, and G the parameter of pair correlation. The analysis of the results of calculation is discussed. (L.B.S.)

12094 AN UNUSUAL NUCLEAR PHOTOREACTION ON C, O, AND Si. Artus, H. (Technische Hochschule, Darmstadt, Ger.). Z. Phys., 189: 355-64(1966). (In German).

The nuclide ^{7}Be was produced by irradiating graphite and water with bremsstrahlung from the Darmstadt 60 Mev linear accelerator. Yield curves and approximate cross sections are presented up to 57 Mev. Integrated cross sections at 57 Mev are 6.0 Mev mbarn for $^{12}C(\gamma,x)^{7}Be$ and about 0.7 Mev mbarn for $^{16}O(\gamma,x)^{7}Be$. At 51.4 Mev maximum bremsstrahlung energy the yield of $^{30}Si(\gamma,2p)^{28}Mg$ is 1.6% of the $^{12}C(\gamma,n)^{11}C$ yield, and about 3.8 times as much ^{24}Na as ^{28}Mg is produced in a natural silicon target. (auth)

12095 THE DISTORTED WAVE ANALYSIS OF STRIPPING REACTIONS AND THE LEVEL STRUCTURE OF ^{53}Cr [Thesis]. Bardwick III, John. Ann Arbor, Mich., Univ. of Michigan, 1964. 96p.

The distorted wave program of Gibbs and Tobocman, developed at Rice University and modified at Los Alamos by Rodberg, Swartz, and Hall was altered to make it compatible with the system in use at The University of Michigan Computing Center and is now one of the standard laboratory tools available for use in the analysis of stripping reactions. As a means of investigating the sensitivity of the optical model parameters, the absolute differential cross sections for 7.8 Mev deuterons scattered elastically from ^{9}Be, ^{24}Mg, ^{25}Mg, ^{26}Mg, ^{27}Al, ^{52}Cr, and ^{197}Au were measured for laboratory angles between 20 and 95°. Optical model potential parameters for the deuteron that fit the above data are determined. The changes in the predicted elastic cross sections that occur as the input param-

eters are varied are investigated. The reaction $^{52}Cr(d,p)^{53}Cr$ was used to study the levels of ^{53}Cr to an excitation of 4.22 Mev. Absolute differential cross sections for nine levels were obtained for laboratory angles between 10° and 90°. The l_n values and reduced widths resulting from the distorted wave analysis of the observed ^{53}Cr levels are listed. The absolute reduced widths predicted by the distorted wave calculation are found to be sensitive to the exact value of R_N, the radius at which the interior and exterior neutron wave functions are matched. The relative reduced widths are much less sensitive, showing variations of the order of 10 percent as R_N is varied from 6.1F to 7.3F. The reduced widths computed for the higher-lying l = 1 levels are consistently less than those computed by the Butler or plane wave theory. (Dissertation Abstr.)

12096 A STUDY OF (d,p) REACTIONS ON LIGHT NUCLEI FROM 200 TO 350 kev [Thesis]. Henkel, Joel Edward. Durham, N. H., Univ. of New Hampshire, 1965. 129p.

The angular distributions of protons from (d,p) reactions on the light nuclei ^{6}Li, ^{9}Be, ^{12}C, ^{14}N, and ^{16}O at deuteron energies below the coulomb barriers were measured and compared with PWBA in the Bhatia form. Applicability of the Born approximation is discussed briefly, followed by development of an expression of PWBA to compare with experiment. The experimental method is discussed in detail. The angular distributions are found to be generally asymmetric about 90 degrees, some with forward peaking, indicating that stripping is important for these reactions. Two distributions show marked structure: $^{9}Be(d,p)^{10}Be$ (g.s.) with a backward peak, and $^{14}N(d,p)^{15}N$(g.s.) with a forward peak. Stripping vs. compound nucleus amplitude ratios are extracted by assuming an isotropic compound nucleus amplitude and fitting the asymmetric component to PWBA in the Bhatia form. A semiclassical model for the ^{9}Be and ^{14}N reactions, using shell structure, is attempted. It is concluded that PWBA cannot reproduce the angular distributions of all of the reactions. A thick target method is used, which gives results similar to those of a thin target method because of the extremely rapid loss of beam energy in the target at these very low energies. (Dissertation Abstr.)

12097 TOTAL GAMMA ABSORPTION IN ^{9}Be, ^{16}O, ^{19}F, AND ^{27}Al AT 20 Mev [Thesis]. Tessler, George. Philadelphia, Univ. of Pennsylvania, 1964. 156p.

The total gamma absorption cross sections were measured for ^{9}Be from 20.04 to 21.24 Mev, ^{16}O from 20.37 to 22.04 Mev, ^{19}F from 19.97 to 20.46 Mev, and ^{27}Al from 20.37 to 20.88 Mev. A direct absorption technique was employed utilizing monochromatic gamma rays from the $^{3}T(p,\gamma)^{4}He$ reaction. Four thallium-activated sodium iodide crystals, each 3 in. diameter by 4 in. long, were used to detect the gamma rays. Absorbers were suspended by thin wires between two of the crystals and the target while the other two crystals served as monitors. The ^{9}Be cross section contained peaks at 20.47 ± .04 Mev and 20.73 ± .04 Mev with integrated cross sections of .45 and .90 Mev-mb respectively. The ^{16}O cross section has a broad resonance at 21.02 ± .04 Mev with an integrated cross section of 10.4 Mev-mb. There is an indication that this resonance is composed of two narrower resonances at about 20.86 Mev and 21.05 Mev. There is some indication of a peak at 20.62 Mev. Above 21.6 Mev, the ^{16}O cross section is rising sharply suggesting the presence of a strong resonance located above 22.04 Mev. The ^{19}F cross section has a peak at 20.09 ± .05 Mev with an integrated cross section of 3.5 Mev-mb. The ^{27}Al cross section showed no structure in the energy region investigated. (Dissertation Abstr.)

12098 BETA-DECAY NUCLEAR MAGNETIC RESONANCE SEARCH FOR THE g FACTORS OF ^{12}B AND ^{110}Ag [Thesis]. Davis, Dan Lee. University Park, New Mexico State Univ., 1965. 164p.

The capture of polarized thermal neutrons by ^{11}B and ^{109}Ag has been found to produce substantial nuclear polarization of the product nuclides, ^{12}B and ^{110}Ag. The resultant "right-left" asymmetry in the ^{12}B beta decay at 77°K was measured. The asymmetry coefficient is $\alpha = -0.142 \pm 0.012$. The asymmetry coefficient for Ag^{110} in AgCl crystals was measured at 4.2°K as $\alpha = -0.080 \pm 0.005$ if only the beta spectrum above 2.20 Mev is observed. The relaxation time for ^{110}Ag nuclei in AgCl at 4.2°K was found to exceed 100 sec. A determination of the beta asymmetry as a function of temperature showed observable polarization at 20°K although the maximum value occurred only for T < 6°K. The effective nuclear polarization is diminished to half the high field value at $H_0 = 600$ gauss for ^{110}Ag and $H_0 = 1500$ gauss for ^{12}B. A search for the nuclear magnetic resonance of each nuclide was unsuccessful. No resonance could be observed over the range g = 0.45−1.20 for ^{12}B and g = 0.23−3.75 for ^{110}Ag. The failure to observe these resonances is attributed to large quadrupolar broadening of the Zeeman lines. (Dissertation Abstr.)

12099 THE ELASTIC AND INELASTIC SCATTERING OF 18-Mev ALPHA PARTICLES FROM ^{9}Be, ^{23}Na, AND ^{31}P [Thesis]. Lucas, Bruce Thomas. Lafayette, Ind., Purdue Univ., 1964. 146p.

The differential cross sections for the elastic and inelastic scattering of α particles from ^{9}Be and ^{23}Na at 18.4 Mev and from ^{31}P at 18.2 Mev were measured using Si surface-barrier detectors. The inelastic differential cross sections correspond to leaving ^{9}Be in its first three excited states at 1.75, 2.43, and 3.04 Mev; ^{23}Na in its first two excited states at 0.439 and 2.080 Mev; and ^{31}P in its first two excited states at 1.265 and 2.232 Mev. All three elastic angular distributions exhibit strong diffraction-like structure with evenly spaced maxima at forward angles. The inelastic cross sections also exhibit oscillatory structure, but generally to a lesser extent. The data were analyzed in terms of the Blair diffraction model, the five-parameter smooth-cutoff model of McIntyre, Wang, and Becker, the sharp-cutoff Akhieser-Pomeranchuk-Blair model, and the PWBA and McCarthy-Pursey theories. A compilation of experimental interaction radii for a series of light nuclei ($6 \leq A \leq 40$) obtained by analysis of elastic α-scattering data was produced. No systematic relation between the radii and the energy of the incident α particle was found. A graphical compilation of σ_E/σ_R ratios for the scattering of 18- to 22.5-Mev α particles from a series of light nuclei ($9 \leqq A \leqq 32$) is presented, and the possible existence of a systematic difference in the large-angle behavior of the cross sections for certain even-even and odd-A nuclei is discussed. (A.G.W.)

12100 NUCLEAR STRUCTURE EFFECT IN NEUTRINO INDUCED NUCLEAR "ELASTIC" REACTIONS [Thesis]. Goulard, Bernard. Philadelphia, Univ. of Pennsylvania, 1964. 91p.

Nuclear effects in the determination of nucleon weak factors from data on reactions of the type $\nu + [Z,A] \rightarrow \mu^{\pm} + [Z \pm 1,A]$ were studied. The first chapter deals with the principles of weak interaction theory and with the applications of these principles to neutrino-induced reactions and to muon capture by nuclei; in particular, various attempts to obtain the induced-pseudoscalar nucleon weak form factor from a comparison of theoretical and experimental muon capture rates are analyzed. Relativistic effects in muon capture by nuclei are calculated; this improves the accuracy of the theoretical expressions for the various capture rates. In the second chapter, the scattering of particles by a collection of nucleons in a nucleus is analyzed in the framework of supermultiplet theory. This formalism is applied to the inelastic electron scattering by nuclei, and its applications to muon capture by Primakoff and others are also outlined. The third chapter starts with a brief review of the first attempts to calculate the effects of nuclear structure on neutrino-induced nuclear reactions. Then, these effects are worked out in detail on the basis of the general theory given in the first and second chapters. The results are displayed as explicit formulas and also graphically for various cases of interest. (Dissertation Abstr.)

12101 A THEORETICAL INVESTIGATION OF THE STABILITY OF ^{5}H [Thesis]. McCarthy, Robert Joseph. Washington, D. C., Catholic Univ. of America, 1965. 83p.

A three-body cluster model consisting of a triton core and two orbital nucleons interacting through local, energy independent two-body potentials is used in a variational calculation to test the proposed existence of a bound ^{5}H. The trial wave function is chosen to be a product of Gaussian functions and is constructed to have the two orbital nucleons in p states relative to the triton core in the absence of any nucleon-nucleon correlation. The introduction of such a correlation brings components of all triton-nucleon angular momentum states into the wave function and all 1s states introduced in this way must be projected out of the wave function since they are forbidden by the Pauli principle. The actual triton-nucleon potentials are non-local and energy dependent but it is shown that they can be replaced by effective potentials derived numerically from wave functions describing the relative motion of a nucleon and a three particle core in various eigenstates of angular momentum, spin, isotopic spin, and energy. The potentials thus derived are fitted with sums of Gaussians and a Gaussian form is also chosen to describe the nucleon-nucleon potential. A check on the accuracy of the calculation is made by calculating the energy of the $^3/_2{}^+$ state of ^{5}He by the same method. The success of the model in calculating the energy of the $^3/_2{}^+$ state of ^{5}He and the lack of any minimum in the variational calculation for ^{5}H provide strong evidence against the existence of a bound ^{5}H. (Dissertation Abstr.)

12102 NUCLEAR DECAY PROCESSES IN THE PRESENCE OF A LASER BEAM [Thesis]. Meyer, James William. Baltimore, Johns Hopkins Univ., 1965. 60p.

The effects on nuclear decay processes of an extremely high-photon-density laser beam are studied to determine whether experiments can be devised to test the validity of quantum electrodynamics at high photon densities, or, assuming the validity of quantum electrodynamics, to obtain information on the interactions controlling the decay process itself. It is found that in the limit of zero laser frequency the total decay rate of an unstable system is unchanged from the total decay rate in the absence of the laser beam. In the appendix this is shown to be a consequence of the gauge invariance of the theory. The differential electron spectrum in beta decay is studied in detail as a function of both energy and angle. It is found that while effects do occur, no practical experiment could be performed even with the largest lasers at present available. Nuclear gamma decay is also discussed. The laser beam is treated as an external field after it is shown that this is equivalent to treating it as a quantized field with certain coherence properties. (Dissertation Abstr.)

12103 QUADRATIC MOMENTUM DEPENDENCE OF NUCLEAR POTENTIAL [Thesis]. Yi, Hsu-shih. Lafayette, Ind., Purdue Univ., 1964. 82p.

Regarding the momentum-dependence of the pion-theoretical potential, Sugawara and Okubo showed that the quadratically momentum-dependent term is $-V_2(\vec{r})\vec{p}^4/4m^2$ H.c., where $V_2(\vec{r})$ is the second-order static potential, m is the nucleon mass and $\vec{p} = -i\vec{\nabla}$, $\vec{\nabla}$ is the gradient with respect to the relative coordinate $\vec{r}$ of the two nucleons. They also showed that pion field theory does not seem to predict any appreciable $\vec{L}.\vec{S}$ potential, $\vec{L} = \vec{r} \times \vec{p}$ and $\vec{S} = (\vec{\sigma}_1 + \vec{\sigma}_2)/2$, $\vec{\sigma}_i$ being the usual spin operator. Two-nucleon scattering data is analyzed in the singlet-even state and the triplet-even state with J = L up to 315 Mev in terms of the potential based on the above theoretical work. The present potential, therefore, consists of a static term and a quadratic term of the form of $-V(\vec{r})\vec{p}^2/4m^2$ + H.c., where the static term and $V(\vec{r})$ are required to approach asymptotically the second-order static potential $V_2(\vec{r})$. The potential contains a hard-core, the radius of which is regarded as an adjustable parameter. The static term and $V(\vec{r})$ in the present potential contain other adjustable parameters that determine the details of the potential in the inner region. All these parameters are adjusted independently for the singlet-even state and the triplet-even state with J = L. No difficulty was found in adjusting these parameters within reasonable ranges to reproduce the empirical phase shifts determined by Breit et al. (YLAM and YLAN3M). The fit to the empirical phase shifts is better than the best potential fits so far obtained by Hamada and Johnston, and by Hull et al. It was confirmed that the above fit cannot be obtained without the quadratic term in the potential. This statement is not affected by adding an $\vec{L}.\vec{S}$ potential to the potential, because an $\vec{L}.\vec{S}$ potential is effectively a static potential in those states in which the phase shifts are analyzed. (Dissertation Abstr.)

12104 THE POLARIZATION OF NUCLEI IN SOLID DEUTERIUM [Thesis]. Waine, Martin. New Haven, Yale Univ., 1965. 95p.

Nuclei of solid deuterium containing trapped deuterium atoms were partially polarized by exciting simultaneous transitions of the paramagnetic centers and the nuclei of their nearest neighbor molecules and by subsequent spin diffusion of the resulting nuclear polarization. Samples were grown by passing deuterium gas at low pressures through a discharge and condensing it in a microwave cavity whose temperature was 4.2°K and which contained a nuclear resonance coil for observing the increase in nuclear polarization. The theory of this method of polarizing nuclei is described for nuclei having spin $^1/_2$, and in greater detail for ortho-deuterium with spin 2. The apparatus is described, and the experimental results are given. Nuclear polarizations of the order of 1% were achieved, but evidence suggests that polarizations of the order of 10% or more should be obtainable. (Dissertation Abstr.)

12105 THE PHOTOPROTON POLARIZATION FROM ^{12}C [Thesis]. Alston III, William Jeffries. New Haven, Yale Univ., 1965. 115p.

The polarization of the photoprotons from the reaction $^{12}C(\gamma,p)$ at 88° ± 3° in the laboratory system was observed with high-pressure helium as an analyzer. The range of proton energies extended from 12 to 18 Mev, corresponding to photons of 30 to 36 Mev. A triple coincidence method, employing before scattering a thin plastic scintillator and after scattering a transmission parallel plate proportional counter followed by a final plastic scintillator, enabled one to observe real 3° coincidences well above the background rate due to accidental coincidences. An additional run with deuterium as a known analyzer with nearly zero polarizing power, gave an indication of the instrumental asymmetry that must be subtracted from the observed L/R asymmetry with helium as analyzer. With an instrumental asymmetry $\epsilon = -21.7\%$, the value of the photo-proton polarization from carbon was found to be +24.9% ± 5.6%. (Dissertation Abstr.)

12106 THE ANGULAR DISTRIBUTION OF NEUTRONS INELASTICALLY SCATTERED FROM THE 0.48 Mev LEVEL OF ^{7}Li [Thesis]. Humphrey, Douglas L. Athens, Ohio, Ohio Univ., 1965. 49p.

The angular distribution of the neutrons inelastically scattered from the first excited state of ^{7}Li was measured to find the dominant mode of interaction. The angular distribution was determined indirectly by analyzing the de-excitation γ rays from ^{7}Li that were in coincidence with the inelastically scattered neutrons. These γ rays are emitted isotropically, thus there is no correlation between the direction of the neutron and the direction of the γ ray. The incident neutron energy was 2.45 Mev. The γ rays were detected by a NaI crystal and the neutrons were detected by a stilbene crystal. Unwanted pulses due to γ rays striking the stilbene were eliminated by a pulse shape discriminator. From the measured angular distribution the conclusion was that direct interaction scattering contributed very little, if any, to the scattering cross section. The large background encountered prevented the conclusion that the angular distribution was symmetric, although the results did not rule out such a possibility. The magnitude of the differential cross section at 90° in the center-of-mass, the approximate position of the maximum, is 0.013 barns per steradian. The error in the absolute cross section was estimated to be 9%. (Dissertation Abstr.)

12107 NUCLEAR POLARIZATION IN THE $^{11}B(d,p)^{12}B$ REACTION [Thesis]. Berlijn, Jean Jacques Henri. Baltimore, Johns Hopkins Univ., 1965. 105p.

Detailed measurements on the nuclear polarization of the β^- active ^{12}B recoil nucleus resulting from the $^{11}B(d,p)^{12}B$ reaction were made. Reaction energies of 1.10, 2.44, and 2.80 Mev were used. The recoil nuclides were stopped on Pilot B, polyetheylene, copper, and solid xenon foils. The up-down asymmetry in the β^- decay of the ^{12}B nuclei was observed at recoil angles of $\pm(53 \pm \frac{1}{2})°$ with respect to the beam direction, which corresponds to the stripping peak for $E_d = 2.80$ Mev. From kinematics calculations relating the proton angle and the ^{12}B recoil angle, it follows that only ^{12}B nuclides in the nuclear ground state were observed. At 1.10 Mev an observation at a mean angle of $\Theta = +45°$ (which corresponds to the stripping peak at $E_d = 1.10$ Mev) was also made, using polyethylene and solid xenon stopping foils. The up-down asymmetry was measured with the stopping foils placed in a perpendicular 500-gauss field. This number was then corrected for by a zero-point measurement taken with only a 15-gauss transverse field turned on. No significant asymmetry was observed using the Pilot B, polyethylene or copper stopping foils. For the solid xenon foil at a reaction energy of 2.44 Mev an asymmetry of $-4.1\% \pm 0.8\%$ was observed. The xenon foil experiment at a reaction energy of 1.10 Mev did not indicate a consistent asymmetry pattern. The one at a reaction energy of 2.80 Mev, on occasion gave comparatively large zero-point measurements. (Dissertation Abstr.)

12108 THE $(n,n'\gamma)$ REACTION IN ^{56}Fe [Thesis]. Benjamin, Richard Walter. Austin, Tex., Univ. of Texas, 1965. 115p.

Gamma-ray angular distributions and $(n,n'\gamma)$ cross sections were measured for gamma rays produced in natural iron by inelastic neutron scattering at inelastic neutron energies ranging from 0.95 to 4.0 Mev. $(n,n'\gamma)$ cross sections were measured at 90° for all the observable gamma rays in iron to 4.0 Mev and for the 0.845 gamma ray to 4.75 Mev. The angular distributions were compared with theoretical predictions of the Satchler formalism using three different sets of neutron penetrabilities. On the basis of theoretical and experimental comparisons of both the shape of the angular distributions and the differential cross sections of the gamma rays an additional energy level at 3.45 Mev is proposed. The following tentative spin and parity assignments were made for levels in the ^{56}Fe nucleus: 3.12 Mev (3^-), 3.45 Mev (1^+), 3.45 Mev (3^+), and 3.60 Mev (2^+). Branching ratios for gamma rays originating at these levels were determined. The $(n,n'\gamma)$ cross sections were also compared successfully with inelastic neutron cross sections measured by Hopkins and Silbert at Los Alamos. (Dissertation Abstr.)

12109 VIBRATIONAL ENERGY SPECTRUM OF THE ATOMIC NUCLEUS ^{112}Cd [Thesis]. Barnes, Peter David. New Haven, Yale Univ., 1965. 146p.

The energy level spectrum of cadmium-112 was investigated with the reaction $^{111}Cd(d,p)^{112}Cd$ as well as the absolute differential cross section for elastic deuteron scattering on natural cadmium. The absolute differential cross section for the population of various levels in ^{112}Cd was analyzed in the framework of the distorted-wave Born approximation, and values of the orbital angular momentum of the captured neutron, l_n, and the spectroscopic factor were assigned. Wave functions suggested by Baranger's microscopic model of nuclear vibrations together with the expansion coefficients for the odd target ground state wave function suggested by Kisslinger and Sorensen were used to calculate the spectroscopic factor for the ground state and first excited state of ^{112}Cd. These values are a factor of three larger in magnitude than the values suggested by the analyzed data. Possible vibrational levels at higher excitation are discussed. The measurement of level energies, l_n, and spectroscopic factors for a number of levels up to 3.3 Mev in excitation are also reported. (Dissertation Abstr.)

12110 MULTIPLE COULOMB EXCITATION STUDIES IN EVEN-EVEN SAMARIUM NUCLEI [Thesis]. Seaman, Gregory Gardner. New Haven, Yale Univ., 1965. 237p.

The spectroscopy of the low-lying collective levels of the even-even samarium nuclei 148, 150, 152, and 154 was studied by detecting the de-excitation gamma radiation following coulomb excitation with oxygen ions up to 65 Mev in energy. Information is presented both on the energy-level structure of these nuclei and the reduced transition probabilities for excitation of some of the levels, and these are discussed within the framework of the existing collective models. The most striking deviations from the simple models occur in ^{152}Sm, and an attempt is made to explain these deviations by first order interband mixing between the ground state band and the beta and gamma vibrational bands. The analysis is performed from measurements of branching ratios of interband transitions. Apparent success in explaining the deviations from the simple axial rotor model is obtained by invoking the hydrodynamic model to calculate the absolute interband transition probability. However, a measurement of the absolute transition probability negates this and other seemingly successful attempts based on the hydrodynamic model. Reduced transition probabilities for vibrational states are obtained for ^{148}Sm and ^{150}Sm, and these new reduced transition probabilities for excitation of even parity states are in fair agreement with the relative magnitudes predicted for pure harmonic oscillations of the nuclear surface. Evidence for collective 3-excitations in the four nuclei is presented, and the measured excitation probabilities are given. (Dissertation Abstr.)

12111 HIGH ENERGY NUCLEAR REACTIONS. Clegg, A. B. Oxford Library of the Physical Sciences. Oxford, Clarendon Press, 1965. 130p. 18s.

Features of nuclear reactions produced by nucleons with energies greater than 100 Mev are described. A detailed account is given of elastic and inelastic scattering and nucleon- and cluster-knockout reactions, whose mechanisms can be understood relatively simply. It is shown how these reactions demonstrate important systematic features of the structure of light nuclei. (M.J.T.)

12112 PROCEEDINGS OF THE NUCLEAR PHYSICS AND SOLID STATE PHYSICS SYMPOSIUM, CALCUTTA, FEBRUARY 8-13, 1965. [VOL. II]. NUCLEAR PHYSICS. Bombay, Atomic Energy Establishment, 1965. 371p. (CONF-650223(Vol.2)).

Separate abstracts were prepared for 58 of the 72 papers included. Eight other papers were previously abstracted for NSA (18: 44815; 19: 12071, 16950, 29296, 29376, 33291, 43298; and 20: 1201). The remaining papers (included only in summary form) deal with the magnetic moment of the 129-kev state in ^{171}Tm, beta-gamma directional correlations in ^{170}Tm, stripping reaction studies of Tl isotopes, internal conversion coefficients of E2 transitions in even-even nuclei, analysis of gamma pulse-height spectra, and measurement of pulsed beam currents in low-energy electron linear accelerators. (G.O.Y.)

For abstracts of individual papers see: 11156, 11514–11517, 11677, 12113–12160, and 12257–12260.

12113 BETA-DECAY AND NUCLEAR STRUCTURE. Steffen, Rolf M. (Tata Inst. of Fundamental Research, Bombay). pp 1-8 of Nuclear Physics and Solid State Physics Symposium, 1965. Nuclear Physics. Bombay, Atomic Energy Establishment, 1965.

The experimental values of the Fermi matrix elements for mixed allowed beta transitions in a number of isotopes were studied together with the anisotropy factor of the beta-gamma directional correlations. The results indicate that the nuclear structure mechanism which reduces the allowed matrix elements is also responsible for an appreciable reduction of the second-forbidden matrix elements. The experimental matrix elements for several first-forbidden beta transitions were compared with the predictions of the CVC theory. (D.C.W.)

12114 K-SELECTION RULE IN THE β-DECAY OF ^{172}Tm. Agarwal, Y. K.; Baba, C. V. K.; Bhattacharjee, S. K. (Tata Inst. of Fundamental Research, Bombay). pp. 9-12 of Nuclear Physics and Solid State Physics Symposium, 1965. Nuclear Physics. Bombay, Atomic Energy Establishment, 1965.

Beta-gamma directional correlation measurements (β_2-79 kev) were made at six beta energies. Analysis using both the shape correction factor and the beta-gamma directional correlation measurements showed that more than 90% of the beta decay takes place by a $\lambda = 2$ type of transition, verifying the K-selection rule. The experimental values of the B_{ij} matrix elements were also in excellent agreement with the ratios predicted by Alaga selection rules. (D.C.W.)

12115 THE MAGNETIC MOMENTS OF THE FIRST EXCITED STATES OF ^{127}I, ^{131}I, AND ^{149}Pm. Tandon, P. N.; Devare, H. G. (Tata Inst. of Fundamental Research, Bombay). pp 13-16 of Nuclear Physics and Solid State Physics Symposium, 1965. Nuclear Physics. Bombay, Atomic Energy Establishment, 1965.

The g factors for the first excited states of ^{127}I, ^{131}I, and ^{149}Pm were measured by the integral method. The experimental values for the magnetic moments were compared with theoretical values. The results indicate that the ^{149}Pm nucleus is quite deformed in its first excited state while it may have a very small deformation in its ground state. (D.C.W.)

12116 NUCLEAR FISSION AS A MARKOV PROCESS. Ramanna, R.; Subramanian, R.; Aiyer, Raju N. (Atomic Energy Establishment, Trombay, Bombay). pp 20-5 of Nuclear Physics and Solid State Physics Symposium, 1965. Nuclear Physics. Bombay, Atomic Energy Establishment, 1965.

It was previously shown that the mass distribution in fission can be obtained by assuming a random transfer of nucleons between the two sides of the fissioning nucleus and by assuming that the asymmetry in thermal fission is due to the shell configuration formed during the process. This theory was extended by treating fission as a Markov process. The transition matrix was obtained from experimental data and from ground-state properties of nuclei. By associating an energy transfer with each nucleon transfer, the deformation energy-mass curve was obtained from the transition matrix. The gap in this curve at the symmetry point was shown to be due to proton transfers. (D.C.W.)

12117 VARIATION OF FISSION THRESHOLD AND THE FISSION FRAGMENT MASS DISTRIBUTION. Nadkarni, D. M. (Atomic Energy Establishment, Trombay, Bombay). pp 33-8 of Nuclear Physics and Solid State Physics Symposium, 1965. Nuclear Physics. Bombay, Atomic Energy Establishment, 1965.

The mechanism of mass division in fission was studied on the basis of some measurements of the kinetic energy distribution and the correlation of mass asymmetry and angular anisotropy of fission fragments in the 4-Mev neutron fission of ^{235}U. (D.C.W.)

12118 A STUDY OF THE Ne(n,p) REACTION AT E_n = 14.1 Mev. Kondaiah, E.; Patell, R. K. (Tata Inst. of Fundamental Research, Bombay). pp 39-41 of Nuclear Physics and Solid State Physics Symposium, 1965. Nuclear Physics. Bombay, Atomic Energy Establishment, 1965.

The reaction Ne(n,p)F at 14.1 Mev was studied using nuclear emulsions placed at the center of an Allan-type camera which was filled with neon. The angular distribution for the energy range $3.3 \geq E_p \geq 7.9$ Mev showed a marked symmetry aroung the 90° center-of-mass angle, with strong forward and backward peaking, indicating the prevalence of a compound process. The cross section for $E_p \geq 3.3$ Mev was also estimated. (D.C.W.)

12119 ^{40}Ca(n,α)^{37}Ar ANGULAR DISTRIBUTION AT En = 4.7 Mev. Bharathi, S. M.; Raheja, U. T.; Lal, B.; Tiwari, P. N.; Kondaisah, E. (Tata Inst. of Fundamental Research, Bombay). pp 42-46 of Nuclear Physics and Solid State Physics Symposium, 1965. Nuclear Physics. Bombay, Atomic Energy Establishment, 1965.

A gas proportional counter telescope was used to study the energy and angular distribution of alpha particles in the reaction ^{40}Ca(n,α)^{37}Ar at 4.7 Mev. (G.O.Y.)

12120 ANALYSIS OF THE ANGULAR DISTRIBUTION FOR ^{16}O(n,α)^{13}C REACTION AT 14 Mev. Chatterjee, M. L. (Saha Inst. of Nuclear Physics, Calcutta). pp 47-53 of Nuclear Physics and Solid State Physics Symposium, 1965. Nuclear Physics. Bombay, Atomic Energy Establishment, 1965.

The angular distribution for the ^{16}O(n,α)^{13}C reaction at 14 Mev was studied using as a target a thin Mylar film positioned between two Ilford K2 plates. Backward peaking of the angular distribution in the region of 4-Mev excitation of ^{13}C indicates that the reaction is mainly governed by the heavy-particle stripping mechanism. Theoretical fits for the angular distribution were calculated using two different values for the orbital angular momentum of the captured neutron in the residual nucleus. (D.C.W.)

12121 FINE STRUCTURE IN THE MASS DISTRIBUTION OF THE FISSION PRODUCTS FROM THE FAST NEUTRON FISSION OF ^{235}U. Mathews, C. K. (Atomic Energy Establishment Trombay, Bombay). pp 54-5 of Nuclear Physics and Solid State Physics Symposium, 1965. Nuclear Physics. Bombay, Atomic Energy Establishment, 1965.

The mass spectrometric method was used to measure isotropic abundances of Ba, Ce, Cs, Nd, Sm, and Xe formed in the fast neutron fission of ^{238}U. Fine structure in the cumulative yields vs mass curve for the fast neutron fission of ^{238}U is discussed along with those for the slow neutron fission of ^{233}U and ^{235}U. It is concluded that while most of the fine structure arises from the variation in the neutron emission probabilities as a function of the mass fragment, some of it could be the result of shell effects in the fission process itself. The origin of this effect is discussed in terms of a modified Whetstone model. (G.O.Y.)

12122 SELF-CONSISTENT CALCULATIONS OF NUCLEAR STRUCTURE. Pal, M. K. (Saha Inst. of Nuclear Physics, Calcutta). pp 56-77 of Nuclear Physics and Solid State Physics Symposium, 1965. Nuclear Physics. Bombay, Atomic Energy Establishment, 1965.

The self-consistent calculations of nuclear structure according to the Hartree-Fock and the Hartree-Fock-Bogoliubov theories are discussed. (G.O.Y.)

12123 GROUND-STATE CORRELATIONS AND THE THEORY OF ONE- AND TWO-PHONON STATES. Raj, Ram; Gambhir, Y. K. (Saha Inst. of Nuclear Physics, Calcutta). pp 78-82 of Nuclear Physics and Solid State Physics Symposium, 1965. Nuclear Physics. Bombay, Atomic Energy Establishment, 1965.

The energies of the first 2^+ (one-phonon) states in Ni isotopes were calculated in the first random-phase approximation (RPA) using quadrupole-quadrupole and Gaussian forces for the residual interaction between quasi-particles. The effect of ground-state correlations was investigated. It was noted that the RPA is not entirely suitable for the description of two-phonon states. The use of the Tamm-Dancoff approximation in which all the four quasi-particle states are treated by simple shell model calculations was proposed. (D.C.W.)

12124 STRUCTURE OF Pr-ISOTOPES. Gambhir, Y. K.; Raj, Ram (Saha Inst. of Nuclear Physics, Calcutta). pp 83-7 of Nuclear Physics and Solid State Physics Symposium, 1965. Nuclear Physics. Bombay, Atomic Energy Establishment, 1965.

The energy level structure of odd (^{141}Pr and ^{143}Pr) and odd-odd (^{144}Pr) Pr isotopes was analyzed using the pairing model equations on taking into account the neutron-proton interaction. (D.C.W.)

12125 THE NILSSON AND THE SELF-CONSISTENT MODELS FOR NUCLEAR DEFORMATIONS. Gunye, M. R.; Gupta, S. Das (Tata Inst. of Fundamental Research, Bombay). pp 88-95 of Nuclear Physics and Solid State Physics Symposium, 1965. Nuclear Physics. Bombay, Atomic Energy Establishment, 1965.

The effects of explicit inclusion of the core on predictions of equilibrium deformations by the Nilsson model and the self-consistent model of Belyaev were studied. It was shown that the core must be taken into account explicitly in the Nilsson model and that the inclusion of the core is unimportant in the self-consistent model. (D.C.W.)

12126 CALCULATION OF EXCHANGE STRIPPING AMPLITUDES. Kumar, Anand (Saha Inst. of Nuclear Physics, Calcutta). pp 96-100 of Nuclear Physics and Solid State Physics Symposium, 1965. Nuclear Physics. Bombay, Atomic Energy Establishment, 1965.

A method was discussed for calculating the stripping amplitude of a deuteron in the reactions $^{9}Be(d,n)^{10}B$ and $^{16}O(n,d)^{15}N$ using the distorted wave Born approximation. (G.O.Y.)

12127 A DISTORTED WAVE BORN APPROXIMATION CALCULATION FOR (^{3}He,p) REACTIONS. Jain, B. K.; Sarma, N. (Atomic Energy Establishment, Trombay, Bombay). pp 101-5 of Nuclear Physics and Solid State Physics Symposium, 1965. Nuclear Physics. Bombay, Atomic Energy Establishment, 1965.

An analysis of the (^{3}He,p) reaction by the distorted-wave Born approximation is outlined. (D.C.W.)

12128 CONFIGURATION MIXING AND INDEPENDENT PARTICLE MOTION. Tewari, S. N. (Saha Inst. of Nuclear Physics, Calcutta). pp 107-12 of Nuclear Physics and Solid State Physics Symposium, 1965. Nuclear Physics. Bombay, Atomic Energy Establishment, 1965.

The density matrices for the J = 3 and J = 4 states of ^{22}Na were evaluated allowing for the mixing of all possible SU_3 symmetries. It was concluded that the intrinsic wave function is a single determinant to the order of 99%, supporting the applicability of the Hartree-Fock method in the 2s-1d shell. The configuration mixing, as measured by the impurity in the single determinantal character, indicates that the intrinsic state is not just the independent particle motion, but there is some residual correlation. The small band mixing indicates that the band-admixed wave function can be adequately described by taking the cranked wave function as the Hartree-Fock solution. (D.C.W.)

12129 IMAGINARY PART OF THE NUCLEAR OPTICAL POTENTIAL AT LOW ENERGIES. Khan, M. Z. Rahman; Ahmed, Israr (Aligharh Muslin Univ., India). pp 119-24 of Nuclear Physics and Solid State Physics Symposium, 1965. Nuclear Physics. Bombay, Atomic Energy Establishment, 1965.

The distribution of the imaginary part of the optical potential for nuclei between A = 55 and 95 was studied using a distorted-wave approximation in which square-well wave functions were taken as the zero-order solution. The results showed that S-wave strength function data for nuclei in this region can be fitted by a variety of surface-peaked distributions. The derivation of information on the radial distribution of the optical potential from low-energy data for individual nuclei was also considered. (D.C.W.)

12130 TRITON PARAMETERS WITH REALISTIC POTENTIALS. Bhakar, B. S.; Mitra, A. N. (Univ. of Delhi). pp 125-6 of Nuclear Physics and Solid State Physics Symposium, 1965. Nuclear Physics. Bombay, Atomic Energy Establishment, 1965.

The binding energy and the probabilities of various angular momentum states of the triton were calculated by regarding the triton as a three-body problem and using separable potentials. The effects of tensor forces were included. (D.C.W.)

12131 NUCLEON-NUCLEON CORRELATION IN L = 0 STATE. Khadkikar, S. B. (Tata Inst. of Fundamental Research, Bombay). pp 127-31 of Nuclear Physics and Solid State Physics Symposium, 1965. Nuclear Physics. Bombay, Atomic Energy Establishment, 1965.

The pairing hamiltonian with pairing interaction G_1 in the L = 0, S = 0, T = 1 state and G_2 in the L = 0, S = 1, T = 0 state was treated using the Bogoliubov variation method. (G.O.Y.)

12132 RECENT RESULTS IN FAST NEUTRON REACTIONS. Chatterjee, Aparesh (Calcutta Univ. Saha Inst. of Nuclear Physics, Calcutta). pp 132-42 of Nuclear Physics and Solid State Physics Symposium, 1965. Nuclear Physics. Bombay, Atomic Energy Establishment, 1965.

Some recent experiments on fast-neutron reactions and scattering are reviewed, including structural effects observed in some of the experiments. (D.C.W.)

12133 SYSTEMATIC MEASUREMENTS OF (n,p) CROSS SECTIONS AT 14.8 Mev. Mitra, B.; Ghose, A. M. (Bose Inst., Calcutta). pp 145-9 of Nuclear Physics and Solid State Physics Symposium, 1965. Nuclear Physics. Bombay, Atomic Energy Establishment, 1965.

The cross sections of (n,p) reactions on ^{27}Al, ^{37}Cl, ^{52}Cr, ^{19}F, ^{16}O, ^{28}Si, ^{23}Na, and ^{51}V at 14.8 Mev were determined. The elimination or reduction of the systematic errors associated with many previous determinations was stressed. (D.C.W.)

12134 CROSS SECTION OF THE REACTION $^{31}P(n,2n)^{30}P$ WITH NEUTRONS OF 14.8 Mev ENERGY. Mitra, B.; Chatterjee, Arun; Ghose, A. M. (Bose Inst., Calcutta). pp 150-3 of Nuclear Physics and Solid State Physics Symposium, 1965. Nuclear Physics. Bombay, Atomic Energy Establishment, 1965.

The cross sections for the reactions $^{31}P(n,\alpha)^{28}Al$ and $^{31}P(n,2n)^{30}P$ at 14.8 Mev were determined in terms of the cross sections for the reactions $^{28}Si(n,p)^{28}Al$ and $^{63}Cu(n,2n)^{62}Cu$, respectively, by irradiating samples of Cu, P, and Si and counting the resultant activities. (D.C.W.)

12135 NEUTRONS ACTIVATION CROSS-SECTION AT 24 Kev II. Chaubey, A. K.; Sehgal, M. L. (Muslim Univ., Aligarh, India). pp 154-7 of Nuclear Physics and Solid State Physics Symposium, 1965. Nuclear Physics. Bombay, Atomic Energy Establishment, 1965.

Neutron activation cross sections at 24 kev were measured for ^{68}Zn, ^{69}Ga, ^{71}Ga, ^{80}Se, ^{79}Br, ^{81}Br, ^{103}Rh, ^{105}Pd, ^{110}Pd, ^{109}Ag, ^{113}In, ^{138}Ba, ^{141}Pr, ^{186}W, ^{185}Re, ^{187}Re, ^{193}Ir, ^{196}Pt; and ^{208}Pb. An Sb–Be photoneutron source was used for the measurement. Theoretical values were obtained using the expression given by R. Booth. In general, there is a good agreement between the experimental and theoretical values. It is found that at the neutron magic numbers, $\sigma_{exp}/\sigma_{theo}$ has a high value. (auth)

12136 LIFE-TIME AND ANGULAR CORRELATION MEASUREMENTS IN THE DECAY OF ^{117}Cd. Pandharipande, V. R.; Prasad, K. G.; Singru, R. M.; Sarma, R. P. (Tata Inst. of Fundamental Research, Bombay). pp 158-60 of Nuclear Physics and Solid State Physics Symposium, 1965. Nuclear Physics. Bombay, Atomic Energy Establishment, 1965.

The energy levels of ^{117}In were investigated by angular correlation measurements in the decay of ^{117}Cd. Parity and spin assignments were made for ^{117}In levels, and the half life of the 750-kev level was measured. (D.C.W.)

12137 LIFE-TIME AND ANGULAR CORRELATION MEASUREMENTS IN ^{199}Au. Prasad, K. G.; Sharma, R. P.; Thosar, B. V. (Tata Inst. of Fundamental Research, Bombay). pp 161-4 of Nuclear Physics and Solid State Physics Symposium, 1965. Nuclear Physics. Bombay, Atomic Energy Establishment, 1965.

The energy levels of ^{199}Au were investigated by angular correlation measurements in the decay of 30-min ^{199}Pt. The half life of the first excited state of ^{199}Au was measured, and level spin and parity assignments were made. Transition multipolarities were also studied. (D.C.W.)

12138 A MAGNETIC COOLING SET-UP FOR STUDIES WITH ORIENTED NUCLEI. Chandra, Girish; Pandharipande, V. R. (Tata Inst. of Fundamental Research, Bombay). pp 165-7 of Nuclear Physics and Solid State Physics Symposium, 1965. Nuclear Physics. Bombay, Atomic Energy Establishment, 1965.

A helium cryostat is described with which a final temperature of 0.011°K is obtained by adiabatic demagnetization of the paramagnetic salt chrome potassium alum. Preliminary results obtained in the polarization of ^{60}Co nuclei in a single crystal of Co using this system are summarized. (D.C.W.)

12139 BETA-GAMMA DIRECTIONAL CORRELATION IN ^{147}Nd. Rao, V. Sehagiri; Lakshminarayana, V. (Andhra Univ., Waltair, India). pp 169-73 of Nuclear Physics and Solid State Physics Symposium, 1965. Nuclear Physics. Bombay, Atomic Energy Establishment, 1965.

Beta-gamma correlations (350 kev-531 kev and 790 kev-91 kev) for the first-forbidden ($\frac{5}{2}^- - \frac{5}{2}^+$) transitions in the decay of ^{147}Nd were studied. (D.C.W.)

12140 GAMMA-GAMMA DIRECTIONAL CORRELATION IN ^{123}Te. Gupta, S. L.; Bajaj, M. M.; Saha, N. K. (Univ. of Delhi). pp 174-7 of Nuclear Physics and Solid State Physics Symposium, 1965. Nuclear Physics. Bombay, Atomic Energy Establishment, 1965.

The ratio E2/M1 for the 159-kev transition in the decay of ^{123m}Te was studied by gamma-gamma directional correlation measurements on the 89 kev−159 kev cascade. The E2 transition lifetime obtained from the results was compared with values obtained from electron-gamma correlations, L-subshell ratios, and Coulomb excitation. (D.C.W.)

12141 STUDY OF ^{37}Cl(p,n)^{37}Ar REACTION MECHANISM. Iyengar, K. V. K.; Gupta, S. K.; Lal, B.; Kondaish, E. (Tata Inst. of Fundamental Research, Bombay). pp 184-8 of Nuclear Physics and Solid State Physics Symposium, 1965. Nuclear Physics. Bombay, Atomic Energy Establishment, 1965.

The excitation function for the production of 1.42-Mev gamma rays in the ^{37}Cl(p,n′γ)^{37}Ar was measured in the energy range from 3.2 to 4.8 Mev, and the angular distribution of the neutron group to the ground state of ^{37}Ar was measured at 5.1, 5.3, and 5.5 Mev. The angular distributions were least squares fitted to a Legendre polynomial series. The results indicate the excitation of mixed parity states and the inapplicability of the statistical assumption for the ^{38}Ar compound nucleus at the excitation reached in the experiment. Evidence for the contribution of some type of direct interaction to the reaction yield was also noted. (D.C.W.)

12142 A STUDY OF NUCLEAR REACTIONS RESULTING FROM PROTON BOMBARDMENT OF ^{27}Al. John, Joseph; Kerekatte, S. S.; Mehta, M. K. (Atomic Energy Establishment, Trombay, Bombay). pp 194-8 of Nuclear Physics and Solid State Physics Symposium, 1965. Nuclear Physics. Bombay, Atomic Energy Establishment, 1965.

The excitation functions for one alpha group from the ^{27}Al(p,α)^{24}Mg reaction and for two proton groups in proton scattering by ^{27}Al were measured from 4 to 5.5 Mev. In many cases, a "resonance" was observed in all the channels. An attempt was made to determine qualitatively whether these are real resonances or Ericson fluctuations. Angular distributions for the (p,α) reaction were measured at six prominent resonances; the observed lack of symmetry about 90° may imply levels of opposite parity if these are resonances. (D.C.W.)

12143 STUDY OF ^{19}F(α,n)^{22}Na REACTION USING A 4π NEUTRON COUNTER. Sekharan, K. K.; Mehta, M. K.; Divatia, A. S. (Atomic Energy Establishment, Trombay, Bombay). pp 199-202 of Nuclear Physics and Solid State Physics Symposium, 1965. Nuclear Physics. Bombay, Atomic Energy Establishment, 1965.

The excitation function of the ^{19}F(α,n)^{22}Na reaction was measured from 2.4 to 5.5 Mev using a 4π neutron counter that consisted of twelve $^{10}BF_3$ counters embedded in a paraffin block. (D.C.W.)

12144 A STUDY OF THE LEVELS OF ^{44}Ti. Betigeri, M. G.; Sarma, N. (Atomic Energy Establishment, Trombay, Bombay). pp 203-8 of Nuclear Physics and Solid State Physics Symposium, 1965. Nuclear Physics. Bombay, Atomic Energy Establishment, 1965.

An attempt was initiated to investigate the energy levels of ^{44}Ti by alpha scattering on ^{40}Ca. Spectra were measured at incident particle energies of 3.5 to 5.5 Mev, and an excitation function for alpha elastic scattering over this energy range was calculated. The resonance behavior of the excitation curve indicated that the data must be analyzed in terms of compound nucleus theory. The development of a computer program for determining the parity and spin assignments of ^{44}Ti energy levels by analysis of the data was begun. (D.C.W)

12145 ENERGY LEVELS OF ^{111}Ag. Pandharipande, V. R.; Singru, R. M.; Sharma, R. P. (Tata Inst. of Fundamental Research, Bombay). pp 211-16 of Nuclear Physics and Solid State Physics Symposium, 1965. Nuclear Physics. Bombay, Atomic Energy Establishment, 1965.

The energy levels of ^{111}Ag were investigated by beta-gamma and gamma-gamma coincidence measurements on the decay of ^{111}Pd and ^{111m}Pd. The relative intensities of the beta transitions were calculated from the gamma intensities. Spin and parity assignments were made for the ^{111}Ag energy levels. (D.C.W.)

12146 ON THE STRUCTURE OF 1.86 and 3.22 Mev STATES OF ^{88}Sr. Shastry, S. (Saha Inst. of Nuclear Physics, Calcutta). pp 222-6 of Nuclear Physics and Solid State Physics Symposium, 1965. Nuclear Physics. Bombay, Atomic Energy Establishment, 1965.

The energy level structure of ^{88}Sr was studied considering only proton excitation and four types of interaction. Level energies, transition energies, and transition probabilities were calculated. The E2-M1 mixing for the transition from the 3.22-Mev (2^+) level to the 1.86-Mev (2^+) level was obtained, together with the E2 transition probability for the transition from the 1.86-Mev level to the 0^+ ground state. (D.C.W.)

12147 STUDIES ON THE LEVEL WIDTHS OF SOME 2^+ STATES. Raju, P. S.; Prasad, A. Durga; Jnanananda, Swami (Andhra Univ., Waltair, India). pp 238-45 of Nuclear Physics and Solid State Physics Symposium, 1965. Nuclear Physics. Bombay, Atomic Energy Establishment, 1965.

The determination of the widths of the 2^+ states of ^{56}Co, ^{46}Ti, and ^{192}Ir by measurement of the cross sections for resonance scattering of gamma rays is analyzed, and an experimental study on ^{46}Ti is summarized. The experimental and theoretical results for ^{46}Ti are compared. (D.C.W.)

12148 DECAY OF ^{183}Hf AND NUCLEAR LEVELS OF ^{183}Ta. Bakhru, H.; Mukherjee, S. K. (Saha Inst. of Nuclear Physics, Calcutta). pp 246-50 of Nuclear Physics and Solid State Physics Symposium, 1965. Nuclear Physics. Bombay, Atomic Energy Establishment, 1965.

The decay of ^{183}Hf and ^{183m}Hf was studied experimentally. On the basis of the results, a decay scheme is proposed for ^{183}Hf. (D.C.W.)

12149 THE ISOTOPE ^{162}Tb AND ITS DECAY CHARACTERISTICS. Bakhru, H.; Mukherjee, S. K. (Saha Inst. of Nuclear Physics, Calcutta). pp 251-5 of Nuclear Physics and Solid State Physics Symposium, 1965. Nuclear Physics. Bombay, Atomic Energy Establishment, 1965.

The decay of ^{162}Tb was investigated through the reactions ^{165}Ho(n,α)^{162}Tb and ^{162}Dy(n,p)^{162}Tb. A value for the half life was obtained. Beta and gamma spectra were measured, as well as beta-gamma and gamma-gamma coincidences. A delay scheme is proposed for ^{162}Tb. (D.C.W.)

12150 "GAMMA RAY ANGULAR CORRELATION STUDIES IN NUCLEAR REACTIONS." Eswaran, M. A.

(Atomic Energy Establishment, Trombay, Bombay). pp 256-77 of Nuclear Physics and Solid State Physics Symposium, 1965. Nuclear Physics. Bombay, Atomic Energy Establishment, 1965.

The study of nuclear energy levels excited in nuclear reactions by a triple correlation method and by a method in which the gamma angular correlation is measured in coincidence with the outgoing particle is discussed. Applications of the techniques to the study of ^{22}Ne and ^{20}Ne levels from the reactions ^{19}F(α,p)^{22}Ne and ^{12}C(C-12,α)^{20}Ne, respectively, are summarized. (D.C.W.)

12151 ON THE HALF LIFE MEASUREMENT OF THE 273 kev LEVEL OF ^{196}Au. Sethi, B.; Mukherjee, S. K. (Saha Inst. of Nuclear Physics, Calcutta). pp 278-81 of Nuclear Physics and Solid State Physics Symposium, 1965. Nuclear Physics. Bombay, Atomic Energy Establishment, 1965.

The half life of the 273-kev level of ^{196}Au was measured using a fast-slow triple coincidence technique. (G.O.Y.)

12152 DECAY OF ^{98}Nb. Gujarathi, S. C.; Mukherjee, S. K. (Saha Inst. of Nuclear Physics, Calcutta). pp 282-6 of Nuclear Physics and Solid State Physics Symposium, 1965. Nuclear Physics. Bombay, Atomic Energy Establishment, 1965.

The decay of short-lived ^{98}Nb was investigated. Half lives of 1.6 and 51 min were measured. Beta and gamma spectra were obtained, and beta-beta and gamma-gamma coincidence measurements were performed as well. A decay scheme is proposed for ^{98}Nb. (D.C.W.)

12153 THE DECAY OF ^{133}Ba. Mangal, P. C.; Sud, S. P. (Panjab Univ., Chandigarh, India). pp 287-91 of Nuclear Physics and Solid State Physics Symposium, 1965. Nuclear Physics. Bombay, Atomic Energy Establishment, 1965.

The decay of ^{133}Ba was investigated using a sum coincidence technique. The relative intensities of the 54- and 276-kev gamma rays were obtained. (D.C.W.)

12154 NUCLEAR STRUCTURE EFFECTS IN THE DECAY OF ^{141}Ce. Brahmavar, S. M. (Panjab Univ., Chandigarh, India); Murthy, A. S. Venkatesha. pp 292-5 of Nuclear Physics and Solid State Physics Symposium, 1965. Nuclear Physics. Bombay, Atomic Energy Establishment, 1965.

The 1-forbidden (M1) transition in the decay of ^{141}Ce was analyzed for nuclear structure effects. (G.O.Y.)

12155 CONFIGURATION MIXING EFFECTS IN SHELL MODEL NUCLEI. Gupta, Raj K. (Panjab Univ., Chandigarh, India). pp 325-30 of Nuclear Physics and Solid State Physics Symposium, 1965. Nuclear Physics. Bombay, Atomic Energy Establishment, 1965.

The energy level structure of ^{14}C was analyzed treating ^{12}C as the core and using a central two-body interaction of the Gaussian type. Configuration assignments were made for the energy levels of ^{14}C. (D.C.W.)

12156 ROTATIONAL BANDS IN ^{82}Kr. Bindal, P. K.; Gupta, Raj K.; Sood, P. C. (Panjab Univ., Chandigarh, India). pp 331-4 of Nuclear Physics and Solid State Physics Symposium, 1965. Nuclear Physics. Bombay, Atomic Energy Establishment, 1965.

The energy level structure of ^{82}Kr was analyzed. Evidence for the K = 2 gamma vibrational band, as well as a ground-state K = 0 rotational band, was obtained. (D.C.W.)

12157 SHELL MODEL CALCULATIONS FOR LEVELS IN ^{91}Nb. Sharma, S. D.; Gupta, Raj K.; Sood, P. C. (Panjab Univ., Chandigarh, India). pp 335-9 of Nuclear Physics and Solid State Physics Symposium, 1965. Nuclear Physics. Bombay, Atomic Energy Establishment, 1965.

The energy level structure of ^{91}Nb was studied using the jj-coupling model. Configuration-mixing effects were not taken into account. Spin the parity assignment were made and the theoretical results were compared with experimental observations. (D.C.W.)

12158 ALPHA-DECAY OF ^{241}Am. Rao, M. Rama (Saha Inst. of Nuclear Physics, Calcutta). pp 340-1 of Nuclear Physics and Solid State Physics Symposium, 1965. Nuclear Physics. Bombay, Atomic Energy Establishment, 1965.

The alpha decay of ^{241}Am was investigated using a low-pressure expansion cloud chamber. The alpha tracks were photographed in a stereo arrangement, and range and energy measurements were made after stereo projection of the photographs. The existence of a 226-kev level in ^{237}Np was also verified. (D.C.W.)

12159 CROSS SECTION MEASUREMENTS OF (p,p'γ) RADIATIONS FROM ^{60}Ni AND ^{62}Ni. Trehan, P. N.; Singhal, N. C. (Punjab Univ., Chandigarh, India). pp 342-7 of Nuclear Physics and Solid State Physics Symposium, 1965. Nuclear Physics. Bombay, Atomic Energy Establishment, 1965.

The gamma yields in proton inelastic scattering by ^{60}Ni and ^{62}Ni at 3.4 to 5.0 Mev were measured. The cross sections for the production of various gamma rays were calculated from the yields. The experimental cross sections for the excitation of various energy levels were compared with theoretical predictions. It was concluded that the 2.30-Mev level of ^{62}Ni is a 2^+ state. (D.C.W.)

12160 "INELASTIC NEUTRON SCATTERING CROSS-SECTIONS IN ^{115}In." Singhal, N. C.; Trehan, P. N. (Panjab Univ., Chandigarh, India). pp 348-52 of Nuclear Physics and Solid State Physics Symposium, 1965. Nuclear Physics. Bombay, Atomic Energy Establishment, 1965.

The cross section for neutron inelastic scattering by ^{115}In was calculated by the method of Feshbach and Hauser using transmission coefficients from the diffused surface potential of Campbell. The theoretical results were compared with some experimental data. On the basis of this comparison, the spin assignments of the 1125- and 1290-kev levels of ^{115}In were studied. (D.C.W.)

Plasma Physics and Thermonuclear Processes

See *also* Fluid Physics and Thermodynamics

12161 (65RL-3940E) SUSTAINED MAGNETIC FIELD THETA PINCH. Weinrich, M.; Westendorp, W. F. (Research Lab., General Electric Co., Schenectady, N. Y.). Apr. 1965. 35p.

The containment of a high-temperature plasma may best be studied in a magnetic field of duration long compared to the life of the plasma. By momentarily suppressing and reversing a low-frequency magnetic field by a highly damped high-frequency field, such a sustained magnetic field may be created. It first produces the high-temperature plasma by θ-pinch action and then contains it for a time limited only by the plasma behavior. Two systems are described with their experimental results. The first has two coils and the two fields form an unsatisfactory superposition of low and high frequency. The second uses a thin-wall coil carrying both low- and high-frequency currents. The fields are better superposed, but streak camera pictures show plasma turbulence that is ascribed to trapped negative fields. A new installation that is now going into operation has a larger stored energy (150 kj) and special circuitry to eliminate field reversal during the preionization interval. This equipment should make it possible to study sustained field θ-pinch operation under conditions that more closely approximate those which have been found to produce quasi-stable, high-temperature plasmas in conventional θ-pinch equipment. (auth)

12162 (65RL-3998E) THEORY OF ION DETECTION FROM A PLASMA IMBEDDED IN A MAGNETIC FIELD. Kilb, R. W. (Research Lab., General Electric Co., Schenectady, N. Y.). July 1965. 14p.

A detailed analysis is made to relate the ion detection rate of an external detector to the ion distribution in a plasma imbedded in a magnetic field. The detection rate is related to the ion velocity distribution function at the surface of the plasma, and to the injection rate into the

velocity phase space loss cone throughout the plasma volume. A rough estimate of the injection rate is found for a classical mirror distribution of large loss-cone angle and low-collision rate. Computations of the ion paths from the plasma surface to the detector entrance hole are made to determine certain parameters needed to interpret a specific θ-pinch experiment. (auth)

12163 (AD-625424) SECOND QUARTERLY PROGRESS REPORT ON PLASMA RESEARCH, 1 APRIL-30 JUNE 1965. (California Univ., Berkeley. Electronics Research Lab.). Contract AF33(615)-1078. 63p. CFSTI $3.00 cy, $0.75 mn.

The heating and stability of plasma in a magnetic mirror machine was investigated, together with the use of laser beams in plasma diagnostics. A computer model for studying the plasma interchange instability was developed; and cyclotron wave propagation in plasma was studied theoretically, together with the nonlinear interaction of an electron with an electromagnetic wave and instabilities of centrifugally-electrostatically focused flow. A method of designing coils for a mirror-quadrupole cusp-type magnetic field was also developed. (D.C.W.)

12164 (ARL-65-129) TIME-SPACE RESOLUTION OF B-FIELDS IN THETA-PINCH PLASMA BY FARADAY ROTATION OF INFRARED MASER RADIATION. Craig, J. P.; Gribble, R. F.; Dougal, A. A. (Texas Univ., Austin). June 1965. Contract AF33(657)-11073. 118p. CFSTI $4.00 cy, $0.75 mn.

A method for experimentally determining the magnetic flux density B as a function of time and space in a dense, extreme temperature, highly dynamic, deuterium plasma was developed. The method employed the 3.39 μ infrared radiation from a He-Ne gas maser as a probe. The plasma electron density and the Faraday rotation of the plane of polarization of the maser beam which propagated through the plasma were measured separately. These two measurements and the laws of propagation of electromagnetic waves in a magnetized plasma were used to deduce the magnetic field B in the plasma. The experimental procedure and instruments are described in some detail. The method was applied to a θ-pinch plasma source. The magnetic field B was measured as a function of time and space with the bias field parallel to the main compression field. (M.O.W.)

12165 (ARL-65-135) INFRARED MASER INTERFEROMETRY FOR TIME AND SPACE RESOLUTION OF ELECTRON DENSITY IN HIGH TEMPERATURE PLASMAS. Gribble, R. F.; Craig, J. P.; Dougal, A. A. (Texas Univ., Austin). July 1965. Contract AF33(657)-11073. 122p. CFSTI $4.00 cy, $0.50 mn.

A 3.39 μ He-Ne maser excited infrared interferometer was utilized for the investigation of time and space resolved electron density in a high temperature, dense plasma formed in the "theta-pinch" geometry. The dense, high temperature plasma is generated in four stages including 16 Mc, 2 Kw pulsed r-f for initial gas breakdown; 1.5 Mc, 100 Mw super high power r-f preheating in the presence of a slowly rising bias magnetic field; and fast magnetic compression in 3.5 μs to a maximum of 72 kG. (M.O.W.)

12166 (CONF-651126-1) HEATING OF VACUUM-WALL BY BREMSSTRAHLUNG RADIATION IN A PULSED THERMONUCLEAR REACTOR. Dean, Stephen O. (Division of Research (AEC), Washington, D. C.). Nov. 22, 1965. 21p. Dep. mn. CFSTI $1.00 cy, $0.50 mn.

From American Physical Society, 7th Annual Meeting of the Division of Plasma Physics, San Francisco.

Calculations for wall surface heating due to absorption of bremsstrahlung radiation in thermonuclear reactors are presented. The particular wall surfaces considered are copper and molybdenum. (M.O.W.)

12167 (COO-1233-24) THERMONUCLEAR PLASMA STUDIES. Quarterly Status Report No. 11. (Wisconsin Univ., Madison. Dept. of Physics). Oct. 31, 1965. Contract AT(11-1)-1233. 13p. Dep. mn; CFSTI $1.00 cy, $0.50 mn.

The development of multipole magnets, components, and instrumentation for thermonuclear plasma studies is reported. (T.F.H.)

12168 (JUL-280-PP) PLASMAEFFEKTE AN EINER IONISIERTEN HELIUMLINIE. (Plasma Effect in an Ionized Helium Line). Berg, H. F. (Kernforschungsanlage, Juelich (West Germany). Institut fuer Plasmaphysik). Aug. 1965. 26p. Dep. mn.

An attempt was made to observe a temperature- and/or density-dependent blue shift of the 4686-Å He II line. A T-tube was used as the plasma source, and the profiles were obtained in single shots using a multi-channel light guide apparatus. No shift was observed within the experimental accuracy of 0.3 Å. (D.C.W.)

12169 (JUL-322-PP) IONIZATION RATE AT HIGHER ELECTRON DENSITIES IN DC FIELDS MEASURED IN AN ELECTRODELESS DISCHARGE. Beerwald, H. (Kernforschungsanlage, Juelich (West Germany). Institut fuer Plasmaphysik). Nov. 1965. 9p. Dep. mn.

A method of measuring the ionization rates of weakly ionized gases in d-c electric fields at electron densities between 10^{11} and 10^{12} cm^{-3} is described in which the growth rate of the electron density is determined by microwave interferometry. Measurements on toroidal discharges in hydrogen and nitrogen are summarized. (D.C.W.)

12170 (LRP-18-65) THE ANOMALOUS SKIN EFFECT IN A PLASMA. Weibel, E. S. (Laboratoire de Recherches sur la Physique des Plasmas, Lausanne (Switzerland)). Nov. 1965. 30p. Dep. mn.

A semi-infinite plasma with a sharp boundary and extending to infinity is treated. The form of the kernel depends on the type of reflection which the electrons suffer at the surface, and on the unperturbed velocity distribution. It is assumed that the electrons are specularly reflected. An arbitrary velocity distribution is assumed for the derivation of the principle equations. The problem is solved explicitly for a Maxwellian distribution using the Boltzmann equation with a relaxation term and Maxwell's equations without displacement current. (J.F.P.)

12171 (MATT-270) INTERPRETATION OF ATOMIC HYDROGEN LIGHT IN THE C STELLARATOR. Hinnov, E.; Bishop, A. S.; Hofmann, F. W. (Princeton Univ., N. J. Plasma Physics Lab.). May 1964. Contract AT(30-1)-1238. 60p. Dep. mn. CFSTI $3.00 cy, $0.75 mn.

All dissociation processes of H_2 which are sufficiently rapid to be of importance in C-Stellarator discharges result in neutral atoms with kinetic energy $\gtrsim$0.5 ev. At these energies, the mean free path of the atoms with respect to ionization and excitation is considerably larger than the radius of the discharge, under typical conditions. Therefore, the observed atomic light must be produced by atoms returning into the discharge from the walls of the vacuum vessel (probably with kinetic energy corresponding to wall temperature). The time delay between production and ionization of atomic hydrogen appears to be influenced also by resonant charge exchange between the inflowing slow atoms and the plasma protons. These conclusions are at least in qualitative agreement with observed time behavior, and measured radial distribution of atomic and molecular hydrogen light. From quantitative measurements of atomic hydrogen light, it appears that a substantial fraction, and perhaps all, of the atoms produced in the discharge return as atoms. It is also deduced from these measurements that the entire power input can be satisfactorily accounted for in terms of the hydrogen ionization, radiation, heating, and charge exchange processes. (auth)

12172 (MATT-302) THE EFFECT OF WEAK COLLISIONS ON ION WAVES. Kulsrud, R.; Shen, C. S. (Princeton Univ., N. J. Plasma Physics Lab.). Oct. 1964. Contract AT(30-1)-1238. 28p. Dep. mn. CFSTI $2.00 cy, $0.50 mn.

The linearized Fokker-Planck equation is solved by an iteration method which assumes the collision term is one order higher than the other terms. It is solved for the case

of ion wave instabilities, where the unperturbed situation consists of a constant electric field, electrons with the Spitzer-Härm distribution, and ions with a Maxwellian distribution of much lower temperature. The effect of collisions on the critical current for instability is determined, and it is found that the electron ion collisions predominate and lower the critical current. The linearized Fokker-Planck equation is also solved for the case of ion waves in a cesium plasma. Here the electrons are taken as an isothermal fluid. The propagation and space damping constants obtained from the first root of the dispersion relation are determined for the situation where the ions have a large mass velocity relative to laboratory frame of reference. A comparison with the experiment of Motley and Wong is made. (auth)

12173 (MATT-315) COOLING SYSTEM FOR MODEL C STELLARATOR. Christie, Robert S. (Princeton Univ., N. J. Plasma Physics Lab.). Dec. 1964. Contract AT(30-1)-1238. 25p. Dep. mn. CFSTI $1.00 cy, $0.50 mn.

The cooling of the C stellarator confining field coils requires a deionized water system of large volume, of consistently high specific resistance, and one which operates well when subjected to widely fluctuating load changes. Some of the problems considered in the design of the system are outlined. The system is described in detail as is the control used. Some operating problems are discussed. (auth)

12174 (MPI-PAE/P1.6/65) A TOROIDAL DEVICE WITH MERIDIAN MAGNETIC CONFINING FIELD OF grad p·grad $\oint$ dl/B > 0. Eckhartt, O.; Gierke, G. v.; Grieger, G. (Max-Planck-Institut fuer Physik und Astrophysik, Munich (West Germany)). Mar. 1965. 72p. Dep. mn.

A toroidal plasma device is described in which are situated a number of equally spaced ring conductors. The currents in the ring conductors can be adjusted in several ways to satisfy the condition that the scalar product of grad p with grad $\oint$ dl/B > 0. The stability of plasma in this configuration is studied. (T.F.H.)

12175 (NASA-CR-348) CYCLOTRON WAVES IN A COLLISIONLESS PLASMA. Wharton, C. B.; Malmberg, J. H. (General Atomic, San Diego, Calif.). Dec. 1965. Contract NAS 7-275. 13p. (CONF-650836-1). CFSTI $1.00 cy, $0.50 mn.

From 7th International Conference on Phenomena in Ionized Gases, Beograd, Yugoslavia.

Experimental studies of plasma waves in a 2 meter long collisionless plasma column, over the frequency range 30 to 520 Mhz, are reported. Special attention is given to the frequencies neighboring the electron cyclotron frequency ω_b. At least three (and perhaps more) distinct waves having resonances at or near ω_b are found. Two waves lie above the cyclotron frequency. One has a velocity greater than that of light and is a forward wave, apparently an electromagnetic waveguide mode, perturbed by the plasma. The other is a slow, backward wave, having a propagation cutoff at the upper hybrid frequency $\omega_{uh} = (\omega_b^2 + \omega_p^2)^{1/2}$, with a dispersion curve resembling that of the C_{01} cyclotron wave. This wave is heavily damped in space, typically 10 to 20 dB per wavelength. The third wave is a slow forward wave, lying below ω_b and resembling a whistler. It is only moderately damped. The measured dispersion curves of these waves are presented, and their relation to the predictions of theory is discussed. (auth)

12176 (NASA-TN-D-3188) BALL LIGHTNING CHARACTERISTICS. Rayle, Warren D. (National Aeronautics and Space Administration, Cleveland, Ohio. Lewis Research Center). Jan. 1966. 39p. CFSTI $2.00 cy, $0.50 mn.

Surveys were conducted to obtain information about ball lightning occurrences. A comparison of the frequency of observation of ball lightning with that of ordinary lightning impact points reveals that ball lightning is not a particularly rare phenomenon. Contrary to widely accepted ideas, the occurrence of ball lightning may be nearly as frequent as that of ordinary cloud-to-ground strokes. Detailed descriptions of 112 ball lightning events were obtained. Correlation techniques applied to the set of descriptions failed to pick out any strong connection between factors such as brightness, size, duration, or color. This result, along with the reported constancy of appearance of the balls, makes it appear unlikely that they represent the slow dissipation of stored energy. Ball lightning diameter estimates follow a log normal distribution. Such a distribution also represents the quantity of charge in lightning strokes and was associated with the field intensities in sferics (electromagnetic disturbances) from thunderstorms. The similarity of these distributions, while certainly not conclusive, suggests that such quantities may be related. Two different categories of events are tentatively identified among those reported. In one the ball appears after a lightning stroke to ground and remains and ends near the ground. In the other the ball is first seen in midair and remains aloft, vanishing without noticeable disturbance. (auth)

12177 (NASA-TN-D-3199) BEHAVIOR OF A SINGLE-TURN MAGNETIC COIL UNDER DYNAMIC LOAD CONDITIONS. Williams, M. D.; Oertel, G. K. (National Aeronautics and Space Administration, Langley Station, Va. Langley Research Center). Jan. 1966. 13p. CFSTI $1.00 cy, $0.50 mn.

In a magnetic plasma compression experiment, a single-turn coil is subjected to magnetic pressure pulses. The energy developing the magnetic pressure pulses is stored in a 1-megajoule capacitor bank and delivered to the coil in a damped ringing electric discharge. The kinetic pressures which can be developed in the coil depend on the coil's ability to contain these pressure pulses and that, in turn, is determined by the coil's mechanical design. Previously, all mechanical designs were based on calculations performed on the assumption that the peak current (and hence magnetic pressure) existed in the coil at all times during the discharge. This approach has a self-contained but unknown safety factor. In actuality, the coil undergoes a dynamic response throughout the discharge and is able to contain higher peak magnetic pressures than those predicted by static stress calculations because of an inertia term which is included in the dynamic response but is neglected in the static response. The dynamic response was mathematically developed and the results were compared with experimental data from a scaled-down model of the larger experiment. (auth)

12178 (NP-15705) ION OSCILLATIONS IN A WEAKLY TURBULENT PLASMA. Ichikawa, Yoshi H. (Illinois Univ., Urbana. Coordinated Science Lab.). Nov. 1965. 35p. (R-271). CFSTI $2.00 cy, $0.50 mn.

Ion oscillations in a high temperature electron-ion plasma with high frequency turbulent fluctuations are investigated by generalizing the quasi-linear theory to a spatially inhomogeneous system. It is found that the feedback effect of the high frequency fluctuation on the low frequency oscillation in the system gives rise to a parametric growth of the ion acoustic mode even if the system has a stable velocity distribution with respect to the ion acoustic mode. (auth)

12179 (NP-15782) THE DIELECTRIC BEHAVIOUR OF A PLASMA AT CYCLOTRON RESONANCE. Rijnhuizen Report 65-25. Schram, D. C. (Stichting voor Fundamenteel Onderzoek der Materie, Jutphaas (Netherlands). Instituut voor Plasma-Fysica). Oct. 1965. 14p. Dep. mn.

An expression for the dielectric tensor $\underline{\underline{\epsilon}}$ of a plasma in a static magnetic field and a circularly polarized standing electromagnetic field, transverse to the static field is obtained. The relativistic mass increase is taken into account in the particle-motion equations leading to $\underline{\underline{\epsilon}}$, so eliminating the singularity at cyclotron resonance ($\omega = \Omega$) appearing in the non-relativistic expression $\epsilon_\perp = \epsilon_0 (1 - \omega_p^2/(\omega^2 - \omega\Omega))$. Also a few considerations about dissipation are given, indicating the importance of collisions and particle escape, particularly in high quality systems. (auth)

12180 (ORNL-P-1556) OBSERVATION OF A MIRROR-LIKE INSTABILITY IN A HOT ELECTRON PLASMA. Ard,

W. B.; Dandl, R. A.; Stetson, R. F. (Oak Ridge National Lab., Tenn.). Aug. 6, 1965. Contract W-7405-eng-26. 15p. (CONF-650806-6). Dep. mn. CFSTI $1.00 cy, $0.50 mn.

From 7th International Conference on Phenomena in Ionized Gases, Belgrade.

Two types of instabilities were observed in a hot electron plasma produced by electron-cyclotron heating in a magnetic mirror. One type results in radial loss of particles across magnetic field lines and appears to be due to the growth of flutes. The other results primarily in loss along magnetic field lines and appears to be due to the mirror instability. Both types are accompanied by r-f oscillations and result in the loss of ~10% of the energy stored in the plasma. (auth)

12181 (UCRL-14467-T) A MONTE CARLO STUDY OF A ONE-COMPONENT PLASMA. [PART] I. Brush, S. G.; Sahlin, H. L.; Teller, E. (Lawrence Radiation Lab., Univ. of California, Livermore). Sept. 28, 1965. Contract W-7405-eng-48. 66p. Dep. mn. CFSTI $3.00 cy, $0.75 mn.

A Monte Carlo study was made of a plasma of heavy ions immersed in a uniform neutralizing background. Systems containing from 32 to 500 particles, with periodic boundary conditions, were used. The results of the study are presented in terms of a dimensionless parameter $\Gamma = (4\pi n/3)^{\frac{1}{3}} [(Ze)^2/kT]$, where n is the ion density (particles per cubic centimeter), T is the temperature (°K), k is the Boltzmann constant, e is the electronic charge, and Z is the atomic number. Thermodynamic properties and pair distribution functions were obtained for values of Γ ranging from 0.05 to 100.0 from the canonical ensemble by the Monte Carlo (MC) method. Two different methods were used to determine the potential energy of a configuration. The first is the "minimum image convention" employed in many previous MC calculations. Each particle is allowed to interact only with each other particle in the basic cell, or with the nearest periodic image of each other particle if the image is closer. In the second method, the interaction of a particle with all the images of the other particles is taken into account by a technique similar to the Ewald procedure used to calculate lattice sums. Energies, and values of the pair distribution function are compared with predictions of various approximate theories for small Γ values. (M.O.W.)

12182 (UCRL-16631) PLASMA KINETIC EQUATIONS [Thesis]. Price, John C. (Lawrence Radiation Lab., Univ. of California, Berkeley). Dec. 20, 1965. Contract W-7405-eng-48. 241p. Dep. mn. CFSTI $6.00 cy, $2.25 mn.

A kinetic equation is derived for a homogeneous field free plasma. This equation effectively joins the theory for a stable system (the Lenard-Balescu equation) and that for an unstable system (the quasilinear equation), for it contains terms from each equation, plus a term rather similar to that of quasilinear theory, but depending only on the one particle distribution function. The derivation follows the formal methods of Dupree, except that the collision term is evaluated for finite time, rather than in the limit $t \to \infty$. The behavior of a large number of terms which appear to oscillate in time is obtained by analytic continuation of various integrals in a manner similar to that used by Landau. It is shown that the kinetic equation satisfies the conservation laws, leads to an H theorem, and correctly reduces to the Lenard-Balescu equation in the asymptotic (long time) limit. The equation is generalized to include the effect of a uniform magnetic field. In a different calculation a collision term is obtained valid to order $1/\ln\Lambda$ for small amplitude waves in a uniform plasma. This result generalizes the ordinary Fokker-Planck equation from the domain $0 \leq \omega \ll \omega_p$, $0 \leq k \ll k_d$ to the domain $0 \leq \omega \ll \Lambda\omega_p$, $0 \leq k \gtrsim k_d$. It is shown that the collisional correction to the behavior of small amplitude waves also appears in the description of fluctuations in a spatially uniform plasma. This correction applies to the kinetic equation described above, so that the collective effects arising from zeros of the dielectric function are affected by collisional damping as well as by Landau damping. (auth)

12183 (ORNL-tr-868) TURBULENT HEATING OF PLASMA BY A DIRECT-DISCHARGE CURRENT. Babykin, M. V.; Gavrin, P. O.; Zavoiskii, E. K.; Nedoseev, S. L.; Rudakov, L. I.; Skoryupin, V. A. (Institut Atomnoi Energii, Gosudarstvennyi Komitet po Ispol'zovaniyu Atomnoi Energii SSSR, Moscow). Translated from paper No. CN-21/154 presented at the Conference on Plasma Physics and Controlled Thermonuclear Research, Culham, England, September 6–10, 1965. 17p. Dep. mn. CFSTI $1.00 cy, $0.50 mn. JCL $1.60 fs, $0.80 mf.

The results of investigations to explain the efficiency of utilization of current instabilities for the heating of plasma (turbulent heating) are presented. Only the turbulent heating of plasma by a current which flows along either a constant or a quasi-stationary magnetic field is considered. It was found that upon the passing of a current of up to 1 kamp/cm^2 along the magnetic field of a mirror trap, which was filled with plasma having a density of from 10^{12} to 10^{13} cm^{-3}, an anomalous resistance was observed. The shapes of the oscillograms of current and noise from the plasma give evidence that the anomalous resistance is connected to a current instability in the plasma. Also the measurement of plasma pressure using the diamagnetic effect shows that an appreciable part of the energy which was stored in the capacitor band remains in the plasma after the turbulent heating. These experimental results can be interpreted on the basis of a nonlinear theory of current instability in a plasma. (J.F.P.)

12184 TRANSIENT AND OSCILLATING SOLUTION OF BOLTZMANN-VLASOV EQUATION IN LINEARIZED PLASMA. Turski, A. J. (Monash Univ., Australia). Ann. Phys., 35: 240-9(Nov. 1965).

The linearized Boltzmann-Vlasov and Poisson equations for a one-dimensional plasma are considered. A Volterra integral equation of convolution type is obtained which is equivalent to the initial value problem for the linearized equations. In order to obtain explicit solutions of Volterra's equation, Lorentz and Maxwell velocity distribution functions of electrons are taken into account. A general class of initial disturbing functions is considered and solutions consisting of an oscillating part, as obtained by Landau, and a transient remainder, which depends on both the initial disturbing function and time are obtained. Asymptotic expansions of this transient remainder and hence the dependence on time for certain initial disturbances, may be obtained, e.g., for a disturbance function vanishing for electron speeds less than some constant α the oscillations tend to zero exponentially while the transient remainder tends to zero as some reciprocal power of time. (auth)

12185 DAMPING AT THE LOWER HYBRID RESONANCE IN A WARM PARTIALLY IONIZED PLASMA. Oakes, M. E.; Schlueter, H. (Univ. of Texas, Austin). Ann. Phys., 35: 396-409(Dec. 1965). (TID-22064).

The refractive index of a plasma in the vicinity of the hybrid ion-electron resonance is determined within a three-fluid model including collision and pressure terms. The importance of collisions with neutrals in suppressing pressure effects is demonstrated for conditions such as those encountered in experiments recently performed by Ransom and Schluter in r-f discharges at the hybrid ion-electron resonance. Refractive indices are given which indicate the transition from the pressure-dominated case to the collision-dominated case. (auth)

12186 ION TEMPERATURE MEASUREMENT OF A STREAMING He PLASMA BY A DOUBLE PROBE METHOD. Kawashima, Nobuki (Japan Atomic Energy Research Inst., Ibaraki). Appl. Phys. Lett., 7: 324-5(Dec. 15, 1965).

In experiments on double probe characteristics where the line passing through the tips of the electrodes of the double probe is either parallel or perpendicular to the plasma stream, it was found that the effect of the shadow of the upstream electrode on the downstream one was significant. The reduction ratio of the ion saturation current for the downstream electrode to that for the upstream electrode was calculated. From that ratio, the ion temper-

ature perpendicular to the plasma stream can be estimated when the stream velocity is known. The method is expected to be useful for ion temperature determination in rather low-density plasma streams as in the ionosphere. (A.G.W.)

12187 KINETIC EQUATION FOR A PLASMA IN A STRONG STATIC MAGNETIC FIELD. Sundaresan, M. K. (Carleton Univ., Ottawa). Can. J. Phys., 44: 247-54 (Jan. 1966).

A kinetic equation for a plasma in a strong static magnetic field B is derived without making any assumptions concerning the isotropy of the one- and two-particle distribution functions in the plane perpendicular to the field. The collision term in the equation is valid to all orders in 1/B and takes complete account of the effect of the strong magnetic field on the collisions. (auth)

12188 WAVE PROPAGATION IN MAGNETOPLASMAS. Sharma, S. R. (Univ. of Rajasthan, Jaipur, India). Can. J. Phys., 44: 255-64(Jan. 1966).

Wave propagation in a fully ionized unbounded magnetoplasma is considered, taking into account the momentum transfer and energy exchange due to collisions. Dispersion relations are examined for wave propagation along and perpendicular to the magnetic field. It is found that there is no additional damping due to temperature relaxation for pure transverse wave propagation. For longitudinal waves dispersion relations are presented which include damping due to temperature relaxation and momentum transfer due to collisions. (auth)

12189 A BEAM-HOT PLASMA INTERACTION AT VERY LOW FREQUENCY. Doucet, Henri (Ecole Polytechnique, Paris). Compt. Rend., 261: 2862-4(Oct. 11, 1965). (In French).

Since the macroscopic theory with scalar pressure takes into consideration the derivatives of the particles, the interaction between a beam of slow electrons and a hot plasma at very low frequency can be described. This theory seems to explain observations made on Cs discharges. (tr-auth)

12190 THEORETICAL INTERPRETATION OF THE EVOLUTION OF THE PLASMA CREATED BY FOCUSING OF A LASER BEAM IN AIR. Champetier, Jean-Louis (CEA, Villeneuve-Saint-Georges, France). Compt. Rend., 261: 3954-7(Nov. 15, 1965). (In French).

The ionized zone is formed by a detonation wave, followed by an expansion wave, a contact discontinuity, and a shock wave. The influence of lateral motion was studied. (tr-auth)

12191 MACROSCOPIC SPACE CHARGE FIELD IN DISTURBED QUASINEUTRAL PLASMA. Pekarek, L.; Masek, K. (Inst. of Physics, Prague). Czech. J. Phys., 15: 644-61(1965).

A method of calculation of the electric field intensity in a quasineutral plasma homogeneity of which is disturbed is found for the case when the problem can be formulated as one-dimensional. The general formula comprising the Ohm's law, ambipolar approximation and higher approximations of the space charge electric field intensity, expressed in terms of deviation n_+ in ion density and its derivatives, is found and the values of the errors of these approximations are derived. Numerical calculations for the sinusoidal as well as for the Gaussian form of the perturbation in the ion concentration are carried out. (auth)

12192 BEAM WIDTH OF TWO ANTENNA SYSTEMS FOR PLASMA DIAGNOSTICS. Datlov, J.; Musil, J.; Zacek, F. (Inst. of Plasma Physics, Prague). Czech. J. Phys., 15: 766-8(1965).

A comparison was made of beam-width measurements for two antenna systems, measuring a plasma column of a reflex discharge about 3λ in diameter within a Pyrex tube. The results are shown for the system consisting of two non-corrected horns and that consisting of two elliptic cylinders irradiated by small sectoral horns. Within the limits of experimental error, the phase shift measured was equal in both cases. Measurements also agreed well with the mean density determined by means of the Langmiur probe technique. (L.B.S.)

12193 ON THE THEORY OF PLASMA INSTABILITY IN AN OSCILLATING DISCHARGE. Vaclavik, J. (Inst. of Plasma Physics, Prague). Czech. J. Phys., 15: 832-7(1965).

The stability of plasma in an oscillating discharge is studied. Within the framework of linear theory, an analysis is given of several types of instabilities in a mixture of hot electrons and cold plasma, caused by the radial inhomogeneity of the density of the hot electrons. (auth)

12194 THE INVERTED ION MAGNETRON PRINCIPLE AND ITS USEFULNESS IN LABORATORY PLASMA PHYSICS AND COSMICAL ELECTRODYNAMICS. Datlov, J. (Inst. for Plasma Physics, Prague). Czech. J. Phys., 15: 858-9(1965).

A mechanism for, and properties of, inverted ion magnetron instabilities observed in studies on plasma rotation are briefly discussed. Applications of the inverted ion magnetron are noted, e.g., in devices of the Burnout type for achieving highly ionized plasma with hot ions accelerated by large electric field gradients. Analogies are made with gravitational mass spiral drift waves and other phenomena, such as radio emission bursts, origin of solar flares, and the origin of the cosmic magnetic field. (L.B.S.)

12195 ON THE STATIONARY STATE OF PLASMA IN A MAGNETOSTATIC AND h-f FIELD. Klima, R. (Inst. of Plasma Physics, Prague). Czech. J. Phys., 16: 16-29 (1966). (In Russian).

Assuming a certain conservativeness of motion of particles along induction lines, a solution is derived for the corresponding Vlasov equation. The electric field in quasineutral plasma is determined from relations for the concentration. The conservativeness of motion of a particle in a nonresonant h-f field is shown by calculating the effective potential. (auth)

12196 A STUDY OF THE RESONANCE CONDITIONS IN ACCELERATING CLUSTERS OF PLASMA IN AN EXTERNAL MAGNETIC FIELD. Jelen, J. (Czech Technical Univ., Podebrady). Czech. J. Phys., 16: 30-41 (1966).

The physical significance is investigated of the so-called "resonance conditions" in accelerating plasmatic clusters between parallel conductors in a strong transversal magnetic field. The problem of acceleration is generally formulated by the Lagrange and Hamiltonian functions and equations. It is shown that an external constant magnetic field does not supply energy during acceleration but only regulates the use of energy from a discharge condenser. The conditions, under which the parameters of the circuit can be found for optimum acceleration of the plasmatic cluster without a complete solution of the equations of motion, are studied. (auth)

12197 A NOTE ON THE INFLUENCE OF RESISTANCE ON THE RESONANCE CONDITIONS IN PLASMA ACCELERATION. Jelen, J.; Hynecek, J. (Czech Technical Univ., Podebrady). Czech. J. Phys., 16: 42-6(1966).

The influence of resistance on the "resonance conditions" in accelerating clusters of plasma of constant mass in an external magnetic field. The plasma structure is not investigated. The dependences of the optimum magnetic field B and the maximum possible cluster velocity on the damping constant δ are found. (auth)

12198 PLASMA INDUCTION ACCELERATOR WITH RADIAL MAGNETIC FIELD. Kracik, J.; Novak, B.; Hanitz, F. (Czech Technical Univ., Prague). Czech. J. Phys., 16: 56-8(1966).

A theoretical investigation was made of the possibility of accelerating plasmatic clusters or shock waves in plasma in a simple tube of circular cross section by an exciting coil with a radial magnetic field, for both pulse operation for constant B_γ and for continuous acceleration for high frequency changes of the exciting current and magnetic induction B_γ. (L.B.S.)

12199 CIRCULAR AUTOSTABLE PATH OF MAGNETOHYDRODYNAMIC PLASMA ACCELERATOR. Kracik, J. (Czech Technical Univ., Prague). Czech. J. Phys., 16: 58-60(1966).

An attempt is made to find an arrangement of a magnetohydrodynamic plasma accelerator whereby a circular and autostable path would be possible. An autostable circular path is considered as a path where the centrifugal force is balanced by a spontaneously produced centric magnetohydrodynamic force. (L.B.S.)

12200 A NEW METHOD OF TIME-SPACE DISPLAY OF WAVE PHENOMENA IN PLASMA. Stirand, O.; Krejci, V.; Laska, L. (Inst. of Physics, Prague). Czech. J. Phys., 16: 65-6(1966).

A new method of time-space display is briefly described for the investigation of complicated wave phenomena or transient processes in plasma. (L.B.S.)

12201 PARTICLE DISTRIBUTION IN THE VICINITY OF A CHARGED SPHERE IN A WEAKLY IONIZED RAREFIED PLASMA. Goryshnik, L. L.; Dyukalov, A. N. (Inst. of Radio Engineering, Academy of Sciences, USSR). Geomagn. Aeronomy (USSR) (Engl. Transl.), 5: 311-19(1965). Translated from Geomagn. Aeronomiya, 3: 401-12(1965).

A general study is made of the trajectories of charged particles in a centrally-symmetric electric field, using the effective surface potential energy introduced in the study. The boundaries of the region in phase space corresponding to bounded particle motion are found. The kinetic equation for the distribution function of finite (i.e., bounded) electrons in a weakly ionized plasma is examined. (auth)

12202 LABORATORY OBSERVATIONS OF A STABLE PLASMA TRAPPED IN A PERMANENT DIPOLAR MAGNETIC FIELD. Quinn, R. G.; Chang, C. C. (Catholic Univ. of America, Washington, D. C.). J. Geophys. Res., 71: 253-62(Jan. 1, 1966).

A method was devised to establish and maintain a stable plasma belt in the field of a permanent dipole magnet. The spherical magnet is made the cathode of a glow discharge, and it is found that a stable plasma belt forms. The effects of various neutral species and pressures are examined. The floating potential was measured at various discharge conditions and latitudes as a function of position. The density of the charged constituents can be varied by changing the applied potential. Evidence of electric and magnetic drifts in the equatorial plane are observed and discussed. The use of Langmuir probes presents a number of difficulties because of the presence of large drift velocities and lack of spatial resolution. The use of different techniques and larger magnets is suggested. The problems inherent in making geophysical comparisons are pointed out. Although exact models are impossible, certain features of the experiment may eventually prove useful in simulating geophysical phenomena. (auth)

12203 ION CYCLOTRON INSTABILITIES IN A BOUNDED BEAM-PLASMA SYSTEM. Hasegawa, Akira (Osaka Univ.). Jap. J. Appl. Phys., 5: 105-12(Jan. 1966).

Ion cyclotron instabilities in a bounded cold beam-plasma system are considered, with an electron beam injected parallel to an applied uniform magnetic field. The conditions and the growth rates of the instabilities of both of the electromagnetic and the electrostatic ion cyclotron waves due to their interactions with the electron beam are obtained. The surface current created by an azimuthal d-c spinning times the radial a-c displacement of the beam is found to have a significant role on the electromagnetic growth rate, while the presence of warm plasma electrons is found to be essential for the electrostatic instability. It is shown that if the direction of the d-c spinning of the beam is in the same sense as that of the plasma ion gyration, the electromagnetic instability is remarkably enhanced. (auth)

12204 TORCH STRUCTURE OF DRIFT INSTABILITY. Vlasov, M. A. JETP Lett. (USSR)(Eng. Transl.), 2: 189-91(Oct. 1, 1965).

Rotating torch structures were observed in a hydrogen discharge at a pressure of 10^{-3} torr and in a magnetic field of 730 gauss. Apparently, the torch is the result of the development of an initial density disturbance on the boundary of the arc column. An analysis of the experimental results indicates that the development of drift instability leads to the appearance of a relatively narrow torch along which the plasma escapes transversely to the field. (D.C.W.)

12205 CONVECTIVE INSTABILITY OF A PLASMA WHICH IS NOT UNIFORM ALONG THE MAGNETIC FIELD. Vdovin, V. L. JETP Lett. (USSR) (Engl. Transl.), 2: 232-5(Oct. 15, 1965).

It is shown that a weakly ionized plasma is subject to its own specific instability resulting from the presence of an axial density gradient. The theoretical description of the instability of a plasma which is not uniform along the magnetic field agrees well with the experimental data on diffusion in a sufficiently broad range of experiments. (G.O.Y.)

12206 ELECTRON HEATING IN THE TN-1 INSTALLATION. Blinov, P. I.; Gavrilov, B. I.; Zakatov, L. P.; Cheremnykh, P. A. JETP Lett. (USSR) (Engl. Transl.), 2: 250-2(Oct. 15, 1965).

An investigation of turbulent heating of a plasma in a magnetic mirror by means of an h-f shock circuit is summarized. (D.C.W.)

12207 ON THE THEORY OF THE SCATTERING OF MAGNETOHYDRODYNAMIC WAVES AT THE END OF A WAVEGUIDE. Kurilko, V. I. Magnit. Gidrodin., No. 3, 44-50(1965). (In Russian).

The problem of the scattering of a MHD wave by the open end of a semi-infinite plasma waveguide is examined, as applied to the case in which the end of the waveguide is covered by a conducting diaphragm. It is shown that in this case the problem of determining the Fourier component of the scattered field reduces to the solution of a system of two boundary-value problems for two unknown functions, which is equivalent to a Fredholm integral equation of the second kind, whose solution can be obtained numerically or, with a small parameter, in the analytic form. (auth)

12208 EXCITATION OF A MAGNETOHYDRODYNAMIC WAVEGUIDE BY A COAXIAL WAVEGUIDE. Kalmykova, S. S.; Kurilko, V. I. Magnit. Gidrodin., No. 3, 51-3(1965). (In Russian).

The problem of matching a cylindrical coaxial waveguide with a semi-infinite plasma waveguide serving as the continuation of the inner core of a coaxial cable with low frequencies ($\omega \ll \omega_{Ci}$, where ω_{Ci} is the ion Larmor frequency) is examined, assuming that the temperature of the plasma may be disregarded if its conductivity is sufficiently large. It is shown that the rigorous problem of finding the Fourier component of the scattered field reduces to the solution of a Fredholm integral equation of the second kind. This solution is derived by an iterative method on the assumption that $\delta = c/\omega_0 \ll b \ll \lambda$ (c is the velocity of light, ω_0 is the plasma frequency, b is the radius of the casing, λ is the wavelength in a vacuum). Analytic formulas for the coaxial-wave reflection factor and the amplitudes of the MHD waves excited in the plasma wave-guide are derived. The dependence of these variables on the constant magnetic field is clarified. It is shown that MHD waves can be effectively excited by a coaxial line only in the presence of sufficiently strong magnetic fields ($\epsilon_\perp - 1 \ll 1$), since otherwise, if the magnetic field is weak, the greater part of the energy of the coaxial wave is expended on exciting the surface plasma wave. (ATD)

12209 USE OF HIGHLY IONIZED PLASMA FOR FABRICATION OF A LASER. Gudzenko, L. I.; Kolesnikov, V. N.; Sobolev, N. N.; Shelepin, L. A. Magnit. Gidrodin., No. 3, 54-6(1965). (In Russian).

The sudden cooling of the free electrons of a highly ionized low-temperature plasma (a condition necessary for the attainment of laser action in such a medium) is discussed. Two methods are proposed: cooling the walls of the container, and the use of heavy particles (ions and neutral atoms of the plasma) to cool the free electrons.

The second method is discussed in detail. In utilizing heavy particles for cooling, two conditions must be satisfied: 1) The electron temperature must be significantly greater than the temperature of the heavy particles ($T_e \gg T$). The temperature T_e must be close to the temperature of the almost totally singly ionized gas, and the temperatures T, to the final cooling temperature of free electrons; and 2) the specific heat of the electrons must be significantly smaller than that of the heavy particles ($C_e \ll C$). The first condition can be realized by heating the gas by means of an electric field. The second condition can be fulfilled only when the electron density is small in comparison with the total density of the gas. This occurs at a practically total ionization of an easy-to-ionize compound of plasma which forms only a small percentage of the total density of a mixture of gases, or, in the case of gas consisting of one component, when the plasma is not ionized completely. In a plasma consisting of a mixture of gases, the hard-to-ionize components form the cooling system, the specific heat of which is high. In addition, the total density cannot be too high lest nonradiative transitions control the population of the discrete lower levels. It is shown that the various cooling methods used in magnetohydrodynamics could probably be used in developing a low-temperature highly ionized plasma laser. (ATD)

12210 ON AMPLIFICATION IN DECAYING PLASMA. Gudzenko, L. I.; Shelepin, L. A. Magnit. Gidrodin., No. 3, 57-60(1965). (In Russian).

The properties of non-equilibrium plasma as a medium amplifying the electromagnetic radiation at frequencies of its discrete spectrum are discussed. A qualitative analysis of three plasma decay stages corresponding to different degrees of ionization is given. It is assumed that the degree of ionization of plasma is essentially higher than its equilibrium value corresponding to average energy of free electrons. (auth)

12211 ROTATION OF LOW-IONIZED GAS IN HOMOPOLAR DEVICE WITH RADIAL MAGNETIC FIELD. Drobyshevskii, E. M.; Chekmarev, I. B. Magnit. Gidrodin., No. 3, 76-80(1965). (In Russian).

An azimuthal movement of glow discharge of plasma between two coaxial dielectric cylinders in crossed radial magnetic and axial electric fields is discussed. Due to nonuniformity of the magnetic field the electron temperature is a function of radius, and the necessity of applying a strong electric field causes the ionic component to gain energy of directional movement in the axis direction of the order 1 to 10 ev. Taking these effects into account the equations of diffusion and movement are solved numerically and the distribution profiles of charged particles concentration, current density and current intensity along the radius are computed. (auth)

12212 KINETIC THEORY OF ELECTROMAGNETIC WAVES IN A LIMITED PLASMA. Kondratenko, A. N. (Physical-Technical Inst., Academy of Sciences, Kharkov, USSR). Nucl. Fusion, 5: 267-71(Dec. 1965). (In Russian).

Propagation of electromagnetic surface waves in an infinite plasma layer is examined in kinetic approximation. The problem is solved with the Fourier method. The dispersion equation obtained is investigated for high-frequency oscillations in which the average thermal velocity of the electrons v_{Tc} and of the ions v_{Ti} is much smaller than the phase velocity of wave V_Φ; and for low-frequency oscillations (ion-acoustic waves) in which $v_{Tc} \gg V_\Phi \gg v_{Ti}$. (TCO)

12213 PLASMA EQUILIBRIUM IN A TOROIDAL CHAMBER WITH A TRAVELING MAGNETIC FIELD. Volkov, T. F. (Kurchatov Inst. of Atomic Energy, Moscow). Nucl. Fusion, 5: 272-5(Dec. 1965). (In Russian).

The displacement was found of the center of a plasma column in a toroidal chamber that is maintained in equilibrium by the average pressure of a high-frequency traveling magnetic field H and the d-c magnetic field $\mathcal{H}$ of the longitudinal surface currents. The traveling h-f magnetic field is created by passing d-c currents with specially selected phases through the annular conductors enveloping the chamber. It is assumed that these conductors do not affect the distribution of the d-c magnetic field, which is assumed to be the same as in a single ideally conducting toroid. The solution is performed in assuming that toroidality is small (expansion in powers with respect to 1/R; R is the large radius of the torus). The conditions for detachment of the column from the chamber walls in a quasi-static regime are evaluated. (TCO)

12214 CERENKOV ABSORPTION OF ALFVEN WAVES AND OF FAST MAGNETOACOUSTIC WAVES IN AN INHOMOGENEOUS PLASMA. Dolgopolov, V. V.; Stepanov, K. N. (Physical-Technical Inst., Academy of Sciences, Kharkov, USSR). Nucl. Fusion, 5: 276-8(Dec. 1965). (In Russian).

Cherenkov electron absorption of low-frequency electromagnetic waves in an inhomogeneous plasma cylinder was investigated. Formulas were obtained for the energy absorbed by plasma, and for the damping factor where there is no resonance layer. A sharp boundary leads to a strong absorption increase. For a resonance layer containing a point at which the radial wave number becomes infinite, a strong absorption increase occurs (if the phase velocity of the wave is the order of thermal electron velocity, then the damping rate is the same order as the frequency). The radial and axial components of the electric field of the wave then increase sharply in the resonance layer. The increase in absorption is caused by the axial component of the electric field. Formulas were derived for the electric field strength inside the resonance layer, for the high-frequency power that is absorbed by the layer; and for the width of the layer. (auth)

12215 PLASMA LOSSES IN A Q-DEVICE. D'Angelo, N.; Goeler, S. V. (Princeton Univ., N. J.). Nucl. Fusion, 5: 279-83(Dec. 1965).

Probe and microwave measurements support the view that the ordinary plasma of a Q-device is suitably described by the equilibrium model. An apparent discrepancy between Motley's results, giving considerable support to the equilibrium model, and those of Grieger and others appears to be resolved by consideration of probe losses. (auth)

12216 LONGITUDINAL DIELECTRIC CONSTANT OF THE CLASSICAL PLASMA. I. Coste, J. (Univ., Paris). Nucl. Fusion, 5: 284-92(Dec. 1965).

Starting from the work of Guernsey on the system of the two first equations of the BBGYK hierarchy, it is shown that an approximate solution of these equations may be found in the limit of high frequency or short wave length, and general expressions are derived for the longitudinal dielectric constant $\epsilon(k,w)$ of the plasma. Limiting cases are considered: zero frequency [equilibrium quantities are derived from $\epsilon(k,0)$]; and frequencies much higher than the inverse relaxation time. (auth)

12217 LONGITUDINAL DIELECTRIC CONSTANT OF THE CLASSICAL PLASMA. II. Coste, J. (Univ., Paris). Nucl. Fusion, 5: 293-8(Dec. 1965).

The contribution of electron-electron correlations to $\epsilon(k,\omega)$ is studied, by considering the case of a one-component plasma. This contribution is compared to that due to the electron-ion correlations. A resonance effect is found at $\omega = 2\omega_p$. From $\epsilon(k,\omega_p)$ a formula is derived for the damping of the plasma oscillations. (auth)

12218 NORMAL MODES OF PLASMA OSCILLATION. Trocheris, Michel (EURATOM-C.E.A., Fontenay-aux-Roses, France). Nucl. Fusion, 5: 299-314(Dec. 1965). (In French).

The problem of electrostatic waves in a uniform collisionless plasma is investigated in the linearized approximation. A new type of normal mode is introduced which can represent damped waves as well as unstable ones, thus preserving the continuity between both kinds of waves. This is possible by considering the distribution function as a linear functional, or as an analytic function defined for

complex values of the velocity. A complete system of such normal modes is formed. The spectrum consists of discrete eigenvalues corresponding to waves, either growing or damped, together with a continuum that may be chosen to have an imaginary part such that it corresponds to rapidly damped transients. An expansion formula is derived and the expansion given by Van Kampen and Case is recovered as a special case. This expansion is used to solve the equation for the distribution function and the relation to the solution by Laplace transformation is discussed. (auth)

12219 ELECTRICAL CONDUCTANCE OF A TURBULENT PLASMA. Petviashvili, V. I.; Ramazashvili, R. R.; Tsintsadze, N. L. (Academy of Sciences, Tbilisi, Georgian SSR). Nucl. Fusion, 5: 315-7(Dec. 1965). (In Russian).

The electrical conductance of a homogeneous, weakly turbulent magnetoactive plasma is investigated under the assumption that oscillation is possible. Under certain conditions the electrical conductance of such a plasma can be anomalously small. This phenomenon can be explained by an effective increase in the frequency of ion-electron collisions that is caused by collective particle interactions. Only low-frequency oscillations (in which both electrons and ions participate) give a significant contribution to turbulent-plasma resistance. A formula was found, through the turbulent oscillation spectrum, for the electrical conductance of the weakly-turbulent plasma. Comparison of the conductance with the anomalous diffusions across the magnetic field shows that they both contain the same quantity (determined by the oscillation spectrum), which can be interpreted as an effective collision frequency; hence the conclusion is drawn that this effective collision frequency will play the role of ordinary collisions in other macroscopic processes also. The effective collision frequency was evaluated for the Drummond-Rosenbluth instability, and with it the width of the weak shock wave in collisionless plasma was found. Also found was the formula for the effective collision frequency of an isotropic plasma. (auth)

12220 EFFECT OF AN ELECTRIC FIELD ON THE SPECTRUM OF OSCILLATIONS IN AN INHOMOGENEOUS PLASMA. Baikov, I. S.; Bogdankevich, L. S.; Rukhadze, A. A. (Lebedev Physical Inst., Moscow). Nucl. Fusion, 5: 318-25(Dec. 1965). (In Russian).

The effect of an inhomogeneous electric field on the spectrum of low-frequency oscillations of a spatially inhomogeneous plasma contained by a strong magnetic field is investigated in the approximation of geometrical optics. The curvature of the lines of force of the containing magnetic field is considered by introducing an effective gravitational field. The cases of a plane and a cylindrical geometry of the inhomogeneous plasma are discussed. Based on the kinetic equation with self-consistent field, expressions are obtained for the longitudinal dielectric permitivity characterizing oscillations derivable from a potential of the electromagnetic field in the plasma. Analysis of the oscillation spectra demonstrated a considerable influence of the inhomogeneous electric field on the low-frequency oscillations of the plasma for the case in which this field is comparable to or greater than the thermal field. (TCO)

12221 EFFECT OF A COLD-PLASMA COMPONENT ON THE STABILITY OF AN INHOMOGENEOUS HOT PLASMA. Baikov, I. S. (Lebedev Inst. of Physics, Moscow). Nucl. Fusion, 5: 326-9(Dec. 1965). (In Russian).

By applying geometrical optics, the effect of a volume component of cold plasma on the low-frequency oscillation spectrum and on the local stability conditions of an inhomogeneous hot plasma contained by a strong magnetic field is investigated. Allowance is made for the curvature of the lines of force of the containing magnetic field by introducing an effective gravitational field. The existence in such a system of a low-frequency oscillation branch is shown, that is "electron" sound, with a frequency proportional to the square root of the ratio of hot to cold plasma densities. For very low cold-plasma densities a hydrodynamic growth of long-wave and short-wave oscillations of the inhomogeneous plasma results from the excitation of an "electron-acoustic" oscillation branch by the gravitational drift of the ions. For higher cold-plasma densities a resonant growth of low-frequency plasma oscillations with frequencies approaching those of the diamagnetic particle drift is observed. Further increases in the cold-plasma density such that the frequency of the electron sound exceeds all the drift frequencies of the plasma, lead to an expansion of the stability region of the inhomogeneous plasma. (auth)

12222 FAUST 1—A HARDCORE DISCHARGE STABILITY EXPERIMENT. Aitken, K. L.; Hopkins, K. J.; Bickerton, R. J.; Hardcastle, R. A.; Reynolds, P. (United Kingdom Atomic Energy Authority, Abingdon, Eng.). Nucl. Fusion, 5: 330-48(Dec. 1965). (CLM-p71).

A hardcore discharge stability experiment is described in which the final configuration is obtained by the radial inward collapse of the plasma sheath from the wall of the tube. By varying the initial conditions an axial field of arbitrary sign can be trapped within the annular plasma column. The construction and mode of operation of the apparatus is fully described. The gas currents were the order of 50 kamp and rod currents were 120 kamp, so that the current in the gas was less than half that in the rod at all times. The general behavior of the discharge was examined and the effects of pressure, preionization and trapped axial field were studied. A detailed examination was made of a representative set of conditions with electric, magnetic and double Langmuir probes. These measurements, together with quantities derived from them, are discussed and the derived values of electron temperature and kinetic pressure are compared with the directly measured values. The validity of the pressure balance analysis is considered in the light of these results. The discharge, without trapped axial field, showed a high degree of reproducibility and the observed fluctuations were of low amplitude (< 10%) and low frequency (~ 500 kc/s) in both electric and magnetic field and in particle density. The last showed a well-defined annular sheath until late in the halfcycle; the radial profiles of azimuthal and axial current densities, kinetic pressure, temperature, and particle density showed good agreement. With trapped axial field, however, the discharge showed a reduction in stability, especially with trapped reverse field which introduces a null in the total axial field. Even with these, the most unstable conditions, the fluctuations were still relatively small (< 20%) and of low frequency (~ 1 Mc/s). The stability of the discharge is quantitatively compared with stability theory and the results are discussed. (auth)

12223 ERRORS IN THE USE OF MASS ANALYZERS IN PLASMA PHYSICS. Fleischmann, H. H. (General Atomics Div., General Dynamics Corp., San Diego, Calif.); Ashby, D. E. T. F.; Larson, A. V. Nucl. Fusion, 5: 349-51(Dec. 1965).

Sources of error are discussed in the use of charged-particle analyzers to determine the ionic species and energies in plasma streams, with particular reference to the widely used electrostatic instrument. Space-charge expansion within the analyzer leads to an upper limit on the size of the entrance aperture. This limit, which depends on the ion energy and density, is less than the proper Debye shielding distance that is often considered a sufficient limit. For ion energies below a few hundred ev and densities above 10^{10} cm^{-3} the aperture requirement is impractical. Therefore the possibility of reducing the plasma density by means of single apertures or multihole screens is considered. These considerations are supported by measurements on plasma gun outputs. The best criteria for proper operation of the analyzer are that the integral over the output spectrum equal the number of incident ions and that the output intensity be proportional to the area of the entrance hole. (auth)

12224 HYDROMAGNETIC WAVES IN A PARTIALLY IONIZED HYDROGEN PLASMA. Malein, A. (United

Kingdom Atomic Energy Authority, Abingdon, Eng.). Nucl. Fusion, 5: 352-8(Dec. 1965). (CLM-P-72).

Further experimental verification of the theory of fast hydromagnetic waves is given. By a suitable choice of plasma conditions the compressional wave is propagated in a partially ionized cylindrical hydrogen plasma at frequencies below the ion cyclotron frequency. The propagation constants of the wave are measured experimentally by observing the phase velocity and attenuation over a fixed distance. Other plasma parameters, with the exception of the neutral density are measured independently. To obtain good experimental agreement with the theoretical curves computed from the measured data, it is necessary to postulate a considerable neutral particle density in the plasma. This gives rise to loading of the wave, observable as a reduction in the Alfvén speed, and also to wave damping not explicable by resistive effects alone. The enhanced loading produced by neutral particles is unaffected by variations in magnetic field and the fitted value of neutral density derived from wave cut-off data is in agreement with that calculated from attenuation measurements. (auth)

12225 ON TWO MODELS PROPOSED FOR EXPLAINING SELF-EXCITED OSCILLATIONS IN AN ALKALI PLASMA. **Enriques, L.; Iannuzzi, M.; Righetti, G. B. (EURATOM-C.N.E.N., Frascati, Italy). Nuovo Cimento (10), 41B: 66-9(1966).**

Remarks are given on the assumptions made in two models, the Landau amplification process and the klystron mechanism, that were previously proposed to explain the observed self-excited oscillations in an alkali plasma. It is concluded that the experimental results are in better agreement with the explanation based on the Landau amplification process. (L.B.S.)

12226 DEPARTURES FROM LOCAL THERMAL EQUILIBRIUM IN A MAGNETICALLY-DRIVEN SHOCK WAVE. **Eckerle, K. L.; McWhirter, R. W. P. (National Bureau of Standards, Washington, D. C.). Phys. Fluids, 9: 81-9(Jan. 1966).**

An experimental study is reported of the time-resolved spectrum of the plasma produced by the magnetically driven shock wave in a T-tube. It is shown that the population densities of the excited levels of helium ions in the plasma depart from the values they would have in local thermal equilibrium. On the other hand if local thermal equilibrium is assumed and the electron temperature estimated for the intensity ratio of He II (4686Å) to He I (5876Å) then in the conditions of the experiment an error of a factor of two in the electron temperature arises. The reason for the departure from local thermal equilibrium was shown to be the rapid rate of change of the plasma conditions (especially the electron temperature). This is so great that the ionization and recombination rates, being slower, cause certain population densities to lag behind the electron density and electron temperature. These rates were found to be consistent with the rates calculated by Bates et al. in their collisional-radiative model for the ionization and recombination of hydrogen-like ions. (auth)

12227 STRUCTURE OF A PERPENDICULAR SHOCK WAVE IN A PLASMA. **Hu, Pung Nien (New York Univ., N. Y. Stevens Inst. of Tech., Hoboken, N. J.). Phys. Fluids, 9: 89-98(Jan. 1966).**

Based on the Boltzmann equations for fully ionized gases, analytic solutions of weak perpendicular shock waves are obtained. The result shows that all weak shock waves (in ionized gases as well as in nonionized gases) have similar profiles given by the hyperbolic-tangent function of the distance. The shock thickness is found to depend on four basic parameters, namely, the mean free path of the gas, the length of penetration, the Larmor radius based on thermal speed, and the mass ratio of electron and ion. From the explicit expression of the shock thickness, various significant cases are derived and discussed. The most interesting case occurs when the mean free path is larger than the electron length of penetration, which is in turn larger than the electron Larmor radius; it is found that both the scaled and the actual shock thickness can be smaller than the length of penetration — a result contrary to that obtained for collisionless plasmas. (auth)

12228 BOUNDARY LAYER OF AN EQUILIBRIUM PLASMA ATMOSPHERE. **Abraham, B. W. (National Aeronautics and Space Administration, Moffett Field, Calif.). Phys. Fluids, 9: 99-101(Jan. 1966).**

An isothermal atmosphere of a fully ionized equilibrium plasma in a gravitational field maintains charge neutrality except near the surface. The atmosphere, held to a spherically symmetric planet or star by a gravitational field, has a charged layer near the surface of approximate width of a Debye length. The charge excess near the boundary is the order of $\epsilon^2 n$ where n is the total density of ions or electrons and ϵ is the ratio of the Debye length to the scale height which is quite small for most atmospheres. The solution is performed by methods used in boundary-layer problems and gives as an example the correction to an equilibrium configuration arising from the presence of boundaries. (auth)

12229 DIELECTRIC PROPERTIES OF A WEAKLY TURBULENT PLASMA. **Ichikawa, Yoshi H. (Univ. of Illinois, Urbana). Phys. Fluids, 9: 111-17(Jan. 1966).**

Generalization of the Herring-Yoshikawa theory was developed to take into account the dynamical effect of turbulent fluctuation on the dielectric properties of the weakly turbulent plasma. According to the hydrodynamic description of electron plasma, the turbulent fluctuation gives rise to appreciable modification of the dielectric properties in the low frequency region and at the frequency of twice of the electron plasma frequency. An expression of the static dielectric constant shows that the characteristic correlation distance of the weakly turbulent plasma becomes longer than the Debye distance of corresponding homogeneous plasma in thermal equilibrium state. Contrary to the hydrodynamic scheme, the integral equation was derived for the induced fluctuation in the kinetic description of the plasma. This integral equation suggests that the turbulent fluctuation may modify the dielectric properties of the turbulent plasma also at the electron plasma frequency. (auth)

12230 KINETIC EQUATION FOR A WARM PLASMA. **Woollett, E. L. (Kansas State Univ., Manhattan). Phys. Fluids, 9: 118-33(Jan. 1966).**

A generalized Balescu-Lenard kinetic equation is derived for a fully ionized, zero-external-field, homogeneous, unbounded plasma which includes relativistic corrections to the thermal motion through terms of order (kT/mc^2). The kinetic equation is constructed in the space of coordinates and relativistic mechanical momenta. The calculation, based on the Darwin Lagrangian, makes use of the multiple time-scale perturbation theory of Frieman and Sandri. Part of the collison integral is expressed in terms of a shielded Lorentz force. The three-body Lorentz force, which appears when the acceleration of a source particle is expressed in terms of the coordinates and velocities of all other particles, does not contribute in the approximation considered. (auth)

12231 LANDAU DAMPING AND THE VELOCITY FOURIER TRANSFORM OF THE INITIAL PERTURBATION. **Denavit, J. (Northwestern Univ., Evanston, Ill.). Phys. Fluids, 9: 134-40(Jan. 1966).**

The linearized Vlasov equation for longitudinal plasma oscillations is solved using the convolution integral for unilateral Fourier transforms. This solution, independent of analyticity conditions on the initial perturbation distribution g(v), is valid for all times. The electric field is given in terms of the Fourier transform H(q) of g(v) with respect to velocity, the wavenumber k, and the Landau poles z_m. The quiescent distribution is assumed Maxwellian. For $t \to \infty$ the solution yields Landau damping if H(q) drops faster than exp $(y_1 q)$ for large q[g(v) analytic], while the results of Weitzner are recovered if H(q) drops as $1/q^n$ [g(v) having $n-2$ continuous derivatives]. For $t \neq \infty$,

Landau damping is shown to take place during a time interval, the limits of which are estimated in terms of the behavior of H(q). (auth)

12232 RELATIVISTIC EFFECTS ON PLASMA STABILITY. Noerdlinger, Peter D. (Univ. of Chicago). Phys. Fluids, 9: 140-2(Jan. 1966).

For an anisotropic uniform plasma in a steady magnetic field, the nonrelativistic theory and Lerche's treatment of highly relativistic plasmas both give instability whenever the pressure $p_\perp$ perpendicular to the magnetic field exceeds $p_\parallel$, the pressure along the field. Here it is shown that the instability persists in weakly relativistic plasmas, in contrast to the implication by Sudan that it vanishes in certain cases. The firehose instability is also investigated for the weakly relativistic plasma; it is slightly stabilized by relativistic effects. (auth)

12233 CRITICAL LENGTH DETERMINATION FOR CONVECTIVE INSTABILITIES IN WEAKLY INHOMOGENEOUS PLASMAS. Aamodt, R. E.; Book, D. L. (General Atomic Div., General Dynamics Corp., San Diego, Calif.). Phys. Fluids, 9: 143-51(Jan. 1966).

A convergent perturbation expansion procedure for determining the reflection coefficient for unstable convective modes in a plasma with small changes in the density is derived. If the total variation of the local wave vector is small, the lowest-order reflection coefficient can be used to determine the critical length of the system. The technique is used to determine the critical length of mirror machines which are subject to the convective loss-cone instability. Even for small rapid or large gentle changes in the local wave vector, critical lengths less than ten e-folding distances can be realized. (auth)

12234 STAGNATION OF ENERGETIC PLASMA. Stuart, G. W. (General Atomic Div., General Dynamics Corp., San Diego, Calif.). Phys. Fluids, 9: 152-61(Jan. 1966).

A finite stream of cool plasma comprised of high A ions incident on a rigid plate, with the stream velocity u_0 between 10^7–10^8 cm/sec is considered. The plate drives a strong ion shock upstream. The ion shock is about a mean free path thick. Overlapping and downstream from the ion shock is a thicker region in which electrons are collisionally heated, multiply by collisional ionization processes, and undergo radiative transition; within the thicker region the directed velocity u continues to decay. The entire structure (stagnation region) is treated in a steady-state shock frame. Except when the stream is very large, most of the energy escapes upstream to infinity as radiation, and the behavior is markedly different from that of the usual shock analysis where radiant flux vanish at infinity, e.g., in the former case material compressions are vastly greater. The atomic populations within the stagnation region are not those of local thermodynamic equilibrium; the more appropriate coronal description predicts a much softened radiation spectrum for $u_0 = 10^8$ cm/sec, but only slight softening for $u_0 = 10^7$ cm/sec. (auth)

12235 FREE-STREAMING PLASMA EXPERIMENTS. Eastlung, B. J.; Chu, C, K. (Columbia Univ., New York). Phys. Fluids, 9: 161-4(Jan. 1966).

Experiments are described with plasma pulses free-streaming from a source plate into a vacuum along a magnetic field. An analytic solution is derived for the pulse shape as a function of position and time in terms of the initial pulse shape at the launching plate. The experimental results agree extremely well with this free-flow theory, in which the initial pulse is assumed to have a Maxwellian velocity distribution. These experiments allow quantitative observations of free-flow phenomena under carefully controlled laboratory conditions. (auth)

12236 PLASMA COLUMN END EFFECTS. Rynn, N. (Princeton Univ., N. J.). Phys. Fluids, 9: 165-76 (Jan. 1966). (MATT-375).

The end effects, or sheaths, of the plasma column of the Q-1 device are analyzed. The analysis utilizes an adaptation of the methods that have been used by Auer and McIntyre to predict the potential distributions in thermionic converters. Poisson's equation is solved under the assumptions of no collisions, no trapping, and a Maxwellian distribution of particles at the emitting boundaries and in the plasma. The model used requires the presence of a potential well in front of each plate. Although simpler than the actual situation with collisions and trapping, the model nevertheless seems to predict, qualitatively, the observed asymmetries in the volt-ampere characteristics, the observed density variations with current flow, and other observed variations with operating conditions. The analysis also indicates a possible explanation for certain of the observed instabilities. (auth)

12237 EFFECT OF WEAK COLLISIONS ON ION WAVES. Kulsrud, R. M.; Shen, C. S. (Princeton Univ., N. J.). Phys. Fluids, 9: 177-86(Jan. 1966).

The linearized Fokker–Planck equation is solved by an iteration method which assumes the collision term is one order higher than the other terms. It is solved for the case of ion wave instabilities, where the unperturbed situation consists of a constant electric field, electrons with the Spitzer–Härm distribution, and ions with a Maxwellian distribution of much lower temperature. The effect of collisions on the critical current for instability is determined, and it is found that the electron–ion collisions predominate and lower the critical current. An attempt is made to justify the use of the Fokker–Planck equation when the distribution functions are nearly unstable. The linearized Fokker–Planck equation is also solved for the case of ion waves in a cesium plasma. Here the electrons are taken as an isothermal fluid. The propagation and time damping constants are obtained as a function of collision rate. Also, the first root of the dispersion relation is applied to the space damping of ion waves in order to make a comparison with the experiment of Motley and Wong. (auth)

12238 BOUNDARY CONDITION EFFECTS IN A MAGNETIC MIRROR COMPRESSION EXPERIMENT. Coensgen, F. H.; Cummins, W. F.; Nexsen, W. E. Jr.; Sherman, A. E. (Univ. of California, Livermore). Phys. Fluids, 9: 187-94(Jan. 1966). (UCRL-12416; UCRL-12416(Rev.1)).

The transition from unstable operation to quasi-stable plasma containment in a plasma-injected magnetic compression experiment was found to be dependent upon the density and lifetime of plasma external to the confinement chamber. Transverse motion of the confined plasma is limited and the magnetic compression proceeds nearly adiabatically, provided the density of the external plasma is greater than ~0.1% of the confined plasma. If the electrical connection to external conducting surfaces is lost after the magnetic compression is well under way (later than 50 μsec after beginning of compression for a magnetic field rise time of 120 μsec), the trapped plasma suddenly moves to the wall between the magnetic mirrors giving dramatic evidence of instability. In any case, during the magnetic compression the shifting external plasma-wall contact results in intermittent particle and/or energy losses from the hot plasma. Later than 100 μsec, the untrapped portion of the injected plasma which has been cooled, neutralized, and contaminated through its interaction with vacuum chamber walls diffuses into the containment chamber. Thus, at all times, there are loss processes in competition with the magnetic compression. (auth)

12239 LOSS RATES OF CHARGED PARTICLES FROM OHMICALLY-HEATED DISCHARGES IN THE C-STELLARATOR. Hinnov, E.; Bishop, A. S. (Princeton Univ., N. J.). Phys. Fluids, 9: 195-8(Jan. 1966). (MATT-356).

Ionization rates in the C-Stellarator discharges of helium and hydrogen, with Ohmic heating, are deduced from measured electron densities, temperatures, and the intensities of certain spectrum lines. Particle loss rates are obtained from the difference between the ionization rates and the observed changes in electron densities. It is shown that the

average charged particle confinement time varies linearly with the confining field and the aperture of the current channel and inversely with the electron temperature. The confinement time is the same for helium and hydrogen and is not explicitly dependent on ohmic heating current or particle density. (auth)

12240 MICROINSTABILITY LIMITATIONS OF THE DCX-1 ENERGETIC PLASMA. Dunlap, J. L.; Haste, G. R.; Nielsen, C. E.; Postma, H.; Reber, L. H. (Oak Ridge National Lab., Tenn.). Phys. Fluids, 9: 199-213 (Jan. 1966). (ORNL-P-1234).

A steady state plasma with an energetic (≈300 kev) proton component is formed by dissociation of part of a 600-kev H_2^+ beam that makes a single pass in the midplane of a 2:1 magnetic mirror field with a central field value of 10 kG. Both gas dissociation and Lorentz dissociation were employed. The potentially accessible density (density expected in the absence of instabilities) with Lorentz dissociation is the larger by more than an order of magnitude. The plasma is stable against flute instabilities, but microinstabilities (ion-electron or negative mass instabilities) are evidenced by radio frequency signals at $\omega > \omega_{ci}$. The lowest density threshold for observation of these signals is 4×10^5 fast protons cm^{-3}. With Lorentz dissociation the microinstabilities eventually eject protons, as observed by detection of these direct losses correlated with microinstability signals and by failure of charge-exchange accountability. The losses are first observed at densities of $5 - 10 \times 10^7$ cm^{-3}; they amount to as much as 0.9 of the proton input current to the plasma; and, along with instability-driven scattering to larger plasma volume, they limit the proton density to $1 - 2 \times 10^8$ cm^{-3}, as much as a factor of 15 below the density expected in the absence of such effects. (auth)

12241 THE RELATIONSHIP OF a.c. RESONANT PROBES TO RESONANT SCATTERING. Leavens, W. M. (National Bureau of Standards, Boulder, Colo.). Phys. Lett., 19: 118-20(Oct. 1, 1965).

The relation between a-c probe resonance and resonant scattering is described, and this relation is used to calculate probe response from previous exact solutions of the linearized Vlasov equation for the resonant scattering problem. The phase and relative magnitude of the a-c current versus the scaled frequency are shown. Although the probe and resonant frequencies are closely related to the plasma frequency at the sheath edge, calculating the actual relation requires essentially full knowledge of the plasma and sheath structure. This relation may be fairly consistent with simple plasmas, such as, mercury arcs and mercury diffusion plasmas. But in other gases such as the ionosphere, the relation may be quite different, which severely impairs the value of resonance probes as a diagnostic tool. (J.F.P.)

12242 NEW HIGH-FREQUENCY EFFECT DUE TO THE DRIFT VELOCITY OF A PLASMA: A PLASMA HF ANALOG OF THE ROENTGEN-EICHENWALD CURRENT. Messiaen, A. M. (Ecole Royale Militaire, Brussels); Vandenplas, P. E. Phys. Lett., 20: 14-15(Jan. 15, 1966).

The mechanism responsible for the coupling between the TE mode and the TM mode excited in a plasma by an incoming plane wave with an exponential time dependence in the absence of a static magnetic induction, was investigated. A resonance peak was observed at the same electron density as that for which the main resonance of the TE mode occurs. Both the position and the angular dependence, but not the magnitude of this resonance (including the complication introduced by a steady axial magnetic field) were very well explained by a cold plasma model. (G.O.Y.)

12243 THEORY OF THE STIMULATED RAMAN EFFECT IN PLASMAS. Comisar, G. G. (Aerospace Corp., El Segundo, Calif.). Phys. Rev., 141: 200-3(Jan. 1966).

The stimulated Raman effect in gaseous plasmas is investigated by means of a coupled-mode analysis. A macroscopic representation for the electron density fluctuations is employed, and is shown to reduce to previous results on the optical pumping of plasmas. The Raman threshold power levels calculated are currently achievable in giant-pulse ruby lasers, but the available laser pulse durations are too brief to allow observable amounts of Raman radiation to build up from the thermal noise background, in the case of ordinary plasmas. However, the effect may possibly be observable in the laser-produced type of plasma. (auth)

12244 INSTABILITIES PRODUCED IN A PLASMA BY A HELICAL PROTON BEAM. Neufeld, Jacob; Wright, Harvel (Oak Ridge National Lab., Tenn.). Phys. Rev., 141: 211-16(Jan. 1966). (ORNL-P-1442).

Instabilities which result from an interaction between a cold plasma immersed in a magnetic field B_0 and an assembly of protons gyrating around the magnetic lines of force (helical proton beam) are analyzed. The special case of transverse electromagnetic waves propagating in the direction parallel to that of B_0 is considered and the instability produced by gyrating protons is compared with the instability produced by protons streaming in the direction of B_0 (linear proton beam). Both a helical and a linear proton beam produce a multiple P instability. There is, however, a difference in the relative rate of growth of the multiply excited P waves. In a linear stream the dominant P instability occurs at the lowest excited frequency, whereas in a helical beam it can occur at the highest excited frequency. Physical conditions under which different types of instability occur are discussed, with particular reference to the frequency ranges and growth rates of the excited waves. (auth)

12245 OPTICAL NONLINEARITIES OF A PLASMA. Bloembergen, N.; Shen, Y. R. (Univ. of California, Berkeley). Phys. Rev., 141: 298-305(Jan. 1966).

Second-harmonic generation and stimulated Raman effects for a plasma are calculated by the same methods that have been used for bound electrons. The nonlinear susceptibility describing the stimulated Raman effect in a gaseous or metallic plasma is 6 to 10 orders of magnitude smaller than the corresponding effect in liquids. This process in a plasma can also be described as the parametric interaction between a damped plasma wave and two light waves. The second-harmonic generation from a plasma boundary is dominated by a surface term which originates from the discontinuity in the normal component of the electric field. It is shown that the observed second-harmonic generation from metallic silver probably stems from bound ion cores in the surface layer rather than from a plasma surface term. (auth)

12246 QUANTUM THEORY OF PHOTON INTERACTION IN A PLASMA. Cheng, H. (Harvard Univ., Cambridge, Mass.); Lee, Y. C. Phys. Rev., 142: 104-14 (Feb. 1966).

The quantum theory of interaction of electromagnetic waves in a plasma is formulated from two different points of view. The first is to consider scattering of light off light (in the form of laser beams) with the plasma acting as a mediator of the interaction; the second is to consider scattering of one of the light beams off a system consisting of the plasma and the other laser beam. Based on the first viewpoint, the light-light scattering cross sections, both elastic and inelastic, are calculated in the lowest order. By summing over the final states of one of the photons, we obtain, based on the above results, the lowest order cross section of scattering of the other photon from the photon-plasma system. In the presence of a second stimulating laser beam, this cross section is enhanced. When both laser beams are very intense, the lowest order perturbation treatment is inadequate. The second viewpoint is then conveniently adopted to include the plasma-laser beam interaction to all orders. The results are discussed and compared with those in previous treatments. Finally, a simple model is considered. In this model, the plasmon is treated as the quantum of a harmonic oscillator which is linearly coupled to a system of phonons. All the previous results are explicitly verified in this model, which is solved exactly. (auth)

12247 OBSERVATION OF NEGATIVE-MASS INSTABILITY IN AN ENERGETIC PROTON PLASMA. Postma, H.; Dunlap, J. L.; Dory, R. A.; Haste, G. R.; Young, R. A. (Oak Ridge National Lab., Tenn.). Phys. Rev. Lett., 16: 265-8(Feb. 14, 1966).

A microinstability was observed in a hot proton plasma which was produced by dissociation of 600-kev H_2^+ injected into a mirror magnetic field. The properties of the instability were studied and were identified with those of the negative mass instability. (D.C.W.)

12248 EXPLOSIVE AND NONEXPLOSIVE ONSETS OF INSTABILITY. Sturrock, P. A. (Stanford Univ., Calif.). Phys. Rev. Lett., 16: 270-3(Feb. 14, 1966).

The stability of a sequence of states is considered. Criteria are established for classifying onsets of instability as explosive or nonexplosive, and it is shown that if a system exhibits an explosive onset of instability, this instability may be triggered. (D.C.W.)

12249 MICROWAVE BRIDGE MEASUREMENT OF PLASMA FREQUENCY. Lutz, B. C.; Lindsay, P. D.; Roemer, L. E. (Univ. of Delaware, Newark). Rev. Sci. Instrum., 37: 168-71(Feb. 1966).

A simple method for determination of plasma frequency is described, utilizing the cutoff effect of a plasma near electron cyclotron resonance. This determination can be made visually or by use of a microwave bridge. (auth)

12250 HIGH SPEED MAGNETICALLY OPERATED PARTICLE OR LIGHT SHUTTER. Kuswa, Glenn (Univ. of Wisconsin, Madison). Rev. Sci. Instrum., 37: 189-90 (Feb. 1966).

A shutter that can close five openings 0.635 × 5.84 cm to straight trajectory particles 240 μsec after it pulsed, and remain closed for 1 msec, was tested in a vacuum and in air. Driving energy is stored in a 15 μF capacitor. The shutter is intended to stop directed residual gas molecules of pulsed plasma guns from entering regions in which plasma properties are being studied. (auth)

12251 ON DISCRETE STATES OF A PLASMA BEAM AND THE TRANSITIONS BETWEEN THEM. Nezlin, M. V.; Solntsev, A. M. Zh. Eksp. Teor. Fiz., 49: 1377-88(Nov. 1965). (In Russian).

It is well known that on decrease of the ratio of the densities of the cold plasma column and fast electron flux which permeates the column, the plasma beam which consists of these two components goes over from a macroscopic stable state to a state with a virtual cathode. The nature of this transition is studied experimentally. It is shown that it occurs as the result of two jumps during which the plasma particles, energy, oscillation frequencies, radial dimensions of the beam and its potential considerably increase. These manifestations of beam instability remain the same even if the fast electron velocity distribution becomes disordered. (auth)

12252 THEORY OF HIGH FREQUENCY STABILIZATION OF SCREW INSTABILITY OF THE ELECTRON-HOLE PLASMA OF A SEMICONDUCTOR. [PART] I. Vladimirov, V. V. Zh. Eksp. Teor. Fiz., 49: 1562-75 (Nov. 1965). (In Russian).

It is shown that high-frequency stabilization of screw instability in semiconductors is due to waves reflected from the ends; this is manifest in the appearance of screw modes, which possess various spatial periods along the sample axis. If the spatial period of the modes is comparable with the sample length, their time correlation during high-frequency current modulation will result in stabilization. It is shown that high-frequency stabilization can arise only in short samples. Some stabilization criteria are introduced. The results of the theoretical treatment are in good agreement with the experiments. The stabilization mechanism considered may be operative in the positive column plasma of a gas discharge. (auth)

12253 EFFECT OF PARTICLE COLLISIONS ON FLUCTUATIONS IN A PLASMA. Sitenko, A. G.; Gurin, A. A. (Inst. of Physics, Academy of Sciences, Ukrainian SSR). Zh. Eksp. Teor. Fiz., 49: 1591-1600(Nov. 1965). (In Russian).

A kinetic theory treatment of plasma fluctuations is presented in which particle pair collisions are taken into account. For description of pair collisions a model collision integral is used in the kinetic equation that satisfies the laws of conservation of number of particles, momentum and energy (Bhatnagar, Gross and Krook model). A single component nonisothermal plasma is investigated. A general expression for the correlation function of random forces is found by applying the fluctuation-dissipation relation. It is demonstrated that if pair collisions are taken into account an additional correlation of random forces in velocity space appears. General formulas are derived for the spectral distributions of particle density fluctuations and temperature fluctuations. The dependence of the shape of the particle density and temperature fluctuation spectra on the magnitude of the effective frequency of pair collisions is investigated. The relation between fluctuations in a non-collisional plasma and fluctuations in hydrodynamics is studied. Scattering of electromagnetic waves on density and temperature fluctuations is considered. It is shown that temperature fluctuations appreciably affect scattering involving small changes of frequency at long wave lengths. (auth)

12254 PROPAGATION OF AN ELECTROMAGNETIC WAVE THROUGH A DIFFUSING PLASMA [Thesis]. Schoendorf, William Harris. Lafayette, Ind., Purdue Univ., 1963. 174p.

The problem of the propagation of an electromagnetic plane wave through a fully ionized diffusing plasma is investigated. The plasma is originally in a homogeneous slab of finite thickness in the x direction and of infinite extent in the y and z directions. The plasma is then allowed to diffuse into a surrounding rarefied neutral gas. The plasma diffuses in an ambipolar fashion. A uniform plane electromagnetic wave, traveling in the direction of increasing x, is then assumed to be normally incident on this diffusing plasma. The electric field within the plasma is obtained from a solution of the hydrodynamical equations and Maxwell's equations. There is no external magnetic field present. It is found that the behavior of the electromagnetic wave is dependent upon the relationship between two critical electron densities. These densities are n_p, the density at which the plasma frequency is equal to the frequency of the electromagnetic wave, and n_c, the density at which the electron-ion collision frequency is equal to the frequency of the electromagnetic wave. At high temperatures n_p is much smaller than n_c, and the incident electromagnetic wave fails to penetrate the plasma beyond the point at which the electron density is equal to n_p. At the other extreme is the low temperature case where n_c is much smaller than n_p. This condition leads to wave attenuation due wholly to collisional effects. In this case, the effect of the plasma frequency on the attenuation of the wave is completely nullified. The intermediate case where n_c and n_p are approximately equal is discussed, and it is seen that the electromagnetic wave is affected by both collisional phenomena and the plasma frequency. (Dissertation Abstr.)

12255 NON-LINEAR OPTICS OF MANY-PARTICLE SYSTEMS. Baym, Gordon; Hellwarth, R. W. (Univ. of Illinois, Urbana). 45p. (CONF-650638-2). ORINS. Gmelin, AED-CONF-65-156-8.

From Physics of Quantum Electronics Conference, San Juan, Puerto Rico.

The non-linear Maxwell equations that describe the coupling of the quantum mechanical Heisenberg representation electromagnetic field operator to the excitations of a uniform many-particle system are developed. It is assumed that these excitations can be treated as harmonic, in the sense that correlations between them can be neglected. An iterative method appropriate for solving these equations when one or more strong beams are incident on the plasma and produce weaker scattered

radiation is given. When the lowest iteration is applied to the optical mixing of two beams by a plasma, a result in agreement with that found by Kroll, Ron and Rostoker is obtained. Equations are then solved for the scattering of one light beam by another in a plasma, a process proposed by DuBois and Gilinsky, and by Platzman, Tzoar, and Buchsbaum; and a result far too small to be observed is found. Finally the stimulated Raman scattering from an electron plasma is studied, and it is found that although it would be difficult to observe with present technology, it is the most likely of these effects to be observed in plasmas in the near future. (auth)

12256 THERMAL AND NON-THERMAL EMISSION FROM PLASMAS. Bekefi, G. (Massachusetts Inst. of Tech., Cambridge). 3p. (CONF-83-3; MIT-1842-12). ORINS.

From International URSI Conference, Tokyo, Sept. 1963.

Experimental and theoretical studies since 1960 on radio and microwave emission from cold and hot plasma and weakly and highly ionized plasma are reviewed briefly. The studies are divided into three groups: nonthermal emission from individual electrons, radiation from collective motions of particles, and interaction between the radiation field and the velocity distribution of plasma electrons. (25 references) (A.G.W.)

12257 DEVELOPMENT OF A SURFACE IONIZATION TYPE ION SOURCE AND ITS USE IN THE DETERMINATION OF IONIZATION POTENTIAL. Dey, S. D. (Saha Inst. of Nuclear Physics, Calcutta). pp 309-15 of Nuclear Physics and Solid State Physics Symposium, 1965. Nuclear Physics. Bombay, Atomic Energy Establishment, 1965.

A three-filament ion source was developed and was used, together with an electrometer circuit, to measure the ionization potential of lithium. (D.C.W.)

12258 COMPLEX REFRACTIVE INDEX OF A MAGNETOPLASMA. Basu, J. (Saha Inst. of Nuclear Physics, Calcutta). pp 353-7 of Nuclear Physics and Solid State Physics Symposium, 1965. Nuclear Physics. Bombay, Atomic Energy Establishment, 1965.

The transmission of a normally incident electromagnetic wave by a magnetoplasma was studied considering both longitudinal and transverse orientation of the magnetic field with respect to the direction of wave propagation. The complex reflection and transmission coefficients were related to the number density, cyclotron frequency, angular wave frequency, and plasma frequency by plotting the complex refractive index on a Smith chart for a few typical values of the electron collision frequency. (D.C.W.)

12259 PROBE MEASUREMENTS OF A COLD CATHODE PENNING DISCHARGE. Bose, D. K.; Nagchaudhuri, B. D.; Sen Gupta, S. N. (Saha Inst. of Nuclear Physics, Calcutta). pp 363-6 of Nuclear Physics and Solid State Physics Symposium, 1965. Nuclear Physics. Bombay, Atomic Energy Establishment, 1965.

A floating double-probe technique was used to study the ion density and electron density and temperature in a cold-cathode Penning discharge. Argon at different pressures was used in the discharge tube, together with magnetic fields of different strengths. The densities and temperature were obtained from the double-probe data by assuming a Maxwellian electron energy distribution. An analysis of current-voltage data obtained with a single Langmiur probe upheld this assumption. (D.C.W.)

12260 ON THE SET-UP OF DUOPLASMATRON FOR AN INTENSE ION BEAM. Bose, D. K.; Majumdar, N. K.; Nagchaudhuri, B. D. pp 367-71 of Nuclear Physics and Solid State Physics Symposium, 1965. Nuclear Physics. Bombay, Atomic Energy Establishment, 1965.

The extraction of intense beams from a duoplasmatron ion source is discussed; and some results obtained with argon are presented, together with the results of a determination of the ion density and the electron density and temperature. (D.C.W.)

Shielding

Refer also to abstracts 11058, 11229, and 11930.

12261 (AFRRI-TN-65-2) THE LOW-ENERGY COMPONENT OF THE TOTAL DOSE FOR DEEP GAMMA PENETRATIONS IN AIR AND WATER. Garrett, C. W. (Armed Forces Radiobiology Research Inst., Bethesda, Md.). Nov. 1965. 21p.

A difference of a factor of two in the buildup factors for infinite water and infinite air at deep penetration distances (e.g., 10 mean free paths) for point isotropic ^{60}Co sources is noted. One possible cause for the discrepancy is the improper accounting of the dose delivered by low-energy photons (energies less than 100 kev) in the infinite air case, which was treated by a Monte Carlo analysis. The possible effects of this cause are presented, showing that lack of present knowledge of the differential number flux density for low-energy photons diffusing in low-Z materials leads to great uncertainty in the fraction of the total dose delivered by the low-energy component. Experimental data indicate that essentially all of the discrepancy between the water and air buildup factors could be attributed to a neglect of the low-energy dose. On the other hand, recent Monte Carlo calculation of the low-energy flux suggests that the cause for the discrepancy must be accounted for by other, at present undetermined, factors. (auth)

12262 (BNL-8721) PASSAGE OF HIGH-ENERGY PARTICLES IN MATTER—NUCLEAR CASCADES INDUCED IN DENSE MEDIA BY 1- AND 3-Gev PROTONS. Shen, S. P. (New York Univ., N. Y. Brookhaven National Lab., Upton, N. Y.). [1964]. Contract AT-30-2-GEN-16. 50p. Dep. mn. CFSTI $2.00 cy, $0.50 mn.

A series of experiments designed to survey the main features of the nuclear cascade induced by monoenergetic protons in thick absorbers were performed using 1- and 3-Bev protons on iron, 1- and 3-Bev protons on material resembling chondritic meteorites, and 1-Bev protons on Plexiglas ($C_5H_8O_2$). The ^{18}F and ^{24}Na activities induced in aluminum foils embedded at various depths in the absorbers were measured. These measurements, usable for detailed comparison with nuclear-cascade calculations, are then roughly translated into the fluxes of the high-energy component (nucleons and pions above 50 Mev) in the cascade. The main results are summarized in families of transition curves, the principal features of which in general depend smoothly on the incident energy, on the energy of the detected component, and on the absorber mass number. A few lateral-spread measurements are also given; in particular, the lateral spread of fast neutrons is, for given large depths, smaller in the 3-Bev-on-Fe cascade than in the 1-Bev-on-Fe cascade, as expected. Albedo of the high-energy component at the bombarded surface is practically nil for the 1-Bev cascades, and is 1 and 0.3 albedo particles per primary proton respectively for the 3-Bev-on-Fe and 3-Bev-on-chondrite cascades. Results of cosmic-ray and astrophysical interest are noted. (auth)

12263 (JINR-P-2479) PROKHOZHDENIE NEITRONOV VYSOKIKH ENERGII V TYAZHELOM BETONE. (Passage of High Energy Neutrons Through Heavy Concrete). Sychev, B. S.; Mal'kov, V. V.; Komochkov, M. M.; Zaitsev, L. N. (Joint Inst. for Nuclear Research, Dubna (USSR)). 1965. 6p. Dep. mn.

The penetration of neutron fluxes with energies of several hundreds of Mev into hematite concrete with different hydrogen contents was investigated. Values for the attenuation lengths of the high-energy neutron fluxes and the storage factors of slowed down neutron fluxes were obtained. (auth)

12264 (MLM-1315) GAMMA SHIELDING REQUIREMENTS FOR ^{238}Pu AND ^{210}Po (REVISED). Foster, K. W. (Mound Lab., Miamisburg, Ohio). Jan. 21, 1966. Contract AT-33-1-GEN-53. 10p. Dep. mn. CFSTI $1.00 cy, $0.50 mn.

Gamma shielding requirements were computed for ^{238}Pu and ^{210}Po. Literature values were used for the gamma energies, their relative abundances, and for the mass absorption coefficients of these decay components in various shielding materials. A point source and isotropic radiation were assumed; self-absorption was not considered. For ^{238}Pu, the greatest shielding thicknesses were required to attenuate the 760-kev component. The following shielding thicknesses are required to reduce the dose rate from a bare 1-kg ^{238}Pu source to less than 2.5 mR/hr at 1 m: 0.85 cm lead, 2.30 cm iron, 0.45 cm uranium, and 10.6 cm concrete. The gamma radiation intensities were computed for 100-w, 1-kw, and 10-kw ^{210}Po heat sources. The thicknesses of uranium required to attenuate the 0.803-Mev gamma radiation from each of the above sources to 1000, 100, 10.0, and 1.0 mR/hr at 1 m were calculated. (auth)

12265 (NP–15697(Vol.1)) DATA COMPILATION AND EVALUATION OF SPACE SHIELDING PROBLEMS. VOLUME I. RANGE AND STOPPING POWER DATA. Hill, C. W.; Ritchie, W. B.; Simpson, K. M. (Lockheed Nuclear Products, Marietta, Ga.). [nd]. Contract NAS-8-11164. 132p. (ER–7777(Vol.1)).

Proton and alpha particle range and stopping-power data are tabulated in the proton energy range of 0.4 Mev to 100 Bev and the alpha energy range of 2 Mev to 100 Bev, for 55 materials. The application of the results to space-vehicle shielding is also noted. (T.F.H.)

12266 (ORNL-tr–918) COMPUTATION OF THE THICKNESS OF CONCRETE SHIELDING WALLS AGAINST GAMMA RADIATION. Hoenig, Arnost. Translated for Oak Ridge National Lab., Tenn., from Inzenyrske Stavby, 7: 3-11(1964). 14p. Dep. mn. JCL $1.60 fs, $0.80 mf.

The basic building materials for shielding walls against radiation are reviewed. The geometry of narrow and broad radiation beams is considered including photon scattering. Dose buildup factors are given as a function of incident gamma energy. Tables of these buildup factors are also given. (J.F.P.)

12267 SECONDARY γ-EMISSION COEFFICIENTS FOR ALUMINUM, COPPER, AND TUNGSTEN. Belov, S. P.; Demin, V. P.; Kazanskii, Yu. A.; Lobakov, A. P.; Popov, V. I. At. Energ. (USSR), 19: 452(Nov. 1965). (In Russian).

The coefficient of secondary gamma emission—the ratio of total capture-gamma flux with energies above threshold emitted from a shielding surface to the total neutron flux leaving the same surface—was determined for Al, Cu, and W, using the RIZ reactor as the neutron source. Measurements were made for gamma quanta over 5 Mev and for shielding thicknesses of 20 cm for Al, 9.5 to 48 cm for Cu, and 5 to 17 cm for W. (M.J.T.)

12268 CHANGES OF SPECTRA OF FAST NEUTRONS AFTER THEIR PASSAGE THROUGH ALUMINIUM, PARAFFIN, AND AQUEOUS MEDIA. Doroshenko, G. G.; Fedorov, V. A.; Leonov, E . S. At. Energ. (USSR), 19: 460-2(Nov. 1965). (In Russian).

Spectra of fast neutrons from a Po–Be source were measured before and after passage through shielding layers of thickness 44 cm for Al, 45 cm for paraffin, and 40 cm for water. Results are presented, showing corrections for resolution of the detector, and are compared with the known energy variations of the neutron total cross section for ^{27}Al, ^{12}C, and ^{16}O, respectively. (M.J.T.)

12269 DIFFERENTIAL ENERGY AND ANGULAR DISTRIBUTION OF SCATTERED GAMMA RAYS THROUGH CONCRETE INCIDENT NORMALLY. Su, Yung-Sung; Chou, Jen-Chang; Lin, Shi-Chien (National Tsing Hua Univ., Hsinchu, Taiwan). Ho Tsu K'o Hsueh, 4: No. 3-4, 39-54(Aug. 1965).

The angular and energy distributions of the gamma radiation emerging from the face of the concrete barrier incident normally with parallel beams from ^{60}Co were first measured by the use of a 3″ × 3″ NaI(Tl) scintillation detector with 256 channels pulse height analyzer. The obtained pulse height distributions were treated by the modified inverse matrix method with the help of IBM-1620 digital computer. The experimental results were compared with theoretical predictions of Monte Carlo calculation and a fairly good agreement was revealed. (auth)

12270 A METHOD OF ANALYSING BETA-RAY ABSORPTION DATA. Otozai, K. (Osaka Univ.); Hayashi, S. Int. J. Appl. Radiat. Isotop., 16: 681-96(Dec. 1965).

A method for analyzing β absorption data by means of a special analyzing paper is proposed. Aluminum absorption data are plotted directly on the paper. On the basis of linear extrapolation, the maximum range and the maximum energy of the β rays are estimated. The results were accompanied by errors no greater than in the Feather method or the Bleuler-Zunti method. The analyzing paper is also useful for semi-quantitative analysis of multicomponent spectra. (auth)

12271 GAMMA-RAY TRANSMISSION THROUGH MULTIPLE LAYERS. Kataoka, Iwao. Nippon Genshiryoku Gakkaishi, 7: 634-44(Nov. 1965). (In Japanese).

Gamma transmission through multiple shields is reviewed. The behavior of photons in stratified slabs is discussed. Several illustrations of energy spectra, angular distributions of photons, and buildup factors in the slabs provide an outline of the phenomena involved. The adaptability of various methods to the γ multilayer problem was examined. The survey included several methods for numerically solving the Boltzmann transport equation, the Monte Carlo method, the successive scattering method, as well as various transmission operator and invariant imbedding methods. Apart from the Monte Carlo method, only a few of the methods were applicable to the multilayer problem of γ rays. Relevant experiments are described. (auth)

12272 RADIATION SHIELDING DEVICE. Adachi, Takeshi (to Tokyo Shibaura Electric Co., Ltd.). Japanese Patent 1964-27180. Nov. 27, 1964. Filed Feb. 28, 1963.

A shield made up of a number of flexible elements, for use around regular shield penetrations, is described. (TCO)

12273 NEUTRON-ABSORPTIVE GLASS. Bishop, Frederic L.; Pinotti, Alfred D. (to Owens-Illinois Glass Co.). U. S. Patent 3,216,808. Nov. 9, 1965. Filed July 12, 1962.

A neutron absorptive glass is prepared by melting a chemically durable glass composition containing 2 to 25 wt % of a neutron-absorbing oxide selected from the group consisting of gadolinium oxide and samarium oxide and mixtures of these, cooling the glass to solidify it, grinding the glass into particulate form, pressing the glass particles into a prescribed shape, and sintering the pressed shape into a semi-fused rigid condition. If the original glass does not contain the neutron-absorbing oxides, they may be added to the ground glass particles to form a homogeneous mixture prior to the pressing operation. (B. L. M.)

Solid State Physics

See also CHEMISTRY — Inorganic and Physical Chemistry
METALS, CERAMICS, AND OTHER MATERIALS — Properties and Structure

Refer also to abstracts 10830, 11276, 11355, 11918, 12073, 12245, and 12252.

12274 (COO–578-18) MAGNETIC PROPERTIES OF INSULATORS. Quarterly Report, May 16–August 15, 1965. Noble, Gordon (IIT Research Inst., Chicago, Ill.). Dec. 10, 1965. Contract AT(11-1)-578. 48p. (IITRI–1184-18). Dep. mn. CFSTI $2.00 cy, $0.50 mn.

The optical absorption constant of the F-center is due to induced transitions. The luminescence is caused by spontaneous transitions between a different set of states. The interaction of the F-center with light is reviewed in order to obtain comparable quantum mechanical transition rates. The observed absorption includes a factor proportional to the frequency. The emitted power per unit energy interval is proportional to the fourth power of frequency. This has significant effects if one compares functions of the equilibrium ionic positions in the relaxed ground state and the relaxed excited state. The correction to the observed peak, width, symmetry and moments is calculated by formula and by numerical methods for absorption and emission of rubidium chloride. The former analytical approximation seems to be preferable. The distribution of expectation values for the operator seems to be wider and more symmetrical than the observed bands at low temperature. The corrections to the emission half width are very significant. Comparable quantities related to the second moment are not appreciably changed. The correct effective frequency is obtained from the uncorrected half widths. The density matrix formalism is applied to the saturation of an inhomogeneously broadened electron paramagnetic resonance line. The sequential saturation, delay and observation technique are analyzed. A set of conditions for the validity of the spin packet model are pointed out. The theory has observable significance when applied to the burning of a hole in a portion of the F-center resonance spectrum at 4°K. Previous models have not adequately explained the depth of the steady state hole as a function of the saturating power. (auth)

12275 (GA-6861) ATOMIC MOTION IN MODERATORS. Young, James A. (General Atomic, San Diego, Calif. John Jay Hopkins Lab. for Pure and Applied Science). Dec. 26, 1965. Contract AT(04-3)-167. 39p. (CONF-660204-3). Dep. mn. CFSTI $2.00 cy, $0.50 mn.

From American Nuclear Society Meeting, San Diego, Calif.

A review of the lattice dynamical properties of Be, BeO, C that are of importance in computing quantities of interest to the study of neutron thermalization is presented. Since all three of these solids have a hexagonal structure a relatively coherent treatment is possible. (auth)

12276 (NYO-3405-4) RESEARCH AND DEVELOPMENT ON SILICON CARBIDE ACTIVE DEVICES. Final Report. Chang, H. C. (Westinghouse Research Labs., Pittsburgh, Pa.). Oct. 1965. Contract AT(30-1)-3405. 97p. Dep. mn. CFSTI $3.00 cy, $0.75 mn.

Research is presented towards the development of junction-gate type unipolar field-effect transistors from silicon carbide which are capable of operating at 500°C in a radiation environment containing gamma rays; and slow and fast neutrons. The transistor designs are based on both abrupt and graded junction theories. A detailed mathematical and computer analysis of the graded junction design is given which approximates more closely the present state-of-the-art aluminum diffused junctions in silicon carbide than the original abrupt junction treatment by Shockley. The thermal growth of SiO_2 on SiC and the chlorine etching of SiC were studied, and the oxidation and etch rates determined. A self-masked diffusion technique was developed which utilizes SiO_2 as a mask for selectively etching regions for aluminum diffusion. This technique can provide precise control in making the device configuration. Preliminary radiation-damage studies with fast and slow neutrons indicate that a SiC unipolar transistor should be operable up to an intergraded neutron flux level of 10^{16} nvt or greater at 500°C. (M.O.W.)

12277 (PAEC(A)IN-656) MOESSBAUER EFFECT. A Literature Search. (Philippine Atomic Energy Commission, Manila). May 1965. 42p. Dep. mn.

A bibliography of the study and applications of the Mössbauer effect was prepared. There are 247 entries included and listed under various fields of study. Each entry includes the personal author, corporate author, title, volume number, and date of publication. Personal author and corporate author indexes are also included. (J.F.P.)

12278 (TID-21570) BAND SHAPE OF THE F-CENTER OPTICAL EMISSION IN RUBIDIUM CHLORIDE. Noble, G. A.; Brada, Y. (IIT Research Inst., Chicago, Ill. Physics Div.). [1964]. Contract AT(11-1)-578. 12p. Dep. mn. CFSTI $1.00 cy, $0.50 mn.

Measurements on the F-center emission band in vacuum-distilled rubidium chloride are reported. The parameters and moments characterizing the emission band at 78 and 4°K were obtained. The shape of the emission band is independent of temperature. From the moments, the Huang-Rhys factor for emission was determined. (auth)

12279 (UCRL-12311) TREATMENT OF PROTON CHANNELLING BY A TRANSVERSE TWO-DIMENSIONAL MODEL. Smith, Harold P. Jr.; Khan, J. M.; Potter, D. L.; Worley, R. D. (Lawrence Radiation Lab., Univ. of California, Livermore). Jan. 12, 1965. Contract W-7405-eng-48. 22p. Dep. mn. CFSTI $1.00 cy, $0.50 mn.

A theoretical model is proposed to describe the channelling of protons along low index channels and is applied to the prediction of x-ray and gamma yield variation as a function of the incident beam vector relative to the channel vector. The model considers only the motion of the proton in the plane perpendicular to the channel vector and does not need to distinguish between directional and planar channelling. However, a simplified version, which considers channelling in a rotationally symmetric directional channel is in good agreement with published data. It is shown that for the simplified version, one can calculate the rotationally averaged interatomic force field directly from the x-ray yield data. (auth)

12280 IMPLANTATION PROFILES FOR 40-kev PHOSPHORUS IONS IN SILICON SINGLE-CRYSTAL SUBSTRATES. Gibbons, James F. (Stanford Electronics Lab., Calif.); El-Hoshy, A.; Manchester, K. E.; Vogel, F. L. Appl. Phys. Lett., 8: 46-8(Jan. 15, 1966).

The doping of semiconductors by ion implantation techniques was investigated. Two single-crystal p-type Si wafers were exposed to a beam of 40-kev ^{31}P ions. In one sample, ^{32}P tracer ions were introduced before exposure to the beam; the tracer ions were introduced into the other sample after exposure to the ^{31}P beam. The concentration profiles of ^{32}P ions in the samples were compared with theoretical profiles calculated for an amorphous Si substrate by the Lindhard theory. (D.C.W.)

12281 STUDY OF THE REFLECTION PROFILES OF X RAYS ON A SILICON CRYSTAL IRRADIATED WITH α RAYS. Burgeat, Jacques; Colella, Roberto (CNET, PCM, Issy-les-Moulineaux, France. CCR EURATOM, Ispra, Italy). Compt. Rend., 261: 2872-5(Oct. 11, 1965). (In French).

The diffraction of x rays is sensitive to crystal imperfections. Point defects, in particular those produced by low-temperature alpha irradiation of silicon crystals, increase the reflective power. The profile of the diffraction rays accompanying this increase of reflective power was studied experimentally. This profile is interpreted as a change of interatomic distance in a thin crystal layer of several microns thickness. (tr-auth)

12282 BOMBARDMENT OF COPPER MONOCRYSTALS WITH OXYGEN IONS OF MEDIUM ENERGY (10 Kev). Meyer, Madeleine; Haymann, Pierre; Trillat, Jean-Jacques (CNRS, Bellevue, France). Compt. Rend., 261: 4353-8 (Nov. 22, 1965). (In French).

The (100) faces of copper monocrystals were bombarded with oxygen ions at 10 kev. The results obtained are the following: the orientation of the cuprous oxide on the copper is modified according to the mode of formation of the oxide (bombardment or heating in oxygen); the degree of orientation of Cu_2O varies with the angle between the ion beam and the (100) plane; and, the best orientation corresponds to an incidence angle of 45°, proving the influence of the channeling process. (tr-auth)

12283 RESONANCE ABSORPTION OF GAMMA-QUANTA IN ONE- AND TWO-DIMENSIONAL CRYSTALS. Dlouha, J.; Rohlena, K. (Charles Univ., Prague). Czech. J. Phys., 15: 686-95(1965).

The resonance absorption of gamma quanta in undisturbed one- and two-dimensional crystals is studied, the form of the resonance lines is determined and the question of the possibility of the existence of the Mössbauer effect is zero with the exception of the case of the perpendicular incidence of gamma rays on the linear chain and for two-dimensional crystals this effect would be possible in addition only at absolute zero temperature. (auth)

12284 APPROXIMATE CALCULATION OF THE SCATTERING CROSS-SECTION AT COLLISION OF TWO ELECTRONS OF LOW ENERGY IN METALS. Malat, V. (Charles Univ., Prague). Czech. J. Phys., 15: 861-2 (1965).

A simple approximation is used to obtain an expression for the scattering phase δ_0 from which the total effective collision cross section of two free electrons in metals can be calculated. A comparison of the approximate values of the phase with those obtained by numerical integration are tabulated for two different values of the screening factor. (L.B.S.)

12285 MOESSBAUER EFFECT OF ^{119}Sn IN SOME TIN COMPOUNDS. Lee, Yih-Fa (National Tsing Hua Univ., Hsinchu, Taiwan). Ho Tsu K'o Hsueh, 4: No. 3-4, 25-37 (Aug. 1965).

The $Mg_2{}^{119m}Sn$ source was synthesized. The absorption spectrum of Mg_2Sn versus $Mg_2{}^{119m}Sn$ source was found to have a half width of only 70% wider than the natural line width. The Mössbauer absorption line spectra of several kinds of tin-containing substance, including high-polymer, crystalline, and amorphous matters, were then studied by means of this source. Their chemical shifts and electric quadrupole splittings were also observed. (auth)

12286 ENERGY LEVELS OF Pu^{3+} IN LANTHANUM TRICHLORIDE. Conway, John G.; Rajnak, K. (Univ. of California, Berkeley). J. Chem. Phys., 44: 348-54(Jan. 1, 1966). (UCRL-16292).

Polarized absorbtion spectra and some Zeeman effect measurements in the region of 20,000–32,000 cm^{-1} are reported for Pu^{3+} in $LaCl_3$. A total of 25 J levels was fitted with an rms deviation of 100 cm^{-1} with the parameters values $E^0 = 14{,}930.5$, $E^1 = 3726.7$, $E^2 = 14.99$, $E^3 = 350.18$, $\zeta = 2260.2$, $\alpha = 36.5$, $\beta = -1171$. The large values of α and β indicate that configuration-interaction effects cannot be neglected in an analysis of the spectra of the high actinides. (auth)

12287 DEUTERON QUADRUPOLE COUPLING IN D_2O. Weissmann, Mariana (Facultad de Ciencias Exactas y Naturales, Buenos Aires). J. Chem. Phys., 44: 422-3 (Jan. 1, 1966).

Coupling constants from wavefunctions obtained previously were computed, in order to discover whether they could account for the structural changes found. The results predict smaller coupling constants for stronger bonds. This effect was observed previously. It is also noted that the quadrupole spin-lattice relaxation time for the nuclear magnetic resonance of deuterons in liquid D_2O could also be explained with a reduced coupling constant due to hydrogen bonding. (J.F.P.)

12288 COLOR CENTERS IN ALUMINOBORATE GLASS. Ghosh, Amal K. (Argonne National Lab., Ill.). J. Chem. Phys., 44: 541-6(Jan. 15, 1966).

Different types of color centers are presented in aluminoborate glass. Some of these are related to impurities, others are possibly due to defects in the glass structure. Radiation induced bands at 520 and 340 mμ are attributed to hole centers. The Fe^{3+} and Pb^{2+} ions present as impurities in a normal melt of aluminoborate glass act as electron traps, while Fe^{2+} ions and Pb^0 (atoms) present in a reduced glass act as hole traps. The reduction of Fe^{3+} ions to Fe^{2+} ions results in decrease of uv absorption around 220mμ. On heating the irradiated glass thermoluminescence along with bleaching of color centers were observed and the relation between the two processes was investigated. Glow peaks were observed at 60° ± 5°C, 165° ± 10°C, and 210° ± 5°C. The high-temperature glow peak is observed only at high gamma-ray exposures (~10^7 R). (auth)

12289 PREPARATION AND LOW-TEMPERATURE MAGNETIC PROPERTIES OF THE TERBIUM OXIDES. MacChesney, J. B.; Williams, H. J.; Sherwood, R. C.; Potter, J. F. (Bell Telephone Labs., Inc., Murray Hill, N. J.). J. Chem. Phys., 44: 596-601(Jan. 15, 1966).

The magnetic properties of terbium oxide phases (Tb_2O_3 cubic and monoclinic polymorphs, $TbO_{1.715}$, $TbO_{1.809}$, $TbO_{1.823}$, and TbO_2) were measured between 1.4° and 300°K. With the exception of $TbO_{1.809}$, each of these phases is observed to order magnetically at low temperatures. The ordering is predominantly antiferromagnetic, several of the lower oxide phases show metamagnetic behavior, wherein the observed moment has a nonlinear dependence upon the applied field at fields above a critical value, approximately 2000 Oe. The phase $TbO_{1.823}$ exhibits a tendency toward ferrimagnetic alignment as evidenced by remanent magnetization at 1.4°K. TbO_2 is antiferromagnetic with a Néel temperature of 3°K. At higher temperatures, in the paramagnetic region all of the oxide phases give effective Bohr magneton numbers close to the expected values for the free ions. (auth)

12290 MAGNETIC-DIPOLE INTENSITIES AND ZEEMAN EFFECT IN Cs_2UCl_6. Johnston, D.; Satten, R.; Wong, E. (Univ. of California, Los Angeles). J. Chem. Phys., 44: 687-91(Jan. 15, 1966).

The oscillator strengths of several magnetic-dipole transitions for U^{4+} in Cs_2UCl_6 were measured, and compared with calculated values using the eigenfunctions previously determined. The Zeeman effect of the only line showing a splitting in a 30-kg field in the photograpi region of the spectrum was observed and $g_{||}$ and $g_{\perp}$ were compared with theoretical values. The second-degree term of the D_{3d} crystalline-field distortion from the large cubic field was obtained. (auth)

12291 ELECTRON SPIN RESONANCE STUDIES OF γ-IRRADIATED FERROELECTRIC METHYLAMMONIUM ALUM CRYSTALS. Kohin, Roger P.; Nadeau, Paul G. (Clark Univ., Worcester, Mass.). J. Chem. Phys., 44: 691-4(Jan. 15, 1966).

The ^{60}Co γ irradiation of methylammonium alum crystals at room temperature produces the $\cdot CH_2NH_3^+$ radical ion which was observed by ESR for the first time. Measurements were made at temperatures between 100° and 300°K. The radical, which undergoes hindered rotation at room temperature, displays isotropic hyperfine splittings of 70 Mc/sec for the two α protons, 53.8 Mc/sec for the three β protons and 11.6 Mc/sec for the β nitrogen. These values are approximately 20% higher than those measured previously in the glycine radical $\cdot CH(CO_2^-)NH_3^+$ in which the CO_2^- group extracts π-electron spin density from the remainder of the molecule. The isoelectronic ethyl radical $\cdot CH_2CH_3$ shows a much larger β-proton splitting and a slightly smaller α-proton splitting, indicating that hyperconjugation is approximately 60% more effective for the CH_3 group. ESR measurements below the ferroelectric Curie temperature (177°K) indicate that below ≈140°K the molecule is rigidly held, but that it begins gradual motion between 140°K and the Curie point. Just at the Curie temperature a transition occurs which liberates additional degrees of freedom and allows virtually free rotation at higher temperatures. (auth)

12292 SPIN-LATTICE RELAXATION IN SOME RARE-EARTH TRICHLORIDES. Mangum, B. W.; Hudson, R. P. (National Bureau of Standards, Washington, D. C.). J. Chem. Phys., 44: 704-13(Jan. 15, 1966).

Studies of spin-lattice relaxation of the ions Ce^{3+}, Nd^{3+}, Sm^{3+}, Ho^{3+}, and Er^{3+} present in low concentrations (0.2% to 2%) in the host lattice of $LaCl_3$ were made in the liquid-helium region by the pulsed-microwave method. The variation of the relaxation time τ with temperature permits separation of the contributions to the relaxation from the two-phonon (resonant and nonresonant) and single-phonon

processes. The substances studied are not "well behaved"; features such as nonexponential decays and variability of the derived values for the splitting between the ground and first excited levels are discussed. Some of the ions exhibit a significant variation of τ with concentration and Nd^{3+} shows an interestingly large anisotropy of τ in the Raman process. (auth)

12293 MONOPULSE GENERATION WITH $CaF_2:U^{3+}$ CRYSTALS. Ermakov, B. A.; Lukin, A. V.; Mak, A. A.; Prilezhaev, D. S. JETP Lett. (USSR) (Engl. Transl.), 2: 239-40(Oct. 15, 1965).

Monopulse generation with $CaF_2:U^{3+}$ crystals at wavelengths of 2.20 and 2.51 μ was observed. (D.C.W.)

12294 JAHN-TELLER EFFECTS IN THE ELECTRON SPIN RESONANCE SPECTRA OF IONS WITH SPIN 1. Stevens, K. W. H. (Univ. of Nottingham, Eng.); Persico, F. Nuovo Cimento (10), 41B: 37-51(1966).

A study is made of the effects of the dynamic Jahn-Teller effect on the electron spin resonance of $S' = 1$ ion in a cubic lattice. The idea that the ion and its near neighbors form a molecule which is almost decoupled from the rest of the lattice is not used and the ion is coupled directly to all the lattice modes. The resulting many-body problem is treated using Green function methods, the emphasis being placed on deriving an expression for the intensity of the spin resonance line. It is found that the spectrum consists of two overlapping lines, in agreement with some of the experimental results available for $S' = 1$ ions in CaO and MgO. (auth)

12295 INTERNAL MAGNETIC FIELD OF IODINE IN IRON. De Waard, H.; Drentje, S. A. (Univ. of Groningen, Netherlands). Phys. Lett., 20: 38-40(Jan. 15, 1966).

The hyperfine magnetic field of iodine in iron was studied by measuring the Zeeman splitting of the 27.7-kev gamma transition of ^{129}I dissolved in iron. This transition was excited in the decay of 33-day ^{129m}Te, which was obtained by irradiating an enriched ^{128}Te sample for one month at a neutron flux of $2 \times 10^{14} cm^{-2} s^{-1}$. (G.O.Y.)

12296 MOESSBAUER EFFECT RESULTING FROM THE REACTION $^{56}Fe(d,p)^{57}Fe$ USING PULSED BEAM TECHNIQUES. Christiansen, J.; Recknagel, E.; Weyer, G. (Hahn-Meitner Institut fuer Kernforschung, Berlin). Phys. Lett., 20: 46-8(Jan. 15, 1966).

The Mössbauer effect of the 14.4-kev gamma radiation of ^{57}Fe was measured after population of the level by the reaction $^{56}Fe(d,p)^{57}Fe$. (G.O.Y.)

12297 TEMPERATURE-DEPENDENT CONCENTRATION QUENCHING OF FLUORESCENCE BY CROSS RELAXATION OF Nd^{3+} IN LaF_3. Asawa, C. K.; Robinson, M. (Hughes Aircraft Co., Malibu, Calif.). Phys. Rev., 141: 251-8(Jan. 1966).

The fluorescence lifetimes of the $^4F_{3/2}$ level of Nd^{3+} in LaF_3 and Nd^{3+} in $LaCl_3$ were measured for various concentrations of Nd^{3+} at 4.2, 77, and 300°K and intermediate temperatures. It is found that the lifetime-concentration curves differ greatly for the two crystals. The optical energy levels of Nd^{3+} in LaF_3 at various concentrations were examined and two sets of levels with precisely overlapping electric dipole transitions were found; no such overlapping transitions were found for the $LaCl_3$ crystal, however. It is suggested that cross relaxation between these levels can account for the strong, temperature-dependent concentration quenching in the LaF_3 crystal. Using rate equations with cross relaxation terms, a one-parameter expression for fluorescence lifetime versus temperature was found which fitted experimental points for the 4.7 and 8.3% concentration crystals reasonably well. Since the overlap of transitions greatly affects cross relaxation rates, the linewidths and lineshifts were examined. Large heterogeneous linewidths and wavelength shifts were observed for the intermediate concentration crystals. The transitions were observed to sharpen in the low-dilution crystals and in the 100%-concentration crystals (NdF_3), but relative shifts in wavelengths are observed. (auth)

12298 INTERNAL FIELD OF ^{57}Fe IN NICKEL FROM 77 deg K TO THE CURIE POINT. Dash, J. G.; Dunlap, B. D.; Howard, D. G. (Univ. of Washington, Seattle). Phys. Rev., 141: 376-8(Jan. 1966).

The internal field of very dilute ^{57}Fe impurities in nickel was measured from 77°K to 0.99 T_c. The temperature dependence of the field is not the same as that of the magnetization, the discrepancy reaching 15% at intermediate temperatures. Correction of both magnetization and internal field to constant volume increases the divergence. Over the entire experimental temperature range, the internal field can be represented by a Brillouin function of the form proposed by Jaccarino, Walker, and Wertheim for ^{55}Mn in iron, indicating quasi-independent localized impurity moments. The empirical exchange field between Fe impurities and the Ni host is larger than the field between Ni ions, in contrast to the relatively weaker coupling of Mn in Fe. Therefore, the conditions for quasi-independent localized moments seem to be fulfilled for the case of the substantially stronger, as well as the weaker, couplings, in accord with a prediction of Callen, Hone, and Heeger. (auth)

12299 THE INFLUENCE OF ANISOTROPIC MOESSBAUER EFFECT ON MAGNETIC HYPERFINE SPLITTINGS IN POLYCRYSTALLINE MATERIALS. Cohen, S. G. (Massachusetts Inst. of Tech., Cambridge); Gielen, Paul; Kaplow, Roy. Phys. Rev., 141: 423-4(Jan. 1966). (MIT-2098-166).

The influence of lattice anisotropy of the recoil-free factor on the intensity of lines observed in recoil-free spectra in polycrystalline materials should be observable for magnetic hyperfine interactions, as well as in the case, previously discussed, of electric quadrupole interactions (Karyagin effect). The modification of line intensities was calculated for some simple cases. (auth)

12300 SPIN-LATTICE RELAXATION IN SOME RARE-EARTH SALTS. I. TEMPERATURE DEPENDENCE. Larson, G. H.; Jeffries, C. D. (Univ. of California, Berkeley). Phys. Rev., 141: 461-78(Jan. 1966).

Measurements are reported of the spin-lattice relaxation rate T_1^{-1} for several magnetically dilute rare-earth ions in the temperature range $1.2° \leq T \leq 5°K$, using the transient recovery of the microwave paramagnetic resonance in the frequency range $8 \leq \nu \leq 18$ Gc/sec. Data are given for Sm^{3+} and Dy^{3+} in the double nitrate $La_2Mg_3(NO_3)_{12} \cdot 24H_2O$; for Pr^{3+}, Sm^{3+}, and Er^{3+} in the ethyl sulfate $La(C_2H_5SO_4) \cdot 9H_2O$; and for Ce^{3+}, Nd^{3+}, Pr^{3+}, Sm^{3+}, Er^{3+}, and Tb^{3+} in the ethyl sulfate $Y(C_2H_5SO_4)_3 \cdot 9H_2O$. The temperature dependence was observed for the direct process $T_1^{-1} \propto T$; for the Orbach process $T_1^{-1} \propto \exp(-\Delta/T)$; and for the Raman process $T_1^{-1} \propto T^7$ or T^9. The magnitudes of the processes are in reasonable agreement with simple theoretical estimates. The observed rates are shown to be independent of paramagnetic ion concentration in the range 0.1 to 1%. For Pr in the ethyl sulfate, a phonon bottleneck rate $T_b^{-1} \propto T^2$ was observed rather than the direct process. In several cases the Orbach process determines a previously unknown value of the crystal-field splitting Δ, while in some cases it shows that the value of Δ in the dilute salt is significantly different from the value determined optically in the concentrated salt. (auth)

12301 MOESSBAUER SCATTERING: THE QUADRUPOLE INTERACTION IN OSMIUM METALS. Grodzins, L.; Chow, Y. W. (Massachusetts Inst. of Tech., Cambridge). Phys. Rev., 142: 86-90(Feb. 1966). (MIT-2098-158).

The Mössbauer scattering of the 137-kev gamma radiation from the first 2+ state of ^{186}Os is reported. The effect, i.e., the Mössbauer intensity-to-background ratio at zero relative velocity between source and scatterer, is, at 15°K, approximately 3:1. The full width at half-maximum of the velocity spectrum is 1.36 ± 0.07 times that theoretically expected. The Debye temperature of the osmium scatterer was determined and appears to increase with increasing temperature, from 4.2 to 80°K. The average value of Θ_D, assuming it to be the same for source and scatterer, is 375 ± 20°K. The angular distribution of the scattered ra-

diation was measured using a three-detector geometry. Assuming that the attenuation of the correlation is due to an axially symmetric electric field gradient (EFG) acting on the quadrupole moment of the 2+ state, the quadrupole interaction, $\omega_E = (35.6 \pm 3.3) \times 10^6$/sec is obtained. From the B(E2) value of the transition, the value the EFG of hexagonal close-packed (hcp) osmium is deduced to be $q = (3.50 \pm 0.50) \times 10^{17}$ V/cm^2. By comparing this value with the lattice contribution to the EFG as well as to the known EFG of hcp rhenium metal, it is concluded that the conduction-electron contribution is significant and probably changes substantially from rhenium to osmium. (auth)

12302 ELECTRONIC SHIELDING PARAMETERS AND ANISOTROPIC MOESSBAUER PATTERNS IN DYSPROSIUM ETHYL SULFATE. **Wickman, H. H.; Nowik, I. (Bell Telephone Labs., Murray Hill, N. J.). Phys. Rev., 142: 115-17(Feb. 1966).**

The Mössbauer effect of the 26-kev gamma transition in ^{161}Dy was employed to study hyperfine interactions in single crystals of DyES at 4.2°K. The Dy nuclei experience a magnetic hyperfine interaction $g_0\beta_N H_{eff}$ of –446 ± 12 Mc, with H_{eff} parallel to the c axis of the crystal. The hyperfine field and Mössbauer patterns (parallel and perpendicular to the c axis) are readily interpreted in terms of the symmetry of the hyperfine interaction from the ground Kramers doublet. The measurement of the electric quadrupole interaction is of interest because the 4*f* contribution to the electric field gradient (EFG) is often dominant in rare-earth ions; however, for the ground doublet of DyES, this gradient is very small. This fact allowed a simple and direct measurement of the lattice contribution to the EFG. From this result the ratio $(1-\gamma_\infty)/(1-\sigma_2)$ was found to be 262, where γ_∞ is the lattice Sternheimer factor and σ_2 represents the shielding of the 4*f* electrons from the crystalline field. The resolution of the paramagnetic hyperfine spectra was interpreted to show that electronic relaxation times were longer than 10^{-8} sec. (auth)

12303 MOESSBAUER EFFECT IN ^{159}Tb. **Woolum, J. C.; Bearden, A. J. (Cornell Univ., Ithaca, N. Y.). Phys. Rev., 142: 143-6(Feb. 1966).**

The linewidth of the Mössbauer resonance of the 58-kev radiation from ^{159m}Tb was measured with ^{159}Dy (as Dy_2O_3) and ^{159}Gd (as Gd_2O_3) sources and Tb_4O_7, Tb metal, and $Tb_2(CO_3)_3$ absorbers, all at 80°K. The measured linewidths, extrapolated to zero absorber thickness, are 5.0 ± 1.4 cm sec^{-1} for the Dy_2O_3-Tb_4O_7 system, 7.9 ± 1.8 cm sec^{-1} for the Dy_2O_3-$Tb_2(Co_3)_3$ system, and 11.5 ± 1.0 cm sec^{-1} for a 22 mg cm^{-2}Tb metallic absorber. A few measurements with a Gd_2O_3-Tb_4O_7 system gave 10.1± 1.0 cm sec^{-1} for a 27 mg cm^{-2}Tb_4O_7 absorber. The extrapolated value for the Dy_2O_3-Tb_4O_7 combination gives a calculated lifetime for this state of $(9.6^{+3}_{-2}) \times 10^{-11}$ sec, in reasonable agreement with the value $(1.3 \pm 0.4) \times 10^{-10}$ sec determined by delayed-coincidence methods. A discussion of linebroadening mechanisms and a comparison with some other rare-earth Mössbauer observations as well as a discussion of the use of this Mössbauer resonance in low-temperature phonon experiments is included. (auth)

12304 POSSIBLE OBSERVATION OF ^{115}In NUCLEAR ELECTRIC HEXADECAPOLE TRANSITIONS. **Mahler, R. J. (National Bureau of Standards, Boulder, Colo.); James, L. W.; Tanttila, W. H. Phys. Rev. Lett., 16: 259-61(Feb. 14, 1966).**

Ultrasonically induced $\Delta m = \pm 3$ ^{115}In nuclear spin transitions were observed in a single crystal of InAs. It was proposed that the $\Delta m = \pm 3$ transitions are due to the ^{115}In nuclear hexadecapole moment. (G.O.Y.)

12305 EVIDENCE FOR THE EXISTENCE OF Cr^{2+} AND Cr^{4+} IN X-IRRADIATED RUBY. **Mason, D. R.; Thorp, J. S. (Univ. of Durham, Eng.). Proc. Phys. Soc., 87: 49-53(Jan. 1966).**

The effect of x irradiation on the spin-lattice relaxation times of transitions between the lowest spin levels of Cr^{3+} in $\alpha-Al_2O_3$ was examined. The values for the first-order transitions at 4.2°K are reduced by a factor of ten after x irradiation. Comparison of the properties of orange rubies grown from the vapor phase and produced by x irradiation of pink ruby indicates that this is due to the conversion of some of the Cr^{3+} into Cr^{4+} and Cr^{2+}. (auth)

12306 F-CENTER PRODUCTION IN ALKALI HALIDES BY ELECTRON-HOLE RECOMBINATION AND A SUBSEQUENT [110] REPLACEMENT SEQUENCE: A DISCUSSION OF THE ELECTRON-HOLE RECOMBINATION. **Pooley, D. (Atomic Energy Research Establishment, Harwell, Eng.). Proc. Phys. Soc., 87: 245-56(Jan. 1966).**

A model for F-center production in alkali halides by ionizing radiation is discussed. The energy required for the formation of the defect is given to an anion in the radiationless recombination of an electron and a hole, which takes place via an exciton state. The primary products of this mechanism are negative ion interstitials and corresponding vacancies. The separation of the ion from the vacancy is achieved by a replacement sequence along a [110] direction. The radiationless transition is discussed in detail, and its properties are seen to explain many hitherto inexplicable results of experiments in F-center production. (auth)

12307 [110] ANION REPLACEMENT SEQUENCES IN ALKALI HALIDES AND THEIR RELATION TO F-CENTER PRODUCTION BY ELECTRON-HOLE RECOMBINATION. **Pooley, D. (Atomic Energy Research Establishment, Harwell, Eng.). Proc. Phys. Soc., 87: 257-62(Jan. 1966).**

It was shown previously that radiationless electron-hole recombination in alkali halides might provide energy for the formation of negative ion vacancies. A [110] replacement sequence provides an efficient method for separation of the interstitial from the vacancy and is particularly suitable for defect formation by electron-hole recombination. Two-body calculations of the replacement thresholds, including only short-range repulsive interactions, are discussed. A computer simulation of the [110] replacement sequence, including the effects of long-range Coulomb forces, was carried out. The results of this simulation indicate that in many of the alkali halides, within broad limits of variation of the interaction forces, replacement thresholds are about 4 to 5 ev. In other alkali halides, such as NaI, much higher values are calculated, while the alkaline earth oxides give values of several tens of electron volts. (auth)

12308 CORRECTIONS FOR X-RAY ABSORPTION BY A CRYSTAL OF ARBITRARY SHAPE. **Wuensch, Bernhardt J. (Massachusetts Inst. of Tech., Cambridge); Prewitt, C. T. Z. Kristallog., 122: 24-59(Oct. 1965). (In German).**

A direct procedure, designed for application in high-speed computation, is described for the determination of x-ray absorption corrections in the equi-inclination Weissenberg, Eulerian orienter, and precession geometries. Crystal shapes with re-entrant angles may be treated. The main restriction on the specimen shape is that it be representable by a combination of functions that may be expressed analytically. Unit vectors are established, relative to the crystal, in the directions of both the incident and diffracted beams for each reflection. These vectors are expressed in terms of reciprocal-cell dimensions in a form that may be evaluated by a computer. Distances from each grid point to the surface of the crystal are determined as multiples of these vectors and are summed to evaluate the transmission factor. (auth)

12309 DIFFRACTION EXPERIMENTS WITH SLOW NEUTRONS. **Landkammer, Franz Josef (Technische Hochschule, Munich). Z. Phys., 189: 113-37(1966). (In German).**

Investigations on the possibility of determining the slow neutron diffraction index of various substances using a neutron interferometer lead to the result that the presence of two separated but completely similar samples (Al, quartz, or bismuth of approximately 1 cm thickness) in the two geometric beams of the interferometer makes the

interference figure disappear. In thin samples of approximately 2 mm thickness the interference figure partially reoccurs again. A series of studies, principally defraction experiments, on simply shaped barriers was carried out in order to prove whether this extinction effect was caused by the beam geometry on the separation layers between the samples. The research did not permit such an explanation; rather in the defraction a process seems to appear which disturbs the coherence. A conceivable process of this type is, for example, an energy change of 10^{-13} ev. A theoretical explanation for such an effect was not found. (tr-auth)

12310 MAGNETIC PROPERTIES OF SINGLE AND POLYCRYSTALLINE PRASEODYMIUM DISELENIDE $PrSe_2$. Chechernikov, V. I.; Pechennikov, A. V.; Kalitin, V. I.; Yarembash, E. I. (Moscow State Univ.). Zh. Eksp. Teor. Fiz., 49: 1399-1401(Nov. 1965). (In Russian).

The magnetic properties of single crystal and polycrystalline praseodymium diselenide are investigated at temperatures between 77 and 300°K. It is found that the magnetic susceptibility is greater in a direction parallel to the single crystal c axis than in the perpendicular direction. It is also shown that the effective atomic magnetic moment P_p of the compound corresponds to the magnetic moment of the triply charged praseodymium ion (3.62 μ_B) and the paramagnetic Curie point Θ_p is negative in both the single crystal and polycrystalline samples in a direction perpendicular to the c axis. (auth)

12311 SPIN DIFFUSION OF NUCLEI IN DOUBLE ELECTRON-NUCLEAR RESONANCE. Dovgopol, S. P.; Izyumova, T. G. (Ural Polytechnic Inst., USSR). Zh. Eksp. Teor. Fiz., 49: 1483-91(Nov. 1965). (In Russian).

Double electron-nuclear resonance in a system with hyperfine interaction is considered. Spin diffusion is assumed to be the mechanism of transfer of excitation from remote nuclei to the paramagnetic centers. The correlation function of the nuclear system is calculated for this relaxation mechanism. Corrections to the relaxation times of the electron system due to spin diffusion are found. The susceptibility of the electron system is calculated. (auth)

12312 BEHAVIOR OF A SEMICONDUCTOR IN A STRONG RESONANCE RADIATION FIELD. Chel'tsov, V. F. Zh. Eksp. Teor. Fiz., 49: 1492-4(Nov. 1965). (In Russian).

The susceptibility $\kappa(\omega)$ of the valence electrons of an intrinsic semiconductor interacting with a free radiation field (stationary state) is determined. The carrier distribution function is found. The saturation effect, which follows from the expression for κ, results in stabilization of the frequencies of the proper field oscillations. (auth)

12313 SUPPRESSION OF INELASTIC CHANNELS IN RESONANCE SCATTERING OF NEUTRONS IN REGULAR CRYSTALS. Kagan, Yu.; Afanas'ev, A. M. Zh. Eksp. Teor. Fiz., 49: 1504-17(Nov. 1965). (In Russian).

A dynamic theory is developed that describes the motion of neutrons in a regular crystal when the interaction between the neutron and a nucleus is predominantly of a resonance nature. The effect of suppression of inelastic channels and the distribution of intensity of the nuclear reaction with varying depth in the crystal are analyzed in detail. The problem is solved by taking into account vibration of the nuclei in the crystal and also spin and isotopic incoherence. (auth)

12314 ON THE INVESTIGATION OF NUCLEAR QUADRUPOLE INTERACTION IN MOSSBAUER EFFECT EXPERIMENTS. Hien, Fam Tsui (Hanoi Teacher's Inst., North Vietnam). Zh. Eksp. Teor. Fiz., 49: 1576-80(Nov. 1965). (In Russian).

Some kinematic effects in resonance absorption and scattering in the presence of nuclear quadrupole interaction are considered. Methods for determining all the characteristic quadrupole interaction parameters from the Mössbauer resonance absorption and scattering spectra in single crystals and polycrystals are proposed. These methods are convenient even in the case when quadrupole interaction is small and results only in a broadening of the Mössbauer lines. (auth)

12315 MOESSBAUER STUDIES OF SOLID SOLUTIONS OF ^{119}Sn IN NOBLE METALS AND OF ^{57}Fe AND ^{119}Sn IN Fe–Sn ALLOYS [Thesis]. Werkheiser, Arthur Henry Jr. Knoxville, Tenn., Univ. of Tennessee, 1965. 198p.

A study of the electronic structure of dilute solid solutions of Sn in Cu, Ag, and Au was performed using the Mössbauer effect isomer shift for ^{119}Sn. The values of the isomer shifts measured with respect to a metallic Sn source were for 7.4% Sn in Cu, -0.741 ± 0.055 mm/sec; for 8.4% Sn in Ag, -0.326 ± 0.045 mm/sec; and for 6.5% Sn in Au, -0.453 ± 0.050 mm/sec. By assuming that the impurity (Sn) in the alloy will present to electrons a square potential well with respect to the rest of the metal, calculations can be performed to determine the size of this effective square well. By use of the Friedel sum rule and the $l = 0$ phase shift calculations of Blatt for the residual resistivity due to Sn, the well depths were determined and found to contain one bound s-state for the Sn impurity in each metal. The s electron density at the nucleus of Sn for the bound states can account for the measured isomer shifts. The nuclei in magnetically ordered materials have large hyperfine magnetic fields due principally to the Fermi contact term for s type electrons. The role of the conduction electrons for Fe–Sn alloys in the production of this field was studied. Measurements of the hyperfine magnetic fields and isomer shifts were made on Fe_3Sn and FeSn. These measurements and measurements on Fe, Fe(1%Sn), Fe(4%Sn) and $FeSn_2$ by other workers in the field were correlated in a simple model where the magnetic polarization of the conduction electrons is proportional to magnetic moment of the 3d band and the hyperfine fields are all assumed negative. In this model, the magnetic polarization of the conduction electrons was found to be negative at the Fe atom in Fe(1%Sn), Fe(4%Sn), and Fe_3Sn. These three alloys are ferromagnetic, and had observed hyperfine splittings such that $|H_{eff}| \simeq 330$ kG. The antiferromagnetic alloys FeSn and $FeSn_2$ had $|H_{eff}|$ considerably lower, near 150 kG, and a positive local conduction electron polarization was required in this model to explain $|H_{eff}|$. No simple correlation was found for the measured effective field in Sn and the conduction electron polarization of the alloy as determined above. (Dissertation Abstr.)

12316 MOESSBAUER EFFECT INVESTIGATIONS OF THE MAGNETIC PROPERTIES OF SINGLE CRYSTAL THULIUM ETHYLSULPHATE [Thesis]. Snively, Frank Thomas. Pasadena, Calif., California Inst. of Tech., 1965. 56p.

Mössbauer effect experiments were performed on a single crystal of paramagnetic thulium ethylsulfate with a magnetic field applied. The effect of the electric field of the surrounding ligands in the crystal, as determined from published optical spectroscopic data, combined with the effect of an externally applied magnetic field, was used to compute the electron wave function of the thulium ion, yielding, within numerical factors, the electric field gradient and magnetic field at the nucleus. The nuclear hyperfine splittings and transition intensities were computed as a function of the ratio of quadrupole interaction energy to the magnetic interaction energy for magnetic fields parallel and perpendicular to the (zz) axis of the electric field gradient tensor. The results of these calculations were compared with experiment. It was found that the ratio of internal magnetic field to external magnetic field varies by a factor of at least 35 as the orientation of the crystal is changed. When the field was applied perpendicular to the z-direction, which gave the maximum internal field, the ratio of internal to external field was found to be 73 ± 7 at 6.5°K. The most significant result is the measurement by a new technique, of the radial integral appearing in the nuclear magnetic hyperfine interaction $\langle r^{-3} \rangle_M$. The numerical value was found to be $\langle r^{-3} \rangle_M = 11.1 \pm 1.0$ atomic units. Other possible applications of the use of magnetic fields with rare earth single crystals in Möss-

bauer effect investigations are discussed. (Dissertation Abstr.)

12317 FLUORESCENT LIFETIMES OF AND ENERGY TRANSFER BETWEEN EXCITED STATES OF RARE EARTH IONS IN CRYSTALS [Thesis]. Barasch, Guy Errol. Baltimore, Johns Hopkins Univ., 1965. 166p.

Fluorescent state lifetimes of rare earth ions in various lattices were measured with a stroboscopic sampling apparatus to a typical accuracy of ±2%. A modified xenon flash lamp pulsing at high repetition rates and a fast monochromator were used to excite ions to known levels. Particular fluorescence transitions were selected by a spectrometer and detected by a pulsed photomultiplier tube. Signals were averaged for long times to discriminate against noise and were recorded on a strip chart. Sampling times were adjusted to obtain a plot of logarithm-intensity versus time for which the inverse slope was the lifetime. A survey study was made of lifetimes at 4.2°, 77°, and 300°K, of all but four of the triply-ionized rare earths (the exceptions were Ce, Pm, Sm, Yb); two doubly-ionized rare earths were studied. The host lattice was most often $LaCl_3$; but YCl_3, La_2O_3, Y_2O_3, LaF_3, $Y_2(WO_4)_3$, $CaWO_4$, CaF_2, various garnets, and some of the pure rare earth chlorides were also used. The lifetimes ranged from 4.8×10^{-6} to 4.8×10^{-3} second. The lifetimes were correlated with the energy gaps below each fluorescent state in an attempt to compare radiative and non-radiative transition probabilities. In $LaCl_3$, non-radiative relaxation in which the lattice accepts an energy E from the ion is dominant for $E < 900$ cm^{-1} and significant for $E < 4000$ cm^{-1}. In YCl_3, partial quenching effects occur in a more restricted energy region: lattice relaxation is dominant for $E < 1500$ cm^{-1} and significant for $E < 2300$ cm^{-1}. The results are discussed in terms of the Debye lattice and possible impurities. The dependence of the measured lifetimes of Pr^{+3} in $LaCl_3$ on temperature and Pr^{+3} concentration was studied. For $^3P_0$, the data are explained by strong reabsorption of $^3P_0 - {}^3H_4$ fluorescence, which enhances the measured lifetimes over ionic lifetimes, and negligible lattice quenching. (Dissertation Abstr.)

12318 FERROMAGNETIC RESONANCE OF ^{3}He-IRRADIATED THIN METAL FILMS [Thesis]. Bailey, Glenn Charles. Washington, D. C., Catholic Univ. of America, 1965. 172p.

Ferromagnetic resonance measurements at 9.5 kmc were made on a number of iron, nickel, and iron–nickel alloy thin films before and (for the first time) after irradiation with 2-Mev ^{3}He particles. The film thicknesses varied from several hundred to several thousand angstroms. The ^{3}He particle flux was about $3 \times 10^{11}/cm^2$ and during the irradiation, the temperature did not exceed 81°C as determined by thin film thermocouples. The resonance field, H_0, and the half-width, ΔH, of the resonance lines were measured at room temperature. In general, H_0 decreased (by about 2 gauss, 20 gauss, and 75 gauss for the iron. Permalloy, and nickel films, respectively) as a result of the irradiation except for the composition range around 34% Ni where H_0 increased (by about 5 gauss). The changes in H_0 can be attributed to $\Delta\sigma$ and $\Delta\sigma_u$ (changes in the isotropic stress, σ, in the plane of the film and in the uniaxial stress, σ_u, in the film), assuming that λ and M (the saturation magnetostrictive constant and magnetization, respectively) do not change with irradiation. Arguments can be given to show that M probably does not change with irradiation. By irradiating films on different substrates (fused quartz, single crystal quartz, soft glass, and copper), it was discovered that the irradiation-induced volume change of the substrate has an effect on the change of σ. A large discontinuity in plots of $\Delta\sigma$ and $\Delta\sigma_u$ vs. composition was found around the $\lambda = 0$ composition (83% Ni) for films all on fused quartz substrates. The irradiation of films with different thicknesses and similar compositions gave no significant changes. However, irradiating the films in different magnetic states (demagnetized, remanent, and magnetically saturated) gave $\Delta\sigma_u$'s that were larger, the larger the magnetic induction of the film during irradiation. Irradiating in a magnetic field also rotated the easy axis of the film into the direction of the field applied during irradiation. In addition, changes in the angular dependence of H_0 and in the half-widths of the resonance lines were found. (Dissertation Abstr.)

12319 AN EPR INVESTIGATION OF VO^{+2} AND X-RAY PRODUCED V^{+2} IN TUTTON SALT [Thesis]. Borcherts, Robert Herman. Ann Arbor, Mich., Univ. of Michigan, 1963. 104p.

The electron paramagnetic resonance (EPR) spectrum of the vanadyl ion (VO^{+2}) in single crystals of $Zn(NH_4)_2(SO_4)_2 \cdot 6H_2O$ was studied and comparison of the x-irradiated VO^{+2} spectrum to V^{+2} in single crystals of $Zn(NH_4)_2(SO_4)_2 \cdot 6H_2O$ was made. Investigation, at 9.3 kmc, of the single crystals containing the vanadyl ion, VO^{+2}, showed that the vanadyl ion substitutes for the divalent zinc ion with its V–O axis oriented in one of three directions. The three directions have a population ratio of 20:5:1 with the larger two population positions having their axes at an angle of 77°48′ to each other and the third position having its V–O axis inclined at an angle of 98° to the other two. The rhombic spin Hamiltonian fits the experimental data well if the x, y principal axes of the g tensor are rotated 23°20′ from the x, y principal axes of the A tensor. The z axes of both tensors are assumed to coincide. The rhombic spin Hamiltonian constants (obtained at room temperature) vary slightly for each of the three positions. The three positions of the V–O axes suggested that the directions of these axes were the (1 1 1) directions of the octahedron of water molecules that surround it. Since the octahedron of water molecules is distorted each of the four positions is ordered in energy and thus in population. The lowest population position was not observed. An alternate description in which the vanadyl ion is surrounded by five water molecules is considered. Also observed was a five-line superhyperfine structure on the vanadyl resonances for a specified orientation of the magnetic field. This structure was found to be due to the protons of the surrounding water molecules. Upon x-irradiation of the crystals containing the vanadyl ion it was found that the x ray, or the subsequent high energy electron it produces, breaks the V–O bond resulting in a V^{+2} EPR spectrum having the same rhombic spin Hamiltonian constants and z axis orientation as crystals grown with V^{+2}. Measurements were also made on the V^{+2} (irradiated VO^{+2}) spectra in $Mg(NH_4)_2(SO_4)_2 \cdot 6H_2O$ and $ZnK_2(SO_4)_2 \cdot 6H_2O$. (A.G.W.)

12320 PROCEEDINGS OF THE NUCLEAR PHYSICS AND SOLID STATE PHYSICS SYMPOSIUM, CALCUTTA, FEBRUARY 8-13, 1965. [VOL. I]. SOLID STATE PHYSICS. Bombay, Atomic Energy Establishment, 1965. 309p. (CONF–650223(Vol.I)).

Separate abstracts were prepared for 8 of the 46 papers included. One other paper was previously abstracted for NSA(19: 22171). The remaining papers deal with studies of crystal structure, magnetic structure, and molecular structure. (G.O.Y.)

For abstracts of individual papers see: 10905 and 12321–12327.

12321 ELECTRON PARAMAGNETIC RESONANCE OF Eu^{2+} IN CdF_2 AND KCl. Lingam, K. V.; Nair, P. G.; Venkataraman, B. (Tata Inst. of Fundamental Research, Bombay). pp 15-21 of Nuclear Physics and Solid State Physics Symposium, 1965. Solid State Physics. Bombay, Atomic Energy Establishment, 1965.

The electron spin resonance of Eu^{2+} in CdF_2 was investigated experimentally, and the spin hamiltonian for Eu^{2+} was evaluated. It was found that the experimental results correspond to Eu^{2+} occupying a substitutional site in the CdF_2 lattice. A preliminary investigation of Eu^{2+} in KCl was also made. (D.C.W.)

12322 COVALENCY EFFECT OF LIGANDS OF RARE EARTH IONS IN CRYSTALS. Raychaudhuri, A. K.; Ray, D. K. (Saha Inst. of Nuclear Physics, Calcutta). pp 53-

61 of Nuclear Physics and Solid State Physics Symposium, 1965. Solid State Physics. Bombay, Atomic Energy Establishment, 1965.

The effects of overlap between the ligand and metal ion wave functions on the crystal field parameters of Pr^{3+} in $PrCl_3$ were studied using hydrogenic wave functions for the rare-earth 4f electron and the ligand electrons. It was found that the overlap effect should be included in paint-model calculations, together with the screening effect of the distortion of the 5s and 5p electrons of the rare earth ion under the crystalline field. (D.C.W.)

12323 NUCLEAR QUADRUPOLAR SHIELDING FACTORS FOR RARE EARTH IONS IN CRYSTALS. Ghatikar, M. N.; Raychaudhuri, A. K.; Ray, D. K. (Saha Inst. of Nuclear Physics, Calcutta). pp 131-5 of Nuclear Physics and Solid State Physics Symposium, 1965. Solid State Physics. Bombay, Atomic Energy Establishment, 1965.

The nuclear quadrupolar shielding factor was calculated for Pr^{3+} and Tm^{3+} with the following excitations: 5p → p; 4p → p; 5p → nf; and 5s → nd. The results show a large amount of shielding. (D.C.W.)

12324 KNIGHT SHIFTS IN RARE-EARTH-TIN INTERMETALLIC COMPOUNDS. Dharmatti, S. S.; Rao, V. Udaya Shankar; Vijayaraghavan, R. (Tata Inst. of Fundamental Research, Bombay). pp 152-6 of Nuclear Physics and Solid State Physics Symposium, 1965. Solid State Physics. Bombay, Atomic Energy Establishment, 1965.

The tin Knight shifts and the magnetic susceptibilities of $CeSn_3$, $LaSn_3$, $NdSn_3$, $PrSn_3$, $SmSn_3$, and USn_3 were measured from room temperature to 100°K. (D.C.W.)

12325 NUCLEAR MAGNETIC RESONANCE IN RARE-EARTH NITRATES A COMPARISON WITH TRANSITION METAL NITRATES. Bose, Monisha; Chatterjee, Nikhilesh; Das, Nemai (Saha Inst. of Nuclear Physics, Calcutta). pp 162-9 of Nuclear Physics and Solid State Physics Symposium, 1965. Solid State Physics. Bombay, Atomic Energy Establishment, 1965.

Nitrogen-14 nuclear magnetic resonance was investigated in transition-metal nitrates with unpaired 3d electrons and rare-earth nitrates with unpaired 4f electrons in concentrated aqueous solutions. (D.C.W.)

12326 THE COMPLETE ABSORPTION TECHNIQUE IN THE MEASUREMENT OF ABSOLUTE RECOIL-LESS FRACTION "F" IN THE MOESSBAUER EFFECT. Fatehally, R.; Sastry, N. P.; Nair, L.; Nagarajan, R. (Tata Inst. of Fundamental Research, Bombay). pp 203-9 of Nuclear Physics and Solid State Physics Symposium, 1965. Solid State Physics. Bombay, Atomic Energy Establishment, 1965.

The "Mössbauer black absorber" technique developed by Dash for Debye-Waller factor measurements is described, together with the extension of the technique to the measurement of the Lamb-Mössbauer factor. (D.C.W.)

12327 NEUTRON DIFFRACTION STUDY OF THE CRYSTAL STRUCTURE OF BERYLLIUM SULPHATE TETRAHYDRATE. Sikka, S. K. (Atomic Energy Establishment Trombay, Bombay). pp 280-5 of Nuclear Physics and Solid State Physics Symposium, 1965. Solid State Physics. Bombay, Atomic Energy Establishment, 1965.

The crystal structure of beryllium sulfate tetrahydrate was investigated using neutron diffraction. Position and temperature parameters were determined, together with bond lengths and angles. (D.C.W.)

REACTOR TECHNOLOGY

General

12328 (ANS–100(Suppl.)) FAST REACTOR TECHNOLOGY. NATIONAL TOPICAL MEETING, DETROIT, MICHIGAN, APRIL 26–28, 1965. (American Nuclear Society, Detroit, Mich.). 118p. (CONF–650417(Suppl.)). American Nuclear Society, Michigan.

Eleven papers and discussions are included; separate abstracts have been prepared for 9. The remaining 2 discussions are of a cursory nature. (T.F.H.)

For abstracts of individual sections see: 11365, 12336, 12345, 12439–12443, and 12512.

12329 (TID–8541) REACTOR TECHNOLOGY. Selected Reviews—1965. Link, Leonard E. (ed.) (Argonne National Lab., Ill.). Jan. 1966. Contract W-31-109-eng-38. 445p. Dep. mn. CFSTI $4.50 cy, $0.75 mn.

Separate abstracts were prepared for the five included sections. (M.O.W.)

For abstracts of individual sections see: 11035, 11241, 12330, 12363, and 12519.

12330 (TID–8541, pp 321-425) SODIUM TECHNOLOGY. Goldmann, Kurt; Minushkin, Bertram (United Nuclear Corp., White Plains, N. Y. Development Div.).

A review is presented of sodium technology that was developed in conjunction with the design, construction, and operation of the following liquid-metal-cooled reactors; SRE, HNPF, EBR-I, EBR-II, EFFBR, LAMPRE-I, DFR, BR-5, and Rapsodie. Reviewed are materials technology, such as materials selections, corrosion, control of sodium purity, and the experience gained in these areas with operating plants. Other aspects of sodium technology, such as sodium components, safe handling procedures, and heat transfer are not covered, or they are only briefly summarized. (M.O.W.)

12331 EXAMINATION OF THE CRITICAL SUPERFICIAL HEAT LOAD AND OF THE BOILING HEAT TRANSFER IN THE CASE OF ORGANIC COOLING AGENTS. Szentgyoergyi, Istvan. Magyar Tud. Akad. Kozp. Fiz. Int. Kozlemen., 13: 259-71(1965). (In Hungarian).

The heat transfer properties of a number of organic coolants, such as diphenyl, diphenyl–diphenyl methane, diphenyl–diphenyl oxide, gas oil, and terphenyl, were investigated with special attention to the superficial boiling heat exchange and the burnout heat flux. A previously described apparatus (KFKI Kozlemen. 11, 21 (1963)) was used for the study of the forced-circulation heat exchange, employing a special pressure-transmitting system for the determination of the vapor pressure of the high-melting di- and terphenyl. The boiling heat transfer of fuel elements immersed in a nonflowing liquid was determined rapidly, requiring less material than needed for the forced-circulation system. Steps were taken to prevent burnout. The burnout heat flux is the chief factor limiting the maximum amount of heat to be removed from a fuel element because the coalescence of the bubbles at the surface forms an insulating layer that results in a sudden increase of the fuel element's temperature and causes its burning. The effect of undercooling, pressure, impurities and flow velocity on the heat exchange was determined. The boiling curves obtained indicated that the ratio of the burnout and transition fluxes is small. Although the heat exchange is improved as the result of the bubble formation, the permissible heat flux in the organic-cooled reactor (taking the safety factor into consideration) is not. It is concluded that only convective heat transfer can be carried out with organic cooling agents. The situation appears to be somewhat more favorable in the case of the little examined terphenyls, especially if they contain radiolytic and pyrolytic polymers because in their case the transition flux is lower and the burnout flux is higher than in the case of the other cooling agents. (TTT)

12332 LEAK TIGHTNESS OF REACTOR BUILDINGS. Crespi, M. A. (Junta de Energia Nuclear, Spain). Nucl. Eng., 10: 434-7(Nov. 1965).

The factors on which the leakage rate of a containment structure depends are outlined, and some methods of measuring leakage rates are discussed. Leakage tests on the JEN-1 reactor building are summarized, and the application of testing methods is discussed. Expressions for the leakage rates of containment structure are included. (D.C.W.)

12333 PROCEDURES FOR CONSIDERING ABNORMAL REACTOR BEHAVIOR IN SITE EVALUATION. Nucl. Eng. Bull., 1-15(Dec. 1963).

Procedures for estimating damage to persons and property in the environs of a reactor plant in the event of an accidental release of activity are presented, and requirements for plant and site compatibility are indicated. The general procedure is to determine the space-time concentration of radioactive materials and the beta-gamma field strengths at the time of, and subsequent to, the accident. From these the potential radiation exposure to individuals is determined and compared with limiting criteria. The possibility of extensive contamination of land, food, water, and industrial complexes from the standpoint of long-range injury, loss of use, and disruption of the lives of regional inhabitants is also considered. A program of onsite meteorological measurements is suggested in an appendix. (A.G.W.)

12334 STATUS OF SPACE-TIME ANALYSIS. Kerlin, T. W. Nucl. Safety, 6: 395-8; 403-4(Summer 1965).

The status of space-time reactor analysis is reviewed. Various analytical methods are described, and commonly used terminology is introduced. Discussions are included on adiabatic approximations, nodal analysis, modal analysis, and flux synthesis. (J.R.D.)

12335 DESIGN PRECEPTS FOR ENGINEERED SAFEGUARDS. Hanauer, S. H. (Univ. of Tennessee, Knoxville). Nucl. Safety, 6: 408-11; 420(Summer 1965).

Engineered safeguards are discussed that are applicable to nuclear power plants to make them acceptable for locations where they would otherwise be unacceptable because of public health and safety. Discussions are included on required reliability, applicability of safety-system concepts, and design precepts. (J.R.D.)

12336 THE U.S. FAST REACTOR PROGRAM—A CURRENT VIEW. Vander Weyden, Allen J. (Atomic Energy Commission, Washington, D. C.). pp 10-14 of ANS–100(Suppl.).

The state of the art of fast reactors in the U. S. is reviewed. (T.F.H.)

12337 REACTOR SAFETY REVIEW ORGANIZATION. Larson, H. J. (General Electric Co., Pleasanton, Calif.). 22p. (CONF-650710–13). ORINS. Gmelin, AED-CONF-65-192-9.

From American Nuclear Society Meeting on Reactor Operating Experience, Jackson Lake Lodge, Wyo.

The present nuclear safety review organization used at the Vallecitos Atomic Laboratory includes two independent internal review groups: a line nuclear safety organization and a management-established review body called the Laboratory Safeguards Group. Functions and procedures of each of these groups are reviewed. Examples of the types of programs reviewed and advantages and disadvantages of this type organization are listed. (A.G.W.)

Auxiliaries and Components

Refer also to abstracts 11110 and 12275.

12338 (GEAP–4911) REACTOR PRIMARY COOLANT SYSTEM RUPTURE STUDY. Quarterly Progress Report No. 1, April–June 1965. (General Electric Co., San Jose, Calif. Atomic Power Equipment Dept.). July 1965. Contract AT(04-3)-189. 84p. Dep. mn; CFSTI $3.00 cy, $0.75 mn.

The reliability effort was devoted to determining the probability of piping failure occurrence. Initial efforts were directed toward formulating a basic reliability model and developing an initial list of those factors which are potential failure causes. A major objective of the stress analysis task is the development of a method for the rational stress and strain analysis of piping components which are, at present, intractable problems. Work was initiated on a digital computer program to handle such problems. The fracture mechanics effort is devoted to extending the technology to define the behavior of ductile materials. A state of the art review was conducted in which the published results of fracture mechanics and plastic instability studies by others is examined. Various testing methods used in evaluating fracture toughness parameters were compared, and an initial test program for evaluating pipe materials was defined. A review of the currently available relationships for describing fatigue crack growth rates was performed. Fatigue crack growth rate data for carbon steel materials were compiled and evaluated. The prototype testing program was reviewed. Experimental requirements were defined and design of a test facility was initiated. (J.R.D.)

12339 (EURFNR–11F) STEAM GENERATORS ASSOCIATED WITH SODIUM-COOLED REACTORS. Robin, M. G. (Commissariat a l'Energie Atomique, Fontenay-Aux-Roses (France). Centre d'Etudes Nucleaires). Translation of report CEAR–156. Nov. 1964. 37p. Dep. mn. CFSTI $2.00 cy, $0.50 mn.

Work Performed under United States–Euratom Fast Reactor Exchange Program.

Problems involved in the choice of a steam generator for use with sodium-cooled reactors are discussed. Consideration is given to vaporization in the case of forced flow of water in a tube, and the principal solutions proposed for realizing once-through steam generators are given. (P.C.H.)

12340 USE OF CONCRETE FOR HIGH-TEMPERATURE REACTOR SHIELDING. Dubrovskii, V. B.; Krasnoyarov, N. V.; Kulakovskii, M. Ya.; Pergamenshchik, B. K.; Pinkhasik, M. S.; Savitskii, V. I. At. Energ. (USSR), 19: 524-9(Dec. 1965). (In Russian).

The possibility of constructing the thermal shielding of a reactor from chromite and chamotte heat-resistant concretes is studied. Neutron fluxes of various intensities (up to 10^{13} n/cm^2 sec, with spectrum close to a fission spectrum), passing through shielding of these materials, are examined. The penetration of neutrons, gamma fluxes, and heat release in the shielding is computed. Temperatures in the shielding are calculated for various neutron fluxes, concrete thicknesses, and cooling conditions. A static calculation of design thermal stresses of shielding of heat-resistant reinforced concrete is carried out. It is determined that reactor shielding can be constructed from heat-resistant reinforced concrete for neutron fluxes up to 10^{13} n/cm^2 sec, temperatures up to 1000 to 1100°C, and temperature drops up to 900°C. (tr-auth)

12341 GAS-COOLED REACTORS—A COMPARISON OF COOLANTS. Deubel, K. L. (Kernforschungszentrum, Karlsruhe, Ger.). Atomkernenergie, 11: 6-14(Jan.-Feb. 1966). (In German).

The criteria determining the thermodynamical suitability of gases as coolants are the heat transfer coefficient and the pumping power. Both criteria were brought into a relationship with each other and the necessary pumping powers for equal heat transfer coefficients as well as the heat transfer coefficients for equal pumping powers were calculated. The temperature rise of the gas may be taken as another criterion. Numerical calculation of the ratios of heat transfer coefficients, pumping powers and temperature rises was carried out for the gases argon, carbon-dioxide, air, nitrogen, steam and hydrogen as related to helium as a reference gas. The comparison was made for turbulent flow in two different assemblies, channels and packed beds of spheres. (auth)

12342 OPTIMIZATION WITH RESPECT TO WEIGHT FOR SHIELDS FOR LARGE REACTORS. Sasse, S. (Technische Hochschule, Hanover). Atomkernenergie, 11: 71-9(Jan.-Feb. 1966). (In German).

A reactor shield of minimum weight is determined. Only arrangements of two materials are discussed; one of which is suitable for attenuation of neutrons but not for γ rays, the other has the opposite attenuation qualities. The optimum shield consists of regions containing either pure materials or a mixture of materials with equal attenuation coefficients for neutrons and γ rays. (auth)

12343 APPROXIMATE METHOD FOR THE EVALUATION OF THE OVER-PRESSURE IN THE PRIMARY CIRCUIT OF A PRESSURIZED WATER REACTOR. Oliveri, E.; Benincasa, G. (Univ., Palermo, Italy). Ing. Nucl., 6: 183-91(July-Aug. 1965). (In Italian).

The function of pressurization is reviewed briefly together with some possibilities of practical devices. The theory of functioning of pressurization developed by Glasser is reported and the difficulty of applying it to concrete cases without the use of electronic computers is shown. Some simplifications to the final equation of the theory are introduced that do not disturb the essence of the phenomenon under examination. These simplifications lead to two equations that are applied alternately (method of finite differences). With them the development of the phenomenon during the phase of water input can be followed in time. A numerical example is given. (tr-auth)

12344 DESIGN OF REACTOR PERIOD METER. Kaneko, Eiji (Hitachi Ltd., Tokyo). Nippon Genshiryoku Gakkaishi, 7: 616-21(Nov. 1965). (In Japanese).

Several design factors of period meters for nuclear reactors are analyzed. Using the results, a transistorized period meter was developed. The input signal level is 0.5 v/decade; the period range is −15 to +3 sec; the stability of the period output for ambient temperature, −10 to +60°C, and a-c line voltage of 85 to 115 v is ±1%; the drift of period output is ±0.1%/10 hr; the hysteresis of the period scram level is ±0.1%; and the stability of the period scram level for ambient temperature, −10 to +60°C, and a-c line voltage of 85 to 115 v is ±11%. (auth)

12345 FIRST RESULTS ON THE COMPARATIVE VALUE OF SODIUM, STEAM AND HELIUM AS FAST REACTOR COOLANTS. Smidt, D. (Kernforschungszentrum, Karlsruhe (West Germany)). pp 27-8 of ANS–100(Suppl.).

Results of a panel discussion on the comparative performances of steam, He, CO_2, and Na as coolants for fast reactors are noted. (T.F.H.)

12346 A NEW CONCEPT FOR NUCLEAR REACTOR CONTAINMENT. Fistedis, Stanley H. (Argonne National Lab., Ill.). New York, American Society of Civil Engineers, 1965, Preprint No. 251, 14p., $0.50. (CONF-651036–2). ORINS.

From American Society of Civil Engineers, Environmental Engineering Conference and Annual Convention, Kansas City, Kan.

In the proposed concept for primary containment of a nuclear reactor, the biological shield is employed in a dual capacity. High strength steel strands are embedded in the concrete in the form of rows of horizontal hoops and vertical strands. The strands are placed in sheaths that prevent bonding to the concrete so that tension applied at one point is manifested in the entire length of the strand. Consideration of the destructive components of the hypothetical accident and the energy that can be absorbed by the proposed arrangement leads to the conclusion that both safety improvement and economy can be achieved in this way. (A.G.W.)

12347 METHOD FOR CONTROL OF NUCLEAR REACTORS. Shimojima, Hikaru (to Nippon Atomic Ind. Group. Co., Ltd.). Japanese Patent 1964-18481. Aug. 31, 1964. Filed Sept. 11, 1961.

A reactor control method is described that employs a hydrophobic slurry containing a neutron absorber for the reactor scram. The scram device consists of a tank containing a slurry of liquid paraffin and boron carbide powder (B_4C), compressed air (or nitrogen) bomb, pipe and valve, and channels for control plates in which the slurry is introduced. Other valves are used to agitate the slurry in the channels to insure homogeneity. Using this system, the reactor can be shut down safely by introducing the slurry into the channels. (TCO)

12348 CONTAINER OF NUCLEAR REACTOR. Kaga, Makio (to Hitachi, Ltd.). Japanese Patent 1964-27164. Nov. 27, 1964. Filed Sept. 7, 1962.

An improved water container for a reactor core is proposed. Using this container, the water level, especially near the container wall, can be kept about the same during accidental shock or vibration. Two plates with a large hole in the center are fixed onto the wall of the water container a little above the water level. The edge of the hole of the lower plate is bent downward, while the upper plate disposed a little distance above the first is simply an annular plate. (TCO)

12349 REACTOR CONTROL-ROD (OR OTHER ROD) DRIVE MECHANISM USING MAGNETIC CLUTCHES. Hamada, Hironari (to Meidensha Electric Mfg. Co., Ltd.). Japanese Patent 1964-27166. Nov. 27, 1964. Filed Mar. 29, 1962.

A rod drive mechanism is proposed in which the driving rod in the pressure tube is driven continuously within the limited space of the pressure tube by electromagnets outside the tube. Two devices, consisting of a movable cylindrical iron tube surrounding the driving rod within the tube which is held by top and bottom springs; a grabbing magnet outside the tube; and two magnets for raising or lowering the movable cylinder, operate in combination for the continuous drive of the drive rod and hence the control rod. (TCO)

12350 RI PRODUCTION AND STORAGE DEVICE. Motomiya, Kimio (to Hitachi, Ltd.). Japanese Patent 1964-27179. Nov. 27, 1964. Filed Aug. 16, 1963.

A pneumatic tube system for use in radioisotope production in a reactor includes a rotary body located between the reactor core and a capsule drawer having a number of storage holes along the circumference; a rod for inserting and withdrawing a capsule; a gear system connected to the rod and operated by a lever; cams with claws free to engage and disengage with the gear system; and a lever system having stoppers for the storage holes, which is engaged with the cams. Insertion, withdrawal, and storage of a sample are all done by means of a change of the handling-angle of the handle for the gear system. (TCO)

Criticality Studies

Refer also to abstracts 11932 and 12507.

12351 (ANL–7033) RIFF RAFF—A PROGRAM FOR COMPUTATION OF RESONANCE INTEGRALS IN A TWO-REGION CELL. Kier, P. H. (Argonne National Lab., Ill.). Aug. 1965. Contract W-31-109-eng-38. 66p. Dep. mn. CFSTI $3.00 cy, $0.75 mn.

A method of computing resonance absorption by a rod in a two-region cylindricalized cell that is not based on the assumption of an asymptotic neutron source distribution is developed and used to write a FORTRAN program RIFF RAFF (RP 359X), for the CDC-3600. An energy range of interest is divided into extremely narrow intervals of equal lethargy width. For each interval, the source distribution in each region is taken to be a three-term polynomial. By using this form for the source and the assumption that neutrons enter the rod isotropically, the reaction rates and the flux distribution for the interval are obtained. The reaction rates are accumulated over specified energy intervals to obtain resonance integrals; the flux distribution is used to obtain the source distribution for intervals at lower energies. RIFF RAFF allows for ten materials in each region. There can be four resonance absorbers in the rod, each having 60 resonances. The nonresonance materials can have 1/v absorption cross sections, with the restriction that for the moderator, the macroscopic absorption cross section must be small compared to the scattering cross section. The running time for a problem with 20 resonances and 4000 fine groups is about 2 min. (auth)

12352 (DP–958) XENON AND SAMARIUM TABLES. Occhipinti, Barbara B. (Du Pont de Nemours (E. I.) and Co., Aiken, S. C. Savannah River Lab.). July 1965. Contract AT(07-2)-1. 222p. Dep. mn. CFSTI $6.00 cy, $1.25 mn.

Tables are presented for calculating the reactivity transients that result from ^{135}Xe or ^{149}Sm poisoning in any thermal reactor that employs ^{235}U as the principal fissionable material. Xenon and samarium concentrations are given as a function of time in units of absorptions per fission neutron. Tables are also given for the change in reactivity held in xenon after step reductions in power. Thermal flux is expressed in units of megawatts from thermal fissions per kilogram of ^{235}U. These tables cover a range of power from 0 to 500 Mw/kg. (auth)

12353 (GA–6734) TEMCO—A FORTRAN PROGRAM FOR COMPUTING TEMPERATURE COEFFICIENTS. Todt, F. W. (General Atomic, San Diego, Calif. John Jay Hopkins Lab. for Pure and Applied Science). Dec. 28, 1965. Contract AT(04-3)-167. 94p. Dep. mn. CFSTI $3.00 cy, $0.75 mn.

TEMCO is a semiautomated procedure for obtaining temperature coefficients. Given cross-section libraries for each temperature to be considered, the code performs a series of one-dimensional diffusion calculations and then uses the results to generate the temperature coefficient. In addition to the temperature coefficient, the factors η, ϵ, p, f, and the temperature derivatives of these quantities are calculated. The code also computes the contribution of each individual nuclide to the temperature derivatives. The program was written in FORTRAN IV for the IBM 7044. (M.O.W.)

12354 (GAMD–6644(Add.)) BLOOST-5: A COMBINED REACTOR KINETICS-HEAT TRANSFER CODE FOR THE IBM-7044. Preliminary Description. Merrill, M. (General Atomic, San Diego, Calif. John Jay Hopkins Lab. for Pure and Applied Science). Nov. 9, 1965. Contract AT(04-3)-167. 5p. Dep. mn. CFSTI $1.00 cy, $0.50 mn.

Modifications were made in BLOOST-5 to permit using the heat transfer subroutines to describe the entire core instead of a single average fuel element. By representing the whole core in a two-dimensional temperature map, the temperatures reached in the hottest elements can be determined and various position-dependent weighting factors can be included in calculating reactivity feedback. Modifications to the program are included. (M.O.W.)

12355 (GAMD–6781) GAPS: A FORTRAN CODE FOR ANALYZING DATA FROM PULSED NEUTRON SOURCE EXPERIMENTS. Brown, J. R.; Van Howe, K. R. (General Atomic, San Diego, Calif. John Jay Hopkins Lab. for Pure and Applied Science). Oct. 11, 1965. Contract AT(04-3)-314. 45p. Dep. mn. CFSTI $2.00 cy, $0.50 mn.

GAPS, a FORTRAN IV-IBM 7044 program, will perform the following operations on the raw data counts obtained on a multichannel analyzer during a pulsed neutron source experiment on a multiplying assembly; make count loss corrections based on an input system resolving time for a Pulsed Neutron Logic Plug-in Unit, background subtraction of the corrected background, least squares fit an exponential to the decay of the fundamental mode, with the

beginning and end points of the fit being input numbers, and perform the integration and iterations required to obtain the subcritical reactivity and the β/Λ by the Garelis and Russell prescription. (M.O.W.)

12356 (IDO–17128) SAMPLING AND ANALYSIS OF FISSION PRODUCTS DURING THE LOSS-OF-FLUID TEST (LOFT). An Interim Report. Hunter, B. R.; Murri, E. L.; Matheney, G. B.; Palmer, J. F. (Phillips Petroleum Co., Idaho Falls, Idaho. Atomic Energy Div.). Dec. 1965. Contract AT(10-1)-205. 114p. Dep. mn. CFSTI $4.00 cy, $0.75 mn.

Numerous sampling systems were proposed for the Loss of Fluid Test (LOFT) program to establish the behavior of fission products within the containment building and the release to the environment. The current design of sampling devices that were proposed for LOFT is described. Considerable emphasis also is given to the problems associated with analyzing the thousands of samples that will become available during the test. Finally, the research and development programs that will be performed prior to LOFT are discussed. (M.O.W.)

12357 (KR–75) BIGG-II—A MULTIGROUP NEUTRON SPECTRUM AND CRITICALITY CODE. Tverbakk, O. P.; Doederlein, J. M. (Institutt for Atomenergi, Kjeller (Norway)). Sept. 1965. 67p. Dep. mn.

A description of the BIGG-II code in FORTRAN-63 for the CDC-3600 computer is presented. BIGG-II is a multigroup neutron spectrum and criticality homogeneous reactor code based on BIGG-I. It applies the B-1 or P-1 approximation with extended Greuling-Goertzel slowing down. Input data requirements were formulated that permit flexibility in the choice of physical approximations applied in homogenizing heterogeneous reactor lattices. A thermal neutron energy group is included. Input data are given explicitly. The calculation of resonance absorption and resonance fission was improved, as compared to BIGG BIGG-I, for better consistency with available resonance integrals. All fundamental nuclear data are contained in a cross-section library. Output is extensive and includes a.o. multigroup flux, leakage and slowing down spectra, elementwise absorption and production and few group diffusion constants, as well as multiplication factor and criticality parameters. (auth)

12358 (LA–3406) SPECTRAL INDICES OF A 4.29 per cent ^{235}U-ENRICHED URANIUM METAL EXPONENTIAL COLUMN. Steinke, R. G. (Los Alamos Scientific Lab., Univ. of California, N. Mex.). Sept. 3, 1965. Contract W-7405-eng-36. 21p. Dep. mn. CFSTI $2.00 cy, $0.50 mn.

The spectral indices or detector ratios and buckling values characteristic of the equilibrium neutron energy spectrum in a 4.29% ^{235}U enriched bulk of uranium metal were investigated. The 21-inch-diameter Los Alamos outdoor exponential column was utilized with the column and "Hydro" source reactor elevated some 11 feet above ground level. (auth)

12359 (ORNL-TM–1195) CRITICALITY OF A SINGLE UNIT OF AQUEOUS URANYL FLUORIDE SOLUTION ENRICHED TO 5 percent IN ^{235}U. Webster, J. Wallace; Johnson, E. B. (Oak Ridge National Lab., Tenn.). July 23, 1965. Contract W-7405-eng-26. 10p. Dep. mn. CFSTI $1.00 cy, $0.50 mn.

As a part of the continuing criticality program with uranium enriched to 5% in ^{235}U, a comparison between theory and experiment was made with regard to the criticality of a volume of aqueous $U(4.98)O_2F_2$ solution (H : ^{235}U = 496) contained in a thin-walled stainless steel cylinder. The solution had a height-to-diameter ratio of about 2.5, thus making the end leakage reasonably small compared to the radial leakage. Computations indicated that the end leakage from the finite system corresponded to only 1.5% in reactivity. One-dimensional calculations, with an approximate correction for end leakage, are therefore valid. The Carlson S_n (DTF) code with the Hansen-Roach 16-group cross sections was used for the calculation. The computed multiplication factor of 1.002 for the critical system lends further confidence to the method and to the cross section set. (auth)

12360 (ORNL-TM–1332) NEUTRON DENSITY FLUCTUATIONS INDUCED BY HYDRAULIC NOISE IN A NUCLEAR POWER REACTOR [Thesis]. Lawrence, Barry R. (Oak Ridge National Lab., Tenn.). [nd]. Contract W-7405-eng-26. 122p. Dep. mn. CFSTI $4.00 cy, $0.75 mn.

Submitted to Univ. of Tennessee, Knoxville.

A compressible fluid model was coupled with reactor dynamics equations to provide a basis for some theoretical studies of the effect of hydraulic noise on the neutron density of a nuclear reactor operating at power. The theory is particularly applicable to the ORNL HFIR and will aid in an understanding of the mechanism by which hydraulic noise induces appreciable neutron density fluctuations in this reactor. The technique is not strictly applicable to reactors in which extensive coolant boiling occurs, since the equations are applicable only to single-phase fluids. (M.O.W.)

12361 (PEL–60) COBRA—A COMPUTER CODE FOR THE CALCULATION OF FUEL DEPLETION IN HETEROGENEOUS NUCLEAR REACTORS. Engelbrecht, C. A.; Fiedeldey, H. (Atomic Energy Board, Pelindaba (South Africa)). Jan. 1965. 48p. Dep. mn.

COBRA is a FORTRAN II computer program for the calculation of burnup in reactor assemblies. A one-group formulation based on a modified four-factor formula and the cell method is used. The thermal utilization is calculated by means of diffusion theory in cylindrical geometry but transport corrections are included for air gaps and cladding cylinders. The streaming effect of air gaps is also taken into account. The burnup routine includes the poisoning effect of fission products as well as the formation of fissile plutonium isotopes. The code is intended for reactors using natural or slightly enriched uranium as fuel. Although a one-group approach is used, the influence of epithermal neutrons on the burnup and the effective multiplication factor is taken into account. The theoretical background of the calculations is presented. COBRA was written for an IBM-704 with an 8K memory capacity. (M.O.W.)

12362 (RFR–193) COMPARISON OF CONTROL ROD CALCULATIONS USING HOMOGENEOUS AND HETEROGENEOUS METHODS. Skardhamar, Torfinn (Aktiebolaget Atomenergi, Stockholm (Sweden)). May 17, 1962. 11p. Dep. mn.

The reactivity effects of fully inserted control rods in different radial configurations in clean, cold cores of the R-3 type were calculated using both the homogeneous method and the heterogeneous method. The results indicate that for fully inserted and symmetrically positioned control rods in a core of the R-3 type, the heterogeneous method of calculation is as adequate as the homogeneous method in determining the reactivity effects of varying the number of fuel elements and control rods. (D.C.W.)

12363 (TID–8541, pp 1-70) THE PHYSICS OF HEAVY-WATER LATTICES. Honeck, H. C. (Brookhaven National Lab., Upton, N. Y.); Crandall, J. L. (Du Pont de Nemours (E. I.) and Co., Aiken, S. C. Savannah River Lab.).

A review of programs in heavy water-lattice physics, including brief descriptions of existing heavy water reactors, the principal experimental programs, and the calculational schemes, is presented. A more detailed description of experimental physics methods, together with an exposition of typical experimental results, is presented. Also a detailed description of the calculational methods and the results of applying these calculations to heavy water lattices is presented. (M.O.W.)

12364 (UJV–1365/65) FLATTENING OF FLUX IN A HETEROGENEOUS SLAB REACTOR. Lelek, V. (Ustav Jaderneho Vyzkumu, Ceskoslovenska Akademie Ved, Rez). 1965. 18p. Dep. mn.

Method of calculation of a reactor with flattened flux by means of the Feinberg-Galanin heterogeneous method is investigated. It appears that the condition of flattened flux leads to the system of transcendental equations for pitches of elements considering the thickness of elements being the same. Elements are considered in the shape of infinite slabs. The equation system for pitches is iteratively solved. The zero approximation are pitches obtained from the homogeneous calculation which is "heterogenized" in a special way. The assumption was made that the resonance escape probability equals one. In accordance with the homogeneous calculation it appears that quantity of elements increases towards the center of the reactor. Compared with the usual result of heterogeneous calculation, critical dimensions decrease and are compensated by the increase of thickness of elements. (auth)

12365 (UJV-1438/65) AN APPLICATION OF THE MODIFIED S_N METHOD FOR INTRACELL THERMAL NEUTRON ABSORPTION DENSITY DISTRIBUTION. Bardos, J.; Vorisek, M. (Ustav Jaderneho Vyzkumu, Ceskoslovenska Akademie Ved, Rez). 1965. 18p. Dep. mn.

Results are presented of the numerical calculations of thermal neutron absorption density distribution in natural uranium-D_2O cells obtained by the S_N method applied to the one velocity Boltzmann equation. The methods of speeding-up the iteration process in connection with the stability and the convergence of the solution are included as well as some other factors which influenced the accuracy of results. The thermalization corrections are taken into account by means of the absorption cross section which is spatially dependent through the effective neutron temperature. Calculations for the case of the constant absorption cross section (effective neutron temperature 298°K) were performed for the sake of comparison. The disadvantage factors obtained from the spatial dependence of the thermal neutron absorption density are compared with the values obtained by other methods. (auth)

12366 (UJV–1439/65) CHANGE OF FLUX IN THE VICINITY OF IRREGULARITIES IN A REGULAR SQUARE LATTICE. Rocek, J. (Ustav Jaderneho Vyzkumu, Ceskoslovenska Akademie Ved, Rez). 1965. 26p. Dep. mn.

A numerical method for solution of the system of equations of a heterogeneous method for describing a regular square infinite lattice where one rod is exchanged for another rod of different qualities is described. A cylindrically symmetrical solution with the axis of symmetry in the perturbation rod which equals zero on the given boundary is sought and the eigenvalue of the problem is determined from this condition. By means of this method the influence of perturbation rod on flux in a heavy water reactor with natural uranium is calculated for a few variants. (auth)

12367 (UJV–1442/65) UEBER DIE VERTEILUNG DER NEUTRONENFLUSSDICHTE IN EINEM ZYLINDRISCHEN REAKTOR MIT TEILWEISE EINGETAUCHTEN REGELSTABEN. (On the Distribution of Neutron Flux Density in a Cylindrical Reactor With Partially Inserted Control Rods). Cermak, J. (Ustav Jaderneho Vyzkumu, Ceskoslovenska Akademie Ved, Rez). 1965. 15p. Dep. mn.

A method of calculating the efficiency of partially inserted control rods is generalized to the case of a reflected reactor with an asymmetric arrangement of rods. The method yields the buckling as well as the thermal-neutron flux and, in the case of the two-group formulation, the fast-neutron flux in the vicinity of channels provided with control rods. The value of both fluxes at any point can also be obtained. (D.C.W.)

12368 (WAPD-T–1737) AN EVALUATION OF A THREE-DIMENSIONAL FLUX SYNTHESIS METHOD AS A NUCLEAR DESIGN TOOL. Flanagan, C. A.; Smith, F. E.; Bogar, G. F.; Rutherford, C. H. (Bettis Atomic Power Lab., West Mifflin, Pa.). Oct. 1964. Contract AT(11-1)-Gen-14. 20p. (CONF-654–100). Dep. mn. CFSTI $1.00 cy, $0.50 mn.

From American Nuclear Society Meeting, San Francisco, Nov.-Dec. 1964.

Research is described towards evaluating the use of the weighted residual flux synthesis method in three-dimensional nuclear design calculations. The evaluation includes comparison of synthesis calculations with direct three-dimensional calculations, a comparison of results from synthesis calculations with experiment, and finally an examination of the practicality of applying the method to depletion calculations involving considerable geometric complexity. (auth)

12369 EVALUATION OF VARIATIONAL METHOD ACCURACY. Erykalov, A. N. At. Energ. (USSR), 19: 462-3(Nov. 1965). (In Russian).

A study is made of a variational method for determining critical reactor dimensions and neutron distributions, with which the upper and lower limits of the eigenvalue of the hermitian operator can be calculated. The high accuracy of the eigenvalues obtained using simple approximations is demonstrated for two examples. The accuracy is computed for a single-group diffusion equation for the case of constant cross section and consinusoidal flux distribution and the case of constant diffusion constant and cosinusoidal absorption and fission cross-section distribution. (M.J.T.)

12370 INFLUENCE OF THEORETICAL CROSS SECTIONS AND THERMAL SPECTRUM MODELS IN THE CALCULATIONS FOR WATER REACTORS CONTAINING PLUTONIUM. Loizzo, P.; Lopez, S.; Tondinelli, L. Comit. Naz. Energia Nucl., Notiz., 11: No. 8-9, 44-7 (Aug.-Sept. 1965). (In Italian).

The problems in the neutron calculation in a reactor containing ^{239}Pu and the difference with ^{235}U are examined. A general scheme for the calculation is proposed and this plan is optimized to the neutron cross section data used. A comparison is made between theory and experimental values for the Hanford critical experiments. (J.S.R.)

12371 THE EXISTENCE OF A DYNAMICS OF THERMAL NEUTRONS. SOME OBSERVATIONS AND CONSEQUENCES. Bucci, Pompeo (CAMEN, Pisa, Italy). Ing. Nucl., 6: 179-82(July-Aug. 1965). (In Italian).

The velocity of a thermal neutron leaving an accelerating source is determined with respect to a fixed target for three cases. The first is when the neutron leaves the source in the direction and on the side of the motion of the system; in the second, the neutron leaves the source in the direction but on the opposite side of the motion; and in the third the neutron leaves the source in a direction forming an angle with that of the motion. The first two cases correspond to an arrangement of the targets perpendicular to the direction of the motion, whereas the third case corresponds to a parallel arrangement. The case of a reactor in motion is also considered for both the perpendicular and the parallel arrangements. (J.S.R.)

12372 EFFECTIVE RESONANCE TEMPERATURE CORRELATION OF UO_2. Sha, William T. (Westinghouse Electric Corp., Pittsburgh). Nucl. Appl., 1: 538-45(Dec. 1965).

The effective resonance temperature (T_{eff}) correlation of UO_2 pellets based on experimental power coefficient data from PWR cores, namely, Yankee, Saxton, BR-3, and Selni, is presented. The correlation can predict the total power defect of reactivity from hot zero power to full power within experimental uncertainties and T_{eff} at any power level within ±80°F (±45°C), a magnitude which constitutes no more than ±6% of the value at full power for current PWR design. With the ±80°F uncertainty in T_{eff}, the magnitude of the power coefficient of reactivity can vary as much as ±30% in the low power region and ±20% in the high power region. This study indicates the temperature drop in the gap between the pellet and clad is much lower than the value calculated for it in the past. (auth)

12373 EIGENVALUE PROBLEMS OF REACTOR THEORY AND SPACE GROUPS. Kunze, Helmut (Technische Hochschule, Karlsruhe, Ger.). Nukleonik, 7: 429-36(Oct. 1965). (In German).

A study was made to determine, using the space group theory, the heterogeneous reactors for which one can detect from the symmetry of the material distribution the existence of a lattice of discrete points at which the site and energy dependence of the neutron flux are separable. The stationary neutron distributions of the heterogeneous and pertinent homogeneous reactors differ from each other in such lattices only by one factor dependent on the energy. A group-theory method for the determination of the degeneration degree of the eigenvalue of the governing equation for the neutron flux was described. (tr-auth)

12374 EFFECTIVE CROSS SECTION FOR CONSIDERATION OF THE RESONANCE SELF-SHIELDING IN GROUP CONSTANTS OF FAST REACTORS. Pucker, N. (Univ. Graz, Ger.). Nukleonik, 7: 436-42(Oct. 1965). (In German).

It is shown with the help of suitably defined effective cross sections how the temperature-dependent resonance self-shielding can be considered in heavy nuclei. This question is of importance for the determination of multigroup constants for fast reactors. Numerical results for ^{238}U and ^{239}Pu were presented. (tr-auth)

12375 SPACE-DEPENDENT FORMULA FOR ROSSI-α MEASUREMENTS. Otsuka, Masuhiko; Iijima, Tsutomu (Japan Atomic Energy Research Inst., Tokai-mura). Nukleonik, 7: 488-91(Oct. 1965).

A generalized formula for Rossi-α measurements is presented, in which the effect of higher-order decay modes and the spatial dependence of detectors are examined. Some modification is necessary to the well-known formula based on a one-point reactor model, even if a system is sufficiently small. (auth)

Design and Feasibility

Refer also to abstract 11222.

12376 NUCLEAR REACTOR. Murota, Kazuo (to Nippon Atomic Ind. Group. Co., Ltd.). Japanese Patent 1964-27163. Nov. 27, 1964. Filed Oct. 19, 1962.

An improved nuclear reactor is proposed in which the reactor core is surrounded by a reflector of a heavy metal having low neutron-moderating and -absorbing cross sections. The reflector is surrounded with a material of high moderating power. When the reactor becomes critical, the heavy metal melts due to the heat from the core. This molten metal serves as thermal shield, and at the time of an accident drops due to gravity to lower the reactivity for safety purposes. (TCO)

Fuels

Refer also to abstracts 10764 and 12407.

12377 (CEND-2863-236) THE DEVELOPMENT AND TESTING OF UO_2 FUEL SYSTEMS FOR WATER REACTOR APPLICATIONS. Progress Report for Period Ending March 31, 1965. Zuromsky, G.; Koziol, J. J.; Chernock, W. P. (Combustion Engineering, Inc., Windsor, Conn. Nuclear Div.). May 1965. Contract AT(30-1)-2863. 27p. (EURAEC-1413). Dep. mn. CFSTI $2.00 cy, $0.50 mn.

Work Performed under United States–Euratom Joint Research and Development Program.

Effort during the present reporting period was concentrated on only two tasks. The effort on the two remaining tasks was aimed at completion of an additional thermal conductivity test on UO_2 with an insulator between the heat sink and the UO_2 and the completion of the projection welding program. The thermal conductivity test was completed and analysis of test data is in progress. A process was developed for the projection welding of 2.13 meter (7 foot) long, 37-tube clusters of stainless steel tubing in a hexagonal arrangement. Tube-to-tube spacing tolerances were defined and a cluster is undergoing 3000 thermal cycle tests at a ΔT from rod to rod typical of that anticipated in a power reactor fuel assembly. Work on projection welding was extended to Zircaloy and results of autoclave tests for five days in 360°C water indicate a uniform black oxide in the region of the weld and the heat affected area. (auth)

12378 ON THE APPLICATION OF CARBIDES IN HIGH-TEMPERATURE REACTORS. Johannsen, K.; Kollekowski, J. (Technische Univ., Berlin). Atomkernenergie, 11: 15-18(Jan.-Feb. 1966). (In German).

The applicability of ceramic carbides for thermal high-temperature reactors, especially, is considered. Beryllium carbide has the best moderating properties followed by the carbides of zirconium and silicon. Unfortunately, the most carbides which are applicable, from nuclear aspects, as fuel matrix decompose at medium temperatures. Therefore, for nuclear reactor applications at very high temperatures, only the carbides of zirconium and niobium seem to be useful. (auth)

12379 USE OF PLUTONIUM IN THERMAL REACTORS. Kinchin, G. H. (United Kingdom Atomic Energy Authority, Winfrith, Eng.). Elec. Rev., 177: 712-14(Nov. 12, 1965).

Consideration is given to the use of ^{239}Pu as fissile material in thermal reactors. The reject fuel from civil power-producing reactors contains plutonium and it is anticipated that in the U.K. about 20 t of ^{239}Pu will be available by 1976. The main differences between the characteristics of reactors fueled with ^{239}Pu and ^{235}U are discussed. From the point of view of reactor design, the factors of major significance which must be taken into account in comparing plutonium and uranium enrichment are noted. A comparison is made of the costs of plutonium and uranium enrichment. Although the feasibility of burning plutonium in thermal reactors has been established, the potential economic gains may be altered by changes in the scale of the forecast generating program and the rate of introduction of fast reactors. (T.C.O.)

12380 OXIDATION BEHAVIOR OF DEFECTIVE FUEL ELEMENTS. Antill, J. E.; Peakall, K. A. (Atomic Energy Research Establishment, Harwell, Eng.). J. Nucl. Energy: Pt. A and B, 19: 935-47(Dec. 1965).

Oxidation of fuel by a reactive coolant inside a defective can was analyzed theoretically. Predictions of the analysis were largely confirmed by results of supporting experimental work on miniature fuel elements. The behavior of unbonded elements containing UC was studied in atmospheres of CO_2, steam, O_2, and an inert gas containing O_2. A similar study was performed for elements containing U. Attack is first governed by the transfer of reactive gas through the defect in the can. As a result of the volume expansion associated with the oxidation, the can normally splits after a period of time, allowing the gas free access to the fuel. Before can rupture the atmosphere inside the can is of paramount importance, and the attack is restricted to a low level if an inert gas atmosphere is maintained at the coolant pressure. Attack is then controlled by a slow inter-diffusion process through the defect which for all practical purposes is independent of total coolant pressure and temperature. With the miniature elements containing UC this condition was achieved in steam, argon containing 30% O_2, and in some instances CO_2. In cases where there is a partial vacuum inside the can and a considerable bulk flow of reactive gas through the defect, the addition of minor amounts (e.g., 10 vol %) of an inert gas to the coolant can be beneficial. (auth)

12381 NUCLEAR FUEL ASSEMBLY. Murota, Kazuo (to Nippon Atomic Ind. Group. Co., Ltd.). Japanese Patent 1964-27161. Nov. 27, 1964. Filed Oct. 3, 1962.

A nuclear fuel assembly is proposed, which provides easy failure detection and replacement. A number of fuel elements are enclosed in the assembly container with coolant flowing through between the elements and through

passages running along the sides of the container for the sample coolant. Coolant sampling exits are provided, and pipes are connected to the passages for drawing the coolant out of the reactor core. A grid supporting the fuel elements is penetrated by the coolant pipes. (TCO)

12382 REACTOR FUEL ELEMENT. Okamoto, Yoshizo (to Japan Atomic Energy Res. Inst.). Japanese Patent 1964-27162. Nov. 27, 1964. Filed Dec. 21, 1962.

An improved fuel bundle consisting of polygonal fuel rods with non-circular fins is proposed for use in gas cooled reactors. The polygonal fuel sheaths with fins fill the whole volume of the coolant passage so that the free path is fully used for heat transfer. The helical flow through the helical fins or vertical fins with skew grooves increases the heat conduction, and the uniform flow obtained by the rows of fins prevents production of hot spots. By orientating the helical fins of the adjacent sheaths in the same direction, the pressure drop of the coolant is reduced. With the fins on the fuel sheath serving as the ribs, no supports are required for the fuel rods to prevent the occurrence of hot spots. (TCO)

12383 HIGH TEMPERATURE THERMIONIC GENERATOR. Pidd, Robert W.; Yang, Ling; Ragone, David V. (to General Dynamics Corp.). U. S. Patent 3,218,487. Nov. 16, 1965. Filed Nov. 15, 1960.

A thermionic converter is patented that has an improved life, avoids permanent loss of hot electrode material, and is capable of efficient operation over extended periods of time at very high temperatures. The converter limits reductions in optical reflection coefficient and increases in the low work function of the cold electrode surface. A fuel body, e.g., any suitable nuclear fuel that is used as a heat source, having improved dimensional stability in use is incorporated in the hot electrode. (B.L.M.)

Power and Power-Breeder Reactors

Refer also to abstracts 10988 and 10990.

12384 (AGN-TM-411) ARMY GAS-COOLED REACTOR SYSTEMS PROGRAM. BOUNCE, AN IBM 7090 CODE TO CALCULATE FLUX DISTRIBUTIONS WITHIN MULTIPLE-PIN FUEL ELEMENTS BY THE METHOD OF SUCCESSIVE GENERATIONS. Wilcox, T. P. (Aerojet-General Nucleonics, San Ramon, Calif.). Nov. 1965. Contract AT(10-1)-880. 106p. Dep. mn. CFSTI $4.00 cy, $0.75 mn.

The BOUNCE code determines the neutron flux distributions within the pin bundle of a multiple-pin fuel element by using the method of successive generations. One energy group is used and all scattering within the pins is considered to be isotropic. Elements with 6, 7, 12, 13, 18, and 19 fuel pins, where each pin is composed of a central fuel pellet surrounded by a cladding material, may be treated by the code. The code neglects the properties of the coolant material around the pins; this, in effect, assumes that the coolant is a gas. The properties of an equivalent solid rod, having the same absorption as the pin bundle, are also determined. The equations of the successive generation method are derived for the cases of a solid rod and the multiple-pin fuel element. Comparison between results calculated by the code and those obtained experimentally for twelve 7- and 19-pin elements reveals good agreement. (auth)

12385 (AGN-TP-149) ML-1 SHIELD STUDY. Whittum, H. O.; Witthaus, J. K. (Aerojet-General Nucleonics, San Ramon, Calif.). [1965]. Contract AT(04-3)-368. 16p. (CONF-651101-50). Dep. mn. CFSTI $1.00 cy, $0.50 mn.

From 13th Conference on Remote Systems Technology, Washington, D. C.

Operational and twenty-four hour shutdown computed dose rates for the ML-1 reactor were compared to measured dose rates and dose rates computed during ML-1 design. The computational methods used and the results from these calculations are discussed. (M.O.W.)

12386 (APDA-176) ANALYSIS OF THE BABCOCK AND WILCOX FULL-SIZE STEAM GENERATOR FOR A SODIUM-WATER REACTION. Chase, W. L.; Ford, J. A.; Friedland, A. J.; Green, D. M.; Kovac, L. R.; Meyers, J. E. (Atomic Power Development Associates, Inc., Detroit, Mich.). Nov. 30, 1965. Contract AT(11-1)-1280. 188p. Dep. mn. CFSTI $5.00 cy, $1.00 mn.

An analysis of the effects of a sodium-water reaction in the steam generator was conducted. A leak in a tube of the unit would cause a sodium-water reaction which would result in the rapid generation of quantities of reaction products, including hydrogen, and high temperatures. The comprehensive mathematical models and supporting experimental tests developed to analyze a sodium-water reaction are discussed and data are presented on the effect of leak size, paths for reaction relief, and leak location on hydrogen pressure. The location and operating conditions for the reaction that would result in the most severe pressure transient from the complete severance of one tube is discussed and illustrated in detail with curves of the reaction data. The phenomena relating to leak propagation, i.e., mechanical damage, temperature softening of the tubes, and wastage, are discussed in terms of the mathematical models developed and the experimental tests conducted. The results from these analyses, coupled with estimates of leak detection, isolation, and dump times, are used to analyze the accidents which would result from initiating leaks of various sizes in the steam generator. (auth)

12387 (APDA-NTS-3) DETERMINATION OF THE SAFETY ROD DROP TIME IN THE ENRICO FERMI REACTOR. Horne, R. E.; Klickman, A. E. (Atomic Power Development Associates, Inc., Detroit, Mich.). Jan. 1965. 39p. Dep. mn.

The safety rod drop tests for the Enrico Fermi reactor were conducted on October 4 and 5, and November 11, 1963. The experimental method was based on an analysis of the flux decay in the reactor after the rod or rods had been dropped. From the data, three sets of results were determined: the time required for the seven safety rods, singly and in specified groups, to be inserted into the reactor; the effect of the reactor temperature and coolant flow rate on the drop time; and the reactivity worths of the rods. During the time a rod was dropped, a high-speed recording oscillograph was used to record the neutron responses of an in-core fission counter, and an ion chamber and BF_3 detector both of which were located outside the reactor in the graphite shield. In addition to recording the flux decay during the drop, the voltages across the latch-open microswitch and the latch magnet were recorded prior to and during the drop so that the exact time of rod release could be determined. Analysis of the results indicated that all measured drop times agreed closely with the predicted values. The time required to insert a safety rod after a manual scram ranged from 588 to 658 msec; the predicted time was 720 msec. Furthermore, no effect on the safety rod drop time was observed when the reactor coolant flow and temperature were varied. The measured worths of the individual safety rods ranged from $1.16 to $1.50, and the reactivity effect of inserting all seven safety rods simultaneously was approximately $8.00. The measured values average about 15% less than predicted. (auth)

12388 (APDA-NTS-6) WORTH MEASUREMENTS OF CORE AND BLANKET SUBASSEMBLY MATERIALS IN THE ENRICO FERMI REACTOR. Ball, G. L.; Daavettila, D. A.; Horne, R. E. (Atomic Power Development Associates, Inc., Detroit, Mich.). Sept. 1965. 45p. Dep. mn.

Measurements were made of the reactivity worths of ^{235}U and ^{238}U in the core, and of fuel and blanket subassemblies in the radial blanket of the Enrico Fermi reactor. The columnar reactivity worths of ^{235}U and ^{238}U were determined at various core positions by means of reactivity measurements made using specially constructed subassemblies. The reactivity worth difference between a core sub-

assembly and a blanket subassembly was determined as a function of position within the inner radial blanket array by substitution measurements. The reactivity worth difference between a blanket subassembly and a sodium-filled dummy subassembly was determined at both inner and outer radial blanket positions, also by substitution measurements. The reactivity determinations were made by means of both critical rod position and positive period measurements. All measured worth values were predicted prior to the test using data from the Core A critical assembly mockup on ZPR-III and/or two-dimensional, first-order perturbation theory analysis. With the exception of the outer radial blanket, where agreement is uniformly poor, both sets of predicted values typically agree with the measured values within about 10 percent; there are a few discrepancies in the order of 20 percent. (auth)

12389 (BAW-1280-28(Vol.1)) PRELIMINARY DESIGN REPORT—PROTOTYPE STEAM GENERATOR. VOL. 1. GENERAL. SODIUM-HEATED STEAM GENERATOR DEVELOPMENT. Clark, J. G. (Babcock and Wilcox Co., Barberton, Ohio. Boiler Div.). June 1, 1965. Contract AT(11-1)-1280. 72p. Dep. mn. CFSTI $3.00 cy, $0.75 mn.

A model of a 1000-Mw(e) steam generator is described. The results of heat-transfer and pressure calculations are included. (D.C.W.)

12390 (BAW-1280-28(Vol.2)) PRELIMINARY DESIGN REPORT—PROTOTYPE STEAM GENERATOR. VOL. 2. STRESS ANALYSIS. SODIUM-HEATED STEAM GENERATOR DEVELOPMENT. Hocking, J. E. (Babcock and Wilcox Co., Barberton, Ohio. Boiler Div.). Nov. 15, 1965. Contract AT(11-1)-1280. 184p. Dep. mn. CFSTI $5.00 cy, $1.00 mn.

An analysis of the structural integrity of the steam generator is summarized. Both steady-state and transient conditions were considered. (D.C.W.)

12391 (BAW-1280-28(Vol.3)) PRELIMINARY DESIGN REPORT—PROTOTYPE STEAM GENERATOR. VOL. 3. EFFECTS OF SODIUM-WATER REACTION ON STEAM GENERATOR. SODIUM-HEATED STEAM GENERATOR DEVELOPMENT. Hocking, J. E. (Babcock and Wilcox Co., Barberton, Ohio. Boiler Div.). Nov. 15, 1965. Contract AT(11-1)-1280. 140p. Dep. mn. CFSTI $4.00 cy, $1.00 mn.

An analysis of the effects of sodium–water reaction in the sodium-heated steam generator is summarized. (D.C.W.)

12392 (BAW-1280-28(Vol.4)) PRELIMINARY DESIGN REPORT—PROTOTYPE STEAM GENERATOR. VOL. 4. SPECIFICATIONS. SODIUM-HEATED STEAM GENERATOR DEVELOPMENT. (Babcock and Wilcox Co., Barberton, Ohio. Boiler Div.). Nov. 15, 1965. Contract AT(11-1)-1280. 52p. Dep. mn. CFSTI $3.00 cy, $0.50 mn.

Specifications for the design, fabrication, and testing of a prototype of a 1000-Mw(e) steam generator are presented. The prototype steam generator is briefly described, and acceptance standards are summarized. (D.C.W.)

12393 (BNL-8748) CONTROL OF REACTIVITY IN HIGH CONVERSION RATIO: PLUTONIUM FUELED, THERMAL POWER REACTORS. Srikantiah, G. (Brookhaven National Lab., Upton, N. Y.). Dec. 1964. Contract AT(30-2)-Gen-16. 35p. Dep. mn. CFSTI $2.00 cy, $0.50 mn.

Methods of long-term reactivity control for plutonium fueled, D_2O moderated reactors are considered which favor high conversion ratios. One method uses annular gaps around the fuel elements which can be selectively filled with the D_2O moderator. Reactivity compensations ranging from 8 to 15% can be achieved with gaps of 6 to 8 cm thickness and a corresponding reduction in conversion ratio of 3 to 5%. In the second method depleted uranium sleeves are utilized around fuel elements in annular regions of the reactor which can be removed as required during long-term operation. Sleeves of only 0.2 cm thickness around fuel elements in the central region of the reactor provide reactivity compensations of up to 10% and actually increase the conversion ratio in the design studied. Average conversion ratios in a large D_2O cooled and moderated reactor using Zircaloy pressure tubes of about 0.90 are obtained at fuel burn up of 10^4 MWD/T. The average conversion ratios would increase to about 0.97 if beryllium based pressure tubes could be developed. (auth)

12394 (BNWL-SA-472) MANAGEMENT OF AMERICIUM IN POWER REACTOR FUELS TO OPTIMIZE PRODUCTION OF ALPHA-EMITTING ISOTOPES. Lang, L. W. (Battelle-Northwest, Richland, Wash. Pacific Northwest Lab.). Dec. 30, 1965. Contract AT(45-1)-1830. 19p. (CONF-660305-1). Dep. mn. CFSTI $1.00 cy, $0.50 mn.

For Presentation at American Nuclear Society Topical Meeting, Augusta, Ga.

The choice of a reactor and the length of irradiation time are unique production determinants in isotope yield from the mixed americium isotopes. Machine calculations were performed for two neutron spectra (those typical of pressurized water reactors (PWR) and heavy water reactors (HWR)), neutron flux (5×10^{13}, 2×10^{14}, and 1×10^{15} nvt) and the period of irradiation (one to 24 months) to determine isotope yields from a specific amount of mixed americium isotope. The calculations indicate that the harder flux spectra typical of pressurized water reactors with short irradiation periods results in a greater production of α-emitting isotopes compared to that produced in a softer neutron spectrum for equivalent or long irradiation times. The data are summarized. (M.O.W.)

12395 (EUR-2552.e) AIREK-PUL—A VERSION OF THE KINETIC CODE AIREK-MOD FOR PERIODICALLY PULSED FAST REACTORS. Inzaghi, A.; Misenta, R. (European Atomic Energy Community, Ispra (Italy). Joint Nuclear Research Center). 1965. 76p. Dep. mn.

The computer program AIREK-PUL, which integrates the kinetic equations for a periodically pulsed fast reactor for two space points and few neutron groups and for one group with an external neutron source, is described. The equations solved by the program are included, together with listings of the three versions of the program. (D.C.W.)

12396 (EURAEC-1505) USE OF PLUTONIUM AS A FUEL IN NUCLEAR REACTORS. Quarterly Report No. 5, January 1–March 31, 1965. (Centre d'Etude de l'Energie Nucleaire, Brussels (Belgium). Societe Belge pour l'Industrie Nucleaire, Brussels). May 1965. Contract 001-64-1-TRUB. 36p. (EUR-2663; BN-6505-01). Dep. mn. CFSTI $2.00 cy, $0.50 mn.

Work Performed under United States–Euratom Joint Research and Development Program.

Further development of PuO_2-UO_2 fuels for the BR-3/Vulcain reactor is discussed in terms of the following: fabrication of powders, fabrication of elements, fabrication methods and control, irradiation testing in the BR-2, BR-3/PWR, and BR-3/Vulcain reactors. Some post irradiation test results are discussed. Space-time measurements were made of the axial and radial diffusion in aluminum-water lattices. Various geometries were used and the results for each are presented. (M.O.W.)

12397 (EURAEC-1506) USE OF PLUTONIUM AS A FUEL IN NUCLEAR REACTORS. Quarterly Report No. 6, April 1–June 30, 1965. (Centre d'Etude de l'Energie Nucleaire, Brussels (Belgium). Societe Belge pour l'Industrie Nucleaire, Brussels). Aug. 1965. Contract 001-64-1-TRUB. 60p. (EUR-2664). Dep. mn. CFSTI $3.00 cy, $0.75 mn.

Work Performed under United States–Euratom Joint Research and Development Program.

Fabrication of PuO_2-UO_2 fuels for the BR-3/Vulcain reactor is discussed. The fuels were irradiation tested in the hydraulic conveyor HR-1 of the BR-2 reactor, in a boiling water capsule, and in the BR-3/Vulcain power re-

actor. Detailed results are presented for the first above test. (M.O.W.)

12398 (GA–6811) EXPERIMENTAL BERYLLIUM OXIDE REACTOR PROGRAM. Quarterly Progress Report for the Period Ending, September 30, 1965. (General Atomic, San Diego, Calif. John Jay Hopkins Lab. for Pure and Applied Science). Sept. 30, 1965. Contract AT(04-3)- 187. 31p. Dep. mn. CFSTI $2.00 cy, $0.50 mn.

Testing of the control rod drive mechanism in helium at the design ambient temperature of 250°F was continued. A discussion of these tests is presented. Systems operational tests and reactor zero power tests were performed. The status of these tests is discussed. Various other development aspects of reactor auxiliaries are discussed. (M.O.W.)

12399 (GEAP–4941) EVESR NUCLEAR SUPERHEAT FUEL DEVELOPMENT PROJECT. Thirteenth Quarterly Report, June–August 1965. Murray, J. L. (General Electric Co., San Jose, Calif. Atomic Power Equipment Dept.). Sept. 1965. Contract AT(04-3)-189. 193p. Dep. mn; CFSTI $5.00 cy, $1.00 mn.

EVESR operation during the period was directed largely toward determining the performance and fission product release from the Mark III fuel element which failed in fuel bundle KB-41. The failed element utilized Incoloy cladding of 0.008-in. thickness. The release of fission products was found to be highly dependent upon both power and steam temperature, and it was possible to maintain reactor operation at 12.5 Mw(t) by overcooling the bundle containing the failed fuel. Fuel bundle KB-41 was examined, and preliminary results and a photograph are included. Fuel bundle ESH-3A containing fuel elements that were previously irradiated in the E-SADE loop in the VBWR was installed in EVESR during the period. Operation of EVESR following a shutdown revealed increased release of fission gas from fuel bundle KB-29 consisting of Mark II annular fuel rods with Type-304 stainless steel cladding. However, the total fission product release from KB-29 is milder than that experienced from KB-41. Continued irradiation of KB-29 is planned. Work was stopped on plans for the ABC fuel irradiation; the work completed is reported. Planning of the Mark V fuel test variables was continued. Three-dimensional diffusion theory physics calculations for the Mark III fuel EVESR core were completed for both the normal and reversed control rod patterns; results are included. (J.R.D.)

12400 (HPR–54) DEVELOPMENT OF A DYNAMICS MODEL FOR HEAVY WATER BOILING REACTORS AND ITS APPLICATION TO THE HBWR. Vollmer, H.; Anderson, A. J. W. (Institutt for Atomenergi, Halden (Norway). OECD Halden Reaktor Prosjekt). Dec. 1964. 143p. Dep. mn.

The presented dynamics model is an improvement and extension of models determining the dynamic behavior of light water boiling reactors. It is a one-dimensional model taking only the axial variations into account. The main improvement consists of an integral calculation of void and void reactivity for space and time dependent steam generation, velocity and density and for space dependent reactivity coefficients. Similarly, coolant temperature and its effect on reactivity is calculated. Furthermore, the pressure calculation was improved. The model is applied to the HBWR second fuel charge and comparison is made between theory and experiments for a variety of conditions to see the influence of power, subcooling, pressure and water level on the dynamic behavior of this reactor. A good agreement is found, and the oscillatory unstable behavior at some conditions is understood quantitatively. (auth)

12401 (JEN–156-DMe/I13) LA SOLDADURA EN LA FABRICACION DE ELEMENTOS COMBUSTIBLES DESTINADOS A UNA EXPERIENCIA EXPONENCIAL. (Welding Procedures Used in the Fabrication of Fuel Elements for the DON Reactor Exponential Experiment). Diaz Beltran, A.; Jaraiz Franco, E.; de las Rivas Diaz, M. (Junta de Energia Nuclear, Madrid (Spain). Division de Metallurgia). 1965. 32p. Dep. mn.

The welding techniques used in the fabrication of UC and UO_2 fuel elements for an exponential experiment in the DON reactor are described. (D.C.W.)

12402 (KFK–369) THE KARLSRUHE REFERENCE DESIGN OF A 1000 MWe SODIUM COOLED FAST BREEDER REACTOR. Haefele, W.; Smidt, D.; Wirtz, K. (Kernforschungszentrum, Karlsruhe (West Germany)). Oct. 1965. 51p. Dep. mn.

A reference design for the proposed 1000-Mw(e) sodium-cooled fast breeder reactor is described in detail. A discussion of possible accidents is presented. (M.O.W.)

12403 (LA–3384) THE MOLTEN PLUTONIUM BURNUP EXPERIMENT. Hannum, W. H.; Kirkbride, L. D. (Los Alamos Scientific Lab., Univ. of California, N. Mex.). Sept. 2, 1965. Contract W-7405-eng-36. 76p. Dep. mn. CFSTI $3.00 cy, $0.75 mn.

A reference core was selected for a Molten Plutonium Burnup Experiment. In this experiment, the fuel, a Pu–Co–Ce alloy, will be contained in sealed Ta–W alloy capsules. The principal purpose of the experiment is to obtain information on the characteristics of molten-Pu fuel during and after high burnup at high rates of fissioning. Present uncertainties prevent a detailed analysis or optimization of performance characteristics. Nevertheless, systems based on the use of this fuel alloy can reasonably be expected to have a very favorable fuel lifetime, short doubling time, and favorable safety characteristics. This experiment will be operated in the Los Alamos Fast Reactor Core Test Facility. (auth)

12404 (NAA-SR–11160) SRE-PEP MODERATOR ELEMENTS. Final Report. Jones, C. E. (Atomics International, Canoga Park, Calif.). Jan. 15, 1966. Contract AT(11-1)-Gen-8. 49p. Dep. mn. CFSTI $2.00 cy, $0.50 mn.

The engineering of the new Zircaloy-2 moderator and reflector elements for the SRE is presented. The design was tested and shown to be more than capable of meeting the design objectives. The central moderator elements contain central process tubes for fuel elements, control rods, and instrumentation; the surrounding reflector elements are solid graphite. The top steel head of the elements incorporate flexible spacing members; the bottom support pedestal includes a slip joint. In case of a failed element the adjacent elements shift laterally to accommodate expansion and removal of the failed element without further core damage. A final proof test of a production element was made. It was thermally cycled 74 times over a temperature ranging from 475 to 1325°F, with gradients between 575 and 675°F along the length of the element. The element was cut open and examined following this environmental exposure, equivalent to approximately 58 years of reactor operation. Upon completion of the test the element was fully integral and subsequent examination of the element showed no deleterious effects. The objectives of the moderator element design were more than confirmed and satisfied by the test program. (auth)

12405 (NAA-SR-Memo–11576) TEST THE GRAPHITE FILLER LOG HANDLING MACHINE. Kennedy, R. S. (Atomics International, Canoga Park, Calif.). Sept. 1, 1965. Contract AT(11-1)-Gen-8. 14p. Dep. mn. CFSTI $1.00 cy, $0.50 mn.

A maintenance remote handling method was developed for replacing a process tube and the graphite moderator surrounding such a tube in a calandria core. The methods used and descriptions of equipment are included. (M.O.W.)

12406 (NAA-SR-Memo–11648) THE NEW HEAT TRANSFER PROTECTION SYSTEM FOR THE SODIUM REACTOR EXPERIMENT. Kline, K. H. (Atomics International, Canoga Park, Calif.). Sept. 14, 1965. Contract AT-11-1-GEN-8. 11p. Dep. mn. CFSTI $1.00 cy, $0.50 mn.

Operation, calibration, and test procedures for the new

heat transfer protection system for the SRE are discussed. The protection system consists of eight channels of instrumentation. There is one chassis of power supplies associated with the instruments which provides regulated d-c power for up-scale burnout, offset, temperature referencing, and calibration. (M.O.W.)

12407 (NEIC-RR-13) BREEDING OF FISSIONABLE FUEL. Taube, M. (Nuclear Energy Information Center, Warsaw (Poland)). 1965. 403p. Dep. mn.

In Polish.

A treatise is presented on basic definitions and handling of fissionable materials; fuel reprocessing; breeder reactor economics; and breeding in thermal, fast, and fused-salt-fueled fast reactors. (T.F.H.)

12408 (NP-15660(Vol.1)) NINE MILE POINT NUCLEAR STATION. VOLUME I. Preliminary Hazards Summary Report. (Niagara Mohawk Power Corp., Syracuse, N. Y.). Apr. 1964. 276p. (DOCKET-50-220 (Vol.1)). Dep. mn. CFSTI $6.00 cy, $1.50 mn.

A preliminary safety analysis is presented which incorporates the results of extensive environmental investigations. The principal architectural and engineering criteria are identified and the descriptions of structures, equipment, and systems upon which this analysis is based represent the design as it is presently conceived. The power plant is described in terms of reactor containment, reactor plant systems, turbine plant systems, control and instrumentation, miscellaneous station systems, shielding and access control, and buildings and structures. Radioactive waste disposal is discussed in terms of liquid, solid, and gaseous wastes. The reactor characteristics are described. A safety analysis was made and the results are presented. (M.O.W.)

12409 (NP-15660(Vol.2)) NINE MILE POINT NUCLEAR STATION. VOLUME II. APPENDIXES. Preliminary Hazards Summary Report. (Niagara Mohawk Power Corp., Syracuse, N. Y.). Apr. 1964. 350p. (DOCKET-50-220(Vol.2)). Dep. mn. CFSTI $7.00 cy, $1.75 mn.

Results of a qualitative study of the meteorology of the Nine Mile Point site are presented in detail. Results from an extensive limnological study of nearby Lake Ontario are presented. The results of an earth-science program and subsequent site evaluation study are included. (M.O.W.)

12410 (NP-15660(Suppl.1)) NINE MILE POINT NUCLEAR STATION. First Supplement to Preliminary Hazards Summary Report. (Niagara Mohawk Power Corp., Syracuse, N. Y.). Aug. 1964. 226p. (DOCKET-50-220 (Suppl.1)). Dep. mn. CFSTI $6.00 cy, $1.25 mn.

The applicants' answers to questions presented by the AEC Division of Reactor Licensing are included. (M.O.W.)

12411 (ORNL-TM-1380) EXAMINATION OF FAILED EXPANSION BELLOWS BETWEEN EGCR CONTAINMENT SHELL AND EXPERIMENTERS CELL 6. Kegley, T. M. Jr.; Tolson, G. M. (Oak Ridge National Lab., Tenn.). Feb. 1966. Contract W-7405-eng-26. 15p. Dep. mn. CFSTI $1.00 cy, $0.50 mn.

A horizontal 42-in.-dia, 0.039-in.-thick expansion bellows of type 304 stainless steel that connected Experimenters Cell 6 to the EGCR containment shell failed due to several leaks at the bottom of the bellows. Examination of the bellows to determine the cause of the failure indicated severe pitting attack which occurred predominantly from the inside of the bellows and the presence of 4.44% Cl^- in scale removed from the inside of the bellows. The failure by severe pitting attack most probably was due to the presence of chloride and to the stagnant condition of the liquid in the bottom of the bellows. (auth)

12412 (TID-22516) QUARTERLY REPORT NO. 13, JULY 1, 1965-SEPTEMBER 30, 1965. (Societe d'Energie Nucleaire Franco-Belge des Ardennes, Chooz-Lez-Givet (France)). 26p. Dep. mn. CFSTI $2.00 cy, $0.50 mn.

The status of the Ardennes power plant is summarized. (D.C.W.)

12413 (TID-22545) SECOND GRADUATE NUCLEAR ENGINEERING DESIGN SEMINAR, PURDUE UNIVERSITY, SUMMER 1965. Summary Report. (Purdue Univ., Lafayette, Ind. Dept. of Nuclear Engineering). Nov. 15, 1965. Contract AT(11-1)-1373. 87p. Dep. mn. CFSTI $3.00 cy, $0.75 mn.

The activities and organization of the second design seminar are summarized, together with design results. Separate abstracts were prepared for three sections of the report. (D.C.W.)

For abstracts of individual sections see: 12414-12416.

12414 (TID-22545, pp 16-52) DESIGN STUDY REPORT ON A 1000 MWe FAST BREEDER REACTOR. Black, Thomas A.; Boggs, J. Vincent; Goktepe, Omer; Ibe, Librado D.; Lee, Jee Won; Martinez-Ginoris, Jose; Webb, Harry W.; Wilson, Robert Lee (Purdue Univ., Lafayette, Ind. Dept. of Nuclear Engineering).

The results of a design study on a 1000-Mw(e) modular-type reactor are presented. The possibility of obtaining a more economical reactor with a reduced height and a different arrangement of blanket, fuel, and reflector materials was stressed. (D.C.W.)

12415 (TID-22545, pp 54-65) STEAM CYCLE CALCULATIONS. Obeid, Mohamed; Mong, B. A. (Purdue Univ., Lafayette, Ind. Dept. of Nuclear Engineering).

An analysis of the steam cycle for a 1000-Mw(e) power plant using a direct-cycle reactor cooled by supercritical steam and moderated by steam and graphite is summarized. (D.C.W.)

12416 (TID-22545, pp 67-80) THERMAL ANALYSIS. Karousakis, Panos (Purdue Univ., Lafayette, Ind.).

An analysis of fluid flow and heat transfer in a 1000-Mw(e) direct-cycle thermal reactor cooled by supercritical steam and moderated by both steam and graphite is summarized. (D.C.W.)

12417 (WCAP-3269-15) LARGE CLOSED-CYCLE WATER REACTOR RESEARCH AND DEVELOPMENT PROGRAM. Progress Report, July 1-September 30, 1965. (Westinghouse Electric Corp., Pittsburgh, Pa. Atomic Power Div.). Contract AT(30-1)-3269. 24p. Dep. mn. CFSTI $1.00 cy, $0.50 mn.

Brief summaries of work accomplished during this period are presented. Most pertinent of these include Zircaloy hydriding in pressurized water, irradiation proof testing of advanced fuel assembly prototypes, fuel swelling studies, and loss of coolant flow analysis. (M.O.W.)

12418 (WCAP-3739) LARGE CLOSED-CYCLE WATER REACTOR RESEARCH AND DEVELOPMENT PROGRAM. Progress Report, April 1-June 30, 1963. (Westinghouse Electric Corp., Pittsburgh, Pa. Atomic Power Div.). Contract AT(30-1)-3269. 362p. Dep. mn. CFSTI $7.00 cy, $1.75 mn.

Various studies were performed in connection with the reactor development program. Detailed results are presented on reactor physics, design and fabrication of the reactor core, chemical shim studies, plant development, and critical experiments. Most prominent among these include light water physics methods, advanced fuel assembly fabrication, biaxial strain fatigue limits of cladding materials, control rod prototype fabrication, chemical studies of soluble neutron poisons, loss of coolant flow analysis, and critical experiment planning and analysis. (M.O.W.)

12419 (EURFNR-1F) REPORT ON ACTIVITIES FOR THE YEAR 1963. (Commissariat a l'Energie Atomique, Saclay (France). Centre d'Etudes Nucleaires. Commissariat a l'Energie Atomique, Cadarache (France). Centre d'Etudes Nucleaires). Translation of French report. 42p. Dep. mn. CFSTI $2.00 cy, $0.50 mn.

Work Performed under United States-Euratom Fast Reactor Exchange Program.

The status of the Rapsodie reactor, the Harmonie research reactor, and the Masurca critical experiment installation is summarized; and the criticality, fuel, kinetics,

and safety studies that were performed in support of these projects are outlined. (D.C.W.)

12420 (EURFNR-9F) GRAND QUEVILLY THERMAL TESTS STATION. 5 MW SODIUM CIRCUIT WITH STEAM GENERATOR SUPERHEATED TO 545 deg C. Robin, Marcel G. (Commissariat a l'Energie Atomique, Saclay (France). Centre d'Etudes Nucleaires). Translation of report CEA-R-2520. July 1964. 55p. Dep. mn. CFSTI $3.00 cy, $0.50 mn.

Work Performed under United States–Euratom Fast Reactor Exchange Program.

An installation developed for testing a sodium-heated steam generator capable of producing steam at 127 bars and 545°C is described, including the test program and a prototype double-wall unit using a K–Na secondary loop. (D.C.W.)

12421 ENERGY CONVERSION AT HIGH TEMPERATURES WITH NUCLEAR REACTORS AS HEAT SOURCES. Pruschek, R. (Technische Hochschule, Stuttgart). Atomkernenergie, 10: 317-26(Sept.-Oct. 1965). (In German).

A survey is given on the requirements and applications of non-conventional energy conversion systems and associated nuclear reactors necessary for them. The characteristic temperature regions for magnetogasdynamic (MGD), magnetofluidodynamic (MFD) and thermionic (TC) conversion are briefly discussed. The individual conversion processes are presented in the familiar way as thermodynamic cycles in temperature-entropy diagrams. The basic schemes of such reactors, necessary for the energy conversion systems, are briefly discussed. (auth)

12422 REMARKS TO THE PROBLEM OF OPTIMUM DESIGN OF NUCLEAR GAS TURBINE POWER PLANTS. Bammert, K. (Technical Univ., Hanover). Atomkernenergie, 11: 1-5(Jan.-Feb. 1966).

The optimum layout of a power plant is characterized by that ratio of heat consumption to construction cost which ensures the cheapest possible production of the kilowatt hour. In order to arrive at such a layout, the effects are examined of the chosen circuit data on the thermal efficiency on one hand and the construction cost of reactor, turbine, compressor, and heat exchanger on the other, and the most important interrelations between these factors are pointed out. (auth)

12423 THE SYSTEM OF FAST REACTORS: REACTOR SYSTEM STUDIES AND PHENIX. Bull. Inform. Sci. Tech. (Paris), No. 95, 79-115(July-Aug. 1965). (In French).

Research into fast neutron type reactors is directed towards the construction of power stations having capacities of about 1,000 Mw(e). The reactor Phenix, whose power should be between 125 and 250 Mw(e) and the construction of which might start in 1969, will represent an intermediate stage between Rapsodie and the large industrial reactors. The development program for the fast neutron reactor system provides for a considerable effort in the essential domain of the reactor fuel and of its canning. Much other theoretical and experimental work is also under way however. This concerns in particular reactor physics, the structure of the reactor and its protection, the handling of the fuels, the energy-recovering circuits. The development of the sodium-water heat-exchangers will be carried out at the Grand Quevilly thermal test station. (auth)

12424 PROJECT CIRENE. Silvestri, Mario. Comit. Naz. Energia Nucl., Notiz., 11: No. 8-9, 33-43(Aug.-Sept. 1965). (In Italian).

A detailed review is given of the Cirene Project, a heavy water reactor with natural uranium fuel. The technical aspects of the reactor are reviewed and then a critical examination is made of the design. (J.S.R.)

12425 TRANSFER FUNCTION ANALYSER FOR THE DRAGON REACTOR. Bredael, I.; Sciuto, F. (CCR-EURATOM, Ispra, Italy). Energia Nucl. (Milan), 12: 628-38(Dec. 1965).

The transfer function analyser was specially designed and built for the Dragon Reactor. The interest of this realisation resides in the measurement accuracy and in the flexibility of use. The equipment, completely transistorized, is based on digital techniques. (auth)

12426 THE SWEDISH AGESTA POWER REACTOR. Abadie-Maumert, F. A. Energie Nucl., 7: 330-2(Sept.-Oct. 1965).

The Agesta power station, brought into service March 8, 1964, is described. The primary power source is a reactor fueled with natural uranium with heavy water as both moderator and coolant. It has a capacity of 65,000 kw(t). The containment, pressure vessel, refuelling bridge, control system, fuel elements, and cooling system are described. (M.C.G.)

12427 THE BRITISH ATOMIC PROGRAMME. Penney, William (United Kingdom Atomic Energy Authority, Harwell, Eng.). Euratom Bull., 4: 98-103(Dec. 1965).

Nuclear research in Britain is reviewed. The nuclear power program is described. Development of advanced gas-cooled reactors, steam-generating heavy water reactors, the Dragon Reactor, and fast reactors is discussed. (M.C.G.)

12428 TOWARDS AN ORGEL PROTOTYPE. Leny, Jean-Claude (EURATOM, Ispra, Italy). Euratom Bull., 4: 122-6(Dec. 1965).

The development of a prototype for ORGEL reactors is considered. The advantages and disadvantages of 80-, 125-, and 300-Mw(e) prototypes are discussed. Economic aspects are considered. From a technical standpoint a 125-Mw(e) plant is suggested as the most suitable. (M.C.G.)

12429 CLEANING FOR NUCLEAR SPECIES IN THE TOKAI ATOMIC POWER STATION. Kunimatsu, Masami (Fuji Electric Mfg. Co., Ltd., Japan). FAPIG (Tokyo), No. 33, 177-80(Aug. 1964). (In Japanese).

Control of nuclear species that affect the operation of an atomic power station is described. These include (1) elements that easily become radioactive (Ne, Mn, Co, Ni, As, Ag, Cd, Sb, etc.), (2) neutron-absorbing elements (Cd, B, Hg, Rh, Au, Ag, etc.), and (3) elements that affect unfavorably reactor materials (Al, Si, Ca, Ni, Cu, Zn, Ag, Sb, Hg, Pb, Bi, etc.). Both mechanical and chemical methods are employed for the purpose. Descriptions are given in detail for the practices at the Tokai atomic power station. (NSA of Japan)

12430 THE AGR FUEL. Greenough, G. B.; Nairn, J. S.; Waine, P. (United Kingdon Atomic Energy Authority, Springfields, Eng.). Nucl. Eng., 10: 426-8(Nov. 1965).

The wrinkling of fuel cans and the ratcheting elongation of fuel pins were studied, together with fission-product release from UO_2 pellets under irradiation. In-pile tests were also conducted using elements obtained to obtain the conditions expected in the Dungeness B reactor. (D.C.W.)

12431 TO BREED OR NOT TO BREED. Caprioglio, P.; De Bacci, M. Nucl. Eng., 10: 429-33(Nov. 1965).

An analysis of the development of the nuclear-power industry during the next fifty years is presented in which the economics of fast breeders and thermal converters, in terms of costs and fuel utilization, is considered in detail. (D.C.W.)

12432 THE DUNGENESS B REPORT. Nucl. Ind., 12: 9-15(Aug. 1965).

A report by the Central Electricity Generating Board on the Dungeness B nuclear station is discussed. The report is essentially a justification for the Board's choice of a version of the British-developed Advanced Gas-Cooled Reactor (AGR) for the two-unit station rather than the closest competitor, boiling water reactors (BWR) designed by the General Electric Co. of the U. S. A table compares the costs of building and operating a 1200-Mw(e) station equipped with each type of reactor. According to the Board's figures, the BWR would have somewhat lower

capital costs than the AGR but considerably higher operating costs. (A.G.W.)

12433 A LOOK AT FAST REACTOR SAFETY. Okrent, David (Argonne National Lab., Ill.). Nucl. Safety, 6: 317-42(Summer 1965).

Major safety features of early fast reactors are briefly reviewed. Discussions are included concerning maximum accident approach to safeguard analyses for these reactors, and safety related operating experiences. Safety characteristics and safety problems associated with large fast reactor design are also discussed with particular attention directed to reactivity coefficients. (J.R.D.)

12434 EMERGENCY COOLING SYSTEMS IN GAS-COOLED REACTORS. Robinson, G. C. Nucl. Safety, 6: 425-32(Summer 1965).

A review of emergency cooling is presented for systems designed to either limit fuel-element failures or prevent meltdown and fission-product release in the event of a depressurization accident. Tabular data on gas-cooled reactors is included along with discussions of reactors moderated by graphite, BeO, and water. (J.R.D.)

12435 HUMBOLDT BAY REACTOR OPERATING EXPERIENCE. Carroll, J. C.; Schuyler, J. O. (Pacific Gas and Electric Co., San Francisco). Nucl. Safety, 6: 441-51; 467(Summer 1965).

Design and operation of the reactor are described. Information is included on equipment performance, testing program for uprating, waste disposal, water chemistry, and maintenance and refueling experience. (J.R.D.)

12436 ACTION ON REACTOR PROJECTS UNDERGOING REGULATORY REVIEW. Nucl. Safety, 6: 454-64; 467-8(Summer 1965).

Recent regulatory actions relative to various reactors are summarized. Information is also included on difficulties or unusual occurrences that were reported to the regulatory staff. (J.R.D.)

12437 CHANGES IN LICENSING REGULATIONS. Nucl. Safety, 6: 464-6; 468(Summer 1965).

Rules and regulations related to reactor licensing being considered for change are tabulated and discussed. (J.R.D.)

12438 TURBINE PRESSURE GOVERNOR CONTROLS REACTOR SYSTEM TEMPERATURES. Lutz, D. E. (Argonne National Lab., Ill.). Power, 110: 59-61(Jan. 1966).

The reactor power levels in Argonne's Experimental Breeder Reactor No. 2 are set manually and do not respond to turbine-generator load fluctuations. In order to maintain steam-drum pressure and temperature, the turbine is operated under control of its initial pressure governor, which senses pressure of the main steam header directly upstream of the turbine stop valve. Design startup and during reactor operation with no turbine load, steam bypasses the turbine and flows directly to the condenser. At 20% steam flow the turbine can be synchronized and put on load. At this point the pressure governor assumes control. An automatic control transfer mechanism was devised to prevent excessive speed increase when the generator is severed from parallel operation with other machines. (A.G.W.)

12439 FAST REACTOR CORE DESIGN AND SAFETY STUDIES IN FRANCE IN THE FEDERAL REPUBLIC OF GERMANY. Zaleski, C. P. (Euratom - CEA, Cadarache, France); Smidt, D. pp 56-72 of ANS-100(Suppl.).

A review is presented of several reference cores developed in France and Germany for conceptual studies of large fast power breeder reactors. Dynamics and safety problems for these cores are investigated. (T.F.H.)

12440 THE IMPACT OF ENERGY REQUIREMENTS ON NUCLEAR POWER DEVELOPMENT. Cisler, Walker L. (Detroit Edison Co., Mich.). pp 6-9 of ANS-100(Suppl.).

A descriptive account is given of the future of the nuclear-energy industry. (T.F.H.)

12441 NUCLEAR POWER PLANT BN-350. Leopunsky, A. I.; Pinkhasik, M. S.; Bagdasarov, Y. E.; Milovidov, I. V.; Poydo, M. S.; Kazatchkovsky, O. D.; Krasnoyarov, N. V.; Troyanov, M. F.; Afrikantov, I. I.; Stekolnikov, V. F. (Inst. of Physics and Power Engineering, Obninsk, USSR). pp 15-26 of ANS-100(Suppl.).

Design characteristics of the BN-350 fast power breeder reactor are reviewed. BN-350 is a 1000-Mw(t), 350-Mw(e) sodium-cooled reactor, under construction on the Mangyshlak Peninsula, on the northeast shore of the Caspian Sea. (T.F.H.)

12442 MIXED CARBIDE FUEL IRRADIATION IN DFR. Russell, L. E. (United Kingdom Atomic Energy Authority, Harwell, Eng.). pp 30 of ANS-100(Suppl.).

Radiation effects on $(U_{0.85}-Pu_{0.15})\ C_x$ are studied in DFR. The carbide samples are in sintered, arc-cast, or powdered form, and are irradiated to about 5% burnup in Nimonic 90 cans lined on the inside with Ta foil. (T.F.H.)

12443 EXPERIMENTAL INVESTIGATION OF THE TEMPERATURE FIELD OF THE FUEL ELEMENTS IN THE CORE AND BLANKET OF THE BN-350 REACTOR USING SIMULATORS. Subbotin, V. I.; Umakov, P. A.; Zhukov, A. V.; Talanov, V. D.; Kudryavtseva, L. K.; Sviridenko, E. Y.; Vasileva, L. V. (Physico-Technical Inst., Obninsk, USSR). pp 73-85 of ANS-100(Suppl.).

BN-350 is a 1000-Mw(t), 350-Mw(e) sodium-cooled fast power breeder reactor under construction on the northeast shore of the Caspian Sea in Russia. A test unit is built to simulate the temperature distributions in the fuel elements of the core and blanket of BN-350. (T.F.H.)

12444 FACILITY BUILDINGS /EGCR/ (Engineering Materials). (Oak Ridge Operations Office (AEC), Tenn. Reactor Div.). (CAPE-976).

385 drawings.

The building complex for the Experimental Gas Cooled Reactor (EGCR) consists of a reactor building, reactor service and turbine buildings, control building, and experimenters' cell. Appurtenant facilities include a river pumping station, chlorination building, helium storage tanks, elevated water storage tank, sewage plant, fire pump house, valve house, stack monitoring house, and a guardhouse. The combined reactor service and turbine buildings consist of a conventional reinforced concrete basement and a steel superstructure. The reactor service building is 457,000 ft^3 in volume and the turbine building is 598,200 ft^3 in volume. The reactor service building contains the spent fuel storage basin, maintenance areas, decontamination and storage areas for radioactive charge and service machine parts, a change room, new fuel storage vault, and an air-lock entrance to the reactor building. The turbine building contains the turbine-generator and steam plant auxiliaries, electric power distribution equipment, a heating and ventilating equipment room, general service shop area, health physics laboratory, first aid room, reactor building air lock, and the auxiliary diesel. The control building, a reinforced concrete structure with concrete block filler walls, contains the main control room for the reactor and steam plants and a 4,800 ft^2 area for the experimenters' control and instrumentation equipment. (For Details, See TID-4100) (M.C.G.)

12445 BUILDING SPECIFICATIONS /EGCR/ (Engineering Materials). (Oak Ridge Operations Office (AEC), Tenn. Reactor Div.). (CAPE-977).

47 specs.

Specifications are given for the buildings of the Experimental Gas Cooled Reactor. (For Details, See TID-4100) (M.C.G.)

12446 PORTABLE BOILING WATER REACTOR, PL-2 (Engineering Materials). (Combustion Engineering Inc., Windsor, Conn. Nuclear Div.). (CAPE-1003).

39 drawings.

The PL-2 reactor described is a factory pre-packaged, modular power plant, which provides 1,300,000 BTU/hr, suitable for central heating, and 800 Kw(e) (net electrical

power). The modules are assembled into air-transportable packages suitable for rapid on-site installation, interconnection, and relocation at minimum costs. The plant is capable of operating satisfactorily as an independent power source or in parallel with other heating and lighting facilities. A number of skids (units) are used in packaging the power plant. These are: reactor module; turbine-generator; condensers (2); feed and condensate; electrical equipment; purification and demineralizer; and waste. The last two are shipped together. The reactor design is a development of the SL-1 prototype. The portable boiling water reactor has a net electrical output ranging to 1,000 Kw and a net space heat output of 400 Kw. The total reactor thermal power is 8.8 Mw; the design life of the core is 3 years. (For Details, See TID-4100) (M.C.G.)

12447 CONTAINMENT FOR WATER REACTOR NUCLEAR POWER PLANTS. PART I. DRY CONTAINMENT. Chave, Charles T. (Stone and Webster Engineering Corp., New York). 39p. (CONF-650829-1). ORINS. Gmelin, AED-CONF-65-199-1.

From American Society of Corrosion Engineers, Power Division Specialty Conference, Denver.

Containment vessels may be classified by type as dry or pressure suppression. In dry containment no water is used to condense the escaping steam. Steel and concrete are the common materials used for dry containment; examples of use of each in existing reactors are cited. General design considerations and strength criteria are suggested. Advantages and disadvantages of use of steel liners in concrete containment vessels, underground containment, and vacuum containment are considered. Possible methods of cooling the core and controlled venting of the containment atmosphere in case of a loss-of-coolant accident are discussed. It is concluded that there is at present no one best method of containment under any and all conditions. Further work on the problem is needed to enhance effectiveness and reduce cost of containment. (A.G.W.)

12448 ELK RIVER REACTOR OPERATIONS. Signorelli, Joseph A. (Nuclear Utility Services, Inc., Washington, D. C.); Campbell, Robert. 8p. (CONF-650710-16). ORINS. Gmelin, AED-CONF-65-192-8.

From American Nuclear Society Meeting on Reactor Operating Experience, Jackson Lake Lodge, Wyo.

The Elk River Reactor Plant was operated at a capacity factor of better than 75% for seven months. Operational problems reviewed briefly concern pulsations in feedwater flow rate, control rod inspection, bolt failure, spurious reactor scrams due to malfunction of a temperature sensing device, and increase in the turbine air ejector discharge activity. Plant radiation levels and primary reactor coolant chemistry are also discussed briefly. (A.G.W.)

12449 DETECTION OF MODERATOR ELEMENT FAILURES IN THE HALLAM NUCLEAR POWER FACILITY. Davidson, R. H. (Consumers Public Power District, Hallam, Neb.). 19p. (CONF-650710-12). ORINS. Gmelin, AED-CONF-65-192-7.

From American Nuclear Society Meeting on Reactor Operating Experience, Jackson Lake Lodge, Wyo.

Moderator elements in the Hallam Nuclear Power Facility are hexagonal graphite logs scalloped at the corners and clad with a 16-mil stainless steel skin. Failure of the skin of these elements and subsequent exposure of the graphite to the sodium coolant was detected by three mechanisms: (1) flux tilt as evidenced by disagreement in the output of the power range nuclear instruments surrounding the core, (2) local power depression as indicated by fuel channel exit temperatures, and (3) reactivity loss determined by daily comparison of measured reactivity with predicted reactivity. Verification of failures was made after reactor shutdown by a technique based on the difference in conductivity between unfailed elements and sodium-saturated graphite. Examination of seven failed elements after removal disclosed that all failures were similar in location. (A.G.W.)

12450 WORK PERFORMED ON FUEL CHANNELS AND THE CORE SUPPORT PLATE AT BIG ROCK POINT NUCLEAR POWER PLANT. Riesland, J. I. (General Electric Co., San Jose, Calif.). 31p. (CONF-650710-10). ORINS. Gmelin, AED-CONF-65-192-26.

From American Nuclear Society Meeting on Reactor Operating Experience, Jackson Lake Lodge, Wyo.

In order to identify the source of a problem involving channel-support tube vibrations in the Big Rock Point reactor, the reactor was shut down and the core was instrumented and subjected to a variety of flow conditions. Tests confirmed that the problem was one of flow distribution inside the vessel, and two courses of action were taken. The first consisted of positive capturing of the channel-support-tube connecting screws to prevent their dislodging as a result of vibration. The second consisted of diffusing the inlet coolant flow by mounting two diffusers on the core support plate. Techniques that could be of value to future projects include use of epoxy resin to attach instruments to stainless steel and Zircaloy-2 surfaces, use of temporary shielding caves, and use of divers to work inside an irradiated reactor vessel. (A.G.W.)

12451 PROFESSIONAL NUCLEAR MATERIALS MANAGEMENT. O'Leary, W. J. (Allis-Chalmers Mfg. Co., Bethesda, Md.); Forcella, A. Vienna, International Atomic Energy Agency, 1965, Preprint No. SM-67/60, 22p. (CONF-650803-37). ORINS.

From IAEA Symposium on Nuclear Materials Management, Vienna.

The scope of nuclear materials management is described for a typical privately operated power reactor in the United States. Because of the high intrinsic value of nuclear materials, appropriate security and accountability must be continually exercised to minimize losses beyond security and accountability for the nuclear materials. Provisions must be made in advance against the following contingencies, and constant control or liaison maintained against deviations from planning during pre-reactor acquisition of fuel and fuel elements, in-reactor utilization of the fuel elements, and post-reactor recovery of fuel values. The fuel element must be designed for economy in manufacture, handling, shipping, and replaceability. For in-reactor operations, the maximum achievable burnup of the fissionable material must be obtained by means of appropriate fuel rearrangement schemes. Down time of the reactor for fuel rearrangement, inspection, etc. must be minimized. In the post-reactor period, when the fuel has reached a predetermined depletion of fissionable material, economical reprocessing and recovery of fissionable values and by-products must be provided. (auth)

12452 MANAGEMENT AND CONTROL OF EBR-II FUEL. Whitham, G. K.; Spalding, T. R.; Feldman, M. J. (Argonne National Lab., Idaho Falls, Idaho). Vienna, International Atomic Energy Agency, 1965, Preprint No. SM-67/21, 23p. (CONF-650803-51). ORINS.

From IAEA Symposium on Nuclear Materials Management, Vienna.

Problems relating to the management and inventory of fuel in the operation of Experimental Breeder Reactor II (EBR-II) are described. The EBR-II plant complex incorporates an on-site facility, adjoining the reactor plant, for pyrometallurgically reprocessing spent fuel. Remote handling is required at every step of the procedure used to accomplish removal, processing, and return to the reactor. The fuel handling mechanisms, as well as the reactor, pumps, and heat exchanger, operate submerged in a large tank containing sodium (86,000 gal) at a temperature of 700°F. A digital computer, which receives data from punched cards, controls these under-sodium transfers. Accurate information on each loading of the 636 reactor grid positions is maintained and controlled by computer tabulation of the punched cards. A complete inventory of fissionable materials is maintained by computer control. Computer analysis and control of the number and frequency of reactor loading changes programs operations to realize maximum plant utilization. In the Fuel Cycle Facility, fuel

burnup information is converted to data that form the basis for replenishment of ^{235}U. The ingot weight of refined fuel plus dross is compared to the incoming fuel weight for process control. When the refined fuel then enters this stage of fabrication, the weight of fuel pins and scrap is carefully accounted for. A punched data card follows the fuel pin through the entire fabrication process, thus furnishing a complete history and data record for each of the 91 elements in a subassembly. Accumulated data on the punched cards are programmed into the computer to provide additional control data for accountability, studies of process efficiency, and statistical control of process variables. (auth)

Process Heat Reactors

12453 (TID-22330(Vol.2)) ENGINEERING AND ECONOMIC FEASIBILITY STUDY FOR A COMBINATION NUCLEAR POWER AND DESALTING PLANT. PHASE III. (Bechtel Corp., San Francisco, Calif.). Dec. 1965. 599p. Dep. mn. CFSTI $4.00 cy, $2.75 mn.

A detailed analysis of the feasibility of dual-purpose plants located at Pelican Point and on Bolsa Island (a man-made island) and of the cost of water from these plants is summarized. Plants using boiling-water and pressurized-water reactors were considered. It is recommended that the Bolsa Island site be selected for the location of the plant. (D.C.W.)

12454 (JPRS-33480) NUCLEAR DESALINATION EQUIPMENT OF LOW CAPACITY. Polushkin, K. K.; Koryakin, Yu. I.; Kuznetsov, S. P.; Grozdov, I. I.; Sirotkin, A. P.; Loginov, A. A.; Khoroshavin, V. D.; Gasnikov, P. E.; Aleksenko, Yu. N. Translation of paper No. SWD/58 presented at the First International Symposium on Desalination of Water, Washington, D. C., October 3–9, 1965. 17p. (TT-65-34054). CFSTI $1.00 cy, $0.50 mn.

The results of a study of desalination plants using organic-cooled reactors of 15, 30, and 70 Mev are presented. (D.C.W.)

Production Reactors

12455 (HW-77921-C) NPR INJECTION PUMP SIMULATION. Swanson, C. D.; Coughren, K. D. (General Electric Co., Richland, Wash. Hanford Atomic Products Operation). June 17, 1963. Contract AT(45-1)-1350. 32p. Dep. mn. CFSTI $2.00 cy, $0.50 mn.

The data necessary to program a simulation of three parallel NPR injection pumps and associated piping upstream of the fill control valves on an EASE 1100 analog computer are presented. (M.O.W.)

12456 (HW-77921-D) NPR PRESSURIZER. Swanson, C. D.; Coughren, K. D. (General Electric Co., Richland, Wash. Hanford Atomic Products Operation). Sept. 25, 1963. Contract AT(45-1)-1350. 38p. Dep. mn. CFSTI $2.00 cy, $0.50 mn.

Data necessary to program a simulation of the NPR primary system pressurizer on an analog computer are presented. The pressure vessel is divided into three sections; a steam region, a spray and condensate region, and a water region. (M.O.W.)

12457 (ORNL-TM-1372) HFIR PRESSURE VESSEL AND STRUCTURAL COMPONENTS MATERIAL SURVEILLANCE PROGRAM. McWherter, J. R.; Schappel, R. E.; McGuffey, J. R. (Oak Ridge National Lab., Tenn.). Jan. 1966. Contract W-7405-eng-26. 46p. Dep. mn. CFSTI $2.00 cy, $0.50 mn.

A review is made of the design considerations and fabrication precautions observed regarding prevention of radio induced brittle fracture for the HFIR pressure vessel. The arrangement of specimens, dosimeters, containers and mounts is described, and the reasoning behind specimen location in the vessel is given. The surveillance program is outlined, and guidelines are established for operation of the vessel. Specifically, it is recommended that a review of vessel operation be made if the NDT of any part occurs at a temperature higher than 60°F below the existing minimum operating temperature. The effects of radiation on beryllium and aluminum components in the high flux near the fuel elements were considered; the surveillance program is described. An in-pile corrosion program was also established to aid in determining the rate of corrosion of materials in the HFIR primary system. The basis for selection of the samples, their size and location, and a recommended schedule for periodic inspection are included. (auth)

Propulsion and Space

See also ENGINEERING — Space Propulsion

Refer also to abstracts 11175 and 11355.

12458 (CONF-640810) PROCEEDINGS OF THE CONFERENCE ON NUCLEAR MARINE PROPULSION HELD AT VIRGINIA POLYTECHNIC INSTITUTE, BLACKSBURG, VIRGINIA, AUGUST 10–13, 1964. (Virginia Polytechnic Inst., Blacksburg). Contract AT(40-1)-3239. 200p. Dep. mn; CFSTI $2.25 cy, $1.25 mn.

Separate abstracts were prepared for 6 of the 15 included papers. Nine papers appeared previously in NSA as 19: 24134, 24155, 24158, 24159, 25739, 25755, 25756, 25757, and 29733. (M.O.W.)

For abstracts of individual papers see: 12459–12464.

12459 (CONF-640810, pp 1-6) A CRITICAL APPRAISAL OF NUCLEAR MERCHANT SHIPS. Holm, Jens T. (Virginia Polytechnic Inst., Blacksburg).

A general discussion of various propulsion systems for merchant ships is presented. In an economic sense, various reactors are considered for propulsion of various size merchant ships. (M.O.W.)

12460 (CONF-640810, pp 7-21) PANEL DISCUSSION: THE ROLE OF NUCLEAR POWER IN THE MERCHANT MARINE. Holm, Jens T.; Gorman, D. L.; Uberti, George; Mott-Smith, H. M. (Virginia Polytechnic Inst., Blacksburg).

A panel consisting of the four authors discuss the overall aspects of ship propulsion by nuclear power. (M.O.W.)

12461 (CONF-640810, pp 105-6) REMARKS CONCERNING THE MARITIME STUDY BY DIVISION OF REACTOR DEVELOPMENT, UNITED STATES ATOMIC ENERGY COMMISSION. Stewart, D. H. (Virginia Polytechnic Inst., Blacksburg).

Reasons for the continued maritime reactor study by the AEC are pointed out. (M.O.W.)

12462 (CONF-640810, pp 122-37) ON THE DESIGN OF JAPANESE NUCLEAR SHIP. Yamaguchi, H. (Virginia Polytechnic Inst., Blacksburg).

The design of a Japanese nuclear-powered oceanographic survey ship is presented. Discussions are presented on the arrangement and compartmentation, structural, design, outfitting, machinery and electrical equipment, automation and remote control, the reactor plant and containment system, and the waste disposal system. (M.O.W.)

12463 (CONF-640810, pp 138-55) THE REACTOR PLANT OF THE RESEARCH SHIP OF GESELLSCHAFT FUER KERNENERGIEVERWERTUNG IN SCHIFFBAU UND SCHIFFAHRT mbH., HAMBURG—GEESTHACHT. Schomer, R. T. (Virginia Polytechnic Inst., Blacksburg).

The design of a German commercial-nuclear-powered ship is discussed in some detail. Primarily, the discussion concerns the reactor and reactor components. (M.O.W.)

12464 (CONF-640810, pp 156-65) PANEL DISCUSSION: LICENSING THE NUCLEAR MERCHANT VESSEL. Beck, Clifford K.; Lill, Harborough I.; MacMillan, John H. (Virginia Polytechnic Inst., Blacksburg).

In consideration of various safety aspects of nuclear-powered ships, the licensing requirements and procedures are discussed. (M.O.W.)

12465 (GA-6807) PRECRITICAL CALCULATIONS FOR THE 3.0 IN. PITCH, BERYLLIUM REFLECTED, TWMR CRITICAL ASSEMBLY. Peak, J. C.; Lovallo, J. M. (General Atomic, San Diego, Calif. John Jay Hopkins Lab. for Pure and Applied Science). Nov. 8, 1965. Contract SNPC-27. 18p. (NASA-CR-54786).

In order to determine the feasibility of an isotopically enriched tungsten, water moderated reactor for use in a nuclear rocket, a critical assembly was fabricated and the necessary precritical neutronic calculations were made. The critical loadings are discussed and the precritical calculations for the 3.0 in pitch core with beryllium reflectors are summarized. (M.O.W.)

12466 (NAA-SR-11642) THE PREDICTED FISSION PRODUCT DECAY OF SNAPSHOT I. Sayer, W. B.; Hart, R. S. (Atomics International, Canoga Park, Calif.). Jan. 15, 1966. Contract AT(11-1)-Gen-8. 17p. Dep. mn. CFSTI $1.00 cy, $0.50 mn.

SNAPSHOT-I was the first flight test of a direct power conversion system utilizing a nuclear reactor as the heat source. The calculated fission product inventory formed during the orbital operation of the SNAP 10A reactor and the predicted decay of this activity and the associated gamma radiation levels are included. A brief system description and summary of the operational phase is included. (auth)

12467 (NAA-SR-11704) METHODS FOR PREDICTING AERODYNAMIC HEATING RATES TO HIGH-VELOCITY BODIES IN THE UPPER ATMOSPHERE. Elliott, R. D. (Atomics International, Canoga Park, Calif.). Jan. 15, 1966. Contract AT(11-1)-Gen-8. 37p. Dep. mn. CFSTI $2.00 cy, $0.50 mn.

The basic physical phenomena associated with aerodynamic heating are described. The methods currently used at AI for predicting heating rates to bodies moving at high velocities through the earth's atmosphere are summarized. The methods described provide the principal input data for the analytical studies of SNAP reentry disintegration in the Aerospace Nuclear Safety Program. (auth)

12468 (NAA-SR-Memo-9916) MONTE CARLO EVALUATION OF FAST NEUTRON FLUXES AND HEATING IN THE S8DS NEUTRON SHIELD. Schweiger, D. F.; Steichen, C. U. (Atomics International, Canoga Park, Calif.). Aug. 27, 1965. Contract AT-11-1-GEN-8. 22p. Dep. mn. CFSTI $1.00 cy, $0.50 mn.

Fast neutron fluxes were calculated for a nominal separation distance of 26 inches between the center of the active core volume and the top of the lithium hydride casting. The maximum fast flux (0.092 to 10.56 Mev) was found to be 2.9×10^5 n/cm^2-sec-watt. At an operating power level of 600 kwt this corresponds to a flux level of 1.74×10^{11} n/cm^2-sec. Fast fluxes were computed down to a depth of 28.75 cm below the top of the casting. A comparison was made between the Monte Carlo results, a removal theory calculation by the QAD program, and a reactor leakage equivalent point source calculation. All three calculations agreed within a factor of three. The Monte Carlo and point source calculation agreed closely. Fast neutron heating rates were computed from the Monte Carlo flux levels. The maximum heating load was estimated to be 2.7×10^{10} Mev/cm^3-sec. This corresponds to 0.0042 watt/cm^3 or 419 Btu/hr-ft^3. (auth)

12469 (NAA-SR-Memo-11630) POST ASSEMBLY ELECTRICAL CHECKOUT OF 10FS-5 IN BUILDING 013. Klinkner, K. C. (Atomics International, Canoga Park, Calif.). Sept. 3, 1965. Contract AT-11-1-GEN-8. 100p. Dep. mn. CFSTI $3.00 cy, $0.75 mn.

The results are presented of the post assembly electrical checkout of 10FS-5. Satisfactory test results were obtained with the exceptions noted. Test results, deviations, and recommendations are presented. The flight system was accepted for acceptance testing in the shock and vibration test facility. (auth)

12470 (SC-R-65-1017) AEROSPACE SAFETY RESULTS FROM A ROVER/NERVA POST-OPERATIONAL DESTRUCT TEST. Berry, R. E. (Sandia Corp., Albuquerque, N. Mex.). Nov. 1965. Contract AT(29-1)-789. 17p. (CONF-651101-54). Dep. mn. CFSTI $1.00 cy, $0.50 mn.

From 13th Conference on Remote Systems Technology, Washington, D. C.

The destruction of a full-scale mockup ROVER/NERVA propulsion engine was performed under the direction of the joint AEC/NASA Space Nuclear Propulsion Office. The data collected included information about the destruct debris velocity, size, weight, and spatial distribution. These data are a satisfactory source term for the computer analysis of the ROVER/NERVA Program safety. (auth)

12471 (SC-RR-65-557) EVALUATION OF MICROSCOPIC-SIZED GRAPHITE AEROSOL FROM A ROVER REACTOR DESTRUCTION TEST, JUNE 1965. Parker, D. R. (Sandia Corp., Albuquerque, N. Mex.). Dec. 1965. Contract AT(29-1)-789. 15p. Dep. mn. CFSTI $1.00 cy, $0.50 mn.

The methods used to evaluate the environmental health aspects of particle dispersion and properties following the destruction of a full-scale model of a ROVER-NERVA reactor are summarized. The methods used to collect airborne samples and to analyze the particles are described. Results on the total number and the size distribution of the particles are included. (D.C.W.)

12472 (SC-RR-65-620) ROVER/NERVA DESTRUCT SYSTEM TEST RESULTS, ABERDEEN PROVING GROUND-3(FINAL REPORT). Berry, R. E.; Martin, J. P. (Sandia Corp., Albuquerque, N. Mex.). Dec. 1965. Contract AT (29-1)-789. 258p. Dep. mn. CFSTI $6.00 cy, $1.25 mn.

A full-scale destruct test of the ROVER/NERVA space propulsion engine was made. In the test, a full-scale mock-up of the ROVER/NERVA was destroyed by four statically emplaced, 105 mm special explosive charges. The information and data obtained from the test were to establish the spatial distribution of particles, the size distribution as a function of the mass, and velocity. The instrumentation for the full-scale destruct test successfully obtained the desired data. Particle sizes up to 20 microns were obtained by air sampling, but these small particles did not contain uranium. Pressure measurements obtained were 23 psi at 20 feet, 8 psi at 30 feet, and 4.2 psi at 40 feet. Graphite debris velocity recorded was 570 fps over 20 feet; however, the debris velocity dropped to 420 fps over 70 feet. Part of the debris from this test was distributed radially, and the remainder was dispersed in five concentrated jets. The metallic components (skin, reflectors, and control drums) were deployed in a symmetrical radial pattern, and each numbered component moved on a radial line from its location prior to the destruct test. The core and graphite reflector did not follow the radial pattern but flowed within the core cavity and were deployed in four horizontal jets, 90° apart, and in a vertical jet. Results are included. (auth)

12473 (TID-22459) N. S. SAVANNAH CONTAINMENT INTEGRITY QUARTERLY LEAK RATE TEST RESULTS, MAY 1964. Taylor, J. H. (Babcock and Wilcox Co., Galveston, Tex. Todd Shipyards Corp., Galveston, Tex.). 22p. (STS-45). Dep. mn. CFSTI $1.00 cy, $0.50 mn.

Two containment leak tests were conducted on the N.S. Savannah. The main objective of the first test was to satisfy the U. S. Coast Guard annual inspection requirements. The second test was of greater technical significance than the first, since it immediately followed a two-day sea trial and was conducted in the "as-is" condition. Results from these tests are presented. (M.O.W.)

12474 (TID-22460) N. S. SAVANNAH OPERATIONS. Quarterly Report, May 1–August 1, 1964. (Babcock and Wilcox Co., Galveston, Tex. Todd Shipyards Corp., Gal-

veston, Tex.). 51p. (STS-51). Dep. mn. CFSTI $3.00 cy, $0.50 mn.

Operation of the ship during this period is discussed. Reports on the reactor compartment ventilation system filter efficiency tests, scrams 42 through 48, and waste disposal are presented. (M.O.W.)

12475 (WANL-PR(B)-009) SPACE POWER PLANT STUDY. Final Report, NAS 5-250. Blinn, H. O.; Hanson, J. P.; Lane, R. H.; Markley, R. A.; Mayer, M. S.; Tauson, P.; Thompson, C. A. (Westinghouse Electric Corp.; Pittsburgh, Pa. Astronuclear Lab.). Dec. 31, 1963. 231p.

The study evaluates cesium and potassium as working fluids in an advanced high-temperature Rankine cycle power conversion system. The evaluation was accomplished by designing the major components of cycles using each working fluid and comparing the results. It is necessary to have as high a maximum cycle temperature as possible in order to minimize power plant weight. The creep of the first turbine rotor is probably the most serious upper temperature limitation on Rankine cycle power plants for space applications. Consequently, this was adopted as a design criterion. With this design basis, the maximum cycle temperature for the system using cesium was higher than for the system using potassium. The study was conducted for 1 Mw shaft output power but it is believed that the conclusions drawn from comparing the two systems on a plant weight basis are generally valid. The total weights of the major components of the power plants compared in this study are 3894 lbs for cesium and 4883 lbs for potassium. This is a consequence of the difference in radiator size. Because of the high expense and long development time of high temperature alkali metal Rankine cycle technology, it is necessary to select the working fluid with the greatest potential as early as possible. For this reason, it is recommended that cesium should be seriously considered for such applications. In addition to the work described above, some reactor and shielding studies were performed. A reactor thermal hydraulic code and a buckling iteration neutron diffusion theory code were written. (auth)

12476 (AD-622352) NUCLEAR ROCKET ENGINE. Ermakov, A. P.; Syrmai, A. G. Translated from pp 114-21 of Atomnaya Energiya i Transport, The Academy of Sciences, Moscow, 1963. 11p. (FTD-TT-65-943). CFSTI.

A brief review of general concepts of nuclear rocket engines is presented. Nuclear electroreactive engines and on-board sources of electric energy are discussed. The operating needs and performances are discussed. (M.O.W.)

12477 PROSPECTS FOR ADVANCED HIGH-THRUST NUCLEAR PROPULSION. Cooper, Ralph S. Astronaut. Aeronaut., 4: 54-9(Jan. 1966). (LA-DC-6961).

Basic technical factors and problem areas are described for concepts that offer the possibility of improved performance as nuclear propulsion systems. Concepts considered include fluidized beds, liquid-core rockets, gas-core schemes, and pulsed nuclear rockets. The fluidized-bed and liquid-core engines appear technically feasible although very little work has been done on them. The gas-core concepts are definitely in the research stage. The open-pulse nuclear rocket has received considerable research effort, short of nuclear tests of ablation, and still appears technically feasible. It is concluded that no clear course is open at present. (30 references). (A.G.W.)

12478 THERMIONIC REACTORS AS POWER SUPPLY OF SPACE CRAFTS. Pruschek, R. (Technische Hochschule, Stuttgart). Atomkernenergie, 10: 327-32(Sept.-Oct. 1965). (In German).

Fast and thermal nuclear reactors with incore-thermionic-converters are discussed with respect to their aptitude as power supply for space vehicles. Two different fields for application are distinguished: auxiliary power supply and electric rocket propulsion. Thermal as well as fast thermionic reactor systems may be used as auxiliary power supply. The choice depends on the required power and on the ratio of transportation to fuel cost. As for electric rocket propulsion, fast thermionic reactor systems could be preferable. (auth)

12479 PARAMETER STUDIES ON THERMAL THERMIONIC REACTORS. Wolf, E.; Haug, W. (Technische Hochschule, Stuttgart). Atomkernenergie, 10: 333-45 (Sept.-Oct. 1965). (In German).

The obtainable specific power (kw/kg) of ZrH- moderated thermionic reactors for space with a total power in the range between 500 and 5000 kw(th) is discussed. Some reactor parameters are optimized with respect to the specific power. The in-core arrangement of the thermionic converters allows a relatively high temperature of waste heat, and thus a low radiator weight may be obtained. On the other hand the in-core arrangement of the converters will decrease the density of the core. The fuel elements will be shielded against thermal neutrons by the converter materials located between moderator and fuel. The effects of converter spacing and shielding properties of some emitter materials on the specific reactor power are discussed. (auth)

12480 ON THE DESIGN OF RADIATORS FOR SPACE. Groll, M. (Technische Hochschule, Stuttgart). Atomkernenergie, 10: 353-8(Sept.-Oct. 1965). (In German).

A radiator for power supply systems for space is briefly described. Plane and arched radiators are compared. The parameters influencing the radiator mass are discussed. The radiator calculation together with a method for optimizing the (rectangular) cooling fins is explained. The results for radiators radiating from one side and from both sides are compared. (auth)

12481 ON THE FEASIBILITY OF ELECTROMAGNETIC PUMPS IN SPACE VEHICLES. Steiner, D. (Technische Hochschule, Stuttgart). Atomkernenergie, 10: 359-62 (Sept.-Oct. 1965). (In German).

The available electromagnetic pumps are discussed with respect to their feasibility for thermionic reactors. The various types of electromagnetic pumps are briefly described. Mass and efficiency of a direct current conduction pump for low output power are estimated. (auth)

12482 DESIGN STUDY OF A NUCLEAR POWER PLANT (TRIKT-50) FOR SPACE FLIGHT. Haug, W.; Fritz, R.; Pruschek, R.; Wolf, E. (Technische Hochschule, Stuttgart). Atomkernenergie, 10: 363-7(Sept.-Oct. 1965). (In German).

The specific weight of a nuclear electric power plant for space flight with an electrical output of 50 kw is estimated. The electric energy is obtained by direct conversion of thermal reactor heat by means of thermionic converters. Some pre-established constructive sketches have resulted in a number of data. The plant is described and the approximate masses of the essential components are given. (auth)

12483 PARAMETER STUDY OF FAST REACTORS WITH INCORE THERMIONIC CONVERTERS (SYSTEM SRIKT). Lutz, D.; Steiner, D.; Unger, H.; Woessner, G. (Technische Hochschule, Stuttgart). Atomkernenergie, 10: 368-74(Sept.-Oct. 1965). (In German).

Fast reactors with convection-cooled incore thermionic converters in the power range of 300 to 10,000 kw(th) are investigated with respect to the application as power supply for space vehicles. For a large number of thermionic reactors, values for power, weight, and specific cost are presented. The use of liquid metals as coolant for fast thermionic reactors in a power supply system for space vehicles is discussed. (auth)

12484 NUCLEAR SPACE POWER UNITS WITHOUT CONVECTIVE HEAT TRANSFER. Unger, H. E. (Technische Hochschule, Stuttgart). Atomkernenergie. 10: 375-7(Sept.-Oct. 1965). (In German).

Advantages and disadvantages of nuclear thermionic space power units without convective cooling are discussed. Systems and projects, which have been studied so far by various institutions, are described and compared. Their investment of fissile material amounts to values of 50 to

1300 kg at a power range of 0.5 to 1000 kw electric. The specific power varies between 1 and 200 w/kg. The latter value seems to be achievable if the systems are intensely developed. (auth)

12485 NUCLEAR CALCULATIONS FOR A FAST REACTOR WITH THE SHAPE OF A HOLLOW CYLINDER WITH THERMIONIC CONVERTERS ON ITS SURFACE. **Unger, H. E. (Technische Hochschule, Stuttgart). Atomkernenergie, 10: 378-82(Sept.-Oct. 1965). (In German).**

The calculation of criticality and neutron flux of a fast, reflected, hollow, cylindric reactor is shown. Neutron spectra for different dimensions and compositions of the core are compared. By averaging the group constants over one of these spectra, data sets for a one- and a four-group diffusion theory are obtained. These are used for the calculation of the criticality and of the spatial distribution of the neutron flux. Improvements due to corrections of the boundary conditions at the cavity are discussed. (auth)

12486 TEMPERATURE DISTRIBUTION IN A FAST REACTOR WITH THERMIONIC CONVERTERS ON ITS SURFACE. **Groll, M.; Pruschek, R. (Technische Hochschule, Stuttgart). Atomkernenergie, 10: 383-91(Sept.-Oct. 1965). (In German).**

A power supply system for space, consisting of a fast reactor and thermionic converters (system SRAST), is investigated. Thermodynamic calculations for the nuclear-calculated reactor with known geometry and flux distribution are carried out. The temperature distribution in the reactor and the produced power are obtained by one- and two-dimensional calculations. The influence of parameters is discussed. (auth)

12487 APPARATUS FOR SIMULATING HEAT TRANSFER FROM THE REACTOR SURFACE TO THERMIONIC CONVERTERS. **Koeppe, A.; Pruschek, R. (Technische Hochschule, Stuttgart). Atomkernenergie, 10: 392-4 (Sept.-Oct. 1965). (In German).**

An apparatus for simulating heat transfer by radiation from the reactor surface to thermionic converters is described. Preliminary investigations on the temperature distribution of heated tantalum plates were carried out. (auth)

12488 THEORETICAL CONSIDERATIONS ON HEAT TRANSFER IN HEAT PIPES. **Schindler, M.; Woessner, G. (Technische Hochschule, Stuttgart). Atomkernenergie, 10: 395-8(Sept.-Oct. 1965). (In German).**

High thermal conductance with small temperature drop may be obtained by evaporating a liquid coolant, conducting the vapor, and subsequent condensation. If the condensate is returned to the evaporator by capillary forces, one will be independent of auxiliary systems as pumps. For heat pipes operating on this principle the physical basis is discussed, and the heat transfer is calculated based on an elementary model. A numerical example is given with regard to waste heat transport from thermionic reactors. (auth)

12489 EMPLOYMENT OF HEAT PIPES FOR THERMIONIC REACTORS. **Ruehle, R.; Steiner, D.; Fritz, R.; Dagbjartsson, S. (Technische Hochschule, Stuttgart). Atomkernenergie, 10: 399-404(Sept.-Oct. 1965). (In German).**

It is shown how heat pipes can be used in thermionic reactors. For this purpose the mass per power ratio of three different systems was calculated: hollow sphere reactors with out-of-core thermionic converters cooled by heat pipes; cylindrical reactors with out-of-core thermionic converters heated and cooled by heat pipes; and radiators with heat pipes instead of cooling fins. For these systems, lower mass per power ratios are obtained with heat pipes. (auth)

12490 THE TECHNICAL ASPECTS OF THE RCN AND THE MUTUAL SIGNIFICANCE OF THE RCN AND THE DUTCH INDUSTRY. **Pelser, J. Atoomenergie Haar Toepass., 7: 211-17(Oct. 1965). (In Dutch).**

Important industrial aspects of the NERO project were explained on the basis of some examples. An indication is also given of the design and construction of a PWR prototype by the Dutch professionals. On this project, they can gain the knowledge and technology necessary for the construction of larger reactors and marine reactors. (tr-auth)

12491 THE STABILITY OF COUPLED-CORE NUCLEAR REACTOR SYSTEMS BY THE SECOND METHOD OF LIAPUNOV [Thesis]. **Murray, Hugh Sutherland. Tucson, Ariz., Univ. of Arizona, 1965. 105p.**

The type of coupled-core system studied includes two or more separate power reactors coupled together for the purpose of achieving an increased system power output. The primary example is that of the proposed clustering of nuclear rocket engines. The equations that describe the dynamics of a coupled-core system contain, because of a time lag in the interdependent portion of the system behavior, variables whose arguments are delayed or retarded in time. It is necessary from a practical standpoint to discover whether or not a projected coupled-core system is inherently stable. Recently, researchers have found that the most universal method of investigating the stability of ordinary differential equations is the Second Method of Liapunov. The Second Method is directly applicable to nonlinear equations. The presence of the time delay, however, necessitates some modifications to the Liapunov approach. The extension of the method is based upon the work performed by Driver, Krasovskii, and Razumikhin on the mathematical features of equations with delay. The time delay is incorporated directly into the Second Method, thus it is certain that the results are conservative due to the sufficiency of the stability conditions. The modified approach is based upon comparing all possible solutions of a system with delay with the known properties of the system without delay. The technique used is to find quadratic Liapunov functions for the linearized, zero-delay system. Stability conclusions can then be made for the linearized system with delay. Finally, the nonlinear terms are added to estimate the regions of stability of the state variables. The results are adequate, from a practical viewpoint, for a simplified two-core example. However, the approach becomes highly restrictive for higher order, more complicated cases, and the results become marginal. The basic stability conclusions combined with simulation studies for the more complicated system, reveal that there are no practical stability problems involved in coupled-core nuclear reactor dynamics. (Dissertation Abstr.)

12492 APPLICATION OF NUCLEAR ELECTRIC PROPULSION TO MANNED MARS MISSIONS. **Brown, Harold; Coates, Gordon L. (General Electric Co.; Philadelphia). New York, American Inst. of Aeronautics and Astronautics, 1965, Preprint No. AIAA 65-414, 30p., $1.00. (CONF-650711-51). ORINS.**

From AIAA 2nd Annual Meeting and Technical Demonstration, San Francisco.

A manned Mars mission is used as an example for a study of the feasibility of manned interplanetary flight using an optimum combination of nuclear rocket and nuclear electric propulsion. Basic data are presented and analytical tools are developed for optimizing the design of the interplanetary vehicle and its trajectory. A particular mission profile, a particular set of powerplant, propulsion, and payload characteristics, and a resultant overall vehicle design concept are considered. The effects of variations in the assumed mission profile and in the vehicle subsystem characteristics are discussed. (A.G.W.)

Research and Test Reactors

Refer also to abstracts 10507, 11061, 11144–11152, 11174, 11241, 11247, and 12398.

12493 (AECL–2514) COMPARISON OF CALCULATED AND MEASURED CRITICAL SIZES FOR SOME

ZED-2 LATTICES. Thibaudeau, J.; Critoph, E. (Atomic Energy of Canada Ltd., Chalk River (Ontario)). Nov. 1965. 30p. (CRRP–1228). Dep. AECL $1.00.

A study of some lattices of 7 and 19-element UO_2 clusters, which was measured in ZED-2, was undertaken to compare the predictions of different programs with measurements. In this study HEX, FLAME, and SYMMETRIZE were used. Using these programs, it was possible to assess the errors associated with most of the approximations contained in each of these programs and derive corrections for them. The measured buckling was finally compared with the bucklings obtained from the programs with these derived corrections applied. (auth)

12494 (BNWL–160) MIGRATION AREA AND MODERATOR REACTIVITY COEFFICIENTS FOR THE H_2O MODERATED, 1.8 wt percent Pu–Al LOADING IN THE PRCF. Uotinen, V. O.; Pitner, A. L.; Stinson, W. P. (Battelle-Northwest, Richland, Wash. Pacific Northwest Lab.). Oct. 1965. Contract AT(45-1)-1830. 15p. Dep. mn; CFSTI $1.00 cy, $0.50 mn.

Reactivity worths of moderator level changes are measured in the Plutonium Recycle Critical Facility (PRCF) for a loading of 1.82 wt. % Pu–Al fuel moderated by H_2O. From these measurements the migration area of the core can be deducted. For an H_2O moderated loading, the main contribution to the migration area comes from the slowing down area for the fast group of neutrons. Therefore, a comparison between experimental and calculational migration areas is a measure of the correctness of methods of calculating fast group parameters. The migration area of the core is determined from the variation of the moderator coefficient of reactivity with moderator height. A value of 42 ± 5 cm^2 is obtained for the migration area of this reactor loading. The value obtained from a diffusion theory calculation using four energy groups is 54 cm^2. (auth)

12495 (EUR–2538.e) THE USE OF PULSED REACTORS IN THE FIELD OF NEUTRON AND SOLID STATE PHYSICS. Kley, W. (European Atomic Energy Community, Ispra (Italy). Joint Nuclear Research Center). May 14, 1965. 61p. (CONF-650568–1). Dep. mn.

From Panel on Kinetics and Applications of Pulsed Reactors Symposium, Vienna.

The neutron source requirements are examined for a particular selection of experiments in the field of neutron and solid state physics. For a number of facilities, the principal design features are given. A quantitative comparison of experiments at a pulsed reactor of the SORA type with those at a very high flux reactor is given. The figure of merit in favor of the SORA type reactor is within the limits of $1 \leq M \leq 40$ for experiments with thermal and subthermal neutrons. In general, the pulsed reactor is better by the flux ratio M = SORA/v.h.f.r. for experiments using the time of flight technique. (auth)

12496 (IDO–16871-5) FUNDAMENTALS IN THE OPERATION OF NUCLEAR TEST REACTORS. VOLUME 5. ADVANCED TEST REACTOR DESIGN AND OPERATION. (Phillips Petroleum Co., Idaho Falls, Idaho. Atomic Energy Div.). Nov. 1965. Contract AT(10-1)-205. 187p. Dep. mn. CFSTI $5.00 cy, $1.00 mn.

A detailed description is presented of the Advanced Test Reactor and its associated facilities. Control components and instrumentation are described. Operating and shutdown procedures are discussed. Other detailed information is presented on supplementary water systems, liquid waste systems, electrical systems, heating and ventilation systems, radiation protection and monitoring, radiation monitoring system, and canal operations. (M.O.W.)

12497 (IDO–17003(Rev.2)) ADDENDUM TO THE SPERT III HAZARDS SUMMARY REPORT—LOW-ENRICHMENT OXIDE CORE. Houghtaling, J. E.; Norberg, J. A.; Haire, J. C. (Phillips Petroleum Co., Idaho Falls, Idaho. Atomic Energy Div.). Oct. 1965. Contract AT (10-1)-205. 98p. Dep. mn. CFSTI $3.00 cy, $0.75 mn.

The important features of a new slightly enriched oxide core, designated the E-core, and the potential problems and hazards of operating this reactor in the Spert III facility are discussed. All features discussed in the previous Spert III Hazards Summary Report still apply. Pertinent mechanical characteristics of the E-core are explained in some detail, as well as changes made to the Spert III control system. Included are the nuclear characteristics of the core as determined both by calculation and extrapolation of previous experimental results. Also, the predicted kinetic behavior for the planned tests and certain accident conditions are discussed. Finally, several accident situations are considered and analyzed to obtain numerical estimates of radiological hazards. It is concluded that the E-core can be operated as proposed and remain within the safety policies of the AEC. (auth)

12498 (IDO–17112, pp 1-51) INSTRUMENTATION ANALYSIS. Wilde, Ned (Phillips Petroleum Co., Idaho Falls, Idaho. Atomic Energy Div.).

Several accident studies were made for various test reactors and critical facilities, using the zero-power kinetic equations. A xenon simulator was completed and was used to estimate the xenon reactivity in Spert III for up-down operation of the reactor. The value of β/l was measured for Spert III, ARMF-1, PBF, ETRC, the Capsule Driver Core, and the ATR critical facility. The kinetic parameters of the SNAP 10A reactor were also measured. A loss-of-flow transient study was performed for LOFT by simulation on an analog computer; flow and pressure transients of the fluid in the LOFT coolant system caused by a rupture in the reactor vessel were also studied. The In-pile Fatigue Testing Experiment to be placed in the ETR was analyzed to determine the amount and rate of contamination of the hydraulic fluid in the actuator. The effects of a rupture in the ETR reactor vessel were also studied, together with the effects of a power failure to the primary coolant pumps. (D.C.W.)

12499 (IDO–17112, pp 52-80) INSTRUMENT COMPONENT AND SYSTEMS DEVELOPMENT. Boland, T. J. (Phillips Petroleum Co., Idaho Falls, Idaho. Atomic Energy Div.).

The development of instrumentation for following the behavior of ATR fuel plates, for the Idaho Chemical Processing Plant, for zero-power reactors, and for test reactors is summarized. The health-physics instrumentation developed is also briefly described, together with a pseudorandom noise generator, a gain stability analyzer, and a program sequence times for the SNAPTRAN-2/10A-1 reactor transient test program. (D.C.W.)

12500 (IDO–17131) SHIFT CREW PERFORMANCE EVALUATION AT NUCLEAR TEST REACTORS. Nertney, R. J. (Phillips Petroleum Co., Idaho Falls, Idaho. Atomic Energy Div.). Dec. 1965. Contract AT(10-1)-205. 17p. Dep. mn. CFSTI $1.00 cy, $0.50 mn.

Results of a study to determine homogeneity of performance by operations shift crews in handling experimental systems at nuclear test reactors are presented. The study was based on rank ordering four operations shift crews at each of two test reactors according to performance quality. Four performance criteria are considered. Results are presented and compared with those obtained in an earlier pilot study. (auth)

12501 (ORNL–TM–1163) FAST AND THERMAL NEUTRON FLUX MEASUREMENTS IN THE ORR AND LITR. O'Brien, H. A. Jr. (Oak Ridge National Lab., Tenn.). Jan. 1966. Contract W-7405-eng-26. 15p. Dep. mn. CFSTI $1.00 cy, $0.50 mn.

Fast- and thermal-neutron flux measurements in the Oak Ridge Research Reactor (ORR) and the Low Intensity Test Reactor (LITR) were made with a precision of ±5%. The fast-neutron flux values were calculated from the ^{54}Mn yields obtained from the $^{54}Fe(n,p)^{54}Mn$ reaction in both natural iron wire and stainless steel targets. The thermal fluxes were measured by the $^{59}Co(n,\gamma)^{60}Co$ reaction in Co–Al alloy targets containing 0.15% cobalt, and in stainless steel targets containing 0.08% cobalt. (auth)

12502 (TID–22547) ADVANCED TEST REACTOR SERVO REGULATOR ROD TEST PROGRAM. ATR Site Tests. Pickett III, R. T. (Babcock and Wilcox Co., Lynchburg, Va. Atomic Energy Div.). Sept. 1965. Contract AT(10-1)-1075. 32p. (ATR-IC–101). Dep. mn. CFSTI $2.00 cy, $0.50 mn.

For Ebasco Services, Inc., New York.

The rod mechanism was set up on a test stand, and the kinetics and heat transfer simulation was tested with step reactivity inputs and sinusoidal reactivity inputs. The step response of the servo rod system and the frequency response of the overall reactor and servo regulator rod system were measured and were compared with previous data. The servo regulator rod system performs as intended except for excessive noise generation. Several modifications are recommended. (D.C.W.)

12503 (AERE-Trans–1043) BEAM TUBE EQUIPMENT FOR THE FRJ-2 (DIDO) COLD NEUTRON SOURCE. Doose, C. (Kernforschungsanlage, Juelich (West Germany)). Translated by J. B. Sykes (Atomic Energy Research Establishment, Harwell, Eng.), from an internal report. 1965. 22p. Dep. BIS $0.30. HMSO 1s. 9d.

The beam tube equipment for the FRJ-2 cold-neutron source is described. The liquid hydrogen moderator is cooled by helium and the vacuum jacket of the beam tube equipment is cooled by heavy water. The cooling systems are described, and safety considerations are summarized. (D.C.W.)

12504 REDUCTION OF RADIOACTIVE EMISSION INTO THE ATMOSPHERE AND RESEARCH ON DEAERATION OF THE WATER OF THE PRIMARY LOOP OF WWR-M REACTOR. Kaminker, D. M.; Konoplev, K. A.; Semenov, Yu. P.; Trenin, V. P. At. Energ. (USSR), 19: 517-21(Dec. 1965). (In Russian).

The purpose and operating principle of the closed deaeration loop of the reactor, the operating experience of the deaeration loop during the first two years, and the results of studies of the deaeration regimes of the primary-loop water are described. It was determined that the deaeration system of the WWR-M reactor is a compound process, furthered by the elimination of the gaseous interfering mixture from the water of the primary loop and hindered by the formation of gas voids with the interfering mixture in the communications of this loop. The closed loop for deaeration and burning of the interfering mixture, developed at the WWR-M reactor, enabled the ejection of radioactive gases into the atmosphere to be decreased to $1/10$ its original value. (tr-auth)

12505 CALCULATION OF THE FAST NEUTRON SPECTRUM IN THE TRIGA MARK-II REACTOR. Berwanger, G. (Oesterreichische Hochschule, Vienna). Atomkernenergie, 11: 35-8(Jan.-Feb. 1966). (In German).

The fast neutron spectrum of the Triga-Mark-II-Reactor was calculated in a simple manner by the assumption of an infinite, homogeneous and water–moderated reactor model. The error was difficult to estimate in the calculation. The error was based on the assumption of a simplified reactor model, but the excellent agreement of the experimental result is shown. (auth)

12506 THE SYSTEM OF FAST REACTORS: RAPSODIE. Bull. Inform Sci. Tech. (Paris), No. 95, 5-45(July-Aug. 1965). (In French).

The building of the fast neutron reactor Rapsodie which has many novel features from the French program point of view, was preceded by a large amount of study and testing. This latter was carried out mainly on full-sized models of the reactor vessel and circuits. Although this research and testing has not led to any fundamental changes in the functional principles of the project, many constructional improvements were nevertheless made. The work led to the choice of the mixed PuO_2–UO_2 rather than the UPuMo alloy which was first considered. The construction of the reactor, planned to be finished in 1966, has itself led to the development of certain techniques, in the following fields for example: resistance of structures to seismic effects, development of thermal and nuclear protection around the reactor, and design of the containment building. Generally speaking the methods, techniques and experimental equipment which were used for the development of the Rapsodie project will be directly applicable to the study of further stages of the fast neutron reactor system. (auth)

12507 THE SYSTEM OF FAST REACTORS: HARMONIE AND MASURCA. Bull. Inform. Sci. Tech. (Paris), No. 95, 47-77(July-Aug. 1965). (In French).

Harmonie, a small source-reactor of 2kw power and Masurca, an installation for studying models of reactors having volumes of between 200 and 6,000 liters, will become, in the field of neutronics an essential part of the equipment required for the study of fast neutron reactors. Harmonie, which was recently finished, has the particular feature that its central section (the assembly made up of the core, the blanket and the reflector) can be lifted above the biological protection. It is thus possible to reduce parasite reflections during experiments in which the reactor neutron flux bombards blocks of various materials. An attempt was made, in designing Masurca, to obtain flexibility, safety of use and a high accuracy in the experimental conditions: temperature, geometry and composition of the media used. Particular attention was paid to safety during the storage and handling of the large amounts of plutonium used. (auth)

12508 ON THE DISTRIBUTION OF SOME FISSION PRODUCTS BETWEEN CORE AND RECOMBINER OF L54M REACTOR. PART 4. DECAY PROBABILITY OF ^{89}Kr AND ^{90}Kr IN RECOMBINER. Lazzarini, E. (CESNEF, Milan). Energia Nucl. (Milan), 12: 625-7(Dec. 1965).

The probabilities that ^{89}Kr and ^{90}Kr decay in the recombiner of L54M reactor, were measured by determining the amounts of ^{89}Sr and ^{90}Sr in the recombiner water. These probabilities, together with those previously obtained for ^{137}Xe, ^{140}Xe, and ^{141}Xe are plotted against the half lives of the nuclides and interpolated with calculated functions. The agreement between experimental and theoretical behaviors is discussed. (auth)

12509 LABORATORY EXAMINATION OF THE PRIMARY WATER CIRCUIT OF REACTORS. Erdey, Anna; Csada, Imre. Magyar Tud. Akad. Kozp. Fiz. Kut. Int. Kozlemen., 13: 241-9(1965). (In Hungarian).

At the time of the construction of the water-cooled, moderated, and reflected Hungarian research reactor, arrangements were made to carry out routinely control analyses of the water in order to ascertain whether it satisfies the preset requirements. Such analyses have been carried out for the past several years since the startup of the reactor. The parameters examined include the conductivity, pH, concentration of suspended particles, dry and calcined residue and the Ca^{2+}, Mg^{2+}, Na^{+}, Al^{3+}, Fe^{3+}, SiO_3^{2-}, SO_4^{2-}, and Cl^{-} concentrations. In addition, the Radiation Protection Section of the plant made occasional activity measurements. Th original water was obtained from power-plant condensates; later, it represented purified water that passed through mixed-bed ion-exchange resins. The β,γ activity varied between 10^{-9} and 10^{-5} C/liter, depending on the period of time since the regeneration and the duration of the operation. The conductivity and the dry and calcined residue of the water was found to increase with the activity but not in direct proportion with it. Contamination of the water was revealed most easily by the activity and the dry residue content; the satisfactory specimens had a dry residue of <2mg/liter. Routine determination of the pH and of the chemical composition of the dissolved material is not justified for routine operational control; it is more important to control the radiolytic products. (TTT)

12510 THE KEWB PROGRAM. Silberberg, M. (Atomics International, Canoga Park, Calif.). Nucl. Safety, 6: 386-95; 403(Summer 1965).

Activities in a program to determine the safety characteristics of small homogeneous reactors (water boilers) are summarized. The facilities for kinetic experiments

on water boilers are described, and experimental and analytical results are discussed. (J.R.D.)

12511 EXPERIMENT ON THE DIRECT CONTROL OF A NUCLEAR REACTOR USING A COMPUTER. Greene, P. J. Rivoluzione Ind., No. 147, 29-31(July-Aug. 1965). (In Italian).

The two-computer system used in the operation control of the NRU reactor at Chalk River is described. The data available to the operator are indicated and the advantages and the disadvantages of the system are considered. (J.S.R.)

12512 FAST REACTOR TEST FACILITY (FARET) AND INITIAL EXPERIMENTAL PROGRAM. Simmons, W. R.; Persiani, P. J.; Bump, T. R. (Argonne National Lab., Ill.). pp 37-55 of ANS-100(Suppl.).

The Fast Reactor Test Facility site, building, containment structure, fuel handling systems, shielding, coolant systems, reactor proper, control systems, experimental capabilities, design specifications, loading, and fuel testing program and objectives are described. (T.F.H.)

12513 DEVELOPMENT AND TESTING OF A FUSIBLE METAL JOINT FOR A FAST REACTOR. Hainzelin, J.; Zaleski, C. P. pp 27-33 of Soudage Tech. Connexes, 19: No. 1-2, 27-33(Jan.-Feb. 1965). (In French).

The eutectic alloy of Bi and Sn (58% Bi, 42% Sn) was chosen as joint material for two rotary closure plugs for the tank of the fast reactor RAPSODIE. Results of mechanical tests (ultimate tensile strength, elongation, compressive strength, cracking, Brinell hardness, and impact strength) on this alloy are given. The application procedure adopted to obtain maximum adherence of the Bi-Sn alloy to adjacent 18-8 stainless steel surfaces is described. Description and results of pressure tests on a mockup of the joint assembly to determine gas tightness of joint in both liquid and solid states are presented. (Rev. Metal Lit.)

12514 ABSOLUTE POWER MEASUREMENTS OF THE FORD NUCLEAR REACTOR. Bullock, J. B. (Univ. of Michigan, Ann Arbor). 20p. (CONF-650710-11). ORINS. Gmelin, AED-CONF-65-192-17.

From American Nuclear Society Meeting on Reactor Operating Experience, Jackson Lake Lodge, Wyo.

In the method described for measuring absolute power level of a pool-type reactor, the pool water system is treated as a calorimeter and measurements are made to determine the rate at which energy is being added to the system. Twelve thermocouples are randomly located in the reactor pool and the reactor is operated at full power without the use of the secondary cooling pump. A computer is used to determine the mean rate of increase of the bulk pool temperature from the thermocouple data. The errors inherent in this method appeared to be reasonably small for systems having low heat losses, and the method was adopted for routine reactor power measurements. (A.G.W.)

12515 NUCLEAR REACTOR. Nakamura, Shoichiro (to Hitachi, Ltd.). Japanese Patent 1964-27167. Nov. 27, 1964. Filed Oct. 4, 1962.

An efficient materials testing reactor is patented. The fuel rods of the reactor are located upright and parallel and the control rods are of the same height as the core and move horizontally through the core. (TCO)

12516 SWIMMING POOL TYPE REACTOR. Yamauchi, Atsuo (to Hitachi Ltd.). Japanese Patent 1964-27171. Nov. 27, 1964. Filed Sept. 19, 1962.

In a swimming pool-type reactor the compartment containing the reactor core at the bottom extends to the surface of the pool so that the water in the compartment is separated from the water in the pool. The cooling water is circulated through the external heat-exchanger and associated parts in a closed loop. In the top of the compartment a warm-water layer is formed to prevent the rising of the heated coolant water from the core. The water layer is supplied with its warm water from the top opening as well as heated by the heater. A pipe for drawing out the warm water to its external tank is installed between the warm water layer and the coolant exit. (TCO)

WASTE DISPOSAL AND PROCESSING

See also BIOLOGY AND MEDICINE — Ecology
CHEMISTRY — Radiochemistry
CHEMISTRY — Separation Processes and Procedures
HEALTH AND SAFETY

Refer also to abstract 11009.

12517 (BNWL–170) RESEARCH AND DEVELOPMENT ACTIVITIES. FIXATION OF RADIOACTIVE RESIDUES. Quarterly Progress Report, July–September 1965. Platt, A. M. (ed.) (Battelle-Northwest, Richland, Wash. Pacific Northwest Lab.). Oct. 1965. Contract AT(45-1)-1830. 40p. Dep. mn. CFSTI $2.00 cy, $0.50 mn.

The calcined-waste containers produced during the Hot Cell Pilot Plant experiments in 1962 and 1963 have generated a maximum pressure of 3 psig. Design verification tests with the prototype spray calciner showed satisfactory performance when producing high melting point powders. Later tests on other feeds showed poor atomization and cake buildup in the calciner. Design of the prototype equipment is complete. Procurement and fabrication of prototype equipment is done except for a few cleanup items and final field-fitting of jumpers. Design verification tests on the pot storage station indicated satisfactory calorimeter performance. A GE-412 computer was successfully used in design verification tests for data collection, calculation, and correlations. Studies continued on fixation of sulfates from acid condensates generated in a glass-making process. Lead sulfate-borax melts produced by a continuous feed melter at 900°C appear to be quite fluid, but exhibited a high (22%) evolution of sulfate. Studies were initiated on incorporation of the neutralized condensate into asphalt. Release rates of up to 2%/hr for ^{137}Cs from a simulated phosphate ceramic waste material were observed from exposures to temperatures up to 1200°C. Release rates of other isotopes which appear to be a thousand-fold lower than for cesium established volatilization as the predominant mode of cesium release. A technique for varying the phosphate content of the simulated ceramic wastes was developed. (auth)

12518 (ORNL-TM–1327) GEOHYDROLOGICAL EVALUATION OF SOLID WASTE STORAGE AREA 6. Lomenick, T. F.; Wyrick, H. J. (Oak Ridge National Lab., Tenn.). Dec. 1965. Contract W-7405-eng-26. 16p. Dep. mn. CFSTI $1.00 cy, $0.50 mn.

The proposed site of Solid Waste Storage Area 6 in Melton Valley is underlain mostly by multicolored shales and interbedded silty limestones that are generally sufficiently weathered to permit easy excavations by power equipment. About 25% of the 70-acre tract is unsuitable for burial, since it lies in areas where the water table is within 6 ft of the land surface. In order to minimize leaching and the subsequent migration of radioactive materials from the buried waste, it is essential that the trenches be constructed so as to suspend the waste above the water table, minimize rainfall infiltration into the holes once they are covered, and provide maximum seepage rates of waters from the trenches. (auth)

12519 (TID–8541, pp 149-248) RADIOACTIVE WASTE MANAGEMENT. Belter, W. G. (Division of Reactor Development and Technology (AEC), Washington, D. C.); Pearce, D. W. (Battelle-Northwest, Richland, Wash. Pacific Northwest Lab.).

A review of highlights of recent waste-management experience in the U. S. and abroad is presented. Advances in technology that have occurred during the past three to four years were summarized. (M.O.W.)

12520 (CEA-tr-A–1490) LE PROBLEME DES DECHETS RADIOACTIFS. (The Problem of Radioactive Wastes). Spitsyn, V. I. Translated into French from Abhandl. Deut. Akad. Wiss. Berlin, Kl. Chem., Geol. Biol., No. 2, 43-61(1960). 58p. Dep. mn; JCL $5.60 fs, $1.94 mf.

Sources of radioactive wastes from industrial and non-industrial installations are discussed and their characteristics are tabulated. The processing of radioactive wastes before burial or storage is summarized, and criticisms of disposal by burial are reviewed. The processing of radioactive wastes at Windscale, Marcoule, and Mol is discussed, and the advantages and disadvantages of methods used by each are emphasized. (J.S.R.)

12521 UNITED STATES AND SOVIET UNION WASTE-DISPOSAL STANDARDS. Parker, F. L. Nucl. Safety, 6: 433-6; 439-40(Summer 1965).

The standards for waste disposal in the two countries are compared. Disposal of liquid, gaseous, and solid wastes is discussed along with findings and conclusions. (J.R.D.)

12522 CURRENT PRACTICES IN THE DISPOSAL OF WASTE RADIOACTIVE GASES FROM NUCLEAR REACTORS. Stolzenbach, C. F. Nucl. Safety, 6: 436-40 (Summer 1965).

A review of information concerning disposal of radioactive gases is presented. Discussions are included of limitations on disposal of waste radioactive gases, source and identity of waste radioactive gases, waste disposal methods, and presently used waste disposal practices. (J.R.D.)

12523 THE EFFECT OF SALT CONCENTRATION IN SOIL SOLUTIONS ON THE RATE OF DIFFUSION OF MICROQUANTITIES OF STRONTIUM IN THE SOIL. Prokhorov, V. M.; Frid, A. S. Radiokhimiya, 7: 496-8 (1965). (In Russian).

The effect of soil composition on the rate of diffusion of radioactive isotopes in the soil was investigated. Experiments were conducted with ^{90}Sr without a carrier. The soil (37 m^2/g, specific surface) was wet with concentrations of $CaCl_2$ solutions ranging from 3.3×10^{-2} to 8.5 g-equiv/l. The soil was moistened to the extent of 30% by weight. To correct for adsorption of Ca^{2+} the equilibrium concentration of $CaCl_2$ was determined by complexometric titration. The diffusion coefficient of ^{90}Sr as a function of the concentration of Ca^{2+} was measured. In the concentration range 4×10^{-3} to 5.8×10^{-1} N the diffusion coefficient of Sr increases by approximately a factor of 13. From 0.6 to 6.6 N the diffusion remains practically constant. (ATD)

12524 WASTE DISPOSAL. Reactor Fuel Process., 8: 172-82(Summer 1965).

Information is reviewed concerning treatment of low- and intermediate-level wastes by incorporation in asphalt. Processes for conversion of high-level-activity wastes to solids are described. Information is also included on recovery of fission products. (J.R.D.)

12525 WASTE WATER AND NUCLEAR ENERGY. Michon, G. (CEN, Fontenay-aux-Roses, France). Rev. Pathol. Gen. Comp., 64: 583-8(1964).

The various origins of waste water produced in the generation of nuclear energy are studied. Thus far radioactive wastes have not been kept minimal in industry. Physical, chemical, and biological tests permit an assessment of the general aspects of such pollution. Biological studies permit better definition of the risks and improvement of pro-

tection of public health, although this is already perfectly satisfactory. (TCO)

12526 ENGINEERING DEVELOPMENT OF A FOAM COLUMN FOR COUNTERCURRENT SURFACE-LIQUID EXTRACTION OF A SURFACE-ACTIVE SOLUTES [Thesis]. Haas, Paul Arnold. Knoxville, Tenn., Univ. of Tennessee, 1965. 241p.

The foam separation process uses differences in surface activity to effect the separation of components of a solution. Engineering problems were solved and methods developed for the design and operation of countercurrent liquid-foam columns. Six- and 24-in.-ID columns were operated to measure contacting efficiency, foam densities, foam drainage, and foam condensation. The experimental results agree with a model for countercurrent liquid-foam flow based on capillary flow through the Plateau borders between foam bubbles. Data for the drainage of the liquid from the foam flowing vertically or horizontally also agree with the same model. The heights of transfer units based on the liquid phase (HTU_x) were about 1 cm for the best conditions of uniform foams of 0.56- to 1.0-mm bubble diameter, liquid flows of 100 gal/sq ft-hr or less, and uniform liquid feed distribution with low inlet velocities. The ability of gas spargers to give uniform foam bubbles was important; spinnerets with 50- or 80-μ-diam holes as used by the rayon industry were superior to porous metal or fritted glass. There was little variation in HTU_x values for countercurrent column lengths of 10 to 28 cm. The major effects of liquid and foam flow rates and of liquid feed distributors on HTU_x values were due to their influence on the extent of channeling. The foams were condensed by means of orifices, air-operated sonic whistles, screen-lined centrifugal foam breakers, or cyclones. The removal of radioactive strontium to decontaminate Oak Ridge National Laboratory low-level waste was shown to be practical if preceded by a precipitation step (head-end step) to decrease the calcium and magnesium concentrations. (Dissertation Abstr.)

12527 METHOD FOR REMOVING RADIOACTIVE SUBSTANCES IN WATER. Kurita, Haruo (to Kurita Ind. Co., Ltd.). Japanese Patent 1965-4720. Mar. 13, 1965. Filed Aug. 24, 1962.

An efficient low-cost method using a modified natural clay mineral is proposed for removing radioactive substances in colloidal state from ordinary waste water. The modified clay is prepared by boiling natural clay mineral, i.e., montmorillonite, in a concentrated aqueous solution of sodium hydroxide, and drying the clay with or without washing. After the radioactive substances are adsorbed from waste water by the exchange reactions, the powder is separated from the water. (TCO)

GENERAL AND MISCELLANEOUS

12528 (BNL–8694) A METHOD FOR SOLVING INTEGER LINEAR PROGRAMMING PROBLEMS BY THE USE OF GENERATING FUNCTIONS. Thurber, James K. (Brookhaven National Lab., Upton, N. Y.). [1960]. Contract AT-30-2-GEN-16. 30p. Dep. mn. CFSTI $2.00 cy, $0.50 mn.

A method is given that is based on a simplification and extension of techniques used to solve simultaneous linear homogeneous diophantine inequalities which are found in the treatise by P. A. MacMahon on Combinatory Analysis. (M.O.W.)

12529 (BNL–8798) A NUMERICAL METHOD FOR THE SOLUTION OF INITIAL VALUE PROBLEMS FOR SYSTEMS OF ORDINARY DIFFERENTIAL EQUATIONS. Cannon, J. R. (Brookhaven National Lab., Upton, N. Y.). [nd]. Contract AT(30-2)-Gen-16. 9p. Dep. mn. CFSTI $1.00 cy, $0.50 mn.

An approximate technique was developed for handling initial value problems of the type $(dx_i/dt) = f_i(t,x_1, \ldots, x_m)$, $0 \leq t \leq T$ $x_i(0) = a_i$, $i = 1, \ldots, m$, where f_i, $i = 1, \ldots, m$, are C^2 in an $m + 1$ dimensional domain D which contains the point $(0, a_1, \ldots, a_m)$ in its interior. The approximation method is presented and its rate of convergence to the solution at the grid points is briefly discussed. Numerical results obtained with the method are discussed. (M.O.W.)

12530 (BNWL–113-10) PLUTONIUM ABSTRACTS. Volume 5, Number 10. (Battelle-Northwest, Richland, Wash. Pacific Northwest Lab.). Nov. 30, 1965. Contract AT(45-1)-1830. 59p. Dep. mn. CFSTI $3.00 cy, $0.75 mn.

References (137) with abstracts on plutonium technology are given to reports and journals published during 1965. The fields covered include: biology and medicine, chemistry, health physics, metallurgy and ceramics, physics, and reactor technology. (P.C.H.)

12531 (BNWL–113-11) PLUTONIUM ABSTRACTS. Volume 5, Number 11. (Battelle-Northwest, Richland, Wash. Pacific Northwest Lab.). Dec. 31, 1965. Contract AT(45-1)-1830. 34p. Dep. mn. CFSTI $2.00 cy, $0.50 mn.

Seventy-three references are given to reports and journals published during 1965. The subjects covered include: biology and medicine; chemistry; health and safety; metallurgy and ceramics; miscellaneous; physics; and reactor technology. (P.C.H.)

12532 (COO–920-8) STERIC INTERFERENCE TO DIFFUSION IN LINDE A ZEOLITE. Rudloff, W.; Brandt, W. W. (Illinois Inst. of Tech., Chicago. Dept. of Chemistry). [1964]. Contract AT(11-1)-920. 5p. Dep. mn. CFSTI $1.00 cy, $0.50 mn.

Diffusion rates of ethane were measured in Li^+, Na^+, and K^+ forms of a Linde A type zeolite with various amounts of water adsorbed prior to the diffusion measurements in order to determine steric interference. It was concluded that additional H_2O molecules present seem to affect the ethane diffusion coefficients through their strong attraction to the mobile cations present. Presumably, the motion of the cations is facilitated, and, therefore, retards the ethane molecules, only little. Data are tabulated. (P.C.H.)

12533 (COO–1020-6) CHELATION AND OLATION REACTIONS OF METAL IONS IN AQUEOUS SOLUTION. PART I. NEW MULTIDENTATE LIGANDS. III. AMINO ACIDS CONTAINING METHYLENEPHOSPHONATE GROUPS. Progress Report. Westerback, S.; Rajan, K. S.; Martell, A. E. (Clark Univ., Worcester, Mass. Dept. of Chemistry. Illinois Inst. of Tech., Chicago. Dept. of Chemistry). 1964. Contract AT(11-1)-1020. 22p. Dep. mn. CFSTI $1.00 cy, $0.50 mn.

Synthesis, properties, and metal chelate formation constants are reported for the new ligands nitriloaceticdi-(methylenephosphonic) acid (NADMP), nitrilo-acetic-β-propionicmethylenephosphonic acid (NAPMP), and N,N, N',N'-ethylenediaminetetra(methylenephosphonic) acid (ENTMP). The stoichiometry of their acid-base and metal ion interactions are deduced from potentiometric data, and the probable structures of the metal chelates formed are inferred by comparison of their metal ion affinities with those of analogous ligands. (auth)

12534 (COO–1198-216) THE BEHAVIOR OF THIRTEEN CHARGE TRANSFER COMPLEXES AT HIGH PRESSURE. Bentley, W. H.; Drickamer, H. G. (Illinois Univ., Urbana). [1964]. Contract AT(11-1)-1198. 62p. Dep. mn; CFSTI $3.00 cy, $0.75 mn.

The effect of pressure to several hundred kilobars was measured on the properties of thirteen complexes containing aromatic molecules. These complexes are classified in four groups: those containing tetracyanoethylene (TCNE), those containing iodine, those involving p-phenylenediamine and halogenated p-benzoquinones, and those involving the halogenated p-benzoquinones and other materials. In all cases the resistance decreased rapidly with increasing pressure at low pressures. A number of complexes exhibited minima in resistance at pressures from 60 to 200 kilobars and an irreversible rise at higher pressures. The nature of the irreversible process could in several cases be postulated from difference in the visible and infrared spectra between the transformed and untransformed complexes. (auth)

12535 (IS-T–61) DIFFUSION OF HYDROGEN IN BARIUM METAL [Thesis]. Hammerberg, Charles Clifford (Ames Lab., Iowa State Univ. of Science and Tech.). Nov. 1965. Contract W-7405-eng-82. 32p. Dep. mn. CFSTI $2.00 cy, $0.50 mn.

The diffusion coefficients for hydrogen in barium metal were measured from 200 to 620°C. D_0 was found to be 4.0×10^{-3} and ΔH was 4.54 kcal. The solubility limit of BaH_2 in barium was determined in the same temperature range and was in agreement with previous measurements. (auth)

12536 (IS-T–66) ELECTROCAPILLARITY STUDIES OF SYMMETRIC ALIPHATIC MOLECULES ON MERCURY [Thesis]. Potter, Gordon Webster Jr. (Ames Lab., Iowa State Univ. of Science and Tech.). Nov. 1965. Contract W-7405-eng-82. 69p. Dep. mn. CFSTI $3.00 cy, $0.75 mn.

Interfacial data were taken for 3-pentanol and 3-pentanone. The adsorption properties for these compounds were very similar to similar data for 1-pentanol giving evidence that reorientations are slight if they do occur. A new method of analysis was used for determining the free energy of adsorption. It was found that a model of inert gas adsorption on solids could be applied successfully to the data. A new charge function was derived and experimental form of the data was shown to be correct by theoretical analysis. No evidence was found for reorientation, but a new model involving the presence of ion within the Inner Helmhotz Region is proposed to account for the variation of the surface excess with polarization. Three-pentanol was observed to be a 2-dimensional analog of a Boyle gas under experimental conditions. (auth)

12537 (LA–3422) THREE-DIMENSIONAL CARTESIAN PARTICLE-IN-CELL CALCULATIONS. Gage, William R.; Mader, Charles L. (Los Alamos Scientific Lab., Univ. of California, N. Mex.). Sept. 10, 1965. Contract W-7405-eng-36. 60p. Dep. mn. CFSTI $3.00 cy, $0.75 mn.

A study of the Particle-In-Cell method of numerically solving hydrodynamic problems in three dimensions is described. The closure of a cubical void in a cubical box was successfully computed. Various methods, including

stereoscopic views, of pictorial description of the particle positions are described. (auth)

12538 (LA-DC-6803) STABILITY OF SOLUTIONS OF THE POLYNOMIAL EQUATION. Clendenin, W. W. (Los Alamos Scientific Lab., Univ. of California, N. Mex.). [1960]. Contract W-7405-eng-36. 17p. Dep. mn; CFSTI $1.00 cy, $0.50 mn.

A complete analysis is carried out of the stability of solutions of the differential equation $dx/dt = -x(x - a_1) \ldots (x - a_n)$, where 0, $a_1 \ldots a_n$ are distinct roots of a real polynominal. It is shown that no periodic solutions exist. Every nonsingular solution of the equation approaches asymptotically one of the nodes either for $t \to \infty$ or for $t \to -\infty$. Moreover, every nonsingular solution which has one point between two nodes remains between them, approaching one asymptotically for $t \to \infty$, and the other for $t \to -\infty$. (auth)

12539 (LA-DC-7692) GMX-2 SPALLING CALCULATIONS. Mader, Charles L. (Los Alamos Scientific Lab., Univ. of California, N. Mex.). Oct. 1965. Contract W-7405-eng-36. 31p. Dep. mn. CFSTI $2.00 cy, $0.50 mn.

The results of some numerical spalling studies on aluminum, copper, iron, and nickel are presented. The equations of state for spall pressures and volumes are briefly discussed. Also spall as a function of tension rate is discussed. (M.O.W.)

12540 (NYO-2882-8) THE SEDIMENTATION OF MANGANESE IN THE OPEN OCEAN. Final Report. Wangersky, Peter J. (Yale Univ., New Haven, Conn. Bingham Oceanographic Lab.). [1965]. Contract AT(30-1)-2882. 13p. Dep. mn. CFSTI $1.00 cy, $0.50 mn.

The distribution of Mn in deep-sea sediments was studied in order to deduce the mechanisms responsible for deposition of Mn in the open ocean. The sediment was separated by chemical fractionation and then analyzed. The Mn content of the residual materials showed a constant linear decrease with depth in core, with occasional limited areas of very high Mn content. An increase in Mn soluble fractions, coupled with a decrease in the Mn content of insoluble fractions, indicated a transfer of Mn, either with depth in core or with time, from a firmly-bound insoluble form to one subject to solution by a gentle buffer. In a second separation, a fraction containing most of the foraminiferal tests was separated from the finer fractions of the sediment and the resulting carbonate solution was analyzed for Ca, Mg, Sr, and Mn. Possible mechanisms for Mn deposition are discussed. (P.C.H.)

12541 (NYO-2929-1) ON THE NATURE OF THE WATER MOVEMENTS IN THE SURFACE LAYER OF THE OCEAN AT OWS STATIONS I AND J SOUTH OF ICELAND. A Preliminary Study. Tufts University Meteorological Studies, Reference No. 64-1. Schell, I. I. (Tufts Univ., Medford, Mass.). Dec. 1964. Contract AT(30-1)-2929. 12p. Dep. mn. CFSTI $1.00 cy, $0.50 mn.

Studies were made on the nature of water movements to the south of Iceland to a depth of 121.9 m (400 ft) as shown by the sea surface to subsurface temperature differences to depths of 30.5, 61.5, and 121.9 m tabulated for different years for the warm (June-Sept.) and cold (Dec.-March) months. For the summer months, a positive correlation between the surface temperature and surface to subsurface differences at two different stations (Juliett and Inida) for all 3 layers. For the winter months, the correlations of the surface to subsurface temperature differences with the air minus sea temperatures at Juliett were negative and positive at India. The results are discussed. (P.C.H.)

12542 (NYO-2929-2) ON THE ORIGIN OF THE FLUCTUATIONS IN THE PERU CURRENT AND RELATED WATER MOVEMENTS OFF THE WEST COAST OF SOUTH AMERICA AND THEIR POSSIBLE PREDICTION. Tufts University Meteorological Studies, Reference No. 64-2. Schell, I. I. (Tufts Univ., Medford, Mass.). Dec. 1964. Contract AT(30-1)-2929. 29p. Dep. mn. CFSTI $2.00 cy, $0.50 mn.

Analyses were made of specified indexes of the atmospheric circulation in the eastern South Pacific between 35 and 50°S westward to longitude 135°W, and also of indexes of the circulation along the west coast of South America north of 40°S, as represented by the pressure differences between selected gridpoints derived from the mean monthly sea level pressure tabulations at standard intersections of latitude and longitude beginning with 1951, in relation to the corresponding sea surface temperature anomalies at 12 stations along the west coast of South America. It is assumed that the character of these anomalies reflects the nature and intensity of the different water movements off the coast. The results indicate that the major controls of the temperatures and presumably the strength of the Peru and Cape Horn currents as well as the upwelling over longer time-intervals and the occasional appearance of El Nino reside in the strength and convergence of the westerlies between 135 and 90°W and 35 and 50°S approximately. (P.C.H.)

12543 (NYO-3018-12) STUDIES ON THE PRODUCTIVITY OF VASCULAR HYDROPHYTES AND THEIR ROLE IN MINERAL CYCLING IN AQUATIC ECOSYSTEMS. Progress Report, January 1-December 31, 1965. Hartman, Richard T. (Pittsburgh Univ., Pa.). Jan. 15, 1966. Contract AT(30-1)-3018. 38p. Dep. mn. CFSTI $2.00 cy, $0.50 mn.

Aquatic vascular plants were studied in three separate aquatic areas. Periodic measurements were made on the size and composition of the standing crop in the communities in order to determine seasonal fluctuations. Autecological investigations were made on selected species. Rates of carbon fixation were measured over full daylight periods at monthly intervals. The relation between incident radiation and rates of carbon fixation at different periods of the day received special attention. Productivity rates were measured for several species of duckweeds using radiocarbon techniques. Special attention was given to the source of the carbon fixed by these plants and to the effect of the absorption of organic compounds on photosynthetic rates. (P.C.H.)

12544 (ORNL-3846) NUMERICAL SOLUTION OF THE LAGRANGE MULTIPLIER PROBLEM WITH SEVERAL CONSTRAINTS. Kam, Francis B. K.; Clark, Francis H. S. (Oak Ridge National Lab., Tenn.). Dec. 1965. Contract W-7405-eng-26. 34p. Dep. mn; CFSTI $2.00 cy, $0.50 mn.

A generalized multiple-constraint Lagrange multiplier program has been written in FORTRAN for the CDC-1604 computer. The program, called XTREME, is an extension of program MAX. XTREME can deal with as many as 25 independent variables. XTREME finds an extreme value for an object function subject to a number of equality constraints, at most one less than the number of independent variables. All second derivatives of the object function and the constraining functions must exist everywhere in the domain of computation. (auth)

12545 (PAEC(A)AR651) ANNUAL REPORT, FISCAL YEAR, 1964-1965. (Philippine Atomic Energy Commission, Manila). 188p. Dep. mn.

Activities in a research and development program devoted to peaceful uses of atomic energy are reported. Results of completed studies in the areas of biology, medicine, chemistry, and health physics are summarized. Research in progress is described, and a bibliography of technical publications originating at the research center is included. Information is also included on reactor operation, radioisotope production, training, regional cooperation, legal and technical activities, library services, and conferences and visits. Organizational charts are also included along with lists of students and licenses issued for radioisotope use. (J.R.D.)

12546 (SC-RR-65-548) THE STRESS POSTPROCESSOR. Martell, C. R. (Sandia Corp., Albuquerque, N. Mex.). Dec. 1965. Contract AT(29-1)-789. 82p. Dep. mn. CFSTI $3.00 cy, $0.75 mn.

Computer routines are described which can be used with

the APT system to obtain weights, centroids, and inertias as well as static and dynamic stress analysis information of solids of revolution. Also, areas, centroids, and inertias of plane areas can be obtained. (auth)

12547 (TID–3043(Rev.2, Suppl.3)) BIBLIOGRAPHIES OF INTEREST TO THE ATOMIC ENERGY PROGRAM. Smith, Richard J.; Voress, Hugh E.; Smelcer, Naomi K. (comps.) (Division of Technical Information Extension (AEC), Oak Ridge, Tenn.). May 1965. 84p. Dep. mn. CFSTI $2.00 cy, $0.75 mn.

Annotated references (422) are given to bibliographies and literature surveys located since the issuance of TID-3043 (Rev. 2, Suppl. 2). The references to report literature are arranged alphanumerically under the issuing organization. Author, subject, and report number-availability indexes are included. (D.C.W.)

12548 (TID–4577(Rev.1)) DESCRIPTIVE CATALOGING GUIDE. (Division of Technical Information Extension (AEC), Oak Ridge, Tenn.). Jan. 1966. 79p. Dep. mn. CFSTI $1.00 cy, $0.75 mn.

Information is given on: preparation of cataloging form and draft tape; preparation of repro copy; program tapes, cataloging elements, and examples for each type of item descriptively cataloged; and composition rules and details of descriptive cataloging elements. (P.C.H.)

12549 (TID–21555) CHEMICAL SPUTTERING OF SOLIDS. Quarterly Report No. 12, June 16–September 16, 1964. Donaldson, Edward E. (Washington State Univ., Pullman. Dept. of Physics). Dec. 17, 1964. Contract AT(45-1)-1548. 15p. Dep. mn. CFSTI $1.00 cy, $0.50 mn.

The adsorption of nitrogen thermally activated at a tungsten filament is reported as a function of filament temperature and gas pressure. The results support the conclusion that the nitrogen molecules strike the tungsten where some are released as atoms which subsequently travel to the walls and stick. Effects due to solubility of nitrogen in tungsten and tungsten evaporation were also observed. (auth)

12550 (TID–22564) CALORIMETRY IN ANHYDROUS ETHYLENEDIAMINE. Progress Report. Huffman, J. C.; Schmidt, F. C. (Indiana Univ. Foundation, Research Div., Bloomington, Ind.). [nd]. Contract AT(11-1)-256. 7p. Dep. mn. CFSTI $1.00 cy, $0.50 mn.

Developments in improving reliability and accuracy of the calorimeter and its supporting equipment are discussed. Preliminary results on use of the heat capacity of the calorimeter itself, together with the specific heat of ethylenediamine solutions, to calculate ΔH_{sol} are discussed. (P.C.H.)

12551 (UCRL–12186) THE SHOALING AND BREAKING OF THE SOLITARY WAVE AND ITS APPLICATIONS. Yee, Kane S. (Lawrence Radiation Lab., Univ. of California, Livermore). Nov. 10, 1964. Contract W-7405-eng-48. 21p. Dep. mn. CFSTI $1.00 cy, $0.50 mn.

The Davies-Packham theory on a symmetrical solitary wave can be used to calculate the behavior of a long wave propagating toward the shore on a shallow beach. The potential energy of the wave is assumed to be conserved in the development. This assumption is made up to the point when the wave breaks at the crest; the wave is assumed to be characterized by a parameter based on the Packham theory if one is "fairly" far away from the shore line. (auth)

12552 (UCRL–12226) CURVE SKETCHING BY DIGITAL COMPUTER. Conn, Richard W.; Von Holdt, Richard E. (Lawrence Radiation Lab., Univ. of California, Livermore). Dec. 2, 1964. Contract W-7405-eng-48. 40p. Dep. mn; CFSTI $2.00 cy, $0.50 mn.

The method of least squares is often used to determine the arbitrary constants in an empirical formula or approximating function. If such a function is not linear in its unknowns, approximate values must first be obtained. Typically they are obtained graphically or as the result of physical supposition or similar experiment. A program written to find first approximations for certain oscilloscope traces by: displaying the trace on a cathode-ray tube (CRT) and, imposing upon it a computer generated curve which employs parameters arbitrarily supplied by an operator in a quest for visual coincidence is described. While the technique proved successful in this application, a greater value may lie in its having indicated a mechanism for further automation. In its present form the method might best be utilized as a tool for studying the behavior of selected approximating functions. (auth)

12553 (UCRL–14359) APPARATUS FOR AUTOMATIC PREPARATIVE GAS CHROMATOGRAPHY. Frazer, J. W.; Morris, C. J. (Lawrence Radiation Lab., Univ. of California, Livermore). Dec. 6, 1965. Contract W-7405-eng-48. 21p. Dep. mn. CFSTI $1.00 cy, $0.50 mn.

A valveless system for compound purification by chromatographic techniques is described, and operational data are given. The sample injection system is pneumatically operated. An inert gas pressure applied for a preset time forces the sample from a reservoir through a capillary needle onto the chromatographic column. By the proper adjustment of the three parameters involved a sample can be admitted in near plug condition. All valves and other moving mechanisms are eliminated from the area between the column exit and the collection traps. This allows the necessary temperature control without the risk of leaks. Trap selection is by means of automatic valves located at the exits of the traps. These valves direct the carrier gas path through the various traps. The trapping logic is programmable. The adjustable parameters are time and detector signal. (P.C.H.)

12554 (UCRL–14473) DESIGN AND CONSTRUCTION OF AQUARIUMS: A BIBLIOGRAPHY. Pierce, Charlie M. (Lawrence Radiation Lab., Univ. of California, Livermore). July 28, 1965. Contract W-7405-eng-48. 8p. Dep. mn. CFSTI $1.00 cy, $0.50 mn.

Forty-nine references are given to journals and books published from 1926 to June 1965. Topics included are the design, construction, and maintenance of aquariums; materials and auxiliary equipment. The references are listed alphabetically by personal author. (P.C.H.)

12555 (WAPD-T–1828) THE INFLUENCE OF THE SYSTEM GEOMETRY ON FRACTURE TOUGHNESS [Thesis]. Johnson, Richard Elwyn (Bettis Atomic Power Lab., Pittsburgh, Pa.). 1965. Contract AT(11-1)-Gen-14. 280p. Dep. mn. CFSTI $6.00 cy, $1.50 mn.

Submitted to Carnegie Inst. of Tech., Pittsburgh, Pa.

Enough reports of variation in plane strain fracture toughness with notch system geometry exist to cast doubt on the applicability of this parameter to component design and on the predictability of fracture mechanics in general. Based on the observation that the greatest variations in fracture toughness were observed in the presence of large bending forces, a load-dependence hypothesis was advanced by Romualdi. To test the hypothesis, an experiment was designed to provide critical data with which to assess the geometry dependence of plane strain fracture toughness. Fracture tests were run using plaster and graphite which, in conjunction with results on metals obtained by others, provided a broad spectrum of inherent material ductility. No significant variation in plane strain fracture toughness dependent on notch system geometry was observed. A corollary to the assertion that plane strain fracture toughness is system geometry independent was noted, namely: a ratio of brittle fracture strengths reflecting a change in system geometry will be material independent for sets of geometrically identical specimens. The fracture data were shown to behave in accordance with the corollary. It was concluded that the methods of fracture mechanics can be employed to obtain laboratory determinations of plane strain fracture toughness that will be applicable to components without regard for differences in system geometries. (auth)

12556 PLACE AND FUNCTION OF THE RCN. Kramer, E. L. Atoomenergie Haar Toepass., 7: 194-7(Oct. 1965). (In Dutch).

A brief review of the facilities and research programs at RCN is presented. (C.E.S.)

12557 THE RCN IN THE PERIOD 1955–1965. Reyseger, W. Atoomenergie Haar Toepass., 7: 198-204(Oct. 1965). (In Dutch).

After a description of the history of the RCN, an insight is given of the financing of the institute. Financing was provided by the state, the professions, the electrical companies, and Euratom. A well-equipped research center resulted. The RCN has available a great concentration of knowledge that can be of much benefit for the development of nuclear energy in the Netherlands. (tr-auth)

12558 URANIUM. Sherman, John (Atomic Industrial Forum Inc., New York). Eng. Mining J., 166: 125-8(Feb. 1965).

Uranium reserves in 1964 and requirements for the metal in the U. S. and other countries are estimated. Uranium production in 1964 continued to decline from levels of the past few years. No important new discoveries were reported in the Free World during 1964, and uranium reserves of the major producing countries continued a gradual decline. There were increases in the reserves of Spain and India. Reserves that will be available on Jan. 1, 1971, with a price of $8 per lb of U_3O_8, are listed. A total of 474,000 tons of U_3O_8 in reserves compares with requirements for the years 1971 to 1980 inclusive of from 250,000 to 365,000 tons. Plans for the construction of nuclear power plants having a combined capacity exceeding 11,000 MW(e) for completion by 1975 were announced and additional installations are being considered for Switzerland and Japan. AEC purchases of uranium from U. S. producers totaled 11,847 short tons of U_3O_8 in 1964. This compared with 14,052 short tons in 1963, a 15.6% reduction. AEC purchases in the four-yr period 1968 to 1970 will be a rate of 7500 tons of U_3O_8 per year from U. S. producers. (BBB)

12559 ASA 1964 COMPILATION OF U. S. NUCLEAR STANDARDS. Nucl. Safety, 6: 354-67(Summer 1965).

The compilation includes listings of sponsoring organization and standards committee, chairmen addresses, codes and standards activities, and status and date of standards. (J.R.D.)

12560 THE MANAGEMENT OF NUCLEAR MATERIALS IN A RESEARCH ESTABLISHMENT. Wright, W. J.; Hocking, D. R. (Australian Atomic Energy Commission, Lucas Heights, New South Wales). Vienna, International Atomic Energy Agency, 1965, Preprint No. SM-67/56, 12p. (CONF-650803–52). ORINS.

From IAEA Symposium on Nuclear Materials Management, Vienna.

The requirements of a materials management scheme in a research establishment were examined with reference to the Australian Atomic Energy Commission's Research Establishment at Lucas Heights. The features that characterize the management of nuclear materials in a research establishment, compared with a production facility, are: less total weight of material is involved; material is dispersed over many areas; there is a large range of chemical and physical forms of material; residence time of material on each project is relatively long; there is a wide variety of operations (experiments) in progress; and there is less formal restraint on the handling of material by the higher qualified staff involved. The factors that determine the probability of an error occurring and the consequences of an undetected error were examined. These data were used as the basis of an inspection procedure, which provides the maximum insurance against error for the least outlay of money. The accounting scheme had to be capable of handling the wide range of materials, operations, and areas involved in research work and of providing material balance reports relating to financial or safety control, or security, as appropriate. Electronic data processing techniques led to improved efficiency and more effective service to the establishment without increasing the number of staff involved. (auth)

12561 TECHNICAL SUPPORT ACTIVITIES OF A NUCLEAR MATERIALS MANAGEMENT PROGRAM. McDowell, S. C. T. (Atomic Energy Commission, Washington, D. C.). Vienna, International Atomic Energy Agency, 1965, Preprint No. SM-67/37, 16p. (CONF-650803–33). ORINS.

From IAEA Symposium on Nuclear Materials Management, Vienna.

The development of the nuclear materials management program in the United States is discussed. The success of the program depended to a large extent on the development of a closely allied technical support effort. A broad spectrum of technical activities evolved: establishment of an Advisory Committee for Standard Reference Materials and Methods of Measurement; preparation and USAEC coordination with the National Bureau of Standards in the development of a series of uranium and plutonium chemical and isotopic standards; research and development programs designed to provide improved measurement techniques; and compilation and publication of a book of selected measurement methods for uranium and plutonium. The need for research and development efforts in areas of mutual interest is examined, and the cooperation of other nations in the development of internationally acceptable standards and methods of measurement is discussed. (auth)

12562 ECONOMIC CRITERIA APPLIED TO THE MANAGEMENT OF NUCLEAR MATERIALS. Shelley, W. J.; Kuehn, M. N. (Mallinckrodt Chemical Works, St. Charles, Mo.). Vienna, International Atomic Energy Agency, 1965, Preprint No. SM-67/38, 13p. (CONF-650803–42). ORINS.

From IAEA Symposium on Nuclear Materials Management, Vienna.

Nuclear materials management systems and factors that influence its costs are discussed. The control system evolved must complement the process, providing the lowest costs of personnel, analysis, and minimum interruption of the operating process. The recording and reporting system should generate maximum subsidiary data and be compatible with the systems employed by suppliers and consumers. Data generated for the control of nuclear materials should be that needed to ensure that no significant losses, theft, misappropriation, or diversion occurs. To ensure optimum costs balanced with adequate nuclear material control needs, some general rules were evolved. Economies were attained by the assignment of nuclear materials management, production control, and cost responsibilities to a single group. (auth)

CORPORATE AUTHOR INDEX

This index contains entries for this period for all report literature and, in addition, for certain published literature items for which it is felt that a corporate approach is especially desirable, e.g., symposia, conference proceedings, and meetings.

Each entry under a corporate author is a shortened version of the title of the publication, followed by the *NSA* volume and abstract number. Report numbers are given in parentheses.

The phrase "Progress report" is abbreviated as "Prog. rpt.," permitting a more rapid and complete alphabetical arrangement of the titles without changing the location of the progress report titles in relation to the other titles.

A

ACADEMIE R. P. R., BUCHAREST. INSTITUTUL DE CERCETARI CHEMICE.
Contribution to the study of molten salts, 20: 10808 (EUR-2466.e, pp 59-80)

ACF INDUSTRIES, INC., ALBUQUERQUE, N. MEX.
Cryogenic and elevated temperature properties of 7039 aluminum plate and weldments, 20: 11263 (ACF-14)

AEROJET-GENERAL CORP., AZUSA, CALIF.
Prog. rpt. on SNAP-8 materials, 1–6/64. II., 20: 11214 (NASA-CR-54717)
Prog. rpt. on SNAP-8 materials, 7–12/64, 20: 11215 (NASA-CR-54718)

AEROJET-GENERAL NUCLEONICS, SAN RAMON, CALIF.
BOUNCE, IBM 7090 code to calculate flux distributions within multiple-pin fuel elements, 20: 12384 (AGN-TM-411)
HECTIC-II—an IBM 7090 FORTRAN computer program, 20: 10989 (IDO-28595(Rev.))
Local film coefficients on ML-1 fuel elements due to boundary layer turbulence promoters, 20: 10988 (CONF-12-5)
Mass transfer analogy studies of shaped turbulence promoter performance, 20: 10993 (TID-22513)
Military vehicles—mission analysis using radioisotope submersible engines, 20: 11187 (AGN-8138)
ML-1 shield study, 20: 12385 (AGN-TP-149)

AKADEMIYA NAUK SSSR, NOVOSIBIRSK. INSTITUT YADERNOI FIZIKI.
Gravitation and finite renormalization in quantum electrodynamics, 20: 11867 (NP-15762)

AKTIEBOLAGET ATOMENERGI, STOCKHOLM (SWEDEN).
Comparison of control rod calculations using homogeneous and heterogeneous methods, 20: 12362 (RFR-193)
Measurement of neutron slowing-down time distribution at 1.46 ev and its space dependence in water, 20: 11927 (AE-208)
Monte Carlo calculations in neutron thermalization in heterogeneous system. II., 20: 11935 (RFR-154)
Scintillometer assembly for geological survey, 20: 11087 (AE-203)
Study of "384"-kev complex γ emission from ^{239}Pu, 20: 11950 (AE-202)
Systematics of absolute γ transition probabilities in deformed odd-A nuclei, 20: 11951 (AE-205)

AMERICAN NUCLEAR SOCIETY, DETROIT, MICH.
Fast reactor technology, suppl., 20: 12328 (ANS-100(Suppl.))

AMES LAB., IOWA STATE UNIV. OF SCIENCE AND TECH.
Comparison of axial-dispersion and radial-diffusion models for fixed-bed catalytic reactor design, 20: 10754 (IS-T-44)
Comparison of rare-earth cathodes in diode ion pump, 20: 10976 (IS-T-46)
Design and performance of long-path oxy-acetylene burner for atomic absorption spectroscopy, 20: 10761 (IS-T-69)
Diffusion of hydrogen in barium metal, 20: 12535 (IS-T-61)
Electrocapillarity studies of symmetric aliphatic molecules on mercury, 20: 12536 (IS-T-66)
Instrumentation for continuous averaging of magnetic spin resonance spectra, 20: 11098 (IS-1312)
Separation of cadmium from lead–bismuth eutectic by distillation, 20: 10762 (IS-T-71)
Separation of high-purity lutetium and ytterbium by ion exchange at 90°C, 20: 10760 (IS-1305)
Vaporization of solid UO_2, 20: 11234 (IS-1300)

AMSTERDAM UNIV. (NETHERLANDS).
Properties of ionic liquids and mixtures, 20: 10804 (EUR-2466.e, pp 9-19)

ARGONNE NATIONAL LAB., ILL.
Automatic analysis of data on kinetics of fast chemical reactions, 20: 10800 (ANL-7113)
Physics of heavy-water lattices, 20: 12363 (TID-8541, pp 1-70)
Radioactive waste management, 20: 12519 (TID-8541, pp 149-248)
Reactor technology, 1965, 20: 12329 (TID-8541)
Remote fabrication of reactor fuels, 20: 11241 (TID-8541, pp 71-148)
RIFFRAFF—program for computation of resonance integrals in two-region cell, 20: 12351 (ANL-7033)
Sodium technology, 20: 12330 (TID-8541, pp 321-425)
Survey of polarized ion sources in Europe, 20: 11379 (ANL-7118)
Transportation of radioactive materials, 20: 11035 (TID-8541, pp 249-319)

ARMED FORCES RADIOBIOLOGY RESEARCH INST., BETHESDA, MD.
Low-energy component of total dose for deep gamma penetrations in air and water, 20: 12261 (AFRRI-TN-65-2)

ATOMENERGIKOMMISSIONEN, RISOE (DENMARK). FORSOEGSINSTITUT.
Bibliography on dispersion-strengthened materials, 1964, 20: 11278 (RISO-48(Suppl.2))
Experimental study of tangential velocity profile in Ranque-Hilsch vortex tube, 20: 10992 (RISO-116)
Pulse-height discriminator, 20: 11064 (RISO-102)

ATOMIC BOMB CASUALTY COMMISSION, HIROSHIMA (JAPAN).
Prog. rpt. on activities, annual, 7/60–6/61, 20: 10595 (ABCC-60-61)

ATOMIC ENERGY BOARD, PELINDABA, PRETORIA (SOUTH AFRICA).
COBRA—computer code for calculation of fuel depletion in heterogeneous nuclear reactors, 20: 12361 (PEL-60)
Electrolytic jet machining method for cutting single crystal and polycrystalline uranium carbide, 20: 11216 (PEL-79)

ATOMIC ENERGY OF CANADA LTD., CHALK RIVER (ONTARIO).
Comparison of calculated and measured critical sizes for some ZED-2 lattices, 20: 12493 (AECL-2514)
Large-volume coaxial germanium gamma-ray spectrometers, 20: 11095 (CRGP-1224)

ATOMIC ENERGY RESEARCH ESTABLISHMENT, HARWELL (ENGLAND).
Extended fire tests on tinplate cans, 20: 11028 (AERE-M-1664)
Extraction by processing solvents of nitrosylruthenium nitrato complexes. III., 20: 10947 (AERE-R-4786)
Response of moving Geiger probe to discrete sources of beta radiation, 20: 11089 (AERE-M-1671)
Study of gas discharges that are expected in closed cycle magneto-hydrodynamic generator, 20: 11541 (AERE-R-5107)

ATOMIC POWER DEVELOPMENT ASSOCIATES, INC., DETROIT, MICH.
Analysis of Babcock and Wilcox full-size steam generator for sodium-water reaction, 20: 12386 (APDA-176)
Determination of safety rod drop time in Enrico Fermi reactor, 20: 12387 (APDA-NTS-3)
Worth measurements of core and blanket subassembly materials in Enrico Fermi reactor, 20: 12388 (APDA-NTS-6)

ATOMIC WEAPONS RESEARCH ESTABLISHMENT, ALDERMASTON (ENGLAND).

Fundamental equations of radiation hydrodynamics, 20: 11766 (AWRE-O-82/65)

ATOMICS INTERNATIONAL, CANOGA PARK, CALIF.

Determination of paired-pulse resolution of random counting systems, 20: 11105 (NAA-SR-Memo-11132)

Interaction of mercury and metal hydrides, 20: 10812 (NAA-SR-Memo-11569)

Methods for predicting aerodynamic heating rates to high-velocity bodies in the upper atmosphere, 20: 12467 (NAA-SR-11704)

Monte Carlo evaluation of fast neutron fluxes and heating in S8DS neutron shield, 20: 12468 (NAA-SR-Memo-9916)

New heat transfer protection system for sodium reactor experiment, 20: 12406 (NAA-SR-Memo-11648)

Post assembly electrical checkout of 10FS-5 in building 013, 20: 12469 (NAA-SR-Memo-11630)

Predicted fission product decay of SNAPSHOT I, 20: 12466 (NAA-SR-11642)

SRE-PEP moderator elements, 20: 12404 (NAA-SR-11160)

Steady-state sodium boiling and hydrodynamics, 20: 10990 (NAA-SR-11586)

Test graphite filler log handling machine, 20: 12405 (NAA-SR-Memo-11576)

Topical report on turbulent lubrication, 20: 10973 (TID-21992)

AUSTRALIAN ATOMIC ENERGY COMMISSION RESEARCH ESTABLISHMENT, LUCAS HEIGHTS.

Large, coaxial, lithium-drift germanium diobe for gamma-ray spectroscopy, 20: 11086 (AAEC/TM-299)

B

BABCOCK AND WILCOX CO., BARBERTON, OHIO. BOILER DIV.

Sodium-heated steam generator, 20: 12389 (BAW-1280-28(Vol.1))

Sodium-heated steam generator: stress analysis, 20: 12390 (BAW-1280-28(Vol.2))

Sodium-heated steam generator: effects of sodium-water reactions, 20: 12391 (BAW-1280-28(Vol.3))

Sodium-heated steam generator: specifications, 20: 12392 (BAW-1280-28(Vol.4))

BABCOCK AND WILCOX CO., GALVESTON, TEX.

NS Savannah containment integrity quarterly leak rate test results, May 1964, 20: 12473 (TID-22459)

Prog. rpt. on NS Savannah operations, 5–8/64, 20: 12474 (TID-22460)

BABCOCK AND WILCOX CO., LYNCHBURG, VA. ATOMIC ENERGY DIV.

Advanced test reactor servo regulator rod test program, 20: 12502 (TID-22547)

BATTELLE MEMORIAL INST., COLUMBUS, OHIO.

Model experimental design for NERVA instrumentation radiation-effects tests, 20: 11175 (NP-15823)

Prog. rpt. on fission-product reactions with and release from fuel-element claddings, 7–9/65, 20: 11212 (BMI-X-10143)

Radiation-induced formation of organometallic compounds with particular emphasis on organotins, 20: 10870 (BMI-1753)

BATTELLE-NORTHWEST, RICHLAND, WASH. PACIFIC NORTHWEST LAB.

Bile salt absorption from irradiated rat intestine, 20: 10599 (BNWL-122, pp 128-30)

Biological effects of ^{131}I in sheep and cattle, 20: 10516 (BNWL-122, pp 49-51)

Biological effects of ^{90}Sr in miniature swine, 20: 10597 (BNWL-122, pp 37-45)

Chemical carcinogens and radionuclide metabolism, 20: 10526 (BNWL-122, pp 91-3)

Chronic effects of inhaled $^{240}PuO_2$ in dogs, 20: 10596 (BNWL-122, pp 1-15)

Computer evaluation of tellurium-iodine contamination events, 20: 10519 (BNWL-122, pp 59-63)

Cycling of ^{90}Sr in molting crayfish, 20: 10515 (BNWL-122, pp 46-8)

Detection of metal overstress by acoustic emission, 20: 11001 (BNWL-SA-438)

Effect of bile on ^{35}S incoporation into intestinal mucopolysaccharides, 20: 10600 (BNWL-122, pp 131-4)

Effect of chronic ingestion of ^{65}Zn in trout, 20: 10528 (BNWL-122, pp 101-6)

Effect of dietary and hormonal manipulations on ^{237}Np-induced fatty livers, 20: 10522 (BNWL-122, pp 79-80)

Effect of DTPA on translocation and excretion of inhaled ^{144}Ce–^{144}Pr oxide in dogs, 20: 10533 (BNWL-122, pp 125-7)

Effect of splenectomy on acute plutonium toxicity, 20: 10524 (BNWL-122, pp 83-4)

Effect of ^{127}I on passage of ^{131}I from cows to man via milk, 20: 10530 (BNWL-122, pp 113-17)

Effects of moisture and air temperature on deposition and retention of $^{131}I_2$ on plants and soil, 20: 10717 (BNWL-122, pp 166-7)

Effects of sulfoxide compound on flour beetles exposed to x rays, 20: 10504 (BNWL-122, pp 142)

Gastrointestinal absorption of ^{144}Ce and ^{147}Pm in miniature swine, 20: 10525 (BNWL-122, pp 85-90)

High temperature creep-rupture properties of Hastelloy X in vacuum, 20: 11266 (BNWL-167)

Influence of fission neutrons on rat reproduction, 20: 10601 (BNWL-122, pp 135-6)

Influence of soil sodium on plant uptake of ^{45}Ca, ^{85}Sr, and ^{137}Cs, 20: 10534 (BNWL-122, pp 168-9)

Liver infiltrates in radiation chimeras, 20: 10505 (BNWL-122, 146-9)

Management of americium in power reactor fuels to optimize production of alpha-emitting isotopes, 20: 12394 (BNWL-SA-472)

Metabolism of ^{137}Cs in trout, 20: 10521 (BNWL-122, pp 73-4)

Migration area and moderator reactivity coefficients for H_2O moderated, 1.8 wt % Pu–Al loading in PRCF, 20: 12494 (BNWL-160)

Milk secretion of ^{65}Zn and ^{115m}Cd in sheep, 20: 10527 (BNWL-122, pp 94-8)

Plutonium abstracts, 20: 12530 (BNWL-113-10)

Plutonium abstracts, 20: 12530 (BNWL-113-11)

Plutonium metallurgy notebook. 20: 11213 (BNWL-37)

Prog. rpt. on biology, annual, 1964, 20: 10503 (BNWL-122)

Prog. rpt. on fixation of radioactive residues, 7–9/65, 20: 12517 (BNWL-170)

Promethium compatibility and encapsulation studies, 20: 11267 (BNWL-SA-488)

Radiation dosimetry of ^{137}Cs in sheep evaluated with thermoluminescent dosimeters, 20: 11091 (BNWL-122, pp 67-72)

Radioactive waste management, 20: 12519 (TID-8541, pp 149-248)

Radioactivity in Alaskan animals and forage plants, 20: 10535 (BNWL-122, pp 176-80)

Radioactivity in northern Alaskan natives and their foods during 1964, 20: 10718 (BNWL-122, pp 172-5)

Radionuclide accumulation and transport by plankton in Columbia River, 20: 10536 (BNWL-122, pp 187-9)

Radionuclide accumulation and productivity of periphyton in Columbia River, 20: 10537 (BNWL-122, pp 190-3)

Reactor effluent monitoring—1964, 20: 10538 (BNWL-122, pp 198-201)

Relationship of annual forage yield and fallout deposition in a cheatgrass community, 20: 11012 (BNWL-122, pp 184-6)

Relationship of ^{137}Cs concentration in feed and rumen contents, 20: 10520 (BNWL-122, pp 64-6)

Remote fabrication of reactor fuels, 20: 11241 (TID-8541, pp 71-148)

Removal of internally deposited plutonium from rats, 20: 10531 (BNWL-122, pp 118-21)

Removal of internally deposited ruthenium from rats, 20: 10532 (BNWL-122, pp 122-4)

Sequence for predicting waste transport by ground water, 20: 11009 (BNWL-SA-406)

Sheep milk production and its ^{131}I content, 20: 10517 (BNWL-122, pp 52-4)

Studies of fallout nuclides in plants and browsing animals of Washington, 20: 11011 (BNWL-122, pp 181-3)

Thyroid uptake of ^{131}I from skin exposure, 20: 10518 (BNWL-122, pp 55-8)

Tissue accumulation of uranium and thorium in rats after inhalation of uranium ore dust, 20: 10514 (BNWL-122, pp 21-4)

Toxicity of copper and x rays in rats, 20: 10598 (BNWL-122, pp 107-9)

Translocation of subcutaneously administered $^{239}PuC_2$, 20: 10523 (BNWL-122, pp 81-2)

Transportation of radioactive materials, 20: 11035 (TID-8541, pp 249-319)

Ultrahigh-speed gross alpha autoradiography, 20: 10529 (BNWL-122, pp 110-12)

Versatile iodine vapor and particle sampler, 20: 11060 (BNWL-122, pp 33-6)

Whole-body retention and biological effects of inhaled ^{144}Ce–^{144}Pr and ^{106}Ru–^{106}Rh oxides in beagles, 20: 10513 (BNWL-122, pp 16-20)

X-ray and fast neutron effects on productivity of flour beetles, 20: 11184 (BNWL-122, pp 137-9)

BECHTEL CORP., SAN FRANCISCO, CALIF.

Engineering and economic feasibility study for combination nuclear power and desalting plant, 20: 12453 (TID-22330(Vol.2))

BERNE UNIV. (SWITZERLAND). PHYSIKALISCHES INSTITUT.

Spallation, fission and neutron capture anomalies in meteoritic krypton and xenon, 20: 11424 (NP-15629)

BETTIS ATOMIC POWER LAB., PITTSBURGH, PA.

Effects of thermal treatment on distribution of alloying elements in Zircaloy-2, 20: 11287 (WAPD-T-1809)

Influence of system geometry on fracture toughness, 20: 12555 (WAPD-T-1828)

BETTIS ATOMIC POWER LAB., WEST MIFFLIN, PA.

Development of photogrammetric techniques for measuring surface contours of small samples, 20: 11068 (WAPD-T-1815)
Evaluation of three-dimensional flux synthesis method as nuclear design tool, 20: 12368 (WAPD-T-1737)

BOEING CO., SEATTLE, WASH.
Response of p-i-n detectors to various nuclear radiation environments, 20: 11173 (D2-84071-1)

BOEING CO., SEATTLE, WASH. AERO-SPACE DIV.
Comparison and evaluation of three automated circuit analysis programs: predict, net-1, and circus, 20: 11172 (AD-623963)

BOEING SCIENTIFIC RESEARCH LABS., SEATTLE, WASH. PLASMA PHYSICS LAB.
Production of large-diameter low-voltage electron beams in absence of magnetic field, 20: 11367 (D1-82-0448)

BRADBERRY (CARROLL E.) AND ASSOCIATES, LOS ALTOS, CALIF.
Transport of radionuclides by ground water, 20: 11010 (HNS-1229-61)

BROOKHAVEN NATIONAL LAB., UPTON, N. Y.
Control of reactivity in high conversion ratio, plutonium fueled, thermal power reactors, 20: 12393 (BNL-8748)
Intermediate resonance absorption, 20: 11928 (BNL-9790)
Method for solution of initial value problems for systems of ordinary differential equations, 20: 12529 (BNL-8798)
Method for solving integer linear programming problems by use of generating functions, 20: 12528 (BNL-8694)
Normal mode analysis of standing wave linacs—field excitation and beam loading in linac cavities, 20: 11381 (BNL-9833)
Passage of high-energy particles in matter—nuclear cascades induced in dense media by 1- and 3-Bev protons, 20: 12262 (BNL-8721)
Physics of heavy-water lattices, 20: 12363 (TID-8541, pp 1-70)
Pulsed phase measuring and control system for RF separator, 20: 11380 (BNL-9772)
Species-diversity problems in plant communities, 20: 10511 (BNL-9836)
Track-segment generator, 20: 11090 (BNL-9749)
Virtual-state eigenvalue problems, 20: 11439 (BNL-8800)
Weather modification: effect on biological equilibrium in plant community, 20: 10510 (BNL-9835)

BUREAU OF MINES, WASHINGTON, D. C.
Corrosion properties of molybdenum, tungsten, vanadium, and some vanadium alloys, 20: 11230 (BM-RI-6715)

C

CALIFORNIA UNIV., BERKELEY. ELECTRONICS RESEARCH LAB.
Prog. rpt. on plasma research, 4–6/65, 20: 12163 (AD-625424)

CALIFORNIA UNIV., LA JOLLA, SAN DIEGO.
Hidden symmetries and the question of massless particles, 20: 11679 (CONF-650927-21)

CAMBRIDGE ELECTRON ACCELERATOR, MASS.
Calculation of radiation effects for bypass, 20: 11384 (CEAL-TM-156)
Synchrotron colliding beam facility at CEA, 20: 11382 (CEAL-TM-151)
Vacuum requirements for bypass, 20: 11385 (CEAL-TM-157)
9-Magnet bypass in target area, 20: 11383 (CEAL-TM-152)

CARNEGIE INST. OF TECH., PITTSBURGH, PA.
Effects of thermal treatment on distribution of alloying elements in Zircaloy-2, 20: 11287 (WAPD-T-1809)
Influence of system geometry on fracture toughness, 20: 12555 (WAPD-T-1828)

CATANIA UNIV. (ITALY). ISTITUTO DI GENETICA.
Prog. rpt. on mutability of polygenes, 1/66, 20: 10603 (IAEA-2466-11)

CEKMECE NUCLEAR RESEARCH CENTER, ATOMIC ENERGY COMMISSION, ISTANBUL (TURKEY).
Effect of tritated thymidine and γ irradiation on mortality of adult Drosophila larvae. II., 20: 10602 (CNAEM-32)

CENTRALNE LABORATORIUM OCHRONY RADIOLOGICZNEJ, WARSAW (POLAND).
Alpha contamination locator with junction radiation detector, 20: 11092 (CLOR-39/D)

CENTRE D'ETUDE DE L'ENERGIE NUCLEAIRE, BRUSSELS (BELGIUM).
Plutonium urinanalysis, 20: 10757 (BLG-353)
Production of ^{192}Ir sources of high specific activity, 20: 11190 (BLG-332)
Prog. rpt. on use of Pu as reactor fuel, 1–3/65, 20: 12396 (EURAEC-1505)
Prog. rpt. on use of Pu as reactor fuel, 4–6/65, 20: 12397 (EURAEC-1506)
Thermal flow-meters for ClF_3, 20: 11059 (BLG-345)
Utilization of radioisotopes for production of electric energy aboard space vehicles, 20: 11188 (BLG-330)

CHICAGO UNIV., ILL. DEPT. OF PHYSICS.
Galilean transformation of continuous energy particle distributions, 20: 11952 (COO-238-46)

CHICAGO UNIV., ILL. INST. FOR COMPUTER RESEARCH.
Algebra for (m,p) switching nets, 20: 11199 (COO-614-34, Sect. IIIC)
Automatic retrieval spark chambers, 20: 11093 (COO-614-34, Sect. IIA)
Duality theorem in combinatorial switching, 20: 11198 (COO-614-34, Sect. IIIB)
Experience with on-line experimentation, 20: 11553 (COO-614-34, Sect. IIC)
Experimental investigation of unnormalized arithmetic, 20: 11196 (COO-614-34, Sect. IIB)
Extension and solution of nonlinear operator equations, 20: 11197 (COO-614-34, Sect. IIIA)
Mu-mesic x-ray experiment, 20: 11440 (COO-614-34, Sect. IID)
Prog. rpt. on computer research, 5/65, 20: 11195 (COO-614-34)

CINCINNATI UNIV., OHIO.
Weak alpha and electron-capture decay in ^{208}Po and ^{209}Po, 20: 11971 (MLM-1251J)

CLARK UNIV., WORCESTER, MASS. DEPT. OF CHEMISTRY.
Chelation and olation reactions of metal ions in aqueous solution. I., 20: 12533 (COO-1020-6)

COLLEGE DE FRANCE, PARIS.
Ion diffusion and migration in molten salts, 20: 10805 (EUR-2466.e, pp 21-30)

COLLEGE DE FRANCE, PARIS. LABORATOIRE DE PHYSIQUE ATOMIQUE ET MOLECULAIRE.
Problem of nuclear interactions of ultra-energetic muons of cosmic radiation, 20: 11975 (PAM-6502)

COLUMBIA UNIV., NEW YORK. ENGINEERING RESEARCH LABS.
Effect of length and pressure on critical heat flux for closely spaced 19-rod bundle in forced convection boiling, 20: 10994 (TID-22539)

COMBUSTION ENGINEERING, INC., WINDSOR, CONN. NUCLEAR DIV.
Prog. rpt. on UO_2 fuel systems, 3/31/65, 20: 12377 (CEND-2863-236)

COMMISSARIAT A L'ENERGIE ATOMIQUE, CADARACHE (FRANCE). CENTRE D'ETUDES NUCLEAIRES.
Prog. rpt. on fast neutrons project, annual, 1963, 20: 12419 (EURFNR-1F)

COMMISSARIAT A L'ENERGIE ATOMIQUE, FONTENAY-AUX-ROSES (FRANCE). CENTRE D'ETUDES NUCLEAIRES.
Steam generators associated with sodium-cooled reactors, 20: 12339 (EURFNR-11F)

COMMISSARIAT A L'ENERGIE ATOMIQUE, GRENOBLE (FRANCE). CENTRE D'ETUDES NUCLEAIRES.
Study of terphenyl substitutes and terphenyl OM2, 20: 10872 (EUR-2517.f)
Synthesis and purification of some alkylphenasthrenes and their spectra, 20: 10861 (CEA-R-2770)
Uranium–hydrogen system, 20: 10801 (CEA-R-2777)

COMMISSARIAT A L'ENERGIE ATOMIQUE, PARIS (FRANCE).
Reactor tanks steels. Irradiation of tensile-test pieces in EL.3 at different temperatures and post-irradiation tests, 20: 11342 (EURAEC-1502)

COMMISSARIAT A L'ENERGIE ATOMIQUE, SACLAY (FRANCE). CENTRE D'ETUDES NUCLEAIRES.
Application of controlled-potential coulometry to determinations in radioactive solutions, 20: 10758 (EUR-2618.f)
Contribution to the study of pitting corrosion of magnesium and its alloys, 20: 11231 (CEA-R-2815)
Grand Quevilly thermal tests station, 20: 12420 (EURFNR-9F)
Prog. rpt. on brittle fracture strength of heavy-gage steel plate, final, 1965, 20: 11240 (EURAEC-1520)
Prog. rpt. on fast neutrons project, annual, 1963, 20: 12419 (EURFNR-1F)
Theoretical and experimental aspects of the neutronic interaction between multiplying media, 20: 11929 (CEA-R-2849)
Use of beams of polarized deuterons and determination of parameters of optical model, 20: 11570 (ANL-Trans-258)

CORNELL UNIV., ITHACA, N. Y.
Efficiency of dislocation climb in metals, 20: 11274 (NYO-3504-2)

D

DEUTSCHES ELEKTRONEN-SYNCHROTRON, HAMBURG (WEST GERMANY).
Calibration measurements on external electron beam 1 to 5 Bev, 20: 11389 (DESY-65/12)
Determination of $\pi\pi$ scattering phase shifts up to 1.3 Bev CMS energy, 20: 11555 (DESY-65/13)
Radiative corrections for e-p scattering for angular and energy coincidence experiments, 20: 11556 (DESY-65/14)

DIVISION OF OPERATIONAL SAFETY (AEC), WASHINGTON, D. C. INDUSTRIAL SAFETY AND FIRE PROTECTION BRANCH.
Industrial accidents in USAEC facilities, 1963–65, 20: 11034 (TID-5360(Suppl.5))

DIVISION OF RAW MATERIALS (AEC), WASHINGTON, D. C.
Reconnaissance for uranium in the Lonquimay area, Province of Malleco,

Chile, 20: 11025 (RME-4552(Rev.))
DIVISION OF REACTOR DEVELOPMENT AND TECHNOLOGY (AEC), WASHINGTON, D. C.
Radioactive waste management, 20: 12519 (TID-8541, pp 149-248)
DIVISION OF RESEARCH (AEC), WASHINGTON, D. C.
Heating of vacuum-wall by bremsstrahlung radiation in pulsed thermonuclear reactor, 20: 12166 (CONF-651126-1)
Summaries of USAEC basic research program in chemistry (off-site), 20: 10755 (TID-4005(Pt. 2a)(2nd ed.))
DIVISION OF TECHNICAL INFORMATION EXTENSION, (AEC), OAK RIDGE, TENN.
Bibliographies of interest to atomic energy program, 20: 12547 (TID-3043(Rev.2, Suppl.3))
Descriptive cataloging guide, 20: 12548 (TID-4577(Rev.1))
Summaries of USAEC basic research program in chemistry (off-site), 20: 10755 (TID-4005(Pt. 2a)(2nd ed.))
DU PONT DE NEMOURS (E. I.) & CO., AIKEN, S. C. SAVANNAH RIVER LAB.
Physics of heavy-water lattices, 20: 12363 (TID-8541, pp 1-70)
Savannah River plant criticality dosimetry system, 20: 11029 (DP-1006)
Thermal neutron diffusion in heavy water, 20: 11931 (CONF-651101-53)
Xenon and samarium tables, 20: 12352 (DP-958)
DU PONT DE NEMOURS (E. I.) AND CO., WILMINGTON, DEL.
Transportation of radioactive materials, 20: 11035 (TID-8541, pp 249-319)

E

EBASCO SERVICES, INC., NEW YORK.
Advanced test reactor servo regulator rod test program, 20: 12502 (TID-22547)
EIDGENOESSISCHES INSTITUT FUER REAKTORFORSCHUNG, WUERENLINGEN (SWITZERLAND).
Contribution to mechanism of dissolution and diffusion of oxygen in zirconium, 20: 11268 (EIR-82)
ENRICO FERMI INST. FOR NUCLEAR STUDIES, UNIV. OF CHICAGO, ILL.
Galilean transformation of continuous energy particle distributions, 20: 11952 (COO-238-46)
Quasi-free proton-proton scattering in light nuclei at 460 Mev, 20: 11948 (AD-624318)
Surface superconductivity in subcritical region, 20: 11891 (COO-264-224)
EUROPEAN ATOMIC ENERGY COMMUNITY.
AIREK-BUL—version of kinetic code AIREK-MOD for periodically pulsed fast reactors, 20: 12395 (EUR-2552.e)
Application of controlled-potential coulometry to determinations in radioactive solutions, 20: 10758 (EUR-2618.f)
Chemical equilibria in molten salts, 20: 10807 (EUR-2466.e, pp 39-57)
Conference on molten salts, plenary lectures, University of Liege, Belgium, 9/64, 20: 10803 (EUR-2466.e)
Construction and calibration of proton recoil type neutron spectrometer, 20: 11096 (EUR-2491.e)
Contribution to the study molten salts, 20: 10808 (EUR-2466.e, pp 59-80)
Ion diffusion and migration in molten salts, 20: 10805 (EUR-2466.e, pp 21-30)
Ion mobilities in molten salts, 20: 10806 (EUR-2466.e, pp 31-8)
Optimization of heat pipe thermionic converters for space power supplies, 20: 11542 (EUR-2534.e)
Plasticity of dispersed-phase type Al–Al_2O_3 alloys, 20: 11269 (EUR-2483.f)
Preparation and purification of tritiated geranyllinalol, 20: 10809 (EUR-2531.f)
Properties of ionic liquids and mixtures, 20: 10804 (EUR-2466.e, pp 9-19)
SR_2–SR_3–SR_4 electron irradiation loop, 20: 10871 (EUR-2288.f)
Study of terphenyl substitutes and terphenyl OM2, 20: 10872 (EUR-2517.f)
Use of pulsed reactors in field of neutron and solid state physics, 20: 12495 (EUR-2538.e)
EUROPEAN ATOMIC ENERGY COMMUNITY, GEEL (BELGIUM). CENTRAL NUCLEAR MEASUREMENTS BUREAU.
Decay of ^{241}Am, 20: 11956 (EUR-2632.d)
EUROPEAN ATOMIC ENERGY COMMUNITY, ISPRA (ITALY). JOINT NUCLEAR RESEARCH CENTER.
AIREK-BUL—version of kinetic code AIREK-MOD for periodically pulsed fast reactors, 20: 12395 (EUR-2552.e)
Construction and calibration of proton recoil type neutron spectrometer, 20: 11096 (EUR-2491.e)
Optimization of heat pipe thermionic converters for space power supplies, 20: 11542 (EUR-2534.e)
Plasticity of dispersed-phase type Al–Al_2O_3 alloys, 20: 11269 (EUR-2483.f)
Use of pulsed reactors in field of neutron and solid state physics, 20: 12495 (EUR-2538.e)
EUROPEAN COMPANY FOR THE CHEMICAL PROCESSING OF IRRADIATED FUELS, MOL (BELGIUM).
Citriflex—decladding of fuel elements clad with zirconium or Zircaloy-2 by an ammonium fluoride-citric acid solution, 20: 11272 (NP-15661)
EUROPEAN ORGANIZATION FOR NUCLEAR RESEARCH, GENEVA (SWITZERLAND).
Contribution to study of closed orbit, 20: 11386 (CERN-65-35)

F

FRANKFORD ARSENAL, PHILADELPHIA, PA.
Ferroelectrics—their electrical behavior during, and subsequent to, ionizing radiations, 20: 11352 (NP-15707)
FREIE UNIVERSITAET, BERLIN (WEST GERMANY). I. PHYSIKALISCHES INSTITUT.
Development of 100-Mev FFAG electron synchrotron, 20: 11391 (NP-15274)
Development of 100-Mev FFAG electron synchrotron, 20: 11392 (NP-15275)

G

GENERAL ATOMIC, SAN DIEGO, CALIF.
Cyclotron waves in collisionless plasma, 20: 12175 (NASA-CR-348)
GENERAL ATOMIC, SAN DIEGO, CALIF. JOHN JAY HOPKINS LAB. FOR PURE AND APPLIED SCIENCE.
Atomic motion in moderators, 20: 12275 (GA-6861)
BLOOST-5: combined reactor kinetics-heat transfer code for IBM-7044, 20: 12354 (GAMD-6644(Add.))
Energy dependence of neutron capture cross section of tungsten isotopes from 0.01 to 10 ev, 20: 11957 (GA-6832)
FASDOP. FORTRAN IV computer program for computing cross sections from resonance parameters, 20: 11958 (GAMD-6562)
GAPS: FORTRAN code for analyzing data from pulsed neutron source experiments, 20: 12355 (GAMD-6781)
GAROL—computer program for evaluating resonance absorption including resonance overlap, 20: 11932 (GA-6637)
Precritical calculations for 3.0 in. pitch, beryllium reflected, TWMR critical assembly, 20: 12465 (GA-6807)
Prog. rpt. on EBOR program, 9/30/65, 20: 12398 (GA-6811)
TEMCO Fortran program for computing temperature coefficients, 20: 12353 (GA-6734)
GENERAL ELECTRIC CO., CINCINNATI, OHIO. NUCLEAR MATERIALS AND PROPULSION OPERATION.
Development and evaluation of a homogeneous W–25Re alloy for 2600°C applications, 20: 11238 (CONF-650449-1)
GENERAL ELECTRIC CO., RICHLAND, WASH. HANFORD ATOMIC PRODUCTS OPERATION.
NPR injection pump simulation, 20: 12455 (HW-77921-C)
NPR pressurizer, 20: 12456 (HW-77921-D)
Proposed chemical flowsheets for decladding and dissolution of PRTR plutonium aluminum fuel, 20: 10948 (HW-76472)
Transportation of radioactive materials, 20: 11035 (TID-8541, pp 249-319)
Utilization of tryptophan by Neurospora, 20: 10540 (HW-SA-3728)
Wescott parameters derived from RBU basic library for Δ-4 cutoff, 20: 11959 (HW-77389)
GENERAL ELECTRIC CO., SAN JOSE, CALIF. ATOMIC POWER EQUIPMENT DEPT.
Prog. rpt. on EVESR nuclear superheat fuel development, 6–8/65, 20: 12399 (GEAP-4941)
Prog. rpt. on reactor primary coolant system rupture study, 4–6/65, 20: 12338 (GEAP-4911)
GENERAL INSTRUMENT CORP., NEWARK, N. J. THERMOELECTRIC DIV.
Prog. rpt. on low power thermoelectric component development, final, 3/65, 20: 11543 (GIC-2605-3)
GEORGIA INST. OF TECH., ATLANTA. ENGINEERING EXPERIMENT STATION.
Prog. rpt. on emission and excitation cross sections, 3–11/65, 20: 11448 (TID-22480)
Prog. rpt. on ionization and charge transfer cross sections, 12/64–11/65, 20: 11447 (TID-22476)
GOSUDARSTVENNYI KOMITET PO ISPOL'ZOVANIYU ATOMNOI ENERGII SSSR.
Levels of nucleus ^{160}Ho from reaction (n,γ), 20: 11982 (LA-tr-65-34)
GOSUDARSTVENNYI KOMITET PO ISPOL'ZOVANIYU ATOMNOI ENERGII SSSR, MOSCOW. INSTITUT TEORETICHESKOI I EKSPERIMENTAL'NOI FIZIKI.
Casimir operators for U(n) and SU(n) groups, 20: 11690 (NP-15764)
Coherent coulombic excitation of nuclei passing through crystals, 20: 11973 (NP-15791)
Green's function for Coulomb potential, 20: 11446 (NP-15794)

Latent symmetry of hydrogen atom, 20: 11445 (NP-15793)
Pulsed ion source with point cathode (needle), 20: 11394 (NP-15766)
Scintillation counter effectiveness in registering neutrons with several Bev energy, 20: 11106 (NP-15786)

GRENOBLE UNIV. (FRANCE).
Synthesis and purification of some alkylphenanthrenes and their spectra, 20: 10861 (CEA-R-2770)
Uranium–hydrogen system, 20: 10801 (CEA-R-2777)

H

HAHN-MEITNER-INSTITUT FUER KERNFORSCHUNG, BERLIN (WEST GERMANY).
Solution of first and second boundary value problems of inner and outer regions for potential equations in R_3 through boundary coverings, 20: 11200 (HMI-B-41)
Stationary supersonic flow in common cone and basis of its numerical calculation, 20: 11767 (HMI-B-42)

HAZLETON-NUCLEAR SCIENCE CORP., PALO ALTO, CALIF.
Transport of radionuclides by ground water, 20: 11010 (HNS-1229-61)

HUGHES RESEARCH LABS., MALIBU, CALIF.
Prog. rpt. on ion rocket engine development, 4–6/65, 20: 11006 (NP-15824)

I

IIT RESEARCH INST., CHICAGO, ILL.
Prog. rpt. on magnetic properties of insulators, 5/16–8/15/65, 20: 12274 (COO-578-18)

IIT RESEARCH INST., CHICAGO, ILL. PHYSICS DIV.
Band shape of F-center optical emission in rubidium chloride, 20: 12278 (TID-21570)

ILLINOIS INST. OF TECH., CHICAGO.
Chelation and olation reactions of metal ions in aqueous solution. III., 20: 10802 (COO-1020-9)

ILLINOIS INST. OF TECH., CHICAGO. DEPT. OF CHEMISTRY.
Chelation and olation reactions of metal ions in aqueous solution. I., 20: 12533 (COO-1020-6)
Steric interference to diffusion in linde A zeolite, 20: 12532 (COO-920-8)

ILLINOIS STATE WATER SURVEY, URBANA.
Ion oscillations in weakly turbulent plasma, 20: 12178 (NP-15705)

ILLINOIS UNIV., URBANA.
Behavior of thirteen charge transfer complexes at high pressure, 20: 12534 (COO-1198-216)
$K_2^0 \rightarrow \pi^- + \pi^+$—a strange decay from a strange particle, 20: 11554 (COO-1195-27)

INDIANA UNIV. FOUNDATION. RESEARCH DIV., BLOOMINGTON, IND.
Calorimetry in anhydrous ethylenediamine, 20: 12550 (TID-22564)

INSTITUT ATOMNOI ENERGII, GOSUDARSTVENNYI KOMITET PO ISPOL'ZOVANIYU ATOMNOI ENERGII SSSR, MOSCOW.
Turbulent heating of plasma by direct-discharge current, 20: 12183 (ORNL-tr-868)

INSTITUT DE RECHERCHES DE LA SIDERUGRIE, ST. GERMAINE-EN-LAYE (FRANCE).
Prog. rpt. on brittle fracture strength of heavy-gage steel plate, final, 1965, 20: 11240 (EURAEC-1520)

INSTITUT FUER KERNPHYSIK, UNIVERSITAET FRANKFURT (WEST GERMANY).
Bibliography on slow neutron detectors, 20: 11088 (AED-C-28-01)

INSTITUTE FOR NUCLEAR STUDY, TOKYO UNIV. (JAPAN).
Shell effects in Coulomb displacement energies of excited states, 20: 11963 (INSJ-91)

INSTITUTE OF NUCLEAR PHYSICS, KRAKOW (POLAND).
Extraction and stability of metal chelates and separation of metal salts by extraction chromatography, 20: 10759 (INP-427/C)

INSTITUTE OF NUCLEAR RESEARCH, WARSAW (POLAND).
Energy levels of ^{9}Be produced in $^{11}B(n,\alpha)^8Li \rightarrow {}^8Be$, 20: 11962 (INR-655/I/PL)
Internal oxidation of Fe–Al alloys, 20: 11232 (INR-644/XIV/PS)
Silicone lithium drifted detectors, 20: 11097 (INR-621/XV/I)
Solutions of superconductivity equations for odd-A nuclei in rare-earth region, 20: 11961 (INR-602/VII/PH)
Tables of functions $x(c,\nu)$ and $x_\pm(c_1,c_2)$ for numerical solution of slab geometry neutron transport problems, 20: 11933 (INR-630/IX-A/PR(Pt.2))

INSTITUTO DE INVESTIGACIONES GEOLOGICAS, SANTIAGO (CHILE).
Reconnaissance for uranium in the Lonquimay area, Province of Malleco, Chile, 20: 11025 (RME-4552(Rev.))

INSTITUTT FOR ATOMENERGI, HALDEN (NORWAY). OECD HALDEN REAKTOR PROSJEKT.
Development of dynamics model for heavy water boiling reactors, 20: 12400 (HPR-54)

INSTITUTT FOR ATOMENERGI, KJELLER (NORWAY).
BIGG-II—multigroup neutron spectrum and criticality code, 20: 12357 (KR-75)
Liquid scintillation determination of ^{239}Pu in pure and contaminated solutions, 20: 10763 (KR-100)

INTERNATIONAL ATOMIC ENERGY AGENCY, VIENNA (AUSTRIA).
Conference on radioisotope techniques in study of protein metabolism, Vienna, 6/64, 20: 10539 (STI/DOC/10/45)
Panel meeting on in-pile dosimetry, Vienna, 7/64, 20: 11110 (STI/DOC/10/46)

INTERNATIONAL CENTRE FOR THEORETICAL PHYSICS, TRIESTE (ITALY).
Green functions from Lie algebras, 20: 11441 (IC/65/94)
Most degenerate representations for compact and non-compact rotation groups, 20: 11682 (IC/65/89)
Non-compact extensions of symmetry groups, 20: 11681 (IC/65/85)
SL(6,c) symmetry, 20: 11680 (IC/65/84)

IONAC CHEMICAL CO., BIRMINGHAM, N. J.
Improved aluminosilicate ion exchangers, 20: 10766 (TID-22511)

J

JET PROPULSION LAB., CALIF. INST. OF TECH., PASADENA.
Particle symmetries, 20: 11688 (JPL-TR-32-797)

JOINT INST. FOR NUCLEAR RESEARCH, DUBNA (USSR).
Passage of high energy neutrons through heavy concrete, 20: 12263 (JINR-P-2479)
Reproduction of kinematical particle parameters by chamber pictures with account of inhomogeneity of magnetic field, energy losses, and coulomb scattering, 20: 11100 (JINR-P-2467)

JOINT INST. FOR NUCLEAR RESEARCH, DUBNA (USSR). LAB OF HIGH ENERGY.
An experimental determination of relative probabilities of $K_2^0 \rightarrow 3\pi^0$ decays, 20: 11561 (JINR-P-2450)
Determination of relative probability of $K_2^0 \rightarrow \pi^\pm + e^\pm + \nu(\bar{\nu})$, 20: 11560 (JINR-P-2449)
Experimental determination of function of spatial neutron distribution around 10 Bev synchrophasotron, 20: 11390 (JINR-P-2446)
Forbidden configurations in a three-photon system, 20: 11686 (JINR-P-2447)
γ-Quanta detecting by using spark chamber and total absorption Cherenkov counter, 20: 11099 (JINR-P-2436)

JOINT INST. FOR NUCLEAR RESEARCH, DUBNA (USSR). LAB. OF NEUTRON PHYSICS.
Computation of multiple interactions for experiments on radiation capture of neutrons, 20: 11967 (JINR-P-2455)

JOINT INST. FOR NUCLEAR RESEARCH, DUBNA (USSR). LAB OF NUCLEAR PROBLEMS.
An experimental determination of relative probabilities of $K_2^0 \rightarrow 3\pi^0$ decays, 20: 11561 (JINR-P-2450)
Analysis of reactions $\pi N \rightarrow \pi_1\pi_2 N'$, 20: 11562 (JINR-P-2454)
Application of electrophotography for measurements of sensitive region of germanium p-i-n detectors, 20: 11102 (JINR-P-2487)
Determination of relative probability of $K_2^0 \rightarrow \pi^\pm + e^\pm + \nu(\bar{\nu})$, 20: 11560 (JINR-P-2449)
Influence of film chamber properties on accuracy of spatial reconstruction of recorded events, 20: 11101 (JINR-P-2468)
Pion production in (n-p) collisions at 600 Mev, 20: 11564 (JINR-P-2462)
Polarized proton target in investigation of low-energy nucleon-nucleon interactions, 20: 11965 (JINR-P-2426)
Revealing of defects in silicon p-i-n detectors, 20: 11103 (JINR-P-2489)

JOINT INST. FOR NUCLEAR RESEARCH, DUBNA (USSR). LAB OF NUCLEAR REACTIONS.
On properties of isotope ^{254}102, 20: 11968 (JINR-P-2470)
Properties of ^{254}No isotope, 20: 11969 (JINR-P-2471)
Proton emitters among Te isotopes, 20: 11964 (JINR-E-2464)

JOINT INST. FOR NUCLEAR RESEARCH, DUBNA (USSR). LAB OF THEORETICAL PHYSICS.
Analytical properties of Euclidean amplitudes, 20: 11687 (JINR-P-2485)
Collective states of nuclei in Tamm-Dancoff method, 20: 11966 (JINR-P-2432)
Determination of spin and parity of Ω^- hyperon, 20: 11563 (JINR-P-2456)
Electromagnetic current and formfactors for meson 35-plet in SL(6,c) symmetry, 20: 11683 (JINR-P-2475)
Equilibrium deformation of heavy nuclei, 20: 11970 (JINR-P-2473)
Internuclear cascades at superhigh energies, 20: 11566 (JINR-P-2472)
Leptonic decay of Ω^- hyperon in the Quark model, 20: 11559 (JINR-P-2445)
Octet of baryon resonances in unitary symmetry scheme, 20: 11685 (JINR-P-2444)
Polarized proton target in investigation of low-energy nucleon-nucleon

interactions, 20: 11965 (JINR-P-2426)
Possibility of specific interactions of muons and ν_μ-neutrinos at superhigh energies, 20: 11558 (JINR-E-2496)
Possible test of CPT invariance in p-p scattering, 20: 11557 (JINR-E-2457)
Proton-antiproton scattering in $SU(6)_w$ symmetry, 20: 11565 (JINR-P-2469)
Relativistic composite model of meson and baryon resonances, 20: 11684 (JINR-P-2442)
Time and energy in quantum mechanics, 20: 11866 (JINR-E-2478)

JUNTA DE ENERGIA NUCLEAR, MADRID (SPAIN). DIVISION DE MATERIALES.
Cleaning of porous filters in fluidized-bed reactors, 20: 10810 (JEN-153-DMe/I-19)

JUNTA DE ENERGIA NUCLEAR, MADRID (SPAIN). DIVISION DE METALLURGIA.
Welding procedures used in fabrication of fuel elements for DON reactor exponential experiment, 20: 12401 (JEN-156-DMe/113)

JUNTA DE ENERGIA NUCLEAR, MADRID (SPAIN). DIVISION DE QUIMICA.
Production of stable isotopes in Spain, 20: 11191 (JEN-150-DQ/I-51)

K

KANSAS STATE UNIV., MANHATTAN.
Hydrogen negative ion, 20: 11453 (UCRL-12230)
Solution of secular equation for electrostatic helium atom, 20: 11451 (UCRL-7941(Rev.1))

KANSAS UNIV., LAWRENCE.
Prog. rpt. on radiochemistry, final, 6/56–5/65, 20: 10933 (TID-22532)

KERNFORSCHUNGSANLAGE, JUELICH (WEST GERMANY).
Beam tube equipment for FRJ-2 (DIDO) cold neutron source, 20: 12503 (AERE-Trans-1043)
Bibliography on dosimetry, 7/65, 20: 11027 (AED-C-21-03)

KERNFORSCHUNGSANLAGE, JUELICH (WEST GERMANY). INSTITUT FUER PLASMAPHYSIK.
Ionization of hydrogen and nitrogen in uniform magnetic field increasing with time, 20: 11768 (JUL-327-PP)
Ionization rate at higher electron densities in d-c fields measured in electrodeless discharge, 20: 12169 (JUL-322-PP)
Plasma effect in an ionized helium line, 20: 12168 (JUL-280-PP)

KERNFORSCHUNGSZENTRUM, KARLSRUHE (WEST GERMANY).
Bibliography on laboratories for work with radioactive, 20: 10977 (KFK-370)
Karlsruhe reference design of 1000 Mw(e) sodium cooled fast breeder reactor, 20: 12402 (KFK-369)

L

LABORATOIRE DE L'ACCELERATEUR LINEAIRE, UNIV. DE PARIS, ORSAY (FRANCE).
Proton form factors from proton observation, 20: 11567 (LAL-1144)

LABORATOIRE DE RECHERCHES SUR LA PHYSIQUE DES PLASMAS, LAUSANNE (SWITZERLAND).
Anomalous skin effect in plasma, 20: 12170 (LRP-18-65)

LABORATORI NAZIONALI DI FRASCATI, COMITATO NAZIONALE PER L'ENERGIA NUCLEARE (ITALY).
Resolution obtainable with some TRC's with electrostatic deflection, 20: 11104 (LNF-65/33)

LABORATORIO DE FISICA E ENGENHARIA NUCLEARES, JUNTA DE ENERGIA NUCLEAR, SACAVEM (PORTUGAL).
Study of the ternary system U–V–Cr, 20: 11271 (LFEN-24)

LABORATORIO GAS IONIZZATI, COMITATO NAZIONALE PER L'ENERGIA NUCLEARE, FRASCATI (ITALY).
Experiment on electrical breakdown in vacuum at laboratorio gas ionizzati, 20: 11769 (LGI-65/30)

LAWRENCE RADIATION LAB., UNIV. OF CALIFORNIA, BERKELEY.
Application of direct digital control to high energy particle accelerators, 20: 11401 (UCRL-16502)
Calculation of characteristics of ω^0 by Faddeev equations, 20: 11568 (UCRL-11749)
Experimental shielding studies at the 6.2-Bev Berkeley Bevatron, 20: 11400 (UCRL-123)
High-temperature compressive deformation equipment, 20: 11285 (UCRL-16434)
Instability of pyruvate-^{14}C, 20: 10934 (UCRL-11743)
ISO—a FORTRAN program for utilizing strong-focusing principle in beta-ray spectrometer design, 20: 11113 (UCRL-16471)
"Monochromatic" neutrino beam from high intensity 200 Bev proton synchrotron, 20: 11398 (UCID-1008)
Plasma kinetic equations, 20: 12182 (UCRL-16631)
Properties and preparation of thin bismuth films, 20: 11280 (UCRL-12001)
Spectra of CaO, 20: 10815 (UCRL-16338)
Variational principle for Faddeev equations, 20: 11692 (UCRL-11768)

LAWRENCE RADIATION LAB., UNIV. OF CALIFORNIA, LIVERMORE.
Analysis of N + ^{4}He reaction and effects of spin coupling n + ^{4}He to d + T, 20: 11978 (UCRL-7961-T)
Analytic continuation of $a(l,s)$ for $Re\, l < N$, 20: 11693 (UCRL-12016-T)
Apparatus for automatic preparative gas chromatography, 20: 12553 (UCRL-14359)
AUTO-DEBUG—machine-level debugging program, 20: 11208 (UCRL-12220)
Cherenkov electromagnetic radiation from nuclear detonation in space, 20: 11807 (UCRL-7495(Rev.1))
Curve sketching by digital computer, 20: 12552 (UCRL-12226)
Design and construction of aquariums: a bibliography, 20: 12554 (UCRL-14473)
Effect of strain rate on mechanical properties of some widely used engineering metals, 20: 11284 (UCRL-14599)
Effect of the planetary system on nearly parabolic comets, 20: 11426 (UCRL-12267)
Elastic and inelastic scattering of protons by ^{18}O, 20: 11979 (UCRL-12152)
Electromagnetic mass of classical electron, 20: 11454 (UCRL-12233)
FORTRAN-FORTRAN, 20: 11207 (UCRL-7737)
Fusion bonding of plasma-sprayed tungsten coatings of steel, 20: 11242 (UCRL-12153)
Helium isoelectronic sequence wave functions, 20: 11450 (UCRL-7842-T)
Hydrodynamic behavior of supernovae explosions, 20: 11425 (UCRL-7777)
Hydrogen negative ion, 20: 11453 (UCRL-12230)
$LiMg_2Tl$: preparation and structure, 20: 11282 (UCRL-12119-T)
Microgram surface density measurements by observation of proton-produced x rays, 20: 11281 (UCRL-12107)
Monte Carlo study of one-component plasma. Pt. 1., 20: 12181 (UCRL-14467-T)
Note on parallelism, 20: 11868 (UCRL-14546)
Paralleling avalanche transistors, 20: 11067 (UCRL-12095-T)
Particle size distribution and bulk permeability of oil shale rubble, 20: 10975 (UCRL-14294)
Positron focusing in accelerating field, 20: 11399 (UCRL-7566(Rev.1))
Production of metastable atoms by electron impact, 20: 11455 (UCRL-14450)
Quantum corrections in Thomas-Fermi model, 20: 11452 (UCRL-12042-T)
Rapid phase transformations in titanium induced by pulse heating, 20: 11283 (UCRL-12142)
Segmented laminar flow and other models for packed-bed longitudinal dispersion, 20: 10995 (UCRL-10696(Rev.) (Pt.1))
Shoaling and breaking of solitary wave and its applications, 20: 12551 (UCRL-12186)
Solution of secular equation for electrostatic helium atom, 20: 11451 (UCRL-7941(Rev.1))
Treatment of proton channelling by a transverse two-dimensional model, 20: 12279 (UCRL-12311)

LIEGE UNIV. (BELGIUM).
Conference on molten salts, plenary lectures, University of Liege, Belgium, 9/64, 20: 10803 (EUR-2466.e)
Ion diffusion and migration in molten salts, 20: 10805 (EUR-2466.e, pp 21-30)
Preparation and purification of tritiated geranyllinalol, 20: 10809 (EUR-2531.f)
Properties of ionic liquids and mixtures, 20: 10804 (EUR-2466.e, pp 9-19)

LOCKHEED–GEORGIA CO., MARIETTA.
Polymeric materials irradiation data submittal, 20: 11344 (N65-35361)

LOCKHEED NUCLEAR PRODUCTS, MARIETTA, GA.
Data compilation and evaluation of space shielding problems, 20: 12265 (NP-15697(Vol.1))
Prog. rpt. on effect of radiation on materials, 7/10/65, 20: 11345 (NASA-CR-54787)

LOS ALAMOS SCIENTIFIC LAB., UNIV. OF CALIFORNIA, N. MEX.
Asymptotic phase and amplitude for modified Coulomb potential in scattering theory, 20: 11689 (LA-DC-6912)
Behavior of coated particles in large nuclear transient (Kiwi TNT), 20: 11343 (LA-3367)
Comparison of different methods of particle size analysis, 20: 11270 (LA-3424)
GMX-2 spalling calculations, 20: 12539 (LA-DC-7692)
Heat content of molten tin, 20: 10811 (LA-DC-6806)
Hydrodynamic model of He(II) neat T_λ, 20: 11892 (LA-DC-6824)
Molten plutonium burnup experiment, 20: 12403 (LA-3384)
Spacing and cesium pressure dependence of electron temperatures and ion densities in thermionic converter, 20: 11544 (LA-DC-7390)
Spectral indices of 4.29 per cent ^{235}U-enriched uranium metal exponential,

20: 12358 (LA-3406)
Stability of solutions of polynomial equation, 20: 12538 (LA-DC-6803)
Survey of Los Alamos and Euratom heat pipe investigations, 20: 11545 (LA-DC-7555)
Three-dimensional cartesian particle-in-cell calculations, 20: 12537 (LA-3422)

LYON UNIV. (FRANCE). INSTITUT DE PHYSIQUE NUCLEAIRE.
Contribution to theoretical study of A(t,p)B reactions, 20: 11972 (NP-15716)

M

MARTIN CO., BALTIMORE, MD. NUCLEAR DIV.
Parametric re-entry ablation study of hypothetical ^{90}Sr fuel forms, 20: 11189 (MND-3062-25)

MARYLAND UNIV., COLLEGE PARK. DEPT. OF PHYSICS AND ASTRONOMY.
Binary-coded digitized hodoscope, 20: 11112 (TID-22553)
Design of scanning template for associating Λ^0 decays with Ξ^0 production vertices, 20: 11111 (TID-22550)
K^-p interactions from 900 to 1100 Mev/c and their bearing on $Y^*(1765)$ and $Y_0^*(1815)$, 20: 11551 (CONF-650837-3)
Study of non-mesic decay of helium hypernuclei, 20: 11977 (TID-22536)

MARYLAND UNIV., COLLEGE PARK. INST. FOR FLUID DYNAMICS AND APPLIED MATHEMATICS.
Approximate formulae for variety of solutions of Thomas-Fermi equation, 20: 11449 (TID-22530)
Chebyshev polynomial approximations for L-membrane eigenvalue problem, 20: 11206 (TID-22529)

MASSACHUSETTS INST. OF TECH., CAMBRIDGE.
Nondestructive analyses of irradiated MITR fuel by γ spectroscopy, 20: 10764 (MITNE-64)

MASSACHUSETTS INST. OF TECH., CAMBRIDGE. DEPT. OF METALLURGY.
Fracture in connection with hot deformation processing of metals, 20: 11265 (AD-626375)

MAX-PLANCK-INSTITUT FUER CHEMIE, MAINZ (WEST GERMANY).
Ion mobilities in molten salts, 20: 10806 (EUR-2466.e, pp 31-8)

MAX-PLANCK-INSTITUT FUER PHYSIK UND ASTROPHYSIK, MUNICH (WEST GERMANY).
Toroidal device with meridian magnetic confining field of grad $p \cdot$ grad ϕ $dl/B > 0$, 20: 12174 (MPI-PAE/P1.6/65)

MECHANICAL TECHNOLOGY INC., LATHAM, N. Y.
Experiments on ultrastable gas journal bearing, 20: 10979 (TID-22528)
Prog. rpt. on gas-bearing Brayton cycle turbocompressor, 9–11/65, 20: 10972 (NYO-3237-4)
Topical report on turbulent lubrication, 20: 10973 (TID-21992)

MICHIGAN STATE UNIV., EAST LANSING.
Optical potentials and high-energy inelastic proton scattering, 20: 11974 (ORNL-P-960)

MIDWESTERN UNIVERSITIES RESEARCH ASSN., STOUGHTON, WIS.
Adjustable current shunt for trimming ampere turns in magnet operating from constant d-c source, 20: 11388 (CONF-650922-29)

MOUND LAB., MIAMISBURG, OHIO.
Bibliography on pentaerythritoltetranitrate, 20: 10862 (MLM-1252)
Gamma shielding requirements for ^{238}Po and ^{210}Po (revised), 20: 12264 (MLM-1315)
Weak alpha and electron-capture decay in ^{208}Po and ^{209}Po, 20: 11971 (MLM-1251J)

MSA RESEARCH CORP., CALLERY, PA.
Effect of high temperature sodium on austenitic and ferritic steels, 20: 11235 (MSAR-65-194)

N

NATIONAL AERONAUTICS AND SPACE ADMINISTRATION, CLEVELAND, OHIO. LEWIS RESEARCH CENTER.
Ball lightning characteristics, 20: 12176 (NASA-TN-D-3188)

NATIONAL AERONAUTICS AND SPACE ADMINISTRATION, LANGLEY STATION, VA. LANGLEY RESEARCH CENTER.
Behavior of single-turn magnetic coil under dynamic load conditions, 20: 12177 (NASA-TN-D-3199)

NATIONAL BUREAU OF STANDARDS, WASHINGTON, D. C.
Engineering method for calculating protection afforded by structures against fallout radiation, 20: 11030 (NBS-MON-76)

NAVAL RADIOLOGICAL DEFENSE LAB., SAN FRANCISCO, CALIF.
An iodine source for beta counting, 20: 10935 (USNRDL-TR-948)
Nuclear-charge distributions of several fission product mass chains, 20: 11980 (USNRDL-TR-935)
Pulsed reactor simulation of underwater nuclear detonations—thermal analysis, 20: 11013 (USNRDL-TR-940)
Total neutron cross sections of copper, iron, and aluminum near 14 Mev, 20: 11949 (AD-625747)
^{115}Pd yield in thermal neutron fission of ^{235}U, 20: 11981 (USNRDL-TR-943)

NAVAL RESEARCH LAB., WASHINGTON, D. C.
Prog. rpt. on metallurgical characteristics of high strength structural materials, 5–7/65, 20: 11273 (NRL-6364)

NERATOOM, N. V., THE HAGUE (NETHERLANDS).
Prog. rpt. on fabrication of pressure vessels, 4–6/65, 20: 11239 (EURAEC-1468)

NEW YORK UNIV., N. Y.
Passage of high-energy particles in matter—nuclear cascades induced in dense media by 1- and 3-Bev protons, 20: 12262 (BNL-8721)

NEW YORK UNIV., N. Y. INST. OF ENVIRONMENTAL MEDICINE.
Empirical sampling using radioactivity as generator randomicity, 20: 11204 (NYO-3136-2, App. 3)
Light bulb statistics, 20: 11205 (NYO-3136-2, App. 4)
Parana pulse-height analysis for radionuclide assay—a FORTRAN program listing, 20: 11202 (NYO-3136-2, App. 1)
Patterns in residuals: test for regression model adequacy in radionuclide assay, 20: 11203 (NYO-3136-2, App. 2)
Prog. rpt. on statistical analysis of environmental and total body x-ray scintillation spectra, 10/64–9/65, 20: 11201 (NYO-3136-2)

NIAGARA MOHAWK POWER CORP., SYRACUSE, N. Y.
Nine Mile Point Nuclear Station. Vol. I., 20: 12408 (NP-15660(Vol.1))
Nine Mile Point Nuclear Station, 20: 12410 (NP-15660(Suppl.1))
Nine Mile Point Nuclear Station. Vol. II., 20: 12409 (NP-15660(Vol.2))

NORDISK INSTITUT FOR TEORETISK ATOMFYSIK, COPENHAGEN (DENMARK).
Quasi-free proton-proton scattering in light nuclei at 460 Mev, 20: 11948 (AD-624318)

NORTH AMERICAN AVIATION, INC., THOUSAND OAKS, CALIF. RESEARCH CENTER.
Chemical equilibria in molten salts, 20: 10807 (EUR-2466.e, pp 39-57)

NUCLEAR ENERGY INFORMATION CENTER, WARSAW (POLAND).
Breeding of fissionable fuel, 20: 12407 (NEIC-RR-13)

O

OAK RIDGE GASEOUS DIFFUSION PLANT, TENN.
Thermal diffusion column shape factors. I., 20: 10949 (K-1469)

OAK RIDGE INST. OF NUCLEAR STUDIES, INC., TENN.
Design of low-background whole-body counting facility, 20: 10724 (ORINS-51)

OAK RIDGE NATIONAL LAB., TENN.
Beam energy measurements at Oak Ridge isochronous cyclotron, 20: 11396 (ORNL-TM-1382)
Criticality of single unit of aqueous uranyl fluoride solution enriched to 5 percent in ^{235}U, 20: 12359 (ORNL-TM-1195)
Decontamination of ORNL molten-salt fluoride-volatility pilot plant after processing irradiated zirconium-uranium alloy fuel, 20: 11032 (ORNL-3891)
Examination of failed expansion bellows between EGCR containment shell and experimenters cell 6, 20: 12411 (ORNL-TM-1380)
Fast and thermal neutron flux measurements in ORR and LITR, 20: 12501 (ORNL-TM-1163)
Geohydrological evaluation of solid waste storage area 6, 20: 12518 (ORNL-TM-1327)
HFIR pressure vessel and structural components material surveillance, 20: 12457 (ORNL-TM-1372)
Improved aluminosilicate ion exchangers, 20: 10766 (TID-22511)
Indexes to Analytical Chemistry Division annual progress reports, 1964–1965, 20: 10765 (ORNL-3904)
Low energy gamma and x-ray from radioactive sources, 20: 10932 (ORNL-P-1928)
Magnetic field storage codes and orbit calculations, 20: 11395 (ORNL-TM-1172(Rev.))
Microstructural examination, 20: 11275 (ORNL-TM-1338)
Neutron density fluctuations induced by hydraulic noise in nuclear power reactor, 20: 12360 (ORNL-TM-1332)
Observation of mirror-like instability in hot electron plasma, 20: 12180 (ORNL-P-1556)
Operations plan—Operation HENRE, 20: 11930 (CEX-65.03)
Optical potentials and high-energy inelastic proton scattering, 20: 11974 (ORNL-P-960)
Possibility of excitation-heating of ions to high temperature, 20: 11770 (ORNL-P-1005)
Preparation of isotope targets by electron-bombardment techniques, 20: 11183 (ORNL-P-1900)
Purification and growth of KCl single crystals, 20: 10813 (ORNL-3906)
R-matrix approach to complex angular momentum and to three-particle interaction, 20: 11691 (ORNL-3914)
REACT and CONVRG FORTRAN subroutines for determining source convergence for 65R Monte Carlo neutron transport code, 20: 11934

(ORNL-TM-1325)
Remote fabrication of reactor fuels, 20: 11241 (TID-8541, pp 71-148)
Solution of Lagrange multiplier problem with several constraints, 20: 12544 (ORNL-3846)

OESTERREICHISCHE STUDIENGESELLSCHAFT FUER ATOMENERGIE G.M.B.H., SEIBERSDORF.
Yields with multiphase isotope separator, 20: 11192 (SGAE-PH-30/1965)

OESTERREICHISCHE STUDIENGESELLSCHAFT FUER ATOMENERGIE G.M.B.H., SIEBERSDORF. ELEKTRONIKINSTITUT.
Univibrator as time element in medium fast coincidence circuit, 20: 11109 (SGAE-E-5/1965)

OHIO STATE UNIV. RESEARCH FOUNDATION, COLUMBUS.
Prog. rpt. on stress corrosion cracking in Fe–Ni–Cr alloy systems, 6–9/65, 20: 11233 (COO-1319-32)

P

PARIS UNIV. (FRANCE).
Application of controlled-potential coulometry to determinations in radioactive solutions, 20: 10758 (EUR-2618.f)

PARIS UNIV. (FRANCE). FACULTE DES SCIENCES.
System of electron grouping at input of linear accelerator, 20: 11393 (NP-15715)

PAVIA UNIV. (ITALY). ISTITUTO DI GENETICA.
Prog. rpt. on mutability of polygenes, 1/66, 20: 10603 (IAEA-2466-11)

PENNSYLVANIA UNIV., PHILADELPHIA. DEPT. OF PHYSICS.
Hidden symmetries and the question of massless particles, 20: 11679 (CONF-650927-21)

PHILIPPINE ATOMIC ENERGY COMMISSION, MANILA.
Bibliography on Moessbauer effect, 20: 12277 (PAEC(A)IN-656)
Bibliography on single crystals, 20: 11276 (PAEC(A)IN-657)
Prog. rpt. annual, 6/64–6/65, 20: 12545 (PAEC(A)AR651)

PHILLIPS PETROLEUM CO. IDAHO FALLS, IDAHO., ATOMIC ENERGY DIV.
Addendum to the Spert III hazards summary report—low-enrichment oxide core, 20: 12497 (IDO-17003(Rev.2))
Fundamentals in operation of nuclear test reactors. V., 20: 12496 (IDO-16871-5)
Instrument component and systems development, 20: 12499 (IDO-17112, pp 52-80)
Instrument development, 20: 11174 (IDO-17112, pp 81-91)
Instrumentation analysis, 20: 12498 (IDO-17112, pp 1-51)
Prog. rpt. on burnup determination of nuclear fuels, 7–9/65, 20: 11960 (IDO-14667)
Prog. rpt. on instrument development, annual, 1964, 20: 11061 (IDO-17112)
Sampling and analysis of fission products during loss-of-fluid test (LOFT), 20: 12356 (IDO-17128)
Shift crew performance evaluation at nuclear test reactors, 20: 12500 (IDO-17131)

PHYLATRON CORP., COLUMBUS, OHIO.
Prog. rpt. on high-sensitivity fast neutron dosimeter, 8–10/65, 20: 11094 (COO-1226-10)

PITKIN (LUCIUS) INC., GRAND JUNCTION, COLO. WESTERN URANIUM PROJECT.
Designs and descriptions of mechanical subsample cutters used in reducing uranium concentrate sample sizes, 20: 10978 (RMO-3006)

PITTSBURGH UNIV., PA.
Prog. rpt. on productivity of vascular hydrophytes and their role in mineral cycling in aquatic ecosystems, annual, 1965, 20: 12543 (NYO-3018-12)

PRINCETON UNIV., N. J.
R-matrix approach to complex angular momentum and to three-particle interaction, 20: 11691 (ORNL-3914)

PRINCETON UNIV., N. J. PLASMA PHYSICS LAB.
Cooling system for model C stellarator, 20: 12173 (MATT-315)
Effect of weak collisions on ion waves, 20: 12172 (MATT-302)
Interpretation of atomic hydrogen light in C stellarator, 20: 12171 (MATT-270)
Theoretical fine structure of He II 4686 A in magnetic fields to 40 kilogauss, 20: 11442 (MATT-280)

PURDUE UNIV., LAFAYETTE, IND.
Thermal analysis, 20: 12416 (TID-22545, pp 67-80)

PURDUE UNIV., LAFAYETTE, IND. DEPT. OF CHEMISTRY.
Charge and mass distribution studies in fission of ^{237}Np and ^{239}Pu by intermediate energy helium ions, 20: 11954 (COO-347-18)
Fission of rhenium at intermediate excitation energy, 20: 11955 (COO-347-19)
Mass and charge distribution studies in fission of ^{197}Au by intermediate energy helium ions, 20: 11953 (COO-347-17)

PURDUE UNIV., LAFAYETTE, IND. DEPT. OF NUCLEAR ENGINEERING.
Design study report on 1000 Mw(e) fast breeder reactor, 20: 12414 (TID-22545, pp 16-52)
Second Graduate Nuclear Engineering Design Seminar, Purdue University, Summer 1965, 20: 12413 (TID-22545)
Steam cycle calculations, 20: 12415 (TID-22545, pp 54-65)
Thermal analysis, 20: 12416 (TID-22545, pp 67-80)

R

RADIO CORP. OF AMERICA, LANCASTER, PA. DIRECT ENERGY CONVERSION DEPT.
Prog. rpt. on thermionic energy converters, 11/64–10/65, 20: 11540 (AD-626444)

RAND CORP., SANTA MONICA, CALIF.
Thermodynamics of the graphite-carbon vapor system, 20: 10799 (AD-625735)

RENSSELAER POLYTECHNIC INST., TROY, N. Y.
Electrical properties of 50-Mev electron-irradiated germanium, 20: 11350 (NP-15611, pp 39-46)
Infrared absorption bands in Si induced by 45-Mev electrons. I., 20: 11347 (NP-15611, pp 5-18)
Infrared studies of 48 Mev electron-irradiated (at 125°K) oxygen-doped germanium, 20: 11348 (NP-15611, pp 19-27)
Lifetime and trapping in 6- to 50-Mev electron-irradiated germanium, 20: 11349 (NP-15611, pp 28-38)
Photoconductivity studies in 10- to 50-Mev electron-irradiated silicon, 20: 11351 (NP-15611, pp 48-89)
Prog. rpt. on radiation damage in semiconductor materials, 2–4/65, 20: 11176 (NP-15835)
Prog. rpt. on radiation damage to semiconductors, 3/15–9/15/65, 20: 11346 (NP-15611)

RESEARCH GROUP, UNITED KINGDOM ATOMIC ENERGY AUTHORITY, WANTAGE (ENGLAND).
Silt movement in an ebb channel, firth of forth, 1965, 20: 11022 (AERE-R-5080)

RESEARCH LAB., GENERAL ELECTRIC CO., SCHENECTADY, N. Y.
Calculation of current and potentials for segmented electrode MHD generator, 20: 11539 (65RL-3888E)
Gravitational instability in vertical magnetic field, 20: 11538 (65RL-3814E(Rev.))
Sustained magnetic field theta pinch, 20: 12161 (65RL-3940E)
Theory of ion detection from plasma imbedded in magnetic field, 20: 12162 (65RL-3998E)

ROCHESTER UNIV., N. Y. DEPT. OF PHYSICS AND ASTRONOMY.
Algebra of currents and magnetic moments of hyperons, 20: 11569 (UR-875-118)
Spark chamber tests of multiple particle detection efficiency, 20: 11114 (UR-875-66)

ROCKY FLATS DIV., DOW CHEMICAL CO., GOLDEN, COLO.
Adhesion tester for evaporated metal films, 20: 11063 (RFP-672)
Evaluation of binders for machinable unfired ceramics, 20: 11277 (RFP-659)
Large area gas proportional detector for low energy photons, 20: 11108 (RFP-637)
Rocky flats body counter, 20: 11107 (RFP-462)
Study of thermistor stability, 20: 11062 (RFP-649)

RUTGERS–THE STATE UNIV. OF NEW JERSEY, NEW BRUNSWICK. SCHOOL OF CERAMICS.
Prog. rpt. on dielectric strength and ferroelectric behavior of ceramics, final, 1/63–6/64, 20: 11279 (SC-DC-64-1477X)

S

SANDIA CORP., ALBUQUERQUE, N. MEX.
Aerospace safety results from ROVER/NERVA post-operational destruct test, 20: 12470 (SC-R-65-1017)
Evaluation of microscopic-sized graphite aerosol from ROVER reactor destruction test, June 1965, 20: 12471 (SC-RR-65-557)
Fast-pulse recording and readout device using tunnel diodes, 20: 11065 (SC-TM-323-62(72))
Ground deposition of microspheres released from 50 kilometers, 20: 11033 (SC-TM-65-398)
Prog. rpt. on dielectric strength and ferroelectric behavior of ceramics, final, 1/63–6/64, 20: 11279 (SC-DC-1477X)
ROVER/NERVA destruct system test results, Aberdeen Proving Ground-3 (final report), 20: 12472 (SC-RR-65-620)
Small orbit betatron, 20: 11397 (SC-RR-65-111)
Stress postprocessor, 20: 12546 (SC-RR-65-548)
^{147}Pm–silicon betavoltaic battery feasibility, 20: 11546 (SC-RR-65-671)

SANDIA CORP., LIVERMORE, CALIF.
Qualification tests of spray-deposited and light-initiated silver acetylide–silver nitrate explosive, 20: 10814 (SCL-DC-65-96)

SOCIETE BELGE POUR L'INDUSTRIE NUCLEAIRE, BRUSSELS.
Prog. rpt. on use of Pu as reactor fuel, 1–3/65, 20: 12396 (EURAEC-1505)

Prog. rpt. on use of Pu as reactor fuel, 4–6/65, 20: 12397 (EURAEC-1506)

SOCIETE D'ENERGIE NUCLEAIRE FRANCO-BELGE DES ARDENNES, CHOOZ-LEZ-GIVET (FRANCE).

Prog. rpt. on Ardennes nuclear power plant, 7–9/65, 20: 12412 (TID-22516)

SOCIETE PROGIL, LYON (FRANCE). LABORATOIRE CENTRAL DE RECHERCHES.

SR_2–SR_3–SR_4 electron irradiation loop, 20: 10871 (EUR-2288.f)

SOUTHWEST RESEARCH INST., SAN ANTONIO, TEX.

Qualification tests of spray-deposited and light-initiated silver acetylide–silver nitrate explosive, 20: 10814 (SCL-DC-65-96)

STANFORD LINEAR ACCELERATOR CENTER, STANFORD UNIV., CALIF.

Insulation structure and coil reliability, 20: 11387 (CONF-650922-28)

Iterative Chebyshev approximation technique for equalizer synthesis, 20: 11066 (SLAC-PUB-146)

STANFORD RESEARCH INST., MENLO PARK, CALIF.

Procedure for evaluating space-charge effects in beam bending magnet system, 20: 11378 (AD-626633)

Secondary ignitions in nuclear attack, 20: 11031 (NP-15708)

STICHTING VOOR FUNDAMENTEEL ONDERZOEK DER MATERIE, JUTPHAAS (NETHERLANDS). INSTITUUT VOOR PLASMA-FYSICA.

Dielectric behavior of plasma at cyclotron resonance, 20: 12179 (NP-15782)

SYRACUSE UNIV., N. Y.

Boson resonances produced in K^-p interactions, 20: 11552 (CONF-651015-3)

T

TENNESSEE UNIV., KNOXVILLE.

Neutron density fluctuations induced by hydraulic noise in nuclear power reactor, 20: 12360 (ORNL-TM-1332)

TEXAS UNIV., AUSTIN.

Infrared maser interferometry for time and space resolution of electron density in high temperature plasmas, 20: 12165 (ARL-65-135)

Time-space resolution of B-fields in theta-pinch plasma by Faraday rotation of infrared maser radiation, 20: 12164

THAYER SCHOOL OF ENGINEERING, DARTMOUTH COLL., HANOVER, N. H.

Bubbly flow in straight pipes, 20: 10991 (NYO-3114-12)

TODD SHIPYARDS CORP., GALVESTON, TEX.

NS Savannah containment integrity quarterly leak rate test results, May 1964, 20: 12473 (TID-22459)

Prog. rpt. on NS Savannah operations, 5–8/64, 20: 12474 (TID-22460)

TRW SPACE TECHNOLOGY LABS., THOMPSON RAMO WOOLDRIDGE INC., REDONDO BEACH, CALIF.

Prog. rpt. on valve technology for spacecraft engines, final, 7/64–8/65, 20: 11007 (NP-15831)

TUFTS UNIV., MEDFORD, MASS.

Nature of water movements in surface layer of ocean at OWS stations I and J south of Iceland, 20: 12541 (NYO-2929-1)

Origin of fluctuations in Peru current, 20: 12542 (NYO-2929-2)

U

UNION CARBIDE CORP., OAK RIDGE, TENN. Y-12 PLANT.

Preparation of highly enriched U_3O_8 for high flux isotope reactor core, 20: 11244 (Y-MA-450)

UNITED AIRCRAFT CORP., EAST HARTFORD, CONN. RESEARCH LABS.

Low-energy electron-cesium atom collision probability investigations, 20: 11444 (NASA-CR-54790(App. 1))

Prog. rpt. on collision probability of electrons and ions with alkali metal atoms, semiannual, 11/65, 20: 11443 (NASA-CR-54790)

UNITED NUCLEAR CORP., WHITE PLAINS, N. Y. DEVELOPMENT DIV.

Sodium technology, 20: 12330 (TID-8541, pp 321-425)

UNITED STATES–EURATOM FAST REACTOR EXCHANGE PROGRAM.

Grand Quevilly thermal tests station, 20: 12420 (EURFNR-9F)

Prog. rpt. on fast neutrons project, annual, 1963, 20: 12419 (EURFNR-1F)

Steam generators associated with sodium-cooled reactors, 20: 12339 (EURFNR-11F)

UNITED STATES–EURATOM JOINT RESEARCH AND DEVELOPMENT PROGRAM.

Bubbly flow in straight pipes, 20: 10991 (NYO-3114-12)

Prog. rpt. on brittle fracture strength of heavy-gage steel plate, final, 1965, 20: 11240 (EURAEC-1520)

Prog. rpt. on fabrication of pressure vessels, 4–6/65, 20: 11239 (EURAEC-1468)

Prog. rpt. on fission-product reactions with and release from fuel-element claddings, 7–9/65, 20: 11212 (BMI-X-10143)

Prog. rpt. on UO_2 fuel systems, 3/31/65, 20: 12377 (CEND-2863-236)

Prog. rpt. on use of Pu as reactor fuel, 4–6/65, 20: 12397 (EURAEC-1506)

Prog. rpt. on use of Pu as reactor fuel, 1–3/65, 20: 12396 (EURAEC-1505)

Reactor tanks steels. Irradiation of tensile-test pieces in EL.3 at different temperatures and post-irradiation tests, 20: 11342 (EURAEC-1502)

USTAV JADERNEHO VYZKUMU, CESKOSLOVENSKA AKADEMIE VED, REZ.

Application of modified S_n method for intracell thermal neutron absorption density distribution, 20: 12365 (UJV-1438/65)

Change of flux in vicinity of irregularities in regular square lattice, 20: 12366 (UJV-1439/65)

Distribution of neutron flux density in cylindrical reactor with partially inserted control rods, 20: 12367 (UJV-1442/65)

Flattening of flux in heterogeneous slab reactor, 20: 12364 (UJV-1365/65)

Precise synchronized measurements of space angle in circular chopper diagram, 20: 11177 (UJV–1388/65)

Specifications of certain steels for nuclear reactor pressure vessels, 20: 11286 (UJV-1405/65)

V

VANDERBILT UNIV., NASHVILLE, TENN.

Internal conversion coefficients in decay of ^{57}Co, 20: 11976 (TID-22504)

VIRGINIA POLYTECHNIC INST., BLACKSBURG.

Conference on nuclear marine propulsion, Blacksburg, Va., 8/64, 20: 12458 (CONF-640810)

Critical appraisal of nuclear merchant ships, 20: 12459 (CONF-640810, pp 1-6)

Design of Japanese nuclear ship, 20: 12462 (CONF-640810, pp 122-37)

Maritime study by Division of Reactor Development, United States Atomic Energy Commission, 20: 12461 (CONF-640810, pp 105-6)

Panel discussion: role of nuclear power in merchant marine, 20: 12460 (CONF-640810, pp 7-21)

Panel discussion: licensing nuclear merchant vessel, 20: 12464 (CONF-640810, pp 156-65)

Reactor plant of research ship of Gesellschaft fuer Kernenergieverwertung, 20: 12463 (CONF-640810, pp 138-55)

W

WASHINGTON STATE UNIV., PULLMAN. DEPT. OF PHYSICS.

Prog. rpt. on chemical sputtering of solids, 6/16–9/16/64, 20: 12549 (TID-21555)

WASHINGTON UNIV., SEATTLE.

Analytic continuation of $a(l,s)$ for $Re\, l < N$, 20: 11693 (UCRL-12016-T)

WESTINGHOUSE ELECTRIC CORP., PITTSBURGH, PA. ASTRO-NUCLEAR LAB.

Forced convection boiling heat transfer to hydrogen, 20: 10996 (WANL-TNR-154)

Prog. rpt. on development of Ta base alloy, 2/20–5/19/65, 20: 11217 (WANL-PR(Q)-007)

Prog. rpt. on evaluation of refractory/austenitic bimetal combinations, 6/22–9/22/65, 20: 11243 (WANL-PR(EE)-001)

Space power plant study, 20: 12475 (WANL-PR(B)-009)

WESTINGHOUSE ELECTRIC CORP., PITTSBURGH, PA. ATOMIC POWER DIV.

Prog. rpt. on large closed-cycle water reactor, 7–9/65, 20: 12417 (WCAP-3269-15)

Prog. rpt. on large closed-cycle water reactor, 4–6/63, 20: 12418 (WCAP-3739)

WESTINGHOUSE RESEARCH LABS., PITTSBURGH, PA.

Research and development on silicon carbide active devices, 20: 12276 (NYO-3405-4)

WISCONSIN UNIV., MADISON. DEPT. OF PHYSICS.

Prog. rpt. on thermonuclear plasma studies, 8–10/65, 20: 12167 (COO-1233-24)

Y

YALE UNIV., NEW HAVEN, CONN. BINGHAM OCEANOGRAPHIC LAB.

Prog. rpt. on sedimentation of Mn in the open ocean, final, 1965, 20: 12540 (NYO-2882-8)

PERSONAL AUTHOR INDEX

Each entry after an author's name is a shortened version of the title of the report or article, followed by the *NSA* volume and abstract number. Report numbers are given in parentheses.

The phrase "Progress report" is abbreviated as "Prog. rpt.," permitting a more rapid and complete alphabetical arrangement of the titles without changing the locatfon of the progress report titles in relation to the other titles.

Because of problems involving the mechanical preparation of this index, all accent marks are omitted. The following changes in spelling have been introduced to reduce some of the confusion which might result from omitting the accents:

ä	becomes	ae
ö		oe
ø		oe
ü		ue (except in transliterated Chinese names)

A

AAMODT, R. E., Critical length determination for convective instabilities in weakly inhomogeneous plasmas, 20: 12233

AARONS, Jules, Enhanced electromagnetic radiation between 500 and 1000 c/s in auroral zone, 20: 11860

AASEN, J. O., Distribution of zeros of grand partition function, 20: 11788

ABADIE-MAUMERT, F. A., Swedish agesta power reactor, 20: 12426

ABBE, W. J., Theory of reggeized bootstraps, 20: 11751

ABDURAKHMANOVA, R. R., Effect of stimulation of the vestibular analyzer on blood coagulability in intact and irradiated dogs, 20: 10682

ABEL, W. R., Thermal equilibrium between liquid ^{3}He and powdered cerium magnesium nitrate at very low temperatures, 20: 11922

ABIODUN, R. A., Approximations for exchange scattering. I., 20: 11505

ABRAHAM, B. W., Boundary layer of equilibrium plasma atmosphere, 20: 12228

ABRAHAM, F., Energy spectrum of charged pions from K^--captures in CF_3Br, 20: 12092

ABRIKOSOV, A. A., Quantum field theoretical methods in statistical physics, 20: 11375

ACHERMAN, W. L., Corrosion properties of molybdenum, tungsten, vanadium, and some vanadium alloys, 20: 11230 (BM-RI-6715)

ACHUTHAN, P., Photoproduction of vector mesons, 20: 11595

ACKERMANN, R. J., Evaporation behavior of neptunium dioxide, 20: 10840

ADACHI, Takeshi, Radiation shielding device, 20: 12272

ADAM, N. V., Computation of geomagnetic field at great heights, 20: 11816

ADAMCOVA, Berta, Relationship of radioresistance and immunoresistance in an experimental tumor, 20: 10634

ADAMS, G. E., Absolute rate constants for reaction of hydroxyl radical with organic compounds, 20: 10916

ADAMS, G. E., Pulse radiolysis of aqueous solutions of thiocyanate ion, 20: 10915

ADAMS, G. E., Radical yields and kinetics in pulse radiolysis of potassium bromide solutions, 20: 10911

ADAMS, G. W., Recent solar cosmic ray events, 20: 11863

ADELMAN, Saul Joseph, Design of scanning template for associating Λ^0 decays with Ξ^0 production vertices, 20: 11111 (TID-22550)

ADITYA, Sukumar, ESR spectra of gaseous ^{129}I and ^{127}I, 20: 11468

ADLER, P., Suitability of neutron sensitive foils for dosimetry of thermal neutrons by means of pocket ion chambers, 20: 11119

ADLER, R. J., Meson exchange effects on electromagnetic structure of deuteron, 20: 11651

AEBERSOLD, J., Measurement of gastro-intestinal protein loss by means of ^{131}I-labeled polyvinylpyrrolidone, 20: 10568

AFANAS'EV, A. M., Suppression of inelastic channels in resonance scattering of neutrons in regular crystals, 20: 12313

AFANAS'EV, V. P., Dosimetric investigations and shielding studies using synchrocyclotron, 20: 10605 (NASA-TT-F-353, pp 21-54)

AFRA, D., Late changes in human brain after intraoperative implantation of ^{60}Co pellets, 20: 10575

AFRIKANTOV, I. I., Nuclear power plant BN-350, 20: 12441

AGARWAL, S. C., Dynamics of Y_1^*, (1815-Mev) $\bar{K}N$ resonance, 20: 11632

AGARWAL, S. P., Survey of cosmic-ray intensity in lower atmosphere, 20: 11521

AGARWAL, Y. K., K-selection rule in β-decay of ^{172}Tm, 20: 12114

AGLINTSEV, K. K., Applied dosimetry, 20: 11058

AGOSTINELLI, Cataldo, Slow steady magnetodynamic movement of electrically conducting viscous fluid in spherical envelope. I., 20: 11776

AGOSTINELLI, Cataldo, Slow steady magnetodynamic movement of electrically conducting viscous fluid in spherical envelope. II., 20: 11777

AGUILAR, J., Studies of background of protons in experiments with neutrinos, 20: 11571

AGUILAR, R., Studies of background of protons in experiments with neutrinos, 20: 11571

AHLUWALIA, S. S., Anion exchange separation of thorium from rare earth elements in acetone–nitric acid medium, 20: 10959

AHMADZADEH, Akbar, Calculation of characteristics of ω^0 by Faddeev equations, 20: 11568 (UCRL-11749)

AHMED, Israr, Imaginary part of nuclear optical potential at low energies, 20: 12129

AIRAPETYANTS, M. G., Eye damage in dogs exposed to radiation in antenatal period of development, 20: 10675

AITKEN, K. L., FAUST 1—hardcore discharge stability experiment, 20: 12222

AIYER, Raju N., Nuclear fission as Markov process, 20: 12116

AJZENBERG-SELOVE, F., Energy levels of light nuclei. VII., 20: 12023

AKABORI, Hiroshi, Electron beam apparatus, 20: 11418

AKASOFU, S.-I., Growth and decay of ring current and polar electrojets, 20: 11829

AKOEV, I. G., Effectiveness of hormone terapy in radiation injuries, 20: 10709

AKSTEIN, E., Cytogenetic studies in chronic myeloid leukemia, 20: 10647

ALBERGOTTI, Jesse C., Total neutron cross sections of copper, iron, and aluminum near 14 Mev, 20: 11949 (AD-625747)

ALBERTI, G., Influence of thermal treatment on rate of ion exchange of zirconium phosphate, 20: 10957

ALDEN, T. H., Magnetic pinning in type-II superconductor, 20: 11894

ALEKSEEV, V. V., Scattering matrix for finite times in interacting particle wave function space, 20: 11761

ALEKSENKO, Yu. N., Nuclear desalination equipment of low capacity, 20: 12454 (JPRS-33480)

ALIEV, N. G., Thermal conductivity of Tm, Yb, and Lu at low temperatures, 20: 11329

AL-KAFAJI, T., Determination of ^{239}Pu content in irradiated nuclear fuel by neutron transmission, 20: 10796

ALLARD, J. F., Upper limit for the partial width $\Gamma(\rho \to \pi\gamma)$, 20: 11618

ALLEMANN, R. T., Promethium compatibility and encapsulation studies, 20: 11267 (BNWL-SA-488)

ALLEN, B. C., Notch-impact behavior of chromium and a chromium–35 at.% rhenium alloy, 20: 11300

ALLISON, Samuel K., Galilean transformation of continuous energy particle distributions, 20: 11952 (COO-238-46)

ALLISON, Samuel K., Laboratory to center-of-mass transformation of particle distributions continuous in energy, 20: 12011

ALM, Robert D., Nuclear submarines—techniques for welding Hy-80, 20: 11261

ALSTER, J., Collective excitations in ^{207}Pb, ^{208}Pb, and ^{209}Bi, 20: 12075
ALSTON III, William Jeffries, Photoproton polarization from ^{12}C, 20: 12105
ALTSCHULER, Sidney Joseph, Spectra emerging from possible cold neutron moderators, 20: 11944
ALY, H. H., Scattering by singular potential r^{-4}, 20: 11706
AMADO, R. D., Theory of triton wave function, 20: 11623
AMALDI, Ugo Jr., (e,e'p) reaction in ^{9}Be nucleus, 20: 11988
AMATO, C. G., Comparison of radiothermoluminescent and radiophotoluminescent dosimeters, 20: 11155
AMBEGAOKAR, Vinay, Accelerated currents in superconductors, 20: 11919
AMME, Robert C., Low-energy ionization of argon atoms by argon atoms, 20: 11477
ANCHEVSKII, E. V., Use of polonium–boron emitter of neutrons in analysis of ores and dressing products for aluminum, 20: 10781
ANDERSON, A. C., Heat capacity of dilute solutions of liquid ^{3}He in ^{4}He at low temperatures, 20: 11920
ANDERSON, A. C., Thermal equilibrium between liquid ^{3}He and powdered cerium magnesium nitrate at very low temperatures, 20: 11922
ANDERSON, A. J. W., Development of dynamics model for heavy water boiling reactors, 20: 12400 (HPR-54)
ANDERSON, J. L., Possible causal violations at radii greater than Schwarzschild radius, 20: 11885
ANDERSON, S. D., Prog. rpt. on instrument development, annual, 1964, 20: 11061 (IDO-17112)
ANDRADE E SILVA, J., Development of particle distribution density during acceleration toward statistical distribution limit, 20: 11408
ANDREEV, G. A., Strengthening metals and alloys by irradiation, 20: 11366
ANDREWS, F. C., Existence of two phases in one-dimensional classical fluids, 20: 11799
ANDREWS, F. C., Theory of droplet formation in one-dimensional fluids, 20: 11800
ANDREWS, R. C., Effect of high temperature sodium on austenitic and ferritic steels, 20: 11235 (NSAR-65-194)
ANISOVICH, V. V., Analytic properties of triangle graphs with decay masses and three-particle production, 20: 11596
ANTILL, J. E., Oxidation behavior of defective fuel elements, 20: 12380
ANTOINE, J.-P., SU_4 mass formula and particle classification schemes, 20: 11753
ANTONIJEVIC, M., Nitrogen metabolism in frog liver after whole-body irradiation. I., 20: 10551
ANTONOV, A. S., Application of electrophotography for measurements of sensitive region of germanium p-i-n detectors, 20: 11102 (JINR-P-2487)
AOKI, Ryozo, Plastic scintillator, 20: 11165
ARD, W. B., Observation of mirror-like instability in hot electron plasma, 20: 12180 (ORNL-P-1556)
ARENDT, F., Development of 100-Mev FFAG electron synchrotron, 20: 11391 (NP-15274)
ARGUTINSKAYA, S. V., Radiation effects on the RDA activity in cellular nuclei and cytoplasm, 20: 10591
ARMENISE, N., Exchange mechanism for $\pi^{+}p \to N^{*}\rho^{0}$ reaction at 2.75 Bev/c, 20: 11605
ARNDT, Richard A., Determination of nucleon-nucleon elastic-scattering matrix. IV., 20: 11622
ARTUS, H., Unusual nuclear photoreaction on C, O, and Si, 20: 12094
ARTYKOV, I. Z., Internuclear cascades at superhigh energies, 20: 11566 (JINR-P-2472)
ARWAS, E. B., Topical report on turbulent lubrication, 20: 10973 (TID-21992)
ASAWA, C. K., Quenching of fluorescence by cross relaxation of Nd^{3+} in LaF_3, 20: 12297
ASHBY, D. E. T. F., Errors in the use of mass analyzers in plasma physics, 20: 12223
ASHENHURST, R. L., Experimental investigation of unnormalized arithmetic, 20: 11196 (COO-614-34, Sect. IIB)
ASHERY, D., Lifetime measurements of some rotational levels by new recoil method, 20: 12020
ASHKIN, M., Radiative absorption cross section of an electron in field of an argon atom, 20: 11478
ASHTON, F., Momentum spectrum of cosmic-ray muons at large Zenith angles, 20: 11526
ASSAF, N., Lifetime measurements of some rotational levels by new recoil method, 20: 12020
AUBREY, B. B., Ion beam measurements of cesium recombination cross sections, 20: 11488
AUSLOOS, P., Gas phase radiolysis and vacuum ultraviolet photolysis of 2- and 3-pentanone, 20: 10895
AUSLOOS, P., H_2S as free-radical interceptor in gas-phase radiolysis and photolysis of propane, 20: 10883
AUXIER, J. A., Operations plan—Operation HENRE, 20: 11930 (CEX-65.03)
AUZINS, Ieva, Synthesis of macroglobulin antibody to bacterial antigen in mice after treatment with Thorotrast, 20: 10617
AVALTRONI, M., Resolution obtainable with some TRC's with electrostatic deflection, 20: 11104 (LNF-65/33)
AVERETT, W. J., Cesium-137 body burdens of Alaskan men, 1965, 20: 10723
AZIMOV, M. A., γ-Quanta detecting by using spark chamber and total absorption Cherenkov counter, 20: 11099 (JINR-P-2436)

B

BAACKE, J., Analysis of πN charge exchange scattering from 4 to 18 Bev/c, 20: 11615
BABA, C. V. K., K-selection rule in β-decay of ^{172}Tm, 20: 12114
BABAEV, Z. R., Electromagnetic properties of mesons in broken SU(6) symmetry, 20: 11727
BABICKY, A., Generalized skeletal response to local radiation injury, 20: 10587
BABIKOV, V. V., Heavy mesons and nucleon-nucleon potentials, 20: 11597
BABYKIN, M. V., Turbulent heating of plasma by direct-discharge current, 20: 12183 (ORNL-tr-868)
BACKOVSKY, J., Most accurate measurements of wavelengths of x-ray spectral lines, 20: 11069
BACON, F. M., Absolute cross sections for single ionization of alkali ions by electron impact. II., 20: 11490
BACONNIER, Y., Contribution to study of closed orbit, 20: 11386 (CERN-65-35)
BACRI, Jean, Initiation of high-frequency electric discharge in rare gases, 20: 11780
BAERNIGHAUSEN, H., Lattice cell and space groups of EuOOH, 20: 10817
BAERNIGHAUSEN, H., Production and crystal data of α-$LiEuO_2$, 20: 10818
BAGDASAROV, Y. E., Nuclear power plant BN-250, 20: 12441
BAIER, V. N., Possible verification of nonconservation of time parity in colliding beam experiments, 20: 11582
BAIKOV, I. S., Effect of electric field on spectrum of oscillations in inhomogeneous plasma, 20: 12220
BAIKOV, I. S., Effect of cold-plasma component on stability of inhomogeneous hot plasma, 20: 12221
BAILEY, Glenn Charles, Ferromagnetic resonance of ^{3}He-irradiated thin metal films, 20: 12318
BAILEY, Peter John, Conveyor systems, 20: 10986
BAILEY, T. L., Inelastic collisions of H_3^+ and N_3^+ ions with hydrogen molecules, 20: 11467
BAINBRIDGE, J. E., Techniques for observing fission gas bubbles in uranium, 20: 11220
BAINES, Bernard Deryck, Conveyor systems, 20: 10986
BAIR, W. J., Chronic effects of inhaled $^{239}PuO_2$ in dogs, 20: 10596 (BNWL-122, pp 1-15)
BAIR, W. J., Effect of DTPA on translocation and excretion of inhaled ^{144}Ce–^{144}Pr oxide in dogs, 20: 10533 (BNWL-122, pp 125-7)
BAIR, W. J., Versatile iodine vapor and particle sampler, 20: 11060 (BNWL-122, pp 33-6)
BAIRD, G. E., Representations of semi-simple Lie groups. V., 20: 11721
BAJAJ, M. M., Gamma-gamma directional correlation in ^{123}Te, 20: 12140
BAKHRU, H., Decay of ^{133}Hf and nuclear levels of ^{133}Ta, 20: 12148
BAKHRU, H., Isotope ^{162}Tb and its decay characteristics, 20: 12149
BALACHANDRAN, A. P., Criteria for solubility of partial-wave dispersion relations, 20: 11699
BALAZS, Louis A. P., Effective nonlocal energy-independent potential and possibility of repulsive core at small distances, 20: 11653
BAL'BUTSEV, E. B., Equilibrium deformation of heavy nuclei, 20: 11970 (JINR-P-2473)
BALIKA, Yu. D., Prophylaxis and therapy of radiation injuries caused by protons, 20: 10699 (NASA-TT-F-353, pp 210-38)
BALL, G. L., Worth measurements of core and blanket subassembly materials in Enrico Fermi reactor, 20: 12388 (APDA-NTS-6)
BALLOU, J. E., Effect of splenectomy on acute plutonium toxicity, 20: 10524 (BNWL-122, pp 83-4)
BALLOU, N. E., Nuclear-charge distributions of several fission product mass chains, 20: 11980 (USNRDL-TR-935)
BALLUFFI, R. W., Efficiency of dislocation climb in metals, 20: 11274 (NYO-3504-2)
BAMBYNEK, W., Decay of ^{241}Am, 20: 11956 (EUR-2632.d)
BAMMERT, K., Problem of optimum design of nuclear gas turbine power plants, 20: 12422
BANBURY, P. C., Energy and orientation effects of electron irradiation in silicon, 20: 11364
BARACHENKOV, V. S., Internuclear cascades at superhigh energies, 20: 11566 (JINR-P-2472)
BARAN, V., Uranates as form of uranyl hydrolytic complexes, 20: 10838
BARANDUN, S., Determination of total clearance of different preparations of gamma-globulin, 20: 10571
BARANDUN, S., Measurement of gastro-intestinal protein loss by means of ^{131}I-labeled polyvinylpyrrolidone, 20: 10568

BARANDUN, S., Metabolism of gamma-globulin in agammaglobulinaemia and hypogammaglobulinaemia, 20: 10572
BARANOV, V. F., Dependence of energy losses averaged over the electron spectrum on β-spectrum energy maximum, atomic number of β emitter, and type of transition, 20: 11037
BARASCH, Guy Errol, Excited states of rare earth ions in crystals, 20: 12317
BARCUS, J. R., Spatial and temporal character of fast variations in auroral-zone x rays, 20: 11826
BARDAKCI, K., Local approximation in renormalizable and non-renormalizable theories. I., 20: 11707
BARDAKCI, K., Local approximations in renormalizable and nonrenormalizable theories. II., 20: 11708
BARDEEN, James Maxwell, Stability and dynamics of spherically symmetric masses in general relativity, 20: 11889
BARDOS, J., Application of modified S_n method for intracell thermal neutron absorption density distribution, 20: 12365 (UJV-1438/65)
BARDWICK III, John, Level structure of ^{53}Cr, 20: 12095
BARDYUKOV, M. E., Thermocouple for measuring temperatures up to 2500°K, 20: 11076
BARENDSEN, G. W., Survival of cells under single and fractionated irradiation and significance of this for radiotherapy of tumors, 20: 10649
BARKMAN, J. R., Preparation of highly enriched U_3O_8 for high flux isotope reactor core, 20: 11244 (Y-MA-450)
BARNES, Peter David, Vibrational energy spectrum of atomic nucleus ^{112}Cd, 20: 12109
BARRETT, Barbara, Consequences of C-violating interactions in η^0 and X^0 decays, 20: 11634
BARRON, Williams, Enhanced electromagnetic radiation between 500 and 1000 c/s in auroral zone, 20: 11860
BARSHAY, S., Decays of Y_1^+ and CP-noninvariant electromagnetic interactions, 20: 11638
BARTLETT, D., Experimental test of time-reversal invariance in decay $K_L \rightarrow \pi^\pm \mu^\mp + \nu$, 20: 11662
BARTON, J. C., Investigation of cosmic rays underground using scintillator stack. I., 20: 11527
BARTON, J. C., Investigation of cosmic rays underground using scintillator stack. II., 20: 11528
BARUT, A. O., Asymptotic behavior of scattering amplitude in left half-plane of complex angular momentum, 20: 11710
BASDEVANT, Jean-Louis, Relativistic three-pion calculation. I., 20: 11639
BASDEVANT, Jean-Louis, Relativistic three-pion calculation. II., 20: 11640
BASDEVANT, Jean-Louis, Relativistic three-pion calculation. III., 20: 11641
BASSICHIS, W. H., Analysis of boson model displaying phase transition, 20: 11801
BASSO, Michael J., Fast neutron detection and flux density measurement, 20: 11169
BASTIDE, J., Liver and kidney of mice during poisoning with uranyl nitrate and carbon tetrachloride, 20: 10548
BASTIDE, P., Liver and kidney of mice during poisoning with uranyl nitrate and carbon tetrachloride, 20: 10548
BASU, G., Resolution in crystal spectra of uranyl acetylacetonate, 20: 10843
BASU, J., Complex refractive index of magnetoplasma, 20: 12258
BATE, G. L., Deformation of transition-state nucleus in energetic fission, 20: 12077
BATYGIN, V. V., Bremsstrahlung on medium electrons and hard Vavilov-Cherenkov radiation, 20: 11670
BAUMANN, N. P., Thermal neutron diffusion in heavy water, 20: 11931 (CONF-651101-53)
BAUMGAERTNER, G., Activation enthalpy of beryllium diffusion in Ni–Be alloys, 20: 11326
BAXENDALE, J. H., Determination of some fast reaction rates using pulsed radiolysis of permanganate solutions, 20: 10914
BAXENDALE, J. H., Formation of Cu^{III} in radiolysis of Cu^{2+} solutions, 20: 10923
BAXENDALE, J. H., Pulse radiolysis of Ag^+ solutions, 20: 10922
BAXENDALE, J. H., Some contributions of electron pulse technique, 20: 10908
BAXENDALE, J. H., Symposium on pulse radiolysis, Manchester, 4/65, 20: 10906
BAXTER, W. G., Development and evaluation of a homogeneous W–25Re alloy for 2600°C applications, 20: 11238 (CONF-650449-1)
BAYM, Gordon, Non-linear optics of many-particle systems, 20: 12255
BEAHN, T. J., Excitation-transfer collisions between rubidium and helium atoms, 20: 11482
BEALL, E. F., Binary-coded digitized hodoscope, 20: 11112 (TID-22553)
BEARDEN, A. J., Moessbauer effect in ^{159}Tb, 20: 12303
BEARDSLEY, G. M., Positron annihilation in superconducting lead, 20: 11912
BEASLEY, T. M., Tissue accumulation of uranium and thorium in rats after inhalation of uranium ore dust, 20: 10514 (BNWL-122, pp 21-4)
BEATTY, R. L., Pyrolytic-carbon coatings on ceramic fuel particles, 20: 11254
BECK, Clifford K., Panel discussion: licensing nuclear merchant vessel, 20: 12464 (CONF-640810, pp 156-65)
BECKER, K., Bibliography on dosimetry, 7/65, 20: 11027 (AED-C-21-03)
BECKER, Kurt M., Burnout conditions for flow of boiling water in vertical 3-rod and 7-rod clusters, 20: 11000
BECKER, Richard L., Alkali-atom-halogen-molecule reactions in molecular beams: the spectator stripping model, 20: 10834
BEERWALD, H., Ionization rate at higher electron densities in d-c fields measured in electrodeless discharge, 20: 12169 (JUL-322-PP)
BEERWALD, Hans, Ionization of hydrogen and nitrogen in uniform magnetic field increasing with time, 20: 11768 (JUL-327-PP)
BEHOUNEK, Frantisek, Analysis of induced atmospheric radioactivity, 20: 11043
BEIDLER, E. A., Fluidized-bed process for production of tungsten, 20: 11255
BEKEFI, G., Thermal and non-thermal emission from plasmas, 20: 12256
BELASHCHENKO, D. K., Mechanism of electroosmosis in liquid metals, 20: 11289 (IS-Trans-26)
BELFORD, R. L., Resolution in crystal spectra of uranyl acetylacetonate, 20: 10843
BELINFANTE, F. J., Kruskal space without wormholes, 20: 11886
BELL, Robert B., Spin-parity determination of Y_1^+ (1765), 20: 11656
BELLEMANS, A., Surface tension of isotopic mixtures, 20: 11787
BELLER, L. S., Determination of paired-pulse resolution of random counting systems, 20: 11105 (NAA-SR-Memo-11132)
BELLON, Louis, Comparison of hydrogen and deuterium bonds by uv absorption spectrometry, 20: 10819
BELOHORSKY, B., Histological findings in corporis uteri following irradiation, 20: 10749
BELOV, K. P., Ferromagnetism and antiferromagnetism of rare-earth metals and alloys, 20: 11340
BELOV, S. P., Secondary γ-emission coefficients for aluminum, copper, and tungsten, 20: 12267
BELTER, W. G., Radioactive waste management, 20: 12519 (TID-8541, pp 149-248)
BELTRAMETTI, E. G., Number of Casimir operators associated with any Lie group, 20: 11609
BELYAKOV, M. A., Use of polonium–boron emitter of neutrons in analysis of ores and dressing products for aluminum, 20: 10781
BEMELMANS, P., Utilization of radioisotopes for production of electric energy aboard space vehicles, 20: 11188 (BLG-330)
BEMIS, C. E. Jr., Decay of ^{132}Te and levels in odd ^{132}I, 20: 12026
BENAKSAS, D., Proton form factors from proton observation, 20: 11567 (LAL-1144)
BENAKSAS, D., Proton form factors from observation of recoil protons, 20: 11628
BEN DANIEL, D. J., Gravitational instability in vertical magnetic field, 20: 11538 (65RL-3814E(Rev.))
BENDT, Philip J., Hydrodynamic model of He(II) near T_λ, 20: 11892 (LA-DC-6824)
BENESOVSKY, F., Octahedral phase structures of transition metals, 20: 11318
BENINCASA, G., Approximate method for evaluation of over-pressure in primary circuit of pressurized water reactor, 20: 12343
BENISTON, M., Energy spectrum of charged pions from K^--captures in CF_3Br, 20: 12092
BENISZ, J., Q-values and cross-sections measurements of (n,α) reaction on some nuclei, 20: 11983
BENJAMIN, Richard Walter, $(n,n'\gamma)$ reaction in ^{56}Fe, 20: 12108
BEN'KOVA, N. P., Computation of geomagnetic field at great heights, 20: 11816
BENN, J., Determination of lifetime and ground-state energy of ^8Be by α-α elastic scattering at 184 kev, 20: 12038
BENO, R. L., Adhesion tester for evaporated metal films, 20: 11063 (RFP-672)
BENOIT-CATTIN, Pierre, Initiation of high-frequency electric discharge in rare gases, 20: 11780
BENSON, J. M., Existence of two phases in one-dimensional classical fluids, 20: 11799
BENSON, Joy L., Isotopic masses of hydrogen, chlorine, barium, cerium, and neodymium, 20: 11494
BENSON, Sidney W., Theory of low-temperature chromatographic separation of hydrogen isotopes, 20: 10939
BENT, G. D., Prog. rpt. on emission and excitation cross sections, 3–11/65, 20: 11448 (TID-22480)
BENTLEY, W. H., Behavior of thirteen charge transfer complexes at high pressure, 20: 12534 (COO-1198-216)
BENVENISTE, J., Measurement of $Fe(\alpha,\alpha')Fe^*$ reactions produced by alpha bombardment, 20: 12056

BEONIO-BROCCHIERI, F., Temperature dependence of ^{240}Pu resonance absorption at 1.05 ev in homogeneous systems, 20: 12001
BERDNIKOV, A. I., Effect of stable cobalt on adsorption of ^{60}Co by peat, 20: 10756
BERG, H. F., Plasma effect in an ionized helium line, 20: 12168 (JUL-280-PP)
BERGGREN, T., Quasi-free proton-proton scattering in light nuclei at 460 Mev, 20: 11948 (AD-624318)
BERGNER, K. G., Examination of radioactivity of food in Baden-Wuerttemberg, 20: 11017
BERINDE, A., Small-angle scattering of protons by ^{24}Mg, 20: 12003
BERLIJN, Jean Jacques Henri, Nuclear polarization in $^{11}B(d,p)^{12}B$ reaction, 20: 12107
BERNARD, A., Rectitis and ileitis after treatment of cervical cancer with radium and x rays, 20: 10654
BERNARD, D. L., Associated particle method for $D(d,n)^3He$ reaction, 20: 11677
BERNHARDT, Heinz, Distribution of radioactive rainfall at dam with help of gamma spectrometry, 20: 11055
BERNSTEIN, J. L., Unit cell and space group of gadolinium molybdate and of scandium tungstate, 20: 10858
BERRY, R. E., Aerospace safety results from Rover/Nerva post-operational destruct test, 20: 12470 (SC-R-65-1017)
BERRY, R. E., Rover/Nerva destruct system test results, Aberdeen proving ground-3(final report), 20: 12472 (SC-RR-65-620)
BERRY, Roger J., Reduced oxygen enhancement ratio for x-ray survival of HeLa cells after treatment with Methotrexate, 20: 10664
BERSON, S. A., Considerations in preparation of ^{131}I-labeled hormones, 20: 10943
BERTINOV, A. I., Magnetic systems of magnetogasdynamic generators, 20: 11548
BERTMAN, B., Thermal conductivity in solid ^3He and ^4He, 20: 11916
BERTMAN, B., Thermal conductivity in isotopic mixtures of solid helium, 20: 11917
BERTOLOTTI, A., Therapeutic use of selective perfusion with radioisotopes with a short half life, 20: 10737
BERTRAND, Jacqueline, Infinitesimal generators of Poincare group in angular momentum base, 20: 11702
BERTRAND, T. E., Beam energy measurements at Oak Ridge isochronous cyclotron, 20: 11396 (ORNL-TM-1382)
BERWANGER, G., Calculation of fast neutron spectrum in Triga Mark-II reactor, 20: 12505
BETHE, H., Theory of Zeeman effect in salts of rare earths, 20: 11456 (AERE-Trans-1041)
BETIGERI, M. G., Study of levels of ^{44}Ti, 20: 12144
BEVENSEE, R. M., Quantum electrodynamics of stimulated emission of radiation. II., 20: 11878
BEYER, W. A., Asymptotic phase and amplitude for modified Coulomb potential in scattering theory, 20: 11689 (LA-DC-6912)
BHAKAR, B. S., Triton parameters with realistic potentials, 20: 12130
BHAMATHI, G., Analysis of light Λ hyperfragments on separable potential model. II., 20: 11594
BHARATHI, S. M., $^{40}Ca(n,\alpha)^{37}Ar$ angular distribution at E_n = 4.7 Mev, 20: 12119
BHATTACHARJEE, S. K., K-selection rule in β-decay of ^{172}Tm, 20: 12114
BIAGINI, C., Therapeutic use of selective perfusion with radioisotopes with a short half life, 20: 10737
BIANCHI, C., Labeling and kinetics of body excretion of ^{131}I-iodothiazide, 20: 10732
BIANU, G., Cytogenetic studies in chronic myeloid leukemia, 20: 10647
BIBERGAL', A. V., Gamma irradiation facilities, 20: 10980 (AEC-tr-6469)
BIBIKOVA, A. F., Biological effect of protons with energies of 510 Mev in multiple irradiation, 20: 10606 (NASA-TT-F-353, pp 55-102)
BIBIKOVA, A. F., Biological effect of protons with energies of 510 Mev during single irradiation, 20: 10607 (NASA-TT-F-353, pp 103-41)
BIBIKOVA, A. F., Prophylaxis and therapy of radiation injuries caused by protons, 20: 10699 (NASA-TT-F-353, pp 210-38)
BICKERTON, R. J., FAUST I—hardcore discharge stability experiment, 20: 12222
BIEDENHARN, L. C., Representations of semi-simple Lie groups. V., 20: 11721
BIEDERMAN, David Leslie, Kinetics of oxidation of graphite by CO_2, 20: 10859
BIEHL, Arthur T., Miniature magnetohydrodynamic generator, 20: 11550
BIESZKIEWCZ, Jan, Internal oxidation of Fe–Al alloys, 20: 11232 (INR-644/XIV/PS)
BIGHAM, C. B., Ratio of direct to cumulative yield of ^{135}Xe in thermal neutron fission of ^{233}U, ^{235}U, ^{239}Pu, and ^{241}Pu, 20: 11990
BILEN'KII, S. M., Determination of spin and parity of Ω^- hyperon, 20: 11563 (JINR-P-2456)
BILENKY, S. M., Possible test of CPT invariance in $\bar{p}$-p scattering, 20: 11557 (JINR-E-2457)
BILENSKII, S. M., Double NN scattering with polarized beam and polarized target, 20: 11671
BILLEREY, Roland, Energy spectra and angular distribution of (n,α) reaction produced on ^{32}S by neutrons at 3.2 Mev, 20: 11993
BILLET, A. B., Testing of space vehicle fluid power controls in nuclear radiation, 20: 11181
BINDAL, P. K., Rotational bands in ^{82}Kr, 20: 12156
BING, Richard J., Determination of coronary flow with positron emitter (^{84}Rb), 20: 10730
BINGHAM, J. A. C., Iterative Chebyshev approximation technique for equalizer synthesis, 20: 11066 (SLAC-PUB-146)
BIRGE, Robert W., Spin-parity determination of Y_1^* (1765), 20: 11656
BISHOP, A. S., Interpretation of atomic hydrogen light in C stellarator, 20: 12171 (MATT-270)
BISHOP, A. S., Loss rates of charged particles from ohmically-heated discharges in C-stellarator, 20: 12239
BISHOP, Frederic L., Neutron-absorptive glass, 20: 12273
BISHOP, W. N., Production of carrier-free ^{132}Cs and ^{129}Cs, 20: 10901
BISI, A., Three-quantum annihilation of positrons in ionic crystals, 20: 11620
BISIACCHI, G., Unitary representations and relativistic coupling coefficients for SL_2, C, 20: 11737
BJOERNHOLM, S., Lifetimes of E3 transitions in odd-mass Ho isotopes, 20: 12017
BLACK, Thomas A., Design study report on 1000 MWe fast breeder reactor, 20: 12414 (TID-22545, pp 16-52)
BLACK, W. C., Thermal equilibrium between liquid ^3He and powdered cerium magnesium nitrate at very low temperatures, 20: 11922
BLACKWELL, Robert T., Modification of radiation damage of bacteria by folic acid antagonists, 20: 10648
BLAGOVESHCHENSKAYA, E. E., Optimum method of recording frequency of free nuclear precession in presence of noise, 20: 11817
BLAIR, J. M., Lithium-lithium scattering, 20: 12053
BLAISE, Jean, New determination of ionization potential from arc spectrum of thulium, 20: 11464
BLAKE, Damon D., Treatment of cancer of cervix by radiation and elective radical hysterectomy, 20: 10726
BLANC, Daniel, Initiation of high-frequency electric discharge in rare gases, 20: 11780
BLANCHET, Jean, Contribution to the study of pitting corrosion of magnesium and its alloys, 20: 11231 (CEA-R-2815)
BLANDER, M., Chemical equilibria in molten salts, 20: 10807 (EUR-2466.e, pp 39-57)
BLANK, J., Solution of Bethe-Goldstone equation for reaction matrix in finite nuclei, 20: 11997
BLANKENBECLER, R., Modified determinantal method, 20: 11700
BLASI, A., Number of Casimir operators associated with any Lie group, 20: 11609
BLIAMPTIS, E. E. E., Symmetry properties of beam handling-magnet systems, 20: 11411
BLICHERT-TOFT, P. H., Decay of $^{191}Pt(3.0\ d)$ to ^{191}Ir, 20: 12009
BLINN, H. O., Space power plant study, 20: 12475 (WANL-PR(B)-009)
BLINOV, P. I., Electron heating in TN-1 installation, 20: 12206
BLOCHER, J. M. Jr., Fluidized-bed process for production of tungsten, 20: 11255
BLOEMBERGEN, N., Optical nonlinearities of plasma, 20: 12245
BLUDMAN, S. A., Hidden symmetries and the question of massless particles, 20: 11679 (CONF-650927-21)
BLUEMCHEN, Gerhard, Determination of coronary flow with positron emitter (^{84}Rb), 20: 10730
BLUESTEIN, I., Neutron measurements in high gamma backgrounds, 20: 11154
BOAG, J. W., Absolute rate constants for reaction of hydroxyl radical with organic compounds, 20: 10916
BOAG, J. W., Pulse radiolysis of aqueous solutions of thiocyanate ion, 20: 10915
BOAG, J. W., Radical yields and kinetics in pulse radiolysis of potassium bromide solutions, 20: 10911
BOCEV, B., Radioactive decay of ^{188}Re, 20: 11998
BOCK, L., Suitability of neutron sensitive foils for dosimetry of thermal neutrons by means of pocket ion chambers, 20: 11119
BOCKRIS, J. O'M., Proton tunneling in hydrogen-evolution reaction, 20: 11372
BODFISH, E., Duality theorem in combinatorial switching, 20: 11198 (COO-614-34, Sect. IIIB)
BODMER, A. R., Hypertriton with S^* state and Λ-N interaction, 20: 12084
BOEHM, H., Penning ion source for mass spectrometers, 20: 11077
BOELUEKBASI, Esin Kent, Effect of tritiated thymidine and γ irradiation on mortality of adult Drosophila larvae. II., 20: 10602 (CNAEM-32)
BOGAR, G. F., Evaluation of three-dimensional flux synthesis method as nuclear design tool, 20: 12368 (WAPD-T-1737)
BOGDANKEVICH, L. S., Effect of electric field on spectrum of oscillations in inhomogeneous plasma, 20: 12220

BOGDANOV, G. F., Use of surface-barrier silicon detectors for measuring fast particle spectra, 20: 11115
BOGGS, J. Vincent, Design study report on 1000 MWe fast breeder reactor, 20: 12414 (TID-22545, pp 16-52)
BOGOLYUBOV, P. N., Relativistic composite model of meson and baryon resonances, 20: 11684 (JINR-P-2442)
BOHN, S. W., Development of photogrammetric techniques for measuring surface contours of small samples, 20: 11068 (WAPD-T-1815)
BOKELUND, H., Economic basis for establishing number of measurements according to value of material, 20: 10967
BOKOV, O. G., Octet of baryon resonances in unitary symmetry scheme, 20: 11685 (JINR-P-2444)
BOLAND, T. J., Instrument component and systems development, 20: 12499 (IDO-17112, pp 52-80)
BOLAND, T. J., Prog. rpt. on instrument development, annual, 1964, 20: 11061 (IDO-17112)
BONA, C., PINETO—FORTRAN code designed for solution of non-linear differential equations in neutrons dynamics, 20: 11946
BONARELLI RULLI, F., Changes of electrophoretic pattern of serum proteins after treatment with ^{32}P, 20: 10581
BONAZZOLA, G. C., Excitation of 4.5 Mev state in ^{27}Al by inelastic scattering of 14 Mev neutrons, 20: 12031
BONNER, B. E., Associated particle method for D(d,n)^{3}He reaction, 20: 11677
BOOK, D. L., Critical length detemination for convective instabilities in weakly inhomogeneous plasmas, 20: 12233
BORCHERTS, Robert Herman, EPR investigation of VO^{2+} and x ray produced V^{2+} in Tutton salt, 20: 12319
BORELLO, T., Analysis of high energy jet showers. III., 20: 11534
BORGGREEN, J., Lifetimes of E3 transitions in odd-mass Ho isotopes, 20: 12017
BORISKINA, N. G., Phase structure of alloys of Ti–Al–Zr system in Ti_3–Al–Zr section, 20: 11334
BORMAN, V. D., Measurements of distribution of pressure behind strong shock waves, 20: 11775
BOROS-GYEVI, Janosne, Investigations in field of radiation-induced solid state polymerization. X., 20: 10897
BOROVSKII, I. B., Detecting superconducting intermetallic compounds, 20: 10767 (AD-620995)
BOSCO, B., Inelastic electron-deuteron scattering and rescattering corrections, 20: 11646
BOSCO, G., Uptake of ^{35}S-sodium sulfate by hepatic tissue of normal and irradiated rats, 20: 10542
BOSE, D. K., Probe measurements of gold cathode Penning discharge, 20: 12259
BOSE, D. K., Set-up of duoplasmatron for intense ion beam, 20: 12260
BOSE, Manisha, Nuclear magnetic resonance in rare earth nitrates comparison with transition metal nitrates, 20: 12325
BOSHOLM, J., Partition chromatography of rare-earth metals with bis-(2-ethylhexyl) hydrogen phosphate. I., 20: 10960
BOTHA, I., Siliconizing to protect molybdenum, 20: 11236
BOTHA, L., Behavior of molybdenum powders during pressing and sintering, 20: 11253
BOTTER, R., Photoionization-efficiency curves for C_2H_2 and C_2D_2, 20: 10867
BOULENGER, R., Plutonium urinanalysis, 20: 10757 (BLG-353)
BOUNIN, J., Automatic retrieval spark chambers, 20: 11093 (COO-614-34, Sect. IIA)
BOUNIN, J., Experience with on-line experimentation, 20: 11553 (COO-614-34, Sect. IIC)
BOUSSARD, Daniel, Measurement of synchronous phase in ion accelerator, 20: 11406
BOWES, William A., Reconnaissance for uranium in the Lonquimay Area, Province of Malleco, Chile, 20: 11025 (RME-4552(Rev.))
BOWMAN, James Talton Jr., Reversion of white-ivory mutant in Drosophila, 20: 10693
BOYD, A. W., Status report on in-pile dosimetry in Canada, 20: 11145
BOYD, R. L. F., Space research in polar regions, 20: 11842
BRAAMS, Reinier, Reactions of hydrated electron with amino acids, peptides and proteins, 20: 10919
BRABY, L. A., Radioactivity in northern Alaskan natives and their foods during 1964, 20: 10718 (BNWL-122, pp 172-5)
BRADA, Y., Band shape of F-center optical emission in rubidium chloride, 20: 12278 (TID-21570)
BRADBURY, B. T., Electron-probe microanalysis of irradiated UO_2, 20: 10787
BRADY, Joseph L., Effect of the planetary system on nearly-parabolic comets, 20: 11426 (UCRL-12267)
BRAESS, D., Inelastic electron-deuteron scattering with final-state interactions, 20: 11666
BRAHMAVAR, S. M., Nuclear structure effects in decay of ^{141}Ce, 20: 12154
BRANDT, W. W., Steric interference to diffusion in Linde A Zeolite, 20: 12532 (COO-920-8)
BRANDT, Werner, Positron annihilation in diatomic crystals, 20: 11655
BRANSON, David, Three particle singularities in scattering amplitudes, 20: 11701
BRAR, S. S., Gamma-ray detection efficiency of annular and well-type sodium iodide crystals, 20: 11127
BRAUN, T., Radiocoulometric titrations, 20: 10769
BRAUNSTEINER, H., Hematologic changes in radiation damage, 20: 10660
BRECHNA, H., Insulation structure and coil reliability, 20: 11387 (CONF-650922-28)
BREDAEL, I., Transfer function analyzer for Dragon reactor, 20: 12425
BREMOND, B., Four-particle correlations in light nuclei, 20: 12013
BRESSANI, T., Excitation of 4.5 Mev state in ^{27}Al by inelastic scattering of 14 Mev neutrons, 20: 12031
BRIDENBAUGH, Peter, Fracture in connection with hot deformation processing of metals, 20: 11265 (AD-626375)
BRINKMAN, H. C., Capture of electrons by α-particles, 20: 11457 (LA-tr-65-29)
BRISCOE, C. V., Positron annihilation in superconducting lead, 20: 11912
BROMLEY, D. A., Isomerism in ^{129}Ba, 20: 12069
BROMLEY, D. A., Low levels of ^{128}Ba from ^{128}La decay, 20: 12068
BROOKS, D., Development of the radio-aurora, 20: 11859
BROOKS, R. A., Rotational magnetic moments of alkali-halide molecules, 20: 11484
BROSSMANN, G., Bibliography on laboratories for work with radioactive materials, 20: 10977 (KFK-370)
BROUT, R., Gravitational ward identity and principle of equivalence, 20: 11888
BROWN, C. L., Transportation of radioactive materials, 20: 11035 (TID-8541, pp 249-319)
BROWN, D. M., Transient absorption from 260-320 nm in certain pulse irradiated aqueous solutions, 20: 10924
BROWN, Harold, Application of nuclear electric propulsion to manned Mars missions, 20: 12492
BROWN, Howard Howland, Hyperfine structure and octopole interaction in stable bromine isotopes, 20: 11502
BROWN, J. R., GAPS: Fortran code for analyzing data from pulsed neutron source experiments, 20: 12355 (GAMD-6781)
BROWN, R. R., Spatial and temporal character of fast variations in auroral-zone x rays, 20: 11826
BRUCE, Daniel W., Cesium-137 body burdens of Alaskan men, 1965, 20: 10723
BRUCKER, G., High-energy radiation damage in silicon transistors, 20: 11182
BRUHAT, Yvonne, Inductive charged fluids of finite conductivity, 20: 11781
BRUHAT, Yvonne, Thermodynamics of charged fluids, 20: 11782
BRUHN, G., Stationary supersonic flow in common cone and basis of its numerical calculation, 20: 11767 (HMI-B-42)
BRUNE, D., Applied gamma-ray spectrometry by germanium semi-conductor detector, 20: 11134
BRUNNER, G., Influence of temperature on scintillations of NaI(Tl), 20: 11118
BRUSH, S. G., Monte Carlo study of one-component plasma. I., 20: 12181 (UCRL-14467-T)
BRUZZESE, E., Changes of electrophoretic pattern of serum proteins after treatment with ^{32}P, 20: 10581
BRUZZESE, E., Effect of 6-mercaptopurine and of x rays on skin homografts, 20: 10506
BRUZZESE, E., Effect of radioactive ^{32}P in the mouse, 20: 10640
BRUZZESE, E., Protection from and repair of biological lesions brought about by ionizing radiations, 20: 10639
BRUZZESE, E., Therapeutic use of selective perfusion with radioisotopes with a short half life, 20: 10737
BRYANT, H. C., High efficiency solid state neutron telescope for 15–35 Mev neutrons, 20: 11139
BRYANT, J. F., Pulse radiolysis of liquid ammonia, 20: 10910
BUBENIK, J., Relationship of radioresistance and immunoresistance in an experimental tumor, 20: 10634
BUCCI, Pompeo, Existence of dynamics of thermal neutrons, 20: 12371
BUCHER, E., Superconductivity of osmium and ruthenium under pressure, 20: 11896
BUCKMAN, R. W. Jr., Prog. rpt. on development of Ta base alloy, 2/20–5/19/65, 20: 11217 (WANL-PR(Q)-007)
BUCKMAN, R. W. Jr., Prog. rpt. on evaluation of refractory/austenitic bimetal combinations, 6/22–9/22/65, 20: 11243 (WANL-PR(EE)-001)
BUDAKOV, L. A., Combined effects of ^{90}Sr, ^{144}Ce, and ^{239}Pu on organs of rats, 20: 10552
BUDINI, P., Green fuactions from lie algebras, 20: 11441 (IC/65/94)
BUDINI, P., Non-compact extensions of symmetry groups, 20: 11681 (IC/65/85)
BUDNITZ, R., Unsuccessful search for excited electron, 20: 11629
BUECHAU, J., Ionospheric plasma density by three different methods,

20: 11847
BUEHLER, R. E., Pulse radiolysis of carbon tetrachloride–benzene mixtures, 20: 10928
BUETTNER, K., Determination of body water with ^{3}H, 20: 10557
BUKOWIECKI, B., Alpha contamination locator with junction radiation detector, 20: 11092 (CLOR-39/D)
BULANOV, P. A., Protective action of polysaccharide from yeast-like microorganism in irradiated mice, 20: 10703
BULLIS, R. H., Prog. rpt. on collision probability of electrons and ions with alkali metal atoms, semiannual, 11/65, 20: 11443 (NASA-CR-54790)
BULLOCK, J. B., Absolute power measurements of Ford nuclear reactor, 20: 12514
BUMP, T. R., Fast reactor test facility (Faret) and ititial experimental program, 20: 12512
BUONERBA, M., Effect of radioactive ^{32}P in the mouse, 20: 10640
BUONERBA, M., Therapeutic use of selective perfusion with radioisotopes with a short half life, 20: 10737
BURDETT, W. J., Mammalian radiation genetics, 20: 10688
BURGE, E. J., Thin liquid sheets at reduced pressure applications in nuclear physics, 20: 11409
BURGEAT, Jacques, Study of reflection profiles of x rays on silicon crystal irradiated with α rays, 20: 12281
BURHOP, E. H. S., Study of K^- meson interaction with nuclei using nuclear emulsion technique, 20: 11991
BURKE, J., Effects of thermal history on kinetics of $\beta \rightarrow \alpha$ phase change in uranium and uranium–chromium alloys, 20: 11311
BURKE, J., M_S temperature for pure uranium, 20: 11315
BURKHOLDER, H., Separation of high-purity lutetium and ytterbium by ion exchange at 90°C, 20: 10760 (IS-1305)
BURNOT, Guy, Improvement of focusing power of electrostatic accelerator tube with very high output, 20: 11405
BURNS, M. P., Plutonium metallurgy notebook, 20: 11213 (BNWL-37)
BUROV, I. V., Magnetic properties of gadolinium alloys with iron, cerium and yttrium, 20: 11341
BURR, John G., Thermal-spike model of low let radiolysis, 20: 10887
BURRICHTER, M., Bone marrow regeneration in rats after sublethal whole-body irradiation, 20: 10681
BURROWS, J. R., Solar flare particles in September 1963, 20: 11852
BURT, W. R. Jr., Fabrication of 20 wt % Ti–V alloy tubing for nuclear fuel cladding, 20: 11258
BURTON, Milton, Excitation transfer and decay processes in multi-component systems, 20: 10927
BUSCHOW, K. H. J., Structures of the rare-earth trialuminides, 20: 11305
BUSS, D. J., Reinvestigation of decays of ^{146}Eu and ^{146}Pm, 20: 12081
BUSSE, C. A., Optimization of heat pipe thermionic converters for space power supplies, 20: 11542 (EUR-2534.e)
BUSSOLATI, C., Three-quantum annihilation of positrons in ionic crystals, 20: 11620
BUSTAD, L. K., Biological effects of ^{131}I in sheep and cattle, 20: 10516 (BNWL-122, pp 49-51)
BUSTAD, L. K., Computer evaluation of tellurium–iodine contamination events, 20: 10519 (BNWL-122, pp 59-63)
BUSTAD, L. K., Effect of ^{127}I on passage of ^{131}I from cows to man via milk, 20: 10530 (BNWL-122, pp 113-17)
BUSTAD, L. K., Gastrointestinal absorption of ^{144}Ce and ^{147}Pm in miniature swine, 20: 10525 (BNWL-122, pp 85-90)
BUSTAD, L. K., Relationship of ^{137}Cs concentration in feed and rumen contents, 20: 10520 (BNWL-122, pp 64-6)
BUSTAD, L. K., Sheep milk production and its ^{131}I content, 20: 10517 (BNWL-122, pp 52-4)
BUT, D. A., Magnetic systems of magnetogasdynamic generators, 20: 11548
BUTLER, C. T., Purification and growth of KCl single crystals, 20: 10813 (ORNL-3906)
BUTLER, G., Mass 13, T = ½ quartet, 20: 12036
BUZZARD, R. J., Prog. rpt. on thermionic energy converters, 11/64–10/65, 20: 11540 (AD-626444)
BYKOV, V. N., Diffusion of uranium in molybdenum, niobium, zirconium, and titanium, 20: 11290

C

CAHILL, L. J. Jr., Transition region magnetic field and polar magnetic disturbances, 20: 11827
CAIN, J. C., Magnetic field data for trapped-particle evaluations, 20: 11834
CALDWELL, P. R. B., Intrapulmonary exchange of $^{15}O_2$ injected intravenously in man, 20: 10547
CALLAHAN, C. M., Ion exchange in fused salts. I., 20: 10958
CALMON, C., Improved aluminosilicate ion exchangers, 20: 10766 (TID-22511)
CAMBOU, Francis, Density of elastic atomic displacements produced in silicon and germanium by protons at 30 Mev to 1 Bev, 20: 11356
CAMERON, A. G. W., Thermonuclear reactions in medium and heavy nuclei, 20: 11989
CAMERON, John R., Gamma camera optimization of light pipe thickness, 20: 11079
CAMPBELL, Robert, Elk river reactor operations, 20: 12448
CAMUS, Pierre, New determination of ionization potential from the arc spectrum of thulium, 20: 11464
CANNON, J. R., Method for solution of initial value problems for systems of ordinary differential equations, 20: 12529 (BNL-8798)
CAPPELLANI, F., Construction and calibration of proton recoil type neutron spectrometer, 20: 11096 (EUR-2491.e)
CAPRIOGLIO, P., To breed or not to breed, 20: 12431
CARDONE, U., Effects of therapeutic doses of radioiodine on coagulative processes, 20: 10679
CAREY, G. H., Chelation and olation reactions of metal ions in aqueous solution. III., 20: 10802 (COO-1020-9)
CARLSEN, F. A. Jr., Pyrolytic-carbon coatings on ceramic fuel particles, 20: 11254
CARLSON, H. C. Jr., Ionospheric heating by magnetic conjugate-point photoelectrons, 20: 11828
CARLSON, R. D., Electron bremsstrahlung from proton-excited targets, 20: 11501
CARMELI, Moshe, Semigenerally covariant equations of motion. II., 20: 11872
CARPENTER, Jack W., Starfish debris measurements from Cosmos 5, 20: 11832
CARROLL, A. S., π-p Charge-exchange processes in region of 2 Bev/c, 20: 11664
CARROLL, J. C., Humboldt Bay reactor operating experience, 20: 12435
CARTER, B. P., Muonic molecules and nucleon-deuteron capture, 20: 11493
CARTER, Brandon, Complete analytic extension of symmetry axis of Kerr's solution of Einstein's equations, 20: 11435
CARTER, Edward L., Parametric re-entry ablation study of hypothetical ^{90}Sr fuel forms, 20: 11189 (MND-3062-25)
CARTER, F. Bayard, Follow-up of patients with adenocarcinoma of cervix and cervical stump, 20: 10727
CARTER, J. P., Corrosion properties of molybdenum, tungsten, vanadium, and some vanadium alloys, 20: 11230 (BM-RI-6715)
CASAS, J., Production of stable isotopes in Spain, 20: 11191 (JEN-150-DQ/I-51)
CASSEL, R. L., Pulsed phase measuring and control system for rf separator, 20: 11380 (BNL-9772)
CASTELLANO, E., Accumulation of radioiodine in the ovaries, 20: 10554
CASTERLINE, J. E., Effect of length and pressure on critical heat flux for closely spaced 19-rod bundle in forced convection boiling, 20: 10994 (TID-22539)
CASWELL, Randall S., Deposition of energy by neutrons in spherical cavities, 20: 11135
CATALAN, R. E., Effect of γ radiation on different cholinesterase preparations, 20: 10586
CATAYEE, G., Variations of –SH groups in human skin after irradiation by cobalt therapy, 20: 10702
CATSCH, Alexander, Elimination of radionuclides, 20: 10556
CATTANI, M., Analysis of high energy jet showers. III., 20: 11534
CAVAGNA, R., Anatomoclinical study of late lesions due to Thorotrast, 20: 10680
CECCHI, P. F., Construction and calibration of proton recoil-type neutron spectrometer, 20: 11096 (EUR-2491.e)
CENEK, Josef, Total radiation in Mileshovka, 20: 11015
CENTI-COLELLA, A., Therapeutic use of selective perfusion with radio-isotopes with a short half life, 20: 10737
CERCEK, B., Pulse radiolysis of aerated aqueous potassium bromide solutions, 20: 10912
CERESARA, S., Recovery of aluminium after neutron irradiation at 78°K, 20: 11362
CERMAK, J., Distribution of neutron flux density in cylindrical reactor with partially inserted control rods, 20: 12367 (UJV-1442/65)
CERNY, J., Mass 13, T = ½ quartet, 20: 12036
CERNY, Joseph, High spin levels preferentially populated by (α,d) reaction, 20: 12061
CERVASEK, Jiri, Specifications of certain steels for nuclear reactor pressure vessels, 20: 11286 (UJV-1405/65)
CESENA, R. A., Pulse radiolysis of liquid ammonia, 20: 10910
CHADAN, K., Sum rules in potential scattering, 20: 11739
CHAGNON, P. R., Spins of excited levels of ^{18}F, 20: 12025
CHAKRAVORTY, A. P., Histological changes in pelvic lymph nodes in cancer of uterine cervix after radiotherapy, 20: 10653
CHALK, J. D., Single-collision approximation, 20: 11742
CHAMBERLAIN, G. E., Inelastic electron scattering from H_2, 20: 11466
CHAMBON, Bernard, Energy spectra and angular distribution of (n,α) reaction produced on ^{32}S by neutrons at 3.2 Mev, 20: 11993
CHAMPETIER, Jean-Louis, Theoretical interpretation of evolution of plasma created by focusing of laser beam in air, 20: 12190
CHAN, C. H., Sum rules for weak axial-vector coupling constants, 20: 11612

CHAN, L. H., Nucleon form factors and their interpretation, 20: 11627
CHANDRA, Girish, Magnetic cooling set-up for studies with oriented nuclei, 20: 12138
CHANDRA, Girish, Study of lifetimes of positronium in teflon irradiated by gamma rays, 20: 10905
CHANG, C. C., Fermi acceleration of charged particles in transition region beyond magnetosphere, 20: 11522
CHANG, C. C., Laboratory observations of stable plasma trapped in permanent dipolar magnetic field, 20: 12202
CHANG, D. B., Additions to paper on interchange stability of Van Allen Belt, 20: 11835
CHANG, F. C., Alpha clusters in spherical nucleus, 20: 12074
CHANG, H. C., Research and development on silicon carbide active devices, 20: 12276 (NYO-3405-4)
CHANG, Shao-lun, Influence of ionizing radiation on cellular response in lymph nodes of rats after immunization, 20: 10685
CHARLESBY, A., Pulse radiolysis studies of aqueous polymer-thiourea systems, 20: 10921
CHASE, B. H., Prog. rpt. on high-sensitivity fast neutron dosimeter, 8–10/65, 20: 11094 (COO-1226-10)
CHASE, L. F. Jr., Lifetime of 1.02-Mev state in ^{23}Ne, 20: 12060
CHASE, W. L., Analysis of Babcock and Wilcox full-size steam generator for sodium–water reaction, 20: 12386 (APDA-176)
CHATTERJEE, Aparesh, Recent results in fast neutron reactions, 20: 12132
CHATTERJEE, Arun, Cross section of reaction ^{31}P(n,2n)^{30}P with neutrons of 14.8 Mev energy, 20: 12134
CHATTERJEE, M. L., Analysis of angular distribution for ^{16}O(n,α)^{13}C reaction at 14 Mev, 20: 12120
CHATTERJEE, Nikhilesh, Nuclear magnetic resonance in rare-earth nitrates comparison with transition metal nitrates, 20: 12325
CHAUBEY, A. K., Neutrons activation cross-section at 24 kev II, 20: 12135
CHAVE, Charles T., Containment for water reactor nuclear power plants. Part I., 20: 12447
CHECHERNIKOV, V. I., Magnetic properties of gadolinium alloys with iron, cerium, and yttrium, 20: 11341
CHECHERNIKOV, V. I., Magnetic properties of single and polycrystalline preseodymium diselenide $PrSe_2$, 20: 12310
CHEKMAREV, I. B., Rotation of low-ionized gas in homopolar device with radial magnetic field, 20: 12211
CHELNOKOV, L. P., On properties of isotope ^{254}102, 20: 11968 (JINR-P-2470)
CHEL'TSOV, V. F., Behavior of semiconductor in strong resonance radiation field, 20: 12312
CHEMLA, N., Ion diffusion and migration in molten salts, 20: 10805 (EUR-2466.e, pp 21-30)
CHEN, Chi-tang, Histochemical effects of x irradiation upon the adrenal cortex, 20: 10576
CHEN, Jin-quan, Effect of pair correlation on α decay in neighborhood of ^{208}Pb, 20: 12093
CHEN, Joseph C. Y., Virtual-state eigenvalue problems. I., 20: 11439 (BNL-8800)
CHEN, K. W., Measurement of proton electromagnetic form factors at high momentum transfers, 20: 11625
CHEN, K. W., Nucleon form factors and their interpretation, 20: 11627
CHEN, K. W., Quasi-elastic electron-deuteron scattering and neutron form factors, 20: 11626
CHENG, H., Quantum theory of photon interaction in plasma, 20: 12246
CHENG, L. J., Infrared absorption bands in Si induced by 45-Mev electrons. I., 20: 11347 (NP-15611, pp 5-18)
CHENG, L. J., Photoconductivity studies in 10- to 50-Mev electron-irradiated silicon, 20: 11351 (NP-15611, pp 48-89)
CHEN-TSAI, C. T., Shell-model calculation of branching ratio of hypernuclear beta-decay, 20: 11999
CHEREMNYKH, P. A., Electron heating in TN-1 installation, 20: 12206
CHERNOCK, W. P., Prog. rpt. on UO_2 fuel systems, 3/31/65, 20: 12377 (CEND-2863-236)
CHERNY, Walter B., Follow-up of patients with adenocarcinoma of cervix and cervical stump, 20: 10727
CHESNAY, Nicole, Influence of distribution function of electrons on spectrum of nonthermal radio sources, 20: 11427
CHEVALLIER, Jacques, Uranium–hydrogen system, 20: 10801 (CEA-R-2777)
CHI, J. W. H., Forced convection boiling heat transfer to hydrogen, 20: 10996 (WANL-TNR-154)
CHIAVASSA, E., Excitation of 4.5 Mev state in ^{27}Al by inelastic scattering of 14 Mev neutrons, 20: 12031
CHIEN, Kuo-cheng, Histochemical effects of x irradiation upon the adrenal cortex, 20: 10576
CHILDS, W. J., Electronic g factors of low levels of Ni I, 20: 11479
CHILDS, W. J., Hyperfine structure of ^{73}Ge in the $^3P_1$ and $^3P_2$ atomic states, 20: 11476
CHILDS, W. J., Hyperfine structure of 9161-cm^{-1} $^2D_{5/2}$ state of ^{197}Au, 20: 11491
CHING, R., Photodisintegration of deuteron from 500 to 1000 Mev, 20: 11631
CHIU, Hong-yee, Neutrino astrophysics, 20: 11436
CHIVERS, H. J. A., Absorption at conjugate points, 20: 11862
CHOI, Kum Duck, Effect of cortisone and x irradiation on mast cells of adrenalectomized albino rats, 20: 10686
CHOPOORIAN, J. A., Photochromism of metal oxides. I., 20: 10837
CHOU, Jen-Chang, Differential energy and angular distribution of scattered gamma rays through concrete incident normally, 20: 12269
CHOU, Yung-tsen, Free-radical processes taking place in irradiated homogenates of animal tissues, 20: 10577
CHOW, Y. W., Moessbauer scattering: quadrupole interaction in osmium metals, 20: 12301
CHRIEN, R. E., Neutron resonance parameters of ^{109}Ag, 20: 12072
CHRISTIAN, J. E., Gross gamma radioactivity in Indiana precipitation, 20: 11020
CHRISTIAN, J. E., Liquid scintillation detector for evaluating phototubes and determining gamma-ray activities, 20: 11128
CHRISTIAN, John E., Determination of gross gamma radioactivity of Indiana soils by large volume liquid scintillation counting, 20: 11019
CHRISTIANSEN, J., Moessbauer effect resulting from reaction ^{56}Fe(d,p)^{57}Fe using pulsed beam techniques, 20: 12298
CHRISTIE, Robert S., Cooling system for model C stellarator, 20: 12173 (MATT-315)
CHU, C. K., Free-streaming plasma experiments, 20: 12235
CIBOIS, E., Reactor tanks steels. Irradiation of tensile-test pieces in EL3 at different temperatures and post-irradiation tests, 20: 11342 (EURAEC-1502)
CIER, Andre, Role of the chemical species released by the radiolysis of water in the saturation of double carbon–carbon bonds, 20: 10875
CIMELLARO, M., Indirect effects of x-ray therapy, 20: 10670
CISLER, Walker L., Impact of energy requirements on nuclear power development, 20: 12440
CLAESON, T., Superconductivity in the alloy system Cd–Hg, 20: 11914
CLANET, Frank, Adsorption of transuranic elements by ion-exchange paper chromatography. I., 20: 10785
CLARK, Francis H. S., Solution of LaGrange multiplier problem with several constraints, 20: 12544 (ORNL-3846)
CLARK, J. G., Sodium-heated steam generator, 20: 12389 (BAW-1280-28 (Vol.1))
CLARK, John W., Method of correlated basis functions, 20: 11492
CLARKE, W. J., Biological effects of ^{90}Sr in miniature swine, 20: 10597 (BNWL-122, pp 37-45)
CLARKE, W. J., Chronic effects of inhaled $^{239}PuO_2$ in dogs, 20: 10596 (BNWL-122, pp 1-15)
CLARKE, W. J., Effect of chronic ingestion of ^{65}Zn in trout, 20: 10528 (BNWL-122, pp 101-6)
CLARKE, W. J., Toxicity of copper and x rays in rats, 20: 10598
CLEGG, A. B., High energy nuclear reactions, 20: 12111
CLEGG, A. B., Possible new octet, 20: 11592
CLENDENIN, W. W., Stability of solutions of polynomial equation, 20: 12538 (LA-DC-6803)
CLINE, J. F., Effects of moisture and air temperature on deposition and retention of $^{131}I_2$ on plants and soil, 20: 10717 (BNWL-122, pp 166-7)
CLINE, J. F., Influence of soil sodium on plant uptake of ^{45}Ca, ^{85}Sr, and ^{137}Cs, 20: 10534 (BNWL-122, pp 168-9)
CLOET, R. L., Silt movement in an EBB channel, Firth of Forth, 1965, 20: 11022 (AERE-R-5080)
CLOUSE, R. J., Nuclearly safe triangular-slab tank for handling enriched uranium, 20: 10981
CLUCHET, Jean, Application of dosimetry by thermoluminescence to radioprotection, 20: 11041
COATES, Gordon L., Application of nuclear electric propulsion to manned Mars missions, 20: 12492
COCHE, A., Semi-conductor detectors of nuclear radiation, 20: 11126
COENSGEN, F. H., Boundary condition effects in magnetic mirror compression experiment, 20: 12238
COHAN, M., Activation analysis of drugs, 20: 10880
COHEN, Alberto, Determination of coronary flow with positron emitter (^{84}Rb), 20: 10730
COHEN, R. C., Isotope shift in muonic K x rays of ^{16}O–^{18}O, ^{40}Ca–^{44}Ca, ^{116}Sn–^{124}Sn, and ^{155}Gd–^{160}Gd, 20: 11480
COHEN, S. G., Influence of anisotropic Moessbauer effect on magnetic hyperfine splittings in polycrystalline materials, 20: 12299
COJOCARU, V., Fission by radiationless transition in μ mesonic atom ^{239}Pu, 20: 12041
COLAN, H., Siliconizing to protect molybdenum, 20: 11236
COLE, Leonard J., Urethan-induced lung tumors in mice: x-radiation dose-dependent inhibition, 20: 10671
COLELLA, Roberto, Study of reflection profiles of x rays on silicon crystal irradiated with α rays, 20: 12281

COLGATE, S. A., Cherenkov electromagnetic radiation from nuclear detonation in space, 20: 11807 (UCRL-7495(Rev. 1))
COLGATE, Stirling A., Hydrodynamic behavior of supernovae explosions, 20: 11425 (UCRL-7777)
COLLI, L. Milazzo, Direct effect and evaporation mechanism in $^{27}Al(d,p)^{28}Al$ and $^{27}Al(d,\alpha)^{25}Mg$ reactions, 20: 12018
COLLIGNON, E., Production of ^{192}Ir sources of high specific activity, 20: 11190 (BLG-332)
COLLINSON, A. J. L., Determination of total alpha activity of drinking water using nuclear emulsion, 20: 11044
COLOMBI, G., C.N.E.N.'s fuel element fabrication and control laboratories at Saluggia, 20: 11247
COLOMBIE, Nicole, Secondary electron emission of iron under bombardment of Ar^+ ions of medium energy, 20: 11462
COLOMBO, R., Autoradiography, 20: 11002
COMAR, C. L., Effects of dietary levels of P and Ca on comparative behavior of Sr and Ca, 20: 10549
COMISAR, G. G., Theory of stimulated Raman effect in plasmas, 20: 12243
COMPTON, D. M. J., Pulse radiolysis of liquid ammonia, 20: 10910
COMPTON, V. B., Occurrence of superconductivity in sulfides, selenides, tellurides of Pt-group metals, 20: 11899
CONDAS, George A., Properties and preparation of thin bismuth films, 20: 11280 (UCRL-12001)
CONDELL, W. J., Excitation-transfer collisions between rubidium and helium atoms, 20: 11482
CONE, A. A., Measurement of proton electromagnetic form factors at high momentum transfers, 20: 11625
CONE, A. A., Quasi-elastic electron-deuteron scattering and neutron form factors, 20: 11626
CONN, Richard W., Curve sketching by digital computer, 20: 12552 (UCRL-12226)
CONRAD, E. E., Mechanism of electroosmosis in liquid metals, 20: 11289 (IS-Trans-26)
CONSTANT, Prog. rpt. on brittle fracture strength of heavy-gage steel plate, final, 1965, 20: 11240 (EURAEC-1520)
CONSTANT, R., Production of ^{192}Ir sources of high specific activity, 20: 11190 (BLG-332)
CONTE, A., Influence of thermal treatment on rate of ion exchange of zirconium phosphate, 20: 10957
CONTZEN, J.-P., Utilization of radioisotopes for production of electric energy aboard space vehicles, 20: 11188 (BLG-330)
CONWAY, John G., Energy levels of Pu^{3+} in lanthanum trichloride, 20: 12286
COOK, C. L., Some SU_n crossing matrices, 20: 11740
COOK, J. E., Response of moving Geiger probe to discharge sources of beta radiation, 20: 11089 (AERE-M-1671)
COOK, J. L., Pyrolytic-carbon coatings on ceramic fuel particles, 20: 11254
COOMBES, Charles A., Scalar pion-nucleon interaction, 20: 11574
COOPER, Leon N., Theory of nonhomogeneous superconductors, 20: 11908
COOPER, Ralph S., Prospects for advanced high-thrust nuclear propulsion, 20: 12477
COPLEY, S. M., High-temperature compressive deformation equipment, 20: 11285 (UCRL-16434)
CORBI, D., Effects of ^{32}P on the urinary excretion of amino acids, 20: 10582
CORDFUNKE, E. H. P., Preparation and properties of uranium fuel, 20: 11245
CORELLI, John C., Prog. rpt. on radiation damage in semiconductor materials, 2–4/65, 20: 11176 (NP-15835)
CORELLI, John C., Prog. rpt. on radiation damage to semiconductors, 3/15–9/15/65, 20: 11346 (NP-15611)
CORNWELL, R. G., Nuclear moments of ^{43}Sc and ^{47}Sc, 20: 12070
CORTELLESSA, Giorgio, (e,e'p) reaction in ^{9}Be nucleus, 20: 11988
CORTI, M., Direct effect and evaporation mechanism in $^{27}Al(d,p)^{28}Al$ and $^{27}Al(d,\alpha)^{25}Mg$ reactions, 20: 12018
COSTE, J., Longitudinal dielectric constant of classical plasma. I., 20: 12216
COSTE, J., Longitudinal dielectric constant of classical plasma. II., 20: 12217
COTE, Roger W., Model experimental design for NERVA instrumentation radiation-effects tests, 20: 11175 (NP-15823)
COTTRELL, Wm. B., Nuclear safety, 20: 11045
COUCHET, G., Time-of-flight mass spectrometry and its applications. I., 20: 10790
COUCHET, G., Time-of-flight mass spectrometry and its applications. II., 20: 10791
COUGHREN, K. D., NPR injection pump simulation, 20: 12455 (HW-77921-C)
COUGHREN, K. D., NPR pressurizer, 20: 12456 (HW-77921-D)
COULSON, C. A., Force fields in KrF_2 and XeF_2, 20: 10829
COULTER, Philip W., N/D calculation with inelastic unitarity of πN scattering, 20: 11643
COURNAND, A., Intrapulmonary exchange of $^{18}O_2$ injected intravenously in man, 20: 10547
COUVILLION, A. J., Prog. rpt. on ion rocket engine development, 4–6/65, 20: 11006 (NP-15824)
COVA, S., Three-quantum annihilation of positrons in ionic crystals, 20: 11620
COWARD, Nathan A., Spectrophotometric study of the Nd^{3+}–NO_3 association, 20: 10848
COX, D. F., Randomization tests for comparing survival curves, 20: 10618
COXELL, H., Survey of cosmic-ray intensity in lower atmosphere, 20: 11521
CRAIG, J. P., Infrared maser interferometry for time and space resolution of electron density in high temperature plasmas, 20: 12165 (ARL-65-135)
CRAIG, J. P., Time-space resolution of B-fields in theta-pinch plasma by Faraday rotation of infrared maser radiation, 20: 12164 (ARL-65-129)
CRAMPTON, S. B., Hyperfine separation of deuterium, 20: 11481
CRANDALL, J. L., Physics of heavy-water lattices, 20: 12363 (TID-8541, pp 1-70)
CRAWFORD, Bevalyn B., Magnitude of K_1^0–K_2^0 mass difference using strong interactions, 20: 11661
CRAWFORD, Frank S. Jr., Magnitude of K_1^0–K_2^0 mass difference using strong interactions, 20: 11661
CRESPI, M. A., Leak tightness of reactor buildings, 20: 12332
CRITOPH, E., Comparison of calculated and measured critical sizes for some ZED-2 lattices, 20: 12493 (AECL-2514)
CRONKITE, Eugene P., Studies of ventromedial hypothalamus with autoradiographic techniques, 20: 10541
CROOKER, T. W., Prog. rpt. on metallurgical characteristics of high strength structural materials, 5–7/65, 20: 11273 (NRL-6364)
CROUTHAMEL, Carl E., Studies of Li hydride systems. II., 20: 10832
CROUTHAMEL, Carl E., Studies of Li hydride systems. III., 20: 10833
CROUTHAMEL, Carl E., Thermodynamic properties of LiH by an electromotive force method, 20: 10849
CRUZ, M. T., Analysis of high energy jet showers. III., 20: 11534
CSADA, Imre, Laboratory examination of primary water circuit of reactors, 20: 12509
CSIKAI, J., Dependence of (n,2n) cross sections on symmetry parameter N-Z, 20: 12040
CSONKA, P. L., Non-dynamical spin and parity determinations, 20: 11611
CULTRERA, G., Uptake of ^{35}S-sodium sulfate by hepatic tissue of normal and irradiated rats, 20: 10542
CUMMINS, W. F., Boundary condition effects in magnetic mirror compression experiment, 20: 12238
CUNNINGHAM, Joseph, Radiation chemistry of ionic solids. IV., 20: 10891
CURATOLA, G., Effect of ^{32}P on the multiplication of germs, 20: 10579
CURATOLA, G., Effect of ^{32}P on bacterial flora of intestine of newborn mouse, 20: 10642
CURATOLA, G., Vitamin B_{12} in lyophilized meat and in meat irradiated with γ-rays of ^{60}Co, 20: 11185
CURNUTTE, B. Jr., Hydrogen negative ion, 20: 11453 (UCRL-12230)
CURNUTTE, B. Jr., Solution of secular equation for electrostatic helium atom, 20: 11451 (UCRL-7941(Rev.1))
CURRANT, J., Absolute rate constants for reaction of hydroxyl radical with organic compounds, 20: 10916
CURRANT, J., Pulse radiolysis of aqueous solutions of thiocyanate ion, 20: 10915
CURWEN, P. W., Prog. rpt. on gas-bearing Brayton cycle turbocompressor, 9–11/65, 20: 10972 (NYO-3237-4)
CUSHING, C. E., Radionuclide accumulation and transport by plankton in Columbia River, 20: 10536 (BNWL-122, pp 187-9)
CUSHING, C. E., Radionuclide accumulation and productivity of periphyton in Columbia River, 20: 10537 (BNWL-122, pp 190-3)

D

DAAVETTILA, D. A., Worth measurements of core and blanket subassembly materials in Enrico Fermi reactor, 20: 12388 (APDA-NTS-6)
DAGBJARTSSON, S., Employment of heat pipes for thermionic reactors, 20: 12489
DAGNAC, Rene, Initiation of high-frequency electric discharge in rare gases, 20: 11780
DAINTON, F. S., Transient absorption from 260-320 nm in certain pulse irradiated aqueous solutions, 20: 10924
DAKHNO, L. G., Analytic properties of triangle graphs with decay masses and three-particle production, 20: 11596
DALLY, E. B., Determination of lifetime and ground-state energy of ^{8}Be by α-α elastic scattering at 184 kev, 20: 12038
DALZIEL, R., Some particular problems in polar ionosphere, 20: 11865
DAMMERS-DE KLERK, A., Properties of ionic liquids and mixtures, 20: 10804 (EUR-2466.e, pp 9-19)
DAMON, Robert A., Fusion bonding of plasma-sprayed tungsten coatings to steel, 20: 11242 (UCRL-12153)
DANDL, R. A., Observation of mirror-like instability in hot electron plasma, 20: 12180 (ORNL-P-1556)

D'ANGELO, N., Plasma losses in Q-device, 20: 12215
DANIELE, G., Therapeutic use of selective perfusion with radioisotopes with a short half life, 20: 10737
DANSGAARD, W., Intrapulmonary exchange of $^{18}O_2$ injected intravenously in man, 20: 10547
DANYSZ, Andrzej, Changes in osmotic resistance of white blood cells in postradiation disease in rats, 20: 10614
DAO WONG, Duc, Proton-antiproton scattering in SU(6)$_w$ symmetry, 20: 11565 (JINR-P-2469)
DARENSKAYA, N. G., Biological effect of protons with energies of 510 Mev in multiple irradiation, 20: 10606 (NASA-TT-F-353, pp 55-102)
DARENSKAYA, N. G., Biological effect of protons with energies of 510 Mev during single irradiation, 20: 10607 (NASA-TT-F-353, pp 103-41)
DARENSKAYA, N. G., Biological effect of proton radiation at 510 Mev, 20: 10612 (NASA-TT-F-353, pp 194-209)
DARENSKAYA, N. G., Biological effect of multiple x irradiation with energies of 180 kv compared with proton irradiation, 20: 10611 (NASA-TT-F-353, pp 185-93)
DAS, A., Complex space-time and geometrization of electromagnetism. III., 20: 11875
DAS, A., Complex space-time and classical field theory. I., 20: 11373
DAS, A., Quantized complex space-time and quantum theory of free fields. II., 20: 11709
DAS, Nemai, Nuclear magnetic resonance in rare-earth nitrates comparison with transition metal nitrates, 20: 12325
DASH, J. G., Internal field of ^{57}Fe in nickel from 77°K to Curie point, 20: 12298
DASPET, Danielle, Density of elastic atomic displacements produced in silicon and germanium by protons at 30 to 1 Bev, 20: 11356
DASTUGUE, G., Liver and kidney of mice during poisoning with uranyl nitrate and carbon tetrachloride, 20: 10548
DATLOV, J., Beam width of two antenna systems for plasma diagnostics, 20: 12192
DATLOV, J., Inverted ion magnetron principle, 20: 12194
DATTA, Bidyut Kumar, Non-static spherically symmetric clusters of particles in general relativity. II., 20: 11869
DATZ, Sheldon, Alkali-atom-halogen-molecular reactions in molecular beams: the spectator stripping model, 20: 10834
DAVIDSON, R. H., Detection of moderator element failures in Hallam nuclear power facility, 20: 12449
DAVIES, J. V., Pulse radiolysis of aqueous carbohydrate solutions, 20: 10920
DAVIES, J. V., Reactions of hydrated electron with glycine and other amino acids and peptides, 20: 10918
DAVIS, Don Lee, g factors of ^{12}B and ^{110}Ag, 20: 12098
DAVISON, W. D., Variational calculations of long-range forces, 20: 11504
DAYTON, R. W., Reactor materials, 20: 11223
DEAN, J. M., Cycling of ^{90}Sr in molting crayfish, 20: 10515 (BNWL-122, pp 46-8)
DEAN, J. M., Metabolism of ^{137}Cs in trout, 20: 10521 (BNWL-122, pp 73-4)
DEAN, Stephen O., Heating of vacuum wall by bremsstrahlung radiation in pulsed thermonuclear reactor, 20: 12166 (CONF-651126-1)
DE BACCI, M., To breed or not to breed, 20: 12431
DEEV, Yu. S., Dosimetric investigations and shielding studies using synchrocyclotron, 20: 10605 (NASA-TT-F-353, pp 21-54)
DE FACIO, W. Brian, Analysis of N + ^{4}He reaction and effects of spin coupling n + ^{4}He to d + T, 20: 11978 (UCRL-7961-T)
DE GROOT, Leslie J., Therapy of thyrotoxicosis, 20: 10747
DEGTYAREV, Yu. G., Cross sections for neutron inelastic interactions with ^{7}Li, ^{12}C, ^{14}N, ^{27}Al, ^{56}Fe, Cu, Pb, ^{235}U, ^{238}U, and ^{239}Pu, 20: 11985
DEITERMAN, Louis Henry Jr., Positron lifetime in lithium ammonia solutions, 20: 11674
DE JAGER, C., Observations of solar particles in interplanetary space, 20: 11438
DE LAFOND, Yann Gervais, Density of elastic atomic displacements produced in silicon and germanium by protons at 30 Mev to 1 Bev, 20: 11356
DE LAS RIVAS DIAZ, M., Welding procedures used in fabrication of fuel elements for DON reactor exponential experiment, 20: 12401 (JEN-156-DMe/113)
DELATTRE, P., Status of dosimetry in France, 20: 11146
DEL FAVERO, C., Protective action of phospholipid extract of spleen on mice subjected to whole-body irradiation, 20: 10704
DEL FAVERO, C., Protective effect of duodenal heparinoid on mouse exposed to lethal dose of whole-body irradiation, 20: 10705
DELUCCHI, A. A., An iodine source for beta counting, 20: 10935 (USNRDL-TR-948)
DELUCCHI, A. A., Nuclear-charge distribution of several fission product mass chains, 20: 11980 (USNRDL-TR-935)
DEMANT, J. T., Electron-probe microanalysis of irradiated UO_2, 20: 10787
DEMETSOPOULLOS, I. C., Determination of total alpha activity of drinking water using nuclear emulsion, 20: 11044
DEMIN, V. P., Secondary γ-emission coefficients for aluminum, copper, and tungsten, 20: 12267
DENAVIT, J., Landau damping and velocity Fourier transform of initial perturbation, 20: 12231
DEN HOED-SIJTSEMA, S., Therapeutic scope of radiation, 20: 10744
DENIS, A., Application of controlled-potential coulometry to determinations in radioactive solutions, 20: 10758 (EUR-2618.f)
DENISOV, Yu. N., Flow near stagnation point in presence of magnetic fields parallel and normal to body surface, 20: 11795
DENNEHY, W., High-energy radiation damage in silicon transistors, 20: 11182
DENNISON, D. H., Solubility of tantalum in eight liquid rare-earth metals, 20: 11306
DEPRAZ, Jean, Energy spectra and angular distribution of (n,α) reaction produced on ^{32}S by neutrons at 3.2 Mev, 20: 11993
DEPTULA, Andrzej, Preparation of UF_6 by fluorination of UF_4, 20: 10852
DERBENEVA, N. A., Biological effect of protons with energies of 510 Mev during single irradiation, 20: 10607 (NASA-TT-F-353, pp 103-41)
DEROW, H., Prog. rpt. on SNAP-8 materials, 1–6/64. II., 20: 11214 (NASA-CR-54717)
DEROW, H., Prog. rpt. on SNAP-8 materials, 7–12/64, 20: 11215 (NASA-CR-54718)
DER SARKISSIAN, M., Study of J = I = 0 $\pi\pi \to N\bar{N}$ amplitude and its effect on πN scattering, 20: 11604
DETENBÉCK, Robert W., Two-step (p,2p) reaction, 20: 12006
DE TOLLIS, B., Contributions of pion pairs and unstable intermediate states to γ-γ scattering, 20: 11600
DETRAZ, C., Mass 13, T = ½ quartet, 20: 12036
DEUBEL, K. L., Gas-cooled reactors—comparison of coolants, 20: 12341
DEURLOO, P. A., Liquid scintillation determination of ^{239}Pu in pure and contaminated solutions, 20: 10763 (KR-100)
DEUTSCH, H., Mixing phenomena in non-stationary glow discharges, 20: 11774
DEUTSCHMANN, M., Rare decay modes of ρ, A_1 and A_2 mesons, 20: 11616
DEVARE, H. G., Magnetic moments of first excited states of ^{127}I, ^{131}I, and ^{149}Pm, 20: 12115
DE VARENNE, D., Variations of –SH groups in human skin after irradiation by cobalt therapy, 20: 10702
DEVONS, S., Isotope shift in muonic K x rays of ^{16}O–^{18}O, ^{40}Ca–^{44}Ca, ^{116}Sn–^{124}Sn, and ^{155}Gd–^{160}Gd, 20: 11480
DE WAARD, H., Internal magnetic field of iodine in iron, 20: 12295
DE WET, R., Thermal flow-meters for ClF_3, 20: 11059 (BLG-345)
DEY, S. D., Development of surface ionization type ion source, 20: 12257
DHARMATTI, S. S., Knight shifts in rare-earth–tin intermetallic compounds, 20: 12324
DI ADDARIO, A., Certain immune indexes in newborn mice treated with ^{32}P, 20: 10580
DI ADDARIO, A., Vitamin B_{12} in lyophilized meat and in meat irradiated with γ-rays of ^{60}Co, 20: 11185
DIAMOND, J. M., Pulse-height discriminator, 20: 11064 (RISO-102)
DIANA, E., Temperature dependence of ^{240}Pu resonance absorption at 1.05 ev in homogeneous systems, 20: 12001
DIAZ BELTRAN, A., Welding procedures used in fabrication of fuel elements for DON reactor exponential experiment, 20: 12401 (JEN-156-DMe/113)
DIBELER, V. H., Photoionization-efficiency curves for C_2H_2 and C_2D_2, 20: 10867
DICKHAUT, R. H., Comparison and evaluation of three automated circuit analysis programs: predict, net-1, and circus, 20: 11172 (AD-623963)
DIENSTBIER, Z., Urinary radiophosphorus ^{32}P levels in rats after single 2,4-dinitrophenol administration prior to 600-r x irradiation, 20: 10666
DIGGELMANN, H., Determination of total clearance of different preparations of gamma-globulin, 20: 10571
DIGGELMANN, H., Interpretation of results of protein turnover studies, 20: 10565
DIGGELMANN, H., Measurement of gastro-intestinal protein loss by means of ^{131}I-labeled polyvinylpyrrolidone, 20: 10568
DIGGELMANN, H., Metabolism of gamma-globulin in agammaglobulinaemia and hypogammaglobulinaemia, 20: 10572
DIGGELMANN, H., Simplified method for clinical study of protein turnover, 20: 10564
DILAY, A. J., Gamma rays from decay of ^{75}Se, 20: 12022
DILLEY, J., Asymptotic behavior of scattering amplitude in left half-plane of complex angular momentum, 20: 11710
DILLON, J. J., Cryogenic and elevated temperature properties of 7039 aluminum plate and weldments, 20: 11264 (ACF-14)
DILLON, Michael A., Excitation transfer and decay processes in multi-component systems, 20: 10927
DI MARCO, N., Gas chromatographic analysis of fatty acids of liver in normal and irradiated rats, 20: 10659

DIMITRIEVA, G. P., Investigation of alloys of Cb–$CbCr_2$–$CbAl_3$ system, 20: 11338
DIMOND, W. J., Development of photogrammetric techniques for measuring surface contours of small samples, 20: 11068 (WAPD-T-1815)
DISANTNIK, Y., Analysis of boson model displaying phase transition, 20: 11801
DISSING, E., Scintillometer assembly for geological survey, 20: 11087 (AE-203)
DIVATIA, A. S., Associated particle method for D(d,n)^{3}He reaction, 20: 11677
DIVATIA, A. S., Study of $^{19}F(\alpha,n)^{22}Na$ reaction using 4 π neutron counter, 20: 12143
DIXON, F. E., Extended fire tests on tinplate cans, 20: 11028 (AERE-M-1664)
DLOUHA, J., Resonance absorption of gamma-quanta in one- and two-dimensional crystals, 20: 12283
DOEDERLEIN, J. M., BIGG-II—multigroup neutron spectrum and criticality code, 20: 12357 (KR-75)
DOERFFLER, W. W., Contribution to mechanism of dissolution and diffusion of oxygen in zirconium, 20: 11268 (EIR-82)
DOLE, Malcolm, Mechanism of decay of vinyl unsaturation during radiolysis of Marlex-50 polyethylene, 20: 10893
DOLEZEL, S., Influence of continuous irradiation and experimental diphtherial intoxication on origin and incidence of non-specific necrotic changes in cardiac muscle, 20: 10631
DOLGOPOLOV, V. V., Cherenkov absorption of Alfven waves and of fast magnetoacoustic waves in inhomogeneous plasma, 20: 12214
DOLGOVA, E. I., Ionospheric-magnetic disturbances in years of maximum solar activity, 20: 11810
DOMANGE, Louis, Solid solutions formed by addition of selenides of rare earths to selenides of fcc NaCl type, 20: 10857
DOMSA, A., Behavior of molybdenum powders during pressing and sintering, 20: 11253
DOMSA, A., Siliconizing to protect molybdenum, 20: 11236
DOMSHLAK, M. P., Biological effect of protons with energies of 510 Mev in multiple irradiation, 20: 10606 (NASA-TT-F-353, pp 55-102)
DOMSHLAK, M. P., Biological effect of multiple x irradiation with energies of 180 kv compared with proton irradiation, 20: 10611 (NASA-TT-F-353, pp 185-93)
DOMSHLAK, M. P., Biological effect of proton radiation at 510 Mev, 20: 10612 (NASA-TT-F-353, pp 194-209)
DONAHUE, D. J., Mean lives of some states in atomic hydrogen, 20: 11474
DONALDSON, Edward E., Prog. rpt. on chemical sputtering of solids, 6/16–9/16/64, 20: 12549 (TID-21555)
DONEDA, G., Gas chromatographic analysis of fatty acids of liver in normal and irradiated rats, 20: 10659
DONETS, E. D., Properties of ^{254}No isotope, 20: 11969 (JINR-P-2471)
DONNELLY, R. J., Growth of pinned quantized vortex lines in helium II, 20: 11905
DOOSE, C., Beam tube equipment for FRJ-2 (DIDO) cold neutron source, 20: 12503 (AERE-Trans-1043)
DOPOTT, Z. M., Spectrographic determination of rare-earth elements of yttrium group with DFS-13 diffraction spectrograph, 20: 10775
DORION, G. H., Photochromism of metal oxides. I., 20: 10837
DORMAN, L. A., Twenty-seven-day variations of geomagnetic field disturbance on zero-days of cosmic-ray intensity, 20: 11818
DORMAN, L. I., Solar cosmic-ray burst of September 28, 1961, 20: 11428
DOROSHENKO, G. G., Changes of spectra of fast neutrons after their passage through aluminum, paraffin, and aqueous media, 20: 12268
DORY, R. A., Observation of negative-mass instability in energetic proton plasma, 20: 12247
DOUCET, Henri, Beam-hot plasma interaction at very low frequency, 20: 12189
DOUGAL, A. A., Infrared maser interferometry for time and space resolution of electron density in high temperature plasmas, 20: 12165 (ARL-65-135)
DOUGAL, A. A., Time-space resolution of B-fields in theta-pinch plasma by Faraday rotation of infrared maser radiation, 20: 12164 (ARL-65-129)
DOUGLASS, R. L., Capture width of vortex lines for negative ions in helium II, 20: 11903
DOVGOPOL, S. P., Spin diffusion of nuclei in double electron-nuclear resonance, 20: 12311
DOWELL, Jerry T., Production of metastable atoms by electron impact, [thesis], 20: 11455 (UCRL-14450)
DOWKER, J. S., Particles of arbitrary spin in curved spaces, 20: 11759
DOWKER, Y. P., Particles of arbitrary spin in curved spaces, 20: 11759
DRAGANIC, I. G., Status report on in-pile dosimetry techniques in Yugoslavia, 20: 11152
DRAGOUN, O., Radioactive decay of ^{188}Re, 20: 11998
DRENNAN, James E., Model experimental design for NERVA instrumentation radiation-effects tests, 20: 11175 (NP-15823)
DRENTJE, S. A., Internal magnetic field of iodine in iron, 20: 12295
DRICKAMER, H. G., Behavior of thirteen charge transfer complexes at high pressure, 20: 12534 (COO-1198-216)
DRICKEY, D., Elastic electron-deuteron scattering, 20: 11644
DRICKEY, D., Proton form factors from proton observation, 20: 11567 (LAL-1144)
DRICKEY, D., Proton form factors from observation of recoil protons, 20: 11628
DRIJARD, D., Upper limit for the partial width $\Gamma(\rho \to \pi\gamma)$, 20: 11618
DRISKO, R. M., Finite-well single-particle wave functions in two-nucleon stripping, 20: 12086
DROBYSHEVSKII, E. M., Rotation of low-ionized gas in homopolar device with radial magnetic field, 20: 12211
DROULERS, Y., Status of dosimetry in France, 20: 11146
DROZHZHIN, V. M., Mesothorium-I concentration in the Black Sea, 20: 10768 (JPRS-33212)
DRUMHELLER, Kirk, Remote fabrication of reactor fuels, 20: 11241 (TID-8541, pp 71-148)
DUARTE, Maria Ivone, Radiorestoring action of fraction extracted from tobacco leaves, 20: 10620
DUBEC, M., Self-consistent determination of πNN and πNN* vertex functions, 20: 11730
DUBOIS, J., Applied gamma-ray spectrometry by germanium semi-conductor detector, 20: 11134
DUBROVSKII, V. B., Concrete for high-temperature reactor shielding, 20: 12340
DUCAUZE, Alain, Energy of ions emitted by metallic target bombarded by laser beam, 20: 11463
DUCK, Ian, Solutions of Aitchison equation for final state interaction, 20: 12016
DUDKIN, V. E., Characteristics of the radiation effect under space flight conditions and ways to determine admissible radiation levels, 20: 10719 (NASA-TT-F-353, pp 3-20)
DUERRSCHNABEL, W., Total emission capacity of niobium, 20: 11314
DUFFAULT-DEVRED, Marylis, Ionization of chromium fluoride and chromium oxide in some fused chlorides and fluorides, 20: 10821
DUMAZET, Gerard, Scattering of protons by neon, 20: 11995
DUNLAP, B. D., Internal field of ^{57}Fe in nickel from 77°K to Curie point, 20: 12298
DUNLAP, J. L., Microinstability limitations of DCX-1 energetic plasma, 20: 12240
DUNLAP, J. L., Observation of negative-mass instability in energetic proton plasma, 20: 12247
DUNNING, J. R. Jr., Measurement of proton electromagnetic form factors at high momentum transfers, 20: 11625
DUNNING, J. R. Jr., Nucleon form factors and their interpretation, 20: 11627
DUNNING, J. R. Jr., Quasi-elastic electron-deuteron scattering and neutron form factors, 20: 11626
DUNNING, J. R. Jr., Unsuccessful search for excited electron, 20: 11629
DUTTON, J., Note on motion of low-energy hydrogen ions in hydrogen, 20: 11805
DYUKALOV, A. N., Particle distribution in vicinity of charged sphere in weakly ionized rarefied plasma, 20: 12201
DZYALOSHINSKII, I. E., Quantum field theoretical methods in statistical physics, 20: 11375

E

EAPEN, J., Metabolism of ^{137}Cs in trout, 20: 10521 (BNWL-122, pp 73-4)
EASLEY, Warren, Nuclear spin and moment of ^{110m}Ag by paramagnetic resonance, 20: 12073
EASTLUND, B. J., Free-streaming plasma experiments, 20: 12235
EBELING, W., Statistical-mechanical derivation of generalized diffusion equation, 20: 11369
EBERHARDT, L. L., Radioactivity in Alaskan animals and forage plants, 20: 10535 (BNWL-122, pp 176-80)
EBERHARDT, L. L., Studies of fallout nuclides in plants and browsing animals of Washington, 20: 11011 (BNWL-122, pp 181-3)
EBERHARDT, P., Spallation, fission and neutron capture anomalies in meteoritic krypton and xenon, 20: 11424 (NP-15629)
EBERT, M., Determination of some fast reaction rates using pulsed radiolysis of permanganate solutions, 20: 10914
EBERT, M., Excitation transfer and decay processes in multi-component systems, 20: 10927
EBERT, M., Formation of Cu^{III} in radiolysis of Cu^{2+} solutions, 20: 10923
EBERT, M., Polarographic study of aqueous oxygenated solutions irradiated with 10 Mev electron pulses, 20: 10909
EBERT, M., Pulse radiolysis of liquid ammonia, 20: 10910
EBERT, M., Pulse radiolysis of aerated aqueous potassium bromide solutions, 20: 10912
EBERT, M., Pulse radiolysis studies of aqueous solutions of nucleic acid and related substances, 20: 10917
EBERT, M., Pulse radiolysis of aqueous carbohydrate solutions, 20: 10920
EBERT, M., Pulse radiolysis studies of aqueous polymer-thiourea systems,

20: 10921
EBERT, M., Pulse radiolysis of Ag^+ solutions, 20: 10922
EBERT, M., Pulse radiolysis study of methylene blue, 20: 10925
EBERT, M., Pulse radiolysis of carbon tetrachloride–benzene mixtures, 20: 10928
EBERT, M., Quenching of excited states formed in pulse radiolysis, 20: 10926
EBERT, M., Radical yields and kinetics in pulse radiolysis of potassium bromide solutions, 20: 10911
EBERT, M., Reactions of hydrated electron with glycine and other amino acids and peptides, 20: 10918
EBERT, M., Reactions of hydrated electron with amino acids, peptides and proteins, 20: 10919
EBERT, M., Some contributions of electron pulse technique, 20: 10908
EBERT, M., Symposium on pulse radiolysis, Manchester, 4/65, 20: 10906
EBERT, M., Technique of pulse radiolysis by optical absorption, 20: 10907
EBERT, M., Transient absorption from 260-320 nm in certain pulse irradiated aqueous solutions, 20: 10924
ECCLES, S. F., Elastic and inelastic scattering of protons by ^{18}O, 20: 11979 (UCRL-12152)
ECCLES, S. F., Strongly excited 2^+ and 3^- states in $^{54,56}Fe$ and $^{58,60,62}Ni$ isotopes, 20: 12065
ECKERLE, K. L., Departures from local thermal equilibrium in magnetically-driven shock waves, 20: 12226
ECKHARTT, D., Toroidal device with meridian magnetic confining field of grad p · grad $\oint dl/B > 0$, 20: 12174 (MPI-PAE/P1.6/65)
EDDY, Hubert A., Mechanisms in acute intestinal radiation syndrome, 20: 10697
EDELMAN, P. Michael, Studies of ventromedial hypothalamus with autoradiographic techniques, 20: 10541
EDELSTEIN, Norman, Nuclear spin and moment of ^{110m}Ag by paramagnetic resonance, 20: 12073
EDER, Leslie, Positron annihilation in diatomic crystals, 20: 11655
EFIMENKO, L. N., Disintegration of tungsten disilicides during oxidation in air, 20: 11237
EFIMENKO, L. N., The high-tungsten section of tungsten–silicon phase diagram, 20: 11296
EFIMOV, G. V., Analytical properties of euclidean amplitudes, 20: 11687 (JINR-P-2485)
EGELAND, Alv, Enhanced electromagnetic radiation between 500 and 1000 c/s in auroral zone, 20: 11860
EHRLICH, R. D., Experience with on-line experimentation, 20: 11553 (COO-614-34, Sect. IIC)
EICHHOLZ, G. G., Corrugated-plate spark counters, 20: 11120
EINFELD, Klaus, Neutron spectra and decay time constants in zirconium hydride, 20: 11943
EISENBUD, Merril, Radiation in perspective, 20: 11047
EISENHAUER, Charles, Engineering method for calculating protection afforded by structures against fallout radiation, 20: 11030 (NBS-MON-76)
EJIRI, Hiroyasu, Shell effects in Coulomb displacement energies of excited states, 20: 11963 (INSJ-91)
EKSTEIN, H., Relativistic combination of internal and spin symmetries in S-matrix formulation, 20: 11755
EL-BAZ, E., Application of simple models of direct interaction to study of reaction $^{28}Si(n,\alpha)^{25}Mg$ at 14.8 Mev, 20: 12002
EL-HOSHY, A., Implantation profiles for 40-kev phosphorus ions in silicon single-crystal substrates, 20: 12280
ELISEEV, B. V., Damping of homogeneous turbulence in magnetic field, 20: 11804
ELISEEV, S. M., Internuclear cascades at superhigh energies, 20: 11566 20: 11566 (JINR-P-2472)
ELK, K., Exact description of elastic scattering processes and deduction of optical nuclear models, 20: 12021
ELLGREN, William K. Jr., Radiative neutron capture in liquid and solid carbon tetrachloride in *n*-hexane, 20: 10938
ELLIOTT, R. D., Methods for predicting aerodynamic heating rates to high-velocity bodies in the upper atmosphere, 20: 12467 (NAA-SR-11704)
ELLIS, Mary K., Liquid scintillation method for determination of solvent-extracted ^{32}P in foods, 20: 10772
EL-NADI, M., Finite-range Coulomb stripping and heavy ion transfer reactions, 20: 12091
ELSNER, N. B., Suppression of grain growth in vapor-deposited tungsten up to 2500°C, 20: 11320
EMANUEL', N. M., Nature of superweak luminescence of irradiated solutions of DNA, 20: 10578
EMMOTT, M. J., Isomer of spin $^{25}/_{2}^+$ in ^{183}Re, 20: 12042
ENDEBROCK, R. W., Reactor materials, 20: 11223
ENGELBRECHT, C. A., COBRA—computer code for calculation of fuel depletion in heterogeneous nuclear reactors, 20: 12361 (PEL-60)
ENGFER, R., Elastic electron scattering from titanium at 53 Mev, 20: 12033
ENGLERT, F., Gravitational ward identity and principle of equivalence, 20: 11888
ENGSTROEM, Arne, Effect of radiation energy on bone tissue, 20: 10628
ENRIQUES, L., Two models proposed for explaining self-excited oscillations in alkali plasma, 20: 12225
EPIK, A. P., Carbon and boron surface saturation in refractory transition metals, 20: 11228
EPLER, E. P., Safety-system reliability vs. performance, 20: 11048
ERDEY, Anna, Laboratory examination of primary water circuit of reactors, 20: 12509
ERDMAN, H. E., Effects of sulfoxide compound on flour beetles exposed to x rays, 20: 10504 (BNWL-122, pp 142)
ERDMAN, H. E., X-ray and fast neutron effects on productivity of flour beetles, 20: 11184
ERICKSON, Glen W., Radiative level shifts. I., 20: 11458
ERMAKOV, A. P., Nuclear rocket engine, 20: 12476 (AD-622352)
ERMAKOV, B. A., Monopulse generation with $CaF_2:U^{3+}$ crystals, 20: 12293
ERMAKOV, V. A., Properties of ^{254}No isotope, 20: 11969 (JINR-P-2471)
ERNST, Frederick J., Linear and nonlinear mass-difference effects in model of baryon multiplets, 20: 11744
ERYKALOV, A. N., Evaluation of variational method accuracy, 20: 12369
ESSMANN, U., Interpretation of electron-microscopic contrast phenomena in vacancy agglomerates of neutron-irradiated copper, 20: 11353 (ANL-Trans-259)
ESWARAN, M. A., "Gamma ray angular correlation studies in nuclear reactions," 20: 12150
EVSEEV, B. A., Crystal structure of compound Zr_5Si_3, 20: 11337

F

FABIAN, A., Effect of ^{90}Sr on certain physiologic indices in Zea mays, 20: 10683
FAELTHAMMAR, C-G., Some aspects of particles and fields in magnetosphere, 20: 11849
FAESSLER, Amand, E2-surface resonance in spherical nuclei, 20: 12024
FAGOT, Bernard, Secondary electron emission of iron under bombardment of Ar^+ ions of medium energy, 20: 11462
FAIER, H., Decays $\pi^0 \to 2\gamma$ and $\eta \to 2\gamma$, 20: 11603
FAINBERG, V. Ya., Quantum field theory equations in axiomatic approach, 20: 11765
FAIRBANK, H. A., Thermal conductivity in isotopic mixtures of solid helium, 20: 11917
FAIRBANK, Henry A., Thermal conductivity in solid ^3He and ^4He, 20: 11916
FAIRCLOTH, R. L., Evaporation behavior of neptunium dioxide, 20: 10840
FAIRFIELD, D. H., Transition region magnetic field and polar magnetic disturbances, 20: 11827
FALECKI, J., Synthesis of salicylic acid ($^{14}COOH$), 20: 10868
FALEEVA, Z. N., Influence of radioinduced chromosome aberrations on vitality of tumor cells, 20: 10677
FALK, Heinz, Optical excitation in negative glow discharge light of hollow cathode discharge, 20: 11773
FALLGATTER, M. B., Mechanism of decay of vinyl unsaturation during radiolysis of Marlex-50 polyethylene, 20: 10893
FARAG, Mohamed Kadri Ahmed, Metabolism of bacteria surviving low-dose γ irradiation of Gulf oysters, 20: 10690
FARINA, A., ECG changes observed in mouse after treatment with ^{32}P, 20: 10643
FARKAS, J., Influence of ionizing radiations on growth of brewing barley, 20: 10619
FARRAR IV, H., Determination of paired-pulse resolution of random counting systems, 20: 11105 (NAA-SR-Memo-11132)
FARWELL, B. E., Prog. rpt. on SNAP-8 materials, 1–6/64. II., 20: 11214 (NASA-CR-54717)
FARWELL, B. E., Prog. rpt. on SNAP-8 materials, 7–12/64, 20: 11215 (NASA-CR-54718)
FATEHALLY, R., Measurement of absolute recoilless fraction "F" in the Moessbauer, 20: 12326
FATKULLIN, M. N., Relationship between E_s at middle and low latitudes and electrodynamic conditions in ionosphere, 20: 11809
FAVUZZI, E., Effect of 6-mercaptopurine and of x rays on skin homografts, 20: 10506
FAW, Richard E., Gamma-ray-induced chlorination of benzene, 20: 10900
FAYYAZUDDIN, Vector-meson decays in U(6) current algebra, 20: 11750
FEATHERSTONE, M., Engineering development of 1200°F sodium vapor trap, 20: 10982
FEDERER, J. I., Vapor deposition and characterization of tungsten–rhenium alloys, 20: 11256
FEDERIGHI, T., Recovery of aluminium after neutron irradiation at 78°K, 20: 11362
FEDORENKO, N. V., Charge exchange of protons in alkaline metal vapor with formation of highly excited hydrogen atoms, 20: 11471
FEDOROV, V. A., Changes of spectra of fast neutrons after their passage

through aluminum, paraffin, and aqueous media, 20: 12268
FEDULOV, V. I., Measurements of distribution of pressure behind strong shock waves, 20: 11775
FELDMAN, M. J., Management and control of EBR-II fuel, 20: 12452
FELDMANN, Hans-Helmut, Measurement of out-of-phase condition of ions in cycle track isochronous cyclotron, 20: 11415
FEL'DSHTEIN, Ya. I., Disturbed solar-diurnal variations at high latitudes during IGY, 20: 11812
FENG, Yue, Histochemical effects of x irradiation upon the adrenal cortex, 20: 10576
FENTIMAN, Allison F. Jr., Radiation-induced formation of organometallic compounds with particular emphasis on organotins, 20: 10870 (BMI-1753)
FERGUSON, I. F., Crystallite size, strain and shape determinations on thoria from x-ray line broadening studies, 20: 11321
FERGUSON, James M., Total neutron cross sections of copper, iron, and aluminum near 14 Mev, 20: 11949 (AD-625747)
FERRARA, A., Therapeutic effect of preserved autologous bone marrow on hematological lesions provoked by radiation, 20: 10706
FERRE, Jean, Initiation of high-frequency electric discharge in rare gases, 20: 11780
FERRELL, Richard A., Fine structure in nuclear resonances, 20: 12087
FERRELL, Richard A., Normal processes which inhibit superconductivity, 20: 11923
FERT, Charles, Secondary electron emission of iron under bombardment of Ar^+ ions of medium energy, 20: 11462
FESSENDEN, Richard W., ESR spectrum of Foo, 20: 10882
FICARI, A., Therapeutic use of selective perfusion with radioisotopes with a short half life, 20: 10737
FIDELIS, I., Regularities in stability constants of some rare earth complexes, 20: 10953
FIEDELDEY, H., COBRA—computer code for calculation of fuel depletion in heterogeneous nuclear reactors, 20: 12361 (PEL-60)
FIELDEN, E. M., Formation of Cu^{III} in radiolysis of Cu^{2+} solutions, 20: 10923
FIELDEN, E. M., Pulse radiolysis of Ag^+ solutions, 20: 10922
FIELDEN, E. M., Reaction of hydrated electron with water, 20: 10894
FIET, O., Prog. rpt. on valve technology for spacecraft engines, final, 7/64–8/65, 20: 11007 (NP-15831)
FILIPESCU, Mihela, Behavior of molybdenum powders during pressing and sintering, 20: 11253
FILIPESCU, N., Solvent and temperature effects on fluorescence emission of europium β-diketonates, 20: 10844
FILIPPOVA, V. N., Effects of whole-body x irradiation on content of iridindiphosphate glucose in liver of rats, 20: 10590
FILLIUS, R. Walker, Trapped protons of inner radiation belt, 20: 11825
FINKELSTEIN, David, High voltage impulse system, 20: 11074
FINKLE, Earl, Military vehicles—mission analysis using radioisotope submersible engines, 20: 11187 (AGN-8138)
FINNEY, P. J., Interaction of 16.3 Bev π^--mesons with complex nuclei, 20: 11602
FIOCCHI, Roberto, Recent developments in uranium isotope separation, 20: 11193
FIORINO, John Angelo, Design and performance of long-path oxy-acetylene burner for atomic absorption spectroscopy, 20: 10761 (IS-T-69)
FISCHER, John E., Lifetime and trapping in 6- to 50-Mev electron-irradiated germanium, 20: 11349 (NP-15611, pp 28-38)
FISTEDIS, Stanley H., New concept for nuclear reactor containment, 20: 12346
FLAHAUT, Jean, Solid solutions formed by addition of selenides of rare earths to selenides of fcc NaCl type, 20: 10857
FLANAGAN, C. A., Evaluation of three-dimensional flux synthesis method as nuclear design tool, 20: 12368 (WAPD-T-1737)
FLECK, C. M., Exact determination of neutron temperature in neutron field variable in time, 20: 11937
FLEISCHMANN, H. H., Errors in the use of mass analyzers in plasma physics, 20: 12223
FLEMING, D., Mass 13, T = ½ quartet, 20: 12036
FLEMING, Gordon N., Physical region decoupling procedure for coupled channel scattering amplitudes, 20: 11711
FLEROV, G. N., On properties of isotope $^{254}102$, 20: 11968 (JINR-P-2470)
FLETCHER, G. H., Combined 5-fluorouracil and cobalt irradiation evaluated by double blind technique, 20: 10725
FLIEDNER, T. M., Bone marrow regeneration in rats after sublethal whole-body irradiation, 20: 10681
FLINTA, Jan E., Burnout conditions for flow of boiling water in vertical 3-rod and 7-rod clusters, 20: 11000
FLORENT, R., Vacuum and cryogenic associated techniques. Application to large bubble chambers, 20: 11141
FLORIN, Roland E., Effect of γ irradiation on polyamide, 20: 10892
FLYNN, E. R., High efficiency solid state neutron telescope for 15–35 Mev neutrons, 20: 11139
FOGEL, P., Collective states of nuclei in Tamm-Dancoff method, 20: 11966 (JINR-P-2432)
FOGEL', Ya. M., Electron loss and formation of slow negative ions in collisions between hydrogen atoms and negative ions with gas molecules, 20: 11509
FOKINA, T. V., Leukocytic reactions to adrenaline in dogs exposed to radiation, 20: 10594
FOLDY, Leslie L., Cartesian tensors in spaces with indefinite metric with applications to relativity, 20: 11879
FOLEY, William A., Urethan-induced lung tumors in mice: x-radiation dose-dependent inhibition, 20: 10671
FORCELLA, A., Professional nuclear materials management, 20: 12451
FORD, J. A., Analysis of Babcock and Wilcox full-size steam generator for sodium–water reaction, 20: 12386 (APDA-176)
FORMANEK, J., Lie group of infinite order as non-trivial coupling of intrinsic and space-time symmetries, 20: 11704
FORSYTH, R. S., Study of "384"-kev complex γ emission from ^{239}Pu, 20: 11950 (AE-202)
FORTI, P., Angular distributions of α-particles leading to first excited states of ^{26}Mg, 20: 12030
FOSSAN, D. B., Lifetime of 1.02-Mev state in ^{23}Ne, 20: 12060
FOSTER, K. W., Gamma shielding requirements for ^{238}Pu and ^{210}Po, 20: 12264 (MLM-1315)
FOWLER, G. N., Absorption of K^- mesons in deuterium, 20: 11599
FOWLER, I. L., Large-volume coaxial germanium gamma-ray spectrometers, 20: 11095 (CRGP-1224)
FOWLER, J. F., Recent progress in radiologic treatment with fast neutrons and mesons, 20: 10736
FOX, J. D., Isobaric analogue states in heavy nuclei. I., 20: 12078
FOX, J. D., Isobaric analogue states in heavy nuclei. II., 20: 12079
FRADKIN, E. S., Application of functional methods in quantum field theory and quantum statistics. II., 20: 11731
FRAHM, H. J., Lifetimes of E3 transitions in odd-mass Ho isotopes, 20: 12017
FRANKE, H., Histochemical detection of glycogen and mucopolysaccharides in brain of guinea pigs after x irradiation, 20: 10638
FRANKEL, S., Roentgenographic development of ^{90}Sr-induced osteogenic sarcoma in the rat, 20: 10652
FRANKEN, P. A., Collision-induced mixing in first excited states of sodium and potassium, 20: 11499
FRANSSON, K., Decay of ^{132}Te and levels in odd ^{132}I, 20: 12026
FRASER, A. R., Fundamental equations of radiation hydrodynamics, 20: 11766 (AWRE-O-82/65)
FRAZER, J. W., Apparatus for automatic preparative gas chromatography, 20: 12553 (UCRL-14359)
FRED, M. S., Electronic g factors of low levels of Ni I, 20: 11479
FREDERICKSON, A. Robb, Prog. rpt. on radiation damage in semiconductor materials, 2–4/65, 20: 11176 (NP-15835)
FREED, C. N., Prog. rpt. on metallurgical characteristics of high strength structural materials, 5–7/65, 20: 11273 (NRL-6364)
FREREJACQUE, D., Proton form factors from proton observation, 20: 11567 (LAL-1144)
FREREJACQUE, D., Proton form factors from observation of recoil protons, 20: 11628
FREUND, Peter G. O., Universality: dynamical principle for theory of hadrons, 20: 11665
FREY, K. W., Radioisotope nephrography during childhood, 20: 10734
FREY, K. W., Radioiodine treatment of benign strumae in endemic goiter region of southern Germany, 20: 10748
FRID, A. S., Effect of salt concentration in soil solutions on rate of diffusion of microquantities of strontium, 20: 12523
FRIDDELL, K. D., Response of P-I-N detectors to various nuclear radiation environments, 20: 11173 (DW-84071-1)
FRIEDBERG, C. E., Experimental test of time-reversal invariance in decay $K_L \to \pi^\pm \mu^+ + \nu$, 20: 11662
FRIEDLAND, A. J., Analysis of Babcock and Wilcox full-size steam generator for sodium–water reaction, 20: 12386 (APDA-176)
FRIEDMAN, Harold L., Thermodynamic excess functions in D_2O and H_2O, 20: 10847
FRIESENHAHN, S. J., Energy dependence of neutron capture cross section of tungsten isotopes from .01 to 10 ev, 20: 11957 (GA-6832)
FRISBY, H., Ultrasonic study of cracks and pores in sintered beryllia, 20: 11324
FRITTS, H. W. Jr., Intrapulmonary exchange of $^{18}O_2$ injected intravenously in man, 20: 10547
FRITZ, R., Design study of nuclear power plant (Trikt-50) for space flight, 20: 12482
FRITZ, R., Employment of heat pipes for thermionic reactors, 20: 12489
FROEHNER, F. H., Energy dependence of neutron capture cross section of tungsten isotopes from .01 to 10 ev, 20: 11957 (GA-6832)
FROMAGE, Francine, Constitution in solution of complex carbonates of rare earths, 20: 10824
FRONSDAL, C., Unitary representations and relativistic coupling coefficients for SL_2, C, 20: 11737

FRONTEROTTA, Gabriele, (e,e'p) reaction in ^{9}Be nucleus, 20: 11988
FRYBERGER, D., Experience with on-line experimentation, 20: 11553 (COO-614-34, Sect. IIC)
FUBINI, A., Construction and calibration of proton recoil type neutron spectrometer, 20: 11096 (EUR-2491.e)
FUJII, I., Application of fast neutron activation method to the determination of oxygen in iron and steel, 20: 10771
FUJITA, S., Thermodynamic evolution equation for quantum statistical gas, 20: 11789
FUKS, S., Surface tension of isotopic mixtures, 20: 11787
FULDE, Peter, Theory of superconductors containing magnetic impurities, 20: 11906
FULLAM, H. T., Promethium compatibility and encapsulation studies, 20: 11267 (BNWL-SA-488)
FULLER, A. B., Design considerations for off-gas system major components, 20: 11050
FUNK, E. G., Decay of ^{191}Pt(3.0 d) to ^{191}Ir, 20: 12009
FUNK, E. G., Half-lives of 2+ rotational states in ^{158}Dy and ^{158}Gd, 20: 12082
FUNK, E. G., Reinvestigation of decays of ^{146}Eu and ^{146}Pm, 20: 12081
FUNYE, M. R., Nilsson and self-consistent models for nuclear deformations, 20: 12125
FURLAN, M., Nitrogen metabolism in frog liver after whole-body irradiation. I., 20: 10551
FURNICA, Gh., Respiratory intake of ^{45}Ca and ^{204}Tl radionuclides, 20: 10546
FURUKAWA, Michiaki, Excitation functions for alpha-particle induced reactions on ^{139}La, 20: 12014
FURUTA, Yutaka, Gamma-ray pulse dosimeter, 20: 11137
FYDELOR, P. J., Pulse radiolysis studies of aqueous polymer-thiourea systems, 20: 10921

G

GABAGLIO, M., C.N.E.N.'s fuel element fabrication and control laboratories at Saluggia, 20: 11247
GABBE, E. E., Inhibition of whole-body incorporation and retention of ^{131}I in man, 20: 10543
GADD, Ivar, Mutations and crop improvement. VI., 20: 10645
GADIOLI, E., Angular distributions of α-particles leading to first excited states of ^{25}Mg, 20: 12030
GAEDKE, R. M., New total-cross-section measurements for reactions $^{14}N(^{14}N,^{13}N)^{15}N$ and $^{10}B(^{14}N,^{13}N)^{11}B$, 20: 12057
GAERTTNER, M., Infrared absorption bands in Si induced by 45-Mev electrons. I., 20: 11347 (NP-15611, pp 5-18)
GAERTTNER, M., Infrared studies of 48 Mev electron-irradiated (at 125°K) oxygen-doped germanium, 20: 11348 (NP-15611, pp 19-27)
GAEUMANN, T., Pulse radiolysis of carbon tetrachloride–benzene mixtures, 20: 10928
GAGE, William R., Three-dimensional cartesian particle-in-cell calculations, 20: 12537 (LA-3422)
GAILLARD, Michel, Scattering of protons by neon, 20: 11995
GALAKTIONOV, Yu. V., Scintillation counter effectiveness in registering neutrons with several Bev energy, 20: 11106 (NP-15786)
GALIMOV, E. M., Method of two standards for eliminating errors in measurement of isotopic composition in mass spectrometer, 20: 10793
GALLAGHER, James P., Determination of coronary flow with positron emitter (^{84}Rb), 20: 10730
GALLIVAN, James B., Ionic processes in γ-irradiated organic solids, 20: 10886
GAMBHIR, Y. K., Ground-state correlations and theory of one- and two-phonon states, 20: 12123
GAMBHIR, Y. K., Structure of Pr-isotopes, 20: 12124
GARRETT, C. W., Low-energy component of total dose for deep gamma penetrations in air and water, 20: 12261 (AFRRI-TN-65-2)
GARVEY, Gerald T., New nuclidic mass relationship, 20: 12090
GARVIN, H. L., Prog. rpt. on ion rocket engine development, 4–6/65, 20: 11006 (NP-15824)
GASNIKOV, P. E., Nuclear desalination equipment of low capacity, 20: 12454 (JPRS-33480)
GATIGNOL, Renee, Structure of shock wave for gas with discrete distributions of velocities, 20: 11779
GAUDEFROY, M., Rectitis and ileitis after treatment of cervical cancer with radium and x rays, 20: 10654
GAUGER, J., Position of south latitude cosmic-ray plateau, 20: 11523
GAUTREAU, R., Possible causal violations at radii greater than Schwarzschild radius, 20: 11885
GAVRILOV, B. I., Electron heating in TN-1 installation, 20: 12206
GAVRIN, P. O., Turbulent heating of plasma by direct-discharge current, 20: 12183 (ORNL-tr-868)
GE, Chzhi-min, Heat resistance of alloys Ti–Al–Mo–V system, 20: 11336
GEBALLE, T. H., Occurrence of superconductivity in sulfides, selenides, tellurides of Pt-group metals, 20: 11899
GEBHARDT, E., Total emission capacity of niobium, 20: 11314
GEER, W. U., Behavior of coated particles in large nuclear transient (KIWI TNT), 20: 11343 (LA-3367)
GEHMAN, B. L., Pulse radiolysis of liquid ammonia, 20: 10910
GEISS, J., Spallation, fission and neutron capture anomalies in meteoritic krypton and xenon, 20: 11424 (NP-15629)
GELEBART, Francois, Absorption spectra of water and heavy water in the ultraviolet, 20: 10823
GEORGE, Marilyn J., ^{90}Sr and ^{137}Cs in Columbia River plume, July 1964, 20: 11023
GERASIMOV, Ya I., Thermodynamics of W, Mo, Ti, Zr, Nb, and Ta and their more important compounds, 20: 10816 (NASA-TT-F-285)
GERBER, H., Determination of total clearance of different preparations of gamma-globulin, 20: 10571
GERMAGNOLI, E., Positron decay in halogen compounds, 20: 11621
GESSNER, R. F., Effects of thermal treatment on distribution of alloying elements in Zircaloy-2, 20: 11287 (WAPD-T-1809)
GEY, Albert, Determination of number of neutrons emitted simultaneously by source, 20: 11947
GHATIKAR, M. N., Nuclear quadrupolar shielding factors for rare earth ions in crystals, 20: 12323
GHEZZI, I., Risk of internal contamination in industries employing ^{137}Cs, 20: 10721
GHIDINI, B., Exchange mechanism for $\pi^+p \to N^{*}\rho^0$ reaction at 2.75 Bev/c, 20: 11605
GHOSE, A. M., Cross section of reaction $^{31}P(n,2n)^{30}P$ with neutrons of 14.8 Mev energy, 20: 12134
GHOSE, A. M., Photoelectric cross section of γ rays for heavy atoms, 20: 11516
GHOSE, A. M., Systematic measurements of (n,p) cross sections at 14.8 Mev, 20: 12133
GHOSH, Amal K., Color centers in aluminoborate glass, 20: 12288
GHOSH, Amal K., Optical spectra of thallium in glasses as related to crystals and solutions, 20: 10830
GIBBONS, James F., Implantation profiles for 40-kev phosphorus ions in silicon single-crystal substrates, 20: 12280
GIBSON, J. W., Critical magnetic fields of superconducting ruthenium isotopes and search for an isotope effect, 20: 11913
GIDAL, George, Measurement of N^{*-}–N^{*++} mass difference, 20: 11624
GIELEN, Paul, Influence of anisotropic Moessbauer effect on magnetic hyperfine splittings in polycrystalline materials, 20: 12299
GIERKE, G. v., Toroidal device with meridian magnetic confining field of grad $p \cdot \text{grad} \oint dl/B > 0$, 20: 12174 (MPI-PAE/P1.6/65)
GIESSEN, B. C., Ordered AB and AB_3 phases in T_6–T_9 alloy systems and modified Mo–Ir phase diagram, 20: 11309
GIGON, Jean, Device for measuring doses of thermal neutrons, 20: 11168
GILBERT, A., Dislocation structure in chromium, chromium–rhenium, and chromium–iron alloys, 20: 11303
GILBERT, A., Notch-impact behavior of chromium and a chromium–35 at.% rhenium alloy, 20: 11300
GILBERT, A., Thermonuclear reactions in medium and heavy nuclei, 20: 11989
GILBERT, C. W., Pulse radiolysis of aerated aqueous potassium bromide solutions, 20: 10912
GILLES, A., Control possibilities on basis of materials balance, 20: 10970
GILLES, Jean-Claude, Preparation of oxynitrides from refractory oxides, 20: 10856
GIRAUD-HERAUD, Francois, Effect of carbon on formation of tempering structures in uranium–molybdenum alloys, 20: 11292
GITLIN, D., Selective permeability of placenta to plasma proteins and protein hormones, 20: 10508
GIUNTINI, C., Intrapulmonary exchange of $^{18}O_2$ injected intravenously in man, 20: 10547
GIVENS, M. Parker, Variation of time-of-flight of electrons through a photomultiplier, 20: 11071
GLABERSON, W. I., Growth of pinned quantized vortex lines in helium II, 20: 11905
GLASS, Laurel E., Mechanism of sterility induced by D_2O in mice, 20: 10550
GLUCKSMANN, Alfred, Can radiosensitivity and histopathology of cervical cancer be correlated? 20: 10739
GOBRON, Roland, Constitution in solution of complex carbonates of rare earths, 20: 10824
GODSHALL, J. L., Prog. rpt. on evaluation of refractory/austenitic bimetal combinations, 6/22–9/22/65, 20: 11243 (WANL-PR(EE)-001)
GOEDEKE, A. D., Recent solar cosmic ray events, 20: 11863
GOEDKOOP, J. A., Scientific work of RCN in national and international contexts, 20: 11355
GOELER, S. V., Plasma losses in Q-device, 20: 12215
GOITEIN, M., Unsuccessful search for excited electron, 20: 11629
GOKTEPE, Omer, Design study report on 1000 MWe fast breeder reactor, 20: 12414 (TID-22545, pp 16-52)
GOLABI, Sayed Mehdi, Solid solutions formed by addition of selenides of

rare earths to selenides of fcc NaCl type, 20: 10857
GOLDANSKII, V. L., Nuclear chemistry, 20: 11377
GOLDANSKII, V. L., Two-proton radioactivity of heavier-than-tin nuclei, 20: 12028
GOLDBERG, I., Precession of satellite orbits and general relativity, 20: 11883
GOLDBERG, Philip, High voltage impulse system, 20: 11074
GOLDMANN, Kurt, Sodium technology, 20: 12330 (TID-8541, pp 321-425)
GOLDRING, G., Lifetime measurements of some rotational levels by new recoil method, 20: 12020
GOLDSTEIN, Gerold, Analytical radiochemistry of technetium, 20: 10940
GOLDSTEIN, Rubin, Intermediate resonance absorption, 20: 11928 (BNL-9790)
GOLFB, J. A., Determination of uranium isotopes by atomic absorption spectrophotometry, 20: 10770
GOL'TSMAN, F. M., Optimum method of recording frequency of free nuclear precession in presence of noise, 20: 11817
GOMBERT, Dieter W., Atomic irradiator, 20: 10987
GOODE, R. J., Prog. rpt. on metallurgical characteristics of high strength structural materials, 5–7/65, 20: 11273 (NRL-6364)
GOODMAN, A. S., Mean lives of some states in atomic hydrogen, 20: 11474
GOODMAN, L. S., Electronic g factors of low levels of Ni I, 20: 11479
GOODMAN, L. S., Hyperfine structure of ^{73}Ge in the $^3P_1$ and $^3P_2$ atomic states, 20: 11476
GOODMAN, L. S., Hyperfine structure of 9161-cm^{-1} $^2D_{5/2}$ state of ^{197}Au, 20: 11491
GOODSPEED, R. C., Prog. rpt. on development of Ta base alloy, 2/20–5/19/65, 20: 11217 (WANL-PR(Q)-007)
GOPINATHAN, K. P., Gamma-gamma directional correlations in ^{149}Pm, 20: 12080
GORDON, Frederick Jr., Definition of space radiation environment, 20: 11840
GORDON, R. G., Kinetic theory of nuclear spin relaxation in gases, 20: 11784
GORDON, R. G., Relations between vibrational spectroscopy and the isotope effect on vapor pressures, 20: 10831
GORDON, Sheffield, Reaction of hydrated electron with water, 20: 10894
GOR'KOV, L. P., Quantum field theoretical methods in statistical physics, 20: 11375
GORMAN, D. L., Panel discussion: role of nuclear power in merchant marine, 20: 12460 (CONF-640810, pp 7-21)
GORYSHNIK, L. L., Particle distribution in vicinity of charged sphere in weakly ionized rarefied plasma, 20: 12201
GOTCH, R. W., Automatic inert gas tungsten arc welding applied to nuclear engineering problems, 20: 11246
GOULARD, Bernard, Nuclear structure effect in neutrino induced nuclear "elastic" reactions, 20: 12100
GOULIANOS, K., Experimental test of time-reversal invariance in decay $K_L \to \pi^2 \mu^+ + \nu$, 20: 11662
GOURLAN, C., Experiment on electrical breakdown in vacuum at Laboratorio Gas Ionizzati, 20: 11769 (LGI-65/30)
GOUTIER, R., Spleen DNA after irradiation of head or of whole body in the rat, 20: 10622
GRACHEV, V. I., Biological effect of multiple x irradiation with energies of 180 kv compared with proton irradiation, 20: 10611 (NASA-TT-F-353, pp 185-93)
GRAHAM, Ruth M., Is cytology a reliable prognosticator of radiosensitivity? 20: 10740
GRAHN, Douglas, Mammalian radiation genetics, 20: 10688
GRANT, N. J., Ordered AB and AB_3 phases in T_8–T_9 alloy systems and modified Mo–Ir phase diagram, 20: 11309
GRANT, Nicholas J., Fracture in connection with hot deformation processing of metals, 20: 11265 (AD-626375)
GRASHCHENKO, S. M., Mesothorium-I concentration in the Black Sea, 20: 10768 (JPRS-33212)
GRAVES-MORRIS, P. R., Fredholm method for Bethe-Salpeter equation, 20: 11757
GRAYBILL, S. E., Observations of magnetically self-focusing electron streams, 20: 11402
GRECO, G., Changes of electrophoretic pattern of serum proteins after treatment with ^{32}P, 20: 10581
GRECO, G., Effect of 6-mercaptopurine and of x rays on skin homografts, 20: 10506
GRECO, G., Effect of radioactive ^{32}P in the mouse, 20: 10640
GRECO, G., Therapeutic use of selective perfusion with radioisotopes with a short half life, 20: 10737
GREEN, D. M., Analysis of Babcock and Wilcox full-size steam generator for sodium–water reaction, 20: 12386 (APDA-176)
GREENDALE, A. E., An iodine source for beta counting, 20: 10935 (USNRDL-TR-948)
GREENDALE, A. E., Nuclear-charge distributions of several fission product mass chains, 20: 11980 (USNRDL-TR-935)
GREENE, Barry, Fracture in connection with hot deformation processing of metals, 20: 11265 (AD-626375)
GREENE, E., Thermal diffusion column shape factors. I., 20: 10949 (K-1469)
GREENE, P. J., Experiment on direct control of nuclear reactor using computer, 20: 12511
GREENOUGH, G. B., AGR fuel, 20: 12430
GREISS, Frank C., Treatment of cancer of cervix by radiation and elective radical hysterectomy, 20: 10726
GRIBBLE, R. F., Infrared maser interferometry for time and space resolution of electron density in high temperature plasmas, 20: 12165 (ARL-65-135)
GRIBBLE, R. F., Time-space resolution of B-fields in theta-pinch plasma by Faraday rotation of infrared maser radiation, 20: 12164 (ARL-65-129)
GRIEGER, G., Toroidal device with meridian magnetic confining field of grad p · grad $\oint dl/B > 0$, 20: 12174 (MPI-PAE/P1.6/65)
GRIEM, Melvin L., Modification of radiation response of tumors by actinomycin D. Clinical evaluation, 20: 10700
GRIFFIN, B. I., Radioactivity in northern Alaskan natives and their foods during 1964, 20: 10718 (BNWL-122, pp 172-5)
GRIFFITH, J. A. R., Thin liquid sheets at reduced pressure applications in nuclear physics, 20: 11409
GRIFFITHS, W., Pulse radiolysis of aqueous carbohydrate solutions, 20: 10920
GRIGOR'EV, Yu. G., Biological effects of 130-Mev protons, 180-kv x rays, and ^{60}Co-γ rays on vestibular apparatus, 20: 10610 (NASA-TT-F-353, pp 157-84)
GRIGOR'EV, Yu. G., Biological effect of proton radiation at 510 Mev, 20: 10612 (NASA-TT-F-353, pp 194-209)
GRIGOR'EV, Yu. G., Characteristics of the radiation effect under space flight conditions and ways to determine admissible radiation levels, 20: 10719 (NASA-TT-F-353, pp 3-20)
GRIMSHAW, J. A., Energy and orientation effects of electron irradiation in silicon, 20: 11364
GRINENKO, V. A., Method of two standards for eliminating errors in measurement of isotopic composition in mass spectrometer, 20: 10793
GRISHANIN, E. I., Measurement of absorption cross section of ^{156}Gd, 20: 11987
GRITZ, K., Histochemical detection of glycogen and mucopolysaccharides in brain of guinea pigs after x irradiation, 20: 10638
GRODZINS, L., Moessbauer scattering: quadrupole interaction in osmium metals, 20: 12301
GROLL, M., Design of radiators for space, 20: 12480
GROLL, M., Temperature distribution in fast reactor with thermionic converters on its surface, 20: 12486
GRONSKAYA, N. F., Reactions of tadpole tissues to x radiation during starvation conditions, 20: 10676
GROOM, Donald Eugene, Λ polarization at 90° in $K^+\Lambda$ photoproduction, 20: 11676
GROSHEV, L. V., Levels of nucleus ^{166}Ho from reaction (n,γ), 20: 11982 (LA-tr-65-34)
GROSSE-RUYKEN, H., Partition chromatography of rare-earth metals with bis-(2-ethylhexyl) hydrogen phosphate. I., 20: 10960
GROSSETETE, B., Elastic electron-deuteron scattering, 20: 11644
GROSSETETE, B., Electrodisintegration of deuteron around $q^2 = 3.5F^{-2}$, 20: 11645
GROSSETETE, B., Inelastic electron-deuteron scattering and rescattering corrections, 20: 11646
GROSSMAN, Lawrence, Effects of uv light on template properties of polycytidylic acid, 20: 10584
GROZDOV, I. I., Nuclear desalination equipment of low capacity, 20: 12454 (JPRS-33480)
GRUNDNER, W. T., Improved aluminosilicate ion exchangers, 20: 10766 (TID-22511)
GRUZIN, P. L., Determination of spectral characteristics of isotope neutron sources by means of paired scintillation crystals of type LiI(Eu), 20: 11116
GSCHNEIDNER, K. A. Jr., Solubility of tantalum in eight liquid rare-earth metals, 20: 11306
GUBAREVA, A. V., Antitumoral resistance in animals subjected to chronic treatment with small doses of ^{90}Sr, 20: 10627
GUDZENKO, L. I., Amplification in decaying plasma, 20: 12210
GUDZENKO, L. I., Use of highly ionized plasma for fabrication of laser, 20: 12209
GUENTHER, K. G., Penning ion source for mass spectrometers, 20: 11077
GUERRIER, Y., Variations of –SH groups in human skin after irradiation by cobalt therapy, 20: 10702
GUISAN, O., Secondary peak at $t = -1$ (Bev/c)^2 in high energy π^-p charge exchange scattering, 20: 11614
GUPTA, K. C., T = ½, ⅓ p- and s-wave Kπ phase shifts, 20: 11648
GUPTA, Raj K., Configuration mixing effects in shell model nuclei, 20: 12155
GUPTA, Raj K., Rotational bands in ^{82}Kr, 20: 12156
GUPTA, Raj K., Shell model calculations for levels in ^{91}Nb, 20: 12157
GUPTA, S. DAS, Nilsson and self-consistent models for nuclear deforma-

tions, 20: 12125
GUPTA, S. K., Study of $^{37}Cl(p,n)^{37}Ar$ reaction mechanism, 20: 12141
GUPTA, S. L., Gamma-gamma directional correlation in ^{123}Te, 20: 12140
GURALNIK, G. S., Algebra of currents and generalized Ademollo-Gatto theorem, 20: 11610
GUREVICH, Yu. B., Effect of conditions of hot plastic deformation on structure and properties of molybdenum, niobium, and titanium, 20: 11249
GURIN, A. A., Effect of particle collisions on fluctuations in plasma, 20: 12253
GURNETT, Donald A., Fractional concentration of hydrogen ions in ionosphere from vlf proton whistler measurement, 20: 11822
GUSBERG, Saul B., Choice of treatment for cervix cancer: radiosensitivity testing, 20: 10741
GUSEV, V. A., Electron loss and formation of slow negative ions in colloids between hydrogen atoms and negative ions with gas molecules, 20: 11509
GUSTAFSON, P. F., Gamma-ray detection efficiency of annular and well-type sodium iodide crystals, 20: 11127
GUSTAFSSON, Ake, Mutations and crop improvement. VI., 20: 10645
GUTHRIE, G. L., Superconducting transition temperature of La_3S_4, 20: 11909
GUYER, R. A., Thermal conductivity in isotopic mixtures of solid helium, 20: 11917
GUYOT, P., Plasticity of dispersed-phase-type $Al-Al_2O_3$ alloys, 20: 11269 (EUR-2483.f)

H

HAACKE, Wolfram, Scintigraphic demonstration of brain tumors with ^{197}Hg-labeled substances, 20: 10733
HAAS, Ann K., Indexes to Analytical Chemistry Division annual progress reports, 1964–1965, 20: 10765 (ORNL-3904)
HAAS, Paul Arnold, Engineering development of foam column for countercurrent surface-liquid extraction of surface-active solutes, 20: 12526
HABERER, Klaus, Distribution of radioactive rainfall at dam with help of gamma spectrometry, 20: 11055
HACKETT, Charles F., Constant speed drive for Moessbauer experiments, 20: 11073
HACKETT, P. L., Toxicity of copper and x rays in rats, 20: 10598
HADDAD, E., Energy dependence of neutron capture cross section of tungsten isotopes from .01 to 10 ev, 20: 11957 (GA-6832)
HADDAD, I. N., Energy and orientation effects of electron irradiation in silicon, 20: 11364
HADEN, C. R., Flux-trapping of RF fields in superconductors, 20: 11926
HAEFELE, W., Karlsruhe reference design of 1000 MWe sodium cooled fast breeder reactor, 20: 12402 (KFK-369)
HAGEDOORN, Hendrik Lourens, Pole shoe assembly for cyclotron electromagnet, 20: 11423
HAGEE, G. R., Weak alpha and electron capture decay in ^{208}Po and ^{209}Po, 20: 11971 (MLM-1251J)
HAINES, Eldon L., Pulse height defect and energy dispersion in semiconductor detectors, 20: 11138
HAINZELIN, J., Testing of fusible metal joint for fast reactor, 20: 12513
HAIRE, J. C., Addendum to the Spert III hazards summary report—low-enrichment oxide core, 20: 12497 (IDO-17003(Rev.2))
HALAMA, H. J., Pulsed phase measuring and control system for rf separator, 20: 11380 (BNL-9772)
HALL, Duane Charles, Internal conversion coefficients in decay of ^{57}Co, 20: 11976 (TID-22504)
HALLING, H., Univibrator as time element in medium fast coincidence circuit, 20: 11109 (SGAE-E-5/1965)
HAMADA, Hironori, Reactor control-rod (or other rod) drive mechanism using magnetic clutches, 20: 12349
HAMILL, William H., Ionic processes in γ-irradiated organic solids, 20: 10886
HAMILTON, J. H., L subshell ratios of pure E2 transitions, 20: 12035
HAMMER, J. M., Ion beam measurements of cesium recombination cross sections, 20: 11488
HAMMERBERG, Charles Clifford, Diffusion of hydrogen in barium metal, 20: 12535 (IS-T-61)
HAMMOND, Carolyn W., Susceptibility of radiation chimeras to experimental Pseudomonas aeruginosa infection, 20: 10669
HANAUER, S. H., Design precepts for engineered safeguards, 20: 12335
HANITZ, F., Plasma induction accelerator with radial magnetic field, 20: 12198
HANNON, John W. G., Beryllium disease, 20: 11038
HANNUM, W. H., Molten plutonium burnup experiment, 20: 12403 (LA-3384)
HANSEN, C. J., Thermonuclear reactions in medium and heavy nuclei, 20: 11989
HANSEN, N. J. Sigurd, Lifetimes of E3 transitions in odd-mass Ho isotopes, 20: 12017
HANSEN, Niels, Bibliography on dispersion-strengthened materials, 1964, 20: 11278 (RISO-48(Suppl.2))
HANSON, G. L., Proposed chemical flowsheets for decladding and dissolution of PRTR plutonium aluminum fuel, 20: 10948 (HW-76472)
HANSON, J. P., Space power plant study, 20: 12475 (WANL-PR(B)-009)
HANSON, W. C., Radioactivity in Alaskan animals and forage plants, 20: 10535 (BNWL-122, pp 176-80)
HANSON, W. C., Radioactivity in northern Alaskan natives and their foods during 1964, 20: 10718 (BNWL-122, pp 172-5)
HANSTEEN, J. M., Magnitudes of some reduced transition probabilities in ^6Li, 20: 12039
HAPPER, William Jr., Nuclear moments of ^{43}Sc and ^{47}Sc, 20: 12070
HARDCASTLE, R. A., FAUST 1—hardcore discharge stability experiment, 20: 12222
HARDER, B. R., Reduction and sintering of hyperstoichiometric carbides in hydrogen, 20: 11252
HARDY, Gyula, Investigations in field of radiation-induced solid state polymerization. IX., 20: 10896
HARDY, Gyula, Investigations in field of radiation-induced solid state polymerization. X., 20: 10897
HARGREAVES, J. K., Absorption at conjugate points, 20: 11862
HARRINGTON, David R., Three-nucleon interaction, 20: 11650
HARRISON, D. E. Jr., Spot patterns and Silsbee chains on Cu single crystal, 20: 11460
HARRISON, E. R., Cosmology without general relativity, 20: 11874
HARROP, Ian Hugh, Crystal field of some monoclinic rare earth chlorides, 20: 10860
HART, Edwin J., Reaction of hydrated electron with water, 20: 10894
HART, R. S., Predicted fission product decay of Snapshot I, 20: 12466 (NAA-SR-11642)
HARTLEY, Craig Sheridan, Strain-aging behavior of Ta, 20: 11331
HARTMAN, Richard T., Prog. rpt. on productivity of vascular hydrophytes and their role in mineral cycling in aquatic ecosystems, annual, 1965, 20: 12543 (NYO-3018-12)
HARTWIG, G., Quasi-elastic electron-deuteron scattering and neutron form factors, 20: 11626
HARTWIG, W. H., Flux-trapping of RF fields in superconductors, 20: 11926
HARUN-AR-RASHID, A. M., One-particle exchange theory of pion photoproduction. I., 20: 11572
HARVEY, Bernard G., High spin levels preferentially populated by (α,d) reaction, 20: 12061
HARVEY, R. A., Computer evaluation of tellurium–iodine contamination events, 20: 10519 (BNWL-122, pp 59-63)
HARWERTH, H. G., Bioptic studies of therapy-induced bone marrow fibroses in chronic myeloid leukemia, 20: 10746
HASBROUCK, M. E., Plutonium metallurgy notebook, 20: 11213 (BNWL-37)
HASEGAWA, Akira, Ion cyclotron instabilities in bounded beam-plasma system, 20: 12203
HASEGAWA, Shun-ichi, Analysis of high energy jet showers. I., 20: 11532
HASEGAWA, Shun-ichi, Analysis of high energy jet showers. IV., 20: 11535
HASEGAWA, Shun-ichi, Analysis of high energy jet showers. II., 20: 11533
HASEGAWA, Shun-ichi, Analysis of high energy jet showers. III., 20: 11534
HASSAN, M. Y. M., Solutions of superconductivity equations for odd-A nuclei in rare-earth region, 20: 11961 (INR-602/VII/PH)
HASTE, G. R., Microinstability limitations of DCX-1 energetic plasma, 20: 12240
HASTE, G. R., Observation of negative-mass instability in energetic proton plasma, 20: 12247
HATTORI, Tadao, Spectrophotometric determination of Y with Arsenazo III, 20: 10773
HAUG, W., Design study of nuclear power plant (Trikt-50) for space flight, 20: 12482
HAUG, W., Parameter studies on thermal thermionic reactors, 20: 12479
HAUGE, E. Hiis, Distribution of zeros of grand partition function, 20: 11788
HAUGE, Robert H., Spectra of CaO, 20: 10815 (UCRL-16338)
HAUNGS, G., Spectrum of monoenergetic Boltzmann equation in plane geometry, 20: 11936
HAUSER, J. J., Proximity effects between superconducting and magnetic films, 20: 11918
HAUTECLOQUE, Simone, Kinetic isotopic effect in the reaction of CCl_3 radicals with molecular H, 20: 10820
HAY, R. D., Heat transfer by circulation of super-critical helium, 20: 11925
HAYASHI, S., Method of analyzing beta-ray absorption data, 20: 12270
HAYBRON, R. M., Optical potentials and high-energy inelastic proton scattering, 20: 11974 (ORNL-P-960)
HAYDEN, Howard C., Low-energy ionization of argon atoms by argon atoms, 20: 11477
HAYMANN, Pierre, Bombardment of copper monocrystals with oxygen ions of medium energy (10 kev), 20: 12282
HAYNES, S. K., Postfocusing acceleration for $\pi\sqrt{2}$ spectrometer, 20: 11153
HAYWOOD, F. F., Operations plan—Operation HENRE, 20: 11930 (CEX-65.03)

HEALY, W. B., Extraction of submicrogram amounts of manganese using ^{54}Mn from bone, milk and teeth solutions, 20: 10950
HEESTAND, R. L., Thermochemical reduction of uranium hexafluoride, 20: 11257
HEIDEMAN, H. G. M., Inelastic electron scattering from H_2, 20: 11466
HEIKKINEN, D. W., Total cross sections and angular distributions of $^{12}C(^6Li,p)^{17}O$, $^{12}C(^6Li,d)^{16}O$, and $^{12}C(^6Li,\alpha)^{14}N$ reactions from 4.5 to 5.5 Mev, 20: 12059
HEIN, R. A., Critical magnetic fields of superconducting ruthenium isotopes and search for an isotope effect, 20: 11913
HEINRICH, H. C., Inhibition of whole-body incorporation and retention of ^{131}I in man, 20: 10543
HEINRICH, Robert R., Thermodynamic properties of LiH by an electromotive force method, 20: 10849
HEINZE, H. G., Radioiodine treatment of benign strumae in endemic goiter region of southern Germany, 20: 10748
HEINZE, H. G., Radioisotope nephrography during childhood, 20: 10734
HELD, Peter Christian, Vaporization of solid UO_2, 20: 11234 (IS-1300)
HELLMAN, O., Generalization of quantum electrodynamics with application to electronproton scattering, 20: 11593
HELLSTROEM, S., Applied gamma-ray spectrometry by germanium semiconductor detector, 20: 11134
HELLWARTH, R. W., Non-linear optics of many-particle systems, 20: 12255
HEMMER, P. C., Distribution of zeros of grand partition function, 20: 11788
HENDRICKS, S. J., Magnetic field data for trapped-particle evaluations, 20: 11834
HENKEL, Joel, Study of (d,p) reactions on light nuclei from 200 to 350 kev, 20: 12096
HENLEY, E. M., n-n And n-p scattering lengths and charge independence, 20: 11649
HENNESSY, J., Upper limit for the partial width $\Gamma(\rho \to \pi\gamma)$, 20: 11618
HENNICO, Alphonse, Segmented laminar flow and other models for packed-bed longitudinal dispersion, 20: 10995 (UCRL-10696(Rev.)(Pt.1))
HEREFORD, Frank L., Recombination luminescence in scintillation of normal and superfluid liquid helium, 20: 11904
HERNBORG, Gunnar, Burnout conditions for flow of boiling water in vertical 3-rod and 7-rod clusters, 20: 11000
HERRERA, J. C., Symmetry properties of beam handling magnet systems, 20: 11411
HERSCHBACK, K., Specimen holder for deuteron irradiation experimeats in metals between 4°K and room temperature, 20: 11410
HERTZBACH, Stanley Shipley, Decay of ρ^0, ω, and ϕ mesons into lepton pairs, 20: 11673
HESS, D. C., Survey of polarized ion sources in Europe, 20: 11379 (ANL-7118)
HETHERINGTON, J. H., Low energy K^--d elastic scattering, 20: 11630
HEWKA, Peter V., $^{17}O(d,p)^{18}O$ reaction and nuclear structure of ^{18}O, 20: 12055
HICKMAN, B. S., Comparison of neutron damage in zinc oxide and beryllium oxide, 20: 11359
HICKMAN, J. S., Prog. rpt. on high-sensitivity fast neutron dosimeter, 8–10/65, 20: 11094 (COO-1226-10)
HICKS, John W., Adjustable current shunt for trimming ampere turns in magnet operating from constant d-c source, 20: 11388 (CONF-650922-29)
HIEN, Fam Tsui, Investigation of nuclear quadrupole interaction in Moessbauer effect experiments, 20: 12314
HILDEBRAND, B., Modulations of generically related galactic cosmic rays, 20: 11525
HILL, C. W., Data compilation and evaluation of space shielding problems, 20: 12265 (NP-15697(Vol.1))
HILLMAN, Manny, Production of carrier-free ^{132}Cs and ^{129}Cs, 20: 10901
HILTZ, R. H., Effect of high temperature sodium on austenitic and ferritic steels, 20: 11235 (MSAR-65-194)
HINDLE, E. D., Preferred orientations in Zircaloy-2 tubing manufactured by various routes, 20: 11251
HINDMARCH, P., Examination of fuel elements irradiated in Calder Hall reactors to 4660 MWD/te or less, 20: 11357
HINNOV, E., Interpretation of atomic hydrogen light in C stellarator, 20: 12171 (MATT-270)
HINNOV, E., Loss rates of charged particles from ohmically-heated discharges in C-stellarator, 20: 12239
HIPP, A. L., Comparison of different methods of particle size analysis, 20: 11270 (LA-3424)
HIRAMOTO, Toshiyuki, Cosmic-ray contribution to background of NaI scintillation spectrometers, 20: 11132
HIRATA, Masashi, Multivariate regression analysis of sex ratio among offspring from irradiated women, 20: 10657
HIREL, Renee, System of electron grouping at input of linear accelerator, 20: 11393 (NP-15715)
HIYAMA, Yoshio, Maximum permissible concentration of radioactive materials in sea water, 20: 11054
HOCKING, D. R., Management of nuclear materials in research establishment, 20: 12560
HOCKING, J. E., Sodium-heated steam generator: stress analysis, 20: 12390 (BAW-1280-28(Vol.2))
HOCKING, J. E., Sodium-heated steam generator: effects of sodium–water reactions, 20: 12391 (BAW-1280-28(Vol.3))
HOEGBERG, T., Monte Carlo calculations in neutron thermalization in heterogeneous system. II., 20: 11935 (RFR-154)
HOEHLER, G., Analysis of πN charge exchange scattering from 4 to 18 Bev/c, 20: 11615
HOENIG, Arnost, Computation of thickness of concrete shielding walls against gamma radiation, 20: 12266 (ORNL-tr-918)
HOER, G., Methods and diagnostic value of radioisotope nephrography, 20: 10753
HOER, G., Radioisotope nephrography during childhood, 20: 10734
HOERZ, G., Total emission capacity of niobium, 20: 11314
HOESE, Fred O., Qualification tests of spray-deposited and light-initiated silver acetylide–silver nitrate explosive, 20: 10814 (SCL-DC-65-96)
HOFFENBERG, R., Studies of protein metabolism with labeled proteins and protein-like substances in nutritional disorders, 20: 10573
HOFFMAN, C. G., Behavior of coated particles in large nuclear transient (KIWI TNT), 20: 11343 (LA-3367)
HOFFMAN, C. M., Activation analysis of drugs, 20: 10880
HOFFMAN, Herbert S., Low energy associated production: $\pi^- + p \to K^0 + \Lambda$, 20: 11589
HOFFMANN, G., Development of 100-Mev FFAG electron synchrotron, 20: 11392 (NP-15275)
HOFMANN, F. W., Interpretation of atomic hydrogen light in C stellarator, 20: 12171 (MATT-270)
HOGE, K. G., Effect of strain rate on mechanical properties of some widely used engineering metals, 20: 11284 (UCRL-14599)
HOGLUND, R. L., Thermal diffusion column shape factors. I., 20: 10949 (K-1469)
HOHMUTH, K., Capture ratio P_L/P_K for electron capture decay of ^{57}Ni, 20: 11984
HOLM, Jens T., Critical appraisal of nuclear merchant ships, 20: 12459 (CONF-640810, pp 1-6)
HOLM, Jens T., Panel discussion: role of nuclear power in merchant marine, 20: 12460 (CONF-640810, pp 7-21)
HOLMES, D. E., Site of attack in radiolysis of pyrimidine compounds, 20: 10899
HOLMES-SIEDLE, A. G., High-energy radiation damage in silicon transistors, 20: 11182
HONECK, H. C., Physics of heavy-water lattices, 20: 12363 (TID-8541, pp 1-70)
HONG, Guy, Positron focusing in accelerating field, 20: 11399 (UCRL-7566(Rev.1))
HOOPER, J. W., Absolute cross sections for single ionization of alkali ions by electron impact. I., 20: 11489
HOOPER, J. W., Absolute cross sections for single ionization of alkali ions by electron impact. II., 20: 11490
HOPKINS, K. J., FAUST 1—hardcore discharge stability experiment, 20: 12222
HORIKAWA, Masazumi, Multivariate regression analysis of sex ratio among offspring from irradiated women, 20: 10657
HORNE, R. E., Determination of safety rod drop time in Enrico Fermi reactor, 20: 12387 (APDA-NTS-3)
HORNE, R. E., Worth measurements of core and blanket subassembly materials in Enrico Fermi reactor, 20: 12388 (APDA-NTS-6)
HORSTMAN, V. G., Biological effects of ^{131}I in sheep and cattle, 20: 10516 (BNWL-122, pp 49-51)
HORSTMAN, V. G., Sheep milk production and its ^{131}I content, 20: 10517 (BNWL-122, pp 52-4)
HOSCHEK, R., Lung x-ray variations by rare earths, 20: 11057
HOUGHTALING, J. E., Addendum to the Spert III hazards summary report—low-enrichment oxide core, 20: 12497 (IDO-17003(Rev.2))
HOUILLER, A., SR_2–SR_3–SR_4 electron irradiation loop, 20: 10871 (EUR-2288.f)
HOWARD, D. G., Internal field of ^{57}Fe in nickel from 77°K to Curie point, 20: 12298
HOWARD, Norman, Treatment of carcinoma of thyroid with radioiodine, 20: 10729
HOWE, C. D., Combined 5-fluorouracil and cobalt irradiation evaluated by double blind technique, 20: 10725
HOWE, D. G., Prog. rpt. on metallurgical characteristics of high strength structural materials, 5–7/65, 20: 11273 (NRL-6364)
HOWES, James E. Jr., Prog. rpt. on fission-product reactions with and release from fuel-element claddings, 7–9/65, 20: 11212 (BMI-X-10143)
HOY, John E., Savannah River plant criticality dosimetry system, 20: 11029 (DP-1006)
HRADIL, M., Radiocoulometric titrations, 20: 10769
HSI, Chang-sung, Determination of spectral characteristics of isotope neutron sources by means of paired scintillation crystals of type LiI(Eu), 20: 11116

HSIEH, J. J. C., Ultrahigh-speed gross alpha autoradiography, 20: 10529 (BNWL-122, pp 110-12)
HSIEH, Tai-ho, Determination of short range order in Ni–Mo alloys, 20: 11325
HSIEN, T. C., Process $\pi^- + p \rightarrow \tilde{p} + d$ and Regge poles, 20: 11590
HSU, H. H., Binary collision expansion of double-time-temperature-dependent Green's functions, 20: 11760
HU, Pung Nien, Structure of perpendicular shock wave in plasma, 20: 12227
HUANG, Rosalind, Study of non-mesic decay of helium hypernuclei, 20: 11977 (TID-22536)
HUBER, H., Hematologic changes in radiation damage, 20: 10660
HUBER, R. W., Prog. rpt. on metallurgical characteristics of high strength structural materials, 5–7/65, 20: 11273 (NRL-6364)
HUDECEK, Milan, Detection of uranium fuel element failures during inactive tests in CO_2 streams, 20: 11003
HUDSON, B., Techniques for observing fission gas bubbles in uranium, 20: 11220
HUDSON, R. P., Spin-lattice relaxation in some rare-earth trichlorides, 20: 12292
HUEGLI, H., Labeling of proteins with ^{131}I, 20: 10942
HUEGLI, H., Preparation of ^{131}I-polyvinylpyrrolidone, 20: 10946
HUFFMAN, J. C., Calorimetry in anhydrous ethylenediamine, 20: 12550 (TID-22564)
HUGHES, Ann M., Mechanism of sterility induced by D_2O in mice, 20: 10550
HUGHES, Harold K., Constant speed drive for Moessbauer experiments, 20: 11073
HUIZENGA, J. R., Deformation of transition-state nucleus in energetic fission, 20: 12077
HUIZENGA, J. R., Nuclear energy levels of ^{56}Fe and ^{59}Co, 20: 12063
HULL, G. W. Jr., Occurrence of superconductivity in sulfides, selenides, tellurides of Pt-group metals, 20: 11899
HULSE, C. O., High-temperature compressive deformation equipment, 20: 11285 (UCRL-16434)
HULTQVIST, Bengt, Electrostatic analysers, 20: 11158
HULTQVIST, Bengt, Height of auroral absorption obtained from satellite observations, 20: 11864
HULUBEI, H., Small-angle scattering of protons by ^{24}Mg, 20: 12003
HUMPHREY, Douglas L., Neutrons inelastically scattered from the 0.48 Mev level of ^{7}Li, 20: 12106
HUNDERE, I. A., Liquid scintillation determination of ^{239}Pu in pure and contaminated solutions, 20: 10763 (KR-100)
HUNGATE, F. P., Effects of moisture and air temperature on deposition and retention of $^{131}I_2$ on plants and soil, 20: 10717 (BNWL-122, pp 166-7)
HUNGATE, F. P., Ultrahigh-speed gross alpha autoradiography, 20: 10529 (BNWL-122, pp 110-12)
HUNSTEIN, W., Bioptic studies of therapy-induced bone marrow fibroses in chronic myeloid leukemia, 20: 10746
HUNT, Dale E., Induced mutation and amino acid protection against uv radiation in Hansenula wingei, 20: 10695
HUNT, Edward L., Ionizing radiation: neutral function and behavior, 20: 10689
HUNTER, B. R., Sampling and analysis of fission products during loss-of-fluid test (LOFT), 20: 12356 (IDO-17128)
HUQ, M., S-wave kaon-pion scattering, 20: 11601
HURWITZ, H. Jr., Gravitational instability in vertical magnetic field, 20: 11538 (65RL-3814E(Rev.))
HUSON, F. R., Upper limit for the partial width $\Gamma(\rho \rightarrow \pi\gamma)$, 20: 11618
HUSZAR, Miklos, Lepton decay of Λ^0 hyperon by modified vector boson propagator, 20: 11588
HUTCHINSON, D., Experimental test of time-reversal invariance in decay $K_L \rightarrow \pi^\pm \mu^\mp + \nu$, 20: 11662
HUTTON, P. H., Detection of metal overstress by acoustic emission, 20: 11001 (BNWL-SA-438)
HYDE, James L., Digital measuring apparatus utilizing radioactive source and detector, 20: 11085
HYNECEK, J., Resonance conditions in plasma acceleration, 20: 12197

I

IANNUZZI, M., Two models proposed for explaining self-excited oscillations in alkali plasma, 20: 12225
IBE, Librado D., Design study report on 1000 MWe breeder reactor, 20: 12414 (TID-22545, pp 16-52)
IBEL, K., Pulse transformer with two separate cores for time-to-pulse-height conversion, 20: 11117
ICHIKAWA, Ryushi, Strontium–calcium discrimination in rainbow trout, 20: 10555
ICHIKAWA, Yoshi H., Dielectric properties of weakly turbulent plasma, 20: 12229
ICHIKAWA, Yoshi H., Ion oscillations in weakly turbulent plasma, 20: 12178 (NP-15705)
IGNATENKO, A., Fission by radiationless transition in μ mesonic atom ^{239}Pu, 20: 12041
IIJIMA, Tsutomu, Space-dependent formula for Rossi-α measurements, 20: 12375
IINUMA, Takeshi A., Cosmic-ray contribution to background of NaI scintillation spectrometers, 20: 11132
IL'IN, R. N., Charge exchange of protons in alkaline metal vapor with formation of highly excited hydrogen atoms, 20: 11471
ILLY, Jozsef, Preparation of deuterium alcoholates, 20: 10850
IMRIS, P., Thermogravimetric study of oxidation of particles of UO_2 prepared from U_3O_8 calcinated under various conditions, 20: 10839
INOUE, Minoru, Flowmeter using neutrons, 20: 11080
INUISHI, Yoshio, Hall effect measurement of radiation effect on p-type silicon, 20: 11360
INUISHI, Yoshio, Radiation damage and annealing of GaAs laser diode, 20: 11178
INZAGHI, A., AIREK-PUL—version of kinetic code AIREK-MOD for periodically pulsed fast reactors, 20: 12395 (EUR-2552.e)
IRODOV, I. E., Collection of problems in atomic and nuclear physics, 20: 11376
IRVING, D. C., REACT and CONVRG FORTRAN subroutines for determining source convergence for Monte Carlo neutron transport code, 20: 11934 (ORNL-TM-1325)
ISACSSON, P., Quasi-free proton-proton scattering in light nuclei at 460 Mev, 20: 11948 (AD-624318)
ISAEV, P. S., Self-consistent calculation of K* resonance parameters, 20: 11669
ISBIN, Herbert S., Gamma-ray-induced chlorination of benzene, 20: 10900
ISIDORI, A., Effects of therapeutic doses of radioiodine on coagulative processes, 20: 10679
ISLAM, M. M., Dynamical inelasticity and high-energy p-p scattering, 20: 11652
ITO, Norio, Radiation shielding concrete incorporating boron carbide, 20: 11229
ITO, Sadato, Hiroshima atomic bomb irradiated patients who entered Hiroshima within the three days postattack period, 20: 10661
ITO, Sadato, Multivariate regression analysis of sex ratio among offspring from irradiated women, 20: 10657
ITOH, Susumu, Cosmic-ray contribution to background of NaI scintillation spectrometers, 20: 11132
IVANCHENKO, I. M., Reproduction of kinematical particle parameters by chamber pictures with account of inhomogeneity of magnetic field, energy losses, and Coulomb scattering, 20: 11100 (JINR-P-2467)
IVANNIKOV, A. T., Re-absorption of bicarbonates by kidneys injured by uranium and secretion of uranium from an organism, 20: 10553
IVANOV, I. I., Influence of ionizing radiation on contractive ability of mitochondria, 20: 10678
IVANOV, K. G., Interpretation of observations of sudden commencements of magnetic storms in space, 20: 11811
IVANOV, V. G., Influence of film chamber properties on accuracy of spatial reconstruction of recorded events, 20: 11101 (JINR-P-2468)
IVANOVSKII, G. F., Zone refining of molybdenum in high vacuum, 20: 11218
IWAMOTO, M., Flux jumps and training effect in multilayer Nb–Zr superconducting coil, 20: 11895
IWASHIA, Fumio, Device for cooling an accelerating tube, 20: 11420
IYENGAR, K. V. K., Study of $^{37}Cl(p,n)^{37}Ar$ reaction mechanism, 20: 12141
IZYUMOVA, T. G., Spin diffusion of nuclei in double electron-nuclear resonance, 20: 12311

J

JABLONOWSKI, Edward J., Prog. rpt. on fission-product reactions with and release from fuel-element claddings, 7–9/65, 20: 11212 (BMI-X-10143)
JACKSON, D. F., Interpretation of (p,2p) reaction in ^{10}B and ^{11}B, 20: 12032
JACOB, Maurice, Consequences of C-violating interactions in η^0 and X^0 decays, 20: 11634
JACOBS, J. M., Interpretation of conductivity of porous and dispersed media with the aid of cubic cellular geometric models, 20: 10997 (AERE-Trans-1038)
JACOBS, K. G., Ionospheric plasma density by three different methods, 20: 11847
JACQUES, Gabriel, Segmented laminar flow and other models for packed-bed longitudinal dispersion, 20: 10995 (UCRL-10696(Rev.)(Pt.1))
JACQUESSON, Jacques, Determination of number of neutrons emitted simultaneously by source, 20: 11947
JADRESIC, A., Pituitary destruction by implantation of ^{90}Y in advanced cases of breast cancer, 20: 10752
JAEGERHUBER, P., Examination of radioactivity of food in Baden-Wuerttemberg, 20: 11017
JAEHNIGEN, U., Ordered AB and AB_3 phases in T_8–T_9 alloy systems and modified Mo–Ir phase diagram, 20: 11309
JAFAR, J. D., Elastic n-p charge-exchange scattering at 8 Bev/c,

20: 11606
JAGADEESAN, K., Hydromagnetic flow against rotating disc, 20: 11778
JAIN, B. K., Distorted wave Born approximation calculation for (^{3}He,p) reactions, 20: 12127
JAKEMAN, E., Nuclear pairing energies with simple interactions, 20: 12049
JAKLEVIC, R. C., Electrodynamic study of Josephson tunneling in superconducting junctions, 20: 11910
JAKLI, Gyoergy, Preparation of deuterium alcoholates, 20: 10850
JAKSIC, B., Asymptotic behavior of phase shift in λ for strongly singular potentials, 20: 11712
JAMES, Frederick Edward, Interactions of positive π mesons with protons at 2 Bev, 20: 11672
JAMES, L. W., Possible observation of ^{115}In nuclear electric hexadecapole transitions, 20: 12304
JANCSO, Gabor, Preparation of deuterium alcoholates, 20: 10850
JARAIZ FRANCO, E., Welding procedures used in fabrication of fuel elements for DON reactor exponential experiment, 20: 12401 (JEN-156-DMe/113)
JARNUM, S., Measurement of gastro-intestinal protein loss by means of ^{131}I-labeled protein, 20: 10567
JARNUM, S., Radioisotope techniques for study of protein turnover, 20: 10561
JASIELSKA, A., Q-values and cross-sections measurements of (n,α) reaction on some nuclei, 20: 11983
JASKOLA, M., Energy levels of ^{8}Be produced in ^{11}B(n,α)^{8}Li → ^{8}Be, 20: 11962 (INR-655/1/PL)
JAWOROWSKI, Z., Half lives and effective equilibrium of RaD(^{210}Pb) and RaF(^{210}Po) in dogs, 20: 10544
JAYET, C., SR_2–SR_3–SR_4 electron irradiation loop, 20: 10871 (EUR-2288.f)
JEEJEEBHOY, K. N., Preparation of ^{3}H-labeled proteins, 20: 10945
JEEJEEBHOY, K. N., Radioisotope techniques for study of protein absorption, 20: 10566
JEFFRIES, C. D., Spin-lattice relaxation in some rare-earth salts. I., 20: 12300
JELEN, J., Accelerating clusters of plasma in external magnetic field, 20: 12196
JELEN, J., Resonance conditions in plasma acceleration, 20: 12197
JENKIN, C. R., Synthesis of macroglobulin antibody to bacterial antigen in mice after treatment with Thorotrast, 20: 10617
JENSEN, Monika, Bibliography on dispersion-strengthened materials, 1964, 20: 11278 (RISO-48(Suppl.2))
JEPSON, M. D., Examination of fuel elements irradiated in Calder Hall reactors to 4660 MWD/te or less, 20: 11357
JESENAK, V., Radiocoulometric titrations, 20: 10769
JESPERSEN, M., Electron density and collision frequency during auroral absorption event, 20: 11848
JEX, H., Bibliography on slow neutron detectors, 20: 11088 (AED-C-28-01)
JIRASEK, L., Occupationally caused bone changes by external radiation burdens, 20: 10637
JNANANANDA, Swami, Absolute photoelectric cross sections of 320-kev γ rays in Pb, Sn, and Ag, 20: 11496
JNANANANDA, Swami, Incoherent scattering of γ rays by K-shell electrons, 20: 11514
JNANANANDA, Swami, Level widths of some 2^+ states, 20: 12147
JOFFRE, Henri, Application of dosimetry by thermoluminescence to radioprotection, 20: 11041
JOHANNIN-GILLES, Andree, Absorption spectra of water and heavy water in the ultraviolet, 20: 10823
JOHANNSEN, K., Application of carbides in high-temperature reactors, 20: 12378
JOHN, Joseph, Study of nuclear reactions resulting from proton bombardment of ^{27}Al, 20: 12142
JOHNSON, Carl E., Studies of Li hydride systems. II., 20: 10832
JOHNSON, Carl E., Studies of Li hydride systems. III., 20: 10833
JOHNSON, Carl E., Thermodynamic properties of LiH by an electromotive force method, 20: 10849
JOHNSON, E. B., Criticality of single unit of aqueous uranyl fluoride solution enriched to 5% in ^{235}U, 20: 12359 (ORNL-TM-1195)
JOHNSON III, J. P., Spot patterns and Silsbee chains on Cu single crystal, 20: 11460
JOHNSON, James E., Separation and recovery of fallout ^{137}Cs from Zr–^{95}Nb in forage samples, 20: 10782
JOHNSON, R. H., Field sampling of ^{131}I in milk with ion exchange cartridges, 20: 10722
JOHNSON, Richard Elwyn, Influence of system geometry on fracture toughness, 20: 12555 (WAPD-T-1828)
JOHNSON, V. P., Rocky Flats body counter, 20: 11107 (RFP-462)
JOHNSON, Walter H. Jr., Isotopic masses of hydrogen, chlorine, barium, cerium, and neodymium, 20: 11494
JOHNSTON, D., Magnetic-dipole intensities and Zeeman effect in Cs_2UCl_6, 20: 12290
JOHNSTON, R. L., Designs and descriptions of mechanical subsample cutters used in reducing uranium concentrate sample sizes, 20: 10978 (RMO-3006)
JOKIPPI, Jack Randolph, Physics of solar wind, 20: 11437
JONES, B. D., Elastic n-p charge-exchange scattering at 8 Bev/c, 20: 11606
JONES, C. E., SRE-PEP moderator elements, 20: 12404 (NAA-SR-11160)
JOON, K., Liquid scintillation determination of ^{239}Pu in pure and contaminated solutions, 20: 10763 (KR-100)
JORDAN, J. A. Jr., Collision-induced mixing in first excited states of sodium and potassium, 20: 11499
JORDAN, W. H., Nuclear safety, 20: 11045
JOSHI, G. C., Regge poles in πN scattering, 20: 11647
JOZEFOWICZ, E. T., Separation of neptunium from neutron irradiated uranium by reversed-phase partition chromatography in the TBP–HNO_3 system, 20: 10954
JUDD, B. R., Hypersensitive transitions in rare-earth ions, 20: 11469
JUDD, B. R., Three-particle operators for equivalent electrons, 20: 11475
JUDY, R. W. Jr., Prog. rpt. on metallurgical characteristics of high strength structural materials, 5–7/65, 20: 11273 (NRL-6364)
JULLIAN, S., Electrodisintegration of deuteron around $q^2 = 3.5F^{-2}$, 20: 11645
JUNG-KOENIG, W., Effect of neutron irradiation on properties of alloy Zr–3Nb–1Sn, 20: 11354

K

KAALEN, J., Therapeutic scope of radiation, 20: 10744
KABAT, Miloslav, Safety and dosimetric problems in exploration of nuclear power plants, 20: 11042
KADANOFF, Leo P., Green's functions and superfluid hydrodynamics, 20: 11898
KAELLEN, G., Momentum-space analyticity properties of Bergman-Weil integral for three point function, 20: 11726
KAESER, H., Metabolism of gamma-globulin in agammaglobulinaemia and hypogammaglobulinaemia, 20: 10572
KAESTNER, H., Capture ratio P_L/P_K for electron capture decay of ^{57}Ni, 20: 11984
KAGA, Makio, Container of nuclear reactor, 20: 12348
KAGAN, Yu., Suppression of inelastic channels in resonance scattering of neutrons in regular crystals, 20: 12313
KAHLER, E. Jack, Radiation-induced formation of organometallic compounds with particular emphasis on organotins, 20: 10870 (BMI-1753)
KAISER, P., Ionospheric plasma density by three different methods, 20: 11847
KAISER, T. R., Development of the radio-aurora, 20: 11859
KAISER, T. R., Low frequency propagation and probe experiments, 20: 11846
KALASHNIKOV, V. K., Flow near stagnation point in presence of magnetic fields parallel and normal to body surface, 20: 11795
KALITIN, V. I., Magnetic properties of single and polycrystalline praseodymium diselenide $PrSe_2$, 20: 12310
KALLOSH, R. E., Quantum field theory equations in axiomatic approach, 20: 11765
KALMA, A. H., Photoconductivity studies in 10- to 50-Mev electron-irradiated silicon, 20: 11351 (NP-15611, pp 48-89)
KALMA, Arne H., Electrical properties of 50-Mev electron-irradiated germanium, 20: 11350 (NP-15611, pp 39-46)
KALMYKOVA, S. S., Excitation of magnetohydrodynamic waveguide by coaxial waveguide, 20: 12208
KAL'NITSKII, R. M., Plasticity and strength of tungsten during short-time tests, 20: 11339
KALUGIN, V. N., Magnetic systems of magnetogasdynamic generators, 20: 11548
KAM, Francis B. K., Solution of LaGrange multiplier problem with several constraints, 20: 12544 (ORNL-3846)
KAMINKER, D. M., Reduction of radioactive emission into atmosphere and deaeration of WWR-M Reactor water, 20: 12504
KAMIYA, Y., Momentum spectrum of cosmic-ray muons at large Zenith angles, 20: 11526
KANARIS, A. D., Isotope shift in muonic K x rays of ^{16}O–^{18}O, ^{40}Ca–^{44}Ca, ^{116}Sn–^{124}Sn, and ^{155}Gd–^{160}Gd, 20: 11480
KANAVETS, V. P., Polarization in elastic p-p scattering at high energies, 20: 11591
KANAYA, H., Observation of partial shrinkage of strata, 20: 11024
KANAZAWA, Teruko, ^{90}Sr and ^{137}Cs in Columbia River plume, July 1964, 20: 11023
KANE, Joseph W., Green's functions and superfluid hydrodynamics, 20: 11898
KANE, R. P., Sidereal component of diurnal variation of cosmic-ray intensity, 20: 11524
KANE, Robert, Fracture in connection with hot deformation processing of

metals, 20: 11265 (AD-626375)
KANEKO, Eiji, Design of reactor period meter, 20: 12344
KANESEKI, N., Flux jumps and training effect in multilayer Nb–Zr superconducting coil, 20: 11895
KANESTROEM, I., Magnitudes of some reduced transition probabilities in ^{6}Li, 20: 12039
KANG, Ik-Ju, Fictitious nature of "core term" in exchange amplitude for electron-atom scattering, 20: 11473
KANO, Yutaka, New phase-space distribution function in statistical theory of electromagnetic field, 20: 11880
KANTZ, Melvin R., Bibliography on pentaerythritoltetranitrate, 20: 10862 (MLM-1252)
KANZAKI, Shizuo, Relay circuit using radiation counter, 20: 11084
KAO, Mei-juan, Effect of pair correlation on α decay in neighborhood of ^{208}Pb, 20: 12093
KAPLAN, Morton, Stopping of energetic copper ions in aluminum, 20: 12085
KAPLOW, Roy, Influence of anisotropic Moessbauer effect on magnetic hyperfine splittings in polycrystalline materials, 20: 12299
KAPOOR, R. N., Reactions of samarium isopropoxide with methylacetoacetate, 20: 10846
KAPULLA, H., Status report on in-pile doimetry in the Federal Republic of Germany, 20: 11147
KAPUSTIN, I. N., Method of determining dead time of nuclear radiation counters, 20: 11125
KARAPETYAN, S. K., Stimulating effect of certain doses of ionizing radiation on ovogenous function of bird ovary, 20: 10626
KARASEK, F. J., Fabrication of 20 wt % Ti–V alloy tubing for nuclear fuel cladding, 20: 11258
KARMOHAPATRO, S. B., Loss of fast negative ions in atomic collisions, 20: 11517
KARNAUKHOV, V. A., Proton emitters among Te isotopes, 20: 11964 (JINR-E-2464)
KARNIKOVA, Eva, Investigation of uranium and zirconium compatibility by means of microanalyser with electron probe, 20: 11316
KAROUSAKIS, Panos, Thermal analysis, 20: 12416 (TID-22545, pp 67-80)
KARPENKO, D. Ye., Vector meson in Coulomb field, 20: 11668
KARPINSKII, O. G., Crystal structure of compound Zr_5Si_3, 20: 11337
KARTASHEVA, L. I., Yield of phenol in radiolysis of aqueous sulfate solutions of benzene containing divalent iron ions and oxygen, 20: 10878
KATAOKA, Iwao, Gamma-ray transmission through multiple layers, 20: 12271
KATSANOS, A. A., Nuclear energy levels of ^{56}Fe and ^{59}Co, 20: 12063
KATSANOS, N. A., Nature of inorganic ^{82}Br in neutron-irradiated bromobenzene, 20: 10890
KATSAURAGI, Yukio, ^{90}Sr and ^{137}Cs in Columbia River plume, July 1964, 20: 11023
KATSUURA, K., Mechanism of decay of vinyl unsaturation during radiolysis of Marlex-50 polyethylene, 20: 10893
KATTCHEE, N., HECTIC-II—IBM 7090 FORTRAN computer program, 20: 10989 (IDO-28595(Rev.))
KATTCHEE, N., Local film coefficients on ML-1 fuel elements due to boundary layer turbulence promoters, 20: 10988 (CONF-12-5)
KATTCHEE, N., Mass transfer analogy studies of shaped turbulence promoter performance, 20: 10993 (TID-22513)
KAUS, P., Theory of reggeized bootstraps, 20: 11751
KAUTZLEBEN, H., Statistical analysis of main part of geomagnetic field. II., 20: 11815
KAUTZLEBEN, H., Statistical analysis of main part of geomagnetic field. I., 20: 11814
KAWAHARA, Masao, Electrode for small dosimeter, 20: 11164
KAWAI, T., Flux jumps and training effect in multilayer Nb–Zr superconducting coil, 20: 11895
KAWAMOTO, Hiroshi, Spectrographic determination of strontium and calcium in bone ash, 20: 10774
KAWARABAYASHI, K., Baryon magnetic-moment sum rules in broken SU_3 and SU_6 symmetries, 20: 11743
KAWASHIMA, Masao, Electron-beam irradiation apparatus, 20: 10984
KAWASHIMA, Nobuki, Ion temperature measurement of streaming He plasma by double probe method, 20: 12186
KAY, M. A., Ion exchange in fused salts. I., 20: 10958
KAYAS, G., Exchange mechanism for $\pi^+ p \to N^* \rho^0$ reaction at 2.75 Bev/c, 20: 11605
KAZANSKII, Yu. A., Secondary γ-emission coefficients for aluminum, copper, and tungsten, 20: 12267
KAZARINOV, Yu. M., Pion production in (n-p) collisions at 600 Mev, 20: 11564 (JINR-P-2462)
KAZATCHKOVSKY, O. D., Nuclear power plant BN-350, 20: 12441
KAZZAZ, A. A., Naphthalene excimer emission, 20: 10854
KEENE, A. R., Administration of radiation safety at Hanford, 20: 11046
KEENE, J. P., Determination of some fast reaction rates using pulsed radiolysis of permanganate solutions, 20: 10914
KEENE, J. P., Formation of Cu^{III} in radiolysis of Cu^{2+} solutions, 20: 10923
KEENE, J. P., Pulse radiolysis studies of carboxyl and related radicals, 20: 10913
KEENE, J. P., Pulse radiolysis studies of aqueous polymer-thiourea systems, 20: 10921
KEENE, J. P., Pulse radiolysis of Ag^+ solutions, 20: 10922
KEENE, J. P., Pulse radiolysis study of methylene blue, 20: 10925
KEENE, J. P., Symposium on pulse radiolysis, Manchester, 4/65, 20: 10906
KEENE, J. P., Technique of pulse radiolysis by optical absorption, 20: 10907
KEENE, J. P., Transient absorption from 260-320 nm in certain pulse irradiated aqueous solutions, 20: 10924
KEGLEY, T. M. Jr., Examination of failed expansion bellows between EGCR containment shell and experimenters cell 6, 20: 12411 (ORNL-TM-1380)
KEHOE, Brandt, Design of scanning template for associating Λ^0 decays with Ξ^0 production vertices, 20: 11111 (TID-22550)
KEIRIM-MARKUS, I. B., Dosimetric investigations and shielding studies using synchrocyclotron, 20: 10605 (NASA-TT-F-353, pp 21-54)
KELLER, J. M., Preparation of highly enriched ^{13}C by thermal diffusion of methane, 20: 11194
KELLER, O. L. Jr., Modified Debye-Scherrer x-ray diffraction camera for radioactive compounds, 20: 11075
KELLERBAUER, A., Thermonuclear injuries, 20: 10701
KELLY, A., Yielding effects in magnesium–0.5% thorium alloy, 20: 11301
KELLY, C. N., Fast-pulse recording and readout device using tunnel diodes, 20: 11065 (SC-TM-323-62(72))
KELSON, Itzhak, New nuclidic mass relationship, 20: 12090
KEMME, J. E., Survey of Los Alamos and Euratom heat pipe investigations, 20: 11545 (LA-DC-7555)
KEMP, T. J., Quenching of excited states formed in pulse radiolysis, 20: 10926
KEMPTHORNE, O., Randomization tests for comparing survival curves, 20: 10618
KENAHAN, C. B., Corrosion properties of molybdenum, tungsten, vanadium, and some vanadium alloys, 20: 11230 (BM-RI-6715)
KENNEDY, R. S., Test graphite filler log handling machine, 20: 12405 (NAA-SR-Memo-11576)
KENNEL, C. F., Limit on stably trapped particle fluxes, 20: 11820
KENT, K. G., Yielding effects in magnesium–0.5% thorium alloy, 20: 11301
KEOUGH, R. F., Gastrointestinal absorption of ^{144}Ce and ^{147}Pm in miniature swine, 20: 10525 (BNWL-122, pp 85-90)
KEREKATTE, S. S., Study of nuclear reactions resulting from proton bombardment of ^{27}Al, 20: 12142
KERLIN, T. W., Status of space-time analysis, 20: 12334
KERNAN, Anne, Measurement of N^{*-}-N^{*++} mass difference, 20: 11624
KERR, J. R. W., Fallout in London rainwater during 1964, 20: 11018
KERRISK, J. F., Behavior of coated particles in large nuclear transient (KIWI-TNT), 20: 11343 (LA-3367)
KERTESZ, Z. I., Effect of gamma radiation upon cherries, 20: 11186
KESSLER, Paul, Problem of nuclear interactions of ultra-energetic muons of cosmic radiation, 20: 11975 (PAM-6502)
KESSLER, W. V., Liquid scintillation detector for evaluating phototubes and determining gamma-ray activities, 20: 11128
KETELAAR, J. A. A., Properties of ionic liquids and mixtures, 20: 10804 (EUR-2466.e, pp 9-19)
KEVAN, Larry, Energy transfer in radiolysis of rare-gas–C_2F_6 mixtures, 20: 10884
KHACHATURYAN, M. N., γ-Quanta detecting by using spark chamber and total absorption Cherenkov counter, 20: 11099 (JINR-P-2436)
KHADKIKAR, S. B., Nucleon-nucleon correlation in L = 0 state, 20: 12131
KHAMIDOV, O. Kh., Metallic compounds of rhenium with rare earth metals, 20: 11298
KHAN, J. M., Microgram surface density measurements by observation of proton-produced x rays, 20: 11281 (UCRL-12107)
KHAN, J. M., Treatment of proton channelling by a transverse two-dimensional model, 20: 12279 (UCRL-12311)
KHAN, M. Z. Rahman, Imaginary part of nuclear optical potential at low energies, 20: 12129
KHANNA, F. C., Solutions of Aitchison equation for final state interaction, 20: 12016
KHANTADZE, A. G., Construction of magnetohydrodynamic model of cyclone. II., 20: 11783
KHANTADZE, A. G., Two-dimensional flow of electrically conducting medium in presence of mass forces and flat magnetic field, 20: 11808
KHELASHVILI, A. A., Asymptotic relations between cross sections for baryon resonance production, 20: 11729
KHOROSHAVIN, V. D., Nuclear desalination equipment of low capacity, 20: 12454 (JPRS-33480)
KHOROSHKOV, V. S., Pulsed ion source with point cathode (needle), 20: 11394 (NP-15788)
KHRIPLOVICH, I. B., Gravitation and finite renormalization in quantum electrodynamics, 20: 11867 (NP-15762)
KIBBLE, T. W. B., Relativistic transformation laws for thermodynamic

variables, 20: 11797
KICHEV, A. Z., Determination of spectral characteristics of isotope neutron sources by means of paired scintillation crystals of type LiI(Eu), 20: 11116
KIEFER, H., Radiophoto-luminescence dosimetry, 20: 11140
KIEFER, John H., Vibrational relaxation of deuterium by a quantitative Schlieren method, 20: 11785
KIEFER, John H., Vibrational relaxation of hydrogen, 20: 11786
KIER, P. H., RIFF RAFF—program for computation of resonance integals in two-region cell, 20: 12351 (ANL-7033)
KILB, R. W., Calculation of current and potentials for segmented electrode MHD generator, 20: 11539 (65RL-3888E)
KILB, R. W., Theory of ion detection from plasma imbedded in magnetic field, 20: 12162 (65RL-3998E)
KILPATRICK, John E., Quantum-mechanical pair-correlation function of ^{4}He gas at low temperatures, 20: 11897
KIM, Sedong, Measurement of N^{*-}-N^{*++} mass difference, 20: 11624
KIMELDORF, Donald J., Ionizing radiation: neutral function and behavior, 20: 10689
KIMONT, E., Engineering development of 1200°F sodium vapor trap, 20: 10982
KINBARA, Seturo, Gamma-ray pulse dosimeter, 20: 11137
KINCHIN, G. H., Plutonium in thermal reactors, 20: 12379
KING, J. S., Neutron scattering in stretch-oriented polyethylene, 20: 10865
KING, James Jr., Theory of low-temperature chromatographic separation of hydrogen isotopes, 20: 10939
KING, John G., Hyperfine structure and octopole interaction in stable bromine isotopes, 20: 11502
KINGSBURY, F. D., Effects of neutron irradiation on stress-rupture properties of high-temperature precipitation hardening alloys, 20: 11358
KIRBY, L. J., Promethium compatibility and encapsulation studies, 20: 11267 (BNWL-SA-488)
KIRCHER, John F., Radiation-induced formation of organometallic compounds with particular emphasis on organotins, 20: 10870 (BMI-1753)
KIRKBRIDE, L. D., Molten plutonium burnup experiment, 20: 12403 (LA-3384)
KIRKO, Igor' Mikhailovich, Magnetohydrodynamics of liquid metals, 20: 11771 (NP-tr-1346)
KIRSCHLER, L. H., Effect of high temperature sodium on austenitic and ferritic steels, 20: 11235 (MSAR-65-194)
KIRST, T. R., Electron probe surface mass spectrometry study of oxygen on molybdenum, 20: 11322
KIRZ, J., Secondary peak at $t = -1$ (Bev/c)^2 in high energy π^-p charge exchange scattering, 20: 11614
KIRZHNITS, D. A., Nonunique solutions for problem on scattering, 20: 11763
KISER, Robert W., Spectrophotometric study of the Nd^{2+}–NO_3 association, 20: 10848
KISS, I., Influence of ionizing radiations on growth of brewing barley, 20: 10619
KITANO, Masami, Symmetry of ^{131}I 4-iodoantipyrine uptake by brain after intravenous injection, 20: 10750
KITAO, Kensuke, Status of reactors for biological and medical use, 20: 10507
KLAS, J., Determination of equivalence point in radiometric precipitation titration by measurement of activity of the precipitate, 20: 10777
KLAS, J., Theoretical considerations on reflection of β radiation in precipitation titration, 20: 10778
KLASSOVSKII, Yu. A., Effectiveness of hormone therapy in radiation injuries, 20: 10709
KLEIN, Melvin P., Nuclear spin and moment of ^{110m}Ag by paramagnetic resonance, 20: 12073
KLEMM, A., Ion mobilities in molten salts, 20: 10806 (EUR-2466.e, pp 31-8)
KLEPPNER, D., Hyperfine separation of deuterium, 20: 11481
KLEY, W., Use of pulsed reactors in field of neutron and solid state physics, 20: 12495 (EUR-2538.e)
KLICKMAN, A. E., Determination of safety rod drop time in Enrico Fermi reactor, 20: 12387 (APDA-NTS-3)
KLIMA, R., Stationary state of plasma in magnetostatic and h-f field, 20: 12195
KLINE, K. H., New heat transfer protection system for sodium reactor experiment, 20: 12406 (NAA-SR-Memo-11648)
KLINKNER, K. C., Post assembly electrical checkout of 10FS-5 in building 013, 20: 12469 (NAA-SR-Memo-11630)
KLYUCHAREV, A. P., Total nuclear decay reactions, 20: 12004
KNIPPING, H. W., Neutron capture therapy, 20: 10728
KNOBLOCH, V., Use of EDTA for radiometric determination of traces of metals by means of electrophoresis, 20: 10792
KNOCHE, Jayne, Electron bremsstrahlung from proton-excited targets, 20: 11501
KNOWLES, Paul H., Reconnaissance for uranium in the Lonquimay Area, Province of Malleco, Chile, 20: 11025 (RME-4552(Rev.))
KOBAYAKAWA, Keizo, Four momentum transfer in jet showers and multi-fireball models, 20: 11530
KOBAYAKAWA, Keizo, Two-center model and four momentum transfer in jets, 20: 11531
KOBAYASHI, Akira, Radiation monitor using magnetic amplifier, 20: 11162
KOBAYASHI, Tetsuro, Theoretical approach to very high energy phenomena, 20: 11529
KOBAYASHI, Tsunehiro, Analysis of high energy jet showers. IV., 20: 11535
KOBISK, E. H., Preparation of isotope targets by electron-bombardment techniques, 20: 11183 (ORNL-P-1900)
KOBLET, H., Determination of total clearance of different preparations of gamma-globulin, 20: 10571
KOBLET, H., Interpretation of results of protein turnover studies, 20: 10565
KOBLET, H., Measurement of gastro-intestinal protein loss by means of ^{131}I-labeled polyvinylpyrrolidone, 20: 10568
KOBLET, H., Metabolism of gamma-globulin in agammaglobulinaemia and hypogammaglobulinaemia, 20: 10572
KOBLET, H., Simplified method for clinical study of protein turnover, 20: 10564
KOCMIERSKA-GRODZKA, Danuta, Changes in osmotic resistance of white blood cells in postradiation disease in rats, 20: 10614
KODA, Shigeyasu, Precipitation on dislocations in beryllium–3% iron alloy, 20: 11299
KODYUKOV, V. M., Applied dosimetry, 20: 11058
KOEHLER, W., Role of resonance activation integral in activation determination of silver, 20: 10789
KOEPPE, A., Apparatus for simulating heat transfer from reactor surface to thermionic converters, 20: 12487
KOESTER, L. J. Jr., Experimental study of reaction ^{3}He$(\gamma,\pi^+)^3$H up to 260 Mev, 20: 12046
KOESTER, Werner, Constitution of systems of europium with silver, cadmium and indium and system cadmium–strontium, 20: 11327
KOFOID, M. J., Production of large-diameter low-voltage electron beams in absence of magnetic field, 20: 11367 (D1-82-0448)
KOHAUPT, R. D., Radiative corrections for e-p scattering for angular and energy coincidence experiments, 20: 11556 (DESY-65/14)
KOHIN, Roger P., Electron spin resonance studies of γ-irradiated ferroelectric methylammonium alum crystals, 20: 12291
KOIAVA, V. K., Twenty-seven-day variations of geomagnetic field disturbance on zero-days of cosmic-ray intensity, 20: 11818
KOK, G., Some aspects of fractionated irradiation in clinical studies, 20: 10743
KOLAR, J., Generalized skeletal response to local radiation injury, 20: 10587
KOLAR, J., Occupationally caused bone changes by external radiation burdens, 20: 10637
KOLDOVSKY, P., Relationship of radioresistance and immunoresistance in an experimental tumor, 20: 10634
KOLESNIK, V. G., γ-Quanta detecting by using spark chamber and total absorption Cherenkov counter, 20: 11099 (JINR-P-2436)
KOLESNIKOV, V. N., Use of highly ionized plasma for fabrication of laser, 20: 12209
KOLLEKOWSKI, J., Application of carbides in high-temperature reactors, 20: 12378
KOLM, H. H., Heat transfer by circulation of super-critical helium, 20: 11925
KOLOUSEK, J., Urinary radiophosphorus ^{32}P levels in rats after single 2,4-dinitrophenol administration prior to 600-r x irradiation, 20: 10666
KOLTUN, D. S., Production and absorption of s-wave pions at low energy by two nucleons, 20: 11642
KOMAI, Kenichiro, Charged-particle accelerator, 20: 11421
KOMAI, Kenichiro, Charged-particle accelerator, 20: 11422
KOMAI, Kenichiro, Travelling-wave type electron accelerator, 20: 11419
KOMOCHKOV, M. M., Passage of high energy neutrons through heavy concrete, 20: 12263 (JINR-P-2479)
KOMURO, Kojiro, Welding method for capsule, 20: 11263
KONDAIAH, E., Study of Ne(n,p) reaction at E_n = 14.1 Mev, 20: 12118
KONDAISAH, E., ^{40}Ca(n,α)^{37}Ar angular distribution at E_n = 4.7 Mev, 20: 12119
KONDAISH, E., Study of ^{37}Cl(p,n)^{37}Ar reaction mechanism, 20: 12141
KONDRATENKO, A. N., Kinetic theory of electromagnetic waves in limited plasma, 20: 12212
KONDRATEV, V., Structure of atoms and molecules, 20: 11512
KONOBEEVSKII, S. T., Strengthening metals and alloys by irradiation, 20: 11366
KONONOV, V. N., Cross sections for fast neutron radiative capture in rhenium and tantalum, 20: 11986
KONOPLEV, K. A., Reduction of radioactive emission into atmosphere and deaeration of WWR-M Reactor water, 20: 12404
KOPANETS, E. G., Excitation function of reaction ^{36}S(p,γ)^{37}Cl in interval E_p = 1.4–2.1 Mev, 20: 12005
KOPP, P. M., Pulse radiolysis studies of aqueous polymer-thiourea systems,

20: 10921
KOPYLOV, G. I., Forbidden configurations in three-photon system, 20: 11686 (JINR-P-2447)
KORDA, Yu. S., Excitation function of reaction $^{36}S(p,\gamma)^{37}Cl$ in interval $E_p = 1.4-2.1$ Mev, 20: 12005
KORECZ, K., Effect of local β irradiation on corneal metabolism of rabbits, 20: 10585
KORIDGE, V. G., Twenty-seven-day variations of geomagnetic field disturbance on zero-days of cosmic-ray intensity, 20: 11818
KORKISCH, J., Anion exchange separation of thorium from rare earth elements in acetone–nitric acid medium, 20: 10959
KORNILOV, I. I., Creep behavior of Ti–Zr–Al–Sn system, 20: 11335
KORNILOV, I. I., Phase equilibrium of alloys in Ti_3Al–Zr section of ternary Ti–Al–Zr system, 20: 11333
KORNILOV, I. I., Phase structure of alloys of Ti–Al–Zr system in Ti_3–Al–Zr section, 20: 11334
KOROLEVA, Yu. I., Radioprotective effects of inert gases and low-molecular narcotics. IV., 20: 10712
KORONCZAY, Laszlo, Investigations in field of radiation-induced solid state polymerization. X., 20: 10897
KORST, W. L., Interaction of mercury and metal hydrides, 20: 10812 (NAA-SR-Memo-11569)
KORYAKIN, Yu. I., Nuclear desalination equipment of low capacity, 20: 12454 (JPRS-33480)
KOSHURNIKOVA, N. A., Combined effects of ^{90}Sr, ^{144}Ce, and ^{239}Pu on organs of rats, 20: 10552
KOSMOWSKI, A., Radioactivity of water and its control, 20: 11021
KOSTIAL, K., Effects of dietary levels of P and Ca on comparative behavior of Sr and Ca, 20: 10549
KOTOV, A. G., Mechanism of non-additive formation of radicals in radiolysis of frozen $CCl_4 + CH_3OH$ solutions, 20: 10879
KOVAC, L. R., Analysis of Babcock and Wilcox full-size steam generator for sodium–water reaction, 20: 12386 (APDA-176)
KOVAL', A. A., Excitation function of reaction $^{36}S(p,\gamma)^{37}Cl$ in interval $E_p = 1.4-2.1$ Mev, 20: 12005
KOVALEV, E. E., Characteristics of the radiation effect under space flight conditions and ways to determine admissible radiation levels, 20: 10719 (NASA-TT-F-353, pp 3-20)
KOVALEV, E. E., Dosimetric investigations and shielding studies using synchrocyclotron, 20: 10605 (NASA-TT-F-353, pp 21-54)
KOVALEV, V. A., Different behavior of uranium and thorium during lithogenesis of many-colored deposits, 20: 11026
KOVOOR, Aries, Radiorestoring action of fraction extracted from tobacco leaves, 20: 10620
KOWALSKA, K., Tables of functions $x(c,\nu)$ and $x_\pm(c_1,c_2)$ for numerical solution of slab geometry neutron transport problems, 20: 11933 (INR-630/IX-A/PR(Pt.2))
KOZIOL, J. J., Prog. rpt. on UO_2 fuel systems, 3/31/65, 20: 12377 (CEND-2863-236)
KOZLOV, V. A., Radioprotective and pharmaceutical effects of β-mercaptopropylamine, 20: 10714
KOZLOV, Yu. P., Free-radical processes taking place in irradiated homogenates of animal tissues, 20: 10577
KRAAK, W., Anion exchange separation between americium and curium and between several lanthanide elements, 20: 10956
KRACIK, J., Circular autostable path of magnetohydrodynamic plasma accelerator, 20: 12199
KRACIK, J., Plasma induction accelerator with radial magnetic field, 20: 12198
KRAMER, E. L., Place and function of RCN, 20: 12556
KRAMER, G., Inelastic electron-deuteron scattering with final-state interactions, 20: 11666
KRAMER, K., Ferroelectrics—their electrical behavior during, and subsequent to, ionizing radiations, 20: 11352 (NP-15707)
KRAMER-AGEEV, E. A., Certain problems in dosimetry around reactors, 20: 11150
KRAMERS, H. A., Capture of electrons by α-particles, 20: 11457 (LA-tr-65-29)
KRAMMER, W. C., Fabrication of 20 wt % Ti–V alloy tubing for nuclear fuel cladding, 20: 11258
KRASILNIKOV, E. Yu., Effects of transverse magnetic field on convective heat transfer in conducting fluid flow in channel, 20: 11793
KRASNANSKY, Victor J., Effect of γ irradiation on polyamide, 20: 10892
KRASNOSHCHEKOVA, R. Ya., Migration of radioactive strontium in soil under influence of electric field, 20: 11053
KRASNOV, A. N., Production of copper, molybdenum, and tungsten powders by atomization with plasma jet, 20: 11219
KRASNOYAROV, N. V., Concrete for high-temperature reactor shielding, 20: 12340
KRASNOYAROV, N. V., Nuclear power plant BN-350, 20: 12441
KREJCI, V., New method of time-space display of wave phenomena in plasma, 20: 12200
KREPS, R. E., Analysis of some pion-pion scattering models, 20: 11637
KREPS, Rodney E., Relativistic three-pion calculation. I., 20: 11639
KREPS, Rodney E., Relativistic three-pion calculation. II., 20: 11640
KREPS, Rodney E., Relativistic three-pion calculation. III., 20: 11641
KRESTOVNIKOV, A. N., Thermodynamics of W, Mo, Ti, Zr, Nb, and Ta and their more important compounds, 20: 10816 (NASA-TT-F-285)
KRIEGER, F. J., Thermodynamics of the graphite–carbon vapor system, 20: 10799 (AD-625735)
KRISCIOKAITIS, R. J., Postfocusing acceleration for $\pi\sqrt{2}$ spectrometer, 20: 11153
KRISHNAMURTHY, E. V., Algebra for (m,p) switching nets, 20: 11199 (COO-614-34, Sect. IIIC)
KRISHNAMURTHY, E. V., Duality theorem in combinatorial switching, 20: 11198 (COO-614-34, Sect. IIIB)
KROEGER, P., Ferroelectrics—their electrical behavior during, and subsequent to, ionizing radiations, 20: 11352 (NP-15707)
KROH, J., Radiation-induced formation of free radicals in styrene-grafted cellulose, 20: 10873
KRUEGER, H., Scattering of laser photons on fast electrons, 20: 11667
KRUER, William L., Spacing and cesium pressure dependence of electron temperatures and ion densities in thermionic converter, 20: 11544 (LA-DC-7390)
KRUGLYAKOVA, K. E., Nature of superweak luminescence of irradiated solutions of DNA, 20: 10578
KRUPNOVA, G. F., Radioprotective effects of inert gases and low-molecular narcotics. IV., 20: 10712
KRUSZEWSKA, Jadwiga, Changes in osmotic resistance of white blood cells in postradiation disease in rats, 20: 10614
KUCHCINSKI, A., Silicon lithium drifted detectors, 20: 11097 (INR-621/XV/1)
KUDRYAVTSEVA, L. K., Temperature field of the fuel elements in core and blanket of BN-350 reactor, 20: 12443
KUEHN, M. N., Economic criteria applied to management of nuclear materials, 20: 12562
KUEHNAU, J. Jr., Inhibition of whole-body incorporation and retention of ^{131}I in man, 20: 10543
KUKAVADZE, G. M., Measurement of absorption cross section of ^{156}Gd, 20: 11987
KUKLIK, A., Radioactive decay of ^{188}Re, 20: 11998
KUKLIN, G. V., Dynamic frequency spectra of short-period cosmic-ray intensity fluctuations, 20: 11518
KUKLIN, G. V., Study of periodic variations of cosmic-ray intensity by means of selective frequency filters, 20: 11519
KUKURUDZYAK, Yu. A., Influence of ionizing radiation on contractive ability of mitochondria, 20: 10678
KULAKOVSKII, M. Yu., Concrete for high-temperature reactor shielding, 20: 12340
KULKARNI, V. G., Study of lifetimes of positronium in teflon irradiated by gamma rays, 20: 10905
KULLANDER, S., Quasi-free proton-proton scattering in light nuclei at 460 Mev, 20: 11948 (AD-624318)
KULSRUD, R., Effect of weak collisions on ion waves, 20: 12172 (MATT-302)
KULSRUD, R. M., Effect of weak collisions on ion waves, 20: 12237
KUMAR, Anand, Calculation of exchange stripping amplitudes, 20: 12126
KUMAR, Kailash, Expanding the exponential, 20: 11209
KUNDU, S. K., Vector-vector-pseudoscalar interactions, 20: 11752
KUNIMATSU, Masami, Cleaning for nuclear species in Tokai atomic power station, 20: 12429
KUNZE, Helmut, Eigenvalue problems of reactor theory and space groups, 20: 12373
KUO, Ke-hsin, Determination of short range order in Ni–Mo alloys, 20: 11325
KURILKO, V. I., Excitation of magnetohydrodynamic waveguide by coaxial waveguide, 20: 12208
KURILKO, V. I., Theory of scattering of magnetohydrodynamic waves at end of waveguide, 20: 12207
KURIMOTO, Sohei, Survey of Nagasaki atomic bombing casualties, 20: 10663
KURITA, Harou, Method for removing radioactive substances in water, 20: 12527
KUSCER, L., Half-space neutron transport with linearly anisotropic scattering, 20: 11939
KUSMA, J. B., Several alloy phases containing yttrium and dysprosium, 20: 11317
KUSWA, Glenn, High speed magnetically operated particle or light shutter, 20: 12250
KUT'IN, V. M., Search for $\pi^0 \to 3\gamma$ decay, 20: 11587
KUYATT, C. E., Inelastic electron scattering from H_2, 20: 11466
KUYATT, C. E., Resonances in electron scattering from H_2, HD, and D_2, 20: 11465
KUZIN, A. M., Effects of α and γ emissions on synthesis of DNA in HeLa cells, 20: 10588
KUZMIN, V. A., Detection of solar neutrinos by means of $^{71}Ga(\nu,e^-)^{71}Ge$

reaction, 20: 11537
KUZNETSOV, S. P., Nuclear desalination equipment of low capacity, 20: 12454 (JPRS-33480)
KUZNETSOVA, S. S., Dosimetric investigations and shielding studies using synchrocyclotron, 20: 10605 (NASA-TT-F-353, pp 21-54)
KUZNETSOVA, T. I., Evaluation of polarization of atom in strong electromagnetic field, 20: 11510
KVELLAND, Ingerid, Mating activity and fertility of Drosophila males, 20: 10644
KWIECINSKI, J., Bootstrap method and Regge poles, 20: 11694
KWON, Toi Su, Effect of cortisone and x irradiation on mast cells of adrenalectomized albino rats, 20: 10686

L

LABERRIGUE-FROLOW, J., Exchange mechanism for $\pi^+ p \to N^+ \rho^0$ reaction at 2.75 Bev/c, 20: 11605
LADAGE, A., Calibration measurements on external electron beam 1 to 5 Bev, 20: 11389 (DESY-65/12)
LADU, M., Certain factors that influence response of photographic dosimeters for roentgen and gamma rays, 20: 11136
LAFOUCRIERE, J., Application of simple models of direct interaction to study of reaction $^{28}Si(n,\alpha)^{25}Mg$ at 14.8 Mev, 20: 12002
LAGU, R. G., Study of lifetimes of positronium in teflon irradiated by gamma rays, 20: 10905
LAGUN, M. A., Effectiveness of hormone therapy in radiation injuries, 20: 10709
LAI, C. S., Meson-baryon scattering in spurion scheme of broken U_{212}-symmetry, 20: 11735
LAKSHMINARAYANA, V., Absolute photoelectric cross sections of 320-kev γ rays in Pb, Sn, and Ag, 20: 11496
LAKSHMINARAYANA, V., Beta-gamma directional correlation in ^{147}Nd, 20: 12139
LAKSHMINARAYANA, V., Compton scattering of low energy γ rays, 20: 11515
LAKSHMINARAYANA, V., Incoherent scattering of γ rays by K-shell electrons, 20: 11514
LAL, B., Study of $^{37}Cl(p,n)^{37}Ar$ reaction mechanism, 20: 12141
LAL, M., Radiative capture of neutrons by cobalt in metal acetylacetonates, 20: 10888
LAMBE, J., Electrodynamic study of Josephson tunneling in superconducting junctions, 20: 11910
LAMBERT, Michel, Scattering of protons by neon, 20: 11995
LAMBRINO, V., Separation of ^{32}P from biological radioactive solutions using ion exchangers, 20: 10780
LAMI, L., Protective action of phospholipid extract of spleen on mice subjected to whole-body irradiation, 20: 10704
LAMI, L., Protective effect of duodenal heparinoid on mouse exposed to lethal dose of whole-body irradiation, 20: 10705
LAND, E. J., Pulse radiolysis study of methylene blue, 20: 10925
LANDINGHAM, Richard L., Fusion bonding of plasma-sprayed tungsten coatings to steel, 20: 11242 (UCRL-12153)
LANDKAMMER, Franz Josef, Diffraction experiments with slow neutrons, 20: 12309
LANDMARK, B., Electron density and collision frequency during auroral absorption event, 20: 11848
LANDRGOT, B., Fracture of pelvis after curative irradiation, 20: 10668
LANDSBERG, L. G., Scintillation counter effectiveness in registering neutrons with several Bev energy, 20: 11106 (NP-15786)
LANDSTROEM, O., Scintillometer assembly for geological survey, 20: 11087 (AE-203)
LANE, R. H., Space power plant study, 20: 12475 (WANL-PR(B)-009)
LANG, Donald W., Angular momentum-dependence of nuclear level density, 20: 12012
LANG, G., Moessbauer effect in some haemoglobin compounds, 20: 10903
LANG, W., Management of americium in power reactor fuels to optimize production of alpha-emitting isotopes, 20: 12394 (BNWL-SA-472)
LANGE, E. A., Prog. rpt. on metallurgical characteristics of high strength structural materials, 5-7/65, 20: 11273 (NRL-6364)
LANGE, R. C., Weak alpha and electron capture decay in ^{208}Po and ^{209}Po, 20: 11971 (MLM-1251J)
LANGE-HESSE, G., Precipitation of solar cosmic ray particles in polar cap regions, 20: 11856
LANGER, H., Determination of body water with ^{3}H, 20: 10557
LANGEROVA, I., Potassium estimation in biologic material by neutron activation analysis, 20: 10776
LANGEVIN, Michel, Nuclear levels of sulfur formed by (α,γ) reaction on silicon, 20: 11994
LANGHAAR, J. W., Transportation of radioactive materials, 20: 11035 (TID-8541, pp 249-319)
LANGNER, Carl G., Qualification tests of spray-deposited and light-initiated silver acetylide-silver nitrate explosive, 20: 10814 (SCL-DC-65-96)
LANGSTROTH, G. F. O., Positron annihilation in magnesium-indium and indium-lead alloys, 20: 11678
LANTELME, F., Ion diffusion and migration in molten salts, 20: 10805 (EUR-2466.e, pp 21-30)
LAPIDUS, L. I., Double NN scattering with polarized beam and polarized target, 20: 11671
LAPITSKII, Yu. Yu., Pulsed ion source with point cathode (needle), 20: 11394 (NP-15788)
LARSEN, E. I., Characteristics and applications of high-density tungsten-based composites, 20: 11291
LARSEN, Sigurd Yves, Quantum-mechanical pair-correlation function of ^{4}He gas at low temperatures, 20: 11897
LARSON, A. V., Errors in the use of mass analyzers in plasma physics, 20: 12223
LARSON, G. H., Spin-lattice relaxation in some rare-earth salts. I., 20: 12300
LARSON, H. J., Reactor safety review organization, 20: 12337
LARZUL, Helene, Absorption spectra of water and heavy water in the ultraviolet, 20: 10823
LASKA, L., New method of time-space display of wave phenomena in plasma, 20: 12200
LASSEN, N. A., Intrapulmonary exchange of $^{18}O_2$ injected intravenously in man, 20: 10547
LATAL, H., Structure of nucleons, 20: 11579
LATTES, C. M. G., Analysis of high energy jet showers. III., 20: 11534
LAUBE, E., Several alloy phases containing yttrium and dysprosium, 20: 11317
LAURENT, Henri, Nuclear levels of sulfur formed by (α,γ) reaction on silicon, 20: 11994
LAURITSEN, T., Energy levels of light nuclei. VII, 20: 12023
LA VALLE, D. E., Purification and growth of KCl single crystals, 20: 10813 (ORNL-3906)
LA VALLE, D. E., Rhenium nitrogen fluoride and rhenium tetrafluoride, 20: 10845
LA VELLE, E. B., Safety requirements for welding stainless steel for nuclear reactor plants, 20: 11259
LAVRENCHIK, E. I., Labile samples as criteria of effectiveness of radioprotection, 20: 10711
LAVRUKHINA, A. K., Nuclear chemistry, 20: 11377
LAW, W. B., Small orbit betatron, 20: 11397 (SC-RR-65-111)
LAWRENCE, Barry R., Neutron density fluctuations induced by hydraulic noise in nuclear power reactor, 20: 12360 (ORNL-TM-1332)
LAWRIE, J. A., Spatial properties of rapid geomagnetic fluctuations, 20: 11833
LAWROSKI, Stephen, Reactor fuel processing, 20: 10962
LAWSON, A. W., Ultrasonic studies in normal and superconducting thallium, 20: 11915
LAZAREV, A. N., Infrared spectra of lanthanum germanates, 20: 10828
LAZAREV, K. F., Mesothorium-I concentration in the Black Sea, 20: 10768 (JPRS-33212)
LAZUTIN, L. L., Solar cosmic rays recorded in stratosphere in September 1963, 20: 11429
LAZZARINI, E., Distribution of some fission products between core and recombiner of L54M reactor. IV. 20: 12508
LEAVENS, W. M., Relationship of a.c. resonant probes to resonant scattering, 20: 12241
LEBEDEV, B. I., Prophylaxis and therapy of radiation injuries caused by protons, 20: 10699 (NASA-TT-F-353, pp 210-38)
LEBEDEV, V. N., Experimental determination of function of neutron distribution around 10 Bev synchrophasotron, 20: 11390 (JINR-P-2446)
LEBEDEVA, G. A., Gastro-intestinal disturbances by radioisotope-induced radiation sickness, 20: 10674
LEBEDINSKII, A. V., Characteristics of the radiation effect under space flight conditions and ways to determine admissible radiation levels, 20: 10719 (NASA-TT-F-353, pp 3-20)
LEBEZ, D., Nitrogen metabolism in frog liver after whole-body irradiation. I., 20: 10551
LE BRET, Prog. rpt. on brittle fracture strength of heavy-gage steel plate, final, 1965, 20: 11240 (EURAEC-1520)
LEE, Jae Won, Design study report on 1000 MWe fast breeder reactor, 20: 12414 (TID-22545, pp 16-52)
LEE, T. Y., Shell-model calculation of branching ratio of hypernuclear beta-decay, 20: 11999
LEE, William, Equipment and techniques for radiation damage studies, 20: 11520
LEE, Y. C., Quantum theory of photon interaction in plasma, 20: 12246
LEE, Yih-Fa, Moessbauer effect of ^{119}Sn in some tin compounds, 20: 12285
LEE, Yu Hao, Life-time of 619 kev state of ^{181}Hf, 20: 12000
LEFKOWITZ, I., Ferroelectrics—their electrical behavior during, and subsequent to, ionizing radiations, 20: 11352 (NP-15707)
LEGAR, F., Polarized proton target in investigation of low-energy nucleon-nucleon interactions, 20: 11965 (JINR-P-2426)
LE GOFF, P., Interpretation of conductivity of porous and dispersed media

with the aid of cubic cellular geometric models, 20: 10997 (AERE-Trans-1038)
LEHMANN, P., Elastic electron-deuteron scattering, 20: 11644
LEHMANN, P., Electrodisintegration of deuteron around $q^2 = 3.5F^{-2}$, 20: 11645
LEIGH, J. R., Isomer of spin $^{25}/_{2}^{+}$ in ^{183}Re, 20: 12042
LEITNER, Jack, Boson resonances produced in K⁻p interactions, 20: 11552 (CONF-851015-3)
LEITTEN, C. F. Jr., Thermochemical reduction of uranium hexafluoride, 20: 11257
LEITTEN, C. F. Jr., Vapor deposition and characterization of tungsten–rhenium alloys, 20: 11256
LELEK, V., Flattening of flux in heterogeneous slab reactor, 20: 12364 (UJV-1365/65)
LEMAIRE, J., Reactor tank steels. Irradiation of tensile-test pieces in EL.3 at different temperatures and post-irradiation tests, 20: 11342 (EURAEC-1502)
LEMANSKI, E. J., Prog. rpt. on low power thermoelectric component development, final, 3/65, 20: 11543 (GIC-2605-3)
LENANDER, Carl J., Low-energy electron scattering from atoms and molecules: a model, 20: 11495
LENGEROVA, Alena, Possibility that thymus-mediated alloantigenic stimulation results in tolerance response, 20: 10632
LENY, Jean-Claude, Toward an ORGEL prototype, 20: 12428
LEONOV, E. S., Changes of spectra of fast neutrons after their passage through aluminum, paraffin, and aqueous media, 20: 12268
LEONOV, V. A., Balance of natural radioactivity in leukemia, 20: 10545
LEOPUNSKY, A. I., Nuclear power plant BN-350, 20: 12441
LEPENDIN, V. I., Measurement of absorption cross section of ^{156}Gd, 20: 11987
LEPRINCE-RINGUET, Louis, Principal results furnished by antiproton-proton annihilations at rest or at low energy, 20: 11575
LE ROUX, Yvonne, Role of the chemical species released by the radiolysis of water in the saturation of double carbon–carbon bonds, 20: 10875
LESHCHINSKII, N. I., Gamma irradiation facilities, 20: 10980 (AEC-tr-6469)
LEUPOLD, M. J., Heat transfer by circulation of super-critical helium, 20: 11925
LEVAVASSEUR, G., Ultrasonic study of cracks and pores in sintered beryllia, 20: 11324
LEVI, Georges, Valence, fundamental, and harmonic vibrations of piperidine $C_5H_{10}NH$ and the N-deuterated piperidine $C_5H_{10}ND$, 20: 10863
LEVIN, F. S., Coupled equations for rearrangement collisions, 20: 12045
LEVIN, F. S., Theory of low-energy scattering of electrons by hydrogen atoms, 20: 11500
LEVINSKII, S. V., Characteristics of the radiation effect under space flight conditions and ways to determine admissible radiation levels, 20: 10719 (NASA-TT-F-353, pp 3-20)
LEVINSON, L. S., Heat content of molten tin, 20: 10811 (LA-DC-6806)
LEVINTOV, I. I., Polarization in elastic p-p scattering at high energies, 20: 11591
LEVI-SETTI, R., Energy spectrum of charged pions from K⁻-captures in CF_3Br, 20: 12092
LEVITIN, R. Z., Ferromagnetism and antiferromagnetism of rare-earth metals and alloys, 20: 11340
LEVITSKII, B. M., Strengthening metals and alloys by irradiation, 20: 11366
LEVY, N. S., Spot patterns and Silsbee chains on Cu single crystal, 20: 11460
LI, A. C., Isomerism in ^{129}Ba, 20: 12069
LI, A. C., Low levels of ^{128}Ba from ^{128}La decay, 20: 12068
LI, Hsing-chun, Influence of ionizing radiation on cellular response in lymph nodes of rats after immunization, 20: 10685
LI, Ming Chiang, Radiative hyperon decays, $\Sigma^{\pm} \to n + \pi^{\pm} + \gamma$, 20: 11633
LIAS, Sharon G., H_2S as free-radical interceptor in gas-phase radiolysis and photolysis of propane, 20: 10883
LIBOFF, Richard L., Brownian motion of charged particles in crossed electric and magnetic fields, 20: 11802
LICHTENSTEIN, Roland M., Prog. rpt. on radiation damage in semiconductor materials, 2–4/65, 20: 11176 (NP-15835)
LICHTMAN, D., Electron probe surface mass spectrometry study of oxygen on molybdenum, 20: 11322
LIEBER, L. F., Radiation-monitoring and -warning system at ORNL, 20: 11049
LIERSE, W., Histochemical detection of glycogen and mucopolysaccharides in brain of guinea pigs after x irradiation, 20: 10638
LIIKALA, R. C., Westcott parameters derived from RBU basic library for Δ-4 cutoff, 20: 11959 (HW-77389)
LILHOLT, Hans, Bibliography on dispersion-strengthened materials, 1964, 20: 11278 (RISO-48(Suppl.2))
LILL, Harborough I., Panel discussion: licensing nuclear merchant vessel, 20: 12464 (CONF-640810, pp 156-65)
LIMIC, N., Asymptotic behavior of phase shift in λ for strongly singular potentials, 20: 11712
LIN, Shi-Chien, Differential energy and angular distribution of scattered gamma rays through concrete incident normally, 20: 12269
LINCOLN, J. Virginia, Geomagnetic and solar data, 20: 11830
LINDERSTROEM-LANG, C. U., Experimental study of tangential velocity profile in Ranque-Hilsch vortex tube, 20: 10992 (RISO-116)
LINDGREN, J. R., Suppression of grain growth in vapor-deposited tungsten up to 2500°C, 20: 11320
LINDNER, R., Diffusion of heavy elements in nuclear fuels: actinides in UO_2, 20: 11312
LINDOP, Patricia J., Life shortening in mice exposed to radiation: effects of age and hypoxia, 20: 10707
LINDSAY, P. D., Microwave bridge measurement of plasma frequency, 20: 12249
LINDSEY, J. S., Experimental branching ratios for ϕ decay, 20: 11619
LINDSTAEDT, Horst Karl, Conveyor systems, 20: 10986
LINEBERGER, W. C., Absolute cross sections for single ionization of alkali ions by electron impact. II., 20: 11490
LINEBERGER, W. G., Absolute cross sections for single ionization of alkali ions by electron impact. I., 20: 11489
LINGAM, K. V., Electron paramagnetic resonance of Eu^{2+} in CdF_2 and KCl, 20: 12321
LINK, Leonard E., Reactor technology, 1965, 20: 12329 (TID-8541)
LIPMAN, N. H., Elastic n-p charge-exchange scattering at 8 Bev/c, 20: 11606
LIPPERHEIDE, R., Final state interaction in decay $^{8}Li \to e^{-} + \nu + 2\alpha$, 20: 12010
LIS, S., Separation of neptunium from neutron irradiated uranium by reversed-phase partition chromatography in the TBP–HNO_3 system, 20: 10954
LISCIA, A., C.N.E.N.'s fuel element fabrication and control laboratories at Saluggia, 20: 11247
LISMAN, Frederick L., Mass and charge distribution studies in fission of ^{197}Au by intermediate energy helium ions, 20: 11953 (COO-347-17)
LITVINOVA, E. G., Dosimetric investigations and shielding studies using synchrocyclotron, 20: 10605 (NASA-TT-F-353, pp 21-54)
LIU, D. H. W., Effect of chronic ingestion of ^{65}Zn in trout, 20: 10528 (BNWL-122, pp 101-6)
LIUZZI, Anthony, Empirical sampling using radioactivity as generator of randomicity, 20: 11204 (NYO-3136-2, App. 3)
LIUZZI, Anthony, Patterns in residuals: test for regression model adequacy in radionuclide assay, 20: 11203 (NYO-3136-2, App. 2)
LIUZZI, Anthony, Prog. rpt. on statistical analysis of environmental and total body x-ray scintillation spectra, 10/64–9/65, 20: 11201 (NYO-3136-2)
LIVAGE, Jacques, Non-stoichiometric zirconia and stabilization of tetragonal zirconia, 20: 11248
LIVINGSTON, J. D., Magnetic pinning in type-II superconductor, 20: 11894
LIVINGSTON, Linda, Studies of ventromedial hypothalamus with auto-radiographic techniques, 20: 10541
LIVINGSTON, M. S., Synchrotron colliding beam facility at CEA, 20: 11382 (CEAL-TM-151)
LJUNGGREN, S., Monte Carlo calculations in neutron thermalization in heterogeneous system. II., 20: 11935 (RFR-154)
LLORET, A., Upper limit for the partial width $\Gamma(\rho \to \pi\gamma)$, 20: 11618
LLOYD, K. B., Prog. rpt. on metallurgical characteristics of high strength structural materials, 5–7/65, 20: 11273 (NRL-6364)
LOBAKOV, A. P., Secondary γ-emission coefficients for aluminum, copper, and tungsten, 20: 12267
LOBANOK, A. G., Protective action of polysaccharide from yeast-like microorganism in irradiated mice, 20: 10703
LOCH, Erwin, Aerostatic externally pressurized gas lubricated thrust bearings, 20: 10974 (AEC-tr-6665)
LOCHAK, G., Development of particle distribution density during acceleration toward statistical distribution limit, 20: 11408
LOCHER, D. W., Radioiodine treatment of benign strumae in endemic goiter region of southern Germany, 20: 10748
LOCHSTET, William A., $^{12}C(\gamma,n)^{11}C$ giant resonance with gamma rays, 20: 12058
LOCK, Frank R., Treatment of cancer of cervix by radiation and elective radical hysterectomy, 20: 10726
LOCKWOOD, Grant J., Production of ions of alkali metals, other metals, and halogen in an rf source, 20: 11374
LOEB, Leonard B., Electrical coronas, their basic physical mechanisms, 20: 11806
LOEBNER, K. E. G., Systematics of absolute γ transition probabilities in deformed odd-A nuclei, 20: 11951 (AE-205)
LOGINOV, A. A., Nuclear desalination equipment of low capacity, 20: 12454 (JPRS-33480)
LOIZZO, P., Calculation of water reactors containing Pu, 20: 12370
LOMBARD, D. B., Particle size distribution and bulk permeability of oil shale rubble, 20: 10975 (UCRL-14294)

LOMENICK, T. F., Geohydrological evaluation of solid waste storage area 6, 20: 12518 (ORNL-TM-1327)
LONG, David M., System qualification procedures for pulsed nuclear environment, 20: 11180
LOOSEMORE, W. R., Status report on in-pile dosimetry in United Kingdom, 20: 11151
LOPEZ, C. A., Dispersion relations in complex angular momentum plane and Sommerfeld-Watson transformation, 20: 11732
LOPEZ, S., Calculation of water reactors containing Pu, 20: 12370
LOPEZ, W. M., Energy dependence of neutron capture cross section of tungsten isotopes from .01 to 10 ev, 20: 11957 (GA-6832)
LOPUSZANSKI, Jan, Quantum field theory with degenerate vacuum and special type of symmetry, 20: 11715
LORENZ, Peter Klaus, Comparison of rare-earth cathodes in diode ion pump, 20: 10976 (IS-T-46)
LORKE, Dietrich, Embryotoxic effects in rats, 20: 10616
LOTTS, A. L., Remote fabrication of reactor fuels, 20: 11241 (TID-8541, pp 71-148)
LOUCKS, T. L., Positron annihilation and electronic structure of rare-earth metals, 20: 11323
LOUW, H. N. J., Electrolytic jet machining method for cutting single crystal and polycrystalline uranium carbide, 20: 11216 (PEL-79)
LOVALLO, J. M., Precritical calculations for 3.0 in. pitch, beryllium reflected, TWNR critical assembly, 20: 12465 (GA-6807)
LOVE, D. L., Nuclear-charge distributions of several fission product mass chains, 20: 11980 (USNRDL-TR-935)
LOVE, T. A., Beam energy measurements at Oak Ridge isochronous cyclotron, 20: 11396 (ORNL-TM-1382)
LOWREY, A. R., Response of P-I-N detectors to various nuclear radiation environments, 20: 11173 (D2-84071-1)
LUCAS, Bruce Thomas, Elastic and inelastic scattering of 18-Mev alpha particles from ^{9}Be, ^{23}Na, and ^{31}P, 20: 12099
LUCAS, Mary, Modification of radiation damage of bacteria by folic acid antagonists, 20: 10648
LUEBS, Eide-Dittmar, Determination of coronary flow with positron emitter (^{64}Rb), 20: 10730
LUIS-ABBOUD, Jose, Comparison of hydrogen and deuterium bonds by uv absorption spectrometry, 20: 10819
LUKASH, N. I., Antitumoral resistance in animals subjected to chronic treatment with small doses of ^{90}Sr, 20: 10627
LUKASZUK, L., Problem of maximum in dispersion theory, 20: 11738
LUKE, Keung P., Photoionization of Cs atoms by solar radiation, 20: 11549
LUKE, T. M., Lee model with unstable v-type particle, 20: 11745
LUKENS, H. R. Jr., Absolute liquid-scintillation rate constants and fluorescence efficiencies, 20: 10902
LUKIN, A. V., Monopulse generation with $CaF_2:U^{3+}$ crystals, 20: 12293
LUMING, M., Integral representation for high-energy scattering amplitudes, 20: 11736
LUNDQVIST, Stig, Positron annihilation in diatomic crystals, 20: 11655
LUO, H. L., Superconductivity in the alloy system Cd–Hg, 20: 11914
LUPFER, David A., Prog. rpt. on dielectric strength and ferroelectric behavior of ceramics, final, 1/63–6/64, 20: 11279 (SC-DC-64-1477X)
LURIE, H., Steady-state sodium boiling and hydrodynamics, 20: 10990 (NAA-SR-11586)
LUTZ, B. C., Microwave bridge measurement of plasma frequency, 20: 12249
LUTZ, D., Parameter study of fast reactors with incore thermionic converters (system Srikt), 20: 12483
LUTZ, D. E., Turbine pressure governor controls reactor system temperatures, 20: 12438
LUTZ, H. F., Elastic and inelastic scattering of protons by ^{18}O, 20: 11979 (UCRL-12152)
LUTZ, H. F., Strongly excited 2^+ and 3^- states in $^{54,56}Fe$ and $^{58,60,62}Ni$ isotopes, 20: 12065
LUTZ, Robert W., Vibrational relaxation of deuterium by a quantitative Schlieren method, 20: 11785
LUTZ, Robert W., Vibrational relaxation of hydrogen, 20: 11786
LUX, F., Role of resonance activation integral in activation determination of silver, 20: 10789
LUZOV, A. A., Dynamic frequency spectra of short-period cosmic-ray intensity fluctuations, 20: 11518
LUZOV, A. A., Study of periodic variations of cosmic-ray intensity by means of selective frequency filters, 20: 11519
LYNCH, Edward J., Transport of radionuclides by ground water, 20: 11010 (HNS-1229-61)
LYON, C. E., Extraction by processing solvents of nitrosylruthenium nitrato complexes. III., 20: 10947 (AERE-R-4786)
LYONS, C. J., Fluidized-bed process for production of tungsten, 20: 11255
LYUBIMOV, G. A., Magnetohydrodynamic boundary layer, 20: 11790
LYUBIMOV, V. A., Scintillation counter effectiveness in registering neutrons with several Bev energy, 20: 11106 (NP-15786)
LYZKOV, A. F., Applied dosimetry, 20: 11058

M

MAC CHESNEY, J. B., Preparation and low-temperature magnetic properties of terbium oxides, 20: 12289
MAC DONALD, William M., Fine structure in nuclear resonances, 20: 12087
MACEK, Robert James, Search for process $K^+ \to \pi^+ + \pi^0 + \gamma$, 20: 11675
MAC GREGOR, Malcolm H., Determination of nucleon-nucleon elastic-scattering matrix. IV., 20: 11622
MACHEN, Donald R., Application of direct digital control to high energy particle accelerators, 20: 11401 (UCRL-16502)
MACKE, W., Exact description of elastic scattering processes and deduction of optical nuclear models, 20: 12021
MAC KENZIE, I. K., Positron annihilation in magnesium–indium and indium–lead alloys, 20: 11678
MAC KEOWN, P. K., Momentum spectrum of cosmic-ray muons at large Zenith angles, 20: 11526
MACKEWICZ, W. V., Local film coefficients on ML-1 fuel elements due to boundary layer turbulence promoters, 20: 10988 (CONF-12-5)
MACKEWICZ, W. V., Mass transfer analogy studies of shaped turbulence promoter performance, 20: 10993 (TID-22513)
MACKINTOSH, A. R., Positron annihilation and electronic structure of rare-earth metals, 20: 11323
MAC MILLAN, John H., Panel discussion: licensing nuclear merchant vessel, 20: 12464 (CONF-640810, pp 156-65)
MADER, Charles L., GMX-2 spalling calculations, 20: 12539 (LA-DC-7692)
MADER, Charles L., Three-dimensional cartesian particle-in-cell calculations, 20: 12537 (LA-3422)
MADEY, R., Precession of satellite orbits and general relativity, 20: 11883
MADSEN, V. A., Strongly excited 2^+ and 3^- states in $^{54,56}Fe$ and $^{58,60,62}Ni$ isotopes, 20: 12065
MAECK, William J., Prog. rpt. on burnup determination of nuclear fuels, 7–9/65, 20: 11960 (IDO-14667)
MAEHLUM, B., Absorption at conjugate points, 20: 11862
MAEHLUM, B., Balloon measurements of solar protons and auroral x-rays, 20: 11855
MAEHLUM, B., Comments on measurements of particle precipitation with Injun satellites, 20: 11851
MAEHLUM, B., Development of the radio-aurora, 20: 11859
MAEHLUM, B., Direct satellite probe measurements of ionospheric irregularities in polar cap, 20: 11845
MAEHLUM, B., Electron density and collision frequency during auroral absorption event, 20: 11848
MAEHLUM, B., Electron-proton spectrometer for rockets using solid state detectors, 20: 11853
MAEHLUM, B., Enhanced electromagnetic radiation between 500 and 1000 c/s in auroral zone, 20: 11860
MAEHLUM, B., Height of auroral absorption obtained from satellite observations, 20: 11864
MAEHLUM, B., Important atmospheric processes in D region, 20: 11843
MAEHLUM, B., Ionospheric plasma density by three different methods, 20: 11847
MAEHLUM, B., Ionospheric effects of particles, 20: 11858
MAEHLUM, B., Longitudinal extent of auroral ionization, 20: 11861
MAEHLUM, B., Low frequency propagation and probe experiments, 20: 11846
MAEHLUM, B., Measurement of charged particles in auroral zone, Andoeya, Norway, 20: 11854
MAEHLUM, B., Methods and results of particle observations, 20: 11850
MAEHLUM, B., Optical effects of particles, 20: 11857
MAEHLUM, B., Precipitation of solar cosmic ray particles in polar cap regions, 20: 11856
MAEHLUM, B., Probe techniques, 20: 11844
MAEHLUM, B., Recent solar cosmic ray events, 20: 11863
MAEHLUM, B., Solar flare particles in September 1963, 20: 11852
MAEHLUM, B., Some aspects of particles and fields in magnetosphere, 20: 11849
MAEHLUM, B., Some particular problems in polar ionosphere, 20: 11865
MAEHLUM, B., Space research in polar regions, 20: 11842
MAEHLUM, B., Symposium on high latitude particles and the ionosphere Alpbach, Tyrol, 1964, 20: 11841
MAEHLUM, Bernt, Methods and results of particle observations, 20: 11850
MAFFEI, G., Hematologic modifications provoked in the mouse, 20: 10641
MAFFEI, G., Therapeutic effect of preserved autologous bone marrow on hematological lesions provoked by radiation, 20: 10706
MAGUIN, Claude, Contribution to theoretical study of A(t,p)B reactions, 20: 11972 (NP-15716)
MAHLER, R. J., Possible observation of ^{115}In nuclear electric hexadecapole transitions, 20: 12304
MAHLUM, D. D., Chemical carcinogens and radionuclide metabolism, 20: 10526 (BNWL-122, pp 91-3)

MAHLUM, D. D., Effect of dietary and hormonal manipulations on ^{237}Np-induced fatty livers, 20: 10522 (BNWL-122, pp 79-80)
MAISONNIER, Ch., Experiment on electrical breakdown in vacuum at Laboratorio Gas Ionizzati, 20: 11769 (LGI-65/30)
MAITA, J. P., Occurrence of superconductivity in sulfides, selenides, tellurides of Pt-group metals, 20: 11899
MAJOR, J. V., Interaction of 16.3 Bev π^--mesons with complex nuclei, 20: 11602
MAJUMDAR, N. K., Set-up of duoplasmatron for intense ion beam, 20: 12260
MAK, A. A., Monopulse generation with $CaF_2:U^{3+}$ crystals, 20: 12293
MAKAROV, A. A., Electromagnetic current and form factors for meson 35-plet in SL(6,c) symmetry, 20: 11683 (JINR-E-2475)
MAKI, Kazumi, Electrodynamics of superconducting alloys in high magnetic fields, 20: 11907
MAKI, Kazumi, Surface superconductivity in subcritical region, 20: 11891 (COO-264-224)
MAKI, Kazumi, Theory of superconductors containing magnetic impurities, 20: 11906
MAKSIMENKO, B. P., Use of surface-barrier silicon detectors for measuring fast particle spectra, 20: 11115
MALAGUTI, R., Anatomoclinical study of late lesions due to Thorotrast, 20: 10680
MALANOSKI, S. B., Experiments on ultrastable gas journal bearing, 20: 10979 (TID-22528)
MALAT, V., Scattering cross-section of two electrons of low energy in metals, 20: 12284
MALEIN, A., Hydromagnetic waves in partially ionized hydrogen plasma, 20: 12224
MALKOV, E. I., Restrictions on elastic scattering cross sections in diffraction peak region, 20: 11764
MAL'KOV, V. V., Passage of high energy neutrons through heavy concrete, 20: 12263 (JINR-P-2479)
MALLEN, Jose-Maria, Beryllium—canning material, 20: 11294
MALLETT, A. J., Nuclearly safe triangular-slab tank for handling enriched uranium, 20: 10981
MALM, H. L., Large-volume coaxial germanium gamma-ray spectrometers, 20: 11095 (CRGP-1224)
MALMBERG, J. H., Cyclotron waves in collisionless plasma, 20: 12175 (NASA-CR-348)
MALMSKOG, S. G., Systematics of absolute γ transition probabilities in deformed odd-A nuclei, 20: 11951 (AE-205)
MALOS, J., Elastic n-p charge-exchange scattering at 8 Bev/c, 20: 11606
MALSKY, S. J., Comparison of radiothermoluminescent and radiophotoluminescent dosimeters, 20: 11155
MALY, L., Radioactive decay of ^{188}Re, 20: 11998
MAMELOVA, L. Ya., Measurement of absorption cross section of ^{156}Gd, 20: 11987
MANCHESTER, K. E., Implantation profiles for 40-kev phosphorus ions in silicon single-crystal substrates, 20: 12280
MANDELBERG, H. I., Excitation-transfer collisions between rubidium and helium atoms, 20: 11482
MANG, Hans J., Comparisons of BCS nuclear wave functions with exact solutions. II., 20: 12050
MANGAL, P. C., Decay of ^{133}Ba, 20: 12153
MANGO, G., Hematologic modifications provoked in the mouse, 20: 10641
MANGO, G., Therapeutic effect of preserved autologous bone marrow on hematological lesions provoked by radiation, 20: 10706
MANGUM, B. W., Spin-lattice relaxation in some rare-earth trichlorides, 20: 12292
MANLEY, Oscar P., Starfish debris measurements from Cosmos 5, 20: 11832
MANN, S., Decontamination of ORNL molten-salt fluoride-volatility pilot plant after processing irradiated zirconium–uranium alloy fuel, 20: 11032 (ORNL-3891)
MANNING, G., Elastic n-p charge-exchange scattering at 8 Bev/c, 20: 11606
MANTEL, Nathan, Light bulb statistics, 20: 11205 (NYO-3136-2, App. 4)
MAPLES, C., Mass 13, T = ½ quartet, 20: 12036
MARCAZZAN, G. M., Direct effect and evaporation mechanism in $^{27}Al(d,p)^{28}Al$ and $^{27}Al(d,\alpha)^{25}Mg$ reactions, 20: 12018
MARCHANT, Y., Citriflex—declading of fuel elements clad with zirconium or Zircaloy-2 by an ammonium fluoride-citric acid solution, 20: 11272 (NP-15661)
MARCUS, Y., Anion exchange of metal complexes. XV., 20: 10995
MAR'IN, N. P., Trajectories of electromagnetic waves in ionized toroid and its effective reflecting surface, 20: 11370
MARINESCU, L., Fission by radiationless transition in μ mesonic atom ^{239}Pu, 20: 12041
MARINI, A., Angular distributions of α-particles leading to first excited states of ^{25}Mg, 20: 12030
MARINOSCI, A., Effects of therapeutic doses of radioiodine on coagulative processes, 20: 10679
MARIWALLA, K. H., Representation of discrete symmetry operators, 20: 11713
MARKLEY, R. A., Space power plant study, 20: 12475 (WANL-PR(B)-009)
MARKOV, M. A., Possibility of specific interactions of muons and ν_μ-neutrinos at superhigh energies, 20: 11558 (JINR-E-2496)
MARRUS, Richard, Optical-pumping transients in ^{87}Rb, 20: 11486
MARSHAK, H., Total cross section for 14-Mev neutrons using aligned ^{165}Ho nuclei, 20: 12089
MARSHALEK, Eugene R., $I^2(I+1)^2$ correction to nuclear rotational spectra, 20: 12088
MARSHALL, W., Moessbauer effect in some haemoglobin compounds, 20: 10903
MARTALOGU, N., Small-angle scattering of protons by ^{24}Mg, 20: 12003
MARTELL, A. E., Chelation and olation reactions of metal ions in aqueous solution. III., 20: 10802 (COO-1020-9)
MARTELL, A. E., Chelation and olation reactions of metal ions in aqueous solution. I., Sect. III, 20: 12533 (COO-1020-6)
MARTELL, C. R., Stress postprocessor, 20: 12546 (SC-RR-65-548)
MARTI, K., Spallation, fission and neutron capture anomalies in meteoritic krypton and xenon, 20: 11424 (NP-15629)
MARTIN, B. R., K_{e4} decay and s-wave π-K scattering, 20: 11654
MARTIN, D. W., Prog. rpt. on ionization and charge transfer cross sections, 12/64–11/65, 20: 11447 (TID-22476)
MARTIN, J. P., Rover/Nerva destruct system test results, Aberdeen proving ground-3(final report), 20: 12472 (SC-RR-65-620)
MARTIN, P. M., Electron-probe microanalysis of irradiated UO_2, 20: 10787
MARTINENGHI, C., Accumulation of radioiodine in the ovaries, 20: 10554
MARTINEZ-GINORIS, Jose, Design study report on 1000 MWe fast breeder reactor, 20: 12414 (TID-22545, pp 16-52)
MARTINOLI, P., Current motion in superconductors carrying alternating currents in transverse magnetic field, 20: 11902
MASCIOLI, G., Effect of radioactive ^{32}P in the mouse, 20: 10640
MASEK, K., Macroscopic space charge field in disturbed quasineutral plasma, 20: 12191
MASHIROV, L. G., Complexes of uranyl perchlorate with neutral ligands, 20: 10825
MASLEY, A. J., Recent solar cosmic ray events, 20: 11863
MASLOVA, E. V., Phase diagram of iron–neodymium system, 20: 11295
MASON, D. R., Existence of Cr^{2+} and Cr^{4+} in x-irradiated ruby, 20: 12305
MASON, J. C., Approximate formulae for variety of solutions of Thomas-Fermi equation, 20: 11449 (TID-22530)
MASON, J. C., Chebyshev polynomial approximations for L-membrane eigenvalue problem, 20: 11206 (TID-22529)
MASSEY, H. S. W., Theory of atomic collisions, 20: 11511
MASSEY, L. M. Jr., Effect of gamma radiation upon cherries, 20: 11186
MASSOT, J. N., Application of simple models of direct interaction to study of reaction $^{28}Si(n,\alpha)^{25}Mg$ at 14.8 Mev, 20: 12002
MASTRYUKOVA, V. M., Biological effect of protons with energies of 126 Mev on corneal epithelia of mice, 20: 10608 (NASA-TT-F-353, pp 142-50)
MATCHETT, William H., Utilization of tryptophan by Neurospora, 20: 10540 (HW-SA-3728)
MATHENEY, G. B., Sampling and analysis of fission products during loss-of-fluid test (LOFT), 20: 12356 (IDO-17128)
MATHEWS, C. K., Fission products from fast neutron fission of ^{238}U, 20: 12121
MATHIS, A., PINETO—FORTRAN code designed for solution of non-linear differential equations in neutrons dynamics, 20: 11946
MATHUR, V. S., Algebra of currents and magnetic moments of hyperons, 20: 11569 (UR-875-118)
MATHUR, V. S., Algebra of currents and generalized Ademollo-Gatto theorem, 20: 11610
MATHUR, V. S., T = ½, ³/₂ p- and s-wave $K\pi$ phase shifts, 20: 11648
MATOUSKOVA, Jirina, Analysis of induced atmospheric radioactivity, 20: 11043
MATSUDA, Shunji, Spectrographic determination of strontium and calcium in bone ash, 20: 10774
MATSUMOTO, Ryuichi, Flow of slurry through pipe. II., 20: 10998
MATTHE, P., Suitability of neutron sensitive foils for dosimetry of thermal neutrons by means of pocket ion chambers, 20: 11119
MATTHEWS, C. M. E., Comments of minimum number of observations required in study of protein turnover, 20: 10563
MATTHEWS, C. M. E., Use of computers in study of protein turnover, 20: 10562
MATTHEWS, Dennis B., Proton tunneling in hydrogen-evolution reaction, 20: 11372
MATTHIAS, B. T., Occurrence of superconductivity in sulfides, selenides, tellurides of Pt-group metals, 20: 11899
MATUS, Lajos, Time-of-flight mass spectrometer, 20: 11072
MATVEEV, V. A., Relativistic composite model of meson and baryon resonances, 20: 11684 (JINR-P-2442)
MATVEEVA, E. N., Scintillation properties of polyphenyls, 20: 11129
MATYASOVA, Jitka, Effect of radiation on deoxyribonucleoproteins in animal tissue. II., 20: 10633
MATYJA, Henryk, Internal oxidation of Fe–Al alloys, 20: 11232 (INR-644/

XIV/PS)
MATYUSHENKO, N. N., Disintegration of tungsten disilicides during oxidation in air, 20: 11237
MATYUSHENKO, N. N., The high-tungsten section of tungsten–silicon phase diagram, 20: 11296
MATZNER, Bruce, Effect of length and pressure on critical heat flux for closely spaced 19-rod bundle in forced convection boiling, 20: 10994 (TID-22539)
MAUNDERS, E. J., Effective cadmium cut-off energies in cylindrical geometry for fissile and 1/V detectors, 20: 11131
MAUSHART, R., Radiophoto-luminescence dosimetry, 20: 11140
MAY, F., Univibrator as time element in medium fast coincidence circuit, 20: 11109 (SGAE-E-5/1965)
MAY, Michael M., Hydrodynamic calculations of general-relativistic collapse, 20: 11434
MAYER, Guy, Device for measuring doses of thermal neutrons, 20: 11168
MAYER, James W., Method of measuring nuclear radiation utilizing semiconductor crystal having lithium compensated intrinsic region, 20: 11170
MAYER, M. S., Space power plant study, 20: 12475 (WANL-PR(B)-009)
MAYER, R., Experimental investigations on cylindrical noble gas-filled thermionic converters for thermionic-reactor, 20: 11547
MAYFIELD, R. M., Fabrication of 20 wt % Ti–V alloy tubing for nuclear fuel cladding, 20: 11258
MAZIERES, Charles, Non-stoichiometric zirconia and stabilization of tetragonal zirconia, 20: 11248
MC ADAM, G. D., Substitutional niobium alloys of high creep strength, 20: 11302
MC AULIFFE, John, Secondary ignitions in nuclear attack, 20: 11031 (NP-15708)
MC AVOY, N., Solvent and temperature effects on fluorescence emission of europium β-diketonates, 20: 10844
MC CABE, John M., Gamma-ray-induced chlorination of benzene, 20: 10900
MC CARTHY, J. T., Weak alpha and electron capture decay in ^{208}Po and ^{209}Po, 20: 11971 (MLM-1251J)
MC CARTHY, Robert Joseph, Theoretical investigation of stability of ^{5}H, 20: 12101
MC CLANAHAN, B. J., Biological effects of ^{131}I in sheep and cattle, 20: 10516 (BNWL-122, pp 49-51)
MC CLANAHAN, B. J., Milk secretion of ^{65}Zn and ^{115m}Cd in sheep, 20: 10527 (BNWL-122, pp 94-8)
MC CLANAHAN, B. J., Sheep milk production and its ^{131}I content, 20: 10517 (BNWL-122, pp 52-4)
MC CLANAHAN, B. J., Translocation of subcutaneously administered $^{239}PuO_2$, 20: 10523 (BNWL-122, pp 81-2)
MC CLEARY, Gail P., Cryogenic design properties of hard carbide alloys, 20: 11293
MC CLELLAN, R. O., Biological effects of ^{90}Sr in miniature swine, 20: 10597 (BNWL-122, pp 37-45)
MC CLELLAN, R. O., Effect of ^{127}I on passage of ^{131}I from cows to man via milk, 20: 10530 (BNWL-122, pp 113-17)
MC CLELLAN, R. O., Gastrointestinal absorption of ^{144}Ce and ^{147}Pm in miniature swine, 20: 10525 (BNWL-122, pp 85-90)
MC CLELLAN, R. O., Radiation dosimetry of ^{137}Cs in sheep evaluated with thermoluminescent dosimeters, 20: 11091 (BNWL-122, pp 67-72)
MC COLM, Douglas, Hyperfine structure of stable lithium isotopes. II., 20: 11498
MC COLM, Douglas W., Hyperfine structure of stable lithium isotopes. I., 20: 11497
MC CORMICK, N. J., Half-space neutron transport with linearly anisotropic scattering, 20: 11939
MC CULLEN, J. D., Nuclear moments of ^{43}Sc and ^{47}Sc, 20: 12070
MC DANIEL, E. W., Absolute cross sections for single ionization of alkali ions by electron impact. I., 20: 11489
MC DIARMID, I. B., Solar flare particles in September 1963, 20: 11852
MC DONALD, K. E., Effect of DTPA on translocation and excretion of inhaled ^{144}Ce–^{144}Pr oxide in dogs, 20: 10533 (BNWL-122, pp 125-7)
MC DONALD, R. E., Lifetime of 1.02-Mev state in ^{23}Ne, 20: 12060
MC DOWELL, S. C. T., Technical support activities of nuclear materials management program, 20: 12561
MC FARLANE, A. S., Measurement of protein synthetic rate, 20: 10559
MC FARLANE, A. S., Preparation of ^{131}I- and ^{125}I-labeled plasma proteins, 20: 10941
MC FARLING, James L., Radiation-induced formation of organometallic compounds with particular emphasis on organotins, 20: 10870 (BMI-1753)
MC GONNAGLE, W. J., Nondestructive methods for determining burnup in nuclear fuel, 20: 11004
MC GUFFEY, J. R., HFIR pressure vessel and structural components material surveillance, 20: 12457 (ORNL-TM-1372)
MC GUIRE, J. B., Interacting fermions in one dimension. II., 20: 11714
MC GURTY, J. A., Development and evaluation of a homogeneous W–25Re alloy for 2600°C applications, 20: 11238 (CONF-650449-1)
MC INERNEY, R. E., Direct satellite probe measurements of ionospheric irregularities in polar cap, 20: 11845
MC KEE, B. T. A., Positron annihilation in magnesium–indium and indium–lead alloys, 20: 11678
MC KEE, R., Mu-mesic x-ray experiment, 20: 11440 (COO-614-34, Sect.IID)
MC KEE, W. E., Prog. rpt. on ion rocket engine development, 4–6/65, 20: 11006 (NP-15824)
MC NALLY, J. Rand Jr., Possibility of excitation-heating of ions to high temperature, 20: 11770 (ORNL-P-1005)
MC WHERTER, J. R., HFIR pressure vessel and structural components material surveillance, 20: 12457 (ORNL-TM-1372)
MC WHIRTER, R. W. P., Departures from local thermal equilibrium in magnetically-driven shock waves, 20: 12226
MEADOWS, H. L., Liquid scintillation detector for evaluating phototubes and determining gamma-ray activities, 20: 11128
MEDVEDEV, B. V., Axiomatic construction of scattering matrix. IV., 20: 11762
MEDVEDEV, M. N., Scintillation properties of polyphenyls, 20: 11129
MEHRAN, F., Rotational magnetic moments of alkali-halide molecules, 20: 11484
MEHTA, M. K., Study of nuclear reactions resulting from proton bombardment of ^{27}Al, 20: 12142
MEHTA, M. K., Study of $^{19}F(\alpha,n)^{23}Na$ reaction using 4 π neutron counter, 20: 12143
MEINEKE, B., Inhibition of whole-body incorporation and retention of ^{131}I in man, 20: 10543
MEISNER, Gerald W., Magnitude of K_1^0–K_2^0 mass difference using strong interactions, 20: 11661
MEIXNER, Johann, Constitution of systems of europium with silver, cadmium and indium and system cadmium–strontium, 20: 11327
MEKERS, J., Production of ^{192}Ir sources of high specific activity, 20: 11190 (BLG-332)
MENABDE, N. E., Viscosity coefficients of isotopes of hydrogen (H_2,D_2), neon (^{20}Ne,^{22}Ne), and helium (^{3}He), 20: 11461
MENDELSOHN, Lawrence B., Asymptotic large-Z atomic wave functions, 20: 11485
MENDICINO, S., Fortran-fortran, 20: 11207 (UCRL-7737)
MENNINGA, Clarence, Fission of thenium at intermediate excitation energy, 20: 11955 (COO-347-19)
MERCER, R. A., Preparation and properties of hydroxy compounds of beryllium, 20: 10836
MERGAULT, Pierre, Ionization of chromium fluoride and chromium oxide in some fused chlorides and fluorides, 20: 10821
MERKEL, G., Measurement of $Fe(\alpha,\alpha')Fe^*$ reactions produced by alpha bombardment, 20: 12056
MERRIAM, M. F., Superconductivity in the alloy system Cd–Hg, 20: 11914
MERRIGAN, Joseph A., Radiative neutron capture in liquid and solid carbon tetrachloride in *n*-hexane, 20: 10938
MERRIHUE, Craig, Xenon and krypton in Bruderheim Meteorite, 20: 11430
MERRILL, M., BLOOST-5: combined reactor kinetics-heat transfer code for IBM-7044, 20: 12354 (GAMD-6644(Add.))
MERRITT, F., Prog. rpt. on valve technology for spacecraft engines, final, 6/64–8/65, 20: 11007 (NP-15831)
MERZ, H., Syntheses of ^{32}S- or ^{35}S-labeled maleimides, 20: 10937 (NP-tr-1323)
MESSIAEN, A. M., Plasma hf analog of the Roentgen-Eichenwald current, 20: 12242
MESTVIRISHVILI, A. N., An experimental determination of relative probabilities of $K_2^0 \to 3\pi^0$ decays, 20: 11561 (JINR-P-2450)
MESTVIRISHVILI, A. N., Determination of relative probability of $K_2^0 \to \pi^\pm + e^\mp + \nu(\bar{\nu})$, 20: 11560 (JINR-P-2449)
MEWISSEN, D. J., Induction of leukemia in C57 BL mouse by tritiated thymidine, 20: 10623
MEYER, Andreas, System aluminum–holmium, 20: 11307
MEYER, James William, Nuclear decay processes in presence of laser beam, 20: 12102
MEYER, Madeleine, Bombardment of copper monocrystals with oxygen ions of medium energy (10 kev), 20: 12282
MEYER, P. E., Bubbly flow in straight pipes, 20: 10991 (NYO-3114-12)
MEYERS, J. E., Analysis of Babcock and Wilcox full-size steam generator for sodium–water reaction, 20: 12386 (APDA-176)
MEYNADIER, Christian, Scattering of protons by neon, 20: 11995
MICALI, G., Possibilities and limitations of treatment of skin radiation injuries, 20: 10658
MICHAEL, B. D., Absolute rate constants for reaction of hydroxyl radical with organic compounds, 20: 10916
MICHAEL, B. D., Pulse radiolysis of aqueous solutions of thiocyanate ion, 20: 10915
MICHAEL, B. D., Radical yields and kinetics in pulse radiolysis of potassium bromide solutions, 20: 10911
MICHIYOSHI, Itoru, Flow of slurry through pipe. II., 20: 10998
MICHON, G., Radioecology and radiological protection, 20: 11039
MICHON, G., Waste water and nuclear energy, 20: 12525
MIDDLETON, Roy, $^{17}O(d,p)^{18}O$ reaction and nuclear structure of ^{18}O,

20: 12055
MIELCZAREK, S. R., Resonances in electron scattering from H_2, HD, and D_2, 20: 11465
MIERAS, Harry, 9-magnet bypass in target area, 20: 11383 (CEAL-TM-152)
MIHALCZO, J. T., REACT and CONVRG FORTRAN subroutines for determining source convergence for 05R Monte Carlo neutron transport code, 20: 11934 (ORNL-TM-1325)
MIHELICH, J. W., Decay of ^{191}Pt(3.0 d) to ^{191}Ir, 20: 12009
MIHELICH, J. W., Half-lives of 2+ rotational states in ^{158}Dy and ^{158}Gd, 20: 12082
MIHELICH, J. W., Reinvestigation of decays of ^{146}Eu and ^{146}Pm, 20: 12081
MIHUL, Et. C., Process $\pi^- + p \rightarrow \bar{p} + d$ and Regge poles, 20: 11590
MIKHAILOV, Yu. D., Effect of alloying on physico-mechanical properties of niobium, 20: 11288 (AD-622477)
MIKHAILUS, F. F., Computation of multiple interactions for experiments on radiation capture of neutrons, 20: 11967 (JINR-P-2455)
MIKHEEV, V. L., On properties of isotope ^{254}102, 20: 11968 (JINR-P-2470)
MILAZZO, M., Direct effect and evaporation mechanism in ^{27}Al(d,p)^{28}Al and ^{27}Al(d,α)^{25}Mg reactions, 20: 12018
MILLER, M. B., On properties of isotope ^{254}102, 20: 11968 (JINR-P-2470)
MILLER, R. H., Automatic retrieval spark chambers, 20: 11093 (COO-614-34, Sect. IIA)
MILLER, R. P., Preparation and properties of hydroxy compounds of beryllium, 20: 10836
MILLER, Richard H., Prog. rpt. on computer research, 5/65, 20: 11195 (COO-614-34)
MILLS, R. G., Suppression of grain growth in vapor-deposited tungsten up to 2500°C, 20: 11320
MILLS, R. L., Phonon-roton model for compressed He II, 20: 11893
MILNER, G. W. C., Appraisal of methods for plutonium and applications to analysis of nuclear materials, 20: 10797
MILOVIDOV, I. V., Nuclear power plant BN-350, 20: 12441
MINAEV, V. M., Determination of spectral characteristics of isotope neutron sources by means of paired scintillation crystals of type LiI(Eu), 20: 11116
MINTURN, Robert E., Alkali-atom-halogen-molecule reactions in molecular beams: the spectator stripping model, 20: 10834
MINUSHKIN, Bertram, Sodium technology, 20: 12330 (TID-8541, pp 321-425)
MIROSHNICHENKO, L. I., Solar cosmic-ray burst of September 28, 1961, 20: 11428
MISENTA, R., AIREK-PUL—version of kinetic code AIREK-MOD for periodically pulsed fast reactors, 20: 12395 (EUR-2552.e)
MISHRA, U. C., Gamma-ray detection efficiency of annular and well-type sodium iodide crystals, 20: 11127
MISRA, M., Some exact solutions of field equations of general relativity, 20: 11877
MISSONI, Guido, Characteristics of synchrotron radiation at 1000 Mev, 20: 11403
MISTURA, L., Shape of coexistence curve in critical region, 20: 11921
MITCHELL, A., Measurement of Fe(α,α')Fe* reactions produced by alpha bombardment, 20: 12056
MITRA, A. N., Triton parameters with realistic potentials, 20: 12130
MITRA, B., Cross section of reaction ^{31}P(n,2n)^{30}P with neutrons of 14.8 Mev energy, 20: 12134
MITRA, B., Systematic measurements of (n,p) cross sections at 14.8 Mev, 20: 12133
MITSUTANI, Akio, Method for production of cis-1,4-polyisoprene, 20: 10929
MIYAKE, Yasuo, ^{90}Sr and ^{137}Cs in Columbia River plume, July 1964, 20: 11023
MIYOSHI, K., Application of fast neutron activation method to the determination of oxygen in iron and steel, 20: 10771
MIZHAILOV, I. N., Equilibrium deformation of heavy nuclei, 20: 11970 (JINR-P-2473)
MIZUNO, Kenichi, Flow of slurry through pipe. II., 20: 10998
MIZUNO, Shoji, Inhibition of protein synthesis in uv-irradiated Mycobacterium smegmatis, 20: 10656
MOCHIZUKI, Nobuyuki, Effects of preoperative irradiation for malignant cell contamination during surgical manipulation, 20: 10735
MODEL, F. S., Photochromism of metal oxides. I., 20: 10837
MODONESI, O., PINETO—FORTRAN code designed for solution of non-linear differential equations in neutrons dynamics, 20: 11946
MOEKEN, H. H. P., Economic basis for establishing number of measurements according to value of material, 20: 10967
MOELLER, E., Measurement of neutron slowing-down time distribution at 1.46 ev and its space dependence in water, 20: 11927 (AE-208)
MOGFORD, J. A., Small orbit betatron, 20: 11397 (SC-RR-65-111)
MOLL, Kendall, Secondary ignitions in nuclear attack, 20: 11031 (NP-15708)
MONEGER, H., SR_2–SR_3–SR_4 electron irradiation loop, 20: 10871 (EUR-2288.f)
MONG, B. A., Steam cycle calculations, 20: 12415 (TID-22545, pp 54-65)
MONGINI TAMAGNINI, C., PINETO—FORTRAN code designed for solution of non-linear differential equations in neutrons dynamics, 20: 11946
MOORE, C. F., Isobaric analogue states in heavy nuclei. I., 20: 12078
MOOREHEAD, Wells Rufus, Effect of x irradiation on endogenous respiration and histone synthesis in Ehrlich ascites tumor cells, 20: 10691
MORA, S., Production and decay of ^{13}B hypernucleus, 20: 12043
MORAGA B., Aldo, Reconnaissance for uranium in the Lonquimay Area, Province of Malleco, Chile, 20: 11025 (RME-4552(Rev.))
MORAVCSIK, M. J., Non-dynamical spin and parity determinations, 20: 11611
MORAVCSIK, Michael J., One-particle exchange theory of pion photoproduction. I., 20: 11572
MOREL DE WESTGAVER, A., Production of ^{192}Ir sources of high specific activity, 20: 11190 (BLG-332)
MOREY, R. E., Prog. rpt. on metallurgical characteristics of high strength structural materials, 5–7/65, 20: 11273 (NRL-6364)
MORITA, Tatsuo, Radiation detector using an electronic discharge phenomenon, 20: 11163
MORIYAMA, Hideo, Studies on x-agent. XLV., 20: 11536
MOROSOV, B. V., Polarization in elastic p-p scattering at high energies, 20: 11591
MOROZOV, I. G., Measurement of absorption cross section of ^{156}Gd, 20: 11987
MOROZUMI, Shotaro, Precipitation on dislocations in beryllium–3% iron alloy, 20: 11299
MORRIS, A. C. Jr., Design of low-background whole-body counting facility, 20: 10724 (ORINS-51)
MORRIS, A. W. H., Heats of solution of some rare-earth elements in liquid tin, 20: 11304
MORRIS, C. J., Apparatus for automatic preparative gas chromatography, 20: 12553 (UCRL-14359)
MORRISON, David L., Prog. rpt. on fission-product reactions with and release from fuel-element claddings, 7–9/65, 20: 11212 (BMI-X-10143)
MORRISON, G. W., REACT and CONVRG FORTRAN subroutines for determining source convergence for 05R Monte Carlo neutron transport code, 20: 11934 (ORNL-TM-1325)
MORRISON, L. K., n-n And n-p scattering lengths and charge independence, 20: 11649
MORSELLI, L., Effects of ^{32}P on the urinary excretion of amino acids, 20: 10582
MOSES, V., Instability of pyruvate-^{14}C, 20: 10934 (UCRL-11743)
MOSKALEV, Yu. I., Combined effects of ^{90}Sr, ^{144}Ce, and ^{239}Pu on organs of rats, 20: 10552
MOSS, Frank E., Recombination luminescence in scintillation of normal and superfluid liquid helium, 20: 11904
MOSZKOWSKI, S. A., Nuclear pairing energies with simple interactions, 20: 12049
MOTEFF, J., Effects of neutron irradiation on stress-rupture properties of high-temperature precipitation hardening alloys, 20: 11358
MOTOMIYA, Kimio, RI production and storage device, 20: 12350
MOTT, N. F., Theory of atomic collisions, 20: 11511
MOTT-SMITH, H. M., Panel discussion: role of nuclear power in merchant marine, 20: 12460 (CONF-640810, pp 7-21)
MOUGNIOT, Jean-Claude, Theoretical and experimental aspects of the neutronic interaction between multiplying media, 20: 11929 (CEA-R-2849)
MUELLER, H. J. W., Scattering by singular potential r^{-4}, 20: 11706
MUELLER, J., Superconductivity of osmium and ruthenium under pressure, 20: 11896
MUELLER, W., Late changes in human brain after intraoperative implantation of ^{60}Co pellets, 20: 10575
MUELLER, William C., Gamma camera optimization of light pipe thickness, 20: 11079
MUELLNER, M., Bibliography on slow neutron detectors, 20: 11088 (AED-C-28-01)
MUENSTER, Horst, Investigations on sodium-air reactions, 20: 10851
MUKHERJEE, S. K., Decay of ^{183}Hf and nuclear levels of ^{183}Ta, 20: 12148
MUKHERJEE, S. K., Decay of ^{96}Nb, 20: 12152
MUKHERJEE, S. K., Half life measurement of 273 kev level of ^{196}Au, 20: 12151
MUKHERJEE, S. K., Isotope ^{162}Tb and its decay characteristics, 20: 12149
MULLER, H. H., Determination of lifetime and ground-state energy of ^{8}Be by α-α elastic scattering at 184 kev, 20: 12038
MUNAKATA, Chusuke, Measurement of homogeneity of semiconductor with electron beam, 20: 11361
MUNICIO, A. M., Effect of γ radiation on different cholinesterase preparations, 20: 10586
MUNRO, I. H., Naphthalene excimer emission, 20: 10854
MURDOCH, Lawrence Bryson, Separation of cadmium from lead–bismuth

eutectic by distillation, 20: 10762 (IS-T-71)
MURGULESCU, I. G., Contribution to the study of molten salts, 20: 10808 (EUR-2466.e, pp 59-80)
MUROTA, Kazuo, Nuclear fuel transport container, 20: 10985
MUROTA, Kazuo, Nuclear reactor, 20: 12376
MUROTA, Kazuo, Nuclear fuel assembly, 20: 12381
MURPHY, Daniel J., Fusion bonding of plasma-sprayed tungsten coatings to steel, 20: 11242 (UCRL-12153)
MURPHY, P. C., Characteristics and applications of high-density tungsten-based composites, 20: 11291
MURRAY, Hugh Sutherland, Stability of coupled-core nuclear reactor systems, 20: 12491
MURRAY, J. L., Prog. rpt. on EVESR nuclear superheat fuel development, 6–8/65, 20: 12399 (GEAP-4941)
MURRAY, J. L., Thyroid uptake of ^{131}I from skin exposure, 20: 10518 (BNWL-122, pp 55-8)
MURRI, E. L., Sampling and analysis of fission products during loss-of-fluid test (LOFT), 20: 12356 (IDO-17128)
MURTAZA, G., Some SU_n crossing matrices, 20: 11740
MURTHY, A. S. Venkatesha, Nuclear structure effects in decay of ^{141}Ce, 20: 12154
MUSIL, J., Beam width of two antenna systems for plasma diagnostics, 20: 12192
MUTO, H., Application of fast neutron activation method to the determination of oxygen in iron and steel, 20: 10771
MYERS, L. S. Jr., Site of attack in radiolysis of pyrimidine compounds, 20: 10899
MYERS, W., Neutron scattering in stretch-oriented polyethylene, 20: 10865

N

NABLO, S. V., Observations of magnetically self-focusing electron streams, 20: 11402
NADAL, J., Organization of basic materials auditing in fuel element fabrication plant, 20: 11262
NADEAU, Paul G., Electron spin resonance studies of γ-irradiated ferroelectric methylammonium alum crystals, 20: 12291
NADKARNI, D. M., Variation of fission threshold and fission fragment mass distribution, 20: 12117
NAGARAJAN, R., Measurement of absolute recoilless fraction "F" in the Moessbauer, 20: 12326
NAGCHAUDHURI, B. D., Probe measurements of gold cathode Penning discharge, 20: 12259
NAGCHAUDHURI, B. D., Set-up of duoplasmatron for intense ion beam, 20: 12260
NAGY, Lajos, Investigations in field of radiation-induced solid state polymerization. IX., 20: 10896
NAIR, L., Measurement of absolute recoilless fraction "F" in the Moessbauer, 20: 12326
NAIR, P. G., Electron paramagnetic resonance of Eu^{2+} in CdF_2 and KCl, 20: 12321
NAIRN, J. S., AGR fuel, 20: 12430
NAKAI, Masaru, Flow of slurry through pipe. II., 20: 10998
NAKAMURA, Shoichiro, Nuclear reactor, 20: 12515
NAKAMURA, Tolhico, Survey of Hiroshima county atomic bombing survivors, 20: 10662
NAKATANI, R. E., Effect of chronic ingestion of ^{65}Zn in trout, 20: 10528 (BNWL-122, pp 101-6)
NAKATANI, R. E., Metabolism of ^{137}Cs in trout, 20: 10521 (BNWL-122, pp 73-4)
NAKATANI, R. E., Reactor effluent monitoring—1964, 20: 10538 (BNWL-122, pp 198-201)
NAKKEN, Karl Ford, X-ray-induced damage to the p-aminobenzoic acid moiety of folic acid, 20: 10904
NAKONECHNIKOV, A. I., Diffusion of uranium in molybdenum, niobium, zirconium, and titanium, 20: 11290
NAMIKI, Mikio, Theoretical approach to very high energy phenomena, 20: 11529
NAQVI, S. I. H., Gamma rays from decay of ^{75}Se, 20: 12022
NARTOVA, T. T., Creep behavior of Ti–Zr–Al–Sn system, 20: 11335
NARTOVA, T. T., Phase equilibrium of alloys in Ti_3Al–Zr section of ternary Ti–Al–Zr system, 20: 11333
NATANSON, L., Energy levels of ^{8}Be produced in $^{11}B(n,\alpha)^{8}Li \rightarrow {}^{8}Be$, 20: 11962 (INR-655/1/PL)
NATH, P., Theory of reggeized bootstraps, 20: 11751
NAUENBERG, Michael, Consequences of C-violating interactions in η^0 and X^0 decays, 20: 11634
NAUMKIN, O. P., Phase diagram and properties of alloys of aluminum–scandium system, 20: 11297
NEAMU, I., Small-angle scattering of protons by ^{24}Mg, 20: 12003
NECHAEV, I. A., Inhibiting effects of x radiation on growth of newborn mice, 20: 10673
NECHIPORENKO, E. P., Disintegration of tungsten disilicides during oxidation in air, 20: 11237
NEDOSEEV, S. L., Turbulent heating of plasma by direct-discharge current, 20: 12183 (ORNL-tr-868)
NEFEDOR, Yu. G., Characteristics of the radiation effect under space flight conditions and ways to determine admissible radiation levels, 20: 10719 (NASA-TT-F-353, pp 3-20)
NEFEDOV, Yu. G., Biological effect of proton radiation at 510 Mev, 20: 10612 (NASA-TT-F-353, pp 194-209)
NEFEDOV, Yu. G., Radiation safety in space flights. Physical and biological studies with high-energy protons, 20: 10604
NEFKENS, B. M. K., $K_1^0 \rightarrow \pi^- + \pi^+$—a strange decay from a strange particle, 20: 11554 (COO-1195-27)
NEILER, J. H., Fragment energy correlation measurements for ^{252}Cf spontaneous fission and ^{235}U thermal-neutron fission, 20: 12076
NELSON, I. C., Effect of ^{127}I on passage of ^{131}I from cows to man via milk, 20: 10530 (BNWL-122, pp 113-17)
NELSON, R. William, Sequence for predicting waste transport by ground water, 20: 11009 (BNWL-SA-406)
NEMENOV, L. L., Analysis of reactions $\pi N \rightarrow \pi_1\pi_2 N'$, 20: 11562 (JINR-P-2454)
NEMETH, Gy., Late eye alterations after irradiation, 20: 10667
NERTNEY, R. J., Shift crew performance evaluation at nuclear test reactors, 20: 12500 (IDO-17131)
NESS, Norman F., Correlated magnetic tail and radiation belt observations, 20: 11831
NEUFELD, Jacob, Instabilities produced in plasma by helical proton beam, 20: 12244
NEUMAN, M., Note on parallelism, 20: 11868 (UCRL-14546)
NEUMANN, M. J., Automatic retrieval spark chambers, 20: 11093 (COO-614-34, Sect. IIA)
NEWLON, C. E., Nuclearly safe triangular-slab tank for handling enriched uranium, 20: 10981
NEWMAN, J. E., Gross gamma radioactivity in Indiana precipitation, 20: 11020
NEWTON, J. O., Isomer of spin $^{25}/_{2}{}^{+}$ in ^{183}Re, 20: 12042
NEXSEN, W. E. Jr., Boundary condition effects in magnetic mirror compression experiment, 20: 12238
NEZLIN, M. V., Discrete states of plasma beam and transitions between them, 20: 12251
NGUYEN, Van Hieu, Asymptotic relations between cross sections for baryon resonance production, 20: 11729
NGUYEN, Van Hieu, Mass renormalization in broken SL(6) symmetry, 20: 11734
NICHOLAE, V., Siliconizing to protect molybdenum, 20: 11236
NICHOLSON, K. P., Time-dependent neutron spectra in graphite, 20: 11940
NICOLAE, V., Behavior of molybdenum powders during pressing and sintering, 20: 11253
NIEDERLE, J., Most degenerate representations for compact and non-compact rotation groups, 20: 11682 (IC/65/89)
NIELSEN, C. E., Microinstability limitations of DXC-1 energetic plasma, 20: 12240
NIFATOV, A. P., Combined effects of ^{90}Sr, ^{144}Ce, and ^{239}Pu on organs of rats, 20: 10552
NIGHAN, W. L., Prog. rpt. on collision probability of electrons and ions with alkali metal atoms, semiannual, 11/65, 20: 11443 (NASA-CR-54790)
NIGHAN, William L., Low-energy electron-cesium atom collision probability investigations, 20: 11444 (NASA-CR-54790(App.1))
NIKOLAEV, A. V., Influence of radius and charge of ion on extraction, 20: 10952
NIKOLAEV, D. S., Mesothorium-I concentration in the Black Sea, 20: 10768 (JPRS-33212)
NISHIKAWA, Kiyoshi, Two-center model and four momentum transfer in jets, 20: 11531
NISHIKAWA, T., Normal mode analysis of standing wave linacs—field excitation and beam loading in linac cavities, 20: 11381 (BNL-9833)
NISSIM-SABAT, C., Isotope shift in muonic K x rays of ^{16}O–^{18}O, ^{40}Ca–^{44}Ca, ^{116}Sn–^{124}Sn, and ^{155}Gd–^{160}Gd, 20: 11480
NOBLE, G. A., Band shape of F-center optical emission in rubidium chloride, 20: 12278 (TID-21570)
NOBLE, Gordon, Prog. rpt. on magnetic properties of insulators, 5/16–8/15/65, 20: 12274 (COO-578-18)
NOERDLINGER, Peter D., Relativistic effects on plasma stability, 20: 12232
NOFRE, Claude, Role of the chemical species released by the radiolysis of water in the saturation of double carbon–carbon bonds, 20: 10875
NOGA, M., Self-consistency condition and πNN-vertex function, 20: 11576
NOGA, M., Self-consistent determination of πNN and πNN* vertex functions, 20: 11730
NORBERG, J. A., Addendum to the Spert III hazards summary report—low-enrichment oxide core, 20: 12497 (IDO-17003(Rev.2))
NOREM, P. C., Theoretical fine structure of He II 4686 A in magnetic fields to 40 kilogauss, 20: 11442 (MATT-280)
NOTARIO, A., Gas chromatographic analysis of fatty acids of liver in

normal and irradiated rats, 20: 10659
NOVAK, B., Plasma induction accelerator with radial magnetic field, 20: 12198
NOWIK, I., Electronic shielding parameters and anisotropic Moessbauer patterns in dysprosium ethyl sulfate, 20: 12302
NOWOTNY, H., Octahedral phase structures of transition metals, 20: 11318
NUSSBAUM, Theodore, Prog. rpt. on dielectric strength and ferroelectric behavior of ceramics, final, 1/63–6/64, 20: 11279 (SC-DC-64-1477X)
NYAGU, D., An experimental determination of relative probabilities of $K_2^0 \to 3\pi^0$ decays, 20: 11561 (JINR-P-2450)
NYAGU, D., Determination of relative probability of $K_2^0 \to \pi^\pm + e^\pm + \nu(\bar{\nu})$, 20: 11560 (JINR-P-2449)
NYMAN, D. H., High temperature creep-rupture properties of hastelloy x in vacuum, 20: 11266 (BNWL-167)

O

OAKES, M. E., Damping at lower hybrid resonance in warm partially ionized plasma, 20: 12185
OAKES, R. J., SU_4 mass formula and particle classification schemes, 20: 11753
OBEID, Mohamed, Steam cycle calculations, 20: 12415 (TID-22545, pp 45-65)
OBERMOSSER, Prog. rpt. on brittle fracture strength of heavy-gage steel plate, final, 1965, 20: 11240 (EURAEC-1520)
O'BRIEN, B. J., Comments on measurements of particle precipitation with Injun satellites, 20: 11851
O'BRIEN, H. A. Jr., Fast and thermal neutron flux measurements in ORR and LITR, 20: 12501 (ORNL-TM-1163)
OCCHIPINTI, Barbara B., Xenon and samarium tables, 20: 12352 (DP-958)
O'CONNELL, R. F., Generalized solutions for massless free fields and consequent generalized conservation laws, 20: 11722
OEHME, Reinhard, Current algebras and suppression of leptonic meson decays with $\delta = 1$, 20: 11659
OERTEL, G. K., Behavior of single-turn magnetic foil under dynamic load conditions, 20: 12177 (NASA-TN-D-3199)
O'FALLON, J. R., Experimental study of reaction $^3He(\gamma,\pi^+)^3H$ up to 260 Mev, 20: 12046
OGAWA, Kazuyuki, Neutron-radiography, 20: 11005
OGIER, W. T., Electron bremsstrahlung from proton-excited targets, 20: 11501
OGIEVETSKY, V. I., Interacting field of spin 2 and Einstein equations, 20: 11871
OGIYEVETSKY, V. I., Theories of interacting fields with spin 1, 20: 11733
OH, Yung Koun, Effect of cortisone and x irradiation on mast cells of adrenalectomized albino rats, 20: 10686
OHSAWA, Akinori, Analysis of high energy jet showers. IV., 20: 11535
OKABE, Shigeru, Beam profile measurement for electron accelerators, 20: 11407
OKAMOTO, Yoshizo, Reactor fuel element, 20: 12382
OKAZAKI, A., Ratio of direct to cumulative yield of ^{135}Xe in thermal neutron fission of ^{233}U, ^{235}U, ^{239}Pu, and ^{241}Pu, 20: 11990
OKAZAKI, Ikio, Ion beam generator, 20: 11083
OKOROKOV, V. V., Coherent coulombic excitation of nuclei passing through crystals, 20: 11973 (NP-15791)
OKRENT, David, Fast reactor safety, 20: 12433
OKUNO, E., Analysis of high energy jet showers. III., 20: 11534
OLDENDORF, William H., Symmetry of ^{131}I 4-iodoantipyrine uptake by brain after intravenous injection, 20: 10750
O'LEARY, W. J., Professional nuclear materials management, 20: 12451
OLESEN, J. K., Electron density and collision frequency during auroral absorption event, 20: 11848
OLIVERI, E., Approximate method for evaluation of over-pressure in primary circuit of pressurized water reactor, 20: 12343
OLNESS, J. W., Beta decay of ^{19}O: states of ^{19}F, 20: 12054
OLSEN, J. L., Current motion in superconductors carrying alternating currents in transverse magnetic field, 20: 11902
OLSEN, J. L., Superconductivity of osmium and ruthenium under pressure, 20: 11896
OLSON, P. A., Reactor effluent monitoring—1964, 20: 10538 (BNWL-122, pp 198-201)
OMELIANENKO, M., Fission by radiationless transition in μ mesonic atom ^{239}Pu, 20: 12041
OMHOLT, A., Optical effects of particles, 20: 11857
OMNES, Roland, Variational principle for Faddeev equations, 20: 11692 (UCRL-11768)
OMORI, Norihiko, Device for lifting and lowering heavy body, 20: 10983
ONO, Joji, Effects of uv light on template properties of polycytidylic acid, 20: 10584
ONO, Masaru, Studies of liquid-liquid partition systems. IV., 20: 10951
ONUFER, Robert J., Prog. rpt. on dielectric strength and ferroelectric behavior of ceramics, final, 1/63–6/64, 20: 11279 (SC-DC-64-1477X)
OPARIN, V. A., Charge exchange of protons in alkaline metal vapor with formation of highly excited hydrogen atoms, 20: 11471
ORESHKO, V. F., Effect of stable cobalt on adsorption of ^{60}Co by peat, 20: 10756
ORGANDZHANYAN, E. E., Influence of marrow injection into spleen on survival and weight of mice, 20: 10713
ORLOV, V. V., Measurement of absorption cross section of ^{156}Gd, 20: 11987
ORLOVA, L. V., Variable radiosensitivity of components of erythrocyte membrane in newborn rat, 20: 10589
ORSINI, C. M., Analysis of high energy jet showers. III., 20: 11534
ORTNER, J., Longitudinal extent of auroral ionization, 20: 11861
ORZHEKHOVSKII, V. L., Effect of conditions of hot plastic deformation on structure and properties of molybdenum, niobium, and titanium, 20: 11249
OSAKIEWICZ, W., Energy levels of ^8Be produced in $^{11}B(n,\alpha)^8Li \to {}^8Be$, 20: 11962 (INR-655/I/PL)
OSBORNE, J. L., Momentum spectrum of cosmic-ray muons at large Zenith angles, 20: 11526
OSMEYER, William E., Parametric re-entry ablation study of hypothetical ^{90}Sr fuel forms, 20: 11189 (MND-3062-25)
OSTER, E., Insulation structure and coil reliability, 20: 11387 (CONF-650922-28)
OTA, Susumu, Electron irradiation method, 20: 11416
OTOZAI, K., Method of analyzing beta-ray absorption data, 20: 12270
OTSUKA, Masuhiko, Space-dependent formula for Rossi-α measurements, 20: 12375
OUTI, Akizi, Analysis of high energy jet showers. II., 20: 11533
OWENS, Herman, ISO—a FORTRAN program for utilizing strong-focusing principle in beta-ray spectrometer design, 20: 11113 (UCRL-16471)
OXLEY, J. H., Fluidized-bed process for production of tungsten, 20: 11255

P

PABST, H. W., Methods and diagnostic value of radioisotope nephrography, 20: 10753
PABST, Y., Pituitary destruction by implantation of ^{90}Y in advanced cases of breast cancer, 20: 10752
PACCA, I. G., Analysis of high energy jet showers. III., 20: 11534
PADEH, B., Cytogenetic studies in chronic myeloid leukemia, 20: 10647
PADERNO, V. N., Refractory carbide alloys, 20: 11330
PAGES, Monique, Adsorption of transuranic elements by ion-exchange paper chromatography. I., 20: 10785
PAK, Soo Yun, Effect of cortisone and x irradiation on mast cells of adrenalectomized albino rats, 20: 10686
PAL, M. K., Self-consistent calculations of nuclear structure, 20: 12122
PALA, J., Influence of γ rays on seed of three species of grass, 20: 10646
PALFALVA, A., Siliconizing to protect molybdenum, 20: 11236
PALFALVI, A., Behavior of molybdenum powders during pressing and sintering, 20: 11253
PALMER, H. E., Radioactivity in northern Alaskan natives and their foods during 1964, 20: 10718 (BNWL-122, pp 172-5)
PALMER, J. R., Sampling and analysis of fission products during loss-of-fluid test (LOFT), 20: 12356 (IDO-17128)
PALMER, R. L., Superconducting transition temperature of La_3S_4, 20: 11909
PALMY, C., Superconductivity of osmium and ruthenium under pressure, 20: 11896
PALOTAY, J. L., Biological effects of ^{90}Sr in miniature swine, 20: 10597 (BNWL-122, pp 37-45)
PALOTAY, J. L., Liver infiltrates in radiation chimeras, 20: 10505 (BNWL-122, pp 146-9)
PALOTAY, J. L., Toxicity of copper and x rays in rats, 20: 10598
PAN, Yu-Li, Spin-parity determination of Y_1^* (1765), 20: 11656
PANASYUK, A. D., Process of activated sintering of tantalum and hafnium carbides, 20: 11250
PANDARESE, F., Resolution obtainable with some TRC's with electrostatic deflection, 20: 11104 (LNF-65/33)
PANDHARIPANDE, V. R., Energy levels of ^{111}Ag, 20: 12145
PANDHARIPANDE, V. R., Life-time and angular correlation measurements in decay of ^{117}Cd, 20: 12136
PANDHARIPANDE, V. R., Magnetic cooling set-up for studies with oriented nuclei, 20: 12138
PANDIT, L. K., Algebra of currents and magnetic moments of hyperons, 20: 11569 (UR-875-118)
PANDIT, L. K., Algebra of currents and generalized Ademollo-Gatto theorem, 20: 11610
PANEK, T., Q-values and cross-sections measurements of (n,α) reaction on some nuclei, 20: 11983
PANTUEV, V. S., γ-Quanta detecting by using spark chamber and total absorption Cherenkov counter, 20: 11099 (JINR-P-2436)
PAPPAS, A., Neutron capture therapy, 20: 10728
PAREISHVILI, E. A., Influence of marrow injection into spleen on survival and weight of mice, 20: 10713

PARHAM, A. G., Elastic n-p charge-exchange scattering at 8 Bev/c, 20: 11606
PARIBOK, V. P., Radioprotective effects of inert gases and low-molecular narcotics. IV., 20: 10712
PARK, J. F., Chronic effects of inhaled $^{239}PuO_2$ in dogs, 20: 10596 (BNWL-122, pp 1-15)
PARK, Kilho, ^{90}Sr and ^{137}Cs in Columbia River plume, July 1964, 20: 11023
PARK, R. S., Fluidized-bed process for production of tungsten, 20: 11255
PARKER, D. R., Evaluation of microscopic-sized graphite aerosol from Rover reactor destruction test, June 1965, 20: 12471 (SC-RR-65-557)
PARKER, F. L., United States and Soviet Union waste-disposal standards, 20: 12521
PARKER, Midgett S., Effect of γ irradiation on polyamide, 20: 10892
PARKER, Robert, Rapid phase transformations in titanium induced by pulse heating, 20: 11283 (UCRL-12142)
PARKER, Roy T., Follow-up of patients with adenocarcinoma of cervix and cervical stump, 20: 10727
PARKS, P. B., Thermal neutron diffusion in heavy water, 20: 11931 (CONF-651101-53)
PARSONS, J. R., Conversion of crystalline germanium to amorphous germanium by ion bombardment, 20: 11363
PARSONS, T. V., Silt movement in an EBB channel, Firth of Forth, 1965, 20: 11022 (AERE-R-5080)
PARTHASARADHI, K., Absolute photoelectric cross sections of 320-kev γ rays in Pb, Sn, and Ag, 20: 11496
PARTHEY, Harry, Chlorinating preparation of fuel elements, 20: 10961
PASOTTI, C., Protective action of phospholipid extract of spleen on mice subjected to whole-body irradiation, 20: 10704
PASOTTI, C., Protective effect of duodenal heparinoid on mouse exposed to lethal dose of whole-body irradiation, 20: 10705
PASTERNACK, Bernard, Empirical sampling using radioactivity as generator of randomicity, 20: 11204 (NYO-3136-2, App. 3)
PASTERNACK, Bernard, Light bulb statistics, 20: 11205 (NYO-3136-2, App. 4)
PASTERNACK, Bernard, Patterns in residuals: test for regression model adequacy in radionuclide assay, 20: 11203 (NYO-3136-2, App. 2)
PASTERNACK, Bernard, Prog. rpt. on statistical analysis of environmental and total body x-ray scintillation spectra, 10/64–9/65, 20: 11201 (NYO-3136-2)
PASZTOR, Endre, Reconstruction of NG 200/1 neutron generator, 20: 11942
PASZYC, Stefan, Photolysis and radiolysis of some simple nitroalkanes. II., 20: 10874
PATANKAR, A. V., Study of lifetimes of positronium in teflon irradiated by gamma rays, 20: 10905
PATELL, R. K., Study of Ne(n,p) reaction at E_n = 14.1 Mev, 20: 12118
PATRIARCA, G., Effect of 6-mercaptopurine and of x rays on skin homografts, 20: 10506
PATRO, A. P., Matrix method for resolution and backscattering corrections in scintillation beta-spectrometry, 20: 11156
PATTISON, J. B. M., Momentum spectrum of cosmic-ray muons at large Zenith angles, 20: 11526
PAVLINOV, L. V., Diffusion of uranium in molybdenum, niobium, zirconium, and titanium, 20: 11290
PAVLOVA, M. P., Balance of natural radioactivity in leukemia, 20: 10545
PAVLYUKEVICH, T. M., Infrared spectra of lanthanum germanates, 20: 10828
PEAK, J. C., Precritical calculations for 3.0 in. pitch, beryllium reflected, TWMR critical assembly, 20: 12465 (GA-6807)
PEAKALL, K. A., Oxidation behavior of defective fuel elements, 20: 12380
PEARCE, D. W., Radioactive waste management, 20: 12519 (TID-8541, pp 149-248)
PEARLSTEIN, L. D., Additions to paper on interchange stability of Van Allen Belt, 20: 11835
PEARSON, J., Fluidized-bed process for production of tungsten, 20: 11255
PECHENNIKOV, A. V., Magnetic properties of single and polycrystalline praseodymium diselenide $PrSe_2$, 20: 12310
PEELLE, R. W., Beam energy measurements at Oak Ridge isochronous cyclotron, 20: 11396 (ORNL-TM-1382)
PEETE, Charles H. Jr., Follow-up of patients with adenocarcinoma of cervix and cervical stump, 20: 10727
PEHL, R. H., Mass 13, T = ½ quartet, 20: 12036
PEHL, Richard H., High spin levels preferentially populated by (α,d) reaction, 20: 12061
PEKAREK, L., Macroscopic space charge field in disturbed quasineutral plasma, 20: 12191
PELSER, J., Technical aspects of RCN and mutual significance of RCN and Dutch industry, 20: 12490
PENG, Ta-tsai, Influence of ionizing radiation on cellular response in lymph nodes of rats after immunization, 20: 10685
PENNEY, William, British atomic program, 20: 12427
PERELOMOV, A. M., Casimir operators for U(n) and SU(n) groups, 20: 11690 (NP-15764)
PERELOMOV, A. M., Green's function for coulomb potential, 20: 11446 (NP-15794)
PERELOMOV, A. M., Latent symmetry of hydrogen atom, 20: 11445 (NP-15793)
PERGAMENSHCHIK, B. K., Concrete for high-temperature reactor shielding, 20: 12340
PERIE, J., Ion diffusion and migration in molten salts, 20: 10805 (EUR-2466.e, pp 21-30)
PERSAUD, Kim, Synthesis and purification of some alkylphenanthrenes and their spectra, 20: 10861 (CEA-R-2770)
PERSIANI, P. J., Fast reactor test facility (Faret) and initial experimental program, 20: 12512
PERSICO, F., Jahn-Teller effects in electron spin resonance spectra of ions with spin 1, 20: 12294
PERSSON, P. E., Monte Carlo calculations in neutron thermalization in heterogeneous system. II., 20: 11935 (RFR-154)
PERTSEV, A. N., Highly effective method of counting ^3H, 20: 11122
PETERSON, Sigfred, Integrity of reactor fuels, 20: 11222
PETERSON, Vincent Z., "Monochromatic" neutrino beam from high intensity 200 Bev proton synchrotron, 20: 11398 (UCID-1008)
PETERSSON, Bengt, Reduction of one-loop Feynman diagram with n verticles in m-dimensional Lorentz space, 20: 11723
PETIT, Pierre, Hyperfrequency spectrograph for study of irradiated substances from 20 to 300°K, 20: 10876
PETOE, G., Dependence of (n,2n) cross sections on symmetry parameter N-Z, 20: 12040
PETRAS, M., Relativistic generalization of dynamic equation for Jost function, 20: 11703
PETRAS, M., Self-consistency condition and πNN-vertex function, 20: 11576
PETRASCU, M., Fission by radiationless transition in μ mesonic atom ^{239}Pu, 20: 12041
PETROV, L. A., Proton emitters among Te isotopes, 20: 11964 (JINR-E-2464)
PETROV, N., An experimental determination of relative probabilities of $K_2^0 \to 3\pi^0$ decays, 20: 11561 (JINR-P-2450)
PETROV, N. I., Determination of relative probability of $K_2^0 \to \pi^\pm + e^\pm + \nu(\bar{\nu})$, 20: 11560 (JINR-P-2449)
PETROVIC, Pavel, Evaluation of atmospheric radiation during 1964, 20: 11016
PETROVIC, Pavel, Simplified method for measuring half-life of radioactive aerosols in stratosphere, 20: 11014
PETRUKHIN, V. I., Search for $\pi^0 \to 3\gamma$ decay, 20: 11587
PETRYSHYN, W. V., Extension and solution of nonlinear operator equations, 20: 11197 (COO-614-34, Sect. IIIA)
PETSCHEK, H. E., Limit on stably trapped particle fluxes, 20: 11820
PETVIASHVILI, V. I., Electrical conductance of turbulent plasma, 20: 12219
PEZHENSKI, A. I., Study of periodic variations of cosmic-ray intensity by means of selective frequency filters, 20: 11519
PFISTER, W., Direct satellite probe measurements of ionospheric irregularities in polar cap, 20: 11845
PFLEIDERER, G., Syntheses of ^{32}S- or ^{35}S-labeled maleimides, 20: 10937 (NP-tr-1323)
PFOTZER, G., Balloon measurements of solar protons and auroral x-rays, 20: 11855
PHAM-MAU-QUAN, Thermodynamics of charged fluids, 20: 11782
PHILIPS, G. C., Associated particle method for D(d,n)^{3}He reaction, 20: 11677
PHILLIPS, A. C., Exact calculation of break-up of deuterons by neutrons, 20: 11607
PHILLIPS G., Appraisal of methods for plutonium and applications to analysis of nuclear materials, 20: 10797
PHILLIPS, G. O., Pulse radiolysis of aqueous carbohydrate solutions, 20: 10920
PHYTHIAN, R., New resonance scattering formalism and its application to electron-hydrogen scattering, 20: 11508
PICCIARELLI, V., Exchange mechanism for $\pi^+ p \to N^{*0} \rho^0$ reaction at 2.75 Bev/c, 20: 11605
PICHA, Jaroslav, Total radiation in Mileshovka, 20: 11015
PICKETT III, R. T., Advanced test reactor servo regulator rod test program, 20: 12502 (TID-22547)
PICKLESIMER, M. L., Microstructural examination, 20: 11275 (ORNL-TM-1338)
PIDD, Robert W., High temperature thermionic generator, 20: 12383
PIERAGOSTINI, F., Recovery of aluminium after neutron irradiation at 78°K, 20: 11362
PIERCE, Charles M., Design and construction of aquariums: a bibliography, 20: 12554 (UCRL-14473)
PIHL, Alexander, X-ray-induced damage to the p-aminobenzoic acid moiety of folic acid, 20: 10904
PIKAEV, A. K., Yield of phenol in radiolysis of aqueous sulfate solutions

of benzene containing divalent iron ions and oxygen, 20: 10878
PIKEL'NER, L. B., Computation of multiple interactions for experiments on radiation capture of neutrons, 20: 11967 (JINR-P-2455)
PIKULEV, A. T., X-radiation effects on central nervous system and skeletal muscles in rats, 20: 10593
PILIPENKO, D. V., Electron loss and formation of slow negative ions in colloids between hydrogen atoms and negative ions with gas molecules, 20: 11509
PILIPETS, D. T., Measurement of absorption cross section of ^{156}Gd, 20: 11987
PINGEL, H., Calibration measurements on external electron beam 1 to 5 Bev, 20: 11389 (DESY-65/12)
PINKHASIK, M. S., Concrete for high-temperature reactor shielding, 20: 12340
PINKHASIK, M. S., Nuclear power plant BN-350, 20: 12441
PINOCHET, J., Organization of basic materials auditing in fuel element fabrication plant, 20: 11262
PINOTTI, Alfred D., Neutron-absorptive glass, 20: 12273
PINSONNEAULT, L. L., Lithium-lithium scattering, 20: 12053
PINTO, Maria do Lourdes, Study of the ternary system U–V–Cr, 20: 11271 (LFEN-24)
PIONTKOVSKII, I. A., Eye damage in dogs exposed to radiation in antenatal period of development, 20: 10675
PIPPIN, C. A., Study of thermistor stability, 20: 11062 (RFP-649)
PISAREVSKII, A. N., Highly effective method of counting ^{3}H, 20: 11122
PITNER, A. L., Migration area and moderator reactivity coefficients for H_2O moderated, 1.8 wt % Pu–Al loading in PRCF, 20: 12494 (BNWL-160)
PITTILLO, Robert F., Modification of radiation damage of bacteria by folic acid antagonists, 20: 10648
PITTMAN, Constance S., Treatment of hyperthyroidism, 20: 10738
PITTMAN, James A. Jr., Treatment of hyperthyroidism, 20: 10738
PIXLEY, R. E., Determination of lifetime and ground-state energy of ^{8}Be by α-α elastic scattering at 184 kev, 20: 12038
PLAJNER, Z., Radioactive decay of ^{188}Re, 20: 11998
PLAKSIN, I. N., Use of polonium–boron emitter of neutrons in analysis of ores and dressing products for aluminum, 20: 10781
PLASIL, V., Precise synchronized measurements of space angle in circular chopper diagram, 20: 11177 (UJV-1388/65)
PLASS, G., Experiments with high energy neutrinos, 20: 11580
PLATT, A. M., Prog. rpt. on fixation of radioactive residues, 7–9/65, 20: 12517 (BNWL-170)
PLOTNIKOVA, E. D., Determination of biological effect of protons with energies of 510 Mev and x rays with energies of 180 kv on hereditary structures, 20: 10609 (NASA-TT-F-353, pp 151-6)
PNEUMAN, G. W., Analogy for laboratory simulation of hydromagnetic phenomena in astrophysics, 20: 11431
POBLETE, M., Pituitary destruction by implantation of ^{90}Y in advanced cases of breast cancer, 20: 10752
POLETTI, G., Positron decay in halogen compounds, 20: 11621
POLIKANOV, S. M., On properties of isotope $^{254}102$, 20: 11968 (JINR-P-2470)
POLIKARPOVA, L. I., Metabolism of ascorbic acid in irradiated adrenal gland, 20: 10715
POLKINGHORNE, J. C., Froissart-Gribov continuation and reggeon unitarity conditions, 20: 11724
POLOV, V. S., Latent symmetry of hydrogen atom, 20: 11445 (NP-15793)
POLUBARINOV, I. V., Interacting field of spin 2 and Einstein equations, 20: 11871
POLUBARINOV, I. V., Theories of interacting fields with spin 1, 20: 11733
POLUSHKIN, K. K., Nuclear desalination equipment of low capacity, 20: 12454 (JPRS-33480)
POMERANTZ, M. A., Survey of cosmic-ray intensity in lower atmosphere, 20: 11521
PONZANO, G., SU_3 vector coupling coefficients, 20: 11741
POOL, James C. T., Mathematical aspects of Weyl correspondence, 20: 11876
POOLE, D. M., Electron-probe microanalysis of irradiated UO_2, 20: 10787
POOLE, M. J., Time-dependent neutron spectra in graphite, 20: 11940
POOLEY, D., F-center production in alkali halides by electron-hole recombination, 20: 12306
POOLEY, D., [110] Anion replacement sequences in alkali halides, 20: 12307
POP, I., Magnetic properties of gadolinium alloys with iron, cerium and yttrium, 20: 11341
POPOV, V. I., Secondary γ-emission coefficients for aluminum, copper, and tungsten, 20: 12267
POPOV, V. S., Casimir operators for U(n) and SU(n) groups, 20: 11690 (NP-15764)
POPOV, V. S., Green's function for coulomb potential, 20: 11446 (NP-15794)
POPPELBAUM, C., Associated particle method for $D(d,n)^{3}He$ reaction, 20: 11677
PORILE, Norbert T., Energy spectra and relative yields of ^{24}Na fragments evaporated in high-energy reactions, 20: 12067
POSTMA, H., Microinstability limitations of DCX-1 energetic plasma, 20: 12240
POSTMA, H., Observation of negative-mass instability in energetic proton plasma, 20: 12247
POTTER, D. L., Microgram surface density measurements by observation of proton-produced x rays, 20: 11281 (UCRL-12107)
POTTER, D. L., Treatment of proton channelling by a transverse two-dimensional model, 20: 12279 (UCRL-12311)
POTTER, Gordon Webster Jr., Electrocapillarity studies of symmetric aliphatic molecules on mercury, 20: 12536 (IS-T-66)
POTTER, J. F., Preparation and low-temperature magnetic properties of terbium oxides, 20: 12289
POTTIE, R. F., Cross sections for ionization by electrons. I. and II., 20: 10885
POULOPOULOS, P. N., Absorption of K^- mesons in deuterium, 20: 11599
POWELL, J. E., Separation of high-purity lutetium and ytterbium by ion exchange at 90°C, 20: 10760 (IS-1305)
POWERS, R. J., Experience with on-line experimentation, 20: 11553 (COO-614-34, Sect. IIC)
POYDO, M. S., Nuclear power plant BN-350, 20: 12441
POZNANSKI, T. W., Roentgenographic development of ^{90}Sr-induced osteogenic sarcoma in the rat, 20: 10652
POZOLOTIN, A. A., Influence of pulsed magnetic fields on cytogenetic effects of irradiation, 20: 10672
PRASAD, A. Durga, Level widths of some 2^+ states, 20: 12147
PRASAD, K. G., Life-time and angular correlation measurements in decay of ^{117}Cd, 20: 12136
PRASAD, K. G., Life-time and angular correlation measurements in ^{199}Au, 20: 12137
PRASAD, S. S., Isotope shift in Li and B^{2+}, 20: 11506
PRASK, H. J., Half-lives of 2^+ rotational states in ^{158}Dy and ^{158}Gd, 20: 12082
PRASLICKA, M., Influence of continuous irradiation and experimental diphtherial intoxication on origin and incidence of non-specific necrotic changes in cardiac muscle, 20: 10631
PRATT, J. N., Heats of solution of some rare-earth elements in liquid tin, 20: 11304
PREDAZZI, E., Integral representation for high-energy scattering amplitudes, 20: 11736
PREISS, I. L., Isomerism in ^{129}Ba, 20: 12069
PREISS, I. L., Low levels of ^{128}Ba from ^{128}La decay, 20: 12068
PRESSLY, R. S., Low energy gamma and x-ray from radioactive sources, 20: 10932 (ORNL-P-1928)
PREWITT, C. T., Corrections for x-ray absorption by crystal of arbitrary shape, 20: 12308
PRIBYL, T., Fracture of pelvis after curative irradiation, 20: 10668
PRICE, John C., Plasma kinetic equations, 20: 12182 (UCRL-16631)
PRICE, Joseph J., Carcinoma of cervix treated during pregnancy and followed by successful pregnancy, 20: 10751
PRILEZHAEV, D. S., Monopulse generation with $CaF_2:U^{3+}$ crystals, 20: 12293
PRINCE, Paul, Paralleling avalanche transistors, 20: 11067 (UCRL-12095-T)
PRO, M. J., Activation analysis of drugs, 20: 10880
PROKHOROV, V. M., Effect of salt concentration in soil solutions on rate of diffusion of microquantities of strontium, 20: 12523
PROKHOROV, V. M., Migration of radioactive strontium in soil under influence of electric field, 20: 11053
PROKOSHKIN, Yu. D., Search for $\pi^0 + 3\gamma$ decay, 20: 11587
PROST, C., Interpretation of conductivity of porous and dispersed media with the aid of cubic cellular geometric models, 20: 10997 (AERE-Trans-1038)
PROTTO, C., Labeling and kinetics of body excretion of ^{131}I-iodothiazide, 20: 10732
PROVENZANO, T. G., Operations plan—Operation HENRE, 20: 11930 (CEX-65.03)
PRUDHOMME, Prog. rpt. on brittle fracture strength of heavy-gage steel plate, final, 1965, 20: 11240 (EURAEC-1520)
PRUSCHEK, R., Apparatus for simulating heat transfer from reactor surface to thermionic converters, 20: 12487
PRUSCHEK, R., Design study of nuclear power plant (Trikt-50) for space flight, 20: 12482
PRUSCHEK, R., Energy conversion at high temperatures with nuclear reactors as heat sources, 20: 12421
PRUSCHEK, R., Experimental investigations on cylindrical noble gas-filled thermionic converters for thermionic-reactor, 20: 11547
PRUSCHEK, R., Temperature distribution in fast reactor with thermionic converters on its surface, 20: 12486
PRUSCHEK, R., Thermionic reactors as power supply of space crafts, 20: 12478
PSHEZHETSKII, S. Ya., Mechanism of non-additive formation of radicals in

radiolysis of frozen CCl_4 + CH_3OH solutions, 20: 10879
PU, Robert T., Spin-parity determination of Y$_1^*$ (1765), 20: 11656
PUCKER, N., Resonance self-shielding in group constants of fast reactors, 20: 12374
PUCKETT, L. J., Prog. rpt. on ionization and charge transfer cross sections, 20: 11447 (TID-22476)
PURSER, F. O. Jr., Cross-section and polarization determinations for $^{12}C(d,n)^{13}N$ reaction from 2.8 to 4.2 Mev, 20: 12044
PUTZ, F., Determination of ^{239}Pu content in irradiated nuclear fuel by neutron transmission, 20: 10796
PUZAK, P. P., Prog. rpt. on metallurgical characteristics of high strength structural materials, 5–7/65, 20: 11273 (NRL-6364)
PYLAEVA, E. N., Heat resistance of alloys Ti–Al–Mo–V system, 20: 11336
PYLAEVA, E. N., Investigation of alloys of ternary Ti–Al–Zr system, 20: 11332

Q

QUARATI, P., Inelastic electron-deuteron scattering and rescattering corrections, 20: 11646
QUEYROUX, Francine, Structure and properties of the intermediary phases of systems formed by lime with rare earth oxides, 20: 10822
QUINCY, R. B. Jr., Purification and growth of KCl single crystals, 20: 10813 (ORNL-3906)
QUINN, R. G., Laboratory observations of stable plasma trapped in permanent dipolar magnetic field, 20: 12202
QUINTANILLA, M., Production of stable isotopes in Spain, 20: 11191 (JEN-150-DQ/I-51)

R

RAAEN, Helen P., Indexes to Analytical Chemistry Division annual progress reports, 1964–1965, 20: 10765 (ORNL-3904)
RABER, M., Criticality control of non-inherently safe systems in fuel processing plant, 20: 10969
RABIDEAU, Sherman W., Oxygen-17 NMR in polycrystalline H_2O and D_2O ice, 20: 10835
RACK, Edward P., Radiative neutron capture in liquid and solid carbon tetrachloride in *n*-hexane, 20: 10938
RACOVEANU, N., Respiratory intake of ^{45}Ca and ^{204}Tl radionuclides, 20: 10546
RACZKA, R., Most degenerate representations for compact and non-compact rotation groups, 20: 11682 (IC/65/89)
RADUTSKII, G. M., Self-consistent calculation of K* resonance parameters, 20: 11669
RAEF, Y., Pulse radiolysis studies of carboxyl and related radicals, 20: 10913
RAGAN, H. A., Biological effects of ^{131}I in sheep and cattle, 20: 10516 (BNWL-122, pp 49-51)
RAGAN, H. A., Biological effects of ^{90}Sr in miniature swine, 20: 10597 (BNWL-122, pp 37-45)
RAGAN, H. A., Milk secretion of ^{65}Zn and ^{115m}Cd in sheep, 20: 10527 (BNWL-122, pp 94-8)
RAGAN, H. A., Relationship of ^{137}Cs concentration in feed and rumen contents, 20: 10520 (BNWL-122, pp 64-6)
RAGAN, H. A., Sheep milk production and its ^{131}I content, 20: 10517 (BNWL-122, pp 52-4)
RAGAN, H. A., Translocation of subcutaneously administered $^{239}PuO_2$, 20: 10523 (BNWL-122, pp 81-2)
RAGONE, David V., High temperature thermionic generator, 20: 12383
RAHAUSEN, A., Pituitary destruction by implantation of ^{90}Y in advanced cases of breast cancer, 20: 10752
RAHEJA, U. T., $^{40}Ca(n,\alpha)^{37}Ar$ angular distribution at E_n = 4.7 Mev, 20: 12119
RAISIC, N., Status report on in-pile dosimetry techniques in Yugoslavia, 20: 11152
RAJ, Ram, Ground-state correlations and theory of one- and two-phonon states, 20: 12123
RAJ, Ram, Structure of Pr-isotopes, 20: 12124
RAJALAKSHMI, K. V., Hydrogen bonds and radioresistance of polynucleotides in solid phase, 20: 10877
RAJAN, K. S., Chelation and olation reactions of metal ions in aqueous solution. I., Sect. III, 20: 12533 (COO-1020-6)
RAJNAK, K., Energy levels of Pu^{3+} in lanthanum trichloride, 20: 12286
RAJU, P. S., Level widths of some 2^+ states, 20: 12147
RAJU, S., Bioptic studies on therapy-induced bone marrow fibroses in chronic myeloid leukemia, 20: 10746
RAKOVIC, M., Potassium estimations in biologic material by neutron activation analysis, 20: 10776
RAM, Budh, Three-baryon states in SU(6) theory, 20: 11756
RAMACCIOTTI, D., Certain factors that influence response of photographic dosimeters for roentgen and gamma rays, 20: 11136
RAMACHANDRAN, R., Quasi-free proton-proton scattering in light nuclei at 460 Mev, 20: 11948 (AD-624318)
RAMANA MURTHY, P. V., Momentum spectrum of cosmic-ray muons at large Zenith angles, 20: 11526
RAMANNA, R., Nuclear fission as Markov process, 20: 12116
RAMAZASHVILI, R. R., Electrical conductance of turbulent plasma, 20: 12219
RAMSEY, N. F., Hyperfine separation of deuterium, 20: 11481
RAMSEY, N. F., Measurement of proton electromagnetic form factors at high momentum transfers, 20: 11625
RAMSEY, N. F., Nucleon form factors and their interpretation, 20: 11627
RAMSEY, N. F., Quasi-elastic electron-deuteron scattering and neutron form factors, 20: 11626
RAMSEY, N. F., Rotational magnetic moments of alkali-halide molecules, 20: 11484
RAMSEY, N. F., Unsuccessful search for excited electron, 20: 11629
RAMSEY, William J., $LiMg_2Tl$: preparation and structure, 20: 11282 (UCRL-12119-T)
RANDONE, G., Positron decay in halogen compounds, 20: 11621
RANKEN, W. A., Survey of Los Alamos and Euratom heat pipe investigations, 20: 11545 (LA-DC-7555)
RANKIN, Bayard, Quantized energy distributions for harmonic oscillator, 20: 11887
RANKIN, Mozelle, Magnetic field storage codes and orbit calculations, 20: 11395 (ORNL-TM-1172(Rev.))
RANNIGER, Klaus, Modification of radiation response of tumors by actinomycin D. Clinical evaluation, 20: 10700
RAO, J. Rama, Compton scattering of low energy γ rays, 20: 11515
RAO, M. Rama, Alpha-decay of ^{241}Am, 20: 12158
RAO, P. V. Ramana, Compton scattering of low energy γ rays, 20: 11515
RAO, V. Sahagiri, Beta-gamma directional correlation in ^{147}Nd, 20: 12139
RAO, V. Udaya Shankar, Knight shifts in rare-earth–tin intermetallic compounds, 20: 12324
RASHID, M. A., Some SU_n crossing matrices, 20: 11740
RASIGNI, Georges, Study of sensitivity and sensitization of photographic emulsions, 20: 11121
RASMUSSEN, John O., Comparisons of BCS nuclear wave functions with exact solutions. II., 20: 12050
RASMUSSEN, Norman C., Nondestructive analyses of irradiated MITR fuel by γ spectroscopy, 20: 10764 (MITNE-64)
RASS, I. T., Peculiarities of oxygen effects in cells of thyroid gland in mice, 20: 10710
RASS, I. T., Radioprotective efficiency of cystamine and its accumulation in mouse thymus cells, 20: 10708
RAUB, Ch. J., Occurrence of superconductivity in sulfides, selenides, tellurides of Pt-group metals, 20: 11899
RAUH, E. G., Evaporation behavior of neptunium dioxide, 20: 10840
RAUTIAN, S. G., Evaluation of polarization of atom in strong electromagnetic field, 20: 11510
RAWER, K., Ionospheric plasma density by three different methods, 20: 11847
RAY, D. K., Covalency effect of ligands of rare earth ions in crystals, 20: 12322
RAY, D. K., Nuclear quadrupolar shielding factors for rare earth ions in crystals, 20: 12323
RAYCHAUDHURI, A. K., Covalency effect of ligands of rare earth ions in crystals, 20: 12322
RAYCHAUDHURI, A. K., Nuclear quadrupolar shielding factors for rare earth ions in crystals, 20: 12323
RAYLE, Warren D., Ball lightning characteristics, 20: 12176 (NASA-TN-D-3188)
RAYNAL, Jacques, Use of beams of polarized deuterons and determination of parameters of optical model, 20: 11570 (ANL-Trans-258)
RAZGA, Z., Influence of ionizing radiations on growth of brewing barley, 20: 10619
RAZMI, M. S. K., Vector-meson decays in U(6) current algebra, 20: 11750
RAZORENOVA, V. A., Biological effect of proton radiation at 510 Mev, 20: 10612 (NASA-TT-F-353, pp 194-209)
READ, Julia, Reduction and sintering of hyperstoichiometric carbides in hydrogen, 20: 11252
READE, P. C., Synthesis of macroglobulin antibody to bacterial antigen in mice after treatment with Thorotrast, 20: 10617
READER, Joseph, Nuclear moments of ^{147}Pm, 20: 12071
READING, D. H., Elastic n-p charge-exchange scattering at 8 Bev/c, 20: 11606
REALE, Armando, (e,e'p) reaction in ^9Be nucleus, 20: 11988
REAVEY, T. A., Field sampling of ^{131}I in milk with ion exchange cartridges, 20: 10722
REBER, L. H., Microinstability limitations of DCX-1 energetic plasma, 20: 12240
RECKNAGEL, E., Moessbauer effect resulting from reaction $^{56}Fe(d,p)^{57}Fe$ using pulsed beam techniques, 20: 12298
REDDI, A. Ramalinga, Incoherent scattering of γ rays by K-shell electrons,

20: 11514
REEH, Helmut, Quantum field theory with degenerate vacuum and special type of symmetry, 20: 11715
REES, James D. Jr., Variation of time-of-flight of electrons through a photomultiplier, 20: 11071
REEVE, E. B., Measurement of synthetic rate of liver-synthesized proteins in animals, 20: 10558
REGIRER, S. A., Electric field in magnetohydrodynamic channel in presence of moving medium with alternating electric conductance, 20: 11803
REICHART, W., Q values of reaction $^{9}Be(p,d)^{8}Be$ and $^{8}Be \rightarrow 2\ ^{4}He$, 20: 12037
REICHELT, Walter H., Spacing and cesium pressure dependence of electron temperatures and ion densities in thermionic converter, 20: 11544 (LA-DC-7390)
REICHERT, W. L., ^{115}Pd yield in thermal neutron fission of ^{235}U, 20: 11981 (USNRDL-TR-943)
REID, C. N., Dislocation structure in chromium, chromium–rhenium, and chromium–iron alloys, 20: 11303
REID, George C., Important atmospheric processes in D region, 20: 11843
REID, George C., Ionospheric effects of particles, 20: 11858
REIN, James E., Prog. rpt. on burnup determination of nuclear fuels, 7–9/65, 20: 11960 (IDO-14667)
REINHOLD, H. S., Interaction between tumor cells and their media under effect of radiation, 20: 10651
REINISCH, B., Ionospheric plasma density by three different methods, 20: 11847
REISING, R. F., Deformation of transition-state nucleus in energetic fission, 20: 12077
REITAN, A., Production and absorption of s-wave pions at low energy by two nucleons, 20: 11642
REKALO, M. P., Photoproduction of mesons on nucleons and SU(6) symmetry, 20: 11581
REMARK, D. G., Cesium-137 body burdens of Alaskan men, 1965, 20: 10723
RENNER, B., Note on mass shell corrections in current algebra calculations, 20: 11613
RERIKH, K. V., Asymptotic relations between cross sections for baryon resonance production, 20: 11729
RESHETOV, G. N., Combined effects of ^{90}Sr, ^{144}Ce, and ^{239}Pu on organs of rats, 20: 10552
REYNOLDS, P., FAUST 1—hardcore discharge stability experiment, 20: 12222
REYNOLDS, W. C., HECTIC-II—IBM 7090 FORTRAN computer program, 20: 10989 (IDO-28595(Rev.))
REYSEGER, W., RCN in period 1955–1965, 20: 12557
RHO, Mannque, Comparisons of BCS nuclear wave functions with exact solutions. II., 20: 12050
RHYKERD, C. L., Gross gamma radioactivity in Indiana precipitation, 20: 11020
RIAZUDDIN, Vector-meson decays in U(6) current algebra, 20: 11750
RICCARDI, A., Accumulation of radioiodine in the ovaries, 20: 10554
RICHARD, P., Isobaric analogue states in heavy nuclei. I., 20: 12078
RICHARDS, L. A., Fallout in London rainwater during 1964, 20: 11018
RICHARDSON, A. C. B., Total cross section for 14-Mev neutrons using aligned ^{165}Ho nuclei, 20: 12089
RICHARDSON, R. W., Numerical study of 8-32-particle eigenstates of pairing hamiltonian, 20: 12051
RICHTER, H., Effect of neutron irradiation on properties of alloy Zr–3Nb–1Sn, 20: 11354
RICKARD, W. H., Influence of soil sodium on plant uptake of ^{45}Ca, ^{85}Sr, and ^{137}Cs, 20: 10534 (BNWL-122, pp 168-9)
RICKARD, W. H., Relationship of annual forage yield and fallout deposition in a cheatgrass community, 20: 11012 (BNWL-122, pp 184-6)
RICKARD, W. H., Studies of fallout nuclides in plants and browsing animals of Washington, 20: 11011 (BNWL-122, pp 181-3)
RICKAYZEN, Gerald, Accelerated currents in superconductors, 20: 11919
RIEDLER, W., Electron-proton spectrometer for rockets using solid state detectors, 20: 11853
RIEDLER, W., Longitudinal extent of auroral ionization, 20: 11861
RIEGER, W., Octahedral phase structures of transition metals, 20: 11318
RIESLAND, J. I., Fuel channels and core support plate at Big Rock Point plant, 20: 12450
RIGAL, M. Th., Liver and kidney of mice during poisoning with uranyl nitrate and carbon tetrachloride, 20: 10548
RIGHETTI, G. B., Two models proposed for explaining self-excited oscillations in alkali plasma, 20: 12225
RIHAN, T. H., Finite-range Coulomb stripping and heavy ion transfer reactions, 20: 12091
RITCHIE, W. B., Data compilation and evaluation of space shielding problems, 20: 12265 (NP-15697(Vol.1))
RIVET, Ernest, High spin levels preferentially populated by (α,d) reaction, 20: 12061
ROACH, W. R., Heat capacity of dilute solutions of liquid ^{3}He in ^{4}He at low temperatures, 20: 11920
ROBERTS, R. W., Ultrahigh vacuum, 20: 11008
ROBERTSHAW, F. C., Effects of neutron irradiation on stress-rupture properties of high-temperature precipitation hardening alloys, 20: 11358
ROBIN, M. G., Steam generators associated with sodium-cooled reactors, 20: 12339 (EURFNR-11F)
ROBIN, Marcel G., Grand Quevilly thermal tests station, 20: 12420 (EURFNR-9F)
ROBINS, R. G., Hydrolysis of uranyl nitrate solutions at elevated temperatures, 20: 10841
ROBINSON, G. C., Emergency cooling systems in gas-cooled reactors, 20: 12434
ROBINSON, H. G., Hyperfine separation of deuterium, 20: 11481
ROBINSON, K. W., Calculation of radiation effects for bypass, 20: 11384 (CEAL-TM-156)
ROBINSON, M., Quenching of fluorescence by cross relaxation of Nd^{3+} in LaF_3, 20: 12297
ROBINSON, W. B., Effect of gamma radiation upon cherries, 20: 11186
ROBSON, D., Isobaric analogue states in heavy nuclei. I., 20: 12078
ROCEK, J., Change of flux in vicinity of irregularities in regular square lattice, 20: 12366 (UJV-1439/65)
RODGERS, S. J., Effect of high temperature sodium on austenitic and ferritic steels, 20: 11235 (MSAR-65-194)
RODRIGO OTERO, A., Cleaning of porous filters in fluidized-bed reactors, 20: 10810 (JEN-153-DMa/I-19)
ROEMER, L. E., Microwave bridge measurement of plasma frequency, 20: 12249
ROFFMAN, Eric H., Complex inhomogeneous Lorentz group and complex angular momentum, 20: 11758
ROGERS, I. W., Investigation of cosmic rays underground using scintillator stack. II., 20: 11528
ROGINSKII, V. A., Mechanism of non-additive formation of radicals in radiolysis of frozen $CCl_4 + CH_3OH$ solutions, 20: 10879
ROGOZKIN, V. D., Prophylaxis and therapy of radiation injuries caused by protons, 20: 10699 (NASA-TT-F-353, pp 210-38)
ROHLENA, K., Resonance absorption of gamma-quanta in one- and two-dimensional crystals, 20: 12283
ROMAN, W. A., Metallographic preparation of some rare-earth metals, 20: 11310
ROMANO, A., Exchange mechanism for $\pi^+ p \rightarrow N^* \rho^0$ reaction at 2.75 Bev/c, 20: 11605
ROMINGER, C. Jules, Carcinoma of cervix treated during pregnancy and followed by successful pregnancy, 20: 10751
RONQVIST, N., Study of "384"-kev complex γ emission from ^{239}Pu, 20: 11950 (AE-202)
ROOS, M., Direct tests of CP invariance, 20: 11608
ROSE, B., Re-normalization of polarization in n-p scattering at medium energies, 20: 11617
ROSEN, Nathan, Mach's principle and mass in expanding universe, 20: 11873
ROSENBERG, T. J., Spatial and temporal character of fast variations in auroral-zone x rays, 20: 11826
ROSENBLUTH, M. N., Additions to paper on interchange stability of Van Allen Belt, 20: 11835
ROSENSTOCK, H. M., Photoionization-efficiency curves for C_2H_2 and C_2D_2, 20: 10867
ROSKIES, Ralph, R-matrix approach to complex angular momentum and to three-particle interaction, 20: 11691 (ORNL-3914)
ROSS, D. A., Design of low-background whole-body counting facility, 20: 10724 (ORINS-51)
ROSS, D. K., Analysis of proposed planetary radar reflection experiment, 20: 11432
ROSS, R., Capture ratio P_L/P_K for electron capture decay of ^{57}Ni, 20: 11984
ROSSTEUTSCHER, Werner, Several T–Zn and T–Cd alloy systems, 20: 11328
ROSTOKER, Gordon, Midlatitude transition bays and their relation to spatial movement of overhead current systems, 20: 11824
ROSWIT, B., Comparison of radiothermoluminescent and radiophotoluminescent dosimeters, 20: 11155
ROTBLAT, J., Life shortening in mice exposed to radiation: effects of age and hypoxia, 20: 10707
ROTH, Lloyd J., Conference on isotopes in experimental pharmacology, Chicago, 6/64, 20: 10509
ROTSHTEIN, A. Ya., Optimum method of recording frequency of free nuclear precession in presence of noise, 20: 11817
ROVINSKI, F. Ya., Adsorption of Ru by natural adsorbents, 20: 10855
ROY, Alain Le, Infrared absorption spectra of deuterated cyclohexane in the solid state, 20: 10864
ROY, S. M., Modified determinantal method, 20: 11700
RUBIN, Philip, Cancer of the cervix state II: comment, 20: 10742
RUBINA, O. G., Scintillation properties of polyphenyls, 20: 11129

RUBINOW, S. I., Asymptotic solution of Schroedinger equation for three body problem, 20: 11459
RUCKENSTEINER, E., Radiological review, 20: 10745
RUDAKOV, L. I., Turbulent heating of plasma by direct-discharge current, 20: 12183 (ORNL-tr-868)
RUDAKOV, V. V., Influence of ionizing radiation on contractive ability of mitochondria, 20: 10678
RUDENKO, N. S., New high voltage power supply for streamer chambers, 20: 11142
RUDLOFF, W., Steric interference to diffusion in Linde A Zeolite, 20: 12532 (COO-920-8)
RUEHLE, M., Interpretation of electron-microscopic contrast phenomena in vacancy agglomerates of neutron-irradiated copper, 20: 11353 (ANL-Trans-259)
RUEHLE, R., Employment of heat pipes for thermionic reactors, 20: 12489
RUGGIERO, Alessandro, Characteristics of synchrotron radiation at 1000 Mev, 20: 11403
RUKHADZE, A. A., Effect of electric field on spectrum of oscillations in inhomogeneous plasma, 20: 12220
RUPPERT, Edmund, Neutron spectra and decay time constants in zirconium hydride, 20: 11943
RUSAKOV, V., An experimental determination of relative probabilities of $K_2^0 \to 3\pi^0$ decays, 20: 11561 (JINR-P-2450)
RUSAKOV, V. A., Determination of relative probability of $K_2^0 \to \pi^\pm + e^\pm + \nu(\bar{\nu})$, 20: 11560 (JINR-P-2449)
RUSSELL, J. R., Purification and growth of KCl single crystals, 20: 10813 (ORNL-3906)
RUSSELL, L. E., Mixed carbide fuel irradiation in DFR, 20: 12442
RUTHERFORD, C. H., Evaluation of three-dimensional flux synthesis method as nuclear design tool, 20: 12368 (WAPD-T-1737)
RUTHERFORD, W. M., Preparation of highly enriched ^{13}C by thermal diffusion of methane, 20: 11194
RUTKEVICH, I. M., Electric field in magnetohydrodynamic channel in presence of moving medium with alternating electric conductance, 20: 11803
RUTKEVICH, N. Yo., Total nuclear decay reactions, 20: 12004
RYAN, D. G., Elastic n-p charge-exchange scattering at 8 Bev/c, 20: 11606
RYAN, James W., Spark chamber tests of multiple particle detection efficiency, 20: 11114 (UR-875-66)
RYBICKI, F., Finite-well, single-particle wave functions in two-nucleon stripping, 20: 12086
RYNDIN, R. M., Determination of spin and parity of Ω^- hyperon, 20: 11563 (JINR-P-2456)
RYNDIN, R. M., Double NN scattering with polarized beam and polarized target, 20: 11671
RYNN, N., Plasma column end effects, 20: 12236
RYZHOV, N. I., Biological effect of multiple x irradiation with energies of 180 kv compared with proton irradiation, 20: 10611 (NASA-TT-F-353, pp 185-93)
RYZHOV, N. I., Biological effect of proton radiation at 510 Mev, 20: 10612 (NASA-TT-F-353, pp 194-209)
RYZHOV, N. I., Characteristics of the radiation effect under space flight conditions and ways to determine admissible radiation levels, 20: 10719 (NASA-TT-F-353, pp 3-20)
RZEWUSKI, J., Functional formulation of S-matrix theory. II., 20: 11695

S

SAAVEDRA, I., Proper time formulation of Dirac electron theory, 20: 11882
SAHA, N. K., Gamma-gamma directional correlation in ^{123}Te, 20: 12140
SAHLIN, H. L., Monte Carlo study of one-component plasma. I., 20: 12181 (UCRL-14467-T)
SAHRI, D. S., Effect of deuteration on Neel temperature of $CoCl_2 \cdot 6H_2O$, 20: 10853
SAJI, Manabu, Radiation damage and annealing of GaAs laser diode, 20: 11178
SAKOVICH, V. A., Dosimetric investigations and shielding studies using synchrocyclotron, 20: 10605 (NASA-TT-F-353, pp 21-54)
SAKUNTALA, M., Study of gas discharges that are expected in closed cycle magnetohydrodynamic generator, 20: 11541 (AERE-R-5107)
SALGANIK, R. I., Radiation effects on the RDA activity in cellular nuclei and cytoplasm, 20: 10591
SALIN, Raymond, Energy spectra and angular distribution of (n,α) reaction produced on ^{32}S by neutrons at 3.2 Mev, 20: 11993
SALMON, G. A., Quenching of excited states formed in pulse radiolysis, 20: 10926
SALVADORI, Paolo, (e,e'p) reaction in ^9Be nucleus, 20: 11988
SALVINSKI, R. J., Prog. rpt. on valve technology for spacecraft engines, final, 7/64–8/65, 20: 11007 (NP-15831)
SAM, D., Nuclear-charge distributions of several fission product mass chains, 20: 11980 (USNRDL-TR-935)
SAMIRALOV, V. S., Electromagnetic properties of mesons in broken SU(6) symmetry, 20: 11727
SAMOSADNYI, V. T., Determination of spectral characteristics of isotope neutron sources by means of paired scintillation crystals of type LiI(Eu), 20: 11116
SAMPAIO, Armando de Oliveira, Study of the ternary system U–V–Cr, 20: 11271 (LFEN-24)
SAMSONOV, G. V., Carbon and boron surface saturation in refractory transition metals, 20: 11228
SAMSONOV, G. V., Production of copper, molybdenum, and tungsten powders by atomization with plasma jet, 20: 11219
SAMUELLI, M., Experiment on electrical breakdown in vacuum at Laboratorio Gas Ionizzati, 20: 11769 (LGI-65/30)
SAMUELS, M. L., Combined 5-fluorouracil and cobalt irradiation evaluated by double blind technique, 20: 10725
SANCHO ROD, J., Cleaning of porous filters in fluidized-bed reactors, 20: 10810 (JEN-153-DMa/I-19)
SANDOMIRSKII, V. B., Transition of semiconductors to superconducting state under influence of field effect, 20: 11901
SANGAL, Satendra P., Complexometric determination of yttrium(III), 20: 10779
SANKHLA, B. S., Reactions of samarium isopropoxide with methylacetoacetate, 20: 10846
SANO, S. I., Observation of partial shrinkage of strata, 20: 11024
SANOCHKIN, Yu. V., Dissipative instability in magnetohydrodynamics, 20: 11794
SANTAGATI, G., Uptake of ^{35}S-sodium sulfate by hepatic tissue of normal and irradiated rats, 20: 10542
SANTORO, R. T., Beam energy measurements at Oak Ridge isochronous cyclotron, 20: 11396 (ORNL-TM-1382)
SANVITO, R., Accumulation of radioiodine in the ovaries, 20: 10554
SARMA, N., Distorted wave Born approximation calculation for $(^3He,p)$ 20: 12127
SARMA, N., Study of levels of ^{44}Ti, 20: 12144
SARMA, R. P., Life-time and angular correlation measurements in decay of ^{117}Cd, 20: 12136
SARUHASHI, Katsuko, ^{90}Sr and ^{137}Cs in Columbia River plume, July 1964, 20: 11023
SARWINSKI, R. E., Heat capacity of dilute solutions of liquid ^3He in ^4He at low temperatures, 20: 11920
SASSE, S., Optimization with respect to weight for shields for large reactors, 20: 12342
SASTRY, N. P., Measurement of absolute recoilless fraction "F" in the Moessbauer effect, 20: 12326
SATCHLER, G. R., Inelastic scattering and nuclear shell model, 20: 12008
SATO, Hideo, Multivariate regression analysis of sex ratio among offspring from irradiated women, 20: 10657
SATTEN, R., Magnetic-dipole intensities and Zeeman effect in Cs_2UCl_6, 20: 12290
SAUER, J., Fracture of pelvis after curative irradiation, 20: 10668
SAUER, Myron C. Jr., Automatic analysis of data on kinetics of fast chemical reactions, 20: 10800 (ANL-7113)
SAVEL'EVA, M. M., Creep behavior of Ti–Zr–Al–Sn system, 20: 11335
SAVEL'EVA, M. M., Phase equilibrium of alloys in Ti_3Al–Zr section of ternary Ti–Al–Zr system, 20: 11333
SAVENKO, I. A., Combined proton spectrometer for space studies, 20: 11123
SAVENKO, I. A., Instrument for recording protons with E = 3 to 14 Mev, α particles, and nuclei of Z > 2, 20: 11124
SAVIRON, J. M., Production of stable isotopes in Spain, 20: 11191 (JEN-150-DQ/I-51)
SAVITSKII, E. M., Metallic compounds of rhenium with rare earth metals, 20: 11298
SAVITSKII, E. M., Phase diagram of iron–neodymium system, 20: 11295
SAVITSKII, E. M., Phase diagram and properties of alloys of aluminum–scandium system, 20: 11297
SAVITSKII, V. I., Concrete for high-temperature reactor shielding, 20: 12340
SAVUN, O. I., Combined proton spectrometer for space studies, 20: 11123
SAVUN, O. I., Instrument for recording protons with E = 3 to 14 Mev, α particles, and nuclei of Z > 2, 20: 11124
SAWERS, J. R. Jr., Cross-section and polarization determinations for $^{12}C(d,n)^{13}N$ reaction from 2.8 to 4.2 Mev, 20: 12044
SAWICKI, J., Microscopic theory of optical-model potential and hole-particle model in nuclear spectroscopy, 20: 12047
SAXENA, R. P., T = ½, ³/₂ p- and s-wave Kπ phase shifts, 20: 11648
SAXENA, R. S., Amperometric studies on compositions of thorium polyvanadates, 20: 10786
SAYER, W. B., Predicted fission product decay of Snapshot I, 20: 12466 (NAA-SR-11642)
SBERTOLI, C., Risk of internal contamination in industries employing ^{137}Cs, 20: 10721
SCADRON, M. D., Non-dynamical spin and parity determinations, 20: 11611
SCALA, A., Gas phase radiolysis and vacuum ultraviolet photolysis of

2- and 3-pentanone, 20: 10895
SCARFONE, Leonard M., Lehmann-Symanzik-Zimmermann formalism in model field theory, 20: 11716
SCARGILL, D., Extraction by processing solvents of nitrosylruthenium nitrato complexes. III., 20: 10947 (AERE-R-4786)
SCHAAL, L. A., Gross gamma radioactivity in Indiana precipitation, 20: 11020
SCHAERF, C., Photodisintegration of deuteron from 500 to 1000 Mev, 20: 11631
SCHAKI, R., Cytogenetic studies in chronic myeloid leukemia, 20: 10647
SCHAPPEL, R. E., HFIR pressure vessel and structural components material surveillance, 20: 12457 (ORNL-TM-1372)
SCHARENBERG, R. P., Pulsed-beam measurement of gyromagnetic ratio of first excited rotational states in ^{172}Yb, ^{174}Yb, and ^{176}Yb, 20: 12064
SCHECK, Florian, Studying dipole-giant resonances in heavy deformed nuclei, 20: 12015
SCHEICHER-GOTTRON, E., Sequelae of radium-irradiated hemangioma, 20: 10687
SCHELL, I. I., Nature of water movements in surface layer of ocean at OWS stations I and J south of Iceland, 20: 12541 (NYO-2929-1)
SCHELL, I. I., Origin of fluctuations in Peru current, 20: 12542 (NYO-2929-2)
SCHERBATSKOY, Serge A., Stabilized scintillation counter using photomultiplier, 20: 11166
SCHERBATSKOY, Serge A., Stabilized scintillation type radiation detector, 20: 11167
SCHEY, Harry M., Quantum corrections in Thomas-Fermi model, 20: 11452 (UCRL-12042-T)
SCHICK, L. H., Low energy K^--d elastic scattering, 20: 11630
SCHIFF, L. I., Analysis of proposed planetary radar reflection experiment, 20: 11432
SCHILLING, Heinz, Beam decomposition in linear or elliptical reflection of polarized plane waves on separation plane between absorbing media, 20: 11368
SCHINDLER, M., Theoretical considerations on heat transfer in heat pipes, 20: 12488
SCHINTLMEISTER, J., Capture ratio P_L/P_K for electron capture decay of ^{57}Ni, 20: 11984
SCHLAILE, H., Analysis of πN charge exchange scattering from 4 to 18 Bev/c, 20: 11615
SCHLAIN, David, Corrosion properties of molybdenum, tungsten, vanadium, and some vanadium alloys, 20: 11230 (BM-RI-6715)
SCHLECHT, Richard G., Hyperfine structure of stable lithium isotopes. I., 20: 11497
SCHLESINGER, H. L., Activation analysis of drugs, 20: 10880
SCHLUETER, H., Damping at lower hybrid resonance in warm partially ionized plasma, 20: 12185
SCHMID, Lawrence A., Scalar formulation of ideal charged gas flow, 20: 11798
SCHMIDT, F. C., Calorimetry in anhydrous ethylenediamine, 20: 12550 (TID-22564)
SCHMIDT, U., Temperature dependence of (n,p) cross section for chemically bound protons, 20: 11938
SCHMITT, H. W., Fragment energy correlation measurements for ^{252}Cf spontaneous fission and ^{235}U thermal-neutron fission, 20: 12076
SCHMITT, R. J., Electrolytic jet machining method for cutting single crystal and polycrystalline uranium carbide, 20: 11216 (PEL-79)
SCHMITZ, F., Diffusion of heavy elements in nuclear fuels: actinides in UO_2, 20: 11312
SCHNITZER, Howard J., Current algebras and meson systems, 20: 11748
SCHNITZER, Howard J., Low energy associated production: $\pi^- + p + K^0 + \Lambda$, 20: 11589
SCHOENDORF, William Harris, Propagation of electromagnetic wave through diffusing plasma, 20: 12254
SCHOEPF, Hans-Georg, Basic concept of general relativistic magnetohydrodynamics for ideal conductors, 20: 11772
SCHOLES, G., Pulse radiolysis studies of aqueous solutions of nucleic acid and related substances, 20: 10917
SCHOMER, R. T., Reactor plant of research ship of Gesellschaft fuer Kernenergieverwertung, 20: 12463 (CONF-640810, pp 138-55)
SCHONFELDER, J. L., Atomic structures and electron scattering in relativistic Hartree approximation, 20: 11507
SCHOONOVER, Edward, AUTO-DEBUG—machine-level debugging program, 20: 11208 (UCRL-12220)
SCHRAM, D. C., Dielectric behaviour of plasma at cyclotron resonance, 20: 12179 (NP-15782)
SCHREIBER, Hans, Basis of neutron biology of human bodies, 20: 10698
SCHROCK, V. E., Pulsed reactor simulation of underwater nuclear detonations—thermal analysis, 20: 11013 (USNRDL-TR-940)
SCHROEDER, Herbert S., Prog. rpt. on dielectric strength and ferroelectric behavior of ceramics, final, 1/63–6/64, 20: 11279 (SC-DC-64-1477X)
SCHROER, B., Local approximation in renormalizable and non-renormalizable theories. I., 20: 11707
SCHROER, B., Local approximations in renormalizable and nonrenormalizable theories. II., 20: 11708
SCHUBERT, Konrad, Several T–Zn and T–Cd alloy systems, 20: 11328
SCHUETZ, H., Air purification techniques currently used in nuclear physics, 20: 11056
SCHULER, Robert H., ESR spectrum of Foo, 20: 10882
SCHULTZ, Harvey A., Scintillations and energy transfer in argon–nitrogen mixtures, 20: 11130
SCHUYLER, J. O., Humboldt Bay reactor operating experience, 20: 12435
SCHWARTZ, Charles, Application of Schwinger variational principle for 20: 11747
SCHWARTZ, Charles, Theory and calculation of scattering with Bethe-Salpeter equation, 20: 11746
SCHWARTZ, Irving L., Studies of ventromedial hypothalamus with autoradiographic techniques, 20: 10541
SCHWARTZ, Judah L., Quantum corrections in Thomas-Fermi model, 20: 11452 (UCRL-12042-T)
SCHWARZSCHILD, Arthur, Lifetimes of first 2+ and 4+ states of ^{192}Pt, 20: 12083
SCHWEIGER, D. F., Monte Carlo evaluation of fast neutron fluxes and heating in S8DS neutron shield, 20: 12468 (NAA-SR-Memo-9916)
SCINTEL, M., Small-angle scattering of protons by ^{24}Mg, 20: 12003
SCIUTO, F., Transfer function analyzer for Dragon reactor, 20: 12425
SCOFIELD, James, Electron-nucleon scattering cross section including all polarization correlations, 20: 11636
SCOSSIROLI, R. E., Prog. rpt. on mutability of polygenes, 1/66, 20: 10603 (IAEA-2466-11)
SCOTT, S. A., New determination of ^{16}N half-life, 20: 12019
SEAMAN, Gregory Gardner, Multiple Coulomb excitation studies in even-even samarium nuclei, 20: 12110
SEATON, M. J., Approximations for exchange scattering. I., 20: 11505
SEHESTED, K., Polarographic study of aqueous oxygenated solutions irradiated with 10 Mev electron pulses, 20: 10909
SEHGAL, B. R., Resonance absorption for heavy moderators in homogeneous media, 20: 11941
SEHGAL, M. L., Neutrons activation cross-section at 24 kev II, 20: 12135
SEIDMAN, D. N., Efficiency of dislocation climb in metals, 20: 11274 (NYO-3504-2)
SEITS, I. F., Effects of whole-body x irradiation on content of iridindiphosphate glucose in liver of rats, 20: 10590
SEKHARAN, K. K., Study of ^{19}F(α,n)^{22}Na reaction using 4 π neutron counter, 20: 12143
SEKINE, Katsuhiko, Initial value problem for elementary and composite particles, 20: 11728
SEKINE, Tatsuya, Studies of liquid-liquid partition systems. IV., 20: 10951
SEMENOV, Yu. P., Reduction of radioactive emission into atmosphere and deaeration of WWR-M Reactor water, 20: 12504
SEMPREBENE, L., Effects of therapeutic doses of radioiodine on coagulative processes, 20: 10679
SEN, P., Matrix method for resolution and backscattering corrections in scintillation beta-spectrometry, 20: 11156
SEN GUPTA, S. N., Probe measurements of gold cathode Penning discharge, 20: 12259
SEPTIER, A., Possibilities of application of superconductors to particle accelerators, 20: 11412
SEQUEIROS, H., Analysis of high energy jet showers. III., 20: 11534
SERBAN D., Respiratory intake of ^{45}Ca and ^{204}Tl radionuclides, 20: 10546
SERBANESCU, Octavian, Radioactivity of mineral RPR waters. XII., 20: 10512
SERLEMITSOS, P., Low-energy electrons in dark magnetosphere, 20: 11823
SERRANO C., Mario, Reconnaissance for uranium in the Lonquimay Area, Province of Malleco, Chile, 20: 11025 (RME-4552(Rev.))
SESHADRI, Indumathi, Analysis of light Λ hyperfragments on separable potential model. II., 20: 11594
SETHI, B., Half life measurement of 273 kev level of ^{196}Au, 20: 12151
SETTE, D., Shape of coexistence curve in critical region, 20: 11921
SEVAN'KAEV, A. V., Biological effects of 130-Mev protons, 180-kv x rays, and ^{60}Co γ rays on vestibular apparatus, 20: 10610 (NASA-TT-F-353, pp 157-84)
SEVERDENKO, V. P., Plasticity and strength of tungsten during short-time tests, 20: 11339
SHA, William T., Effective resonance temperature correlation of UO_2, 20: 12372
SHADIEV, N., Levels of neucleus ^{166}Ho from reaction (n,γ), 20: 11982 (LA-tr-65-34)
SHAFRANOV, M. D., Scintillation properties of polyphenyls, 20: 11129
SHAKHOV, A. S., Thermodynamics of W, Mo, Ti, Zr, Nb, and Ta and their more important compounds, 20: 10816 (NASA-TT-F-285)
SHAND, J. B., Motion of positrons, 20: 11660
SHANKAR, J., Radiative capture of neutrons by cobalt in metal acetylacetonates, 20: 10888
SHANNON, R. O., Biological effects of ^{131}I in sheep and cattle, 20: 10516

(BNWL-122, pp 49-51)
SHANNON, R. O., Relationship of ^{137}Cs concentration in feed and rumen contents, 20: 10520 (BNWL-122, pp 64-6)
SHANSHIASHVILI, L. G., Concerning rotation of helium II near λ point, 20: 11900
SHAPIRO, I. M., Influence of radioinduced chromosome aberrations on vitality of tumor cells, 20: 10677
SHAPIRO, Irwin I., Testing general relativity with radar, 20: 11433
SHARAPOV, E. I., Computation of multiple interactions for experiments on radiation capture of neutrons, 20: 11967 (JINR-P-2455)
SHARMA, O. P., Amperometric studies on compositions of thorium polyvanadates, 20: 10786
SHARMA, R. P., Energy levels of ^{111}Ag, 20: 12145
SHARMA, R. P., Life-time and angular correlation measurements in ^{199}Au, 20: 12137
SHARMA, R. P., Radiosensitizing effects of N-ethylmalemide on Vicia faba, 20: 10624
SHARMA, S. D., Shell model calculations for levels in ^{91}Nb, 20: 12157
SHARMA, S. R., Wave propagation in magnetoplasmas, 20: 12188
SHASTRY, S., Structure of 1.86 and 3.22 Mev states of ^{88}Sr, 20: 12146
SHATASHVILI, L. Kh., Twenty-seven-day variations of geomagnetic field disturbance on zero-days of cosmic-ray intensity, 20: 11818
SHAVRIN, P. I., Combined proton spectrometer for space studies, 20: 11123
SHAW, Gordon L., N/D calculation with inelastic unitarity of πN scattering, 20: 11643
SHAW, Patricia, Pulse radiolysis studies of aqueous solutions of nucleic acid and related substances, 20: 10917
SHAWHAN, Stanley D., Experimental observations of proton whistlers from Injun 3 vlf data, 20: 11821
SHAWHAN, Stanley D., Fractional concentration of hydrogen ions in ionosphere from vlf proton whistler measurement, 20: 11822
SHCHEGOLEV, V. A., Properties of ^{254}No isotope, 20: 11969 (JINR-P-2471)
SHCHELKACHEV, A. V., ϕ Meson and low-energy interactions of elementary particles, 20: 11598
SHCHERBININ, E. V., Integral methods in electroconducting fluid jet theory, 20: 11792
SHCHERBININ, E. V., Plane magnetohydrodynamic flow, 20: 11791
SHEFSIEK, P. K., Prog. rpt. on thermionic energy converters, 11/64–10/65, 20: 11540 (AD-626444)
SHELEPIN, L. A., Amplification in decaying plasma, 20: 12210
SHELEPIN, L. A., Use of highly ionized plasma for fabrication of laser, 20: 12209
SHELLEY, W. J., Economic criteria applied to management of nuclear materials, 20: 12562
SHELLEY, W. J., Generation of quantitative data while sampling ores and concentrates, 20: 10968
SHELUPSKY, David, Translations of discrete Bose-Einstein operators, 20: 11717
SHEN, C. S., Effect of weak collisions on ion waves, 20: 12172 (MATT-302)
SHEN, C. S., Effect of weak collisions on ion waves, 20: 12237
SHEN, C. S., Fermi acceleration of charged particles in transition region beyond magnetosphere, 20: 11522
SHEN, Pu, Life-time of 619 kev state of ^{181}Hf, 20: 12000
SHEN, S. P., Passage of high-energy particles in matter—nuclear cascades induced in dense media by 1- and 3-Bev protons, 20: 12262 (BNL-8721)
SHEN, Y. R., Optical nonlinearities of plasma, 20: 12245
SHERMAN, A. E., Boundary condition effects in magnetic mirror compression experiment, 20: 12238
SHERMAN, John, Uranium, 20: 12558
SHERMAN, R. L., Modified Debye-Scherrer x-ray diffraction camera for radioactive compounds, 20: 11075
SHERWOOD, B. A., Experience with on-line experimentation, 20: 11553 (COO-614-34, Sect. IIC)
SHERWOOD, R. C., Preparation and low-temperature magnetic properties of terbium oxides, 20: 12289
SHESKOLSKAYA, A. Yu., Gravimetric method for determination of large amounts of niobium and tungsten present together, 20: 10794
SHEVCHENKO, A. N., Interpretation of absorption spectra of some organic uranyl complexes, 20: 10827
SHIBATA, Toru, Analysis of high energy jet showers. IV., 20: 11535
SHIELDS, W. R., Accuracy of isotopic analysis by thermal ionization, 20: 10795
SHIMANOVSKAYA, K. B., Antitumoral resistance in animals subjected to chronic treatment with small doses of ^{90}Sr, 20: 10627
SHIMOJIMA, Hikaru, Method for control of nuclear reactors, 20: 12347
SHIMURA, K., Application of fast neutron activation method to the determination of oxygen in iron and steel, 20: 10771
SHIN, Ernest E. H., Space-time theory of elementary particles. I., 20: 11718
SHIN, Ernest E. H., Space-time theory of elementary particles. II., 20: 11719
SHIRLEY, D. A., Nuclear spin and moment of ^{110m}Ag by paramagnetic resonance, 20: 12073
SHIROKOV, M. I., Time and energy in quantum mechanics, 20: 11866 (JINR-E-2478)
SHISHKIN, G. V., Angular asymmetry of μ decay and neutral weak current ($\nu_e \nu_\mu$), 20: 11578
SHISHKIN, G. V., Discrimination of nonpolarized state in lepton radiation produced by neutrino interactions with matter, 20: 11577
SHIZUMI, Kiyoshi, Hiroshima atomic bomb irradiated patients who entered Hiroshima within the three days postattack period, 20: 10661
SHUCHATOWITZ, Joshua, High voltage impulse system, 20: 11074
SHUCK, A. B., Remote fabrication of reactor fuels, 20: 11241 (TID-8541, pp 71-148)
SHUCK, David Leroy, Comparison of axial-dispersion and radial-diffusion models for fixed-bed design, 20: 10754 (IS-T-44)
SHUKLA, S. K., Ion exchange paper chromatography of Tc(IV), Tc(V), and Tc(VII) in HCl, 20: 10783
SHUMILOV, S. N., Total nuclear decay reactions, 20: 12004
SHURIN, A. K., Investigation of alloys of Cb–$CbCr_2$–$CbAl_3$ system, 20: 11338
SIEKIERSKI, S., Regularities in stability constants of some rare earth complexes, 20: 10953
SIEKIERSKI, S., Separation of some fission products from uranium(VI) by reversed-phase partition chromatography, 20: 10784
SIEKIERSKI, S., Separation of neptunium from neutron irradiated uranium by reversed-phase partition chromatography in the TBP–HNO_3 system, 20: 10954
SIGNORELLI, Joseph A., Elk River reactor operations, 20: 12448
SIKKA, S. K., Neutron diffraction study of crystal structure of beryllium sulphate tetrahydrate, 20: 12327
SILBERBERG, M., Kinetic experiments on water boilers program, 20: 12510
SILBERBERG, R., Modulations of generically related galactic cosmic rays, 20: 11525
SILVER, A. H., Electrodynamic study of Josephson tunneling in superconducting junctions, 20: 11910
SILVER, A. H., Macroscopic quantum interference effects through superconducting point contacts, 20: 11911
SILVERT, William, Theory of nonhomogeneous superconductors, 20: 11908
SILVESTRI, Mario, Project Cirene, 20: 12424
SIL'VESTROV, L. V., γ-Quanta detecting by using spark chamber and total absorption Cherenkov counter, 20: 11099 (JINR-P-2436)
SIMMONS, W. R., Fast reactor test facility (Faret) and initial experimental program, 20: 12512
SIMMS, P. C., Nuclear matrix elements in first-forbidden 2.2-Mev β transition of ^{140}La, 20: 12066
SIMONOFF, G. N., Production of ^{32}P and ^{33}P by high energy protons, 20: 12034
SIMONOV, Yu. N., Pion production in (n,p) collisions at 600 Mev, 20: 11564 (JINR-P-2462)
SIMONS, E. M., Reactor materials, 20: 11223
SIMPSON, J. Arol, Resonances in electron scattering from H_2, HD, and D_2, 20: 11465
SIMPSON, K. M., Data compilation and evaluation of space shielding problems, 20: 12265 (NP-15697(Vol.1))
SINANOGLU, Oktay, Quantum numbers and masses of mesons as quark-antiquark systems, 20: 11657
SINGHAL, N. C., Cross section measurements of (p,p′γ) radiation from ^{60}Ni and ^{62}Ni, 20: 12159
SINGHAL, N. C., Inelastic neutron scattering cross sections in ^{115}In, 20: 12160
SINGRU, R. M., Energy levels of ^{111}Ag, 20: 12145
SINGRU, R. M., Life-time and angular correlation measurements in decay of ^{117}Cd, 20: 12136
SINGRU, R. M., Nuclear matrix elements in first-forbidden 2.2-Mev β transition of ^{140}La, 20: 12066
SINHA, S. P., 2-2′-Dipyridyl complexes of rare earths. III., 20: 10842
SINITSYN, N. M., Adsorption of Ru by natural adsorbents, 20: 10855
SINITSYN, V. I., Gamma irradiation facilities, 20: 10980 (AEC-tr-6469)
SIRACKY, J., Histological findings in corporis uteri following irradiation, 20: 10749
SIROTKIN, A. P., Nuclear desalination equipment of low capacity, 20: 12454 (JPRS-33480)
SITENKO, A. G., Effect of particle collisions on fluctuations in plasma, 20: 12253
SIVINTSEV, Yu. V., Applied dosimetry, 20: 11058
SIX, J., Upper limit for the partial width $\Gamma(\rho \to \pi\gamma)$, 20: 11618
SIZMAN, R., Activation enthalpy of beryllium diffusion in Ni–Be alloys, 20: 11326
SKALKA, M., Effect of radiation on deoxyribonucleoproteins in animal tissue. II., 20: 10633
SKARDHAMAR, Torfinn, Comparison of control rod calculations using homogeneous and heterogeneous methods, 20: 12362 (RFR-193)
SKLADANOWSKI, Z., Solutions of superconductivity equations for odd-A

nuclei in rare-earth region, 20: 11961 (INR-602/VII/PH)
SKLYAROVA, Z. N., Spectrographic determination of rare-earth elements of yttrium group with DFS-13 diffraction spectrograph, 20: 10775
SKORYUPIN, V. A., Turbulent heating of plasma by direct-discharge current, 20: 12183 (ORNL-tr-868)
SKOVLI, Gunnar, Beta-spectrometer for low-energy electrons, 20: 11157
SLATTERY, G. F., Preferred orientations in Zircaloy-2 tubing manufactured by various routes, 20: 11251
SLAVIERO, G., Gas chromatographic analysis of fatty acids of liver in normal and irradiated rats, 20: 10659
SLAVIERO, G. E., Uptake of ^{35}S-sodium sulfate by hepatic tissue of normal and irradiated rats, 20: 10542
SLEPTSOV, V. M., Production of copper, molybdenum, and tungsten powders by atomization with plasma jet, 20: 11219
SMELCER, Naomi K., Bibliographies of interest to atomic energy program, 20: 12547 (TID-3043(Rev.2, Suppl.3))
SMIDT, D., Fast reactor core design and safety studies in France in Federal Republic of Germany, 20: 12439
SMIDT, D., First results on comparative value of sodium, steam and helium as fast reactor coolants, 20: 12345
SMIDT, D., Karlsruhe reference design of 1000 KWe sodium cooled fast breeder reactor, 20: 12402 (KFK-369)
SMIRENNYI, L. N., Characteristics of the radiation effect under space flight conditions and ways to determine admissible radiation levels, 20: 10719 (NASA-TT-F-353, pp 3-20)
SMIRENNYI, L. N., Dosimetric investigations and shielding studies using synchrocyclotron, 20: 10605 (NASA-TT-F-353, pp 21-54)
SMITH, Alan R., Experimental shielding studies at 6.2-Bev Berkeley bevatron, 20: 11400 (UCRL-16323)
SMITH, C. V., GAROL—computer program for evaluating resonance absorption including resonance overlap, 20: 11932 (GA-6637)
SMITH, D. B., Silt movement in an EBB channel, Firth of Forth, 1965, 20: 11022 (AERE-R-5080)
SMITH, F., Engineering development of 1200°F sodium vapor trap, 20: 10982
SMITH, F. E., Evaluation of three-dimensional flux synthesis method as nuclear design tool, 20: 12368 (WAPD-T-1737)
SMITH, G. A., Experimental branching ratios for ϕ decay, 20: 11619
SMITH, Harold P. Jr., Treatment of proton channelling by a transverse two-dimensional model, 20: 12279 (UCRL-12311)
SMITH, J. H., Experimental study of reaction $^3He(\gamma,\pi^+)^3H$ up to 260 Mev, 20: 12046
SMITH, James H., Introduction to special relativity, 20: 11890
SMITH, Richard J., Bibliographies of interest to atomic energy program, 20: 12547 (TID-3043(Rev.2, Suppl.3))
SMITH, V. H., Removal of internally deposited plutonium from rats, 20: 10531 (BNWL-122, pp 118-21)
SMITH, V. H., Removal of internally deposited ruthenium from rats, 20: 10532 (BNWL-122, pp 122-4)
SMITH, Wm. T. Jr., Rhenium nitrogen fluoride and rhenium tetrafluoride, 20: 10845
SMITHERS, D. W., Treatment of carcinoma of thyroid with radioiodine, 20: 10729
SMRZ, Pavel, Absorptive corrections to nucleon exchange term in elastic πN scattering, 20: 11573
SNIVELY, Frank Thomas, Magnetic properties of single crystal Tm ethylsulphate, 20: 12316
SNYDER, M. D., Versatile iodine vapor and particle sampler, 20: 11060 (BNWL-122, pp 33-6)
SOBOLEV, N. N., Use of highly ionized plasma for fabrication of laser, 20: 12209
SOERAAS, F., Measurement of charged particles in auroral zone, Andoeya, Norway, 20: 11854
SOKOLOVA, I. K., Dosimetric investigations and shielding studies using synchrocyclotron, 20: 10605 (NASA-TT-F-353, pp 21-54)
SOKURSKII, Yu. N., Strengthening metals and alloys by irradiation, 20: 11366
SOLDATENKOVA, L. I., Effects of whole-body x irradiation on content of iridindiphosphate glucose in liver of rats, 20: 10590
SOLE, M. J., Electrolytic jet machining method for cutting single crystal and polycrystalline uranium carbide, 20: 11216 (PEL-79)
SOLNTSEV, A. M., Discrete states of plasma beam and transitions between them, 20: 12251
SOLOMON, Y., Development of photogrammetric techniques for measuring surface contours of small samples, 20: 11068 (WAPD-T-1815)
SOLOV'EV, E. S., Charge exchange of protons in alkaline metal vapor with formation of highly excited hydrogen atoms, 20: 11471
SOLOV'EV, L. D., Electromagnetic properties of mesons in broken SU(6) symmetry, 20: 11727
SOLOV'EV, V. V., Charge asymmetry in radiative decays of K and ρ mesons upon violation of CP invariance, 20: 11584
SOLOVIEV, L. D., ϕ Meson and low-energy interactions of elementary particles, 20: 11598
SOLTYSIK, Edward A., Reorientation of H atoms by proton impact, 20: 11503
SONDEREGGER, P., Analysis of πN charge exchange scattering from 4 to 18 Bev/c, 20: 11615
SONDEREGGER, P., Secondary peak at $t = -1$ (Bev/c)^2 in high energy π^-p charge exchange scattering, 20: 11614
SOOD, P. C., Rotational bands in ^{82}Kr, 20: 12156
SOOD, P. C., Shell model calculations for levels in ^{91}Nb, 20: 12157
SORKIN, Rodney B., Use of microelectronic circuitry in space radiation environment, 20: 11179
SOSHIN, L. D., Highly effective method of counting ^3H, 20: 11122
SOSI, S., Labeling and kinetics of body excretion of ^{131}I-iodothiazide, 20: 10732
SOSNOVSKII, A. T., Investigation of particular microelements in x-ray dermatitis, 20: 10625
SOUFFRIN, Suzanne, Influence of distribution function of electrons on spectrum of nonthermal radio sources, 20: 11427
SOVKA, Jerry A., Nondestructive analyses of irradiated MITR fuel by γ spectroscopy, 20: 10764 (MITNE-64)
SOWDEN, R. G., Reduction and sintering of hyperstoichiometric carbides in hydrogen, 20: 11252
SPAID, J. F., Effect of gamma radiation upon cherries, 20: 11186
SPALDING, T. R., Management and control of EBR-II fuel, 20: 12452
SPALTHOFF, W., Effect of neutron irradiation on properties of alloy Zr–3Nb–1Sn, 20: 11354
SPANJERSBERG, Genevieve, Effect of x rays on growth of tissue cells of Topinambour, 20: 10621
SPANNER, J. C., Detection of metal overstress by acoustic emission, 20: 11001 (BNWL-SA-438)
SPEISER, D., SU_4 mass formula and particle classification schemes, 20: 11753
SPERBER, Daniel, Competition between neutron and gamma emission from nuclear states with high spin, 20: 12048
SPITSYN, V. I., Influence of radioactive additions of labeled atoms on mechanisms of reactions, 20: 10936 (CEA-tr-A-1855)
SPITSYN, V. I., Problem of radioactive wastes, 20: 12520 (CEA-tr-A-1490)
SPLICHAL, William F. Jr., Savannah River Plant criticality dosimetry system, 20: 11029 (DP-1006)
SPLITTSTOESSER, D. F., Effect of gamma radiation upon cherries, 20: 11186
SPRINZAK, A., Lifetime measurements of some rotational levels by new recoil method, 20: 12020
SRIKANTIAN, G., Control of reactivity in high conversion ratio, plutonium fueled, thermal power reactors, 20: 12393 (BNL-8748)
SRINIVASAN, S. K., Photoproduction of vector mesons, 20: 11595
SRIVASTAVA, Y. N., Theory of reggeized bootstraps, 20: 11751
STACK, John D., Polarization as test for Regge behavior in backward $\pi^\pm$p scattering, 20: 11663
STAEHLE, R. W., Prog. rpt. on stress corrosion cracking in Fe–Ni–Cr alloy systems, 6–9/65, 20: 11233 (COO-1319-32)
STANEK, F. W., Pulse transformer with two separate cores for time-to-pulse-height conversion, 20: 11117
STARKE, E., Effect of neutron irradiation on properties of alloy Zr–3Nb–1Sn, 20: 11354
STARY, J., Use of EDTA for radiometric determination of traces of metals by means of electrophoresis, 20: 10792
STARZYCKI, S., Influence of γ rays on seed of three species of grass, 20: 10646
STAUB, H. H., Determination of lifetime and ground-state energy of ^8Be by α-α elastic scattering at 184 kev, 20: 12038
STAUB, H. H., Q values of reaction $^9Be(p,d)^8Be$ and $^8Be \rightarrow 2\ ^4He$, 20: 12037
STAVISSKII, Yu. Ya., Cross sections for fast neutron radiative capture in rhenium and tantalum, 20: 11986
STEELE, R. M., Rhenium nitrogen fluoride and rhenium tetrafluoride, 20: 10845
STEFFEN, R. M., Nuclear matrix elements in first-forbidden 2.2-Mev β transition of ^{140}La, 20: 12066
STEFFEN, Rolf M., Beta-decay and nuclear structure, 20: 12113
STEICHEN, C. U., Monte Carlo evaluation of fast neutron fluxes and heating in S8DS neutron shield, 20: 12468
STEINBERG, R., Rare decay modes of ρ, A_1 and A_2 mesons, 20: 11616
STEINER, D., Employment of heat pipes for thermionic reactors, 20: 12489
STEINER, D., Feasibility of electromagnetic pumps in space vehicles, 20: 12481
STEINER, D., Parameter study of fast reactors with incore thermionic converters (system Srikt), 20: 12483
STEINKE, R. G., Spectral indices of 4.29% ^{235}U-enriched uranium metal exponential column, 20: 12358 (LA-3406)
STEKOLNIKOV, V. F., Nuclear power plant BN-350, 20: 12441
STEPANOV, K. N., Cherenkov absorption of Alfven waves and of fast magnetoacoustic waves in inhomogeneous plasma, 20: 12214
STEPHENS, William E., $^{12}C(\gamma,n)^{11}C$ giant resonance with gamma rays,

20: 12058
STERNBERG, S., Contribution to the study of molten salts, 20: 10808 (EUR-2466.e, pp 59-80)
STETSON, R. F., Observation of mirror-like instability in hot electron plasma, 20: 12180 (ORNL-P-1556)
STEUER, M., Exact determination of neutron temperature in neutron field variable in time, 20: 11937
STEVENS, C. A., FASDOP, Fortran IV computer program for computing cross sections from resonance parameters, 20: 11958 (GAMD-6562)
STEVENS, C. A., GAROL—computer program for evaluating resonance absorption including resonance overlap, 20: 11932 (GA-6637)
STEVENS, J., Elastic and inelastic scattering of protons by ^{18}O, 20: 11979 (UCRL-12152)
STEVENS, K. W. H., Jahn-Teller effects in electron spin resonance spectra of ions with spin 1, 20: 12294
STEWART, A. L., Isotope shift in Li and B^{2+}, 20: 11506
STEWART, A. T., Motion of positrons, 20: 11660
STEWART, A. T., Positron annihilation in superconducting lead, 20: 11912
STEWART, D. H., Maritime study by division of reactor development, United States Atomic Energy Commission, 20: 12461 (CONF-640810, pp 105-6)
STIEF, L. J., Vacuum-ultraviolet photochemistry. IV., 20: 10881
STINSON, W. P., Migration area and moderator reactivity coefficients for H_2O moderated, 1.8 wt % Pu–Al loading in PRCF, 20: 12494 (BNWL-160)
STIRAND, O., New method of time-space display of wave phenomena in plasma, 20: 12200
STODTMEISTER, R., Bone marrow regeneration in rats after sublethal whole-body irradiation, 20: 10681
STOKER, Michael, Regulation of growth and orientation in hamster cells transformed by polyoma virus, 20: 10684
STOLZENBACK, C. F., Current practices in disposal of waste radioactive gases from reactors, 20: 12522
STONE, Philip M., Polarization potentials for low-energy scattering: e^+-H and e^--Li, 20: 11487
STORCH, D., Fortran-fortran, 20: 11207 (UCRL-7737)
STORNELLI, R., Certain immune indexes in newborn mice treated with ^{32}P, 20: 10580
STORNELLI, R., Variations of lactic acid dehydrogenase and malic acid dehydrogenase in liver and spleen of irradiated rats, 20: 10583
STORNELLI, R., Vitamin B_{12} in lyophilized meat and in meat irradiated with γ-rays of ^{60}Co, 20: 11185
STOTT, D. A., Determination of some fast reaction rates using pulsed radiolysis of permanganate solutions, 20: 10914
STRAND, R. C., Track-segment generator, 20: 11090 (BNL-9749)
STRAND, T. G., Accurate analytical Hartree-Fock potentials for neutral atoms as sum of Yukawa terms, 20: 11472
STRASHENKO, S. I., Determination of biological effect of protons with energies of 510 Mev and x rays with energies of 180 kv on hereditary structures, 20: 10609 (NASA-TT-F-353, pp 151-6)
STRAUSS, M., Generalized Lorentz transformation, 20: 11870
STREETON, R. J. W., Extraction by processing solvents of nitrosyl-ruthenium nitrato complexes. III., 20: 10947 (AERE-R-4786)
STROM, P. O., Nuclear-charge distributions of several fission product mass chains, 20: 11980 (USNRDL-TR-935)
STRONSKI, Ignacy, Extraction and stability of metal chelates and separation of metal salts by extraction chromatography, 20: 10759 (INP-427/C)
STRUDLER, P. M., Isomerism in ^{129}Ba, 20: 12069
STRUDLER, P. M., Low levels of ^{128}Ba from ^{128}La decay, 20: 12068
STRUMINSKII, B. V., Relativistic composite model of meson and baryon resonances, 20: 11684 (JINR-P-2442)
STRZHIZHOVSKII, A. D., Biological effect of protons with energies of 126 Mev on corneal epithelia of mice, 20: 10608 (NASA-TT-F-353, pp 142-50)
STUART, B. O., Tissue accumulation of uranium and thorium in rats after inhalation of uranium ore dust, 20: 10514 (BNWL-122, pp 21-4)
STUART, B. O., Whole-body retention and biological effects of inhaled ^{144}Ce–^{144}Pr and ^{106}Ru–^{106}Rh oxides in beagles, 20: 10513 (BNWL-122, pp 16-20)
STUART, G. W., Stagnation of energetic plasma, 20: 12234
STUESSI, H., Q values of reaction $^9Be(p,d)^8Be$ and $^8Be \rightarrow 2\ ^4He$, 20: 12037
STURROCK, P. A., Explosive and nonexplosive onsets of instability, 20: 12248
STURROCK, P. A., Stochastic acceleration, 20: 11837
SU, Yung-Sung, Differential energy and angular distribution of scattered gamma rays through concrete incident normally, 20: 12269
SUBBOTIN, V. I., Temperature field of the fuel elements in core and blanket of BN-350 reactor, 20: 12443
SUBRAHMANYAM, V., Stopping of energetic copper ions in aluminum, 20: 12085
SUBRAMANIAN, R., Nuclear fission as Markov process, 20: 12116
SUCHER, J., Fictitious nature of "core term" in exchange amplitude for electron-atom scattering, 20: 11473
SUD, S. P., Decay of ^{133}Ba, 20: 12153
SUEMATSU, Shigeru, Negative ion generating device, 20: 11082
SUEMATSU, Shigeru, Particle accelerator, 20: 11417
SUGLOBOV, D. N., Complexes of uranyl perchlorate with neutral ligands, 20: 10825
SUIT, H. D., Combined 5-fluorouracil and cobalt irradiation evaluated by double blind technique, 20: 10725
SUKHOTIN, L. N., Excitation function of reaction $^{36}S(p,\gamma)^{37}Cl$ in interval $E_p = 1.4 - 2.1$ Mev, 20: 12005
SUKHOV, A. M., On properties of isotope $^{254}102$, 20: 11968 (JINR-P-2470)
SULLIVAN, D. J., $^9Be(^3He,\alpha)$ reactions to 16.63 and 16.92 Mev states of ^8Be, 20: 12027
SULLIVAN, M. F., Bile salt absorption from irradiated rat intestine, 20: 10599 (BNWL-122, pp 128-30)
SULLIVAN, M. F., Effect of bile on ^{35}S incorporation into intestinal mucopolysaccharides, 20: 10600 (BNWL-122, pp 131-4)
SULLIVAN, M. F., Influence of fission neutrons on rat reproduction, 20: 10601 (BNWL-122, pp 135-6)
SUMMERFIELD, G. C., Neutron scattering in stretch-oriented polyethylene, 20: 10865
SUNDARESAN, M. K., Kinetic equation for plasma in strong static magnetic field, 20: 12187
SUNDBERG, O., Quasi-free proton-proton scattering in light nuclei at 460 Mev, 20: 11948 (AD-624318)
SUNDERMAN, Duane N., Prog. rpt. on fission-product reactions with and release from fuel-element claddings, 7–9/65, 20: 11212 (BMI-X-10143)
SUTHERLAND, G., Fortran-fortran, 20: 11207 (UCRL-7737)
SUTTON, H. C., Radical yields and kinetics in pulse radiolysis of potassium bromide solutions, 20: 10911
SUZUKI, Mahiko, Branching ratios into $K_{\mu 2}$, $K_{\rho e 3}$, and $K_{e 4}$ in partially conserved axial-vector current, 20: 11658
SUZUKI, T., Effect of pressure on the radiation-induced solid state polymerization of acrylamide, 20: 10898
SVECHNIKOV, V. N., Investigation of alloys of Cb–$CbCr_2$–$CbAl_3$ system, 20: 11338
SVESHNIKOV, A. A., Biological effects of 130-Mev protons, 180-kv x rays, and ^{60}Co γ rays on vestibular apparatus, 20: 10610 (NASA-TT-F-353, pp 157-84)
SVIRIDENKO, E. Y., Temperature field of the fuel elements in core and blanket of BN-350 reactor, 20: 12443
SWAIN, J. E., Helium isoelectronic sequence wave functions, 20: 11450 (UCRL-7842-T)
SWAIN, J. E., Hydrogen negative ion, 20: 11453 (UCRL-12230)
SWAIN, J. E., Solution of secular equation for electrostatic helium atom, 20: 11451 (UCRL-7941(Rev.1))
SWALLOW, A. J., Pulse radiolysis of aerated aqueous potassium bromide solutions, 20: 10912
SWALLOW, A. J., Pulse radiolysis studies of carboxyl and related radicals, 20: 10913
SWALLOW, A. J., Pulse radiolysis studies of aqueous polymer-thiourea systems, 20: 10921
SWALLOW, A. J., Pulse radiolysis study of methylene blue, 20: 10925
SWALLOW, A. J., Reactions of hydrated electron with glycine and other amino acids and peptides, 20: 10918
SWALLOW, A. J., Symposium on pulse radiolysis, Manchester, 4/65, 20: 10906
SWANSON, A. A., Effect of radiation of lenticular epithelial enzymes in young rabbits, 20: 10630
SWANSON, C. D., NPR injection pump simulation, 20: 12455 (HW-77921-C)
SWANSON, C. D., NPR pressurizer, 20: 12456 (HW-77921-D)
SWARTZ, D. L., Prog. rpt. on high-sensitivity fast neutron dosimeter, 8–10/65, 20: 11094 (COO-1226-10)
SWARTZ, J. M., Prog. rpt. on high-sensitivity fast neutron dosimeter, 8–10/65, 20: 11094 (COO-1226-10)
SYCHEV, B. S., Passage of high energy neutrons through heavy concrete, 20: 12263 (JINR-P-2479)
SYCHKOV, M. A., Characteristics of the radiation effect under space flight conditions and ways to determine admissible radiation levels, 20: 10719 (NASA-TT-F-353, pp 3-20)
SYCHKOV, M. A., Dosimetric investigations and shielding studies using synchrocyclotron, 20: 10605 (NASA-TT-F-353, pp 21-54)
SYDORENKO, I. D., Effect of ionizing and uv radiation on corn seeds, 20: 10613 (NP-tr-1344)
SYKES, J. B., Beam tube equipment for FRJ-2 (DIDO) cold neutron source, 20: 12503 (AERE-Trans-1043)
SYRMAI, A. G., Nuclear rocket engine, 20: 12476 (AD-622352)
SZABO, Arpad, Radioactivity of mineral RPR waters. XII., 20: 10512
SZABO, F., Status report on in-pile dosimetry in hungary, 20: 11148
SZE, Shih-yuan, Effect of pair correlation on α decay in neighborhood of ^{208}Pb, 20: 12093
SZENTGYOERGYI, Istvan, Examination of critical superficial heat load and of boiling heat transfer in case of organic cooling agents, 20: 12331
SZIRMAK, E., Effect of local β irradiation on corneal metabolism of

rabbits, 20: 10585
SZUCHNIK, A., Synthesis of salicylic acid (^{14}COOH), 20: 10868
SZYMANSKI, Z., Calculation of parity impurities in ^{203}Tl, 20: 12007
SZYMANSKI, Z., Solutions of superconductivity equations for odd-A nuclei in rare-earth region, 20: 11961 (INR-602/VII/PH)

T

TABATA, Tatsuo, Beam profile measurement for electron accelerators, 20: 11407
TABATA, Y., Effect of pressure on the radiation-induced solid state polymerization of acrylamide, 20: 10898
TAKEDA, Kenichi, Method for stabilizing vitamin B_1–hydrochloride, 20: 10931
TAKEI, Sachio, Plasma jet generator, 20: 10798
TALANOV, V. D., Temperature field of the fuel elements in core and blanket of BN-350 reactor, 20: 12443
TALPOVA, H., Potassium estimations in biologic material by neutron activation analysis, 20: 10776
TAMURA, T., Total cross section for 14-Mev neutrons using aligned ^{165}Ho nuclei, 20: 12089
TANAKA, Eiichi, Cosmic-ray contribution to background of NaI scintillation spectrometers, 20: 11132
TANAKA, Toshikatsu, Hall effect measurement of radiation effect on p-type silicon, 20: 11360
TANDON, P. N., Magnetic moments of first excited states of ^{127}I, ^{131}I, and ^{149}Pm, 20: 12115
TANEMURA, Takashi, Performance of x-ray spectroanalyzer using ^{147}Pm beta-ray source, 20: 11133
TANG, Kwong-tin, Elastic and reactive scattering in (H,H_2) system [thesis], 20: 11513
TANG, Y. S., Liquid-metal boiling heat transfer, 20: 10999
TANGHERLINI, F. R., Consistency of subtraction method for gravitational mass, 20: 11884
TANTTILA, W. H., Possible observation of ^{115}In nuclear electric hexadecapole transitions, 20: 12304
TARASENKO, A. G., Radioprotective efficiency of cystamine and its accumulation in mouse thymus cells, 20: 10708
TARASOV, N. D., Effect of alloying on physico-mechanical properties of niobium, 20: 11288 (AD-622477)
TARJANNE, Pekka, Bootstrap approach to strong interaction symmetries, 20: 11705
TARR, C. O., Development and evaluation of a homogeneous W–25Re alloy for 2600°C applications, 20: 11238 (CONF-650449-1)
TARUSOV, B. N., Free-radical processes taking place in irradiated homogenates of animal tissues, 20: 10577
TAUBE, M., Breeding of fissionable fuel, 20: 12407 (NEIC-RR-13)
TAUSON, P., Space power plant study, 20: 12475 (WANL-PR(B)-009)
TAVENDALE, A. J., Large, coaxial, lithium-drift germanium diode for gamma-ray spectroscopy, 20: 11086 (AAEC/TM-299)
TAYLOR, G. O., Prog. rpt. on ionization and charge transfer cross sections, 20: 11447 (TID-22476)
TAYLOR, J. H., N.S. Savannah containment integrity quarterly leak rate test results, May 1964, 20: 12473 (TID-22459)
TAYLOR, John R., Spin and isospin in S-matrix theory, 20: 11720
TEITLER, S., Isotopic space, complex conjugation, and U_3 symmetry for particles, 20: 11725
TELEGDI, V. L., Experience with on-line experimentation, 20: 11553 (COO-614-34, Sect. IIC)
TELLER, E., Monte Carlo study of one-component plasma. I., 20: 12181 (UCRL-14467-T)
TEMES, G. C., Iterative Chebyshev approximation technique for equalizer synthesis, 20: 11066 (SLAC-PUB-146)
TEMPLETON, W. M., Corrugated-plate spark counters, 20: 11120
TENGERDY, Catherine, Separation and recovery of fallout ^{137}Cs from Zr–^{95}Nb in forage samples, 20: 10782
TENISHEVA, T. F., Infrared spectra of lanthanum germanates, 20: 10828
TEPPER, F., Effect of high temperature sodium on austenitic and ferritic steels, 20: 11235 (MSAR-65-194)
TER-AKOPYAN, G. M., Proton emitters among Te isotopes, 20: 11964 (JINR-E-2464)
TEREKHOVA, V. F., Phase diagram of iron–neodymium system, 20: 11295
TEREKHOVA, V. T., Phase diagram and properties of alloys of aluminum–scandium system, 20: 11297
TERENT'EV, M. V., Charge asymmetry in radiative decays of K and ρ mesons upon violation of CP invariance, 20: 11584
TERRY, Claude Emory Jr., Effects of acriflavine on uv-induced lethality and photoreactivation in Neurospora, 20: 10716
TESSLER, George, Total gamma absorption in ^{9}Be, ^{16}O, ^{19}F, and ^{27}Al at 20 Mev, 20: 12097
TETER, A. R., Evaluation of binders from machinable unfired ceramics, 20: 11277 (RFP-659)
TEWARI, S. N., Configuration mixing and independent particle motion, 20: 12128
THANKAPPAN, V. K., ^{27}Al and excited-core model, 20: 12052
THEUERER, H. C., Proximity effects between superconducting and magnetic films, 20: 11918
THIBAUDEAU, J., Comparison of calculated and measured critical sizes for some ZED-2 lattices, 20: 12493 (AECL-2514)
THOMAS, E. W., Emission and excitation cross sections, 20: 11448 (TID-22480)
THOMPSON, C. A., Space power plant study, 20: 12475 (WANL-PR(B)-009)
THOMPSON, M. G., Investigation of cosmic rays underground using scintillator stack. II., 20: 11528
THOMPSON, R. C., Prog. rpt. on biology, annual, 1964, 20: 10503 (BNWL-122)
THOMPSON, S. A., Prog. rpt. on ion rocket engine development, 4–6/65, 20: 11006 (NP-15824)
THORN, R. J., Evaporation behavior of neptunium dioxide, 20: 10840
THORP, J. S., Existence of Cr^{2+} and Cr^{4+} in x-irradiated ruby, 20: 12305
THOSAR, B. V., Life-time and angular correlation measurements in ^{199}Au, 20: 12137
THOSAR, B. V., Study of lifetimes of positronium in teflon irradiated by gamma rays, 20: 10905
THURBER, James K., Method for solving integer linear programming problems by use of generating functions, 20: 12528 (BNL-8694)
THURSTON, M. O., Prog. rpt. on high-sensitivity fast neutron dosimeter, 8–10/65, 20: 11094 (COO-1226-10)
TIETZ, T., Accurate analytical Hartree-Fock potentials for neutral atoms as sum of Yukawa terms, 20: 11472
TIKHONIN, F. F., Leptonic decay of Ω^- hyperon in the Quark model, 20: 11559 (JINR-P-2445)
TIPPIE, J. W., Pulsed-beam measurement of gyromagnetic ratio of first excited rotational states in ^{172}Yb, ^{174}Yb, and ^{176}Yb, 20: 12064
TIWARI, P. N., ^{40}Ca(n,α)^{37}Ar angular distribution at E_n = 4.7 Mev, 20: 12119
TOADER, M., Respiratory intake of ^{45}Ca and ^{204}Tl radionuclides, 20: 10546
TOCCA, M., Variations of lactic acid dehydrogenase and malic acid dehydrogenase in liver and spleen of irradiated rats, 20: 10583
TODT, F. W., TEMCO Fortran program for computing temperature coefficients, 20: 12353 (GA-6734)
TOELGYESSY, J., Radiocoulometric titrations, 20: 10769
TOLMIE, Ronald W., Radioisotope identifier, 20: 11171
TOLSON, G. M., Examination of failed expansion bellows between EGCR containment shell and experimenters cell 6, 20: 12411 (ORNL-TM-1380)
TOMAZIC, B., Separation of some fission products from uranium(VI) by reversed-phase partition chromatography, 20: 10784
TOMBROPOULOS, E. G., Effect of DTPA on translocation and excretion of inhaled ^{144}Ce–^{144}Pr oxide in dogs, 20: 10533 (BNWL-122, pp 125-7)
TOMPKINS, D. R., Generalized solutions for massless free fields and consequent generalized conservation laws, 20: 11722
TONDINELLI, L., Calculation of water reactors containing Pu, 20: 12370
TONON, Gianfranco, Energy of ions emitted by metallic target bombarded by laser beam, 20: 11463
TORGESON, David R., Instrumentation for continuous averaging of magnetic spin resonance spectra, 20: 11098 (IS-1312)
TORRACCA, E., Influence of thermal treatment on rate of ion exchange of zirconium phosphate, 20: 10957
TOTH, K. S., New total-cross-section measurements for reactions ^{14}N(^{14}N,^{13}N)^{15}N and ^{10}B(^{14}N,^{13}N)^{11}B, 20: 12057
TOWNDROW, E. F., Syntheses of ^{32}S- or ^{35}S-labeled maleimides, 20: 10937 (NP-tr-1323)
TOWNSEND, R. D., Effects of thermal history on kinetics of $\beta \rightarrow \alpha$ phase change in uranium and uranium–chromium alloys, 20: 11311
TOWNSEND, R. D., M_S temperature for pure uranium, 20: 11315
TRAMMELL, G. T., Single-collision approximation, 20: 11742
TREACY, P. B., ^{9}Be(^{3}He,α) reactions to 16.63 and 16.92 Mev states of ^{8}Be, 20: 12027
TREHAN, P. N., Cross section measurements of (p,p′γ) radiations from ^{60}Ni and ^{62}Ni, 20: 12159
TREHAN, P. N., Inelastic neutron scattering cross sections in ^{115}In, 20: 12160
TREHERNE, Jacqueline, Study of γ radiations emitted during transmutations of ^{227}Th (RdAc) toward ^{223}Ra (AcX), 20: 11992
TRENIN, V. P., Reduction of radioactive emission into atmosphere and deaeration of WWR-M Reactor water, 20: 12504
TRIDON, J., Exchange mechanism for $\pi^+ p \rightarrow N^* \rho^0$ reaction at 2.75 Bev/c, 20: 11605
TRIFU, M., Effect of ^{90}Sr on certain physiologic indices in Zea mays, 20: 10683
TRILLAT, Jean-Jacques, Bombardment of copper monocrystals with oxygen ions of medium energy (10-kev), 20: 12282
TRINCHER, K. S., Variable radiosensitivity of components of erythrocyte membrane in newborn rat, 20: 10589
TRIPATHY, K. C., Photoproduction processes and SU(6) symmetry,

20: 11635
TROCHERIS, Michel, Normal modes of plasma oscillation, 20: 12218
TROLLOPE, R., Null fields in Einstein-Maxwell field theory, 20: 11881
TROTT, N. G., Treatment of carcinoma of thyroid with radioiodine, 20: 10729
TROYANOV, M. F., Nuclear power plant BN-350, 20: 12441
TRUMPY, B., Measurement of charged particles in auroral zone, Andoeya, Norway, 20: 11854
TRUONG, Tran N., Consequences of C-violating interactions in η^0 and X^0 decays, 20: 11634
TRURAN, J. W., Thermonuclear reactions in medium and heavy nuclei, 20: 11989
TSAI, C. H., Binary collision expansion of double-time-temperature-dependent Green's functions, 20: 11760
TSAKADZE, D. S., Concerning rotation of helium II near λ point, 20: 11900
TSCHETTER, M. J., Solubility of tantalum in eight liquid rare-earth metals, 20: 11306
TSINOBER, A. B., Plane magnetohydrodynamic flow, 20: 11791
TSINTSADZE, N. L., Electrical conductance of turbulent plasma, 20: 12219
TSUDA, Yutaka, Method for producing biphenyl and triphenyl, 20: 10930
TSUKAHARA, Iwao, Spectrophotometric determination of Y with Arsenazo III, 20: 10773
TSUKAMOTO, W. T., Site of attack in radiolysis of pyrimidine compounds, 20: 10899
TSUKAMURA, Michio, Inhibition of protein synthesis in uv-irradiated Mycobacterium smegmatis, 20: 10656
TSUKAMURA, Michio, Modification of distribution of ^{35}S-labeled mycobacterial vaccine in mouse organs by x irradiation, 20: 10655
TSUKAMURA, Sumio, Modification of distribution of ^{35}S-labeled mycobacterial vaccine in mouse organs by x irradiation, 20: 10655
TSUMORI, Kunihiko, Beam profile measurement for electron accelerators, 20: 11407
TSUNO, Nobuo, Precipitation on dislocations in beryllium–3% iron alloy, 20: 11299
TSVETAEV, A. A., Thermocouple for measuring temperatures up to 2500°K, 20: 11076
TSYTKO, S. P., Excitation function of reaction $^{36}S(p,\gamma)^{37}Cl$ in interval $E_p = 1.4 - 2.1$ Mev, 20: 12005
TULIS, Jerry John, Effect of ionizing radiation on Pasteurella tularensis, 20: 10694
TURCHINI, J. P., Liver and kidney of mice during poisoning with uranyl nitrate and carbon tetrachloride, 20: 10548
TURKIEWICZ, J., Energy levels of ^8Be produced in $^{11}B(n,\alpha)^8Li \rightarrow {}^8Be$, 20: 11962 (INR-655/I/PL)
TURSKI, A. J., Transient and oscillating solution of Boltzmann-Vlasov equation in linearized plasma, 20: 12184
TVERBAKK, O. P., BIGG-II—multigroup neutron spectrum and criticality code, 20: 12357 (KR-75)
TYMPL, M., Uranates as form of uranyl hydrolytic complexes, 20: 10838
TYREE, W. H., Large area gas proportional detector for low energy photons, 20: 11108 (RFP-637)
TYREN, H., Quasi-free proton-proton scattering in light nuclei at 460 Mev, 20: 11948 (AD-624318)
TYRRELL, M. W., Determination of total alpha activity of drinking water using nuclear emulsion, 20: 11044
TYURMINA, L. O., Computation of geomagnetic field at great heights, 20: 11816
TYUTIN, I. V., Effect of mass splitting within baryon octet on BB scattering, 20: 11586

U

UBERTI, George, Panel discussion: role of nuclear power in merchant marine, 20: 12460 (CONF-640810, pp 7-21)
UEBERALL, H., Giant resonance in inelastic electron scattering, 20: 12029
UEYANAGI, Hideo, Scintillation scanner, 20: 11161
UGLESIAS, J., Production of stable isotopes in Spain, 20: 11191 (JEN-150-DQ/I-51)
ULEHLA, I., Solution of Bethe-Goldstone equation for reaction matrix in finite nuclei, 20: 11997
ULWICK, J. C., Direct satellite probe measurements of ionospheric irregularities in polar cap, 20: 11845
UL'YANOV, R. A., Effect of alloying on physico-mechanical properties of niobium, 20: 11288 (AD-622477)
UMAKOV, P. A., Temperature field of the fuel elements in core and blanket of BN-350 reactor, 20: 12443
UMEMURA, Yasuo, Carriers of continuous measures in Hilbertian norm, 20: 11211
UMEMURA, Yasuo, Measures on infinite dimensional vector spaces, 20: 11210
UMREIKO, D. S., Interpretation of absorption spectra of some organic uranyl complexes, 20: 10827
UNGER, E., Effect of x irradiation on take and growth of Guerin tumor. II., 20: 10665
UNGER, H., Parameter study of fast reactors with incore thermionic converters (ayatem Srikt), 20: 12483
UNGER, H. E., Calculations for fast reactor with shape of hollow cylinder with thermionic converters on its surface, 20: 12485
UNGER, H. E., Nuclear space power units without convective heat transfer, 20: 12484
UOTINEN, V. O., Migration area and moderator reactivity coefficients for H_2O moderated, 1.8 wt % Pu–Al loading in PRCF, 20: 12494 (BNWL-160)
URBAN, Eugene W., Critical Stoermer conditions in quadrupole and double ring-current fields, 20: 11836
URBAN, P., Structure of nucleons, 20: 11579
URBANEK, E., Influence of continuous irradiation and experimental diphtherial intoxication on origin and incidence of non-specific necrotic changes in cardiac muscle, 20: 10631
URGEL, M., Production of stable isotopes in Spain, 20: 11191 (JEN-150-DQ/I-51)
URTILE, S., Free-radical processes taking place in irradiated homogenates of animal tissues, 20: 10577
USPENSKAYA, M. S., Blood serum cholinesterase changes in dogs exposed to irradiation, 20: 10592
USTINOV, V. I., Method of two standards for eliminating errors in measurement of isotopic composition in mass spectrometer, 20: 10793
UYEKI, E. M., Liver infiltrates in radiation chimeras, 20: 10505 (BNWL-122, pp 146-9)

V

VACLAVIK, J., Theory of plasma instability in oscillating discharge, 20: 12193
VAINSON, A. A., Effects of α and γ emissions on synthesis of DNA in HeLa cells, 20: 10588
VALENTIN, N., Plutonium urinanalysis, 20: 10757 (BLG-353)
VAN BUREN, J. P., Effect of gamma radiation upon cherries, 20: 11186
VAN CAENGGHEM, J., Citriflex—decladding of fuel elements clad with zirconium or Zircaloy-2 by an ammonium fluoride-citric acid solution, 20: 11272 (NP-15661)
VANCE, Dennis W., Inelastic collisions of H_f^+ and N_f^+ ions with hydrogen molecules, 20: 11467
VANDENPLAS, P. E., Plasma hf analog of the Roentgen-Eichenwald current, 20: 12242
VAN DER HEIJDEN, W. A., Anion exchange separation between americium and curium and between several lanthanide elements, 20: 10956
VAN DER RAAY, H. B., Elastic n-p charge-exchange scattering at 8 Bev/c, 20: 11606
VANDER WEYDEN, Allen J., U. S. fast reactor program—current view, 20: 12336
VAN DE VORST, Albert, Hydrogen bonds and radioresistance of polynucleotides in solid phase, 20: 10877
VAN-GIAI, Nguyen, Microscopic theory of optical-model potential and hole-particle model in nuclear spectroscopy, 20: 12047
VAN HOOK, W. Alexander, Vapor pressures of deuterated ethanes, 20: 10866
VAN HOWE, K. R., GAPS: Fortran code for analyzing data from pulsed neutron source experiments, 20: 12355 (GAMD-6781)
VANICEK, Oldrich, Investigation of uranium and zirconium compatibility by means of microanalyser with electron probe, 20: 11316
VAN VUCHT, J. H. N., Structures of the rare-earth trialuminides, 20: 11305
VAN VUCHT, J. H. N., Structures of $GdFe_3$, $GdNi_3$, $GdCo_3$ and corresponding yttrium compounds, 20: 11308
VANYASHIN, V. S., Contribution to theory of weak interaction, 20: 11583
VARDANYAN, V. A., Stimulating effect of certain doses of ionizing radiation on ovogenous function of bird ovary, 20: 10626
VARGA, Zoltan, Determination of coronary flow with positron emitter (^{84}Rb), 20: 10730
VARVOGLIS, A. G., Nature of inorganic ^{82}Br in neutron-irradiated bromobenzene, 20: 10890
VAS, K., Influence of ionizing radiations on growth of brewing barley, 20: 10619
VASILEVA, L. V., Temperature field of the fuel elements in core and blanket of BN-350 reactor, 20: 12443
VASKU, J., Influence of continuous irradiation and experimental diphtherial intoxication on origin and incidence of non-specific necrotic changes in cardiac muscle, 20: 10631
VDOVENKO, V. M., Complexes of uranyl perchlorate with neutral ligands, 20: 10825
VDOVIN, V. L., Convective instability of plasma which is not uniform along magnetic field, 20: 12205
VEILLET, J. J., Upper limit for the partial width $\Gamma(\rho \rightarrow \pi\gamma)$, 20: 11618
VELINSKY, Libor Jiri, Iron-free double focusing beta-ray spectrometer, 20: 11143
VENKATARAMAN, B., Electron paramagnetic resonance of Eu^{2+} in CdF_2

and KCl, 20: 12321
VENKATESWARLU, K., Hydrogen bonds and radioresistance of polynucleotides in solid phase, 20: 10877
VENKATESWARLU, K. S., Radiative capture of neutrons by cobalt in metal acetylacetonates, 20: 10888
VENUTI, Gloria Campos, (e,e'p) reaction in ^{9}Be nucleus, 20: 11988
VERESS, Imre, Reconstruction of NG 200/1 neutron generator, 20: 11942
VERKHOROBIN, L. F., Disintegration of tungsten disilicides during oxidation in air, 20: 11237
VERKHOROBIN, L. F., The high-tungsten section of tungsten–silicon phase diagram, 20: 11296
VERLY, W., Preparation and purification of tritiated geranyllinalol, 20: 10809 (EUR-2531.f)
VERMA, B. G., Reflection of hydromagnetic shock on rigid wall, 20: 11796
VERMEULEN, Theodore, Segmented laminar flow and other models for packed-bed longitudinal dispersion, 20: 10995 (UCRL-10696(Rev.) (Pt.1))
VERNOTTE, Jean, Nuclear levels of sulfur formed by (α,γ) reaction on silicon, 20: 11994
VERSTER, Nico Frederick, Pole shoe assembly for cyclotron electromagnet, 20: 11423
VERTOGRADOV, L. S., Proton emitters among Te isotopes, 20: 11964 (JINR-E-2464)
VESIN, P., Protein metabolism in digestive diseases, 20: 10570
VEYRIE, Pierre, Energy of ions emitted by metallic target bombarded by laser beam, 20: 11463
VEZZETTI, David J., Asymptotic solution of Schroedinger equation for three body problem, 20: 11459
VICTOR, Laurence Joseph, Correlations between auroral and geomagnetic micropulsations, 20: 11839
VIDAL, C., Production of ^{32}P and ^{33}P by high energy protons, 20: 12034
VIEHBOECK, F. P., Yields with multiphase isotope separator, 20: 11192 (SGAE-PH-30/1965)
VIEU, Charles, Study of γ radiations emitted during transmutations of ^{227}Th (RdAc) toward ^{223}Ra (AcX), 20: 11992
VIGNERON, L., Exchange mechanism for $\pi^{+}p \rightarrow N^{*}\rho^{0}$ reaction at 2.75 Bev/c, 20: 11605
VIJAYARAGHAVAN, R., Knight shifts in rare-earth–tin intermetallic compounds, 20: 12324
VINARNICK, L., Transportation of radioelements, 20: 11040
VINDUSKA, M., Lg ft-values of forbidden beta-transitions, 20: 11996
VINH MAU, N., Microscopic theory of optical-model potential and hole-particle model in nuclear spectroscopy, 20: 12047
VISHNEVSKII, V. F., Reproduction of kinematical particle parameters by chamber pictures with account of inhomogeneity of magnetic field, energy losses, and Coulomb scattering, 20: 11100 (JINR-P-2467)
VLADIMIROV, V. V., Theory of high frequency stabilization of screw instability of electron-hole plasma of semiconductor. I., 20: 12252
VLASOV, M. A., Torch structure of drift instability, 20: 12204
VLCEK, Jiri, Detection of uranium fuel element failures during inactive tests in CO_2 streams, 20: 11003
VOGEL, F. L., Implantation profiles for 40-kev phosphorus ions in silicon single-crystal substrates, 20: 12280
VOGT, Glenda S., Biological effects of ^{90}Sr in miniature swine, 20: 10597 (BNWL-122, pp 37-45)
VOICULESCU, G., Fission by radiationless transition in μ mesonic atom ^{239}Pu, 20: 12041
VOJTISKOVA, Marta, Possibility that thymus-mediated alloantigenic stimulation results in tolerance response, 20: 10632
VOJVODIC, S., Effects of dietary levels of P and Ca on comparative behavior of Sr and Ca, 20: 10549
VOLKENSHTEIN, N. V., Thermal conductivity of Tm, Yb, and Lu at low temperatures, 20: 11329
VOLKOV, T. F., Plasma equilibrium in toroidal chamber with traveling magnetic field, 20: 12213
VOLKOVA, M. A., Investigation of alloys of ternary Ti–Al–Zr system, 20: 11332
VOLLMER, H., Development of dynamics model for heavy water boiling reactors, 20: 12400 (HPR-54)
VONACH, H. K., Nuclear energy levels of ^{56}Fe and ^{59}Co, 20: 12063
VON BAEYER, Hans C., Absorptive corrections to nucleon exchange term in elastic πN scattering, 20: 11573
VON EHRENSTEIN, D., Survey of polarized ion sources in Europe, 20: 11379 (ANL-7118)
VON HALLE, E., Thermal diffusion column shape factors. I., 20: 10949 (K-1469)
VON HOLDT, Richard E., Curve sketching by digital computer, 20: 12552 (UCRL-12226)
VON WEDELSTAEDT, Ekart, Elimination of radionuclides, 20: 10556
VORESS, Hugh E., Bibliographies of interest to atomic energy program, 20: 12547 (TID-3043(Rev.2, Supp.3))
VORISEK, M., Application of modified S_n method for intracell thermal neutron absorption density distribution, 20: 12365 (UJV-1438/65)
VOS, O., Possibilities for recovery after x irradiation in the living organism and significance of recovery processes in irradiation of tumors, 20: 10650
VOURVOPOULOS, G., Isobaric analogue states in heavy nuclei. II., 20: 12079
VRABEC, R., Occupationally caused bone changes by external radiation burdens, 20: 10637
VRIENS, L., Binary-encounter electron-atom collision theory, 20: 11483

W

WADA, W. W., Baryon magnetic-moment sum rules in broken SU_3 and SU_6 symmetries, 20: 11743
WAGEN, D., Engineering development of 1200°F sodium vapor trap, 20: 10982
WAINE, Martin, Polarization of nuclei in solid deuterium, 20: 12104
WAINE, P., AGR fuel, 20: 12430
WAINWRIGHT, W. W., How much radiation does the patient receive per set of dental radiographs? 20: 10720
WAJDOWICZ, A., Effect of uv rays on erythropoietic activity of the kidney, 20: 10635
WALDMANN, T. A., Measurement of gastro-intestinal protein loss by means of ^{51}Cr-albumin and ^{67}Cu-caeruloplasmin, 20: 10569
WALDMANN, T. A., Preparation of ^{51}Cr-albumin, 20: 10944
WALDRON, M. B., Electron probe micro analysis of irradiated UO_2, 20: 11365
WALDSTEIN, Peter, Oxygen-17 NMR in polycrystalline H_2O and D_2O ice, 20: 10835
WALI, Kameshwar C., Linear and nonlinear mass-difference effects in model of baryon multiplets, 20: 11744
WALICKI, M., Radiation-induced formation of free radicals in styrene-grafted cellulose, 20: 10873
WALKER, D. C., Transient absorption from 260-320 nm in certain pulse irradiated aqueous solutions, 20: 10924
WALKER, J. A., Photoionization-efficiency curves for C_2H_2 and C_2D_2, 20: 10867
WALKER, J. K., Measurement of proton electromagnetic form factors at high momentum transfers, 20: 11625
WALKER, J. K., Nucleon form factors and their interpretation, 20: 11627
WALKER, J. K., Quasi-elastic electron-deuteron scattering and neutron form factors, 20: 11626
WALKER, J. K., Unsuccessful search for excited electron, 20: 11629
WALKER, W. H., Ratio of direct to cumulative yield of ^{135}Xe in thermal neutron fission of ^{233}U, ^{235}U, ^{239}Pu, and ^{241}Pu, 20: 11990
WALLACE, L. A., Cryogenic and elevated temperature properties of 7039 aluminum plate and weldments, 20: 11264 (ACF-14)
WALLIS, G. B., Bubbly flow in straight pipes, 20: 10991 (NYO-3114-12)
WALTER, F. J., Fragment energy correlation measurement for ^{252}Cf spontaneous fission and ^{235}U thermal-neutron fission, 20: 12076
WALTER, R. L., Cross-section and polarization determinations for ^{12}C(d,n)^{13}N reaction from 2.8 to 4.2 Mev, 20: 12044
WAMPLER, Stanley N., Liquid scintillation method for determination of solvent-extracted ^{32}P in foods, 20: 10772
WANG, Chen-hai, Influence of ionizing radiation on cellular response in lymph nodes of rats after immunization, 20: 10685
WANGERSKY, Peter J., Prog. rpt. on sedimentation of Mn in the open ocean, final, 1965, 20: 12540 (NYO-2882-8)
WARD, D., Isomer of spin $^{25}/_{2}^{+}$ in ^{183}Re, 20: 12042
WARD, Gerald M., Separation and recovery of fallout ^{137}Cs from Zr–^{95}Nb in forage samples, 20: 10782
WARD, J. F., Site of attack in radiolysis of pyrimidine compounds, 20: 10899
WARDMAN, P., Quenching of excited states formed in pulse radiolysis, 20: 10926
WARNKE, D. F., Ground deposition of microspheres released from 50 kilometers, 20: 11033 (SC-TM-65-398)
WARNOCK, Robert L., Linear and nonlinear mass-difference effects in model of baryon multiplets, 20: 11744
WATANABA, Mineo, Hiroshima atomic bomb irradiated patients who entered Hiroshima within the three days postattack period, 20: 10661
WATANABE, Hitoshi, Heat treatment of dilute U–Fe alloys, 20: 11319
WATANABE, Masanori, Device for transmission of pulses to high voltage circuit, 20: 11081
WATANABE, Mineo, Multivariate regression analysis of sex ratio among offspring from irradiated women, 20: 10657
WATERLOW, J. C., Study of protein metabolism in relation to nutrition, 20: 10574
WATERLOW, J. C., Use of ^{15}N for study of protein metabolism, 20: 10560
WATSON, C. E., Isobaric analogue states in heavy nuclei. I., 20: 12078
WATSON, C. R., Radiation dosimetry of ^{137}Cs in sheep evaluated with thermoluminescent dosimeters, 20: 11091 (BNWL-122, pp 67-72)
WATSON, D. G., Radioactivity in Alaskan animals and forage plants, 20: 10535 (BNWL-122, pp 176-80)
WATSON, E. C., Computer evaluation of tellurium–iodine contamination

events, 20: 10519 (BNWL-122, pp 59-63)
WATSON, E. C., Effect of ^{127}I on passage of ^{131}I from cows to man via milk, 20: 10530 (BNWL-122, pp 113-17)
WATSON, James R., Susceptibility of radiation chimeras to experimental Pseudomonas aeruginosa infection, 20: 10669
WEBB, Donald Harris, Multiple-transition effects in superconducting filamentary crystals of tin, 20: 11924
WEBB, Harry W., Design study report on 1000 MWe fast breeder reactor, 20: 12414 (TID-22545, pp 16-52)
WEBER, H., Rare decay modes of ρ, A_1 and A_2 mesons, 20: 11616
WEBSTER, J. Wallace, Criticality of single unit of aqueous uranyl fluoride solution enriched to 5% in ^{235}U, 20: 12359 (ORNL-TM-1195)
WEIBEL, E. S., Anomalous skin effect in plasma, 20: 12170 (LRP-18-65)
WEIL, Raoul, Ultrasonic studies in normal and superconducting thallium, 20: 11915
WEINBERG, A. F., Suppression of grain growth in vapor-deposited tungsten up to 2500°C, 20: 11320
WEINRICH, M., Sustained magnetic field theta pinch, 20: 12161 (65RL-3940E)
WEINZIERL, P., Determination of ^{239}Pu content in irradiated nuclear fuel by neutron transmission, 20: 10796
WEISS, H. V., ^{115}Pd yield in thermal neutron fission of ^{235}U, 20: 11981 (USNRDL-TR-943)
WEISSMANN, Mariana, Deuteron quadrupole coupling in D_2O, 20: 12287
WEISZ, Prog. rpt. on brittle fracture strength of heavy-gage steel plate, final, 1965, 20: 11240 (EURAEC-1520)
WEISZ, M., Reactor tank steels. Irradiation of tensile-test pieces in EL.3 at different temperatures and post-irradiation tests, 20: 11342 (EURAEC-1502)
WEISZ, Michel, Beryllium—canning material, 20: 11294
WELLNER, Marcel, Self-energy loop of charged vector meson, 20: 11749
WELLS, T. C., Creep behavior of magnesium–aluminum–zirconium alloy at 450°C, 20: 11313
WENDER, M., Changes in content of cerebral lipids during normal development of guinea pigs and after prenatal x irradiation, 20: 10636
WENDLAND, W., Solution of first and second boundary value problems of inner and outer regions for potential equations in R_3 through boundary coverings, 20: 11200 (HMI-B-41)
WERKHEISER, Arthur Henry Jr., Moessbauer studies of solid solutions of ^{119}Sn in noble metals, 20: 12315
WERTHAMER, N. R., Proximity effects between superconducting and magnetic films, 20: 11918
WEST, R. W., Proton emission in 42-Mev alpha-particle bombardments of several elements, 20: 12062
WESTENDORP, W. F., Sustained magnetic field theta pinch, 20: 12161 (65RL-3940E)
WESTER, P. O., Concentration of 24 trace elements in human heart tissue determined by neutron activation analysis, 20: 10869
WESTERBACK, S., Chelation and olation reactions of metal ions in aqueous solution. I., Sect. III, 20: 12533 (COO-1020-6)
WESTHAUS, Paul, Method of correlated basis functions, 20: 11492
WESTHEAD, James W., Prog. rpt. on radiation damage in semiconductor materials, 2–4/65, 20: 11176 (NP-15835)
WEYER, G., Moessbauer effect resulting from reaction $^{56}Fe(d,p)^{57}Fe$ using pulsed beam techniques, 20: 12296
WEYERS, C., Plutonium urinanalysis, 20: 10757 (BLG-353)
WHANG, D. H., Inhibition of whole-body incorporation and retention of ^{131}I in man, 20: 10543
WHARTON, C. B., Cyclotron waves in collisionless plasma, 20: 12175 (NASA-CR-348)
WHEATLEY, J. C., Heat capacity of dilute solutions of liquid ^3He in ^4He at low temperatures, 20: 11920
WHEATLEY, J. C., Thermal equilibrium between liquid ^3He and powdered cerium magnesium nitrate at very low temperatures, 20: 11922
WHITE, C. W., Thermal conductivity in isotopic mixtures of solid helium, 20: 11917
WHITE, Clark W., Thermal conductivity in solid ^3He and ^4He, 20: 11916
WHITE, R., SL(6,c) symmetry, 20: 11680 (IC/65/84)
WHITE, Richard H., Hydrodynamic behavior of supernovae explosions, 20: 11425 (UCRL-7777)
WHITE, Richard H., Hydrodynamic calculations of general-relativistic collapse, 20: 11434
WHITEHEAD, A. Bruce, Pulse height defect and energy dispersion in semiconductor detectors, 20: 11138
WHITFIELD, James F., How radiation causes cell death, 20: 10629
WHITHAM, G. K., Management and control of EBR-II fuel, 20: 12452
WHITTAKER, R. H., Species-diversity problems in plant communities, 20: 10511 (BNL-9836)
WHITTAKER, R. H., Weather modification: effect on biological equilibrium in plant community, 20: 10510 (BNL-9835)
WHITTUM, H. O., ML-1 shield study, 20: 12385 (AGN-TP-149)
WICKMAN, H. H., Electronic shielding parameters and anisotropic Moessbauer patterns in dysprosium ethyl sulfate, 20: 12302
WICKMAN, H. Hollis, Nuclear spin and moment of ^{110m}Ag by paramagnetic resonance, 20: 12073
WIELAND, T., Syntheses of ^{32}S- or ^{35}S-labeled maleimides, 20: 10937 (NP-tr-1323)
WILCKE, O., Late changes in human brain after intraoperative implantation of ^{60}Co pellets, 20: 10575
WILCOX, T. P., BOUNCE, IBM 7090 code to calculate flux distributions within multiple-pin fuel elements, 20: 12384 (AGN-TM-411)
WILDE, N., Prog. rpt. on instrument development, annual, 1964, 20: 11061 (IDO-17112)
WILDE, NED, Instrumentation analysis, 20: 12498 (IDO-17112, pp 1-51)
WILDE, P. F., Desaga scanner: new scanner for radioactive substances on thin-layer chromatograms, 20: 10788
WILDER, D. R., Vaporization of solid UO_2, 20: 11234 (IS-1300)
WILKENS, M., Interpretation of electron-microscopic contrast phenomena in in vacancy agglomerates of neutron-irradiated copper, 20: 11353 (ANL-Trans-259)
WILKINSON, D. H., Beta decay of ^{19}O: states of ^{19}F, 20: 12054
WILLARD, H. James Jr., Prog. rpt. on radiation damage in semiconductor materials, 2–4/65, 20: 11176 (NP-15835)
WILLARD, John E., ESR spectra of gaseous ^{129}I and ^{127}I, 20: 11468
WILLARD, William Kenneth, Effects of x rays on Aedes aegypti population dynamics, 20: 10692
WILLIAMS, Donald J., Correlated magnetic tail and radiation belt observations, 20: 11831
WILLIAMS, E. M., Note on motion of low-energy hydrogen ions in hydrogen, 20: 11805
WILLIAMS, H. J., Preparation and low-temperature magnetic properties of terbium oxides, 20: 12289
WILLIAMS, I. R., New total-cross-section measurements for reactions $^{14}N(^{14}N,^{13}N)^{15}N$ and $^{10}B(^{14}N,^{13}N)^{11}B$, 20: 12057
WILLIAMS, M. D., Behavior of single-turn magnetic coil under dynamic load conditions, 20: 12177 (NASA-TN-D-3199)
WILLIAMS, R. W., Positron annihilation and electronic structure of rare-earth metals, 20: 11323
WILLIS, Charles R., Model of interacting radiation and matter. II., 20: 11470
WILLMORE, A. P., Probe techniques, 20: 11844
WILLSON, R. L., Pulse radiolysis studies of aqueous solutions of nucleic acid and related substances, 20: 10917
WILSON, Charles R., Gamma camera optimization of light pipe thickness, 20: 11079
WILSON, Daniel W., Separation and recovery of fallout ^{137}Cs from Zr–^{95}Nb in forage samples, 20: 10782
WILSON, Margaret D., Solar flare particles in September 1963, 20: 11852
WILSON, Richard, Measurement of proton electromagnetic form factors at high momentum transfers, 20: 11625
WILSON, Richard, Nucleon form factors and their interpretation, 20: 11627
WILSON, Richard, Quasi-elastic electron-deuteron scattering and neutron form factors, 20: 11626
WILSON, Richard, Unsuccessful search for excited electron, 20: 11629
WILSON, Robert G., Effects of uv light on template properties of poly-cytidylic acid, 20: 10584
WILSON, Robert Lee, Design study report on 1000 MWe fast breeder reactor, 20: 12414 (TID-22545, pp 16-52)
WILSON, S. A., Ultrahigh-speed gross alpha autoradiography, 20: 10529 (BNWL-122, pp 110-12)
WILSON, Virginia H., Production of carrier-free ^{132}Cs and ^{129}Cs, 20: 10901
WINDLE, W. F., ^{147}Pm-silicon betavoltaic battery feasibility, 20: 11546 (SC-RR-65-671)
WINICK, H., Vacuum requirements for bypass, 20: 11385 (CEAL-TM-157)
WINKLER, H., Determination of lifetime and ground-state energy of ^8Be by α-α elastic scattering at 184 kev, 20: 12038
WINTER, G., Capture ratio P_L/P_K for electron capture decay of ^{57}Ni, 20: 11984
WINTERNITZ, P., Electromagnetic current and form factors for meson 35-plet in SL(6,c) symmetry, 20: 11683 (JINR-E-2475)
WINTERNITZ, P., Polarized proton target in investigation of low-energy nucleon-nucleon interactions, 20: 11965 (JINR-P-2426)
WIRTZ, K., Karlsruhe reference design of 1000 MWe sodium cooled fast breeder reactor, 20: 12402 (KFK-369)
WISE, Benjamin Nathan, Morphogenesis in Euplotes. I and II., 20: 10696
WIT, Romuald, New restriction on forward scattering amplitude in local field theory, 20: 11697
WIT, Romuald, Validity of Martin's physical sum rule for forward scattering amplitude, 20: 11696
WITTE, Kathleen, Quantum-mechanical pair-correlation function of ^4He gas at low temperatures, 20: 11897
WITTE, S., Possibilities of bone marrow transfusion in treatment of bone marrow diseases, 20: 10731
WITTHAUS, J. K., ML-1 shield study, 20: 12385 (AGN-TP-149)
WIZA, Joseph L., $^{17}O(d,p)^{18}O$ reaction and nuclear structure of ^{18}O,

20: 12055
WNUK, Stephen P. Jr., Progress in high-temperature and radiation resistant strain-gage development, 20: 11070
WOCHNER, R. D., Measurement of gastro-intestinal protein loss by means of ^{51}Cr-albumin and ^{67}Cu-caeruloplasmin, 20: 10569
WOESSNER, G., Parameter study of fast reactors with incore thermionic converters (system Srikt), 20: 12483
WOESSNER, G., Theoretical considerations on heat transfer in heat pipes, 20: 12488
WOGMAN, Ned Allen, Charge and mass distribution studies in fission of ^{237}Np and ^{239}Pu by intermediate energy helium ions, 20: 11954 (COO-347-18)
WOLF, E., Design study of nuclear power plant (Trikt-50) for space flight, 20: 12482
WOLF, E., Parameter studies on thermal thermionic reactors, 20: 12479
WOLF, Guenter, Determination of $\pi\pi$ scattering phase shifts up to 1.3 Bev CMS energy, 20: 11555 (DESY-65/13)
WOLFENDALE, A. W., Momentum spectrum of cosmic-ray muons at large Zenith angles, 20: 11526
WOLFSON, Y., Lifetime measurements of some rotational levels by new recoil method, 20: 12020
WONG, E., Magnetic-dipole intensities and Zeeman effect in Cs_2UCl_6, 20: 12290
WOOD, D. H., Effect of ^{127}I on passage of ^{131}I from cows to man via milk, 20: 10530 (BNWL-122, pp 113-17)
WOOD, R., Fallout in London rainwater during 1964, 20: 11018
WOOD, Scott E., Studies of Li hydride systems. II., 20: 10832
WOOD, Scott E., Studies of Li hydride systems. III., 20: 10833
WOODS, S. W., Prog. rpt. on biology, annual, 1964, 20: 10503 (BNWL-122)
WOOLLETT, E. L., Kinetic equation for warm plasma, 20: 12230
WOOLLEY, Carolyn, Modification of radiation damage of bacteria by folic acid antagonists, 20: 10648
WOOLUM, J. C., Moessbauer effect in ^{159}Tb, 20: 12303
WORLEY, R. D., Microgram surface density measurements by observation of proton-produced x rays, 20: 11281 (UCRL-12107)
WORLEY, R. D., Treatment of proton channelling by a transverse two-dimensional model, 20: 12279 (UCRL-12311)
WRIGHT, Charles N., Savannah River plant criticality dosimetry system, 20: 11029 (DP-1006)
WRIGHT, Harvel, Instabilities produced in plasma by helical proton beam, 20: 12244
WRIGHT, Jon, Variational principle for Faddeev equations, 20: 11692 (UCRL-11768)
WRIGHT, W. J., Management of nuclear materials in research establishment, 20: 12560
WU, Keh-li, Influence of ionizing radiation on cellular response in lymph nodes of rats after immunization, 20: 10685
WU, Tsung-fan, An experimental determination of relative probabilities of $K_2^0 \to 3\pi^0$ decays, 20: 11561 (JINR-P-2450)
WU, Tsung-fan, Determination of relative probability of $K_2^0 \to \pi^\pm + e^\pm + \nu(\bar{\nu})$, 20: 11560 (JINR-P-2449)
WU, Yung-Chi, Thermodynamic excess functions in D_2O and H_2O, 20: 10847
WUENSCH, Bernhardt J., Corrections for x-ray absorption by crystal of arbitrary shape, 20: 12308
WYANT, Robert E., Radiation-induced formation of organometallic compounds with particular emphasis on organotins, 20: 10870 (BMI-1753)
WYLER, Eugene N., Model experimental design for NERVA instrumentation radiation-effects tests, 20: 11175 (NP-15823)
WYMAN, M., Null fields in Einstein-Maxwell field theory, 20: 11881
WYRICK, H. J., Geohydrological evaluation of solid waste storage area 6, 20: 12518 (ORNL-TM-1327)

Y

YADAVALLI, S. V., Procedure for evaluating space-charge effects in beam bending magnet system, 20: 11378 (AD-626633)
YAGER, Robert H., Liquid scintillation method for determination of solvent-extracted ^{32}P in foods, 20: 10772
YAJIMA, Nobuo, Analysis of high energy jet showers. I., 20: 11532
YAJIMA, Nobuo, Analysis of high energy jet showers. II., 20: 11533
YAJIMA, Nobuo, Analysis of high energy jet showers. III., 20: 11534
YAJIMA, Nobuo, Analysis of high energy jet showers. IV., 20: 11535
YAKOVLEV, B. M., Combined proton spectrometer for space studies, 20: 11123
YAKUBOVICH, L. S., X-radiation effects on central nervous system and skeletal muscles in rats, 20: 10593
YALOW, R. S., Considerations in preparation of ^{131}I-labeled hormones, 20: 10943
YAMAGATA, Noboru, Spectrographic determination of strontium and calcium in bone ash, 20: 10774
YAMAGUCHI, H., Design of Japanese nuclear ship, 20: 12462 (CONF-640810, pp 122-37)
YAMAMOTO, Hiroshi, Method for separation of aluminum cladding from spent fuel element, 20: 10971
YAMAMOTO, Manabu, Plasma jet generator, 20: 10798
YAMAMOTO, Okimu, Hiroshima atomic bomb irradiated patients who entered Hiroshima within the three days postattack period, 20: 10661
YAMAMOTO, Toshimi, Spectrophotometric determination of Y with Arsenazo III, 20: 10773
YAMANAKA, Jiro, Determination of coronary flow with positron emitter (^{84}Rb), 20: 10730
YAMAUCHI, Atsuo, Swimming pool type reactor, 20: 12516
YANG, John Y., Thermal-spike model of low let radiolysis, 20: 10887
YANG, Kuei-chen, Influence of ionizing radiation on cellular response in lymph nodes of rats after immunization, 20: 10685
YANG, Ling, High temperature thermionic generator, 20: 12383
YAREMBASH, E. I., Magnetic properties of single and polycrystalline praseodymium diselenide $PrSe_2$, 20: 12310
YAROSHENKO, A. P., Vector meson in Coulomb field, 20: 11668
YASUKAWA, T., Annealing effects in neutron irradiated crystalline cobalt complexes. I., 20: 10889
YAVIN, A. I., Experimental study of reaction ^{3}He$(\gamma,\pi^+)^3$H up to 260 Mev, 20: 12046
YEE, K. S., Cherenkov electromagnetic radiation from nuclear detonation in space, 20: 11807 (UCRL-7495(Rev. 1))
YEE, Kane S., Shoaling and breaking of solitary wave and its applications, 20: 12551 (UCRL-12186)
YELLIN, Joseph, Optical-pumping transients in ^{87}Rb, 20: 11486
YENNIE, Donald R., Radiative level shifts. I., 20: 11458
YI, Hsu-shih, Quadratic momentum dependence of nuclear potential, 20: 12103
YIOU, T. P., Exchange mechanism for $\pi^+p \to N^*\rho^0$ reaction at 2.75 Bev/c, 20: 11605
YODH, G. B., K^-p interactions from 900 to 1100 Mev/c and their bearing on $Y^*(1765)$ and $Y_0^*(1815)$, 20: 11551 (CONF-650837-3)
YOSHIDA, S., Growth and decay of ring current and polar electrojets, 20: 11829
YOST, Kenneth John, Methodology for neutron resonance calculations, 20: 11945
YOUNG, James A., Atomic motion in moderators, 20: 12275 (GA-6861)
YOUNG, R. A., Observation of negative-mass instability in energetic proton plasma, 20: 12247
YOUNGBLOOD, E. L., Decontamination of ORNL molten-salt fluoride-volatility pilot plant after processing irradiated zirconium–uranium alloy fuel, 20: 11032 (ORNL-3891)
YUANG, Rung-fang, Analysis of reactions $\pi N \to \pi_1\pi_2 N'$, 20: 11562 (JINR-P-2454)
YUROVSKII, A. V., Instrument for recording protons with E = 3 to 14 Mev, α particles, and nuclei of Z > 2, 20: 11124
YUSKESELIEVA, L. G., Application of electrophotography for measurements of sensitive region of germanium p-i-n detectors, 20: 11102 (JINR-P-2487)
YUSKESELIEVA, L. G., Revealing of defects in silicon p-i-n detectors, 20: 11103 (JINR-P-2489)

Z

ZACEK, F., Beam width of two antenna systems for plasma diagnostics, 20: 12192
ZAGER, B. A., On properties of isotope ^{254}102, 20: 11968 (JINR-P-2470)
ZAGORSKAYA, T. N., Zone refining of molybdenum in high vacuum, 20: 11218
ZAGORSKI, Z. P., Polarographic study of aqueous oxygenated solutions irradiated with 10 Mev electron pulses, 20: 10909
ZAHN, L. L., Transportation of radioactive materials, 20: 11035 (TID-8541, pp 249-319)
ZAIO, A., Certain immune indexes in newborn mice treated with ^{32}P, 20: 10580
ZAIO, A., Effect of ^{32}P on the multiplication of germs, 20: 10579
ZAIO, A., Effect of ^{32}P on bacterial flora of intestine of newborn mouse, 20: 10642
ZAITSEV, A. N., Disturbed solar-diurnal variations at high latitudes during IGY, 20: 11812
ZAITSEV, L. N., Passage of high energy neutrons through heavy concrete, 20: 12263 (JINR-P-2479)
ZAITSEVA, S. A., Some characteristics of relationship between auroras and magnetic disturbances, 20: 11819
ZAJIC, Vladimir, Detection of uranium fuel element failures during inactive tests in CO_2 streams, 20: 11003
ZAKATOV, L. P., Electron heating in TN-1 installation, 20: 12206
ZAKHAROV, V. I., Effect of mass splitting within baryon octet on BB scattering, 20: 11586
ZALESKI, C. P., Fast reactor core design and safety studies in France in Federal Republic of Germany, 20: 12439

ZALESKI, C. P., Testing of fusible metal joint for fast reactor, 20: 12513
ZALESKI, Edward J., Determination of coronary flow with positron emitter (^{84}Rb), 20: 10730
ZALEWSKI, Kacper, Angular momentum conservation in statistical model of multiple production of particles, 20: 11698
ZALOGIN, G. N., Flow near stagnation point in presence of magnetic fields parallel and normal to body surface, 20: 11795
ZAMBONI, F., Q values of reaction ^{8}Be(p,d)^{8}Be and ^{8}Be → 2 ^{4}He, 20: 12037
ZANETTI, A., Gas chromatographic analysis of fatty acids of liver in normal and irradiated rats, 20: 10659
ZAPPA, L., Three-quantum annihilation of positrons in ionic crystals, 20: 11620
ZAVODSKY, Dusan, Evaluation of atmospheric radiation during 1964, 20: 11016
ZAVOISKII, E. K., Turbulent heating of plasma by direct-discharge current, 20: 12183 (ORNL-tr-868)
ZEL'DOVICH, Ya. B., Masses of particles (resonances) with strangeness S = −4 and S = +1, 20: 11585
ZEMACH, Charles, Theory and calculation of scattering with Bethe-Salpeter equation, 20: 11746
ZHIZHINA, G. P., Nature of superweak luminescence of irradiated solutions of DNA, 20: 10578
ZHUKOV, A. V., Temperature field of the fuel elements in core and blanket of BN-350 reactor, 20: 12443
ZHUKOV, V. A., Analysis of reactions $\pi N \to \pi_1 \pi_2 N'$, 20: 11562 (JINR-P-2454)
ZIEGENBALG, H., Treatment of radiation damage of skin, 20: 10615
ZIEGLER, W. A., Generation of quantitative data while sampling ores and concentrates, 20: 10968
ZIEMER, P. L., Gross gamma radioactivity in Indiana precipitation, 20: 11020
ZIEMER, P. L., Liquid scintillation detector for evaluating phototubes and determining gamma-ray activities, 20: 11128
ZIEMER, Paul L., Determination of gross gamma radioactivity of Indiana soils by large volume liquid scintillation counting, 20: 11019
ZIESKE, P., Production of large-diameter low-voltage electron beams in absence of magnetic field, 20: 11367 (D1-82-0448)
ZIJP, W., Status report on in-pile radiation metrology in Netherlands, 20: 11149
ZIMMERMAN, J. E., Macroscopic quantum interference effects through superconducting point contacts, 20: 11911
ZIMMERMAN, Robert L., Analytic continuation of $a(l,s)$ for $\mathrm{Re}\, l < N$, 20: 11693 (UCRL-12016-T)
ZIMMERMAN, Robert L., Equivalent field theories and elementary-particle democracy, 20: 11754
ZINGL, H., Structure of nucleons, 20: 11579
ZINK, J. W., Electromagnetic mass of classical electron, 20: 11454 (UCRL-12233)
ZMUIDZINAS, Jonas Stasys, Particle symmetries, 20: 11688 (JPL-TR-32-797)
ZNAMENSKAYA, K. M., Prophylaxis and therapy of radiation injuries caused by protons, 20: 10699 (NASA-TT-F-353, pp 210-38)
ZNAMIROVSCHI, V., Effect of ^{90}Sr on certain physiologic indices in Zea mays, 20: 10683
ZOLLER, P., Current motion in superconductors carrying alternating currents in transverse magnetic field, 20: 11902
ZONN, Z. N., Growing of cerium aluminate single crystals, 20: 10826
ZUBAREV, A. L., Electromagnetic current and form factors for meson 35-plet in SL(6,c) symmetry, 20: 11683 (JINR-E-2475)
ZUCCARO, D. E., Prog. rpt. on ion rocket engine development, 4–6/65, 20: 11006 (NP-15824)
ZUROMSKY, G., Prog. rpt. on UO_2 fuel systems, 3/31/65, 20: 12377 (CEND-2863-236)
ZUYKOV, N. V., Thermocouple for measuring temperatures up to 2500°K, 20: 11076
ZVENIGOROSKY, A., Time-of-flight mass spectrometry and its applications. I., 20: 10790
ZVENIGOROSKY, A., Time-of-flight mass spectrometry and its applications. II., 20: 10791
ZYBIN, K. Yu., Properties and nature of geomagnetic micropulsations with periods from 10 sec to several minutes, 20: 11813

SUBJECT INDEX

Main entries in this index are generally specific materials, things, and processes. These are followed by modifiers that describe the properties of, and processes applied to, the main entries.

The number preceding the colon is the *NSA* volume number, and the number following is the abstract number. The designation (R) following the abstract number indicates that the abstract is of a progress report; (P) indicates a patent; and (T) indicates a translation. Abstracts for reports other than progress reports carry no letter designation. References to report numbers, where appropriate, are included after the abstract number of the citation. Published literature (journal article or book) is identifiable by the absence of a report number.

The user should bear in mind that the ideas presented in the original literature, rather than key words, have been indexed. The indexers have tried to select what seemed the most probable and logical place to look for typical information. Since it is not possible to anticipate where a user would look for information, numerous cross references are included in cumulative indexes to assist him in his search.

Experience in using an index of this type will be the best guide in obtaining the desired information, and a consideration of synonymous or closely related terms will prove valuable.

Information must be so indexed as to be of the greatest use to the greatest number of users. This requires that a topic be indexed to headings that most specifically describe it and not ordinarily to the headings that describe its ultimate use, nor to the general class headings that include the specific headings. For example, information on the treatment of thyroid disease with I-131 would be indexed under Thyroid Gland and under Iodine Isotopes I-131, but not necessarily under Radiotherapy. A study of the effects of x radiation on hair would be indexed under both X Radiation and Hair. However, the information would not be indexed under the experimental animal, e.g., Rats, unless the report discusses the effects on rat hair as compared with the effect on the hair of other animals.

The broad, general class headings are used only for general information or for comprehensive reports or articles.

Subject Heading Styles

Generally, the direct form of subject entry is used rather than inverted headings, e.g., Amino Acids rather than Acids, Amino; Helium Isotopes He-4 rather than Helium—isotopes He-4 or Helium—He-4 isotopes. Note, however, that in some cases parenthetic modifying terms or inverted headings of the form Neutrons, Fast are used in preference to a direct entry that would result in the scattering of information. Organic compounds are usually entered in the index in the inverted form so that substituted compounds can be listed near the parent compound; e.g., Benzene, Bromo- rather than Bromobenzene. In general, the style of nomenclature used is that of Chemical Abstracts, except that some items listed in that publication as subheadings are elevated to form part of the main heading; e.g., Butyric Acid, Methyl Ester rather than Butyric Acid—methyl ester.

Alphabetization

Main headings are alphabetized word-by-word. A parenthetic qualifier following a main heading is disregarded in alphabetizing unless there are two or more headings identical except for the parenthetic qualifier, in which case the qualifier determines the order. Headings involving Greek letters are arranged as if the names of the letters were spelled out.

Examples:

M-Capture
  see Electron Capture
Magnesium
Magnesium Alloys
Manganese Fluorides
Manganese(II) Fluorides
Mesons
Mesons (π)
Mesons (ρ)
3-Pentanol, 2,4-Dimethyl-
2-Pentanol, 2-Methyl-
2-Pentanol, 4-Methyl-

Nomenclature of Inorganic Compounds

Inorganic compounds are indexed in the direct form, listing cations in the order of increasing valence in the case of polycationic salts of varying valence and in alphabetic order for polycationic salts in which all cations have the same valence; e.g., Sodium Aluminum Silicates and Potassium Sodium Sulfates.

Multicomponent Alloys and Other Systems

Multicomponent alloys, except well-known trade names, are indexed under a main heading in the form "element alloy" for each element in the alloy. The modifier begins with element symbols for each component arranged alphabetically as if the English name for the element were spelled out.

Example: Copper-Gold Alloy is indexed
  Copper Alloys
    Cu-Au...
  Gold Alloys
    Cu-Au...

Well-known alloys such as Zircaloy-2 are indexed directly to the trade name; cross references referring from each component of the alloy to the entry for the trade name appear in cumulative indexes.

Multicomponent systems of non-metallic elements are indexed in a manner similar to alloys except the main heading used contains the word "Systems" in place of "Alloys."

Example: Silicon–Tungsten Systems are indexed
  Silicon Systems
    Si-W...
  Tungsten Systems
    Si-W...

Multicompound systems and mixtures of compounds are indexed under the main heading for each component com-

pound; the modifiers begin with an alphabetical listing of compound formulas.

Example: Lead Titanate–Lead Zirconate is indexed
Lead Titanates
$PbTiO_3$-$PbZrO_3$...
Lead Zirconates
$PbTiO_3$-$PbZrO_3$...

A mixed system of compounds and elements is indexed using a combined form of the above conventions, e.g., a dispersion of copper and alumina would be indexed

Aluminum Oxides
Al_2O_3-Cu...
Copper Systems
Al_2O_3-Cu..

Physical States and Configurations of Materials

Specification of the physical state, if other than normal, or geometric configuration of the material is included in the modifying phrase, i.e., liquid metals would be indexed to the metal with "liquid" in the modifier, and carbon crucibles would be indexed to Carbon with "crucibles" appropriately placed in the modifier and also to Crucibles if appropriate.

Modifying Phrases

The modifiers appearing under a main heading are written specifically to describe the relation of the item being indexed to that main heading. The modifier, therefore, will generally contain more useful information about that relation than will a title or a phrase written to be used under every main heading assigned to the item. Effort is exerted to begin the modifier with the word judged to be of greatest use to the greatest number of users; this, however, does not obviate the need to consider all modifiers under the main heading(s) of interest.

Modifiers are usually intended to form a meaningful phrase when combined with the main heading. Some are intended to be read following the main heading, e.g., the entry Hydrogen—sorption by charcoal is read "hydrogen sorption by charcoal"; however, as a result of placing the important word first, many modifiers must be arranged for smooth reading, e.g., Formaldehyde—yields in radiolysis of ethyl ether, effects of deuterium on is read "effects of deuterium on formaldehyde yields in radiolysis of ethyl ether" and Uranium—crystal structure of, effect of cooling rate on allotropic transformations in is read "effect of cooling rate on allotropic transformations in crystal structure of uranium." Prepositions are sometimes omitted if no ambiguity results.

Special characters are added to modifiers in the field of physics; if the modifier does not establish the experimental or theoretical character of a reference, a symbol (E), (T), or (E/T) is placed immediately after the modifying phrase and before the journal reference number. The value of this identification has been established by the American Institute of Physics.

A

A-286 ALLOY
radiation effects on stress-rupture properties of, neutron, 20: 11358
ABSORPTION SPECTRA
excited states in radiolysis, quenching of, 20: 10926
ABSTRACTS
on plutonium, 20: 12530 (BNWL-113-10)
ACCELERATOR TUBES
description for electrostatic generators, (T), 20: 11405
wall temperature differences in, device for minimizing, 20: 11420(P)
ACCELERATORS
beam control in, pulse amplifiers for, 20: 11414
beam density in, statistical distribution limit for, (T), 20: 11408
beam focusing in, electron and positron, (T), 20: 11399 (UCRL-7566 (Rev.1))
beam phase measurement in ion, synchronous, 20: 11406
design of charged-particle, 20: 11421(P)
design of charged-particle, 20: 11422(P)
design of electron, with automatic field scanning device, 20: 11416(P)
design of traveling-wave electron, 20: 11419(P)
radiation absorption in electron, method for secondary, 20: 11418(P)
storage ring beam orbit calculations for, computer programs for, 20: 11395 (ORNL-TM-1172(Rev.))
ACCIDENTS
cesium-137 release in industrial, hazards from, 20: 10721
evaluation in reactor siting, proposed standards for, 20: 12333
survey of, in USAEC facilities, 1963–64, 20: 11034 (TID-5360(Suppl.5))
ACETIC ACID
corrosive effects on molybdenum, tungsten, and vanadium at 35, 60, and 100°C, 20: 11230 (BM-RI-6715)
ACETIC ACID, [(CARBOXYMETHYLIMINO) BIS(ETHYLENENITRILO)] TETRA-
complexes with uranium(IV) in aqueous solutions, potentiometry of, 20: 10802(R) (COO-1020-9)
effects on excretion of inhaled cerium-144 in dogs, 20: 10533(R) (BNWL-122, pp 125-7)
effects on excretion of inhaled praseodymium-144 in dogs, 20: 10533(R) (BNWL-122, pp 125-7)
effects on plutonium excretion in rats, 20: 10531(R) (BNWL-122, pp 118-21)
ACETIC ACID, CHLORO-
corrosive effects on molybdenum, tungsten, and vanadium at 35, 60, and 100°C, 20: 11230 (BM-RI-6715)
ACETIC ACID, CHLORO-, VINYL ESTER
radioinduced polymerization with acrylic acid, 20: 10897
ACETIC ACID, (1,2-CYCLOHEXYLENEDINITRILO)TETRA- COMPLEXES
with uranium(IV) in aqueous solutions, potentiometry of, 20: 10802(R) (COO-1020-9)
ACETIC ACID, [ETHYLENEBIS[(CARBOXYMETHYLIMINO)ETHYLENE-NITRILO]]TETRA-
chelates of, toxicity in mice, 20: 10556
properties as cerium and yttrium elimination agent in mice, 20: 10556
ACETIC ACID, (ETHYLENEDIAMINE) TETRA-
analytical uses for radiometric determination of traces of metals by electrophoresis, 20: 10792
use in radiotherapy of dysprosium-165-labeled, 20: 10737
with uranium(IV) in aqueous solutions, potentiometry of, 20: 10802(R) (COO-1020-9)
ACETIC ACID, (ETHYLENEDIAMINE) TETRA-, SODIUM SALTS
effects on serum transaminase activity in mice, 20: 12545(R) (PAEC(A)AR651)
ACETIC ACID, (*N*-HYDROXYETHYLETHYLENEDIAMINE) TRI- COMPLEXES
with uranium(IV) in aqueous solutions, potentiometry of, 20: 10802(R) (COO-1020-9)
ACETIC ACID, [(2-HYDROXYETHYL)IMINO]DI-
complexes with uranium(IV) in aqueous solutions, potentiometry of, 20: 10802(R) (COO-1020-9)
ACETIC ACID, IMINODI-
complexes with uranium(IV) in aqueous solutions, potentiometry of, 20: 10802(R) (COO-1020-9)
ACETIC ACID, NITRILOTRI- COMPLEXES
with uranium(IV) in aqueous solutions, potentiometry of, 20: 10802(R) (COO-1020-9)
ACETOACETIC ACID, METHYL ESTER
reactions with samarium isopropoxide, 20: 10846
ACETONE, THENOYLTRIFLUORO-
solvent properties for europium, 20: 10951
ACETONITRILE
complexes with uranyl perchlorate, preparation of, 20: 10825
ACETYLENE
photoionization-efficiency curves for normal and deuterated, 20: 10867
ACRIFLAVINE
effects on uv-induced lethality and photoreactivation in Neurospora, 20: 10716
ACRYLAMIDE
radioinduced polymerization of, effects of pressure on solid-state, 20: 10898
ACRYLIC ACID
radioinduced polymerization with vinyl chloroacetate, 20: 10897
ACTINIDES
diffusion in sintered uranium dioxide at 1250 to 1600°C, 20: 11312
energy level transition probabilities in deformed odd A, for A ≥ 227, (E/T), 20: 11951 (AE-205)
separation of trivalent, by ion exchange or solvent extraction, 20: 10955
ACTINIUM ISOTOPES Ac-227
performance as space vehicle power supply, 20: 11188 (BLG-330)
ACTINOMYCIN
radiosensitivity effects on tumors in man and rats, 20: 10700
ACTIVATION ANALYSIS
method for trace-element, in muscle, 20: 10869
of biological materials, use in pharmacological studies, 20: 10509
performance of foil, in pocket chambers, 20: 11119
use for nondestructive determination of burnup in nuclear fuels, 20: 11004
use of, for identification of trace elements that determine source of manufacture of drugs, 20: 10880
ADENINE
radiolysis of copolymers of, with adenine, 20: 10877
radiolysis of, yields from, 20: 10877
ADENOSINEPHOSPHORIC ACIDS
effects on irradiated polycytidylic acid, 20: 10584
ADRENAL GLANDS
effects of removal of rat, on response to cortisone, 20: 10686
effects on intestinal radiation syndrome in rats, 20: 10697
radiation effects on ascorbic acid metabolism in rat, protective effects of cystamine and mercamine against, 20: 10715
radiation effects on rat, x, 20: 10576
radiosensitivity effects of rat, 20: 10686
ADRENAL HORMONES
effects on fat accumulation induced by neptunium-237 in rat liver, 20: 10522(R) (BNWL-122, pp 79-80)
effects on intestinal radiation syndrome in rats, 20: 10697
ADRENALINE
radiation effects on leukocytic reaction to, in dogs, x, 20: 10594
ADVANCED REACTIVITY MEASUREMENT FACILITY
neutron kinetics, 20: 12498(R) (IDO-17112, pp 1-51)
ADVANCED TEST REACTOR
control components and instrumentation, 20: 12496 (IDO-16871-5)
control system for, testing of, 20: 12502 (TID-22547)
design and operation, 20: 12496 (IDO-16871-5)
fuel element testing for, instrumentation for, 20: 12499(R) (IDO-17112, pp 52-80)
AEROSOLS
half-life of radioactive, in stratosphere, 20: 11014
AGE
effects on activity of alanine–2-oxoglutarate and aspartate-2-oxoglutarate-aminotransferase in x-irradiated rats, 20: 10593
radiosensitivity effects of, in mice, 20: 10707
AIR
corrosive effects on uranium–10 molybdenum alloys, 20: 11224
corrosive effects on molybdenum–titanium–uranium alloys, 20: 11224
effects on fatigue crack propagation in nickel–chromium–molybdenum–vanadium steel, 20: 11273(R) (NRL-6364)
electron capture by alpha particles in, (T), 20: 11457(T) (LA-tr-65-29)
filtration in nuclear plants, 20: 11056
gamma buildup factors for, calculation of, (T), 20: 12261 (AFRRI-TM-65-2)
heat transfer coefficients for, 20: 12341
laser beam reactions in, plasma production in, (T), 20: 12190
reactions with molybdenum–niobium alloys at 1000 to 1200°C, effects of composition on, 20: 11227
reactions with sodium in reactors, model for processes in, (T), 20: 10851
reactions with Stellite 6B at 1600°F, 20: 11215(R) (NASA-CR-54718)
reactions with tungsten disilicide at 600 to 1100°C, 20: 11237
sampling for radioactive and stable iodine, 20: 11060(R) (BNWL-122, pp 33-6)
ALARM SYSTEMS
design of relay, using radiation counters, 20: 11084(P)
ALASKA
cesium-137 content in natives of, whole-body, 1965, 20: 10723
fallout monitoring, 1963 and 1964, 20: 10535(R) (BNWL-122, pp 176-80)
fallout monitoring, 1964, 20: 10718(R) (BNWL-122, pp 172-5)
ALBUMINS
effects on radioinduced luminescence of desoxyribonucleic acid,

20: 10578
labeling with chromium-51, 20: 10944
labeling with iodine-131, 20: 10942
labeling with tritium, 20: 10945
metabolism of labeled, data interpretation for, 20: 10565
properties of chromium-51-labeled, 20: 10944
properties of tritium-labeled, 20: 10566
radiosensitivity of, in erythrocyte membranes of newborn rats, 20: 10589
use of chromium-51-labeled, in measuring gastrointestinal protein loss, 20: 10569
use of iodine-131-labeled, in measuring intestinal protein absorption, 20: 10566
use of iodine-131-labeled, in measuring gastrointestinal protein loss, 20: 10567
use of iodine-131-labeled, for determining effects of nutritional disorders on protein metabolism, 20: 10573

ALCOHOLATES
preparation of deuterium-labeled, 20: 10850

ALCOHOLS
reactions of aliphatic, with hydroxyl radicals, 20: 10916

ALKALI METAL HALIDES
interactions with positrons in crystals, annihilation, 20: 11377
positron annihilation in, three-quantum, (E), 20: 11620
positron capture by defects in crystals of, 20: 11377
radioinduced F-centers by electron-hole recombination, (T), 20: 12306
radioinduced F-centers in, by [110] anion replacement sequences, (T), 20: 12307

ALKALI METAL IONS
production of, r-f source for, 20: 11374

ALKALI METALS
oscillations in plasma of, models for self-excited, (T), 20: 12225
proton reactions with atoms of, production of highly excited hydrogen atoms by charge-exchange, (E), 20: 11471(T)

ALKALINE EARTH METALS
proton reactions with atoms of, production of highly excited hydrogen atoms by charge-exchange, (E), 20: 11471(T)

ALKALINE EARTH OXIDES
positron annihilation in, three-quantum, (E), 20: 11620

ALLOYS
dislocation climb in, efficiency of, 20: 11274 (NYO-3504-2)
dispersion-strengthened, bibliography on, 20: 11278 (RISO-48(Suppl.2))
electrodynamics of superconducting, in strong magnetic fields, (T), 20: 11907
strengthening by irradiation, 20: 11366

ALPHA BEAMS
use in radiotherapy, 20: 10736

ALPHA PARTICLES
angular distributions and energy spectra from sulfur-32 (n,α_0) reactions at 3.2 Mev, (E), 20: 11993
angular distributions from neutron reactions with silicon-28 at 14.8 Mev, (E/T), 20: 12030
attenuation in argon–nitrogen mixtures, energy transfer and scintillations in, 20: 11130
cluster structure in polonium-212, (E), 20: 12074
detection and measurement in solutions, using nuclear emulsions, 20: 11044
detection and measurement using junction detectors, 20: 11092 (CLOR-39/D)
detection and measurement of, from uranium-238 in tissues, 20: 10514(R) (BNWL-122, pp 21-4)
detection and measurement of, from thorium-230 in tissues, 20: 10514(R) (BNWL-122, pp 21-4)
detection and measurement of, use of time-to-pulse height converter with scintillation counters for, 20: 11117
detection and measurement of, silicon surface-barrier detector for, 20: 11124(T)
detection using corrugated-plate spark chambers, 20: 11120
detection using lithium-drifted silicon diodes, 20: 11097 (INR-621/XV/I)
effects on DNA synthesis in HeLa cells, 20: 10588
effects on gastrointestinal tract during chronic radiation sickness, 20: 10674
effects on liquid helium scintillation, recombination luminescence in, (E), 20: 11904
effects on x-ray diffraction by silicon crystals, 20: 12281
electron capture by, in air, (T), 20: 11457(T) (LA-tr-65-29)
emission in beta decay of lithium-8, energy distribution of, (T), 20: 12010
emission in decay of astatine and polonium isotopes, effect of pair correlation on, (T), 20: 12093
reactions (α,d) with nuclei at 42 to 53 Mev, deuteron energy spectra from, 20: 12061
reactions (α,d) with carbon-12 at 42 to 53 Mev, deuteron energy spectra from, (E), 20: 12061
reactions (α,γ) with silicon-28 and -30 at 3.2 to 4.3 Mev, energy levels from, (E), 20: 11994
reactions (α,n), (α,pn), $(\alpha,3n)$, $(\alpha,4n)$ at 11 to 40 Mev, excitation functions for, (E/T), 20: 12014
reactions (α,n) with fluorine-19 at 2.4 to 5.5 Mev, excitation function for, (E), 20: 12143
reactions (α,n) and $(\alpha,4n)$ with iodine-129 at 35 Mev, cesium-129 and -132 production in, (E), 20: 10901
reactions $(\alpha,2n)$ with iodine-127 at 35 Mev, cesium-129 production from, (E), 20: 10901
reactions with nuclei at 42 Mev, proton emission in, (E), 20: 12062
scattering by alpha particles, beryllium-8 binding energy and lifetime from elastic, (E), 20: 12038
scattering by beryllium-9, phosphorus-31, and sodium-23 at 18 Mev, elastic and inelastic, (E), 20: 12099
scattering by calcium-40 at 3.5 to 5.5 Mev, elastic, (E), 20: 12144
scattering by iron at 21, 27.5, and 47.9 Mev, statistical-theory analysis of inelastic, (E), 20: 12056
scattering by lead-207, -208, and bismuth-209, collective excitations in inelastic, (E), 20: 12075
shielding against, tabulation of materials for, 20: 12265 (NP-15697 (Vol.1))

ALUMINUM
beta absorption by, paper for linear plotting of data on, 20: 12270
beta energy losses in, dependence of, on beta-energy maximum and Z of emitter, (T), 20: 11037
coating with niobium by chemical vapor deposition, 20: 11260
compatibility with urania, 20: 11224
copper recoil ion stopping in, ranges and range-straggling for energetic, (E), 20: 12085
corrosion by distilled water, kinetics of, 20: 11227
corrosion by formic, hydrochloric, and oxalic acids at 35°C, galvanic, 20: 11230 (BM-RI-6715)
corrosion by sea water, sodium chloride, and sodium hydroxide, galvanic, 20: 11230 (BM-RI-6715)
determination in ores and enriched products, effects of silicon on activation, 20: 10781
dislocation climb in, efficiency of, 20: 11274 (NYO-3504-2)
dissolution of fuel cladding of, molten-salt, 20: 10971(P)
effects of alloying additions of, on oxidation rates of niobium, tantalum, and tungsten, 20: 11227
effects on creep of magnesium, 20: 11313
effects on stability of delta-phase plutonium–gallium alloys, 20: 11224
gamma incoherent scattering by electrons of, at 100 to 280 kev, (E), 20: 11515
neutron capture by, secondary gamma emission from, (E), 20: 12267
neutron diffraction by, extinction effect in slow, (E), 20: 12309
neutron scattering total cross sections at 12 to 14 Mev, (E), 20: 11949 (AD-625747)
neutron transmission through energy spectra after fast, (E), 20: 12268
pressure spalling of, properties of, (T), 20: 12539 (LA-DC-7692)
proton channeling in, transverse two-dimensional model for, (T), 20: 12279 (UCRL-12311)
radiation effects on low-cycle fatigue and tensile properties of, at cryogenic temperatures, 20: 11345(R) (NASA-CR-54787)
radiation effects on electric properties of, recovery mechanism for neutron, 20: 11362
use as lining in electron beam apparatus, 20: 11418(P)

ALUMINUM ALLOYS
fracture toughness properties of types 5083-0, 5086-H112, and 6061-T651, 20: 11273(R) (NRL-6364)
mechanical properties of, effects of strain rate on, 20: 11284 (UCRL-14599)
mechanical properties of 7039 plate and weldments at −423 to 400°F, 20: 11264 (ACF-14)
welded joints between copper and type 6061, effects of heat treatments on pressure, 20: 11215(R) (NASA-CR-54718)
welding to nickel of type 6061-T6, cold-pressure, 20: 11214(R) (NASA-CR-54717)
Al–Ce, crystal structure of intermetallic compound $CeAl_3$ in, 20: 11305
Al–Cr–Co–Fe–Mo–Ni–Ti, stress-rupture properties of Udimet 700, at high temperatures and strain rates, 20: 11265 (AD-626375)
Al–Cr–Nb, oxidation at 1100°C, effects of composition on, 20: 11338
Al–Cr–Nb, phase studies, 20: 11338
Al–Dy, crystal structure of intermetallic compound $DyAl_3$ in, 20: 11305
Al–Er–Gd, crystal structure of intermetallic compound $(Gd_xEr_{1-x})Al_3$ in, 20: 11305
Al–Er–Y, crystal structure of intermetallic compound $(Y_xEr_{1-x})Al_3$ in, 20: 11305
Al–Fe, oxidation by oxygen at 800 to 1050°C, kinetics of internal, 20: 11232 (INR-644/XIV/PS)
Al–Fe–U, phase transformations in, effects of aluminum and iron content

on, 20: 11224
Al–Ga–Pu, tensile properties and thermal expansion of delta-stabilized plutonium-base, 20: 11224
Al–Ho, crystal structure of intermetallic compound $HoAl_3$ in, 20: 11305
Al–Ho, phase diagram of, evidence for intermetallic compounds in, 20: 11307
Al–La, crystal structure of intermetallic compound $LaAl_3$ in, 20: 11305
Al–Li, swelling from helium precipitation in, mechanism of, 20: 11224
Al–Mg–Zr, creep rates, 20: 11313
Al–Mo–Sn–Ti–V, fracture toughness properties of titanium-base, effects of heat treatments on, 20: 11273(R) (NRL-6364)
Al–Mo–Ti, fracture toughness of weldments of titanium-base, effects of heat treatments on, 20: 11273(R) (NRL-6364)
Al–Mo–Ti, fracture toughness of plasmarc welds in titanium-base, 20: 11273(R) (NRL-6364)
Al–Mo–Ti, fracture toughness of titanium-base, effects of composition and heat treatments on, 20: 11273(R) (NRL-6364)
Al–Mo–Ti–V, corrosion cracking by salts at 550 to 600°F, stress-, 20: 11227
Al–Mo–Ti–V, thermal stability of, effects of composition on, 20: 11336
Al–Nb, phase studies, 20: 11338
Al–Nb–Ta–Ti, fracture toughness of plasmarc welds in titanium-base, 20: 11273(R) (NRL-6364)
Al–Nd, crystal structure of intermetallic compound $NdAl_3$ in, 20: 11305
Al–Pr, crystal structure of intermetallic compound $PrAl_3$ in, 20: 11305
Al–Pu, decladding and dissolution of PRTR fuel elements of, flowsheets for, 20: 10948 (HW-76472)
Al–rare earth, crystal structure of intermetallic compounds in, 20: 11305
Al–Sc, phase diagram, 20: 11297
Al–Sc, tensile properties, effects of composition on, 20: 11297
Al–Sn–Ti, fracture toughness of plasmarc welds in titanium-base, 20: 11273(R) (NRL-6364)
Al–Sn–Ti, mechanical properties of, effects of strain rate on, 20: 11284 (UCRL-14599)
Al–Sn–Ti, radiation effects on low-cycle fatigue and tensile properties at cryogenic temperatures, 20: 11345(R) (NASA-CR-54787)
Al–Sn–Ti–V, fracture toughness properties of titanium-base, plane-strain, 20: 11273(R) (NRL-6364)
Al–Sn–Ti–Zr, creep properties of, effects of composition on, 20: 11335
Al–Tb, crystal structure of intermetallic compound $TbAl_3$ in, 20: 11305
Al–Ti, thermal stability of $TiAl_3$, effects of molybdenum, niobium, and vanadium alloying additions on, 20: 11335
Al–Ti–V, corrosion by cesium at 400°C, 20: 11227
Al–Ti–V, fracture toughness properties of titanium-base, 20: 11273(R) (NRL-6364)
Al–Ti–V, fracture toughness of plasmarc welds in titanium-base, 20: 11273(R) (NRL-6364)
Al–Ti–V, fracture toughness properties of titanium-base, plane-strain, 20: 11273(R) (NRL-6364)
Al–Ti–V, mechanical properties of, effects of strain rate on, 20: 11284 (UCRL-14599)
Al–Ti–V, radiation effects on low-cycle fatigue and tensile properties at cryogenic temperatures, 20: 11345(R) (NASA-CR-54787)
Al–Ti–V, tensile properties of, effects of exposure to cesium at 650°C on, 20: 11227
Al–Ti–Zr, phase studies and properties of, 20: 11332
Al–Ti–Zr, phase studies and properties of, 20: 11333
Al–Ti–Zr, phase studies and properties of, 20: 11334
Al–U, properties as oxidation-protection coating on uranium, 20: 11224
Al–Y, crystal structure of intermetallic compound YAl_3 in, 20: 11305

ALUMINUM CHLORIDES
corrosive effects on molybdenum, tungsten, and vanadium at 35, 60, and 100°C, 20: 11230 (BM-RI-6715)

ALUMINUM IONS
energy levels of, (T), 20: 11450 (UCRL-7842-T)
production of, τ-f source for, 20: 11374

ALUMINUM ISOTOPES Al-26
energy levels, (E), 20: 12061

ALUMINUM ISOTOPES Al-27
deuteron elastic scattering at 7.8 Mev by, cross sections for, (E), 20: 12095
deuteron reactions (d,α) and (d,p) at 1.5 to 3 Mev, direct effect and evaporation mechanism in, (E/T), 20: 12018
energy levels in, excited-core model for low-lying, (T), 20: 12052
gamma total absorption cross sections near 20 Mev, (E), 20: 12097
neutron inelastic scattering at 14 Mev, excitation of 4.5-Mev state by, (E), 20: 12031
neutron nonelastic reactions at 8.1 Mev, cross sections for, (E), 20: 11985
neutron reactions (n,p) at 14.8 Mev, cross sections for, (E), 20: 12133
proton inelastic scattering at 4 to 5.5 Mev, (E), 20: 12142
proton reactions (p,2p) at 460 Mev, (E/T), 20: 11948 (AD-624318)
proton reactions (p,α) at 4 to 5.5 Mev, (E), 20: 12142

ALUMINUM ISOTOPES Al-28
energy levels, (E), 20: 12061

ALUMINUM OXIDE SLURRIES
flow in pipes, friction coefficient for, 20: 10998

ALUMINUM OXIDES
compatibility with urania, 20: 11224
corrosion by cesium at 400°C of Lucalox, Al-300, and synthetic sapphire, 20: 11227
radioinduced swelling of, fission fragment, 20: 11227
tensile strength for machining, effects of PVA binders on, 20: 11277 (RFP-659)
tensile strength for machining, effects of binders on, 20: 11277 (RFP-659)
use in chromatographic separation of hydrogen isotopes at 77.4°K, 20: 10939
Al–Al_2O_3, plastic formation mechanisms of dispersed phase SAP, 20: 11269 (EUR-2483.f)
Al_2O_3–SiO_2, preparation and properties of, for use in cesium ion exchange from waste solutions, 20: 10766 (TID-22511)

ALUMINUM OXYNITRIDES
preparation, properties, and structure, 20: 10856

ALUMINUM SYSTEMS
Al–Al_2O_3, plastic deformation mechanisms of dispersed phase SAP, 20: 11269 (EUR-2483.f)
Al–B_4C, development of foils of, 20: 11226
Al–H_2O, neutron diffusion in plutonium-fueled lattices of, thermal, (E), 20: 12396(R) (EURAEC-1505)
Al–Si–U, properties of splat-cooled, 20: 11224

ALUMINUM, TRIALKYL-
use as catalyst in isoprene polymerization, 20: 10929(P)

AMERICIUM
diffusion in sintered uranium dioxide at 1250 to 1600°C, 20: 11312
separation from curium by ion exchange, 20: 10956

AMERICIUM ALLOYS
Am–Pu, phase studies, 20: 11224

AMERICIUM ISOTOPES
use in reactor fuels for producing α-emitting isotopes, 20: 12394 (BNWL-SA-472)

AMERICIUM ISOTOPES Am-241
alpha decay, (E), 20: 12158
alpha decay of, conversion electron intensities from, (E), 20: 11956 (EUR-2632.d)
helium ion fission at 42.8 Mev, deformation of transition-state nucleus in, (E), 20: 12077
neutron cross section of, Westcott parameters for, (T), 20: 11959 (HW-77389)
neutron reactions with, curium-242 and plutonium-238 production in, (E), 20: 12394 (BNWL-SA-472)

AMERICIUM ISOTOPES Am-242
neutron cross section of, Westcott parameters for, (T), 20: 11959 (HW-77389)

AMERICIUM ISOTOPES Am-243
helium ion fission at 42.8 Mev, deformation of transition-state nucleus in, (E), 20: 12077
neutron cross section of, Westcott parameters for, (T), 20: 11959 (HW-77389)
neutron reactions with, curium-244 production in, (E), 20: 12394 (BNWL-SA-472)
nitrogen-15 reactions (N-15,4n) at 75 to 90 Mev, nobelium-254 production in, (E), 20: 11969 (JINR-P-2471)

AMIDE POLYMERS
radiation effects on, ESR and spectroscopic studies of gamma, 20: 10892

AMINES
solvent properties for actinides and lanthanides, 20: 10955

AMINO ACIDS
determination in mouse urine, methods for, 20: 10582
radiation effects on mouse urinary excretion of, β, 20: 10582
radiolysis of aqueous solutions of, reaction of hydrated electron in, 20: 10919
radiolysis of aqueous solutions of, pulsed-electron, 20: 10917
radiolysis of aqueous solutions of, reaction of hydrated electron in, 20: 10918
radiosensitivity effects on *Hansenula wingei*, 20: 10695
synthesis of labeled, by biochemical methods, 20: 12545(R) (PAEC(A)AR651)

AMMETERS
design and performance for electron beam measurements, 20: 11392 (NP-15275)

AMMONIA
neutron moderation by, at 77 and 300°K, (E), 20: 11944
positron lifetime in, (E), 20: 11674
radiolysis of liquid, pulsed-electron, 20: 10910

NH_3–Li, positron lifetime in, (E), 20: 11674
AMMONIUM ALUMINUM SULFATES
methyl- radiation effects on ferroelectric, ESR studies of gamma, (E), 20: 12291
AMMONIUM CHLORIDES
corrosive effects on molybdenum, tungsten, and vanadium at 35, 60, and 100°C, 20: 11230 (BM-RI-6715)
effects on porosity of sintered hafnium and tantalum carbides, 20: 11250
AMMONIUM COMPOUNDS
neutron moderation by, at 77 and 300°K, (E), 20: 11944
AMMONIUM FLUORIDES
solvent properties for uranium–zirconium alloys, 20: 10964
AMMONIUM HYDROXIDES
corrosive effects on molybdenum, tungsten, and vanadium at 35 and 60°C, 20: 11230 (BM-RI-6715)
radioinduced reactions with coconut oil, gamma, 20: 12545(R) (PAEC(A)AR651)
AMMONIUM MAGNESIUM SULFATES
radioinduced vanadium ions in vanadyl-containing, EPR spectra of, 20: 12319
AMMONIUM ZINC SULFATES
radioinduced vanadium ions in vanadyl-containing, EPR spectra of, 20: 12319
vanadyl ion EPR spectra in, 20: 12319
AMPLIFIERS
design for accelerator beam control, engineering drawings for, 20: 11414
stability of pulse, system for determining, 20: 12499(R) (IDO-17112, pp 52-80)
use of magnetic, in radiation monitoring device, 20: 11162(P)
AMYGDALIN
effects in combination with cystamine on radiosensitivity of dogs and rats, 20: 10699(T) (NASA-TT-F-353, pp 210-38)
ANILINE
radiolysis mechanisms of, 20: 12545(R) (PAEC(A)AR651)
ANIMAL CELLS
effects of cortisone on mesenteric mast cells in normal and adrenalectomized rats, 20: 10686
radiation effects on mesenteric mast cells in normal and adrenalectomized rats, x, 20: 10686
radiation effects on histone synthesis and respiration in Ehrlich ascites tumor, x, 20: 10691
radiation effects on thyroid, protective effects of anoxia against, 20: 10710
radiation effects on, mechanisms of, 20: 10629
radiation effects on cultured, single and fractionated γ and x, 20: 10649
radiation effects on DNA-ase activity in cell nuclei and cytoplasm of, 20: 10591
radiation effects on survival of cultured, effects of anoxia and antimetabolite drug on x, 20: 10664
radioinduced chromosomal aberrations in Ehrlich ascites tumor, effects on survival of, 20: 10677
radiosensitivity of, x, 20: 10650
ANIMAL REPRODUCTION
effects of ingested deuterium oxide on, of mice, 20: 10550
radiation effects on rat, fission neutrons, 20: 10601(R) (BNWL-122, pp 135-6)
ANIMAL RESPIRATION
oxygen exchange between alveolar gas and pulmonary capillary blood, tracer study, 20: 10547
ANIMALS
book: *Problems of Radiation Safety in Space Flights. Physical and Biological Studies with High-Energy Protons*, 20: 10604(T) (NASA-TT-F-353)
radiation effects on, test for protective effects of AET against, 20: 10711
radioactivity in herbivorous Alaskan, 1963 and 1964, 20: 10535(R) (BNWL-122, pp 176-80)
radioactivity in herbivorous, effects of diet on, 20: 11011(R) (BNWL-122, pp 181-3)
ANOXIA
protective effects of, against radiation injuries in mice, effects of age, 20: 10707
radiosensitivity effects on thyroid cells in mice, 20: 10710
radiosensitivity effects on HeLa cells in culture, 20: 10664
ANTENNAS
use of multiple, in cosmic noise absorption studies, 20: 11862
ANTIBIOTICS
production by radioinduced mutants of *Hansenula wingei*, 20: 10695
ANTIBODIES
formation in mice, effects of, 20: 10617
labeling with tritium, 20: 10945
ANTIGENS
immune response to, in mice, 20: 10617
injection into thymus, effects on immune reactions, 20: 10632
ANTIMONY CHLORIDES
separation from salts by extraction chromatography using organic phosphorus compounds, 20: 10759 (INP-427/C)
ANTIMONY ISOTOPES Sb-132
half life, (E), 20: 11980 (USNRDL-TR-935)
ANTIMONY ISOTOPES Sb-133
half life, (E), 20: 11980 (USNRDL-TR-935)
ANTINEUTRINOS
interactions with nucleons, nonpolarized lepton state from, (T), 20: 11577
ANTINUCLEONS
interactions with mesons (π) and nucleons, ABC anomaly for amplitudes of, (T), 20: 11604
ANTIPROTONS
interactions with protons, $SU(6)_w$ symmetry for cross sections of, (T), 20: 11565 (JINR-P-2469)
interactions with protons, meson-resonance production in annihilation, (E), 20: 11575
interactions with protons, CPT invariance in, (T), 20: 11557 (JINR-E-2457)
ANTIPYRINE
complexes with uranyl perchlorate, preparation of, 20: 10825
ARCHAEOLOGICAL SPECIMENS
analysis methods for, 20: 12545(R) (PAEC(A)AR651)
ARCO CHEMICAL PLANT
instrumentation development, 20: 12499(R) (IDO-17112, pp 52-80)
ARGON
alpha stopping in, energy transfer and scintillations from, 20: 11130
argon reactions at 30 to 2900 ev, ionization cross sections for, (E), 20: 11477
diffusion in potassium halide single crystals, 20: 11224
electric discharge in, diagnostics of Penning, (E), 20: 12259
electron elastic scattering at low energies, free-electron wave functions for, (T), 20: 11495
electron reactions with atomic, metastable excitation in, (E), 20: 11455 (UCRL-14450)
heat transfer coefficients for, 20: 12341
helium-atom and -ion scattering by, electrons and ions from, 20: 11447(R) (TID-22476)
photon absorption by electrons in atomic field of, cross section for, (T), 20: 11478
Ar–C_2F_6, energy transfer in gamma radiolysis of, 20: 10884
ARGON IONS
energy levels of, (T), 20: 11450 (UCRL-7842-T)
reactions with iron at 10 to 100 kev, secondary-electron emission in, (E), 20: 11462
sputtering on copper single crystals, (T), 20: 11460
ARGON ISOTOPES Ar-38
production and separation of, method for, 20: 11191 (JEN-150-DQ/I-51)
ARGON ISOTOPES Ar-40
alpha reactions (α,d) at 42 to 53 Mev, deuteron energy spectra from, (E), 20: 12061
proton reactions (p,2p) at 460 Mev, (E/T), 20: 11948 (AD-624318)
ARGON SYSTEMS
Ar–D_2, vibrational relaxation in shock tubes, Schlieren method for, 20: 11785
Ar–H_2, vibrational relaxation in shock tubes, laser Schlieren method for, 20: 11786
Ar–K, excitation transfer in first excited state of potassium, cross sections for collision-induced, (E), 20: 11499
Ar–N, alpha stopping in, energy transfer and scintillations from, 20: 11130
Ar–Na, excitation transfer in first excited states of sodium, cross sections for collision-induced, (E), 20: 11499
ARGONNE FAST REACTOR EXPERIMENT TEST
design and operations of, 20: 12512
ARMY REACTORS
neutron flux distributions in, computer program for, 20: 12384 (AGN-TM-411)
ARMY REACTORS (ML-1)
heat transfer from fuel elements with boundary-layer turbulence promoters, 20: 10988 (CONF-12-5)
radiation levels from, (E/T), 20: 12385 (AGN-TP-149)
ARMY REACTORS (PL-2)
design of, engineering drawings for, 20: 12446
ARSENAZO III
analytical use for spectrophotometric determination of yttrium, 20: 10773
ARSENIC ISOTOPES As-75
energy levels from selenium-75 decay, spin of, (E), 20: 12022
ASCORBIC ACID
radiation effects on adrenal metabolism of, in rats, protective effects of

cystamine and mercamine against, 20: 10715
ASPHALT
incorporation of condensate waste into, effects of radioactivity levels on, 20: 12517(R) (BNWL-170)
incorporation of waste in, 20: 12524
ASTATINE
production in high-energy reactions on bismuth and lead, 20: 11377
ASTATINE ISOTOPES
alpha decay of odd-even, effect of pair correlation on, (T), 20: 12093
ASTROPHYSICS
book: *Neutrino Astrophysics*, 20: 11436
hydromagnetic phenomena in, laboratory simulation of, (T), 20: 11431
ATLANTIC OCEAN
movement south of Iceland, nature of surface-layer, 20: 12541 (NYO-2929-1)
ATMOSPHERE
charged-particle reactions in, ionization from, (T), 20: 11857
cosmic nucleon intensity in lower, (E), 20: 11521
cyclone motion in, MHD model for, 20: 11783(T)
effects on alkyltin yields in radiolysis of mixtures of 1-bromobutane or 1-bromopentane with tin, 20: 10870 (BMI-1753)
electron and proton energy and pitch angle distributions in auroral zone, (E), 20: 11854
fallout monitoring in, criteria for, 20: 11043
magnetohydrodynamic flow of electric-conducting medium in, (T), 20: 11808(T)
research in polar regions of, review of, 20: 11842
solar particle precipitation in polar regions of, vlf phase recording network for determining, 20: 11856
solar radiation in polar cap regions of, detection from absorption events, 20: 11863
ATOMIC BEAMS
production of excited hydrogen, by proton charge-exchange in metal vapors, (E), 20: 11471(T)
ATOMIC ENERGY
bibliography on, 20: 12547 (TID-3043(Rev.2, Suppl.3))
development in Netherlands, 20: 12556
development in Netherlands, 20: 12557
research programs on, in Philippine Islands, 20: 12545(R) (PAEC(A)AR651)
safety hazards of, perspective on, 20: 11047
ATOMIC ENERGY COMMISSION
accidents in facilities of, 1963–64, survey of, 20: 11034 (TID-5360 (Suppl.5))
descriptive cataloging guide for, 20: 12548 (TID-4577(Rev.1))
reactor licensing rules by, changes in, 20: 12437
regulatory actions on U. S. reactors, 20: 12436
research projects in chemistry, summaries of basic off-site, 20: 10755 (TID-4005(Pt.2a)(2nd ed.))
ATOMIC ENERGY, LEGAL ASPECTS
regulations on radioisotope transport, 20: 11040
ATOMIC EXPLOSIONS
effects on population of Hiroshima, 1961 survey, 20: 10661
effects on population of Hiroshima, 1961 survey, 20: 10662
effects on population of Nagasaki, statistical analysis of, 20: 10663
fire hazards from, evaluation of secondary, 20: 11031 (NP-15708)
radiation effects on sex ratio of offspring of exposed women, 20: 10657
simulation of underwater, using pulsed reactors, 20: 11013 (USNRDL-TR-940)
ATOMIC MODELS
quantum corrections in Thomas-Fermi, (T), 20: 11452 (UCRL-12042-T)
ATOMIC PHYSICS
book: *A Collection of Problems in Atomic and Nuclear Physics*, 20: 11376(T)
book: *The Theory of Atomic Collisions*, 20: 11511
ATOMIC STRUCTURE
book: *The Structure of Atoms and Molecules*, 20: 11512(T)
electron configurations in, three-particle operators for, (T), 20: 11475
field calculations of, relativistic Hartree approximation for, (T), 20: 11507
ATOMS
book: *The Structure of Atoms and Molecules*, 20: 11512(T)
book: *The Theory of Atomic Collisions*, 20: 11511
electron reactions with, binary-encounter collision theory for, 20: 11483
electron scattering at low energies, free-electron wave functions for, (T), 20: 11495
electron scattering by, core term in exchange amplitude for, (T), 20: 11473
electron scattering by heavy, relativistic Hartree approximation for, (T), 20: 11507
energy levels of, formulation and lowest order Lamb shift for, 20: 11458
energy levels of, virtual-state, (T), 20: 11439 (BNL-8800)
interactions of two-level, with radiation from gaseous lasers, 20: 11470
motion in moderators, (T), 20: 12275 (GA-6861)
photoelectric cross sections for heavy, method for measuring, 20: 11516
polarization in strong electromagnetic fields, (T), 20: 11510
potential at zero temperature, Thomas-Fermi method for, (T), 20: 11449 (TID-22530)
potentials for neutral, Yukawa terms for accurate analytic Hartree-Fock, 20: 11472
reactions of hot, in condensed organic matter, 20: 11377
reactions with atoms and ions, variational calculations of long-range, (T), 20: 11504
reactions with atoms, electrons, and ions, quantum mechanical theories for, 20: 11511
reactions with negative ions, (T), 20: 11517
wave functions for, asymptotic large-z, (T), 20: 11485
AUDITORY ORGANS
radiotherapy of hemangioma in, effects of, 20: 10687
AURORAL STORMS
absorption event structure, electron precipitation mechanism for, (E/T), 20: 11861
charged-particle precipitation correlations with, (E), 20: 11851
correlation with geomagnetic mircopulsations, 20: 11839
electron and proton energy spectra in ionosphere during, spectrometer for measuring, 20: 11853
electron density and collision frequency in ionospheric F region during absorption event, (E), 20: 11848
excitation mechanisms for optical, (T), 20: 11857
intensity of, relation to magnetic disturbances, 20: 11819(T)
light intensity from, (E), 20: 11851
occurrence of radio aurora, correlations with geomagnetic storms, (E), 20: 11859
properties of, experiments for determining, 20: 11865
x-ray intensity during, (E), 20: 11855
AUSTRALIA
nuclear materials management in research establishment at Lucas Heights, 20: 12560
AUTORADIOGRAPHY
methods using nuclear emulsions, 20: 11002
technique for high-speed alpha, 20: 10529(R) (BNWL-122, pp 110-12)
use in drug distribution studies, 20: 10509
AZULENE
complexes with ethenetetracarbonitrile, effects of pressure on properties of, 20: 12534 (COO-1198-216)

B

BACTERIA
distribution of heat-killed *Mycobacterium smegmatis* in mice, 20: 10655
immune reactions to *Mycobacterium tuberculosis* in mice, 20: 10655
radiation effects on, from Gulf oysters, gamma, 20: 10690
radiation effects on growth and reproduction in Aerobacter and Salmonella, 20: 10579
radiation effects on activity of, in mice, β, 20: 10580
radiation effects on populations of, in mouse intestine, β, 20: 10642
radiation effects on protein synthesis in *Mycobacterium smegmatis*, uv, 20: 10656
radiation effects on mouse susceptibility to infection by Pseudomonas, x, 20: 10669
radiosensitivity of *Pasteurella tularensis*, effects of cell concentrations, deuterium substitution, and radioprotective compounds on gamma, 20: 10694
radiosensitivity of, effects of folic acid analogs on, 20: 10648
BALLOONS
use for investigating auroral and polar cap phenomena, 20: 11855
BARIUM
determination in irradiated uranium dioxide, 20: 10787
diffusion of hydrogen in, at 200 to 620°C, 20: 12535 (IS-T-61)
separation from fused salts by ion exchange, tracer studies of, 20: 10958
separation from uranium by reversed-phase partition chromatography, 20: 10784
BARIUM ISOTOPES
atomic mass, (E/T), 20: 11494
BARIUM ISOTOPES Ba-128
energy levels from lanthanum 128 decay, (E), 20: 12068
BARIUM ISOTOPES Ba-129
energy levels in, isomeric, (E), 20: 12069
BARIUM ISOTOPES Ba-133
decay, (E), 20: 12153
BARIUM ISOTOPES Ba-137
internal conversion spectrum of, (E), 20: 11143
BARIUM ISOTOPES Ba-138
neutron activation cross section at 24 kev, (E), 20: 12135
BARIUM ISOTOPES Ba-140
content in ocean fish, effects of content in sea water on, 20: 11054

determination in irradiated MITR fuel elements by gamma spectroscopy, 20: 10764 (MITNE-64)
BARIUM SULFATES
radiation effects from radium or sulfur-35 on sorption of aqueous organic dye solutions by, 20: 10936(T) (CEA-tr-A-1855)
BARIUM TITANATES
dielectric properties of, effects of preparation on, 20: 11279(R) (SC-DC-64-1477X)
BARLEY
radiation control of insect pests on, x, 20: 10619
radiation effects on sprouting of, 20: 10619
BARYONS
interactions with leptons, weak, (T), 20: 11583(T)
interactions with baryons, mass splitting effects in, (T), 20: 11586(T)
interactions with mesons, spurion scheme of broken U(L12) symmetry for, 20: 11735
mass of supermultiplet, in quark model, (T), 20: 11585
photoproduction on nucleons, SU(6) sum rules for, (T), 20: 11635
symmetries for, magnetic moment sum rules in broken SU(3) and SU(6), (T), 20: 11743
symmetry for three-body states of, SU(6), 20: 11756
symmetry for, mass-difference effects in model of multiplets in SU(3), (T), 20: 11744
BARYONS, RESONANCE
decay of $Y_0^*(1405)$, CP-noninvariant electromagnetic interactions in, (T), 20: 11638
decay of $\frac{1}{2}^-$ octet of, SU(3) symmetry for, 20: 11685 (JINR-P-2444)
mass and width of N^{*-} and N^{*--}, differences in, (E), 20: 11624
mass of supermultiplet, in quark model, (T), 20: 11585
model for $\Lambda(1668)$, SU(3)-group $\frac{1}{2}^-$-octet, 20: 11685 (JINR-P-2444)
model for, relativistic composite quark, (T), 20: 11684 (JINR-P-2442)
parity, spin, and width of Y_{03}^*, (T), 20: 11632
photoproduction on nucleons, SU(6) sum rules for, (T), 20: 11635
production of $J^P = \frac{3}{2}^-$, I = 1, in strong interactions, (T), 20: 11592
production of N* in meson (π)–nucleon interactions at 290 to 905 Mev, cross sections for, (T), 20: 11562 (JINR-P-2454)
production of $N^{*+}(1237)$, in meson (π^+)-proton interactions at 2.75 Bev/c, (E/T), 20: 11605
production of $N^*(1670)$, in meson (π^+)-proton interactions at 2 Bev/c, (E), 20: 11672
production of $Y^*(1765)$ and $Y_0^*(1815)$ in meson (K^-)-proton interactions at 900 to 1100 Mev/c, (E), 20: 11551 (CONF-650337-3)
production of $Y_{03}^*(1815)$ in meson (K)-nucleon interactions, (T), 20: 11632
production of Y^*, in meson (K^-) capture by deuterium, (T), 20: 11599
production of, asymptotic relations between cross sections for, (T), 20: 11729
properties of $Y^*(1765)$ and $Y_0^*(1815)$, (E), 20: 11551 (CONF-650337-3)
properties of $Y_1^*(1765)$, (E), 20: 11656
BEANS
radioinduced chromosomal aberrations in roots of, protective effects of nitrogen against, 20: 10712
radioinduced mutations in, effects of, on disease resistance, 20: 12545(R) (PAEC(A)AR651)
BEARINGS
analysis of externally-pressurized gas-lubricated thrust, (E/T), 20: 10974(T) (AEC-tr-6665)
design of coupled rotor-, using liquid-metal lubrication, 20: 10973 (TID-21992)
BEHAVIOR
book: *Ionizing Radiation: Neural Function and Behavior*, 20: 10689
BELGIAN REACTOR-2
fuel irradiation testing in hydraulic conveyor of, plutonium, 20: 12397(R) (EURAEC-1506)
BELGIAN REACTOR-3
fuel element fabrication and testing for Vulcain core studies in, 20: 12396(R) (EURAEC-1505)
fuel element fabrication and testing for Vulcain core studies in, 20: 12397(R) (EURAEC-1506)
BELLOWS
inspection of failed expansion, between EGCR containment shell and experimenters cell, 20: 12411 (ORNL-TM-1380)
BENTONITES
properties for use in ion exchange separation of phosphorus-32 from biological solutions, 20: 10780
BENZENE
positron decay in halogen derivatives of, (E), 20: 11621
radiolysis of, effects of ferrous ions and sulfates on phenol yields from, 20: 10878
benzene–CCl_4, pulsed-electron radiolysis of, 20: 10928
benzene–Cl, radioinduced reactions in, hexachlorocyclohexane production in γ, 20: 10900
benzene–cyclohexane–*p*-terphenyl, excitation transfer and decay processes in radiolysis of, 20: 10927
benzene–N_2O–H_2O, production of biphenyl–terphenyl mixtures in radiolysis of, 20: 10930(P)
BENZENE, BROMO-
radiolysis of, yields of inorganic bromine-82 in, 20: 10890
BENZENE, BUTYL-
effects on fat accumulation induced by neptunium-237 in rat liver, 20: 10522(R) (BNWL-122, pp 79-80)
BENZENES
vibronic interactions in deuterated, calculations of, 20: 12545(R) (PAEC(A)AR651)
BENZOIC ACID
corrosive effects on molybdenum, tungsten, and vanadium at 35, 60, and 100°C, 20: 11230 (BM-RI-6715)
BENZOQUINONE
effects on radioinduced polymerization of triallyl, cyanurate, 20: 10896
BERYLLIUM
compression properties of ultrahigh-purity single-crystal, 20: 11225
crystal lattice dynamics, (T), 20: 12275 (GA-6861)
crystallization and grain growth of, effects of oxide distribution and impurity level on, 20: 11225
diffusion in beryllium–nickel alloys, enthalpy of, 20: 11326
effects on hydrogen distribution in Zircaloy, 20: 11221
extrusion, 20: 11225
inclusions and precipitates in, 20: 11225
joining components of, solid-state, 20: 11260
mechanical properties of, for use as fuel cans, 20: 11294
preferred orientation in wrought, effects of recrystallization on, 20: 11225
proton reactions at 1.6 Mev, electron bremsstrahlung from, (E/T), 20: 11501
BERYLLIUM ALLOYS
Be–Ca, compatibility with carbon dioxide, 20: 11225
Be–Ca, properties as fuel element cladding, 20: 11225
Be–Fe, precipitation of $Be_{11}Fe$ on dislocations in, 20: 11299
Be–Mg, compatibility with carbon dioxide, 20: 11225
Be–Ni, diffusion of beryllium in, enthalpy of, 20: 11326
Be–U, properties of splat-cooled, 20: 11224
BERYLLIUM HYDROXIDES
preparation and properties of, 20: 10836
$Be(OH)_2$–$Ca(OH)_2$, preparation and properties of, 20: 10836
$Be(OH)_2$–$Sr(OH)_2$, preparation and properties of, 20: 10836
BERYLLIUM IONS
energy levels of, (T), 20: 11450 (UCRL-7842-T)
BERYLLIUM ISOTOPES Be-6
energy levels, 20: 12023
BERYLLIUM ISOTOPES Be-7
energy levels, 20: 12023
production in bremsstrahlung reactions with carbon-12 and oxygen-16 at 25 to 57 Mev, cross sections and yield curves for, (E), 20: 12094
BERYLLIUM ISOTOPES Be-8
binding energy, (E), 20: 12037
binding energy and lifetime of ground-state, (E), 20: 12038
energy levels, 20: 12023
energy levels, (E), 20: 11962 (INR-655/I/PL)
energy-level parities and spins from helium-3 reactions (He-3,α) with beryllium-9 at 3 Mev, (E), 20: 12027
BERYLLIUM ISOTOPES Be-9
alpha scattering at 18 Mev, (E), 20: 12099
deuteron elastic scattering at 7.8 Mev by, cross sections for, (E), 20: 12095
deuteron reactions (d,n) with, exchange stripping amplitudes of, (T), 20: 12126
deuteron reactions (d,p) at 200 to 350 kev, proton angular distributions in, (E), 20: 12096
electron reactions (e,e'p) at 407 Mev, lithium-8 energy levels from, (E), 20: 11988
energy levels from proton reactions (p,2p) with boron-10, (E/T), 20: 12032
gamma total absorption cross section near 20 Mev, (E), 20: 12097
helium-3 reactions (He-3,α) at 3 Mev, beryllium-8 level, parities and spins from, (E), 20: 12027
proton reactions (p,2p) at 460 Mev, (E/T), 20: 11948 (AD-624318)
proton reactions (p,d) at 1.66 Mev, Q-value for, (E), 20: 12037
BERYLLIUM ISOTOPES Be-10
energy levels, 20: 12023
energy levels from proton reactions (p,2p) with boron-11, (E), 20: 12032
BERYLLIUM OXIDE REACTOR EXPERIMENT
design of emergency cooling systems for, 20: 12434
development, July–Sept. 1965, 20: 12398 (GA-6811)
BERYLLIUM OXIDES
compatibility with urania, 20: 11224
crack and pore distribution in sintered, ultrasonic study of, 20: 11324
crystal lattice dynamics of, (T), 20: 12275 (GA-6861)
deposition on urania particles, method for, 20: 11224

performance for neutron shielding, 20: 12475 (WANL-PR(B)-009)
radiation effects on, fast-neutron, 20: 11225
radioinduced swelling of, fission fragment, 20: 11227
BeO–ThO_2, phase studies, 20: 11225
BERYLLIUM POISONING
pathology of, in man, 20: 11038
BERYLLIUM SULFATES
crystal structure of hydrated, (E), 20: 12327
BERYLLIUM SYSTEMS
C–Be–U, properties of splat-cooled, 20: 11224
BETA DECAY
branching ratio for light hypernuclei, shell-model calculations for, (T), 20: 11999
laser beam effects on, (E/T), 20: 12102
transitions in, effect of interference and nuclear charge on, log ft values of forbidden, (T), 20: 11996
transitions in, matrix elements for allowed and first-forbidden, (E/T), 20: 12113
BETA PARTICLES
absorption by aluminum, paper for linear plotting of data on, 20: 12270
detection and measurement of low-energy, scintillation method for, 20: 11122
detection of, response of moving G-M ratemeter for, 20: 11089 (AERE-M-1671)
detection using lithium-drifted silicon diodes, 20: 11097 (INR-621/XV/I)
effects on amino acid excretion in mouse urine, 20: 10582
effects on animals, carcinogenic, effects of chemical carcinogens on, 20: 10627
effects on bacterial growth and reproduction, 20: 10579
effects on bacterial population in mouse intestine, 20: 10642
effects on blood coagulation, 20: 10679
effects on blood picture and bone marrow in mice, 20: 10641
effects on bone, carcinogenic, 20: 10628
effects on corneal metabolism in rabbits, 20: 10585
effects on desoxyribonucleotide content in mouse spleen and thymus, 20: 10633
effects on electrophoretic pattern of serum proteins in mice, 20: 10581
effects on gastrointestinal tract during chronic radiation sickness, 20: 10674
effects on growth and pH in maize seedlings, effects of dose on, 20: 10683
effects on hemangiomas in children, therapeutic, 20: 10745
effects on immunity in mice, 20: 10580
effects on mice, model for, 20: 10640
effects on myocardium in mice, 20: 10643
effects on pituitary gland, effects on mammary carcinoma of, 20: 10752
effects on rat bones, tumorigenic, 20: 10652
effects on swine of, from ingested strontium-90, leukemogenic, 20: 10597(R) (BNWL-122, pp 37-45)
effects on swine of, from ingested strontium-90, carcinogenic, 20: 10597(R) (BNWL-122, pp 37-45)
energy losses in aluminum and tissue, dependence of, on beta-energy maximum and Z of emitter, (T), 20: 11037
leukemogenic effects in mice of, from injected tritium, 20: 10623
reactions with liquid phosphors, fluorescence efficiencies for, 20: 10902
reflection in precipitation titration, analysis by, 20: 10778
use in production of x rays, methods for, 20: 12545(R) (PAEC(A)AR651)
BETA SOURCES
effects of mixed, on rats, 20: 10552
performance of promethium-147, in x-ray spectroanalyzer, 20: 11133
preparation of silver iodide, method for, 20: 10935 (USNRDL-TR-948)
BETA SPECTRA
corrections to scintillation, matrix method for backscattering and resolution, 20: 11156
BETA SPECTROMETERS
acceleration equipment for $\pi\sqrt{2}$, postfocusing, 20: 11153
design and performance for measuring electron spectra during auroral storms, 20: 11853
design and performance of double-focusing iron-free, 20: 11143
design and performance of miniaturized double-focusing, for low-energy auroral electrons, 20: 11157
design of automatic scanning, 20: 11159(P)
design of, computer program for, 20: 11113 (UCRL-16471)
focusing effect of post acceleration system of Vanderbilt, (E), 20: 11976 (TID-22504)
performance of well-type plastic-scintillation, for determining absolute photoelectric cross sections, 20: 11496
BETAINES
storage of tritiates, self-radiolysis during, 20: 10809 (EUR-2531.f)
BETATRONS
design and performance of small orbit, 20: 11397 (SC-RR-65-111)
BEVATRON
control of, PDP-5 digital computer for, 20: 11401 (UCRL-16502)
shielding configurations for, neutron spectra from, (E/T), 20: 11400 (UCRL-16323)
BIBLIOGRAPHIES
on aquarium design and construction, 20: 12554 (UCRL-14473)
on atomic energy literature, 20: 12547 (TID-3043(Rev.2, Suppl.3))
on chemical, photographic, and solid state detectors, 20: 11027 (AED-C-21-03)
on design specifications for gamma irradiation facilities, 20: 10980(T) (AEC-tr-6469)
on design, equipment, and construction of laboratories for work with radioactive materials, 20: 10977 (KFK-370)
on dispersion-strengthened materials, 20: 11278 (RISO-48(Suppl.2))
on fast reactors, 20: 12433
on fuel processing, 20: 10965
on fused salt thermodynamics and transport phenomena, 20: 10808 (EUR-2466.e, pp 59-80)
on Mössbauer effect, 20: 12277 (PAEC(A)-IN-656)
on nuclear propulsion concepts, 20: 12477
on pentaerythritol tetranitrate and its homologs, 20: 10862 (MLM-1252)
on phase equilibria in hydrogen–uranium systems, 20: 10801 (CEA-R-2777)
on plutonium, 20: 12530 (BNWL-113-10)
on plutonium, 20: 12531 (BNWL-113-11)
on production of plutonium, thorium, uranium, and their compounds, 20: 10966
on progress reports of Analytical Chemistry Division at ORNL, 20: 10765 (ORNL-3904)
on reactor cooling systems, 20: 12434
on reactor fuels and reactor analysis, 20: 11222
on reactor hazards and safeguards, 20: 11052
on research projects in chemistry, 20: 10755 (TID-4005(Pt.2a)(2nd ed.))
on secondary ignitions in nuclear attack, 20: 11031 (NP-15708)
on separation of metal ions and salts by extraction chromatography, 20: 10759 (INP-427/C)
on single crystals, 20: 11276 (PAEC(A)IN-657)
on slow neutron detectors, 20: 11088 (AED-C-28-01)
on thermal and nonthermal emission from plasmas, 20: 12256
on thermodynamic properties of molybdenum, niobium, tantalum, titanium, tungsten, and zirconium and their compounds, 20: 10816(T) (NASA-TT-F-285)
on waste disposal, 20: 12522
on waste disposal, 20: 12524
BIG ROCK POINT POWER REACTOR
fuel channel-support tube vibrations in, correction of, 20: 12450
BILE
effects on mucus synthesis in rat intestine, tracer study, 20: 10600(R) (BNWL-122, pp 131-4)
BILE ACIDS
radiation effects on intestinal absorption of, in rats, x, 20: 10599(R) (BNWL-122, pp 128-30)
BINDERS
effects on tensile strength of alumina powders for machining, 20: 11277 (RFP-659)
BINDING ENERGY
calculation for closed-shell nuclei, Bethe-Goldstone equation for, 20: 11997
BIOLOGICAL MATERIALS
analysis for potassium, activation, 20: 10776
neutron interactions with, 20: 10698
radiation effects on, mechanism for, 20: 10639
BIOLOGICAL MODELS
of kinetics of uranium-235 fission product distribution in tissues, computer analysis of data, 20: 10519(R) (BNWL-122, pp 59-63)
BIOLOGICAL STRESS
effects on heart muscle, pathological, 20: 10631
BIOLOGICAL SYSTEMS
activation analysis of, use in pharmacological studies, 20: 10509
deuterium effects on, 20: 10509
effects of drugs on, tracer studies, 20: 10509
radiation effects on dog and rat, multiple-dose high-energy proton, 20: 10606(T) (NASA-TT-F-353, pp 55-102)
radiation effects on dog and rat, single-dose high-energy proton, 20: 10607(T) (NASA-TT-F-353, pp 103-41)
radiation effects on dog and rat, comparison of RBE of gamma, proton, and x-ray, 20: 10612(T) (NASA-TT-F-353, pp 194-209)
BIOLOGY
research in, uses of reactors in, 20: 10507
BIOMETRY
kinetics of distribution of uranium-235 fission products in tissues, 20: 10519(R) (BNWL-122, pp 59-63)
statistical methods for mixed radionuclide counting, 20: 11201(R) (NYO-3136-2)
statistical methods for mixed radionuclide counting, 20: 11203(R)

(NYO-3136-2, App. 2)
statistical methods for mixed radionuclide counting, 20: 11204(R) (NYO-3136-2, App. 3)
BIOSYNTHESIS
rate of urea, carbon-14-labeled carbonate for measuring, 20: 10559
tritium-labeling of proteins by, 20: 10945
BIPHENYL
radiation effects on, at −196°C, decay of trapped electrons from, 20: 10886
biphenyl–terphenyl, method for radiation production of, 20: 10930(P)
BIPYRIDINES
complexes with europium and terbium, effects of methyl group on, 20: 10842
BISMUTH
charged-particle reactions at high energies, astatine production in, 20: 11377
neutron diffraction by, extinction effect in slow, (E), 20: 12309
preparation and properties of films of, for thickness-optical transmission relation evaluation, 20: 11280 (UCRL-12001)
proton reactions at 1.84 Bev, sodium-24 energy spectra and yield in, (T), 20: 12067
BISMUTH ALLOYS
Bi–Pb, vacuum distillation of cadmium from eutectic of, 20: 10762 (IS-T-71)
Bi–Sn, development as fusible metal joint for fast reactors, 20: 12513
BISMUTH ISOTOPES Bi-206
preparation of carrier-free, method for, 20: 10759 (INP-427/C)
BISMUTH ISOTOPES Bi-208
energy levels, 20: 11971 (MLM-1251J)
BISMUTH ISOTOPES Bi-209
alpha inelastic scattering at 42 Mev, collective excitations in, (E), 20: 12075
energy levels, 20: 11971 (MLM-1251J)
BISMUTH ISOTOPES Bi-210
internal conversion spectrum of, (E), 20: 11143
BISMUTH ISOTOPES Bi-212
preparation from thorium-238 decay products, method for, 20: 10759 (INP-427/C)
BISMUTH NITRATES
separation from salt mixtures by extraction chromatography using organic phosphorus compounds, 20: 10759 (INP-427/C)
BISMUTH TELLURIDES
coating with chromium, cobalt, and nickel, electrolytic, 20: 11543(R) (GIC-2605-3)
performance of thermoelectric couples of, 20: 11543(R) (GIC-2605-3)
BLACK SEA
analysis for radium-224 and -228, methods for, 20: 10768(T) (JPRS-33212)
radioactivity from radium-224 and -228 in, 20: 10768(T) (JPRS-33212)
radium, radon, and uranium contents of, 20: 10512
BLADDER
radiotherapy of carcinomas of, effects of dose fractionation, x, 20: 10743
BLOOD
calcium-45 content in human, after respiratory uptake, 20: 10546
glucose content of, effects on appetite inhibition, 20: 10541
thallium-204 content in human, after respiratory uptake, 20: 10546
BLOOD CIRCULATION
measurement of brain, using iodine-131-iodoantipyrine and external counting, 20: 10750
measurement of coronary, tracer method for, 20: 10730
BLOOD COAGULATION
radiation effects on dog, effects of stimulating vestibular analyzer on, 20: 10682
radiation effects on, therapeutic radioiodine, 20: 10679
BLOOD FORMATION
radiation effects on rat, electron-beam, 20: 10681
BLOOD PICTURE
radiation effects on, in rats, x, 20: 10598(R) (BNWL-122, pp 107-9)
radiation effects on rat, electron-beam, 20: 10681
radiation effects on mouse, protective effects of splenic phospholipids against, 20: 10704
radiation effects on mouse, protective effects of heparin against, 20: 10705
radiation effects on human, 20: 10660
BLOOD PLASMA
labeling proteins in, review of procedures for iodine isotope, 20: 10941
labeling proteins in, methods and uses for, 20: 10561
placental selectivity for proteins in, effects on survival of newborn of, 20: 10508
proteins in, metabolism in pathologic subjects, tracer study, 20: 10570
BLOOD PLATELETS
radiation effects on human, 20: 10660
radiation effects on, therapeutic radioiodine, 20: 10679
BLOOD SERUM
labeling albumins in, iodine-131, 20: 10942
labeling proteins in, chromium-51, 20: 10944
radiation effects on opsonic activity of mouse, β, 20: 10580
radiation effects on electrophoretic patterns of proteins in mouse, β, 20: 10581
radiation effects on cholinesterase activity in dog, effects of fractionated doses on proton, 20: 10592
BLOOD VESSELS
radiation effects on celiac, after Thorotrast carotidography, 20: 10680
BODY WATER
determination of, using tritium oxide, 20: 10557
BOILERS
design for cesium and potassium Rankine cycles, 20: 12475 (WANL-PR(B)-009)
design for sodium-cooled reactors, problems in, 20: 12339(T) (EURFNR-11F)
design of sodium-heated, for nuclear power plants, 20: 12389 (BAW-1280-28(Vol.1))
development of sodium-heated, 20: 12392 (BAW-1280-28(Vol.4))
failures in steam-water, transient properties of, (T), 20: 12418(R) (WCAP-3739)
sodium–water reaction effects in, 20: 12386 (APDA-176)
sodium-water reactions in sodium-heated, 20: 12391 (BAW-1280-28 (Vol.3))
stress analysis of sodium-heated, 20: 12390 (BAW-1280-28(Vol.2))
testing of sodium-heated superheat, 20: 12420(T) (EURFNR-9F)
welded joints in, procedures for tube-to-tube-sheet, 20: 11214(R) (NASA-CR-54717)
welded joints in, procedures for tube-to-tube-sheet, 20: 11215(R) (NASA-CR-54718)
BOILING
burnout conditions for water flow in vertical 3- and 7-rod clusters, (E/T), 20: 11000
critical heat flux for 19-rod bundle in forced convection, 20: 10994 (TID-22539)
heat transfer and burnout in organic-coolant, 20: 12331
heat transfer and critical heat flux for sodium, in forced convection, 20: 10990 (NAA-SR-11586)
heat transfer to, hydrogen in two-phase flow, 20: 10996 (WANL-TNR-154)
BOILING REACTORS
cooling system pipes of, reliability of, 20: 12338(R) (GEAP-4911)
economic comparison with gas-cooled reactors for Dungeness B station, 20: 12432
reactivity of heavy water, model for determining, (T), 20: 12400 (HPR-54)
BONDING
strength of vapor-deposited metal-to-metal, tensile tester for measuring, 20: 11063 (RFP-672)
BONE FRACTURES
radioinduced pelvic, after radiotherapy for uterine adenocarcinomas, 20: 10668
BONE MARROW
diseases of, effects of marrow transfusion on, 20: 10731
effects of DMSO and low-temperature preserved, on radioinduced lesions in dogs, 20: 10706
effects of grafts of, on radiation injuries, 20: 10688
radiation effects on rat, electron-beam, 20: 10681
radiation effects on mouse, β, 20: 10641
radioinduced fibrosis in, of leukemia patients, 20: 10746
transfusions of, effects on bone marrow diseases, 20: 10731
BONE TUMORS
radioinduced by strontium-90, effects of chemical carcinogens on, 20: 10627
radioinduced rat, β, 20: 10652
BONES
analysis of ash of, for calcium and strontium, spectrographic, 20: 10774
radiation effects on guinea pig femur, γ, 20: 10615
radiation effects on, pathological, chronic low-dose exposure, 20: 10637
separation of manganese from solutions of ashes of, by solvent extraction, 20: 10950
BORATE GLASS
radioinduced color centers in alumino-, effect of lead and iron ions on gamma, (E), 20: 12288
thallium absorption and emission spectra in alumino-, (E), 20: 10830
BORON
diffusion in molybdenum, niobium, tantalum, titanium, tungsten, and zirconium surfaces, 20: 11228
use for automatic control of closed-cycle water reactors, 20: 12418(R) (WCAP-3739)
BORON CARBIDES
compatibility with copper, AISI 4130 steel, and types 304 and 430 stain-

less steel, 20: 11226
use as aggregate in concrete shielding, 20: 11229(P)
Al–B_4C, development of foils of, 20: 11226
B_4C–paraffin, use in reactor control systems, 20: 12347
B_4C–UO_2, development of fuel rods of, 20: 11226

BORON IONS
energy levels of, (T), 20: 11450 (UCRL-7842-T)
spectra of divalent, isotope shift of 2s and 2p levels of, (T), 20: 11506

BORON ISOTOPES B-7
energy levels, 20: 12023

BORON ISOTOPES B-9
energy levels, 20: 12023

BORON ISOTOPES B-10
effects on atomic spectra of doubly-ionized boron, isotope-shift, (T), 20: 11506
energy levels, 20: 12023
nitrogen-14 reactions (N-14, N-13) with, total cross sections for, (E), 20: 12057
production and separation of, method for, 20: 11191 (JEN-150-DQ/I-51)
proton reactions (p,2p) at 460 Mev, (E/T), 20: 11948 (AD-624318)
proton reactions (p,2p) with, beryllium-9 levels from, (E/T), 20: 12032
reactions with cobalt-59 and manganese-55, copper recoil ions from, (E), 20: 12085
reactions with nitrogen-14, alpha-particle clusters in, (E), 20: 12004(T)

BORON ISOTOPES B-11
deuteron reactions (d,p) at 1.10, 2.44, and 2.80 Mev, recoil nucleus polarization in, (E), 20: 12107
effects on atomic spectra of doubly-ionized boron, isotope-shift, (T), 20: 11506
neutron capture by, polarization of boron-12 from, (E), 20: 12098
production and separation of, method for, 20: 11191 (JEN-150-DQ/I-51)
proton reactions (p,2p) at 460 Mev, (E/T), 20: 11948 (AD-624318)
proton reactions (p,2p) with, beryllium-10 levels from, (E/T), 20: 12032
reactions with cobalt-59 and manganese-55, copper recoil ions from, (E), 20: 12085

BORON ISOTOPES B-12
polarization in boron-11 (d,p) reactions, (E), 20: 12107
polarization of, from neutron capture by boron-11, (E), 20: 12098

BORON OXIDES
B_2O_3–CdO–In_2O_3, properties of neutron-absorbing glasses of, as reactor control-rod material, 20: 11226

BORON SYSTEMS
B–H_2O, corrosive effects on control rod and fuel cladding, 20: 12418(R) (WCAP-3739)
B–Nb, mechanical properties of, effects of composition on, 20: 11288(T) (AD-622477)
B–UO_2, preparation of sintered pellets of, with controlled composition, 20: 11224
B–W, grain growth in arc-melted, 20: 11226

BOSONS
decay of spin-0 and -1, forbidden configurations for 3-photon, (T), 20: 11686 (JINR-P-2447)
decay of, model for radiative, (T), 20: 11752
interactions of systems of, quantum field theoretical methods for, 20: 11375(T)
interactions of, binary collision expansion of double-time-temperature-dependent Green's functions for, (T), 20: 11760
interactions with fermions, functional methods in quantum field theory and quantum statistics for, (T), 20: 11731
model of, with phase transition, 20: 11801
model with unstable V-type particle for, solution for Lee, (T), 20: 11745
thermodynamic evolution equation for gases of, 20: 11789

BRAIN
blood circulation in, measurements using iodine-131-iodoantipyrine and external counting, 20: 10750
glucose uptake by hypothalamus of mouse, tracer study, 20: 10541
gold uptake by hypothalamus of mouse, tracer study, 20: 10541
radiation effects on biochemical properties of homogenates of mouse, γ, 20: 10577
radiation effects on lipid content of developing guinea pig, x, 20: 10636
radiation effects on guinea pig, histochemical, x, 20: 10638

BRAIN TUMORS
localization of, using mercury-197-labeled compounds and scintillation counting, 20: 10733
radioinduced by deposited strontium-90, 20: 10628
radiotherapy of, combined surgery and cobalt-60, 20: 10575

BRAKES
design for master-slave manipulator, engineering drawings for, 20: 11078

BRAZING ALLOYS
development for refractory metals and alloys, 20: 11260

BREEDER REACTORS
design of 1000-Mw(e) fast sodium-cooled, 20: 12402 (KFK-369)

BREMSSTRAHLUNG
effects on vacuum-wall in thermonuclear reactors, heating, (T), 20: 12166 (CONF-651126-1)
emission of electron, from proton reactions with beryllium at 1.6 Mev, (E/T), 20: 11501
production on medium electrons and hard Vavilov-Cherenkov radiation, (T), 20: 11670
reactions (γ,π^+) with helium-3 at 180 to 260 Mev, cross sections for, (E), 20: 12046
reactions (γ,2p) with silicon-30 at 51.4 Mev, magnesium-28 yields from, (E), 20: 12094
reactions with carbon-12 and oxygen-16 at 25 to 57 Mev beryllium-7 yields from, (E), 20: 12094
reactions with copper and molybdenum, heating effects of, (T), 20: 12166 (CONF-651126-1)

BREMSSTRAHLUNG SOURCES
preparation of low-energy, methods for, 20: 10932 (ORNL-P-1928)

BREN OPERATION
facilities and objectives for Operation HENRE, 20: 11930 (CEX-65.03)

BRITISH REACTORS
development for power review on, 20: 12427

BROMANIL
complexes with 3,8-diaminopyrene and phenylenediamines, effects of pressure on properties of, 20: 12534 (COO-1198-216)

BROMINE
mesons (K^-) capture at 600 Mev/c by, hyperons (Λ) production and trapping in, (E), 20: 12092
reactions with cesium in crossed molecular beams, spectator stripping model for, 20: 10834

BROMINE IONS
yields of molecular, in electron-pulse radiolysis of aerated aqueous solutions of potassium bromide, 20: 10912

BROMINE ISOTOPES Br-79
hyperfine structure of ground state of, magnetic octopole interaction in, (T), 20: 11502
neutron activation cross section at 24 kev, (E), 20: 12135

BROMINE ISOTOPES Br-81
hyperfine structure of ground state of, magnetic octopole interaction in, (T), 20: 11502
neutron activation cross section at 24 kev, (E), 20: 12135
neutron reactions (n,γ) in carbon tetrachloride and *n*-hexane ground-state and isomeric bromine-82 production from, 20: 10938

BROMINE ISOTOPES Br-82
decay of isomeric, in carbon tetrachloride and *n*-hexane, 20: 10938
production at PRR, methods for, 20: 12545(R) (PAEC(A)AR651)
reactions of recoil, in neutron-irradiated cobalt bromide complexes, 20: 10889
reactions of recoil, in bromobenzene, 20: 10890

BROMINE SYSTEMS
Br–CCl_4, radiation chemistry of, processes of bromine-81 (n,γ), 20: 10938
Br–hexane, radiation chemistry of, processes of bromine-81 (n,γ), 20: 10938

BROOKHAVEN ALTERNATING-GRADIENT SYNCHROTRON
beam deflection systems for, design of phase-stabilization circuits in, (E), 20: 11380 (BNL-9772)

BUBBLE CHAMBERS
development of, cryogenic and vacuum techniques for, 20: 11141
events in, accuracy of spatial reconstruction of, 20: 11101 (JINR-P-2468)
photograph scanning template for associating hyperons (Λ^0) with hyperon (Ξ^0) production vertices, 20: 11111 (TID-22550)
track pictures from, particle kinematics from, (T), 20: 11100 (JINR-P-2467)

BUBBLES
detection in uranium, evaluation of techniques for, 20: 11220

1,3-BUTADIENE, 2-METHYL- POLYMERS
production of *cis*-1,4-, using irradiated titanium chloride–trialkylaluminum catalyst, 20: 10929(P)

BUTANE, 1-BROMO-
1-bromobutane–Sn, radiation effects on alkyltin yields in, 20: 10870 (BMI-1753)

1,3-BUTANEDIONE, 1-PHENYL-
solvent properties for europium, 20: 10951

1,3-BUTANEDIONE, 4,4,4-TRIFLUORO-1-(2-FURYL)-
solvent properties for europium, 20: 10951

1,3-BUTANEDIONE, 4,4,4-TRIFLUORO-1-PHENYL-
solvent properties for europium, 20: 10951

BUTYL ETHER
complexes with uranyl perchlorate, preparation of, 20: 10825

BUTYL PHOSPHATE COMPLEXES
with uranyl perchlorate, preparation of, 20: 10825

BUTYL PHOSPHATES
solvent properties for actinides and lanthanides, effects of ion charge and radius on, 20: 10952
solvent properties for nitrosylruthenium nitrato and nitro complexes,

20: 10947 (AERE-R-4786)
$Ce(NO_3)_4$–TBP–$UO_2(NO_3)_2$–H_2O, phase diagram, 20: 10952
HCl–TBP, solvent properties for metal chlorides, 20: 10759 (INP-427/C)

C

CABLES
radiation effects on, transient, 20: 11174(R) (IDO-17112, pp 81-91)
CADARACHE REACTORS (RAPSODIE)
construction, 20: 12506
development, 20: 12419(T,R) (EURFNR-1F)
joints for, development of fusible metal, 20: 12513
CADMIUM
deuteron elastic scattering by, differential cross sections for, (E), 20: 12109
gamma incoherent scattering by electrons of, at 100 to 280-kev, (E), 20: 11515
neutron transmission in filters of, for fissile and 1/v detectors with cylindrical geometry, (T), 20: 11131
radioinduced ionization of, cross sections for electron, 20: 10885
separation from bismuth–lead eutectic by high-vacuum single-stage distillation, equipment for, 20: 10762 (IS-T-71)
separation from salts by extraction chromatography using organic phosphorus compounds, 20: 10759 (INP-427/C)
CADMIUM ALLOYS
Cd–Dy–Hg, phase studies, 20: 11317
Cd–Eu, phase studies, 20: 11327
Cd–Hf, crystal structure of intermetallic compounds in, 20: 11328
Cd–Hg, superconducting transition temperature of, effect of ordering on, (E), 20: 11914
Cd–Sr, phase studies, 20: 11327
Cd–Zr, crystal structure of intermetallic compounds in, 20: 11328
CADMIUM FLUORIDES
europium ion paramagnetic resonance in, (E/T), 20: 12321
CADMIUM IONS
reactions with permanganate ions during pulse-radiolysis of solutions, 20: 10914
CADMIUM ISOTOPES
content in ocean fish, effects of content in sea water on, 20: 11054
CADMIUM ISOTOPES Cd-111
deuteron reactions (d,p) with, cross sections for, (E), 20: 12109
CADMIUM ISOTOPES Cd-112
energy levels of, (E), 20: 12109
CADMIUM ISOTOPES Cd-115
secretion of, in milk of sheep, 20: 10527(R) (BNWL-122, pp 94-8)
CADMIUM ISOTOPES Cd-117
beta decay, (E), 20: 12136
CADMIUM NITRATES
separation from salt mixtures by extraction chromatography using organic phosphorus compounds, 20: 10759 (INP-427/C)
CADMIUM OXIDES
B_2O_3–CdO–In_2O_3, properties of neutron-absorbing glasses of, as reactor control-rod material, 20: 11226
CdO–In_2O_3, properties of neutron-absorbing glasses of, as reactor control-rod material, 20: 11226
CALCIUM
content in diet, effects on calcium-45 and strontium-90 uptake by rats, 20: 10549
content in open-ocean silts, 20: 12540(R) (NYO-2882-8)
determination in bone ash, spectrographic, 20: 10774
effects on strontium-90 diffusion in soil, 20: 12523
meson (μ^-) capture by, isotope effects on K x-ray emission from, (E), 20: 11480
radiation effects on skeletal metabolism of, in rats, x, 20: 10587
separation from salts by solvent extraction using Schiff bases in chloroform, 20: 10759 (INP-427/C)
uptake by rats, effects of calcium and phosphorus content in diet, tracer study, 20: 10549
CALCIUM ALLOYS
Be–Ca, compatibility with carbon dioxide, 20: 11225
Be–Ca, properties as fuel element cladding, 20: 11225
CALCIUM CHLORIDES
separation from salts by extraction chromatography using organic phosphorus compounds, 20: 10759 (INP-427/C)
CALCIUM COMPLEXES
with methylenephosphonic acid derivatives, preparation and properties of, 20: 12533 (COO-1020-6)
CALCIUM FLUORIDES
analysis for rare earths, spectrographic, 20: 10775
laser emission by uranium-doped crystals of, monopulse, (E), 20: 12293(T)
rare-earth-ion fluorescent lifetimes in crystals of, 20: 12317
CALCIUM HYDROXIDES
$Be(OH)_2$–$Ca(OH)_2$, preparation and properties of, 20: 10836
CALCIUM ISOTOPES Ca-40
alpha elastic scattering at 3.5 to 5.5 Mev, (E/T), 20: 12144
alpha reactions (α,d) at 42 to 53 Mev, deuteron energy spectra from, (E), 20: 12061
helium-3 reactions (He-3,p) at 12 Mev, (T), 20: 12086
meson (μ^-) capture by, K x-ray emission from, (E), 20: 11480
neutron reactions (n,α) with, Q-values for, (E), 20: 11983
neutron reactions (n,α) at 4.7 Mev, alpha angular distributions in, (E), 20: 12119
proton reactions (p,2p) at 460 Mev, (E/T), 20: 11948 (AD-624318)
CALCIUM ISOTOPES Ca-43
neutron reactions (n,α) with, Q-values for, (E), 20: 11983
CALCIUM ISOTOPES Ca-44
meson (μ^-) capture by, K x-ray emission from, (E), 20: 11480
CALCIUM ISOTOPES Ca-45
radiation effects on skeletal uptake of chloride-incorporated, in rats, x, 20: 10587
uptake of, combined with thallium-204 by human respiratory tract, 20: 10546
CALCIUM OXIDES
electron spin resonance spectra of spin-1 ions in, Jahn-Teller effects in, (T), 20: 12294
spectra of isotopic shifts of oxygen-18 in, infrared, 20: 10815 (UCRL-16338)
spectra of, vibrational and rotational infrared, 20: 10815 (UCRL-16338)
CaO–Dy_2O_3, phase diagrams, 20: 10822
CaO–Yb_2O_3, phase diagrams, 20: 10822
CALCIUM SELENIDES
CaSe–Ce_2Se_3, phase studies, 20: 10857
CaSe–Dy_2Se_3, phase studies, 20: 10857
CaSe–Er_2Se_3, phase studies, 20: 10857
CaSe–Gd_2Se_3, phase studies, 20: 10857
CaSe–Ho_2Se_3, phase studies, 20: 10857
CaSe–La_2Se_3, phase studies, 20: 10857
CaSe–Lu_2Se_3, phase studies, 20: 10857
CaSe–Nd_2Se_3, phase studies, 20: 10857
CaSe–Pr_2Se_3, phase studies, 20: 10857
CaSe–rare earth selenides, phase studies, 20: 10857
CaSe–Sm_2Se_3, phase studies, 20: 10857
CaSe–Tm_2Se_3, phase studies, 20: 10857
CaSe–Yb_2Se_3, phase studies, 20: 10857
CaSe–Y_2Se_3, phase studies, 20: 10857
CALCIUM TUNGSTATES
rare-earth-ion fluorescent lifetimes in crystals of, 20: 12317
CALDER HALL REACTORS
economic analysis of Dungeness B, 20: 12432
fuel element development for Dungeness B, 20: 12430
fuel element performance, 20: 11357
CALIFORNIUM ISOTOPES Cf-249
helium ion fission at 42.8 Mev, deformation of transition-state nucleus in, (E), 20: 12077
CALIFORNIUM ISOTOPES Cf-252
fission of, fragment mass-energy correlations from spontaneous, (E), 20: 12076
CALORIMETERS
development for measuring thermodynamic properties of ethylenediamine solutions, 20: 12550 (TID-22564)
performance for electron beam energy calibration measurements, 20: 11389 (DESY-65/12)
CAMBRIDGE SYNCHROTRON
beam bypass of, vacuum requirements for, 20: 11385 (CEAL-TM-157)
beam bypass system of, magnet criteria for, 20: 11383 (CEAL-TM-152)
beam collision facility for, design of, 20: 11382 (CEAL-TM-151)
synchrotron radiation effects for bypass, calculation of, (T), 20: 11384 (CEAL-TM-156)
CAMERAS
properties of, affecting accuracy of spatial reconstruction of recorded events, 20: 11101 (JINR-P-2468)
CAMPHOR
complexes with uranyl perchlorate, preparation of, 20: 10825
CARBAMIC ACID, DIETHYLDITHIO-, SODIUM SALTS
solvent properties for manganese, tracer studies of, 20: 10950
CARBAMIC ACID, ETHYL ESTER
effects on bone marrow of leukemia patients, fibrotic, 20: 10746
CARBOHYDRATES
radiolysis of aqueous solutions of, role of hydrated electrons in, 20: 10920
CARBON
coating on ceramic fuel particles, deposition-condition effects on properties of, 20: 11254
compatibility with water vapor at 1000°C of coatings of pyrolytic, on carbide fuel particles, 20: 11224
crystal lattice dynamics, (T), 20: 12275 (GA-6861)
diffusion in molybdenum, titanium, tungsten, and zirconium surfaces,

20: 11228
diffusion in uranium monocarbide at 1200 to 2100°C, 20: 11224
effects on formation of tempering structures in molybdenum–uranium alloys, 20: 11292
effects on tantalum and tantalum alloys corrosion by plutonium–cobalt–cerium alloys, 20: 11224
effects on tensile properties of tungsten and tantalum–tungsten single crystals, 20: 11227
fixation by vascular hydrophytes, effects of daylight on, 20: 12543(R) (NYO-3018-12)
gamma incoherent scattering by electrons of, at 100 to 280 kev, (E), 20: 11515
neutron four-group cross sections, 20: 12485
performance of coatings of pyrolytic, on carbide and oxide fuels, irradiation, 20: 11224
radiation effects on fixation of, by vascular hydrophytes, 20: 12543(R) (NYO-3018-12)
radioinduced swelling in, irradiated at 150 to 650°C, fast-neutron, 20: 11225
radioinduced swelling of pyrolytic, fission fragment, 20: 11227
reactions with Armco iron and chromium–molybdenum steel in sodium at 1200°F, 20: 11235 (MSAE-65-194)
reactions with types 304 and 316 stainless steels in sodium at 1200°F, 20: 11235 (MSAE-65-194)
structure of pyrolytic, effects of methane concentration on, 20: 11224
structure of pyrolytic, effects of deposition temperature on, 20: 11225
surface density determination of thin films of, from x-ray production cross sections, 20: 11281 (UCRL-12107)

CARBON ARCS
ion heating in, (E/T), 20: 11770 (ORNL-P-1005)

CARBON DIOXIDES
compatibility with beryllium–calcium and beryllium–magnesium alloys, 20: 11225
corrosive effects on uranium–10 molybdenum alloys, effects of reactor radiation on, 20: 11224
heat transfer coefficients for, 20: 12341
radiolysis of deaerated aqueous solutions of, pulsed-electrons, 20: 10913
reactions with graphite at 960 to 1200°C, kinetics of, 20: 10859
reactions with tantalum at 500 to 700°C, mechanisms of, 20: 11227
reactions with uranium carbide in defective fuel elements, oxidation, (E/T), 20: 12380

CARBON IONS
energy levels of, (T), 20: 11450 (UCRL-7842-T)
heating of, excitation method for, (E/T), 20: 11770 (ORNL-P-1005)

CARBON ISOTOPES C-9
energy levels, 20: 12023

CARBON ISOTOPES C-10
energy levels, 20: 12023

CARBON ISOTOPES C-12
alpha reactions (α,d) at 42 to 53 Mev, deuteron energy spectra from, (E), 20: 12061
bremsstrahlung reactions at 25 to 57 Mev, beryllium-7 yields from, (E), 20: 12094
deuteron reactions (d,n) at 2.8 to 4.2 Mev, cross sections and polarization in, (E), 20: 12044
deuteron reactions (d,p) at 200 to 350 kev, proton angular distributions in, (E), 20: 12096
electron inelastic scattering by, giant resonances in, (T), 20: 12029
gamma reactions (γ,n) at 22 to 26 Mev, cross sections for, (E), 20: 12058
gamma reactions (γ,p) at 30 to 36 Mev, proton polarization from, (E), 20: 12105
lithium-6 reactions (Li-6,α), (Li-6,d) and (Li-6,p) at 4.5 to 5.5 Mev, cross sections for, (E), 20: 12059
neutron nonelastic reactions at 13 to 21 Mev, cross sections for, (E), 20: 11985
nucleon scattering at 20 Mev, optical potential for, (T), 20: 12047
production and separation of, method for, 20: 11191 (JEN-150-DQ/I-51)
proton inelastic scattering at 156 Mev, cross sections for, (T), 20: 11974 (ORNL-P-960)
proton reactions (p,2p) at 460 Mev, (E/T), 20: 11948 (AD-624318)

CARBON ISOTOPES C-13
enrichment of, by thermal diffusion of labeled methane, 20: 11194
production and separation of, method for, 20: 11191 (JEN-150-DQ/I-51)

CARBON ISOTOPES C-14
effects on decomposition of pyruvate, 20: 10934 (UCRL-11743)
energy level structure of, configuration mixing effects in, (T), 20: 12155
incorporation in salicylic acid, 20: 10868
use of carbonate-incorporated, for measuring synthetic rate of urea, 20: 10559
use of carbonate-incorporated, in combination with nitrogen-15-labeled urea for measuring rate of urea synthesis, 20: 10559

CARBON MONOXIDES
effects on carbon dioxide–graphite reactions at 960 to 1200°C, 20: 10859
hydrogen reactions at 3 to 30 kev, electron loss and formation of slow anions in, (E), 20: 11509
radiolysis of deaerated aqueous solutions of, pulsed-electrons, 20: 10913
reactions with tantalum at 500 to 700°C, mechanisms of, 20: 11227
vapor pressure of, vibrational spectroscopy and isotope effect on, 20: 10831

CARBON STEEL
boronization of, procedure for, 20: 11260
fatigue crack growth in, 20: 12338(R) (GEAP-4911)
radiation damage and recovery in, neutron, 20: 11227
radiation effects on wear resistance of, neutron, 20: 11227
radiation hardening of, combined effects of carbon content and irradiation temperature on fast-neutron, 20: 11342 (EURAEC-1502)
welding of, automatic inert gas tungsten arc, 20: 11246

CARBON SYSTEMS
C–Be–U, properties of splat-cooled, 20: 11224
C–Ce–Th, phase studies, 20: 11224
C–Ce–U, phase studies, 20: 11224
C–graphite, thermodynamic properties to 6000°K of solid and vaporous, 20: 10799 (AD-625735)
C–Hf–Re–Ta–W, preparation and properties of dispersion-strengthened, 20: 11217(R) (WANL-PR(Q)-007)
C–Hf–Ta–W, bonding of T-222, to Inconel 600 and types 321 and 347 stainless steels, explosive, 20: 11243(R) (WANL-PR(EE)-001)
C–Mo–Ti–Zr, stress-rupture properties of TZC, at high temperatures and strain rates, 20: 11265 (AD-626375)
C–Pu–Th, phase studies and properties of, 20: 11224
C–U, properties of splat-cooled, 20: 11224

CARBON TETRACHLORIDE
radiolysis of frozen methanol solutions of, formation of stabilized radicals in, 20: 10879
toxicity in mice, 20: 10548
benzene–CCl_4, pulsed-electron radiolysis of, 20: 10928
Br–CCl_4, radiation chemistry of, processes of bromine-81 (n,γ), 20: 10938

CARBON TETRAFLUORIDE
radiolysis of, ESR spectrum of oxygen fluorides from electron, 20: 10882

CARBONATES
radiation effects on strength of, proton, 20: 10605(T) (NASA-TT-F-353, pp 21-54)
use of carbon-14-labeled, for measuring synthetic rate of urea, 20: 10559

CARBONYL COMPOUNDS
reactions with hydroxyl radicals, rate constants for, 20: 10916

CARBOX PROCESS
performance for carbide fuels, 20: 10965

CARBOXYL GROUP
yields in pulse-radiolysis, 20: 10913

CARCINOGENS
effects of chemical, on induction of bone sarcomas by strontium-90, 20: 10627
effects of diacetylaminofluorene on deposition of cerium-144 in rat liver, 20: 10526(R) (BNWL-122, pp 91-3)
effects of diacetylaminofluorene on deposition of praseodymium-144 in rat liver, 20: 10526(R) (BNWL-122, pp 91-3)
effects of diacetylaminofluorene on deposition of plutonium-238 in rat liver, 20: 10526(R) (BNWL-122, pp 91-3)
effects of dimethylaminoazobenzene on deposition of cerium-144 in rat liver, 20: 10526(R) (BNWL-122, pp 91-3)
effects of dimethylaminoazobenzene on deposition of plutonium-238 in rat liver, 20: 10526(R) (BNWL-122, pp 91-3)
effects of dimethylaminoazobenzene on deposition of praseodymium-144 in rat liver, 20: 10526(R) (BNWL-122, pp 91-3)

CARCINOMAS
radiation effects on urethan-induced, in mice, x, 20: 10671
radioinduced lung, after inhalation of plutonium-239 oxide particles, 20: 10596(R) (BNWL-122, pp 1-15)
radiosensitivity of, effects of 5-fluorouracil, 20: 10725
radiotherapy of bladder, effects of dose fractionation on x, 20: 10743
radiotherapy of cervical, complications and survival rate after, 20: 10726
radiotherapy of cervical, evaluation of results, 20: 10727
radiotherapy of cervical, histological evaluation of radium, 20: 10749
radiotherapy of cervical, during pregnancy, 20: 10751
radiotherapy of cervical, review of indirect effects of, 20: 10670
radiotherapy of laryngeal, 20: 10744
radiotherapy of pharyngeal, y, 20: 10725
radiotherapy of thyroid, using iodine-131, 20: 10729
radiotherapy of uterine adeno-, pelvic fracture induced by, 20: 10668
surgery of cervical, evaluation of results, 20: 10727
therapy of mammary, by yttrium-90 pituitary destruction, 20: 10752

CASCADE SHOWERS
model for internuclear, above 10 Bev, (T), 20: 11566 (JINR-P-2472)
properties of 1- to 3-Bev proton-induced, in dense media, (E), 20: 12262 (BNL-8721)

CASEIN
use of iodine-131-labeled calcium, in measuring intestinal protein absorption, 20: 10566
CATHODE-RAY TUBES
performance for scanning spark chamber photograms, 20: 11104 (LNF-65/33)
CATHODES
performance of rare earth, in ion pumps, 20: 10976 (IS-T-46)
CATTLE
iodine-131 content in tissues of, after ingestion, 20: 10516(R) (BNWL-122, pp 49-51)
iodine-131 content of milk, effects of dietary content of radioactive and stable iodine, 20: 10530(R) (BNWL-122, pp 113-17)
iodine-131 content of milk, effects of dietary content of radioactive and stable iodine, 20: 10530(R) (BNWL-122, pp 113-17)
CAVES
design, equipment, and construction of, bibliography on, 20: 10977 (KFK-370)
use of temporary, for work in reactor vessels, 20: 12450
CAVITY RESONATORS
beam loading and field excitation in linac, (T), 20: 11381 (BNL-9833)
radiation emission from, quantum electrodynamics of stimulated, 20: 11878
CELLULOSE
radioinduced grafting of styrene to, 20: 10873
radiolysis of styrene-grafted, free radical yields in, 20: 10873
CENTRIFUGAL PUMPS
design for cesium and potassium Rankine cycles, 20: 12475 (WANL-PR(B)-009)
CERAMIC MATERIALS
creep properties at high temperatures, design of apparatus for measurement of, 20: 11285 (UCRL-16434)
dispersion-strengthened, bibliography on, 20: 11278 (RISO-48(Suppl.2))
fabrication by hot isostatic pressing, 20: 11260
fracture toughness testing, effects of geometry on, 20: 12555 (WAPD-T-1828)
CERIUM
determination in irradiated uranium dioxide, 20: 10787
effects on stability of delta-phase plutonium–gallium alloys, 20: 11224
heat of solution in liquid tin at 631 to 634°K, 20: 11304
magnetic properties, 20: 11340
separation from other elements by solvent extraction using TBP, 20: 10952
separation from uranium by reversed-phase partition chromatography, 20: 10784
CERIUM ALLOYS
Al–Ce, crystal structure of intermetallic compound $CeAl_3$ in, 20: 11305
Ce–Co–Pu, analysis for plutonium, review of methods for, 20: 10797
Ce–Co–Pu, burnup studies on, core design for, 20: 12403 (LA-3384)
Ce–Co–Pu, corrosive effects on tantalum and tantalum alloys, effects of carbon, on, 20: 11224
Ce–Ga–Pu, tensile properties and thermal expansion of delta-stabilized plutonium-base, 20: 11224
Ce–Gd, magnetic properties of, effects of composition and temperature on, 20: 11341
Ce–Sn, tin Knight shift and magnetic susceptibility of $CeSn_3$, 20: 12324
CERIUM ALUMINATES
preparation of single crystals of, 20: 10826
CERIUM IONS
spin-lattice relaxation of trivalent, in lanthanum chlorides, (E), 20: 12292
spin-lattice relaxation in yttrium ethyl sulfates, (E), 20: 12300
CERIUM ISOTOPES
atomic mass, (E/T), 20: 11494
CERIUM ISOTOPES Ce-140
determination in uranium-233 and -235 fission products, (E), 20: 11960(R) (IDO-14667)
CERIUM ISOTOPES Ce-141
beta decay of, l-forbidden transitions in, (T), 20: 12154
CERIUM ISOTOPES Ce-142
determination in uranium-233 and -235 fission products, (E), 20: 11960(R) (IDO-14667)
CERIUM ISOTOPES Ce-144
absorption by swine, gastrointestinal, 20: 10525(R) (BNWL-122, pp 85-90)
content in ocean fish, effects of content in sea water on, 20: 11054
determination in irradiated MITR fuel elements by gamma spectroscopy, 20: 10764 (MITNE-64)
determination in uranium-233 and -235 fission products, (E), 20: 11960(R) (IDO-14667)
diffusion from simulated solid wastes, 20: 12517(R) (BNWL-170)
effects of combined plutonium-239 or strontium-90 and, on rats, 20: 10552
effects of inhaled oxide particles of, pathological, 20: 10513(R) (BNWL-122, pp 16-20)
effects on gastrointestinal tract during chronic radiation sickness, 20: 10674
effects on plutonium determination in fission product solutions, 20: 10763 (KR-100)
elimination from mice using TTHA chelates, 20: 10556
elimination of combined plutonium-239 or strontium-90 and, in rats, 20: 10552
excretion of inhaled, effects of DTPA in dogs, 20: 10533(R) (BNWL-122, pp 125-7)
metabolism in rats, effects of chemical carcinogens on, 20: 10526(R) (BNWL-122, pp 91-3)
performance as space vehicle power supply, 20: 11188 (BLG-330)
CERIUM NITRATES
$Ce(NO_3)_4$–TBP–$UO_2(NO_3)_2$–H_2O, phase diagram, 20: 10952
CERIUM OXIDES
distribution of inhaled particles of, in dogs, 20: 10513(R) (BNWL-122, pp 16-20)
CERIUM SELENIDES
CaSe–Ce_2Se_3, phase studies, 20: 10857
CERIUM SYSTEMS
C–Ce–Th, phase studies, 20: 11224
C–Ce–U, phase studies, 20: 11224
CESIUM
cesium ion reactions with atomic, probability of, (E), 20: 11443 (NASA-CR-54790)
corrosive effects on metals and ceramics at 400°C, 20: 11227
determination in irradiated urania pellets using electron microprobe analysis, 20: 11365
effects on tensile properties of heat-resisting metals and alloys at 650 and 1200°C, 20: 11227
electron reactions with atoms of, probability of, (E), 20: 11443(R) (NASA-CR-54790)
electron reactions with atoms of, probability of, (E), 20: 11444 (NASA-CR-54790(App. 1))
ion wave propagation in plasma of, effect of weak collisions on, (T), 20: 12172 (MATT-302)
ion-wave propagation in plasma of, effect of weak collision rate on, (T), 20: 12237
performance as working fluid for Rankine cycles, 20: 12475 (WANL-PR(B)-009)
photoionization of atoms of, by solar radiation, (T), 20: 11549
proton reactions with atoms of, production of highly excited hydrogen atoms by charge-exchange, (E), 20: 11471(T)
reactions with bromine in crossed molecular beams, spectator stripping model for, 20: 10834
separation from fused salts by ion exchange, tracer studies of, 20: 10958
separation from iodine and thallium, 20: 10901
separation from uranium by reversed-phase partition chromatography, 20: 10784
separation from waste solutions by ion exchange on alumina–silica, 20: 10766 (TID-22511)
CESIUM CHLORIDES
magnetic moment of molecular, rotational, (E), 20: 11484
CESIUM FLUORIDES
magnetic moment of molecular, rotational, (E), 20: 11484
CESIUM IONS
electron recombination cross sections for atomic and molecular, (E), 20: 11488
reactions with cesium atoms, probability of, (E), 20: 11443(R) (NASA-CR-54790)
CESIUM ISOTOPES Cs-129
production of carrier-free, in alpha reactions (α,2n) with iodine-127 and (α,4n) with iodine-129 at 35 Mev, (E), 20: 10901
CESIUM ISOTOPES Cs-132
production of carrier-free, in alpha reactions (α,n) with iodine-129 at 35 Mev, 20: 10901
CESIUM ISOTOPES Cs-133
energy levels, (E), 20: 12153
CESIUM ISOTOPES Cs-134
determination in irradiated MITR fuel elements by gamma spectroscopy, 20: 10764 (MITNE-64)
gamma activity of, discrimination in presence of cesium-137, 20: 11134
CESIUM ISOTOPES Cs-137
content in Alaskan deer, 1963 and 1964, 20: 10535(R) (BNWL-122, pp 176-80)
content in Alaskan forage plants, 1963 and 1964, 20: 10535(R) (BNWL-122, pp 176-80)
content in Alaskan natives, whole-body, 1964, 20: 10718(R) (BNWL-122, pp 172-5)
content in Alaskan natives, whole-body, 1965, 20: 10723
content in Columbia River plume, 20: 11023
content in diet of sheep, effects on content in rumen, 20: 10520(R) (BNWL-122, pp 64-6)

content in fallout, 1964, 20: 11018
content in forage plants, effects of precipitation on, 20: 11012(R) (BNWL-122, pp 184-6)
content in German milk, effects of precipitation on, 20: 11017
content in German rye and wheat, effects of precipitation on, 20: 11017
content in ocean fish, effects of content in sea water on, 20: 11054
content in sheep rumen, effects of content in diet on, 20: 10520(R) (BNWL-122, pp 64-6)
determination in irradiated MITR fuel elements by gamma spectroscopy, 20: 10764 (MITNE-64)
determination in plants by gamma spectroscopy following dissolution in sodium hydroxide, 20: 10782
determination in uranium-233 and -235 fission products, (E), 20: 11960(R) (IDO-14667)
diffusion from simulated solid wastes, 20: 12517(R) (BNWL-170)
dosimetry of gamma radiation from ingested, using *in vivo* thermoluminescent detector, 20: 11091(R) (BNWL-122, pp 67-72)
effects on man after accidental exposure, 20: 10721
effects on plutonium determination in fission product solutions, 20: 10763 (KR-100)
metabolism of intravenously injected, in rainbow trout, 20: 10521(R) (BNWL-122, pp 73-4)
performance as space vehicle power supply, 20: 11188 (BLG-330)

CESIUM ISOTOPES Cs-144
content in fallout, 1964, 20: 11018

CESIUM NITRATES
radiolysis of, at 77, 300, and 400°K, effects of pressure on, 20: 10891

CESIUM URANIUM CHLORIDES
uranium ion spectra in, M1 transitions and Zeeman effect in, (E), 20: 12290

CHARGED PARTICLE BEAMS
acceleration of, statistical distribution limit for density in, (T), 20: 11408
deflection of, engineering drawings of electrostatic steering system for, 20: 11413
transport in deflecting magnet systems, symmetry properties for, (T), 20: 11411

CHARGED PARTICLES
acceleration in electromagnetic fields, mechanisms of, (T), 20: 11837
acceleration of, design of accelerator for, 20: 11421(P)
acceleration of, design of apparatus for, 20: 11422(P)
containment in radiation belts, interchange stability of, (T), 20: 11835
emission from solar flares, 20: 11438
energy and rigidity spectra of solar flare, in polar regions, (E), 20: 11855
interactions in ionosphere, (E), 20: 11850
interactions with magnetospheric electric and magnetic fields, 20: 11849
motion in fluids in crossed electric and magnetic fields, Brownian, (T), 20: 11802
motion in plasma in magnetostatic and h-f field, (T), 20: 12195
precipitation in ionosphere, correlations with auroral storms, (E), 20: 11851
properties of ionospheric high-latitude, conference on, 20: 11841
reactions in ionospheric polar D region, review of, (T), 20: 11843
reactions with bismuth and lead at high energies, astatine production in, 20: 11377
reactions with heavy and medium nuclei, rates for, (T), 20: 11989
reactions with nuclei at high energies, fragmentation in, 20: 11377
reactions with nuclei, finite-range Coulomb stripping and heavy-ion transfer, (T), 20: 12091
scattering by atoms, Fredholm equations for resonance potential, (T), 20: 11508

CHEMICAL ANALYSIS
beta reflection in precipitation titration, 20: 10778
Mössbauer effect for, problems in, 20: 11377
progress reports of ORNL Analytical Chemistry Division, author and keyword indexes of, 20: 10765 (ORNL-3904)
radiometric precipitation titration methods, 20: 10777

CHEMICAL ENGINEERING
design of fixed-bed catalytic reactors, models for, 20: 10754 (IS-T-44)
fluid flow in porous media, geometric model for predicting exchanger efficiency for, (T), 20: 10997(T) (AERE-Trans-1038)

CHEMICAL RADIATION DETECTORS
bibliography on, 20: 11027 (AED-C-21-03)

CHEMISTRY
book: *Nuclear Chemistry*, in Russian, 20: 11377
research projects in, summaries on basic off-site, 20: 10755 (TID-4005 (Pt.2a)(2nd ed.))

CHERENKOV DETECTORS
performance as trigger for spark chambers, for detecting meson (π^0)-decay photons, 20: 11099 (JINR-P-2436)

CHERENKOV RADIATION
emission from nuclear detonation in space, mechanism for coherent, (T), 20: 11807 (UCRL-7495(Rev.1))
emission in charged-particle interactions with electrons, (T), 20: 11670

CHICKENS
radiation effects on egg production by, x, 20: 10626

CHILE
uranium reconnaissance in Lonquimay area in, 20: 11025 (RME-4552 (Rev.))

CHIMERAS
radiation effects on Pseudomonas susceptibility in mouse, x, 20: 10669
response of liver to immune reactions to donor cells in mouse-rat radiation, 20: 10505(R) (BNWL-122, pp 146-9)

CHLORANIL
complexes with 3,8-diaminopyrene and phenylenediamines, effects of pressure on properties of, 20: 12534 (COO-1198-216)

CHLORIDE IONS
corrosive effects on magnesium and its alloys, electrochemistry of pitting, 20: 11231 (CEA-R-2815)

CHLORINE
chlorine ion reactions with atoms of, charge-exchange, (T), 20: 11517
glow discharge in impure, optical excitation in negative, (E/T), 20: 11773

CHLORINE FLUORIDES
flow rate of gaseous, design and calibration of flowmeters for measuring, 20: 11059 (BLG-345)

CHLORINE IONS
energy levels of, (T), 20: 11450 (UCRL-7842-T)
reactions with chlorine atoms at 25 to 90 kev, charge-exchange, (T), 20: 11517

CHLORINE ISOTOPES
atomic mass, (E/T), 20: 11494

CHLORINE ISOTOPES Cl-34
energy levels, (E), 20: 12061

CHLORINE ISOTOPES Cl-37
energy levels, (E), 20: 12005(T)
neutron reactions (n,p) at 14.8 Mev, cross sections for, (E), 20: 12133
proton reactions (p,n) with mechanism for, (E/T), 20: 12141

CHLORINE SYSTEMS
benzene–Cl, radioinduced reactions in, hexachlorocyclohexane production in γ, 20: 10900

CHLOROFORM
bonding in, comparison of, deuterium and hydrogen, 20: 10819
solvent properties of, with 8-hydroxy-5-quinolinesulfonic acid and Schiff bases for metals, 20: 10759 (INP-427/C)

CHOLINESTERASES
radiation effects on activity of, in dog serum, proton, 20: 10592
radioinduced inactivation of, in biological materials, effects of purity on γ, 20: 10586

CHROMATOGRAPHY
developments in radio gas, 20: 10933(R) (TID-22532)
equipment for compound purification by gas, 20: 12553 (UCRL-14359)
radioactive material scanning in thin-layer, instrument for, 20: 10788

CHROMIC ACID
corrosive effects on molybdenum, tungsten, and vanadium at 35, 60, and 100°C, 20: 11230 (BM-RI-6715)

CHROMIUM
crystal structure of, dislocations in, 20: 11303
deposition from fused salt mixtures, electro-, 20: 11260
deposition on bismuth telluride, electrolytic, 20: 11543(R) (GIC-2605-3)
determination in fission product and irradiated fuel solutions by controlled-potential coulometry, 20: 10758 (EUR-2618.f)
effects of alloy additions of, on mechanical properties of niobium, 20: 11302
electron interaction effects in films of, superimposed on superconducting lead films, (E), 20: 11918
transition temperature of, notch-impact, 20: 11300
x-ray spectra of, performance of spectroanalyzer with promethium-147 beta source for K, 20: 11133

CHROMIUM ALLOYS
Al–Cr–Co–Fe–Mo–Ni–Ti, stress-rupture properties of Udimet 700, at high temperatures and strain rates, 20: 11265 (AD-626375)
Al–Cr–Nb, oxidation at 1100°C, effects of composition on, 20: 11338
Al–Cr–Nb, phase studies, 20: 11338
Cr–Co–Mo–Ni–W, erosion by mercury vapor at 640°F of Stellite 6B, 20: 11214(R) (NASA-CR-54717)
Cr–Co–Mo–Ni–W, oxidation by air at 1600°F of Stellite 6B, 20: 11215(R) (NASA-CR-54718)
Cr–Fe, crystal structure of, dislocations in, 20: 11303
Cr–Fe, diffusion of fission products in, effects of concentrations on, 20: 11212(R) (BMI-X-10143)
Cr–Fe–Mo–V, erosion by mercury vapor at 640°F of Lapelloy, 20: 11214(R) (NASA-CR-54717)
Cr–Fe–Ni, diffusion of fission products in, effects of concentrations on, 20: 11212(R) (BMI-X-10143)
Cr–Fe–Ni, mechanism of stress corrosion cracking of, in sodium chloride, 20: 11233(R) (COO-1319-32)

Cr–Nb, mechanical properties of, effects of composition on, 20: 11288(T) (AD-622477)
Cr–Ni, analysis for yttrium using Arsenazo-III, spectrophotometric, 20: 10773
Cr–Ni–stainless steel, strain fatigue limits of, biaxial, 20: 12418(R) (WCAP-3739)
Cr–Re, crystal structure of, dislocations in, 20: 11303
Cr–Re, transition temperature of, notch-impact, 20: 11300
Cr–U, phase transformations in, effects of heat treatments on kinetics of $\beta \rightarrow \alpha$, 20: 11311
Cr–U–V, phase studies on, 20: 11271 (LFEN-24)

CHROMIUM CHLORIDES
reactions with fused alkali metal chlorides and fluorides, 20: 10821
reactions with lanthanum oxides in fused chlorides and fluorides, 20: 10821

CHROMIUM FLUORIDES
ionization in fused chlorides and fluorides, 20: 10821

CHROMIUM IONS
radiation effects on content in rubies, x, 20: 12305
reactions with permanganate ions during pulse-radiolysis of solutions, 20: 10914

CHROMIUM ISOTOPES Cr-51
incorporation in serum albumins, 20: 10944
production at PRR, methods for, 20: 12545(R) (PAEC(A)AR651)
use of albumin-incorporated, in measuring gastrointestinal protein loss, 20: 10569

CHROMIUM ISOTOPES Cr-52
deuteron elastic scattering at 7.8 Mev by, cross sections for, (E), 20: 12095
deuteron reactions (d,p) with, cross sections for, (E), 20: 12095
neutron reactions (n,p) at 14.8 Mev, cross sections for, (E), 20: 12133

CHROMIUM ISOTOPES Cr-53
energy level structure, (E/T), 20: 12095

CHROMIUM OXIDES
ionization in fused chlorides and fluorides, 20: 10821

CHROMIUM STEEL
boronization of, procedure for, 20: 11260
thermal stress fatigue of Croloy 2¼, 20: 11227
Cr–Mo, carburization by high-carbon sodium at 1200°F, 20: 11235 (MSAE-65-194)
Cr–Mo, compatibility with boron carbide of AISI 4130, 20: 11226
Cr–Mo, corrosion by flowing sodium at 1000 to 1200°F, equation for, 20: 11227
Cr–Mo, corrosion by mercury vapor at 1250°F, 20: 11214(R) (NASA-CR-54717)
Cr–Mo, creep at 1325°F, effects of welding on, 20: 11215(R) (NASA-CR-54718)
Cr–Mo, hardness of welded, effects of heat treatments on, 20: 11215(R) (NASA-CR-54718)
Cr–Mo, mechanical properties of, effects of exposure to high- and low-oxygen sodium on, 20: 11227
Cr–Mo, tensile properties of, effects of welding on, 20: 11214(R) (NASA-CR-54717)
Cr–Mo, welding of, automatic inert gas tungsten arc, 20: 11246
Cr–Mo, welding to type 316 stainless steel, weld-filler metal for, 20: 11214(R) (NASA-CR-54717)
Cr–Mo–Ni, fracture toughness properties of 12% maraging, 20: 11273(R) (NRL-6364)
Cr–Mo–Ni, hardness of welded type 4340, effects of heat treatments on, 20: 11215(R) (NASA-CR-54718)
Cr–Mo–Ni, radiation hardening in low-alloy, effects of irradiation temperature on fast-neutron, 20: 11342 (EURAEC-1502)
Cr–Mo–Ni, welding techniques for HY-80, 20: 11261
Cr–Mo–Ni–V, fatigue crack propagation in, effects of air or salt water environment on, 20: 11273(R) (NRL-6364)
Cr–Mo–Ti, corrosion by flowing sodium at 1000 to 1200°F, equation for, 20: 11227
Cr–W–V, erosion by mercury vapor at 640°F of 18-4-1 tool, 20: 11214(R) (NASA-CR-54717)

CHROMIUM SYSTEMS
Cr–O–Zr, phase studies, 20: 11227
Cr–PuC–UC, analysis for plutonium, review of methods for, 20: 10797

CHROMOSOMES
anomalies of, in leukemia patients, 20: 10647
effects of N-ethylmaleimide on, in Vicia roots, genetic, 20: 10624
radiation effects on bean root, protective effects of nitrogen against aberrant, 20: 10712
radioinduced aberrations in, effects of magnetic fields on, 20: 10672
radioinduced aberrations in, effects on survival of Ehrlich ascites tumor cells of, 20: 10677
radiosensitivity of Vicia root, effects of N-ethylmaleimide on x, 20: 10624

CIRCUITS
design for phase stabilization of r-f beam deflectors in Brookhaven AGS, (E), 20: 11380 (BNL-9772)
design of relay, using radiation counters, 20: 11084(P)
design of, iterative Chebyshev approximation technique for, 20: 11066 (SLAC-PUB-146)
radiation effects on, computer programs for analysis of, 20: 11172 (AD-623963)
radiation effects on microelectronic, 20: 11179
testing of SNAP-10FS-5, shock and vibration, 20: 12469 (NAA-SR-Memo-11630)

CITRIC ACID
corrosive effects on molybdenum, tungsten, and vanadium at 35, 60, and 100°C, 20: 11230 (BM-RI-6715)

CITRIFLEX PROCESS
use for decladding of Zircaloy-2 and zirconium-clad fuel elements, advantages, 20: 11272 (NP-15661)

CIVILIAN DEFENSE
fire hazards in nuclear attack, evaluation of secondary, 20: 11031 (NP-15708)
shelter protection against fallout, engineering method for calculating, 20: 11030 (NBS-MON-76)

CLAYS
geochemistry of thorium and uranium in, in Lower Triassic deposits, Pripyat Basin, USSR, 20: 11026
ruthenium-106 sorption by, 20: 10855
sorptive properties for radioactive substances in waste waters, 20: 12527(P)

CLOUD CHAMBERS
track pictures from, particle kinematics from, (T), 20: 11100 (JINR-P-2467)

COATINGS
decontamination and radiation resistance of protective, 20: 10964

COAXIAL CABLES
design of equalized, 20: 11066 (SLAC-PUB-146)

COBALT
deposition on bismuth telluride, electrolytic, 20: 11543(R) (GIC-2605-3)
diffusion in molybdenum, coefficient for, 20: 11227
effects of alloying additions of, on oxidation rates of niobium, tantalum, and tungsten, 20: 11227
effects of binder of, on cryogenic properties of titanium and tungsten carbides, 20: 11293
proton reactions with, phosphorus-32 and -33 production in, (E), 20: 12034
separation from salts by solvent extraction using 8-mercaptoquinoline in chloroform, 20: 10759 (INP-427/C)
solubility in potassium, 20: 11227

COBALT ALLOYS
Al–Cr–Co–Fe–Mo–Ni–Ti, stress-rupture properties of Udimet 700, at high temperatures and strain rates, 20: 11265 (AD-626375)
Ce–Co–Pu, analysis for plutonium, review of methods for, 20: 10797
Ce–Co–Pu, burnup studies on, core design for, 20: 12403 (LA-3384)
Ce–Co–Pu, corrosive effects on tantalum and tantalum alloys, effects of carbon on, 20: 11224
Co–Gd, crystal structure of intermetallic compound $GdCo_3$ in, 20: 11308
Co–Th, phase studies, 20: 11224
Co–Y, crystal structure of intermetallic compound YCo_3 in, 20: 11308
Cr–Co–Mo–Ni–W, erosion by mercury vapor at 640°F of Stellite 6B, 20: 11214(R) (NASA-CR-54717)
Cr–Co–Mo–Ni–W, oxidation by air at 1600°F of Stellite 6B, 20: 11215(R) (NASA-CR-54718)

COBALT CHLORIDES
effects on porosity of sintered hafnium and tantalum carbides, 20: 11250
separation from salts by extraction chromatography using organic phosphorus compounds, 20: 10759 (INP-427/C)

COBALT(II) CHLORIDES
Neel temperature of hexahydrate of, effect of deuteration on, 20: 10853

COBALT COMPLEXES
halopentammine, radiation effects on, annealing of, 20: 10889
with 2,4-pentanedione, radiation effects on, gamma and thermal annealing of neutron, 20: 10888
with 2,4-pentanedione, cobalt-58m decay in, 20: 10888

COBALT IONS
reactions with permanganate ions during pulse-radiolysis of solutions, 20: 10914

COBALT ISOTOPES Co-56
energy levels of, width of 2^+, 20: 12147

COBALT ISOTOPES Co-57
decay of, conversion coefficients for, (E), 20: 11976 (TID-22504)

COBALT ISOTOPES Co-58
decay of isomeric, in cobalt acetylacetonate, effects from, 20: 10888
production at PRR, methods for, 20: 12545(R) (PAEC(A)AR651)

COBALT ISOTOPES Co-59

alpha reactions at 42 Mev, proton emission in, (E), 20: 12062
energy levels, (E), 20: 12063
ion reactions with, copper recoil ions from heavy, (E), 20: 12085
proton reactions (p,2p) at 460 Mev, (E/T), 20: 11948 (AD-624318)
proton reactions (p,α) at 10.965 Mev, iron-56 energy levels from, (E), 20: 12063
proton reactions (p,p') at 8.972 Mev, energy levels from, (E), 20: 12063

COBALT ISOTOPES Co-60
adsorption by peat, 20: 10756
content in ocean fish, effects of content in sea water on, 20: 11054
nuclear orientation by adiabatic demagnetization, (E), 20: 12138
production at PRR, methods for, 20: 12545(R) (PAEC(A)AR651)
reactions of recoil, in neutron-irradiated cobalt complexes, 20: 10889
use in measurement of strata shrinkage, 20: 11024

COBALT OXIDES
magnetic structure, (E), 20: 11355
radiation effects on, fast neutron, (E), 20: 11355

COBALT STEEL
Co–Mo–Ni, mechanical properties of, effects of strain rate on, 20: 11284 (UCRL-14599)
Co–Ni, fracture toughness properties of, effects of carbon content on, 20: 11273(R) (NRL-6364)

COILS
magnetic pressure pulse effects on single-turn, 20: 12177 (NASA-TN-D-3199)

COINCIDENCE CIRCUITS
timing element for medium-fast, univibrator performance as, 20: 11109 (SGAE-E-5/1965)

COINCIDENCE COUNTERS
design and performance of binary-coded digitized hodoscope, 20: 11112 (TID-22553)
design of scintillation, for protons, 20: 11123(T)
use in tracer studies of coronary blood flow, 20: 10730

COLUMBIA RIVER
mixing with Pacific Ocean waters, tracer study on, 20: 11023
phosphorus-32 uptake and accumulation by plankton in, 20: 10536(R) (BNWL-122, pp 187-9)
phosphorus-32 uptake and accumulation by plankton in, 20: 10537(R) (BNWL-122, pp 190-3)
zinc-65 uptake and accumulation by plankton in, 20: 10536(R) (BNWL-122, pp 187-9)
zinc-65 uptake and accumulation by plankton in, 20: 10537(R) (BNWL-122, pp 190-3)

COMETS
trajectories of, planetary system effects on, (T), 20: 11426 (UCRL-12267)

COMPRESSORS
performance of gas-bearing closed-Brayton cycle turbo-, 20: 10972(R) (NYO-3237-4)

COMPUTER PROGRAMS
AIPMAN-I, for pulse resolution of random counters, FORTRAN II for IBM 709/7090/94, 20: 11105 (NAA-SR-Memo-11132)
AIREK-PUL, for solution of kinetics equations for periodically pulsed fast reactors, 20: 12395 (EUR-2552.e)
AUTO-DEBUG, for computer operating efficiency, in FORTRAN for IBM 7094, 20: 11208 (UCRL-12220)
BIGG-II, for neutron spectra and criticality of homogeneous reactors, FORTRAN 63, for CDC-3600, 20: 12357 (KR-75)
BLOOST-5, for reactor kinetics and heat transfer analysis, FORTRAN IV for IBM 7044, 20: 12354 (GAMD-6644(Add.))
BOUNCE, for neutron flux distributions in multiple-pin fuel elements, IBM 7090, 20: 12384 (AGN-TM-411)
CHLOE, for digitization of photographic oscilloscope traces of fast chemical reactions, for CDC-3600, 20: 10800 (ANL-7113)
COBRA, for fuel burnup in heterogeneous reactors, FORTRAN II for IBM-704, 20: 12361 (PEL-60)
CONVRG, subroutine for source convergence for 05R neutron transport code, FORTRAN, 20: 11934 (ORNL-TM-1325)
FASDOP, for neutron cross sections from Breit-Wigner resonance parameters, in FORTRAN IV, 20: 11958 (GAMD-6562)
for analysis of radiation effects on circuits, 20: 11172 (AD-623963)
for curve sketching, for first approximations for oscilloscope traces, 20: 12552 (UCRL-12226)
for distorted wave analysis of stripping reactions, 20: 12095
GAPS, for data analysis of pulsed neutron source experiments, FORTRAN IV for IBM 7044, 20: 12355 (GAMD-6781)
GAROL, for neutron resonance absorption, IBM 7044, 20: 11932 (GA-6637)
HECTIC-II, for heat transfer analysis of gas or liquid-cooled reactor passages, FORTRAN for IBM 7090, 20: 10989 (IDO-28595(Rev.))
ISO, for beta spectrometer design, FORTRAN II, 20: 11113 (UCRL-16471)
LRSPC, for performance of shielding materials for cosmic alpha particles and protons, 20: 12265 (NP-15697(Vol.1))
MADCAP, for particle orbits in storage rings, FORTRAN for CDC 1604, 20: 11395 (ORNL-TM-1172(Rev.))
PAPA, for piping stress analysis, 20: 12338(R) (GEAP-4911)
PARANA, for pulse-height analysis for radionuclide assay data, FORTRAN II for IBM-7094, 20: 11202(R) (NYO-3136-2, App. 1)
PINETO, for nonlinear differential equations in neutron dynamics, FORTRAN for IBM 7090, 20: 11946
REACT, subroutine for source convergence for 05R neutron transport code, FORTRAN, 20: 11934 (ORNL-TM-1325)
REST-I, for pulse resolution of random counters, FORTRAN II for IBM 709/7090/94, 20: 11105 (NAA-SR-Memo-11132)
RIFF RAFF, for resonance integrals in two-region cell, FORTRAN for CDC-3600, 20: 12351 (ANL-7033)
STORE, for particle orbits in storage rings, FORTRAN for CDC 1604, 20: 11395 (ORNL-TM-1172(Rev.))
STRESS, for machine tool control, 20: 12546 (SC-RR-65-548)
TEMCO, for reactor temperature coefficients, FORTRAN IV for IBM 7044, 20: 12353 (GA-6734)
use in neutron resonance calculations, 20: 11945
XTREME, numerical solutions of Lagrange multiplier problems, FORTRAN for CDC-1604, (T), 20: 12544 (ORNL-3846)

COMPUTERS
compilers for, properties of FORTRAN II, 20: 11207 (UCRL-7737)
logic switching networks of, duality theorem for combinatorial, 20: 11198(R) (COO-614-34, Sect. IIIB)
logic switching networks of, algebra for, (m,p), 20: 11199(R) (COO-614-34, Sect. IIIC)
performance for control of 200-Bev protron synchrotron, 20: 11401 (UCRL-16502)
performance of PDP-5 digital, for Bevatron control, 20: 11401 (UCRL-16502)
research, 20: 11195(R) (COO-614-34)
use for analysis of data on kinetics of fission product distribution in tissues, 20: 10519(R) (BNWL-122, pp 59-63)
use for evaluating engineering prototypes for waste processing by solidification, 20: 12517(R) (BNWL-170)
use for NRU Reactor control, 20: 12511
use for unnormalized arithmetic investigations, 20: 11196(TR) (COO-614-34, Sect. IIB)
use in plasma protein studies, 20: 10562
use on-line for electron moments spectra in meson (μ) decay in spark chambers, 20: 11553(R) (COO-614-34, Sect. IIC)
use on-line for mu-mesic atom x-ray spectra analysis, 20: 11440(R) (COO-614-34, Sect. IID)
use with spark chambers, 20: 11093(R) (COO-614-34, Sect. IIA)

CONCRETE AGGREGATES
shield design using boron carbide, 20: 11229(P)

CONCRETES
gamma attenuation in, (T), 20: 12264 (MLM-1315)
gamma scattering in, energy and angular distributions of, 20: 12269
neutron attenuation and moderation in hematite, high-energy, (E), 20: 12263 (JINR-P-2479)
performance of reinforced chamotte and chromite, for reactor thermal shielding, (T), 20: 12340
use for gamma shielding, dose buildup and thickness for, 20: 12266(T) (ORNL-tr-918)
use in containment of water-cooled power reactors, 20: 12447
use of reinforced, in reactor containment, 20: 12346

CONDENSERS
design for cesium and potassium Rankine cycles, 20: 12475 (WANL-PR(B)-009)

CONES
supersonic flow in common, numerical calculation of stationary, 20: 11767 (HMI-B-42)

CONFERENCES
see also introduction to Report Number Index
Dosimetry, Panel on In-Pile, Vienna, July 1964, 20: 11110 (STI/DOC/10/46)

CONNECTIVE TISSUE
effects of cortisone on mast cells in rats, 20: 10686
radiation effects on mast cells in rats, x, 20: 10686

CONNECTORS (ELECTRIC)
welded joints between component piping and Conoseal flange, stress relief of, 20: 11214(R) (NASA-CR-54717)

CONVEYERS
design for irradiation facilities, 20: 10986(P)

COPPER
bremsstrahlung reactions with, heating effects of, (T), 20: 12166 (CONF-651126-1)
compatibility with boron carbide, 20: 11226
corrosion by formic, hydrochloric, and oxalic acids at 35°C, galvanic, 20: 11230 (BM-RI-6715)
corrosion by sea water, sodium chloride, and sodium hydroxide,

galvanic, 20: 11230 (BM-RI-6715)
effects on iron content in rat erythrocytes, tracer study, 20: 10598(R) (BNWL-122, pp 107-9)
effects on leukocyte number in rats, 20: 10598(R) (BNWL-122, pp 107-9)
gamma incoherent scattering by electrons of, at 100 to 280-kev, (E), 20: 11515
light absorption by, mechanism of photographic sensitivity from, (T), 20: 11121
neutron capture by, secondary gamma emission from, (E), 20: 12267
neutron nonelastic reactions at 8.1 Mev, cross sections for, (E), 20: 11985
neutron scattering total cross section at 12 to 14 Mev, (E), 20: 11949 (AD-625747)
oxygen-ion reactions at 10 kev on (100) faces, cuprous oxide formation in, (E), 20: 12282
preparation of spherical particles of, by plasma jet atomization, 20: 11219
pressure spalling of, properties of, (T), 20: 12539 (LA-DC-7692)
proton channeling in, transverse two-dimensional model for, (T), 20: 12279 (UCRL-12311)
proton reactions at 1.84 Bev, sodium-24 energy spectra and yield in, (T), 20: 12067
radioinduced vacancy agglomerates in, interpretation of contrast phenomena in neutron, 20: 11353(T) (ANL-Trans-259)
separation from salts by solvent extraction using Schiff bases in chloroform, 20: 10759 (INP-427/C)
separation from salts by solvent extraction using 8-mercaptoquinoline in chloroform, 20: 10759 (INP-427/C)
sputtering of single crystals of, by argon ions, (T), 20: 11460
tin-119 Mössbauer effect in, 20: 12315
toxicity of, in rats, 20: 10598(R) (BNWL-122, pp 107-9)
welded joints between type 6061 aluminum alloy and, effects of heat treatments on pressure, 20: 11215(R) (NASA-CR-54718)

COPPER ALLOYS
Cu–Ni–W, mechanical properties of sintered composites of tungsten-base, 20: 11291
Cu–Y, analysis for yttrium using Arsenazo-III, spectrophotometric, 20: 10773

COPPER CHLORIDES
corrosive effects on molybdenum and tungsten at 35, 60, and 100°C, 20: 11230 (BM-RI-6715)
separation from salt mixtures by extraction chromatography using organic phosphorus compounds, 20: 10759 (INP-427/C)

COPPER COMPLEXES
with methylenephosphonic acid derivatives, preparation and properties of, 20: 12533 (COO-1020-6)

COPPER COUPLES
Cu/Nb/stainless steel, diffusion in bimetallic tubing of, with copper diffusion barrier, inter-, 20: 11215(R) (NASA-CR-54718)

COPPER IONS
radio-oxidation of divalent, in aqueous solutions, pulsed-electron, 20: 10923
reactions with permanganate ions during pulse-radiolysis of solutions, 20: 10914

COPPER ISOTOPES Cu-60
ranges of recoil ions of, in aluminum, (E), 20: 12085

COPPER ISOTOPES Cu-61
ranges of recoil ions of, in aluminum, (E), 20: 12085

COPPER ISOTOPES Cu-63
alpha reactions at 42 Mev, proton emission in, (E), 20: 12062

COPPER ISOTOPES Cu-64
production at PRR, methods for, 20: 12545(R) (PAEC(A)AR651)

COPPER ISOTOPES Cu-65
alpha reactions at 42 Mev, proton emission in, (E), 20: 12062

COPPER ISOTOPES Cu-67
use of ceruloplasmin-incorporated, in measuring gastrointestinal protein loss, 20: 10569

COPPER NITRATES
nitrogen-14 NMR in, (E), 20: 12325

COPPER OXIDES
effects on photolysis of nitroethane, 20: 10874
production and orientation in oxygen-ion reactions with copper at 10 kev, (E), 20: 12282

COPPER SYSTEMS
Cu–Si, deposition on molybdenum for oxidation protection, 20: 11236

CORONENE
complexes with iodine, effects of pressure on properties of, 20: 12534 (COO-1198-216)

CORROSION LOOPS
cleaning procedure for mercury, 20: 11215(R) (NASA-CR-54718)

CORROSION-RESISTANT ALLOYS
strengthening by irradiation, 20: 11366

CORTISONE
effects on mesenteric mast cells in normal and adrenalectomized rats, 20: 10686

COSMIC ALPHA PARTICLES
shielding against, tabulations of materials for, 20: 12265 (NP-15697(Vol.1))

COSMIC MESONS
intensities from high-energy reactions, meson (μ) spectra from K/π ratio of, (E), 20: 11526
intensity variations from 1954 to 1964, sidereal component of diurnal, 20: 11524
production in high-energy jet showers, analysis of multiple, (E/T), 20: 11534

COSMIC MESONS (μ)
interactions with nucleons in lead at high energies, electromagnetic, (E), 20: 11528
momentum spectra at large zenith angles, (E), 20: 11526
reactions with nuclei, (T), 20: 11975 (PAM-6502)

COSMIC MESONS (π)
intensities from high-energy reactions, meson (μ) spectra from K/π ratio of, (E), 20: 11526

COSMIC NEUTRONS
intensity in lower atmosphere, (E), 20: 11521
intensity in southern latitudes, plateau in, 20: 11523
intensity variations from 1954 to 1964, sidereal component of diurnal, 20: 11524

COSMIC NUCLEONS
intensity in lower atmosphere, (E), 20: 11521
momentum distribution of recoil, in high-energy jets, (T), 20: 11535

COSMIC PARTICLES
intensity in southern latitudes, plateau in, 20: 11523
interactions of high-energy, review on theory of, 20: 11529

COSMIC PROTONS
book: *Problems of Radiation Safety in Space Flights. Physical and Biological Studies with High-Energy Protons*, 20: 10604(T) (NASA-TT-F-353)
detection and measurement of, design of spectrometer telescope for, 20: 11123(T)
detection and measurement at 3 to 14 Mev, silicon surface-barrier detector for, 20: 11124(T)
momentum distribution of recoil, in high-energy jets, (T), 20: 11535
shielding against, tabulations of materials for, 20: 12265 (NP-15697(Vol.1))

COSMIC RADIATION
absorption of cosmic noise in atmosphere, use of multiple antennas for investigating, 20: 11862
composition and origin of galactic, 20: 11377
detection and measurement underground, liquid scintillator stack for, 20: 11527
effects on space vehicle materials, 20: 11520
hazards of, in space flight, 20: 10719(T) (NASA-TT-F-353, pp 3-20)
intensity modulation of generically related galactic, method of analysis for, (T), 20: 11525
intensity variations of, frequency spectra of short-period, (T), 20: 11518(T)
intensity variations of, selective frequency filters for diurnal, 20: 11519(T)
intensity variations from 1954 to 1964, sidereal component of diurnal, 20: 11524
intensity variations of, correlation with geomagnetic field 27-day variations, 20: 11818(T)
noise absorption correlations with solar flare proton flux, (E), 20: 11852

COSMIC SHOWERS
analysis of high-energy jet, (E/T), 20: 11534
kinematic analysis of high-energy, Monte Carlo test of, 20: 11533
kinematic analysis of jet, 20: 11532
model for four momentum transfers in jet, two-center, 20: 11531
models for four-momentum transfers in, multifireball, 20: 11530
nucleon momentum distributions in high-energy jet, recoil, (T), 20: 11535
theory on high-energy, review of, 20: 11529

COSMOLOGY
mass in expanding universe, (T), 20: 11873
model of universe without general relativity, (T), 20: 11874
universes in, subtraction method for gravitational mass in Einstein and de Sitter, 20: 11884

COULOMETRY
radiometric end-point determination in, 20: 10769

COUNTERCURRENT SEPARATION PROCESSES
development of liquid-foam, 20: 12526

CREATINE
radiation effects on excretion of, by man, 20: 12545(R) (PAEC(A)AR651)

CREEP
properties of ceramic materials at high temperatures, design of apparatus

for measurement of, 20: 11285 (UCRL-16434)
CRITICAL ASSEMBLIES
criticality of TWMR, (T), 20: 12465 (GA-6807)
criticality studies of uranium dioxide–water moderated, computer methods for, 20: 12418(R) (WCAP-3739)
design of Masurca, 20: 12507
development of Masurca, 20: 12419(T,R) (EURFNR-1F)
instrumentation for, development of, 20: 11061(R) (IDO-17112)
neutron diffusion in plutonium-fueled aluminum-water, thermal, (E), 20: 12396(R) (EURAEC-1505)
neutron Doppler coefficient for uranium, calculation of, 20: 11945
neutron kinetics of ATR and ETR, 20: 12498(R) (IDO-17112, pp 1-51)
neutron source experiments with, computer program for data analysis of pulsed, 20: 12355 (GAMD-6781)
CRITICALITY STUDIES
calculations for water moderated assemblies, computer, 20: 12418(R) (WCAP-3739)
neutron cross sections and thermal spectra in plutonium–uranium-water systems, 20: 12370
reactor physics calculation methods in, for fuel processing plants, 20: 10969
CRUSTACEA
strontium-90 distribution in molting crayfish, 20: 10515(R) (BNWL-122, pp 46-8)
yttrium-90 distribution in molting crayfish, 20: 10515(R) (BNWL-122, pp 46-8)
CRYOGENICS
materials for, properties and uses of titanium and tungsten carbides as, 20: 11293
system for, forced-circulation, 20: 11925
use in bubble chamber development, 20: 11141
CRYOSTATS
design for adiabatic demagnetization, 20: 12138
design for deuteron irradiation experiments in metals, 20: 11410
CRYSTAL STRUCTURE
conference, 20: 12320
CRYSTALS
bibliography on single, 20: 11276 (PAEC(A)IN-657)
dislocations in, properties of, 20: 11331
gamma resonance absorption in one- and two-dimensional, (T), 20: 12283
ion reactions with, coherent Coulomb excitation in, (T), 20: 11973 (NP-15791)
neutron resonance scattering in regular, inelastic channels in, (T), 20: 12313
proton channeling in, transverse two-dimensional model for, (T), 20: 12279 (UCRL-12311)
radiation absorption and emission by F centers in, (T), 20: 12274(R) (COO-578-18)
rare earth ion electric field parameters in, (T), 20: 12322
rare earth ion nuclear quadrupole shielding factors in, (T), 20: 12323
x-ray absorption by, corrections for, (T), 20: 12308
CURIUM
separation from americium by ion exchange, 20: 10956
CURIUM ISOTOPES Cm-242
neutron cross section of, Westcott parameters for, (T), 20: 11959 (HW-77389)
performance as space vehicle power supply, 20: 11188 (BLG-330)
production in heavy-water and pressurized-water reactors from mixed americium isotopes, 20: 12394 (BNWL-SA-472)
CURIUM ISOTOPES Cm-243
neutron cross section of, Westcott parameters for, (T), 20: 11959 (HW-77389)
CURIUM ISOTOPES Cm-244
helium ion fission at 42.8 Mev, deformation of transition-state nucleus in, (E), 20: 12077
neutron cross section of, Westcott parameters for, (T), 20: 11959 (HW-77389)
performance as space vehicle power supply, 20: 11188 (BLG-330)
production in heavy-water and pressurized-water reactors from mixed americium isotopes, 20: 12394 (BNWL-SA-472)
CYCLOALKANES
reactions with recoil tritium atoms, yields in, 20: 10933(R) (TID-22532)
CYCLOALKENES
radiolysis products of, 20: 12545(R) (PAEC(A)AR651)
CYCLOHEXANE
naphthalene emission spectra in, 20: 10854
neutron reactions (n,p) in, temperature dependence of cross sections for, (E), 20: 11938
spectra of, at 77°K, deuterium effects on infrared, 20: 10864
benzene–cyclohexane–*p*-terphenyl, excitation transfer and decay processes in radiolysis of, 20: 10927
CYCLOHEXANOL
hydrogenation of, effects of catalytic radioactivity on, 20: 10936(T) (CEA-tr-A-1855)
CYCLOHEXANONE
solvent properties for technetium, 20: 10940
CYCLOTRON RADIATION
detection and measurement, (E), 20: 12163(R) (AD-625424)
effects on CEA beam bypass operation, 20: 11385 (CEAL-TM-157)
effects on storage ring bypass in CEA, (T), 20: 11384 (CEAL-TM-156)
emission by electrons at 1,000 Mev, angular, power, and spectral distributions for, (E), 20: 11403
propagation in collisionless plasma, dispersion relations for, (E), 20: 12175 (NASA-CR-348)
CYCLOTRONS
ion path in isochronous, measurement of out-of-phase condition of, 20: 11415(P)
magnet pole shoe assembly for, 20: 11423(P)
CYSTEINE
radiosensitivity effects on *Pasteurella tularensis*, 20: 10694
reactions with sulfur-35-labeled *N*-(*N*-acetyl-4-sulfamoyl)maleimide, 20: 10937(T) (NP-tr-1323)
CYTIDYLIC ACIDS
radiation effects on template properties of polymers of, uv, 20: 10584
CYTOLOGY
radiation effects on, of cervical cancers, 20: 10741
radiation effects on, of cervical cancers, 20: 10742
CYTOPLASM
radiation effects on pH of maize, effects of dose on β, 20: 10683
radiation effects on DNA-ase activity in animal, 20: 10591
CZECHOSLOVAKIA
fallout monitoring in, 1964, 20: 11016
radiation monitoring in, 1951 to 1960, 20: 11015

D

DATA RECORDING SYSTEMS
design of fast-pulse, using tunnel diodes, 20: 11065 (SC-TM-323-62(72))
DATA TABULATIONS
energy level transition probabilities in deformed odd-A nuclei, (E/T), 20: 11951 (AE-205)
gamma buildup factors for concrete shielding, 20: 12266(T) (ORNL-tr-918)
geomagnetic and solar activity parameters for August 1965, 20: 11830
neutron transport equation for slab geometry, 20: 11933 (INR-630/IX-A/PR(Pt.2))
polarization in nucleon reactions with nuclei at 0.1 to 25 Mev, 20: 11965 (JINR-P-2426)
radiation source efficiencies and spectra, bremsstrahlung, gamma, and x, 20: 10932 (ORNL-P-1928)
samarium-149 and xenon-135 concentrations in uranium-235 fueled thermal reactors, 20: 12352 (DP-958)
shielding characteristics of materials for cosmic alpha particles and protons, 20: 12265 (NP-15697(Vol.1))
water boiling burnout conditions in 3- and 7-rod clusters, 20: 11000
wave function constants for helium isoelectronic sequence, 20: 11450 (UCRL-7842-T)
Westcott parameters for americium, curium, plutonium, and uranium isotopes, 20: 11959 (HW-77389)
DECONTAMINATION
method for, of ORNL molten-salt fluoride-volatility plant, 20: 11032 (ORNL-3891)
DEER
cesium-137 content in Alaskan caribou, moose, and reindeer, 1963 and 1964, 20: 10535(R) (BNWL-122, pp 176-80)
cesium-137 content of reindeer in Alaska, 1965, 20: 10723
strontium-90 content in Alaskan caribou, moose, and reindeer, 1963 and 1964, 20: 10535(R) (BNWL-122, pp 176-80)
DEFEROXAMINE
effects on plutonium excretion in rats, 20: 10531(R) (BNWL-122, pp 118-21)
DEHYDROGENASES
radiation effects on lactic- and malic-acid, in extracts of rat liver and spleen, x, 20: 10583
DEUTERIUM
bonding in chloroform, comparison of, with hydrogen, 20: 10819
deuteron reactions (d,n) with, use in studies of neutron-deuteron interactions, 20: 11677
effects on biological systems, 20: 10509
effects on infrared spectra of cyclohexane, 20: 10864
effects on photoionization of acetylene, 20: 10867
effects on reactions of CCl_3 radicals with hydrogen, 20: 10820
effects in recoil tritium reactions, 20: 10933(R) (TID-22532)
effects on valence vibration spectra of piperidine, 20: 10863
electron density in plasma of, laser interferometer measurement of, (E), 20: 12165 (ARL-65-135)

electron scattering at 11 to 13 ev by molecular, resonances in, (E), 20: 11465
exchange and transfer in photolysis and radiolysis of deuterated propane–hydrogen sulfide mixtures, (E), 20: 10883
exchange with hydrogen in hydrated cobalt(II) chlorides, effect of Neel temperature on, 20: 10853
heating of plasma of, direct-discharge current for turbulent, (E), 20: 12183(T) (ORNL-tr-868)
hyperfine separation of, determination using hydrogen maser, (E), 20: 11481
incorporation in alcoholates by exchange, 20: 10850
incorporation in ethane, effects on vapor pressure from, 20: 10866
magnetic field in theta-pinch plasma of, laser determination of, (E), 20: 12164 (ARL-65-129)
meson (K^-) capture by, Y^* production in, (T), 20: 11599
molecular vibrational relaxation in shock tubes, Schlieren method for, 20: 11785
nuclear polarization in solid, method for, 20: 12104
proton reactions (p,γ) at 25 kev, cross sections from ($p_\mu d$) wave functions, (T), 20: 11493
proton tunneling in evolution reactions of, quantum mechanical rates for, (T), 20: 11372
radiosensitivity effects on, *Pasteurella tularensis*, 20: 10694
viscosity coefficients at −195 to +25°C, isotope effects on, (E), 20: 11461

DEUTERIUM HYDRIDES
electron scattering at 11 to 13 ev, resonances in, (E), 20: 11465
D_2–DH, surface tension of, (T), 20: 11787
DH–H_2, surface tension of, (T), 20: 11787

DEUTERIUM SYSTEMS
Ar–D_2, vibrational relaxation in shock tubes, Schlieren method for, 20: 11785
D_2–DH, surface tension of, (T), 20: 11787
D–H, analysis of elastic and reactive scattering in, 20: 11513
D_2–H_2, surface tension of, (T), 20: 11787

DEUTERON BEAMS
polarization and uses of, formalism for, (T), 20: 11570(T) (ANL-Trans-258)
use in radiotherapy, 20: 10736

DEUTERONS
coupling in heavy water, constants for quadrupole, (T), 20: 12287
effects on metals, specimen holder for investigating, 20: 11410
electromagnetic structure of, review of, (T), 20: 11579
electromagnetic structure of, $\pi\rho$ exchange effects on, (T), 20: 11651
energy spectra from (α,d) reactions with nuclei, high-spin levels from, (E), 20: 12061
interactions with nucleons, breakup, (T), 20: 11607
interactions with protons, neutron form factors from inelastic, (E), 20: 11626
interactions with gamma rays at 500 to 1000 Mev, resonance production from disintegration, (E), 20: 11631
interactions with electrons, properties of elastic, (E), 20: 11644
interactions with electrons, disintegration spectrum for inelastic, (E/T), 20: 11645
interactions with electrons, scattering and rescattering corrections for inelastic, (T), 20: 11646
interactions with electrons, neutron electromagnetic structure from, (T), 20: 11666
interactions with mesons (K^-) below 300 Mev/c, effects of $\bar{K}^0$–K^- and n-p mass differences on, (T), 20: 11630
potential calculations for, optical model, 20: 11570(T) (ANL-Trans-258)
reactions (d,α) and (d,p) with aluminum-27 at 1.5 to 3 Mev, direct effect and evaporation mechanism in, (E/T), 20: 12018
reactions (d,n) with deuterium, use in studies of neutron-deuteron interactions, (E), 20: 11677
reactions (d,n) with carbon-12 at 2.8 to 4.2 Mev, cross sections and polarization in, (E), 20: 12044
reactions (d,n) with beryllium-9, exchange stripping amplitudes of, (T), 20: 12126
reactions (d,p) and (d,t) with thallium-203 and thallium-205, (E), 20: 12112
reactions (d,p) with light nuclei at 200 to 350 kev, proton angular distributions in, (E), 20: 12096
reactions (d,p) with neon-22, lifetime of neon-23 1.02-Mev level from, (E), 20: 12060
reactions (d,p) with boron-11 at 1.10, 2.44, and 2.80 Mev, recoil nucleus polarization in, (E), 20: 12107
reactions (d,p) with cadmium-111, cross sections for, (E), 20: 12109
reactions (d,p) with oxygen-17 at 10 Mev, oxygen-18 energy levels from, (E), 20: 12055
reactions with tritium, spin coupling to neutron–helium-4 reaction channels, (T), 20: 11978 (UCRL-7961-T)
scattering by cadmium, differential cross sections for elastic, (E), 20: 12109
scattering by nuclei at 7.8 Mev, cross sections and optical model parameters for elastic, (E/T), 20: 12095

DIDO REACTORS
experimental facilities of FRJ-2, cold neutron beam tube, 20: 12503(T) (AERE-Trans-1042)

DIET
calcium content of rat, effects on uptake of calcium-45 and strontium-90, 20: 10549
calcium uptake from, by trout, tracer study, 20: 10555
cesium-137 content in sheep, effects on content in rumen, 20: 10520(R) (BNWL-122, pp 64-6)
cesium-137 content of Alaskan, effects of caribou meat on, 20: 10723
iodine content of cattle, effects on iodine-131 content of milk, 20: 10530(R) (BNWL-122, pp 113-17)
iodine-131 content of cattle, effects on content in milk, 20: 10530(R) (BNWL-122, pp 113-17)
phosphorus content of rat, effects on uptake of calcium-45 and strontium-90, 20: 10549
radioactivity in forage, effects on browsing animals, 20: 11011(R) (BNWL-122, pp 181-3)
radioactivity of Alaskan, effects of caribou meat on, 20: 10718(R) (BNWL-122, pp 172-5)
radiosensitivity effects on tadpole tissues, 20: 10676
strontium uptake from, by trout, tracer study, 20: 10555

DIFFERENTIAL EQUATIONS
solution of Bethe-Salpeter equation, Fredholm method for, (T), 20: 11757
solution of nonlinear, computer program for, 20: 11946
solution of partial, method for, 20: 11206 (TID-22529)
solutions of polynomial, stability of, (T), 20: 12538 (LA-DC-6803)

DIFFUSERS
installation in Big Rock Point reactor vessel, 20: 12450

DIODES
fabrication and performance of germanium p-i-n, for gamma spectrometers, 20: 11095 (CRGP-1224)
of cesium photoionization in, by solar radiation, (T), 20: 11549
radiation effects on gallium arsenide laser, gamma, (E), 20: 11178

DIRECT ENERGY CONVERSION DEVICES
bibliography, 20: 12421
materials for, review of, 20: 12421

DISASTERS
data review on AEC nuclear, for 1964, 20: 11051

DISEASES
incidence of, in Hiroshima population exposed to atomic bomb, 1961 survey, 20: 10661
radiography of epileptic, effects on blood vessels, liver, and spleen of Thorotrast, 20: 10680
tracer techniques for studying tropical intestinal, 20: 10566

DISKS
hydromagnetic flow against rotating, equations for, 20: 11778

DISTILLATION APPARATUS
design for cadmium separation from bismuth–lead eutectic, 20: 10762 (IS-T-71)

DOGS
distribution of inhaled cerium-144 oxide particles in, 20: 10513(R) (BNWL-122, pp 16-20)
distribution of inhaled praseodymium-144 oxide particles in, 20: 10513(R) (BNWL-122, pp 16-20)
distribution of inhaled ruthenium-106 oxide particles in, 20: 10513(R) (BNWL-122, pp 16-20)
distribution of inhaled rhodium-106 oxide particles in, 20: 10513(R) (BNWL-122, pp 16-20)
effects of inhaled cerium-144 oxide particles in, pathological, 20: 10513(R) (BNWL-122, pp 16-20)
effects of inhaled praseodymium-144 oxide particles in, pathological, 20: 10513(R) (BNWL-122, pp 16-20)
effects of inhaled ruthenium-106 oxide particles in, pathological, 20: 10513(R) (BNWL-122, pp 16-20)
effects of inhaled rhodium-106 oxide particles in, pathological, 20: 10513(R) (BNWL-122, pp 16-20)
effects of inhaled plutonium-239 oxide particles on, pathological, 20: 10596(R) (BNWL-122, pp 1-15)
excretion of inhaled cerium-144 by, effects of DTPA, 20: 10533(R) (BNWL-122, pp 125-7)
excretion of inhaled praseodymium by, effects of DTPA, 20: 10533(R) (BNWL-122, pp 125-7)
lead-210 biological half-life in, 20: 10544
polonium-210 biological half-life in, 20: 10544
proton distribution in phantoms of, 20: 10605(T) (NASA-TT-F-353, pp 21-54)
radiation effects on blood coagulation in, effects of stimulating vestibular analyzer on, 20: 10682
radiation effects on, protective effects of chemical compounds against,

20: 10699(T) (NASA-TT-F-353, pp 210-38)
radiation effects on, effects of bone marrow preserved with DMSO and low temperature on γ, 20: 10706
radiation effects on cholinesterase activity in serum of, effects of fractionated doses on proton, 20: 10592
radiation effects on leukocytic reaction to adrenaline in, 20: 10594
radiation effects on, multipledose energy proton, 20: 10606(T) (NASA-TT-F-353, pp 55-102)
radiation effects on, single-dose high-energy proton, 20: 10607(T) (NASA-TT-F-353, pp 103-41)
radiation effects on, comparison of RBE of gamma, proton, and x-ray, 20: 10612(T) (NASA-TT-F-353, pp 194-209)
radiation effects on eyes of, after fetal exposure, effects of age on x, 20: 10675
radiation effects on, protective effects of MEA against, 20: 10714
radiation effects on vestibular apparatus in, gamma, proton, and x-ray, 20: 10610(T) (NASA-TT-F-353, pp 157-84)
radiation effects on, RBE of proton and x-ray, 20: 10611(T) (NASA-TT-F-353, pp 185-93)

DOMINIC OPERATION
electron flux from Starfish burst, 20: 11840

DOSIMETERS
bibliography on chemical, photographic, and solid state, 20: 11027 (AED-C-21-03)
book: *Applied Dosimetry*, 20: 11058(T)
design of glass, for thermal neutrons, 20: 11168(P)
development of glass, 20: 12545(R) (PAEC(A)AR651)
development of in-pile, 20: 11144
development of in-pile, 20: 11146
development of in-pile, 20: 11147
development of in-pile, 20: 11148
development of in-pile, 20: 11149
development of in-pile, 20: 11151
development of in-pile, 20: 11152
development of solid-state, for fast neutrons, 20: 11094(R) (COO-1226-10)
development of thermoluminescent, 20: 11041
electrode design for small, 20: 11164(P)
evaluation of, for high-energy synchrocyclotron protons, 20: 10605(T) (NASA-TT-F-353, pp 21-54)
holder for fluoroglass-rod, 20: 11160(P)
performance of in-pile, conference on, 20: 11110 (STI/DOC/10/46)
performance of organic scintillator, for pulsed gamma radiation, 20: 11137
performance of photoluminescent and thermoluminescent, for medical uses, 20: 11155
performance of spherical-cavity, for neutrons, (T), 20: 11135
response of photographic-film, 20: 11136
sensitivity of neutron foil, 20: 11119
use of in-pile, status in Canada, 20: 11145
use of phosphate–glass photoluminescent, 20: 11140

DOUBLE BONDS
saturation in aqueous solution radiolysis, effects of chemical species on, 20: 10875

DOUNREAY FAST REACTOR
design, 20: 12433
fuel irradiation testing in, plutonium carbide–uranium carbide, 20: 12442

DROSOPHILA
radiation effects on reversion of white-ivory mutant in, x, 20: 10693
radiation effects on mortality in larvae of, gamma and/or tritiated thymidine, 20: 10602 (CNAEM-32)
radiation effects on mating activity of male, x, 20: 10644

DRUGS
analysis for trace elements that determine source of manufacture, activation, 20: 10880
biochemical effects of, tracer studies, 20: 10509
biotransformation of, tracer studies, 20: 10509
leukemia induction by cancer chemotherapeutic, 20: 10647
preparation of iodine-131-iodothiazide, 20: 10732
preparation of labeled, for experimental uses, 20: 10509
radiosensitivity effects of antimetabolite, Methotrexate, on HeLa cells in culture, 20: 10664
use for therapy of hyperthyroidism, 20: 10738

DYES
radiation effects from radium or sulfur-35 on sorption of, by barium sulfate, 20: 10936(T) (CEA-tr-A-1855)

DYSPROSIUM
magnetic properties, 20: 11340
metallography of, specimen preparation for, 20: 11310
solvent properties for tantalum, thermodynamics of, 20: 11306
vapor pressure at 850 to 1075°C, 20: 11226

DYSPROSIUM ALLOYS
Al–Dy, crystal structure of intermetallic compound $DyAl_3$ in, 20: 11305
Cd–Dy–Hg, phase studies, 20: 11317
Dy–Re, phase studies, 20: 11298

DYSPROSIUM CARBONATES
complexes of, composition in solution of, 20: 10824

DYSPROSIUM CHLORIDES
crystal field of hydrated, 20: 10860

DYSPROSIUM ETHYL SULFATES
dysprosium-161 Mössbauer effect in, electronic shielding parameters from, (E), 20: 12302

DYSPROSIUM IONS
spectra of trivalent, in hydrated chloride lattices, 20: 10860
spin-lattice relaxation in magnesium lanthanum nitrates, (E), 20: 12300

DYSPROSIUM ISOTOPES Dy-158
energy levels from terbium-158 decay, lifetime of 2⁺ rotational, (E), 20: 12082

DYSPROSIUM ISOTOPES Dy-160
energy levels in, lifetime of 86.8 kev, (E), 20: 12082

DYSPROSIUM ISOTOPES Dy-161
Mössbauer effect in dysprosium ethyl sulfate, electronic shielding parameters from, (E), 20: 12302

DYSPROSIUM ISOTOPES Dy-162
energy levels, (E), 20: 12149

DYSPROSIUM ISOTOPES Dy-165
use in radiotherapy of versenate-incorporated, 20: 10737

DYSPROSIUM NITRATES
nitrogen-14 NMR in, (E), 20: 12325

DYSPROSIUM OXIDES
CaO–Dy_2O_3, phase diagrams, 20: 10822

DYSPROSIUM SELENIDES
CaSe–Dy_2Se_3, phase studies, 20: 10857

E

EARTH
satellite orbits about, general relativity tests by precession of, (T), 20: 11883

ECOLOGY
diversity problems in plant communities, 20: 10511 (BNL-9836)
effects of precipitation and temperature on plant communities, 20: 10510 (BNL-9835)
mineral cycling in aquatic ecosystems, role of vascular hydrophytes in, 20: 12543(R) (NYO-3018-12)
radiation protection standards in, 20: 11039

EGGS
radiation effects on *Aëdes aegypti*, x, 20: 10692
radiation effects on production of, by chickens, x, 20: 10626

ELASTOMERS
radiation effects on, 20: 11181

ELECTRIC ARCS
ion heating in, (E/T), 20: 11770 (ORNL-P-1005)

ELECTRIC CHARGES
Coulomb potential of, Green's function for, (T), 20: 11446 (NP-15794)

ELECTRIC CONDENSERS
magnetohydrodynamics for ideal, basic concept of general relativistic, (T), 20: 11772

ELECTRIC CURRENTS
effects of direct-discharge on plasma turbulent heating, (E), 20: 12183(T) (ORNL-tr-868)
production of large pulse, using parallel avalanche transistors, 20: 11067 (UCRL-12095-T)

ELECTRIC DISCHARGE
book: *Electrical Coronas: Their Basic Physical Mechanisms*, 20: 11806
diagnostics in cold-cathode Penning, using Langmuir floating double probes, (E), 20: 12259
initiation of h-f rare-gas, in longitudinal magnetic field, (E/T), 20: 11780
plasma stability in oscillating, (T), 20: 12193
plasma stability in low-pressure arc, (E), 20: 12204(T)
properties of, in MHD cells, (E/T), 20: 11541 (AERE-R-5107)
theories for vacuum, review of, 20: 11769 (LGI-65/30)
transverse magnetic field effects on vacuum, (E), 20: 11769 (LGI-65/30)
use in radiation detectors, 20: 11163(P)

ELECTRIC FIELDS
charged-particle Brownian motion in fluids in crossed magnetic and, (T), 20: 11802
charged-particle interactions in magnetospheric, (T), 20: 11849
effects on low-frequency oscillations in inhomogeneous plasma, 20: 12220
effects on migration of strontium-89 in soil, 20: 11053
effects on radiolysis of 2-pentanone and 3-pentanone, 20: 10895
effects on superconductors, accelerated energy and matter currents from, 20: 11919
intensity in disturbed quasineutral plasma, (T), 20: 12191
plasma ionization rate in d-c, weakly ionized, (E), 20: 12169 (JUL-322-PP)

ELECTRIC INSULATORS
voids in, effects on magnet coil performance, 20: 11387 (CONF-650922-28)
ELECTRIC PROBES
characteristics of Langmuir double, in streaming plasma, 20: 12186
effects on particle distributions in weakly ionized rarefied plasma, (T), 20: 12201(T)
theory for a-c resonance, relation to scattering resonances in plasma, 20: 12241
use in polar ionosphere diagnostics, evaluation of, 20: 11844
use of impedance, for ionospheric charged-particle density measurements, 20: 11847
use of Langmuir floating, double plasma diagnostics for, 20: 12259
use of r-f impedance, in ionospheric profile determinations, 20: 11846
use of r-f standing wave impedance, for ionospheric electron density measurements, 20: 11845
ELECTRODES
design of insulated, for small dosimeters, 20: 11164(P)
development of collector, for thermionic cells, 20: 11540(R) (AD-626444)
ELECTROMAGNETIC FIELDS
atom polarization in strong, (T), 20: 11510
charged-particle acceleration in, mechanisms of, (T), 20: 11837
conservation laws for, generalized, 20: 11722
Einstein-Maxwell null equations for, 20: 11881
interactions with two-level atoms, model for, 20: 11470
plasma skin effect in sinusoidally varying, (T), 20: 12170 (LRP-18-65)
statistical theory of, phase-space distribution function in, 20: 11880
ELECTROMAGNETIC LENSES
design for neutrino beam facility of 200-Bev proton synchrotron, (T), 20: 11398 (UCID-1008)
ELECTROMAGNETIC PUMPS
review of, for thermionic space reactors, 20: 12481
ELECTROMAGNETIC WAVES
absorption in inhomogeneous plasma, Cherenkov electron, (T), 20: 12214
amplification in decaying plasma, (T), 20: 12210
beam decomposition of polarized plane, on separation plane between absorbing media, (T), 20: 11368
emission from solar flares, 20: 11438
interactions with electrons, (T), 20: 12163(R) (AD-625424)
propagation in auroral zone atmosphere, proton gyro-frequency radiation mechanism for, (E/T), 20: 11860
propagation in fully ionized unbounded plasma, in magnetic field, (T), 20: 12188
propagation in infinite plasma, kinetic theory of, 20: 12212
propagation in ionized diffusing plasma, 20: 12254
propagation of transverse, in plasma, (T), 20: 12163(R) (AD-625424)
scattering by density and temperature fluctuations in, (T), 20: 12253
scattering by plasma column, drift velocity effect in, (E/T), 20: 12242
scattering resonances in plasma, a-c resonant probe relation to, (T), 20: 12241
trajectories in ionized toroids, (T), 20: 11370(T)
transmission by plasma in magnetic fields, 20: 12258
ELECTROMAGNETISM
geometrization and complex space-time in, (T), 20: 11875
ELECTRON BEAMS
effects on aerated aqueous potassium bromide solutions, kinetics of, 20: 10912
effects on aqueous solutions of amino acids, peptides, and proteins, 20: 10919
effects on aqueous solutions of carbohydrates, 20: 10920
effects on aqueous solutions of ethylene oxide polymer–thiourea, 20: 10921
effects on aqueous solutions of cupric ions, kinetic studies of, 20: 10923
effects on aqueous solutions of thiocyanate ions, 20: 10915
effects on aqueous solutions of nucleic acids and related substances, 20: 10917
effects on aqueous solutions of glycine, other amino acids, and peptides, 20: 10918
effects on aqueous solutions, uv-absorption peaks from, 20: 10924
effects on carbon precipitation in alpha-iron, 20: 11227
effects on deaerated solutions of carboxyl-containing solutes, kinetic studies of, 20: 10913
effects on hematopoiesis in rats, 20: 10681
effects on liquid ammonia, 20: 10910
effects on metallic ion–permanganate solutions, 20: 10914
effects on mixtures of benzene–carbon tetrachloride, 20: 10928
effects on n- and p-type silicon, transient, (E), 20: 11176(R) (NP-15835)
effects on oxygen-saturated neutral solutions of potassium bromide, kinetics of, 20: 10911
effects on solutions of silver ions, kinetic studies of, 20: 10922
effects on solution of methylene blue, kinetic studies of, 20: 10925
energy of, performance of instruments for measuring, 20: 11389 (DESY-65/12)
focusing in accelerating magnetic fields, (T), 20: 11399 (UCRL-7566 (Rev.1))
focusing of partially neutralized relativistic, self-, (E), 20: 11402
interaction with ion-cyclotron waves in cold plasma, (T), 20: 12203
interaction with laser beams at high energies, energy spectra and polarization from Compton, (T), 20: 11667
interactions with hot plasma at low frequency, macroscopic theory for, 20: 12189
monitoring of linear accelerator, profile, 20: 11407
production for irradiation facilities, 20: 11416(P)
production of large-diameter, low-voltage, (E), 20: 11367 (D1-82-0448)
production of, techniques and equipment for, 20: 10907
radiolysis using, survey of, 20: 10908
reactions with lithium ions at 75.6 to 800 ev, cross sections for single ionization in, (E), 20: 11489
reactions with sodium and potassium ions to 1 kev, cross sections for single ionization in, (E), 20: 11490
trajectories in bending magnet systems, space-charge effects on, (T), 20: 11378 (AD-626633)
use of pulsed, to determine rate constants for hydroxyl radical reaction with organic compounds, 20: 10916
uses for strengthening metals and alloys, 20: 11366
ELECTRON MULTIPLIER TUBES
design of, for time-of-flight mass spectrometers, 20: 10791
ELECTRON PAIRS
production in meson (ρ^0), (ω), and (ϕ) decay, branching ratios for, (E), 20: 11673
ELECTRON SOURCES
development of low-voltage, (E), 20: 11367 (D1-82-0448)
ELECTRON TUBES
plasma rotation in inverted ion magnetron, 20: 12194
ELECTRONIC EQUIPMENT
performance in pulsed radiation environment, qualification procedure for, 20: 11180
radiation effects on microcircuits for space, 20: 11179
ELECTRONS
absorption of secondary, in electron beam apparatus, 20: 11418(P)
acceleration at earth's bow shock front, (T), 20: 11437
acceleration in transition region beyond magnetosphere, Fermi, (T), 20: 11522
acceleration of, design of traveling-wave device for, 20: 11419(P)
capture by alpha particles in air, (T), 20: 11457(T) (LA-tr-65-29)
decay of trapped, in gamma-irradiated biphenyl and 3-methylpentane, 20: 10886
density and collision frequency in ionospheric F region, during auroral absorption event, (E), 20: 11848
density in high temperature plasma, laser interferometer measurement of, (E), 20: 12165 (ARL-65-135)
density in ionospheric F2 polar region, irregularities in, (E), 20: 11845
density in plasma, effects on electromagnetic wave propagation, 20: 12254
density profiles in ionospheric D region, 20: 11846
detection and measurement of ~5-kev, equipment for, 20: 11153
distribution in nonthermal radio stars, effects on energy spectra of, (T), 20: 11427
effects of solvated, on methylene blue in pulse-radiolysis, 20: 10925
effects of 3-Mev, on microelectronic circuitry, 20: 11179
effects on aqueous oxygenated solutions, 20: 10909
effects on carbon tetrafluoride, ESR spectrum of oxygen fluorides from, 20: 10882
effects on electric properties of germanium, 20: 11350(R) (NP-15611, pp 39-46)
effects on germanium, homogeneity measurements from, 20: 11361
effects on heat-transfer surfaces and terphenyls, design of loops for studying, 20: 10871 (EUR-2288.f)
effects on monocrystals at 1.5 Mev, electron resonance studies of, at 20 to 300°K, 20: 10876
effects on p-i-n junction detectors, pulsed and steady-state, 20: 11173 (D2-84071-1)
effects on photoconductivity of silicon, (E), 20: 11351(R) (NP-15611, pp 48-89)
effects on silicon transistors, 20: 11182
effects on silicon, energy and orientation dependence of damage from, 20: 11364
effects on sulfate solutions of benzene, 20: 10878
electromagnetic self-energy and wave function renormalization constant for, (T), 20: 11867 (NP-15762)
emission from argon-ion reactions with iron, secondary, (E), 20: 11462
energy absorption in inhomogeneous plasma, (T), 20: 12214
energy and intensity in Van Allen belt, 20: 11840
energy and intensity distributions of, from Starfish explosion, 20: 11840
energy and pitch angle distributions for auroral-zone, (E), 20: 11854
energy in plasma, double probe method for measuring, 20: 12186

energy spectra in ionosphere during auroral storms, spectrometer for measuring, 20: 11853
energy spectra in ionosphere, spectrometer for measuring, 20: 11157
flux of stably trapped, in magnetosphere, (T), 20: 11820
heating in magnetic mirror machines, cyclotron, (T), 20: 12163(R) (AD-625424)
heating in magnetic mirrors, turbulent, (E), 20: 12206(T)
interactions in metals at low energy, cross section for free, (T), 20: 12284
interactions in plasma, effect on longitudinal dielectric constant, (T), 20: 12217
interactions of, bremsstrahlung production from, (T), 20: 11670
interactions with protons, radiative corrections for, (T), 20: 11556 (DESY-65/14)
interactions with positrons, invariance violations in, (T), 20: 11582(T)
interactions with protons, quantum electrodynamic theory for, 20: 11593
interactions with protons at 1.0 to 6.0 Bev, absolute cross sections and electromagnetic form factors from elastic, (E), 20: 11625
interactions with deuterons, neutron form factors from inelastic, (E), 20: 11626
interactions with protons at 5.0 Bev, heavy electron productions from, (E), 20: 11629
interactions with nucleons, cross sections for, (T), 20: 11636
interactions with deuterons, properties of elastic, (E), 20: 11644
interactions with deuterons, disintegration spectrum for inelastic, (E/T), 20: 11645
interactions with deuterons, scattering and rescattering corrections for inelastic, (T), 20: 11646
interactions with deuterons, neutron electromagnetic structure from, (T), 20: 11666
interactions with electromagnetic waves, (T), 20: 12163(R) (AD-625424)
interactions with positrons, photon angular correlations for momentum distribution of annihilation, 20: 11377
light scattering by, in plasma, (T), 20: 12255
mass of, electromagnetic and electrostatic, (T), 20: 11454 (UCRL-12233)
motion in electromagnetic and gravitational fields, scalar formulation of ideal, 20: 11798
photon absorption in field of argon atom cross section for, (T), 20: 11478
precipitation in auroral regions, absorption events from, (E/T), 20: 11861
precipitation in ionosphere, correlations with geomagnetic storms, (E), 20: 11851
precipitation in ionosphere, auroral absorption height from rate of, (E), 20: 11864
production in helium-atom and -ion scattering by molecules, 20: 11447(R) (TID-22476)
production of heavy, in electron-proton interactions at 5.0 Bev, (E), 20: 11629
properties of fast ionospheric, (E), 20: 11850
reactions (e,e'p) with beryllium-9, lithium-8 energy levels from, (E), 20: 11988
reactions in atmosphere, ionization from, (T), 20: 11857
reactions in ionosphere, direct ionization from, (T), 20: 11858
reactions of hydrated, with amino acids, peptides, and proteins, 20: 10919
reactions of hydrated, in radiolysis of aqueous solutions of silver ions, 20: 10922
reactions of hydrated, with water in pulse radiolysis, 20: 10894
reactions of hydrated, with nucleic acids and related substances, 20: 10917
reactions of hydrated, with glycine, other amino acids, and peptides, 20: 10918
reactions of hydrated, in radiolysis of aqueous ethylene oxide polymer–thiourea, 20: 10921
reactions of hydrated, with D-glucose, 20: 10920
reactions with atoms, binary-encounter collision theory for, 20: 11483
reactions with cadmium, tellurium, and zinc, ionization cross sections for, 20: 10885
reactions with cesium atoms, probability of, (E), 20: 11443(R) (NASA-CR-54790)
reactions with cesium atoms, probability of, (E), 20: 11444 (NASA-CR-54790(App. 1))
reactions with germanium at 6 to 50 Mev, defect lifetime and trapping from, 20: 11349(R) (NP-15611, pp 28-38)
reactions with heavy deformed nuclei at high energy, dipole-giant resonances from, (T), 20: 12015
reactions with oxygen-doped germanium at 48 Mev, infrared spectroscopy of, 20: 11348(R) (NP-15611, pp 19-27)
reactions with rare gas atoms, metastable excitation in, (E), 20: 11455 (UCRL-14450)
reactions with silicon at 45 Mev, analysis of infrared absorption bands from, 20: 11347(R) (NP-15611, pp 5-18)
scattering by argon, nitrogen, and oxygen at low energies, model for elastic, (T), 20: 11495
scattering by atoms, core term in exchange amplitude for, (T), 20: 11473
scattering by atoms at low energies, free-electron wave functions for, (T), 20: 11495
scattering by atoms at low energies, exchange effects on, (T), 20: 11500
scattering by atoms, Fredholm equations for resonance potential, (T), 20: 11508
scattering by atoms and ions, quantum mechanical theories for, 20: 11511
scattering by carbon-12 and oxygen-16, giant resonances in inelastic, (T), 20: 12029
scattering by deuterium, deuterium hydrides, and hydrogen at 11 to 13 ev, resonances in, (E), 20: 11465
scattering by heavy atoms, relativistic Hartree approximation for, (T), 20: 11507
scattering by homonuclear diatomic molecules at low energies, method for prediction of, (T), 20: 11495
scattering by hydrogen at 13.7 to 50.7 ev, energy-loss spectra and excitation cross sections for, (E), 20: 11466
scattering by hydrogen ground state, variational principle for elastic exchange, (T), 20: 11505
scattering by hydrogen, Fredholm equations for resonance, (T), 20: 11508
scattering by lithium, polarization potentials for, (T), 20: 11487
scattering by nuclei, elastic, (T), 20: 12100
scattering by polyethylene, proton electromagnetic form factors from elastic, (E), 20: 11567 (LAL-1144)
scattering by polyethylene, proton electric and magnetic form factors from elastic, (E), 20: 11628
scattering by spherical nuclei, for detection of E2 surface resonances, (T), 20: 12024
scattering by titanium at 53 Mev, cross sections and nuclear radius from, (E), 20: 12033
solvation in liquid ammonia pulse radiolysis, kinetics of, 20: 10910
synchrotron radiation emission from 1,000 Mev, (E), 20: 11403
temperature in cesium thermionic converters, pressure and spacing effects on, (E), 20: 11544 (LA-DC-7390)
temperature of conjugate-point photo-, in ionospheric F-region, 20: 11828
theory of, Lamiltonian formulation of Dirac, 20: 11882
trapping of low-energy, in dark magnetosphere, 20: 11823
velocity distribution from magnetic mirror machine, system for measuring, 20: 12163(R) (AD-625424)
velocity in photomultiplier tubes, gas lasers for measuring time-of-flight, 20: 11071

ELECTROPHORESIS
behavior of chromium-51-labeled albumins in, 20: 10944
radiation effects on patterns of mouse serum protein, β, 20: 10581

ELECTROSTATIC ANALYZERS
use for plasma measurements, errors in, 20: 12223

ELECTROSTATIC FIELDS
use for deflection of charged-particle beams, engineering drawings of equipment for, 20: 11413

ELECTROSTATIC GENERATORS
beam focusing power of tube for, with high output, (T), 20: 11405

ELECTROSTATIC LENSES
design of, engineering drawings for, 20: 11413

ELEMENTARY PARTICLES
coupling constants of, sum rules for weak axial-vector, (T), 20: 11612
decay of spin-1, vertex function for spin-0 particle emission in, (T), 20: 11737
field theories for composite and bootstrap, (T), 20: 11754
field theory for, Lehmann-Symanzik-Zimmermann formalism in, 20: 11716
interactions of spin ½, formulation of S-matrix theory for, 20: 11695
interactions of, asymptotic phase and amplitude for modified Coulomb potential in, (T), 20: 11689 (LA-DC-6912)
interactions of, Aitchison equation for final-state, (T), 20: 12016
interactions of, bootstrap method and Regge poles for, (T), 20: 11694
interactions of, Bethe-Salpeter equation for dynamics of strong, (T), 20: 11746
interactions of, baryon loops for vector-vector-pseudoscalar, (T), 20: 11752
interactions of, C and T invariance in electromagnetic, (T), 20: 11582(T)
interactions of, Cutkosky rule for analytical properties of Euclidean amplitudes for, 20: 11687 (JINR-P-2485)
interactions of, dispersion relations for maximum strengths of, (T), 20: 11738
interactions of, review of bootstrap theory for, (T), 20: 11705
interactions of, Reggeized bootstraps for, (T), 20: 11751
interactions of, R-matrix for three-body, (T), 20: 11691 (ORNL-3914)
interactions of, solubility of partial-wave dispersion relations for, 20: 11699
interactions of, sum rules in potential, 20: 11739
interactions of, SU(n) generalized crossing matrices for, (T), 20: 11740
interactions of, SU(3) vector coupling coefficients for, (T), 20: 11741

interactions of, Schwinger variational principle for, (T), 20: 11747
interactions of, solution of Bethe-Salpeter equation for, 20: 11757
isospin and spin in S-matrix theory for, 20: 11720
kinematics of, calculation from track photographs, 20: 11100 (JINR-P-2467)
mass renormalization in broken SL(6) symmetry for, 20: 11734
mass shell corrections in current algebra calculations, (T), 20: 11613
model for arbitrary spin, in curved spaces, covariant, 20: 11759
model for, infinitesimal generators of Poincaré group for zero-mass representations in, 20: 11702
parity and spin of, nondynamical methods for determining, (T), 20: 11611
production of, angular momentum conservation in statistical model for multiple, (T), 20: 11698
scattering amplitudes for, singularities in three-body, (T), 20: 11701
scattering by nucleons in nuclei, (T), 20: 12100
scattering of, nonunique solutions for nonrelativistic, 20: 11763
symmetries, (T), 20: 11688 (JPL-TR-32-797)
symmetries for Goldstone theorem for, (T), 20: 11679 (CONF-650927-21)
symmetries for, S-matrix formulation from relativistic combination of internal and spin, (T), 20: 11755
symmetries of, Casimir operators of Lie groups for, (T), 20: 11609
symmetries of, infinite order Lie group for coupling of intrinsic and space-time, (T), 20: 11704
symmetry for, current renormalization in $\bar{W}_3$, (T), 20: 11610
symmetry for, degenerate representations for compact and noncompact rotation groups in, (T), 20: 11682 (IC/65/89)
symmetry for, isotopic space and complex conjugation in U(3), 20: 11725
symmetry for, mass formula and classification schemes from SU(4) and SU(8), (T), 20: 11753
symmetry for, SL(6,c), (T), 20: 11680 (IC/65/84)
symmetry for, sum rules from photoproduction processes in SU(6), 20: 11635
symmetry for, unitary representations and relativistic coupling constants in SL(2,C), 20: 11737
symmetry for, Wigner operators for SU(3), 20: 11721
symmetry groups for, noncompact extensions of, (T), 20: 11681 (IC/65/85)
symmetry groups for, Casimir operators for SU(n) and U(n), (T), 20: 11690 (NP-15764)
symmetry operators for, representation of discrete, (T), 20: 11713
theory for equivalence between composite and, 20: 11728
theory of strongly interacting, 20: 11665
theory of, Born reciprocity principle in space-time, 20: 11718
theory of, complex Minkowski space formalism of space-time, 20: 11719

ELEMENTS
determination of trace, in heart muscle, activation, 20: 10869
determination of trace, in drugs for identification of manufacturer, activation, 20: 10880
metabolism of trace, effects of radiodermatitis in rabbits, 20: 10625
performance as shielding for cosmic alpha particles and protons, 20: 12265 (NP-15697(Vol.1))
photoelectric cross sections of heavy, method for measuring, 20: 11516

ELK RIVER POWER REACTOR
operation review, 20: 12448

EMBRYOS
radioinduced dominant lethals in rat, proton and x-ray, 20: 10609(T) (NASA-TT-F-353, pp 151-6)

ENGINEERING TEST REACTOR
coolant flow in, transients in, 20: 12498(R) (IDO-17112, pp 1-51)

ENZYMES
labeling with tritium, 20: 10945
radiation effects on activity of, in mice, 20: 12545(R) (PAEC(A)AR651)
radiation effects on activity of phosphoglucomutase and pyrophosphorilase, in rat liver, x, 20: 10590
radiation effects on aspartate–2-oxoglutarate-aminotransferase, in rat CNS and skeletal muscle, effects of age on x, 20: 10593
radiation effects on activity of lenticular epithelial, in rabbits, x, 20: 10630

EPITHELIUM
radiation effects on corneal, in mice, 20: 10608(T) (NASA-TT-F-353, pp 142-50)
radiation effects on enzymes of lenticular, x, 20: 10630
radiation effects on tadpole corneal, effects of starvation during irradiation on x, 20: 10676

ERBIUM
electron structure of, analysis using positron annihilation, (E), 20: 11323
magnetic properties, 20: 11340
metallography of, specimen preparation for, 20: 11310
performance of cathodes of, in diode ion pumps, 20: 10976 (IS-T-46)
solvent properties for tantalum, thermodynamics of, 20: 11306

ERBIUM ALLOYS
Al–Er–Gd, crystal structure of intermetallic compound $(Gd_xEr_{1-x})Al_3$ in, 20: 11305
Al–Er–Y, crystal structure of intermetallic compound $(Y_xEr_{1-x})Al_3$ in, 20: 11305
Er–Re, phase studies, 20: 11298

ERBIUM CARBONATES
complexes of, composition in solution of, 20: 10824

ERBIUM CHLORIDES
crystal field of hydrated, 20: 10860

ERBIUM IONS
spectra of trivalent, in hydrated chloride lattices, 20: 10860
spin-lattice relaxation of trivalent, in lanthanum chlorides, (E), 20: 12292
spin-lattice relaxation in yttrium ethyl sulfates, (E), 20: 12300
spin-lattice relaxation in lanthanum ethyl sulfates, (E), 20: 12300

ERBIUM SELENIDES
CaSe–Er_2Se_3, phase studies, 20: 10857

ERYTHROCYTES
radiation effects on membranes of, in newborn rats, 20: 10589
radiation effects on human, 20: 10660
radiation on content in mice, β, 20: 10641

ERYTHROPOIESIS
production of erythropoietic factor by kidney, 20: 10635
radiation effects on rat, 20: 10709

ESTERS
reactions with hydroxyl radicals, rate constants for, 20: 10916

ETHANE
diffusion in lithium, potassium, and sodium forms of Linde A zeolite, steric effects in, 20: 12532 (COO-920-8)
vapor pressures of deuterated, 20: 10866

ETHANE, 1,2-DICHLORO-
effects on carbon dioxide–graphite reactions at 960 to 1200°C, 20: 10859

ETHANE, HEXAFLUORO-
Ar–C_2F_6, energy transfer in gamma radiolysis of, 20: 10884
C_2F_6–Kr, energy transfer in gamma radiolysis of, 20: 10884
C_2F_6–Ne, energy transfer in gamma radiolysis of, 20: 10884
C_2F_6–Xe, energy transfer in gamma radiolysis of, 20: 10884
He–C_2F_6, energy transfer in gamma radiolysis of, 20: 10884

ETHANE, NITRO-
photolysis of, effects of cupric oxide on, 20: 10874
radiolysis of, mechanisms of gamma, 20: 10874

ETHANETHIOL, 2-AMINO-
hydrochloride, effects on serum transaminase activity in mice, 20: 12545(R) (PAEC(A)AR651)
pharmaceutical effects in animals, 20: 10714
radiosensitivity effects on *Pasteurella tularensis*, 20: 10694
radiosensitivity effects in animals, 20: 10714
radiosensitivity effects on ascorbic acid metabolism in rats, 20: 10715

ETHENETETRACARBONITRILE
complexes with azulene, naphthalene, and perylene, effects of pressure on properties of, 20: 12534 (COO-1198-216)

ETHER, BIS(2-BUTOXYETHYL)
solvent properties for nitrosylruthenium nitrato and nitro complexes, 20: 10947 (AERE-R-4786)

ETHYLAMINE, 2,2'-DITHIOBIS-
effects in combination with amygdalin on radiosensitivity of dogs and rats, 20: 10699(T) (NASA-TT-F-353, pp 210-38)
effects on radiosensitivity of dogs and rats, 20: 10699(T) (NASA-TT-F-353, pp 210-38)
protective effects of, against radiation injuries in mice, 20: 10708
radiosensitivity effects on ascorbic acid metabolism in rats, 20: 10715
uptake by mouse thymus cells, tracer study, 20: 10708

ETHYLENE
ethylene–ethylene polymer, performance of spherical-cavity neutron dosimeters of, (T), 20: 11135

ETHYLENE, CHLORO- POLYMERS
radiation effects on electric and physical properties of, gamma and neutron, 20: 11344 (N65-35361)

ETHYLENE OXIDE POLYMERS
radiolysis of aqueous solution of, with and without thiourea additive, 20: 10921

ETHYLENE POLYMERS
electron elastic scattering by, proton electromagnetic form factors from, (E), 20: 11567 (LAL-1144)
electron elastic scattering by, proton electric and magnetic form factors from, (E), 20: 11628
neutron scattering by stretch-oriented, frequency limit of stretch-bend acoustic mode from, 20: 10865
radiolysis of, decay of vinyl unsaturation during, 20: 10893
ethylene–ethylene polymer, performance of spherical-cavity neutron dosimeters of, (T), 20: 11135

ETHYLENE, TETRAFLUORO- POLYMERS
positronium lifetime in irradiated, effects of free radicals on, 20: 10905
radiation effects on electric and physical properties of, gamma and

neutron, 20: 11344 (N65-35361)
ETHYLENEDIAMINE
thermal capacity of aqueous solutions of, use of calorimeter for measuring, 20: 12550 (TID-22564)
EUROPIUM
determination of radioactive, by electrophoresis, use of EDTA in, 20: 10792
magnetic properties, 20: 11340
separation from aqueous solutions by solvent extraction using acetylacetone derivatives, 20: 10951
separation from other cations by partition chromatography, tracer studies of, 20: 10960
separation from uranium by reversed-phase partition chromatography, 20: 10784
EUROPIUM ALLOYS
Cd–Eu, phase studies, 20: 11327
Eu–Ag, phase studies, 20: 11327
Eu–In, phase studies, 20: 11327
EUROPIUM CARBONATES
complexes of, composition in solution of, 20: 10824
EUROPIUM COMPLEXES
dipyridyl, fluorescence of, effects of methyl group on, 20: 10842
EUROPIUM COMPOUNDS
fluorescence of diketonates, effects of solvents and temperature on, 20: 10844
EUROPIUM HYDROXIDE OXIDES
crystal structure, 20: 10817
EUROPIUM IONS
electron paramagnetic resonance of divalent, in cadmium fluoride and potassium chloride, (E), 20: 12321
EUROPIUM ISOTOPES Eu-146
decay of, samarium-146 energy levels at 1381 kev from, (E), 20: 12081
EUROPIUM ISOTOPES Eu-153
oxygen-ion reactions at 35 Mev, lifetime of rotational levels from, (E), 20: 12020
EXHAUST SYSTEMS
design, 20: 11050
EXPERIMENTAL BREEDER REACTOR-II
design, 20: 12433
fuel control and management for, 20: 12452
fuel cycle facility operation for, 20: 10965
fuel fabrication for, review of, 20: 11241 (TID-8541, pp 71-148)
steam pressure control system for, 20: 12438
EXPERIMENTAL GAS COOLED REACTOR
building complex for, specifications for, 20: 12445
building complex for, engineering drawings of, 20: 12444
containment failure in, inspection of expansion bellows, 20: 12411 (ORNL-TM-1380)
EXPLOSIVES
tests on spray-deposited and light-initiated silver acetylide–silver nitrate, 20: 10814 (SCL-DC-65-96)
EXPONENTIAL PILES
neutron decay constants in water-moderated plutonium–uranium dioxide, (E), 20: 12397(R) (EURAEC-1506)
spectral indices of 4.29% enriched uranium metal, (E), 20: 12358 (LA-3406)
EXTRACTION APPARATUS
development of countercurrent liquid-foam, 20: 12526
EYES
radiation effects on corneal metabolism in rabbit, β, 20: 10585
radiation effects on lenticular epithelial enzymes of rabbit, x, 20: 10630
radiation effects on, after therapy of bulbar cavity tumor, 20: 10667
radiation effects on dog, exposed during fetal stages, 20: 10675
radiation effects on corneal epithelia in mice, 126-Mev proton, 20: 10608(T) (NASA-TT-F-353, pp 142-50)

F

FALLOUT
analysis for fission products in, 1964, 20: 11018
contamination of forage plants by, effects of elevation, precipitation, and season on, 20: 11011(R) (BNWL-122, pp 181-3)
content in German milk, effects of precipitation on, 20: 11017
content in German rye and wheat, effects of precipitation on, 20: 11017
distribution in water above dam, 1963, 20: 11055
monitoring in Alaska, 1963 and 1964, 20: 10535(R) (BNWL-122, pp 176-80)
monitoring in Alaska, 1964, 20: 10718(R) (BNWL-122, pp 172-5)
monitoring in atmosphere, criteria for, 20: 11043
monitoring in Czechoslovakia, 1964, 20: 11016
monitoring in Great Britain, 1964, 20: 11018
monitoring in Washington, 1963 and 1964, 20: 11011(R) (BNWL-122, pp 181-3)
monitoring in Washington, 1961 through 1964, 20: 11012(R) (BNWL-122, pp 184-6)
surface water contamination by, hazards to man from, 20: 11021
FAST REACTORS
coolants for, comparison of carbon dioxide, helium, sodium, and steam, 20: 12345
core design and safety analyses of large power breeders, 20: 12439
criticality calculations for hollow cylindrical thermionic, 20: 12485
design of 1000-Mw(e) sodium-cooled breeder, 20: 12402 (KFK-369)
design of 1000-Mw(e) sodium-cooled, 20: 12433
design of 350-Mw(e) sodium-cooled BN-350 power breeder, 20: 12441
design parameters for thermionic space, 20: 12483
design study for 1000-Mw(e) power-breeder, 20: 12414 (TID-22545, pp 16-52)
development, 20: 12419(T,R) (EURFNR-1F)
development in Great Britain, review of, 20: 12427
development in U. S., review, 20: 12336
development of Phenix, 20: 12423
development of, conference on, 20: 12328 (ANS-100(Suppl.))
fuel development for power breeders, 20: 12407 (NEIC-RR-13)
fuel element temperature distributions in 350-Mw(e) sodium-cooled BN-350 power breeder, 20: 12443
heat transfer in thermionic, calculation for heat-pipe, 20: 12489
kinetics equations for periodically pulsed, computer program for solution of, 20: 12395 (EUR-2552.e)
neutron dynamics in, computer program for solution of equations for, 20: 11946
neutron resonance self-shielding in, effective cross section for, (T), 20: 12374
properties of thermionic, for space power, 20: 12478
safety analyses for large sodium-cooled, 20: 12433
temperature distribution in thermionic, for space, 20: 12486
FATIGUE
modes in reactor cooling system pipes, 20: 12338(R) (GEAP-4911)
testing of irradiated materials at cryogenic temperatures, in-pile loop design for, 20: 11345(R) (NASA-CR-54787)
FATS
accumulation in rat liver, effects of neptunium-237 on, 20: 10522(R) (BNWL-122, pp 79-80)
FATTY ACIDS
radiation effects on content of, in rat liver, 20: 10659
FEEDBACK SYSTEMS
design for motor speed control, 20: 11073
FERMI FAST BREEDER REACTOR
control rod drop tests in, 20: 12387 (APDA-NTS-3)
design, 20: 12433
reactivity with calculations for, 20: 12388 (APDA-NTS-6)
FERMIONS
interactions in attractive potential, energies and wavefunctions for, (T), 20: 11714
interactions in many-body systems of, method of correlated basis functions for, (T), 20: 11492
interactions of systems of, quantum field theoretical methods for, 20: 11375(T)
interactions of, binary collision expansion of double-time-temperature-dependent Green's functions for, (T), 20: 11760
interactions with bosons, functional methods in quantum field theory and quantum statistics for, (T), 20: 11731
model with unstable V-type particle for, solution for Lee, (T), 20: 11745
superconductivity in degenerate gas of, suppression of Cooper pairing in, (T), 20: 11923
thermodynamic evolution equation for quantum statistical, 20: 11789
FETUSES
iodine-131 uptake by sheep, effects of stable iodine on, 20: 10516(R) (BNWL-122, pp 49-51)
radiation effects on rat, pathological, x, 20: 10616
radiation effects on lipid content in brain of developing guinea pig, x, 20: 10636
radiation effects on dog eyes, effects of age at exposure on x, 20: 10675
FFAG ACCELERATORS
beam current measurement of 100-Mev electron, monitor for, 20: 11392 (NP-15275)
magnet coils of, variable shunt design for, 20: 11388 (CONF-650922-29)
magnetic field calculations for 100-Mev electron, 20: 11391 (NP-15274)
FIBRINOGEN
radiation effects on content in man of, beta, 20: 10679
FIELD THEORY
Bethe-Salpeter equation in, Fredholm method for solving, 20: 11757
book: *Quantum Field Theoretical Methods in Statistical Physics*, 20: 11375(T)
Bose-Einstein operator translations in quantum, discrete, 20: 11717
boson-fermion interactions in, functional methods in quantum statistics and quantum, (T), 20: 11731

conservation laws for mossless free fields in, generalized, 20: 11722
dispersion relations for maximum interaction strengths in, 20: 11738
Euclidean amplitudes in quantum, Cutkosky rule for analytical properties of, 20: 11687 (JINR-P-2485)
Feynman diagrams in m-dimensional Lorentz space, reduction of one-loop, 20: 11723
field elimination from langrangian for bootstrap, (T), 20: 11754
field interactions in, spin-1 vector, (T), 20: 11733
formalism for particles of arbitrary spin in curved spaces, covariant, 20: 11759
formalism of quantum, with degenerate vacuum state and symmetry, 20: 11715
gauge transformations and complex space-time for classical, 20: 11373
Lee model in, Lehmann-Symanzik-Zimmermann formalism in, 20: 11716
matrix elements in renormalizable and nonrenormalizable, 20: 11708
matrix elements in renormalizable and nonrenormalizable quantum, 20: 11707
momentum-space analyticity properties of Bergman-Weil integral in, 20: 11726
quantum, equations in axiomatic formulation of, 20: 11765
Regge poles in Froissart-Gribov continuation, unitary conditions for, 20: 11724
scattering amplitude in local, restriction on forward, (T), 20: 11697
space-time quantization for free-fields in, complex, 20: 11709
symmetry operators for Dirac and Klein-Gordon fields, representation of discrete, 20: 11713

FILMS
preparation of isotope radiation-target, using vacuum evaporation-condensation, 20: 11183 (ORNL-P-1900)
superconducting transition temperature of superposed, (T), 20: 11908
surface density of, determination of, from x-ray production cross sections, 20: 11281 (UCRL-12107)

FILTERS
design of air, for industrial use, 20: 11056
use of air, in nuclear plants, 20: 11056

FINNED TUBES
radiation from rectangular-fin, 20: 12480

FIRES
effects on tinplate cans, for radioisotope containment, 20: 11028 (AERE-M-1664)
hazards from, in nuclear attack, secondary, 20: 11031 (NP-15708)

FISH
aquarium design and construction for, bibliography on, 20: 12554 (UCRL-14473)
cesium-137 metabolism in rainbow trout, 20: 10521(R) (BNWL-122, pp 73-4)
effects of Hanford reactor effluent on growth of salmon, 20: 10538(R) (BNWL-122, pp 198-201)
effects of zinc-65 on, chronic ingestion in trout, 20: 10528(R) (BNWL-122, pp 101-6)
phosphorus-32 content in salmon reared in Hanford reactor effluent, 20: 10538(R) (BNWL-122, pp 198-201)
radioactivity of ocean, effects of sea water contamination on, 20: 11054
uptake of calcium from diet and water by trout, tracer study, 20: 10555
uptake of strontium from diet and water by trout, tracer study, 20: 10555
zinc-65 content in salmon reared in Hanford reactor effluent, 20: 10538(R) (BNWL-122, pp 198-201)

FISSION
mass division in, (T), 20: 12117
theory of, using Markov process, 20: 12116

FISSION CHAMBERS
neutron cadmium cut-off energies for, in cylindrical geometry, (T), 20: 11131

FISSION FRAGMENTS
angular distribution anisotropy ratios from helium-ion induced fission of $Z \geq 90$ nuclei at 42.8 Mev, (E), 20: 12077
effects on dimension of ceramic materials, 20: 11227
ejection and re-ejection by, dynamic equilibrium of uranium, 20: 11224
energy and mass distributions from californium-252 spontaneous and uranium-235 thermal-neutron fission, (E), 20: 12076

FISSION PRODUCTS
activity in irradiated MITR fuel elements, 20: 10764 (MITNE-64)
activity of, effects on waste incorporation into asphalt, 20: 12517(R) (BNWL-170)
analysis for hydrogen peroxide, iodine-129, and metals by controlled-potential coulometry, 20: 10758 (EUR-2618.f)
analysis in urania pellets, electron microprobe, 20: 11365
analysis of uranium-233 and -235, 20: 11960(R) (IDO-14667)
buildup in SNAP-10A core during orbit, predicted, (T), 20: 12466 (NAA-SR-11642)
determination in irradiated MITR fuel elements by gamma spectroscopy, 20: 10764 (MITNE-64)
diffusion from crystals, equations for effects of crystal geometry on gaseous, 20: 11227
diffusion from simulated solid wastes, 20: 12517(R) (BNWL-170)
diffusion from uranium monocarbide at 900 to 2100°C, gaseous, 20: 11224
diffusion from urania, mechanisms of temperature-dependent gaseous, 20: 11224
diffusion in chromium–iron alloys, effects of concentrations on, 20: 11212(R) (BMI-X-10143)
diffusion in chromium–iron–nickel alloys, effects of concentrations on, 20: 11212(R) (BMI-X-10143)
diffusion in iron–nickel alloys, effects of concentrations on, 20: 11212(R) (BMI-X-10143)
diffusion in thoria–urania compacts, effects of stress on gaseous, 20: 11224
diffusion in urania, relation between grain growth and gaseous, 20: 11224
diffusion in urania, effects of stress on gaseous, 20: 11224
distribution in tissues of, biological model and computer analysis of kinetics, 20: 10519(R) (BNWL-122, pp 59-63)
injection into space from Starfish explosion, analysis of Cosmos-5 data on, 20: 11832
release in LOFT, sampling and analysis of, 20: 12356 (IDO-17128)
separation from uranium by reversed-phase partition chromatography, 20: 10784
separation from wastes, processes for, 20: 12524
separation of technetium from, by solvent extraction, 20: 10940
solubility and drip temperature in Purex process wastes, effects of rare metals on, 20: 12517(R) (BNWL-170)
yields from uranium-233 and -235 thermal fission, (E), 20: 11960(R) (IDO-14667)
yields in fast neutron, fission of uranium-238, fine structure in mass distribution of, (E), 20: 12121

FISSIONABLE MATERIAL
handling of, book on, 20: 12407 (NEIC-RR-13)

FLAMES
oxyacetylene, burner design and performance for atomic absorption spectroscopy using, 20: 10761 (IS-T-69)

FLOWMETERS
design and calibration of, for measuring gaseous chlorine trifluoride flow, 20: 11059 (BLG-345)
design of neutron radiometric, 20: 11080(P)

FLUID FLOW
critical heat flux for 19-rod bundle in forced convection boiling, 20: 10994 (TID-22539)
electric-field distribution in isotropic MHD, with alternating conductivity, 20: 11803
equations of relativistic inductive charged, 20: 11781
friction coefficients for slurry, in pipes, 20: i0998
hydrodynamic equations for radiative, derivation of, (T), 20: 11766 (AWRE-O-52/65)
in supercritical steam-cooled reactors, 20: 12416 (TID-22545, pp 67-80)
magnetic field convective diffusion in, laboratory simulation for astrophysics, (T), 20: 11431
magnetohydrodynamic equations for small-velocity in weak fields, (T), 20: 11776
magnetohydrodynamic, velocity in spherical envelope, (T), 20: 11777
magnetohydrodynamic, model for rotational, 20: 11783(T)
magnetohydrodynamic, plane, (T), 20: 11791
magnetohydrodynamic inviscid, near stagnation point, 20: 11795
magnetohydrodynamic, in atmosphere, (T), 20: 11808(T)
model for predicting, in porous media, (T), 20: 10997(T) (AERE-Trans-1038)
phenomena in bubbly, in straight pipes, (T), 20: 10991 (NYO-3114-12)
turbulence in conducting incompressible MHD, damping of homogeneous, (T), 20: 11804
two-phase hydrogen and nitrogen, in straight circular tube, 20: 10996 (WANL-TNR-154)

FLUID FLOW (LAMINAR)
magnetohydrodynamic, integral methods for, 20: 11792
magnetohydrodynamic boundary layer in, (T), 20: 11790
models of segmented, for packed-bed longitudinal dispersion, 20: 10995 (UCRL-10696(Rev.)(Pt.1))

FLUID FLOW (TURBULENT)
heat transfer in conducting channel, effects of transverse magnetic field on convective, 20: 11793

FLUID PROPELLANTS
valve development for space propulsion systems, 20: 11007(R) (NP-15831)

FLUIDIZATION
fluid flow in packed-bed longitudinal dispersion, model for segmented laminar, 20: 10995 (UCRL-10696(Rev.)(Pt.1))

FLUIDS
charged-particle Brownian motion in, in crossed fields, (T), 20: 11802
critical point for, coexistence curve near, (T), 20: 11921
droplet formation in one-dimensional, (T), 20: 11800

equations of relativistic inductive charged, 20: 11781
magnetohydrodynamic model for rotating, 20: 11783(T)
phases in one-dimensional classical, (T), 20: 11799
thermodynamics of relativistic charged, with electromagnetic induction and thermal exchange, (T), 20: 11782
FLUORANIL
complexes with 3,8-diaminopyrene and tetramethylphenylenediamine, effects of pressure on properties of, 20: 12534 (COO-1198-216)
FLUORIDE VOLATILITY PROCESSES
corrosive effects on ORNL pilot plant for, 20: 10965
plant for processing irradiated uranium–zirconium alloy fuel, decontamination of ORNL, 20: 11032 (ORNL-3891)
FLUORINE
reactions with uranium tetrafluoride, 20: 10852
FLUORINE IONS
energy levels of, (T), 20: 11450 (UCRL-7842-T)
FLUORINE ISOTOPES F-18
distribution in EVESR coolant and moderator, 20: 12399(R) (GEAP-4941)
energy levels, (E), 20: 12061
energy levels from helium-3 reactions (He-3,$p\gamma$) with oxygen-16 at 3.6 to 4.0 Mev, spins of, 20: 12025
FLUORINE ISOTOPES F-19
alpha reactions (α,n) at 2.4 to 5.5 Mev, excitation function for, (E), 20: 12143
energy levels from oxygen-19 beta decay, (E/T), 20: 12054
gamma total absorption cross sections near 20 Mev, (E), 20: 12097
neutron reactions (n,p) at 14.8 Mev, cross sections for, (E), 20: 12133
FOLIC ACID
analogs, radiosensitivity effects on Escherichia coli, 20: 10648
analogs, radiosensitivity effects on bacteria, 20: 10648
radioinduced degradation of, x, 20: 10904
FOOD
analysis for phosphorus-32 by scintillation counting following solvent extraction, 20: 10772
FORMALDEHYDE POLYMERS
radiation effects on strength of, proton, 20: 10605(T) (NASA-TT-F-353, pp 21-54)
FORMATES
effects on radiolysis of aqueous solutions of methylene blue, 20: 10925
FORMIC ACID
corrosive effects on molybdenum, tungsten, and vanadium at 35, 60, and 100°C, 20: 11230 (BM-RI-6715)
corrosive effects on molybdenum, tungsten, or vanadium coupled with aluminum or copper, galvanic, 20: 11230 (BM-RI-6715)
radiolysis of deaerated aqueous solutions of, pulsed-electrons, 20: 10913
FRACTURE TESTS
development for pipes, 20: 12338(R) (GEAP-4911)
FREE RADICALS
effects on lifetime of positronium in irradiated Teflon, 20: 10905
formation in radiolysis of styrene-grafted cellulose, 20: 10873
radioinduced in tissue homogenates, γ, 20: 10577
reactions of CCl_3, with deuterium and hydrogen, 20: 10820
yields from radiolysis of carbon tetrachloride in methanol, 20: 10879
FRENCH REACTORS
design of Harmonie and Masurca, 20: 12507
development of Phenix, 20: 12423
FROGS
radiation effects on nitrogen excretion by isolated liver of, γ, 20: 10551
radiation effects on tissues in tadpole, effects of starvation during irradiation on x, 20: 10676
FRUITS
radiation effects on mango, gamma, 20: 12545(R) (PAEC(A)AR651)
radiation processing of sweet cherries, effects of, on storage life, 20: 11186
FUMARIC ACID
radiolysis of aqueous solutions of, gamma, 20: 10875
FUNGI
radiosensitivity of, effects of tobacco leaf extract on x, 20: 10620
FUSED SALTS
equilibria in, use of thermodynamics for calculating chemical, 20: 10807 (EUR-2466.e, pp 39-57)
ion mobilities in, review on, 20: 10806 (EUR-2466.e, pp 31-8)
ion transfer in, model of, 20: 10805 (EUR-2466.e, pp 21-30)
ion transfer in, review on, 20: 10808 (EUR-2466.e, pp 59-80)
properties of, conference on, 20: 10803 (EUR-2466.e)
thermodynamic properties of, review on, 20: 10808 (EUR-2466.e, pp 59-80)

G

GADOLINIUM
electron interaction effects in films of, superimposed on superconducting lead films, (E), 20: 11918
magnetic properties, 20: 11340
meson (μ^-) capture by, isotope effects on K x-ray emission from, (E), 20: 11480
metallography of, specimen preparation for, 20: 11310
separation from other elements by solvent extraction using TBP, 20: 10952
solvent properties for tantalum, thermodynamics of, 20: 11306
vapor pressure at 1120 to 1310°C, 20: 11226
GADOLINIUM ALLOYS
Al–Er–Gd, crystal structure of intermetallic compound $(Gd_xEr_{1-x})Al_3$ in, 20: 11305
Ce–Gd, magnetic properties of, effects of composition and temperature on, 20: 11341
Co–Gd, crystal structure of intermetallic compound $GdCo_3$ in, 20: 11308
Gd–Fe, crystal structure of intermetallic compound $GdFe_3$ in, 20: 11308
Gd–Fe, magnetic properties of, effects of composition and temperature on, 20: 11341
Gd–Ni, crystal structure of intermetallic compound $GdNi_3$ in, 20: 11308
Gd–Pb, electron interaction effects in films of, superimposed on superconducting lead films, (E), 20: 11918
Gd–Re, phase studies, 20: 11298
Gd–Y, magnetic properties of, effects of composition and temperature on, 20: 11341
GADOLINIUM CARBIDES
GdC_2–UC_2, phase studies, 20: 11224
GADOLINIUM CARBONATES
complexes of, composition in solution of, 20: 10824
GADOLINIUM CHLORIDES
spectra of hydrated, 20: 10860
GADOLINIUM IONS
use of trivalent, as probe in crystal field studies, 20: 10860
GADOLINIUM ISOTOPES Gd-155
meson (μ^-) capture by, K x-ray emission from, (E), 20: 11480
GADOLINIUM ISOTOPES Gd-156
neutron absorption cross sections at 0.025 ev, (E), 20: 11987
GADOLINIUM ISOTOPES Gd-158
energy levels from terbium-158 decay, lifetime of 2^+ rotational, (E), 20: 12082
GADOLINIUM ISOTOPES Gd-160
meson (μ^-) capture by, K x-ray emission from, (E), 20: 11480
GADOLINIUM MOLYBDATES
crystal structure, 20: 10858
GADOLINIUM NITRATES
nitrogen-14 NMR in, (E), 20: 12425
GADOLINIUM OXIDES
use as neutron absorber in glasses, 20: 12273(P)
GADOLINIUM SELENIDES
CaSe–Gd_2Se_3, phase studies, 20: 10857
GALLIUM ALLOYS
Al–Ga–Pu, tensile properties and thermal expansion of delta-stabilized plutonium-base, 20: 11224
Ce–Ga–Pu, tensile properties and thermal expansion of delta-stabilized plutonium-base, 20: 11224
Ga–Pu, stability of delta-phase, effects of aluminum, cerium, or zinc additions on, 20: 11224
Ga–Pu, strength at −32 to 500°C, effects of iron impurities on, 20: 11224
Ga–Pu–Zn, tensile properties and thermal expansion of delta-stabilized plutonium-base, 20: 11224
GALLIUM ARSENIDES
radiation effects on laser diode of, gamma, 20: 11178
GALLIUM ISOTOPES Ga-69
energy levels of, resonances in proton reactions (p,p) and (p,n) with zinc-68 as isobaric analog, (E), 20: 12079
neutron activation cross section at 24 kev, (E), 20: 12135
GALLIUM ISOTOPES Ga-71
neutrino reactions (ν,e$^-$) with, detection of solar neutrinos by, (T), 20: 11537
neutron activation cross section at 24 kev, (E), 20: 12135
GAMMA CAMERAS
light pipe thickness optimization, (T), 20: 11079
GAMMA DECAY
laser beam effects on, (E/T), 20: 12102
GAMMA RADIATION
absorption by nuclei at 20 Mev, total cross sections for, (E), 20: 12097
absorption cross section for detection of E2 surface resonances in spherical nuclei, (T), 20: 12024
absorption in one- and two-dimensional crystals, resonance, (T), 20: 12283
angular correlations from neodymium-149 decay, (E), 20: 12080
angular distribution from iron-56 (n,n'γ) reactions, (E), 20: 12108
attenuation in concrete, iron, lead, and uranium, (T), 20: 12264 (MLM-1315)

detection and measurement of, from Indiana soils, 20: 11019
detection and measurement of, in Indiana precipitation, 20: 11020
detection and measurement in geological surveys, scintillation detector for, 20: 11087 (AE-203)
detection and measurement of, from internally-deposited isotopes, performance of *in vivo* thermoluminescent detector for, 20: 11091(R) (BNWL-122, pp 67-72)
detection and measurement using scintillation detector, statistical analysis of pulse-height distribution, 20: 11201 (NYO-3136-2)
detection and measurement using scintillation detector, statistical analysis of pulse-height distribution, 20: 11203(R) (NYO-3136-2, App. 2)
detection and measurement of, using scintillation detector, statistical analysis of pulse-height distribution, 20: 11204(R) (NYO-3136-2, App. 3)
detection and measurement of, from cesium-137 deposited in man, whole-body, 20: 10723
detection and measurement of, efficiency of sodium iodide scintillation crystals for, 20: 11127
detection and measurement of, design of liquid scintillation counter for, 20: 11128
detection of, design of plastic scintillator with imbedded metal foil for, 20: 11165(P)
detection of, scintillation properties of polyphenyls for, (E), 20: 11129
dose buildup factors for air and water, calculation of, (T), 20: 12261 (AFRRI-TM-65-2)
dose to personnel from accidental cesium-137 exposure, 20: 10721
dosimetry in event of accident at Savannah River Plant, equipment and methods for, 20: 11029 (DP-1006)
dosimetry of in-pile, conference on, 20: 11110 (STI/DOC/10/46)
dosimetry of in-pile, status in Canada, 20: 11145
dosimetry of in-pile, status in France, 20: 11146
dosimetry of pulsed, using organic scintillator, 20: 11137
effects of therapeutic doses on skin, protective effects of sulfur and glutathione, 20: 10702
effects of, combined with surgery on brain tumors, 20: 10575
effects on ammonolysis of coconut oil, 20: 12545(R) (PAEC(A)AR651)
effects on animal cells in culture, single and fractionated doses, 20: 10649
effects on aqueous fumaric acid, 20: 10875
effects on auditory tissues after hemangioma therapy, 20: 10687
effects on bacteria in Gulf oysters, 20: 10690
effects on beans and rice, 20: 12545(R) (PAEC(A)AR651)
effects on benzene–chlorine mixtures, hexachlorocyclohexane production by, 20: 10900
effects on biphenyl and 3-methylpentane at −196°C, 20: 10886
effects on carcinomas of cervix, therapeutic, 20: 10727
effects on carcinoma of cervix during pregnancy, 20: 10751
effects on cervical cancers of, from radium implants, 20: 10739
effects on cervical carcinomas, histological evaluation of, 20: 10749
effects on cholinesterase activity of biological specimens, effects of purity on, 20: 10586
effects on crystals of alkali metal nitrates under pressure at 77, 300, and 400°K, 20: 10891
effects on deuterated propane–hydrogen sulfide mixtures, (E), 20: 10883
effects on development and growth of maize following seed exposure, 20: 10613(T) (NP-tr-1344)
effects on DNA synthesis in HeLa cells, 20: 10588
effects on dogs and rats, protective effects of chemical compounds against, 20: 10699(T) (NASA-TT-F-353, pp 210-38)
effects on dogs and rats, RBE of, 20: 10612(T) (NASA-TT-F-353, pp 194-209)
effects on dogs, effects of bone marrow preserved with DMSO and low temperature on, 20: 10706
effects on electric and physical properties of polymeric materials, 20: 11344 (N65-35361)
effects on electric properties of ferroelectric materials, 20: 11352 (NP-15707)
effects on Escherichia coli, effects of folic acid analogs on, 20: 10648
effects on femurs and soft tissues in guinea pigs, 20: 10615
effects on ferroelectric methylammonium alum crystals, ESR studies on, (E), 20: 12291
effects on fluorocarbon–rare gas mixtures, energy transfer in, 20: 10884
effects on frozen solutions of carbon tetrachloride in methanol, 20: 10879
effects on gallium arsenide-laser diode electric properties, (E), 20: 11178
effects on gastrointestinal tract during chronic radiation sickness, 20: 10674
effects on grain- and vegetable-infesting insects, 20: 12545(R) (PAEC(A)AR651)
effects on grass, effects of dose rate on structural, 20: 10646
effects on heart muscle, pathological, γ, 20: 10631
effects on immune reactions in mice, 20: 10632
effects on man after accidental cesium-137 exposure, 20: 10721
effects on man, biological, 20: 10701
effects on mango ripening, 20: 12545(R) (PAEC(A)AR651)
effects on medical x-ray film, 20: 12545(R) (PAEC(A)AR651)
effects on neutron-irradiated cobalt acetylacetonate, 20: 10888
effects on nitroethane, 20: 10874
effects on nitrogen excretion by isolated frog liver, 20: 10551
effects on p-i-n junction detectors, pulsed and steady-state, 20: 11173 (D2-84071-1)
effects on p-type silicon, Hall effect measurement of, 20: 11360
effects on pharyngeal carcinomas, therapeutic, 20: 10725
effects on polyamides, 20: 10892
effects on polyethylene, 20: 10893
effects on polymerization of triallyl cyanurate, 20: 10896
effects on polymerization of acrylamide at 1 to 5000 atm and 28 to 70°C, 20: 10898
effects on polynucleotides in solid phase, 20: 10877
effects on pyrimidine compounds in aqueous solution, 20: 10899
effects on silicon transistors, 20: 11182
effects on small intestine after cervical cancer therapy, 20: 10654
effects on snails, 20: 12545(R) (PAEC(A)AR651)
effects on storage life of sweet cherries, 20: 11186
effects on sulfate solutions of benzene, 20: 10878
effects on thermoluminescence in aluminoborate glass containing lead and iron impurities, (E), 20: 12288
effects on tissues, biochemical, 20: 10577
effects on toluene, thermal-spike model for, 20: 10887
effects on vestibular apparatus in dogs and rabbits, 20: 10610(T) (NASA-TT-F-353, pp 157-84)
effects on vitamin B_{12} in meat, effects of lyophilization on γ, 20: 11185
effects on 1-bromobutane and 1-bromopentane mixtures with tin, alkyltin yields in, 20: 10870 (BMI-1753)
effects on 2-pentanone and 3-pentanone, 20: 10895
effects on, *Pasteurella tularensis*, effects of cell concentration, deuterium substitution, and radioprotective compounds on, 20: 10694
effects with and without tritiated thymidine on mortality in Drosophila larvae, 20: 10602 (CNAEM-32)
emission by samarium nuclei excited by oxygen ions, (E), 20: 12110
emission from neutron capture by aluminum, copper, and tungsten, secondary, (E), 20: 12267
emission in decay of compound nuclei, effect of spin on, (T), 20: 12048
emission in neutron inelastic scattering by lithium-7, (E), 20: 12106
interactions with deuterons at 500 to 1,000 Mev, resonance production from disintegration, (E), 20: 11631
interactions with protons, polarization of hyperons (Λ) from, (E), 20: 11676
polarization in thallium-203 energy-level transitions, circular, (T), 20: 12007
reactions (γ,n) with carbon-12 at 22 to 26 Mev, cross sections for, (E), 20: 12058
reactions (γ,p) with carbon-12 at 30 to 36 Mev, proton polarization from, (E), 20: 12105
reactions with lead, silver, and tin at 320 kev, absolute photoelectric cross sections for, (E), 20: 11496
scattering by electrons of aluminum, cadmium, carbon, and copper at 100 to 280 kev, incoherent, (E), 20: 11515
scattering by K-shell electrons of lead, samarium, and tantalum at 320 kev, incoherent, (E), 20: 11514
scattering by spherical nuclei, for detection of E2 surface resonances, (T), 20: 12024
scattering in concretes, energy and angular distributions of, 20: 12269
transmission by multilayer shielding, (T), 20: 12271
uses for strengthening metals and alloys, 20: 11366

GAMMA SHIELDING
properties of concrete, 20: 12266(T) (ORNL-tr-918)

GAMMA SOURCES
design specifications for, 20: 10980(T) (AEC-tr-6469)
preparation of low-energy, methods for, 20: 10932 (ORNL-P-1928)

GAMMA SPECTRA
analysis of pulse-height, method for, 20: 12112

GAMMA SPECTROMETERS
performance of germanium semiconductor, 20: 11134
performance of large coaxial lithium-drifted germanium, (E), 20: 11086 (AAEC/TM-299)
performance of lithium-ion-drift germanium, for irradiated fuel element analysis, 20: 10764 (MITNE-64)
performance using germanium p-i-n diodes, 20: 11095 (CRGP-1224)
radiation background of scintillation, cosmic, 20: 11132

GARNETS
rare-earth-ion fluorescent lifetimes in, 20: 12317

GAS COOLED REACTORS
coolant heat-transfer coefficients for, comparison of, 20: 12341

coolants for fast, comparison of carbon dioxide, helium, and steam, 20: 12345
design of emergency cooling systems for, 20: 12434
design optimization for, 20: 12422
development in great Britain, review of, 20: 12427
economic comparison with boiling water reactors for Dungeness B station, 20: 12432
fuel element design for, 20: 12382(P)
heat transfer in, computer program for calculating, 20: 10989 (IDO-28595(Rev.))
performance of urania elements in, 20: 11222
GAS FLOW
in electromagnetic and gravitational fields, scalar formulation of ideal charged, 20: 11798
measurement of chlorine trifluoride, design and calibration of flowmeters for, 20: 11059 (BLG-345)
GASES
diffusion of particles in, generalized equations for, (T), 20: 11369
glow discharge in impure, optical excitation in negative, (E/T), 20: 11773
nuclear spin relaxation in dilute, (T), 20: 11784
partition function for, distribution of zeros of grand, (T), 20: 11788
separation in thermal diffusion columns, shape factors for, 20: 10949 (K-1469)
shock propagation in, with discrete velocity distributions, (T), 20: 11779
superconductivity in degenerate fermion, suppression of Cooper pairing in, (T), 20: 11923
thermodynamic evolution equation for quantum statistical, 20: 11789
gas–liquid, phenomena in bubbly flow of, (T), 20: 10991 (NYO-3114-12)
GASTROINTESTINAL TRACT
cesium-137 content in rumen of sheep, effects of content in diet on, 20: 10520(R) (BNWL-122, pp 64-6)
protein loss in, use of iodine-131-labeled albumin for measuring, 20: 10567
protein loss in, use of iodine-131-labeled polyvinylpyrrolidone for measuring, 20: 10568
protein loss in, use of chromium-51-labeled albumin and copper-67-labeled ceruloplasmin for measuring, 20: 10569
radiation effects on, chronic α, β, and γ, 20: 10674
GEIGER-MUELLER TUBES
response of moving, to discrete beta sources, 20: 11089 (AERE-M-1671)
GENETICS
effects on growth in γ-irradiated newborn mice, 20: 10673
radiation effects on variability of, in maize and wheat, 20: 10603(R) (IAEA-2466-11)
radiation effects on mammalian, review, 20: 10688
radioinduced dominant lethals in rats, proton and x-ray, 20: 10609(T) (NASA-TT-F-353, pp 151-6)
GEOCHEMISTRY
Mössbauer effect for problems in, 20: 11377
reactions of hot atoms in, 20: 10933(R) (TID-22532)
GEOLOGY
evaluation of ground storage at ORNL, 20: 12518 (ORNL-TM-1327)
radiation measurements in, scintillation detector for gamma, 20: 11087 (AE-203)
GEOMAGNETIC FIELDS
charged-particle interactions in, (T), 20: 11849
configuration of transition-region, effects of polar magnetic disturbances on, (E), 20: 11827
configuration of, current systems and midlatitude transition bays, in, 20: 11824
decay and growth of polar-electrojet and ring-current, (E/T), 20: 11829
distributions at 1000, 5000, and 10,000 km, computation of, 20: 11816(T)
disturbance of, 27-day variations of, 20: 11818(T)
electron Fermi acceleration in transition region of, (T), 20: 11522
fluctuations of, spatial properties of rapid, (E), 20: 11833
intensity data for August 1965, 20: 11830
intensity index correlations with solar flare proton flux, (E), 20: 11852
intensity of epoch 1960.0 of, data for trapped-particle evaluations from, 20: 11834
measurement of, method of free nuclear precession for, 20: 11817(T)
pulsations in, properties and proposed mechanisms for micro-, 20: 11839
pulsations of, mechanism and properties of micro-, (E/T), 20: 11813(T)
structure of, statistical analysis of, (T), 20: 11814(T)
structure of, statistical analysis of world magnetic charts for, 20: 11815(T)
structures of, Störmer conditions in axially symmetric, 20: 11836
variation at high latitudes during IGY, solar-diurnal, 20: 11812(T)
variations of, correlation with auroras, 20: 11819(T)
GEOMAGNETIC STORMS
commencement of, shock wave effects on sudden, (T), 20: 11811(T)
effects on decay and growth of polar electrojets and ring currents, (E/T), 20: 11829
effects on magnetosphere tail and electron distribution in radiation belts, (E), 20: 11831
effects on structure variations of Van Allen belts, (T), 20: 11838
electron precipitation correlations with, (E), 20: 11851
occurrence during years of maximum solar activity, 20: 11810(T)
occurrence of, correlations with radio aurora, (E), 20: 11859
GERMAN REACTORS
design of 1000-Mw(e) sodium-cooled fast breeder, 20: 12402 (KFK-369)
GERMANIUM
fabrication and performance of p-i-n diodes of, for gamma spectrometers, 20: 11095 (CRGP-1224)
performance in heavy ion detectors, energy dispersion and pulse height defect in, (T), 20: 11138
performance of detectors of, in applied gamma spectrometry, 20: 11134
performance of large coaxial lithium-drifted semiconductors of, for gamma spectroscopy, (E), 20: 11086 (AAEC/TM-299)
preparation of crystal of, for use in gamma spectrometer, 20: 10764 (MITNE-64)
properties and use of diodes of, for radiation detection, 20: 11126
radiation effects on p-i-n junctions of, electron, gamma, and x, 20: 11173 (D2-84071-1)
radiation effects on electric properties of, 50-Mev electron, 20: 11350(R) (NP-15611, pp 39-46)
radiation effects on atomic displacements in, by protons at 30 Mev to 1 Bev, 20: 11356
radiation effects on, homogeneity measurements from electron, 20: 11361
radioinduced damage in, oxygen ion, 20: 11363
radioinduced defects in, lifetime and trapping from electron, 20: 11349(R) (NP-15611, pp 28-38)
radioinduced defects in oxygen-doped, infrared spectroscopy of electron, 20: 11348(R) (NP-15611, pp 19-27)
sensitive region in p-i-n detectors of, determination of width of, 20: 11102 (JINR-P-2487)
GERMANIUM ISOTOPES Ge-71
nuclear magnetic dipole moment of, (E), 20: 11476
GERMANIUM ISOTOPES Ge-73
hyperfine structure constants for $^3P_1$ and $^3P_2$ atomic states of, (E), 20: 11476
GERMANIUM OXIDES
GeO_2–La_2O_3, spectra of compounds formed in, infrared, 20: 10828
GERMANIUM OXYNITRIDES
preparation, 20: 10856
GERMANY
fallout contamination of food and milk in, 20: 11017
fallout distribution in water at dam, 1963, 20: 11055
GLASS
fabrication of neutron-absorptive, 20: 12273(P)
radiation effects on, proton, 20: 10605(T) (NASA-TT-F-353, pp 21-54)
response to gamma radiation, effects of boron on, 20: 12545(R) (PAEC(A)AR651)
thallium absorption and emission spectra in fused silica, (E), 20: 10830
use in thermal-neutron dosimeters, 20: 11168(P)
GLASS TEXTILES
radiation effects on electric and physical properties of fiber glass, gamma and neutron, 20: 11344 (N65-35361)
GLOBULIN
metabolism of gamma-, in a gamma globulinemic subjects, 20: 10572
metabolism of iodine-131-labeled gamma-, tracer study in man, 20: 10571
use of iodine-131-labeled, for determining effects of nutritional disorders on protein metabolism, 20: 10573
GLOW DISCHARGES
mixing in non-stationary, frequency dependence of a-c, 20: 11774
optical excitation in hollow cathode, (E/T), 20: 11773
GLUCOSE
content in blood, effects on appetite inhibition, 20: 10541
effects on fat accumulation induced by neptunium-237 in rat liver, 20: 10522(R) (BNWL-122, pp 79-80)
radiolysis of aqueous solutions of D-, role of hydrated electrons in, 20: 10920
uptake by hypothalamus of mice, tracer study, 20: 10541
GLUCOSE PHOSPHATES
radiation effects on content of, in rat liver, x, 20: 10590
GLUTAMIC ACID, ACETYL-L-PHENYLALANYL-L-
solvent partition between butanol–chloroform and water, 20: 10809 (EUR-2531.f)
GLUTAMIC ACID, *N*-(*p*-AMINOBENZOYL)-
radioinduced degradation of, x, 20: 10904
GLUTATHIONE
protective effects of, against radiation injuries of skin, γ, 20: 10702
GLYCEROL
radiosensitivity effects on *Pasteurella tularensis*, 20: 10694
GLYCINE

radiolysis of aqueous solutions of, reaction of hydrated electron in, 20: 10918

GLYCINE, *N*-(*p*-AMINOBENZOYL)-
radioinduced degradation of, x, 20: 10904

GLYCOGEN
radiation effects on content of, in rat adrenal glands, x, 20: 10576
radiation effects on content in rats, x, 20: 10590
radiation effects on content in brain tissues of guinea pigs, x, 20: 10638

GLYCOLYSIS
radiation effects on rabbit corneal, β, 20: 10585

GOITER
radiotherapy of, using iodine-131, 20: 10748

GOLD
dislocation climb in, efficiency of, 20: 11274 (NYO-3504-2)
light absorption by, mechanism of photographic sensitivity from, (T), 20: 11121
proton reactions with, phosphorus-32 and -33 production in, (E), 20: 12034
tin-119 in Mössbauer effect in, 20: 12315
uptake by hypothalamus of mice, tracer study, 20: 10541

GOLD ALLOYS
Au–Th, phase studies, 20: 11224

GOLD ISOTOPES Au-196
energy levels of, half life of 273-kev, (E), 20: 12151

GOLD ISOTOPES Au-197
deuteron elastic scattering at 7.8 Mev by, cross sections for, (E), 20: 12095
helium ion reactions at 33 to 40 Mev, charge and mass distributions in fission, (E), 20: 11953 (COO-347-17)
hyperfine structure, (E), 20: 11491
nuclear electric quadrupole moment, (E), 20: 11491

GOLD ISOTOPES Au-198
production at PRR, methods for, 20: 12545(R) (PAEC(A)AR651)

GOLD ISOTOPES Au-199
energy levels, (E), 20: 12137

GOLD ORES
analysis, activation, 20: 12545(R) (PAEC(A)AR651)

GONADS
iodine-131 accumulation by ovaries, 20: 10554
radiation dose to ovaries, from tracer dose of iodine-131, 20: 10554
radiation effects of mouse testicular, model for β, 20: 10640
radiosensitivity of, 20: 10747

GRAPHITE
coating with Zircaloy-2, creep-fit, 20: 12404 (NAA-SR-11160)
diffusion of thorium in pyrolytic, effects of structure on, 20: 11224
fabrication by hot isostatic pressing, 20: 11260
neutron energy spectra after fast-pulse injection in, time-dependent, (E/T), 20: 11940
oxidation by carbon dioxide at 960 to 1200°C, kinetics of, 20: 10859
particle dispersion and size distribution from explosive destruction of NERVA mockup, 20: 12471 (SC-RR-65-557)
radiation effects on thermal expansion of pyrolytic, effects of annealing on neutron, 20: 11225
radiation effects on Poisson's ratio of PGA, fast-neutron, 20: 11225
radiation effects on tensile-strain limits of, neutron, 20: 11225
radioinduced shrinking in, neutron, (E), 20: 11355
radioinduced swelling in pyrolytic, effects of annealing on neutron, 20: 11225
radioinduced swelling in, irradiated at 150 to 650°C, fast-neutron, 20: 11225
radioinduced swelling of, fission fragment, 20: 11227
reactions with hydrogen at 1550 to 2260°C, 20: 11225
reactions with steam, 20: 11225
C–graphite, thermodynamic properties to 6000°K of solid and vaporous, 20: 10799 (AD-625735)

GRAPHITE (IMPREGNATED)
performance and properties, 20: 11222

GRAPHITE COUPLES
graphite/Mg, corrosion pitting by chloride ions, 20: 11231 (CEA-R-2815)

GRAPHITE MODERATED REACTORS
design of emergency cooling systems for, 20: 12434

GRAPHITE SYSTEMS
graphite–U, neutron spectra in, for 0, 0.011, and 0.099 bucklings, 20: 12485

GRASS
growth and morphology of, after seed γ-irradiation, 20: 10646
radiation effects on germination of seed of, effects of dose rate on γ, 20: 10646

GRAVITATION
Einstein equations for, Kerr solution of, (T), 20: 11435
field theory of, Einstein-Maxwell null, 20: 11881
formalism for arbitrary-spin particles in curved spaces, covariant, 20: 11759
interactions of spin-2 field of, Einstein equations for, 20: 11871
interactions with scalar fields, Ward identity for equivalence principle from, (T), 20: 11888
mass in expanding universe, (T), 20: 11873
mass in nonquasi-rectangular coordinates, subtraction method for, 20: 11884
particle motion in field of, equations for, (T), 20: 11872
particle-cluster motion in field of, general relativity theory for, 20: 11869
plasma equilibrium in field of, boundary-layer charge in, (T), 20: 12228

GREAT BRITAIN
fallout monitoring, 1964, 20: 11018
reactor development in, review of, 20: 12427

GROUND
deposition of microspheres released from 50 km on, effects of wind on, 20: 11033 (SC-TM-65-398)

GROUND WATERS
mineral cycling in aquatic ecosystems, role of vascular hydrophytes in, 20: 12543(R) (NYO-3018-12)
radioisotope transport by, hazards of, (T), 20: 11010 (HNS-1229-61)
waste transport by, sequence for predicting, 20: 11009 (BNWL-SA-406)

GUINEA PIGS
effects on brain of guinea pig, histochemical, 20: 10638
radiation effects on femurs and soft tissues in, γ, 20: 10615
radiation effects on, protective effects of MEA against, 20: 10714
radiation effects on brain lipid content of, x, 20: 10636

H

HAFNIUM
deposition from fused salt mixtures, electro-, 20: 11260
effects of alloy additions of, on mechanical properties of niobium, 20: 11302
separation from salts by solvent extraction using 8-mercaptoquinoline in chloroform, 20: 10759 (INP-427/C)

HAFNIUM ALLOYS
Cd–Hf, crystal structure of intermetallic compounds in, 20: 11328
Hf–Nb–W–Y, development and evaluation of C-129Y, 20: 11227
Hf–Zn, crystal structure of intermetallic compounds in, 20: 11328

HAFNIUM CARBIDES
sintering of, effects of ammonium and cobalt chlorides on porosity following, 20: 11250
HfC–NbC, preparation and properties, 20: 11330
HfC–TaC, preparation and properties, 20: 11330
HfC–TiC, preparation and properties, 20: 11330
HfC–ZrC, preparation and properties, 20: 11330

HAFNIUM CHLORIDES
separation from salts by extraction chromatography using organic phosphorus compounds, 20: 10759 (INP-427/C)

HAFNIUM ISOTOPES Hf-181
energy levels in, lifetime of 619-kev, (E), 20: 12000

HAFNIUM ISOTOPES Hf-183
decay, (E), 20: 12148

HAFNIUM SYSTEMS
C–Hf–Re–Ta–W, preparation and properties of dispersion-strengthened, 20: 11217(R) (WANL-PR(Q)-007)
C–Hf–Ta–W, bonding of T-222, to Inconel 600 and types 321 and 347 stainless steels, explosive, 20: 11243(R) (WANL-PR(EE)-001)

HALDEN BOILING REACTOR
reactivity of, model for determining, (T), 20: 12400 (HPR-54)

HALIDES
solvent properties of molten, aluminum cladding, 20: 10971(P)

HALLAM POWER REACTOR
moderator element failure detection in, 20: 12449

HALOGEN COMPOUNDS
positron decay in, (E), 20: 11621

HALOGENS
production of ions of, r-f source for, 20: 11374

HALOHYDROCARBONS
positron decay in, (E), 20: 11621

HAMBURG ELECTRON SYNCHROTRON
beam energy calibration of, performance of instruments for, 20: 11389 (DESY-65/12)

HANDBOOKS AND MANUALS
descriptive cataloging guide, 20: 12548 (TID-4577(Rev.1))

HANDLING AND STORAGE
system design for reactor radioisotope, pneumatic, 20: 12350(P)

HANFORD PRODUCTION REACTORS (N)
pressurizer for, computer simulation of, 20: 12456 (HW-77921-D)
pumps for, computer simulation of injection, 20: 12455 (HW-77921-C)

HANFORD WORKS, RICHLAND, WASH.
safety program at, 20: 11046

HASTELLOY C
compatibility and encapsulation with neodymium, promethium, and samarium oxides, 20: 11267 (BNWL-SA-488)

HASTELLOY X
compatibility and encapsulation with neodymium, promethium, and samarium oxides, 20: 11267 (BNWL-SA-488)
creep rupture at 1950 and 2100°F *in vacuo*, 20: 11266 (BNWL-167)
HAYNES 25 ALLOY
compatibility and encapsulation with neodymium, promethium, and samarium oxides, 20: 11267 (BNWL-SA-488)
HEALTH PHYSICS
analysis for trace elements, activation, 20: 10869
book: *Applied Dosimetry*, 20: 11058(T)
dosimetry system for accidents at Savannah River Plant, 20: 11029 (DP-1006)
regulations for gamma defectoscopy in Bulgaria, 20: 11036(T) (JPRS-33502)
survey of accidents in USAEC facilities, 1963–64, 20: 11034 (TID-5360 (Suppl.5))
HEART
blood circulation in, tracer method for measuring, 20: 10730
effects of diphtherial toxins on muscle of, pathological, 20: 10631
microscopy of muscles of rat, 20: 10631
radiation effects on myocardium, pathological, γ, 20: 10631
radiation effects on myocardium in mouse, β, 20: 10643
radiosensitivity effects of stimulating vestibular analyzer in dog, on blood coagulation, 20: 10682
HEAT-RESISTING ALLOYS
brazing of, development of alloys for, 20: 11260
strengthening by irradiation, 20: 11366
HEAT TRANSFER
analysis for gas or liquid-cooled reactor passages, computer program for, 20: 10989 (IDO-28595(Rev.))
by 19-rod fuel elements, 20: 10994 (TID-22539)
calculation of evaporation-condensation, in tubes, 20: 12488
calculation of heat-pipe, for thermionic reactors, 20: 12489
critical heat flux for sodium in forced convection two-phase boiling, 20: 10990 (NAA-SR-11586)
effects of surface profile on, 20: 10993 (TID-22513)
from ML-1 fuel elements with boundary-layer turbulence promoters, 20: 10988 (CONF-12-5)
in boiling liquid metals, review of, 20: 10999
in reactors, computer program for, 20: 12354 (GAMD-6644(Add.))
in supercritical steam-cooled reactors, 20: 12416 (TID-22545, pp 67-80)
properties of organic-coolant, 20: 12331
radiation effects on surfaces in, design of loop for studying electron, 20: 10871(EUR-2288.f)
to hydrogen and nitrogen in straight circular tubes during chill-down, 20: 10996 (WANL-TNR-154)
HEAT TRANSFER SYSTEMS
design for simulating reactor radiant heat transfer, 20: 12487
design of cryogenic, using forced circulation of supercritical helium, 20: 11925
development for thermoionic converters, 20: 11545 (LA-DC-7555)
performance of syphon loops, for thermoelectric cells, (E/T), 20: 11543(R) (GIC-2605-3)
performance optimization for thermionic converters, 20: 11542 (EUR-2534.e)
HEAVY WATER REACTORS
control of high conversion ratio plutonium fueled, methods for, 20: 12393 (BNL-8748)
criticality calculations for, review of, 20: 12363 (TID-8541, pp 1-70)
design and technical aspects of Cirene, 20: 12424
development in Great Britain, review of, 20: 12427
neutron absorption density distributions in, calculation of thermal, (T), 20: 12365 (UJV-1438/65)
neutron flux variations in, method for calculating, (T), 20: 12366 (UJV-1439/65)
neutron kinetics of, review of, 20: 12363 (TID-8541, pp 1-70)
reactivity of boiling, model for determining, (T), 20: 12400 (HPR-54)
HELIUM
diffusion in irradiated zirconium, 20: 11227
electric discharges in C-Stellarator, particle-loss rates for, (E), 20: 12239
electron reactions with atomic, metastable excitation in, (E), 20: 11455 (UCRL-14450)
energy levels of, solution of secular equation for, (T), 20: 11451 (UCRL-7941(Rev.1))
heat transfer coefficients for, 20: 12341
helium-atom and -ion scattering by, electrons and ions from, 20: 11447(R) (TID-22476)
hydrodynamic model of liquid II, near T_λ, (T), 20: 11892 (LA-DC-6824)
ion temperature in plasma of, double probe method for measuring, 20: 12186
ion trapping by vortex lines in liquid II, negative –, (E), 20: 11903
magnetic susceptibility of, wave-function calculations of, (T), 20: 11485
model for compressed liquid II, phonon-roton, (T), 20: 11893
precipitation in aluminum–lithium alloys, mechanisms of swelling from, 20: 11224
proton scattering at 0.15 to 1 Mev, cross sections for atomic, 20: 11448(R) (TID-22480)
radioinduced scintillation of liquid, recombination luminescence in alpha, (E), 20: 11904
reactions with atoms and ions, variational calculations of long-range, (T), 20: 11504
reactions with excited rubidium atoms, cross sections for excitation transfer in, (E), 20: 11482
rotation of liquid II, near lambda point, (E), 20: 11900(T)
spectra of shock-produced plasma of, deviations from local thermal equilibrium in, (E), 20: 12226
spectral line shift in plasma of, (E), 20: 12168 (JUL-280-PP)
use of supercritical, in forced circulation heat transfer system, 20: 11925
vortex lines in liquid II, growth of pinned quantized, (T), 20: 11905
wave functions for atoms of, (T), 20: 11459
He–C_2F_6, energy transfer in gamma radiolysis of, 20: 10884
HELIUM IONS
effects on ferromagnetic resonance of iron, nickel, and iron–nickel alloys, 20: 12318
energy levels of, (T), 20: 11450 (UCRL-7842-T)
reactions with atoms and ions, variational calculations of long-range, (T), 20: 11504
reactions with gold-197 at 33 to 40 Mev, charge and mass distributions in fission, (E), 20: 11953 (COO-347-17)
reactions with neptunium-237 and plutonium-239, charge and mass distributions in fission, (E), 20: 11954 (COO-347-18)
reactions with nuclei ($Z \geq 90$) at 42.8 Mev, fission-fragment anisotropy ratios from, (E), 20: 12077
reactions with rhenium-185 and rhenium-187 at 40.9 Mev, fission, (E), 20: 11955 (COO-347-19)
scattering by di- and monatomic molecules, electrons and ions from, 20: 11447(R) (TID-22476)
spectra of, fine structure of 4686 Å line of, (T), 20: 11442 (MATT-280)
HELIUM ISOTOPES He-3
bremsstrahlung reactions (γ,π^+) at 180 to 260 Mev, cross sections for, (E), 20: 12046
effects on ferromagnetic resonance of iron, nickel, and iron–nickel alloys, 20: 12318
reactions (He-3, He-6) with oxygen-16 at 65.3 Mev, (E), 20: 12036
reactions (He-3,α) with beryllium-9 at 3 Mev, beryllium-8 level parities and spins, (E), 20: 12027
reactions (He-3, Li-6) with oxygen-16 at 65.3 Mev, (E), 20: 12036
reactions (He-3,pγ) with oxygen-16 at 3.6 to 4.0 Mev, fluorine-18 excited levels from, (E), 20: 12025
reactions (He-3,p) with calcium-40 at 12 Mev, (T), 20: 12086
reactions (He-3,p) with nuclei, distorted-wave Born approximation for, (T), 20: 12127
solubility in helium-4 at low temperatures, (E), 20: 11920
symmetry for, SU(6), 20: 11756
theory of liquid, correlated basis functions in, 20: 11492
thermal conductivity of solid, (E), 20: 11916
transmission through geomagnetic and interplanetary fields, comparison with helium-4, (E), 20: 11525
viscosity coefficients at –195 to +25°C, isotope effects on, (E), 20: 11461
He-3–He-4, thermal capacity of liquid, at low temperatures, (E), 20: 11920
He-3–He-4, thermal conductivity of solid, lattice distortion effects on, (E), 20: 11917
He-3–$MgCe(NO_3)_5$, thermal relaxation time at low temperatures, (E), 20: 11922
HELIUM ISOTOPES He-4
critical point for, coexistence curve near, (T), 20: 11921
neutron reactions with, spin coupling to deuteron-tritium reaction channels, (T), 20: 11978 (UCRL-7961-T)
nuclear reactions with, spin coupling analysis for, (T), 20: 11978 (UCRL-7961-T)
particle pair-correlation function for gas of, (T), 20: 11897
proton reactions (p,2p) at 460 Mev, (E/T), 20: 11948 (AD-624318)
solvent properties for helium-3 at low temperatures, (E), 20: 11920
thermal conductivity of solid, (E), 20: 11916
transmission through geomagnetic and interplanetary fields, comparison with helium-3, (E), 20: 11525
He-3–He-4, thermal capacity of liquid, at low temperatures, (E), 20: 11920
He-3–He-4, thermal conductivity of solid, lattice distortion effects on, (E), 20: 11917
HELIUM ISOTOPES He-5
energy levels, 20: 12023

energy of 3/2 + state, calculation of, (T), 20: 12101
HELIUM ISOTOPES He-6
energy levels, 20: 12023
HELIUM SYSTEMS
He–K, excitation transfer in first excited state of potassium, cross sections for collision-induced, (E), 20: 11499
He–Na, excitation transfer in first excited states of sodium, cross sections for collision-induced, (E), 20: 11499
HEMATOPOIETIC SYSTEM
radioinduced lesions in dogs, effects of preserved bone marrow on, 20: 10706
HEMOGLOBIN
Mössbauer effect in iron(II) and (III) compounds of iron-57-enriched rat, 20: 10903
HEPARIN
radiosensitivity effects in mice, 20: 10705
HETEROGENEOUS REACTORS
fuel burnup in, computer program for calculating, 20: 12361 (PEL-60)
neutron flux flattening in, calculation of, (T), 20: 12364 (UJV-1365/65)
1,6,10,14-HEXADECATETRAEN-3-ol, 3,7,11,15-TETRAMETHYL-
preparation and purification of tritiated, 20: 10809 (EUR-2531.f)
HEXANE
neutron moderation by, at 77 and 300°K, (E), 20: 11944
Br–hexane, radiation chemistry of, processes of bromine-81 (n,γ), 20: 10938
HIGH-ALTITUDE EXPLOSIONS
Cherenkov radiation from, in space, (T), 20: 11807 (UCRL-7495(Rev.1))
electrons from Starfish, energy and intensity distributions of, 20: 11840
fission debris from Starfish, analysis of Cosmos-5 data on, 20: 11832
HIGH ENERGY INJECTION DEVICES
plasma losses due to microinstabilities in DCX-1, hydrogen, (E), 20: 12240
HIGH TEMPERATURE GAS COOLED REACTOR EXPERIMENT
development of, review of, 20: 12427
reactivity transfer function analyzer for, performance of, 20: 12425
HIGH TEMPERATURE SEPARATION PROCESSES
flowsheets for fast breeder fuels, 20: 10965
HILSCH TUBES
velocity profile in Ranque-, tangential, 20: 10992 (RISO-116)
HIROSHIMA
atomic bomb survivors in population of, 1961 survey, 20: 10662
effects of atomic explosion on population of, 1961 survey, 20: 10661
medical survey of population of, exposed to 1945 atomic bomb, 1961, 20: 10595(R) (ABCC-60-61)
HISTOLOGY
of cancers of cervix, use in evaluation of prognosis and results of radiotherapy, 20: 10739
HOISTS
design, 20: 10983(P)
HOLMIUM
electron structure of, analysis using positron annihilation, (E), 20: 11323
magnetic properties, 20: 11340
metallography of, specimen preparation for, 20: 11310
proton reactions with, phosphorus-32 and -33 production in, (E), 20: 12034
solvent properties for tantalum, thermodynamics of, 20: 11306
HOLMIUM ALLOYS
Al–Ho, crystal structure of intermetallic compound $HoAl_3$ in, 20: 11305
Al–Ho, phase diagram of, evidence for intermetallic compounds in, 20: 11307
Ho–Re, phase studies, 20: 11298
HOLMIUM CARBONATES
complexes of, composition in solution of, 20: 10824
HOLMIUM CHLORIDES
crystal field of hydrated, 20: 10860
HOLMIUM IONS
spectra of trivalent, in hydrated chloride lattices, 20: 10860
spin-lattice relaxation of trivalent, in lanthanum chlorides, (E), 20: 12292
HOLMIUM ISOTOPES Ho-159
energy levels of, parity and spin of, (E), 20: 12017
isomeric transitions in, lifetime of E3, (E), 20: 12017
HOLMIUM ISOTOPES Ho-161
energy levels of, parity and spin of, (E), 20: 12017
isomeric transitions in, lifetime of E3, (E), 20: 12017
HOLMIUM ISOTOPES Ho-163
energy levels of, parity and spin of, (E), 20: 12017
isomeric transitions in, lifetime of E3, (E), 20: 12017
HOLMIUM ISOTOPES Ho-165
neutron reactions (n,γ) with, gamma spectra from thermal, (E), 20: 11982(T) (LA-tr-65-34)
neutron total cross section at 14 Mev, deformation effects on, (E), 20: 12089
HOLMIUM ISOTOPES Ho-166
energy levels of, excitation energies for, (E), 20: 11982(T) (LA-tr-65-34)
HOLMIUM SELENIDES
CaSe–Ho_2Se_3, phase studies, 20: 10857
HOMOGENEOUS REACTORS
criticality and neutron spectra of, computer program for, 20: 12357 (KR-75)
HORMONES
labeling with iodine-131, review of procedures for, 20: 10943
placental selectivity for protein, effects on survival of newborn of, 20: 10508
HUMBOLDT BAY POWER REACTOR
design and operation, 20: 12435
HYDRAULIC FLUIDS
radiation effects on, 20: 11181
HYDRAULICS
radiation effect on system components in, 20: 11181
HYDRAZYL, DIPHENYLPICRYL-
effects on radioinduced polymerization of triallyl, cyanurate, 20: 10896
HYDRIDES
reactions with mercury, review on, 20: 10812 (NAA-SR-Memo-11569)
HYDROAROMATIC COMPOUNDS
reactions with hydroxyl radicals, rate constants for, 20: 10916
HYDROCARBONS
reactions with recoil tritium atoms, mechanisms of, 20: 10933(R) (TID-22532)
HYDROCHLORIC ACID
corrosive effects on zirconium–platinum alloy, effects of platinum content on, 20: 11227
corrosive effects on molybdenum, tungsten, and vanadium at 35, 60, and 100°C, 20: 11230 (BM-RI-6715)
corrosive effects on vanadium-base alloys at low temperatures, 20: 11230 (BM-RI-6715)
corrosive effects on molybdenum, tungsten, or vanadium coupled with aluminum or copper, galvanic, 20: 11230 (BM-RI-6715)
reactions with Zircaloy-2 and zirconium, hydrogen sorption during, 20: 11227
HCl–TBP, solvent properties for metal chlorides, 20: 10759 (INP-427/C)
HYDRODYNAMICS
calculation of three-dimensional, particle-in-cell method for, (T), 20: 12537 (LA-3422)
evaluation for sodium-cooled reactors, 20: 10990 (NAA-SR-11586)
properties of supernova explosions, (T), 20: 11425 (UCRL-7777)
thermodynamic Green functions for superfluid, 20: 11898
HYDROGEN
atomic mass, (E/T), 20: 11494
bonding in chloroform, comparison of, with deuterium, 20: 10819
Coulomb potential of, Green's function for, (T), 20: 11446 (NP-15794)
diffusion in barium at 200 to 620°C, 20: 12535 (IS-T-61)
distribution in zirconium alloys, 20: 11221
effects in recoil tritium reactions, 20: 10933(R) (TID-22532)
effects on brittleness of Zircaloy-2 and zirconium–2.5 niobium alloy, 20: 11227
effects on carbon dioxide–graphite reactions at 960 to 1200°C, 20: 10859
effects on mechanical properties of zirconium alloys, 20: 11221
effects on mechanical properties of zirconium, combined oxygen and, 20: 11227
electric discharges in C Stellarator, light emission during, (E), 20: 12171 (MATT-270)
electric discharges in C-Stellarator, particle-loss rates for, (E), 20: 12239
electron elastic exchange scattering by ground-state, variational principle for, (T), 20: 11505
electron inelastic scattering at 13.7 to 50.7 ev, energy-loss spectra and excitation cross sections for, (E), 20: 11466
electron resonance scattering by, Fredholm equations for, (T), 20: 11508
electron scattering at 11 to 13 ev by molecular, resonances in, (E), 20: 11465
electron scattering at low energies by atomic, exchange effects on, (T), 20: 11500
energy levels in atomic, mean lives of excited, (E), 20: 11474
flow in straight circular tubes during chill-down, two-phase, 20: 10996 (WANL-TNR-154)
heat transfer coefficients for, 20: 12341
heat transfer to boiling, in straight circular tubes, 20: 10996 (WANL-TNR-154)
helium-atom and -ion scattering by, electrons and ions from, 20: 11447(R) (TID-22476)
hydrogen-ion cross sections and mobility in, positive low-energy, (E), 20: 11805
hydromagnetic waves in partially ionized plasma of, (E/T), 20: 12224
ion reactions with molecular, cross sections for inelastic, (E), 20: 11467
ionization in uniform inceasing magnetic field, (E), 20: 11768 (JUL-

327-PP)
ionization rates in d-c electric field, (E), 20: 12169 (JUL-322-PP)
kinetics of systems of atomic, Green functions from Lie algebras for, (T), 20: 11441 (IC/65/94)
molecular vibrational relaxation in shock tubes, laser Schlieren method for, 20: 11786
positron scattering by, polarization potentials for, (T), 20: 11487
production by sodium–water reaction in steam generator, 20: 12386 (APDA-176)
production of highly excited atoms of, by proton change exchange in alkaline metal vapors, (E), 20: 11471(T)
proton reactions with atomic, amplitude for reorientation from, (T), 20: 11503
proton tunneling in evolution reactions of, quantum mechanical rates for, (T), 20: 11372
reactions with atoms and ions, variational calculations of long-range, (T), 20: 11504
reactions with carbon monoxide, nitrogen oxide, and oxygen at 3 to 30 kev, electron loss and anion formation in, (E), 20: 11509
reactions with CCl_3^- radicals, deuterium effects on kinetics of, 20: 10820
reactions with graphite at 1550 to 2260°C, 20: 11225
reactions with Zircaloy-2 and Zircaloy-4 in water, 20: 11221
reactions with Zircaloy-2, 20: 11225
scattering in atom-molecule systems of, quantum mechanical analysis of elastic and reactive, (T), 20: 11513
sorption by Zircaloy-2 during aqueous corrosion, effects of environment on, 20: 11227
sorption by Zircaloy-2 and zirconium from hydrochloric acid, 20: 11227
spectra of, symmetry for continuous and discrete, (T), 20: 11445 (NP-15793)
stability in DCX-1, (E), 20: 12240
symmetry groups for atomic, noncompact extensions of, (T), 20: 11681 (IC-65/85)
viscosity coefficients at −195 to +25°C, isotope effects on, (E), 20: 11461
yields from gamma radiolysis of toluene, thermal-spike model for, 20: 10887

HYDROGEN IONS
energy levels of, (T), 20: 11450 (UCRL-7842-T)
energy levels of negative, secular equation for, (T), 20: 11453 (UCRL-12230)
mobility of low-energy positive, in hydrogen gas, (E), 20: 11805
production of negative, apparatus for, 20: 11082(P)
reactions with atoms and ions, variational calculations of long-range, (T), 20: 11504
scattering by hydrogen molecules at 3 to 100 ev, cross sections for inelastic, (E), 20: 11467

HYDROGEN ISOTOPES
separation by chromatography using aluminum oxide column at 77.4°K, 20: 10939

HYDROGEN ISOTOPES H-5
stability of, variational calculation of, (T), 20: 12101

HYDROGEN PEROXIDES
determination in fission product solutions by controlled-potential coulometry, 20: 10758 (EUR-2618.f)
effects on radioinduced luminescence of desoxyribonucleic acid, 20: 10578
radiolysis of dilute solutions of, formation of hydroxyl radicals in pulsed-electron, 20: 10924
yields in electron-pulse radiolysis of aerated aqueous potassium bromide solutions, 20: 10912

HYDROGEN SULFIDES
H_2S–propane-d_8, photolysis and radiolysis of, deuterium-transfer reactions in, (E), 20: 10883

HYDROGEN SYSTEMS
Ar–H_2, vibrational relaxation in shock tubes, laser Schlieren method for, 20: 11786
D–H, analysis of elastic and reactive scattering in, 20: 11513
D_2–H_2, surface tension of, (T), 20: 11787
DH–H_2, surface tension of, (T), 20: 11787
H–Nb–Zr, phase studies, 20: 11225
H–U–UH_n, phase studies and thermodynamic properties below 430°C, 20: 10801 (CEA-R-2777)

HYDROLOGY
evaluation of ground storage at ORNL, 20: 12518 (ORNL-TM-1327)

HYDROMAGNETIC WAVES
absorption in inhomogeneous plasma, Cherenkov electron, (T), 20: 12214
propagation in partially ionized hydrogen plasma, (E/T), 20: 12224
scattering by open end of semi-infinite plasma waveguide, 20: 12207
scattering of shock, on rigid wall, (T), 20: 11796

HYDROPEROXIDES
yields from irradiated desoxyribonucleic acid, 20: 10578

HYDROXYL RADICAL
radioinduced in aqueous nitrous oxide solutions, absorption spectrum of, 20: 10924
reactions with nucleic acids and related substances, rates of, 20: 10917
reactions with organic compounds, rate constants for, 20: 10916

HYPERFRAGMENTS
beta decay of light, shell-model calculation of branching ratio for, (T), 20: 11999
decay of $_{\Lambda}He^5$ nonmesic, (E), 20: 11977 (TID-22536)
hyperon (Λ) binding energies in $_{\Lambda}H^3$ and $_{\Lambda}H^4$, hyperon (Λ) nucleon scattering cross section from, (T), 20: 11594
production of $_{\Lambda}$ Br, (E), 20: 12092
properties of $_{\Lambda}B^{13}$, (E), 20: 12043
properties of $_{\Lambda}H^3$, Λ-N interaction cross sections from, (T), 20: 12084
symmetry for $_{\Lambda}H^3$, SU(6), 20: 11756

HYPERONS
interactions with nucleons, mass splitting effects in, (T), 20: 11586(T)

HYPERONS (Λ)
interactions with nucleons, analysis of light hyperfragments for cross sections for, (T), 20: 11594
interactions with nucleons in hypertritons, cross sections for, (T), 20: 12084
magnetic moments of, algebra of currents of, (T), 20: 11569 (UR-875-118)
photoproduction on protons, polarization in, (E), 20: 11676
production and trapping in meson (K^-) capture by bromine at 600 Mev/c, 20: 12092

HYPERONS (Λ^o)
binding energy in $_{\Lambda}B^{13}$, (E), 20: 12043
decay of, modified vector-boson propagator for leptonic, (T), 20: 11588
emission in hyperon (Ξ^o) decay in bubble chambers, scanning template for associating, 20: 11111 (TID-22550)

HYPERONS (Ω^-)
decay of, quark model for leptonic, (T), 20: 11559 (JINR-P-2445)
parity and spin from decay in meson (K^-)-proton interactions, (T), 20: 11563 (JINR-P-2456)

HYPERONS (Σ^-)
decay of, models for radiative-meson (π), (T), 20: 11633

HYPERONS (Σ^+)
decay of, models for radiative-meson (π), (T), 20: 11633
magnetic moments of, algebra of currents of, (T), 20: 11569 (UR-875-118)

HYPERONS ($\bar{\Xi}^o$)
production in bubble chambers, scanning template for associating hyperons (Λ^o) with vertices of, 20: 11111 (TID-22550)

HYPERTHYROIDISM
radiotherapy of, using iodine-131, 20: 10747
radiotherapy using iodine-131, 20: 10738
therapy of, in children, 20: 10738
therapy using drugs, 20: 10738

I

ICE
oxygen-17 nuclear magnetic resonance spectra in, 20: 10835

ICE-d_2
oxygen-17 nuclear magnetic resonance spectra in, 20: 10835

IGNEOUS ROCKS
geochemistry of thorium and uranium in, in Lower Triassic deposits, Pripyat Basin, USSR, 20: 11026

IMMUNE REACTIONS
effects of prednisolone on, in mice, 20: 10655
effects of Thorotrast on, in mice, 20: 10617
effects of thymus on tolerance response, 20: 10632
of sarcoma cells, effects of irradiation in suspension before injection in mice, 20: 10634
radiation effects on, to rat tissue transplants in mice, 20: 10505(R) (BNWL-122, pp 146-9)
radiation effects on, to bone marrow transfusions, 20: 10731
radiation effects on, in mice, γ, 20: 10632
radiation effects on, in mice, x, 20: 10655

IMMUNITY
radiation effects on mouse, β, 20: 10580

IMMUNIZATION
radiation effects on cellular response of rat lymph nodes after diphtheria, 20: 10685

IN-PILE LOOPS
development of, for low-cycle fatigue and tensile testing of irradiated materials, 20: 11345(R) (NASA-CR-54787)

INCOLOY
thermal stress fatigue of type 800, 20: 11227

INCONEL
bonding of type 600, to niobium, tantalum, and FS-85 and T-222 alloys, explosive, 20: 11243(R) (WANL-PR(EE)-001)

INDEXES
of progress reports of ORNL Analytical Chemistry Division using

permuted titles, 20: 10765 (ORNL-3904)
INDIANA
radioactivity of precipitation in, determination of gamma, 20: 11020
radioactivity of soils in, determination of gamma, 20: 11019
INDIUM
compatibility with types 316 and 410 stainless steel at 1300°F, 20: 11215(R) (NASA-CR-54718)
corrosion by low-melting-point metals, 20: 11227
INDIUM ALLOYS
Eu–In, phase studies, 20: 11327
In–Hg, magnetic properties of superconducting, containing iron particles, 20: 11894
In–Mg, positron annihilation in, temperature dependence of, 20: 11678
In–Pb, positron annihilation in, temperature dependence of, 20: 11678
In–Pu, phase studies, 20: 11224
In–Sn, r-f field trapping in superconducting, 20: 11926
INDIUM ARSENIDES
indium-115 nuclear spin transitions in single crystals of, (E), 20: 12304
INDIUM ISOTOPES In-113
electron spectra of, Auger, 20: 11153
neutron activation cross section at 24 kev, (E), 20: 12135
INDIUM ISOTOPES In-115
energy levels, (T), 20: 12160
neutron inelastic scattering by, cross sections for, (T), 20: 12160
nuclear spin transitions in single crystals of indium arsenides, (E), 20: 12304
INDIUM ISOTOPES In-117
energy levels, (E), 20: 12136
INDIUM OXIDES
B_2O_3–CdO–In_2O_3, properties of neutron-absorbing glasses of, as reactor control-rod material, 20: 11226
CdO–In_2O_3, properties of neutron-absorbing glasses of, as reactor control-rod material, 20: 11226
INDOLE, 3-(2-AMINOETHYL)-5-METHOXY-
effects on radiosensitivity of dogs and rats, 20: 10699(T) (NASA-TT-F-353, pp 210-38)
INDOLE-3-PYRUVIC ACID
formation in tryptophan metabolism in *Neurospora crassa*, 20: 10540 (HW-SA-3728)
5-INDOLOL, 3-(2-AMINOETHYL)-
effects on radiosensitivity of dogs and rats, 20: 10699(T) (NASA-TT-F-353, pp 210-38)
INDUSTRIAL HYGIENE
in beryllium processing plants, 20: 11038
pulmonary deposition of rare earth dusts during occupational exposure, 20: 11057
INFECTIONS
vaccination against *Mycobacterium tuberculosis*, in mice, using heat-killed *M. smegmatis*, 20: 10655
INOR-8
bonding to tantalum and FS-85 niobium-base alloy, explosive, 20: 11243(R) (WANL-PR(EE)-001)
INSECTS
effects of sulfoxide compounds on radiosensitivity of *Tribolium confusum* and *T. castaneum*, 20: 10504(R) (BNWL-122, pp 142)
radiation control of flour beetle, *Tribolium castaneum*, 20: 11184(R) (BNWL-122, pp 137-9)
radiation control of, infesting barley, 20: 10619
radiation effects on grain- and vegetable-infesting, gamma, 20: 12545(R) (PAEC(A)AR651)
radiosensitivity of *Tribolium castaneum*, effects of age, sex, temperature, and dose of fast neutrons and x, 20: 11184(R) (BNWL-122, pp 137-9)
INSTRUMENTATION
design and performance for SRE power expansion program, 20: 12406 (NAA-SR-Memo-11648)
design for use in targets for proton beams, 20: 11448(R) (TID-22480)
development for critical facilities and test reactors, 20: 11061(R) (IDO-17112)
development for radiation-monitoring and -warning at ORNL, 20: 11049
development for reactor safety, 20: 12335
INSULIN
labeling with tritium, 20: 10945
INTERFEROMETERS
performance of laser, for plasma electron density measurement, (E), 20: 12165 (ARL-65-135)
INTERMETALLIC COMPOUNDS
production by diffusion in superconductors, method for determining, 20: 10767(T) (AD-620995)
INTERNATIONAL ATOMIC ENERGY AGENCY
research in Philippine Islands under, 20: 12545(R) (PAEC(A)AR651)
INTESTINE
radiation effects on absorption of bile salts by rat, x, 20: 10599(R) (BNWL-122, pp 128-30)
radiation effects on mucus synthesis in rat, x, 20: 10600(R) (BNWL-122, pp 131-4)
radiation effects on bacterial population in mouse, β, 20: 10642
radiation effects on, after cervical cancer therapy, 20: 10654
radiation injuries to rat, effects of adrenal factors in x, 20: 10697
IODIDE IONS
magnetic field in iron, hyperfine, (E), 20: 12295
IODIDES
determination using radiocoulometric methods, 20: 10769
IODINE
reactions with potassium in crossed molecular beams, spectator stripping model for, 20: 10834
sampling in air, 20: 11060(R) (BNWL-122, pp 33-6)
separation from cesium and thallium, 20: 10901
IODINE BROMIDES
reactions with rubidium in crossed molecular beams, spectator stripping model for, 20: 10834
IODINE COMPLEXES
with coronene, perylene, and pyrene, effects of pressure on properties of, 20: 12534 (COO-1198-216)
IODINE ISOTOPES
distribution in EVESR coolant and moderator, 20: 12399(R) (GEAP-4941)
effects of therapeutic doses of radioactive, on blood coagulation of, 20: 10679
incorporation in plasma proteins, review of procedures for, 20: 10941
IODINE ISOTOPES I-127
alpha reactions (α,2n) at 35 Mev, cesium-129 production from, (E), 20: 10901
electron spin resonance spectra of gaseous, (E), 20: 11468
energy levels of, magnetic moments of, (E), 20: 12115
IODINE ISOTOPES I-128
production at PRR, methods for, 20: 12545(R) (PAEC(A)AR651)
IODINE ISOTOPES I-129
alpha reactions (α,n) and (α,4n) at 35 Mev, cesium-129 and -132 production from, (E), 20: 10901
determination in fission product solutions by controlled-potential coulometry, 20: 10758 (EUR-2618.f)
electron spin resonance spectra of gaseous, (E), 20: 11468
magnetic field in iron, hyperfine, (E), 20: 12295
IODINE ISOTOPES I-131
content in German milk, effects of precipitation on, 20: 11017
content in ocean fish, effects of content in sea water on, 20: 11054
content in thyroid gland of sheep, long-term ingestion study, 20: 10516(R) (BNWL-122, pp 49-51)
content in tissues of cattle, after ingestion, 20: 10516(R) (BNWL-122, pp 49-51)
deposition on plants, effects of moisture and temperature on, 20: 10717(R) (BNWL-122, pp 166-7)
deposition on soil, effects of moisture and temperature on, 20: 10717(R) (BNWL-122, pp 166-7)
distribution in tissues of rats, 20: 10554
energy levels of, magnetic moments of, (E), 20: 12115
incorporation in human albumin, 20: 10942
incorporation in hormones, review of procedures for, 20: 10943
incorporation in polyvinylpyrrolidone, method for, 20: 10946
incorporation into iodothiazide, 20: 10732
production at PRR, methods for, 20: 12545(R) (PAEC(A)AR651)
properties of protein-incorporated, 20: 10566
radiation effects on uptake of, by polyvinylpyrrolidone, uv, 20: 10946
retention on plants of deposited, effects of moisture and temperature on, 20: 10717(R) (BNWL-122, pp 166-7)
retention on soil of deposited, effects of moisture and temperature on, 20: 10717(R) (BNWL-122, pp 166-7)
sampling in air, 20: 11060(R) (BNWL-122, pp 33-6)
secretion in sheep milk, 20: 10517(R) (BNWL-122, pp 52-4)
separation from milk of, field use of ion exchange cartridges for, 20: 10722
uptake and retention in man, inhibition of whole-body, 20: 10543
uptake by thyroid gland of, from skin exposure of swine, 20: 10518(R) (BNWL-122, pp 55-8)
uptake of human thyroid gland of, from milk, 20: 10530(R) (BNWL-122, pp 113-17)
use as tracer for brain blood circulation measurements, 20: 10750
use for radiotherapy of goiter, 20: 10748
use for therapy of thyroid carcinomas, 20: 10729
use for therapy of hyperthyroidism, 20: 10738
use in gamma-globulin metabolism studies, 20: 10571
use in gamma-globulin metabolism studies, 20: 10572
use in therapy of hyperthyroidism, 20: 10747
use of albumin- and calcium caseinate-incorporated, in measuring intestinal protein absorption, 20: 10566
use of albumin-incorporated, in measuring gastrointestinal protein loss,

20: 10567
use of albumin-incorporated, for determining effects of nutritional disorders on protein metabolism, 20: 10573
use of γ-globulin-incorporated, for determining effects of nutritional disorders on protein metabolism, 20: 10573
use of polyvinylpyrrolidone-incorporated, for measuring gastrointestinal protein loss, 20: 10568
use of protein-incorporated, in protein metabolism studies, 20: 10562
IODINE ISOTOPES I-132
distribution in tissues of, following ingestion of tellurium-132, biological model for, 20: 10519(R) (BNWL-122, pp 59-63)
energy levels from technetium-132 decay, parity and spin of, (E), 20: 12026
IODINE ISOTOPES I-133
diffusion from urania at 800 to 1600°C, coefficients for, 20: 11224
IODINE ISOTOPES I-135
diffusion from urania at 800 to 1600°C, coefficients for, 20: 11224
ION BEAMS
focusing power of tube for electrostatic accelerator with high output, (T), 20: 11405
measurements on out-of-phase, in isochronous cyclotrons, 20: 11415(P)
motion in accelerators, synchronous phase measurements for, 20: 11406
production of intense, using duoplasmatron source, 20: 12260
production of stable high-intensity, device for, 20: 11083(P)
trajectories in bending magnet systems, space-charge effects on, (T), 20: 11378 (AD-626633)
uses for strengthening metals and alloys, 20: 11366
ION EXCHANGE MATERIALS
diffusion of ethane in zeolitic, steric effects in, 20: 12532 (COO-920-8)
efficiency of, in fused sodium nitrate, tracer studies of, 20: 10958
sorptive properties of alumina–silica for cesium in waste solutions, 20: 10766 (TID-22511)
use of cartridges of, for separation of iodine-131 from milk, 20: 10722
ION PUMPS
cathode performance in diode, rare earth, 20: 10976 (IS-T-46)
ION SOURCES
current-voltage characteristics of Penning, for mass spectrometers, 20: 11077
design, 20: 11083(P)
design and performance of r-f, 20: 11374
design for negative ions, 20: 11082(P)
development of polarized, review of European, 20: 11379 (ANL-7118)
development of r-f, 20: 12163(R) (AD-625424)
performance of cold-cathode pulsed, 20: 11394 (NP-15788)
performance of duoplasmatron, 20: 12260
use of surface-ionization, in measurement of ionization potentials, 20: 12257
IONIZATION CHAMBERS
use with neutron-sensitive foils and pocket dosimeters, 20: 11119
IONIZATION POTENTIALS
measurement using surface-ionization ion source, 20: 12257
IONOSPHERE
charged particle interactions in, (E), 20: 11850
charged particle processes in polar D region of, review, 20: 11843
charged-particle density in, simultaneous methods for measuring, (E), 20: 11847
charged-particle properties in polar, evaluation of electric probes for measurement of, 20: 11844
conference, 20: 11841
disturbances in, during years of maximum solar activity, 20: 11810(T)
electromagnetic wave scattering resonances in, a-c resonant probe relation to, (T), 20: 12241
electron and proton reactions in, direct ionization from, (T), 20: 11858
electron density and collision frequency in F region of, during auroral absorption event, (E), 20: 11848
electron density irregularities in polar cap above F2 layer maximum, (E), 20: 11845
electron density profiles in D region of, low frequency r-f propagation from rockets for measuring, 20: 11846
electron density profile in D region of, theory for r-f impedance probe measurements of, 20: 11846
electron precipitation in, auroral absorption height from rate of, (E), 20: 11864
electron properties in, fast, (E), 20: 11850
heating in upper F region of, by photoelectron streaming from sunlit conjugate ionosphere, (E), 20: 11828
ionization in auroral, longitudinal extent of, (E/T), 20: 11861
ionization layers in low and middle latitudes, sporadic-E, (T), 20: 11809(T)
properties of polar, experiments for determining, 20: 11865
proton content in, from vlf whistler measurement, 20: 11822
radio wave absorption in, auroral and polar cap, (T), 20: 11858
x-ray intensity pulsations in auroral zone, spatial and time, (E), 20: 11826
IONS
calculation of chemical equilibria in fused salts using, 20: 10807 (EUR-2466.e, pp 39-57)
density in cesium thermionic converters, pressure and spacing effects on, (E), 20: 11544 (LA-DC-7390)
detection of, mass spectrometers for, 20: 10791
diffusion and migration of, in fused salts, review on, 20: 10808 (EUR-2466.e, pp 59-80)
diffusion and migration in fused salts, model of, 20: 10805 (EUR-2466.e, pp 21-30)
diffusion and mobilities of, in fused salts, review on, 20: 10806 (EUR-2466.e, pp 31-8)
electron spin resonance spectra in cubic lattices, Jahn-Teller effects in, (T), 20: 12294
emission in laser-beam reactions with metals, energy and intensity of, (E), 20: 11463
energy levels of, wave functions for calculating, (T), 20: 11450 (UCRL-7842-T)
escape rate from magnetically confined plasma, (T), 20: 12162 (65RL-3998E)
heating of, excitation method for, (E/T), 20: 11770 (ORNL-P-1005)
interactions with positrons in condensed media, Hartree-Fock method for annihilation, 20: 11377
motion in electromagnetic and gravitational fields, scalar formulation of ideal, 20: 11798
motion in plasma, effects of weak collisions on, (T), 20: 12172 (MATT-302)
oscillation in weakly turbulent plasma, (T), 20: 12178 (NP-15705)
production in helium-atom and -ion scattering by molecules, 20: 11447(R) (TID-22476)
production in high-energy proton reactions, 20: 11377
reactions of heavy, with nuclei, mechanisms of, 20: 11377
reactions of negative, with atoms, (T), 20: 11517
reactions with atoms and ions, variational calculations of long-range, (T), 20: 11504
reactions with atoms, electrons, and ions, quantum mechanical theories for, 20: 11511
reactions with crystals, coherent Coulomb excitation in, (T), 20: 11973 (NP-15791)
reactions with nuclei, finite-range Coulomb stripping and heavy-ion transfer, (T), 20: 12091
reactions with semiconductors, doping effect in, (E), 20: 12280
temperatures in plasma, double probe method for measuring, 20: 12186
wave functions for, asymptotic large-z, (T), 20: 11485
IRIDIUM
compatibility and encapsulation with neodymium, promethium, and samarium oxides, 20: 11267 (BNWL-SA-488)
effects of alloy additions of, on mechanical properties of niobium, 20: 11302
performance as collector electrode for thermionic cells, 20: 11540(R) (AD-626444)
IRIDIUM ALLOYS
Ir–Mo, phase studies, 20: 11309
Ir–Nb, mechanical properties of, effects of composition on, 20: 11288(T) (AD-622477)
Ir–Nb, phase studies, 20: 11227
Ir–W, phase studies, 20: 11309
IRIDIUM COMPOUNDS
superconductivity in chalcogenide, (E), 20: 11899
IRIDIUM ISOTOPES Ir-191
energy levels from electron-capture decay of platinum-191, (E), 20: 12009
IRIDIUM ISOTOPES Ir-192
energy levels of, width of 2⁺, 20: 12147
production of high-specific-activity sources of, equipment and method for, 20: 11190 (BLG-332)
IRIDIUM ISOTOPES Ir-193
neutron activation cross section at 24 kev, (E), 20: 12135
IRIDIUM TELLURIDES
superconductivity in, (E), 20: 11899
IRON
alpha inelastic scattering at 21, 27.5, and 47.9 Mev, statistical-theory analysis of, (E), 20: 12056
analysis for oxygen, activation, 20: 10771
argon-ion reactions at 10 to 100 kev, secondary-electron emission in, (E), 20: 11462
carburization of Armco, by high-carbon sodium at 1200°F, 20: 11235 (MSAE-65-194)
determination in fission product and irradiated fuel solutions by controlled-potential coulometry, 20: 10758 (EUR-2618.f)
diffraction patterns of powdered, neutron, 20: 12545(R) (PAEC(A)AR651)
effects of alloying additions of, on oxidation rates of niobium, tantalum,

and tungsten, 20: 11227
effects on strength of plutonium–gallium alloys at –32 to 500°C, 20: 11224
electron interaction effects in films of, superimposed on superconducting lead films, (E), 20: 11918
gamma attenuation in, (T), 20: 12264 (MLM-1315)
magnetic field at iodine nuclei in, hyperfine, 20: 12295
magnetic properties of particles of, in superconducting indium–mercury alloys, 20: 11894
neutron scattering total cross sections at 12 to 14 Mev, (E), 20: 11949 (AD-625747)
pressure spalling of, properties of, (T), 20: 12539 (LA-DC-7692)
proton reactions at 1 to 3 Bev, cascades in, (E), 20: 12262 (BNL-8721)
radiation effects on ferromagnetic resonance of thin films of, helium-3, 20: 12318
radiation effects on carbon precipitation in alpha-phase, electrons and fast neutron, 20: 11227
separation from salts by extraction chromatography using organic phosphorus compounds, 20: 10759 (INP-427/C)
separation from salts by solvent extraction using Schiff bases in chloroform, 20: 10759 (INP-427/C)
separation from salts by solvent extraction using 8-mercaptoquinoline in chloroform, 20: 10759 (INP-427/C)
solubility in potassium at 871°F, effects of crucible material on, 20: 11227
stress-rupture properties of Ferrovac E and Armco, at high temperatures and strain rates, 20: 11265 (AD-626375)
x-ray spectra of, performance of spectroanalyzer with promethium-147 beta source for K, 20: 11133

IRON ALLOYS
Al–Cr–Co–Fe–Mo–Ni–Ti, stress-rupture properties of Udimet 700, at high temperatures and strain rates, 20: 11265 (AD-626375)
Al–Fe, oxidation by oxygen at 800 to 1050°C, kinetics of internal, 20: 11232 (INR-644/XIV/PS)
Al–Fe–U, phase transformations in, effects of aluminum and iron content on, 20: 11224
Be–Fe, precipitation of $Be_{11}Fe$ on dislocations in, 20: 11299
Cr–Fe, crystal structure of, dislocations in, 20: 11303
Cr–Fe, diffusion of fission products in, effects of concentrations on, 20: 11212(R) (BMI-X-10143)
Cr–Fe–Mo–V, erosion by mercury vapor at 640°F of Lapelloy, 20: 11214(R) (NASA-CR-54717)
Cr–Fe–Ni, diffusion of fission products in, effects of concentrations on, 20: 11212(R) (BMI-X-10143)
Cr–Fe–Ni, mechanism of stress corrosion cracking of, in sodium chloride, 20: 11233(R) (COO-1319-32)
Fe–Nd, phase diagram, 20: 11295
Fe–Ni, diffusion of fission products in, effects of concentrations on, 20: 11212(R) (BMI-X-10143)
Fe–Ni, radiation effects on ferromagnetic resonance of thin films of, helium-3, 20: 12318
Fe–Ni–W, mechanical properties of, effects of strain rate on, 20: 11284 (UCRL-14599)
Fe–Ni–W, mechanical properties of sintered composites of tungsten-base, 20: 11291
Fe–Sn, iron-57 and tin-119 Mössbauer effects in, 20: 12315
Fe–U, heat treatment, 20: 11319
Fe–Y, crystal structure of intermetallic compound YFe_3 in, 20: 11308
Gd–Fe, crystal structure of intermetallic compound $GdFe_3$ in, 20: 11308
Gd–Fe, magnetic properties of, effects of composition and temperature on, 20: 11341
Mo–Fe, electron interaction effects in films of, superimposed on superconducting lead films, (E), 20: 11918

IRON CHLORIDES
corrosive effects on molybdenum and tungsten at 35, 60, and 100°C, 20: 11230 (BM-RI-6715)
corrosive effects on vanadium-base alloys at low temperatures, 20: 11230 (BM-RI-6715)

IRON COMPLEXES
with methylenephosphonic acid derivatives, preparation and properties of, 20: 12533 (COO-1020-6)

IRON COMPOUNDS
Mössbauer effect in iron-57-enriched, in rat hemoglobin, 20: 10903

IRON COUPLES
Fe/Nb/stainless steel/V, diffusion in bimetallic tubing of, with iron and vanadium diffusion barriers, inter-, 20: 11215(R) (NASA-CR-54718)
Fe/Nb–Zr/stainless steel/V, diffusion in bimetallic tubing of, with iron and vanadium diffusion barriers, inter-, 20: 11215(R) (NASA-CR-54718)
Fe/Nb/stainless steel, diffusion in bimetallic tubing of, with iron diffusion barrier, inter-, 20: 11215(R) (NASA-CR-54718)
Fe/stainless steel/Ta, diffusion in bimetallic tubing of, with iron diffusion barrier, inter-, 20: 11215(R) (NASA-CR-54718)
Fe/stainless steel/Ta/V, diffusion in bimetallic tubing of, with iron and vanadium diffusion barriers, inter-, 20: 11215(R) (NASA-CR-54718)
Fe/Zr–Zr/stainless steel, diffusion in bimetallic tubing of, with iron diffusion barrier, inter-, 20: 11215(R) (NASA-CR-54718)

IRON HYDROXIDES
diffraction patterns of, neutron, 20: 12545(R) (PAEC(A)AR651)

IRON IONS
effects on phenol yields from radiolysis of sulfate solutions of benzene, 20: 10878

IRON ISOTOPES
content in ocean fish, effects of content in sea water on, 20: 11054

IRON ISOTOPES Fe-54
proton scattering at 19 Mev, excited 2⁺ and 3⁻ levels from, (E/T), 20: 12065
triton reactions (t,p) at 12 Mev, (T), 20: 12086

IRON ISOTOPES Fe-56
energy levels, (E), 20: 12063
energy levels of, parity and spin of, (E), 20: 12108
neutron nonelastic reactions at 8.1 to 21 Mev, cross sections for, (E), 20: 11985
neutron reactions (n,n′γ) at 0.95 to 4 Mev, cross sections and gamma angular distributions for, (E), 20: 12108
proton reactions (p,p′) at 10.965 Mev, energy levels from, (E), 20: 12063
proton scattering at 19 Mev, excited 2⁺ and 3⁻ levels from, (E/T), 20: 12065

IRON ISOTOPES Fe-57
hyperfine field in nickel at 77°K to curie point, internal, (E), 20: 12298
Mössbauer effect in iron(II) and (III) compounds of, in rat hemoglobin, 20: 10903
Mössbauer effect in stainless steel, (E), 20: 12296
Mössbauer effects in iron–tin alloys, 20: 12315

IRON ISOTOPES Fe-59
production at PRR, methods for, 20: 12545(R) (PAEC(A)AR651)

IRON SYSTEMS
Fe–PuC–UC, analysis for plutonium, review of methods for, 20: 10797

IRRADIATION FACILITIES
beam control in electron, 20: 11416(P)
conveyor system for, 20: 10986(P)
design, 20: 10987(P)
design specifications for gamma, 20: 10980(T) (AEC-tr-6469)
operation at PRR, 20: 12545(R) (PAEC(A)AR651)
target rotation in electron-beam, device for, 20: 10984(P)

ISOTOPE EFFECTS
of deuterium on infrared spectra of cyclohexane, 20: 10864
of deuterium on photoionization of acetylene, 20: 10867
of deuterium on valence vibration spectra of piperidine, 20: 10863
on reactions of CCl_3 radicals with hydrogen, 20: 10820
on superconductivity of osmium and ruthenium, correlation with pressure effects, 20: 11896
on thermodynamic properties of electrolytes in heavy water, 20: 10847

ISOTOPE SEPARATION METHODS
yields in multiphase mass spectrometric, 20: 11192 (SGAE-PH-30/1965)

ISOTOPES
abundance of, elimination of errors in mass spectrometric measurements of, 20: 10793

J

JAPAN
land subsidence at Niigata in, measurement of, 20: 11024

JOINTS
properties of bismuth–tin eutectic fusible-metal, 20: 12513

JOURNAL BEARINGS
design and stability of grooved, gas-lubricated, (E/T), 20: 10979 (TID-22528)

K

KIDNEYS
effects of iodothiazide on excretory function of, 20: 10732
function tests of, using iodine-131-iodothiazide, 20: 10732
function tests on, evaluation of radioisotope, 20: 10734
function tests on, evaluation of radioisotope, 20: 10753
radiation effects on rat, pathological, x, 20: 10598(R) (BNWL-122, pp 107-9)
radiation effects on production of erythropoietic factor in rat, uv, 20: 10635
uranium elimination from, effects on sulfanilamides on, 20: 10553

KRYPTON
content in Bruderheim meteorite, 20: 11430
electron reactions with atomic, metastable excitation in, (E), 20: 11455 (UCRL-14450)
C_2F_6–Kr, energy transfer in gamma radiolysis of, 20: 10884

KRYPTON FLUORIDES

molecular vibrations of, bond-bond interaction constants for, 20: 10829
KRYPTON ISOTOPES
determination in meteorites as indication of fission, neutron capture, and spallation anomalies, (E/T), 20: 11424 (NP-15629)
production and separation of stable, method for, 20: 11191 (JEN-150-DQ/I-51)
KRYPTON ISOTOPES Kr-80
content in Bruderheim meteorite, 20: 11430
KRYPTON ISOTOPES Kr-82
content in Bruderheim meteorite, 20: 11430
energy level structure of, rotational and vibrational bands in, (T), 20: 12156
KRYPTON ISOTOPES Kr-83
content in Bruderheim meteorite, 20: 11430
determination in uranium-233 and -235 fission products, (E), 20: 11960(R) (IDO-14667)
KRYPTON ISOTOPES Kr-84
content in Bruderheim meteorite, 20: 11430
determination in uranium-233 and -235 fission products, (E), 20: 11960(R) (IDO-14667)
KRYPTON ISOTOPES Kr-85
determination in uranium-233 and -235 fission products, (E), 20: 11960(R) (IDO-14667)
diffusion from urania at 800 to 1600°C, coefficients for, 20: 11224
KRYPTON ISOTOPES Kr-86
content in Bruderheim meteorite, 20: 11430
determination in uranium-233 and -235 fission products, (E), 20: 11960(R) (IDO-14667)
KRYPTON ISOTOPES Kr-87
diffusion from urania at 800 to 1600°C, coefficients for, 20: 11224
KRYPTON ISOTOPES Kr-88
diffusion from urania at 800 to 1600°C, coefficients for, 20: 11224
KRYPTON ISOTOPES Kr-89
decay probability in recombiner of L54M reactor, (E), 20: 12508
KRYPTON ISOTOPES Kr-90
decay probability in recombiner of L54M reactor, (E), 20: 12508
KRYPTON SYSTEMS
Kr–Na, excitation transfer in first excited states of sodium, cross sections for collision-induced, (E), 20: 11499

L

LABORATORIES
nuclear materials management in research, Lucas Heights, Australia, 20: 12560
LABORATORY EQUIPMENT
development for use in caves, bibliography on, 20: 10977 (KFK-370)
LACTIC ACID
corrosive effects on vanadium at 35, 60, and 100°C, 20: 11230 (BM-RI-6715)
LAMINATES
gamma transmission by, (T), 20: 12271
LANTHANUM
heat of solution in liquid tin at 632°K, 20: 11304
separation from other elements by solvent extraction using TBP, 20: 10952
separation from uranium by reversed-phase partition chromatography, 20: 10784
spectra of, burner design for atomic absorption, 20: 10761 (IS-T-69)
LANTHANUM ALLOYS
Al–La, crystal structure of intermetallic compound $LaAl_3$ in, 20: 11305
La–Nb, mechanical properties of, effects of composition on, 20: 11288(T) (AD-622477)
La–Sn, tin Knight shift and magnetic susceptibility of $LaSn_3$, 20: 12324
LANTHANUM CARBONATES
complexes of, composition in solution of, 20: 10824
LANTHANUM CHLORIDES
neodymium ion fluorescence in, mechanism of concentration quenching of, 20: 12297
plutonium trivalent ion energy levels in, (E), 20: 12286
rare-earth ion spin-lattice relaxation in trivalent, (E), 20: 12292
rare-earth-ion fluorescent lifetimes in crystals of, 20: 12317
LANTHANUM ETHYL SULFATES
rare-earth ion spin-lattice relaxation in, (E), 20: 12300
LANTHANUM FLUORIDES
neodymium ion fluorescence in, mechanism of concentration quenching of, 20: 12297
rare-earth-ion fluorescent lifetimes in crystals of, 20: 12317
LANTHANUM GERMANATES
spectra of $La_2(GeO_4)O$ and $La_2(Ge_2O_7)$, infrared, 20: 10828
LANTHANUM ISOTOPES La-128
beta decay of, barium-128 energy levels from, (E), 20: 12068
LANTHANUM ISOTOPES La-139
alpha reactions (α,n), (α,pn), (α,3n), (α,4n) at 11 to 40 Mev, excitation functions for, (E/T), 20: 12014
LANTHANUM ISOTOPES La-140
beta transition of, nuclear matrix elements in 2.2 Mev, (E/T), 20: 12066
content in ocean fish, effects of content in sea water on, 20: 11054
determination in irradiated MITR fuel elements by gamma spectroscopy, 20: 10764 (MITNE-64)
use as tracer in studies on silt movement, 20: 11022 (AERE-R-5080)
LANTHANUM NITRATES
separation from salt mixtures by extraction chromatography using organic phosphorus compounds, 20: 10759 (INP-427/C)
LANTHANUM OXIDES
rare-earth-ion fluorescent lifetimes in crystals of, 20: 12317
reactions with chromium chlorides in fused chlorides and fluorides, 20: 10821
reactions with fused alkali metal chlorides and fluorides, 20: 10821
GeO_2–La_2O_3, spectra of compounds formed in, infrared, 20: 10828
LANTHANUM SELENIDES
CeSe–La_2Se_3, phase studies, 20: 10857
LANTHANUM SULFIDES
superconducting transition temperature of, (E), 20: 11909
LARVAE
radiation effects on *Aëdes aegypti*, x, 20: 10692
radiation effects on mortality in Drosophila, gamma and/or tritiated thymidine, 20: 10602 (CNAEM-32)
LARYNX
radiotherapy of carcinomas of, 20: 10744
LEAD
charged-particle reactions at high energies, astatine production in, 20: 11377
effects of superconducting films of, on electron interactions in superimposed magnetic films, (E), 20: 11918
electron interaction effects in superimposed films of magnetic and superconducting, (E), 20: 11918
gamma attenuation in, (T), 20: 12264 (MLM-1315)
gamma incoherent scattering by K-shell electrons of, at 320 kev, (E), 20: 11514
gamma reactions at 320 kev, absolute photoelectric cross sections for, (E), 20: 11496
meson (π^-) reactions at 15 Bev/c, meson (ρ) production in, (E), 20: 11618
neutron nonelastic reactions at 8.1 Mev, cross sections for, (E), 20: 11985
photoelectric cross section of, (E), 20: 11516
positron annihilation in normal and superconducting, photon angular correlation from, (E), 20: 11912
superconducting point contacts of, macroscopic quantum interference effects in, (E/T), 20: 11911
LEAD ALLOYS
Bi–Pb, vacuum distillation of cadmium from eutectic of, 20: 10762 (IS-T-71)
Gd–Pb, electron interaction effects in films of, superimposed on superconducting lead films, (E), 20: 11918
In–Pb, positron annihilation in, temperature dependence of, 20: 11678
LEAD ISOTOPES Pb-204
energy levels, 20: 11971 (MLM-1251J)
LEAD ISOTOPES Pb-205
energy levels, 20: 11971 (MLM-1251J)
LEAD ISOTOPES Pb-207
alpha inelastic scattering at 42 Mev, collective excitations in, (E), 20: 12075
LEAD ISOTOPES Pb-208
alpha inelastic scattering at 42 Mev, collective excitations in, (E), 20: 12075
neutron activation cross section at 24 kev, (E), 20: 12135
LEAD ISOTOPES Pb-210
biological half-life in dogs, 20: 10544
equilibrium with polonium-210 in dogs, 20: 10544
LEAD ISOTOPES Pb-212
preparation from thorium-228 decay products, method for, 20: 10759 (INP-427/C)
reactions of recoil atoms of, 20: 10933(R) (TID-22532)
LEAD NITRATES
separation from salt mixtures by extraction chromatography using organic phosphorus compounds, 20: 10759 (INP-427/C)
LEAD TITANATES
$PbTiO_3$–$PbZrO_3$, dielectric properties of, effects of preparation on, 20: 11279(R) (SC-DC-64-1477X)
LEAD ZIRCONATES
$PbTiO_3$–$PbZrO_3$, dielectric properties of, effects of preparation on, 20: 11279(R) (SC-DC-1477X)
LEAKS
measurement in reactor containment structures, 20: 12332

LEPTONS
interactions with baryons, weak, (T), 20: 11583(T)
production of nonpolarized, in antineutrino- and neutrino-nucleon interactions, (T), 20: 11577
LEUKEMIA
chemotherapy using urethan, effects on bone marrow of, 20: 10746
chromosome anomalies in patients with, 20: 10647
effects on metabolism in children, 20: 10545
incidence in population of Nagasaki, 20: 10595(R) (ABCC-60-61)
incidence in population of Hiroshima, 20: 10595(R) (ABCC-60-61)
induced by cancer therapeutic drugs, 20: 10647
radioinduced in man, x, 20: 10647
radioinduced in mice, by injected tritium, 20: 10623
radioinduced in swine, by beta particles from ingested strontium-90, 20: 10597(R) (BNWL-122, pp 37-45)
radiotherapy of, effects on bone marrow of x, 20: 10746
therapy using bone marrow transfusions, 20: 10731
LEUKOCYTES
radiation effects on reaction of, to adrenaline in dogs, 20: 10594
radiation effects on thymocytes, mechanisms of, 20: 10629
radiation effects on human, 20: 10660
radiation effects on osmotic resistance of rat, 20: 10614
radiation on content in mice, β, 20: 10641
LEVEL INDICATORS
development of radiometric, 20: 12545(R) (PAEC(A)AR651)
LIFE SPANS
radiation effects on swine, from exposed sires, x, 20: 10618
LIGHT
absorption by electrons in field of argon atom, cross section for, (T), 20: 11478
absorption by rubidium-87, excited-state disorientation cross section for, (E), 20: 11486
effects of natural, on carbon fixation by vascular hydrophytes, 20: 12543(R) (NYO-3018-12)
effects on patterns of X-agent, 20: 11536
effects on radiation damage in Neurospora, 20: 10716
interactions with F centers in crystals, (T), 20: 12274(R) (COO-578-18)
interactions with gaseous and metallic plasma, second-harmonic generation and Raman effects in, (T), 20: 12245
mixing of beams of, in plasma, (T), 20: 12255
reflection from Schwarzschild source, (T), 20: 11885
scattering by light in plasma, (T), 20: 12255
scattering in plasma, stimulated Raman effect in, (T), 20: 12243
LIGHTNING
occurrence and properties of ball, 20: 12176 (NASA-TN-D-3188)
LINEAR ACCELERATORS
beam currents in low-energy electron, method of measuring pulsed, 20: 12112
beam grouping at input of electron, (T), 20: 11393 (NP-15715)
beam phase measurement in ion, synchronous, 20: 11406
beam profile measurement for electron, 20: 11407
cavity resonators of, beam loading and field excitation in, (T), 20: 11381 (BNL-9833)
design, 20: 11417(P)
development of, superconductor use in, 20: 11412
magnetic field optimization in, equations for, 20: 11386 (CERN-65-35)
LIPIDS
radiation effects on content of, in rat adrenal glands, x, 20: 10576
radiation effects on mouse liver, protective effects of splenic phospholipids against, 20: 10704
radiation effects on mouse, protective effects of heparin against, 20: 10705
radiation effects on content of, in brain of guinea pigs, x, 20: 10636
LIPOPROTEINS
radiosensitivity of, in erythrocyte membranes of newborn rats, 20: 10589
LIQUID FLOW
magnetohydrodynamic properties of metal, (T), 20: 11771(T) (NP-tr-1346)
LIQUID METAL COOLED REACTORS
boiler design for, problems associated with, 20: 12339(T) (EURFNR-11F)
coolant reactions with air in sodium, model for processes in, (T), 20: 10851
coolant technology for, review of sodium, 20: 12330 (TID-8541, pp 321-425)
coolants for fast, evaluation of sodium, 20: 12345
design of 1000-Mw(e) fast breeder sodium, 20: 12402 (KFK-369)
design of 1000-Mw(e), 20: 12433
design of 350-Mw(e) sodium-cooled BN-350 power breeder, 20: 12441
design parameters for thermionic space, 20: 12483
development of Phenix, 20: 12423
fuel element temperature distributions in 350-Mw(e) sodium-cooled BN-350 power breeder, 20: 12443
safety analyses for, 20: 12433
safety of sodium, heat transfer, hydrodynamic effects, and void formations in, 20: 10990 (NAA-SR-11586)
LIQUICS
diffusion of particles in, generalized equations for, (T), 20: 11369
gas–liquid, phenomena in bubbly flow of, (T), 20: 10991 (NYO-3114-12)
LITHIUM
electron scattering by, polarization potentials for, (T), 20: 11487
heat transfer by, in turbulent flow, 20: 12483
ionization potential, (E), 20: 12257
proton reactions with atoms of, production of highly excited hydrogen atoms by charge-exchange, (E), 20: 11471(T)
spectra of, isotope shift of 2s and 2p levels of, (T), 20: 11506
LITHIUM ALLOYS
Al–Li, swelling from helium precipitation in, mechanism of, 20: 11224
Li–Mg–Tl, preparation, properties, and structure of intermetallic compound $LiMg_2Tl$ in, 20: 11282 (UCRL-12119-T)
LITHIUM BROMIDES
magnetic moment of molecular, rotational, (E), 20: 11484
LiBr–KBr, ion transfer in fused, 20: 10805 (EUR-2466.e, pp 21-30)
LiBr–LiH, phase studies, 20: 10833
LITHIUM CHLORIDES
magnetic moment of molecular, rotational, (E), 20: 11484
thermodynamic properties of, in heavy water, 20: 10847
LITHIUM EUROPIUM OXIDES
preparation and crystal structure of alpha-, 20: 10818
LITHIUM FLUORIDES
magnetic moment of molecular, rotational, (E), 20: 11484
reactions of fused, with chromium fluoride or lanthanum oxide, 20: 10821
LITHIUM HYDRIDES
neutron fluxes and heating in shielding of, fast, (T), 20: 12468 (NAA-SR-Memo-9916)
performance for neutron shielding, 20: 12475 (WANL-PR(B)-009)
positron annihilation in, three-quantum, (E), 20: 11620
positron annihilation in, photon angular correlations from, (T), 20: 11655
thermodynamic properties of, emf studies of, 20: 10849
LiBr–LiH, phase studies, 20: 10833
LiH–LiI, phase studies, 20: 10833
LiH–NaCl, phase studies, 20: 10832
LITHIUM IODIDES
performance of paired lithium-6 and -7 enriched europium-activated, for neutron spectra, 20: 11116
LiH–LiI, phase studies, 20: 10833
LITHIUM IONS
electron reactions at 75.6 to 800 ev, cross sections for single ionization in, (E), 20: 11489
energy levels of, (T), 20: 11450 (UCRL-7842-T)
magnetic susceptibility of, wave-function calculations of, (T), 20: 11485
reactions with atoms and ions, variational calculations of long-range, (T), 20: 11504
LITHIUM ISOTOPES Li-5
energy levels, 20: 12023
LITHIUM ISOTOPES Li-6
alpha-deuteron cluster representation of, (T), 20: 12039
deuteron reactions (d,p) at 200 to 350 kev, proton angular distributions in, (E), 20: 12096
effects on lithium atomic spectra, isotope-shift, (T), 20: 11506
energy levels, 20: 12023
hyperfine structure of, (E), 20: 11497
hyperfine structure of, (T), 20: 11498
lithium-6 elastic scattering at 3.2 to 7.0 Mev, cross sections for, (E), 20: 12053
nuclear properties, (T), 20: 11498
proton reactions (p,2p) at 460 Mev, (E/T), 20: 11948 (AD-624318)
reactions (Li-6,α), (Li-6,d) and (Li-6,p) with carbon-12 at 4.5 to 5.5 Mev, cross sections for, (E), 20: 12059
reactions with cobalt-59 and manganese-55, copper recoil ions from, (E), 20: 12085
LITHIUM ISOTOPES Li-7
effects on lithium atomic spectra, isotope-shift, (T), 20: 11506
energy levels, 20: 12023
hyperfine structure of, (E), 20: 11497
hyperfine structure of, (T), 20: 11498
lithium-7 elastic scattering at 4.0 to 6.5 Mev, cross sections for, (E), 20: 12053
neutron inelastic scattering at 2.45 Mev, angular distributions from, (E), 20: 12106
neutron nonelastic reactions at 13 to 21 Mev, cross sections for, (E), 20: 11985
nuclear properties, (T), 20: 11498
proton reactions (p,2p) at 460 Mev, (E/T), 20: 11948 (AD-624318)
LITHIUM ISOTOPES Li-8
beta decay of, alpha energy distribution from, (T), 20: 12010
energy levels, (E), 20: 11988

energy levels, 20: 12023
LITHIUM NITRATES
$LiNO_3$–$AgNO_3$, electrochemical and thermochemical properties of fused, 20: 10804 (EUR-2466.e, pp 9-19)
$LiNO_3$–KNO_3, ion transfer in fused, 20: 10805 (EUR-2466.e, pp 21-30)
LITHIUM SYSTEMS
NH_3–Li, positron lifetime in, (E), 20: 11674
LITTER SIZES
radiation effects on rat, fission neutrons, 20: 10601(R) (BNWL-122, pp 135-6)
LIVER
fat accumulation in rat, effects of neptunium-237 on, 20: 10522(R) (BNWL-122, pp 79-80)
protein synthesis in animal, tracer study of rate of, 20: 10558
radiation effects on rat, pathological, x, 20: 10598(R) (BNWL-122, pp 107-9)
radiation effects on human, after Thorotrast carotidography, 20: 10680
radiation effects on lipid content in mouse, protective effects of splenic phospholipids against, 20: 10704
radiation effects on lipid content in mouse, protective effects of heparin against, 20: 10705
radiation effects on uptake of sulfur-35-labeled sodium sulfate by rat, 20: 10542
radiation effects on nitrogen excretion by isolated frog, y, 20: 10551
radiation effects on lactic- and malic-acid dehydrogenases in extracts of rat, x, 20: 10583
radiation effects on fatty acid and total lipid content of rat, 20: 10659
radiation effects on biochemical properties of homogenates of mouse, y, 20: 10577
radiation effects on iridindiphosphate content in rat, x, 20: 10590
response to immune reactions to donor cells in mouse-rat radiation chimeras, 20: 10505(R) (BNWL-122, pp 146-9)
LOOPS
performance of thermal syphon, for thermoelectric cells, (E/T), 20: 11543(R) (GIC-2605-3)
LOS ALAMOS MOLTEN PLUTONIUM REACTOR EXPERIMENTS
core design for fuel burnup studies, 20: 12403 (LA-3384)
LUBRICATION
theory for, liquid-metal, 20: 10973 (TID-21992)
LUMINESCENCE
conference, 20: 11371
LUMINESCENT DETECTORS
design of, using powdered lithium fluoride in Teflon capsules, for internal gamma dosimetry, 20: 11091(R) (BNWL-122, pp 67-72)
performance for medical uses, 20: 11155
properties and uses of phosphate–glass, in dosimetry, 20: 11140
LUNGS
effects of inhaled plutonium-239 oxide particles on, pathological, 20: 10596(R) (BNWL-122, pp 1-15)
oxygen exchange in alveoli and capillaries of, 20: 10547
radiation dose to, from inhaled uranium ore aerosols, 20: 10514(R) (BNWL-122, pp 21-4)
radiography of, effects of deposited rare earth dusts on, 20: 11057
LUTETIUM
separation from other elements by solvent extraction using TBP, 20: 10952
separation from ytterbium by ion exchange at 90°C, 20: 10760 (IS-1305)
solvent properties for tantalum, thermodynamics of, 20: 11306
thermal conductivity at 2 to 100°K, (E), 20: 11329
LUTETIUM CARBONATES
complexes of, composition in solution of, 20: 10824
LUTETIUM SELENIDES
CaSe–Lu_2Se_3, phase studies, 20: 10857
LYMPH CELLS
radiation effects on rat, after diphtheria immunization, 20: 10685
LYMPH SYSTEM
radiation effects on nodes in rat, after diphtheria immunization, 20: 10685
radiation effects on pelvic, after cervical cancer therapy, 20: 10653

M

MACHINE TOOLS
programming of numerically controlled, STRESS postprocessor for, 20: 12546 (SC-RR-65-548)
MAGNESIUM
content in open-ocean silts, 20: 12540(R) (NYO-2882-8)
corrosion by chloride ions, electrochemistry of pitting, 20: 11231 (CEA-R-2815)
corrosion by sea water, sodium chloride, and sodium hydroxide, galvanic, 20: 11230 (BM-RI-6715)
creep of, effects of aluminum and zirconium on, 20: 11313
neutron scattering total cross sections at 12 to 14 Mev, (E), 20: 11949 (AD-625747)
proton reactions with atoms of, production of highly excited hydrogen atoms by charge-exchange, (E), 20: 11471(T)
use as lining in electron beam apparatus, 20: 11418(P)
MAGNESIUM ALLOYS
corrosion by chloride ions, electrochemistry of pitting, 20: 11231 (CEA-R-2815)
Al–Mg–Zr, creep rates, 20: 11313
Be–Mg, compatibility with carbon dioxide, 20: 11225
In–Mg, positron annihilation in, temperature dependence of, 20: 11678
Li–Mg–Tl, preparation, properties, and structure of intermetallic compound $LiMg_2Tl$ in, 20: 11282 (UCRL-12119-T)
Mg–Sn, tin-119 Mössbauer effect in, 20: 12285
Mg–Th, ductility in, mechanisms of, 20: 11301
MAGNESIUM CESIUM NITRATES
He-3–$MgCe(NO_3)_5$, thermal relaxation time at low temperatures, (E), 20: 11922
MAGNESIUM CHLORIDES
$MgCl_2$–NaCl, corrosive effects on titanium-base alloys at 550 to 600°F, stress, 20: 11227
MAGNESIUM COUPLES
graphite/Mg, corrosion pitting by chloride ions, 20: 11231 (CEA-R-2815)
Mg/Pt, corrosion pitting by chloride ions, 20: 11231 (CEA-R-2815)
Mg/stainless steel, corrosion pitting by chloride ions, 20: 11231 (CEA-R-2815)
MAGNESIUM IONS
energy levels of, (T), 20: 11450 (UCRL-7842-T)
MAGNESIUM ISOTOPES Mg-24
alpha reactions (α,d) at 42 to 53 Mev, deuteron energy spectra from, (E), 20: 12061
deuteron elastic scattering at 7.8 Mev by, cross sections for, (E), 20: 12095
proton inelastic scattering at small angles, (E), 20: 12003(T)
MAGNESIUM ISOTOPES Mg-25
deuteron elastic scattering at 7.8 Mev by, cross sections for, (E), 20: 12095
energy levels, (T), 20: 12002
MAGNESIUM ISOTOPES Mg-26
alpha reactions (α,d) at 42 to 53 Mev, deuteron energy spectra from, (E), 20: 12061
deuteron elastic scattering at 7.8 Mev by, cross sections for, (E), 20: 12095
MAGNESIUM ISOTOPES Mg-28
production in bremsstrahlung reactions (γ,2p) with silicon-30 at 51.4 Mev, cross sections and yield curves for, (E), 20: 12094
MAGNESIUM LANTHANUM NITRATES
rare-earth ion spin-lattice relaxation in, (E), 20: 12300
MAGNESIUM OXIDES
compatibility with urania, 20: 11224
electron spin resonance spectra of spin-1 ions in, Jahn-Teller effects in, 20: 12294
mechanical properties of, effects of grain boundaries on, 20: 11227
radioinduced swelling of, fission fragment, 20: 11227
tensile strength for machining, effects of PVA binders on, 20: 11277 (RFP-659)
MAGNESIUM SULFATES
$MgSO_4$–Na_2SO_4, effects of sulfur-35 on exchange reactions in, 20: 10936(T) (CEA-tr-A-1855)
MAGNET COILS
insulation structure effects on performance of, 20: 11387 (CONF-650922-28)
shunt resistor for paralleling large, design of variable, 20: 11388 (CONF-650922-29)
training effect in multilayer superconducting, (E), 20: 11895
MAGNETIC FIELDS
calculations for 100-Mev FFAG accelerators, 20: 11391 (NP-15274)
charged-particle beam bending in, space-charge effects on, (T), 20: 11378 (AD-626633)
charged-particle Brownian motion in fluids in crossed electric and, (T), 20: 11802
configuration of dipole-interplanetary transition-region, effects of polar disturbances on, (E), 20: 11827
determination in theta-pinch plasmas using lasers, (E), 20: 12164 (ARL-65-129)
effects of longitudinal, on h-f discharge initiation in rare gases, (E/T), 20: 11780
effects of transverse, on electric discharge in vacuum, (E), 20: 11769 (LGI-65/30)
effects of uniform increasing, on ionization of hydrogen and nitrogen, (E), 20: 11768 (JUL-327-PP)
effects of uniform, magnetohydrodynamic viscous fluid flow in spherical envelope, (T), 20: 11777
effects of weak, on viscous fluid flow, (T), 20: 11776

effects on convective heat transfer in turbulent conducting fluid flow in channels, 20: 11793
effects on hydromagnetic flow against rotating disks, 20: 11778
effects on radioinduced chromosomal aberrations, 20: 10672
effects on surface superconductivity, (T), 20: 11891 (COO-264-224)
electron focusing in accelerating, (T), 20: 11399 (UCRL-7566(Rev.1))
plasma acceleration in external, resonance conditions for, (T), 20: 12196
plasma acceleration in external, resonance conditions for, (T), 20: 12197
plasma containment in sustained theta pinch, (E), 20: 12161 (65RL-3940E)
plasma containment and stability in toroidal, 20: 12174 (MPI-PAE/P1.6/65)
plasma containment in permanent dipole, stable, (E), 20: 12202
plasma flow in, free-streaming pulsed, (E), 20: 12235
positron focusing in accelerating, (T), 20: 11399 (UCRL-7566(Rev.1))
structure of interplanetary, correlations with solar flare proton flux, (E), 20: 11852
trapping in superconductors, r-f, 20: 11926

MAGNETIC MIRROR MACHINES
design using quadrupole fields, 20: 12163(R) (AD-625424)
electron cyclotron heating in, (T), 20: 12163(R) (AD-625424)
electron velocity distribution from, system for measuring, 20: 12163(R) (AD-625424)
plasma column end effects in Q-1 device, (T), 20: 12236
plasma compression in, boundary condition effects in, (E), 20: 12238
plasma free-streaming experiments in Q device, (E), 20: 12235
plasma instabilities in, critical length determination for convective-loss-cone, (T), 20: 12233

MAGNETIC MIRRORS
electron heating in, turbulent, (E), 20: 12206(T)
plasma containment and properties in, (E/T), 20: 12163(R) (AD-625424)
plasma negative-mass instability in, hot proton, (E), 20: 12247

MAGNETIC RESONANCE
crystal lattice effects in electron para-, (T), 20: 12274(R) (COO-578-18)

MAGNETITES
diffraction patterns of powdered, neutron, 20: 12545(R) (PAEC(A)AR651)

MAGNETO-OPTICAL ROTATION
use of laser beam, for determination of plasma magnetic fields, (E), 20: 12164 (ARL-65-129)

MAGNETOHYDRODYNAMIC CELLS
current and potentials for segmented electrode, calculation of, (T), 20: 11539 (65RL-3888E)
design of miniature, for production of short high-energy pulses, 20: 11550(P)
electric discharges in closed-cycle, properties of, (E/T), 20: 11541 (AERE-R-5107)
magnet system designs for, 20: 11548
plasma instability in vertical field, gravitational, (T), 20: 11538 (65RL-3814E(Rev.))
thermodynamic analysis of, 20: 12421

MAGNETOHYDRODYNAMICS
electric-field distribution in flow of isotropic fluid with alternating conductivity, (T), 20: 11803
fluid flow in integral methods for, 20: 11792
fluid flow in spherical envelope, equations for, (T), 20: 11776
fluid flow in spherical envelope in, (T), 20: 11777
fluid flow in, damping of homogeneous turbulence in, (T), 20: 11804
fluid flow in, plane, (T), 20: 11791
fluid flow in, theory of laminar boundary layer in, 20: 11790
fluid flow near stagnation point, two-dimensional inviscid, (T), 20: 11795
hydromagnetic flow against a rotating disk, equations for, 20: 11778
plasma waveguide excitation by coaxial waveguide, 20: 12208
properties of liquid metals, (T), 20: 11771(T) (NP-tr-1346)
stability in, effect of energy dissipation and temperature dependence of transfer coefficients on, (T), 20: 11794
theory for ideal conductors, general relativistic, 20: 11772

MAGNETOMETERS
signal analysis of free nuclear precession, for geomagnetic field measurements, 20: 11817(T)

MAGNETOSPHERE
charged-particle acceleration by electromagnetic fields in, (T), 20: 11837
charged-particle interactions with fields of, (T), 20: 11849
electron and proton stable trapping in, limiting fluxes of, (T), 20: 11820
electron trapping in dark, low-energy, 20: 11823
solar wind effects on boundary on, (T), 20: 11838
variations in tail of, correlations with radiation-belt changes during magnetic storms, (E), 20: 11831

MAGNETS
charged-particle beam transport in deflecting systems of, symmetry properties for, (T), 20: 11411
design for CEA beam bypass system, 20: 11383 (CEAL-TM-152)
design for magnetohydrodynamic generators, 20: 11548
pole shoe assembly design for, 20: 11423(P)

MAIZE
radiation effects on growth and pH in seedlings of, effects of dose on β, 20: 10683
radiation effects on genetic variability in, 20: 10603(R) (IAEA-2466-11)
radiation effects on development and growth of, by seed exposure to gamma, uv, and x rays, 20: 10613(T) (NP-tr-1344)

MALEIMIDE
N-(*N*-acetyl-4-sulfamoyl)-, reactions between cysteine and sulfur-35-labeled, 20: 10937(T) (NP-tr-1323)
substituted, preparation of sulfur-35-labeled, 20: 10937(T) (NP-tr-1323)

MALEIMIDE, *N*-ETHYL-
radiosensitivity effects on chromosomes in Vicia roots, 20: 10624

MALIC ACID
production in gamma radiolysis of aqueous fumaric acid, 20: 10875

MAMMALS
radiation effects on, review of genetic, 20: 10688

MAMMARY GLAND
therapy of carcinomas of, by yttrium-90 pituitary destruction, 20: 10752

MAN
analysis for plutonium and uranium, design of counter for, 20: 11107 (RFP-462)
calcium-45 uptake by respiratory tract in, combined thallium-204 and, 20: 10546
cesium-137 content in, in Alaska, whole-body, 1964, 20: 10718(R) (BNWL-122, pp 172-5)
cesium-137 content in Alaskan, whole-body, 1965, 20: 10723
effects of leukemia on metabolism of children, 20: 10545
excretion of β-aminoisobutyric acid, 20: 12545(R) (PAEC(A)AR651)
gamma-globulin metabolism in, tracer study, 20: 10571
gamma-globulin metabolism in a gamma globulinemic, tracer study, 20: 10572
hyperthyroidism in, therapy in children, 20: 10738
iodine-131 uptake by thyroid gland of, from milk, 20: 10530(R) (BNWL-122, pp 113-17)
iodine-131 whole-body incorporation and retention in, inhibition of, 20: 10543
pathology of berylliosis in, 20: 11038
radiation doses to, 1951 to 1960, evaluation of, 20: 11015
radiation effects on, from thermonuclear explosions, 20: 10701
radiation effects on creatine excretion by, 20: 12545(R) (PAEC(A)AR651)
radiation effects on blood picture in, 20: 10660
radiation hazards to, in space flight, 20: 10719(T) (NASA-TT-F-353, pp 3-20)
radiation protection of, in contaminated environments, 20: 11039
radiosensitivity of tumors in, effects of antinomycin on, 20: 10700
thallium-204 uptake by respiratory tract in, combined calcium-45 and, 20: 10546

MAN (STANDARD)
chemical composition of organs and tissues, 20: 10698

MANGANESE
content and deposition in open-ocean silts, 20: 12540(R) (NYO-2882-8)
separation from salts by solvent extraction using 8-mercaptoquinoline in chloroform, 20: 10759 (INP-427/C)
separation from solutions of bone, milk, and teeth ash by solvent extraction using sodium diethyldithiocarbamate, tracer studies of, 20: 10950

MANGANESE ALLOYS
Mg–Zn, phase studies by neutron diffraction, 20: 12545(R) (PAEC(A)AR651)

MANGANESE CHLORIDES
separation from salts by extraction chromatography using organic phosphorus compounds, 20: 10759 (INP-427/C)

MANGANESE COMPLEXES
with methylenephosphonic acid derivatives, preparation and properties of, 20: 12533 (COO-1020-6)

MANGANESE ISOTOPES Mn-54
content in fallout, 1964, 20: 11018

MANGANESE ISOTOPES Mn-55
ion reactions with, copper recoil ions from heavy, (E), 20: 12085
neutron reactions (n,γ) at 200 to 525 ev, multiple scattering in, (T), 20: 11967 (JINR-P-2455)

MANGANESE NITRATES
nitrogen-14 NMR in, (E), 20: 12325

MANGANESE STEEL
Mn–Mo, radiation hardening of A302B, effects of irradiation temperature on fast-neutron, 20: 11342 (EURAEC-1502)
Mn–Mo, radiation effects on impact strength of A-302B, combined stress and fast neutron, 20: 11227
Mn–Mo, thermal stress fatigue of A-302B, 20: 11227

MARITIME PRESSURIZED WATER REACTOR
containment leak rate testing, 20: 12473 (TID-22459)

operation, May–Aug. 1964, 20: 12474(R) (TID-22460)
MARITIME REACTORS
design of German pressurized-water, 20: 12463 (CONF-640810, pp 138-55)
design of Japanese, 20: 12462 (CONF-640810, pp 122-37)
development of NERO, 20: 12490
development of NERO, 20: 11355
economics, 20: 12459 (CONF-640810, pp 1-6)
fuel element fabrication and testing for, 20: 12397(R) (EURAEC-1506)
fuel element testing for Vulcain, (E), 20: 12396(R) (EURAEC-1505)
research, 20: 12461 (CONF-640810, pp 105-6)
MASERS
resonant modes for, quantum electrodynamics in theory of, 20: 11878
MASERS (OPTICAL)
beam interactions with electrons, energy spectra and polarization from Compton, (T), 20: 11667
beam interactions in plasma, quantum theory for, (T), 20: 12246
beam reactions in air, plasma production in, (T), 20: 12190
beam reactions with metals, energy and intensity of ions from, (E), 20: 11463
development using highly ionized plasma, 20: 12209
effects on nuclear decay processes, (E/T), 20: 12102
performance for magnetic field determination in theta-pinch plasma, (E), 20: 12164 (ARL-65-129)
radiation effects on gallium arsenide diode, gamma, 20: 11178
radiation emission from gaseous, interactions with matter, 20: 11470
use for plasma electron density measurements, (E), 20: 12165 (ARL-65-135)
use in determining electron time-of-flight in photomultiplier tubes, 20: 11071
use in plasma diagnostics, (E), 20: 12163(R) (AD-625424)
use of hydrogen, for determining hyperfine separation of deuterium, (E), 20: 11481
uses in welding, 20: 11260
MASS LAW
for nuclides, (T), 20: 12090
MASS SPECTROMETERS
design and construction of time-of-flight, 20: 11072
design and uses of time-of-flight, 20: 10790
design and uses of time-of-flight, 20: 10791
ion source for, current-voltage characteristics of Penning, 20: 11077
performance of multiphase, 20: 11192 (SGAE-PH-30/1965)
use for measurement of isotopic composition of samples, elimination of errors in, 20: 10793
MATERIALS TESTING
for space vehicles, 20: 11520
fracture toughness of ceramics and metals, effects of geometry on, 20: 12555 (WAPD-T-1828)
methods for, development of nondestructive, 20: 11260
neutron radiography procedure for, 20: 11005(P)
use of acoustic emission for, of overstress in reactor pressure systems, 20: 11001 (BNWL-SA-438)
MATERIALS TESTING REACTOR MOCKUP
neutron flux measurements in, fast and thermal, (E), 20: 12501 (ORNL-TM-1163)
MATHEMATICS
Boolean logic combinatorial switching in, duality theorem for, (T), 20: 11198(R) (COO-614-34, Sect. IIIB)
Cartesian tensors in spaces with indefinite metric for relativity theory, 20: 11879
differential equations in, numerical solution to initial valve, (T), 20: 12529 (BNL-8798)
diophantine inequalities in, generating functions for solving, (T), 20: 12528 (BNL-8694)
functions of noncommuting operators, expansions of exponential, 20: 11209
Lagrange multiplier problems in, numerical solutions for, (T), 20: 12544 (ORNL-3846)
Lie groups in elementary-particle physics, Casimir operators of, (T), 20: 11609
Lie groups in, representations of semisimple, 20: 11721
operator equations in, extension and solution of nonlinear, (T), 20: 11197(R) (COO-614-34, Sect. IIIA)
potential equations in, solution of boundary value using boundary coverings, 20: 11200 (HMI-B-41)
unnormalized, computer study of, 20: 11196(TR) (COO-614-34, Sect. IIB)
MATING
radiation effects on, of Drosophila, x, 20: 10644
MATTER
distributions of, dynamics and stability of spherically-symmetric, 20: 11889
radiation interactions with, laser, 20: 11470
radiation reactions with, equations for, 20: 11889
MEATS
cesium-137 content of caribou, effects on radioactivity of diet in Alaska, 20: 10723
radiation effects on vitamin B_{12} in, effects of lyophilization on γ, 20: 11185
radioactivity in caribou, in Alaska, 1964, 20: 10718(R) (BNWL-122, pp 172-5)
MECHANICS
gauge transformations and complex space-time for classical fields in, 20: 11373
Lagrange multiplier problems in, numerical solutions for, (T), 20: 12544 (ORNL-3846)
Weyl correspondence between quantum and classical systems, mathematics of, 20: 11876
MEDICINE
research in, uses of reactors in, 20: 10507
MEMBRANES
radiation effects on erythrocyte, in newborn rats, 20: 10589
vibration of L-shaped, method for analysis of, 20: 11206 (TID-22529)
MERCAPTO GROUP
effects on fluorescence of europium and terbium dipyridyl complexes, 20: 10842
MERCHANT VESSELS
nuclear-powered, design of German, 20: 12463 (CONF-640810, pp 138-55)
nuclear-powered, economics of, 20: 12459 (CONF-640810, pp 1-6)
nuclear-powered, licensing of, 20: 12464 (CONF-640810, pp 156-65)
nuclear-powered, research on, 20: 12458 (CONF-640810)
nuclear-powered, role of, 20: 12460 (CONF-640810, pp 7-21)
MERCURY
corrosive effects on type 316 stainless and 9 chromium–1 molybdenum steels at 1250°F, 20: 11214(R) (NASA-CR-54717)
electromagnetic wave scattering resonances in plasma of, a-c resonant probe relation to, (T), 20: 12241
erosive effects on turbine blade and nozzle materials at 640°F, 20: 11214(R) (NASA-CR-54717)
photoelectric cross section of, (E), 20: 11516
reactions with metal hydrides, review on, 20: 10812 (NAA-SR-Memo-11569)
sorptive properties for 3-pentanol and 3-pentanone, effects of molecular symmetry on, 20: 12536 (IS-T-66)
MERCURY ALLOYS
Cd–Dy–Hg, phase studies, 20: 11317
Cd–Hg, superconducting transition temperature of, effect of ordering on, (E), 20: 11914
Hg–Rb, formation and properties of, 20: 11215(R) (NASA-CR-54718)
Hg–Y–Zn, phase studies, 20: 11317
In–Hg, magnetic properties of superconducting, containing iron particles, 20: 11894
MERCURY CHLORIDES
corrosive effects on molybdenum, tungsten, and vanadium at 35, 60, and 100°C, 20: 11230 (BM-RI-6715)
corrosive effects on vanadium-base alloys at low temperatures, 20: 11230 (BM-RI-6715)
MERCURY IONS
production of, r-f source for, 20: 11374
MERCURY ISOTOPES Hg-197
use as tracer for brain tumor localization, 20: 10733
MESIC ATOMS
fission of plutonium-239 (μ), by radiationless transitions, (E), 20: 12041
x-ray emission from (μ^-), isotope effects on K, (E), 20: 11480
x-ray emission from (μ), computer analysis of, 20: 11440(R) (COO-614-34, Sect. IID)
MESIC MOLECULES
wave functions for (pμd), nucleon-deuteron capture cross section from, (T), 20: 11493
MESONS
decay of spin-0 and -1, forbidden configurations for 3-photon, (T), 20: 11686 (JINR-P-2447)
decay of, $\Delta S = 1$ leptonic, (T), 20: 11659
decays of vector, U(6) current algebra for, (T), 20: 11750
electromagnetic properties in broken SU(6) symmetry, (T), 20: 11727(T)
energy loop of charged vector, Lagrangian field theory for self-, (T), 20: 11749
exchange of heavy, in nucleon-nucleon interactions, (T), 20: 11597
form factors for, in SL(6,c) symmetry, (T), 20: 11683 (JINR-E-2475)
interactions of scalar, determinantal method for N/D equations for, (T), 20: 11700
interactions with baryons, spurion scheme of broken U(L12) symmetry for, 20: 11735
model for spin-2, in SL(6) symmetry, 20: 11734
motion of vector, in Coulomb field, (T), 20: 11668
photoproduction of vector, amplitude for, (T), 20: 11595

photoproduction on nucleons, SU(6) symmetry for, (T), 20: 11581(T)
photoproduction on nucleons, SU(6) sum rules for, (T), 20: 11635
quark model for, SU(6) symmetry in, (T), 20: 11657
symmetries for systems of, current algebras for, (T), 20: 11748
MESONS, RESONANCE
decay of A_1 and A_2, (E), 20: 11616
mass and width of K*, self-consistent calculation of, 20: 11669
model for, relativistic composite quark, (T), 20: 11684 (JINR-P-2442)
production in meson (π) interactions, Faddeev equations for, (T), 20: 11568 (UCRL-11749)
production in three-body meson (π) interactions, model for relativistic, (T), 20: 11641
production of (740), in meson (π^-)–(π^+) interactions, (T), 20: 11555 (DESY-65/13)
production of $C^0(1215)$, $D^0(1290)$, and $E^0(1410)$ in proton-antiproton annihilations, (E), 20: 11575
production of E, in relativistic three-body meson (π) interactions, (T), 20: 11640
production of N*(1238), in meson (π^+)-proton interactions at 2 Bev/c, (E), 20: 11672
properties and symmetry of f*(1500) and K**(1410), 20: 11552 (CONF-651015-3)
properties of η'(960) and ϕ(1020), review of, 20: 11552 (CONF-651015-3)
MESONS (η)
decays of, C-violating interactions in, (T), 20: 11634
MESONS (η^0)
decay rates of, vector-meson and ω–ϕ mixing models for 2γ and $\pi\pi\gamma$, (T), 20: 11603
production in meson (π^+)-proton interactions at 2 Bev/c, (E), 20: 11672
MESONS (K)
decay of, branching ratios for leptonic, (T), 20: 11658
decay of, charge asymmetry in radiative 2π, (T), 20: 11584(T)
form factors for, meson (ϕ) contribution to, (T), 20: 11598
interactions with mesons (K) and (π), resonance production in, (E), 20: 11575
interactions with mesons (π), iterative self-consistent solutions for S-wave, 20: 11601
interactions with nucleons, $Y_0^*(1815)$ production from, (T), 20: 11632
interactions with mesons (π), p- and s-wave phase shifts for, (T), 20: 11648
interactions with mesons (π), meson (K_{e4}) decay for analysis of low-energy s-wave, (T), 20: 11654
MESONS (K^-)
capture by bromine at 600 Mev/c, hyperons (Λ) production and trapping in, (E), 20: 12092
capture by deuterium, Y* production in, (T), 20: 11599
interactions with protons, $J^P = \frac{1}{2}^+$, Y = 0, I = 0 and 1 octet in strong, (T), 20: 11592
interactions with deuterons below 300 Mev/c, effects of $\bar{K}^0$–K^- and n-p mass differences on, (T), 20: 11630
interactions with protons, angular distributions from phase shifts for, (T), 20: 11648
interactions with neutrons at 828 to 1112 Mev/c, $Y_1^*(1765)$ resonance in, (E), 20: 11656
interactions with protons at 900 to 1100 Mev/c, Y*(1765) and $Y_0^*(1815)$ from, (E), 20: 11551 (CONF-650337-3)
interactions with protons, properties of meson resonance produced in, 20: 11552 (CONF-651015-3)
interactions with protons, hyperon (Ω^-) spin-parity from, (T), 20: 11563 (JINR-P-2456)
reactions with emulsion nuclei, review on, 20: 11991
MESONS (K^0)
decay of K_2^0, relative probability for $e\pi\nu$, (E), 20: 11560 (JINR-P-2449)
decay of K_2^0, 2π, (E/T), 20: 11554 (COO-1195-27)
decay of, CP invariance in 2π, (T), 20: 11608
decay of, relative probability of 3π, (E), 20: 11561 (JINR-P-2450)
decay of, testing of time-reversal invariance by, (E), 20: 11662
mass difference (K_1^0–K_2^0), (E), 20: 11661
MESONS (K^+)
decay ($\pi^+ + \pi^0 + \gamma$), upper limit for, (E), 20: 11675
photoproduction on protons, (E), 20: 11676
MESONS (K_{e4})
decay of, s-wave meson (K)-meson (π) interactions in, (T), 20: 11654
MESONS ($K_{\mu 3}^0$)
decay of, relative probability of, (E), 20: 11561 (JINR-P-2450)
MESONS (μ)
capture by nuclei, (T), 20: 12100
decay in spark chambers, on-line measurement of electron momenta spectra in, 20: 11553(R) (COO-614-34, Sect. IIC)
decay of, beta spectra calculation in, (E), 20: 11093(R) (COO-614-34, Sect. IIA)
decay of, modified vector-boson propagator for leptonic, (T), 20: 11588
interactions above 10^{12} ev, model for, (T), 20: 11558 (JINR-E-2496)
pair production in meson (ρ^0), (ω), and (ϕ) decay, branching ratios for, (E), 20: 11673
MESONS (μ^-)
capture by calcium, gadolinium, oxygen, and tin, isotopic shift of K x-ray transitions in, (E), 20: 11480
decay of, weak neutrino current hypothesis for angular asymmetry of, (T), 20: 11578
MESONS (μ^+)
decay of, weak neutrino current hypothesis for angular asymmetry of, (T), 20: 11578
polarization for studying chemical-reaction mechanisms, 20: 11377
MESONS (ω)
decay of, branching ratios for lepton-pair, (E), 20: 11673
photoproduction on nucleons, angular distributions for, (T), 20: 11595
MESONS (ω^0)
production in meson (π^+)-proton interactions at 2 Bev/c, (E), 20: 11672
production in meson (π) interactions, Faddeev equations for, (T), 20: 11568 (UCRL-11749)
MESONS (ϕ)
decay of, branching ratios for, (E), 20: 11619
decay of, branching ratios for lepton-pair, (E), 20: 11673
interactions with nucleons, coupling constant for, (T), 20: 11598
properties of, review of, 20: 11552 (CONF-651015-3)
MESONS (π)
exchange effects of, on deuteron electromagnetic structure, (T), 20: 11651
interactions of, effects on potential for nucleon three-body interactions, (T), 20: 11650
interactions with nucleons at 290 to 905 Mev, cross sections for N* production in, (T), 20: 11562 (JINR-P-2454)
interactions with mesons (K) and (π), resonance production in, (E), 20: 11575
interactions with nucleons, self-consistency conditions for πNN-vertex function in, (T), 20: 11576
interactions with nucleons, triangle graphs for three-particle production in, (T), 20: 11596
interactions with nucleons, meson (ϕ)-nucleon coupling in, (T), 20: 11598
interactions with mesons (π) and nucleons, ABC anomaly for amplitudes of, (T), 20: 11604
interactions with mesons (π), model analysis for, (T), 20: 11637
interactions with mesons (π), relativistic calculation for three-body, (T), 20: 11639
interactions with mesons (π), resonance from relativistic three-body, (T), 20: 11640
interactions with mesons (π), relativistic spinless resonances in three-body, (T), 20: 11641
interactions with nucleons, Regge poles for, (T), 20: 11647
interactions with mesons (K), p- and s-wave phase shifts for, (T), 20: 11648
interactions with mesons (π), momentum-space calculation for meson (ρ) exchange in, (T), 20: 11653
interactions with mesons (K), meson (K_{e4}) decay for analysis of low-energy s-wave, (T), 20: 11654
interactions with mesons (π), amplitudes for, (T), 20: 11694
interactions with nucleons, self-consistent methods for vertex functions for, (T), 20: 11730
interactions with mesons (π), meson (ω^0) and resonance production in, (T), 20: 11568 (UCRL-11749)
interactions with mesons (K), iterative self-consistent solutions for S-wave, 20: 11601
interactions with nucleons, N/D calculation with inelastic unitarity for, (T), 20: 11643
photoproduction on nucleons, one-particle exchange theory of, 20: 11572
production and absorption of s-wave, in proton-proton interactions, (T), 20: 11642
MESONS (π^-)
effects on γ–γ scattering, (T), 20: 11600
interactions with mesons (π^+) below 1.3 Bev, phase shifts for elastic, (T), 20: 11555 (DESY-65/13)
interactions with nucleons at low energies, cross sections for scalar, (T), 20: 11574
interactions with protons, scalar model for branching ratio of $n\pi$ and $n\gamma$, (T), 20: 11574
interactions with protons, resonance model for low-energy, (T), 20: 11589
interactions with protons, fermion Regge trajectories for, (T), 20: 11590
interactions with nucleons in emulsions at 16.3 Bev, angular distributions from, (E/T), 20: 11602
interactions with protons at high energies, charge-exchange, (E), 20: 11614
interactions with protons at high energies, charge-exchange, (T), 20: 11615
interactions with protons, test for Regge behavior in backward, (T), 20: 11663

interactions with protons at 1.70 to 2.50 Bev/c, charge exchange in, (E/T), 20: 11664
interactions with protons, decay of mesons (ρ^0), (ω), and (ϕ) from, (E), 20: 11673
interactions with protons, forward amplitude for, (T), 20: 11697
production in neutron-proton interactions at 600 Mev, angular distributions and cross sections for, (E), 20: 11564 (JINR-P-2462)
reactions with emulsion nuclei at 16.3 Bev, angular distributions from, (E/T), 20: 11602
use in radiotherapy, 20: 10736

MESONS (π^0)
decay of, detection of photons in, 20: 11099 (JINR-P-2436)
decay of, three-photon, (E), 20: 11587(T)
decay rates of, vector-meson dominant and ω–ϕ mixing models for 2γ, (T), 20: 11603
production in meson (K^+) decay ($\pi^+ + \pi^0 + \gamma$), upper limit for, (E), 20: 11675
production in neutron-proton interactions at 600 Mev, cross sections for, (E), 20: 11564 (JINR-P-2462)

MESONS (π^+)
effects on γ–γ scattering, (T), 20: 11600
interactions with mesons (π^-) below 1.3 Bev, phase shifts for elastic, (T), 20: 11555 (DESY-65/13)
interactions with protons at 4 and 8 Bev, absorptive corrections to nucleon exchange term in, (T), 20: 11573
interactions with protons at 2.75 Bev/c, exchange mechanism for $p\pi\pi n$, (E/T), 20: 11605
interactions with protons, test for Regge behavior in backward, (T), 20: 11663
interactions with protons at 2 Bev/c, cross sections for inelastic, (E), 20: 11672
interactions with protons, forward amplitude for, (T), 20: 11697
interactions with protons at 8 Bev/c, resonances in, (E), 20: 11616
photoproduction on helium-3 at 180 to 260 Mev, cross sections for, (E), 20: 12046
production in meson (K^+) decay ($\pi^+ + \pi^0 + \gamma$), upper limit for, (E), 20: 11675
production in neutron-proton interactions at 600 Mev, angular distributions and cross sections for, (E), 20: 11564 (JINR-P-2462)
reactions with lead at 15 Bev/c, meson (ρ) production in, (E), 20: 11618

MESONS (ρ)
decay, (E), 20: 11616
decay of, charge asymmetry in radiative 2π, (T), 20: 11584(T)
decay of, partial width for $\pi\gamma$, (E), 20: 11618
exchange effects of, on deuteron electromagnetic structure, (T), 20: 11651
exchange in meson (π)-meson (π) interactions, momentum-space calculation for, (T), 20: 11653
width of, from $\pi\pi$ elastic interaction phase shifts, (T), 20: 11555 (DESY-65/13)

MESONS (ρ^0)
decay of, branching ratios for lepton-pair, (E), 20: 11673
production in meson (π^+)-proton interactions at 2.75 Bev/c, (E/T), 20: 11605
production in meson (π^+)-proton interactions at 2 Bev/c, (E), 20: 11672

MESONS (ρ^+)
production in meson (π^+)-proton interactions at 2 Bev/c, (E), 20: 11672

MESONS (X^0)
decays of, C-violating interactions in, (T), 20: 11634
properties of, review of, 20: 11552 (CONF-651015-3)

METABOLIC DISEASES
plasma protein metabolism in patients with, tracer study, 20: 10570

METABOLISM
effects of leukemia on, in children, 20: 10545
research on protein, criteria for, 20: 10563
tracer techniques for research on, nitrogen-15, 20: 10560

METAL COATINGS
bonding strength of vapor-deposited, tensile tester for measuring, 20: 11063 (RFP-672)

METAL COMPACTS
packing efficiency of, equations for, 20: 11260

METAL-FOIL DETECTORS
use for nondestructive determination of burnup in nuclear fuel, 20: 11004

METALLIC FILMS
electron interaction effects from superimposed magnetic and superconducting, (E), 20: 11918

METALLIC FILTERS
cleaning of porous, in fluidized beds, 20: 10810 (JEN-153-DMa/I-19)

METALLIC FOILS
performance of neutron-sensitive, in pocket ion chambers, 20: 11119
use of high-atomic-number, in plastic scintillators for gamma detection, 20: 11165(P)

METALLOGRAPHY
cutting uranium-base ceramic crystals, electrolytic jet machining method for, 20: 11216 (PEL-79)

METALLURGY
microstructural examination in, evaluation of, 20: 11275 (ORNL-TM-1338)

METALS
dislocation climb in, efficiency of, 20: 11274 (NYO-3504-2)
dispersion-strengthened, bibliography on, 20: 11278 (RISO-48(Suppl.2))
effects of precious, on solubility and drip temperature of fission products in Purex process wastes, 20: 12517(R) (BNWL-170)
electron scattering in, cross section for free, (T), 20: 12284
electroosmosis in liquid, mechanism of, (T), 20: 11289(T) (IS-Trans-26)
fracture toughness testing, effects of geometry on, 20: 12555 (WAPD-T-1828)
heat transfer in boiling liquid, review of, 20: 10999
laser-beam reactions with, energy and intensity of ions from, (E), 20: 11463
lubricity of liquid, in coupled rotor-bearings, 20: 10973 (TID-21992)
magnetohydrodynamic properties of liquid, (T), 20: 11771(T) (NP-tr-1346)
overstress in, use of acoustic emission for detection of, 20: 11001 (BNWL-SA-438)
plastic deformation of, theory of, 20: 11331
positron thermalization in, (E), 20: 11660
radiation effects on, specimen holder for investigating deuteron, 20: 11410
strengthening by irradiation, 20: 11366

METEORITES
analysis for krypton and xenon isotopes for indication of fission, neutron capture, and spallation anomalies, (E/T), 20: 11424 (NP-15629)
krypton and xenon content in chondrules and minerals of Bruderheim, 20: 11430
nuclear reactions in, krypton and xenon isotopic content as indicators of, (E/T), 20: 11424 (NP-15629)
proton reactions at 1 to 3 Bev, cascades in, (E), 20: 12262 (BNL-8721)
proton reactions with nuclei in, 20: 11377

METEOROLOGY
effects of precipitation and temperature on plant communities, 20: 10510 (BNL-9835)
program for reactor sites, 20: 12333

METHACRYLIC ACID, METHYL ESTER POLYMERS
design of Lucite light pipes for gamma cameras, thickness optimization for, (T), 20: 11079
neutron moderation by, at 20, 77, and 300°K, (E), 20: 11944
proton reactions at 1 Bev, cascades in, (E), 20: 12262 (BNL-8721)

METHANE
effects on carbon dioxide–graphite reactions at 960 to 1200°C, 20: 10859
thermal diffusion of carbon-13-labeled, enrichment in, 20: 11194

METHANE, NITRO-
complexes with uranyl perchlorate, preparation of, 20: 10825

METHANESULFONIC ACID, ETHYL ESTER
preparation from ethyl iodide and silver methanesulfonate, 20: 10809 (EUR-2531.f)

METHANOL
complexes with uranyl perchlorate, preparation of, 20: 10825
radiolysis of frozen carbon tetrachloride solutions of, formation of stabilized radicals in, 20: 10879

METHYL SULFOXIDE
effects of bone marrow preserved with, on radioinduced lesions in dogs, 20: 10706

METHYLENE BLUE
radiolysis of aqueous solutions of, with and without formate ions, 20: 10925

MICE
cerium-144 removal from, using TTHA chelates, 20: 10556
cystamine uptake by thymus cells of, *in vivo* and *in vitro*, 20: 10708
effects of ingested deuterium oxide on sterility of, 20: 10550
effects of irradiated *Schistosoma japonicum* cercariae on, 20: 12545(R) (PAEC(A)AR651)
effects of prednisolone on distribution of mycobacterial vaccine in, 20: 10655
effects of thymus on tolerance response in, 20: 10632
glucose uptake by hypothalamus of, tracer study, 20: 10541
gold uptake by hypothalamus of, tracer study, 20: 10541
immune reactions in, effects of Thorotrast on, 20: 10617
immunoresistant sarcoma cells in, 20: 10634
liver response to syngenic and xenogenic tissue transplants, 20: 10505(R) (BNWL-122, pp 146-9)
physiology of appetite inhibition and obesity in, tracer study, 20: 10541
pneumonia incidence in laboratory, 20: 12545(R) (PAEC(A)AR651)
radiation effects on immune reactions to rat tissue transplants in, 20: 10505(R) (BNWL-122, pp 146-9)
radiation effects on, protective effects of heparin against, 20: 10705
radiation effects of thyroid cells in, protective effects of anoxia against,

20: 10710
radiation effects on, protective effects of splenic marrow transplants against, 20: 10713
radiation effects on, protective effects of MEA against, 20: 10714
radiation effects on serum transaminase activity in, x, 20: 12545(R) (PAEC(A)AR651)
radiation effects on biochemical properties of tissue homogenates from, γ, 20: 10577
radiation effects on immunity in, β, 20: 10580
radiation effects on electrophoretic patterns of serum proteins of, β, 20: 10581
radiation effects on amino acid excretion in urine of, β, 20: 10582
radiation effects on corneal epithelia in, 126-Mev proton, 20: 10608(T) (NASA-TT-F-353, pp 142-50)
radiation effects on immune reactions in, γ, 20: 10632
radiation effects on desoxyribonucleotide content in bone marrow, spleen, and thymus of, β and γ, 20: 10633
radiation effects on, model for β, 20: 10640
radiation effects on blood picture and bone marrow in, β, 20: 10641
radiation effects on myocardium in, β, 20: 10643
radiation effects on distribution of mycobacterial vaccine in, 20: 10655
radiation effects on Pseudomonas susceptibility in, x, 20: 10669
radiation effects on urethan-induced tumors in, effects of dose on x, 20: 10671
radiation effects on growth in newborn, effects of dose and strain on, 20: 10673
radiation effects on bacterial population in intestine of, β, 20: 10642
radiation injuries in, protective effects of polysaccharide prepared from yeast cultures, 20: 10703
radiation injuries of, protective effects of anoxia against, effects of age, 20: 10707
radiation injuries in, protective effects of cystamine, 20: 10708
radioinduced leukemia in, after tritium injection, 20: 10623
radioresistant sarcoma cells in, 20: 10634
toxic effects of carbon tetrachloride in, 20: 10548
toxic effects of uranyl nitrate in, 20: 10548
toxicity of TTHA chelates in, 20: 10556
yttrium-91 removal from, using TTHA chelates, 20: 10556

MICHIGAN RESEARCH REACTOR
power level measurements in, calorimetric method for, 20: 12514

MICROÖRGANISMS
effects of, on decomposition of vascular hydrophytes in aquatic ecosystems, 20: 12543(R) (NYO-3018-12)

MICROWAVE EQUIPMENT
hydromagnetic wave scattering by open end of semi-infinite plasma waveguide, 20: 12207
magnetohydrodynamic waveguide excitation by coaxial waveguide, 20: 12208
waveguide space harmonics in linear accelerators, coefficients for iris-loaded, (E), 20: 11393 (NP-15715)

MICROWAVES
emission from plasma, review of nonthermal and thermal, 20: 12256
transmission by plasma in magnetic fields, (T), 20: 12258
use for plasma column, diagnostics beam width of antenna systems in, (E), 20: 12192
use in measurement of plasma ionization rates, 20: 12169 (JUL-322-PP)
use in plasma frequency diagnostics, bridge for, 20: 12249

MILK
cadmium-115 secretion in sheep, 20: 10527(R) (BNWL-122, pp 94-8)
cesium-137 content in German, effects of precipitation on, 20: 11017
iodine-131 content in German, effects of precipitation on, 20: 11017
iodine-131 content of, effects of dietary content of radioactive and stable iodine on, 20: 10530(R) (BNWL-122, pp 113-17)
iodine-131 secretion in sheep, 20: 10517(R) (BNWL-122, pp 52-4)
iodine-131 separation from, field use of ion exchange cartridges for, 20: 10722
iodine-131 uptake from, by human thyroid gland, 20: 10530(R) (BNWL-122, pp 113-17)
production by sheep, tracer study, 20: 10517(R) (BNWL-122, pp 52-4)
separation of manganese from solutions of ashes of, by solvent extraction, 20: 10950
strontium-89 content in German, effects of precipitation on, 20: 11017
strontium-90 content in German, effects of precipitation on, 20: 11017
zinc-65 secretion in sheep, 20: 10527(R) (BNWL-122, pp 94-8)

MINERAL METABOLISM
radiation effects on rat skeletal, tracer study of x, 20: 10587

MITOCHONDRIA
radiation effects on contractive ability of, 20: 10678

MOLECULAR STRUCTURE
book: *The Structure of Atoms and Molecules*, 20: 11512(T)
conference, 20: 12320

MOLECULES
book: *The Structure of Atoms and Molecules*, 20: 11512(T)
electron scattering at low energies by homonuclear diatomic, method for prediction of, (T), 20: 11495
energy levels of, virtual-state, (T), 20: 11439 (BNL-8800)
nuclear spin relaxation for linear, in dilute gases, (T), 20: 11784
spectroscopy of, neutron, 20: 11377
vapor pressure of diatomic, vibrational spectroscopy and isotope effect on, 20: 10831

MOLTEN SALT REACTORS
fuel development for power breeders, 20: 12407 (NEIC-RR-13)

MOLYBDENUM
bremsstrahlung reactions with, heating effects of, (T), 20: 12166 (CONF-651126-1)
coating with copper–silicon eutectic for oxidation protection, 20: 11236
coating with rhenium, electrolytic, 20: 11260
compatibility and encapsulation with neodymium, promethium, and samarium oxides, 20: 11267 (BNWL-SA-488)
compatibility with uranium, 20: 11224
corrosion by ammonium hydroxide, sodium hydroxide, and sodium hypochlorite at 35 and 60°C, 20: 11230 (BM-RI-6715)
corrosion by cesium at 400°C, 20: 11227
corrosion by chloride solutions at 35, 60, and 100°C, 20: 11230 (BM-RI-6715)
corrosion by formic, hydrochloric, and oxalic acids at 35°C, galvanic, 20: 11230 (BM-RI-6715)
corrosion by nitric acid at 35°C, galvanic, 20: 11230 (BM-RI-6715)
corrosion by sea water, sodium chloride, and sodium hydroxide, galvanic, 20: 11230 (BM-RI-6715)
corrosion of, by acids and bases, crevice, galvanic, and spray, 20: 11230 (BM-RI-6715)
crystal structure of single-crystal, effects of plastic deformation on, 20: 11227
deformation of, effects of strain rate on, 20: 11227
deposition from fused salt mixtures, electro-, 20: 11260
determination in fission product and irradiated fuel solutions by controlled-potential coulometry, 20: 10758 (EUR-2618.f)
determination in irradiated uranium dioxide, 20: 10787
diffusion in, self-, 20: 11227
diffusion of boron and carbon in surface of, 20: 11228
diffusion of cobalt and niobium in, coefficient for, 20: 11227
diffusion of uranium in, temperature dependence of, 20: 11290
ductile-to-brittle transition in, effects of grain size and temperature on, 20: 11227
ductility, 20: 11227
effects of alloy additions of, on mechanical properties of niobium, 20: 11302
effects of alloying additions of, on thermal stability of $TiAl_3$, 20: 11335
fracture properties of recrystallized and wrought stress-relieved, 20: 11227
mechanical properties and structure of, effects of hot rolling in air, argon, and vacuum on, 20: 11249
performance as collector electrode for thermionic cells, 20: 11540(R) (AD-626444)
preparation of spherical particles of, by plasma jet atomization, 20: 11219
radiation effects on microstructure of, neutron, 20: 11227
refining of, zone, 20: 11218
sintering procedure for, 20: 11253
sorptive properties for oxygen, (E), 20: 11322
tensile properties of, effects of exposure to cesium at 1200°C on, 20: 11227
tensile properties of, effects of working reduction, stress-relief annealing, and grain size on, 20: 11227
thermodynamic properties, 20: 10816(T) (NASA-TT-F-285)
transition temperature in recrystallized, tensile-ductility, 20: 11227
x-ray spectra of, performance of spectroanalyzer with promethium-147 beta source for K, 20: 11133

MOLYBDENUM ALLOYS
corrosion by inorganic and organic acids at 35, 60, and 100°C, 20: 11230 (BM-RI-6715)
Al–Cr–Co–Fe–Mo–Ni–Ti, stress-rupture properties of Udimet 700, at high temperatures and strain rates, 20: 11265 (AD-626375)
Al–Mo–Sn–Ti–V, fracture toughness properties of titanium-base, effects of heat treatments on, 20: 11273(R) (NRL-6364)
Al–Mo–Ti, fracture toughness of weldments of titanium-base, effects of heat treatments on, 20: 11273(R) (NRL-6364)
Al–Mo–Ti, fracture toughness of plasmarc welds in titanium-base, 20: 11273(R) (NRL-6364)
Al–Mo–Ti, fracture toughness of titanium-base, effects of composition and heat treatments on, 20: 11273(R) (NRL-6364)
Al–Mo–Ti–V, corrosion cracking by salts at 550 to 600°F, stress-, 20: 11227
Al–Mo–Ti–V, thermal stability of, effects of composition on, 20: 11336
Cr–Co–Mo–Ni–W, erosion by mercury vapor at 640°F of Stellite 6B,

20: 11214(R) (NASA-CR-54717)
Cr–Co–Mo–Ni–W, oxidation by air at 1600°F of Stellite 6B, 20: 11215(R) (NASA-CR-54718)
Cr–Fe–Mo–V, erosion by mercury vapor at 640°F of Lapelloy, 20: 11214(R) (NASA-CR-54717)
Ir–Mo, phase studies, 20: 11309
Mo–Fe, electron interaction effects in films of, superimposed on superconducting lead films, (E), 20: 11918
Mo–Nb, creep strength of, effects of composition on, 20: 11302
Mo–Nb, mechanical properties of, effects of composition on, 20: 11288(T) (AD-622477)
Mo–Nb, oxidation by air at 1000 to 1200°C, effects of composition on, 20: 11227
Mo–Nb–W, creep strength of, effects of composition on, 20: 11302
Mo–Ni, short-range order in, x-ray diffuse-scattering determination of, (E), 20: 11325
Mo–Pu–U, analysis for plutonium, review of method for, 20: 10797
Mo–Re, compatibility and encapsulation with neodymium, promethium, and samarium oxides, 20: 11267 (BNWL-SA-488)
Mo–Rh, phase studies, 20: 11309
Mo–Ta, electric conductivity of, effects of composition on, 20: 11227
Mo–Ta, mechanical properties of single-crystal, 20: 11227
Mo–Ta–W, fabrication of tantalum-base, process development for, 20: 11260
Mo–Ti, erosion by mercury vapor at 640°F, 20: 11214(R) (NASA-CR-54717)
Mo–Ti, tensile properties of, effects of working reduction, stress-relief annealing, and grain size on, 20: 11227
Mo–Ti–U, corrosion cracking in air, stress-, 20: 11224
Mo–Ti–Zr, erosion by mercury vapor at 640°F of TZM, 20: 11214(R) (NASA-CR-54717)
Mo–U, corrosion cracking in air, stress-, 20: 11224
Mo–U, crystal structure of tempered, effects of carbon on, 20: 11292
Mo–U, mechanical properties of, effects of strain rate on, 20: 11284 (UCRL-14599)
Mo–U, mechanical properties of, effects of dynamic tensile loads on, 20: 11224
Mo–U, radiation effects on corrosion rate of, by carbon dioxide and nitrogen, reactor, 20: 11224

MOLYBDENUM BROMIDES
thermodynamic properties, 20: 10816(T) (NASA-TT-F-285)

MOLYBDENUM CARBIDES
thermodynamic properties, 20: 10816(T) (NASA-TT-F-285)

MOLYBDENUM CHLORIDES
thermodynamic properties, 20: 10816(T) (NASA-TT-F-285)

MOLYBDENUM COUPLES
Mo/Ni/Nb/stainless steel, diffusion in bimetallic tubing of, with molybdenum and nickel diffusion barriers, inter-, 20: 11215(R) (NASA-CR-54718)
Mo/Ni/Nb–Zr/stainless steel, diffusion in bimetallic tubing of, with molybdenum and nickel diffusion barriers, inter-, 20: 11215(R) (NASA-CR-54718)
Mo/Ni/stainless steel/Ta, diffusion in bimetallic tubing of, with molybdenum and nickel diffusion barriers, inter-, 20: 11215(R) (NASA-CR-54718)

MOLYBDENUM FLUORIDES
thermodynamic properties, 20: 10816(T) (NASA-TT-F-285)

MOLYBDENUM IODIDES
thermodynamic properties, 20: 10816(T) (NASA-TT-F-285)

MOLYBDENUM ISOTOPES
proton reactions (p,n) and (p,p) with, isobaric analog states from, (E), 20: 12078

MOLYBDENUM ISOTOPES Mo-92
neon-20 reactions at 100 Mev, delayed proton emission in, (E), 20: 11964 (JINR-E-2464)
proton reactions (p,n) and (p,p) with, isobaric analog states from, (E), 20: 12078

MOLYBDENUM ISOTOPES Mo-94
neon-20 reactions at 100 Mev, delayed proton emission in, (E), 20: 11964 (JINR-E-2464)
proton reactions (p,n) and (p,p) with, isobaric analog states from, (E), 20: 12078

MOLYBDENUM ISOTOPES Mo-95
proton reactions (p,n) and (p,p) with, isobaric analog states from, (E), 20: 12078

MOLYBDENUM ISOTOPES Mo-96
proton reactions (p,n) and (p,p) with, isobaric analog states from, (E), 20: 12078

MOLYBDENUM ISOTOPES Mo-97
proton reactions (p,n) and (p,p) with, isobaric analog states from, (E), 20: 12078

MOLYBDENUM ISOTOPES Mo-98
energy levels, (E), 20: 12152
proton reactions (p,n) and (p,p) with, isobaric analog states from, (E), 20: 12078

MOLYBDENUM ISOTOPES Mo-99
content in ocean fish, effects of content in sea water on, 20: 11054

MOLYBDENUM ISOTOPES Mo-100
proton reactions (p,n) and (p,p) with, isobaric analog states from, (E), 20: 12078

MOLYBDENUM NITRIDES
thermodynamic properties, 20: 10816(T) (NASA-TT-F-285)

MOLYBDENUM OXIDES
thermodynamic properties, 20: 10816(T) (NASA-TT-F-285)

MOLYBDENUM STEEL
Co–Mo–Ni, mechanical properties of, effects of strain rate on, 20: 11284 (UCRL-14599)
Cr–Mo, carburization by high-carbon sodium at 1200°F, 20: 11235 (COO-65-194)
Cr–Mo, compatibility with boron carbide of AISI 4130, 20: 11226
Cr–Mo, corrosion by flowing sodium at 1000 to 1200°F, equation for, 20: 11227
Cr–Mo, corrosion by mercury vapor at 1250°F, 20: 11214(R) (NASA-CR-54717)
Cr–Mo, creep at 1325°F, effects of welding on, 20: 11215(R) (NASA-CR-54718)
Cr–Mo, hardness of welded, effects of heat treatments on, 20: 11215(R) (NASA-CR-54718)
Cr–Mo, mechanical properties of, effects of exposure to high- and low-oxygen sodium on, 20: 11227
Cr–Mo, tensile properties of, effects of welding on, 20: 11214(R) (NASA-CR-54717)
Cr–Mo, welding of, automatic inert gas tungsten arc, 20: 11246
Cr–Mo, welding to type 316 stainless steel, weld-filler metal for, 20: 11214(R) (NASA-CR-54717)
Cr–Mo–Ni, fracture toughness properties of 12% maraging, 20: 11273(R) (NRL-6364)
Cr–Mo–Ni, hardness of welded type 4340, effects of heat treatments on, 20: 11215(R) (NASA-CR-54718)
Cr–Mo–Ni, radiation hardening in low-alloy, effects of irradiation temperature on fast-neutron, 20: 11342 (EURAEC-1502)
Cr–Mo–Ni, welding techniques for HY-80, 20: 11261
Cr–Mo–Ni–V, fatigue crack propagation in, effects of air or salt water environment on, 20: 11273(R) (NRL-6364)
Cr–Mo–Ti, corrosion by flowing sodium at 1000 to 1200°F, equation for, 20: 11227
Mn–Mo, radiation hardening of A302B, effects of irradiation temperature on fast-neutron, 20: 11342 (EURAEC-1502)
Mn–Mo, radiation effects on impact strength of A-302B, combined stress and fast neutron, 20: 11227
Mn–Mo, thermal stress fatigue of A-302B, 20: 11227

MOLYBDENUM SULFIDES
thermodynamic properties, 20: 10816(T) (NASA-TT-F-285)

MOLYBDENUM SYSTEMS
C–Mo–Ti–Zr, stress-rupture properties of TZC, at high temperatures and strain rates, 20: 11265 (AD-626375)
Mo–PuC–UC, analysis for plutonium, review of methods for, 20: 10797
Mo–UO_2, chlorination, 20: 10961

MONTE CARLO METHOD
use in one-component plasma analysis, 20: 12181 (UCRL-14467-T)

MOON
satellite orbits about, general relativity tests by precession of, (T), 20: 11883

MOSQUITOES
radiation effects on population dynamics of *Aëdes aegypti*, x, 20: 10692

MÖSSBAUER EFFECT
bibliography on, 20: 12277 (PAEC(A)IN-656)
effects on magnetic hyperfine splitting in polycrystalline materials, (T), 20: 12299
in one- and two-dimensional crystals, (T), 20: 12283
in osmium-186 137-kev level, quadrupole interaction for, (E), 20: 12301
in terbium-159 isomeric state width of 58-kev resonance from, (E), 20: 12303
measurement of recoilless fraction in, technique for, 20: 12326
measurement of, constant speed drive for, 20: 11073
spectra in crystals, effect of nuclear quadrupole interaction on, 20: 12314
use in analytical chemistry and geochemistry, 20: 11377
use in study of magnetic properties of rare earth single crystals, 20: 12316
use in tin solid solution and iron–tin alloy studies, 20: 12315

MOTORS
control of synchronous, in neutron choppers, 20: 11177 (UJV-1388/65)
speed control circuit for, using feedback system, 20: 11073

MUCOPROTEINS
radiation effects on synthesis of, in rat intestine, x, 20: 10600 (BNWL-122, pp 131-4)

MULTIPLICATION FACTOR
calculation of, methods for, (E/T), 20: 11929 (CEA-R-2849)
MUONIUM
properties of, chemical and physical, 20: 11377
MUSCLES
microscopy of heart, 20: 10631
radiation effects on activity of alanine–2-oxoglutarate and aspartate–2-oxoglutarate-aminotransferase in rat, x, 20: 10593
radiation effects on mouse myocardial, β, 20: 10643
MUTAGENS
chemical, effects on oats, genetic, 20: 10645
MUTATIONS
chemically induced in oats, use in crop improvement, 20: 10645
radiation effects on reversion of white-ivory, in Drosophila, x, 20: 10693
radioinduced in oats, use in crop improvement, 20: 10645
radioinduced in yeast, antibiotic production by, 20: 10695
radioinduced lethal, in *Tribolium castaneum*, fast neutron and x, 20: 11184(R) (BNWL-122, pp 137-9)

N

NAGASAKI
medical survey of population of, exposed to 1945 atomic bomb, 1961, 20: 10595(R) (ABCC-60-61)
population exposed to atomic bomb, statistical analysis of, 20: 10663
NAPHTHALENE
complexes with ethenetetracarbonitrile, effects of pressure on properties of, 20: 12534 (COO-1198-216)
NAPHTHALENES
spectra in cyclohexane and toluene solutions of, excimer emission, 20: 10854
NEODYMIUM
atomic mass, (E/T), 20: 11494
effects on hydrogen distribution in Zircaloy, 20: 11221
heat of solution in liquid tin at 828°K, 20: 11304
magnetic properties, 20: 11340
performance of cathodes of, in diode ion pumps, 20: 10976 (IS-T-46)
NEODYMIUM ALLOYS
Al–Nd, crystal structure of intermetallic compound $NdAl_3$ in, 20: 11305
Nd–Sn, tin Knight shift and magnetic susceptibility of $NdSn_3$, 20: 12324
NEODYMIUM CARBONATES
complexes of, composition in solution of, 20: 10824
NEODYMIUM IONS
fluorescence in lanthanum-chlorides and -fluorides, mechanism of concentration quenching of, (E/T), 20: 12297
spectra of, effects of nitrate ions on, 20: 10848
spin-lattice relaxation of trivalent, in lanthanum chlorides, (E), 20: 12292
spin-lattice relaxation in yttrium ethyl sulfates, (E), 20: 12300
NEODYMIUM ISOTOPES Nd-143
determination in uranium-233 and -235 fission products, (E), 20: 11960(R) (IDO-14667)
NEODYMIUM ISOTOPES Nd-144
determination in uranium-233 and -235 fission products, (E), 20: 11960(R) (IDO-14667)
energy transitions in, from promethium-144 beta decay, (E), 20: 12081
NEODYMIUM ISOTOPES Nd-145
determination in uranium-233 and -235 fission products, (E), 20: 11960(R) (IDO-14667)
NEODYMIUM ISOTOPES Nd-146
determination in uranium-233 and -235 fission products, (E), 20: 11960(R) (IDO-14667)
energy level transitions in, from promethium-146 decay of, (E), 20: 12081
NEODYMIUM ISOTOPES Nd-147
beta transitions in, first-forbidden, (E), 20: 12139
NEODYMIUM ISOTOPES Nd-148
determination in uranium-233 and -235 fission products, (E), 20: 11960(R) (IDO-14667)
NEODYMIUM ISOTOPES Nd-149
beta decay of, γ-γ directional correlations from, (E), 20: 12080
NEODYMIUM ISOTOPES Nd-150
determination in uranium-233 and -235 fission products, (E), 20: 11960(R) (IDO-14667)
NEODYMIUM NITRATES
nitrogen-14 NMR in, (E), 20: 12325
spectra of, in aqueous solutions, absorption, 20: 10848
NEODYMIUM OXIDES
compatibility and encapsulation with alloys and metals, 20: 11267 (BNWL-SA-488)
NEODYMIUM SELENIDES
CaSe–Nd_2Se_3, phase studies, 20: 10857
NEON
electron reactions with atomic, metastable excitation in, (E), 20: 11455 (UCRL-14450)
neutron reactions (n,p) at 14.1 Mev, (E), 20: 12118
C_2F_6–Ne, energy transfer in gamma radiolysis of, 20: 10884
NEON IONS
energy levels of, (T), 20: 11450 (UCRL-7842-T)
NEON ISOTOPES Ne-20
alpha reactions (α,d) at 42 to 53 Mev, deuteron energy spectra from, (E), 20: 12061
energy levels, (E), 20: 12150
production and separation of, method for, 20: 11191 (JEN-150-DQ/I-51)
proton scattering at 1.5 to 2.8 Mev, angular distributions and excitation curves from, (E), 20: 11995
reactions with molybdenum-92 and -94 at 100 Mev, delayed proton emission in, (E), 20: 11964 (JINR-E-2464)
viscosity coefficients at −195 to +25°C, isotope effects on, (E), 20: 11461
NEON ISOTOPES Ne-21
production and separation of, method for, 20: 11191 (JEN-150-DQ/I-51)
NEON ISOTOPES Ne-22
deuteron reactions (d,p) with, lifetime of neon-23 1.02-Mev level from, (E), 20: 12060
energy levels, (E), 20: 12150
production and separation of, method for, 20: 11191 (JEN-150-DQ/I-51)
reactions (Ne-22,6n) with uranium-238 at 112 to 135 Mev, nobelium-254 production in, (E), 20: 11969 (JINR-P-2471)
viscosity coefficients at −195 to +25°C, isotope effects on, (E), 20: 11461
NEON ISOTOPES Ne-23
energy levels in, lifetime of 1.02 Mev, (E), 20: 12060
NEON SYSTEMS
Ne–K, excitation transfer in first excited state of potassium, cross sections for collision-induced, (E), 20: 11499
Ne–Na, excitation transfer in first excited states of sodium, cross sections for collision-induced, (E), 20: 11499
NEPTUNIUM
diffusion in sintered uranium dioxide at 1250 to 1600°C, 20: 11312
separation from irradiated uranium by reversed-phase partition chromatography, 20: 10954
NEPTUNIUM ALLOYS
Fe–Nd, phase diagram, 20: 11295
NEPTUNIUM ISOTOPES Np-237
effects of injected, on fat accumulation in rat liver, 20: 10522(R) (BNWL-122, pp 79-80)
energy level transitions in, conversion electron intensities from, (E), 20: 11956 (EUR-2632.d)
energy levels, (E), 20: 12158
helium ion fission at 42.8 Mev, deformation of transition-state nucleus in, (E), 20: 12077
helium ion reactions at 20.0 to 40.5 Mev, charge and mass distributions in fission, (E), 20: 11954 (COO-347-18)
NEPTUNIUM OXIDES
evaporation *in vacuo* at 1850 to 2475°K, thermodynamics of, 20: 10840
preparation of thin-film radiation targets of, using evaporation-condensation, 20: 11183 (ORNL-P-1900)
NERVE CELLS
glucose metabolism in glioi, effects on appetite inhibition, 20: 10541
NERVOUS SYSTEM
book: *Ionizing Radiation: Neural Function and Behavior*, 20: 10689
radiation effects on activity of alanine–2-oxoglutarate and aspartate–2-oxoglutarate-aminotransferase in rat, x, 20: 10593
radiation effects on vestibular apparatus in dogs and rabbits, gamma, proton, and x-ray, 20: 10610(T) (NASA-TT-F-353, pp 157-84)
NETHERLANDS
nuclear industry in, development of, 20: 12557
nuclear research in, review of, 20: 12556
NEUROSPORA
metabolism of tryptophan by, indolepyruvic acid formation in, 20: 10540 (HW-SA-3728)
radiation effects on, mechanisms of repair of uv, 20: 10716
radiosensitivity of, effects of acriflavine on, 20: 10716
NEUTRINO BEAMS
production of monochromatic, using 200-Bev proton synchrotron, (T), 20: 11398 (UCID-1008)
NEUTRINOS
detection using gallium-71 (ν,e−) reactions, (T), 20: 11537
interaction of, proton background in CERN experiments on, (E), 20: 11571
interactions of high-energy, review of experiments on, 20: 11580
interactions with nucleons, nonpolarized lepton state from, (T), 20: 11577
reactions with nuclei, nuclear structure effects in, (T), 20: 12100
NEUTRINOS (ν_e)
interactions in meson ($\mu^\pm$) decay, weak-current, (T), 20: 11578
NEUTRINOS (ν_μ)

interactions above 10^{12} ev, model for, (T), 20: 11558 (JINR-E-2496)
interactions in meson (μ^2) decay, weak-current, (T), 20: 11578
NEUTRON-ABSORPTION ANALYSIS
use for nondestructive determination of burnup in nuclear fuels, 20: 11004
NEUTRON ACTIVATION CROSS SECTIONS
measurement for nuclei with $68 \leq A \leq 208$ at 24 kev, (E), 20: 12135
NEUTRON BEAMS
energy spectra in time-variable, method for determining exact, (T), 20: 11937
NEUTRON CROSS SECTIONS
calculation from Breit-Wigner resonance parameters, computer program for, 20: 11958 (GAMD-6562)
Westcott parameters of americium, curium, plutonium, and uranium isotopes, (T), 20: 11959 (HW-77389)
NEUTRON-DIFFRACTION ANALYSIS
extinction and interference effects for crystalline, 20: 12309
NEUTRON SHIELDING
preparation of glass, 20: 12273(P)
NEUTRON SOURCES
construction of NG 200/1, 20: 11942
design for Operation HENRE, 20: 11930 (CEX-65.03)
emission from, method for determining simultaneous, 20: 11947(P)
equipment for FRJ-2 cold beam, 20: 12503(T) (AERE-Trans-1042)
performance of pulsed research reactors as, 20: 12495 (EUR-2538.e)
use in critical assembly experiments, computer program for data analysis from, 20: 12355 (GAMD-6781)
NEUTRON SPECTRA
calculation in homogeneous reactors, computer program for, 20: 12357 (KR-75)
calculation of thermal, in plutonium–uranium fueled water reactors, (T), 20: 12370
measurement using lithium–iodide europium-activated phosphors, 20: 11116
NEUTRON SPECTROMETERS
control of synchronous motors in chopper, 20: 11177 (UJV-1388/65)
design and performance of solid-state, for 15- to 35-Mev neutrons, 20: 11139
design of proton-recoil, for fast neutrons, 20: 11096 (EUR-2491.e)
development and performance of, 20: 12545(R) (PAEC(A)AR651)
NEUTRON SPECTROSCOPY
use for molecules, 20: 11377
NEUTRONS
absorption by nuclei in homogeneous media with heavy moderators, resonance, (T), 20: 11941
absorption by plutonium-240 at 1.05 ev in homogeneous systems, temperature dependence of resonance, (T), 20: 12001
absorption by uranium-238 in homogeneous media with heavy moderators, resonance, (T), 20: 11941
absorption in reactors, computer program for calculating, 20: 11932 (GA-6637)
absorption in thorium metals and thorium dioxides, computer program for calculating resonance, 20: 11932 (GA-6637)
absorption in two-region cells, computer program for calculating resonance, 20: 12351 (ANL-7033)
absorption of, intermediate resonance, (T), 20: 11928 (BNL-9790)
book: *Neutrino Astrophysics*, 20: 11436
capture by aluminum, copper, and tungsten, secondary gamma emission from, (E), 20: 12267
capture by manganese-55 at 200 to 525 ev, multiple scattering corrections for radiative, (T), 20: 11967 (JINR-P-2455)
capture by nuclei, multiple scattering corrections for radiative, (T), 20: 11967 (JINR-P-2455)
decay constants for plutonium fueled uranium-water lattices, (E), 20: 12397(R) (EURAEC-1506)
decay of, modified vector-boson propagator for leptonic, (T), 20: 11588
density fluctuations in reactors, hydraulic noise effects on, (T), 20: 12360 (ORNL-TM-1332)
detection and measurement of, cadmium cut-off energies for fission and 1/v detectors for, (T), 20: 11131
detection and measurement in high gamma backgrounds, 20: 11154
detection of Bev-range, performance of scintillation counters for, 20: 11106 (NP-15786)
detection using corrugated-plate spark chambers, 20: 11120
diffusion in reactors, accuracy of variational method for, (T), 20: 12369
diffusion in zirconium hydrides, decay-time constants and spectra for, (E), 20: 11943
dosimetry in event of accident at Savannah River Plant, equipment and methods for, 20: 11029 (DP-1006)
dosimetry of in-pile, conference on, 20: 11110 (STI/DOC/10/46)
dosimetry of in-pile, review of, 20: 11144
dosimetry of in-pile, status in Canada, 20: 11145
dosimetry of in-pile, status in France, 20: 11146
dosimetry of in-pile, status in Germany, 20: 11147
dosimetry of in-pile, status in Hungary, 20: 11148
dosimetry of in-pile, status in Netherlands, 20: 11149
dosimetry of in-pile, methods for, 20: 11150
dosimetry of in-pile, status in United Kingdom, 20: 11151
dosimetry of in-pile, status in Yugoslavia, 20: 11152
effects on bromobenzene, 20: 10890
effects on carbon steel, 20: 11227
effects on cobalt acetylacetonate, annealing of, 20: 10888
effects on cobalt halopentammine complexes, annealing of, 20: 10889
effects on corrosion and mechanical properties of zirconium–niobium–tin alloy and Zircaloy-2, 20: 11354
effects on crystal structure of zinc oxide, 20: 11359
effects on dimensions and thermal expansion of pyrolytic graphite, effects of annealing on, 20: 11225
effects on electric and physical properties of polymeric materials, 20: 11344 (N65-35361)
effects on electric properties of aluminum, mechanism for recovery from, 20: 11362
effects on fission-product distributions in urania pellets, 20: 11365
effects on man, biological, 20: 10698
effects on medical x-ray film, 20: 12545(R) (PAEC(A)AR651)
effects on microstructure of uranium at 4.5°K, 20: 11224
effects on microstructure of molybdenum, 20: 11227
effects on silicon carbide transistors, 20: 12276 (NYO-3405-4)
effects on stress-rupture properties of A-286 alloy and René 41, 20: 11358
effects on tensile-strain limits of graphite, 20: 11225
effects on vacancy agglomerate induction in copper, interpretation of contrast phenomena in, 20: 11353(T) (ANL-Trans-259)
effects on wear resistance of carbon steel, 20: 11227
emission in decay of compound nuclei, effect of spin on, (T), 20: 12048
emission in helium hypernuclei nonmesic decay, (E), 20: 11977 (TID-22536)
emission of, determination of simultaneous, 20: 11947(P)
energy loss in polyethylene–ethylene spherical-cavity dosimeters, (T), 20: 11135
energy spectra in nonstationary beams, method for determining exact, 20: 11937
energy spectra in graphite after fast-pulse injection, time-dependent, (E/T), 20: 11940
flux distribution around 10-Bev synchrophasotron, spatial, (E), 20: 11390 (JINR-P-2446)
flux distributions in multiple-pin fuel elements, computer program for, 20: 12384 (AGN-TM-411)
flux flattening in heterogeneous reactors, calculation of, (T), 20: 12364 (UJV-1365/65)
flux in reactors, performance of synthesis method for calculating, (E/T), 20: 12368 (WAPD-T-1737)
flux in reactors, group-theory method for eigenvalue problems in, (T), 20: 12373
flux variations in square lattices, method for calculating, (T), 20: 12366 (UJV-1439/65)
form factors from deuteron-electron interactions, electromagnetic, (T), 20: 11666
form factors of, from triton wave function, (T), 20: 11623
form factors of, from deuteron-electron inelastic interactions, (E), 20: 11626
form factors of, from electron-deuteron elastic interactions, (E), 20: 11644
interactions with protons at 600 Mev, meson (π) production in, (E), 20: 11564 (JINR-P-2462)
interactions with deuterons, breakup, (T), 20: 11607
interactions with protons at medium energies, polarization in, (T), 20: 11617
interactions with protons, elastic-scattering matrix from phase-shift analyses of, (E/T), 20: 11622
interactions with neutrons, N^{*-} production from, (E), 20: 11624
interactions with neutrons, charge independence and lengths for, (T), 20: 11649
interactions with protons, charge independence and lengths for, (T), 20: 11649
interactions with mesons (K^-) at 828 to 1112 Mev/c, $Y_1^*(1765)$ resonance in, (E), 20: 11656
interactions with biological materials, 20: 10698
interactions with protons at 2 Bev/c, differential cross sections for elastic charge-exchange, (E), 20: 11606
kinetics in reactors, computer program for, 20: 12354 (GAMD-6644 (Add.))
kinetics in reactors, computer program for solution of equations for, 20: 11946
lifetime in reactors, space-dependent formula for Rossi-α measurements of, (T), 20: 12375
moderation in fluids, flow measurement using, 20: 11080(P)

oscillations in spherical nuclei, E2 surface, (T), 20: 12024
reactions (n,a_0) with sulfur-32 at 3.2 Mev, angular and energy distributions from, (E), 20: 11993
reactions (n,a) at 14.8 Mev, direct interaction models for, (T), 20: 12002
reactions (n,a) with phosphorus-31 at 14.8 Mev, cross section for, (E), 20: 12134
reactions (n,a) with silicon-28 at 14.8 Mev, angular distributions from, (E/T), 20: 12030
reactions (n,a) with calcium-40 at 4.7 Mev, alpha angular distributions in, (E), 20: 12119
reactions (n,a) with oxygen-16 at 14 Mev, angular distribution for, (E/T), 20: 12120
reactions (n,d) with oxygen-16, exchange amplitudes for, (T), 20: 12126
reactions (n,γ) with bromine-81 in carbon tetrachloride and *n*-hexane, ground-state and isomeric bromine-82 production from, 20: 10938
reactions (n,n'γ) with iron-56 at 0.95 to 4 Mev, cross sections and gamma angular distributions from, (E), 20: 12108
reactions (n,p) with light nuclei at 14.8 Mev, cross sections for, (E), 20: 12133
reactions (n,p) with neon at 14.1 Mev, (E), 20: 12118
reactions (n,2n) with phosphorus-31 at 14.8 Mev, cross section for, (E), 20: 12134
reactions (n,2n) with nuclei, cross sections for, (E/T), 20: 12040
reactions in plutonium–uranium fueled water reactors, cross sections for, (T), 20: 12370
reactions with americium-241 and -243, curium-242, and -244 and plutonium-238 production in, (E), 20: 12394 (BNWL-SA-472)
reactions with heavy and medium nuclei, rates for, (T), 20: 11989
reactions with helium-4, spin coupling to deuteron-tritium reaction channels, (T), 20: 11978 (UCRL-7961-T)
reactions with holmium-165 at 14 Mev, total cross sections for, (E), 20: 12089
reactions with plutonium-239 and uranium-238, cross sections for resonance self-shielding in, (T), 20: 12374
reactions with technetium-99, cross sections for, 20: 10940
reactions with tungsten-182, -183, -184, and -186 at .01 to 10 ev, capture cross sections for, (E), 20: 11957 (GA-6832)
reactions with uranium dioxide pellets, effective resonance temperature correlation for, 20: 12372
reactions with uranium-235, fission fragment energy and mass distributions in, (E/T), 20: 12117
resonance calculations for, methodology for, 20: 11945
scattering by aluminum, copper, iron, and magnesium at 12 to 14 Mev, total cross sections for, (E), 20: 11949 (AD-625747)
scattering by indium-115, cross sections for inelastic, 20: 12160
scattering by lithium-7 at 2.45 Mev, angular distributions from inelastic, (E), 20: 12106
scattering by stretch-oriented polyethylene, frequency limit of stretch-bend acoustic mode from, 20: 10865
scattering in regular crystals, inelastic channels in resonance, (T), 20: 12313
scattering on aluminum-27 at 14 Mev, excitation of 4.5-Mev state by inelastic, (E), 20: 12031
slowing down in water, space- and time-dependent density for, (E), 20: 11927 (AE-208)
spectra from moderators at 20 to 80°K, (E), 20: 11944
thermalization in moderators, (T), 20: 12275 (GA-6861)
thermalization in heterogeneous systems, Monte Carlo calculations of, (T), 20: 11935 (RFR-154)
transmission in silver-109 at 30 ev to 20 kev, resonance parameters for, (E), 20: 12072
transport equation for slab geometry, solutions for, 20: 11933 (INR-630/IX-A/PR(Pt.2))
transport of, computer programs for determining source convergence for, 20: 11934 (ORNL-TM-1325)
transport theory for, Boltzmann equation for anisotropic scattering in, 20: 11936
transport with linearly anisotropic scattering, equations for half-space, 20: 11939
use for therapy, 20: 10728
uses for strengthening metals and alloys, 20: 11366

NEUTRONS, COLD

production of, moderator materials for, (E), 20: 11944
reactions (n,p) in cyclohexane, temperature dependence of cross sections for, (E), 20: 11938

NEUTRONS, FAST

attenuation and moderation in hematite concrete, (E), 20: 12263 (JINR-P-2479)
detection and measurement of, proton-recoil spectrometer for, 20: 11096 (EUR-2491.e)
detection and measurement of 15- to 35-Mev, design and performance of solid state spectrometer for, 20: 11139
dosimetry of, development of solid-state device for, 20: 11094(R) (COO-1226-10)
effects on aluminum and titanium alloys and metals at cryogenic temperatures, in-pile loops for testing, 20: 11345(R) (NASA-CR-54787)
effects on carbon precipitation in alpha-iron, 20: 11227
effects on cobalt oxides, (E), 20: 11355
effects on dimensions of carbon and graphite irradiated at 150 to 650°C, 20: 11225
effects on electric properties of ferroelectric materials, 20: 11352 (NP-15707)
effects on hardness of carbon steels, combined effects of carbon content and irradiation temperature on, 20: 11342 (EURAEC-1502)
effects on hardness of A302B and nickel–chromium–molybdenum steels, effects of irradiation temperature on, 20: 11342 (EURAEC-1502)
effects on impact strength of A-302B steel, combined stress and, 20: 11227
effects on Poisson's ratio of PGA graphite, 20: 11225
effects on *Tribolium castaneum*, genetic, 20: 11184(R) (BNWL-122, pp 137-9)
energy spectra of, measurement using lithium–iodide europium-activated phosphors, 20: 11116
flux and heating in SNAP-8DS shielding, calculation of, (T), 20: 12468 (NAA-SR-Memo-9916)
flux in LITR and ORR, measurement of, (E), 20: 12501 (ORNL-TM-1163)
flux of, NMR measurement of, 20: 11169(P)
reactions (n,γ) with rhenium and tantalum at 30 to 170 kev, cross sections for, (E), 20: 11986
reactions with nuclei at 8 to 21 Mev, cross sections for nonelastic, (E), 20: 11985
reactions with nuclei, use in nuclear structure analysis, 20: 12132
reactions with uranium-238, fine structure in mass distribution of fission fragments from, (E), 20: 12121
spectra in Triga Mark-II, (T), 20: 12505
transmission through aluminum, paraffin, and water, energy spectra from, (E), 20: 12268
use in radiotherapy, 20: 10736

NEUTRONS, FISSION

effects on rat reproduction, 20: 10601(R) (BNWL-122, pp 135-6)

NEUTRONS, THERMAL

absorption by gadolinium-156, cross section for, (E), 20: 11987
absorption density distributions in heavy water reactors, calculation of, (T), 20: 12365 (UJV-1438/65)
capture by boron-11 and silver-109, polarization of product nuclei in, (E), 20: 12098
detectors for, bibliography on, 20: 11088 (AED-C-28-01)
diffraction by aluminum, bismuth, and quartz, extinction effect in, (E), 20: 12309
diffusion in heavy water, (E/T), 20: 11931 (CONF-651101-53)
diffusion in plutonium-fueled aluminum-water lattices, (E), 20: 12396(R) (EURAEC-1505)
dosimeter for, deformable-glass, 20: 11168(P)
dosimetry of, performance of foils in pocket ion chambers for, 20: 11119
effects of microstructure of urania single crystals, 20: 11224
emission from accelerating sources, kinetics of, (T), 20: 12371
flux and multiplication in Saxton reactor, subcritical, 20: 12418(R) (WCAP-3739)
flux in LITR and ORR, measurement of, (E), 20: 12501 (ORNL-TM-1163)
reactions (n,a) with calcium-40 and -43 and oxygen-17, Q-values for, (E), 20: 11983
reactions (n,a) with potassium-39, sulfur-32, and -33, cross sections and Q-values for, (E), 20: 11983
reactions (n,f) with uranium-235, fragment charge distribution in, (E), 20: 11980 (USNRDL-TR-935)
reactions (n,γ) with holmium-165, gamma spectra from, (E), 20: 11982(T) (LA-tr-65-34)
reactions with plutonium-239 and -241 and uranium-233 and -235, xenon-135 yields from fission, (E), 20: 11990
reactions with uranium-233 and -235, capture-to-fission ratios for, (E), 20: 11960(R) (IDO-14667)
reactions with uranium-233 and -235, fission yields from, (E), 20: 11960(R) (IDO-14667)
reactions with uranium-235, palladium-115 yields from fission, (E), 20: 11981 (USNRDL-TR-943)
reactions with uranium-235, fission-fragment mass-energy correlations from, (E), 20: 12076
spectra in plutonium–uranium fueled water reactors, (T), 20: 12370
use in weld radiography, 20: 11005(P)

NICKEL

corrosion by cesium at 400°C, 20: 11227
corrosion by sodium chloride, determination of rate of, by tracers, 20: 12545(R) (PAEC(A)AR651)
corrosion by water of, plates of plutonium–aluminum fuel elements, 20: 11227

deposition on bismuth telluride, electrolytic, 20: 11543(R) (GIC-2605-3)
determination using radiocoulometric methods, 20: 10769
diffraction patterns of powdered, neutron, 20: 12545(R) (PAEC(A)AR651)
effects of alloying additions of, on oxidation rates of niobium, tantalum, and tungsten, 20: 11227
effects of binder of, on cryogenic properties of titanium and tungsten carbides, 20: 11293
electron interaction effects in films of, superimposed on superconducting lead films, (E), 20: 11918
energy levels in, g-factors of low, (E/T), 20: 11479
iron-57 internal field in, at 77°K to Curie point, 20: 12298
performance as collector electrode for thermionic cells, 20: 11540(R) (AD-626444)
pressure spalling of, properties of, (T), 20: 12539 (LA-DC-7692)
radiation effects on ferromagnetic resonance of thin films of, helium-3, 20: 12318
separation from salts by solvent extraction using Schiff bases in chloroform, 20: 10759 (INP-427/C)
solubility in potassium, 20: 11227
welding to type 6061-T6 aluminum alloy, cold-pressure, 20: 11214(R) (NASA-CR-54717)
x-ray spectra of, performance of spectroanalyzer with promethium-147 beta source for K, 20: 11133

NICKEL ALLOYS
Al–Cr–Co–Fe–Mo–Ni–Ti, stress-rupture properties of Udimet 700, at high temperatures and strain rates, 20: 11265 (AD-626375)
Be–Ni, diffusion of beryllium in, enthalpy of, 20: 11326
Cr–Co–Mo–Ni–W, erosion by mercury vapor at 640°F of Stellite 6B, 20: 11214(R) (NASA-CR-54717)
Cr–Co–Mo–Ni–W, oxidation by air at 1600°F of Stellite 6B, 20: 11215(R) (NASA-CR-54718)
Cr–Fe–Ni, diffusion of fission products in, effects of concentrations on, 20: 11212(R) (BMI-X-10143)
Cr–Fe–Ni, mechanism of stress corrosion cracking of, in sodium chloride, 20: 11233(R) (COO-1319-32)
Cr–Ni, analysis for yttrium using Arsenazo-III, spectrophotometric, 20: 10773
Cr–Ni–stainless steel, strain fatigue limits of, biaxial, 20: 12418(R) (WCAP-3739)
Cu–Ni–W, mechanical properties of sintered composites of tungsten-base, 20: 11291
Fe–Ni, diffusion of fission products in, effects of concentrations on, 20: 11212(R) (BMI-X-10143)
Fe–Ni, radiation effects on ferromagnetic resonance of thin films of, helium-3, 20: 12318
Fe–Ni–W, mechanical properties of, effects of strain rate on, 20: 11284 (UCRL-14599)
Fe–Ni–W, mechanical properties of sintered composites of tungsten-base, 20: 11291
Gd–Ni, crystal structure of intermetallic compound $GdNi_3$ in, 20: 11308
Mo–Ni, short-range order in, x-ray diffuse-scattering determination of, (E), 20: 11325
Ni–Ta, crystallization, 20: 11227
Ni–Y, crystal structure of intermetallic compound YNi_3 in, 20: 11308

NICKEL CHLORIDES
separation from salt mixtures by extraction chromatography using organic phosphorus compounds, 20: 10759 (INP-427/C)

NICKEL COUPLES
Mo/Ni/Nb/stainless steel, diffusion in bimetallic tubing of, with molybdenum and nickel diffusion barriers, inter-, 20: 11215(R) (NASA-CR-54718)
Mo/Ni/Nb–Zr/stainless steel, diffusion in bimetallic tubing of, with molybdenum and nickel diffusion barriers, inter-, 20: 11215(R) (NASA-CR-54718)
Mo/Ni/stainless steel/Ta, diffusion in bimetallic tubing of, with molybdenum and nickel diffusion barriers, inter-, 20: 11215(R) (NASA-CR-54718)

NICKEL IONS
reactions with permanganate ions during pulse-radiolysis of solutions, 20: 10914

NICKEL ISOTOPES
energy levels of, one- and two-phonon, (T), 20: 12123

NICKEL ISOTOPES Ni-57
decay of, K/L ratio for electron-capture, (E), 20: 11984

NICKEL ISOTOPES Ni-58
alpha reactions at 42 Mev, proton emission in, (E), 20: 12062
proton scattering at 19 Mev, excited 2^+ and 3^+ levels from, (E/T), 20: 12065

NICKEL ISOTOPES Ni-60
alpha reactions at 42 Mev, proton emission in, (E), 20: 12062
proton reactions (p,p′γ) at 3.4 to 5 Mev, cross sections for, (E), 20: 12159
proton scattering at 19 Mev, excited 2^+ and 3^+ levels from, (E/T), 20: 12065

NICKEL ISOTOPES Ni-62
alpha reactions at 42 Mev, proton emission in, (E), 20: 12062
proton reactions (p,p′γ) at 3.4 to 5 Mev, cross sections for, (E), 20: 12159
proton scattering at 19 Mev, excited 2^+ and 3^+ levels from, (E/T), 20: 12065

NICKEL ISOTOPES Ni-63
production at PRR, methods for, 20: 12545(R) (PAEC(A)AR651)

NICKEL ISOTOPES Ni-65
production at PRR, methods for, 20: 12545(R) (PAEC(A)AR651)

NICKEL STEEL
Co–Mo–Ni, mechanical properties of, effects of strain rate on, 20: 11284 (UCRL-14599)
Co–Ni, fracture toughness properties of, effects of carbon content on, 20: 11273(R) (NRL-6364)
Cr–Mo–Ni, fracture toughness properties of 12% maraging, 20: 11273(R) (NRL-6364)
Cr–Mo–Ni, hardness of welded type 4340, effects of heat treatments on, 20: 11215(R) (NASA-CR-54718)
Cr–Mo–Ni, radiation hardening in low-alloy, effects of irradiation temperature on fast-neutron, 20: 11342 (EURAEC-1502)
Cr–Mo–Ni, welding techniques for HY-80, 20: 11261
Cr–Mo–Ni–V, fatigue crack propagation in, effects of air or salt water environment on, 20: 11273(R) (NRL-6364)

NINE MILE POINT POWER REACTOR
design and safety analysis of, 20: 12408 (NP-15660(Vol.1))
hazards analysis, 20: 12408 (NP-15660(Vol.1))
hazards analysis, 20: 12410 (NP-15660(Suppl.1))
site evaluation analysis, 20: 12409 (NP-15660(Vol.2))

NIOBIUM
alpha reactions at 42 Mev, proton emission in, (E), 20: 12062
bonding to Inconel 600 and types 321 and 347 stainless steels, explosive, 20: 11243(R) (WANL-PR(EE)-001)
deposition from fused salt mixtures, electro-, 20: 11260
deposition on aluminum and uranium, chemical vapor, 20: 11260
determination in niobium–tungsten alloys, gravimetric, 20: 10794
diffusion in molybdenum, coefficient for, 20: 11227
diffusion of boron in surface of, 20: 11228
diffusion of uranium in, temperature dependence of, 20: 11290
effects of alloying additions of, on thermal stability of $TiAl_3$, 20: 11335
emissivity of, at 1200 to 2300°C, 20: 11314
fabrication by hot isostatic pressing, 20: 11260
internal friction of, effects of nitrogen and oxygen on, 20: 11227
mechanical properties and structure of, effects of hot rolling in air, argon, and vacuum on, 20: 11249
mechanical properties of, effects of alloying additions on, 20: 11288(T) (AD-622477)
mechanical properties of, effects of alloy additions on, 20: 11302
oxidation by air at 500 to 900°C, effects of alloying additions on, 20: 11227
oxidation by oxygen at 1200 to 1700°C, effects of pressure on, 20: 11227
properties of bimetal tubes for type 316 stainless steel and, 20: 11214(R) (NASA-CR-54717)
solubility in potassium, 20: 11227
superconducting point contacts of, macroscopic quantum interference effects in, (E/T), 20: 11911
tensile properties of, effects of exposure to cesium at 1200°C on, 20: 11227
tensile properties of single-crystal, effects of strain rate and temperature on, 20: 11227
thermodynamic properties, 20: 10816(T) (NASA-TT-F-285)

NIOBIUM ALLOY COUPLES
Fe/Nb–Zr/stainless steel/V, diffusion in bimetallic tubing of, with iron and vanadium diffusion barriers, inter-, 20: 11215(R) (NASA-CR-54718)
Fe/Nb–Zr/stainless steel, diffusion in bimetallic tubing of, with iron diffusion barrier, inter-, 20: 11215(R) (NASA-CR-54718)
Mo/Ni/Nb–Zr/stainless steel, diffusion in bimetallic tubing of, with molybdenum and nickel diffusion barriers, inter-, 20: 11215(R) (NASA-CR-54718)
Nb/Nb–Ti, diffusion at 1300 to 2000°C, inter-, 20: 11227
Nb–Zr/stainless steel, diffusion in bimetallic tubing of, inter-, 20: 11215(R) (NASA-CR-54718)

NIOBIUM ALLOYS
Al–Cr–Nb, oxidation at 1100°C, effects of composition on, 20: 11338
Al–Cr–Nb, phase studies, 20: 11338
Al–Nb, phase studies, 20: 11338
Al–Nb–Ta–Ti, fracture toughness of plasmarc welds in titanium-base, 20: 11273(R) (NRL-6364)
Cr–Nb, mechanical properties of, effects of composition on, 20: 11288(T) (AD-622477)
Hf–Nb–W–Y, development and evaluation of C-129Y, 20: 11227
Ir–Nb, mechanical properties of, effects of composition on,

20: 11288(T) (AD-622477)
Ir–Nb, phase studies, 20: 11227
La–Nb, mechanical properties of, effects of composition on, 20: 11288(T) (AD-622477)
Mo–Nb, creep strength of, effects of composition on, 20: 11302
Mo–Nb, mechanical properties of, effects of composition on, 20: 11288(T) (AD-622477)
Mo–Nb, oxidation by air at 1000 to 1200°C, effects of composition on, 20: 11227
Mo–Nb–W, creep strength of, effects of composition on, 20: 11302
Nb–Pd, mechanical properties of, effects of composition on, 20: 11288(T) (AD-622477)
Nb–Re, mechanical properties of, effects of composition on, 20: 11288(T) (AD-622477)
Nb–Rh, phase studies, 20: 11227
Nb–Sn–Zr, radiation effects on corrosion and mechanical properties of, neutron, 20: 11354
Nb–Sn–Zr, stability of martensite structure in zirconium-base, 20: 11227
Nb–Ta, mechanical properties of, effects of composition on, 20: 11288(T) (AD-622477)
Nb–Ta–W, creep strength of, effects of composition on, 20: 11302
Nb–Ta–W–Zr, bonding to Hastelloy N, Inconel 600, and types 321 and 347 stainless steels of FS-85, explosive, 20: 11243(R) (WANL-PR(EE)-001)
Nb–Ti, mechanical properties of, effects of composition on, 20: 11288(T) (AD-622477)
Nb–Ti–V, corrosion by acids and bases of vanadium-base, 20: 11230 (BM-RI-6715)
Nb–Ti–W, creep strength of, effects of composition on, 20: 11302
Nb–U, phase studies, 20: 11224
Nb–V, corrosion by acids and bases of vanadium-base, 20: 11230 (BM-RI-6715)
Nb–W, analysis for niobium and tungsten, gravimetric, 20: 10794
Nb–W, creep strength of, effects of composition on, 20: 11302
Nb–W, mechanical properties of, effects of composition on, 20: 11288(T) (AD-622477)
Nb–W–Zr, erosion by mercury vapor of Cb-752, 20: 11214(R) (NASA-CR-54717)
Nb–Zn, crystal structure of intermetallic compounds in, 20: 11328
Nb–Zr, bonding to types 321 and 347 stainless steels, explosive, 20: 11243(R) (WANL-PR(EE)-001)
Nb–Zr, brittleness of, effects of hydrogen on, 20: 11227
Nb–Zr, mechanical properties of, effects of composition on, 20: 11288(T) (AD-622477)
Nb–Zr, oxidation by oxygen at 400 to 600°C, kinetics and mechanisms of, 20: 11227
Nb–Zr, properties of bimetal tubes of type 316 stainless steel and, 20: 11214(R) (NASA-CR-54717)
Nb–Zr, superconducting point contacts of, macroscopic quantum interference effects in, (E/T), 20: 11911
Nb–Zr, training effect in coil of superconducting, (E), 20: 11895

NIOBIUM BORIDES
thermodynamic properties, 20: 10816(T) (NASA-TT-F-285)

NIOBIUM BROMIDES
thermodynamic properties, 20: 10816(T) (NASA-TT-F-285)

NIOBIUM CARBIDES
performance in high-temperature reactor fuels, 20: 12378
thermodynamic properties, 20: 10816(T) (NASA-TT-F-285)
HfC–NbC, preparation and properties, 20: 11330
NbC–TaC, preparation and properties, 20: 11330
NbC–ZrC, preparation and properties, 20: 11330

NIOBIUM CHLORIDES
thermodynamic properties, 20: 10816(T) (NASA-TT-F-285)

NIOBIUM COUPLES
Cu/Nb/stainless steel, diffusion in bimetallic tubing of, with copper diffusion barrier, inter-, 20: 11215(R) (NASA-CR-54718)
Fe/Nb/stainless steel, diffusion in bimetallic tubing of, with iron diffusion barrier, inter-, 20: 11215(R) (NASA-CR-54718)
Fe/Nb/stainless steel/V, diffusion in bimetallic tubing of, with iron and vanadium diffusion barriers, inter-, 20: 11215(R) (NASA-CR-54718)
Mo/Ni/Nb/stainless steel, diffusion in bimetallic tubing of, with molybdenum and nickel diffusion barriers, inter-, 20: 11215(R) (NASA-CR-54718)
Nb/Nb–Ti, diffusion at 1300 to 2000°C, inter-, 20: 11227
Nb/stainless steel, diffusion in bimetallic tubing of, inter-, 20: 11215(R) (NASA-CR-54718)

NIOBIUM FLUORIDES
thermodynamic properties, 20: 10816(T) (NASA-TT-F-285)

NIOBIUM HYDRIDES
thermodynamic properties, 20: 10816(T) (NASA-TT-F-285)

NIOBIUM ISOTOPES Nb-91
energy level structure in shell model, (T), 20: 12157

NIOBIUM ISOTOPES Nb-94
gamma activity of, discrimination in presence of niobium-95, 20: 11134

NIOBIUM ISOTOPES Nb-95
determination in irradiated MITR fuel elements by gamma spectroscopy, 20: 10764 (MITRE-64)
effects on plutonium determination in fission product solutions, 20: 10763 (KR-100)
gamma activity of, discrimination in presence of niobium-94, 20: 11134

NIOBIUM ISOTOPES Nb-98
decay, (E), 20: 12152

NIOBIUM NITRIDES
thermodynamic properties, 20: 10816(T) (NASA-TT-F-285)

NIOBIUM OXIDES
phase transformations, 20: 11227
thermodynamic properties, 20: 10816(T) (NASA-TT-F-285)

NIOBIUM SILICIDES
thermodynamic properties, 20: 10816(T) (NASA-TT-F-285)

NIOBIUM SULFIDES
thermodynamic properties, 20: 10816(T) (NASA-TT-F-285)

NIOBIUM SYSTEMS
B–Nb, mechanical properties of, effects of composition on, 20: 11288(T) (AD-622477)
H–Nb–Zr, phase studies, 20: 11225
Nb–O–Ti, crystal structure of $TiNb_{24}O_{62}$, 20: 11227
Nb–Si, mechanical properties of, effects of composition on, 20: 11288(T) (AD-622477)

NITRIC ACID
corrosive effects on molybdenum, tungsten, and vanadium at 35, 60, and 100°C, 20: 11230 (BM-RI-6715)
corrosive effects on vanadium-base alloys at low temperatures, 20: 11230 (BM-RI-6715)
corrosive effects on molybdenum, tungsten, or vanadium coupled with titanium, galvanic, 20: 11230 (BM-RI-6715)
solvent properties for irradiated thoria–urania fuels, 20: 10964

NITROGEN
alpha stopping in, energy transfer and scintillations from, 20: 11130
corrosive effects on uranium–10 molybdenum alloys, effects of reactor radiation on, 20: 11224
effects on alkyltin yields in radiolysis of mixtures of 1-bromobutane or 1-bromopentane with tin, 20: 10870 (BMI-1753)
effects on internal friction of niobium, 20: 11227
electron elastic scattering at low energies, free-electron wave functions for, (T), 20: 11495
flow in straight circular tubes during chill-down, two-phase, 20: 10996 (WANL-TNR-154)
heat transfer coefficients for, 20: 12341
heat transfer to boiling, in straight circular tubes, 20: 10996 (WANL-TNR-154)
helium-atom and -ion scattering by, electrons and ions from, 20: 11447(R) (TID-22476)
ionization in uniform increasing magnetic yield, (E), 20: 11768 (JUL-327-PP)
ionization rates in d-c electric fields, (E), 20: 12169 (JUL-322-PP)
radiation effects on excretion of, by isolated frog liver, γ, 20: 10551
radiosensitivity effects on chromosomes in bean roots, 20: 10712
sorption of thermally activated, by tungsten filament, 20: 12549(R) (TID-21555)

NITROGEN IONS
energy levels of, (T), 20: 11450 (UCRL-7842-T)
scattering by hydrogen molecules at 3 to 100 ev, cross sections for inelastic, (E), 20: 11467

NITROGEN ISOTOPES N-14
alpha reactions (α,d) at 42 to 53 Mev, deuteron energy spectra from, (E), 20: 12061
boron-10 reactions with, alpha-particle clusters in, (E), 20: 12004(T)
deuteron reactions (d,p) at 200 to 350 kev, proton angular distributions in, (E), 20: 12096
energy levels, (E), 20: 12061
neutron nonelastic reactions at 13 to 21 Mev, cross sections for, (E), 20: 11985
nitrogen-14 reactions (N-14, N-13) with, total cross sections for, (E), 20: 12057
nuclear magnetic resonance in rare-earth nitrates and transition-metal nitrates, 20: 12325
production and separation of, method for, 20: 11191 (JEN-150-DQ/I-51)
proton reactions (p,2p) at 460 Mev, (E/T), 20: 11948 (AD-624318)
reactions (N-14, N-13) with boron-10 and nitrogen-14, total cross sections for, (E), 20: 12057

NITROGEN ISOTOPES N-15
alpha reactions (α,d) at 42 to 53 Mev, deuteron energy spectra from, (E), 20: 12061
production and separation of, method for, 20: 11191 (JEN-150-DQ/I-51)
proton reactions (p,t) at 43.7 Mev, (E), 20: 12036

proton reactions (p,He-3) at 43.7 Mev, (E), 20: 12036
reactions (N-15,4n) with americium-243 at 75 to 90 Mev, nobelium-254 production in, (E), 20: 11969 (JINR-P-2471)
use in nutritional research, 20: 10560
use of urea-incorporated, combined with carbon-14-labeled carbonate for measuring rate of urea synthesis, 20: 10559

NITROGEN ISOTOPES N-16
half life, (E), 20: 12019

NITROGEN OXIDES
hydrogen reactions at 3 to 30 kev, electron loss and formation of slow anions in, (E), 20: 11509
benzene–N_2O–H_2O, production of biphenyl–terphenyl mixtures in radiolysis of, 20: 10930(P)
N_2O–H_2O, radioinduced hydroxyl radicals in, 20: 10924

NITROGEN SYSTEMS
Ar–N, alpha stopping in, energy transfer and scintillations from, 20: 11130

NOBELIUM ISOTOPES No-254
alpha decay of, energy and half life of, (E), 20: 11968 (JINR-P-2470)
alpha decay of, half life for, (E), 20: 11969 (JINR-P-2471)
production in americium-243 (N-15,4n) and uranium-238 (Ne-22,6n) reactions, (E), 20: 11969 (JINR-P-2471)

NOISE
use of acoustic emission for detection of metal overstress in reactor pressure systems, 20: 11001 (BNWL-SA-438)

NRU REACTOR
control of, two-computer system for direct, 20: 12511

NRX REACTOR
neutron dosimetry in, 20: 11145

NUCLEAR BATTERIES
feasibility of promethium-147–silicon, 20: 11546 (SC-RR-65-671)

NUCLEAR EMULSIONS
meson (K^-) reactions in, review on, 20: 11991
meson (π^-) reactions at 16.3 Bev, angular distributions from, (E/T), 20: 11602
sensitivity and sensitization of, role of metals in, (T), 20: 11121
use for measurement of alpha activity in solutions, 20: 11044
use in autoradiography, 20: 11002

NUCLEAR ENGINEERING
compilation of U. S. nuclear standards for 1964, 20: 12559

NUCLEAR MAGNETIC RESONANCE
use in fast-neutron flux measurement, 20: 11169(P)

NUCLEAR MATERIALS MANAGEMENT
burnup measurements on fuels for, nondestructive methods of, 20: 11004
criticality control in fuel processing operations, use of reactor physics calculation methods in, 20: 10969
economic aspects, 20: 10967
economic criteria for, 20: 12562
inventory in reactor accidents, 20: 12333
isotopic analysis by mass spectroscopy, errors in, 20: 10795
methods for, in processing ores and concentrates, 20: 10968
methods of, based on materials balance, 20: 10970
methods of, for EBR-II fuel, 20: 12452
methods of, for power reactors, 20: 12451
methods of, for research establishment, Lucas Heights, Australia, 20: 12560
methods of, in fuel element fabrication plant, 20: 11262
plutonium-239 determination in irradiated fuels, 20: 10796
program for, in United States, technical support activities of, 20: 12561

NUCLEAR MODELS
energy level density in independent-particle, angular-momentum dependence of, (T), 20: 12012
nuclear structure of odd-A nuclei in superfluid, 20: 11961 (INR-602/VII/PH)

NUCLEAR MODELS (OPTICAL)
deuteron and nucleon potential calculations in, (T), 20: 11570(T) (ANL-Trans-258)
potential parameters for deuterons, 20: 12095
potentials in elastic scattering, S-matrix formalism for, 20: 12021
potentials in, for nuclear spectroscopy, 20: 12047
potentials in, radial distribution of imaginary part of, (T), 20: 12129
use for proton inelastic scattering calculations, 20: 11974 (ORNL-P-960)

NUCLEAR MODELS (SHELL)
configuration mixing effects in carbon-14, (T), 20: 12155
energy level structure of niobium-91, (T), 20: 12157
scattering analysis in, inelastic, 20: 12008

NUCLEAR PHYSICS
book: *A Collection of Problems in Atomic and Nuclear Physics*, 20: 11376(T)
conference, 20: 12112

NUCLEAR POWER
development, 20: 12431

NUCLEAR POWER PLANTS
boilers for, design of sodium-heated, 20: 12389 (BAW-1280-28(Vol.1))
boilers for, development of sodium-heated, 20: 12392 (BAW-1280-28(Vol.4))
coolant cycle analysis for, using supercritical steam-cooled reactors, 20: 12415 (TID-22545, pp 54-65)
design of TRIKT-50 thermionic, for space, 20: 12482
design optimization of gas-turbine, 20: 12422
development for space, 20: 12484
development in Great Britain, review of, 20: 12427
development of, review of uranium requirements for, 20: 12558
economic comparison of boiling-water and gas-cooled reactors for, 20: 12432
economics of, analysis of future, 20: 12440
radiation dosimetry and safety problems in, 20: 11042
use in manned space flight, 20: 12492
use offshore for desalination of sea water, 20: 12453 (TID-22330 (Vol.2))

NUCLEAR REACTIONS
amplitudes for final-state interactions in, Aitchison equation for, 20: 12016
book: *High Energy Nuclear Reactions*, 20: 12111
equations for finite-range Coulomb stripping and heavy-ion transfer, 20: 12091
gamma and neutron emission from compound nucleus in, (T), 20: 12048
gamma angular correlations in, use in energy level structure analysis, (E/T), 20: 12150
mechanism of direct, at high energies, 20: 11377
particle energy distribution from, Galilean transformation of continuous, (T), 20: 11952 (COO-238-46)
particle energy distributions in, laboratory to center-of-mass transformation for continuous, (T), 20: 12011
properties of stellar, book on, 20: 11436
resonances in, fine structure in, (T), 20: 12087
stripping, computer program for distorted wave analysis of, 20: 12095
theories for, quantum, 20: 11511
theory for (He-3,p), distorted-wave Born approximation in, 20: 12127
theory of rearrangement, coupled equations for, 20: 12045
theory of two-step (p,2p), 20: 12006
wave functions in two-nucleon stripping, (T), 20: 12086

NUCLEAR SPECTRA
correction to rotational, (T), 20: 12088
theory of, optical-model potential and hole-particle model for, 20: 12047

NUCLEAR SPIN
relaxation in dilute gases, (T), 20: 11784

NUCLEAR STRUCTURE
analysis for tritons, using separable potentials, (T), 20: 12130
analysis using beta decay data, (E/T), 20: 12113
analysis using fast neutron reactions and scattering, 20: 12132
configuration mixing in sd-shell nuclei, (T), 20: 12128
effects on neutrino reactions with nuclei, (T), 20: 12100
energy level calculations for praseodymium isotopes, nucleon interactions in, 20: 12124
energy levels of light nuclei, shell effects in Coulomb displacement energies of, (T), 20: 11963 (INSJ-91)
energy levels of nuclei, one- and two-phonon, (T), 20: 12123
nucleon pairing correlations in $L = 0$ state, 20: 12131
theory for odd-A nuclei with $62 \leq Z \leq 76$, 20: 11961 (INR-602/VII/PH)
theory of, self-consistent calculations in, (T), 20: 12122

NUCLEAR THEORY
deformations of nuclei, models for calculating equilibrium, 20: 12125
nuclear potentials in, quadratic momentum dependence of, 20: 12103
wave functions in ,particle-number conserving method for BCS, 20: 12050

NUCLEI
alpha scattering by light ($6 \leq A \leq 40$), data compilation on, (E), 20: 12099
beta transitions in, allowed and first-forbidden, (E/T), 20: 12113
binding energies of closed-shell, Bethe-Goldstone equation for, (T), 20: 11997
charged-particle and neutron reactions with heavy and medium, rates of, (T), 20: 11989
charged-particle reactions at high energies, fragmentation in, 20: 11377
charged-particle reactions with, finite range Coulomb stripping and heavy-ion transfer in, (T), 20: 12091
configuration mixing effects in shell-model, (T), 20: 12155
decay of $Z > 50$, two-proton, (T), 20: 12028
decay rates of, effects of laser beam on, (E/T), 20: 12102
deformation in heavy, space symmetry of wave functions for equilibrium, (T), 20: 11970 (JINR-P-2473)
deformations of, models for calculating equilibrium, (T), 20: 12125
detection and measurement of >2, silicon surface-barrier detector for, 20: 11124(T)
electron reactions with heavy deformed, dipole-giant resonances from high-energy, (T), 20: 12015

energy level density of, independent particle model for angular-momentum dependence of, (T), 20: 12012
energy level structure of, analysis using gamma angular correlations in nuclear reactions, (E/T), 20: 12150
energy level structure of closed-shell, (T), 20: 12157
energy level structure of deformed even-even, rotational, (T), 20: 12088
energy level transition probabilities in deformed odd A actinide and rare earth, (E/T), 20: 11951 (AE-205)
energy level transitions in even-even, L subshell ratios of E2, 20: 12035
energy level transition probabilities in even-even, E2, (E), 20: 12083
energy level transitions in even-even, conversion coefficients of E2, (E), 20: 12112
energy levels in even-even $142 \leq A \leq 152$, energy systematics from 3^- and 4^+, 20: 12081
energy levels in, eigenstates of pairing hamiltonian for single-particle, 20: 12051
energy levels of light, shell effects in Coulomb displacement energies of, (T), 20: 11963 (INSJ-91)
energy levels of $5 \leq A \leq 10$, 20: 12023
energy levels of, method for measuring widths of 2^+, 20: 12147
energy levels of, Tamm-Dancoff method for collective, (T), 20: 11966 (JINR-P-2432)
energy levels of, nucleon pairing correlations in L = 0, (T), 20: 12131
energy levels of, one- and two-phonon, (T), 20: 12123
energy-level lifetimes, B (E2) values and deformation parameters for $60 \leq Z \leq 68$ even-even rotational, 20: 12082
fission of, theory using Markov process, 20: 12116
gamma and neutron emission in decay of compound, effect of spin on, (T), 20: 12048
helium-3 reactions (He-3,p) with, distorted-wave Born approximation for, (T), 20: 12127
ion reactions with, mechanisms of heavy, 20: 11377
mass law, (T), 20: 12090
mass of A = 13 $T = 3/2$, testing of isobaric mass multiplet equation on, (E/T), 20: 12036
meson (K^-) reactions with emulsion, review on, 20: 11991
meson (μ) capture by, (T), 20: 12100
meson (μ) reactions with, cosmic, (T), 20: 11975 (PAM-6502)
meson (π^-) reactions at 16.3 Bev, angular distributions from, (E/T), 20: 11602
neutrino reactions with, nuclear structure effects in, (T), 20: 12100
neutron radiative capture by, multiple scattering corrections for, (T), 20: 11967 (JINR-P-2455)
neutron reactions with, structure analysis using fast, 20: 12132
neutron reactions (n,p) with light, at 14.8 Mev, (E), 20: 12133
neutron reactions (n,2n) with, cross sections for, (E/T), 20: 12040
neutron resonance absorption in homogeneous media with heavy moderators, (T), 20: 11941
nuclear structure of odd-A, with $62 \leq Z \leq 76$, (T), 20: 11961 (INR-602/VII/PH)
nucleon E2 surface resonance in spherical, (T), 20: 12024
nucleon interactions in, correlated basis functions for, (T), 20: 11492
nucleon pairing correlations in light, four-body, (T), 20: 12013
nucleon pairing interactions in, (T), 20: 12049
nucleon reactions at 0.1 to 25 Mev, data tabulations on polarization in, 20: 11965 (JINR-P-2426)
nucleon reactions at high energies, mechanisms of, 20: 12111
particle inelastic scattering by, shell model for, 20: 12008
particle scattering by nucleons of, (T), 20: 12100
polarization in solid deuterium, method for, 20: 12104
potentials at low energies, radial distribution of imaginary part of optical, (T), 20: 12129
properties of, review of, 20: 11512(T)
proton interactions in light, at 460 Mev, (E/T), 20: 11948 (AD-624318)
proton reactions (p,2p) with, two-step, (T), 20: 12006
proton reactions at high energies, ion production in, 20: 11377
proton reactions with, in meteorites, 20: 11377
radii of closed-shell, Bethe-Goldstone equation for, (T), 20: 11997
spin diffusion in electron-nuclear double resonance, (T), 20: 12311
structure of sd-shell, configuration mixing and independent particle motion in, (T), 20: 12128
triton reactions (t,p) with, properties of, (T), 20: 11972 (NP-15716)
wave functions for, particle-number conserving-method for BCS, 20: 12050

NUCLEI (CELLS)
radiation effects on DNA-ase activity in animal, 20: 10591

NUCLEIC ACIDS
reactions with hydrated electrons and hydroxyl radicals, rates of, 20: 10917

NUCLEONS
electromagnetic structure of, review of, (T), 20: 11579
form factors for, meson (ϕ) contribution to, (T), 20: 11598
form factors of, corrections for inelastic deuteron-electron interaction effects on, (T), 20: 11646
form factors of, vector meson model for, (T), 20: 11627
interactions in nuclei, correlated basis functions for, (T), 20: 11492
interactions in praseodymium isotopes, (T), 20: 12124
interactions of, meson (π)-interaction effects on potential for three-body, (T), 20: 11650
interactions of, with polarized beam and target, (T), 20: 11671
interactions with cosmic mesons (μ) in lead at high energies, electromagnetic, (E), 20: 11528
interactions with mesons (π) at 290 to 905 Mev, cross sections for N* production in, (T), 20: 11562 (JINR-P-2454)
interactions with photons, meson (π) production in, (T), 20: 11572
interactions with mesons (π^-) at low energies, cross sections for scalar, (T), 20: 11574
interactions with mesons (π), self-consistency condition for πNN-vertex function in, 20: 11576
interactions with antineutrinos and neutrinos, nonpolarized lepton state from, (T), 20: 11577
interactions with hyperons, mass splitting effects in, (T), 20: 11586(T)
interactions with hyperon (Λ), analysis of light hyperfragments for cross sections for, (T), 20: 11594
interactions with photons, vector meson production in, (T), 20: 11595
interactions with mesons (π), triangle graphs for three-particle production in, (T), 20: 11596
interactions with nucleons, heavy-meson exchange in, (T), 20: 11597
interactions with mesons (π), meson (ϕ)-nucleon coupling in, (T), 20: 11598
interactions with mesons (ϕ), coupling constants for, (T), 20: 11598
interactions with mesons (π^-) in emulsions at 16.3 Bev, angular distributions from, (E/T), 20: 11602
interactions with antinucleons and mesons (π), ABC anomaly for amplitudes of, (T), 20: 11604
interactions with photons, SU(6) symmetry for particle production in, (T), 20: 11635
interactions with electrons, cross sections for, (T), 20: 11636
interactions with mesons (π), N/D calculation with inelastic unitarity for, (T), 20: 11643
interactions with mesons (π), Regge poles for, (T), 20: 11647
interactions with mesons(π), self-consistent method for vertex functions for, (T), 20: 11730
interactions with photons, SU(6) symmetry for meson production in, (T), 20: 11581(T)
interactions with mesons (K), $Y_0^*(1815)$ production from, (T), 20: 11632
interactions with nucleons, data tabulations on polarization in low-energy, 20: 11965 (JINR-P-2426)
interactions with cosmic mesons (μ), (T), 20: 11975 (PAM-6502)
interactions with hyperons (Λ) in hypertritons, cross sections for, (T), 20: 12084
pairing correlations in light nuclei, four-body, (T), 20: 12013
pairing correlations in L = 0 states, (T), 20: 12131
pairing interactions in nuclei, (T), 20: 12049
particle scattering by, in nuclei, (T), 20: 12100
potential calculations for, optical model, 20: 11570(T) (ANL-Trans-258)
production in meson (π^+)-proton interactions at 2 Bev/c, (E), 20: 11672
reactions with helium-4, spin coupling analysis for, (T), 20: 11978 (UCRL-7961-T)
reactions with nuclei at 0.1 to 25 Mev, data tabulations on polarization in, 20: 11965 (JINR-P-2426)
reactions with nuclei at high energies, mechanisms of, 20: 12111
scattering by carbon-12 at 20 Mev, optical potential for, (T), 20: 12047
scattering of, quadratic momentum dependence of nuclear potential in, 20: 12103

NUCLEOSIDES
pyrimidine, radiolysis of aqueous solutions of, γ, 20: 10899
reactions with hydrated electrons and hydroxyl radicals, rates of, 20: 10917

NUCLEOTIDES
pyrimidine, radiolysis of aqueous solutions of, γ, 20: 10899
reactions with hydrated electrons and hydroxyl radicals, rates of, 20: 10917

O

OATS
chemically induced mutations of, use in crop improvement, 20: 10645
radioinduced mutations of, use in crop improvement, 20: 10645

OCEANOGRAPHY
fluctuations in Peru current and related water movements off west coast of South America, 20: 12542 (NYO-2929-2)
ocean mixing of river waters, tracer study on, 20: 11023
surface water movement south of Iceland, nature of, 20: 12541 (NYO-2929-1)

OIL SHALES
nuclear explosions in, permeability and size distribution of fragments

from, (T), 20: 10975 (UCRL-14294)
OILS
analysis of used motor, activation, 20: 12545(R) (PAEC(A)AR651)
radioinduced ammonolysis of coconut, gamma, 20: 12545(R) (PAEC(A)AR651)
radioinduced hydrolysis of coconut, 20: 12545(R) (PAEC(A)AR651)
radiolysis products of coconut, 20: 12545(R) (PAEC(A)AR651)
saponification of coconut, using sodium hydroxide, tracer study of, 20: 12545(R) (PAEC(A)AR651)
OPTICAL SYSTEMS
design for flying-spot analysis of particle tracks, 20: 11090 (BNL-9749)
design of light pipes for gamma cameras, thickness optimization for, (T), 20: 11079
photogrammetry method for contour measurements on small irradiated surfaces, 20: 11068 (WAPD-T-1815)
ORES
analysis for aluminum, effects of silicon on activation, 20: 10781
ORGANIC ACIDS
reactions with hydroxyl radicals, rate constants for, 20: 10916
ORGANIC COMPOUNDS
atom reactions in condensed systems of, hot, 20: 11377
purification by gas chromatography, valveless apparatus for, 20: 12553 (UCRL-14359)
ORGANIC COOLED REACTORS
heat transfer and burnout in boiling, 20: 12331
use in small desalination plants, 20: 12454(T) (JPRS-33480)
ORGANS
chemical composition of, in man, 20: 10698
neutron interactions with, 20: 10698
radiation effects on dog and rat, multiple-dose high-energy proton, 20: 10606(T) (NASA-TT-F-353, pp 55-102)
radiation effects on dog and rat, single-dose high-energy proton, 20: 10607(T) (NASA-TT-F-353, pp 103-41)
radiation effects on dog and rat, comparison of RBE of gamma, proton, and x-ray, 20: 10612(T) (NASA-TT-F-353, pp 194-209)
ORGEL REACTOR
development of, review of prototype concepts for, 20: 12428
ORNL HIGH FLUX ISOTOPE REACTOR
fuel for, preparation of enriched uranium(IV-VI) oxide, 20: 11244 (Y-MA-450)
neutron density fluctuations in, hydraulic noise effects on, (T), 20: 12360 (ORNL-TM-1332)
pressure vessel of, corrosion and radioinduced brittle fracture in, 20: 12457 (ORNL-TM-1372)
ORNL RELATIVISTIC ISOCHRONOUS CYCLOTRON
beam energies in, (E), 20: 11396 (ORNL-TM-1382)
ORNL RESEARCH REACTOR
neutron flux measurements in, fast and thermal, (E), 20: 12501 (ORNL-TM-1163)
OSCILLATORS
performance of univibrator as timing element in coincidence circuits, 20: 11109 (SGAE-E-5/1965)
OSCILLOGRAPHS
digitization of, on fast chemical reaction, computer program for, 20: 10800 (ANL-7113)
performance for spark chamber photogram scanning, 20: 11104 (LNF-65/33)
OSMIUM
effects of alloy additions of, on mechanical properties of niobium, 20: 11302
osmium-186 Mössbauer effect in, quadrupole interaction for, (E), 20: 12301
superconductivity of, correlation between isotope and pressure effects on, 20: 11896
OSMIUM ISOTOPES Os-186
Mössbauer effect in 137-kev level of, quadrupole interaction for, (E), 20: 12301
OSMIUM ISOTOPES Os-188
energy levels, (E), 20: 11998
oxygen-ion scattering at 35 Mev, lifetime of 2^+ levels from, (E), 20: 12020
OSMOSIS
electro-, mechanism in liquid metals, (T), 20: 11289(T) (IS-Trans-26)
1,3,4-OXADIAZOLE, 2-(4-BIPHENYLYL)-5-PHENYL-
radioinduced fluorescence efficiency and quenching in, rate constants for β, 20: 10902
OXALIC ACID
corrosive effects on molybdenum, tungsten, and vanadium at 35, 60, and 100°C, 20: 11230 (BM-RI-6715)
corrosive effects on molybdenum, tungsten, or vanadium coupled with aluminum or copper, galvanic, 20: 11230 (BM-RI-6715)
OXAZOLE, DIPHENYL-
radioinduced fluorescence efficiency and quenching in, rate constants for β, 20: 10902
OXIDES
tensile strength for machining powdered, effects of binders on, 20: 11277 (RFP-659)
OXYGEN
consumption in animals, effects of MEA on, 20: 10714
determination in iron and steel, activation, 20: 10771
diffusion in zirconium, coefficient and mechanism of, 20: 11268 (EIR-82)
effects on alkyltin yields in radiolysis of mixtures of 1-bromobutane or 1-bromopentane with tin, 20: 10870 (BMI-1753)
effects on creep of type 304 stainless steel at 815°C, 20: 11227
effects on gamma radiolysis of alkali metal nitrates, 20: 10891
effects on internal friction of niobium, 20: 11227
effects on mechanical properties of zirconium, combined hydrogen and, 20: 11227
effects on strain-aging in tantalum, 20: 11331
effects on stress corrosion of chromium–iron–nickel alloys in sodium chloride, 20: 11233(R) (COO-1319-32)
electron elastic scattering at low energies, free-electron wave functions for, (T), 20: 11495
exchange of alveolar gaseous and pulmonary capillary, tracer study, 20: 10547
hydrogen reactions at 3 to 30 kev, electron loss and formation of slow anions in, (E), 20: 11509
meson (μ^-) capture by, isotope effects on K x-ray emission from, 20: 11480
production of thin flowing sheets of liquid, for radiation target use, 20: 11409
radiation effects on consumption of, in rabbit cornea, β, 20: 10585
reactions with iron–aluminum alloys at 800 to 1050°C, kinetics of internal, 20: 11232 (INR-644/XIV/PS)
reactions with niobium at 1200 to 1700°C, effects of pressure on, 20: 11227
reactions with tungsten at 1600°C, effects of crystal orientation on, 20: 11227
reactions with uranium carbide in defective fuel elements, oxidation, (E/T), 20: 12380
reactions with zirconium and zirconium–niobium alloy at 400 to 600°C, kinetics and mechanisms of, 20: 11227
solubility in zirconium, 20: 11268 (EIR-82)
sorption on molybdenum, (E), 20: 11322
OXYGEN FLUORIDES
spectra of, from electron radiolysis of carbon tetrafluoride, ESR, 20: 10882
OXYGEN IONS
effects on germanium at 100 kev, damage from, 20: 11363
energy levels of, (T), 20: 11450 (UCRL-7842-T)
reactions with copper (100) faces at 10 kev, cuprous oxide formation in, (E), 20: 12282
reactions with dysprosium-163 at 35 Mev, lifetime of rotational levels from, (E), 20: 12020
reactions with europium-153 at 35 Mev, lifetime of rotational levels from, (E), 20: 12020
reactions with osmium-188 at 35 Mev, lifetime of 2^+ levels from, (E), 20: 12020
reactions with samarium-152 at 35 Mev, lifetime of 2^+ levels from, (E), 20: 12020
reactions with samarium isotopes to 65 Mev, excitation in, (E), 20: 12110
OXYGEN ISOTOPES O-13
mass of ground-state, (E), 20: 12036
OXYGEN ISOTOPES O-15
alpha reactions (α,d) at 42 to 53 Mev, deuteron energy spectra from, (E), 20: 12061
OXYGEN ISOTOPES O-16
bremsstrahlung reactions at 35 to 57 Mev, beryllium-7 yields from, (E), 20: 12094
deuteron reactions (d,p) at 200 to 350 kev, proton angular distributions in, (E), 20: 12096
electron inelastic scattering by, giant resonances in, (T), 20: 12029
energy levels, (E), 20: 12061
gamma total absorption cross section near 20 Mev, (E), 20: 12097
helium-3 reactions (He-3, He-6) at 65.3 Mev, (E), 20: 12036
helium-3 reactions (He-3,pγ) at 3.6 to 4.0 Mev, fluorine-18 excited levels from, (E), 20: 12025
helium-3 reactions (He-3, Li-6) at 65.3 Mev, (E), 20: 12036
meson (μ^-) capture by, K x-ray emission from, (E), 20: 11480
neutron reactions (n,p) at 14.8 Mev, cross sections for, (E), 20: 12133
neutron reactions (n,α) at 14 Mev, angular distribution for, (E/T), 20: 12120
neutron reactions (n,d) with exchange amplitudes for, (T), 20: 12126
proton reactions (p,n) at 30 and 50 Mev, target development for, 20: 11409
proton reactions (p,2p) at 460 Mev, (E/T), 20: 11948 (AD-624318)

triton reactions (t,p) with, properties of, (T), 20: 11972 (NP-15716)
OXYGEN ISOTOPES O-17
deuteron reactions (d,p) at 10 Mev, oxygen-18 energy levels from, (E), 20: 12055
neutron reactions (n,α) with, Q-values for thermal, (E), 20: 11983
nuclear magnetic resonance spectra of, in polycrystalline ice and ice-d_2, 20: 10835
OXYGEN ISOTOPES O-18
energy levels from deuteron reactions (d,p) with oxygen-17 at 10 Mev, (E), 20: 12055
meson (μ^-) capture by, K x-ray emission from, (E), 20: 11480
proton scattering at 7.89 to 16.28 Mev, cross sections for, (E/T), 20: 11979 (UCRL-12152)
spectra of isotopic shifts of, in C=O, infrared, 20: 10815 (UCRL-16338)
OXYGEN ISOTOPES O-19
beta decay of, fluorine-19 energy levels from, (E/T), 20: 12054
OXYGEN SYSTEMS
Cr–O–Zr, phase studies, 20: 11227
Nb–O–Ti, crystal structure of $TiNb_{24}O_{62}$, 20: 11227
O–Na_2SO_4, effects of sulfur-35 on exchange reactions in, 20: 10936(T) (CEA-tr-A-1855)
OYSTERS
radiation effects on bacteria in, gamma, 20: 10690

P

PACIFIC OCEAN
fluctuations in Peru current and related water movements off west coast of South America, 20: 12542 (NYO-2929-2)
mixing of Columbia River water in, 20: 11023
PALLADIUM
alpha reactions at 42 Mev, proton emission in, (E), 20: 12062
PALLADIUM ALLOYS
Nb–Pd, mechanical properties of, effects of composition on, 20: 11288(T) (AD-622477)
PALLADIUM COMPOUNDS
superconductivity in chalcogenide, (E), 20: 11899
PALLADIUM ISOTOPES Pd-108
neutron activation cross section at 24 kev, (E), 20: 12135
PALLADIUM ISOTOPES Pd-110
neutron activation cross section at 24 kev, (E), 20: 12135
PALLADIUM ISOTOPES Pd-111
decay, (E), 20: 12145
PALLADIUM ISOTOPES Pd-115
half life, (E), 20: 11981 (USNRDL-TR-943)
yield from uranium-235 thermal fission, 20: 11981 (USNRDL-TR-943)
PALLADIUM SELENIDES
superconductivity in, (E), 20: 11899
PALLADIUM TELLURIDES
superconductivity in, (E), 20: 11899
PANCREAS
disorder of, tracer techniques for studying, 20: 10566
PARAFFIN
neutron moderation by, at 20, 77, and 300°K, (E), 20: 11944
neutron transmission through energy spectra after fast, (E), 20: 12268
B_4C-paraffin, use in reactor control systems, 20: 12347
PARTICLE COLLECTORS
design, for radioactive and stable iodine, 20: 11060(R) (BNWL-122, pp 33-6)
PARTICLE STATISTICS
for quantum gases, thermodynamic evolution equation in, 20: 11789
PARTICLE TRACKS
analysis by flying-spot methods, track-segment generator for, 20: 11090 (BNL-9749)
particle kinematics from chamber pictures, (T), 20: 11100 (JINR-P-2467)
PARTICLE TRAJECTORIES
space-charge effects on, in bending magnet systems, (T), 20: 11378 (AD-626633)
PARTICLES
acceleration at shock fronts, model for, 20: 11437
deposition of microspheres released from 50 km, effects of wind on, 20: 11033 (SC-TM-65-398)
diffusion in gases, liquids, and solids, generalized equations for, (T), 20: 11369
distribution of graphite, from explosive destruction of NERVA mockup, 20: 12471 (SC-RR-65-557)
motion of gravitating cluster of, general relativity theory for, 20: 11869
permeability and size distribution of, from underground explosions in oil shale, (T), 20: 10975 (UCRL-14294)
PATENTS
on fuel processing, list of, 20: 10963
PEACH BOTTOM POWER REACTOR
heat transfer and neutron kinetics in, computer program for, 20: 12354 (GAMD-6644(Add.))
PEAT
cobalt-60 adsorption by, 20: 10756
ruthenium-106 sorption by, 20: 10855
PENTAERYTHRITOL TETRANITRATE
bibliography on, 20: 10862 (MLM-1252)
PENTANE, 1-BROMO-
1-bromopentane–Sn, radiation effects on alkyltin yields in, 20: 10870 (BMI-1753)
PENTANE, 3-METHYL-
radiation effects on, at –196°C, decay of trapped electrons from, 20: 10886
2,4-PENTANEDIONE
solvent properties for europium, 20: 10951
2,4-PENTANEDIONE COMPLEXES
uranyl, spectra of single-crystal, vibrational structure of, 20: 10843
with cobalt, cobalt-58m decay in, 20: 10888
with cobalt, radiation effects on, gamma and thermal annealing of neutron, 20: 10888
2,4-PENTANEDIONE, TRIFLUORO-
solvent properties for europium, 20: 10951
3-PENTANOL
sorption by mercury, effects of molecular symmetry on, 20: 12536 (IS-T-66)
2-PENTANONE
photolysis of, tracer studies of, 20: 10895
radiolysis of, tracer studies of, 20: 10895
3-PENTANONE
photolysis of, tracer studies of, 20: 10895
radiolysis of, tracer studies of, 20: 10895
sorption by mercury, effects of molecular symmetry on, 20: 12536 (IS-T-66)
PEPTIDES
radiolysis of aqueous solutions of, reactions of hydrated electrons in, 20: 10919
radiolysis of aqueous solutions of di- and tri-, pulsed-electron, 20: 10917
radiolysis of aqueous solutions of, reaction of hydrated electron in, 20: 10918
PERCHLORIC ACID
radiolysis of aqueous oxygenated solutions of, polarographic studies of 10-Mev-electron, 20: 10909
PERMANGANATES
reactions with metallic ions, kinetic studies of, using pulse-radiolysis, 20: 10914
PERSONNEL
accidents to, in USAEC facilities, 1963–64, survey of, 20: 11034 (TID-5360(Suppl.5))
dosimetry system for, in event of accident at Savannah River Plant, 20: 11029 (DP-1006)
radiation effects on industrial, from accidental cesium-137 exposure, 20: 10721
radiation monitoring of, photoluminescent dosimeters for, 20: 11140
training at Philippine Atomic Research Center, 20: 12545(R) (PAEC(A)AR651)
PERYLENE
complexes with ethenetetracarbonitrile and iodine, effects of pressure on properties of, 20: 12534 (COO-1198-216)
PHANTOMS
preparation of dog and rat, for radiation distribution studies, 20: 10605(T) (NASA-TT-F-353, pp 21-54)
PHARMACEUTICALS
preparation of labeled, 20: 10509
use of labeled, in compartment analysis and dynamic measurements, 20: 10509
PHARMACOLOGY
book: *Isotopes in Experimental Pharmacology*, 20: 10509
PHARYNX
radiotherapy of carcinomas of, γ, 20: 10725
PHENANTHRENE
alkyl-, preparation and properties of, 20: 10872 (EUR-2517.f)
methyl derivatives of, preparation, purification, and spectra of, 20: 10861
preparation, purification, and spectra of, 20: 10861 (CEA-R-2770)
PHENOL, DINITRO-
effects on urinary excretion of injected phosphorus-32 in x-irradiated rats, 20: 10666
radiosensitivity effects on animal cells, 20: 10629
PHENOLS
yields from radiolysis of sulfate solutions of benzene, 20: 10878
PHENYLENEDIAMINE
complexes with bromanil, chloranil, and fluoranil, effects of pressure on properties of, 20: 12534 (COO-1198-216)
p-PHENYLENEDIAMINE, N,N,N',N'-TETRAMETHYL-
complexes with bromanil and chloranil, effects of pressure on properties

of, 20: 12534 (COO-1198-216)
PHILIPPINE ISLANDS
nuclear power development in, economic and technical aspects on, 20: 12545(R) (PAEC(A)AR651)
PHILIPPINE RESEARCH REACTOR
operation of, pool water analysis after prolonged, 20: 12545(R) (PAEC(A)AR651)
radiological monitoring during operation, 20: 12545(R) (PAEC(A)AR651)
PHOSPHATE GLASS
properties and uses in radiation dosimetry, 20: 11140
thallium absorption and emission spectra in, (E), 20: 10830
PHOSPHATES
radiation effects on mouse, protective effects of heparin against, 20: 10705
radiation effects on content of, in rat adrenal glands, x, 20: 10576
solubility and temperature of waste solutions of, containing fission product and process oxides, 20: 12517(R) (BNWL-170)
PHOSPHATIDES
radiosensitivity effects of splenic, in mice, 20: 10704
PHOSPHINE OXIDE, TRIOCTYL-
solvent properties for metal chlorides and nitrates, 20: 10759 (INP-427/C)
PHOSPHONIC ACID, CARBOXYETHYLCARBOXYMETHYLIMINO-METHYLENE-
complexes with calcium, copper, iron, and manganese, preparation and properties of, 20: 12533 (COO-1020-6)
PHOSPHONIC ACID, CARBOXYMETHYLIMINODIMETHYLENE-
complexes with calcium, copper, iron, and manganese, preparation and properties of, 20: 12533 (COO-1020-6)
PHOSPHONIC ACID, [ETHYLENEBIS(NITRILODIMETHYLENE)]TETRA-
complexes with calcium, copper, iron, and manganese, preparation and properties of, 20: 12533 (COO-1020-6)
PHOSPHONIC ACID, PHENYL-, BIS(2-ETHYLHEXYL) ESTER
complexes with rare earths, stability of, 20: 10953
PHOSPHORIC ACID
corrosive effects on molybdenum, tungsten, and vanadium at 35, 60, and 100°C, 20: 11230 (BM-RI-6715)
corrosive effects on vanadium-base alloys at low temperatures, 20: 11230 (BM-RI-6715)
PHOSPHORS
design of plastic, with imbedded metal foil, 20: 11165(P)
performance of organic, for pulsed gamma radiation dosimetry, 20: 11137
PHOSPHORUS
content in diet, effects on calcium-45 and strontium-90 uptake by rats, 20: 10549
separation from solutions by ion exchange, 20: 10780
PHOSPHORUS IONS
reactions with silicon single crystals, doping effect in, (E), 20: 12280
PHOSPHORUS ISOTOPES P-30
energy levels, (E), 20: 12061
PHOSPHORUS ISOTOPES P-31
alpha scattering at 18 Mev, (E), 20: 12099
neutron reactions (n,2n) at 14.8 Mev, cross section for, (E), 20: 12134
neutron reactions (n,α) at 14.8 Mev, cross section for, 20: 12134
proton reactions (p,2p) at 460 Mev, (E/T), 20: 11948 (AD-624318)
radiosensitivity effects on Aerobacter and Salmonella, 20: 10579
PHOSPHORUS ISOTOPES P-32
content in salmon, reared in Hanford reactor effluent, 20: 10538(R) (BNWL-122, pp 198-201)
determination in biological solutions, 20: 10780
determination in food by scintillation counting following solvent extraction, 20: 10772
effects on amino acid excretion in mouse urine, 20: 10582
effects on bacterial growth and reproduction, 20: 10579
effects on bacterial population in mouse intestine, 20: 10642
effects on blood picture and bone marrow in mice, 20: 10641
effects on electrophoretic pattern of serum proteins in mice, 20: 10581
effects on immunity in mice, 20: 10580
effects on mice, model for, 20: 10640
effects on myocardium in mice, 20: 10643
production at PRR, methods for, 20: 12545(R) (PAEC(A)AR651)
production in proton reactions with cobalt, gold, holmium, rhenium, silver, thorium, and uranium, (E), 20: 12034
radiation effects on urinary excretion of injected, in rats, effects of dinitrophenol on x, 20: 10666
uptake and accumulation by plankton, seasonal variations, 20: 10536(R) (BNWL-122, pp 187-9)
uptake by coconut trees, use of, in fertilizer studies, 20: 12545(R) (PAEC(A)AR651)
use in hemangioma therapy, 20: 10745
PHOSPHORUS ISOTOPES P-33
production in proton reactions with cobalt, gold, holmium, rhenium, silver, thorium, and uranium, (E), 20: 12034
PHOTOELECTRIC EFFECT
cross sections for heavy atoms, method for measuring, 20: 11516
PHOTOGRAPHIC FILM
particle track analysis in, using flying-spot methods with track-segment generator, 20: 11090 (BNL-9749)
sensitivity and sensitization of, role of metals in, (T), 20: 11121
PHOTOGRAPHIC FILM DETECTORS
bibliography on chemical, photographic, and solid state, 20: 11027 (AED-C-21-03)
calibration of personnel-monitoring, 20: 12545(R) (PAEC(A)AR651)
response of, factors affecting, 20: 11136
PHOTOGRAPHY
photogrammetry method for contour measurements on small irradiated surfaces, 20: 11068 (WAPD-T-1815)
PHOTOMULTIPLIER TUBES
electron time-of-flight variations in, gas laser method for measuring, 20: 11071
testing of, design of liquid scintillator tank for, 20: 11128
PHOTONS
detection and measurement from meson (π^0) decay, Cherenkov counter-spark chamber system for, 20: 11099 (JINR-P-2436)
dosimetry of, use of thermoluminescent detectors for, 20: 11041
emission in charged-particle interactions with electrons, (T), 20: 11670
emission in spin-0 and -1 boson decay, forbidden configurations in, (T), 20: 11686 (JINR-P-2447)
interactions with nucleons, meson (π) production in, (T), 20: 11572
interactions with nucleons, SU(6) symmetry for meson production in, (T), 20: 11581(T)
interactions with nucleons, vector meson production in, (T), 20: 11595
interactions with photons, contributions of unstable intermediate states and meson (π) pairs to, (T), 20: 11600
interactions with nucleons, SU(6) symmetry for particle production in, (T), 20: 11635
production in meson (K^+) decay ($\pi^+ + \pi^0 + \gamma$), upper limit for, (E), 20: 11675
PHOTOSYNTHESIS
use of carbon sources in, by duckweeds, 20: 12543(R) (NYO-3018-12)
PHYSICS
book: *Quantum Field Theoretical Methods in Statistical Physics*, 20: 11375(T)
stability of sequence of states, (T), 20: 12248
PHYSIOLOGY
compartment analysis and dynamic measurements, tracer techniques for, 20: 10509
of appetite and obesity in mice, tracer study, 20: 10541
PIEZOELECTRIC CRYSTALS
radiation effects on electric properties of, fast-neutron and gamma, 20: 11352 (NP-15707)
PINCH DEVICES
plasma hardcore discharge stability in Faust-1, 20: 12222
PINCH EFFECT
magnetic field from theta, laser determination of, (E), 20: 12164 (ARL-65-129)
plasma containment in sustained magnetic field theta, (E), 20: 12161 (65RL-3940E)
PIPE JOINTS
performance in reactors, reliability of, 20: 12338(R) (GEAP-4911)
PIPERIDINE
spectra of, deuterium effects on valence vibration, 20: 10863
PIPES
failure in reactors, model development for, 20: 12338(R) (GEAP-4911)
fluid flow in, phenomena in bubbly, (T), 20: 10991 (NYO-3114-12)
fracture mechanisms of, 20: 12338(R) (GEAP-4911)
heat transfer properties of thermionic converter, 20: 11545 (LA-DC-7555)
slurry flow in, friction coefficients for, 20: 10998
PITUITARY GLAND
radioinduced destruction of, effects on mammary carcinoma of beta, 20: 10752
PITUITARY HORMONES
effects on fat accumulation induced by neptunium-237 in rat liver, 20: 10522(R) (BNWL-122, pp 79-80)
PLACENTA
diffusion through human, plasma protein and protein hormone, 20: 10508
PLANETS
effects on trajectories of parabolic comets, (T), 20: 11426 (UCRL-12267)
radar reflection from, for general relativity test, (T), 20: 11432
radar reflection from, general relativity test from solar gravitational effects on, (T), 20: 11433
satellite orbits about, general relativity tests by precession of, (T), 20: 11883
PLANKTON
phosphorus-32 uptake and accumulation by Columbia River, 20: 10537(R)

(BNWL-122, pp 190-3)
phosphorus-32 uptake and accumulation by Columbia River, 20: 10536(R) (BNWL-122, pp 187-9)
radium, radon, and uranium uptake by, in Black Sea and Lake Techirghiol, 20: 10512
zinc-65 uptake and accumulation by Columbia River, 20: 10536(R) (BNWL-122, pp 187-9)
zinc-65 uptake and accumulation by Columbia River, 20: 10537(R) (BNWL-122, pp 190-3)

PLANT CELLS
radiation effects on pH of maize, effects of dose on β, 20: 10683
radiation effects on growth of Topinambour, x, 20: 10621
radiosensitivity of chromosomes in Vicia, effects of N-ethylmaleimide on x, 20: 10624

PLANTS
analysis for cesium-137 by gamma spectroscopy following dissolution in sodium hydroxide, 20: 10782
cesium-137 content in Alaskan forage, 1963 and 1964, 20: 10535(R) (BNWL-122, pp 176-80)
cesium-137 content in forage, effects of precipitation on, 20: 11012(R) (BNWL-122, pp 184-6)
diversity problems in communities of, 20: 10511 (BNL-9836)
effects of precipitation and temperature on communities of, 20: 10510 (BNL-9835)
iodine-131 deposition and retention on, effects of moisture and temperature on, 20: 10717(R) (BNWL-122, pp 166-7)
phosphorus-32 uptake and accumulation by Columbia River, 20: 10537(R) (BNWL-122, pp 190-3)
photosynthesis by duckweed, carbon sources used in, 20: 12543(R) (NYO-3018-12)
productivity of vascular hydrophytes, 20: 12543(R) (NYO-3018-12)
radioactivity in forage, effects of elevation, precipitation, and season on, 20: 11011(R) (BNWL-122, pp 181-3)
role of vascular hydrophytes in mineral cycling in aquatic ecosystems, 20: 12543(R) (NYO-3018-12)
strontium-90 content in Alaskan forage, 1963 and 1964, 20: 10535(R) (BNWL-122, pp 176-80)
uptake of calcium-45 from soil by, effects of sodium content on, 20: 10534(R) (BNWL-122, pp 168-9)
uptake of cesium-137 from soil by, effects of sodium content on, 20: 10534(R) (BNWL-122, pp 168-9)
uptake of strontium-85 from soil by, effects of sodium content on, 20: 10534(R) (BNWL-122, pp 168-9)
zinc-65 uptake and accumulation by Columbia River, 20: 10537(R) (BNWL-122, pp 190-3)

PLASMA
acceleration in external magnetic field, resonance conditions for, (T), 20: 12196
acceleration in external magnetic field, resonance conditions for, (T), 20: 12197
acceleration with radial magnetic field, induction, (T), 20: 12198
charged-particle losses from C-Stellarator, (E), 20: 12239
containment and stability in toroidal devices, (E/T), 20: 12174 (MPI-PAE/P1.6/65)
containment in sustained magnetic field theta pinch, (E), 20: 12161 (65RL-3940E)
containment of stable, in permanent dipole magnetic field, (E), 20: 12202
cyclotron waves in collisionless, dispersion relations for, (E), 20: 12175 (NASA-CR-348)
diagnostics of, beam width of antenna systems in microwave, (E), 20: 12192
diagnostics using laser beams, (E), 20: 12163(R) (AD-625424)
diagnostics using Langmuir floating double probes, (E), 20: 12259
dielectric constant of, equations for longitudinal, (T), 20: 12216
dielectric constant of, effect of electron-electron correlations on longitudinal, (T), 20: 12217
dielectric properties at cyclotron resonance, (T), 20: 12179 (NP-15782)
dielectric properties of weakly turbulent, (T), 20: 12229
electric charge at boundary layer of equilibrium, in gravitational field, (T), 20: 12228
electric conductivity of turbulent, (T), 20: 12219
electric currents in semi-infinite, anomalous skin effect for, (T), 20: 12170 (LRP-18-65)
electric-field intensity in disturbed quasineutral, (T), 20: 12191
electromagnetic wave propagation in, (T), 20: 12163(R) (AD-625424)
electromagnetic waves in infinite, kinetic theory of, 20: 12212
electromagnetic wave scattering resonances in, a-c resonant probe relation to, (T), 20: 12241
electromagnetic wave scattering by column of, drift velocity effect in, (E/T), 20: 12242
electromagnetic wave scattering by density and temperature fluctuations in, (T), 20: 12253
electromagnetic-wave propagation in fully ionized diffusing, 20: 12254
electromagnetic-wave transmission by, in magnetic fields, (T), 20: 12258
electron density in, laser interferometer measurement of, (E), 20: 12165 (ARL-65-135)
electron heating in magnetic mirrors, turbulent, (E), 20: 12206(T)
electron-ion resonance in three-fluid model, damping at hybrid, (T), 20: 12185
electrostatic analyzers for, errors in use of, 20: 12223
electrostatic waves in uniform collisionless, normal modes of, (T), 20: 12218
experimental facilities for, magnetically operated shutter, 20: 12250
flow of pulsed, in magnetic fields, (E), 20: 12235
frequency of, microwave bridge for measurement of, 20: 12249
heating by direct-discharge current, turbulent, (E), 20: 12183(T) (ORNL-tr-868)
hydromagnetic wave scattering by open end of semi-infinite waveguide for, 20: 12207
hydromagnetic waves in partially ionized hydrogen, (E/T), 20: 12224
interactions with electron beams at low frequency, macroscopic theory for, 20: 12189
ion loss rate from magnetically confined, (T), 20: 12162 (65RL-3998E)
ion oscillations in weakly turbulent, (T), 20: 12178 (NP-15705)
ion temperature measurement in, double probe method for, 20: 12186
ion wave propagation in, effect of weak collisions on, (T), 20: 12172 (MATT-302)
ion-wave instabilities in, effect of weak collisions on, (T), 20: 12237
ionization rate of weakly ionized, in electric fields, (E), 20: 12169 (JUL-322-PP)
kinetic equation for, in strong static magnetic field, (T), 20: 12187
kinetic equation for warm, generalized Balescu-Lenard, 20: 12230
kinetics of homogeneous field-free, equation for, (T), 20: 12182 (UCRL-16631)
laser-beam interactions in, quantum theory for, (T), 20: 12246
light interactions in, stimulated Raman effect in, (T), 20: 12243
light interactions with gaseous and metallic, second-harmonic generation and Raman effects in, (T), 20: 12245
losses in Q-device, 20: 12215
magnetic compression of, effects on single-turn coil of energy from, (E), 20: 12177 (NASA-TN-D-3199)
magnetic compression in mirror system, boundary condition effects in, (E), 20: 12238
magnetic field of theta-pinch, time-space resolution using lasers, (E), 20: 12164 (ARL-65-129)
magnetohydrodynamic accelerator for, circular autostable path of, (T), 20: 12199
magnetohydrodynamic waveguide excitation by coaxial waveguide, 20: 12208
microwave emission from, review of nonthermal and thermal, 20: 12256
motion in magnetostatic and h-f fields, stationary state of, (T), 20: 12195
motion of glow discharge, between coaxial dielectric cylinders in crossed fields, (T), 20: 12211
of electromagnetic wave amplification in decaying, (T), 20: 12210
optical effects in, equations for non-linear, (T), 20: 12255
oscillations in alkali, models for self-excited, (T), 20: 12225
oscillations in inhomogeneous, effect of electric field on spectra of, 20: 12220
oscillations in, Landau damping of longitudinal, (T), 20: 12231
oscillations in, linearized Boltzmann-Vlason equation for, (T), 20: 12184
particle density and temperature fluctuation in, effect of collisions on, (T), 20: 12253
particle distribution near charged sphere in weakly ionized rarefied, (T), 20: 12201(T)
production for thermonuclear studies, summary of, 20: 12167(R) (COO-1233-24)
production in air by focused laser beam, (T), 20: 12190
properties in Q-1 device, end effects on, (T), 20: 12236
proton beam interactions with cold, instabilities from helical, (T), 20: 12244
radio wave emission from, review of nonthermal and thermal, 20: 12256
reactions with rigid plates, stagnation layer formation in, (T), 20: 12234
rotation of, inverted ion magnetron instability in, 20: 12194
shock structure in, transverse, (T), 20: 12227
shock structure in finite, one-dimensional, (T), 20: 12234
spectra of shock-produced helium, deviations from local thermal equilibrium in, (E), 20: 12226
spectral line shift in helium, (E), 20: 12168 (JUL-280-PP)
stability, (T), 20: 12248
stability, (T), 20: 12163(R) (AD-625424)
stability in arc discharges at low pressures, (E), 20: 12204(T)
stability in electron-beam, ion-cyclotron, (T), 20: 12203
stability in Faust-1 device, hardcore discharge, (E), 20: 12222

stability in hot electron, properties of, (E), 20: 12180 (ORNL-P-1556)
stability in magnetic fields, relativistic effects on, (T), 20: 12232
stability in oscillating discharge, (T), 20: 12193
stability in toroidal chamber with traveling magnetic field, (T), 20: 12213
stability of beam of, discrete states in, (E), 20: 12251
stability of hot proton, in magnetic mirrors, (E), 20: 12247
stability of inhomogeneous hot, effect of cold-plasma component on, (T), 20: 12221
stability of nonuniform, in magnetic field, (T), 20: 12205(T)
stability of positive-column gas-discharge, mechanism for screw, (T), 20: 12252
stability of weakly inhomogeneous, critical length determination for convective, (T), 20: 12233
thermodynamic properties and pair distribution functions for one-component, (T), 20: 12181 (UCRL-14467-T)
use of highly ionized, for lasers, 20: 12209
wave absorption in inhomogeneous, by Cherenkov electrons, (T), 20: 12214
wave phenomena in, method of time-space display of, 20: 12200
wave propagation in fully ionized unbounded, in magnetic field, (T), 20: 12188

PLASMA JETS
design for spectroscopic analysis, 20: 10798(P)
development of induction, with radial magnetic field, (T), 20: 12198
development of MHD, with circular autostable path, (T), 20: 12199
experimental facilities for, magnetically operated shutter, 20: 12250
operation of, resonance conditions for, (T), 20: 12196
operation of, resonance conditions for, (T), 20: 12197

PLASTIC-FILM DETECTORS
response to gamma radiation and neutrons, 20: 12545(R) (PAEC(A)AR651)

PLASTICS
radiation effects on, proton, 20: 10605(T) (NASA-TT-F-353, pp 21-54)

PLATES
plasma reactions with rigid, stagnation layer formation in, (T), 20: 12234
shock wave scattering from rigid, hydromagnetic, (T), 20: 11796

PLATINUM
alpha reactions at 42 Mev, proton emission in, (E), 20: 12062

PLATINUM ALLOYS
Pt–Zr, corrosion by hydrochloric acid, effects of platinum content on, 20: 11227

PLATINUM COMPOUNDS
superconductivity in chalcogenide, (E), 20: 11899

PLATINUM COUPLES
Mg/Pt, corrosion pitting by chloride ions, 20: 11231 (CEA-R-2815)

PLATINUM ISOTOPES Pt-191
decay of, iridium-191 energy levels from electron-capture, (E), 20: 12009

PLATINUM ISOTOPES Pt-192
energy levels in, lifetimes of 2^+ and 4^+, (E), 20: 12083

PLATINUM ISOTOPES Pt-198
neutron activation cross section at 24 kev, (E), 20: 12135

PLATINUM ISOTOPES Pt-199
beta decay, (E), 20: 12137

PLATINUM METALS
superconductivity in compounds with chalcogenides, (E), 20: 11899

PLATINUM TELLURIDES
superconductivity in, (E), 20: 11899

PLUTONIUM
bibliography on, 20: 12530 (BNWL-113-10)
bibliography on, 20: 12531 (BNWL-113-11)
corrosion and corrosive properties of, compilation of, 20: 11213 (BNWL-37)
detection in man, design of counter for, 20: 11107 (RFP-462)
determination in nuclear materials, review of methods for, 20: 10797
determination in urine, method for, 20: 10757 (BLG-353)
diffusion in sintered uranium dioxide at 1250 to 1600°C, 20: 11312
diffusion of gamma-phase, self-, 20: 11224
excretion by rats, effects of deferoxamine on, 20: 10531(R) (BNWL-122, pp 118-21)
excretion by rats, effects of DTPA on, 20: 10531(R) (BNWL-122, pp 118-21)
mechanical properties of, compilation of, 20: 11213 (BNWL-37)
phase transformation kinetics, 20: 11213 (BNWL-37)
physical properties of, compilation of, 20: 11213 (BNWL-37)
production and refining of metallic, 20: 10966
radiation damage in alpha-, beta-, and delta-phase, at 4.5°K, self-, 20: 11224
radiation damage in alpha-phase, annealing of self-, 20: 11224
radiation effects on physical properties of, compilation of, 20: 11213 (BNWL-37)
separation from mixed oxides by salt cycle process, 20: 10965
separation from nitric acid solutions by ion-exchange paper chromatography, 20: 10785
separation from waste materials, 20: 10966
solvent properties for tungsten at 700 to 1000°C, 20: 11224
vapor pressure at 1100 to 1800°K, 20: 11224

PLUTONIUM ALLOYS
corrosion and corrosive properties of, compilation of, 20: 11213 (BNWL-37)
crystal structure of, compilation of, 20: 11213 (BNWL-37)
mechanical properties of, compilation of, 20: 11213 (BNWL-37)
phase diagrams of, compilation of, 20: 11213 (BNWL-37)
phase transformation kinetics in, compilation of, 20: 11213 (BNWL-37)
physical properties of, compilation of, 20: 11213 (BNWL-37)
radiation effects on physical properties of, compilation of, 20: 11213 (BNWL-37)
Al–Ga–Pu, tensile properties and thermal expansion of delta-stabilized plutonium-base, 20: 11224
Al–Pu, decladding and dissolution of PRTR fuel elements of, flowsheets for, 20: 10948 (HW-76472)
Am–Pu, phase studies, 20: 11224
Ce–Co–Pu, analysis for plutonium, review of methods for, 20: 10797
Ce–Co–Pu, burnup studies on, core design for, 20: 12403 (LA-3384)
Ce–Co–Pu, corrosive effects on tantalum and tantalum alloys, effects of carbon on, 20: 11224
Ce–Ga–Pu, tensile properties and thermal expansion of delta-stabilized plutonium-base, 20: 11224
Ga–Pu, stability of delta-phase, effects of aluminum, cerium, or zinc additions on, 20: 11224
Ga–Pu, strength at −32 to 500°C, effects of iron impurities on, 20: 11224
Ga–Pu–Zn, tensile properties and thermal expansion of delta-stabilized plutonium-base, 20: 11224
In–Pu, phase studies, 20: 11224
Mo–Pu–U, analysis for plutonium, review of methods for, 20: 10797
Pu–Sc, phase studies, 20: 11224
Pu–Ti–U, strength of, ultimate compressive, 20: 11224
Pu–U, analysis for plutonium, review of methods for, 20: 10797

PLUTONIUM BORIDES
crystal structures, 20: 11224

PLUTONIUM CARBIDES
preparation, 20: 10966
Cr–PuC–UC, analysis for plutonium, review of methods for, 20: 10797
Fe–PuC–UC, analysis for plutonium, review of methods for, 20: 10797
Mo–PuC–UC, analysis for plutonium, review of methods for, 20: 10797
PC–UC, analysis for plutonium, review of methods for, 20: 10797
PuC–UC, radiation effects on, measurement in DFR, 20: 12442
Pu_2C_3–UC, reduction and sintering in hydrogen, 20: 11252

PLUTONIUM IONS
energy levels of trivalent, in lanthanum trichloride, (E), 20: 12286

PLUTONIUM ISOTOPES Pu-238
gamma shielding for thermal radiation sources using, (T), 20: 12264 (MLM-1315)
metabolism in rats, effects of chemical carcinogens on, 20: 10526(R) (BNWL-122, pp 91-3)
performance as space vehicle power supply, 20: 11188 (BLG-330)
production in heavy-water and pressurized-water reactors from mixed americium isotopes, 20: 12394 (BNWL-SA-472)
toxicity of, in rats, 20: 10524(R) (BNWL-122, pp 83-4)

PLUTONIUM ISOTOPES Pu-239
determination in fission product and pure solutions by liquid scintillation counting, 20: 10763 (KR-100)
determination in irradiated nuclear fuel by neutron transmission techniques, 20: 10796
distribution in tissues of swine, 20: 10523(R) (BNWL-122, pp 81-2)
distribution of, from inhaled oxide particles, 20: 10596(R) (BNWL-122, pp 1-15)
effects of combined cerium-144 or strontium-90 and, on rats, 20: 10552
effects of inhaled oxide particles of, pathological, 20: 10596(R) (BNWL-122, pp 1-15)
elimination of combined cerium-144 or strontium-90 and, in rats, 20: 10552
fission of μ-mesic atoms of, by radiationless transitions, (E), 20: 12041
gamma counting of, proportional detector for whole-body, 20: 11108 (RFP-637)
gamma spectra of, 384-kev peak in, (E), 20: 11950
helium ion fission at 42.8 Mev, deformation of transition-state nucleus in, (E), 20: 12077
helium ion reactions at 21.5 and 32.0 Mev, charge and mass distributions in fission, (E), 20: 11954 (COO-347-18)
neutron cross section of, Westcott parameters for, (T), 20: 11959 (HW-77389)
neutron fission reactions, cumulative and direct xenon-135 yields in thermal, (E), 20: 11990
neutron nonelastic reactions at 13 to 21 Mev, cross sections for, (E), 20: 11985

neutron resonance self-shielding in fast reactors, effective cross sections for, (T), 20: 12374
toxicity of, in rats, 20: 10524(R) (BNWL-122, pp 83-4)
use as thermal reactor fuel, economic and technical aspects of, 20: 12379

PLUTONIUM ISOTOPES Pu-240
helium ion fission at 42.8 Mev, deformation of transition-state nucleus in, (E), 20: 12077
neutron cross section of, Westcott parameters for, (T), 20: 11959 (HW-77389)
neutron resonance absorption at 1.05 ev in homogeneous systems, temperature dependence of, (T), 20: 12001

PLUTONIUM ISOTOPES Pu-241
neutron cross section of, Westcott parameters for, (T), 20: 11959 (HW-77389)
neutron fission reactions, cumulative and direct xenon-135 yields in thermal, (E), 20: 11990

PLUTONIUM ISOTOPES Pu-242
helium ion fission at 42.8 Mev, deformation of transition-state nucleus in, (E), 20: 12077
neutron cross section of, Westcott parameters for, (T), 20: 11959 (HW-77389)

PLUTONIUM NITRATES
distribution in tissues of swine, 20: 10523(R) (BNWL-122, pp 81-2)

PLUTONIUM NITRIDES
preparation, 20: 10966

PLUTONIUM OXIDES
distribution in tissues of swine, 20: 10523(R) (BNWL-122, pp 81-2)
distribution of inhaled particles of, in dogs, 20: 10596(R) (BNWL-122, pp 1-15)
preparation of thin-film radiation targets of, using evaporation-condensation, 20: 11183 (ORNL-P-1900)
preparation of, nuclear materials management in, 20: 10967

PLUTONIUM(IV) OXIDES
production and properties of, 20: 10966
PuO_2–UO_2, analysis for plutonium, review of method for, 20: 10797
PuO_2–UO_2, fabrication and testing for BR-3/Vulcain, 20: 12397(R) (EURAEC-1506)
PuO_2–UO_2, fabrication and testing for BR-3/Vulcain, 20: 12396(R) (EURAEC-1505)
PuO_2–UO_2, fabrication of, review of remote, 20: 11241 (TID-8541, pp 71-148)
PuO_2–UO_2–H_2O, neutron decay constants in lattices of, (E), 20: 12397(R) (EURAEC-1506)

PLUTONIUM PHOSPHIDES
preparation, 20: 10966

PLUTONIUM POISONING
effects of splenectomy on, in rats, 20: 10524(R) (BNWL-122, pp 83-4)

PLUTONIUM RECYCLE CRITICAL FACILITY
reactivity of water-moderated metal cores in, 20: 12494 (BNWL-160)

PLUTONIUM RECYCLE TEST REACTOR
fuel element decladding and dissolution for, flowsheets for, 20: 10948 (HW-76472)
fuel fabrication for, review of, 20: 11241 (TID-8541, pp 71-148)

PLUTONIUM SYSTEMS
C–Pu–Th, phase studies and properties of, 20: 11224
Pu–U–H_2O, neutron cross sections and thermal spectra in, 20: 12370

PNEUMATIC SYSTEMS
design for radioisotope handling at reactors, 20: 12350(P)

POCKET CHAMBERS
performance of neutron-sensitive foils in, 20: 11119

POLONIUM ISOTOPES
alpha decay of even-even, effect of pair correlation on, (T), 20: 12093

POLONIUM ISOTOPES Po-208
decay of, properties of alpha and electron-capture, (E), 20: 11971 (MLM-1251J)

POLONIUM ISOTOPES Po-209
decay of, properties of alpha and electron-capture, (E), 20: 11971 (MLM-1251J)

POLONIUM ISOTOPES Po-210
biological half-life in dogs, 20: 10544
effects on gastrointestinal tract during chronic radiation sickness, 20: 10674
equilibrium with lead-210 in dogs, 20: 10544
gamma shielding for thermal radiation sources using, (T), 20: 12264 (MLM-1315)
performance as space vehicle power supply, 20: 11188 (BLG-330)

POLONIUM ISOTOPES Po-212
alpha clusters in, (E), 20: 12074

POLYCRYSTALS
magnetic hyperfine splitting in, effect of anisotropic Mössbauer effect on, 20: 12299

POLYMERS
radiation effects on electric and physical properties of, gamma and neutron, 20: 11344 (N65-35361)

POLYPHENYL ETHERS
analytical procedures for evaluation of Mix-4P3E, as lubricant-coolant, 20: 11215(R) (NASA-CR-54718)
performance of Mix-4P3E, as lubricant-coolant for liquid metal pump motor, 20: 11215(R) (NASA-CR-54718)

POLYPHENYLS
scintillation properties of, gamma, (E), 20: 11129

POLYPHOSPHATES
radiosensitivity effects on *Aerobacter aerogenes*, 20: 10579

POLYSACCHARIDES
protective effects of yeast, against radiation injuries of mice, x, 20: 10703
radiation effects on content in brain tissues of guinea pigs, x, 20: 10638

POPULATIONS
effects of atomic explosion on Hiroshima, 1961 survey, 20: 10661
effects of atomic explosion on Hiroshima, 1961 survey, 20: 10662
of Hiroshima, medical survey of, for effects of radiation from 1945 atomic bomb, 1961, 20: 10595(R) (ABCC-60-61)
of Nagasaki, medical survey of, for effects of radiation from 1945 atomic bomb, 1961, 20: 10595(R) (ABCC-60-61)
radiation effects on *Aëdes aegypti*, x, 20: 10692
statistical analysis of Nagasaki, exposed to atomic bomb, 20: 10663

POROUS MATERIALS
exchange efficiency in relation to operation and structure of, cubic cellular geometric model for predicting, (T), 20: 10997(T) (AERE-Trans-1038)

POSITRON BEAMS
focusing in accelerating magnetic fields, (T), 20: 11399 (UCRL-7566 (Rev.1))

POSITRONIUM
lifetime in irradiated Teflon, effects of free radicals on, 20: 10905

POSITRONS
annihilation in alkali halides, alkaline earth oxides, and lithium hydrides, three-quantum, (E), 20: 11620
annihilation in halogen compounds, (E), 20: 11621
annihilation in indium–lead and indium–magnesium alloys, temperature dependence of, 20: 11678
annihilation in lithium hydride, photon angular correlations from, (T), 20: 11655
annihilation in normal and superconducting lead, photon angular correlation from, (E), 20: 11912
capture by defects in alkali-halide crystals, 20: 11377
interactions in alkali-halide crystals, annihilation, 20: 11377
interactions in ionic media, Hartree-Fock method for annihilation, 20: 11377
interactions with electrons, invariance violations in, (T), 20: 11582(T)
interactions with electrons, photon angular correlations for momentum distribution of annihilation, 20: 11377
lifetime in ammonia and lithium ammonia solutions, (E), 20: 11674
scattering by hydrogen, polarization potentials for, (T), 20: 11487
thermalization in metals, (E), 20: 11660

POTASSIUM
determination in animal tissues, activation method for, 20: 10776
performance as working fluid for Rankine cycles, 20: 12475 (WANL-PR(B)-009)
proton reactions with atoms of, production of highly excited hydrogen atoms by charge-exchange, (E), 20: 11471(T)
reactions with iodine in crossed molecular beams, spectator stripping model for, 20: 10834
solvent properties for iron at 871°F, effects of crucible material on, 20: 11227
solvent properties for cobalt, nickel, niobium, and tantalum, 20: 11227

POTASSIUM BROMIDES
diffusion of argon in single-crystal, 20: 11224
radiolysis of aerated aqueous solution of, kinetics in electron-pulse, 20: 10912
radiolysis of oxygen-saturated neutral solutions of, kinetics in pulsed-electron of, 20: 10911
LiBr–KBr, ion transfer in fused, 20: 10805 (EUR-2466.e, pp 21-30)

POTASSIUM CHLORIDES
diffusion of argon in single-crystal, 20: 11224
europium ion paramagnetic resonance in, (E), 20: 12331
preparation of high-purity single-crystal, 20: 10813 (ORNL-3906)
reactions of fused, with chromium fluoride or lanthanum oxide, 20: 10821

POTASSIUM FLUORIDES
diffusion of argon in single-crystal, 20: 11224

POTASSIUM IODIDES
magnetic moment of molecular, rotational, (E), 20: 11484

POTASSIUM IONS
electron reactions below threshold to 1 kev, cross sections for single ionization in, (E), 20: 11490

POTASSIUM ISOTOPES K-39

neutron reactions (n,α) at 0.025 ev, cross sections and Q-values for, (E), 20: 11983
POTASSIUM ISOTOPES K-42
energy levels, (E), 20: 12061
gamma activity of, discrimination in presence of sodium-24, 20: 11134
production at PRR, methods for, 20: 12545(R) (PAEC(A)AR651)
POTASSIUM NITRATES
radiolysis of, at 77, 300, and 400°K, effects of pressure on, 20: 10891
KNO_3–$AgNO_3$, electrochemical and thermochemical properties of fused, 20: 10804 (EUR-2466.e, pp 9-19)
KNO_3–$NaNO_3$, ion transfer in fused, 20: 10805 (EUR-2466.e, pp 21-30)
$LiNO_3$–KNO_3, ion transfer in fused, 20: 10805 (EUR-2466.e, pp 21-30)
POTASSIUM SULFATES
K_2SO_4–SO_3, effects of sulfur-35 exchange on reactions in, 20: 10936(T) (CEA-tr-A-1855)
POTASSIUM SYSTEMS
Ar–K, excitation transfer in first excited state of potassium, cross sections for collision-induced, (E), 20: 11499
He–K, excitation transfer in first excited state of potassium, cross sections for collision-induced, (E), 20: 11499
Ne–K, excitation transfer in first excited state of potassium, cross sections for collision-induced, (E), 20: 11499
POTASSIUM ZINC SULFATES
radioinduced vanadium ions in vanadyl-containing, EPR spectra of, 20: 12319
POWDER COMPACTS
packing efficiency of, equations for, 20: 11260
tensile strength for machining oxide, effects of binders on, 20: 11277 (RFP-659)
POWDERS
size measurements on, equipment and methods for, 20: 11270 (LA-3424)
POWER BREEDER REACTORS
core design and safety analyses of large fast, 20: 12439
design of 350-Mw(e) sodium-cooled BN-350, 20: 12441
design study for 1000-Mw(e) fast, 20: 12414 (TID-22545, pp 16-52)
economics, 20: 12431
fuel development for fast and thermal, 20: 12407 (NEIC-RR-13)
fuel element temperature distributions in 350-Mw(e) sodium-cooled BN-350, 20: 12443
POWER BURST FACILITY
fuel element deformations in, devices for measuring, 20: 11174(R) (IDO-17112, pp 81-91)
neutron kinetics, 20: 12498(R) (IDO-17112, pp 1-51)
POWER CYCLES
component design for Rankine, liquid metal, 20: 12475 (WANL-PR(B)-009)
performance of closed-Brayton, for gas-bearing turbocompressors, 20: 10972(R) (NYO-3237-4)
performance of Rankine, using cesium and potassium, 20: 12475 (WANL-PR(B)-009)
pump designs for Rankine, cesium and potassium, 20: 12475 (WANL-PR(B)-009)
POWER REACTORS
boiler design for sodium-cooled, problems associated with, 20: 12339(T) (EURFNR-11F)
containment of water-cooled, 20: 12447
control of plutonium fueled heavy water, methods for, 20: 12393 (BNL-8748)
control rod design and hydraulic analysis for closed-cycle water, (T), 20: 12418(R) (WCAP-3739)
control rods for closed-cycle water, feasibility of boron automatic, 20: 12418(R) (WCAP-3739)
coolant cycle analysis for supercritical steam-cooled, 20: 12415 (TID-22545, pp 54-65)
coolant loss accidents in closed-cycle water, flow analysis of, (T), 20: 12418(R) (WCAP-3739)
criticality calculations for hollow cylindrical thermionic, 20: 12485
criticality studies of uranium dioxide–water moderated, computer methods for, 20: 12418(R) (WCAP-3739)
design bases of direct-conversion, review of, 20: 12421
design parameters for thermionic zirconium hydride-moderated, 20: 12479
design parameters for thermionic space, 20: 12483
development in Great Britain, review of, 20: 12427
development of fast, review, 20: 12336
development of large closed-cycle water, 20: 12417(R) (WCAP-3269-15)
development of large closed-cycle water, 20: 12418(R) (WCAP-3739)
development of Phenix, 20: 12423
economics of, analysis of future, 20: 12440
fuel matrices for high-temperature, use of carbides as, 20: 12378
heat transfer in thermionic, calculation for heat-pipe, 20: 12489
loading closed-cycle water, using automatic boron control, 20: 12418(R) (WCAP-3739)
neutron density fluctuations in, hydraulic noise effects on, (T), 20: 12360 (ORNL-TM-1332)
nuclear materials management for, 20: 12451
properties of thermionic, for space power, 20: 12478
safety evaluation for sodium-cooled, heat transfer, hydrodynamics, and void formations in, 20: 10990 (NAA-SR-11586)
site criteria for, 20: 11045
stability of coupled-core, 20: 12491
temperature distribution in thermionic, for space, 20: 12486
thermal analysis of supercritical steam-cooled, 20: 12416 (TID-22545, pp 67-80)
weight of TRIKT-50, analysis of, 20: 12482
POWER SUPPLIES
properties of thermionic, for space vehicles, 20: 12478
radiator design for space, 20: 12480
use of radioisotope, for space vehicles, 20: 11188 (BLG-330)
PRASEODYMIUM
heat of solution in liquid tin at 724 to 768°K, 20: 11304
PRASEODYMIUM ALLOYS
Al–Pr, crystal structure of intermetallic compound $PrAl_3$ in, 20: 11305
Pr–Re, phase studies, 20: 11298
Pr–Sn, tin Knight shift and magnetic susceptibility of $PrSn_3$, 20: 12324
PRASEODYMIUM CARBONATES
complexes of, composition in solution of, 20: 10824
PRASEODYMIUM CHLORIDES
praseodymium ion electric field parameters in crystals of, trivalent, (T), 20: 12322
PRASEODYMIUM IONS
electric field parameters in praseodymium chloride crystals, (T), 20: 12322
fluorescent lifetime in lanthanum chloride, effects of concentration and temperature on, 20: 12317
nuclear quadrupole shielding factors for trivalent, in crystals, 20: 12323
spin-lattice relaxation in lanthanum ethyl sulfates, (E), 20: 12300
spin-lattice relaxation in yttrium ethyl sulfates, (E), 20: 12300
PRASEODYMIUM ISOTOPES
energy level calculations for, nucleon interactions in, (T), 20: 12124
PRASEODYMIUM ISOTOPES Pr-141
energy level calculations for, nucleon interactions in, (T), 20: 12124
energy level transitions in, nuclear structure effects in l-forbidden, (T), 20: 12154
neutron activation cross section at 24 kev, (E), 20: 12135
PRASEODYMIUM ISOTOPES Pr-143
energy level calculations for, nucleon interactions in, (T), 20: 12124
PRASEODYMIUM ISOTOPES Pr-144
determination in irradiated MITR fuel elements by gamma spectroscopy, 20: 10764 (MITNE-64)
effects of inhaled oxide particles of, pathological, 20: 10513(R) (BNWL-122, pp 16-20)
effects on plutonium determination in fission product solutions, 20: 10763 (KR-100)
energy level calculations for, nucleon interactions in, (T), 20: 12124
excretion of inhaled, effects of DTPA in dogs, 20: 10533(R) (BNWL-122, pp 125-7)
metabolism in rats, effects of chemical carcinogens on, 20: 10526(R) (BNWL-122, pp 91-3)
PRASEODYMIUM NITRATES
nitrogen-14 NMR in, (E), 20: 12325
PRASEODYMIUM OXIDES
distribution of inhaled particles of, in dogs, 20: 10513(R) (BNWL-122, pp 16-20)
PRASEODYMIUM SELENIDES
magnetic properties of single and polycrystalline, 20: 12310
CaSe–Pr_2Se_3, phase studies, 20: 10857
PRECIPITATION, ATMOSPHERIC
effects on ecology of plant communities, 20: 10510 (BNL-9835)
effects on fallout content of food and milk in Germany, 20: 11017
PREDNISOLONE
effects on distribution of heat-killed *Mycobacterium smegmatis* in mice, 20: 10655
PREGNANCY
radiation effects on sex ratio of offspring of women exposed during, 20: 10657
radiotherapy of cervical carcinoma during, 20: 10751
PRESSURE
effects on spalling of aluminum, copper, iron, and nickel, calculations for, (T), 20: 12539 (LA-DC-7692)
effects on superconductivity of osmium and ruthenium, correlation with isotope effects, 20: 11896
measurement of, radiometric digital apparatus for, 20: 11085(P)
PRESSURE SYSTEMS
metal overstress in, use of acoustic emission for detection of, 20: 11001 (BNWL-SA-438)
PRESSURE VESSELS
design and strength criteria for reactor containment, 20: 12447

design for liquid-cooled reactor, 20: 12348(P)
properties of steels used for, 20: 11286 (UJV-1405/65)
radioinduced brittle fracture of HFIR, inspection program for, 20: 12457 (ORNL-TM-1372)

PRESSURIZED WATER REACTORS
coolant pressurization function for primary circuit in, overpressure approximation from, (T), 20: 12343
cooling system pipes of, reliability of, 20: 12338(R) (GEAP-4911)
design and construction of prototype, 20: 12490
fuel burnup in large, stainless steel and zirconium clad, 20: 12418(R) (WCAP-3739)

PROMETHIUM ISOTOPES Pm-144
beta decay of, gamma transitions in neodymium-144 from, (E), 20: 12081

PROMETHIUM ISOTOPES Pm-146
beta decay of, samarium-146 energy levels at 1381 kev from, (E), 20: 12081
decay of, gamma transitions in neodymium-146 from, (E), 20: 12081

PROMETHIUM ISOTOPES Pm-147
absorption by swine, gastrointestinal, 20: 10525(R) (BNWL-122, pp 85-90)
content in fallout, 1964, 20: 11018
nuclear moments of, E2 and M1, (E), 20: 12071
performance as beta source for silicon nuclear batteries, 20: 11546 (SC-RR-65-671)
performance as beta source in x-ray spectroanalyzer, 20: 11133
performance as space vehicle power supply, 20: 11188 (BLG-330)

PROMETHIUM ISOTOPES Pm-149
energy levels from neodymium-149 decay, (E), 20: 12080
energy levels of, magnetic moments of, (E), 20: 12115

PROMETHIUM OXIDES
compatibility and encapsulation with alloys and metals, 20: 11267 (BNWL-SA-488)

PROPANE
H_2S–propane-d_8, photolysis and radiolysis of, deuterium-transfer reactions in, (E), 20: 10883

PROPENE POLYMERS
radiation effects on strength of, proton, 20: 10605(T) (NASA-TT-F-353, pp 21-54)

PROPERDIN
radiation effects on mouse serum content of, β, 20: 10580

PROPERTIES
determination from microstructural examination, evaluation of, 20: 11275 (ORNL-TM-1338)

PROPIONIC AICD, 3-AMINO-2-METHYL-
excretion by man, 20: 12545(R) (PAEC(A)AR651)

PROPIOPHENONE, p-AMINO-
effects on radiosensitivity of dogs and rats, 20: 10699(T) (NASA-TT-F-353, pp 210-38)

PROPORTIONAL DETECTORS
design of gas-flow, for whole-body gamma counting, 20: 11108 (RFP-637)
performance of spherical-cavity, in neutron dosimetry, (T), 20: 11135
use in scanning radioactive materials on thin-layer chromatograms, 20: 10788

PROPULSION
electric and rocket, for manned Mars mission, 20: 12492
electric, properties of fast and thermal thermionic reactors for, 20: 12478
ion engines for space, development of, 20: 11006(R) (NP-15824)
ion, mission requirements for manned interplanetary flight, 20: 12492
nuclear, review of advanced concepts of, 20: 12477
systems for submarine, radioisotope, 20: 11187 (AGN-8138)

PROTACTINIUM
diffusion in sintered uranium dioxide at 1250 to 1600°C, 20: 11312

PROTACTINIUM CHLORIDES
separation from salts by extraction chromatography using organic phosphorus compounds, 20: 10759 (INP-427/C)

PROTACTINIUM ISOTOPES Pa-231
helium ion fission at 42.8 Mev, deformation of transition-state nucleus in, (E), 20: 12077

PROTEINS
gastrointestinal loss of, use of iodine-131-labeled albumin for measuring, 20: 10567
gastrointestinal loss of, use of iodine-131-labeled polyvinylpyrrolidone for measuring, 20: 10568
gastrointestinal loss of, use of chromium-51-labeled albumin and copper-57-labeled ceruloplasmin for measuring, 20: 10569
labeling of plasma, review of procedures for iodine isotope, 20: 10941
labeling of plasma, studies using iodine, 20: 10561
labeling plasma, methods and uses for, 20: 10561
labeling with tritium, review of methods for, 20: 10945
metabolism in subjects with nutritional disorders of, tracer study, 20: 10573
metabolism of labeled, method for determining, 20: 10564
metabolism of plasma, in pathologic subjects, tracer study, 20: 10570
metabolism of, conference on radioisotope study of, 20: 10539 (STI/DOC/10/45)
metabolism of, criteria for, research on, 20: 10563
metabolism of, effects of nutritional state on, tracer study, 20: 10574
placental selectivity for human plasma, effects on survival of newborn of, 20: 10508
placental selectivity for human hormone, effects on survival of newborn of, 20: 10508
properties of iodine-131-labeled, 20: 10566
radiation effects on synthesis of histone, in Ehrlich ascites tumor cells, x, 20: 10691
radiation effects on electrophoretic patterns of mouse serum, β, 20: 10581
radiation effects on synthesis of, in *Mycobacterium smegmatis*, uv, 20: 10656
radiation effects on synthesis of, after cervical carcinoma therapy, 20: 10670
radiolysis of aqueous solutions of, reactions of hydrated electrons in, 20: 10919
synthesis in animal, liver, tracer study of rate of, 20: 10558
synthesis in *Neurospora crassa*, effects of temperature and tryptophan metabolism on, 20: 10540 (HW-SA-3728)
use of iodine-131-labeled, in metabolism studies, 20: 10562

PROTON BEAMS
effects on cholinesterase activity in dog serum, effects of fractionated doses on, 20: 10592
interactions with cold plasma, instabilities from helical, (T), 20: 12244
use in radiotherapy, 20: 10736

PROTON SHIELDING
performance at 0.4 Mev to 100 Bev, tabulations of, 20: 12265 (NP-15697(Vol.1))

PROTON SPECTROMETERS
design and performance for measuring proton spectra during auroral storms, 20: 11853
design of scintillation, with electron discrimination, 20: 11123(T)

PROTONS
angular distributions from (d,p) reactions with light nuclei at 200 to 350 kev, (E), 20: 12096
content in ionosphere, from vlf whistler measurements, 20: 11822
distribution in dog and rat phantoms, 20: 10605(T) (NASA-TT-F-353, pp 21-54)
distributions in inner radiation belt, energy and spatial, 20: 11825
dosimetry of high-energy, from synchrocyclotron, methods for, 20: 10605(T) (NASA-TT-F-353, pp 21-54)
effects of high-energy, on shielding materials for space craft, 20: 10605(T) (NASA-TT-F-353, pp 21-54)
effects on atomic displacements in germanium and silicon at 30 Mev to 1 Bev, 20: 11356
effects on corneal epithelia in mice at 126 Mev, 20: 10608(T) (NASA-TT-F-353, pp 142-50)
effects on dogs and rats, protective effects of chemical compounds against, 20: 10699(T) (NASA-TT-F-353, pp 210-38)
effects on dogs and rats, multiple-dose high-energy, 20: 10606(T) (NASA-TT-F-353, pp 55-102)
effects on dogs and rats, single-dose high-energy, 20: 10607(T) (NASA-TT-F-353, pp 103-41)
effects on dogs and rats, RBE of, 20: 10611(T) (NASA-TT-F-353, pp 185-93)
effects on dogs and rats, RBE of, 20: 10612(T) (NASA-TT-F-353, pp 194-209)
effects on dominant lethal induction in rats, 20: 10609(T) (NASA-TT-F-353, pp 151-6)
effects on vestibular apparatus in dogs and rabbits, 20: 10610(T) (NASA-TT-F-353, pp 157-84)
electromagnetic radiation emission from, in auroral zone atmosphere, 20: 11860
emission in alpha reactions with nuclei at 42 Mev, (E), 20: 12062
emission in decay of $Z > 50$ nuclei, (T), 20: 12028
emission in helium hypernuclei nonmesic decay, (E), 20: 11977 (TID-22536)
emission in neon-20 reactions with molybdenum-92 and -94 at 100 kev, delayed, (E), 20: 11964 (JINR-E-2464)
energy and intensity in Van Allen belt, 20: 11840
energy and pitch angle distributions for auroral-zone, (E), 20: 11854
energy spectra and flux during PCA event, (T), 20: 11858
energy spectra in ionosphere during auroral storms, spectrometer for measuring, 20: 11853
flux from solar flares, correlations with cosmic noise absorption and geomagnetic and interplanetary fields, (E), 20: 11852
flux of stably trapped, in magnetosphere, (T), 20: 11820
form factors of, electric and magnetic, (E), 20: 11567 (LAL-1144)
form factors of, from triton wave function, (T), 20: 11623
form factors of, from electron elastic scattering by polyethylene, (E), 20: 11628

interactions of, elastic-scattering matrix from phase-shift analyses of, (E/T), 20: 11622
interactions with mesons (K⁻) at 900 to 1100 Mev/c, Y*(1765) and Y₁*(1815) from, (E), 20: 11551 (CONF-650337-3)
interactions with electrons, radiative corrections for, (T), 20: 11556 (DESY-65/14)
interactions with mesons (K⁻), hyperon (Ω⁻) spin-parity from, (T), 20: 11563 (JINR-P-2456)
interactions with neutrons at 600 Mev, meson (π^0) production in, (E), 20: 11564 (JINR-P-2462)
interactions with antiprotons, SU(6)$_w$ symmetry for cross sections of, (T), 20: 11565 (JINR-P-2469)
interactions with mesons (π^+) at 4 and 8 Bev, absorptive corrections to nucleon exchange term in, (T), 20: 11573
interactions with mesons (π^-), scalar model for branching ratio of $n\pi$ and $n\gamma$, (T), 20: 11574
interactions with antiprotons, meson-resonance production in annihilation, (E), 20: 11575
interactions with mesons (π^-), resonance model for low-energy, (T), 20: 11589
interactions with mesons (π^-), fermion Regge trajectories for, (T), 20: 11590
interactions with protons at 4.9 and 8.5 Bev, polarization in elastic, (E), 20: 11591
interactions with mesons (K⁻), $J^P = \frac{1}{2}^+$, Y = 0, I = 0 and 1 octet in strong, (T), 20: 11592
interactions with electrons, quantum electrodynamic theory for, 20: 11593
interactions with mesons (π^+) at 2.75 Bev/c, exchange mechanism for $p\pi\pi\pi$, (E/T), 20: 11605
interactions with neutrons at 8 Bev/c, differential cross sections for elastic charge-exchange, (E), 20: 11606
interactions with mesons (π^-) at high energies, charge-exchange, (E), 20: 11614
interactions with mesons (π^-) at high energies, charge-exchange, (T), 20: 11615
interactions with mesons (π^+) at 8 Bev/c, resonances in, (E), 20: 11616
interactions with neutrons at medium energies, polarization in, (T), 20: 11617
interactions with neutrons, elastic-scattering matrix from phase-shift analyses of, (E/T), 20: 11622
interactions with protons, N*₊₊ production from, (E), 20: 11624
interactions with electrons at 1.0 to 6.0 Bev, absolute cross sections and electromagnetic form factors from elastic, (E), 20: 11625
interactions with electrons at 5.0 Bev, heavy electron production from, (E), 20: 11629
interactions with protons, s-wave meson (π^0) production and absorption in, (T), 20: 11642
interactions with mesons (K⁻), angular distributions from phase shifts for, (T), 20: 11648
interactions with neutrons, charge independence and lengths for, (T), 20: 11649
interactions with protons at high energies, dynamical inelasticity calculations for, (T), 20: 11652
interactions with mesons ($\pi^\pm$), test for Regge behavior in backward, (T), 20: 11663
interactions with mesons (π^-) at 1.70 to 2.50 Bev/c, charge exchange in, (E/T), 20: 11664
interactions with mesons (π^+) at 2 Bev/c, cross sections for inelastic, (E), 20: 11672
interactions with mesons ($\pi^\pm$), forward amplitude for, (T), 20: 11697
interactions with gamma radiation, polarization of hyperons (Λ) from, (E), 20: 11676
interactions with mesons (K⁻), properties of meson resonances produced in, 20: 11552 (CONF-651015-3)
interactions with antiprotons, CPT invariance in, (T), 20: 11557 (JINR-E-2457)
interactions with mesons (π^-), decay of mesons (ρ^0), (ω), and (ϕ) from, (E), 20: 11673
interactions with protons in light nuclei at 460 Mev, (E/T), 20: 11948 (AD-624318)
interactions with nucleons, use of polarized proton target for low-energy, 20: 11965 (JINR-P-2426)
motion in ionosphere, whistlers from, (E), 20: 11821
oscillations in spherical nuclei, E2 surface, (T), 20: 12024
photoproduction on carbon-12, polarization from, (E), 20: 12105
production by leakage neutrons in neutrino interactions, (E), 20: 11571
reactions (p,α) with aluminum-27 at 4 to 5.5 Mev, (E), 20: 12142
reactions (p,α) with cobalt-59 at 10.965 Mev, iron-56 energy levels from, (E), 20: 12063
reactions (p,d) with beryllium-9 at 1.66 Mev, Q value for, (E), 20: 12037
reactions (p,γ) with deuterium at 25 kev, cross sections for (pμd) wave functions, (T), 20: 11493
reactions (p,γ) with sulphur-36 at 1.4 to 2.1 Mev, excitation function for, (E), 20: 12005(T)
reactions (p,He-3) with nitrogen-15 at 43.7 Mev, (E), 20: 12036
reactions (p,n) and (p,p) with molybdenum isotopes, isobaric analog states from, (E), 20: 12078
reactions (p,n) and (p,p) with zinc-68, isobaric analog states of gallium-69 from, (E), 20: 12079
reactions (p,n) with oxygen-16 at 30 and 50 Mev, target development for, 20: 11409
reactions (p,n) with chlorine-37, mechanism for, (E/T), 20: 12141
reactions (p,p′) with cobalt-59 at 8.972 Mev, energy levels from, (E), 20: 12063
reactions (p,p′) with iron-56 at 10.965 Mev, energy levels from, (E), 20: 12063
reactions (p,p′γ) with nickel-60 and -62 at 3.4 to 5 Mev, cross sections for, (E), 20: 12159
reactions (p,t) with nitrogen-15 at 43.7 Mev, (E), 20: 12036
reactions (p,2p) with light nuclei at 460 Mev, (E/T), 20: 11948 (AD-624318)
reactions (p,2p) with nuclei, two-step, (T), 20: 12006
reactions (p,2p) with boron-10, beryllium-9 levels from, (E/T), 20: 12032
reactions (p,2p) with boron-11, beryllium-10 levels from, (E/T), 20: 12032
reactions in atmosphere, ionization from, (T), 20: 11857
reactions in crystalline solids, model for channeling in, (T), 20: 12279 (UCRL-12311)
reactions in ionosphere, direct ionization from, (T), 20: 11858
reactions with alkali-metal and alkaline-earth atoms, production of highly excited hydrogen atoms by charge-exchange, (E), 20: 11471(T)
reactions with beryllium at 1.6 Mev, electron bremsstrahlung from, (E/T), 20: 11501
reactions with bismuth, copper, and silver at 1.84 Bev, sodium-24 energy spectra and yields in, (T), 20: 12067
reactions with cobalt, gold, holmium, rhenium, silver, thorium, and uranium, phosphorus-32 and -33 production in, (E), 20: 12034
reactions with films, surface density determination by x-ray production in, 20: 11281 (UCRL-12107)
reactions with hydrogen atoms, amplitude for reorientation from, (T), 20: 11503
reactions with iron, meteorites, and Plexiglas at 1 to 3 Bev, cascades in, (E), 20: 12262 (BNL-8721)
reactions with nuclei in meteorites, 20: 11377
reactions with nuclei at high energies, ion production in, 20: 11377
scattering by aluminum-27 at 4 to 5.5 Mev, inelastic, (E), 20: 12142
scattering by carbon-12 at 156 Mev, cross sections for inelastic, (T), 20: 11974 (ORNL-P-960)
scattering by helium at 0.15 to 1 Mev, cross sections for atomic, 20: 11448(R) (TID-22480)
scattering by iron-54 and -56, nickel-58, -60, and -62 at 19 Mev, excited 2⁺ and 3⁺ levels from, (E/T), 20: 12065
scattering by magnesium-24 at small angles, inelastic, (E), 20: 12003(T)
scattering by neon-20 at 1.5 to 2.8 Mev, angular distributions and excitation curves, (E), 20: 11995
scattering by oxygen-18 at 7.89 to 16.28 Mev, cross sections for, (E/T), 20: 11979 (UCRL-12152)
shielding against, tabulation of materials for, 20: 12265 (NP-15697 (Vol.I))
tunneling in hydrogen evolution reactions, quantum mechanical theory for, (T), 20: 11372

PROTOZOA
morphogenesis in Euplotes, 20: 10696
radiation effects on developmental mechanisms in Euplotes, 20: 10696

PSEUDOUREA, 2-(2-AMINOETHYL)-2-THIO-
effects on radiosensitivity of dogs and rats, 20: 10699(T) (NASA-TT-F-353, pp 210-38)
effects on serum transaminase activity in irradiated mice, 20: 12545(R) (PAEC(A)AR651)
radiosensitivity effects in animals, test for, 20: 10711

PULSE ANALYZERS
description of 400-channel, for magnetic spin resonance spectrometers, 20: 11098 (IS-1312)
design and testing of time-to-pulse height converter, 20: 11117
design of fast-pulse recording and readout device using tunnel diodes, 20: 11065 (SC-TM-323-62(72))
design of pulse-height discriminator, 20: 11064 (RISO-102)

PULSE COLUMNS
design and performance of solvent extraction, 20: 10964

PULSE GENERATORS (ELECTRONICS)
design and performance of high-voltage, 20: 11074
design of pseudorandom noise source, 20: 12499(R) (IDO-17112, pp 52-80)
design of, with short rise-time for high-voltage circuits, 20: 11081(P)
development using avalanche transistors, 20: 11067 (UCRL-12095-T)

PULSE TRANSFORMERS
design and performance of, for production of high current voltage pulses,

20: 11074
design and testing of, for time-to-pulse height conversion, 20: 11117
PULSES
production of high current and voltage, design and performance of transformer system for, 20: 11074
PUMPS
design for supercritical helium, 20: 11925
PUMPS (LIQUID METAL)
performance of Mix-4P3E polyphenyl ether as lubricant-coolant for, 20: 11215(R) (NASA-CR-54718)
PUPAE
radiation effects on *Aëdes aegypti*, x, 20: 10692
PUREX PROCESS
development, 20: 10964
fission product drip temperature and solubility in, effects of rare metals on, 20: 12517(R) (BNWL-170)
waste calcination in, tests on prototype equipment for, 20: 12517(R) (BNWL-170)
PURINES
radiolysis of aqueous solutions of, pulsed-electron, 20: 10917
6-PURINETHIOL
effects of, combined with x radiation on skin graft survival in rats, 20: 10506
effects on survival of skin homografts in rats, 20: 10506
PYRENE
complexes with iodine, effects of pressure on properties of, 20: 12534 (COO-1198-216)
3,8-diamino-, effects of pressure on complexes with bromanil and chloranil, 20: 12534 (COO-1198-216)
PYRIDINE COMPLEXES
with uranyl perchlorate, preparation of, 20: 10825
PYRIDINES
radiolysis products of, 20: 12545(R) (PAEC(A)AR651)
PYRIMIDINES
nucleosides of, radiolysis of aqueous solutions of, γ, 20: 10899
nucleotides of, radiolysis of aqueous solutions of, γ, 20: 10899
radiolysis of aqueous solutions of, γ, 20: 10899
radiolysis of aqueous solutions of, pulsed-electron, 20: 10917
PYRROLIDONE, VINYL- POLYMERS
labeling with iodine-131, method for, 20: 10946
radiation effects on iodine-131 uptake by, uv, 20: 10946
use of iodine-131-labeled, for measuring gastrointestinal protein loss, 20: 10568
PYRUVATES
stability of carbon-14-labeled, chromatographic analysis of, 20: 10934 (UCRL-11743)

Q

QUANTOMETERS
performance for electron beam energy calibration measurements, 20: 11389 (DESY-65/12)
QUANTUM ELECTRODYNAMICS
gravitation and finite renormalization in, (T), 20: 11867 (NP-15762)
radiation emission from cavity resonators, equations for stimulated, 20: 11878
validity at high photon densities, laser beam study of, (E/T), 20: 12102
QUANTUM MECHANICS
book: *Quantum Field Theoretical Methods in Statistical Physics*, 20: 11375(T)
formalism for arbitrary-spin particles in relativistic, covariant, 20: 11759
Green functions from Lie algebras, (T), 20: 11441 (IC/65/94)
operators in, energy and time, (T), 20: 11866 (JINR-E-2478)
oscillators in, energy distributions for one-dimensional harmonic, (T), 20: 11887
Schroedinger equation for three-body problem, asymptotic solution of, (T), 20: 11459
symmetry operators for nonrelativistic, representation of discrete, 20: 11713
Weyl correspondence between classical and, mathematics of, 20: 11876
QUARTZ
neutron diffraction by, extinction effect in slow, (E), 20: 12309
5-QUINOLINESULFONIC ACID, 8-HYDROXY-
preparation of sulfur-35-labeled, 20: 10759 (INP-427/C)
solvent properties of, in chloroform for metals, 20: 10759 (INP-427/C)
use of sulfur-35-labeled, for determining distribution coefficients of complexes, 20: 10759 (INP-427/C)

R

RABBITS
effects of radiodermatitis on trace element metabolism in, 20: 10625
radiation effects on, protective effects of MEA against, 20: 10714
radiation effects on corneal metabolism in, β, 20: 10585
radiation effects on vestibular apparatus in, gamma, proton, and x-ray, 20: 10610(T) (NASA-TT-F-353, pp 157-84)
radiation effects on lenticular epithelial enzymes of, x, 20: 10630
RADAR
reflection from planets, for general relativity test, (T), 20: 11432
reflection from planets, general relativity test from solar gravitational effects on, (T), 20: 11433
RADIATION
book: *Ionizing Radiation: Neural Function and Behavior*, 20: 10689
dose estimation in reactor accidents, 20: 12333
dosimetry of, factors in photographic-film, 20: 11136
dosimetry of, use of lymphocytes in circulating blood for biological, 20: 10629
effects of ascorbic acid metabolism in rat adrenals, protective effects of cystamine and mercamine against, 20: 10715
effects of preoperative exposure to, on dissemination of cancer cells, 20: 10735
effects on animal cells in culture, single and fractionated doses, 20: 10649
effects on animals, test for protective effects of AET against, 20: 10711
effects on biological materials, mechanism for, 20: 10639
effects on biological materials, research on recovery from, 20: 10639
effects on blood coagulation in dogs, effects of stimulating vestibular analyzer on, 20: 10682
effects on bones of chronic, low-dose exposure, pathological, 20: 10637
effects on carbon fixation by vascular hydrophytes, 20: 12543(R) (NYO-3018-12)
effects on catalytic properties of titanium chloride in isoprene polymerization, 20: 10929(P)
effects on chromosomes, effects of magnetic fields on aberrant, 20: 10672
effects on chromosomes in Ehrlich ascites tumor cells, effects on survival of aberrant, 20: 10677
effects on DNA-ase activity in cell nuclei and cytoplasm of animal cells, 20: 10591
effects on electronic systems, procedure for evaluation of, 20: 11180
effects on erythrocyte membranes in newborn rats, 20: 10589
effects on eyes, after therapy of bulbar cavity tumor, 20: 10667
effects on F-center production in alkali halides by electron-hole recombination, (T), 20: 12306
effects on F-center production in alkali halides by [110] anion replacement sequences, (T), 20: 12307
effects on Hiroshima population of atomic bomb, 1961 survey, 20: 10662
effects on human blood picture, 20: 10660
effects on human survival, after cervical carcinoma therapy, 20: 10726
effects on immune reactions to bone marrow transfusions, 20: 10731
effects on mammals, review of genetic, 20: 10688
effects on mice, protective effects of splenic phospholipids against, 20: 10704
effects on mice, protective effects of heparin against, 20: 10705
effects on mice, protective effects of splenic marrow transplants against, 20: 10713
effects on microelectronic circuitry, 20: 11179
effects on pelvic lymph nodes after cervical cancer therapy, 20: 10653
effects on population of Hiroshima and Nagasaki, medical survey on, 20: 10595(R) (ABCC-60-61)
effects on rat lymph node cells after diphtheria immunization, 20: 10685
effects on rats, protective effects of hormones against, 20: 10709
effects on sex ratio of offspring of women exposed during pregnancy, 20: 10657
effects on skin after radiotherapy, 20: 10658
effects on space vehicle materials, 20: 11520
effects on space vehicle hydraulic systems, 20: 11181
effects on thyroid cells in mice, protective effects of anoxia against, 20: 10710
effects on uptake of sulfur-35-labeled sodium sulfate by rat liver, 20: 10542
effects on uterine adenocarcinomas, pelvic fractures induced by, 20: 10668
effects on vaginal cytology, 20: 10740
effects on vitamin B_{12}-hydrochloride, stabilizing, 20: 10931(P)
emission from cavity resonators, quantum electrodynamics of stimulated, 20: 11878
hazards to public, analysis of, 20: 11047
reactions with matter, equations for, 20: 11889
RADIATION CHEMISTRY
activation energies in, thermal-spike model for low, 20: 10887
aqueous solution, transient absorption in uv region from, 20: 10924
chemical species in water radiolysis, effects of, on carbon double bond saturation, 20: 10875
decomposition of aqueous solutions of carbohydrates, role of hydrated

electron in, 20: 10920
equipment and methods for pulse, 20: 10907
excitation transfer and decay in multicomponent system, 20: 10927
excited state quenching in, 20: 10926
intermediate species in pulsed-electron radiolysis of aqueous oxygenated solutions, 20: 10909
pulse radiolysis, survey of some contributions of, 20: 10908
rate constants for hydroxyl radical reaction with organic compounds, 20: 10916
reaction rates in metallic ion–permanganate solutions, 20: 10914
reaction rates in aqueous solutions of nucleic acids and related substances, 20: 10917
reactions in aqueous solutions of amino acids, peptides, and proteins, 20: 10919
reactions of hydrated electron with glycine, other amino acids, 20: 10918
symposium on pulse radiolysis, 20: 10906

RADIATION DETECTION INSTRUMENTS
design of low-background whole-body counter, 20: 10724 (ORINS-51)
design of transistorized, for reactor period measurement, 20: 12344
design using magnetic amplifier, 20: 11162(P)
development for monitoring, 20: 12499(R) (IDO-17112, pp 52-80)
performance in nuclear power plants, 20: 11042
use in polar region space research, 20: 11842

RADIATION DETECTION INSTRUMENTS (PULSE TYPE)
computer program for pulse-height analysis, 20: 11202(R) (NYO-3136-2, App. 1)
counting statistics for, regression model adequacy in mixed radionuclide assay, 20: 11203(R) (NYO-3136-2, App. 2)
dead time determination for, 20: 11125(T)
design and performance for neutron detection in high gamma backgrounds, 20: 11154
design for radioisotope identification, 20: 11171(P)
design for two-dimensional scanning and automatically recorded scintigram, 20: 11161(P)
design of scintillation, for detecting alpha-source contamination in man, 20: 11107 (RFP-462)
design of scintillator, for stabilized operation, 20: 11166(P)
resolution time of, determination of paired-pulse, (T), 20: 11105 (NAA-SR-Memo-11132)
statistical analysis of pulse-height distribution of, 20: 11201(R) (NYO-3136-2)
statistical analysis of pulse-height distributions from mixed radionuclides, 20: 11204(R) (NYO-3136-2, App. 3)

RADIATION DETECTORS
bibliography on, thermal-neutron, 20: 11088 (AED-C-28-01)
design using electric discharge phenomenon, 20: 11163(P)
performance of Hanford personnel-monitoring, 20: 11046

RADIATION INJURIES
mechanisms in *Pasteurella tularensis*, 20: 10694
pathology of bone, induced by chronic, low-dose exposure, 20: 10637
protection against, effects of polysaccharide prepared from yeast cultures in mice, 20: 10703
protection against, chemicals for, 20: 10688
protection against, in dogs and rats using chemical compounds, 20: 10699(T) (NASA-TT-F-353, pp 210-38)
protection against skin, during gamma therapy, effects of sulfur and glutathione, 20: 10702
protection against, effects of anoxia in mice, effects of age, 20: 10707
protection against, effects of cystamine in mice, 20: 10708
rat intestinal, effects of adrenal factors on, 20: 10697
recovery mechanisms for, in normal and neoplastic animal cells, 20: 10650
repair in Neurospora, mechanisms of, 20: 10716
therapy of, using bone marrow, 20: 10688

RADIATION MONITORING
environmental, at PRR, 20: 12545(R) (PAEC(A)AR651)
equipment for, magnetic amplifier for, 20: 11162(P)
methods for industrial personnel working with cesium-137, 20: 10721
system for ORNL, design of laboratory-wide, 20: 11049

RADIATION PROTECTION
book: *Problems of Radiation Safety in Space Flights. Physical and Biological Studies with High-Energy Protons*, 20: 10604(T) (NASA-TT-F-353)
mechanisms for, 20: 10639
methods for, in occupational exposure, 20: 10660
methods of, in nuclear power plants, 20: 11042
regulations for gamma defectoscopy in Bulgaria, 20: 11036(T) (JPRS-33502)
research in, 20: 10639
standards for, in contaminated environments, 20: 11039
standards for, of personnel, 20: 11045
standards for, of personnel at Hanford, 20: 11046

RADIATION SICKNESS
development in dogs and rats by protons and x rays, 20: 10611(T) (NASA-TT-F-353, pp 185-93)
gastrointestinal disturbances during chronic, 20: 10674
pathology of, induced by exposure to thermonuclear explosion, 20: 10701

RADIATION SOURCES
use in digital measuring apparatus, 20: 11085(P)

RADIATION TARGET CANS
welding method for, 20: 11263(P)

RADIATION TARGETS
design for proton-beam atomic reactions with gases, 20: 11448(R) (TID-22480)
development for production of x rays by beta bombardment, 20: 12545(R) (PAEC(A)AR651)
preparation of thin-film isotope, using vacuum evaporation-condensation, 20: 11183 (ORNL-P-1900)
production of thin liquid sheets for, 20: 11409
sample holder for deuteron, design of, 20: 11410

RADIATORS
design for cesium and potassium Rankine cycles, 20: 12475 (WANL-PR(B)-009)
design for space power supplies, 20: 12480

RADIO WAVES
absorption in ionosphere, auroral and polar cap, (T), 20: 11858
emission from plasma, review of nonthermal and thermal, 20: 12256
use of low frequency, in ionospheric D region density profile measurements from rockets, 20: 11846
use of vlf phase recordings for determining solar particle precipitation in polar cap regions, 20: 11856

RADIOACTIVE CONTAMINATION
estimation in reactor accidents, 20: 12333

RADIOACTIVE MATERIALS
control of, at Hanford, 20: 11046
disposal of gaseous, methods for, 20: 12522
inventory of, in reactor accidents, 20: 12333
laboratory design, equipment, and construction for, bibliography on, 20: 10977 (KFK-370)
packaging and transportation of, 20: 11045
separation from waste waters by sorption by clay minerals, 20: 12527(P)

RADIOACTIVITY
content in surface waters, control measures for, 20: 11021
determination in Indiana soils by scintillation counting, 20: 11019
determination in Indiana precipitation by scintillation counting, 20: 11020

RADIOAPPLICATORS
use of cobalt-60 bead, for brain tumor therapy, 20: 10575

RADIOBIOLOGY
book: *Ionizing Radiation: Neural Function and Behavior*, 20: 10689

RADIOCHEMICAL PROCESSING PLANTS
decontamination of ORNL molten-salt fluoride-volatility, 20: 11032 (ORNL-3891)

RADIODERMATITIS
effects on trace element metabolism in rabbits, 20: 10625

RADIODIAGNOSIS
dosimetry in, performance of photoluminescent and thermoluminescent dosimeters in, 20: 11155

RADIOFREQUENCY SPECTROMETERS
pulse analyzers for magnetic spin resonance, 400-channel, 20: 11098 (IS-1312)
use for ionospheric charged particle density measurements, 20: 11847

RADIOGRAPHY
effects of diagnostic, on sex ratio of offspring of women exposed during pregnancy, 20: 10657
method using thermal neutrons, 20: 11005(P)
radiation dose from dental, 20: 10720
regulations for industrial gamma, in Bulgaria, 20: 11036(T) (JPRS-33502)

RADIOISOTOPES
conference on, in protein metabolism studies, 20: 10539 (STI/DOC/10/45)
flow and dispersion in rocks, effects of ground water on, (T), 20: 11010 (HNS-1229-61)
identification of, device for, 20: 11171(P)
incorporation in plasma proteins, methods and uses for, 20: 10561
production and uses of, 20: 10933(R) (TID-22532)
production at PRR, summary on, 20: 12545(R) (PAEC(A)AR651)
production in reactors, design of pneumatic handling system for, 20: 12350(P)
production in reactors, 20: 10507
shipping in United States, review of general aspects of, 20: 11035 (TID-8541, pp 249-319)
sorption by soils, 20: 12545(R) (PAEC(A)AR651)
surface water contamination by, hazards to man from, 20: 11021
transport by flowing ground water, hazards of, (T), 20: 11010 (HNS-

1229-61)
transport of, regulations on, 20: 11040
use in power supplies for space vehicles, 20: 11188 (BLG-330)
RADIOLOGICAL WARFARE
radiation hazards of, 20: 10701
RADIOMETRIC ANALYSIS
titration methods of, determination of equivalence point in, 20: 10777
RADIOPROTECTIVE COMPOUNDS
effectiveness of amino acid, against uv radiation, 20: 10695
effects of AET, on serum transaminase activity in irradiated mice, 20: 12545(R) (PAEC(A)AR651)
efficiency of 2,4-dinitrophenol, 20: 10629
review of chemical, 20: 10688
RADIOSENSITIVITY
effects of amino acids on yeast-cell, 20: 10695
of animal cells, x, 20: 10650
of cervical cancers, cytological appraisal of, 20: 10739
of cervical cancers, cytological appraisal of, 20: 10740
of cervical cancers, cytological appraisal of, 20: 10741
of cervical cancers, cytological appraisal of, 20: 10742
of Escherichia coli, effects of folic acid analogs on, 20: 10648
of fungi, effects of tobacco leaf extract on, 20: 10620
of sarcoma cells, effects of irradiation in suspension before injection in mice, 20: 10634
of *Tribolium castaneum*, effects of age, sex, temperature, and dose of fast neutrons and x, 20: 11184(R) (BNWL-122, pp 137-9)
of Tribolium, effects of sulfoxide compounds on, 20: 10504(R) (BNWL-122, pp 142)
of tumors, effects of single and fractionated dose of γ and x, 20: 10649
of tumors, effects of dose fractionation, x, 20: 10651
RADIOSTERILIZATION
bacterial metabolism in oysters following, 20: 10690
equipment for, design of, 20: 10986(P)
of flour beetle, *Tribolium castaneum*, 20: 11184(R) (BNWL-122, pp 137-9)
RADIOTHERAPY
dosimetry in, performance of photoluminescent and thermoluminescent dosimeters in, 20: 11155
dysprosium-165-labeled versenate in, 20: 10737
effects of cervical carcinomas, review of indirect, 20: 10670
histological evaluation of radium, for cervical carcinomas, 20: 10749
selectivity in neutron-capture, 20: 10728
sources for, α, deuteron, fast neutron, meson, and proton, 20: 10736
RADIUM
content in plankton, sediments, and waters of Black Sea and Lake Techirghiol, 20: 10512
effects on cervical carcinomas, histological evaluation of, 20: 10749
effects on small intestine after cervical cancer therapy, 20: 10654
radiation effects from, on sorption of aqueous organic dye solutions by barium sulfate, 20: 10936(T) (CEA-tr-A-1855)
use as gamma source for therapy of cervical carcinomas, 20: 10727
use as gamma source for therapy of cervical cancers, 20: 10739
use of implants of, as γ source for treatment of cervical carcinoma during pregnancy, 20: 10751
RADIUM ISOTOPES Ra-223
energy level transition spectra from thorium-227 decay, (E), 20: 11992
RADIUM ISOTOPES Ra-224
content in coastal waters of Black Sea, 20: 10768(T) (JPRS-33212)
determination in Black Sea, method for, 20: 10768(T) (JPRS-33212)
RADIUM ISOTOPES Ra-228
content in Black Sea, factors affecting, 20: 10768(T) (JPRS-33212)
determination in Black Sea, method for, 20: 10768(T) (JPRS-33212)
RADON
content in plankton, sediments, and waters of Black Sea and Lake Techirghiol, 20: 10512
RAIN WATER
analysis for fallout fission products in, London, 1964, 20: 11018
radioactivity of Indiana, determination of gamma, 20: 11020
RARE EARTH ALLOYS
Al-rare earth, crystal structure of intermetallic compounds in, 20: 11305
RARE EARTH CHLORIDES
rare-earth-ion fluorescent lifetimes in crystals of, 20: 12317
RARE EARTH COMPLEXES
carbonate, composition in solution of, 20: 10824
with bis(2-ethylhexyl)phenylphosphonate, stability of, 20: 10953
RARE EARTH HYDRIDES
reactions with mercury, review on, 20: 10812 (NAA-SR-Memo-11569)
RARE EARTH IONS
electric field parameters crystals, (T), 20: 12322
energy transfer between excited states of, in crystals, 20: 12317
fluorescent lifetimes in crystals, 20: 12317
nuclear quadrupole shielding factors in crystals, (T), 20: 12323
spectra of, hypersensitive transitions in absorption, 20: 11469
RARE EARTH ISOTOPES
nuclear structure in superfluid model, (T), 20: 11961 (INR-602/VII/PH)
RARE EARTH NITRATES
nitrogen-14 NMR in, 20: 12325
RARE EARTH SALTS
spectra of, Zeeman effect in, (T), 20: 11456(T) (AERE-Trans-1041)
RARE EARTH SELENIDES
CaSe–rare earth selenides, phase studies, 20: 10857
RARE EARTHS
determination in fluorites, spectrographic, 20: 10775
electron structure of, analysis using positron annihilation, (E), 20: 11323
energy level transition probabilities in deformed odd A, for $153 \leq A \leq 181$, (E/T), 20: 11951 (AE-205)
inhalation of dusts of, during occupational exposure, 20: 11057
magnetic properties, 20: 11340
metallography of, specimen preparation for, 20: 11310
origin in solar system, 20: 11377
separation by ion exchange or solvent extraction, 20: 10955
separation by ion exchange in columns in aluminum nitrate media, 20: 10956
separation by partition chromatography using bis(2-ethylhexyl)phenylphosphonate, 20: 10953
separation by partition chromatography, 20: 10960
separation by solvent extraction using TBP, effects of ion charge and radius on, 20: 10952
separation from thorium by ion exchange, 20: 10959
RARE GASES
distribution in EVESR coolant and moderator, 20: 12399(R) (GEAP-4941)
electric discharges in, effect of longitudinal magnetic induction on initiation of h-f, (E/T), 20: 11780
electron beam production in, large-diameter, low-voltage, (E), 20: 11367 (D1-82-0448)
RATE METERS
response of moving G-M, to discrete beta sources, 20: 11089 (AERE-M-1671)
RATS
calcium-45 uptake by bones of, effects of calcium and phosphorus content in diet on, 20: 10549
cerium-144 metabolism in, effects of chemical carcinogens on, 20: 10526(R) (BNWL-122, pp 91-3)
distribution of inhaled uranium ore aerosols in tissues of, 20: 10514(R) (BNWL-122, pp 21-4)
effects of cortisone on mesenteric mast cells in normal and adrenalectomized, 20: 10686
effects of diphtherial toxins on heart muscle of, pathological, 20: 10631
effects of neptunium-237 of fat accumulation in liver of, 20: 10522(R) (BNWL-122, pp 79-80)
elimination of mixed β emitters from, 20: 10552
hemoglobin of, Mössbauer effect in iron-57-enriched iron(II) and (III) compounds in, 20: 10903
iodine-131 distribution in tissues of, 20: 10554
plutonium excretion by, effects of deferoxamine on, 20: 10531(R) (BNWL-122, pp 118-21)
plutonium excretion by, effects of DTPA on, 20: 10531(R) (BNWL-122, pp 118-21)
plutonium poisoning in, effects of splenectomy on, 20: 10524(R) (BNWL-122, pp 83-4)
plutonium-238 metabolism in, effects of chemical carcinogens on, 20: 10526(R) (BNWL-122, pp 91-3)
pneumonia incidence in laboratory, 20: 12545(R) (PAEC(A)AR651)
praseodymium-144 metabolism in, effects of chemical carcinogens on, 20: 10526(R) (BNWL-122, pp 91-3)
proton distribution in phantoms of, 20: 10605(T) (NASA-TT-F-353, pp 21-54)
radiation effects on, pathological, x, 20: 10598(R) (BNWL-122, pp 107-9)
radiation effects on intestinal absorption of bile salts in, x, 20: 10599(R) (BNWL-122, pp 128-30)
radiation effects on mucus synthesis in intestine of, x, 20: 10600(R) (BNWL-122, pp 131-4)
radiation effects on reproduction in, fission neutrons, 20: 10601(R) (BNWL-122, pp 135-6)
radiation effects on hematopoiesis in, electron-beam, 20: 10681
radiation effects on lymph node cells in, after diphtheria immunization, 20: 10685
radiation effects on mesenteric mast cells in normal and adrenalectomized, 20: 10686
radiation effects on, protective effects of chemical compounds against, 20: 10699(T) (NASA-TT-F-353, pp 210-38)
radiation effects on, protective effects of hormones against, 20: 10709
radiation effects on, protective effects of MEA against, 20: 10714
radiation effects on ascorbic acid metabolism in, protective effects of

cystamine and mercamine against, 20: 10715
radiation effects combined with 6-purinethiol on skin graft survival in, x, 20: 10506
radiation effects on uptake of sulfur-35-labeled sodium sulfate by liver tissue in, 20: 10542
radiation effects on, mixed β, 20: 10552
radiation effects on adrenal cortex in, x, 20: 10576
radiation effects on lactic- and malic-acid dehydrogenases in liver and spleen extracts from, x, 20: 10583
radiation effects on calcium uptake by skeletons in, tracer study of x, 20: 10587
radiation effects on erythrocyte membranes in newborn, 20: 10589
radiation effects on iridindiphosphate glucose content in liver of, x, 20: 10590
radiation effects on activity of alanine–2-oxoglutarate and aspartate–2-oxoglutarate-aminotransferase in, x, 20: 10593
radiation effects on, multipledose energy proton, 20: 10606(T) (NASA-TT-F-353, pp 55-102)
radiation effects on, single-dose high-energy proton, 20: 10607(T) (NASA-TT-F-353, pp 103-41)
radiation effects on, RBE of proton and x-ray, 20: 10611(T) (NASA-TT-F-353, pp 185-93)
radiation effects on, comparison of RBE of gamma, proton, and x-ray, 20: 10612(T) (NASA-TT-F-353, pp 194;209)
radiation effects on osmotic resistance of leukocytes of, x, 20: 10614
radiation effects on fetuses of, pathological, x, 20: 10616
radiation effects on desoxyribonuclease activity in spleen, x, 20: 10622
radiation effects on myocardium of, pathological, γ, 20: 10631
radiation effects on desoxyribonucleotide content in bone marrow, spleen, and thymus of, β and γ, 20: 10633
radiation effects on production of erythropoietic factor in kidney of, uv, 20: 10635
radiation effects on fatty acid and total lipid content of, liver of, 20: 10659
radiation effects on growth of tumor transplants in, 20: 10665
radiation injuries to intestines of, effects of adrenal factors on, x, 20: 10697
radioinduced dominant lethals in, proton and x-ray, 20: 10609(T) (NASA-TT-F-353, pp 151-6)
radioinduced osteosarcomas in, β, 20: 10652
radiosensitivity of tumors in, effects of actinomycin on, 20: 10700
ruthenium-106 excretion by, effects of various treatments on, 20: 10532(R) (BNWL-122, pp 122-4)
skin graft survival in, effects of 6-purinethiol on, 20: 10506
strontium-90 uptake by bones of, effects of calcium and phosphorus content of diet on, 20: 10549
toxic effects of copper in, 20: 10598(R) (BNWL-122, pp 107-9)

REACTION MECHANISMS
analysis of chemical, by depolarization of mesons (μ^+), 20: 11377
kinetics of, in carboxyl production in pulse-radiolysis, 20: 10913
kinetics of, in pulse radiolysis of potassium bromide solutions, 20: 10911
kinetics of, in pulse-radiolysis of aerated aqueous potassium bromide solutions, 20: 10912
kinetics of, in pulse-radiolysis of permanganate–metallic ion solutions, 20: 10914
kinetics of, in pulse-radiolysis of thiocyanate solutions, 20: 10915
kinetics of aqueous carbohydrate radiolysis, 20: 10920
kinetics of fast, computer program for digitization of photographic oscilloscope traces of, 20: 10800 (ANL-7113)
rate constants for, use of pulse radiolysis in measuring, 20: 10908
rate constants for hydroxyl radical–organic compound, 20: 10916
rate constants in pulse radiolysis of solution of methylene blue, 20: 10925
rate constants in sulfuric and perchloric acid solution radiolysis, 20: 10909
rates of hydrated electron and hydroxyl radical reactions with nucleic acids and related substances, 20: 10917
rates of hydrated electron reactions with glycine, other amino acids, and peptides, 20: 10918
rates of hydrated-electron, with amino acids, peptides, and proteins, 20: 10919

REACTOR COMPONENTS
development for ARMF and ATR critical facility, 20: 12499(R) (IDO-17112, pp 52-80)
failure of, probabilistic analysis of, 20: 11048
instrumentation development, 20: 11061(R) (IDO-17112)
instrumentation for NERVA, radiation effects on, 20: 11175 (NP-15823)

REACTOR CONTROL ELEMENTS
properties of boron oxide–cadmium oxide–indium oxide glasses as, 20: 11226
properties of cadmium oxide–indium oxide glasses as, 20: 11226

REACTOR CONTROL RODS
design and hydraulics for closed-cycle water reactors, 20: 12418(R) (WCAP-3739)
drive mechanism design for, 20: 12349(P)
drive testing for PBF and SPERT III, instrumentation for, 20: 11174(R) (IDO-17112, pp 81-91)
effectiveness of safety, in Fermi Fast Breeder Reactor, 20: 12387 (APDA-NTS-3)
efficiency of partially inserted, in cylindrical reflected reactor, (T), 20: 12367 (UJV-1442/65)
feasibility of boron automatic, for closed-cycle water reactors, 20: 12418(R) (WCAP-3739)
reactivity effects of, methods for calculating, 20: 12362 (RFR-193)
worth evaluation of, computer calculations for, 20: 12418(R) (WCAP-3739)

REACTOR CONTROL SYSTEMS
design using liquid paraffin-boron carbide powder for scram, 20: 12347
development for ATR critical facility, 20: 12499(R) (IDO-17112, pp 52-80)

REACTOR COOLANTS
analyses for chemical and radioactive contamination, 20: 12509
deaeration of water, in WWR-M reactor, 20: 12504
heat transfer coefficients for gaseous, comparison of, 20: 12341
heat-transfer properties of organic, 20: 12331
performance in fast reactors, 20: 12433
performances of gas and sodium, for fast reactors, 20: 12345

REACTOR COOLING SYSTEMS
development for large closed-cycle water reactors, 20: 12418(R) (WCAP-3739)
flow diffusion in Big Rock Point, equipment for, 20: 12450
pipe failures in, probability of, 20: 12338(R) (GEAP-4911)
pressure and temperature control system for, 20: 12438

REACTOR ENGINEERING
cooling system reliability studies, 20: 12338(R) (GEAP-4911)
design studies for 1000-Mw(e) fast-breeder and supercritical steam-cooled reactors, 20: 12413 (TID-22545)
spacetime reactor analysis methods, 20: 12334

REACTOR FUEL ALLOYS
burnup studies on plutonium, core design for, 20: 12403 (LA-3384)

REACTOR FUEL ELEMENTS
analysis for hydrogen peroxide, iodine-129, and metals by controlled-potential coulometry, 20: 10758 (EUR-2618.f)
analysis for plutonium-239 by neutron transmission techniques, 20: 10796
analysis of irradiated MITR, by gamma spectroscopy, 20: 10764 (MITNE-64)
burnout heat flux in open lattice cores, (E/T), 20: 12418(R) (WCAP-3739)
burnup in, nondestructive methods for determination of, 20: 11004
burnup of stainless steel and zirconium clad, in PWR, 20: 12418(R) (WCAP-3739)
cladding wear testing in boron-water solutions, 20: 12418(R) (WCAP-3739)
critical heat flux for 19-rod, in forced-convection boiling, 20: 10994 (TID-22539)
deformations of PBF, devices for measuring, 20: 11174(R) (IDO-17112, pp 81-91)
design and development of EVESR Mark V, 20: 12399(R) (GEAP-4941)
design and mechanical testing of water-cooled, 20: 12418(R) (WCAP-3739)
design and testing of advanced Bonus, 20: 12399(R) (GEAP-2941)
design of enclosed-assembly, 20: 12381(P)
design of EVESR Mark IV, 20: 12399(R) (GEAP-4941)
design of polygonal, with helical fins, 20: 12382(P)
development and testing of EVESR ESH-3A, 20: 12399(R) (GEAP-4941)
development of Dungeness B, 20: 12430
development of Rapsodie, 20: 12419(T,R) (EURFNR-1F)
fabrication and control of, CNEN laboratory for, Saluggia, Italy, 20: 11247
fabrication for exponential experiment in DON reactor, welding techniques for, 20: 12401 (JEN-156-DMe/113)
fabrication of, nuclear materials management in, 20: 11262
failure of, radiometric detection of uranium release in, 20: 11003
heat transfer and burnout of boiling organic cooled, 20: 12331
heat transfer from ML-1, with boundary-layer turbulence promoters, 20: 10988 (CONF-12-5)
heat transfer properties of, effects of surface profile on, 20: 10993 (TID-22513)
oxidation in defective, by reactive coolant, (E/T), 20: 12380
pressure measurements using strain gages, 20: 11174(R) (IDO-17112, pp 81-91)
processing aluminum-clad, by dissolution in molten salts, 20: 10971(P)
processing of irradiated, nuclear materials management in, 20: 10967
processing of, criticality control in, 20: 10969

radiation effects on EVESR bundles KB-29 and KB-41, 20: 12399(R) (GEAP-4941)
testing in carbon dioxide streams, method for detecting uranium release in, 20: 11003
testing in EVESR, flux wire data from, 20: 12399(R) (GEAP-4941)
testing of ATR, instrumentation for, 20: 12499(R) (IDO-17112, pp 52-80)

REACTOR FUEL ELEMENTS (CERAMIC)
coatings for particles, deposition-condition effects on properties of pyrolytic carbon, 20: 11254
development of urania, containing boron carbide dispersions, 20: 11226
neutron buckling in 7- and 19-element clusters of uranium dioxide, (E/T), 20: 12493 (AECL-2514)
neutron resonance temperature correlation for pellets of uranium dioxide, effective, (T), 20: 12372
performance and properties of mixed oxide, 20: 11222
preparation of uranium dioxide, hexafluoride thermochemical reduction for, 20: 11257
processing of molybdenum–uranium dioxide, chlorination, 20: 10961
radiation effects on plutonium carbide–uranium carbide, 20: 12442
welding of wire spacers to stainless steel and Zircaloy cladding of, projection, 20: 12377(R) (CEND-2863-236)

REACTOR FUEL ELEMENTS (DISPERSION)
performance and properties of stainless steel–urania, 20: 11222
preparation, 20: 11224

REACTOR FUEL ELEMENTS (THERMOELECTRIC)
design, 20: 12482
design of high-temperature, 20: 12383(P)
properties of, effects of emitter materials on, 20: 12479

REACTOR FUEL PINS
neutron flux distributions in multiple, computer program for, 20: 12384 (AGN-TM-411)

REACTOR FUEL RODS
neutron resonance absorption by, computer program for calculating, 20: 12351 (ANL-7033)
transport of spent, design of container for, 20: 10985(P)

REACTOR FUELS
burnup in heterogeneous reactors, computer program for calculating, 20: 12361 (PEL-60)
canning of, properties of beryllium for, 20: 11294
cladding for, fabrication of titanium–vanadium alloy, 20: 11258
development for power breeders, 20: 12407 (NEIC-RR-13)
fabrication of, review of remote, 20: 11241 (TID-8541, pp 71-148)
materials for, evaluation of carbide, 20: 12378
performance and properties of metal-base, 20: 11222
performance of carbide, metallic, and oxide, in fast reactors, 20: 12433
processing of carbide, methods for, 20: 10964
processing of spent, methods for, 20: 10962
processing of, commercial and economic aspects of, 20: 10963
radiation effects on coated uranium carbide and uranium dioxide particles, 20: 11343 (LA-3367)
shipping of spent, casks for, 20: 10963
volatility separation processes for spent, 20: 10965

REACTOR MATERIALS
corrosion and radioinduced brittle fracture of HFIR, 20: 12457 (ORNL-TM-1372)
purity of, methods for controlling, 20: 12429
research progress on, *Technical Progress Reviews*, Winter 1965–1966, 20: 11223

REACTOR MATRICES
neutron physics analyses of EVESR Mark III, 20: 12399(R) (GEAP-4941)
reactivity of EVESR Mark IV, 20: 12399(R) (GEAP-4941)

REACTOR MODERATORS
crystal lattice dynamics of, (T), 20: 12275 (GA-6861)

REACTOR SAFETY
accident studies for critical facilities and test reactors, 20: 12498(R) (IDO-17112, pp 1-51)
analyses for sodium-cooled fast reactors, 20: 12433
analysis of accident consequences, procedure for, 20: 12333
containment concept using steel strands in biological shield, 20: 12346
control systems design for, 20: 12335
cooling system failure probability, 20: 12338(R) (GEAP-4911)
core cooling and venting in coolant-loss accidents, 20: 12447
evaluation for sodium-cooled reactors, two-phase heat transfer, hydrodynamic effects, and void formations in, 20: 10990 (NAA-SR-11586)
hazards analysis for EVESR Mark IV core, 20: 12399(R) (GEAP-4941)
review organization at Vallecitos Atomic Laboratory, 20: 12337
studies for Masurca critical assembly and Rapsodie reactor, 20: 12419(T,R) (EURFNR-1F)
use of acoustic emission for detecting metal overstress, 20: 11001 (BNWL-SA-438)
use of probabilistic methods for development of, 20: 11048

REACTOR SAFETY EXPERIMENTS
control-rod drive testing for SPERT III, instrumentation for, 20: 11174(R) (IDO-17112, pp 81-91)
coolant flow in LOFT, transients in, 20: 12498(R) (IDO-17112, pp 1-51)
core design for SPERT III, low enrichment oxide, 20: 12497 (IDO-17003(Rev.2))
fission product release in LOFT, sampling and analysis of, 20: 12356 (IDO-17128)
fuel cladding strain in SPERT I, measurement of, 20: 11174(R) (IDO-17112, pp 81-91)
neutron kinetics of SPERT III, 20: 12498(R) (IDO-17112, pp 1-51)
operation of KEWB, 20: 12510

REACTOR SHIELDING
design for optimum weight, 20: 12342
design of biological, containing steel strands for accident containment, 20: 12346
neutron fluxes and heating in SNAP-8DS, (T), 20: 12468 (NAA-SR-Memo-9916)
performance of beryllium oxide and lithium hydride, 20: 12475 (WANL-PR(B)-009)

REACTORS
containment of, using steel strands in biological shield, 20: 12346
containment structure leak testing, 20: 12332
control-rod reactivity effects in, methods for calculating, 20: 12362 (RFR-193)
design of heavy liquid-metal-reflected, 20: 12376(P)
design of, performance of flux synthesis methods for, (E/T), 20: 12368 (WAPD-T-1737)
design seminar, 20: 12413 (TID-22545)
development, technological review of, 20: 12329 (TID-5541)
experimental facilities for radioisotope-production, pneumatic tube system, 20: 12350(P)
gamma and neutron dosimetry for, conference on, 20: 11110 (STI/DOC/10/46)
heat transfer and neutron kinetics in, computer program for, 20: 12354 (GAMD-6644(Add.))
heat transfer from surfaces in, to thermionic converters, simulation of radiant, 20: 12487
heat transfer in liquid-cooled, computer program for, 20: 10989 (IDO-28595(Rev.))
heat transfer in thermionic, evaporation-condensation, (T), 20: 12488
licensing of, rule changes for U. S., 20: 12437
neutron density fluctuations in, hydraulic noise effects on, (T), 20: 12360 (ORNL-TM-1332)
neutron diffusion in, accuracy of variational method for, (T), 20: 12369
neutron dosimetry in, methods for, 20: 11150
neutron flux distribution in cylindrical, with partially inserted control rods, (T), 20: 12367 (UJV-1442/65)
neutron flux eigenvalue problems of, group-theory method for, (T), 20: 12373
neutron flux in, performance of synthesis method for calculating, (E/T), 20: 12368 (WAPD-T-1737)
neutron flux variations in, method for calculating, (T), 20: 12366 (UJV-1439/65)
neutron kinetics in moving, thermal, 20: 12371
neutron lifetime in, space-dependent formula for Rossi-α measurements for, (T), 20: 12375
neutron resonance absorption in, computer program for calculating, 20: 11932 (GA-6637)
pressure vessel for liquid cooled, 20: 12348(P)
pumps for thermionic space, review of electromagnetic, 20: 12481
reactivity measurements servo-controlled regulating rods, 20: 12499(R) (IDO-17112, pp 52-80)
reactivity period meter for, development of transistorized, 20: 12344
reactivity temperature coefficients of, computer program for calculating, 20: 12353 (GA-6734)
reactivity transfer function measurements in, equipment for, 20: 11154
regulatory actions on U. S., summary on, 20: 12436
site evaluation for, procedures for considering accidents in, 20: 12333
thermal shielding of high-temperature, reinforced chamotte and chromite concretes for, (T), 20: 12340
thermionic cells for, performance of cylindrical rare gas-filled, 20: 11547
xenon buildup in, simulator for studying, 20: 12498(R) (IDO-17112, pp 1-51)

RECOIL IONS
ranges of copper, in aluminum, (E), 20: 12085

RELATIVITY THEORY
book: *Introduction to Special Relativity*, 20: 11890
Cartesian tensors in spaces with indefinite metric for, 20: 11879
field equations in, exact solutions of Einstein-Maxwell, 20: 11877
formalism for particles of arbitrary spin in curved spaces, 20: 11759
gravitational mass of moving particle cluster in, 20: 11869
Kruskal space without wormholes, (T), 20: 11886
light reflection from Schwarzschild source, (T), 20: 11885
Lorentz transformation in, generalized, (T), 20: 11870

mass in expanding universe, (T), 20: 11873
masses in general, dynamics and stability of spherically symmetric, 20: 11889
parallelism in general, 20: 11868 (UCRL-14546)
test of general, radar reflection from planets for, (T), 20: 11432
test of general, solar gravitational effects on radar reflection from planets for, (T), 20: 11433
tests of, precession of satellite orbits as, (T), 20: 11883

RELAYS
circuit design for alarm, using radiation counters, 20: 11084(P)

REMOTE-CONTROL EQUIPMENT
brake assembly for, engineering drawings of, 20: 11078

RENÉ-41
mechanical properties of fusion-welded, 20: 11260
radiation effects on stress-rupture properties of, neutron, 20: 11358

RESEARCH REACTORS
coolant analysis for chemical and radioactive contamination, 20: 12509
coolant deaeration in WWR-M, 20: 12504
criticality of ZED-2, computer calculation of, 20: 12493 (AECL-2514)
design and uses of SORA, for neutron and solid state physics, 20: 12495 (EUR-2538.e)
design of Harmonie, 20: 12507
design of materials-testing, 20: 12515(P)
development of Harmonie, 20: 12419(T,R) (EURFNR-1F)
experimental facilities of FRJ-2, cold neutron beam tube, 20: 12503(T) (AERE-Trans-1042)
fuel element fabrication for Avogadro, 20: 11247
gamma and neutron dosimetry in, status in France, 20: 11146
krypton-89 and -90 decay probability in recombiner of L54M, (E), 20: 12508
neutron dosimetry for, review of in-pile, 20: 11144
neutron dosimetry in, status in Germany, 20: 11147
neutron dosimetry in, status in Hungary, 20: 11148
neutron dosimetry in, status in Netherlands, 20: 11149
neutron dosimetry in, status in United Kingdom, 20: 11151
neutron dosimetry in, status in Yugoslavia, 20: 11152
neutron spectra in Triga Mark-II, fast, (T), 20: 12505
operation of, shift crew performance for, 20: 12500 (IDO-17131)
performance and uses of pulsed, for neutron and solid state physics, 20: 12495 (EUR-2538.e)
radioactivity release from WWR-M, reduction of, 20: 12504
use in biology and medicine, 20: 10507

RESINS
use of epoxy, in instrument attachment to reactor fuel-channel tubes, 20: 12450

RESISTORS
design of variable shunt, for accelerator magnet coils, 20: 11388 (CONF-650922-29)
stability of thermistors, 20: 11062 (RFP-649)

RESPIRATION
radiation effects on endogenous, in Ehrlich ascites tumor cells, x, 20: 10691

RESPIRATORY TRACTS
calcium-45 uptake by human, combined thallium-204 and, 20: 10546
effects of beryllium aerosols on, of man, 20: 11038
thallium-204 uptake by human, combined calcium-45 and, 20: 10546

RETICULO-ENDOTHELIAL SYSTEM
radioinduced stimulation of, effects on fibrinogen levels of, 20: 10679

RHENIUM
compatibility and encapsulation with neodymium, promethium, and samarium oxides, 20: 11267 (BNWL-SA-488)
deposition on molybdenum and tungsten, electro-, 20: 11260
diffusion in single-crystal tungsten, 20: 11227
effects of alloy additions of, on mechanical properties of niobium, 20: 11302
fabrication by hot isostatic pressing, 20: 11260
neutron reactions (n,γ) at 30 to 170 kev, cross sections for, (E), 20: 11986
proton reactions with, phosphorus-32 and -33 production in, (E), 20: 12034

RHENIUM ALLOYS
Cr–Re, crystal structure of, dislocations in, 20: 11303
Cr–Re, transition temperature of, notch-impact, 20: 11300
Dy–Re, phase studies, 20: 11298
Er–Re, phase studies, 20: 11298
Gd–Re, phase studies, 20: 11298
Ho–Re, phase studies, 20: 11298
Mo–Re, compatibility and encapsulation with neodymium, promethium, and samarium oxides, 20: 11267 (BNWL-SA-488)
Nb–Re, mechanical properties of, effects of composition on, 20: 11288(T) (AD-622477)
Pr–Re, phase studies, 20: 11298
Re–Tb, phase studies, 20: 11298
Re–W, deposition of, properties of vapor, 20: 11256
Re–W, extrusion of, process development for, 20: 11260
Re–W, fabrication and properties for use at 2600°C, 20: 11238 (CONF-650449-1)

RHENIUM FLUORIDE NITRIDES
preparation and properties of, 20: 10845

RHENIUM FLUORIDES
preparation and properties of, 20: 10845
ReF_6–WF_6, reduction to rhenium–tungsten alloy using hydrogen, 20: 11256

RHENIUM ISOTOPES Re-183
properties of isomeric, (E), 20: 12042

RHENIUM ISOTOPES Re-185
helium ion reactions at 40.9 Mev, fission, (E), 20: 11955 (COO-347-19)
neutron activation cross section at 24 kev, (E), 20: 12135

RHENIUM ISOTOPES Re-187
helium ion reactions at 40.9 Mev, fission, (E), 20: 11955 (COO-347-19)
neutron activation cross section at 24 kev, (E), 20: 12135

RHENIUM ISOTOPES Re-188
decay scheme, (E), 20: 11998

RHENIUM SYSTEMS
C–Hf–Re–Ta–W, preparation and properties of dispersion-strengthened, 20: 11217(R) (WANL-PR(Q)-007)

RHODIUM
alpha reactions at 42 Mev, proton emission in, (E), 20: 12062

RHODIUM ALLOYS
Mo–Rh, phase studies, 20: 11309
Nb–Rh, phase studies, 20: 11227
Rh–W, phase studies, 20: 11309

RHODIUM COMPOUNDS
superconductivity in chalcogenide, (E), 20: 11899

RHODIUM ISOTOPES Rh-103
neutron activation cross section at 24 kev, (E), 20: 12135

RHODIUM ISOTOPES Rh-106
determination in irradiated MITR fuel elements by gamma spectroscopy, 20: 10764 (MITNE-64)
effects of inhaled oxide particles of, pathological, 20: 10513(R) (BNWL-122, pp 16-20)
effects on plutonium determination in fission product solutions, 20: 10763 (KR-100)

RHODIUM OXIDES
distribution of inhaled particles of, in dogs, 20: 10513(R) (BNWL-122, pp 16-20)

RIBONUCLEASE, DEOXY-
radiation effects on activity of, in cell nuclei and cytoplasm of animal cells, 20: 10591
radiation effects on activity in spleen, x, 20: 10622

RIBONUCLEIC ACID
radiation effects on content of, in rat adrenal glands, x, 20: 10576

RIBONUCLEIC ACID, DESOXY-
radiation effects on HeLa-cell, synthesis of α and γ, 20: 10588
radiation effects on synthesis of, after cervical carcinoma therapy, 20: 10670
radioinduced luminescence of, role of hydroperoxides in, 20: 10578

RIBONUCLEOTIDES, DESOXY-
radiation effects on content in radiosensitive tissues, β and γ, 20: 10633

RICE
radiation effects on Bengawan and Peta varieties of, gamma, 20: 12545(R) (PAEC(A)AR651)

ROCKET MOTORS
properties of, review, 20: 12476(T) (AD-622352)

ROCKET REACTORS
criticality of TWMR, (T), 20: 12465 (GA-6807)
design optimization for interplanetary manned flight, 20: 12492
review of advanced, 20: 12477
stability of coupled-core, 20: 12491

ROCKET REACTORS (KIWI)
particle dispersion and size distribution from explosive destruction of NERVA mockup, 20: 12471 (SC-RR-65-557)
radiation effects on coated fuel particles for, transient, 20: 11343 (LA-3367)
radiation effects on linear-displacement transducers in NERVA, model for studying, 20: 11175 (NP-15823)
safety testing of, destructive, 20: 12472 (SC-RR-65-620)
testing of ROVER/NERVA mockup, debris distribution from destructive, 20: 12470 (SC-R-65-1017)

ROCKETS
propulsion systems for, review of advanced nuclear, 20: 12477

ROCKS
radioactivity of, scintillation detector for measuring gamma, 20: 11087 (AE-203)
radioisotope dispersion and flow in, effects of ground water on, (T), 20: 11010 (HNS-1229-61)

ROOTS

development of grass, following seed γ-irradiation, 20: 10646
radioinduced chromosomal aberrations in bean, protective effects of nitrogen against, 20: 10712
radiosensitivity of chromosomes in Vicia, effects of N-ethylmaleimide on x, 20: 10624
RUBIDIUM
reactions with helium atoms, cross sections for excitation transfer in, (E), 20: 11482
reactions with iodine bromide in crossed molecular beams, spectator stripping model for, 20: 10834
separation from fused salts by ion exchange, tracer studies of, 20: 10958
superconducting critical field and transition temperature of, isotope effect on, (E), 20: 11913
RUBIDIUM ALLOYS
Hg–Rb, formation and properties of, 20: 11215(R) (NASA-CR-54718)
RUBIDIUM CHLORIDES
color centers in, band shape of optical emission from F, (E), 20: 12278 (TID-21570)
magnetic moment of molecular, rotational, (E), 20: 11484
radiation absorption and emission by F centers in, (T), 20: 12274(R) (COO-578-18)
RUBIDIUM FLUORIDES
magnetic moment of molecular, rotational, (E), 20: 11484
RUBIDIUM ISOTOPES Rb-84
use as tracer for coronary blood flow, 20: 10730
RUBIDIUM ISOTOPES Rb-87
light absorption by, excited-state disorientation cross sections for, (E), 20: 11486
RUBIDIUM NITRATES
radiolysis of, at 77, 300, and 400°K, effects of pressure on, 20: 10891
$RbNO_3$–$AgNO_3$, electrochemical and thermochemical properties of fused, 20: 10804 (EUR-2466.e, pp 9-19)
RUBIES
radiation effects on chromium divalent and tetravalent ion content in, x, 20: 12305
RUPTURE
mechanisms of pipe, 20: 12338(R) (GEAP-4911)
RUSSIAN REACTORS
design of 350-Mw(e) sodium-cooled BN-350 power breeder, 20: 12441
fuel element temperature distributions in 350-Mw(e) sodium-cooled BN-350 power breeder, 20: 12443
RUTHENIUM
corrosion by low-melting-point metals, 20: 11227
determination in irradiated uranium dioxide, 20: 10787
effects of alloy additions of, on mechanical properties of niobium, 20: 11302
superconductivity of, correlation between isotope and pressure effects on, 20: 11896
RUTHENIUM ALLOYS
Ru–U, phase studies, 20: 11224
RUTHENIUM COMPOUNDS
superconductivity in chalcogenide, (E), 20: 11899
RUTHENIUM ISOTOPES Ru-103
content in ocean fish, effects of content in sea water on, 20: 11054
RUTHENIUM ISOTOPES Ru-106
diffusion from simulated solid wastes, 20: 12517(R) (BNWL-170)
effects of inhaled oxide particles of, pathological, 20: 10513(R) (BNWL-122, pp 16-20)
effects on plutonium determination in fission product solutions, 20: 10763 (KR-100)
excretion by rats, effects of various treatments on, 20: 10532(R) (BNWL-122, pp 122-4)
sorption of complexes of, by sand, 20: 10855
sorption of complexes of, by clays, 20: 10855
sorption of complexes of, by soils, 20: 10855
sorption of complexes of, by peat, 20: 10855
sorption of complexes of, by sludge, 20: 10855
RUTHENIUM NITROSYL NITRATES
separation by solvent extraction using Butex or TBP, 20: 10947 (AERE-R-4786)
RUTHENIUM OXIDES
distribution of inhaled particles of, in dogs, 20: 10513(R) (BNWL-122, pp 16-20)
RYE
cesium-137 content in German, effects of precipitation on, 20: 11017
strontium-89 and -90 content in German, effects of precipitation on, 20: 11017

S

SAFETY
book: *Problems of Radiation Safety in Space Flights. Physical and Biological Studies with High-Energy Protons*, 20: 10604(T) (NASA-TT-F-353)
in AEC 1964 operations, nuclear incident related to, 20: 11051
program for Operation HENRE, 20: 11930 (CEX-65.03)
re-entry ablation of strontium-90 fuel capsules for space power plants, 20: 11189 (MND-3062-25)
regulations for gamma defectoscopy in Bulgaria, 20: 11036(T) (JPRS-33502)
review of Hanford program for, 20: 11046
SALICYLIC ACID
labeling with carbon-14, 20: 10868
SALTS
separation by extraction chromatography using organic phosphorus compounds, 20: 10759 (INP-427/C)
SAMARIUM
gamma incoherent scattering by K-shell electrons of, at 320 kev, (E), 20: 11514
heat of solution in liquid tin at 828°K, 20: 11304
magnetic properties, 20: 11340
separation from other elements by solvent extraction using TBP, 20: 10952
SAMARIUM ALLOYS
Sm–Sn, tin Knight shift and magnetic susceptibility of $SmSn_3$, 20: 12324
SAMARIUM CARBONATES
complexes of, composition in solution of, 20: 10824
SAMARIUM IONS
spin-lattice relaxation in lanthanum ethyl sulfates, (E), 20: 12300
spin-lattice relaxation of trivalent, in lanthanum chlorides, (E), 20: 12292
spin-lattice relaxation in magnesium lanthanum nitrates, (E), 20: 12300
spin-lattice relaxation in yttrium ethyl sulfates, (E), 20: 12300
SAMARIUM ISOPROPOXIDE
reactions with methyl acetoacetate, 20: 10846
SAMARIUM ISOTOPES
excitation of even-even, by oxygen ions to 65 Mev, (E), 20: 12110
SAMARIUM ISOTOPES Sm-146
energy levels at 1381 kev from decay of europium-146 and promethium-146, 20: 12081
SAMARIUM ISOTOPES Sm-147
determination in uranium-233 and -235 fission products, (E), 20: 11960(R) (IDO-14667)
SAMARIUM ISOTOPES Sm-149
determination in uranium-233 and -235 fission products, (E), 20: 11960(R) (IDO-14667)
reactor criticality effects of, tables for calculating transients from, 20: 12352 (DP-958)
SAMARIUM ISOTOPES Sm-151
determination in uranium-233 and -235 fission products, (E), 20: 11960(R) (IDO-14667)
SAMARIUM ISOTOPES Sm-152
determination in uranium-233 and -235 fission products, (E), 20: 11960(R) (IDO-14667)
oxygen-ion scattering at 35 Mev, lifetime of 2^+ levels from, (E), 20: 12020
SAMARIUM ISOTOPES Sm-154
determination in uranium-233 and -235 fission products, (E), 20: 11960(R) (IDO-14667)
SAMARIUM NITRATES
nitrogen-14 NMR, (E), 20: 12325
SAMARIUM OXIDES
compatibility and encapsulation with alloys and metals, 20: 11267 (BNWL-SA-488)
use as neutron absorber in glasses, 20: 12273(P)
SAMARIUM SELENIDES
CaSe–Sm_2Se_3, phase studies, 20: 10857
SAMPLING
equipment for, of uranium concentrates, 20: 10978 (RMO-3006)
SAN ONOFRE POWER REACTOR
coolant loss accidents in, flow analysis of, (T), 20: 12418(R) (WCAP-3739)
fuel assembly design and testing for, 20: 12418(R) (WCAP-3739)
fuel assembly for, mechanical testing of, 20: 12418(R) (WCAP-3739)
SANDS
geochemistry of thorium and uranium in, in Lower Triassic deposits, Pripyat Basin, USSR, 20: 11026
ruthenium-106 sorption by, 20: 10855
SANDSTONE
geochemistry of thorium and uranium in, in Lower Triassic deposits, Pripyat Basin, USSR, 20: 11026
SAP (SINTERED ALUMINUM PRODUCTS)
plasticity of dispersed-phase, mechanisms of, 20: 11269 (EUR-2483.f)
SARCOMAS
induction of immunoresistance in mouse, by irradiation of cells in suspension before injection, 20: 10634
radioinduced in bone, by strontium-90 and chemical carcinogens,

20: 10627
radioinduced in swine, by beta particles from ingested strontium-90, 20: 10597(R) (BNWL-122, pp 37-45)
radioinduced radioresistant mouse, induction by exposure of cells in suspension before injection, 20: 10634
SATELLITES
orbits about celestial bodies as tests of general relativity, precession of, (T), 20: 11883
radiation doses to, in various orbits, 20: 11840
SAVANNAH RIVER PLANT
dosimetry system for use in event of accidents at, 20: 11029 (DP-1006)
SAXTON POWER REACTOR
control rod cladding for, corrosion testing of, 20: 12418(R) (WCAP-3739)
coolant sampling in, chemical and radiochemical analysis of, 20: 12418(R) (WCAP-3739)
fuel assemblies for, irradiation proof testing of, 20: 12417(R) (WCAP-3269-15)
fuel assembly design for irradiation testing in, 20: 12418(R) (WCAP-3739)
kinetic experiments in, instrumentation development for, 20: 12418(R) (WCAP-3739)
neutron flux and multiplication in subcritical, thermal, 20: 12418(R) (WCAP-3739)
SCANDIUM
solvent properties for tantalum, thermodynamics of, 20: 11306
SCANDIUM ALLOYS
Al–Sc, phase diagram, 20: 11297
Al–Sc, tensile properties, effects of composition on, 20: 11297
Pu–Sc, phase studies, 20: 11224
SCANDIUM CARBONATES
complexes of, composition in solution of, 20: 10824
SCANDIUM ISOTOPES Sc-42
energy level scheme, (E), 20: 12061
SCANDIUM ISOTOPES Sc-43
nuclear moments of, E2 and M1, (E), 20: 12070
SCANDIUM ISOTOPES Sc-47
nuclear moments of, E2 and M1, (E), 20: 12070
SCANDIUM TUNGSTATES
crystal structure, 20: 10858
SCATTERING
amplitude for three-body, variational principle for Faddeev equations for, (T), 20: 11692 (UCRL-11768)
amplitude in left half-plane of complex angular momentum, asymptotic behavior of, 20: 11710
amplitudes at high energies, integral representation for, (T), 20: 11736
amplitudes for final-state interactions in, Aitchison equation for, 20: 12016
amplitudes for, singularities in three-particle, (T), 20: 11701
amplitudes in complex angular momentum plane, partial wave, (T), 20: 11693 (UCRL-12016-T)
amplitudes in, Cutkosky rule for Feynman graphs for, 20: 11687 (JINR-P-2485)
amplitudes in, physical sum rule for forward, (T), 20: 11696
amplitudes in, physical region decoupling method for coupled channel, 20: 11711
amplitudes in, relativistic generalization of dynamic equation for Jost function for, 20: 11703
amplitudes in, single-collision approximation for, (T), 20: 11742
Bethe-Salpeter equation for, (T), 20: 11746
Bethe-Salpeter equation in, Fredholm method for solving, 20: 11757
cross sections in diffraction peat region, restrictions on elastic, (T), 20: 11764
dispersion relations in, solubility of partial-wave, 20: 11699
Green's function for, binary collision expansion of double-time-temperature-dependent, 20: 11653
dependent, 20: 11760
matrix theory of, langrangian form of, 20: 11762
model for nonrelativistic particles, nonunique solutions for, 20: 11763
potential, R-matrix approach to complex angular momentum and three-particle, (T), 20: 11691 (ORNL-3914)
potential, repulsive core in effective nonlocal energy-independent, (T),
potential, Schwinger variational principle for, (T), 20: 11747
potential, sum rules in, 20: 11739
potentials in asymptotic phase and amplitude for modified Coulomb, (T), 20: 11689 (LA-DC-6912)
potentials in elastic, S-matrix formalism for optical model, 20: 12021
potentials in, asymptotic form of phase shift for strongly singular, (T), 20: 11712
potentials in, Regge trajectories and S-matrix for singular, 20: 11706
Regge poles in Froissart-Gribov continuation, unitary conditions for, 20: 11724
S-matrix for finite times in interacting-particle wave-function space, 20: 11761
S-matrix for, relativistic combination of internal and spin symmetries in, (T), 20: 11755
S-matrix in complex angular momentum plane for, Sommerfeld-Watson transformation and dispersion relations for, (T), 20: 11732
S-matrix invariance under complex inhomogeneous Lorentz group, complex angular momentum in, (T), 20: 11758
S-matrix theory for, isospin and spin in, 20: 11720
theory of, determinantal method for N/D equations in, (T), 20: 11700
SCHIFF BASES
solvent properties of, in chloroform for metals, 20: 10759 (INP-427/C)
SCINTILLATION DETECTORS
construction, performance, and testing of stack of, for cosmic-ray measurements underground, 20: 11527
design for gamma activity measurements in geological surveys, 20: 11087 (AE-203)
design for two-dimensional scanning and automatically recorded scintigram, 20: 11161(P)
design of horizontally directional, for well logging, 20: 11024
design of liquid, for gamma measurements and phototube testing, 20: 11128
design with continuous sensitivity variation compensation, 20: 11167(P)
efficiency for low-energy beta counting, 20: 11122
efficiency of liquid, for beta particles, 20: 10902
efficiency of sodium iodide, for gamma radiation, 20: 11127
performance for Bev-range neutrons, 20: 11106 (NP-15786)
performance of lithium–iodide europium-activated, for neutron spectra, 20: 11116
performance of organic, for pulsed gamma radiation dosimetry, 20: 11137
performance of plastic well-type, for determining absolute photoelectric cross sections, 20: 11496
radiation background of sodium iodide, cosmic, 20: 11132
use for gamma counting, 20: 11201(R) (NYO-3136-2)
use for gamma counting, 20: 11204(R) (NYO-3136-2, App. 3)
SCOTLAND
silt movement in ebb channel, Firth of Forth, 20: 11022 (AERE-R-5080)
SEA WATER
corrosive effects on molybdenum and tungsten coupled with aluminum, copper, or magnesium, galvanic, 20: 11230 (BM-RI-6715)
desalination using offshore nuclear power plant, feasibility of, 20: 12453 (TID-22330(Vol.2))
desalination using small organic-cooled reactors, 20: 12454(T) (JPRS-33480)
effects on fatigue crack propagation in nickel–chromium–molybdenum–vanadium steel, 20: 11273(R) (NRL-6364)
movement of surface, south of Iceland, 20: 12541 (NYO-2929-1)
radioactivity of, effects of waste disposal practices on, 20: 11054
radioactivity of, effects on radioactivity of sea foods, 20: 11054
SEED
radiation effects on growth and development of maize, gamma, uv, and x-ray, 20: 10613(T) (NP-tr-1344)
radiation effects on germination of grass, γ, 20: 10646
SEEDLINGS
radiation effects on growth and pH in maize, effects of dose on β, 20: 10683
radiation effects on barley, x, 20: 10619
SEIGNETTOELECTRIC MATERIALS
radiation effects on electric properties of, fast-neutron and gamma, 20: 11352 (NP-15707)
SELENIUM ISOTOPES Se-75
decay of, gamma spectra from, (E), 20: 12022
SELENIUM ISOTOPES Se-80
neutron activation cross section at 24 kev, (E), 20: 12135
SEMICONDUCTOR DETECTORS
defects in silicon p-i-n, determination of, 20: 11103 (JINR-P-2489)
design and performance for measuring electron and proton spectra during auroral storms, 20: 11853
design of lithium-drifted silicon, 20: 11170(P)
performance for heavy ions, energy dispersion and pulse height defect in, (T), 20: 11138
performance of germanium, in gamma spectrometers, 20: 11095 (CRGP-1224)
performance of germanium, in applied gamma spectrometry, 20: 11134
performance of junction, for alpha monitoring, 20: 11092 (CLOR-39/D)
performance of lithium-drifted silicon, for α and β particles, 20: 11097 (INR-621/XV/I)
performance of silicon surface-barrier, for particle spectra from 10 to 200 kev, 20: 11115
performance of silicon, for recording protons, α particles, and nuclei ($Z > 2$), 20: 11124(T)
properties and uses of, review on, 20: 11126
radiation effects on p-i-n, electron, gamma, and x, 20: 11173 (D2-84071-1)

sensitive region in germanium p-i-n determination of width of, 20: 11102 (JINR-P-2487)
SEMICONDUCTORS
electron susceptibility in, effect of resonance radiation field on valence, (T), 20: 12312
electron-hole plasma of, h-f stabilization of screw instability in, (T), 20: 12252
ion reactions with, doping effect in, (E), 20: 12280
performance of large coaxial lithium-drifted germanium, for gamma spectroscopy, (E), 20: 11086 (AAEC/TM-299)
radiation damage by high-energy electrons and protons, research on, (E), 20: 11346(R) (NP-15611)
radiation effects on, homogeneity measurements from electron, 20: 11361
radioinduced damage in n- and p-type silicon, transient electron, (E), 20: 11176(R) (NP-15835)
superconducting transition in, induction using field effect, (T), 20: 11901(T)
SENA POWER REACTOR
development status, 20: 12412(R) (TID-22516)
SEPARATION PROCESSES
shape factors for thermal diffusion columns, 20: 10949 (K-1469)
SERVOMECHANISMS
radiation effects on hydraulic, for space vehicles, 20: 11181
SEWAGE
labeling using gold-198, 20: 12545(R) (PAEC(A)AR651)
SEX
ratio of offspring of women irradiated during pregnancy, 20: 10657
SHEEP
cadmium-115 secretion in milk of, 20: 10527(R) (BNWL-122, pp 94-8)
cesium-137 content of rumen of, effects of cesium content in diet, 20: 10520(R) (BNWL-122, pp 64-6)
dosimetry of gamma radiation from ingested cesium-137 in, performance of *in vivo* thermoluminescent detector for, 20: 11091(R) (BNWL-122, pp 67-72)
iodine-131 content in tissues of, long-term ingestion study, 20: 10516(R) (BNWL-122, 49-51)
milk production by, tracer study, 20: 10517(R) (BNWL-122, pp 52-4)
zinc-65 secretion in milk of, 20: 10527(R) (BNWL-122, pp 94-8)
SHIELDED CONTAINERS
description of, 20: 10963
design for transporting spent reactor fuel rods, 20: 10985(P)
effects of fire on tinplate cans for radioisotope containment, 20: 11028 (AERE-M-1664)
SHIELDING
design of concrete, using boron carbide aggregate, 20: 11229(P)
design of flexible, 20: 12272(P)
design of, methods and tables for, 20: 11058(T)
gamma transmission by multilayer, (T), 20: 12271
performance for 2-Mev to 100-Bev alpha particles, tabulations of, 20: 12265 (NP-15697(Vol. 1))
SHIELDING MATERIALS
performance for cosmic alpha particles and protons, tabulations of, 20: 12265 (NP-15697(Vol. 1))
performance of reinforced chamotte and chromite, for reactor thermal shielding, (T), 20: 12340
SHIPPING
hazards in, of solidified high-level waste, 20: 12517(R) (BNWL-170)
review of radioisotope, in United States, 20: 11035 (TID-8541, pp 249-319)
SHIPS
design of Japanese nuclear-powered, 20: 12462 (CONF-640810, pp 122-37)
nuclear-powered, licensing of, 20: 12464 (CONF-640810, pp 156-65)
nuclear-powered, role of, 20: 12460 (CONF-640810, pp 7-21)
SHOCK WAVES
acceleration at fronts of, model for Fermi, 20: 11437
effects on geomagnetic storm sudden commencement, (T), 20: 11811(T)
pressure distribution on front of strong, from electric-discharge shock tube, 20: 11775
propagation in gases with discrete velocity distributions, (T), 20: 11779
scattering of hydromagnetic, on rigid wall, (T), 20: 11796
structure in finite plasma, one-dimensional, (T), 20: 12234
structure in plasma, (T), 20: 12227
transport in ideal fluids, jump conditions for, 20: 11889
SILICON
defects in p-i-n detectors of, determination of, 20: 11103 (JINR-P-2489)
design of lithium-drifted detector of, 20: 11170(P)
development of dosimeters of, for fast neutrons, 20: 11094(R) (COO-1226-10)
effects of, on activation determination of aluminum in ores, 20: 10781
performance in betavoltaic batteries, 20: 11546 (SC-RR-65-671)
performance in heavy ion detectors, energy dispersion and pulse height defect in, (T), 20: 11138
performance of surface-barrier, as 10 to 200 kev particle detector, 20: 11115
performance of surface-barrier detectors of, 20: 11124(T)
phosphorus ion reactions with single crystals of, doping effect in, (E), 20: 12280
preparation of lithium-drifted, 20: 11097
properties and use of diodes of, for radiation detection, 20: 11126
radiation effects on p-i-n junctions of, electron, gamma, and x, 20: 11173 (D2-84071-1)
radiation effects on transistors of, electron and gamma, 20: 11182
radiation effects on x-ray diffraction by crystalline, alpha, 20: 12281
radiation effects on photoconductivity of, electron, (E), 20: 11351(R) (NP-15611, pp 48-89)
radiation effects on atomic displacements in, by protons at 30 Mev to 1 Bev, 20: 11356
radiation effects on p-type, Hall effect measurement of gamma, 20: 11360
radioinduced damage in n- and p-type, transient electron, (E), 20: 11176(R) (NP-15835)
radioinduced damage in, energy and orientation dependence of electron, 20: 11364
radioinduced defects in, infrared absorption bands of electron, 20: 11347(R) (NP-15611, pp 5-18)
SILICON CARBIDES
compatibility with urania, 20: 11224
development of junction-gate type field-effect transistors of, 20: 12276 (NYO-3405-4)
radiation effects on transistors of, neutron, 20: 12276 (NYO-3405-4)
radioinduced swelling of, fission fragment, 20: 11227
SILICON IONS
energy levels of, (T), 20: 11450 (UCRL-7842-T)
SILICON ISOTOPES Si-28
alpha reactions (α,γ) at 3.2 to 4.3 Mev, energy levels from, (E), 20: 11994
alpha reactions (α,d) at 42 to 53 Mev, deuteron energy spectra from, (E), 20: 12061
energy levels in, model of proton-hole coupling of to, (T), 20: 12052
neutron reactions (n,α) at 14.8 Mev, direct interaction models for, (T), 20: 12002
neutron reactions (n,p) at 14.8 Mev, cross sections for, (E), 20: 12133
neutron reactions (n,α) at 14.8 Mev, angular distributions from, (E/T), 20: 12030
proton reactions (p,2p) at 460 Mev, (E/T), 20: 11948 (AD-624318)
triton reactions (t,p) with, properties of, (T), 20: 11972 (NP-15716)
SILICON ISOTOPES Si-30
alpha reactions (α,γ) at 3.2 to 4.3 Mev, energy levels from, (E), 20: 11994
bremsstrahlung reactions (γ,2p) at 51.4 Mev, magnesium-28 yields from, (E), 20: 12094
SILICON OXIDES
radioinduced swelling of, fission fragment, 20: 11227
Al_2O_3–SiO_2, preparation and properties of, for use in cesium ion exchange from waste solutions, 20: 10766 (TID-22511)
SILICON SYSTEMS
Al–Si–U, properties of splat-cooled, 20: 11224
Cu–Si, deposition on molybdenum for oxidation protection, 20: 11236
Nb–Si, mechanical properties of, effects of composition on, 20: 11288(T) (AD-622477)
Si–W, phase diagram, 20: 11296
SILICONE POLYMERS
radiation effects on electric and physical properties of, gamma and neutron, 20: 11344 (N65-35361)
SILTS
analysis for calcium, magnesium, and strontium, 20: 12540(R) (NYO-2882-8)
manganese content of open-ocean, mechanism of deposition of, 20: 12540(R) (NYO-2882-8)
movement in ebb channel, Firth of Forth, tracer study on, 20: 11022 (AERE-R-5080)
radium, radon, and uranium contents of, in Black Sea and Lake Techirghiol, 20: 10512
ruthenium-106 sorption by, 20: 10855
SILVER
determination of, silver-109 neutron resonance activation integral for, (E), 20: 10789
gamma reactions at 320 kev, absolute photoelectric cross sections for, (E), 20: 11496
light absorption by, mechanism of photographic sensitivity from, (T), 20: 11121
light scattering by bound electrons in, second-harmonic generation and Raman effects in, (T), 20: 12245
proton reactions at 1.84 Bev, sodium-24 energy spectra and yield in, (T),

20: 12067
proton reactions with, phosphorus-32 and -33 production in, (E), 20: 12034
reactions with permanganate ions during pulse-radiolysis of solutions, 20: 10914
tin-119 Mössbauer effect in, 20: 12315

SILVER ACETYLIDES
Ag_2C_2–$AgNO_3$, qualification tests on spray-deposited and light-initiated explosives of, 20: 10814 (SCL-DC-65-96)

SILVER ALLOYS
Ag–Th, phase studies, 20: 11224
Eu–Ag, phase studies, 20: 11327

SILVER IODIDES
preparation of beta sources of, method for, 20: 10935 (USNRDL-TR-948)

SILVER IONS
radiolysis of, aqueous solutions of, 20: 10922

SILVER ISOTOPES Ag-109
neutron activation cross section at 24 kev, (E), 20: 12135
neutron capture by, resonance integral of, (T), 20: 10789
neutron capture by, polarization of silver-110 from, (E), 20: 12098
neutron transmission at 30 ev to 20 kev, resonance parameters for, (E), 20: 12072
nuclear moment and spin of isomeric, (E), 20: 12073

SILVER ISOTOPES Ag-110
polarization of, from neutron capture by silver-109, (E), 20: 12098

SILVER ISOTOPES Ag-111
energy levels, (E), 20: 12145

SILVER NITRATES
Ag_2C_2–$AgNO_3$, qualification tests on spray-deposited and light-initiated explosives of, 20: 10814 (SCL-DC-65-96)
$AgNO_3$–$NaNO_3$, electrochemical and thermochemical properties of fused, 20: 10804 (EUR-2466.e, pp 9-19)
KNO_3–$AgNO_3$, electrochemical and thermochemical properties of fused, 20: 10804 (EUR-2466.e, pp 9-19)
$LiNO_3$–$AgNO_3$, electrochemical and thermochemical properties of fused, 20: 10804 (EUR-2466.e, pp 9-19)
$RbNO_3$–$AgNO_3$, electrochemical and thermochemical properties of fused, 20: 10804 (EUR-2466.e, pp 9-19)

SINGLE CRYSTALS
deformation in, resolution of stresses in, 20: 11331
radiation effects on, electron resonance study of, at 20 to 300°K, 20: 10876

SKELETON
radiation effects on calcium uptake by rat, tracer study of x, 20: 10587
radiation effects on developing, in rat fetuses, x, 20: 10616
strontium-90 uptake by rat, effects of calcium and phosphorus content of diet on, 20: 10549

SKIN
iodine-131 absorption by swine, 20: 10518(R) (BNWL-122, pp 55-8)
radiation effects on tadpole tail, effects of starvation during irradiation on x, 20: 10676
radiation injuries of, protective effects of sulfur and glutathione against γ, 20: 10702
radiosensitivity of, effects of content of sulfhydryl radicals on γ, 20: 10702

SKIN GRAFTING
effects of 6-purinethiol on rat, 20: 10506
immune reactions to, in mice, 20: 10632
radiation effects combined with 6-purinethiol on rat, x, 20: 10506

SKIN LESIONS
radioinduced, treatment of, 20: 10658

SLURRIES
flow through pipes, Bingham viscosity and yield stress for, 20: 10998

SNAILS
radiation effects on, gamma, 20: 12545(R) (PAEC(A)AR651)

SNOW
radioactivity of Indiana, determination of gamma, 20: 11020

SODIUM
boiling heat transfer and critical heat flux for, in forced convection, 20: 10990 (NAA-SR-11586)
corrosive effects on steels at 1000 to 1200°F of flowing, equation for, 20: 11227
effects of high-carbon, on mechanical properties of type 316 stainless steel, at 1200°F, 20: 11235 (MSAE-65-194)
effects on creep rate of type 316 stainless steel at 1200°F, 20: 11227
effects on mechanical properties of chromium–molybdenum steel, 20: 11227
heat transfer by 900°K, in tubes, 20: 12488
heat transfer by, in turbulent flow, 20: 12483
positron thermalization in, (E), 20: 11660
properties as reactor coolant, technological review of, 20: 12330 (TID-8541, pp 321-425)
proton reactions with atoms of, production of highly excited hydrogen atoms by charge-exchange, (E), 20: 11471(T)
reactions with air in reactors, model for processes in, (T), 20: 10851
reactions with water in steam generators, 20: 12386 (APDA-176)
reactions with water in sodium-heated steam generators, 20: 12391 (BAW-1280-28(Vol.3))
separation from fused salts by ion exchange, tracer studies of, 20: 10958
soil content of, effects on strontium-85 uptake by plants, 20: 10534(R) (BNWL-122, pp 168-9)
soil content of, effects on calcium-45 uptake by plants, 20: 10534(R) (BNWL-122, pp 168-9)
soil content of, effects on cesium-137 uptake by plants, 20: 10534(R) (BNWL-122, pp 168-9)
technology for fast reactors, 20: 12419(T,R) (EURFNR-1F)
thermal properties of solidified wastes of, 20: 12517(R) (BNWL-170)

SODIUM ACID CARBONATES
radiolysis of deaerated aqueous solutions of, pulsed-electrons, 20: 10913

SODIUM CHLORIDES
corrosive effects on molybdenum and tungsten at 35, 60, and 100°C, 20: 11230 (BM-RI-6715)
corrosive effects on molybdenum and tungsten coupled with aluminum, copper, or magnesium, galvanic, 20: 11230 (BM-RI-6715)
corrosive effects on magnesium and its alloys, electrochemistry of pitting, 20: 11231 (CEA-R-2815)
effects on stress corrosion cracking in chromium–iron–nickel alloys, 20: 11233(R) (COO-1319-32)
reactions of fused, with chromium fluoride or lanthanum oxide, 20: 10821
thermodynamic properties of, in heavy water, 20: 10847
LiH–NaCl, phase studies, 20: 10832
$MgCl_2$–NaCl, corrosive effects on titanium-base alloys at 550 to 600°F, stress-, 20: 11227

SODIUM FLUORIDES
reactions of fused, with chromium fluoride or lanthanum oxide, 20: 10821

SODIUM FORMATES
radiolysis of deaerated aqueous solutions of, pulsed-electrons, 20: 10913

SODIUM GRAPHITE REACTORS
calandria core maintenance tools for, development of remote, 20: 12405 (NAA-SR-Memo-11576)

SODIUM HYDROXIDES
corrosive effects on molybdenum, tungsten, and vanadium at 35 and 60°C, 20: 11230 (BM-RI-6715)
corrosive effects on vanadium-base alloys at low temperatures, 20: 11230 (BM-RI-6715)
corrosive effects on molybdenum and tungsten coupled with aluminum, copper, or magnesium, galvanic, 20: 11230 (BM-RI-6715)
corrosive effects on magnesium and its alloys, electrochemistry of pitting, 20: 11231 (CEA-R-2815)
reactions with coconut oil, tracer study of, 20: 12545(R) (PAEC(A)AR651)

SODIUM HYPOCHLORITES
corrosive effects on molybdenum, tungsten, and vanadium at 35 and 60°C, 20: 11230 (BM-RI-6715)

SODIUM IODIDES
efficiency of crystals of, in scintillation detectors, 20: 11127
magnetic moment of molecular, rotational, (E), 20: 11484
radiation background of scintillation spectrometer of, cosmic, 20: 11132
scintillation efficiency of thallium-activated, effect of temperature on, 20: 11118
thermodynamic properties of, in heavy water, 20: 10847

SODIUM IONS
electron reactions below threshold to 1 kev, cross sections for single ionization in, (E), 20: 11490
energy levels of, (T), 20: 11450 (UCRL-7842-T)

SODIUM ISOTOPES Na-22
energy levels, (E), 20: 12061
nuclear structure of, configuration mixing and independent particle motion in, (T), 20: 12128

SODIUM ISOTOPES Na-23
alpha scattering at 18 Mev, (E), 20: 12099
neutron reactions (n,p) at 14.8 Mev, cross sections for, (E), 20: 12133

SODIUM ISOTOPES Na-24
energy spectra and yields in proton reactions with copper, silver, and bismuth at 1.84 Bev, (T), 20: 12067
production at PRR, methods for, 20: 12545(R) (PAEC(A)AR651)

SODIUM MOLYBDATES
photosensitivity of, effects of titanium dioxide on, 20: 10837

SODIUM NITRATES
effects of fused, on efficiency of mineral ion exchangers, 20: 10958
radiolysis of, at 77, 300, and 400°K, effects of pressure on, 20: 10891
$AgNO_3$–$NaNO_3$, electrochemical and thermochemical properties of fused, 20: 10804 (EUR-2466.e, pp 9-19)
KNO_3–$NaNO_3$, ion transfer in fused, 20: 10805 (EUR-2466.e, pp 21-30)

SODIUM REACTOR EXPERIMENT
heat transfer protection system for, operation and testing of, 20: 12406 (NAA-SR-Memo-11648)

moderator and reflector elements for, design and performance of Zircaloy-2 clad, 20: 12404 (NAA-SR-11160)
SODIUM SULFATES
radiation effects on uptake of sulfur-35-labeled, by rat liver, 20: 10542
$MgSO_4$–Na_2SO_4, effects of sulfur-35 on exchange reactions in, 20: 10936(T) (CEA-tr-A-1855)
Na_2SO_4–SO_3, effects of sulfur-35 on exchange reactions in, 20: 10936(T) (CEA-tr-A-1855)
O–Na_2SO_4, effects of sulfur-35 on exchange reactions in, 20: 10936(T) (CEA-tr-A-1855)
SODIUM SYSTEMS
Ar–Na, excitation transfer in first excited states of sodium, cross sections for collision-induced, (E), 20: 11499
He–Na, excitation transfer in first excited states of sodium, cross sections for collision-induced, (E), 20: 11499
Kr–Na, excitation transfer in first excited states of sodium, cross sections for collision-induced, (E), 20: 11499
Na–Xe, excitation transfer in first excited states of sodium, cross sections for collision-induced, (E), 20: 11499
Ne–Na, excitation transfer in first excited states of sodium, cross sections for collision-induced, (E), 20: 11499
SODIUM TUNGSTATES
photosensitivity of, effects of titanium dioxide on, 20: 10837
SOILS
calcium-45 uptake by plants from, effects of sodium content on, 20: 10534(R) (BNWL-122, pp 168-9)
cesium-137 uptake by plants from, effects of sodium content on, 20: 10534(R) (BNWL-122, pp 168-9)
iodine-131 deposition and retention on, effects of moisture and temperature on, 20: 10717(R) (BNWL-122, pp 166-7)
radioactivity of Indiana, determination of gamma, 20: 11019
ruthenium-106 sorption by, 20: 10855
sorptive properties for radioisotopes, 20: 12545(R) (PAEC(A)AR651)
strontium-85 uptake by plants from, effects of sodium content on, 20: 10534(R) (BNWL-122, pp 168-9)
strontium-89 diffusion in, effects of electric field on, 20: 11053
strontium-90 diffusion in, effects of calcium on, 20: 12523
SOLAR FLARES
charged-particle energy and rigidity spectra in polar regions from, (E), 20: 11855
particles from, diffusion model for propagation of, 20: 11428(T)
properties of, (T), 20: 11438
proton fluxes from, correlations with cosmic noise absorption and geomagnetic and interplanetary fields, (E), 20: 11852
radiation emission from, corpuscular and electromagnetic, 20: 11438
SOLAR RADIATION
composition of solar wind, 20: 11437
detection of neutrino, by gallium-71 (ν,e$^-$) reactions, (T), 20: 11537
effects of solar wind, on magnetospheric boundary, (T), 20: 11838
hazards of, in space flight, 20: 10719(T) (NASA-TT-F-353, pp 3-20)
intensity of flare-associated, during Sept. 1963, 20: 11429(T)
measurement in polar cap regions using absorption events, (E), 20: 11863
precipitation in polar cap regions, vlf phase recording network for determining, 20: 11856
propagation of particles from flare, diffusion model for, 20: 11428(T)
properties of solar wind, (E), 20: 11438
reactions with cesium atoms, ionization from, (T), 20: 11549
SOLIDS
conference, 20: 12320
diffusion of particles in, generalized equations for, (T), 20: 11369
dosimetry using, bibliography on, 20: 11027 (AED-C-21-03)
proton channeling in crystalline, transverse two-dimensional model for, (T), 20: 12279 (UCRL-12311)
SOLUTIONS
decontamination from phosphorus-32 by ion exchange, 20: 10780
radiolysis of aqueous, reactions of hydrated electron with water in pulse, 20: 10894
SONIC INSPECTION
methods of ultra-, for sintered beryllium oxide, 20: 11324
SOVIET UNION
waste disposal standards in, comparison of, with U.S., 20: 12521
SPACE
radiation environment in, 20: 11181
space environment in, definition of, 20: 11840
SPACE FLIGHT
book: *Problems of Radiation Safety in Space Flights. Physical and Biological Studies with High-Energy Protons*, 20: 10604(T) (NASA-TT-F-353)
fission product decay in SNAPSHOT I, 20: 12466 (NAA-SR-11642)
mission profile for manned Mars, using nuclear electric and rocket propulsion, 20: 12492
radiation hazards to man in, 20: 10719(T) (NASA-TT-F-353, pp 3-20)
SPACE VEHICLES
design for manned Mars mission, 20: 12492
materials testing, 20: 11520
power plant design for, TRIKT-50, 20: 12482
power plants for, parameters of fast thermionic-reactor, 20: 12483
power plants for, review of nuclear, 20: 12484
power plants for, temperature distribution in fast thermionic reactor, 20: 12486
power supplies for, use of radioisotope, 20: 11188 (BLG-330)
power supplies for, properties of, 20: 12476(T) (AD-622352)
power supplies for, thermionic reactors for, 20: 12478
power supply for, design of hydride-moderated thermionic reactor, 20: 12479
power supply for, radiator design for, 20: 12480
power systems for, heat transfer pipes performance for, (T), 20: 11542 (EUR-2534.e)
power systems for, re-entry ablation of strontium-90 fuel capsules for, 20: 11189 (MND-3062-25)
propulsion of, development of ion engines for, 20: 11006(R) (NP-15824)
propulsion of, properties of fast and thermal thermionic reactors for, 20: 12478
propulsion systems for, propellant valve development for, 20: 11007(R) (NP-15831)
radiation effects on hydraulic systems for, 20: 11181
re-entry heating rates for, methods for calculating, (T), 20: 12467 (NAA-SR-11704)
shielding against cosmic alpha particles and protons, tabulations for, 20: 12265 (NP-15697(Vol.1))
use in high-latitude studies, 20: 11842
SPANISH REACTORS (DON)
fuel element fabrication for exponential experiment in, welding techniques for, 20: 12401 (JEN-156-DMe/113)
SPANISH REACTORS (JEN-1)
containment structure leak testing, 20: 12332
SPARK CHAMBERS
development and performance of automatic retrieval, 20: 11093(R) (COO-614-34, Sect. IIA)
operation of corrugated-plate, for alpha and neutron detection, 20: 11120
performance for multiple particle detection, 20: 11114 (UR-875-66)
performance of Cherenkov-counter triggered, for detecting meson (π^0)-decay photons, 20: 11099 (JINR-P-2436)
photograph scanning system for, performance of cathode-ray tube, 20: 11104 (LNF-65/33)
power supply for streamer, performance of high-voltage, (E/T), 20: 11142
track pictures from, particle kinematics from, (T), 20: 11100 (JINR-P-2467)
SPECTROMETERS
burner for atomic absorption, design and performance of long-path oxy-acetylene, 20: 10761 (IS-T-69)
description of electrostatic deflection, for ionospheric particles, 20: 11158
design of hyperfrequency, for study of irradiated single crystals at 20 to 300°K, 20: 10876
SPECTROSCOPY
source for, design of plasma-jet, 20: 10798(P)
use for nondestructive determination of burnup in nuclear fuels, 20: 11004
SPERM
effects of ingested deuterium oxide on mouse, 20: 10550
SPLEEN
radiation effects on rat, pathological, x, 20: 10598(R) (BNWL-122, pp 107-9)
radiation effects on human, after Thorotrast carotidography, 20: 10680
radiation effects on biochemical properties of homogenates of mouse, γ, 20: 10577
radiation effects on lactic- and malic-acid dehydrogenases in extracts of rat, x, 20: 10583
radiation effects on desoxyribonuclease activity in rat, x, 20: 10622
radiation effects on mouse, model for β, 20: 10640
radiosensitivity effects of phospholipid extracts of, in mice, 20: 10704
radiosensitivity effects of marrow transplants into mouse, 20: 10713
STABLE ISOTOPES
production in Spain, 20: 11191 (JEN-150-DQ/I-51)
STACK DISPOSAL
gas-handling system for, design of, 20: 11050
STAINLESS STEEL
bonding to refractory metals and alloys of types 321 and 347, explosive, 20: 11243(R) (WANL-PR(EE)-001)
boronization of, procedure for, 20: 11260
carburization of types 304 and 316, by high-carbon sodium at 1200°F, 20: 11235 (MSAE-65-194)
compatibility and encapsulation with neodymium, promethium, and samarium oxides, 20: 11267 (BNWL-SA-488)
compatibility with indium at 1300°F of types 316 and 410, 20: 11215(R)

(NASA-CR-54718)
compatibility with urania, 20: 11224
compatibility with boron carbide of types 304 and 430, 20: 11226
corrosion by cesium at 400°C of types 17-4PH, 17-7PH, and AM 350, 20: 11227
corrosion by flowing sodium at 1000 to 1200°F of type 316, equation for, 20: 11227
corrosion by mercury vapor at 1250°C of type 316, 20: 11214(R) (NASA-CR-54717)
corrosion properties of, effects of metal purity on, 20: 11227
creep in argon–oxygen environment at 815°C of type 304, effects of oxygen content on, 20: 11227
creep rate in air, helium, and sodium at 1200°F of type 316, 20: 11227
erosion by mercury vapor at 640°F of type 347, 410, 17-4PH, and PH15-7Mo, 20: 11214(R) (NASA-CR-54717)
iron-57 Mössbauer effect in, (E), 20: 12296
mechanical properties of type 316, effects of high-carbon sodium on, at 1200°F, 20: 11235 (MSAE-65-194)
performance as fuel element cladding in large PWR, 20: 12418(R) (WCAP-3739)
properties of bimetal tubes for niobium or niobium–1 zirconium alloy and type 316, 20: 11214(R) (NASA-CR-54717)
properties of type 310, as weld-filler metal, 20: 11214(R) (NASA-CR-54717)
radiation effects on stress-rupture of 20/25/Nb-stabilized, combined heat treatment and in-reactor, 20: 11227
strain fatigue limit of Type 304, biaxial, 20: 12418(R) (WCAP-3739)
tensile properties of type 302, effects of exposure to cesium at 650°C on, 20: 11227
thermal stress fatigue of types 304, 304L, and 403, 20: 11227
welding for nuclear reactor plants, safety requirements for, 20: 11259
welding of fuel element spacer to, projection, 20: 12377(R) (CEND-2863-236)
welding of types 304 and 321, automatic inert gas tungsten arc, 20: 11246
welding to 9 chromium–1 molybdenum steel of type 316, weld-filler metal for, 20: 11214(R) (NASA-CR-54717)
Cr–Ni–stainless steel, strain fatigue limits of, biaxial, 20: 12418(R) (WCAP-3739)
stainless steel–UO_2, fabrication by roll bonding, 20: 11260

STAINLESS STEEL COUPLES
Cu/Nb/stainless steel, diffusion in bimetallic tubing of, with iron diffusion barrier, inter-, 20: 11215(R) (NASA-CR-54718)
Fe/Nb/stainless steel, diffusion in bimetallic tubing of, with iron diffusion barrier, inter-, 20: 11215(R) (NASA-CR-54718)
Fe/Nb/stainless steel/V, diffusion in bimetallic tubing of, with iron and vanadium diffusion barriers, inter-, 20: 11215(R) (NASA-CR-54718)
Fe/Nb–Zr/stainless steel, diffusion in bimetallic tubing of, with iron diffusion barrier, inter-, 20: 11215(R) (NASA-CR-54718)
Fe/Nb–Zr/stainless steel/V, diffusion in bimetallic tubing of, with iron and vanadium diffusion barriers, inter-, 20: 11215(R) (NASA-CR-54718)
Fe/stainless steel/Ta, diffusion in bimetallic tubing of, with iron diffusion barrier, inter-, 20: 11215(R) (NASA-CR-54718)
Fe/stainless steel/Ta/V, diffusion in bimetallic tubing of, with iron and vanadium diffusion barriers, inter-, 20: 11215(R) (NASA-CR-54718)
Mg/stainless steel, corrosion pitting by chloride ions, 20: 11231 (CEA-R-2815)
Mo/Ni/Nb/stainless steel, diffusion in bimetallic tubing of, with molybdenum and nickel diffusion barriers, inter-, 20: 11215(R) (NASA-CR-54718)
Mo/Ni/Nb–Zr/stainless steel, diffusion in bimetallic tubing of, with molybdenum and nickel diffusion barriers, inter-, 20: 11215(R) (NASA-CR-54718)
Mo/Ni/stainless steel/Ta, diffusion in bimetallic tubing of, with molybdenum and nickel diffusion barriers, inter-, 20: 11215(R) (NASA-CR-54718)
Nb/stainless steel, diffusion in bimetallic tubing of, inter-, 20: 11215(R) (NASA-CR-54718)
Nb–Zr/stainless steel, diffusion in bimetallic tubing of, inter-, 20: 11215(R) (NASA-CR-54718)
stainless steel/Ta, diffusion in bimetallic tubing of, inter-, 20: 11215(R) (NASA-CR-54718)

STANDARDS
compilation of U. S. nuclear, 1964 ASA, 20: 12559
isotopic compositions of 16 uranium isotope, by National Bureau of Standards, 20: 10795

STARS
collapse of, hydrodynamic calculations of general-relativistic, (T), 20: 11434
collapse of, Kerr solution of Einstein equations for, (T), 20: 11435
energy spectra of nonthermal radio, effect of electron distribution function on, (T), 20: 11427
explosions of, hydrodynamic properties of supernova, (T), 20: 11425 (UCRL-7777)
properties of, book on, 20: 11436

STATISTICS
computer program for pulse-height analysis for radionuclide assay data, 20: 11202(R) (NYO-3136-2, App. 1)
multivariate regression analysis of sex ratio among offspring from irradiated women, 20: 10657
regression model adequacy in radionuclide assay, test for, 20: 11203(R) (NYO-3136-2, App. 2)
theory for electromagnetic fields, phase-space distribution function in, 20: 11880
use for analysis of pulse-height distribution data from gamma scintillation counting, 20: 11201(R) (NYO-3136-2)
use for estimating probability of light bulb failure, 20: 11205(R) (NYO-3136-2, App. 4)
use in analysis of pulse-height distribution from scintillation counting of mixed radionuclides, 20: 11204(R) (NYO-3136-2, App. 3)

STEAM
heat transfer coefficients for, 20: 12341
pressure control system for, in EBR-2, 20: 12438
reactions with graphite, 20: 11225
reactions with uranium carbide in defective fuel elements, oxidation, (E/T), 20: 12380

STEEL
analysis for oxygen, activation, 20: 10771
brittle fracture properties of, bend test to measure effects of welding on, 20: 11240(R) (EURAEC-1520)
brittle fracture properties of, effects of weld distribution and size on, 20: 11240(R) (EURAEC-1520)
coating by plasma-sprayed tungsten, fusion-bonding of, 20: 11242 (UCRL-12153)
erosion by mercury vapor at 640°F of Dynacut tool, 20: 11214(R) (NASA-CR-54717)
properties of welded joints in thick plates of 1.2 MD07, 20: 11239(R) (EURAEC-1468)
properties of, used for reactor pressure vessel, 20: 11286 (UJV-1405/65)
use in containment of water-cooled power reactors, 20: 12447
use of strands of, in reactor biological shield for accident containment, 20: 12346

STELLARATORS (C)
cooling system for, design and operation of, 20: 12173 (MATT-315)
electric discharges in, light emission by hydrogen during, (E), 20: 12171 (MATT-270)
electric discharges in, particle-loss rates for, (E), 20: 12239

STEROIDS
radiation effects on mouse, protective effects of heparin against, 20: 10705

4,4'-STILBENEDIOL, α,α'-DIETHYL-
radiosensitivity effects in rats, 20: 10709

STRAIN GAGES
development of high-temperature, radiation-resistant, 20: 11070
use in pressure measurements on reactor fuel elements, 20: 11174(R) (IDO-17112, pp 81-91)

STRATIGRAPHY
measurement of strata shrinkage, cobalt-60 method for, 20: 11024

STRATOSPHERE
radioactive aerosols in, half life of, 20: 11014

STRESS ANALYSIS
of reactor cooling system piping, computer code for, 20: 12338(R) (GEAP-4911)
of sodium-heated steam generator, 20: 12390 (BAW-1280-28(Vol.2))

STRONTIUM
content in open-ocean silts, 20: 12540(R) (NYO-2882-8)
determination in bone ash, spectrographic, 20: 10774
separation from salts by solvent extraction using 8-mercaptoquinoline in chloroform, 20: 10759 (INP-427/C)
separation from uranium by reversed-phase partition chromatography, 20: 10784
separation from waste solutions using countercurrent liquid-foam columns, 20: 12526

STRONTIUM ALLOYS
Cd–Sr, phase studies, 20: 11327

STRONTIUM CHLORIDES
separation from salts by extraction chromatography using organic phosphorus compounds, 20: 10759 (INP-427/C)

STRONTIUM HYDROXIDES
$Be(OH)_2$–$Sr(OH)_2$, preparation and properties of, 20: 10836

STRONTIUM ISOTOPES Sr-85
diffusion from simulated solid wastes, 20: 12517(R) (BNWL-170)
uptake by rats, effects of calcium and phosphorus content in diet, tracer study, 20: 10549

STRONTIUM ISOTOPES Sr-88

energy level structure, (T), 20: 12146
STRONTIUM ISOTOPES Sr-89
content in German milk, effects of precipitation on, 20: 11017
content in German rye and wheat, effects of precipitation on, 20: 11017
diffusion in soil, effects of electric field on, 20: 11053
STRONTIUM ISOTOPES Sr-90
content in Alaskan deer, 1963 and 1964, 20: 10535(R) (BNWL-122, pp 176-80)
content in Alaskan forage plants, 1963 and 1964, 20: 10535(R) (BNWL-122, pp 176-80)
content in Columbia River plume, 20: 11023
content in fallout, 1964, 20: 11018
content in German milk, effects of precipitation on, 20: 11017
content in German rye and wheat, effects of precipitation on, 20: 11017
content in ocean fish, effects of content in sea water on, 20: 11054
diffusion in soil, effects of calcium on, 20: 12523
distribution in tissues of molting crayfish, 20: 10515(R) (BNWL-122, pp 46-8)
effects of combined cerium-144 or plutonium-239 and, on rats, 20: 10552
effects of ingested, in miniature swine, pathological, 20: 10597(R) (BNWL-122, pp 37-45)
effects on animals, carcinogenic, effects of chemical carcinogens on, 20: 10627
effects on corneal metabolism in rabbits, 20: 10585
effects on gastrointestinal tract during chronic radiation sickness, 20: 10674
effects on rat bones, tumorigenic, 20: 10652
elimination of combined cerium-144 or plutonium-239 and, in rats, 20: 10552
performance as space vehicle power supply, 20: 11188 (BLG-330)
re-entry ablation of fuel capsules of, for space power plants, 20: 11189 (MND-3062-25)
uptake by bone, effects on tumor incidence, 20: 10628
use in hemangioma therapy, 20: 10745
STRUCTURES
protection against fallout in, engineering method for calculating, 20: 11030 (NBS-MON-76)
STYRENE
radioinduced grafting to cellulose, 20: 10873
STYRENE POLYMERS
radiation effects on strength of, proton, 20: 10605(T) (NASA-TT-F-353, pp 21-54)
with cellulose, radiolysis of, free radical yields in, 20: 10873
SUBMARINES
propulsion using radioisotope systems, 20: 11187 (AGN-8138)
SUCCINIC ACID
production in gamma radiolysis of aqueous fumaric acid, 20: 10875
SULFANILAMIDE
effects on uranium elimination from kidneys, 20: 10553
SULFATES
effects on phenol yields from radiolysis of benzene, 20: 10878
properties of waste solutions of, versus sulfate-free samples, 20: 12517(R) (BNWL-170)
SULFOXIDES
radiosensitivity effects on *Tribolium confusum* and *T. castaneum*, 20: 10504(R) (BNWL-122, pp 142)
SULFUR
protective effects of, against radiation injuries of skin, γ, 20: 10702
SULFUR ISOTOPES S-32
alpha reactions (α,d) at 42 to 53 Mev, deuteron energy spectra from, (E), 20: 12061
energy levels from silicon (α,γ) reactions at 3.2 to 4.3 Mev, (E), 20: 11994
neutron reactions (n,α) at 0.025 and 0.035 ev, cross sections and Q-values for, (E), 20: 11983
neutron reactions (n,α_0) at 3.2 Mev, angular and energy distributions from, (E), 20: 11993
proton reactions (p,2p) at 460 Mev, (E/T), 20: 11948 (AD-624318)
SULFUR ISOTOPES S-33
neutron reactions (n,α) at 0.025 and 0.035 ev, cross sections and Q-values for, (E), 20: 11983
SULFUR ISOTOPES S-34
energy levels from silicon (α,γ) reactions at 3.2 to 4.3 Mev, (E), 20: 11994
SULFUR ISOTOPES S-35
incorporation in maleimides, method for, 20: 10937(T) (NP-tr-1323)
production at PRR, methods for, 20: 12545(R) (PAEC(A)AR651)
radiation effects from, on physicochemical properties of solid systems, 20: 10936(T) (CEA-tr-A-1855)
radiation effects from, on sorption of aqueous organic dye solutions by barium sulfate, 20: 10936(T) (CEA-tr-A-1855)
radiation effects on uptake of sodium sulfate-incorporated, by rat liver, 20: 10542
SULFUR ISOTOPES S-36
proton reactions (p,γ) at 1.4 to 2.1 Mev, excitation function for, (E), 20: 12005(T)
SULFUR SYSTEMS
S–U, phase studies, 20: 11224
SULFUR TRIOXIDES
K_2SO_4–SO_3, effects of sulfur-35 exchange on reactions in, 20: 10936(T) (CEA-tr-A-1855)
Na_2SO_4–SO_3, effects of sulfur-35 on exchange reactions in, 20: 10936(T) (CEA-tr-A-1855)
SULFURIC ACID
corrosive effects on molybdenum, tungsten, and vanadium at 35, 60, and 100°C, 20: 11230 (BM-RI-6715)
corrosive effects on vanadium-base alloys at low temperatures, 20: 11230 (BM-RI-6715)
radiolysis of aqueous oxygenated solutions of, polarographic studies of 10-Mev-electron, 20: 10909
SUN
activity in August 1965, data for, 20: 11830
corona of, effects of radial diffusion on composition of, 20: 11437
effects on low-energy cosmic rays, (E), 20: 11525
effects on radar reflection from planets for general relativity test, gravitational, (T), 20: 11433
nuclear reactions in flare regions of, (T), 20: 11438
particle emission from, mechanisms of, (T), 20: 11438
satellite orbits about, general relativity tests by precession of, (T), 20: 11883
SUPERCONDUCTIVITY
book: *Quantum Field Theoretical Methods in Statistical Physics*, 20: 11375(T)
magnetic field effects on surface, (T), 20: 11891 (COO-264-224)
properties of degenerate fermion gas, suppression of Cooper pairing in, (T), 20: 11923
SUPERCONDUCTORS
analysis for intermetallic compounds, method of, 20: 10767(T) (AD-620995)
critical field and transition temperature of rubidium, isotope effect on, (E), 20: 11913
current motion in, in transverse magnetic fields, (E), 20: 11902
electric field effects on, accelerated energy and matter currents from long-wavelength, (T), 20: 11919
electrodynamics of alloy, in strong magnetic fields, (T), 20: 11907
electron interaction effects in magnetic films superimposed on, (E), 20: 11918
electron tunneling in junctions of, electrodynamics of Josephson, (E), 20: 11910
flux pinning in bulk type-II, (E/T), 20: 11911
magnetic field of rotating, (E/T), 20: 11911
magnetic flux jumps in niobium–zirconium alloy, training effects from, (E), 20: 11895
magnetic flux trapping in, r-f, 20: 11926
magnetic pinning in type II, (E), 20: 11894
positron annihilation in lead, photon angular correlation from, (E), 20: 11912
properties of platinum–metal chalcogenide, (E), 20: 11899
quantum interference effects in point contacts of macroscopic, (E/T), 20: 11911
theory of nonhomogeneous, 20: 11908
theory of, containing magnetic impurities, 20: 11906
transition effects in filamentary tin crystals, 20: 11924
transition in semiconductors, induction using field effect, (T), 20: 11901(T)
transition temperature of lanthanum sulfide, (E), 20: 11909
transition temperature of cadmium–mercury alloy, effects of ordering on, (E), 20: 11914
ultrasonic-wave attenuation in thallium, (E/T), 20: 11915
use in particle accelerators, 20: 11412
SUPERFLUIDITY
hydrodynamics of, thermodynamic Green functions for, 20: 11898
SUPERSONIC FLOW
calculations of stationary, in common cones, 20: 11767 (HMI-B-42)
SURFACE WATERS
fallout distribution in, at dam, effects of time of year and plankton on, 20: 11055
radioactivity in, control measures for, 20: 11021
radium, radon, and uranium contents of Lake Techirghiol, 20: 10512
SURFACES
contour measurements on small irradiated, development of photogrammetry method for, 20: 11068 (WAPD-T-1815)
heat transfer by, effects of profile on, 20: 10993 (TID-22513)
SURGERY
effects of preoperative irradiation on dissemination of cancer cells by, 20: 10735

effects of, combined with γ radiation on brain tumors, 20: 10575
SWEDISH REACTORS (R-3)
control-rod reactivity effects in, 20: 12362 (RFR-193)
description, 20: 12426
SWIMMING POOL REACTORS
design of compartmented, 20: 12516(P)
SWINE
cerium-144 absorption by, gastrointestinal, 20: 10525(R) (BNWL-122, pp 85-90)
effects of ingested strontium-90 on miniature, pathological, 20: 10597(R) (BNWL-122, pp 37-45)
iodine-131 uptake by thyroid gland of, from skin exposure, 20: 10518(R) (BNWL-122, pp 55-8)
plutonium-239 distribution in tissues of, 20: 10523(R) (BNWL-122, pp 81-2)
promethium-147 absorption by, gastrointestinal, 20: 10525(R) (BNWL-122, pp 85-90)
radiation effects on, biological, 20: 10618
SYNCHROCYCLOTRONS
dosimetry of, methods for, 20: 10605(T) (NASA-TT-F-353, pp 21-54)
SYNCHROTRONS
control of 200-Bev proton, computer, 20: 11401 (UCRL-16502)
development of CERN proton, 20: 11404
experimental facilities of 200-Bev proton, for neutrino beam production, (T), 20: 11398 (UCID-1008)
neutron spatial distribution around 10-Bev synchrophasotron, (E), 20: 11390 (JINR-P-2446)
synchrotron radiation from beam of Frascati, (E), 20: 11403
SYSTEMS FOR NUCLEAR AUXILIARY POWER
criticality and shielding studies for, 20: 12475 (WANL-PR(B)-009)
radioisotope evaluation for space, 20: 11188 (BLG-330)
re-entry heating rates for, methods for calculating, (T), 20: 12467 (NAA-SR-11704)
testing of SNAPTRAN 2/10A-1, program sequence times for transient, 20: 12499(R) (IDO-17112, pp 52-80)
SYSTEMS FOR NUCLEAR AUXILIARY POWER (SNAP-8)
development of component materials for, 20: 11214(R) (NASA-CR-54717)
development of component materials for, 20: 11215(R) (NASA-CR-54718)
shielding of, neutron fluxes and heating in, (T), 20: 12468 (NAA-SR-Memo-9916)
SYSTEMS FOR NUCLEAR AUXILIARY POWER (SNAP-10)
control and instrumentation circuits for 10FS-5, shock testing of, 20: 12469 (NAA-SR-Memo-11630)
fission product inventory for 10A orbit, 20: 12466 (NAA-SR-11642)
kinetics of 10A, 20: 12498(R) (IDO-17112, pp 1-51)

T

TACHOMETERS
use in motor speed control circuit, 20: 11073
TANKS
design for handling enriched uranium slurries, 20: 10981
TANTALUM
bonding to Hastelloy N, Inconel 600, and types 321 and 347 stainless steels, explosive, 20: 11243(R) (WANL-PR(EE)-001)
compatibility with urania, 20: 11224
corrosion by plutonium–cobalt–cerium alloys, effects of carbon on, 20: 11224
crystallographic orientation in, development of preferred, 20: 11227
deposition from fused salt mixtures, electro-, 20: 11260
diffusion of boron in surface of, 20: 11228
effects of alloy additions of, on mechanical properties of niobium, 20: 11302
fabrication by hot isostatic pressing, 20: 11260
gamma incoherent scattering by K-shell electrons of, at 320 kev, (E), 20: 11514
magnetic flux trapping in superconducting, r-f, 20: 11926
mechanical properties of, effects of strain rate on, 20: 11284 (UCRL-14599)
neutron reactions (n,γ) at 30 to 170 kev, cross sections for, (E), 20: 11986
oxidation by air at 500 to 900°C, effects of alloying additions on, 20: 11227
oxidation by carbon monoxide and carbon dioxide at 500 to 700°C, mechanisms of, 20: 11227
performance as collector electrode for thermionic cells, 20: 11540(R) (AD-626444)
solubility in liquid rare earth metals, thermodynamics of, 20: 11306
solubility in potassium, 20: 11227
strain-aging in polycrystalline and single-crystal, (E/T), 20: 11331
superconducting point contacts of, macroscopic quantum interference effects in, (E/T), 20: 11911
tensile properties of, effects of exposure to cesium at 1200°C on, 20: 11227
thermodynamic properties, 20: 10816(T) (NASA-TT-F-285)
TANTALUM ALLOYS
brazing of, development of alloys for, 20: 11260
corrosion by plutonium–cobalt–cerium alloys, effects of carbon on, 20: 11224
development of dispersion-strengthened, 20: 11217(R) (WANL-PR(Q)-007)
Al–Nb–Ta–Ti, fracture toughness of plasmarc welds in titanium-base, 20: 11273(R) (NRL-6364)
Mo–Ta, electric conductivity of, effects of composition on, 20: 11227
Mo–Ta, mechanical properties of single-crystal, 20: 11227
Mo–Ta–W, fabrication of tantalum-base, process development for, 20: 11260
Nb–Ta, mechanical properties of, effects of composition on, 20: 11288(T) (AD-622477)
Nb–Ta–W, creep strength of, effects of composition on, 20: 11302
Nb–Ta–W–Zr, bonding to Hastelloy N, Inconel 600, and types 321 and 347 stainless steels of FS-85, explosive, 20: 11243(R) (WANL-PR(EE)-001)
Ni–Ta, crystallization, 20: 11227
Ta–W, fabrication of tantalum-base, process development for, 20: 11260
Ta–W, tensile properties of single-crystal, effects of carbon additions and heat treatments on, 20: 11227
Ta–W–Zr, fabrication of tantalum-base, process development for, 20: 11260
Ta–Zn, crystal structure of intermetallic compounds in, 20: 11328
TANTALUM BROMIDES
thermodynamic properties, 20: 10816(T) (NASA-TT-F-285)
TANTALUM CARBIDES
sintering of, effects of ammonium and cobalt chlorides on porosity following, 20: 11250
thermodynamic properties, 20: 10816(T) (NASA-TT-F-285)
HfC–TaC, preparation and properties, 20: 11330
NbC–TaC, preparation and properties, 20: 11330
TANTALUM CHLORIDES
thermodynamic properties, 20: 10816(T) (NASA-TT-F-285)
TANTALUM FLUORIDES
thermodynamic properties, 20: 10816(T) (NASA-TT-F-285)
TANTALUM HYDRIDES
thermodynamic properties, 20: 10816(T) (NASA-TT-F-285)
TANTALUM COUPLES
Fe/stainless steel/Ta, diffusion in bimetallic tubing of, with iron diffusion barrier, inter-, 20: 11215(R) (NASA-CR-54718)
Fe/stainless steel/Ta/V, diffusion in bimetallic tubing of, with iron and vanadium diffusion barriers, inter-, 20: 11215(R) (NASA-CR-54718)
Mo/Ni/stainless steel/Ta, diffusion in bimetallic tubing of, with molybdenum and nickel diffusion barriers, inter-, 20: 11215(R) (NASA-CR-54718)
stainless steel/Ta, diffusion in bimetallic tubing of, inter-, 20: 11215(R) (NASA-CR-54718)
TANTALUM IODIDES
thermodynamic properties, 20: 10816(T) (NASA-TT-F-285)
TANTALUM NITRIDES
thermodynamic properties, 20: 10816(T) (NASA-TT-F-285)
TANTALUM OXIDES
thermodynamic properties, 20: 10816(T) (NASA-TT-F-285)
TANTALUM SILICIDES
thermodynamic properties, 20: 10816(T) (NASA-TT-F-285)
TANTALUM SYSTEMS
C–Hf–Re–Ta–W, preparation and properties of dispersion-strengthened, 20: 11217(R) (WANL-PR(Q)-007)
C–Hf–Ta–W, bonding of T-222, to Inconel 600 and types 321 and 347 stainless steels, explosive, 20: 11243(R) (WANL-PR(EE)-001)
TARTARIC ACID
corrosive effects on vanadium at 35, 60, and 100°C, 20: 11230 (BM-RI-6715)
production in gamma radiolysis of aqueous fumaric acid, 20: 10875
TECHNETIUM
determination by radiochemical methods, 20: 10940
separation from sulfuric acid solution by solvent extraction using cyclohexanone, 20: 10940
TECHNETIUM ALLOYS
Tc–W, preparation, 20: 11260
TECHNETIUM IONS
separation of tetra-, penta-, and hexavalent, by ion exchange paper chromatography, 20: 10783
TECHNETIUM ISOTOPES Tc-99
beta counting methods for, 20: 10940
half life and specific activity of, 20: 10940
neutron reactions with, cross sections for, 20: 10940
TECHNICAL REPORTS
by Philippine Atomic Research Center personnel, 20: 12545(R)

(PAEC(A)AR651)
descriptive cataloging guide for, 20: 12548 (TID-4577(Rev.1))
on reactor hazards and safeguards, 20: 11052
TEETH
radiography of, radiation dose from, 20: 10720
separation of manganese from solutions of ashes of, by solvent extraction, 20: 10950
TELLURIUM
radioinduced ionization of, cross sections for electron, 20: 10885
TELLURIUM CHLORIDES
separation from salts by extraction chromatography using organic phosphorus compounds, 20: 10759 (INP-427/C)
TELLURIUM ISOTOPES Te-109
proton emission from, half-life for, (E), 20: 11964 (JINR-E-2464)
TELLURIUM ISOTOPES Te-111
proton emission from, half-life for, (E), 20: 11964 (JINR-E-2464)
TELLURIUM ISOTOPES Te-123
decay of isomeric, transition multipolarity in, (E), 20: 12140
TELLURIUM ISOTOPES Te-132
beta decay of, iodine-132 energy levels from, (E), 20: 12026
distribution in tissues of ingested, biological model for, 20: 10519(R) (BNWL-122, pp 59-63)
TEMPERATURE
effects on alkyltin yields in radiolysis of mixtures of 1-bromobutane or 1-bromopentane with tin, 20: 10870 (BMI-1753)
effects on ecology of plant communities, 20: 10510 (BNL-9835)
effects on positron annihilation in indium–lead and indium–magnesium alloys, 20: 11678
effects on scintillation in sodium iodide crystals, 20: 11118
measurement of, radiometric digital apparatus for, 20: 11085(P)
reduction of animal, using MEA, 20: 10714
TEMPERATURE CONTROL
equipment for, in accelerator tubes, 20: 11420(P)
TENSILE PROPERTIES
testing of irradiated materials at cryogenic temperatures, in-pile loop design for, 20: 11345(R) (NASA-CR-54787)
TERBIUM
magnetic properties, 20: 11340
separation from uranium by reversed-phase partition chromatography, 20: 10784
solvent properties for tantalum, thermodynamics of, 20: 11306
TERBIUM ALLOYS
Al–Tb, crystal structure of intermetallic compound $TbAl_3$ in, 20: 11305
Re–Tb, phase studies, 20: 11298
TERBIUM CARBONATES
complexes of, composition in solution of, 20: 10824
TERBIUM CHLORIDES
separation from salts by extraction chromatography using organic phosphorus compounds, 20: 10759 (INP-427/C)
TERBIUM COMPLEXES
dipyridyl, fluorescence of, effects of methyl group on, 20: 10842
TERBIUM IONS
spin-lattice relaxation in yttrium ethyl sulfates, (E), 20: 12300
TERBIUM ISOTOPES Tb-158
decay of, lifetime of 2^+ rotational states in dysprosium-158 and gadolinium-158 from, (E), 20: 12082
TERBIUM ISOTOPES Tb-159
lifetime of isomeric, (E), 20: 12303
Mössbauer effect in isomeric, width of 58-kev resonance from, (E), 20: 12303
TERBIUM ISOTOPES Tb-162
decay, (E), 20: 12149
TERBIUM NITRATES
nitrogen-14 NMR, (E), 20: 12325
TERBIUM OXIDES
magnetic properties at 1.4 to 300°K, 20: 12289
preparation, 20: 12289
TEREPHTHALIC ACID, ETHYLENE POLYMER ESTERS
radiation effects on strength of, proton, 20: 10605(T) (NASA-TT-F-353, pp 21-54)
radiation effects on electric and physical properties of, gamma and neutron, 20: 11344 (N65-35361)
TERPHENYL
pyrolysis of, rate of, 20: 10872 (EUR-2517.f)
radioinduced fluorescence efficiency and quenching in *p*-, rate constants for β, 20: 10902
radiolysis at 200 to 450°C, rate of, 20: 10872 (EUR-2517.f)
radiolysis of, design of loop for studying electron, 20: 10871 (EUR-2288.f)
benzene–cyclohexane–*p*-terphenyl, excitation transfer and decay processes in radiolysis of, 20: 10927
biphenyl–terphenyl, method for radiation production of, 20: 10930(P)
THALLIUM
spectra in aluminaborate, fused silica, and phosphate glasses, optical, (E), 20: 10830
ultrasonic-wave attenuation in normal and superconducting, (E/T), 20: 11915
THALLIUM ALLOYS
Li–Mg–Tl, preparation, properties, and structure of intermetallic compound $LiMg_2Tl$ in, 20: 11282 (UCRL-12119-T)
THALLIUM ISOTOPES Tl-202
energy levels, (E), 20: 12112
THALLIUM ISOTOPES Tl-203
deuteron reactions (d,p) and (d,t) with, (E), 20: 12112
energy level transitions in, parity admixtures and circular polarization of, (T), 20: 12007
THALLIUM ISOTOPES Tl-204
energy levels, (E), 20: 12112
uptake of, combined with calcium-45 by human respiratory tract, 20: 10546
THALLIUM ISOTOPES Tl-205
deuteron reactions (d,p) and (d,t) with, (E), 20: 12112
THALLIUM ISOTOPES Tl-206
energy levels, (E), 20: 12112
THERMAL INSULATION
testing of silica aerogel, for thermoelectric cells, 20: 11543(R) (GIC-2605-3)
THERMAL RADIATION
emission from fluids, hydrodynamic equations for, (T), 20: 11766 (AWRE-O-52/66)
transfer in reactors, simulation of, 20: 12487
THERMAL RADIATION SHIELDING
concretes for high-temperature reactor, reinforced chamotte and chromite, 20: 12340
THERMAL RADIATION SOURCES
gamma shielding for, using plutonium-238 and polonium-210, (T), 20: 12264 (MLM-1315)
THERMAL REACTORS
criticality studies, 20: 12475 (WANL-PR(B)-009)
design parameters for thermionic zirconium hydride-moderated, 20: 12479
economic and technique aspects of plutonium fuel for, 20: 12379
fuel development for power breeders, 20: 12407 (NEIC-RR-13)
properties of thermionic, for space power, 20: 12478
reactivity transients from samarium-149 and xenon-135 poisons in, tables for calculating, 20: 12352 (DP-958)
THERMIONIC CELLS
cesium atom photoionization in, by solar radiation, (T), 20: 11549
design of high-temperature, 20: 12383(P)
electron temperature and ion density in cesium, pressure and spacing effects on, (E), 20: 11544 (LA-DC-7390)
heat transfer pipes for, properties of, 20: 11545 (LA-DC-7555)
heat transfer to, from reactor surfaces, simulation of radiant, 20: 12487
performance of cylindrical rare gas-filled, effects of emitter location on, 20: 11547
performance of, parametric equation for, 20: 11540(R) (AD-626444)
performance of, using heat transfer pipes, (T), 20: 11542 (EUR-2534.e)
thermodynamic analysis of, 20: 12421
use in fast- and thermal-reactor space power supplies, 20: 12478
THERMOCOUPLES
design of graphite-carbon, for measuring temperature to 3000°K, 20: 11076
THERMODYNAMICS
book: *Quantum Field Theoretical Methods in Statistical Physics*, 20: 11375(T)
calculation of chemical equilibria in fused salts using, 20: 10807 (EUR-2466.e, pp 39-57)
energy variables in, relativistic transformation laws for total, 20: 11797
THERMOELECTRIC CELLS
component development for low power, 20: 11543(R) (GIC-2605-3)
development of bismuth telluride, 20: 11543(R) (GIC-2605-3)
heat transfer system for, performance of syphon loop, (E/T), 20: 11543(R) (GIC-2605-3)
insulation testing for, 20: 11543(R) (GIC-2605-3)
performance of bismuth telluride, 20: 11543(R) (GIC-2605-3)
THERMOLUMINESCENT DETECTORS
performance for medical uses, 20: 11155
use of, for photon dosimetry at 10 kev to 10 Mev, 20: 11041
THERMONUCLEAR EXPLOSIONS
radiation hazards from, 20: 10701
THERMONUCLEAR REACTORS
bremsstrahlung heating of vacuum-wall of, (T), 20: 12166 (CONF-651126-1)
development of, summary of, 20: 12167(R) (COO-1233-24)
plasma losses in Q-device, 20: 12215
THIOCYANATES
radiolysis of aqueous solutions of, kinetics of pulsed-electron, 20: 10915

THORIUM
determination by amperometric titration precipitating ortho-vanadate, 20: 10786
diffusion in pyrolytic graphite, effects of structure on, 20: 11224
diffusion in sintered uranium dioxide at 1250 to 1600°C, 20: 11312
neutron resonance absorption in, computer program for calculating, 20: 11932 (GA-6637)
proton reactions with, phosphorus-32 and -33 production in, (E), 20: 12034
separation from other elements by solvent extraction using TBP, 20: 10952
separation from rare earths by ion exchange, 20: 10959
separation from salts by solvent extraction using 8-mercaptoquinoline in chloroform, 20: 10759 (INP-427/C)
THORIUM ALLOYS
hardness at 600 and 750°C, 20: 11224
Ag–Th, phase studies, 20: 11224
Au–Th, phase studies, 20: 11224
Co–Th, phase studies, 20: 11224
Mg–Th, ductility in, mechanisms of, 20: 11301
THORIUM CARBIDES
preparation of spheres of, 20: 11224
ThC_2–UC_2, fabrication of, review of, 20: 11241 (TID-8541, pp 71-148)
THORIUM CHLORIDES
separation from salt mixtures by extraction chromatography using organic phosphorus compounds, 20: 10759 (INP-427/C)
THORIUM HALIDES
separation from salts by extraction chromatography using organic phosphorus compounds, 20: 10759 (INP-427/C)
THORIUM ISOTOPES Th-227
alpha decay of, gamma spectra from, (E), 20: 11992
THORIUM ISOTOPES Th-228
decay of, preparation of bismuth-212 and lead-212 from products of, 20: 10759 (INP-427/C)
performance as space vehicle power supply, 20: 11188 (BLG-330)
THORIUM ISOTOPES Th-230
determination in tissues, radiochemical, 20: 10514(R) (BNWL-122, pp 21-4)
helium ion fission at 42.8 Mev, deformation of transition-state nucleus in, (E), 20: 12077
radiation dose in lungs from, in inhaled uranium ores, 20: 10514(R) (BNWL-122, pp 21-4)
THORIUM ISOTOPES Th-232
helium ion fission at 42.8 Mev, deformation of transition-state nucleus in, (E), 20: 12077
THORIUM MINERALS
geochemistry of, in igneous rocks of Lower Triassic deposits, Pripyat Basin, USSR, 20: 11026
THORIUM OXIDES
crystal structure of, x-ray line broadening studies on, (E), 20: 11321
preparation of thin-film radiation targets of, using evaporation-condensation, 20: 11183 (ORNL-P-1900)
THORIUM(IV) OXIDES
effects on immune reactions in mice, 20: 10617
effects on man after carotidography, 20: 10680
effects on mice, pathological, 20: 10617
neutron resonance absorption in, computer program for calculating, 20: 11932 (GA-6637)
BeO–ThO_2, phase studies, 20: 11225
ThO_2–UO_2, fabrication of, review of, 20: 11241 (TID-8541, pp 71-148)
ThO_2–UO_2, fission gas diffusion in, effects of stress on, 20: 11224
ThO_2–UO_2, radiation effects on dissolution of, by nitric acid, 20: 10964
ThO_2–W, tensile properties of, effects of strain rate and temperature on, 20: 11227
THORIUM SYSTEMS
C–Ce–Th, phase studies, 20: 11224
C–Pu–Th, phase studies and properties of, 20: 11224
THORIUM VANADATES
preparation by amperometric titration of thorium compounds with alkali metal vanadates, 20: 10786
THRESHOLD DETECTORS
neutron cadmium cut-off energies for boron 1/v, in cylindrical geometry, (T), 20: 11131
THULIUM
energy levels, (E), 20: 11464
ionization potential, (E), 20: 11464
magnetic properties, 20: 11340
solvent properties for tantalum, thermodynamics of, 20: 11306
thermal conductivity at 2 to 100°K, (E), 20: 11329
THULIUM CARBONATES
complexes of, composition in solution of, 20: 10824
THULIUM CHLORIDES
crystal field of hydrated, 20: 10860
THULIUM ETHYL SULFATES
magnetic properties of single-crystal, Mössbauer effect study of, 20: 12316
THULIUM IONS
electron wave function of, 20: 12316
nuclear quadrupole shielding factors for trivalent, in crystals, 20: 12323
spectra of trivalent, in hydrated chloride lattices, 20: 10860
THULIUM ISOTOPES Tm-170
beta decay of, β-γ directional correlations in, (E), 20: 12112
THULIUM ISOTOPES Tm-171
energy levels of, magnetic moments of 129-kev, (E), 20: 12112
THULIUM ISOTOPES Tm-172
beta decay of, K-selection rule in, (E/T), 20: 12114
THULIUM SELENIDES
CaSe–Tm_2Se_3, phase studies, 20: 10857
THYMIDINE
effects of tritiated, with and without gamma radiation on mortality in Drosophila larvae, 20: 10602 (CNAEM-32)
THYMUS GLAND
effects on tolerance response, 20: 10632
injection of antigens into grafts of, effects on immune reactions, 20: 10632
physiology of, 20: 10632
radiation effects on mouse, model for β, 20: 10640
uptake of cystamine by mouse, tracer study *in vivo* and *in vitro*, 20: 10708
THYROID GLAND
iodine-131 content of sheep, long-term ingestion study, 20: 10516(R) (BNWL-122, pp 49-51)
iodine-131 uptake by, from skin exposure of swine, 20: 10518(R) (BNWL-122, pp 55-8)
iodine-131 uptake by human, from milk, 20: 10530(R) (BNWL-122, pp 113-17)
radiation effects on function of rat, 20: 10709
radiation effects on cells in mouse, protective effects of anoxia against, 20: 10710
radiodiagnosis of diseases of, radiation dose to ovaries from iodine-131, 20: 10554
radioinduced tumors of, incidence of, 20: 10747
radiotherapy of carcinomas of, using iodine-131, 20: 10729
THYROXINE
radiosensitivity effects in rats, 20: 10709
TIN
distribution in Zircaloy-2, effects of thermal treatment on, 20: 11287 (WAPD-T-1809)
effects of fire on cans of, for radioisotope containment, 20: 11028 (AERE-M-1664)
enthalpy at 1222 to 1745°K, 20: 10811 (LA-DC-6806)
gamma reactions at 320 kev, absolute photoelectric cross sections for, (E), 20: 11496
Knight shifts in rare-earth-tin compounds, 20: 12324
magnetic flux trapping in superconducting impure, r-f, 20: 11926
meson (μ^-) capture by, isotope effects on K x-ray emission from, (E), 20: 11480
solvent properties for rare earth metals, thermodynamics of, 20: 11304
superconducting point contacts of, macroscopic quantum interference effects in, (E/T), 20: 11911
superconducting transitions in filamentary crystals of, 20: 11924
TIN ALLOYS
Al–Mo–Sn–Ti–V, fracture toughness properties of titanium-base, effects of heat treatments on, 20: 11273(R) (NRL-6364)
Al–Sn–Ti, fracture toughness of plasmarc welds in titanium-base, 20: 11273(R) (NRL-6364)
Al–Sn–Ti, mechanical properties of, effects of strain rate on, 20: 11284 (UCRL-14599)
Al–Sn–Ti, radiation effects on low-cycle fatigue and tensile properties at cryogenic temperatures, 20: 11345(R) (NASA-CR-54787)
Al–Sn–Ti–V, fracture toughness properties of titanium-base, plane-strain, 20: 11273(R) (NRL-6364)
Al–Sn–Ti–Zr, creep properties of, effects of composition on, 20: 11335
Bi–Sn, development as fusible metal joint for fast reactors, 20: 12513
Ce–Sn, tin Knight shift and magnetic susceptibility of $CeSn_3$, 20: 12324
Fe–Sn, iron-57 and tin-119 Mössbauer effects in, 20: 12315
In–Sn, r-f field trapping in superconducting, 20: 11926
La–Sn, tin Knight shift and magnetic susceptibility of $LaSn_3$, 20: 12324
Mg–Sn, tin-119 Mössbauer effect in, 20: 12285
Nb–Sn–Zr, radiation effects on corrosion and mechanical properties of, neutron, 20: 11354
Nb–Sn–Zr, stability of martensite structure in zirconium-base, 20: 11227
Nd–Sn, tin Knight shift and magnetic susceptibility of $NdSn_3$, 20: 12324
Pr–Sn, tin Knight shift and magnetic susceptibility of $PrSn_3$, 20: 12324
Sm–Sn, tin Knight shift and magnetic susceptibility of $SmSn_3$, 20: 12324
Sn–U, tin Knight shift and magnetic susceptibility of USn_3, 20: 12324

TIN CHLORIDES
separation from salts by extraction chromatography using organic phosphorus compounds, 20: 10759 (INP-427/C)
TIN COMPOUNDS
alkyl-, yields in radiolysis of 1-bromobutane and 1-bromopentane mixtures with tin, 20: 10870 (BMI-1753)
TIN ISOTOPES Sn-116
meson (μ^-) capture by, K x-ray emission from, (E), 20: 11480
TIN ISOTOPES Sn-119
Mössbauer effect in magnesium–tin alloys, 20: 12285
Mössbauer effects in iron–tin alloys, 20: 12315
Mössbauer studies in copper, gold, and silver, 20: 12315
TIN ISOTOPES Sn-124
meson (μ^-) capture by, K x-ray emission from, (E), 20: 11480
TIN ISOTOPES Sn-131
half life, (E), 20: 11980 (USNRDL-TR-935)
TIN ISOTOPES Sn-132
half life, (E), 20: 11980 (USNRDL-TR-935)
TIN ISOTOPES Sn-133
half life, (E), 20: 11980 (USNRDL-TR-935)
TIN SYSTEMS
1-bromobutane–Sn, radiation effects on alkyltin yields in, 20: 10870 (BMI-1753)
1-bromopentane–Sn, radiation effects on alkyltin yields in, 20: 10870 (BMI-1753)
TISSUE CULTURES
growth in Polyoma-infected hamster, effects of x-irradiated non-infected cells on, 20: 10684
radiation effects on hamster, effects of viral transformation on x, 20: 10684
radiation effects on animal cells in, single and fractionated γ and x, 20: 10649
radiation effects on survival of HeLa cells in, effects of anoxia and antimetabolite drug on x, 20: 10664
radiation effects on DNA synthesis in HeLa cell, α and γ, 20: 10588
TISSUE HOMOGENATES
radiation effects on, biochemical, 20: 10577
TISSUE TRANSPLANTS
radiation effects on immune reactions of mice to rat, 20: 10505(R) (BNWL-122, pp 146-9)
radiosensitivity effects of splenic marrow, in mice, 20: 10713
TISSUES
analysis for thorium-230, radiochemical, 20: 10514(R) (BNWL-122, pp 21-4)
analysis for uranium-238, radiochemical, 20: 10514(R) (BNWL-122, pp 21-4)
beta energy losses in, dependence of, on beta-energy maximum and Z of emitter, (T), 20: 11037
chemical composition of, in man, 20: 10698
iodine-132 distribution in, following ingestion of tellurium-132, biological model for, 20: 10519(R) (BNWL-122, pp 59-63)
neutron interactions with, 20: 10698
radiation effects on growth of coleoptile and radicle, in maize seedlings, effects of dose on β, 20: 10683
radiation effects on dog and rat, multiple-dose high-energy proton, 20: 10606(T) (NASA-TT-F-353, pp 55-102)
radiation effects on dog and rat, single-dose high-energy proton, 20: 10607(T) (NASA-TT-F-353, pp 103-41)
radiation effects on dog and rat, comparison of RBE of gamma, proton, and x-ray, 20: 10612(T) (NASA-TT-F-353, pp 194-209)
radiation effects on guinea pig soft, γ, 20: 10615
tellurium-132 distribution in, following ingestion, biological model for, 20: 10519(R) (BNWL-122, pp 59-63)
TITANIUM
corrosion by nitric acid at 35°C, galvanic, 20: 11230 (BM-RI-6715)
diffusion of boron and carbon in surface of, 20: 11228
diffusion of uranium in, temperature dependence of, 20: 11290
effects of alloy additions of, on mechanical properties of niobium, 20: 11302
effects of alloying additions of, on oxidation rates of niobium, tantalum, and tungsten, 20: 11227
electron elastic scattering at 53 Mev, cross sections and nuclear radius from, (E), 20: 12033
mechanical properties and structure of, effects of hot rolling in air, argon, and vacuum on, 20: 11249
phase transformation in, latent heat of alpha-to-beta, 20: 11283 (UCRL-12142)
radiation effects on low-cycle fatigue and tensile properties of, at cryogenic temperatures, 20: 11345(R) (NASA-CR-54787)
tensile properties of, effects of exposure to cesium at 650°C on, 20: 11227
thermodynamic properties, 20: 10816(T) (NASA-TT-F-285)
TITANIUM ALLOY COUPLES
Nb/Nb–Ti, diffusion at 1300 to 2000°C, inter-, 20: 11227
TITANIUM ALLOYS
Al–Cr–Co–Fe–Mo–Ni–Ti, stress-rupture properties of Udimet 700, at high temperatures and strain rates, 20: 11265 (AD-626375)
Al–Mo–Sn–Ti–V, fracture toughness properties of titanium-base, effects of heat treatments on, 20: 11273(R) (NRL-6364)
Al–Mo–Ti, fracture toughness of weldments of titanium-base, effects of heat treatments on, 20: 11273(R) (NRL-6364)
Al–Mo–Ti, fracture toughness of plasmarc welds in titanium-base, 20: 11273(R) (NRL-6364)
Al–Mo–Ti, fracture toughness of titanium-base, effects of composition and heat treatments on, 20: 11273(R) (NRL-6364)
Al–Mo–Ti–V, corrosion cracking by salts at 550 to 600°F, stress-, 20: 11227
Al–Mo–Ti–V, thermal stability of, effects of composition on, 20: 11336
Al–Nb–Ta–Ti, fracture toughness of plasmarc welds in titanium-base, 20: 11273(R) (NRL-6364)
Al–Sn–Ti, fracture toughness of plasmarc welds in titanium-base, 20: 11273(R) (NRL-6364)
Al–Sn–Ti, mechanical properties of, effects of strain rate on, 20: 11284 (UCRL-14599)
Al–Sn–Ti, radiation effects on low-cycle fatigue and tensile properties at cryogenic temperatures, 20: 11345(R) (NASA-CR-54787)
Al–Sn–Ti–V, fracture toughness properties of titanium-base, plane-strain, 20: 11273(R) (NRL-6364)
Al–Sn–Ti–Zr, creep properties of, effects of composition on, 20: 11335
Al–Ti, thermal stability of $TiAl_3$, effects of molybdenum, niobium, and vanadium alloying additions on, 20: 11335
Al–Ti–V, corrosion by cesium at 400°C, 20: 11227
Al–Ti–V, fracture toughness properties of titanium-base, 20: 11273(R) (NRL-6364)
Al–Ti–V, fracture toughness of plasmarc welds in titanium-base, 20: 11273(R) (NRL-6364)
Al–Ti–V, fracture toughness properties of titanium-base, plane-strain, 20: 11273(R) (NRL-6364)
Al–Ti–V, mechanical properties of, effects of strain rate on, 20: 11284 (UCRL-14599)
Al–Ti–V, radiation effects on low-cycle fatigue and tensile properties at cryogenic temperatures, 20: 11345(R) (NASA-CR-54787)
Al–Ti–V, tensile properties of, effects of exposure to cesium at 650°C on, 20: 11227
Al–Ti–Zr, phase studies and properties of, 20: 11332
Al–Ti–Zr, phase studies and properties of, 20: 11333
Al–Ti–Zr, phase studies and properties of, 20: 11334
Mo–Ti, erosion by mercury vapor at 640°F, 20: 11214(R) (NASA-CR-54717)
Mo–Ti, tensile properties of, effects of working reduction, stress-relief annealing, and grain size on, 20: 11227
Mo–Ti–U, corrosion cracking in air, stress-, 20: 11224
Mo–Ti–Zr, erosion by mercury vapor at 640°F of TZM, 20: 11214(R) (NASA-CR-54717)
Nb–Ti, mechanical properties of, effects of composition on, 20: 11288(T) (AD-622477)
Nb–Ti–V, corrosion by acids and bases of vanadium-base, 20: 11230 (BM-RI-6715)
Nb–Ti–W, creep strength of, effects of composition on, 20: 11302
Pu–Ti–U, strength of, ultimate compressive, 20: 11224
Ti–V, corrosion by acids and bases of vanadium-base, 20: 11230 (BM-RI-6715)
Ti–V, fabrication of tubing of, for reactor fuel cladding, 20: 11258
Ti–V, fabrication of TV-20, process development for, 20: 11260
Ti–Zn, crystal structure of intermetallic compounds in, 20: 11328
TITANIUM BROMIDES
thermodynamic properties, 20: 10816(T) (NASA-TT-F-285)
TITANIUM CARBIDES
properties and uses at cryogenic temperatures, 20: 11293
thermodynamic properties, 20: 10816(T) (NASA-TT-F-285)
HfC–TiC, preparation and properties, 20: 11330
TITANIUM CHLORIDES
thermodynamic properties, 20: 10816(T) (NASA-TT-F-285)
use of irradiated, as catalyst in isoprene polymerization, 20: 10929(P)
TITANIUM FLUORIDES
thermodynamic properties, 20: 10816(T) (NASA-TT-F-285)
TITANIUM IODIDES
thermodynamic properties, 20: 10816(T) (NASA-TT-F-285)
TITANIUM ISOTOPES Ti-44
energy levels, 20: 12144
TITANIUM ISOTOPES Ti-46
energy levels of, width of 2^+, (E/T), 20: 12147
TITANIUM NITRIDES
thermodynamic properties, 20: 10816(T) (NASA-TT-F-285)
TITANIUM OXIDES
effects on photochromism of molybdates and tungstates, 20: 10837

thermodynamic properties, 20: 10816(T) (NASA-TT-F-285)
TITANIUM OXYNITRIDES
preparation, properties, and structure, 20: 10856
TITANIUM STEEL
Cr–Mo–Ti, corrosion by flowing sodium at 1000 to 1200°F, equation for, 20: 11227
TITANIUM SULFIDES
thermodynamic properties, 20: 10816(T) (NASA-TT-F-285)
TITANIUM SYSTEMS
C–Mo–Ti–Zr, stress-rupture properties of TZC, at high temperatures and strain rates, 20: 11265 (AD-626375)
Nb–O–Ti, crystal structure of $TiNb_{24}O_{62}$, 20: 11227
TOBACCO
radiosensitivity effects of extract from leaves of, on fungi, x, 20: 10620
TOKAI-MURA POWER REACTOR
materials for, methods for control of nuclear species in, 20: 12429
TOLUENE
naphthalene emission spectra in, 20: 10854
radioinduced fluorescence efficiency and quenching in, rate constants for β, 20: 10902
radiolysis of, thermal-spike model for low LET, 20: 10887
TOPOLOGY
Hilbert spaces in, continuous measures on, 20: 11211
vector spaces in, measures on infinite dimensional, 20: 11210
TOXINS
effects of diphtherial, on heart muscle, pathological, 20: 10631
radiation effects on rat resistance to bacterial, 20: 10709
TRACER TECHNIQUES
for sewage, 20: 12545(R) (PAEC(A)AR651)
TRACER TECHNIQUES (AGRICULTURE)
for coconut tree nutrition, 20: 12545(R) (PAEC(A)AR651)
TRACER TECHNIQUES (BIOLOGY)
conference on, for protein metabolism, 20: 10539 (STI/DOC/10/45)
for determining synthesis rate of liver proteins, carbon-14, 20: 10558
for high-speed alpha autoradiography, 20: 10529(R) (BNWL-122, pp 110-12)
for measuring rate of urea synthesis, carbon-14, 20: 10559
for nutritional research, nitrogen-15, 20: 10560
for plasma protein studies, 20: 10561
for plasma protein studies, computer analysis of, 20: 10562
for studies of snails, 20: 12545(R) (PAEC(A)AR651)
TRACER TECHNIQUES (CHEMISTRY)
for study of saponification of coconut oil using sodium-24, 20: 12545(R) (PAEC(A)AR651)
TRACER TECHNIQUES (GEOLOGY)
for silt movement, lanthanum-140, 20: 11022 (AERE-R-5080)
TRACER TECHNIQUES (MEDICINE)
development for pharmacological studies, 20: 10509
for brain blood circulation, 20: 10750
for brain tumor localization, 20: 10733
for coronary blood flow measurements, 20: 10730
for determining body water, tritium oxide, 20: 10557
for determining effects of nutritional state on protein metabolism, 20: 10574
for determining metabolism of labeled proteins, 20: 10564
for determining metabolism of labeled albumins, 20: 10565
for determining the effect of nutritional disorders on protein metabolism, iodine-131, 20: 10573
for gamma-globulin metabolism in man, 20: 10571
for gamma-globulin metabolism iodine-131, 20: 10572
for kidney function, evaluation of, 20: 10753
for kidney function, evaluation of, 20: 10734
for measuring gastrointestinal protein loss, criteria for, 20: 10567
for measuring intestinal protein absorption, 20: 10566
for metabolism of plasma proteins and protein-like substances, 20: 10570
for oxygen exchange measurements in man, 20: 10547
for pancreatic disorders, 20: 10566
for tropical intestinal diseases, 20: 10566
TRACER TECHNIQUES (METALLURGY)
for measuring corrosion rates of nickel, 20: 12545(R) (PAEC(A)AR651)
TRACER TECHNIQUES (OCEANOGRAPHY)
for river water mixing processes, 20: 11023
TRANSDUCERS
design of digital energy, for measuring apparatus, 20: 11085(P)
radiation effects on, transient, 20: 11174(R) (IDO-17112, pp 81-91)
radiation effects on linear-displacement, in NERVA engines, 20: 11175 (NP-15823)
TRANSFORMATION TEMPERATURES
critical points of fluids, coexistence curve near, (T), 20: 11921
TRANSISTORS
circuit for paralleling avalanche, for high current pulses, 20: 11067 (UCRL-12095-T)
development of field-effect silicon carbide junction-gate type, 20: 12276 (NYO-3405-4)
radiation effects on silicon carbide, neutron, 20: 12276 (NYO-3405-4)
radiation effects on, in microelectronic circuits, 20: 11179
radiation effects on silicon, electron and gamma, 20: 11182
TRANSITION METAL ALLOYS
phase studies, multicomponent, 20: 11318
TRANSURANIC ELEMENTS
isotope analysis of, survey of errors in mass spectrometric, 20: 10795
TRAPS
development of 1200°F sodium-vapor, 20: 10982
TREES
coir dust from coconut, pyrolysis products from, 20: 12545(R) (PAEC(A)AR651)
nutrition of coconut, tracer studies on, 20: 12545(R) (PAEC(A)AR651)
radiation effects on coconut, 20: 12545(R) (PAEC(A)AR651)
s-TRIAZINE, 2,4,6-TRIS-(ALLYLOXY)-
radioinduced polymerization of, effects of *p*-benzoquinone and diphenylpicrylhydrazil on gamma, 20: 10896
TRIOCTYLAMINE
solvent properties for metal chlorides, 20: 10759 (INP-427/C)
TRITIUM
beta decay of, scintillation method for measuring, 20: 11122
deuteron reactions with, spin coupling to neutron–helium-4 reaction channels, (T), 20: 11978 (UCRL-7961-T)
effects in thymidine with and without gamma radiation on mortality in Drosophila larvae, 20: 10602 (CNAEM-32)
effects on leukemia induction in mice, of injected, 20: 10623
incorporation in proteins, review of methods for, 20: 10945
production in high-energy proton reactions, 20: 11377
properties of albumin-incorporated, 20: 10566
proton tunneling in evolution reactions of, quantum mechanical rates for, (T), 20: 11372
reactions of recoil atoms of, 20: 10933(R) (TID-22532)
reactions of recoil atoms of, with hydrocarbons, 20: 10933(R) (TID-22532)
symmetry for, SU(6), 20: 11756
TRITONS
binding energy of, meson (π)-interaction effects on, (T), 20: 11650
reactions (t,p) with nuclei, properties of, (T), 20: 11972 (NP-15716)
reactions (t,p) with oxygen-16 and silicon-28, properties of, (T), 20: 11972 (NP-15716)
reactions (t,p) with iron-54 at 12 Mev, (T), 20: 12086
structure of, analysis using separable potentials, (T), 20: 12130
wave function for, nucleon form factor from bound-state, (T), 20: 11623
TRYPTOPHAN
metabolism in *Neurospora crassa*, indolepyruvic acid formation in, 20: 10540 (HW-SA-3728)
TUBERCULOSIS
vaccination against *Mycobacterium tuberculosis* infection in mice using heat-killed *M. smegmatis*, 20: 10655
TUBES
heat transfer in, for thermionic reactors, (T), 20: 12488
heat transfer in, for thermionic reactors, 20: 12489
heat transfer to boiling hydrogen and nitrogen in straight circular, during chill-down, 20: 10996 (WANL-TNR-154)
welding to tube sheets in boilers, methods for, 20: 11214(R) (NASA-CR-54717)
welding to tube sheets in boilers, method for, 20: 11215(R) (NASA-CR-54718)
TUMORS
plasma proteins substances metabolism in patients with malignant, tracer study, 20: 10570
radiation effects on histone synthesis and respiration in Ehrlich ascites, x, 20: 10691
radiation effects on growth of transplanted in rats, x, 20: 10665
radioinduced chromosomal aberrations in Ehrlich ascites, effects on cellular survival of, 20: 10677
radioinduced skin, after radiotherapy, 20: 10658
radioinduced thyroid, incidence of, 20: 10747
radiosensitivity of human and rat, effects of antinomycin on, 20: 10700
radiosensitivity of cervical, cytological appraisal of, 20: 10741
radiosensitivity of, x, 20: 10650
radiosensitivity of, effects of single and fractionated dose of γ and x, 20: 10649
radiosensitivity, effects of dose fractionation, x, 20: 10651
radiotherapy of auditory hemangioma, injuries from, 20: 10687
radiotherapy of bulbar, effects on eyes of, 20: 10667
radiotherapy of cervical, cytological appraisal of, 20: 10742
radiotherapy of cervical, γ, 20: 10739
radiotherapy of cervical, cytological evaluation using vaginal smears, 20: 10740
radiotherapy of cervical, cytological appraisal of, 20: 10741

radiotherapy of cervical, effects on pelvic lymph nodes of, 20: 10653
radiotherapy of cervical, effects on small intestine of γ and x, 20: 10654
radiotherapy of hemangiomas in children, β, 20: 10745
radiotherapy of, preoperative, effects on dissemination of cancer cells, 20: 10735
TUNGSTEN
coating on steel, fusion-bonding of plasma-sprayed, 20: 11242 (UCRL-12153)
coating with rhenium, electrolytic, 20: 11260
compatibility with urania, 20: 11224
corrosion by ammonium hydroxide, sodium hydroxide, and sodium hypochlorite at 35 and 60°C, 20: 11230 (BM-RI-6715)
corrosion by cesium at 400°C, 20: 11227
corrosion by chloride solutions at 35, 60, and 100°C, 20: 11230 (BM-RI-6715)
corrosion by formic, hydrochloric, and oxalic acids at 35°C, galvanic, 20: 11230 (BM-RI-6715)
corrosion by nitric acid at 35°C, galvanic, 20: 11230 (BM-RI-6715)
corrosion by sea water, sodium chloride, and sodium hydroxide, galvanic, 20: 11230 (BM-RI-6715)
corrosion of, by acids and bases, crevice, galvanic, and spray, 20: 11230 (BM-RI-6715)
deposition from fused salt mixtures, electro-, 20: 11260
determination in niobium–tungsten alloys, gravimetric, 20: 10794
diffusion of boron and carbon in surface of, 20: 11228
diffusion of rhenium and tungsten in single-crystal, 20: 11227
effects of alloy additions of, on mechanical properties of niobium, 20: 11302
extrusion of thin-walled hemispheres of, process development for high-deformation-rate, 20: 11260
fabrication by hot isostatic pressing, 20: 11260
grain growth in arc-melted, 20: 11226
grain growth suppression in vapor-deposited, up to 2500°C, 20: 11320
neutron capture by, secondary gamma emission from, (E), 20: 12267
oxidation by air at 500 to 900°C, effects of alloying additions on, 20: 11227
oxidation by oxygen at 1600°C, effects of crystal orientation on, 20: 11227
particle size measurements on powdered, equipment and methods for, 20: 11270 (LA-3424)
performance as collector electrode for thermionic cells, 20: 11540(R) (AD-626444)
preparation of high-purity, fluidized-bed process for, 20: 11255
preparation of spherical particles of, by plasma jet atomization, 20: 11219
solubility in plutonium at 700 to 1000°C, 20: 11224
sorptive properties for thermally activated nitrogen, effects of pressure and temperature on, 20: 12549(R) (TID-21555)
spectra of, burner design for atomic absorption, 20: 10761 (IS-T-69)
tensile properties of high-purity powder-metallurgy, effects of strain rate and temperature on, 20: 11227
tensile properties of single-crystal, effects of carbon additions and heat treatments on, 20: 11227
tensile properties of powder-metallurgy, effects of strain rate and temperature on, 20: 11339
thermodynamic properties, 20: 10816(T) (NASA-TT-F-285)
transition temperature of polycrystalline, ductile-to-brittle, 20: 11227
TUNGSTEN ALLOYS
brazing of, development of alloys for, 20: 11260
corrosion by inorganic and organic acids at 35, 60, and 100°C, 20: 11230 (BM-RI-6715)
Cr–Co–Mo–Ni–W, erosion by mercury vapor at 640°F of Stellite 6B, 20: 11214(R) (NASA-CR-54717)
Cr–Co–Mo–Ni–W, oxidation by air at 1600°F of Stellite 6B, 20: 11215(R) (NASA-CR-54718)
Cu–Ni–W, mechanical properties of sintered composites of tungsten-base, 20: 11291
Fe–Ni–W, mechanical properties of, effects of strain rate on, 20: 11284 (UCRL-14599)
Fe–Ni–W, mechanical properties of sintered composites of tungsten-base, 20: 11291
Hf–Nb–W–Y, development and evaluation of C-129Y, 20: 11227
Ir–W, phase studies, 20: 11309
Mo–Nb–W, creep strength of, effects of composition on, 20: 11302
Mo–Ta–W, fabrication of tantalum-base, process development for, 20: 11260
Nb–Ta–W, creep strength of, effects of composition on, 20: 11302
Nb–Ta–W–Zr, bonding to Hastelloy N, Inconel 600, and types 321 and 347 stainless steels of FS-85, explosive, 20: 11243(R) (WANL-PR(EE)-001)
Nb–Ti–W, creep strength of, effects of composition on, 20: 11302
Nb–W, analysis for niobium and tungsten, gravimetric, 20: 10794
Nb–W, creep strength of, effects of composition on, 20: 11302
Nb–W, mechanical properties of, effects of composition on, 20: 11288(T) (AD-622477)
Nb–W–Zr, erosion by mercury vapor of Cb-752, 20: 11214(R) (NASA-CR-54717)
Re–W, deposition of, properties of vapor, 20: 11256
Re–W, extrusion of, process development for, 20: 11260
Re–W, fabrication and properties for use at 2600°C, 20: 11238 (CONF-650449-1)
Rh–W, phase studies, 20: 11309
Ta–W, fabrication of tantalum-base, process development for, 20: 11260
Ta–W, tensile properties of single-crystal, effects of carbon additions and heat treatments on, 20: 11227
Ta–W–Zr, fabrication of tantalum-base, process development for, 20: 11260
Tc–W, preparation, 20: 11260
TUNGSTEN BROMIDES
thermodynamic properties, 20: 10816(T) (NASA-TT-F-285)
TUNGSTEN CARBIDES
corrosion by cesium at 400°C, 20: 11227
properties and uses at cryogenic temperatures, 20: 11293
thermodynamic properties, 20: 10816(T) (NASA-TT-F-285)
TUNGSTEN CHLORIDES
thermodynamic properties, 20: 10816(T) (NASA-TT-F-285)
TUNGSTEN FLUORIDES
reduction to metal, fluidized-bed process for, 20: 11255
thermodynamic properties, 20: 10816(T) (NASA-TT-F-285)
ReF_6–WF_6, reduction to rhenium–tungsten alloy using hydrogen, 20: 11256
TUNGSTEN HALIDES
separation from salts by extraction chromatography using organic phosphorus compounds, 20: 10759 (INP-427/C)
TUNGSTEN IODIDES
thermodynamic properties, 20: 10816(T) (NASA-TT-F-285)
TUNGSTEN ISOTOPES W-182
energy levels in, lifetime of 100.1 at 1289 kev, 20: 12082
neutron capture cross sections at .01 to 10 ev, (E), 20: 11957 (GA-6832)
TUNGSTEN ISOTOPES W-183
neutron capture cross sections at .01 to 10 ev, (E), 20: 11957 (GA-6832)
TUNGSTEN ISOTOPES W-184
neutron capture cross sections at .01 to 10 ev, (E), 20: 11957 (GA-6832)
TUNGSTEN ISOTOPES W-186
neutron activation cross section at 24 kev, (E), 20: 12135
neutron capture cross sections at .01 to 10 ev, (E), 20: 11957 (GA-6832)
TUNGSTEN OXIDES
thermodynamic properties, 20: 10816(T) (NASA-TT-F-285)
TUNGSTEN SILICIDES
oxidation by air at 600 to 1100°C, effects of preparation method on, 20: 11237
TUNGSTEN STEEL
Cr–W–V, erosion by mercury vapor at 640°F of 18-4-1 tool, 20: 11214(R) (NASA-CR-54717)
TUNGSTEN SULFIDES
thermodynamic properties, 20: 10816(T) (NASA-TT-F-285)
TUNGSTEN SYSTEMS
B–W, grain growth in arc-melted, 20: 11226
C–Hf–Re–Ta–W, preparation and properties of dispersion-strengthened, 20: 11217(R) (WANL-PR(Q)-007)
C–Hf–Ta–W, bonding of T-222, to Inconel 600 and types 321 and 347 stainless steels, explosive, 20: 11243(R) (WANL-PR(EE)-001)
Si–W, phase diagram, 20: 11296
ThO_2–W, tensile properties of, effects of strain rate and temperature on, 20: 11227
TURBINES
design for liquid metal Rankine cycles, 20: 12475 (WANL-PR(B)-009)
performance of gas-bearing closed-Brayton cycle turbocompressors, 20: 10972(R) (NYO-3237-4)
pressure governor control system for, 20: 12438

U

ULTRASONICS
attenuation in normal and superconducting thallium, (E/T), 20: 11915
ULTRAVIOLET RADIATION
effects on developmental mechanisms in Euplotes, 20: 10696
effects on development and growth of maize following seed exposure, 20: 10613(T) (NP-tr-1344)
effects on *Hansenula wingei*, antibiotic-producing mutagenic, 20: 10695
effects on iodine-131 uptake by polyvinylpyrrolidone, 20: 10946
effects on Neurospora, mechanisms of repair of, 20: 10716
effects on production of erthropoietic factor in rat kidney, 20: 10635
effects on protein synthesis in *Mycobacterium smegmatis*, tracer study, 20: 10656
effects on template properties of polycytidylic acid, 20: 10584

reactions with water at 1470 Å, primary decomposition processes in, 20: 10881
UNDERGROUND EXPLOSIONS
particle permeability and size distribution from, in oil shale, (T), 20: 10975 (UCRL-14294)
UNDERWATER EXPLOSIONS
simulation of atomic, using pulsed reactors, 20: 11013 (USNRDL-TR-940)
UNITED STATES
waste disposal standards in, comparison of, with Russia, 20: 12521
URACIL
radiolysis of copolymers of, with adenine, 20: 10877
radiolysis of, yields from, 20: 10877
URACIL, 5-FLUORO-
effects on radiosensitivity of pharyngeal carcinomas, 20: 10725
URANATES
properties as form of uranyl hydrolytic complexes, 20: 10838
URANIUM
bubble detection in, evaluation of techniques for, 20: 11220
coating with niobium by chemical vapor deposition, 20: 11260
coatings for, development of oxidation-protection, 20: 11224
compatibility with zirconium at 500 to 900°C, 20: 11316
content in plankton, sediments, and waters of Black Sea and Lake Techirghiol, 20: 10512
detection in man, design of counter for, 20: 11107 (RFP-462)
determination in carbon dioxide streams in fuel element test loops, 20: 11003
determination in fission product and irradiated fuel solutions by controlled-potential coulometry, 20: 10758 (EUR-2618.f)
diffusion in molybdenum, niobium, titanium, and zirconium, temperature dependence of, 20: 11290
diffusion in sintered uranium dioxide at 1250 to 1600°C, 20: 11312
diffusion in zirconium, 20: 11316
ductility of irradiated, effects of stress on tensile creep, 20: 11224
effects on plutonium determination in fission product solutions, 20: 10763 (KR-100)
ejection and re-ejection of fission fragments, dynamic equilibrium of, 20: 11224
electric conductivity of irradiated, kinetics of annealing of increased, 20: 11224
elimination from kidneys, effects of sulfamilamides on, 20: 10553
gamma attenuation in, (T), 20: 12264 (MLM-1315)
isotope analysis of, survey of errors in mass spectrometric, 20: 10795
neutron Doppler coefficient for, calculation of, 20: 11945
phase transformations in, effects of heat treatments on kinetics of $\beta \rightarrow \alpha$, 20: 11311
phase transformation in, 20: 11315
production and properties of, as reactor fuel, 20: 11245
production of, nuclear materials management in, 20: 10970
proton reactions with, phosphorus-32 and -33 production in, (E), 20: 12034
radiation effects on microstructure of, reactor, 20: 11357
radioinduced defects in, at 4.5°K, neutron, 20: 11224
radioinduced swelling in, mechanisms of, 20: 11224
recovery by skull-reclamation process, 20: 10965
separation from fission products by reversed-phase partition chromatography, 20: 10784
separation from mixed oxides by salt cycle process, 20: 10965
separation from other elements by solvent extraction using TBP, 20: 10952
separation of neptunium from irradiated, by reversed-phase partition chromatography, 20: 10954
spectral indices of 4.29% enriched exponential column of, (E), 20: 12358 (LA-3406)
URANIUM ALLOYS
criticality of highly enriched, in water systems, 20: 10969
Al–Fe–U, phase transformations in, effects of aluminum and iron content on, 20: 11224
Al–U, properties as oxidation-protection coating on uranium, 20: 11224
Be–U, properties of splat-cooled, 20: 11224
Cr–U, phase transformations in, effects of heat treatments on kinetics of $\beta \rightarrow \alpha$, 20: 11311
Cr–U–V, phase studies on, 20: 11271 (LFEN-24)
Fe–U, heat treatment, 20: 11319
Mo–Pu–U, analysis for plutonium, review of method for, 20: 10797
Mo–Ti–U, corrosion cracking in air, stress-, 20: 11224
Mo–U, corrosion cracking in air, stress-, 20: 11224
Mo–U, crystal structure of tempered, effects of carbon on, 20: 11292
Mo–U, mechanical properties of, effects of strain rate on, 20: 11284 (UCRL-14599)
Mo–U, mechanical properties of, effects of dynamic tensile loads on, 20: 11224
Mo–U, radiation effects on corrosion rate of, by carbon dioxide and nitrogen, reactor, 20: 11224
Nb–U, phase studies, 20: 11224
Pu–Ti–U, strength of, ultimate compressive, 20: 11224
Pu–U, analysis for plutonium, review of methods for, 20: 10797
Ru–U, phase studies, 20: 11224
Sn–U, tin Knight shift and magnetic susceptibility of USn_3, 20: 12324
U–Zr, decontamination of fluoride-volatility plant after processing irradiated, 20: 11032 (ORNL-3891)
U–Zr, dissolution by ammonium fluoride, 20: 10964
URANIUM CARBIDES
cutting crystals of, electrolytic jet machining method for, 20: 11216 (PEL-79)
diffusion of carbon in, at 1200 to 2100°C, 20: 11224
fission gas diffusion from, at 900 to 2100°C, 20: 11224
oxidation in defective fuel elements by reactive coolants, (E/T), 20: 12380
performance as fuel, 20: 11222
radiation effects on coated particles of, 20: 11343 (LA-3367)
reduction and sintering in hydrogen, 20: 11252
Cr–PuC–UC, analysis for plutonium, review of methods for, 20: 10797
Fe–PuC–UC, analysis for plutonium, review of methods for, 20: 10797
GdC_2–UC_2, phase studies, 20: 11224
Mo–PuC–UC, analysis for plutonium, review of methods for, 20: 10797
PC–UC, analysis for plutonium, review of methods for, 20: 10797
PuC–UC, radiation effects on, measurement in DFR, 20: 12442
Pu_2C_3–UC, reduction and sintering in hydrogen, 20: 11252
ThC_2–UC_2, fabrication of, review of, 20: 11241 (TID-8541, pp 71-148)
U–UC, phase studies and kinetics of hydrogenation of, 20: 10801 (CEA-R-2777)
URANIUM CHLORIDES
separation from salt mixtures by extraction chromatography using organic phosphorus compounds, 20: 10759 (INP-427/C)
URANIUM COMPLEXES
hydroxy, preparation and properties, 20: 10838
with acetic acid compounds in aqueous solutions, potentiometry of, 20: 10802(R) (COO-1020-9)
with 2,4-pentanedione, spectra of single-crystal, vibrational structure of, 20: 10843
URANIUM COMPOUNDS
preparation and properties, 20: 11245
URANIUM CONCENTRATES
processing of, nuclear materials management in, 20: 10968
sampling of, design of equipment for, 20: 10978 (RMO-3006)
URANIUM DEPOSITS (CHILE)
reconnaissance of Lonquimay area, 20: 11025 (RME-4552(Rev.))
URANIUM(IV) FLUORIDES
fluorination to uranium hexafluoride, 20: 10852
URANIUM(VI) FLUORIDES
preparation and properties of, 20: 10965
preparation by fluorination of uranium tetrafluoride, 20: 10852
reduction to uranium dioxide, thermochemical, 20: 11257
URANIUM HALIDES
separation from salts by extraction chromatography using organic phosphorus compounds, 20: 10759 (INP-427/C)
URANIUM HYDRIDES
H–U–UH_n, phase studies and thermodynamic properties below 430°C, 20: 10801 (CEA-R-2777)
URANIUM IONS
spectra in cesium uranium chlorides, M1 transitions in, (E), 20: 12290
URANIUM ISOTOPES
separation of, theory and economics of methods for, 20: 11193
URANIUM ISOTOPES U-232
performance as space vehicle power supply, 20: 11188 (BLG-330)
URANIUM ISOTOPES U-233
helium ion fission at 42.8 Mev, deformation of transition-state nucleus in, (E), 20: 12077
neutron capture-to-fission ratios for, thermal, (E), 20: 11960(R) (IDO-14667)
neutron fission of, yields from thermal, (E), 20: 11960(R) (IDO-14667)
neutron fission reactions, cumulative and direct xenon-135 yields in thermal, (E), 20: 11990
URANIUM ISOTOPES U-234
energy levels of, Tamm-Dancoff method for collective, (T), 20: 11966 (JINR-P-2432)
helium ion fission at 42.8 Mev, deformation of transition-state nucleus in, (E), 20: 12077
URANIUM ISOTOPES U-235
burnup in PWR, stainless steel and zirconium cladding effects on, 20: 12418(R) (WCAP-3739)
determination by atomic absorption spectrophotometry, 20: 10770
fission products of, distribution in tissues of, biological model and computer analysis of kinetics, 20: 10519(R) (BNWL-122, pp 59-63)
helium ion fission at 42.8 Mev, deformation of transition-state nucleus in, (E), 20: 12077

neutron capture-to-fission ratios for, thermal, (E), 20: 11960(R) (IDO-14667)
neutron cross section of, Westcott parameters for, (T), 20: 11959 (HW-77389)
neutron fission of, yields from thermal, (E), 20: 11960(R) (IDO-14667)
neutron fission of, fragment charge distribution in thermal, (E), 20: 11980 (USNRDL-TR-935)
neutron fission of, palladium-115 yields from thermal, (E), 20: 11981 (USNRDL-TR-943)
neutron fission of, fragment mass-energy correlations from thermal, (E), 20: 12076
neutron fission of, fragment energy and mass distributions in, (E/T), 20: 12117
neutron fission reactions, cumulative and direct xenon-135 yields in thermal, (E), 20: 11990
neutron four-group cross sections, 20: 12485
neutron nonelastic reactions at 8.1 Mev, cross sections for, (E), 20: 11985
neutron spectra in, for 0, 0.011, and 0.099 bucklings, 20: 12485
radioinduced vaporization of beads of, *in vacuo* and in water, 20: 11013 (USNRDL-TR-940)

URANIUM ISOTOPES U-236
helium ion fission at 42.8 Mev, deformation of transition-state nucleus in, (E), 20: 12077
neutron cross section of, Westcott parameters for, (T), 20: 11959 (HW-77389)

URANIUM ISOTOPES U-238
determination by atomic absorption spectrophotometry, 20: 10770
determination in tissues, radiochemical, 20: 10514(R) (BNWL-122, pp 21-4)
helium ion fission at 42.8 Mev, deformation of transition-state nucleus in, (E), 20: 12077
neon-22 reactions (Ne-22,6n) at 112 to 135 Mev, nobelium-254 production in, (E), 20: 11969 (JINR-P-2471)
neutron cross section of, Westcott parameters for, (T), 20: 11959 (HW-77389)
neutron fission of, fine structure in mass distribution from fast, (E), 20: 12121
neutron nonelastic reactions at 8.1 to 21 Mev, cross sections for, (E), 20: 11985
neutron resonance self-shielding in fast reactors, effective cross sections for, (T), 20: 12374
neutron resonance absorption in homogeneous media with heavy moderators, (T), 20: 11941
radiation dose in lungs from, in inhaled uranium ores, 20: 10514(R) (BNWL-122, pp 21-4)

URANIUM MINERALS
geochemistry of, in igneous rocks of Lower Triassic deposits, Pripyat Basin, USSR, 20: 11026
reactions of hot atoms in, 20: 10933(R) (TID-22532)

URANIUM NITRATES
preparation of, nuclear materials management in, 20: 10967
separation from salt mixtures by extraction chromatography using organic phosphorus compounds, 20: 10759 (INP-427/C)

URANIUM NITRIDES
preparation and sintering, 20: 11224

URANIUM ORES
distribution of inhaled aerosols of, in rats, 20: 10514(R) (BNWL-122, pp 21-4)
processing, 20: 11245
processing of, nuclear materials management in, 20: 10968
processing of, nuclear materials management in, 20: 10970

URANIUM OXIDES
preparation of thin-film radiation targets of, using evaporation-condensation, 20: 11183 (ORNL-P-1900)
reduction to uranium dioxide, 20: 10966
vaporization mechanisms, 20: 11234 (IS-1300)

URANIUM(IV) OXIDES
analysis of irradiated, use of electron probe microanalyzer for, 20: 10787
coating with beryllia, method for, 20: 11224
compatibility with materials for carbon dioxide-cooled reactors, 20: 11224
diffusion of actinides in sintered compacts of, at 1250 to 1600°C, 20: 11312
fission gas diffusion from, coefficients for, 20: 11224
fission gas diffusion in, relation between grain growth and, 20: 11224
fission gas diffusion in, effects of stress on, 20: 11224
fission gas diffusion from, mechanisms of temperature-dependent, 20: 11224
formation of hydrates of, in hydrolysis of uranyl nitrates, 20: 10841
neutron buckling in 7- and 19-element fuel clusters of, (E/T), 20: 12493 (AECL-2514)
neutron resonance temperature correlation for pellets of, effective, (T), 20: 12372
oxidation of particles of, thermogravimetric studies of, 20: 10839
performance in gas-cooled reactors and water reactors, 20: 11222
preparation by calcination of uranium(IV-VI) oxides, 20: 10839
preparation for reactor fuels, hexafluoride thermochemical reduction for, 20: 11257
preparation of single-crystal, 20: 11224
production by reduction of higher oxides, 20: 10966
radiation effects on coated particles of, 20: 11343 (LA-3367)
radiation effects on, fission-product distributions from neutron, 20: 11365
radioinduced defects in single-crystal, thermal-neutron, 20: 11224
thermal conductivity, 20: 12377(R) (CEND-2863-236)
vaporization mechanisms, 20: 11234 (IS-1300)
B_4C–UO_2, development of fuel rods of, 20: 11226
B–UO_2, preparation of sintered pellets of, with controlled composition, 20: 11224
Mo–UO_2, chlorination, 20: 10961
PuO_2–UO_2, analysis for plutonium, review of method for, 20: 10797
PuO_2–UO_2, fabrication and testing for BR-3/Vulcain, 20: 12397(R) (EURAEC-1506)
PuO_2–UO_2, fabrication and testing for BR-3/Vulcain, 20: 12396(R) (EURAEC-1505)
PuO_2–UO_2, fabrication of, review of remote, 20: 11241 (TID-8541, pp 71-148)
PuO_2–UO_2–H_2O, neutron decay constants in lattices of, (E), 20: 12397(R) (EURAEC-1506)
stainless steel–UO_2, fabrication by roll bonding, 20: 11260
ThO_2–UO_2, fabrication of, review of, 20: 11241 (TID-8541, pp 71-148)
ThO_2–UO_2, fission gas diffusion in, effects of stress on, 20: 11224
ThO_2–UO_2, radiation effects on dissolution of, by nitric acid, 20: 10964
UO_3–$UO_2(NO_3)_2$–H_2O, phase studies, 20: 10841

URANIUM(IV-VI) OXIDES
calcination of, preparation of uranium dioxide by, 20: 10839
preparation of enriched, for use as fuel in HFIR, 20: 11244 (Y-MA-450)

URANIUM(VI) OXIDES
conversion to urania, 20: 10966

URANIUM RESERVES
evaluation of, 1964, 20: 12558

URANIUM SLURRIES
handling of, design of tank for, 20: 10981

URANIUM SYSTEMS
Al–Si–U, properties of splat-cooled, 20: 11224
C–Be–U, properties of splat-cooled, 20: 11224
C–Ce–U, phase studies, 20: 11224
C–U, properties of splat-cooled, 20: 11224
graphite–U, neutron spectra in, for 0, 0.011, and 0.099 bucklings, 20: 12485
H–U–UH_n, phase studies and thermodynamic properties below 430°C, 20: 10801 (CEA-R-2777)
Pu–U–H_2O, neutron cross sections and thermal spectra in, 20: 12370
S–U, phase studies, 20: 11224
U–UC, phase studies and kinetics of hydrogenation of, 20: 10801 (CEA-R-2777)

URANYL CARBONATES
sorption in kidneys, effects of sulfanilamides on, 20: 10553

URANYL FLUORIDES
critical dimensions of aqueous enriched, (E/T), 20: 12359 (ORNL-TM-1195)

URANYL IONS
separation from salts by solvent extraction using Schiff bases in chloroform, 20: 10759 (INP-427/C)

URANYL NITRATE COMPLEXES
spectra of, absorption and luminescence, 20: 10827

URANYL NITRATES
hydrolysis of, precipitation of uranium trioxide hydrates in, 20: 10841
toxicity in mice, 20: 10548
$Ce(NO_3)_4$–TBP–$UO_2(NO_3)_2$–H_2O, phase diagram, 20: 10952
UO_3–$UO_2(NO_3)_2$–H_2O, phase studies, 20: 10841

URANYL PERCHLORATES
complexes with neutral ligands, preparation of, 20: 10825

UREA
synthesis of, carbon-14-labeled carbonate for measuring rate of, 20: 10559
use of nitrogen-15-labeled, combined with carbon-14-labeled carbonate for measuring rate of urea synthesis, 20: 10559

UREA, THIO-
radiolysis of aqueous solutions of, with ethylene oxide polymer, 20: 10921

URETHAN POLYMERS
radiation effects on electric and physical properties of, gamma and neutron, 20: 11344 (N65-35361)

URETHANS

radioinduced inhibition of mouse tumors induced by, x, 20: 10671
URINE
analysis for amino acids, methods for, 20: 10582
analysis for plutonium, method for, 20: 10757 (BLG-353)
calcium-45 content in human, after respiratory uptake, 20: 10546
radiation effects on amino acid excretion in mouse, β, 20: 10582
radiation effects on excretion of injected phosphorus-32 in rat, effects of dinitrophenol on x, 20: 10666
thallium-204 content in human, after respiratory uptake, 20: 10546
UTERUS
radiotherapy of carcinomas of, complications and survival rate after, 20: 10726
radiotherapy of carcinomas of, histological evaluation of radium, 20: 10749
radiotherapy of carcinomas of, review of indirect effects of x, 20: 10670
radiotherapy of cervical carcinomas, evaluation of results, 20: 10727
radiotherapy of cervical cancers, y, 20: 10739
radiotherapy of cervical cancers, evaluation of prognosis and results by cytological studies of vaginal smears, 20: 10740
radiotherapy of cervical cancers, cytological appraisal of, 20: 10741
radiotherapy of cervical cancers, cytological appraisal of, 20: 10742
radiotherapy of cervical carcinoma during pregnancy, 20: 10751
radiotherapy of cervical cancer in, effects on small intestine of y and x, mice, x, 20: 10655
radiotherapy of cervical cancer in, effects on pelvic lymph nodes of, 20: 10653

V

VACCINES
radiation effects on distribution of heat-killed *Mycobacterium smegmatis* in 20: 10654
VACUUM
electric discharge in, review of theories for, 20: 11769 (LGI-65/30)
electric discharge in, transverse magnetic field effects on, (E), 20: 11769
technology of ultrahigh, review of, 20: 11008
use in containment of water-cooled power reactors, 20: 12447
VACUUM GAGES
review of ultrahigh, 20: 11008
VACUUM PUMPS
review of ultrahigh, 20: 11008
VACUUM SEALS
review of ultrahigh, 20: 11008
VACUUM SYSTEMS
development for CEA beam bypass, 20: 11385 (CEAL-TM-157)
review of ultrahigh, 20: 11008
VACUUM TECHNIQUES
use in bubble chamber development, 20: 11141
uses of ultrahigh, review of, 20: 11008
VACUUM VALVES
review of ultrahigh, 20: 11008
VAGINA
cytology of, use in evaluation of prognosis and results of radiotherapy of cervical cancers, 20: 10740
radiation effects on benign cells of, 20: 10740
VALLECITOS SUPERHEAT REACTOR
coolant and moderator chemistry, 20: 12399(R) (GEAP-4941)
operation summary for June–Aug. 1965, 20: 12399(R) (GEAP-4941)
safety organization for, 20: 12337
VALVES
development for space propulsion systems using liquid propellants, 20: 11007(R) (NP-15831)
VAN ALLEN RADIATION BELTS
electron-distribution variations during magnetic storms, correlations with magnetosphere tail, (E), 20: 11831
particle energies and intensities in, 20: 11840
proton energy and spatial distributions in inner, 20: 11825
stability of, interchange, (T), 20: 11835
structure variations during geomagnetic storms, (T), 20: 11838
VANADIUM
corrosion by ammonium hydroxide, sodium hydroxide, and sodium hypochlorite at 35 and 60°C, 20: 11230 (BM-RI-6715)
corrosion by chloride solutions at 35, 60, and 100°C, 20: 11230 (BM-RI-6715)
corrosion by formic, hydrochloric, and oxalic acids at 35°C, galvanic, 20: 11230 (BM-RI-6715)
corrosion by nitric acid at 35°C, galvanic, 20: 11230 (BM-RI-6715)
corrosion of, by acids and bases, crevice, galvanic, and spray, 20: 11230 (BM-RI-6715)
deposition from fused salt mixtures, electro-, 20: 11260
effects of alloy additions of, on mechanical properties of niobium, 20: 11302
effects of alloying additions of, on thermal stability of $TiAl_3$, 20: 11335
effects on hydrogen distribution in Zircaloy, 20: 11221
superconducting point contacts of, macroscopic quantum interference effects in, (E/T), 20: 11911
VANADIUM ALLOYS
corrosion by inorganic and organic acids at 35, 60, and 100°C, 20: 11230 (BM-RI-6715)
Al–Mo–Sn–Ti–V, fracture toughness properties of titanium-base, effects of heat treatments on, 20: 11273(R) (NRL-6364)
Al–Mo–Ti–V, corrosion cracking by salts at 550 to 600°F, stress-, 20: 11227
Al–Mo–Ti–V, thermal stability of, effects of composition on, 20: 11336
Al–Sn–Ti–V, fracture toughness properties of titanium-base, plane-strain, 20: 11273(R) (NRL-6364)
Al–Ti–V, corrosion by cesium at 400°C, 20: 11227
Al–Ti–V, fracture toughness of plasmarc welds in titanium-base, 20: 11273(R) (NRL-6364)
Al–Ti–V, fracture toughness properties of titanium-base, plane-strain, 20: 11273(R) (NRL-6364)
Al–Ti–V, fracture toughness properties of titanium-base, 20: 11273(R) (NRL-6364)
Al–Ti–V, mechanical properties of, effects of strain rate on, 20: 11284 (UCRL-14599)
Al–Ti–V, radiation effects on low-cycle fatigue and tensile properties at cryogenic temperatures, 20: 11345(R) (NASA-CR-54787)
Al–Ti–V, tensile properties of, effects of exposure to cesium at 650°C on, 20: 11227
Cr–Fe–Mo–V, erosion by mercury vapor at 640°F of Lapelloy, 20: 11214(R) (NASA-CR-54717)
Cr–U–V, phase studies on, 20: 11271 (LFEN-24)
Nb–Ti–V, corrosion by acids and bases of vanadium-base, 20: 11230 (BM-RI-6715)
Nb–V, corrosion by acids and bases of vanadium-base, 20: 11230 (BM-RI-6715)
Ti–V, corrosion by acids and bases of vanadium-base, 20: 11230 (BM-RI-6715)
Ti–V, fabrication of tubing of, for reactor fuel cladding, 20: 11258
Ti–V, fabrication of TV-20, process development for, 20: 11260
V–Y, corrosion by acids and bases of vanadium-base, 20: 11230 (BM-RI-6715)
VANADIUM OXYNITRIDES
preparation, 20: 10856
VANADIUM COUPLES
Fe/Nb/stainless steel/V, diffusion in bimetallic tubing of, with iron and vanadium diffusion barriers, inter-, 20: 11215(R) (NASA-CR-54718)
Fe/stainless steel/Ta/V, diffusion in bimetallic tubing of, with iron and vanadium diffusion barriers, inter-, 20: 11215(R) (NASA-CR-54718)
VANADIUM IONS
radioinduced in ammonium magnesium sulfates, ammonium zinc sulfates, and potassium zinc sulfates, EPR spectra of, 20: 12319
VANADIUM ISOTOPES V-51
neutron reactions (n,p) at 14.8 Mev, cross sections for, (E), 20: 12133
proton reactions (p,2p) at 460 Mev, (E/T), 20: 11948 (AD-624318)
VANADIUM STEEL
mechanical properties of, effects of strain rate on, 20: 11284 (UCRL-14599)
Cr–Mo–Ni–V, fatigue crack propagation in, effects of air or salt water environment on, 20: 11273(R) (NRL-6364)
Cr–W–V, erosion by mercury vapor at 640°F of 18-4-1 tool, 20: 11214(R) (NASA-CR-54717)
VANADYL IONS
radiation effects on, in ammonium zinc sulfate, x, 20: 12319
spectra in ammonium zinc sulfate, EPR, 20: 12319
VINYL ALCOHOL POLYMERS
effects as binder on tensile strength of oxides for machining, 20: 11277 (RFP-659)
VIRUSES
hamster cells infected with Polyoma, effects of x-irradiated non-infected cells on, 20: 10684
VITAMIN B_1
hydrochloride, irradiation method for stabilization of, 20: 10931(P)
VITAMIN B_{12}
radiation effects on, in meat, effects of lyophilization on y, 20: 11185
VOLATILITY SEPARATION PROCESSES
development of, for spent fuels, 20: 10965

W

WASHINGTON
fallout monitoring, 1963 and 1964, 20: 11011(R) (BNWL-122, pp 181-3)
fallout monitoring, 1961 through 1964, 20: 11012(R) (BNWL-122, pp 184-6)
WASTE DISPOSAL
burial and storage, processing for, 20: 12520(T) (CEA-tr-A-1490)
ground storage at ORNL, geohydrology evaluation of, 20: 12518

(ORNL-TM-1327)
ground, ground water transport effects on, 20: 11009 (BNWL-SA-406)
incorporation in asphalt, 20: 12524
marine, effects on radioactivity of sea foods, 20: 11054
methods for gases, 20: 12522
methods for Humboldt Bay Power Reactor, 20: 12435
methods for, review of, 20: 12519 (TID-8541, pp 149-248)
standards in U.S. and U.S.S.R., comparison of, 20: 12521
storage, pressure in calcined waste pots for, 20: 12517(R) (BNWL-170)

WASTE PROCESSING
incorporation in asphalt, effects of radioactivity levels on, 20: 12517(R) (BNWL-170)
method for low-level, liquid-foam, 20: 12526
method for PW-1 and PW-2, effects of melter products on, 20: 12517(R) (BNWL-170)
methods for, at Marcoule, Mol, and Windscale, 20: 12520(T) (CEA-tr-A-1490)
methods for, burial and storage, 20: 12520(T) (CEA-tr-A-1490)
methods for, review of, 20: 12519 (TID-8541, pp 149-248)
solidification condensate treatment, 20: 12517(R) (BNWL-170)
solidification, design of engineering prototypes for, 20: 12517(R) (BNWL-170)
solidification, design verification tests on prototype equipment for, 20: 12517(R) (BNWL-170)
solidification, flow diagram for engineering prototypes for, 20: 12517(R) (BNWL-170)
solidification, methods for high-level materials, 20: 12524
solidification, tests on in-tank, 20: 12517(R) (BNWL-170)
solidification, use of computers for evaluation of engineering prototype for, 20: 12517(R) (BNWL-170)

WASTE SOLUTIONS
decontamination using clay minerals, 20: 12527(P)
effects of Hanford reactor, on growth of salmon, 20: 10538(R) (BNWL-122, pp 198-201)
fission product diffusion from simulated solid, 20: 12517(R) (BNWL-170)
hazards of radioactive aqueous, assessment of, 20: 12525
origin of radioactive aqueous, in nuclear industry, 20: 12525
properties of sulfate-bearing versus sulfate-free samples of, 20: 12517(R) (BNWL-170)
solubility and drip temperature of, effects of temperature and time on, 20: 12517(R) (BNWL-170)
solubility and temperature of phosphate, containing fission product and process oxides, 20: 12517(R) (BNWL-170)
sources of, industrial and non-industrial, 20: 12520(T) (CEA-tr-A-1490)
thermal properties of solidified, 20: 12517(R) (BNWL-170)
transport by ground water, sequence for predicting, 20: 11009 (BNWL-SA-406)
transport of solidified, hazards in, 20: 12517(R) (BNWL-170)

WATER
boiling burnout conditions for flow in vertical 3- and 7-rod clusters, (E/T), 20: 11000
calcium uptake from, by trout, tracer study, 20: 10555
containment of, dry, 20: 12447
corrosive effects on aluminum, kinetics of, 20: 11227
corrosive effects on nickel plating on plutonium–aluminum fuel elements, 20: 11227
decontamination using clay minerals, 20: 12527(P)
gamma buildup factors for, calculation of, (T), 20: 12261 (AFRRI-TM-65-2)
neutron moderation by, at 20, 77, and 300°K, (E), 20: 11944
neutron slowing down in, space- and time-dependent density for, (E), 20: 11927 (AE-208)
neutron transmission through energy spectra after fast, (E), 20: 12268
photolysis at 1470 Å, primary processes in, 20: 10881
production of thin flowing sheets for radiation target use, 20: 11409
radioactive waste solutions of, assessment of industrial hazards from, 20: 12525
radiolysis in solutions with fumaric acid, gamma, 20: 10875
radiolysis of, formation of hydroxyl radicals in pulsed-electron, 20: 10924
reactions of hydrated electron with, in pulse radiolysis, 20: 10894
reactions with sodium in steam generator, 20: 12386 (APDA-176)
reactions with sodium in sodium-heated steam generators, 20: 12391 (BAW-1280-28(Vol.3))
spectra of, uv absorption, 20: 10823
strontium uptake from, by trout, tracer study, 20: 10555
$Al–H_2O$, neutron diffusion in plutonium-fueled lattices of, thermal, (E), 20: 12396(R) (EURAEC-1505)
benzene–N_2O–H_2O, production of biphenyl–terphenyl mixtures in radiolysis of, 20: 10930(P)
$B–H_2O$, corrosive effects on control rod and fuel cladding, 20: 12418(R) (WCAP-3739)
$Ce(NO_3)_4$–TBP–$UO_2(NO_3)_2$–H_2O, phase diagram, 20: 10952
$N_2O–H_2O$, radioinduced hydroxyl radicals in, 20: 10924
$PuO_2–UO_2–H_2O$, neutron decay constants in lattices of, (E), 20: 12397(R) (EURAEC-1506)
$Pu–U–H_2O$, neutron cross sections and thermal spectra in, 20: 12370
$UO_3–UO_2(NO_3)_2–H_2O$, phase studies, 20: 10841

WATER-d_2
deuteron quadrupole in, constants for, (T), 20: 12287
effects of ingested, on sterility of mice, 20: 10550
neutron diffusion in, thermal, (E/T), 20: 11931 (CONF-651101-53)
neutron moderation by, at 77 and 300°K, (E), 20: 11944
spectra of, uv absorption, 20: 10823
thermodynamic properties of electrolytes in, 20: 10847

WATER-t_2
use in determining body water, 20: 10557

WATER COOLED REACTORS
control rods for closed-cycle, feasibility of boron automatic, 20: 12418(R) (WCAP-3739)
coolant analysis for chemical and radioactive contamination, 20: 12509
coolant loss accidents in closed-cycle power, flow analysis of, (T), 20: 12418(R) (WCAP-3739)
development of large closed-cycle power, 20: 12417(R) (WCAP-3269-15)
development of large closed-cycle power, 20: 12418(R) (WCAP-3739)
fuel element welding development for, 20: 12377(R) (CEND-2863-236)
loading closed-cycle power, using automatic boron control, 20: 12418(R) (WCAP-3739)
performance of urania elements in, 20: 11222

WATER MODERATED REACTORS
design of emergency cooling systems for, 20: 12434
development of large closed-cycle power, 20: 12417(R) (WCAP-3269-15)
development of large closed-cycle power, 20: 12418(R) (WCAP-3739)
neutron cross sections and thermal spectra in plutonium-uranium-fueled, 20: 12370
reactivity of aluminum–plutonium fueled, 20: 12494 (BNWL-160)

WATER SUPPLIES
alpha activity due to radium and decay products, measurement of, using nuclear emulsions, 20: 11044

WATER VAPOR
compatibility with pyrolytic-carbon-coated carbide fuel particles at 1000°C, 20: 11224

WATER WAVES
motion of solitary breaking and shoaling, (T), 20: 12551 (UCRL-12186)

WELDED JOINTS
properties of, in thick plates of 1.2 MD07 steel, 20: 11239(R) (EURAEC-1468)
stress relief of, between Conoseal flange and component piping, 20: 11214(R) (NASA-CR-54717)

WELDING
development of explosive, 20: 11260
development of projection, for fuel element spacing, 20: 12377(R) (CEND-2863-236)
effects on brittle fracture of thick steel plates, bend test for measurement of, 20: 11240(R) (EURAEC-1520)
methods for capsule, 20: 11263(P)
procedures for tube-to-tube-sheets in boilers, 20: 11214(R) (NASA-CR-54717)
procedures for tube-to-tube-sheet, in boilers, 20: 11215(R) (NASA-CR-54718)
safety requirements for, stainless steel for nuclear reactor plants, 20: 11259
uses of lasers for, 20: 11260

WELDS
radiography of, method for neutron, 20: 11005(P)

WELL LOGGING
method for strata shrinkage measurement using cobalt-60, 20: 11024

WHEAT
cesium-137 content in German, effects of precipitation on, 20: 11017
radiation effects on genetic variability in, 20: 10603(R) (IAEA-2466-11)
strontium-89 and -90 content in German, effects of precipitation on, 20: 11017

WHISTLERS
frequency of proton, from vlf data, (E), 20: 11821
frequency of vlf proton, hydrogen ion ionospheric content from crossover, 20: 11822

WIND
effects on ground deposition of microspheres released from 50 km, 20: 11033 (SC-TM-65-398)
motion in conducting atmosphere, MHD equations for, 20: 11808(T)

WORMS
radiation effects on virulence of *Schistosoma japonicum* cercariae in mice, x, 20: 12545(R) (PAEC(A)AR651)

X

X AGENT
patterns of, effects of light on, 20: 11536
X RADIATION
absorption by crystals, corrections for, (T), 20: 12308
absorption in electron beam apparatus, provision for, 20: 11418(P)
diffraction by alpha-irradiated silicon crystals, 20: 12281
effects of, combined with 6-purinethiol on skin graft survival in rats, 20: 10506
effects on activity of alanine–2-oxoglutarate and aspartate–2-oxoglutarate-aminotransferase in rat CNS and muscles, 20: 10593
effects on activity of lenticular epithelial enzymes in rabbits, 20: 10630
effects on adrenal cortex in rats, histochemical, 20: 10576
effects on animal cells, biological, 20: 10650
effects on barley seedlings, 20: 10619
effects on bone marrow of leukemia patients, fibrotic, 20: 10746
effects on brain of guinea pig, histochemical, 20: 10638
effects on carcinomas of cervix, therapeutic, 20: 10727
effects on carcinoma of bladder, effects of dose fractionation on therapeutic, 20: 10743
effects on carcinoma of cervix during pregnancy, 20: 10751
effects on chromium divalent and tetravalent ion content in rubies, 20: 12305
effects on chromosomes in Vicia roots, effects of N-ethylmaleimide on, 20: 10624
effects on contractive ability of mitochondria, 20: 10678
effects on desoxyribonuclease activity in rat spleen, 20: 10622
effects on desoxyribonucleotide content of mouse and rat bone marrow, spleen, and thymus, single and repeated exposure, 20: 10633
effects on development and growth of maize following seed exposure, 20: 10613(T) (NP-tr-1344)
effects on distribution of heat-killed *Mycobacterium smegmatis* in mice, 20: 10655
effects on dogs and rats, protective effects of chemical compounds against, 20: 10699(T) (NASA-TT-F-353, pp 210-38)
effects on dogs and rats, RBE of, 20: 10611(T) (NASA-TT-F-353, pp 185-93)
effects on dogs and rats, RBE of, 20: 10612(T) (NASA-TT-F-353, pp 194-209)
effects on dominant lethal induction in rats, 20: 10609(T) (NASA-TT-F-353, pp 151-6)
effects on egg production by chickens, 20: 10626
effects on endogenous respiration and histone synthesis in Ehrlich ascites tumor cells, 20: 10691
effects on eyes of dogs exposed during fetal stages, 20: 10675
effects on folic acid, 20: 10904
effects on fungi, physiological, 20: 10620
effects on genetic variability in maize and wheat, 20: 10603(R) (IAEA-2466-11)
effects on growth of tissue cells of Topinambour, 20: 10621
effects on growth of tumor transplants in rats, 20: 10665
effects on growth in newborn mice, effects of dose and strain on, 20: 10673
effects on immune reactions of mice to rat tissue transplants, 20: 10505(R) (BNWL-122, pp 146-9)
effects on immune properties of sarcoma cells in suspension, 20: 10634
effects on intestinal absorption of bile salts in rats, 20: 10599(R) (BNWL-122, pp 128-30)
effects on iridindiphosphate glucose content in rat liver, 20: 10590
effects on lactic- and malic-acid dehydrogenases in extracts of rat liver and spleen, 20: 10583
effects on leukocytic reaction to adrenaline in dogs, 20: 10594
effects on lipid content of brain of guinea pigs, 20: 10636
effects on man after cervical carcinoma therapy, review of indirect, 20: 10670
effects on man, leukemogenic, 20: 10647
effects on mating activity of male Drosophila, 20: 10644
effects on mesenteric mast cells in normal and adrenalectomized rats, 20: 10686
effects on mineral metabolism in rat skeleton, localized-exposure, 20: 10587
effects on mucus synthesis in rat intestine, 20: 10600 (BNWL-122, pp 131-4)
effects on non-infected hamster cells, effects on contacted Polyoma-infected cells, 20: 10684
effects on oats, genetic, 20: 10645
effects on osmotic resistance of rat leukocytes, 20: 10614
effects on *p*-aminobenzoic acid conjugates, 20: 10904
effects on p-i-n junction detectors, pulsed and steady-state, 20: 11173 (D2-84071-1)
effects on polynucleotides in solid phase, 20: 10877
effects on population dynamics of mosquitoes, 20: 10692
effects on Pseudomonas susceptibility in mouse chimeras, 20: 10669
effects on Pseudomonas susceptibility in mice, 20: 10669
effects on radioresistance of sarcoma cells in suspension, 20: 10634
effects on rat fetuses, pathological, 20: 10616
effects on rat intestine, effects of adrenal factors on, 20: 10697
effects on rats, pathological, 20: 10598(R) (BNWL-122, pp 107-9)
effects on reproduction of Tribolium, effects of sulfoxide compounds on, 20: 10504(R) (BNWL-122, pp 142)
effects on reproduction of *Tribolium castaneum*, 20: 11184(R) (BNWL-122, pp 137-9)
effects on reversion of white-ivory mutants in Drosophila, 20: 10693
effects on serum transaminase activity in mice, 20: 12545(R) (PAEC(A)AR651)
effects on sex ratio of women exposed during diagnostic radiography, 20: 10657
effects on small intestine after cervical cancer therapy, 20: 10654
effects on survival of tumor cells in culture, effects of anoxia and anti-metabolite drug on, 20: 10664
effects on swine, biological, 20: 10618
effects on tadpole tissues, effects of starvation during irradiation on, 20: 10676
effects on *Tribolium castaneum*, genetic, 20: 11184(R) (BNWL-122, pp 137-9)
effects on tumor cells, biological, 20: 10650
effects on tumor cells, biological, 20: 10651
effects on urethan-induced tumors in mice, effects of dose on inhibitory, 20: 10671
effects on urinary excretion of injected phosphorus-32 in rats, effects of dinitrophenol on, 20: 10666
effects on vanadyl ions in ammonium zinc sulfate, 20: 12319
effects on vestibular apparatus in dogs and rabbits, 20: 10610(T) (NASA-TT-F-353, pp 157-84)
effects on viral-transformed hamster cells, 20: 10684
effects on virulence of *Schistosoma japonicum* cercariae in mice, 20: 12545(R) (PAEC(A)AR651)
emission from mu-mesic atoms, computer analysis of, 20: 11440(R) (COO-614-34, Sect. IID)
emission from proton reactions with beryllium at 1.6 Mev from electron acceleration and bremsstrahlung, (E/T), 20: 11501
intensity during auroral storms, (E), 20: 11855
intensity pulsations of auroral-zone, spatial and time, (E), 20: 11826
production by proton bombardment, use of, in determining film surface density, 20: 11281 (UCRL-12107)
production of beta-induced, 20: 12545(R) (PAEC(A)AR651)
wavelengths of, errors in measurement of, 20: 11069
X-RAY CAMERAS
design modification for Debye-Scherrer diffraction, for powder patterns of alpha emitters, 20: 11075
X-RAY-DIFFRACTION ANALYSIS
equipment for alpha-active powder design modification for, 20: 11075
X-RAY FLUORESCENCE ANALYSIS
use for nondestructive determination of burnup in nuclear fuel, 20: 11004
X-RAY SOURCES
preparation of low-energy, methods for, 20: 10932 (ORNL-P-1928)
X-RAY SPECTROMETERS
performance, 20: 11069
performance using promethium-147 beta source for K x-ray spectra, 20: 11133
XENON
buildup in reactors, simulator for studying, 20: 12498(R) (IDO-17112, pp 1-51)
content in Bruderheim meteorite, 20: 11430
determination in irradiated urania pellets using electron microprobe analysis, 20: 11365
electron reactions with atomic, metastable excitation in, (E), 20: 11455 (UCRL-14450)
C_2F_6–Xe, energy transfer in gamma radiolysis of, 20: 10884
XENON FLUORIDES
molecular vibrations of, bond-bond interaction constants for, 20: 10829
XENON ISOTOPES
determination in meteorites as indication of fission, neutron capture, and spallation anomalies, (E/T), 20: 11424 (NP-15629)
XENON ISOTOPES Xe-124
content in Bruderheim meteorite, 20: 11430
XENON ISOTOPES Xe-126
content in Bruderheim meteorite, 20: 11430
XENON ISOTOPES Xe-128
content in Bruderheim meteorite, 20: 11430
XENON ISOTOPES Xe-129
content in Bruderheim meteorite, 20: 11430
XENON ISOTOPES Xe-130
content in Bruderheim meteorite, 20: 11430

XENON ISOTOPES Xe-131
content in Bruderheim meteorite, 20: 11430
determination in uranium-233 and -235 fission products, (E), 20: 11960(R) (IDO-14667)
XENON ISOTOPES Xe-132
content in Bruderheim meteorite, 20: 11430
determination in uranium-233 and -235 fission products, (E), 20: 11960(R) (IDO-14667)
XENON ISOTOPES Xe-133
diffusion from urania at 800 to 1600°C, coefficients for, 20: 11224
XENON ISOTOPES Xe-134
content in Bruderheim meteorite, 20: 11430
determination in uranium-233 and -235 fission products, (E), 20: 11960(R) (IDO-14667)
XENON ISOTOPES Xe-135
diffusion from urania at 800 to 1600°C, coefficients for, 20: 11224
production in thermal-neutron fission, cumulative and direct yields in, (E), 20: 11990
reactor criticality effects of, tables for calculating transients from, 20: 12352 (DP-958)
XENON ISOTOPES Xe-136
content in Bruderheim meteorite, 20: 11430
XENON SYSTEMS
Na–Xe, excitation transfer in first excited states of sodium, cross sections for collision-induced, (E), 20: 11499

Y

YANKEE POWER REACTOR
coolant sampling in, analysis of, 20: 12418(R) (WCAP-3739)
criticality studies, 20: 12418(R) (WCAP-3739)
YEASTS
protective effects of polysaccharide prepared from, against radiation injuries of mice, x, 20: 10703
radioinduced antibody production in, uv, 20: 10695
radiosensitivity of, effects of amino acids in culture on, 20: 10695
YTTERBIUM
heat of solution in liquid tin at 770°K, 20: 11304
performance of cathodes of, in diode ion pumps, 20: 10976 (IS-T-46)
separation from lutetium by ion exchange at 90°C, 20: 10760 (IS-1305)
separation from other elements by solvent extraction using TBP, 20: 10952
thermal conductivity at 2 to 100°K, (E), 20: 11329
YTTERBIUM CARBONATES
complexes of, composition in solution of, 20: 10824
YTTERBIUM CHLORIDES
crystal field of hydrated, 20: 10860
YTTERBIUM IONS
spectra of trivalent, in hydrated chloride lattices, 20: 10860
YTTERBIUM ISOTOPES Yb-170
energy levels on, lifetime of 84.2 kev, (E), 20: 12082
YTTERBIUM ISOTOPES Yb-172
energy levels in, gyromagnetic ratio of first-excited rotational, (E), 20: 12064
YTTERBIUM ISOTOPES Yb-174
energy levels in, gyromagnetic ratio of first-excited rotational, (E), 20: 12064
energy levels in, lifetime of 76.5 kev, (E), 20: 12082
YTTERBIUM ISOTOPES Yb-176
energy levels in, gyromagnetic ratio of first-excited rotational, (E), 20: 12064
YTTERBIUM OXIDES
CaO–Yb_2O_3, phase diagrams, 20: 10822
YTTERBIUM SELENIDES
CaSe–Yb_2Se_3, phase studies, 20: 10857
YTTRIUM
determination in copper–yttrium and chromium–nickel alloys using Arsenazo-III, spectrophotometric, 20: 10773
determination of radioactive, by electrophoresis, use of EDTA in, 20: 10792
determination of, complexometric, 20: 10779
effects on hydrogen distribution in Zircaloy, 20: 11221
effects on oxidation of zirconia, 20: 11227
electron structure of, analysis using positron annihilation, (E), 20: 11323
performance of cathodes of, in diode ion pumps, 20: 10976 (IS-T-46)
separation from other elements by solvent extraction using TBP, 20: 10952
separation from salts by solvent extraction using 8-mercaptoquinoline in chloroform, 20: 10759 (INP-427/C)
separation from uranium by reversed-phase partition chromatography, 20: 10784
YTTRIUM ALLOYS
Al–Er–Y, crystal structure of intermetallic compound $(Y_xEr_{1-x})Al_3$ in, 20: 11305
Al–Y, crystal structure of intermetallic compound YAl_3 in, 20: 11305
Co–Y, crystal structure of intermetallic compound YCo_3 in, 20: 11308
Cu–Y, analysis for yttrium using Arsenazo-III, spectrophotometric, 20: 10773
Fe–Y, crystal structure of intermetallic compound YFe_3 in, 20: 11308
Gd–Y, magnetic properties of, effects of composition and temperature on, 20: 11341
Hf–Nb–W–Y, development and evaluation of C-129Y, 20: 11227
Hg–Y–Zn, phase studies, 20: 11317
Ni–Y, crystal structure of intermetallic compound YNi_3 in, 20: 11308
V–Y, corrosion by acids and bases of vanadium-base, 20: 11230 (BM-RI-6715)
YTTRIUM CARBONATES
complexes of, composition in solution of, 20: 10824
YTTRIUM CHLORIDES
rare-earth-ion fluorescent lifetimes in crystals of, 20: 12317
separation from salts by extraction chromatography using organic phosphorus compounds, 20: 10759 (INP-427/C)
YTTRIUM ETHYL SULFATES
rare-earth ion spin-lattice relaxation in, (E), 20: 12300
YTTRIUM ISOTOPES Y-90
distribution in tissues of molting crayfish, 20: 10515(R) (BNWL-122, pp 46-8)
effects on pituitary gland, effects on mammary carcinoma of, 20: 10752
preparation of carrier-free, method for, 20: 10759 (INP-427/C)
use in hemangioma therapy, 20: 10745
YTTRIUM ISOTOPES Y-91
content in fallout, 1964, 20: 11018
elimination from mice using TTHA chelates, 20: 10556
YTTRIUM OXIDES
rare-earth-ion fluorescent lifetimes in crystals of, 20: 12317
YTTRIUM SELENIDES
CaSe–Y_2Se_3, phase studies, 20: 10857
YTTRIUM TUNGSTATES
rare-earth-ion fluorescent lifetimes in crystals of, 20: 12317

Z

ZINC
effects on stability of delta-phase plutonium–gallium alloys, 20: 11224
radioinduced ionization of, cross sections for electron, 20: 10885
separation from salts by extraction chromatography using organic phosphorus compounds, 20: 10759 (INP-427/C)
separation from salts by solvent extraction using Schiff bases in chloroform, 20: 10759 (INP-427/C)
ZINC ALLOYS
Ga–Pu–Zn, tensile properties and thermal expansion of delta-stabilized plutonium-base, 20: 11224
Hf–Zn, crystal structure of intermetallic compounds in, 20: 11328
Hg–Y–Zn, phase studies, 20: 11317
Mg–Zn, phase studies by neutron diffraction, 20: 12545(R) (PAEC(A)AR651)
Nb–Zn, crystal structure of intermetallic compounds in, 20: 11328
Ta–Zn, crystal structure of intermetallic compounds in, 20: 11328
Ti–Zn, crystal structure of intermetallic compounds in, 20: 11328
Zn–Zr, crystal structure of intermetallic compounds in, 20: 11328
ZINC CHLORIDES
separation from salt mixtures by extraction chromatography using organic phosphorus compounds, 20: 10759 (INP-427/C)
separation from salts by extraction chromatographic using organic phosphorus compounds, 20: 10759 (INP-427/C)
ZINC ISOTOPES Zn-65
content in ocean fish, effects of content in sea water on, 20: 11054
content in salmon, reared in Hanford reactor effluent, 20: 10538(R) (BNWL-122, pp 198-201)
effects of chronic ingestion of, in trout, 20: 10528(R) (BNWL-122, pp 101-6)
secretion of, in milk of sheep, 20: 10527(R) (BNWL-122, pp 94-8)
uptake and accumulation by plankton, seasonal variations, 20: 10536(R) (BNWL-122, pp 187-9)
ZINC ISOTOPES Zn-68
neutron activation cross section at 24 kev, (E), 20: 12135
proton reactions (p,n) and (p,p) with, isobaric analog states of gallium-69 from, (E), 20: 12079
ZINC OXIDES
radiation effects on crystal structure of, neutron, 20: 11359
ZIRCALOY-2
brittleness of, effects of hydrogen on, 20: 11227
creep and stress-rupture properties at 300°C, 20: 11227
crystallographic orientations in tubing of, effects of fabrication method on preferred, 20: 11251

dissolution by Citriflex process, chemistry of, 20: 11272 (NP-15661)
dissolution of cladding of, on aluminum–plutonium fuel elements, flowsheet for, 20: 10948 (HW-76472)
distribution of alloying elements in, effects of thermal treatment on, 20: 11287 (WAPD-T-1809)
hydridation, 20: 11225
hydridation of, in water, 20: 11221
mechanical properties of, effects of hydrogen on, 20: 11221
mechanical testing of, effects of embrittling factors in, 20: 11227
performance as SRE moderator and reflector cladding, 20: 12404 (NAA-SR-11160)
radiation effects on corrosion and mechanical properties of, neutron, 20: 11354
sorptive properties for hydrogen during aqueous corrosion, effects of environment on, 20: 11227
sorptive properties for hydrogen from hydrochloric acid, 20: 11227
thermal stress fatigue, 20: 11227
welding of fuel element spacer to, projection, 20: 12377(R) (CEND-2863-236)

ZIRCALOY-4
fatigue strength of, effects of superimposed strain on bending, 20: 11227
hydridation of, in water, 20: 11221
strain fatigue limit of fuel cladding of, biaxial, 20: 12418(R) (WCAP-3739)

ZIRCONIUM
compatibility with urania, 20: 11224
compatibility with uranium at 500 to 900°C, 20: 11316
corrosion by steam at 500°C, effects of surface contamination on, 20: 11227
deposition from fused salt mixtures, electro-, 20: 11260
diffusion in uranium, 20: 11316
diffusion of boron and carbon in surface of, 20: 11228
diffusion of helium in irradiated, 20: 11227
diffusion of oxygen in, coefficient and mechanism of, 20: 11268 (EIR-82)
diffusion of uranium in, temperature dependence of, 20: 11290
dissolution by Citriflex process, chemistry of, 20: 11272 (NP-15661)
effects of alloy additions of, on mechanical properties of niobium, 20: 11302
effects of alloying additions of, on oxidation rates of niobium, tantalum, and tungsten, 20: 11227
effects on creep of magnesium, 20: 11313
mechanical properties of, combined effects of hydrogen and oxygen on, 20: 11227
neutron four-group cross sections, 20: 12485
oxidation by oxygen at 400 to 600°C, kinetics and mechanisms of, 20: 11227
performance as fuel element cladding in large PWR, 20: 12418(R) (WCAP-3739)
separation from uranium by reversed-phase partition chromatography, 20: 10784
solvent properties for oxygen, 20: 11268 (EIR-82)
sorptive properties for hydrogen from hydrochloric acid, 20: 11227
thermodynamic properties, 20: 10816(T) (NASA-TT-F-285)

ZIRCONIUM ALLOY COUPLES
Fe/Nb–Zr/stainless steel, diffusion in bimetallic tubing of, with iron diffusion barrier, inter-, 20: 11215(R) (NASA-CR-54718)
Fe/Nb–Zr/stainless steel/V, diffusion in bimetallic tubing of, with iron and vanadium diffusion barriers, inter-, 20: 11215(R) (NASA-CR-54718)
Mo/Ni/Nb–Zr/stainless steel, diffusion in bimetallic tubing of, with molybdenum and nickel diffusion barriers, inter-, 20: 11215(R) (NASA-CR-54718)
Nb–Zr/stainless steel, diffusion in bimetallic tubing of, inter-, 20: 11215(R) (NASA-CR-54718)

ZIRCONIUM ALLOYS
mechanical properties of, effects of hydrogen on, 20: 11221
Al–Mg–Zr, creep rates, 20: 11313
Al–Sn–Ti–Zr, creep properties of, effects of composition on, 20: 11335
Al–Ti–Zr, phase studies and properties of, 20: 11332
Al–Ti–Zr, phase studies and properties of, 20: 11333
Al–Ti–Zr, phase studies and properties of, 20: 11334
Cd–Zr, crystal structure of intermetallic compounds in, 20: 11328
Mo–Ti–Zr, erosion by mercury vapor at 640°F of TZM, 20: 11214(R) (NASA-CR-54717)
Nb–Sn–Zr, radiation effects on corrosion and mechanical properties of, neutron, 20: 11354
Nb–Sn–Zr, stability of martensite structure in zirconium-base, 20: 11227
Nb–Ta–W–Zr, bonding to Hastelloy N, Inconel 600, and types 321 and 347 stainless steels of FS-85, explosive, 20: 11243(R) (WANL-PR(EE)-001)
Nb–W–Zr, erosion by mercury vapor of Cb-752, 20: 11214(R) (NASA-CR-54717)
Nb–Zr, bonding to types 321 and 347 stainless steels, explosive, 20: 11243(R) (WANL-PR(EE)-001)
Nb–Zr, brittleness of, effects of hydrogen on, 20: 11227
Nb–Zr, mechanical properties of, effects of composition on, 20: 11288(T) (AD-622477)
Nb–Zr, oxidation by oxygen at 400 to 600°C, kinetics and mechanisms of, 20: 11227
Nb–Zr, properties of bimetal tubes of type 316 stainless steel and, 20: 11214(R) (NASA-CR-54717)
Nb–Zr, superconducting point contacts of, macroscopic quantum interference effects in, (E/T), 20: 11911
Nb–Zr, training effect in coil of superconducting, (E), 20: 11895
Pt–Zr, corrosion by hydrochloric acid, effects of platinum content on, 20: 11227
Ta–W–Zr, fabrication of tantalum-base, process development for, 20: 11260
U–Zr, decontamination of fluoride-volatility plant after processing irradiated, 20: 11032 (ORNL-3891)
U–Zr, dissolution by ammonium fluoride, 20: 10964
Zn–Zr, crystal structure of intermetallic compounds in, 20: 11328

ZIRCONIUM BROMIDES
thermodynamic properties, 20: 10816(T) (NASA-TT-F-285)

ZIRCONIUM CARBIDES
performance in high-temperature reactor fuels, 20: 12378
thermodynamic properties, 20: 10816(T) (NASA-TT-F-285)
HfC–ZrC, preparation and properties, 20: 11330
NbC–ZrC, preparation and properties, 20: 11330

ZIRCONIUM CHLORIDES
thermodynamic properties, 20: 10816(T) (NASA-TT-F-285)

ZIRCONIUM FLUORIDES
thermodynamic properties, 20: 10816(T) (NASA-TT-F-285)

ZIRCONIUM HYDRIDES
neutron diffusion in, decay-time constants and spectra for, (E), 20: 11943

ZIRCONIUM IODIDES
thermodynamic properties, 20: 10816(T) (NASA-TT-F-285)

ZIRCONIUM ISOTOPES Zr-95
content in fallout, 1964, 20: 11018
determination in irradiated MITR fuel elements by gamma spectroscopy, 20: 10764 (MITNE-64)
effects on plutonium determination in fission product solutions, 20: 10763 (KR-100)
energy level transitions in, branching ratio for, (E), 20: 11134

ZIRCONIUM NITRIDES
thermodynamic properties, 20: 10816(T) (NASA-TT-F-285)

ZIRCONIUM OXIDES
oxidation at 450 to 900°C, effects of yttrium additions on, 20: 11227
preparation and stability of black nonstoichiometric, 20: 11248
radioinduced swelling of, fission fragment, 20: 11227
tensile strength for machining, effects of PVA binders on, 20: 11277 (RFP-659)
thermodynamic properties, 20: 10816(T) (NASA-TT-F-285)

ZIRCONIUM OXYNITRIDES
preparation, properties, and structure, 20: 10856

ZIRCONIUM PHOSPHATES
ion exchange properties of, effects of heat treatments on, 20: 10957

ZIRCONIUM SILICIDES
crystal structure of Zr_5Si_3, 20: 11337

ZIRCONIUM SULFIDES
thermodynamic properties, 20: 10816(T) (NASA-TT-F-285)

ZIRCONIUM SYSTEMS
C–Mo–Ti–Zr, stress-rupture properties of TZC, at high temperatures and strain rates, 20: 11265 (AD-626375)
Cr–O–Zr, phase studies, 20: 11227
H–Nb–Zr, phase studies, 20: 11225

ZIRCONS
tensile strength for machining, effects of PVA binders on, 20: 11277 (RFP-659)

REPORT NUMBER INDEX

Reports, conference papers and proceedings, numbered translations, and patents abstracted during the period are included in this index. Each item is listed by report number; this is followed by the abstract number and a brief notation regarding public availability. The index entries show which reports are on file in the depository libraries, which reports have been published in open-literature journals (journal citation given), and which reports can be purchased (source and price). Whenever a report is identified by more than one number, cross references from secondary to primary report numbers are cited.

The report number codes apply to AEC reports unless designated otherwise. Non-AEC reports are identified by parenthetical notes after the report codes; e.g., (non-AEC), (British), (Canadian), (French). The note (Misc.) identifies those codes used for both USAEC and non-AEC reports. Patents are listed under the heading "PATENTS"; the country of origin is included in parentheses.

A comprehensive listing of both AEC and non-AEC report codes is contained in TID-85(5th Rev.), *Report Number Series Used by the Division of Technical Information in Cataloging Reports*. This information is also included in the Cumulative Report Number Index (issued annually).

Public Availability of USAEC Reports

All USAEC reports abstracted in *NSA* are available to the public through one or more of the following sources:

(1) Depository libraries in the United States, in other countries, and in international agencies. A list of these depositories appears on the inside covers of each issue of *NSA*.

(2) Scientific and technical journals or other publications.

(3) Microcard Editions, Inc., in Microcard and micronegative form. Orders and inquiries should be sent to: Accounting and Shipping Department, West Salem, Wisconsin 54669.

(4) Clearinghouse for Federal Scientific and Technical Information, U. S. Department of Commerce, Springfield, Virginia 22151.

(5) Superintendent of Documents, U. S. Government Printing Office, Washington, D. C. 20402.

Public Availability of Non-AEC Reports

U. S. Reports. Many reports of U. S. Government agencies are available to the public from the Clearinghouse for Federal Scientific and Technical Information (CFSTI). This availability is given when known. Such reports should be ordered by AD number or NASA-N number. If availability is not shown, inquiries may be directed to CFSTI. In the case of NP numbers, inquiries should be by title and author.

Non-U. S. Reports. Many reports of atomic energy establishments of other countries are deposited in the libraries listed on the inside covers of each issue of *NSA*.

Additionally, the following have made their reports available as indicated.

AUSTRALIA

Australian Atomic Energy Commission Research Establishment. Available upon request from the Library, Australian Atomic Research Establishment, Private Mail Bag, Sutherland, New South Wales, Australia.

BELGIUM

Centre d'Étude de l'Énergie Nucléaire. Available upon request to individuals and organizations, from the Centre d'Étude de l'Énergie Nucléaire (CEN), 31, Rue Belliard, Bruxelles, Belgium.

CANADA

Atomic Energy of Canada Limited. For sale by the Technical Information Officer, Atomic Energy of Canada Limited, Chalk River, Ontario, Canada. Copies are also deposited in libraries in the United Kingdom.

National Research Council of Canada. Available from the National Research Council of Canada, Ottawa 2, Ontario, Canada.

DENMARK

Atomic Energy Commission Research Establishment, Risø. Available on exchange from the Library, Danish Atomic Energy Commission, Risø, Roskilde, Denmark. Also for sale by Jul. Gjellerup, Booksellers, 87 Sölvgade, København K., Denmark.

Danatom. Available on loan from Research Establishment, Risø, Roskilde, Denmark. Copies are available from Danatom, Aurehøjvej 2, Hellerup, Denmark.

EURATOM

Reports from the Commission of the European Atomic Energy Community are available from: Presses academiques europeennes, 98, chaussee de Charleroi, Brussels 6, Belgium; and Office central de vente des publications des Communautes eurodeennes 2, place de Metz, Luxemburg.

FRANCE

Commissariat à l'Énergie Atomique. Inquiries for reports numbered 1-2199 should be addressed to Commissariat à l'Énergie Atomique, Service Central de Documentation, Centre d'Études Nucléaires de Saclay, Boite Postale No. 2, Gif-sur-Yvette (S. et O.), France. Reports numbered 2200 and above are available from La Documentation Francaise, 16 Rue Lord-Byron, Paris VIII, France.

Service Central de Protection contre les Rayonnements Ionisants. Copies are available from Ministère de la Santé Publique, Service Central de Protection contre les Rayonnements Ionisants, B. P. n° 35—LE VESINET (S. et O.), France.

GERMANY

Deutsches Elektronen-Synchrotron DESY. Copies are available from Deutsches Elektronen-Synchrotron Desy, Dokumentation, 2000 Hamburg-Gr. Flottbek 1, Notkestieg 1, Germany.

Gesellschaft für Kernforschung mbH (KFK). Copies are available from Gesellschaft für Kernforschung mbH, 75 Karlsruhe, Postfach 947, Germany. Copies are also deposited in many national nuclear centers in the world.

Kernforschungsanlage. Copies may be ordered from Zentralbibliothek der Kernforschungsanlage Jülich, Jülich, Bundesrepublik Deutschland.

Hahn-Meitner-Institute für Kernforschung. Available without charge from Hahn-Meitner-Institute für Kernforschung Berlin, Bibliothek, Glienicker Strasse 100, 1 Berlin

39, Germany. Copies are deposited in many national nuclear centers in the world.

Johann-Wolfgang-Goethe Universität, Frankfurt Am Main, Institut für Kernphysik, (IKF). Copies are available from Gmelin Institut, 40-42 Varrentrappstrasse, Frankfurt (Main), West Germany.

ISRAEL

Israel Atomic Energy Commission. Available without charge from Ministry of Defence/Atomic Energy Commission, Soreq Research Establishment, Yavne, Israel. Copies are deposited in libraries in Israel and in other countries.

ITALY

Centro Informazioni Studi Esperienze (CISE). For sale at CISE Press Office, Casella Postale 3986, Milano, Italy. Copies are deposited in libraries in Italy.

Comitato Nazionale per l'Energia Nucleare. Copies are available from Comitato Nazionale per l'Energia Nucleare, Divisione Affari Internazionali e Studi Economici, Ufficio Pubblicazioni, Via Belisario, 15, Roma, Italy.

JAPAN

Japan Atomic Energy Research Institute (JAERI). Available from the Staff Supply Cooperative of Japan Atomic Energy Research Institute (JAERI), 1-1 Tamura-Cho, Shiba, Minato-Ku, Tokyo, Japan. Copies are deposited in depositories in Tokyo, Nagoya, and Osaka.

Nagoya University. Copies are available from Research Information Center, Institute of Plasma Physics, Nagoya University, Nagoya, Japan.

University of Tokyo. Available free of charge from Institute for Nuclear Study, University of Tokyo, Tanashi-Machi, Kitatama-gun, Tokyo, Japan.

NETHERLANDS

Reactor Centrum Nederland. For sale by Reactor Centrum Nederland, 112 Scheveningseweg, 's-Gravenhage, The Netherlands. Copies are deposited in university libraries in Holland and in many national nuclear centers in the world.

NEW ZEALAND

Institute of Nuclear Sciences. Copies are available from Librarian, Institute of Nuclear Sciences, D.S.I.R., Private Bag, Lower Hutt, New Zealand. Copies are deposited in other countries.

NORWAY

Forsvarets Forskningsinstitutt. Copies available from Norwegian Defence Research Establishment, Library, P. O. Box 25, Kjeller, Norway.

Institutt for Atomenergi. "KR" reports are available on an exchange basis from the Library, Institutt for Atomenergi, Box 40, Kjeller, Norway. Other series are not generally available to the public.

Norwegian Reactor School. Copies are available from The Library, Institutt for Atomenergi, P. O. Box 40, Kjeller, Norway.

PAKISTAN

Atomic Energy Center. Copies are available from Atomic Energy Center, P. O. Box 658, Lahore, (West Pakistan).

POLAND

Reports of the Polish nuclear institutes are published by the Nuclear Energy Information Center of the Government Commissioner for Use of Nuclear Energy. Copies are available from Ośrodek Informacji o Energii Jądrowej, Warszawa, PKiN, Poland.

SPAIN

Junta de Energia Nuclear. "JEN" reports are available without charge from Servicio de Documentation, Junta de Energia Nuclear, Ciudad Universitaria, Madrid (3), Spain.

SWEDEN

Aktiebolaget Atomenergi. "AE" reports are for sale from Aktiebolaget Atomenergi, Library Section, Box 43041, Stockholm 43, Sweden. Bibliographies and literature surveys of the VDDIT- series may be obtained from Aktiebolaget Atomenergi, Information Office, Scientific and Technical Information, Box 43041, Stockholm 43, Sweden. Other series are not generally available to the public. Organizations in the atomic energy field may obtain copies from Aktiebolaget Atomenergi. Microcopy of AE reports is available from the International Documentation Centre, Tumba, Sweden.

SWITZERLAND

CERN European Organization for Nuclear Research. Available without charge from CERN European Organization for Nuclear Research, Geneva 23, Switzerland. Copies are deposited in libraries in 13 countries.

Eidgenössisches Institut für Reaktorforschung. "EIR" reports are available from Eidgenössiches Institut für Reaktorforschung, c/o Bibliothek, Würenlingen/Ag, Switzerland.

TURKEY

Turkish Atomic Energy Commission. Copies are available free of charge from T.A.E.C., Çekmece Nuclear Research Center, P. O. Box 1, Airport, Istanbul, Turkey.

UNITED KINGDOM

United Kingdom Atomic Energy Authority. Some reports are for sale in the United States by the British Information Service (BIS), 845 Third Avenue, New York, N. Y. 10022. United Kingdom reports generally may be purchased from Her Majesty's Stationery Office, London. Copies not for sale by Her Majesty's Stationery Office may be purchased in microcopy form from Micro Methods Limited, East Ardsley, Wakefield, Yorks, England. Report copies are deposited in a large number of libraries in England.

Conferences

Published conference proceedings as well as individual unpublished papers from conferences are included in this index. A CONF number is assigned to the conference if published proceedings are received and also if only a single paper is received. The base number used is year-month-sequence. Thus, the number CONF-650101 would indicate that the conference was held in 1965, in January, and that this was the first January 1965 conference so received. This number would be assigned to complete published proceedings, or if individual papers are received, the base number would be extended to include a paper number, i.e., CONF-650101-1. As additional papers are received, they will be assigned consecutive numbers in the series, CONF-650101-1, 2, 3, 4, etc. This numbering system ensures that all papers received from a conference will be associated with that conference in this index.

If published proceedings are received after the receipt of individual papers, the complete proceedings will be abstracted and the abstract number will appear in this index with the base CONF number.

Abbreviations Used in Availability Column

AECL	For sale by Atomic Energy of Canada Ltd., Chalk River, Ontario, Canada.
BIS	For sale by British Information Service, 845 Third Avenue, New York, N. Y. 10022
CFSTI	For sale by the Clearinghouse for Federal Scientific and Technical Information, U. S. Department of Commerce, Spring-

field, Virginia 22151. The symbol "cy" indicates that the format of the item sold may be either a printed document or a photographic reproduction (two-thirds of original size) depending upon the availability of printed stock. The indicated price is for either format. The symbol "mn" is used to indicate that copy is also available in the form of micronegatives (microfiche).

Dep. — AEC reports: Full-size copy is on deposit in the depository libraries both inside and outside the United States. These reports are also for sale by Microcard Editions, Inc., Accounting and Shipping Department, West Salem, Wisconsin 54669.

Non-AEC reports: Full-size copy on deposit in the depository libraries in the United States only.

Dep.(mc) — Same as for Dep., except copy is in Microcard form.

Dep.(mn) — Same as for Dep., except copy is in micronegative (microfiche) form.

DSIR — For sale by the National Lending Library for Science and Technology (D.S.I.R.), Boston Spa, Yorkshire, England.

DTI Extension — Available from the U. S. Atomic Energy Commission, Division of Technical Information Extension, P. O. Box 62, Oak Ridge, Tennessee 37830.

EM — Blueprints and microcopy of AEC engineering drawings are available from Clearinghouse for Federal Scientific and Technical Information, U. S. Department of Commerce, Springfield, Virginia 22151. Current prices of the CAPE- packages may be obtained from this address. TID-4100, available from the Division of Technical Information Extension, P. O. Box 62, Oak Ridge, Tennessee 37831, contains information on all the CAPE- packages for sale.

Gmelin — Available at a nominal charge and under the AED- number shown from Atomic Energy Documentation Center, Gmelin Institute, 40-42 Varrentrappstrasse Frankfurt (Main), West Germany.

GPO — For sale by the Superintendent of Documents, Government Printing Office, Washington, D. C. 20402.

HMSO — Her Majesty's Stationery Office, London.

IAEA — Available from the International Atomic Energy Agency, Vienna, Austria, and from its sales agencies in various countries throughout the world. A list of these agencies is found in each STI/DOC and STI/PUB publication.

JCL — For sale by the Special Libraries Association Translation Center, John Crerar Library, 35 West 33rd Street, Chicago, Illinois 60616.

LC — For sale by the Library of Congress, Photoduplication Service, Washington, D. C. 20540.

NAS — National Academy of Sciences, National Research Council, Washington, D. C. 20418.

NRC — For sale by the National Research Council of Canada, Ottawa, Ontario, Canada.

ORINS — Available on interlibrary loan from the Library, Oak Ridge Associated Universities, Post Office Box 117, Oak Ridge, Tennessee 37830.

OTS — See CFSTI.

UKAEA, London — Available from United Kingdom Atomic Energy Authority, 11 Charles II Street, London, S. W. 1.

UN — United Nations Bookshop, United Nations Headquarters, New York, New York.

USGS — Available free of charge from the U. S. Geological Survey, Washington, D. C. 20242.

[The symbols "ph," "mf," and "fs" are used to designate that copy is available only in photostat, microfilm, or facsimile form. The symbol "mn" is used to designate that copy is available in micronegative (microfiche) form. The symbol "cy" is used to designate full size or photographically enlarged copy (two-thirds of original size).]

Report No.	Abstract No.	Availability
NUMERICAL	**(Misc.)**	
65RL-3814E(Rev.)	20-11538	
65RL-3888E	20-11539	
65RL-3940E	20-12161	
65RL-3998E	20-12162	
AAEC-TM–	**(Australian)**	
299	20-11086	Dep. mn
ABCC–		
60-61	20-10595	Dep. mn. CFSTI $3.00 cy, $0.75 mn
ACF–		
14	20-11264	Dep. mn. CFSTI $2.00 cy, $0.50 mn
412-262	20-11264	See ACF-14
AD–	**(Misc.)**	
620995	20-10767	CFSTI $1.00 cy, $0.50 mn. JCL $1.10 fs, $0.80 mf
622352	20-12476	CFSTI
622477	20-11288	CFSTI $1.00 cy, $0.50 mn
623963	20-11172	CFSTI $1.00 cy, $0.50 mn
624318	20-11948	
625424	20-12163	CFSTI $3.00 cy, $0.75 mn
625735	20-10799	CFSTI $2.00 cy, $0.50 mn
625747	20-11949	CFSTI $1.00 cy, $0.50 mn
626375	20-11265	CFSTI $2.00 cy, $0.50 mn
626444	20-11540	CFSTI $4.00 cy, $0.75 mn
626633	20-11378	CFSTI $1.00 cy, $0.50 mn
AE–	**(Non-AEC)**	
202	20-11950	Dep. mn
203	20-11087	Dep. mn
205	20-11951	Dep. mn
208	20-11927	Dep. mn
AEC-tr–	**(For complete listing see TID-4025)**	
6469	20-10980	CFSTI $4.00 cy, $0.75 mn
6665	20-10974	Dep. mn; JCL $12.50 fs, $5.60 mf
AECL–	**(Canadian)**	
2374	20-11990	Can. J. Phys., 44: 237-46(1966)
2504	20-11095	See CRGP-1224
2514	20-12493	Dep. AECL $1.00
AED-C–	**(Non-AEC)**	
21-03	20-11027	Dep. mn
28-01	20-11088	Dep. mn
AEEW-R–	**(British)**	
403	20-11131	J. Nucl. Energy: Pt. A and B, 19: 959-69(1965)
AERE-M–	**(British)**	
1664	20-11028	Dep. BIS $1.40. HMSO 7s.
1671	20-11089	Dep. BIS $0.80. HMSO 4s.
AERE-R–	**(British)**	
4786	20-10947	Dep. BIS $0.60. HMSO 3s.
4842	20-11940	J. Nucl. Energy: Pt. A and B, 19: 949-57(1965)
4845	20-10787	J. Nucl. Mater., 17: 227-36(1965)
4877	20-11252	J. Nucl. Mater., 17: 203-14(1965)
4965	20-11220	J. Nucl. Mater., 17: 237-44(1965)
5080	20-11022	Dep. BIS $0.80. HMSO 4s.
5107	20-11541	Dep. BIS $2.00. HMSO 10s.
AERE-Trans–	**(British)**	
1038	20-10997	Dep. BIS $2.00. HMSO 10s.
1041	20-11456	Dep. BIS $0.60. HMSO 3s.
1043	20-12503	Dep. BIS $0.30. HMSO 1s. 9d.
AFCRL–	**(Non-AEC)**	
65-787	20-10764	See MITNE-64
AFRRI-TN–	**(Non-AEC)**	
65-2	20-12261	
AGN–	**(Misc.)**	
8138	20-11187	Dep. mn. CFSTI $2.00 cy, $0.50 mn
AGN-TM–		
411	20-12384	Dep. mn. CFSTI $4.00 cy, $0.75 mn
AGN-TP–		
149	20-12385	Dep. mn. CFSTI $1.00 cy, $0.50 mn
AN-AGCR–		
223	20-10988	See CONF-12-5
919	20-10993	See TID-22513
ANL–		
7033	20-12351	Dep. mn. CFSTI $3.00 cy, $0.75 mn
7113	20-10800	Dep. mn. CFSTI $1.00 cy, $0.50 mn
7118	20-11379	Dep. mn. CFSTI $4.00 cy, $0.75 mn
ANL-Trans–		
258	20-11570	Dep. mn; JCL $9.60 fs, $3.65 mf
259	20-11353	Dep. mn; JCL $1.60 fs, $0.80 mf
ANS–	**(Non-AEC)**	
100(Suppl.)	20-12328	
APDA–	**(Misc.)**	
176	20-12386	Dep. mn. CFSTI $5.00 cy, $1.00 mn
APDA-NTS–	**(Non-AEC)**	
3	20-12387	Dep. mn
6	20-12388	Dep. mn
ARL–	**(Non-AEC)**	
65-129	20-12164	CFSTI $4.00 cy, $0.75 mn
65-135	20-12165	CFSTI $4.00 cy, $0.50 mn
ATR-IC–		
101	20-12502	See TID-22547
AWRE-O–	**(British)**	
82/65	20-11766	Dep. BIS $0.80. HMSO 4s. 0d.
BAW–	**(Misc.)**	
1280-28(Vol.1)	20-12389	Dep. mn. CFSTI $3.00 cy, $0.75 mn
1280-28(Vol.2)	20-12390	Dep. mn. CFSTI $5.00 cy, $1.00 mn
1280-28(Vol.3)	20-12391	Dep. mn. CFSTI $4.00 cy, $1.00 mn
1280-28(Vol.4)	20-12392	Dep. mn. CFSTI $3.00 cy, $0.50 mn
BLG–	**(Belgian)**	
330	20-11188	Dep. mn
332	20-11190	Dep. mn
345	20-11059	Dep. mn
353	20-10757	Dep. mn
BM-RI–	**(Misc.)**	
6715	20-11230	Bureau of Mines Free
BMI–	**(Misc.)**	
1753	20-10870	Dep. mn. CFSTI $2.00 cy, $0.50 mn
BMI-X–		
10143	20-11212	Dep. mn; CFSTI $1.00 cy, $0.50 mn
BN–	**(Misc.)**	
428	20-11206	See TID-22529
430	20-11449	See TID-22530
6505-01	20-12396	See EURAEC-1505
BNL–		
8694	20-12528	Dep. mn. CFSTI $2.00 cy, $0.50 mn
8721	20-12262	Dep. mn. CFSTI $2.00 cy, $0.50 mn
8748	20-12393	Dep. mn. CFSTI $2.00 cy, $0.50 mn
8798	20-12529	Dep. mn. CFSTI $1.00 cy, $0.50 mn
8800	20-11439	Dep. mn. CFSTI $1.00 cy, $0.50 mn
8958	20-10541	Ann. N. Y. Acad. Sci., 131: 485-501(1965)
9132	20-11714	J. Math. Phys., 7: 123-32(1966)
9136	20-11941	J. Nucl. Energy: Pt. A and B, 19: 921-34(1965)
9356	20-10901	Nucl. Appl., 1: 556-9(1965)
9412	20-12072	Phys. Rev., 141: 1129-32(1966)
9429	20-12083	Phys. Rev., 141: 1206-14(1966)
9430	20-11500	Phys. Rev., 142: 33-45(1966)
9462	20-12045	Phys. Rev., 141: 858-62(1966)
9465	20-12054	Phys. Rev., 141: 966-74(1966)
9470	20-12067	Phys. Rev., 141: 1082-8(1966)
9749	20-11090	Dep. mn; CFSTI $2.00 cy, $0.50 mn

Report No.	Abstract No.	Availability
9772	20-11380	Dep. mn; CFSTI $1.00 cy, $0.50 mn
9790	20-11928	Dep. mn. CFSTI $1.00 cy, $0.50 mn
9833	20-11381	Dep. mn. CFSTI $3.00 cy, $0.50 mn
9835	20-10510	Dep. mn. CFSTI $1.00 cy, $0.50 mn
9836	20-10511	Dep. mn. CFSTI $1.00 cy, $0.50 mn
BNWL–		
37	20-11213	Dep. mn. CFSTI $6.00 cy, $1.25 mn
113-10	20-12530	Dep. mn. CFSTI $3.00 cy, $0.75 mn
113-11	20-12531	Dep. mn. CFSTI $2.00 cy, $0.50 mn
122	20-10503	Dep. mn. CFSTI $6.00 cy, $1.25 mn
160	20-12494	Dep. mn; CFSTI $1.00 cy, $0.50 mn
167	20-11266	Dep. mn. CFSTI $1.00 cy, $0.50 mn
170	20-12517	Dep. mn; CFSTI $2.00 cy, $0.50 mn
BNWL-SA–		
406	20-11009	ORAU
438	20-11001	Dep. mn. CFSTI $1.00 cy, $0.50 mn
472	20-12394	Dep. mn. CFSTI $1.00 cy, $0.50 mn
488	20-11267	Dep. mn. CFSTI $1.00 cy, $0.50 mn
CAPE–		
976	20-12444	
977	20-12445	
1003	20-12446	
1091	20-11078	
1216	20-11413	
1217	20-11414	
CEA-R–	**(French)**	
2770	20-10861	Dep. mn
2777	20-10801	Dep. mn
2815	20-11231	Dep. mn
2849	20-11929	Dep. mn
CEA-tr–	**(French)**	
A-1490	20-12520	Dep. mn; JCL $5.60 fs, $1.94 mf
A-1855	20-10936	Dep. mn; JCL $4.60 fs, $1.43 mf
CEAL-TM–		
151	20-11382	Dep. mn; CFSTI $2.00 cy, $0.50 mn
152	20-11383	Dep. mn; CFSTI $1.00 cy, $0.50 mn
156	20-11384	Dep. mn; CFSTI $1.00 cy, $0.50 mn
157	20-11385	Dep. mn; CFSTI $2.00 cy, $0.50 mn
CEND–	**(Misc.)**	
2863-236	20-12377	Dep. mn. CFSTI $2.00 cy, $0.50 mn
CERN–	**(European Organization for Nuclear Research)**	
65-35	20-11386	Dep. mn
CEX–		
65.03	20-11930	Dep. mn; CFSTI $1.00 cy, $0.50 mn
CLM-P–	**(British)**	
71	20-12222	Nucl. Fusion, 5: 330-48(1965)
72	20-12224	Nucl. Fusion, 5: 352-8(1965)
CLOR–	**(Polish)**	
39/D	20-11092	Dep. mn
CNAEM–	**(Turkish)**	
32	20-10602	Dep. mn
CONF-12–	**(American Nuclear Society 8th Annual Meeting, Boston, June 1962)**	
5	20-10988	Dep. mn. CFSTI $1.00 cy, $0.50 mn
CONF-83–	**(International URSI Conference, Tokyo, Sept. 1963)**	
3	20-12256	ORINS
CONF-412–	**(Thermal Conductivity Conference, Gatlinburg, Tenn., Oct. 1963)**	
2	20-11275	See ORNL-TM-1338
CONF-621–	**20-11110**	**(IAEA Panel on In-Pile Dosimetry, Vienna, July 1964) See STI/DOC/10/46**
CONF-654–	**19-2907 19-6030**	**(American Nuclear Society Meeting, San Francisco, Nov. 30–Dec. 3, 1964) Proceedings**
100	20-12368	See WAPD-T-1737
CONF-758–	**(American Physical Society Meeting, New York, Jan. 22–25, 1965)**	
54	20-11153	ORINS. Gmelin, AED-CONF-65-003-101
55	20-11926	ORINS. Gmelin, AED-CONF-65-003-99
CONF-640307–	**20-11841**	**(Symposium on High Latitude Particles and the Ionosphere, Alpbach, Tyrol, Austria, Mar. 19–26, 1964)**
CONF-640628–	**20-10509**	**(Conference on Isotopes in Experimental Pharmacology, Chicago, Aug. 7–9, 1964)**
CONF-640629–	**20-10539**	**(Symposium on Radioisotope Techniques in the Study of Protein Metabolism, Vienna, June 1–5, 1964) See STI/DOC/10/45**
CONF-640711–	**(27th Portugo-Spanish Conference on Progress in Sciences, Bilbao, Spain, July 20–24, 1964)**	
5	20-11271	See LFEN-24
CONF-640810–	**20-12458**	**(Conference on Nuclear Marine Propulsion, Blacksburg, Va., Aug. 10–13, 1964) Dep. mn; CFSTI $2.25 cy, $1.25 mn**
CONF-640922–	**20-10803**	**(Symposium Discussions on Molten Salts, Liège, Sept. 16–17, 1964) See EUR-2466.e**
CONF-650223–	**(Symposium on Nuclear Physics, Calcutta, Sept. 11–13, 1965)**	
Vol.1	20-12320	
Vol.2	20-12112	
CONF-650417–	**19-35725**	**(American Nuclear Society, National Topical Meeting on Fast Reactor Technology, Detroit, Apr. 26–28, 1965) See ANS-100**
Suppl.	20-12328	See ANS-100(Suppl.)
CONF-650447–	**20-10906**	**(Symposium on Pulse Radiolysis, Manchester, England, Apr. 21–23, 1965)**
CONF-650449–	**(6th Annual Structures and Metals Conference, Palm Springs, Calif., Apr. 5–7, 1965)**	
1	20-11238	Dep. mn. CFSTI $1.00 cy, $0.50 mn
CONF-650501–	**19-47907**	**(The Application of Computing Methods to Reactor Problems, Argonne, Ill., May 17–19, 1965) See ANL-7050**
20	20-11946	ORINS. Gmelin, AED-CONF-65-115-13
CONF-650568–	**(Panel on Kinetics and Applications of Pulsed Reactors Symposium, Vienna, May 17–21, 1965)**	
1	20-12495	See EUR-2538.e
CONF-650602–	**(American Nuclear Society 11th Annual Meeting, Gatlinburg, Tenn., June 20–24, 1965)**	
64	20-10982	ORAU, Gmelin, AED-CONF-65-125-36
CONF-650616–	**(Health Physics Society, Annual Meeting, Los Angeles, June 14–17, 1965)**	
10	20-11155	ORINS. Gmelin, AED-CONF-65-153-5
CONF-650638–	**(Physics of Quantum Electronics Conference, San Juan, Puerto Rico, June 28–30, 1965)**	
2	20-12255	ORINS. Gmelin, AED-CONF-65-156-8
CONF-650647–	**(Society of Nuclear Medicine, 12th Annual Meeting, Bal Harbour, Fla., June 19, 1965)**	
3	20-11079	ORINS. Gmelin, AED-CONF-65-197-2
CONF-650707–	**(IEEE Annual Conference on Nuclear and Space Radiation Effects, Ann Arbor, Mich., July 12–15, 1965)**	
12	20-11179	ORINS. Gmelin, AED-CONF-65-152-12
13	20-11840	ORINS. Gmelin, AED-CONF-65-152-7
14	20-11180	ORINS. Gmelin, AED-CONF-65-152-10
16	20-11182	ORINS

Report No.	Abstract No.	Availability
CONF-650710–	19-43507	(American Nuclear Society, Meeting on Reactor Operating Experience, Jackson Lake Lodge, Wyo., July 28–30, 1965)
9	20-11154	ORINS. Gmelin, AED-CONF-65-192-25
10	20-12450	ORINS. Gmelin, AED-CONF-65-192-26
11	20-12514	ORINS. Gmelin, AED-CONF-65-192-17
12	20-12449	ORINS. Gmelin, AED-CONF-65-192-7
13	20-12337	ORINS. Gmelin, AED-CONF-65-192-9
16	20-12448	ORINS. Gmelin, AED-CONF-65-192-8
CONF-650711–		(AIAA 2nd Annual Meeting and Technical Demonstration, San Francisco, July 26–29, 1965)
51	20-12492	ORINS
CONF-650719–		(4th Annual Reliability and Maintainability Conference, Los Angeles, July 28–30, 1965)
1	20-11181	ORINS. Gmelin, AED-CONF-65-190-2
CONF-650721–		(Positron Annihilation Conference, Detroit, July 27–29, 1965)
2	20-11678	ORINS. Gmelin, AED-CONF-65-211-9
CONF-650802–		(Cryogenic Engineering Conference, Houston, Tex., Aug. 23–25, 1965)
8	20-11925	ORINS. Gmelin, AED-CONF-65-193-6
CONF-650803–		(IAEA Symposium on Nuclear Materials Management, Vienna, Aug. 30–Sept. 3, 1965)
22	20-10970	ORINS
30	20-10797	ORINS
31	20-10967	ORINS
33	20-12561	ORINS
35	20-11004	ORINS
37	20-12451	ORINS
38	20-11262	ORINS
39	20-10969	ORINS
42	20-12562	ORINS
43	20-10968	ORINS
44	20-10795	ORINS
50	20-10796	ORINS
51	20-12452	ORINS
52	20-12560	ORINS
CONF-650806–		(7th International Conference on Phenomena in Ionized Gases, Belgrade, Aug. 22–27, 1965)
6	20-12180	See ORNL-P-1556
CONF-650829–		(American Society of Corrosion Engineers, Power Division Specialty Conference, Denver, Aug. 18–20, 1965)
1	20-12447	ORINS. Gmelin, AED-CONF-65-199-1
CONF-650836–		(7th International Conference on Phenomena in Ionized Gases, Beograd, Yugoslavia, Aug. 22–27, 1965)
1	20-12175	See NASA-CR-348
2	20-11768	See JUL-327-PP
CONF-650837–		(Boulder Conference on Particle Physics, Boulder, Colo., Aug. 9–20, 1965)
3	20-11551	Dep. mn. CFSTI $2.00 cy, $0.50 mn
CONF-650839–		(Conference on Nuclear Physics, Melbourne, Aug. 23–25, 1965)
1	20-11086	See AAEC/TM-299
CONF-650922–		(1st International Symposium on Magnet Technology, Stanford, Calif., Sept. 8–10, 1965)
28	20-11387	Dep. mn. CFSTI $2.00 cy, $0.50 mn
29	20-11388	Dep. mn. CFSTI $1.00 cy, $0.50 mn
CONF-650927–		(American Physical Society, Honolulu, Hawaii, Sept. 2–4, 1965)
21	20-11679	Dep. mn. CFSTI $2.00 cy, $0.50 mn
CONF-650950–		(International Statistical Inst., 35th Session, Belgrad, Sept. 14–22, 1965)
1	20-11204	See NYO-3136-2, App. 3
CONF-651015–		(American Physical Society, Chicago, Oct. 7, 1965)
3	20-11552	Dep. mn. CFSTI $1.00 cy, $0.50 mn
CONF-651023–		(Symposium on Radioisotope Instruments in Industry and Geophysics, Warsaw, Oct. 18–22, 1965)
17	20-11024	ORINS
CONF-651036–		(American Society of Civil Engineers, Environmental Engineering Conference and Annual Convention, Kansas City, Kans., Oct. 18–22, 1965)
2	20-12346	ORINS
CONF-651039–		(Conference on Programming for Flying Spot Devices, Columbia, N. Y., Oct. 26–29, 1965)
3	20-11090	See BNL-9749
CONF-651049–		(IEEE Thermionic Conversion Specialist Conference, San Diego, Calif., Oct. 25–27, 1965)
2	20-11544	See LA-DC-7390
3	20-11545	See LA-DC-7555
CONF-651055–		(Preparation and Standardization of Isotopic Targets and Foils Conference, Harwell, England, Oct. 20–21, 1965)
2	20-11183	See ORNL-P-1900
CONF-651058–		(Allerton Conference on Circuit and System Theory, Urbana, Ill., Oct. 20–22, 1965)
1	20-11066	See SLAC-PUB-146
CONF-651101–	20-3647 20-9102	(American Nuclear Society, Winter Meeting, Washington, D. C., Nov. 15–18, 1965) (Revised 11-8-65)
50	20-12385	See AGN-TP-149
53	20-11931	Dep. mn. CFSTI $2.00 cy, $0.50 mn
54	20-12470	See SC-R-65-1017
CONF-651109–		(1st Symposium on Accelerator Radiation Dosimetry and Experience, Upton, N. Y., Nov. 3–5, 1965)
20	20-11400	See UCRL-16323
CONF-651126–		(American Physical Society, 7th Annual Meeting of the Division of Plasma Physics, San Francisco, Nov. 8–11, 1965)
1	20-12166	Dep. mn; CFSTI $1.00 cy, $0.50 mn
CONF-651130–		(DECUS Symposium, Stanford, Calif., Nov. 29–30, 1965)
1	20-11401	See UCRL-16502
CONF-651207–		(American Water Resources Assn., 1st Annual Meeting, Chicago, Dec. 2, 1965)
1	20-11009	See BNWL-SA-406
CONF-651211–		(American Assn. for the Advancement of Science, Berkeley, Calif., Dec. 28, 1965)
1	20-10511	See BNL-9836
2	20-10510	See BNL-9835
CONF-660203–		(National Topical Meeting on Reactor Physics in the Resonance and Thermal Regions, San Diego, Calif., Feb. 7–9, 1966)
3	20-11928	See BNL-9790
CONF-660204–		(American Nuclear Society Meeting, San Diego, Calif., Feb. 7–9, 1966)
3	20-12275	See GA-6861
CONF-660207–		(Radioisotope Applications in Aerospace Symposium, Dayton, Ohio, Feb. 15–17, 1966)
2	20-10932	See ORNL-P-1928
CONF-660305–		(American Nuclear Society, Topical Meeting, Augusta, Ga., Mar. 21–23, 1966)
1	20-12394	See BNWL-SA-472
2	20-11267	See BNWL-SA-488
CONF-661001–		(14th Conference on Remote Systems Technology, Pittsburgh, Oct. 30–Nov. 4, 1966)
1	20-11068	See WAPD-T-1815
COO–		
32-112	20-11468	J. Chem. Phys., 44: 833-4(1966)
238-46	20-11952	Dep. mn. CFSTI $3.00 cy, $0.50 mn
264-224	20-11891	Dep. mn. CFSTI $1.00 cy, $0.50 mn
264-260	20-11735	Nuovo Cimento (10), 41A: 1-11(1966)
264-263	20-11907	Phys. Rev., 141: 331-5(1966)

Report No.	Abstract No.	Availability
264-294	20-11665	Phys. Rev. Lett., 16: 291-5(1966)
347-17	20-11953	Dep. mn. CFSTI $6.00 cy, $1.50 mn
347-18	20-11954	Dep. mn. CFSTI $6.00 cy, $1.50 mn
347-19	20-11955	Dep. mn. CFSTI $5.00 cy, $1.00 mn
498-44	20-12009	Nucl. Phys., 77: 513-26(1966)
498-45	20-12081	Phys. Rev., 141: 1193-9(1966)
498-46	20-12082	Phys. Rev., 141: 1200-5(1966)
578-18	20-12274	Dep. mn. CFSTI $2.00 cy, $0.50 mn
614-34	20-11195	Dep. mn; CFSTI $6.00 cy, $1.25 mn
920-8	20-12532	Dep. mn. CFSTI $1.00 cy, $0.50 mn
1020-6	20-12533	Dep. mn. CFSTI $1.00 cy, $0.50 mn
1020-9	20-10802	Dep. mn. CFSTI $1.00 cy, $0.50 mn
1195-27	20-11554	Dep. mn; CFSTI $1.00 cy, $0.50 mn
1198-216	20-12534	Dep. mn; CFSTI $3.00 cy, $0.75 mn
1198-325	20-11922	Phys. Rev. Lett., 16: 273-5(1966)
1198-326	20-11920	Phys. Rev. Lett., 16: 263-4(1966)
1226-10	20-11094	Dep. mn. CFSTI $1.00 cy, $0.50 mn
1233-24	20-12167	Dep. mn; CFSTI $1.00 cy, $0.50 mn
1261-7	20-11743	Phys. Rev., 141: 1322-4(1966)
1319-32	20-11233	Dep. mn. CFSTI $3.00 cy, $0.50 mn
1371-4	20-11458	Ann. Phys., 35: 271-313(1965)
1371-17	20-11630	Phys. Rev., 141: 1314-20(1966)
1420-114	20-12066	Phys. Rev., 141: 1078-81(1966)
CRGP–	**(Canadian)**	
1224	20-11095	AECL $1.00
CRRP–	**(Canadian)**	
1228	20-12493	See AECL-2514
D–	**(Misc.)**	
1-82-0448	20-11367	
2-84071-1	20-11173	
DESY–	**(German)**	
65/12	20-11389	Dep. mn
65/13	20-11555	Dep. mn
65/14	20-11556	Dep. mn
DOCKET	**(Misc.)**	
50-220(Vol.1)	20-12408	See NP-15660(Vol.1)
50-220(Suppl.1)	20-12410	See NP-15660(Suppl.1)
50-220(Vol.2)	20-12409	See NP-15660(Vol.2)
DP–		
958	20-12352	Dep. mn. CFSTI $6.00 cy, $1.25 mn
1006	20-11029	Dep. mn. CFSTI $2.00 cy, $0.50 mn
DUBNA REPORTS	**(Russian)**	
See JINR (Russian)		
EFINS–	**(Misc.)**	
64-59	20-11891	See COO-264-224
65-3	20-11952	See COO-238-46
65-112	20-11665	See COO-264-294
EIR–	**(Swiss)**	
82	20-11268	Dep. mn
ER–	**(Misc.)**	
7777(Vol.1)	20-12265	See NP-15697(Vol.1)
7887	20-11344	See N65-35361
ETR–	**(Belgian)**	
170	20-11272	See NP-15661
EUR–	**(European Atomic Energy Community)**	
2288.f	20-10871	Dep. mn
2391	20-11239	See EURAEC-1468
2466.e	20-10803	Dep. mn
2483.f	20-11269	Dep. mn
2491.e	20-11096	Dep. mn
2517.f	20-10872	Dep. mn
2531.f	20-10809	Dep. mn
2534.e	20-11542	Dep. mn
2538.e	20-12495	Dep. mn
2552.e	20-12395	Dep. mn
2618.f	20-10758	Dep. mn
2632.d	20-11956	Dep. mn
2660	20-11342	See EURAEC-1502
2663	20-12396	See EURAEC-1505
2664	20-12397	See EURAEC-1506
2672	20-11240	See EURAEC-1520

Report No.	Abstract No.	Availability
EURAEC–		
1413	20-12377	See CEND-2863-236
1468	20-11239	Dep. mn. CFSTI $2.00 cy, $0.50 mn
1496	20-11212	See BMI-X-10143
1502	20-11342	Dep. mn. CFSTI $3.00 cy, $0.75 mn
1505	20-12396	Dep. mn. CFSTI $2.00 cy, $0.50 mn
1506	20-12397	Dep. mn. CFSTI $3.00 cy, $0.75 mn
1520	20-11240	Dep. mn. CFSTI $2.00 cy, $0.50 mn
1530	20-10991	See NYO-3114-12
EURFNR–	**(Misc.)**	
1F	20-12419	Dep. mn. CFSTI $2.00 cy, $0.50 mn
9F	20-12420	Dep. mn. CFSTI $3.00 cy, $0.50 mn
11F	20-12339	Dep. mn. CFSTI $2.00 cy, $0.50 mn
FTD-TT–	**(Non-AEC)**	
65-184	20-10767	For translation see AD-620995
65-915	20-11288	For translation see AD-622477
65-943	20-12476	For translation see AD-622352
GA–	**(Misc.)**	
6637	20-11932	Dep. mn. CFSTI $4.00 cy, $1.00 mn
6734	20-12353	Dep. mn. CFSTI $3.00 cy, $0.75 mn
6807	20-12465	
6811	20-12398	Dep. mn; CFSTI $2.00 cy, $0.50 mn
6832	20-11957	
6861	20-12275	Dep. mn. CFSTI $2.00 cy, $0.50 mn
GAMD–	**(Misc.)**	
6562	20-11958	Dep. mn. CFSTI $1.00 cy, $0.50 mn
6644(Add.)	20-12354	Dep. mn. CFSTI $1.00 cy, $0.50 mn
6781	20-12355	Dep. mn. CFSTI $2.00 cy, $0.50 mn
GE-TM–		
65-2-18	20-11238	See CONF-650449-1
GEAP–	**(Misc.)**	
4911	20-12338	Dep. mn; CFSTI $3.00 cy, $0.75 mn
4941	20-12399	Dep. mn; CFSTI $5.00 cy, $1.00 mn
GIC–		
2605-3	20-11543	Dep. mn. CFSTI $4.00 cy, $1.00 mn
HMI-B–	**(German)**	
41	20-11200	Dep. mn
42	20-11767	Dep. mn
HNS–		
1229-61	20-11010	Dep. mn; CFSTI $3.00 cy, $0.75 mn
HPR–	**(Norwegian)**	
54	20-12400	Dep. mn
HW–		
76472	20-10948	ORAU
77389	20-11959	Dep. mn. CFSTI $1.00 cy, $0.50 mn
77921-C	20-12455	Dep. mn. CFSTI $2.00 cy, $0.50 mn
77921-D	20-12456	Dep. mn. CFSTI $2.00 cy, $0.50 mn
HW-SA–		
3728	20-10540	Dep. mn. CFSTI $2.00 cy, $0.50 mn
IA–	**(Non-AEC)**	
1020	20-10955	J. Inorg. Nucl. Chem., 28: 209-19(1966)
IAEA–	**(International Atomic Energy Agency)**	
2466-11	20-10603	Dep. mn. CFSTI $2.00 cy, $0.50 mn
IBJ–	**(Polish)**	
See INR		
IC–	**(Misc.)**	
65/84	20-11680	Dep. mn
65/85	20-11681	Dep. mn
65/89	20-11682	Dep. mn
65/94	20-11441	Dep. mn
IDO–		
14667	20-11960	Dep. mn. CFSTI $2.00 cy, $0.50 mn
16871-5	20-12496	Dep. mn. CFSTI $5.00 cy, $1.00 mn

Report No.	Abstract No.	Availability
17003(Rev.2)	20-12497	Dep. mn. CFSTI $3.00 cy, $0.75 mn
17112	20-11061	Dep. mn. CFSTI $4.00 cy, $1.00 mn
17128	20-12356	Dep. mn. CFSTI $4.00 cy, $0.75 mn
17131	20-12500	Dep. mn. CFSTI $1.00 cy, $0.50 mn
28595(Rev.)	20-10989	Dep. mn. CFSTI $2.00 cy, $0.75 mn
IFJ–	**(Polish)**	
See INP		
IITRI–	**(Misc.)**	
1184-18	20-12274	See COO-578-18
INP–	**(Polish)**	
427/C	20-10759	Dep.
INR–	**(Non-AEC)**	
602/VII/PH	20-11961	Dep.
621/XV/I	20-11097	
630/IX-A/PR (Pt.2)	20-11933	Dep.
644/XIV/PS	20-11232	
655/I/PL	20-11962	
INSJ–	**(Japanese)**	
91	20-11963	Dep. mn
IONAC–		
5002	20-10766	See TID-22511
IPST-Cat.–	**(Russian)**	
1247	20-10980	For translation see AEC-tr-6469
IS–		
1231	20-11306	J. Less-Common Metals, 10: 108-15(1966)
1300	20-11234	Dep. mn. CFSTI $4.00 cy, $0.75 mn
1305	20-10760	Dep. mn. CFSTI $1.00 cy, $0.50 mn
1312	20-11098	Dep. mn. CFSTI $1.00 cy, $0.50 mn
IS-T–		
44	20-10754	Dep. mn. CFSTI $3.00 cy, $0.75 mn
46	20-10976	Dep. mn. CFSTI $3.00 cy, $0.50 mn
61	20-12535	Dep. mn. CFSTI $2.00 cy, $0.50 mn
66	20-12536	Dep. mn. CFSTI $3.00 cy, $0.75 mn
69	20-10761	Dep. mn. CFSTI $3.00 cy, $0.75 mn
71	20-10762	Dep. mn. CFSTI $3.00 cy, $0.75 mn
IS-Trans–		
26	20-11289	Dep. mn. CFSTI $1.00 cy, $0.50 mn. JCL $1.10 fs, $0.80 mf
JEN–	**(Spanish)**	
150-DQ/I-51	20-11191	Dep. mn
153-DMa/I-19	20-10810	Dep. mn
156-DMe/113	20-12401	Dep. mn
JINR–	**(Russian)**	
E-2457	20-11557	Dep. mn
E-2464	20-11964	Dep. mn
E-2475	20-11683	Dep. mn
E-2478	20-11866	Dep. mn
E-2496	20-11558	Dep. mn
P-2426	20-11965	Dep. mn
P-2432	20-11966	Dep. mn
P-2436	20-11099	Dep. mn
P-2442	20-11684	Dep. mn
P-2444	20-11685	Dep. mn
P-2445	20-11559	Dep. mn
P-2446	20-11390	Dep. mn
P-2447	20-11686	Dep. mn
P-2449	20-11560	Dep. mn
P-2450	20-11561	Dep. mn
P-2454	20-11562	Dep. mn
P-2455	20-11967	Dep. mn
P-2456	20-11563	Dep. mn
P-2462	20-11564	Dep. mn
P-2467	20-11100	Dep. mn
P-2468	20-11101	Dep. mn
P-2469	20-11565	Dep. mn
P-2470	20-11968	Dep. mn
P-2471	20-11969	Dep. mn
P-2472	20-11566	Dep. mn
P-2473	20-11970	Dep. mn
P-2479	20-12263	Dep. mn
P-2485	20-11687	Dep. mn
P-2487	20-11102	Dep. mn
P-2489	20-11103	Dep. mn
JPL-TR–	**(Non-AEC)**	
32-797	20-11688	
JPRS–	**(Non-AEC)**	
33212	20-10768	CFSTI $1.00 cy, $0.50 mn
33480	20-12454	CFSTI $1.00 cy, $0.50 mn
33502	20-11036	CFSTI $1.00 cy, $0.50 mn
JUL–	**(German)**	
280-PP	20-12168	Dep. mn
322-PP	20-12169	Dep. mn
327-PP	20-11768	Dep. mn
K–		
1469	20-10949	Dep. mn. CFSTI $4.00 cy, $1.00 mn
KFK–	**(German)**	
369	20-12402	Dep. mn
370	20-10977	Dep. mn
KR–	**(Norwegian)**	
75	20-12357	Dep. mn
100	20-10763	Dep. mn
LA–		
3367	20-11343	Dep. mn. CFSTI $3.00 cy, $0.75 mn
3384	20-12403	Dep. mn. CFSTI $3.00 cy, $0.75 mn
3406	20-12358	Dep. mn. CFSTI $2.00 cy, $0.50 mn
3422	20-12537	Dep. mn. CFSTI $3.00 cy, $0.75 mn
3424	20-11270	Dep. mn. CFSTI $2.00 cy, $0.50 mn
LA-DC–		
6803	20-12538	Dep. mn; CFSTI $1.00 cy, $0.50 mn
6806	20-10811	Dep. mn. CFSTI $1.00 cy, $0.50 mn
6824	20-11892	Dep. mn. CFSTI $1.00 cy, $0.50 mn
6912	20-11689	Dep. mn. CFSTI $1.00 cy, $0.50 mn
6929	20-11139	Rev. Sci. Instrum., 37: 215-23(1966)
6961	20-12477	Astronaut. Aeronaut., 4: 54-9(1966)
7241(Rev.)	20-10835	J. Chem. Phys., 44: 1304-5(1966)
7269	20-11893	Ann. Phys., 35: 410-25(1965)
7384	20-11785	J. Chem. Phys., 44: 658-67(1966)
7390	20-11544	Dep. mn; CFSTI $1.00 cy, $0.50 mn
7459	20-11897	J. Chem. Phys., 44: 213-20(1966)
7480	20-11786	J. Chem. Phys., 44: 668-72(1966)
7555	20-11545	Dep. mn; CFSTI $1.00 cy, $0.50 mn
7692	20-12539	Dep. mn. CFSTI $2.00 cy, $0.50 mn
LA-tr–		
65-29	20-11457	Dep. mn. JCL $1.60 fs, $0.80 mf
65-34	20-11982	Dep. mn. CFSTI $1.00 cy, $0.50 mn. JCL $1.60 fs, $0.80 mf
LAC-ER–	**(Non-AEC)**	
8231	20-11345	See NASA-CR-54787
LAL–	**(French)**	
1144	20-11567	Dep. mn
LFEN–	**(Portuguese)**	
24	20-11271	Dep. mn
LGI–	**(Italian)**	
65/30	20-11769	Dep. mn
LNF–	**(Italian)**	
65/33	20-11104	Dep. mn
LRP–	**(Swiss)**	
18-65	20-12170	Dep. mn
MATT–		
270	20-12171	Dep. mn. CFSTI $3.00 cy, $0.75 mn
280	20-11442	Dep. mn. CFSTI $2.00 cy, $0.50 mn
302	20-12172	Dep. mn. CFSTI $2.00 cy, $0.50 mn
315	20-12173	Dep. mn. CFSTI $1.00 cy, $0.50 mn
356	20-12239	Phys. Fluids, 9: 195-8(1966)
375	20-12236	Phys. Fluids, 9: 165-76(1966)

Report No.	Abstract No.	Availability
MIT–	**(Misc.)**	
65TR37	20-10979	See TID-22528
1842-12	20-12256	See CONF-83-3
2098-158	20-12301	Phys. Rev., 142: 86-90(1966)
2098-166	20-12299	Phys. Rev., 141: 423-4(1966)
MITNE–	**(Misc.)**	
64	20-10764	CFSTI $6.00 cy, $1.25 mn
MLM–		
1251J	20-11971	Dep. mn. CFSTI $2.00 cy, $0.50 mn
1252	20-10862	Dep. mn. CFSTI $1.00 cy, $0.50 mn
1298J	20-11194	J. Chem. Phys., 44: 723-9(1966)
1315	20-12264	Dep. mn. CFSTI $1.00 cy, $0.50 mn
MND–	**(Misc.)**	
3062-25	20-11189	Dep. mn. CFSTI $5.00 cy, $1.00 mn
MPI-PAE–	**(German)**	
P1.6/65	20-12174	Dep. mn
MSAR–	**(Misc.)**	
65-194	20-11235	Dep. mn. CFSTI $4.00 cy, $1.00 mn
MTI–	**(Misc.)**	
65TR64	20-10972	See NYO-3237-4
N–	**(Misc.)**	
65-35361	20-11344	
NAA-SR–		
11160	20-12404	Dep. mn. CFSTI $2.00 cy, $0.50 mn
11586	20-10990	Dep. mn. CFSTI $3.00 cy, $0.50 mn
11642	20-12466	Dep. mn. CFSTI $1.00 cy, $0.50 mn
11704	20-12467	Dep. mn. CFSTI $2.00 cy, $0.50 mn
NAA-SR-Memo–		
9916	20-12468	Dep. mn. CFSTI $1.00 cy, $0.50 mn
11132	20-11105	Dep. mn. CFSTI $4.00 cy, $0.75 mn
11569	20-10812	Dep. mn. CFSTI $1.00 cy, $0.50 mn
11576	20-12405	Dep. mn. CFSTI $1.00 cy, $0.50 mn
11630	20-12469	Dep. mn. CFSTI $3.00 cy, $0.75 mn
11648	20-12406	Dep. mn. CFSTI $1.00 cy, $0.50 mn
NASA-CR–	**(Misc.)**	
348	20-12175	CFSTI $1.00 cy, $0.50 mn
54658	20-11217	See WANL-PR(Q)-007
54717	20-11214	
54718	20-11215	
54786	20-12465	See GA-6807
54787	20-11345	
54790	20-11443	
54790(App.1)	20-11444	
67342	20-11344	See N65-35361
NASA-TN–	**(Misc.)**	
D-3188	20-12176	CFSTI $2.00 cy, $0.50 mn
D-3199	20-12177	CFSTI $1.00 cy, $0.50 mn
NASA-TT–	**(Non-AEC)**	
F-285	20-10816	CFSTI $6.00 cy, $1.25 mn
F-353	20-10604	CFSTI $6.00
NBS-MON–	**(Misc.)**	
76	20-11030	GPO $0.20
NEIC-RR–	**(Polish)**	
13	20-12407	Dep. mn
NP–	**(AEC File No. for Non-AEC Reports)**	
15274	20-11391	Dep. mn
15275	20-11392	Dep. mn
15611	20-11346	
15629	20-11424	Dep. mn
15660(Vol.1)	20-12408	Dep. mn. CFSTI $6.00 cy, $1.50 mn
15660(Suppl.1)	20-12410	Dep. mn. CFSTI $6.00 cy, $1.25 mn
15660(Vol.2)	20-12409	Dep. mn. CFSTI $7.00 cy, $1.75 mn
15661	20-11272	Dep. mn. CFSTI $1.00 cy, $0.50 mn
15697(Vol.1)	20-12265	
15705	20-12178	CFSTI $2.00 cy, $0.50 mn
15707	20-11352	CFSTI $4.00 cy, $1.00 mn
15708	20-11031	CFSTI $6.00 cy, $1.25 mn
15715	20-11393	Dep. mn
15716	20-11972	Dep. mn
15762	20-11867	Dep. mn
15764	20-11690	Dep. mn
15782	20-12179	Dep. mn
15786	20-11106	Dep. mn
15788	20-11394	Dep. mn
15791	20-11973	Dep. mn
15793	20-11445	Dep. mn
15794	20-11446	Dep. mn
15823	20-11175	
15824	20-11006	
15831	20-11007	
15835	20-11176	CFSTI $2.00 cy, $0.50 mn
NP-tr–	**(AEC File No. for Non-AEC Translations)**	
1323	20-10937	Dep. mn; JCL $2.60 fs, $0.98 mf
1344	20-10613	CFSTI $1.00 cy, $0.50 mn
1346	20-11771	Consultants Bureau. $17.50
NRL–	**(Misc.)**	
6364	20-11273	CFSTI $3.00 cy, $0.75 mn
NYO–		
2262-101	20-11634	Phys. Rev., 141: 1342-9(1966)
2882-8	20-12540	Dep. mn. CFSTI $1.00 cy, $0.50 mn
2929-1	20-12541	Dep. mn. CFSTI $1.00 cy, $0.50 mn
2929-2	20-12542	Dep. mn. CFSTI $2.00 cy, $0.50 mn
3018-12	20-12543	Dep. mn. CFSTI $2.00 cy, $0.50 mn
3114-12	20-10991	Dep. mn. CFSTI $2.00 cy, $0.50 mn
3136-2	20-11201	Dep. mn; CFSTI $5.00 cy, $1.00 mn
3237-4	20-10972	Dep. mn; CFSTI $4.00 cy, $0.75 mn
3399-12	20-11699	Ann. Phys., 35: 209-39(1965)
3405-4	20-12276	Dep. mn. CFSTI $3.00 cy, $0.75 mn
3504-2	20-11274	Dep. mn. CFSTI $3.00 cy, $0.75 mn
ORINS–		
51	20-10724	Dep. mn. CFSTI $3.00 cy, $0.50 mn
ORNL–		
3846	20-12544	Dep. mn; CFSTI $2.00 cy, $0.50 mn
3891	20-11032	Dep. mn. CFSTI $2.00 cy, $0.50 mn
3904	20-10765	Dep. mn. CFSTI $3.00 cy, $0.75 mn
3906	20-10813	Dep. mn. CFSTI $2.00 cy, $0.50 mn
3914	20-11691	Dep. mn. CFSTI $3.00 cy, $0.75 mn
ORNL-P–	**(Misc.)**	
960	20-11974	Dep. mn. CFSTI $1.00 cy, $0.50 mn
999	20-11254	Nucl. Appl., 1: 560-6(1965)
1005	20-11770	Dep. mn. CFSTI $1.00 cy, $0.50 mn
1017	20-11256	Nucl. Appl., 1: 575-80(1965)
1234	20-12240	Phys. Fluids, 9: 199-213(1966)
1442	20-12244	Phys. Rev., 141: 211-16(1966)
1536	20-12076	Phys. Rev., 141: 1146-60(1966)
1556	26-12180	Dep. mn. CFSTI $1.00 cy, $0.50 mn
1615	20-12057	Phys. Rev., 141: 996-1002(1966)
1617	20-11650	Phys. Rev., 141: 1494-6(1966)
1695	20-12008	Nucl. Phys., 77: 481-512(1966)
1717	20-10834	J. Chem. Phys., 44: 1149-59(1966)
1755	20-11075	Rev. Sci. Instrum., 37: 240(1966)
1878	20-12089	Phys. Rev. Lett., 16: 194-7(1966)
1900	20-11183	Dep. mn. CFSTI $1.00 cy, $0.50 mn
1920	20-12247	Phys. Rev. Lett., 16: 265-8(1966)
1928	20-10932	Dep. mn. CFSTI $2.00 cy, $0.50 mn
ORNL-TM–		
1163	20-12501	Dep. mn. CFSTI $1.00 cy, $0.50 mn
1172(Rev.)	20-11395	Dep. mn. CFSTI $1.00 cy, $0.50 mn
1195	20-12359	Dep. mn. CFSTI $1.00 cy, $0.50 mn
1325	20-11934	Dep. mn. CFSTI $1.00 cy, $0.50 mn
1327	20-12518	Dep. mn. CFSTI $1.00 cy, $0.50 mn
1332	20-12360	Dep. mn; CFSTI $4.00 cy, $0.75 mn
1338	20-11275	Dep. mn. CFSTI $1.00 cy, $0.50 mn
1372	20-12457	Dep. mn. CFSTI $2.00 cy, $0.50 mn
1380	20-12411	Dep. mn. CFSTI $1.00 cy, $0.50 mn
1382	20-11396	Dep. mn. CFSTI $1.00 cy, $0.50 mn
ORNL-tr–		
868	20-12183	Dep. mn. CFSTI $1.00 cy, $0.50 mn. JCL $1.60 fs, $0.80 mf
918	20-12266	Dep. mn. JCL $1.60 fs, $0.80 mf

Report No.	Abstract No.	Availability
PAEC(A)AR–	**(Philippines)**	
651	20-12545	Dep. mn
PAEC(A)IN–	**(Philippines)**	
656	20-12277	Dep. mn
657	20-11276	Dep. mn
PAM–	**(French)**	
6502	20-11975	Dep. mn
PAN–	**(Polish)**	**(This series of reports was terminated in 1965. Subsequent reports are identified by the code INR.)**
PATENTS	**(British)**	**(4s. 6d. each, U. K. Patent Office)**
1,012,912	20-11159	
1,012,919	20-11160	
PATENTS	**(German)**	
1,202,914	20-11415	
PATENTS	**(Japanese)**	
1964-12695	20-10983	
1964-12700	20-11416	
1964-14183	20-11080	
1964-14949	20-11005	
1964-15099	20-10984	
1964-18226	20-11263	
1964-18481	20-12347	
1964-18499	20-11081	
1964-18500	20-11417	
1964-21420	20-11082	
1964-23458	20-10985	
1964-24285	20-10929	
1964-24780	20-11161	
1964-24897	20-11229	
1964-24985	20-11418	
1964-25940	20-11083	
1964-26197	20-10930	
1964-26654	20-11084	
1964-26655	20-11162	
1964-26932	20-11163	
1964-26933	20-11164	
1964-26934	20-11165	
1964-27161	20-12381	
1964-27162	20-12382	
1964-27163	20-12376	
1964-27164	20-12348	
1964-27166	20-12349	
1964-27167	20-12515	
1964-27171	20-12516	
1964-27173	20-10971	
1964-27179	20-12350	
1964-27180	20-12272	
1964-30370	20-11419	
1964-30372	20-11420	
1964-30373	20-11421	
1964-30374	20-11422	
1965-2154	20-10931	
1965-4720	20-12527	
PATENTS	**(U. S.)**	**($0.25 each, U. S. Patent Office)**
3,216,808	20-12273	
3,218,460	20-11166	
3,218,487	20-12383	
3,223,842	20-11085	
3,224,562	20-10986	
3,225,195	20-11167	
3,225,196	20-11168	
3,225,197	20-11169	
3,225,198	20-11170	
3,225,199	20-11171	
3,225,200	20-11947	
3,225,203	20-10987	
3,225,227	20-11550	
3,225,245	20-10798	
3,225,270	20-11423	
PEL–	**(South African)**	
60	20-12361	Dep. mn
79	20-11216	Dep. mn
R–	**(Misc.)**	
271	20-12178	See NP-15705
1779	20-11352	See NP-15707
RFP–		
462	20-11107	Dep. mn. CFSTI $1.00 cy, $0.50 mn
637	20-11108	Dep. mn. CFSTI $1.00 cy, $0.50 mn
649	20-11062	Dep. mn. CFSTI $1.00 cy, $0.50 mn
659	20-11277	Dep. mn. CFSTI $1.00 cy, $0.50 mn
672	20-11063	Dep. mn. CFSTI $1.00 cy, $0.50 mn
RFR–	**(Swedish)**	
154	20-11935	Dep. mn
193	20-12362	Dep. mn
RISO–	**(Danish)**	
48(Suppl.2)	20-11278	Dep. mn
102	20-11064	Dep. mn
116	20-10992	Dep. mn
RM–	**(Misc.)**	
3326-1-PR	20-10799	See AD-625735
RME–		
4552(Rev.)	20-11025	Dep. mn; CFSTI $1.00 cy, $0.50 mn
RMO–		
3006	20-10978	Dep. mn. CFSTI $2.00 cy, $0.50 mn
RRL–		
2310-161	20-10882	J. Chem. Phys., 44: 434-7(1966)
SC-DC–		
64-1477X	20-11279	Dep. mn. CFSTI $4.00 cy, $1.00 mn
SC-R–		
65-1017	20-12470	Dep. mn. CFSTI $1.00 cy, $0.50 mn
SC-RR–		
65-111	20-11397	Dep. mn. CFSTI $3.00 cy, $0.50 mn
65-548	20-12546	Dep. mn. CFSTI $3.00 cy, $0.75 mn
65-557	20-12471	Dep. mn. CFSTI $1.00 cy, $0.50 mn
65-620	20-12472	Dep. mn. CFSTI $6.00 cy, $1.25 mn
65-671	20-11546	Dep. mn. CFSTI $1.00 cy, $0.50 mn
SC-TM–		
65-398	20-11033	Dep. mn. CFSTI $2.00 cy, $0.50 mn
323-62(72)	20-11065	Dep. mn. CFSTI $1.00 cy, $0.50 mn
SCL-DC–		
65-96	20-10814	Dep. mn. CFSTI $4.00 cy, $0.75 mn
SGAE-E–	**(Austrian)**	
5/1965	20-11109	Dep. mn
SGAE-PH–	**(Austrian)**	
30/1965	20-11192	Dep.
SLAC-PUB–		
146	20-11066	Dep. mn. CFSTI $1.00 cy, $0.50 mn
STI-DOC–	**(International Atomic Energy Agency)**	
10/45	20-10539	IAEA: $4.50; S 115.50; £ 1.13.0; F Fr 22,-; DM 19.25.
10/46	20-11110	IAEA: $2.50; S 52.50; 15/-stg; F Fr 10,-; DM 8,-.
STS–		
45	20-12473	See TID-22459
51	20-12474	See TID-22460
T–	**(Misc.)**	
A2049-26	20-10974	For translation see AEC-tr-6665
TID–		
3043(Rev.2, Suppl.3)	20-12547	Dep. mn. CFSTI $2.00 cy, $0.75 mn
4005(Pt.2a) (2nd ed.)	20-10755	Dep. mn. CFSTI $1.75 cy, $1.00 mn
4577(Rev.1)	20-12548	Dep. mn. CFSTI $1.00 cy, $0.75 mn
5360(Suppl.5)	20-11034	Dep. mn. CFSTI $3.00 cy, $0.50 mn
8541	20-12329	Dep. mn. CFSTI $4.50 cy, $2.00 mn

Report No.	Abstract No.	Availability
21420	20-11677	pp 297-302 of Nuclear Physics and Solid State Physics Symposium, 1965. Nuclear Physics. Bombay, Atomic Energy Establishment, 1965.
21555	20-12549	Dep. mn. CFSTI $1.00 cy, $0.50 mn
21570	20-12278	Dep. mn. CFSTI $1.00 cy, $0.50 mn
21913	20-12016	Nucl. Phys., 77: 609-18(1966)
21992	20-10973	Dep. mn. CFSTI $4.00 cy, $0.75 mn
22064	20-12185	Ann. Phys., 35: 396-409(1965)
22076	20-12048	Phys. Rev., 141: 927-32(1966)
22113	20-11742	Phys. Rev., 141: 815-24(1966)
22233	20-11649	Phys. Rev., 141: 1489-93(1966)
22330(Vol.2)	20-12453	Dep. mn. CFSTI $4.00 cy, $2.75 mn
22340	20-11490	Phys. Rev., 141: 165-73(1966)
22341	20-11489	Phys. Rev., 141: 151-64(1966)
22459	20-12473	Dep. mn. CFSTI $1.00 cy, $0.50 mn
22460	20-12474	Dep. mn. CFSTI $3.00 cy, $0.50 mn
22476	20-11447	Dep. mn; CFSTI $2.00 cy, $0.50 mn
22480	20-11448	Dep. mn; CFSTI $2.00 cy, $0.50 mn
22504	20-11976	Dep. mn. CFSTI $3.00 cy, $0.75 mn
22511	20-10766	Dep. mn. CFSTI $3.00 cy, $0.75 mn
22513	20-10993	Dep. mn. CFSTI $2.00 cy, $0.50 mn
22516	20-12412	Dep. mn. CFSTI $2.00 cy, $0.50 mn
22528	20-10979	Dep. mn. CFSTI $2.00 cy, $0.50 mn
22529	20-11206	Dep. mn. CFSTI $2.00 cy, $0.50 mn
22530	20-11449	Dep. mn. CFSTI $1.00 cy, $0.50 mn
22532	20-10933	Dep. mn. CFSTI $2.00 cy, $0.50 mn
22536	20-11977	Dep. mn. CFSTI $3.00 cy, $0.75 mn
22539	20-10994	Dep. mn. CFSTI $2.00 cy, $0.50 mn
22545	20-12413	Dep. mn. CFSTI $3.00 cy, $0.75 mn
22547	20-12502	Dep. mn. CFSTI $2.00 cy, $0.50 mn
22550	20-11111	Dep. mn. CFSTI $1.00 cy, $0.50 mn
22553	20-11112	Dep. mn. CFSTI $1.00 cy, $0.50 mn
22564	20-12550	Dep. mn. CFSTI $1.00 cy, $0.50 mn
TT–	**(Canadian)**	
65-33787	20-10768	See JPRS-33212
65-34054	20-12454	See JPRS-33480
65-34076	20-11036	See JPRS-33502
65-50025	20-10613	For translation see NP-tr-1344
65-50111	20-10816	For translation see NASA-TT-F-285
UACRL-D–	**(Non-AEC)**	
920243-18	20-11443	See NASA-CR-54790
UCID–		
10028	20-11398	Dep. mn. CFSTI $2.00 cy, $0.50 mn
UCLA–		
12-570	20-10899	Nature, 208: 1086-7(1965)
UCRL–		
7495(Rev.1)	20-11807	Dep. mn. CFSTI $2.00 cy, $0.50 mn
7566(Rev.1)	20-11399	Dep. mn. CFSTI $1.00 cy, $0.50 mn
7737	20-11207	Dep. mn. CFSTI $1.00 cy, $0.50 mn
7777	20-11425	Dep. mn. CFSTI $4.00 cy, $0.75 mn
7842-T	20-11450	Dep. mn. CFSTI $2.00 cy, $0.50 mn
7941(Rev.1)	20-11451	Dep. mn. CFSTI $1.00 cy, $0.50 mn
7961-T	20-11978	Dep. mn. CFSTI $3.00 cy, $0.75 mn
10696(Rev.)(Pt.1)	20-10995	Dep. mn. CFSTI $2.00 cy, $0.50 mn
11743	20-10934	Dep. mn. CFSTI $1.00 cy, $0.50 mn
11749	20-11568	Dep. mn. CFSTI $1.00 cy, $0.50 mn
11768	20-11692	Dep. mn. CFSTI $1.00 cy, $0.50 mn
11773	20-11497	Phys. Rev., 142: 11-13(1966)
12001	20-11280	Dep. mn. CFSTI $1.00 cy, $0.50 mn
12016-T	20-11693	Dep. mn. CFSTI $2.00 cy, $0.50 mn
12042-T	20-11452	Dep. mn. CFSTI $2.00 cy, $0.50 mn
12095-T	20-11067	Dep. mn. CFSTI $1.00 cy, $0.50 mn
12107	20-11281	Dep. mn. CFSTI $1.00 cy, $0.50 mn
12110-T	20-11572	Ann. Phys., 35: 331-50(1965)
12119-T	20-11282	Dep. mn. CFSTI $1.00 cy, $0.50 mn
12142	20-11283	Dep. mn. CFSTI $1.00 cy, $0.50 mn
12152	20-11979	Dep. mn. CFSTI $2.00 cy, $0.50 mn
12153	20-11242	Dep. mn. CFSTI $1.00 cy, $0.50 mn
12186	20-12551	Dep. mn. CFSTI $1.00 cy, $0.50 mn
12220	20-11208	Dep. mn; CFSTI $2.00 cy, $0.50 mn
12226	20-12552	Dep. mn; CFSTI $2.00 cy, $0.50 mn
12230	20-11453	Dep. mn. CFSTI $1.00 cy, $0.50 mn
12233	20-11454	Dep. mn. CFSTI $1.00 cy, $0.50 mn
12267	20-11426	Dep. mn. CFSTI $1.00 cy, $0.50 mn
12311	20-12279	Dep. mn. CFSTI $1.00 cy, $0.50 mn
12416	20-12238	Phys. Fluids, 9: 187-94(1966)
12416(Rev.1)	20-12238	See UCRL-12416
14252-T	20-11622	Phys. Rev., 141: 873-88(1966)
14256-T	20-11604	Nuovo Cimento (10), 41A: 132-41(1966)
14294	20-10975	Dep. mn. CFSTI $1.00 cy, $0.50 mn
14305	20-12065	Phys. Rev., 141: 1067-77(1966)
14348	20-11636	Phys. Rev., 141: 1352-3(1966)
14359	20-12553	Dep. mn. CFSTI $1.00 cy, $0.50 mn
14384-T	20-11754	Phys. Rev., 141: 1554-9(1966)
14450	20-11455	Dep. mn. CFSTI $2.00 cy, $0.50 mn
14467-T	20-12181	Dep. mn; CFSTI $3.00 cy, $0.75 mn
14473	20-12554	Dep. mn. CFSTI $1.00 cy, $0.50 mn
14491-T	20-11611	Phys. Lett., 20: 67-70(1966)
14546	20-11868	Dep. mn. CFSTI $1.00 cy, $0.50 mn
14599	20-11284	Dep. mn. CFSTI $2.00 cy, $0.50 mn
16002	20-12073	Phys. Rev., 141: 1132-5(1966)
16065	20-11486	Phys. Rev., 141: 130-6(1966)
16096	20-11624	Phys. Rev., 141: 1261-7(1966)
16096(Rev.)	20-11624	See UCRL-16096
16125	20-11498	Phys. Rev., 142: 14-19(1966)
16200	20-12061	Phys. Rev., 141: 1021-32(1966)
16233	20-11639	Phys. Rev., 141: 1398-1403(1966)
16255	20-11640	Phys. Rev., 141: 1404-9(1966)
16292	20-12286	J. Chem. Phys., 44: 348-54(1966)
16321	20-11475	Phys. Rev., 141: 4-14(1966)
16323	20-11400	Dep. mn. CFSTI $3.00 cy, $0.75 mn
16331	20-11641	Phys. Rev., 141: 1409-12(1966)
16338	20-10815	Dep. mn. CFSTI $2.00 cy, $0.50 mn
16380	20-11469	J. Chem. Phys., 44: 839-40(1966)
16434	20-11285	Dep. mn. CFSTI $1.00 cy, $0.50 mn
16451	20-11656	Phys. Rev. Lett., 16: 203-7(1966)
16471	20-11113	Dep. mn. CFSTI $1.00 cy, $0.50 mn
16502	20-11401	Dep. mn. CFSTI $1.00 cy, $0.50 mn
16527	20-11619	Phys. Lett., 20: 93-6(1966)
16631	20-12182	Dep. mn. CFSTI $6.00 cy, $2.25 mn
UJV–	**(Czechoslovakian)**	
1365/65	20-12364	Dep. mn
1388/65	20-11177	Dep. mn
1405/65	20-11286	Dep. mn
1438/65	20-12365	Dep. mn
1439/65	20-12366	Dep. mn
1442/65	20-12367	Dep. mn
UR–		
875-66	20-11114	Dep. mn. CFSTI $1.00 cy, $0.50 mn
875-88	20-11642	Phys. Rev., 141: 1413-18(1966)
875-114	20-11610	Phys. Lett., 20: 64-7(1966)
875-118	20-11569	Dep. mn. CFSTI $1.00 cy, $0.50 mn
USNRDL-TR–	**(Misc.)**	
929	20-11949	See AD-625747
935	20-11980	Dep. mn. CFSTI $2.00 cy, $0.50 mn
940	20-11013	Dep. mn. CFSTI $2.00 cy, $0.50 mn
943	20-11981	Dep. mn. CFSTI $1.00 cy, $0.50 mn
948	20-10935	Dep. mn. CFSTI $1.00 cy, $0.50 mn
WANL-PR–	**(Misc.)**	
(B)-009	20-12475	
(EE)-001	20-11243	
(Q)-007	20-11217	
WANL-TNR–	**(Misc.)**	
154	20-10996	
WAPD-T–		
1737	20-12368	Dep. mn. CFSTI $1.00 cy, $0.50 mn
1809	20-11287	Dep. mn. CFSTI $2.00 cy, $0.50 mn
1815	20-11068	Dep. mn. CFSTI $1.00 cy, $0.50 mn
1828	20-12555	Dep. mn. CFSTI $6.00 cy, $1.50 mn
WCAP–	**(Misc.)**	
3269-15	20-12417	Dep. mn. CFSTI $1.00 cy, $0.50 mn
3739	20-12418	Dep. mn. CFSTI $7.00 cy, $1.75 mn
Y-MA–		
450	20-11244	Dep. mn. CFSTI $1.00 cy, $0.50 mn

DEPOSITORIES OF USAEC REPORTS

In Countries Other than the U.S.

ARGENTINA
Buenos Aires, Comisión Nacional de Energía Atómica
AUSTRALIA
Canberra, Australian National Library
Sutherland, New South Wales, Australian Atomic Energy Commission
AUSTRIA
Vienna, Zentral Bibliothek der Physikalischen Institute der Universität
BELGIUM
Mol-Donk, Centre d'Etude de l'Energie Nucleaire
BOLIVIA
La Paz, Comisión Nacional de Energiá Nuclear
BRAZIL
Rio de Janeiro, Instituto Brasileiro de Bibliografia e Documentacao
São Paulo, Instituto de Energia Atomica, Cidade Universitaria São Paulo
BURMA
Rangoon, Union of Burma Applied Research Institute, Atomic Energy Center Library
CANADA
Hamilton, McMaster University
Ottawa, National Research Council Library
Vancouver, University of British Columbia
CHILE
Santiago, Instituto de Fisica y Matematicas, Universidad de Chile
CHINA
Hsinchu, Taiwan, Free China, National Tsing Hua University
COLOMBIA
Bogota, Instituto De Asuntos Nucleares
COSTA RICA
San Pedro, University of Costa Rica Library
DENMARK
Risö, Danish Atomic Energy Commission
ECUADOR
Quito, Escuela Politécnica Nacional
EL SALVADOR
San Salvador, Universidad de El Salvador, Biblioteca de Energia Nuclear
FINLAND
Helsinki, Teknillisen Korkeakoulun Kirjasto
FRANCE
Gif-sur-Yvette, Centre d'Etudes Nucléaires de Saclay
Paris, Académie des Sciences
GERMANY
Berlin, Hahn-Meitner-Institut für Kernforschung Berlin
Frankfurt/Main, Gmelin-Institut
Munich, Technische Hochschule, Bibliothek
GHANA
Accra, University College of Ghana
GREECE
Athens, Nuclear Research Center "Democritus"
GUATEMALA
Guatemala, Comisión Nacional de Energía Nuclear
INDIA
Bombay, Department of Atomic Energy
IRAN
Tehran, Tehran University Nuclear Centre
IRAQ
Baghdad, Iraqi Atomic Energy Commission
IRELAND
Dublin, University College
ISRAEL
Rehovoth, Israel Atomic Energy Commission
ITALY
Rome, Centro di Studi Nucleari della Casaccia
Rome, Comitato Nazionale per l'Energia Nucleare
JAPAN
Tokyo, National Diet Library
KOREA
Seoul, Office of Atomic Energy
LEBANON
Beirut, Lebanese National Council for Scientific Research
LUXEMBOURG
Luxembourg, Ministry of Transport and Electricity
MALAYSIA
Kuala Lumpur, University of Malaysia
MEXICO
Mexico, D.F., Comisión Nacional de Energía Nuclear
NETHERLANDS
The Hague, Reactor Centrum Nederland
NEW ZEALAND
Lower Hutt, Institute of Nuclear Sciences
NIGERIA
Ibadan, University of Ibadan
NORWAY
Lillestrøm, Institutt för Atomenergi
PAKISTAN
Lahore, West Pakistan, Atomic Energy Centre
PERU
Lima, Junta de Control de Energia Atomica
PHILIPPINE REPUBLIC
Manila, Philippine Atomic Energy Commission
POLAND
Warsaw, Biura Pelnomocnika Rzadu do Spraw Wykorzystania Energii Jadrowej
PORTUGAL
Sacavem, Junta de Energía Nuclear
REPUBLIC OF SOUTH AFRICA
Pretoria, Atomic Energy Board Library
REPUBLIC OF THE CONGO
Leopoldville, Université Lovanium
SPAIN
Madrid, Junta de Energía Nuclear, Biblioteca Documentación y Publicaciones, Ciudad Universitaria
SWEDEN
Nyköping, Aktiebolaget Atomenergi
SWITZERLAND
Zürich, Eidgenössische Technische Hochschule, Bibliothek
THAILAND
Bangkok, Office of the Thai Atomic Energy Commission, Department of Science
TURKEY
Ankara, Turkish Atomic Energy Commission, Atomic Energy Library
UNITED ARAB REPUBLIC
Cairo, Atomic Energy Commission
UNITED KINGDOM
Birmingham, Central Library
Boston Spa, National Lending Library for Science and Technology
Bristol, Central Library
Kingston upon Hull, Central Library
Liverpool, Central Library
London, Central Library, Acton
London, National Reference Library
London, Science Museum Library, South Kensington
Manchester, Central Library
Newcastle upon Tyne, Central Library
Nottingham, Central Library
Sheffield, Central Library
URUGUAY
Montevideo, Comision Nacional de Energia Atomica
VENEZUELA
Caracas, Instituto Venezolano de Investigaciones Científicas
VIET-NAM
Saigon, Atomic Energy Office
YUGOSLAVIA
Belgrade, Federal Commission for Nuclear Energy

In International Agencies

AUSTRIA
Vienna, International Atomic Energy Agency
BELGIUM
Brussels, La Bibliotheque EURATOM
FRANCE
Paris, European Nuclear Energy Agency, O.E.C.D.
ITALY
Ispra, EURATOM Research Center
SWITZERLAND
Geneva, United Nations Library

UNITED STATES
GOVERNMENT PRINTING OFFICE
DIVISION OF PUBLIC DOCUMENTS
WASHINGTON, D.C. 20402

OFFICIAL BUSINESS

POSTAGE AND FEES PAID
U.S. GOVERNMENT PRINTING OFFICE

TECHNICAL PROGRESS REVIEWS

The Division of Technical Information, U. S. Atomic Energy Commission, also publishes the Technical Progress Reviews, a series of five quarterly journals on nuclear technology. These journals, compiled by specialists and recognized authorities, summarize, evaluate, and reference the progress of development in five important fields.

Isotopes and Radiation Technology P. S. Baker, A. F. Rupp, and associates, Oak Ridge National Laboratory. Reviews AEC-sponsored projects and related significant worldwide developments in radioisotopes and radiation technology.

Nuclear Safety Wm. B. Cottrell, W. H. Jordan, and associates, Oak Ridge National Laboratory. Covers topics relevant to the analysis and control of hazards associated with nuclear reactors and with operations involving fissionable materials and the products of nuclear fission.

Power Reactor Technology Argonne National Laboratory. Reviews research, development, design practices, and operating experiences associated with power reactors, including aerospace applications.

Reactor Fuel Processing Stephen Lawroski and associates, Argonne National Laboratory. Reviews all aspects of the fuel-processing field, including aqueous and nonaqueous processing and waste disposal.

Reactor Materials R. W. Dayton, E. M. Simons, and associates, Battelle Memorial Institute. Covers the properties, behavior, and fabrication processes of materials used in nuclear reactors and associated equipment.

Availability

SUBSCRIPTION RATE: The Technical Progress Reviews may be purchased from the Superintendent of Documents, U. S. Government Printing Office, Washington, D. C. 20402, at $2.50 per year for each subscription or $0.70 per issue.

POSTAGE: Postpaid within the United States, Canada, Mexico, and all Central and South American countries except Argentina, Brazil, British and French Guiana, Surinam, and British Honduras. For these Central and South American countries and all other countries, add $0.75 per year or $0.20 per single issue.

REMITTANCE: Payment should be by check, money order, or document coupons and MUST accompany order. Remittances from foreign countries should be made by international money order or draft on an American bank payable to the Superintendent of Documents or by UNESCO book coupons.